GEOLOGICAL SURVEY OF WESTERN AUSTRALIA

BULLETIN 132

THE KIMBERLITES AND LAMPROITES OF WESTERN AUSTRALIA

DEPARTMENT OF MINES
WESTERN AUSTRALIA

THE KIMBERLITES AND LAMPROITES OF WESTERN AUSTRALIA

Frontispiece

Oblique aerial view, looking north, of the Argyle Pipe prior to disturbance by mining. The pipe occupies the narrow valley in the centre of the photograph. To the east and southeast is the Razor Ridge, of Hensman Sandstone, unconformably overlying well-bedded Revolver Creek Formation. The main hill is the East Ridge, composed of Lissadell Formation sandstones, silstones and shales dipping 30°-40° to the north (GSWA 22555) (Photo: CRAE).



GEOLOGICAL SURVEY OF WESTERN AUSTRALIA

Bulletin 132

THE KIMBERLITES AND LAMPROITES OF WESTERN AUSTRALIA

by

A.L. Jaques[1], J.D. Lewis[2] and C.B. Smith[3]

1. Bureau of Mineral Resources, Canberra, A.C.T.
2. Geological Survey of Western Australia, Perth, W.A.
3. C.R.A. Exploration Pty. Ltd., Belmont, W.A.

Government Printing Office
Perth, 1986

MINISTER FOR MINERALS AND ENERGY
THE HONOURABLE DAVID PARKER, M.L.A.

DIRECTOR GENERAL OF MINES
D.R. KELLY

DIRECTOR OF THE GEOLOGICAL SURVEY
A.F. TRENDALL

NATIONAL LIBRARY OF AUSTRALIA CATALOGUING-IN-PUBLICATION ENTRY

Jaques, A.L. (Alan Lynton), 1949-
The kimberlites and lamproites of Western Australia.

Bibliography
ISBN 0 7309 0802 X.

1. Kimberlite — Western Australia. 2. Lamporite — Western Australia. 3. Diamonds — Western Australia. I. Lewis, J.D. (John David), 1936-. II. Smith, C.B. (Christopher Brian), 1939-. III. Geological Survey of Western Australia. IV. Title. (Series: Bulletin (Geological Survey of Western Australia); no. 132).

552'.3

ISSN 0085-8145

FOREWORD

The discovery of diamonds in the Kimberley region of Western Australia — first, the sub-economic deposits of Ellendale in 1976, followed by the rich Argyle pipe in 1979 — was the culmination of an extensive exploration effort by a number of mining companies. That the host rocks are ultrapotassic lamproites, rather than "classical" kimberlites, has transformed the appreciation of these petrological curiosities, not only in Australia but worldwide. It is as a direct result of these discoveries, and the interest they have generated, that Western Australia has been privileged to host the Fourth International Kimberlite Conference of 1986.

This bulletin is intended primarily to present the field and laboratory work of the authors, one of whom has been engaged in the Western Australian diamond exploration programme almost from its inception. About one hundred and fifty lamproite, kimberlite, and alkali picrite bodies are now known, and the history of exploration for diamond is fully documented. All presently known lamproites and kimberlites in Western Australia are described, and an account given of their structural setting, petrography, mineralogy and chemistry. Modern research on the petro-genesis of lamproites and their diamond content is at an early stage, and treatment of these topics is necessarily brief and tentative. Thus, a secondary intention of this bulletin is to stimulate research on these interesting, if rare, rock types.

This important bulletin is the first Geological Survey publication to have joint authors from industry, the Bureau of Mineral Resources, and the Survey, affirming and exemplifying the increasing need for cooperative geological effort between different groups. Many of the basic data have been obtained by mining companies, and their active assistance is acknowledged with gratitude. Without this fruitful cooperation this publication would not have been possible. It is to be hoped that this will become more frequent in the future, to the benefit of the mining industry and the people of Western Australia.

A.F. Trendall
DIRECTOR
GEOLOGICAL SURVEY

CONTENTS

Foreword v
Summary xv

CHAPTER 1 INTRODUCTION

Introduction 1
Acknowledgements 1
Previous investigations 2
Alluvial diamonds at Nullagine 2
Early work on the Fitzroy Lamproites 2
Diamond exploration of the 1970's 3
Early diamond exploration in the Kimberley area 3
The Kalumburu Joint Venture 4
Diamondiferous lamproites in the West Kimberley 7
The Argyle diamond deposits 12
Post-Argyle exploration in the Kimberley area 13
Exploration south of the Kimberley area 14
Nomenclature 15

CHAPTER 2 THE STRUCTURAL SETTING OF WEST AUSTRALIAN KIMBERLITE AND LAMPROITE PROVINCES

Evolution of the structural framework of Western Australia 18
The Archaean nucleii 18
Proterozoic mobile belts and progressive cratonization 18
Phanerozoic rifting of the western continental margin 20
Kimberlite and lamproite provinces 20
North Kimberley Province 20
East Kimberley Province 21
West Kimberley Province 21
Wandagee Province (Carnarvon Basin) 21
Discussion 22

CHAPTER 3 THE NORTH KIMBERLEY PROVINCE

Physiography, regional geology, and structure 24
Age of intrusion 24
Geology of the kimberlites 24
Skerring Pipe 24
Wishywashy Dyke 26
Hadfields Dyke 27
KGB2 Dyke 27
Jump Up Dyke 28
Pteropus Breccia Pipe 28
Mineralogy 29
Skerring Pipe 30
Wishywashy, Hadfields, and Jump Up Dykes 33
KGB2 Dyke 34
Pteropus Breccia Pipe 34

CHAPTER 4 THE EAST KIMBERLEY PROVINCE

Regional geology and structure 36
Age of intrusion 37
Argyle Pipe, AK-1 37
Local stratigraphy 37
Geology of the Arygle Pipe 40
Shape of the pipe 40
Contact relations 41

Diatreme lithologies ... 41
Eruptive sequence ... 43
Petrography ... 45
Mineralogy ... 51
Xenoliths ... 54
Geochemistry ... 55
Lamproite and lamprophyre dykes ... 59
Lissadell Road Dykes ... 59
Bow Hill Dykes ... 60
Kimberlitic dykes ... 65
Maude Creek Dyke ... 65
Devils Elbow Dykes ... 67
Other dyke occurrences ... 69

CHAPTER 5 THE WEST KIMBERLEY PROVINCE

Distribution of pipes and mode of emplacement ... 71
Mode of emplacement ... 71
The age of intrusion ... 74
The Ellendale Field ... 75
Geology and structure of the field ... 75
Structure ... 77
Geology ... 78
The lamproite intrusions ... 80
Mount North ... 83
Mount Percy ... 89
81 Mile Vent ... 93
Ellendale 2 ... 100
Ellendale 4 ... 102
Ellendale 4, Satellite pipe ... 111
Ellendale 6 ... 112
Ellendale 7 ... 114
Ellendale 9 ... 117
Ellendale 11 ... 125
Ellendale 16 ... 128
Ellendale 23 ... 130
Ellendale 31 ... 131
Ellendale 37 ... 132
Ellendale 38 ... 133
Other lamproite intrusions ... 134
Ellendale 8 ... 135
Ellendale 10 ... 135
Ellendale 12 ... 135
Ellendale 13 ... 135
Ellendale 14 ... 136
Ellendale 15 ... 136
Ellendale 17 ... 137
Ellendale 18 ... 137
Ellendale 19 ... 138
Ellendale 21 ... 138
Ellendale 22 ... 139
Ellendale 24 ... 139
Ellendale 25 ... 139
Ellendale 26 ... 139
Ellendale 27 ... 140
Ellendale 33 ... 140
Ellendale 34 ... 140
Ellendale 35 ... 140
Ellendale 36 ... 141
Ellendale 39 ... 141
Ellendale 40 ... 141
Ellendale 41 ... 141
Ellendale 42 ... 141
Ellendale 43 ... 142
Ellendale 44 ... 142
Ellendale 45 ... 142
Ellendale 46 ... 142
Water Reserve Pipe ... 142
Sill "A" ... 142

The Eastern Lennard Shelf Field 142
Geology and structure 143
Big Spring 143
Big Spring West 146
Cajaput Creek 146
Mount Rose 146
McKinrick Hill 149
Old Leopold Hill 150
Old Leopold West 151
Prairie Hill East 151
Brooking Creek 154
J J Bore 155
Unexposed lamproites 155
Hooper West 155
Brooking Gorge 156
J K Yard 156
Stoney Creek 156
The Calwynyardah Field 156
Geology and structure 156
Calwynyardah 157
Laymans Bore East 159
Laymans Bore West 160
Hansons Bore 160
Minor lamproite intrusions 160
Metters Bore 160
Merrilees Bore 161
Billys Bore 161
Fishers Dam 161
The Noonkanbah Field 161
Geology and structure 162
Mount Abbott 163
Mount Noreen 165
Mount Gytha 166
Machells Pyramid 167
Mount Cedric 169
Mount Cedric North 174
Mount Ibis 174
Fishery Hill 177
Noonkanbah Hill 179
Howes Hill 182
Mamilu Hill 183
Hills Cone 185
"P" Hill 187
Djada Hill 189
The Sisters 192
Walgidee Hills 194
White Rocks 199
Minor lamproite intrusions 201
19 Bore No. 1 201
19 Bore No. 2 201
20 Bore 201
33 Bore 202
Mamilu West 202
Mount Cedric South 202
BHPM-2 202
Kalyeeda 202
Isolated intrusions in the Fitzroy Valley 203
Rice Hill 203
Bruten 204
Oscar 207
Concealed lamproite intrusions 208
Nerrima 208
Gumhole 208
Spielers Bore 208
Camarotoechia Creek 209
Mineral Chemistry 209
Olivine 209
Phlogopite 210
Diopside 214
Leucite 215

Amphibole 216
Chrome spinel 216
Apatite 218
Priderite and other titanates 218
Other phases 219
Xenocryst phases 220
Mantle xenoliths 222
Chemistry 223
Major elements 223
Trace elements 225
Isotopic compositions 227

CHAPTER 6 THE WANDAGEE PROVINCE (CARNARVON BASIN)

Regional geology and structural setting 229
Geology of the diatremes and intrusions 231
Petrography 233
Sills and dykes 233
Pyroclastics 233
Mineralogy 234
Olivine 234
Clinopyroxene 234
Spinels 234
Mica 235
Other phases 235
Xenocryst suite 235
Chemistry 237

CHAPTER 7 DIAMONDS

Argyle diamonds 239
Lamproite diamonds 239
Alluvial diamonds 242
West Kimberley diamonds 243
Lamproite diamonds 243
Alluvial diamonds 244
Kimberley Plateau diamonds 244
Nullagine diamonds 244
Wandagee diamonds 246
Comparison of lamproite and kimberlite diamonds 246

CHAPTER 8 PETROGENESIS

Relationships between the kimberlitic and lamproitic rocks of Western Australia 247
Petrological and mineralogical differences 247
Low pressure fractionation 248
High pressure crystallization 248
Contrasting magma types 250
Xenoliths and the nature of the upper mantle beneath the Kimberley and Carnarvon Basin regions 251
Origin of the magma 252
Mantle sources 252
Conditions of formation 252
Conclusions 253
REFERENCES 257

APPENDICES

Appendix 1. Mineral and chemical analyses (methods) 255
Appendix 2. Mineral and chemical analyses (results) ..... (microfiche in pocket)

ILLUSTRATIONS

PLATES (in pocket)

1. Lamproite intrusions of the West Kimberley Region
2. Lamproite intrusions of the Ellendale Field
3. Lamproite intrusions of the Noonkanbah Field
4. Kimberlitic intrusions of the Carnarvon Basin

FIGURES

1. Oblique aerial view of the Argyle Pipe ..... *(frontispiece)*
2. Stream-gravel sampling from a trap site in the North Kimberley 5
3. Laboratory flow sheet for processing gravel samples 6
4. Aeromagnetic anomalies of the Ellendale area 8
5. Annual expenditure on exploration of the Kalumburu and Ashton Joint Ventures 8
6. Size distribution and diamond content of the Ellendale pipes 11
7. Argyle Diamond Mines processing facility 13
8. Tectonic units of Western Australia and location of kimberlite and lamproite provinces 17
9. Location of kimberlites in the North Kimberley Province 23
10. Sketch map of the Skerring Pipe 25
11. Nb *versus* Zr plot for some West Australian kimberlites and lamproites 26
12. Geological sketch map of the Wishywashy Dyke 26
13. Geological sketch map of the Hadfields Dyke 27
14. Geology and gravity contours of the Pteropus Breccia Pipe 29
15. $MgTiO_3$-$FeTiO_3$-Fe_2O_3 plot for ilmenite macrocrysts from the North and East Kimberley 31
16. Ilmenite-silica graphic intergrowth, Skerring Pipe 31
17. Clustering of Skerring garnets on an MgO-FeO-CaO plot 31
18. CaO *versus* Cr_2O_3 plot for Skerring Garnets 32
19. Ca-Mg-Fe plot for Skerring pyroxenes 32
20. Spinel prism plots for spinels from the Skerring Pipe 33
21. Plot of Fe^{2+}/Mg face of the oxidized spinel prism for spinels from Skerring Pipe 34
22. Location of kimberlites and lamproites in the East Kimberley Province 35
23. Geological map and cross sections of the Argyle Pipe 38
24. Slickensides on the Gap Fault, Argyle 40
25. Bedded "sandy" tuff in drill core 42
26. Dyke of phlogopite-olivine lamproite 42
27. Polished drill core of tuffs from the Argyle Pipe 44
28. Polished slab and drill core of tuffs from the Argyle Pipe 46
29. Photomicrographs of contact breccia and tuff from Argyle Pipe 48
30. Photomicrographs of tuff from Argyle Pipe 49
31. Photomicrographs of "non-sandy" tuff from Argyle Pipe 50
32. Spinel-pyroxene pseudomorph after garnet 54
33. Variation of SiO_2 with MgO for Argyle lamproites and country rocks 56
34. Variation of K_2O/Na_2O with K_2O/Al_2O_3 for Argyle lamproites 56
35. Variation of major elements with 100 Mg/(Mg + FeO) for Argyle lamproites and country rocks 57
36. Variation of trace elements with 100 Mg/Mg+FeO) for Argyle lamproites and country rocks 58
37. Zr/Nb *versus* Ti/Zr diagram for Argyle lamproites 59
38. Geological sketch map of the Lissadell Road Dykes 60
39. Geological map of the Bow Hill Dykes 61
40. Detailed section through the Bow Hill and Lissadell Road dykes 62
41. Photomicrographs of the Bow Hill Dyke 63
42. Geological sketch map of the Maude Creek Dyke 65
43. Photomicrograph of Maude Creek kimberlite 66
44. Spinel prism plot of groundmass spinels from Maude Creek Dyke 66
45. Plot of Fe^{2+}/Mg face of the oxidized spinel prism for groundmass spinels from Maude Creek Dyke 67
46. $MgTiO_3$-$FeTiO_3$-Fe_2O_3 plot for ilmenite macrocrysts from Maude Creek and Duck Creek dykes 67
47. Ca-Mg-Fe plot for clinopyroxene macrocrysts from Maude Creek Dyke 67
48. MgO-FeO-CaO plot of garnets from Maude Creek 68
49. CaO *versus* Cr_2O_3 plot for garnets from Maude Creek 68
50. CaO *versus* Cr_2O_3 plot for garnets from Devils Elbow No 3 Dyke 69
51. 100 Mg/(Mg+Fe^{2+}) *versus* Cr/(Cr+Al) for chromite from Devils Elbow No 3 Dyke 69
52. Distribution of lamproites in the West Kimberley Province, and a summary of K-Ar isotopic ages 74
53. Seismic profiles across the Lennard Shelf 76
54. Depth to Magnetic Basement of part of the Lennard Shelf 77
55. Panoramic view of Windjana Gorge 79
56. Exhumed karst in the Nullara Formation 81

57. Geological map of Mount North 82
58. Bedded "sandy" lapilli-tuffs, Mount North 84
59. Mount North from the north 85
60. Mount north from the west 85
61. Photomicrographs of tuff and lamproite from Mount North 87
62. Geological map of Mount Percy 90
63. Geological map of 81 Mile Vent 94
64. 81 Mile Vent, oblique view from the southwest 95
65. Screen of tuff-breccia between sills, 81 Mile Vent 95
66. Structures in the pyroclastic deposits of 81 Mile Vent 97
67. Photomicrographs of tuff and lamproite from 81 Mile Vent 98
68. Geology and total magnetic intensity of Ellendale 2 101
69. Geological map of Ellendale 4 103
70. Bedded tuffs exposed in an exploration pit 104
71. Structural contours of Ellendale 4 105
72. Photomicrographs of tuffs from Ellendale 4 106
73. Photomicrographs of olivine lamproite from Ellendale 4 108
74. Variation of SiO_2 and Ni with MgO for olivine lamproites from Ellendale 4 111
75. Variation of Nb with Zr and Zr/La with Ti/Zr for olivine lamproites of Ellendale 4 111
76. Geological map of Ellendale 4, Satellite pipe 112
77. Geological map of Ellendale 6 113
78. Grant Group sandstone ridge around Ellendale 6 113
79. Geological map of Ellendale 7 114
80. Photomicrographs of tuffs and lamproite from Ellendale 7 116
81. Ferruginized and silicified lapilli-tuff 117
82. Geology and ground magnetic contours of Ellendale 9 119
83. Photomicrographs of tuffs from Ellendale 9 120
84. Photomicrographs of olivine lamproite from Ellendale 9 122
85. Variation of SiO_2, Ni, and Zr/Nb ratio with MgO for olivine lamproites from Ellendale 9 125
86. Geological map of Ellendale 11 126
87. Photomicrographs of tuff and olivine lamproite from Ellendale 11 127
88. Geological map of Ellendale 16 129
89. Geological map of Ellendale 31 131
90. Ellendale 38 from the east 133
91. Geological map of Ellendale 38 134
92. Geological map of the Big Spring area 144
93. Borehole logs, Big Spring 5 145
94. Geological map of Mount Rose 147
95. Geological map of McKinrick Hill 148
96. McKinrick Hill from the south 148
97. Geological map of Old Leopold Hill 149
98. Old Leopold Hill from the east 150
99. Geological map of Prairie Hill East 151
100. The main plug of Prairie Hill East from the northwest 152
101. Satellite vent of Prairie Hill East 152
102. Geological map of Calwynyardah area 157
103. Geological map of Calwynyardah 158
104. Photomicrographs of Calwynyardah lamproites 159
105. Geological map of Mount Abbott 164
106. Geological map of Mount Gytha 166
107. Geological map of Machells Pyramid 168
108. Machells Pyramid from the southeast 168
109. Geological map of Mount Cedric 170
110. Breccia of vesicular lamproite, Mount Cedric 171
111. Centre II of Mount Cedric 172
112. Photomicrograph of olivine-rich lamproite, Mount Cedric 173
113. Geological map of Mount Ibis 175
114. Photomicrograph of olivine-rich lamproite, Mount Ibis 176
115. Geological map of Fishery Hill 178
116. Fishery Hill from the south 178
117. Geological map of Noonkanbah Hill 180
118. Noonkanbah Hill from the south 181
119. Sandstone breccia, Noonkanbah Hill 181
120. Geological map of Howes Hill 182
121. Geological map of Mamilu Hill 184
122. Geological map of Hills Cone 186
123. Geological map of "P" Hill 188
124. "P" Hill from the north 189
125. Geological map of Djada Hill 190
126. Djada Hill from the west 191
127. Columnar jointing, Djada Hill 191
128. Geological map of The Sisters 193

129. Geological map, and contours of Ni and MgO, Walgidee Hills ... 196
130. Photomicrographs of Walgidee Hills lamproites ... 197
131. Geological map of White Rocks ... 200
132. Photomicrograph of tuff from 19 Bore No. 2 ... 202
133. Geological map of Rice Hill ... 203
134. Photomicrographs of lamproite from Rice Hill ... 204
135. Geological map of Bruten ... 206
136. Bruten from the northwest ... 206
137. Geological map of Oscar ... 207
138. Photomicrograph of vitrophyric olivine-leucite lamproite ... 208
139. Compositions of xenocrystal and phenocrystal olivine in West Kimberley lamproites ... 210
140. Chemical profiles across xenocrystal and phenocrystal olivine from an olivine lamproite ... 211
141. Variation of NiO content in xenocrystal and phenocrystal olivine from West Kimberley lamproites ... 211
142. Variation in composition of West Kimberley micas ... 212
143. Variation of F content of West Kimberley micas ... 213
144. Compositional variation of West Kimberley phenocryst and groundmass pyroxene ... 215
145. Composition of leucite in West Kimberley lamproites. ... 215
146. Compositional variation of amphiboles in West Kimberley lamproites ... 217
147. Compositional variation of pyroxenes and amphiboles from Rice Hill ... 220
148. Compositional variation of xenocryst spinels and spinels from West Kimberley peridotite xenoliths ... 221
149. Composition of chrome diopside xenocrysts from West Kimberley lamproites ... 222
150. CaO *versus* Cr_2O_3 in Cr-bearing garnets from the West Kimberley ... 222
151. Major element *versus* MgO variation in West Kimberley lamproites ... 224
152. Trace element *versus* MgO variation in West Kimberley lamproites ... 226
153 Chondrite-normalized REE diagram for West Kimberley lamproites and southern African kimberlites ... 227
154. Structural divisions of the Carnarvon Basin ... 229
155. Structure and gravity trends of the Wandagee area ... 230
156. Photomicrographs of Wandagee alkali picrites and tuffs ... 232
157. Morphology of Argyle and Ellendale diamonds ... 239
158. Colour of Argyle and Ellendale diamonds ... 240
159. Photographs of Argyle and Ellendale diamonds ... 241
160. Diamonds from Morelli's Fox, King George River ... 245

TABLES

1. Diamonds recovered from Big Spring ... 7
2. New lamproites found in the West Kimberley Province, 1977-1982 (excluding Ellendale Field) ... 10
3. Results of evaluation of Ellendale 4, 7, 9, and 11 ... 11
4. Estimated reserves of diamondiferous alluvial gravel at Argyle, prior to mining ... 12
5. Alluvial diamond production from Argyle ... 12
6. Argyle, AK-1, Pipe, ore reserves ... 13
7. Diamonds recovered by Gem Exploration and Minerals Ltd from the Ord River ... 14
8. Diamonds recovered by Bow River Joint Venture from Limestone Creek ... 14
9. U-Pb and fission-track zircon ages from the North Kimberley ... 24
10. Analysis of massive kimberlite from Skerring Pipe ... 25
11. Trace-element analyses of the Hadfields and Wishywashy dykes ... 27
12. Analysis of KGB 2 Dyke ... 28
13. Trace-element geochemistry of the Pteropus Breccia Pipe and host-rock sandstone ... 30
14. Concentrate minerals and their abundance in kimberlites from the North Kimberley Province ... 30
15. Representative analyses of ilmenite from the Skerring Pipe ... 30
16. Representative analyses of garnet macrocrysts from the Skerring Pipe ... 32
17. Representative analyses of clinopyroxenes from the Skerring Pipe ... 32
18. Representative analyses of macrocryst spinels from the Skerring Pipe ... 33
19. Representative analyses of groundmass oxides in the Skerring Pipe ... 34
20. Rb-Sr and K-Ar ages of the Argyle Pipe ... 37
21. Rb-Sr and K-Ar ages of the Bow Hill Dykes ... 37
22. Representative analyses of mica from the Argyle Pipe ... 52
23. Representative analyses of groundmass spinel from the Argyle Pipe ... 53
24. Representative analyses of Argyle lamproites and associated country rocks ... 56
25. Representative analyses of mica in Bow Hill Dykes ... 63
26. Representative analyses of pyroxenes, amphibole, clinozoisite, apatite, perovskite, and garnet from the Bow Hill Dykes ... 64
27. Representative analyses of groundmass spinels from the Bow Hill Dykes ... 64
28. Analyses of East Kimberley lamproitic and kimberlitic dykes ... 64
29. Representative analyses of ilmenite and spinels from Maude Creek, Duck Creek, and Devil's Elbow No 3 dykes ... 66
30. Representative analyses of diopside and garnet from Maude Creek and Devil's Elbow No 3 dykes ... 68
31. Representative analyses of Mount North lampoites ... 89
32. Representative analyses of Mount Percy lamproites ... 93
33. Representative analyses of 81 Mile Vent lamproites ... 100
34. Representative analyses of Ellendale 2 lamproites ... 102
35. Representative analyses of Ellendale 4, and Ellendale 4 Satellite lamproite and pyroclastics ... 110
36. Representative analyses of Ellendale 7 lamproites ... 118

37. Representative analyses of Ellendale 9 lamproites 124
38. Representative analyses of Ellendale 11 lamproites 128
39. Representative analyses of Ellendale 16 lamproites 130
40. Representative analyses of Ellendale 23, 31, and 38 lamproites 132
41. Representative analyses of lamproites from Big Spring 146
42. Representative analyses of Eastern Lennard Shelf lamproites 154
43. Representative analyses of Machells Pyramid and Mount Gytha lamproites 169
44. Representative analyses of Mount Cedric lamproites 174
45. Representative analyses of Mount Ibis lamproites 177
46. Representative analyses of Fishery Hill lamproites 179
47. Representative analyses of Noonkanbah Hill lamproites 183
48. Representative analyses of Howes Hill lamproites 183
49. Representative analyses of Mamilu Hill lamproites 185
50. Representative analyses of Hills Cone lamproites 187
51. Representative analyses of "P" Hill lamproites 189
52. Representative analyses of Djada Hill lamproites 192
53. Representative analyses of The Sisters lamproites 195
54. Representative analyses of Walgidee Hills lamproites 198
55. Representative analyses of White Rocks lamproites 201
56. Representative analyses of isolated lamproites in the Fitzroy Valley 205
57. Representative analyses of olivine 210
58. Representative analyses of phlogopite 213
59. Representative analyses of diopside 214
60. Representative analyses of leucite 215
61. Representative analyses of potassic richterite 216
62. Representative analyses of spinels and ilmenite 217
63. Representative analyses of titanates and Ti and Zr silicates 218
64. Representative analyses of alkali pyroxenes 219
65. Representative analyses of sanidine 220
66. Representative analyses of xenocryst phases 221
67. Average mineral composition of mantle xenoliths from Ellendale 7 223
68. Details of Wandagee diatremes, sills and dykes 231
69. Representative analyses of silicate phases in the alkali picrites 234
70. Representative analyses of groundmass spinels 235
71. Summary of macrocryst minerals recovered in concentrates from the Wandagee diatremes 236
72. Representative analyses of xenocrysts phases from the Wandagee diatremes 236
73. Representaive analyses of Wandagee intrusions 237
74. Quality of Argyle Diamonds 240
75. Syngenetic mineral inclusions from Argyle diamonds 240
76. Representative analyses of olivine inclusions in diamonds 240
77. Representative analyses of pyroxene inclusions in diamonds 242
78. Representative analyses of garnet inclusions in diamonds 242
79. Representative analyses of chromite, kyanite, and rutile inclusions in diamonds 242
80. Syngenetic mineral inclusions from Ellendale diamonds 243
81. Carbon isotope measurements on West Australian lamproite diamonds 246
82. Comparison of major- and trace-element data for West Australian kimberlites and lamproites 249

SUMMARY

Chapter 1: Diamonds were first found in Western Australia at Nullagine, in the Pilbara District, in 1895; their source is still unknown. Leucite lamproites of Miocene age in the West Kimberley region were first studied in the 1930's, and their affinity with kimberlites noted. Exploration for diamonds in the West Kimberley began in the late 1960's; pyrope garnet and picroilmenite were recovered from Mount Abbott, but no diamonds. Nine small diamonds were recovered from the Lennard River but the result was not repeatable. Many companies became involved, but the most successful diamond search has been that of the Kalumburu/Ashton Joint Venture, which discovered kimberlite dykes and pipes in the North and East Kimberley, diamondiferous olivine lamproite in the Ellendale area of the West Kimberley, and the rich lamproitic Argyle Pipe in the East Kimberley. The exploration and evaluation of these deposits is fully described. In the Carnarvon Basin a group of small sills, dykes, and pipes of alkali picrite, carrying traces of diamond, was also discovered.

Chapter 2: A brief account of the structural evolution of Western Australia is given, particularly the cratonization of the West Australian Shield and the North Australian Craton. The kimberlite and lamproite provinces are related to these structures. The kimberlite dykes and pipes of the North Kimberley Province ($\approx$ 800 Ma) intrude gently folded platform cover of the Kimberley Basin, and are probably related to a marginal downwarp of the Kimberley Block towards the Bonaparte Basin. The East Kimberley Province kimberlite and lamprophyre dykes ($\approx$ 800 Ma), and the lamproitic Argyle Pipe ($\approx$ 1 150 Ma), are related to major faults in the Halls Creek Mobile Zone, which was cratonized at about 1 800 Ma. In the West Kimberley Province, the leucite and olivine lamproites are of Miocene age ($\approx$ 20 Ma) and straddle the Proterozoic King Leopold Mobile Zone (cratonized $\approx$ 1 800 Ma) and the Fitzroy Trough (Devonian-Jurassic). The basement of the Fitzroy Trough is probably an extension of the King Leopold Mobile Zone, and the lamproites may be related to major basement faults active into the Early Jurassic, or to passage of the Australian continent over a "hot spot". The Wandagee diatremes are related to a major rift fault and basement horst block in the Phanerozoic Carnarvon Basin. The age of the Wandagee diatremes is the same as the age of continental breakup (160 Ma).

The principal structural setting for kimberlite and lamproite intrusion in Western Australia is within Early Proterozoic mobile zones marginal to Archaean nucleii, although the mobile zones may be covered by Phanerozoic sediments. The belts had been cratonized, but were still subject to brittle fracture and faulting. Major strike-slip faults, active over a long period, have formed the principal conduits for the rise of kimberlitic and lamproitic magma.

Chapter 3: The North Kimberley Province is known to contain four small kimberlite dykes and two pipes, and the presence of other dykes is probable. The dykes are very thin (< 1 m wide), thoroughly altered, and are marked at the surface by a wide dispersion of indicator minerals, chiefly picroilmenite. The age of the dykes is about 800 Ma. The Skerring pipe is an expansion, 450 m long and 75 m wide, on a dyke at least 3.5 km long, and contains massive, altered porphyritic kimberlite containing abundant macrocrysts of picroilmenite, garnet, and chrome diopside. A second variety of kimberlite, packed with xenoliths of country-rock shale, is also present. The Pteropus Breccia Pipe is about 2 ha in area and contains a breccia of country-rock sandstone with small dykes and stringers of altered kimberlitic material. Diamond has been recovered in a number of drainage gravel samples but only single stones have been obtained from one dyke and the Pteropus pipe. The mineralogy and chemistry of heavy-mineral concentrates, particularly picroilmenite, garnet, chromite, and clinopyroxene from the Skerring pipe, is discussed.

Chapter 4: The East Kimberley Province occupies part of the Halls Creek Mobile Zone and contains kimberlite and lamproite bodies of at least two ages. All intrusions are closely related to major faults in the mobile zone. The lamproitic Argyle Pipe is dated between 1 048 Ma and 1 153 Ma, and is intruded close to the Halls Creek Fault into sediments of the Carr Boyd Group, which are only marginally older. The Bow Hill Dykes are lamprophyric in character, dated at about 800 Ma, and related to the Bow Hill Fault; while a number of micaceous kimberlite dykes, similar to those of the North Kimberley Province and probably the same age ($\approx$ 800 Ma), are related to the Greenvale Fault.

The diamond-rich Argyle Pipe is an elongate body, 2 km long and from 150 m to 500 m wide, that was intruded into sandstone, siltstone, and shale of the Carr Boyd Group. At its northern end, the pipe is bowl-shaped; the remainder is a steeply dipping dyke-like body cut by several faults. The pipe is filled by a faulted and disrupted sequence of pyroclastics, with subordinate dykes of olivine-phlogopite lamproite. Two types of pyroclastic deposit are present — "sandy" tuff containing abundant quartz grains of wall-rock origin in addition to juvenile lamproitic ash and lapilli; and "non-sandy" tuff composed almost entirely of lamproitic material. Both pyroclastic types are fully described, and the model developed for the eruptive sequence is similar to that for the formation of maars, a model which involves the explosive interaction of rising magma and groundwater. The "sandy" tuffs are often well-bedded and are inferred to have resulted from base-surge eruptions, while the "non-sandy" tuffs are possibly the result of magma extruding into a crater lake.

The rock-type present in the Argyle Pipe is olivine lamproite, sometimes with minor leucite present, although alteration has destroyed much of the primary mineralogy. Analyses of phlogopite and spinel are presented, and the primary and secondary mineralogy described. Xenocryst minerals are described, and also rare mantle xenoliths of harzburgite from the "non-sandy" tuff. The chemistry of the rocks is complicated by the inclusion of much country- rock quartz, but nevertheless the magma is shown to be ultrapotassic, MgO-rich, and similar in composition to the olivine lamproite of the West Kimberley.

The Lissadell Road Dykes are small and thoroughly altered and silicified. They are diamond-rich, similar to, and probably related to, the Argyle Pipe.

The Bow Hill Dykes are a suite of micaceous ultrabasic lamprophyres emplaced, *en echelon,* over a strike length of 19 km, into the Bow Granite. Two main rock types are present — olivine-phlogopite lamprophyre, similar in appearance to the micaceous kimberlite dykes, and garnet-phlogopite pegmatite, found as veins within the dykes. The garnets of the pegmatites are distinctive, consisting of dark red-brown melanite cores and colourless andradite rims. The chemistry and mineralogy of the dykes, particularly the Zr-rich garnets, is compared with alnöite, and the dykes shown to have carbonatitic affinities.

The kimberlitic dykes of the western part of the province are micaceous, usually < 1.5 m wide, characterized by the presence of picroilmenite and pyrope macrocrysts, and some carry a few diamonds. Dykes from Maude Creek and the Devils Elbow area are described, and the chemistry of the macrocryst minerals is reported.

Chapter 5: The West Kimberley Province occupies an area about 150 km diameter covering parts of the King Leopold Mobile Zone, and adjacent parts of the Lennard Shelf and Fitzroy Trough on the northern margin of the Canning Basin. Over one hundred intrusions of leucite-rich and olivine-rich lamproites are known; they are concentrated in two large fields, the Ellendale and Noonkanbah Fields, and two smaller groups, the Eastern Lennard Shelf and Calwynyardah Fields. The intrusions are Miocene in age (18-23 Ma), and become progressively younger from north to south. This possibly results from the Australian continent passing northward over a mantle "hot spot" at rate of about 30 mm/a. Most of the bodies are relatively small diatremes, in which an early phase of explosive volcanism was followed by the rise of magma to form a lava lake or blister within the open vent, or a plug in the neck of the volcano. Separate dykes and sills are less common. Drilling of a number of the bodies has shown that the vents flare rapidly from a narrow conduit a few hundred metres below the present land surface to give a "champagne glass" shaped vent. The large vents are filled with bedded pyroclastics, the result of phreatomagmatic activity and base-surge deposition of fine-grained pyroclastics. This model is similar to that for maar volcanism but relies on groundwater in the sediments rather than the ingress of surface water.

In the Ellendale Field, a total of 48 lamproite vents occurs in an area about 40 km long by 15 km wide on the northern margin of the Canning Basin. They intrude a faulted basement block of the underlying King Leopold Mobile Zone, which is overlain by relatively thin Paleozoic sediments. Lamproite intrusion was probably influenced by the nearby Oscar Fault, which was active from Proterozoic times through to the Jurassic. A small number of lamproites appear to be directly related to this, and another fault, along the base of the Napier Range. The larger lamproite vents of the Ellendale Field are described in detail, with brief notes on the unexposed smaller bodies.

Mount North forms a prominent hill 90 m high, and consists of a central magmatic core of coarse phlogopite-leucite lamproite, thin sills of olivine-leucite lamproite, and well-bedded "sandy" lapilli-tuff. Erosion has exposed the central core, which displays prominent columnar jointing.

Mount Percy contains a small body of lamproite and lamproite lapilli-tuff in a vent which is filled mostly with brecciated sandstone. Tangential dykes of brecciated sandstone in the surrounding country rock suggest that the vent enlarged itself by spalling large blocks of country rock into the vent.

The 81 Mile Vent is similar to Mount North; it consists of a central core of phlogopite-leucite lamproite and a number of concentric sills intruding a bedded pyroclastic succession. The tuffs are well exposed and show a variety of structures consistent with an origin from base-surge type volcanism. The rocks of 81 Mile Vent are notable for consistently high LREE contents compared with other lamproites, and extreme Rb abundances ($> 7\,000$ ppm).

Ellendale 4 is a large unexposed vent of 76 ha, formed by the coalescing of a number of adjacent smaller vents. Extensive drilling has revealed a group of vents, each "champagne glass" shaped, and filled with a variety of fine-grained, bedded pyroclastic deposits. A central magmatic core, similarly "champagne glass" shaped, is of olivine lamproite which probably formed a lava lake within the open vent. The rock type is distinctive and contains abundant olivine macrocrysts — with undulose extinction and other solid-state deformation textures — and olivine microphenocrysts, all in a fine-grained groundmass of diopside, phlogopite and spinels. More slowly cooled and evolved central portions of the mass also contain poikilitic phlogopite, interstitial potassic richterite, and a little altered leucite. The pyroclastic deposits contain diamond at an average grade of about 14 CM/100 t, but the grade in the magmatic core is only about 0.5 CM/100 t.

Ellendale 4 is typical of a number of other concealed olivine lamproite pipes which contain diamond at grades > 1 CM/100 t; these include Ellendale 7, 9, and 11. In general the larger and more MgO-rich bodies contain higher diamond grades, but a few stones have been recovered from a number of concealed leucite-rich pipes.

Ellendale 7 is distinctive in that olivine lamproite has intruded an earlier leucite lamproite pipe, and both types of fragments are present in the pyroclastic deposits. Marked differences in isotopic ratios preclude a comagmagtic relationship between the two rock types.

The Eastern Lennard Shelf Field comprises a scattered group of leucite lamproite plugs that intrude the Lennard Granite, and a number of pipes, including the olivine lamproites of Big Spring, which intrude Devonian limestone of the Lennard Shelf. The intrusions appear to be structurally controlled and related to major faults in the crystalline basement. The Big Spring pipes are up to 10 ha in area and were the site of the first recovery of diamond from an olivine lamproite pipe.

The lamproite intrusions of the Calwynyardah Field are probably structurally related to the major northern boundary faults of the Fitzroy Trough. Two large, and five small, concealed lamproites are emplaced in an area of less than 50 km^2. The Calwynyardah pipe is 124 ha in area, the largest known pipe in Western Australia after Walgidee Hills. Drilling has shown it to be "champagne glass" shaped and pyroclast filled, except for a small plug and sills of olivine-leucite lamproite. The pipe contains a thick central wedge of reworked silty tuff interbedded with thin lignite horizons — the result of deposition within a crater lake. With similar reworked

tuffs at the nearby Laymans Bore East pipe, this is the only direct evidence of post-eruption crater lakes in the lamproite volcanoes. All the pipes of the Calwynyardah area contain sparse diamond.

Lamproites of the Noonkanbah Field are located in the central part of the Fitzroy Trough and intrude rocks of Permian to Triassic age, mostly on the southern limb of the Quanbun Syncline. The intrusions are probably related to structures within the Proterozoic basement, which is nowhere exposed. With the exception of Mount Abbott, all the intrusions are leucite-rich. Small numbers of diamonds have been recovered from Mount Abbott and from a few unexposed lamproites.

Mount Abbott is a large (≈ 90 ha), poorly exposed vent, containing a coarse sandstone breccia with angular blocks >1 m across, "sandy" tuff composed of quartz grains and minor amounts of lamproite, and lamproite lapilli-tuff. The summit of the hill is formed by a large mass of relatively undisturbed sandstone. The lamproite is olivine-rich and contains none of the minerals characteristic of lamproite. A few diamonds and abundant indicator minerals have been recovered from bulk samples.

Machells Pyramid is a prominent landmark and consists of a "spine" of xenolith-bearing diopside-leucite lamproite that has intruded unbedded pyroclastics. A similar "spine" of welded agglomeratic lamproite forms the summit of "P" Hill.

Mount Cedric is a composite vent. The main hill consists of a central core of olivine-leucite lamproite overlying coarse tuffs and breccias. A second intrusive centre consists of a partial cone-sheet of fine-grained olivine-leucite lamproite surrounding central intrusions of diopside – potassic-richterite – leucite lamproite and olivine-rich lamproite. This last intrusion carries abundant olivine macrocrysts with undulose extinction and, along with similar rocks from Mount Ibis and The Sisters Southwest, forms a distinct class of magnesia-rich leucite lamproites with MgO between 14 and 19%.

Walgidee Hills is the largest lamproite body in the West Kimberley, and has a diameter of about 3 km. Most of the area is underlain by poorly exposed, coarse-grained, altered lamproite. Only a narrow marginal zone of brecciated country-rock is present. The central part of the body is most notable for the rare minerals contained in pegmatoid veins and patches: priderite, jeppeite, wadeite, shcherbakovite, and potassic richterite.

A number of isolated lamproites are also found in the West Kimberley Province: most notably Rice Hill, a 45 m-thick sill of coarse-grained, phlogopite-leucite lamproite; and Oscar, a small dyke of olivine-leucite lamproite containing an unaltered glassy groundmass.

Analyses and variation diagrams for the major mineral species contained in the lamproites are given. Olivine, both macrocysts and microphenocrysts, lies in the range $Mg_{92-92.5}$ with high Ni, and low Cr, Ti, and Al contents. The macrocrysts often show marginal reverse zoning. Phlogopite phenocrysts often show strongly coloured rims, rich in Ti and Fe; and groundmass mica is usually tetraferriphlogopite. A feature of the micas is their high TiO_2 (1-12%) and F (up to 7%) contents. The strongly pleochroic amphibole is titanian potassic richterite — characterized by high Mg/(Mg + Fe), TiO_2 (2-7%), and alkalis ($Na_2O + K_2O > 8\%$). Other minerals discussed include diopside, leucite, chromite, apatite, titanates, and Ti-Zr silicates. A brief account is also given of xenocryst minerals from heavy-mineral concentrates and the mineralogy of the rarely occuring mantle xenoliths.

Chemically, the West Kimberley lamproites are characterized by high K_2, TiO_2, P_2O_5, ZrO_2, and BaO, and very low Na_2O. The suite forms a continuum from the ultrabasic, peridotitic composition of olivine lamproite, to the more basic leucite lamproite. The greatest variation is in MgO (<5%-29%) and variation diagrams based on 470 analyses are plotted for major and trace elements *versus* MgO. The lamproites are rich in LREE and "incompatible" elements (Ba, Rb, Sr, P, Zr, Nb), and have a high initial $^{87}Sr/^{86}Sr$ ratio and low $^{143}Nd/^{144}Nd$ ratio.

Chapter 6: A group of 14 small diatremes and 8 sills and dykes of alkali picrite are known from the Wandagee area of the Phanerozoic Carnarvon Basin. The pipes intrude close to the Wandagee Fault System, a major rift fault close to the eastern margin of the basin. The age of the intrusions is 160 ± 10 Ma, similar to the age of the breakup of Gondwana. The diatremes are steep-sided, pipe-shaped bodies filled with olivine-rich pyroclastics, and contain very sparse diamond. The sills and dykes are of alkali picrite, and contain olivine macrocrysts and abundant olivine phenocrysts in a diopside-rich matrix. The rocks are rich in MgO (up to 28%), contain abundant Ni and Cr, but are poor in alkalis, and have low levels of "incompatible" elements.

Chapter 7: A brief account of the diamonds and diamond inclusion minerals from Argyle and Ellendale pipes is given. From Argyle the stones are strongly resorbed dodecahedral forms, and brown is the dominant colour. Diamond grades are high (>5 CM/t), but the content of industrial stones is also high. Syngenetic mineral inclusions are dominantly from the eclogitic suite. From Ellendale the diamonds are typically rounded dodecahedral forms with a distinctive shiny surface, and yellow in colour. The gem content is high, but the overall diamond grades are low. The ultramafic and eclogitic suites of syngenetic mineral inclusions are present in equal proportions. A comparison with kimberlitic diamonds shows no differences from those recovered from lamproites.

Chapter 8: The differences and similarities between the kimberlitic and lamproitic rocks of Western Australia are re-examined to assist in determining petrogenesis. Unlike kimberlitic pipes, glassy and vesicular pyroclasts are common in the lamproitic vents, and magmatic rocks are present in the crater zone. Mineralogically the lamproites contain phases that are atypical of kimberlites, notably leucite, potassic richterite, priderite, and wadeite. The wide range of composition of the lamproites is the result of low-pressure fractionation and the separation of olivine, chrome spinel, diopside, phlogopite, and perovskite; although there was probably more than one parent magma. High-pressure crystallization is more evident in the kimberlitic dykes of the North and East Kimberley; this is indicated by the relatively common occurrence of macrocrysts of picroilmenite, titanian pyrope, pyroxene, spinel and zircon. Such macrocrysts are rare or absent in lamproites.

In Western Australian lamproite and kimberlite pipes, mantle xenoliths are rare and often altered. Rock types present have been interpreted to include dunite, garnet peridotite, garnet lherzolite, and harzburgite.

No eclogitic xenoliths are known, but inclusions in diamonds, and heavy mineral concentrates, contain minerals of the eclogitic suite. It is concluded that the mantle beneath the Kimberley region is refractory, depleted, and possibly contains some eclogite.

Lamproite, like kimberlite, is considered to be a small-volume partial melt that formed deep in the mantle. The West Kimberley lamproites, however, like micaceous kimberlites, are derived from a source which has also undergone long-term enrichment in Rb/Sr and Nd/Sm. Melting took place under H_2O- and HF-rich, CO_2-poor conditions, probably of a phlogopite-rich, metasomatized harzburgitic or lherzolitic mantle.

CHAPTER 1

INTRODUCTION

Diamonds were first recorded in Western Australia in 1895 (Groom, 1896) when a few small stones were found by gold prospectors near Nullagine in the Pilbara region. Despite continued speculation as to their source, it was not until the mid-1960's that serious exploration for diamonds began. A state-wide exploration effort by a number of mining companies culminated in October 1979 with the discovery, by the Ashton Joint Venture, of the Argyle Pipe, AKI, in the East Kimberley District. This body, grading 7 CM/t (metric carats/tonne) is the richest diamond pipe in the world in terms of quantity although about 90% of production is industrial diamonds.

Mining of alluvial gravels associated with the Argyle Pipe began in January 1983; and, in the first full year of production, 6 154 639 CM of diamond, valued at over $60 million, was obtained from 1 068 052 t of gravel, a grade of 5.76 CM/t. Open-pit production from the pipe itself began in December 1985, and annual production is planned to build up to about 25 million CM.

Thus, in the short space of twenty years, diamond in Western Australia has been transformed from a mineralogical curiosity to a commercial mining operation contributing significantly to the State's income from mineral wealth. In terms of quantity of production, the Argyle mine is the largest diamond mine in the world; and Australia has become the largest producer of natural industrial diamonds, and a significant producer of gem-quality stones.

Mineral exploration has discovered several dozen diamond-bearing intrusions, some with definite kimberlitic affinities, but most associated with previously known leucite-lamproite bodies. Altogether, more than one hundred such bodies are now known, including diatremes, plugs, sills, and dykes. Most of the intrusions are located in the Kimberley region in the north of Western Australia; but a small group with distinctive characteristics has also been found in the northern Carnarvon Basin. No source has yet been found for the diamonds recovered from the Nullagine area on the southeastern margin of the Pilbara Block.

The affinity of leucite-lamproite and kimberlite was originally proposed by Prider (Wade and Prider, 1940; Prider, 1960) in studies of the intrusions in the Fitzroy valley, Western Australia. Recent exploration work has shown that the diamond-bearing olivine-rich rocks of this suite, although they show many similarities, differ from true kimberlites. In the Ivory Coast, alluvial diamond fields are associated with dykes of phlogopite-leucite lamproite (fitzroyite) (Knopf, 1970); and the diamond-bearing intrusion at Prairie Creek, Arkansas, is also a member of the lamproite suite (Scott-Smith and Skinner, 1984 a,b). From preliminary work on the Western Australian intrusions by Atkinson and others (1982, 1984a), Jaques and others (1982, 1984a), Smith (1984a), Gregory (1984), and Hall and Smith (1984), it is now widely recognized that lamproites form a new class of diamond-bearing rocks, allied to, but different from the classical kimberlites of southern Africa and the U.S.S.R. In Western Australia, the complete range of such rocks — from basic leucite-rich to ultrabasic olivine-rich types — is now known and provides an ideal study area for ultrapotassic volcanism.

This study is to provide: an account of the geology of the individual lamproite and other kimberlitic intrusions in Western Australia; a description of their regional setting; and a review of their petrology, mineralogy, and chemistry.

Isotopic geochemistry and age data, largely the work of other authors, will be reviewed, and a brief account of diamonds, in both pipe and alluvial deposits, will be given. The various chapters of the bulletin have usually been written by one author but each has been reviewed by the other authors so that individual credits are not possible.

ACKNOWLEDGEMENTS

This bulletin would not have been possible without access to the reports of, and support of personnel from, many mining companies. In particular, the staff of C.R.A. Exploration Pty Ltd (operators for the Ashton Joint Venture), Argyle Diamond Mines Pty Ltd, B.H.P. Co Ltd, B.P. Minerals, Gem Exploration and Minerals Ltd, and Stockdale Exploration Ltd, are acknowledged. For assistance in the field, advice, and comment on various parts of the manuscript, we wish to thank W.J. Atkinson, G.L. Boxer, C.L. Geach, G.P. Gregory, M.J. Gunn, E.A. Haebig, F.E. Hughes, I.D. Kerr, A. Meakins, and A.C. Moore. In particular, the contribution of G.L. Boxer to the description of the geology of the Argyle Pipe is acknowledged. Dr J. Ferguson, formerly of the Bureau of Mineral Resources, is acknowledged for his contribution and support in the early part of this project.

Chemical analyses have been made by J. Pike, T. Slezak, W. Pappas, and J. Haldane of the B.M.R.; and N. Marsh and C. Dodd, of the W.A. Government Chemical Laboratories.

Diagrams and maps have been drawn by Manjeet Kumar, Carol Locke, and Frank Martin, of the W.A. Mines Department.

This bulletin is a cooperative effort between State and Federal bodies, and was prepared with the full participation of industry. The authors wish to acknowledge the encouragement of the Directors of the Geological Survey of W.A. and the Bureau of Mineral Resources, and in particular Mr. J. Collier, Managing Director of C.R.A.E., for permitting C.B.S. to participate.

PREVIOUS INVESTIGATIONS

Large-scale exploration for diamond did not begin in Western Australia until the late 1960's; but, apart from the Nullagine diamonds, there had been important work by Prider (Wade & Prider, 1940; Prider, 1960) suggesting the kimberlitic affinities of lamproites in the West Kimberley area. Until exploration began, there were no published reports — known to the authors — of diamonds in the Kimberley; but, in view of developments, the personal report of Fr. Sanz of the Kalumburu Mission that, in 1906, he was given a diamond that had been recovered by an Aborigine from the Drysdale River, cannot be entirely discounted (G.P. Gregory, pers. comm.). The unconfirmed rumour that the Brockman expedition of 1902 discovered diamonds in the north Kimberley remains entirely speculative.

Alluvial diamonds at Nullagine

Diamonds were first discovered in 1895 at Nullagine in Western Australia, by gold prospectors working what are now thought to be Tertiary conglomerates. The diamonds were recovered from the gravel remaining in the stamper boxes after crushing to release gold. The initial report by Groom (1896) recorded 17 small diamonds; and in 1900, a further 25 small diamonds were recovered from 230 tons of conglomerate from a location 1.6 km north of the township. In succeeding years, diamonds — including a 3.5 carat stone in 1915 — were occasionally found by fossickers. These early records are detailed by Simpson (1951), who also notes that between 1901 and 1903 customs records show an export of "precious stones" valued at £2,011. As no other gems were known at this time the "precious stones" are presumed to be Nullagine diamonds.

No systematic exploration for alluvial diamonds, or for their source rock, took place at Nullagine before 1965. In that year, Dr John Jeppe was granted a Temporary Reserve to explore for diamonds; and in 1967, he was joined by C.R.A. Exploration Pty Ltd. In 1970, exploration was continued by Mining Advisers Pty Ltd; the reserve was finally relinquished in April 1971. An area of over 4 000 km^2 was explored by stream sampling and photogeology, and resulted in the recovery of 20 small diamonds, the largest being 1.03 CM.

The geology of the Nullagine area has been described by Carter (1974), and it appears that all the diamonds recovered have come from the Brooks Hill Beds, or from gravel washed from the beds. The Brooks Hill Beds — of Tertiary age — form elongate limonite-capped mesas which stand up to 45 m above the valley floor and consist of fluviatile sands, gravels, and conglomerates, variably ferruginized (Carter, 1974). The deposits are probably an older alluvium from a paleo-channel of the Nullagine River. The diamond-bearing gravels are not of sufficient extent, or sufficiently rich, to warrant a major exploration effort, and thus far the source of the diamonds has not been discovered. Continued exploration for alluvial gold deposits will probably produce a few more diamonds (Hutton, 1985) and may eventually lead to the discovery of the source rock. Recent exploration has been on a regional scale, and several companies have conducted stream-gravel surveys over much of the Pilbara Block. One such survey by BHP recovered indicator minerals, possibly from a Proterozoic sandstone, north of Nullagine (M.J. Gunn, pers. comm.).

Early work on the Fitzroy Lamproites

The lamproites of the Fitzroy valley and adjacent Lennard Shelf areas provided Western Australia with its first major diamond find when the Ellendale Field was discovered in 1976. The majority of intrusions to be described in this bulletin are located in this area, which in recent years has become the "type locality" for lamproite magmatism. A number of intrusions, however, have been known for many years.

The first geologist to investigate the area was E.T. Hardman in 1883. He travelled up the Fitzroy River, visiting Mount Abbott, Mount Hardman, and possibly Machell's Pyramid. In the report of the expedition (Hardman, 1884), all these hills are noted as composed of sandstone, grit, and ironstones which weathered to form spheroidal and concretionary structures. There is no evidence that he visited all the hills; and, at a distance, Hardman appears to have mistaken intrusive lamproite plugs for ironstone. Machell's Pyramid, for example, is described as "a curious pyramidal mass of reddish sandstone rising rather abruptly from the surrounding plain. The debris from the pyramid forms a steep *talus* around it." Nevertheless, Hardman provided the first description of what is now known to be a lamproitic body:

> Mount Abbott is a low hog-backed hill, slightly pointed at top, and is formed of fine grey and brown sandstone, highly indurated at times, very massively bedded, but showing thin laminae, all more or less colored, in patches, green. The dip is N. at 30°. The rocks in this neighborhood show considerable signs of disturbance. (Hardman, 1884, p.15).

The green colour of the sandstones, which is now known to be a characteristic marginal effect of lamproite intrusion, was tested for copper, but Hardman concluded that it was caused by the presence of "proto-silicate of iron".

The first recognition of lamproite in the Fitzroy area followed the examination of rock samples collected by W.V. Fitzgerald, who traversed the Kimberley region north and east of the Napier and Oscar Ranges (Fitzgerald, 1907). One specimen was described by

Farquharson (1920) as a "mica leucitite" from a locality given as "Lennard River, near Mount Eliza", and he expressed doubt as to its genuineness, likening it to similar alkaline rocks from Java. The thin section (GSWA 64605) is of a phlogopite-leucite lamproite consisting of small flakes of phlogopite, up to 1mm long, set in a very fine-grained leucite-rich groundmass with small prisms of priderite. Small xenoliths of granite and shale are also present. The rock is similar to many other leucite-lamproites of the region, and the xenoliths are those to be expected of a dyke or plug intruding the King Leopold Mobile Zone. The curiosity remains, however, that the location given is 45 km northeast of the nearest exposed lamproite at Mount North and it has not been rediscovered during recent mineral exploration work.

The discovery of the lamproite intrusions of the Noonkanbah area, close to the Fitzroy River, followed the beginning of oil exploration in the Kimberley region. Farquharson (1922) briefly noted mica-leucitite lavas, leucitite agglomerates and tuffs, and fine green tuffs from "Freney's Oil Find". The intrusions then known were noted on the maps of Wade (1924) and included Rice Hill, Machell's Pyramid, Fishery Hill, Noonkanbah Hill, "P" Hill, and Bruten's Hill. In the text there is a footnote that:

> Lamprophyres and Leucite-bearing lavas break through the Upper Carboniferous Rocks and form a line of volcanic necks sometimes associated with small local flows... T. Blatchford...considers these lavas to be of Tertiary Age because of their resemblance to the lavas of this age in the Dutch East Indies. (Wade, 1924, p.9).

In a note by Simpson (1925), it is recorded that these intrusions were first discovered by Blatchford and Talbot of the Geological Survey, and that J.E. Wells had reported similar rocks at Mount North. In the same report, Simpson provides an analysis of a rock from Barjar Hill (now known as Djada Hill), remarking on the high titanium and barium content of the rock. The rocks were described and note was made of small needles of rutile, now known to be priderite, and — from B.E. Hill (Rice Hill) — titaniferous augite with yellow to violet pleochroism, an obvious misidentification of potassic richterite. In a final report on oil prospects in the Kimberley area, Blatchford (1927) added Mount Gytha, Mount Cedric, Mount Ibis, and Djada Hill, to the list of known intrusions, together with "a hill one mile south of Paradise" which is otherwise unknown. The rocks are described as necks or elongated vents, the baking of marginal shales and sandstones is noted as also the lack of evidence for surface flows.

Thorough investigation of the lamproite intrusions came with the work of Wade and Prider (1940). In 1934-5, Wade, while engaged in oil exploration, discovered several more intrusions in the Noonkanbah area, and made sketch maps of the 19 bodies then known. The mineralogy, petrology, and chemistry of the rocks, was investigated by Prider. A complex nomenclature based on local names was erected, and it was noted that the magma was rich in "incompatible" elements — K, Ti, Zr, P, Ba, Sr, V, and F. The kimberlitic affinities of the magma were noted and a petrogenesis by removal of olivine from a mica-peridotite magma proposed. This, and subsequent studies, discovered three new minerals, wadeite, $K_2ZrSi_2O_{12}$ (Prider, 1939), priderite $(K,Ba)(Ti,Fe)_8O_{13}$ (Norrish, 1951) and jeppeite, $(K,Ba)_2(Ti,Fe)_6O_{13}$ (Pryce and others, 1984); and potashrich varietes of richterite (Prider 1939) and batisite (Prider, 1965).

In his 1960 paper, Prider presents detailed maps of a number of the intrusions and develops further his ideas on the derivation of the lamproite magma from a mica peridotite parent, concluding that "They appear to be genetically related to an ultrabasic magma... probably closely related to kimberlites,". In addition, a Rb-Sr model age of 144 ± 7 Ma is given — suggesting a Jurassic age for the intrusions. Further age determinations were given by Kaplan and others (1967) for Mount North: a Rb-Sr isochron age of 150 ± 4 Ma was interpreted as the age of intrusion; and K-Ar ages of 32-37 Ma assumed to be the age of uplift of the surrounding peneplain. There is, however, no evidence for Oligocene uplift in the Mount North area; and Wellman (1972) presented further K-Ar ages for three lamproite bodies of 17-21 Ma (Eary Miocene) which he interpreted as the age of emplacement. More recent work by Jaques and others (1984b), giving dates of 17-24 Ma, confirms the Miocene age of the West Kimberley lamproites.

Additional lamproites discovered during oil exploration work were reported by Prider (1960) at Mount Percy, near Mount North, and — as sills — in the Nerrima 1 well north of the Fitzroy River. Systematic regional mapping by BMR-GSWA field parties has recorded a new group of lamproites intruding the Leopold Mobile Zone, including Old Leopold Hill (Harms, 1959), Mount Rose, McKinrick Hill, Prairie Hill East, and Big Spring (Derrick and Gellatly, 1972). The last authors also describe 81 Mile Vent, a lamproite in the vicinity of Mount North.

DIAMOND EXPLORATION OF THE 1970's

Exploration for diamonds in Australia using modern techniques began in the southeastern States in the 1960's, based on the known occurrence of small deposits of alluvial diamonds (MacNevin, 1977) and the presence of basic and ultrabasic diatremes. This has led to the discovery of kimberlite dykes and small pipes in South Australia, and numerous para-kimberlitic diatremes elsewhere (Stracke and others, 1979; Ferguson and Sheraton, 1979), but no economic diamond deposits. Exploration in Western Australia, beginning in 1965, and based on the known occurrence of alluvial diamonds at Nullagine, has already been described. New ground was not broken until exploration began in the Kimberley area.

Early diamond exploration in the Kimberley area

In 1967 a consortium of three small exploration companies, Exoil N.L., Transoil N.L., and Petromin N.L., were granted a Temporary Reserve, TR 4665H, of about 670 km^2 on the northern margin of the Lennard

Shelf some 100 km east of Derby. Grab samples of alluvium and lamproitic material from Mount North were examined for diamonds and kimberlitic indicator minerals. In addition, a number of lamproite intrusions in the Noonkanbah area, together with alluvium in the Fitzroy River channel west of Mount Abbott, were sampled. A combined aeromagnetic and radiometric survey of 1 770 line-kilometres was flown in 1968 over TR 4665H, but the results were not thought to be encouraging and there was no ground follow-up. At this stage, no diamond or indicator mineral had been identified; but in October 1969, samples of alluvium from the bed of the Lennard River, in the vicinity of Police Camp Pool (see Plate 2), weighing about 1 t in total, produced a concentrate of ilmenite and 9 small diamonds totalling 1.65 CM. A follow-up survey in 1970, taking fifteen 1 t samples from the same locality, produced more ilmenite, which was not tested for kimberlitic affinities, but no diamond. The origin of the nine small diamonds is problematic; but it should be noted that Police Camp Pool is only a few kilometres north of the Ellendale area, which contains diamondiferous lamproites. The aeromagnetic survey south of the Lennard River noted several anomalies over these bodies; but they were not investigated. A full account of the operation can be found in Haynes (1971) who concluded:

> ... despite all efforts by a South African leading authority in diamond exploration no further diamonds were found and no minerals normally associated with diamonds were observed... In view of these conclusions it can only be assumed that results of the early sampling were not representative of the area from which the samples were taken.

Exploration by Stellar Minerals N.L. extended from 1968 to 1971 (Jeppe, 1971) and concentrated on the known lamproite bodies in the Noonkanbah area, and at Mount North and Mount Percy on the Lennard Shelf. Bulk sampling of the lamproites was combined with soil and stream sediment sampling, shallow drilling, and ground magnetic and radiometric surveys. Geophysical surveys were discontinued when initial tests failed to give useful results. No diamonds were found; but, in two cases, kimberlitic indicator minerals were recovered. In the initial investigation, small grains of pyrope garnet were recovered from pits in the northeast intrusion of The Sisters and from Mount Abbott; and a few grains of ilmenite, from stream sediments on Mount Abbott. The MgO content of the ilmenite ranged up to 5.5%, suggesting the possibility of a kimberlitic origin. A partial analysis of pyrope from Mount Abbott gave MgO, 18.9%; CaO, 4.2%; Cr_2O_3, 3.5%; and FeO, 6.7% — equivalent to a group 9 chrome pyrope, the common kimberlitic pyrope of Dawson and Stephens (1975). This was the first recognition of kimberlitic indicator minerals in Western Australia and was obtained from material which Jeppe recognized as a weathered olivine-rich tuffisite breccia similar to "yellow ground" kimberlite. Subsequent investigations discovered five more localities within the Mount Abbott body with similar tuffs and tuff-breccias containing phlogopite, pyrope, picroilmenite, and picrochromite. Bulk sampling operations on the Mount Abbott lamproite treated about 200 t but no diamonds were recovered and Stellar's prospecting operations then ceased. A few diamonds were later recovered from Mount Abbott by the Ashton Joint Venture.

During the same period a number of other companies explored for diamond in the Kimberley area. Stockdale Prospecting Ltd., for example, carried out drainage sampling in the West Kimberley, but with negative results. Most directed their attention to the leucite lamproites of the Fitzroy valley, but a few companies extended reconnaissance prospecting northwards into the Proterozoic Kimberley Basin. In 1971, Selection Trust Ltd collected 119 drainage samples, each of about 13 kg of -2 mm material, from 20 700 km^2 of the Sturt Block, east of Halls Creek. Few good trap sites were found and no diamonds or indicator minerals. Almost all prospecting was carried out on "open ground" without public reporting of results. Lawrence (1971) has, however, described one such survey carried out by the Bureau de Recherches Géologiques et Minières (BRGM).

The BRGM survey covered some 100 000 km^2 of the west Kimberley, from the Fitzroy valley to the central and western parts of the Kimberley Basin. Alluvial prospecting was used; 2 to 20 m^3 bulk samples of stream gravel were taken from drainage lines every 25 km, giving a sample density of 1:1 000 km^2. The samples were excavated by hand or back-hoe, ideally from bedrock crevices or pot-holes. After transport to a central washing plant, the heavy minerals were concentrated by a jig of BRGM design. Each concentrate was then examined for diamond and kimberlite indicator minerals (IM). Lawrence gives no results for the programme, but in view of the lack of announced discoveries, or signs of detailed follow-up work, this survey and other similar surveys throughout the Kimberley area at this time were presumably unsuccessful in locating targets of economic interest.

The Kalumburu Joint Venture

The most successful diamond search in Western Australia has been that of the Kalumburu Joint Venture and its successor, the Ashton Joint Venture. Both major diamond discoveries, Ellendale and Argyle, were made by this consortium; and, because of its success, the exploration programme will be described in detail.

The chain of events commenced in 1971 when Tanganyika Holdings Ltd. (now known officially as Tanks) considered area selection for diamond exploration and carried out photogeological interpretation and reconnaissance field work in the Kimberley to test the methods under consideration. Tanks' area selection criteria (Atkinson and others, 1984a,b) were based on the African model where economic kimberlite sources of diamond are restricted to cratons stable for at least 1 500 Ma (Clifford, 1966). In South Africa, and also in the Siberian shield (Yakutia), a zonal arrangement is seen (Dawson, 1970, 1980) in which a diamondiferous kimberlite area is

surrounded by non-diamondiferous kimberlites, and alkalic intrusions such as olivine melilitite and carbonatite occur in the circum-cratonic fold belts. In Western Australia, there are three ancient cratonic nuclei: the Yilgarn, the Pilbara (with alluvial diamonds at Nullagine), and the Kimberley. Tanks had confirmed the presence of the kimberlitic indicators, pyrope and chrome diopside, at Mount Abbott, and recognized the similarity of the West Kimberley leucite lamproites to an outer zone of alkalic rocks or barren kimberlites surrounding a hypothetical diamondiferous zone within the Kimberley Basin — a little-disturbed platform cover over a shield area as old as or older than the surrounding mobile zones.

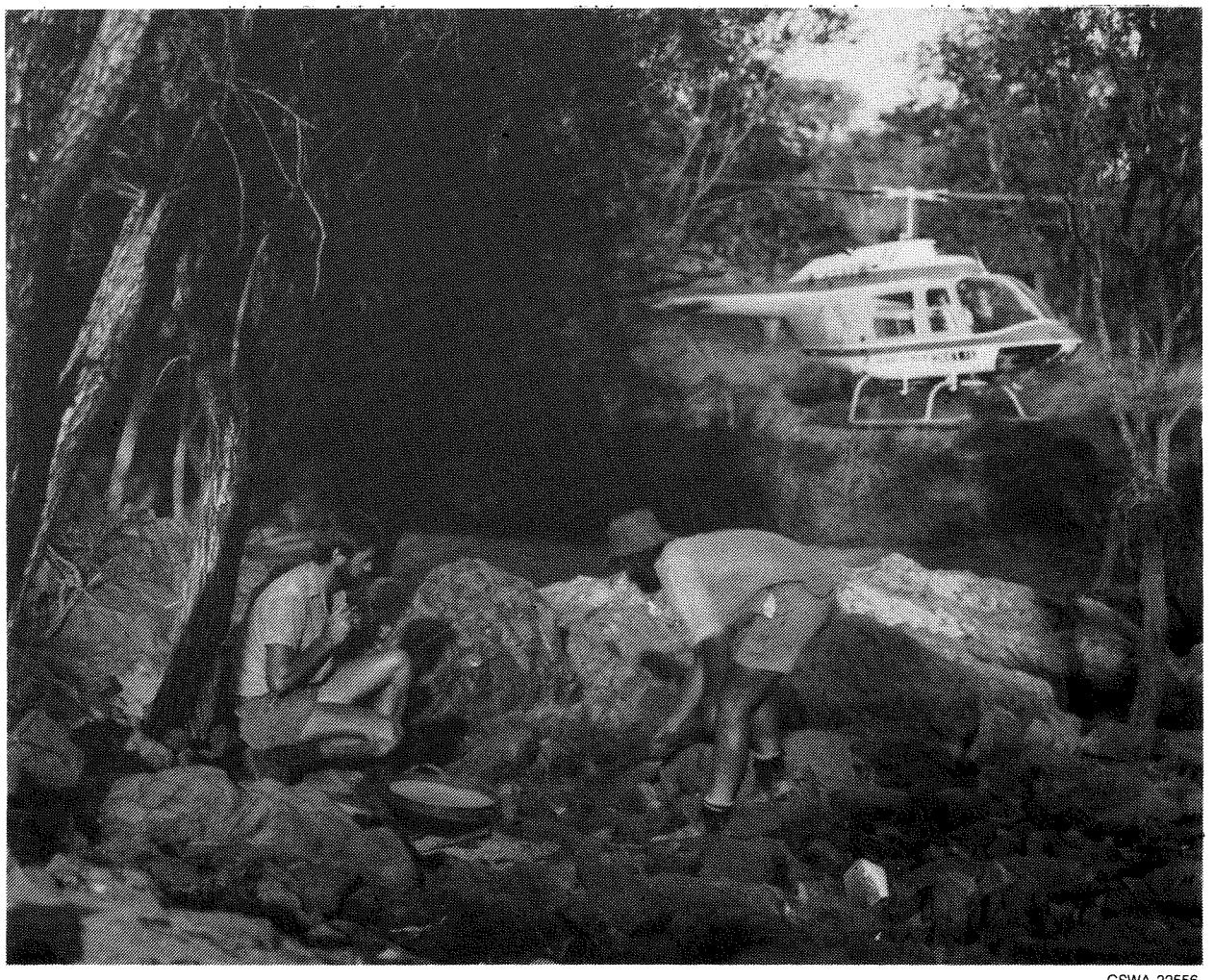
Many other factors were considered during area selection, particularly their suitability for practical methods of exploration. In 1971, Tanks concluded that the Kimberley Block was the prime geological target and eminently suitable for stream-gravel sampling. This method is rapid and cost-effective for the reconnaissance coverage of large well-drained areas. It was decided to include within the area those parts of the surrounding fold belts and Lennard Shelf in which suitable drainages were present.

To carry out this programme, the Kalumburu Joint Venture was formed in 1972: it consisted of Sibeka (a Belgian company with diamond interests in Africa), A.O. Australia Pty Ltd (a subsidiary of the London Tin Corporation), Jennings Mining Ltd, Northern Mining NL, and Tanks — each with a 20% interest and with Tanks as manager.

The initial reconnaissance consisted of the helicopter-borne collection of some 1 000 gravel samples of about 8 kg, each taken from trap sites at 15 km intervals along major drainage lines. The area sampled covered the whole of the Kimberley Block, about 200 000 km^2, bounded in the southwest by the Lennard Shelf, in the south by the 19°S latitude, and in the east by the Great Northern Highway, which lies within the Halls Creek Mobile Zone (Fig. 2). This artificial eastern boundary was created as a result of budgetary constraints in 1972, and thus excluded the Argyle deposit, 15 km east of the highway!

The samples were shipped to Perth and processed through tetrabromoethane (TBE) to recover heavy minerals for inspection. Early samples were searched down to 0.2 mm grain size, later increased to 0.4 mm to speed up the process. The target of the sampling was a kimberlite province, and the minimum for success would be the recovery of one IM grain from one sample — enough to justify detailed follow-up work in a wide region around the sample.

The initial programme indicated three possible kimberlitic provinces. In the north Kimberley, diamonds



GSWA 22556

Figure 2. Stream-gravel sampling from a trap site in the North Kimberley area (Photo: CRAE).

and IM were recovered from one sample in Pteropus Creek; and further diamonds were found in check samples from the King George River. In the east Kimberley, picroilmenite was identified in the Wilson River; and, in the west Kimberley, pyrope was recovered from a creek near Mount Percy. This success suggested that detailed stream sampling should be used to trace the indicators back to their kimberlitic sources. During 1974, sampling commenced in the north Kimberley at 5 km intervals using a gravel sample size of 40 kg. The method was also applied to the Wilson River area; and, in subsequent years, has been extended throughout the Kimberley region as basic coverage.

Field screening of the gravel samples at 4 mm reduced the bulk of each sample to about 20 kg for shipment to Perth for processing. Prior to 1974, the samples had been subjected to minimal processing — TBE separation followed by examination under binocular microscope, usually by the geological staff. In 1974, with about 30 t of samples being generated per annum, it became necessary to design and construct a special laboratory for the processing and analysis of the samples. The laboratory flow sheet adopted (Fig. 3) owes a great deal to the practice of the Australian beach-sand mining industry. Test work by the Engineering Section of the Western Australian Government Chemical Laboratories showed the efficiency of the Wilfley table in preparing heavy mineral concentrates which retained the IM while allowing the advantage of unsized feed. The Wilfley table concentrates are then further upgraded by heavy liquid separation using TBE, and electromagnetic and high tension separations, to reduce the sample to a small fraction requiring final hand sorting by trained mineral observers.

Quality control of the laboratory process is in the hands of graduate staff who confirm the identification of the minerals recorded. At this level, experience is supplemented by optical mineralogy, x-ray techniques, and the use of a scanning electron microscope equipped with an energy dispersive analyzer.

The success of a diamond exploration programme based on kimberlitic indicator minerals depends not only on the quality of the field work, but equally on the efficiency of the associated mineralogical laboratory. In recent years in Australia a number of diamond laboratories have been established along similar lines by companies seeking this commodity.

The detailed stream sampling in the north Kimberley during 1974 and 1975 traced diamond and kimberlitic zircon back towards a cut-off point in Pteropus Creek. Abundant chromite, and occasional pyrope and picroilmenite, were also found, and some chromite in Pteropus Creek above the cut-off point suggested more than one kimberlitic source. Loam sampling, ground magnetometry, and radiometric measurements, were then made on a 200 × 100 m grid in the area surrounding the cut-off. Field examination in early 1976 of a small radiometric anomaly near the IM cut-off in Pteropus Creek located a rubbly, partly lateritized outcrop of vuggy sandstone breccia containing visible

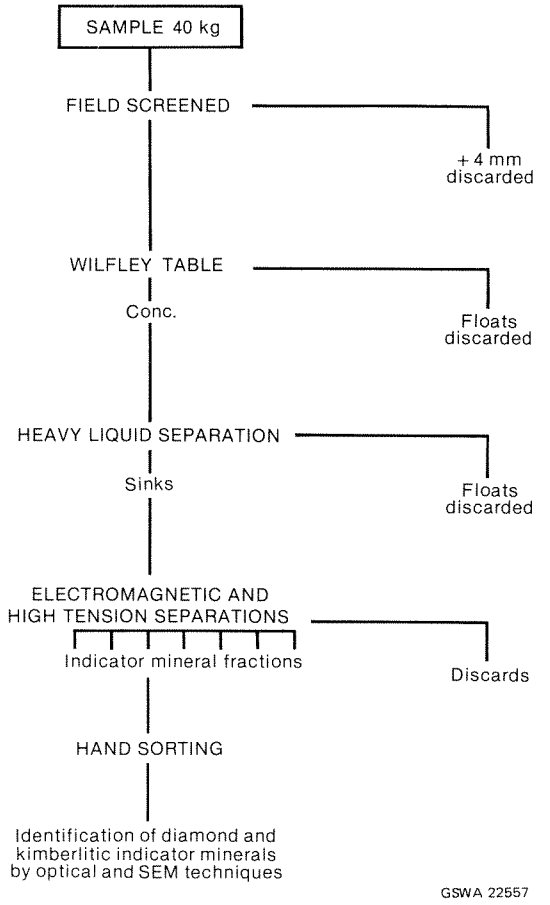


Figure 3. Laboratory flow sheet for processing gravel samples.

chromite and zircon. This was the first kimberlitic pipe found on the Kimberley plateau, and the first in Western Australia to be proved diamondiferous, even though only one diamond has been recovered from the rock itself, and the pipe is only 2 ha in area. The name "Pteropus", for the creek and the pipe, is informal and comes from the large Fruit Bat or Flying Fox, *Pteropus scapulatus,* large colonies of which roost in the Pandanus palms fringing the creek.

Further north on the King George River, follow-up work on diamond, picroilmenite, and minor pyrope indicators, outlined two areas for loaming on 100 m square grids. On the first day of the programme, samplers picked up macrocrysts of picroilmenite several centimetres across; and, on the following day, silicified and lateritized outcrops of the Skerring kimberlite were located. The Skerring, of 1.75 ha, was discovered in September 1976, and was the first pipe in Western Australia to show all the hallmarks of a classical kimberlite. It contains abundant pyrope, picroilmenite, chrome diopside, and mantle nodules, but none of the suite of minerals characteristic of lamproites — such as wadeite, priderite or richterite. However, no diamonds were recovered from 55 m^3 of bulk samples of the kimberlite.

Subsequent work in the north Kimberley has located a number of kimberlitic dykes and stringers, notably Hadfield's, Wishywashy, Jump-up, and KGB2. Most are characterized by an abundance of picroilmenite and pyrope indicators, but most prominent in KGB2 is Nb-

Cr-rutile; none of these dykes have been proven to contain diamonds.

In the east Kimberley, pyrope and picroilmentite occurrences in the Wilson River were traced back to the Duck Creek and Lightening Creek dykes. Neither dyke has been bulk sampled, but the absence of diamond from stream and loam samples suggests that they are not prospective. In 1977, further micaceous kimberlite dykes of the classical type were found at Maude Creek and Devils Elbow. The 7 m-wide Maude Creek dyke yielded four small diamonds from bulk sampling, making it the only known diamondiferous classical kimberlite in Western Australia.

Diamondiferous lamproites in the west Kimberley

Derrick and Gellatly (1972) suggested that the small breccia outcrop at Big Spring was part of a cryptovolcanic structure similar to Mount Abbott. Sampling of soil and creek alluvium in the vicinity of the outcrop by the Kalumburu Joint Venture yielded chrome diopside, chrome pyrope, abundant chromite, and rare diamond. In May 1976, hand excavations, auger drilling, and geological mapping, coupled with grid loaming and soil geochemistry, demonstrated that the breccia outcrop was a large xenolith set within an unexposed 360 m-diameter, (10.4 ha), olivine-rich, magmatic, "kimberlitic" pipe. Throughout 1976, the Big Spring pipe was used as a testing ground for exploration methods. Infra-red photography showed the pipe to be characterized by anomalous faint pink tones, probably reflecting the growth pattern of the grasses covering the pipe. Ground follow-up of similar anomalies immediately to the east located Big Spring No. 2 (3.7 ha), No. 3 (2.2 ha) and No. 4 (2.2 ha) (Fig. 92).

Grid loam sampling and soil geochemistry showed that the soil overlying the pipes was characterized by concentrations of chromite and other indicators, and by anomalously high contents of Ni, Co, and Cr (Hughes and Smith, 1977). Follow-up of anomalous soil geochemistry 0.5 km south of the pipes revealed Big Spring No. 5 (1.1 ha).

A number of geophysical methods were tested over Big Spring No. 1. Good responses were recorded by the magnetic, and turam methods; lesser success was obtained with radiometric, gravity, and resistivity methods; but the moving source E.M. produced no response (Jenke, 1983).

Bulk sampling of the pipes (1977-1982) included magmatic and tuffaceous rocks, overburden, and adjacent creek gravels. The material was treated using a diamond pan and heavy-media separation plant (HMS), with the results given in Table 1. The indicated grade of <0.1 CM/100 t, and the small size of the diamonds recovered, shows that the pipes have no economic value.

TABLE 1. DIAMONDS RECOVERED FROM BIG SPRING

Tonnes treated	*Diamonds recovered*	*Carats recovered*	*Mean stone size (CM)*	*Largest stone (CM)*
650	52	0.55	0.01	0.11

Nevertheless, the Big Spring discovery was most important in that it demonstrated the occurrence of diamondiferous pipes of economic size in Western Australia; and it was the first pipe known in which diamonds were associated with rocks of the lamproite suite. The discovery enabled a study of the geological, petrographic, and geochemical peculiarities of the ultramafic host rocks. The rock-type was first named "kimberlite", although its properties indicated that it was different from the classical kimberlites of southern Africa and other parts of the Kimberley district of Western Australia. These ultramafic lamproites are now known as olivine lamproite following the definition of Jaques and others (1984a).

Follow-up of the pyrope occurrence in a creek northeast of Mount Percy, the first indication of kimberlitic rocks in that area, soon defined a trail of abundant chromite and occasional pyrope and diamond that led back to a cut-off point in a creek near the Oscar Range. At this point, it was possible to hand-jig and field-recover diamonds direct from pot-holes in the creek bed. Loaming of the adjacent country showed that the diamonds and indicators emanated from a very large composite circular structure that was readily visible on air photographs. Thus the 76 ha olivine lamproite pipe, Ellendale 4, became in November 1976 the first diamondiferous pipe to be discovered in the Ellendale Field.

As a result of the success of the ground-based geophysical test work at Big Spring, an airborne magnetic and radiometric survey was carried out in 1977 over some 3 500 km^2 of the Lennard Shelf (Jenke, 1983). Flight-line spacing was 250 m and flight height 80 m. The Palaeozoic sandstones, shales, and limestones of the Lennard Shelf gave a suitably quiet and steady magnetic background against which the lamproites of Big Spring and Ellendale 4 stood out with marked dipolar response. The survey revealed a number of similar dipolar anomalies and to protect these discoveries mineral title was immediately applied for in the form of mineral claims and temporary reserves covering about 900 km^2. Part of the contoured aeromagnetic map is shown in Fig. 4.

The aeromagnetic anomalies were investigated by a programme of ground magnetometry, geological mapping, auger and rotary drilling, and heavy-mineral loam and geochemical soil sampling. From one anomaly, now known as Ellendale 9, a geologist, Frank Hughes, was even able to pick up a 1.75 CM diamond from an adjacent drainage wash! By the end of 1977, a small amount of ground from four of the anomalies, which had been demonstrated to represent large pipes, had been processed through an HMS plant; and diamonds had been recovered from three of them.

It is convenient at this point to review another aspect of diamond exploration, expenditure and company structure. Annual expenditure of the Kalumburu Joint

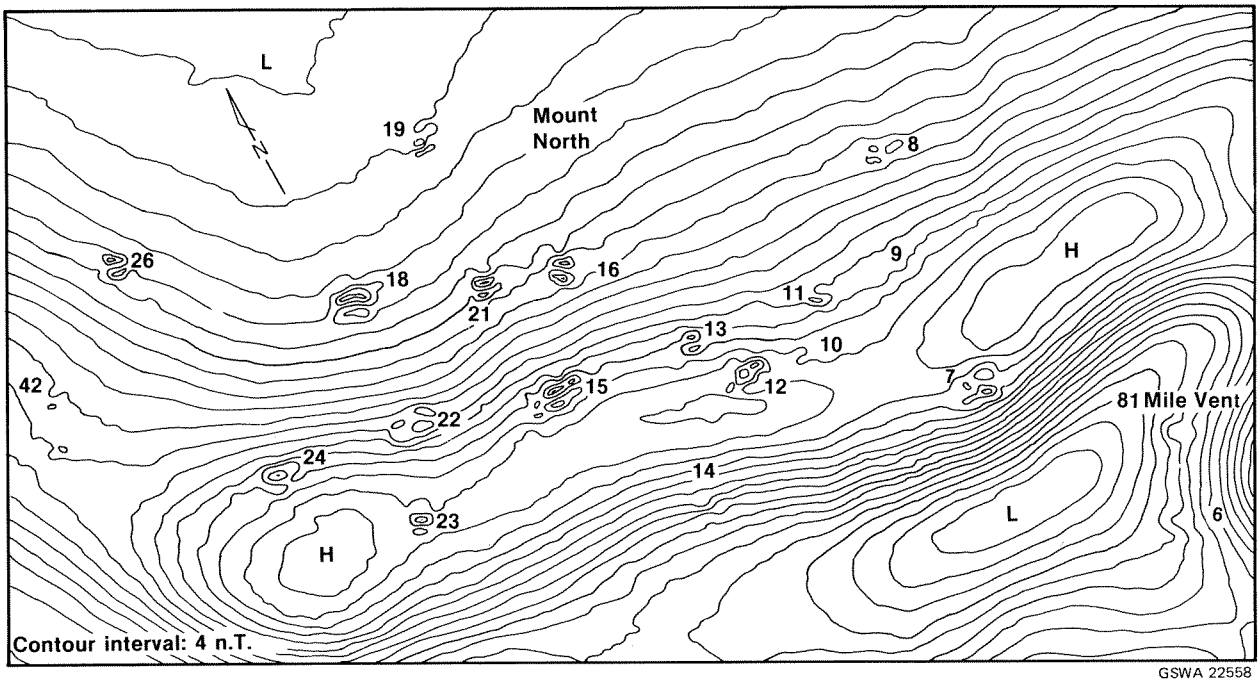


Figure 4. Aeromagnetic anomalies of the Ellendale area (after Hughes, 1978).

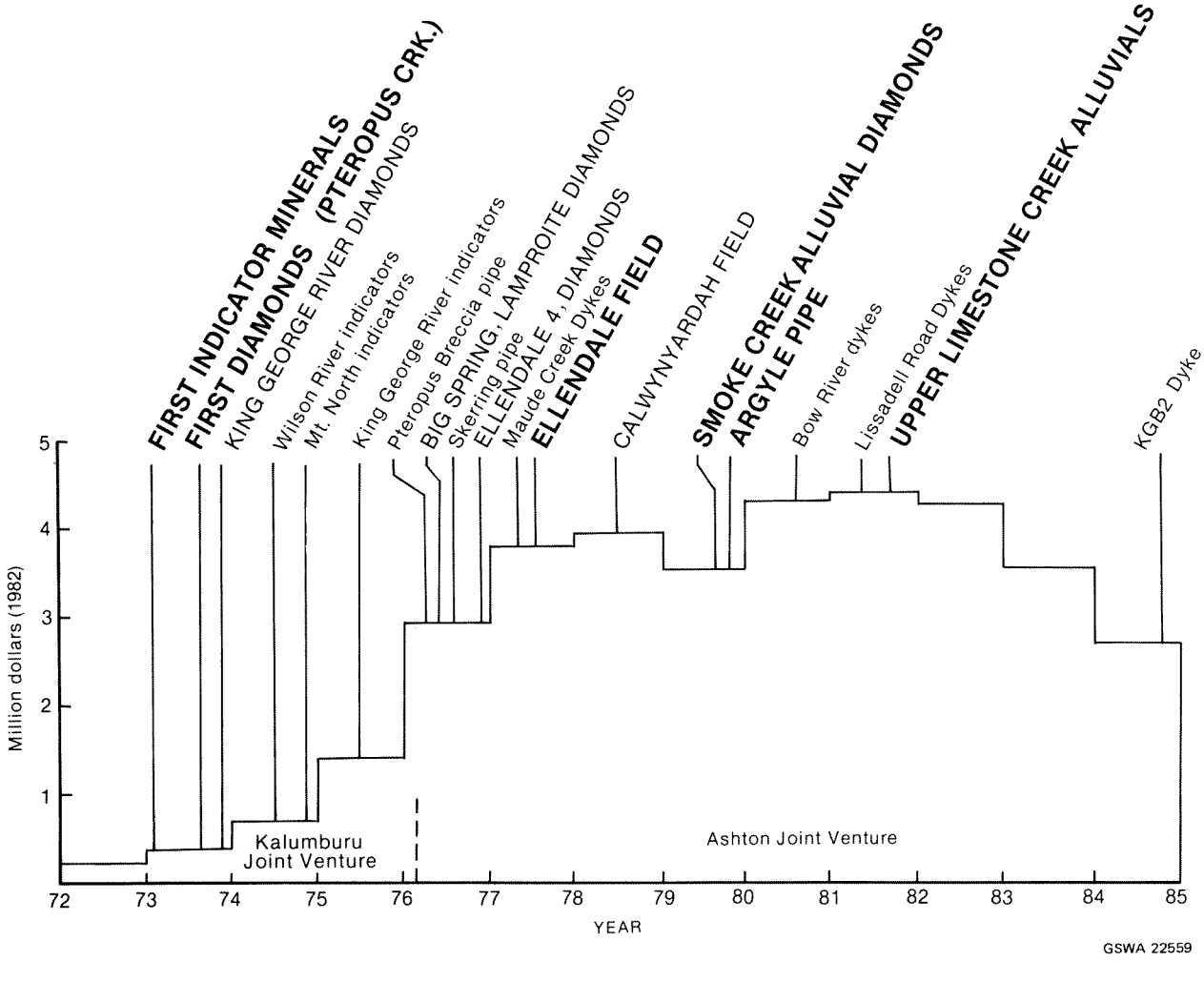


Figure 5. Annual expenditure on exploration of the Kalumburu and Ashton Joint Ventures, 1972-1985, in 1982 dollars; and the sequence of significant discoveries.

Venture had been virtually doubling each year (Fig. 5); and a total of $1.1 million had to be funded for 1974 and 1975. The rate of expenditure, although supported by promising results, was becoming unacceptable to the Joint Venturers, who decided to seek an additional partner to provide funds and broaden the exploration expertise. In February 1976, CRA Exploration joined the Venture, now renamed the Ashton Joint Venture (AJV), on agreement to a staged funding of $1.6 million to earn a 35% interest. As the major shareholder, CRA Exploration took over the project management on 1 January 1977. Substantial changes have seen Sibeka and Jennings Mining Ltd sell their holdings; the Tanks interest has been merged with A O (Australia) Pty Ltd to form the Ashton Mining Group; and Northern Mining NL was eventually sold to the Western Australian Diamond Trust. The current structure of the Ashton Joint Venture is: CRA Exploration 56.8%, Ashton Mining 38.2% and the Western Australian Diamond Trust 5%.

Until the end of 1977, the Kalumburu/Ashton Joint Venture had been able to explore without publicity, and had the diamond exploration scene in the Kimberley area virtually to itself. However, in March 1978, CRA Exploration issued the first quarterly press release on the Ashton Joint Venture, which announced the discovery of "prospects containing kimberlite-like material ... Many of these prospects are probably pipes, and preliminary tests indicate some to be diamond bearing." News of the find sparked a rush to peg mineral claims, and the west Kimberley was soon full of frenzied, competitive exploration activity involving companies both large and small. At Ellendale, the AJV's temporary reserves were soon surrounded by competitors mineral claims; and every known leucite lamproite in the Lennard Shelf and Fitzroy Trough was soon held under mineral title. Astute prospectors pegged mineral claims over a water reserve which had been excluded from the Ellendale temporary reserve; subsequently Seltrust located two concealed lamproite bodies within the claims. Others pegged the telegraph line and stockroute reserves, which traversed the Ellendale reserve, but to the south of the lamproite intrusions. At about this time, preliminary studies of indicator minerals from Western Australia were published by Mosig (1980), and new exploration tools, particularly Landsat imagery, were researched, (Longman, 1980). Such imagery, while important for structural interpretation, has not proved successful in locating kimberlites or lamproites in Western Australia.

A number of major companies had actually formulated exploration programmes prior to the announcement of the Ellendale discovery. For example, both Stockdale and BHP had applied for tenements in the Forrest River Aboriginal Reserve of the North Kimberley in 1977 but were denied access after objections from the local Aboriginal community. Nevertheless, the exploration programmes actually commenced in 1978 and early 1979. In the west Kimberley many aeromagnetic surveys were flown over the Fitzroy Trough and Lennard Shelf areas.

Amax examined many of the known lamproite bodies, and identified a number of anomalies (Gellatly, 1979) which were later drilled by Seltrust under a joint venture. With another partner, Amax found the Hooper West pipe in the eastern Lennard Shelf area.

On its own account, Seltrust flew an aeromagnetic survey of 1200 km^2 along the Lennard River northwest of Ellendale, in a search for lamproite pipes and concealed gravels marking the sites of former river channels. This search failed to recover either indicator minerals or diamond; but, in the Fitzroy valley, Seltrust did discover the lamproite pipes at Camarotoechia Creek and Spielers Bore, as well as the Water Reserve lamproites at Ellendale.

The gravels of the Fitzroy River attracted the attention of BHP, who washed several thousand tonnes from terraces downstream from the Noonkanbah lamproite field, with negative results. A similar project on the Meda and May Rivers and the lower part of the Lennard River showed similar negative results. Presuming an older age for the lamproites than is now accepted, Carpentaria Exploration examined many of the Tertiary conglomerates of the Fitzroy Valley, but failed to find sufficient encouragement to warrant full scale exploration.

One of the few exploration programmes to examine new ground was that of Stockdale Prospecting Ltd in the Dukes Dome area, south of the Fitzroy River, an area of well-dissected Permian rocks with many good trap sites (Marx, 1982). Gravel sampling, begun in 1978, was followed by photogeology, aeromagnetic survey, and ground-magnetic follow-up of anomalies. Garnets were recovered from a number of samples, and a single diamond of 0.0015 CM. Follow-up work suggests that the diamond may have been derived from Permian tillites with a northerly provenance. This survey also suggests that the lamproite marked by Crowe and Towner (1981) southeast of Mount Tuckfield on the Noonkanbah map sheet does not exist.

The major discovery of this period of activity was a group of concealed lamproite vents at Calwynyardah and Laymans Bore by the AJV. The Calwynyardah pipe, at 128 ha, is the largest new lamproite found in the west Kimberley. None of these new discoveries, however, carried more than a trace of diamond, and those recovered were usually less than 1 mm in size. During prospecting operations on previously known leucite lamproites, Seltrust recovered a diamond from Mount Ibis, and the AJV showed that Mount Abbott lamproite carries a few small diamonds. The other exposed lamproites are believed to be barren.

Exploration activity in the west Kimberley since 1977 has failed to discover further significant diamond deposits, either pipe or alluvial; but a large number of lamproites, usually small and concealed beneath soil or alluvium, have been found. A number of these bodies have been shown to carry trace diamonds; brief details will be found in Table 2.

TABLE 2. NEW LAMPROITES FOUND IN THE WEST KIMBERLEY PROVINCE, 1977-1982 (EXCLUDING THE ELLENDALE FIELD)

	Size (ha)	*Lamproite type*	*Diamonds found*
1. Eastern Lennard Shelf Field:			
Big Spring No 1	10.4	Olivine	yes
Big Spring No 2	2.2	Olivine	no
Big Spring No 3	3.7	Olivine	no
Big Spring No 4	1.1	Olivine	yes
Big Spring No 5	2.2	Olivine	yes
Big Spring West	v. small	Leucite	no
Cajaput Creek	< 1	Leucite	no
Brooking Creek	< 1	Leucite	no
J J Bore	?	?	no
Hooper West	2	Leucite	no
Brooking Gorge	0.1	Leucite	no
J K Yard	1.8	Leucite	no
J K Yard East	1.6	Leucite	no
J K Yard Southeast	0.3	Leucite	no
Stoney Creek	1	Leucite	no
Old Leopold West	?	Leucite	no
2. Calwynyardah Field:			
Calwynyardah	128	Olivine	yes
Laymans Bore East	103	Olivine	yes
Laymans Bore West	12,16	Leucite	yes
Hansons Bore	8.6	Leucite	no
Metters Bore No 1	2.5	Leucite	yes
Metters Bore No 3	2.5	Leucite	yes
Metters Bore No 6	2.0	Leucite	yes
Merrilees Bore	0.8	?	yes
Billys Bore West	1.6	Leucite	yes
Billys Bore East	0.3	?	no
Fishers Dam	0.5	?	no
3. Noonkanbah Field:			
19 Bore No 1	3.7	?	no
19 Bore No 2	0.8	Olivine	no
20 Bore No 2	3.4	?	yes
33 Bore	28,8	Leucite	yes
Mount Cedric North	0.3	Leucite	no
Mount Cedric South	1.8	Leucite	no
Mount Noreen	6.3	Leucite	yes
Mamilu West	v.small	Leucite	no
Howes Hill West	v.small	Leucite	no
Kalyeeda	2	Leucite	no
BHPM 2	3.3	Leucite	no
4. Miscellaneous areas:			
Spielers Bore	2.5	Leucite	no
Camaratoechia Creek	3.5	Leucite	yes
Gumhole	1.2,1	Leucite	no

By the end of 1978, continuing work at Ellendale had located 32 lamproite pipes, of which 17 were leucite bearing, 12 were olivine lamproites, and 3 were of mixed rock types or intermediate between the two (Smith, 1978a). The number of lamproites known in the Ellendale Field has since been increased to 46. To evaluate these pipes, the AJV established a central washing plant consisting of hammer mill, scrubber, and HMS plant with a 20 t/hr cyclone operating on a −13mm to +0.8mm feed. HMS plant concentrates were passed to an adjacent sorthouse where they were upgraded by electromagnetic separation, and ball milling if required, before final hand picking of the diamonds. The plant was commissioned in August 1978 and operated until mid-1980, by which time 181 067 t of ground had been treated for the recovery of approximately 15 300 CM of diamonds.

Details of the Ellendale evaluation work are given by Atkinson and others (1984b); each lamproite was subjected to a programme of up to six stages:

(1) *Initial geological investigation:* Mapping, geophysics, and scout rotary air blast drilling, were undertaken on a 100 m grid. These established the boundaries of the lamproite and the rock types present. In conjunction with core dilling, they showed that most lamproites occupied shallow vents filled with a basal tuffaceous sequence overlain by a magmatic lamproite which emerged from a central narrow feeder (Figs 69 and 82). Bulk sampling showed the tuffs to have generally higher diamond grades.

(2) *Scout pitting to determine presence or absence of diamonds:* From 2 to 7 samples, depending on the size of the lamproite and the rock types present, were dug by CAT 245 excavator or drilled with a 1 m-diameter auger and trucked for treatment to the central washing plant. Sample size was 200 t. Three-quarters of the Ellendale lamproites tested were shown to contain diamonds (Fig. 6). The more olivine-rich lamproites were the most diamondiferous. Where diamonds were recovered the programme proceeded to stage 3.

(3) *Detailed bulk sampling:* To determine grade, pits were dug on a one sample per 2 ha grid. Four lamproites, Ellendale 4, 7, 9, and 11, yielded grades of 1 CM/100 t or better, and warranted further work. At Ellendale 4 and 9, large samples totalling several thousand cubic metres were dug and processed to provide parcels of 5 000 CM or more for valuation of the diamonds. The Ellendale stones are mostly dodecahedra of excellent crystal structure (Hall and Smith, 1984). The predominant colour is "cape" yellow; and the gem content, 60%, with very little board. Values are given in Table 3.

(4) *Air core and diamond drilling:* To investigate vent geometry and geology at depth, 302 holes totalling 22 764 m were drilled in the four most prospective lamproites. The drilling enabled computation of available volumes of tuff and magmatic lamproite.

(5) *Large diameter drilling:* To determine diamond content at depth, bulk samples from depths up to 200 m were taken from 1 m-diameter holes drilled with a Wirth reverse circulation rig using toothed

roller bits. Holes to 30 m depth were also sunk using a Hughes Tool Company Williams auger. Hole spacing in higher grade tuff was 50-100 m, and samples of about 25 m length were processed. Drill samples totalling 5 695 m^3 were obtained from vents 4, 9, and 11; and treated through the central washing plant.

(6) *Preliminary feasibility studies:* Ellendale 4 and 9 have diamond grades that locally approach economic levels. Preliminary feasibility studies showed that the magmatic lamproite had such low grades that it could only be considered as waste. The extensive thick cover of magmatic rock reduces the economic potential for opencut mining of the underlying tuff. The limited areas of higher grade tuff available at surface are not considered payable today, but should diamond prices improve, then limited mining operations may become possible. Some details from the evaluation programme are given in Table 3.

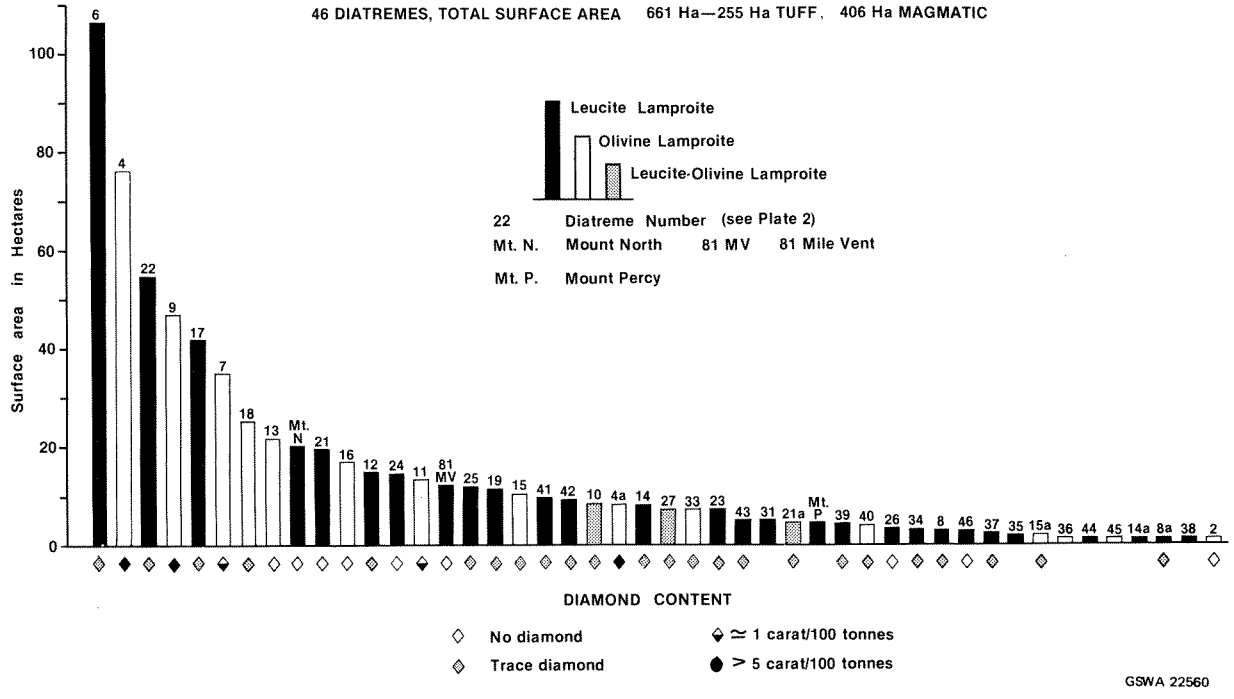


Figure 6. Size distribution, and diamond content, of the Ellendale pipes (modified after Atkinson and others, 1984a).

TABLE 3. RESULTS OF EVALUATION OF ELLENDALE 4,7,9 AND 11

Vent and rock type	*Surface area (ha)*	*Diamond recovered (CM)*	*Largest stone (CM)*	*Mean stone size (CM)*	*Value 1980 (US$/CM)*	*Grade (CM/100t)*
Ellendale 4:						
Magmatic lamproite	58	—	—	0.10	—	0.5
Higher grade tuff	18	—	—	0.10	—	14
Total	**76**	**6 600**	**6.15**	—	**67**	—
Ellendale 7:						
Higher grade tuff	24	—	—	—	—	1
Total	**36**	**48**	**2.66**	**0.16**	—	**<1**
Ellendale 9:						
Magmatic lamproite	26	—	—	0.20	—	—
Higher grade tuff	20	—	—	0.21	—	5
Total	**46**	**6 100**	**6.47**	—	**96**	—
Ellendale 11:						
Higher grade tuff	4	—	—	—	—	1
Total	**13**	**53**	**6.23**	**0.09**	—	**<1**

The Argyle diamond deposits

During the late 1970's, although most attention was directed to the west Kimberley, the AJV continued reconnaissance work elsewhere. Stream sampling was undertaken in that part of the east Kimberley east of the Great Northern Highway. This road had formed an arbitrary boundary to exploration since 1972 when budget restraints had caused the area to the east to be omitted from the first pass sampling. For reconnaissance stream sampling, the AJV now used a sample interval of 5 km, thus 3 routine gravel samples of 40 kg each were collected along the length of Smoke Creek to the west of Lake Argyle. On 28 August 1979, the laboratory in Perth recovered 2 diamonds from the first of these samples, and during the following two days 4 and 5 diamonds respectively from the other two samples (Atkinson and others 1984b).

During September, follow-up work recovered more and more diamonds upstream from the discovery sites, and it was soon recognized that the Upper Smoke Creek and Lower Smoke Creek gravels constituted diamond deposits that would probably be mined.

Chromite also occurs with the diamonds in Smoke Creek, but the diamonds alone formed a clear trail that led 20 km upstream to the 50 ha Argyle (AK1) pipe, discovered on 2 October 1979. Tuffaceous lamproite formed recognizable outcrops in the stream bed and valley sides in the discovery area.

Drainage from the southern end of the Argyle pipe leads south and eastwards into Limestone Creek, where the economic potential of the associated diamondiferous alluvials was recognized during detailed stream sampling the following year.

The evaluation of the Argyle diamond deposits has been described by Meakins (1983) and Atkinson and others (1984b). The Upper Smoke Creek and Limestone Creek alluvials were trenched on lines 200 m apart; and samples of 11 m^3 each were taken at regular intervals and processed through an HMS plant (some early samples were processed by diamond pan). Only reconnaissance evaluation has been carried out on the Lower Smoke Creek deposits: trench lines were at 2 km intervals. The indications are that the Lower Smoke Creek deposits are markedly lower in grade than those of Upper Smoke Creek and Limestone Creek. Reserves of diamondiferous alluvial gravel prior to mining are given in Table 4. In addition, there is a limited amount of diamondiferous scree and overburden from the Argyle pipe; this is being treated with the alluvials.

TABLE 4. ESTIMATED RESERVES OF DIAMONDIFEROUS ALLUVIAL GRAVEL AT ARGYLE, PRIOR TO MINING

Location	*Category*	*Tonnage (t)*	*Grade (CM/t)*	*Total (CM)*
Upper Smoke Creek	Probable	580 000	4.6	2 668 000
Limestone Creek	Proven	1 700 000	3.6	6 120 000
Limestone Creek	Probable	330 000	3.0	990 000

Alluvial mining commenced in January 1983 and is planned to continue at a rate of 4000 t/d until the start of mining of the Argyle pipe. Figures for the first three years of production are given in Table 5.

TABLE 5. ALLUVIAL DIAMOND PRODUCTION FROM ARGYLE

	1983	*1984*	*(a) 1985*
Ore processed (t)	1 068 052	1 473 714	1 087 799
Diamonds recovered (CM)	6 200 227	5 689 546	4 685 970
Recovery grade (CM/t)	5.81	3.86	4.31

(a) Production for period January to September, 1985

The evaluation of the Argyle pipe was carried out by a variety of physical methods involving pitting and drilling:

(1) *Pitting on 100 m centres:* Mapping of the pits, surface outcrop, and drill-core logging (see below), determined the three fundamental geological divisions of the pipe, the early high-grade "sandy" tuff (about 5 CM/t overall), the later low-grade (< 1 CM/t) "Non-sandy" tuff phase in the northern part of the pipe, and the thin, late stage lamproite dykes.

Initial pit size averaged 16 m^3 (38 t), which was adequate for calculation of grades at surface. This size was increased to 200-600 m^3 to check grade reliability, to yield large parcels of diamonds for valuation, and to provide metallurgical data.

(2) *Diamond drilling:* The pipe geometry and geological structure at depth were determined by diamond drilling. A total of 30 463 m were drilled from 182 holes spaced on lines 50-100 m apart. This drilling also enabled calculation of available tonnages of ore.

(3) *Large diameter core drilling (LDC):* LDC drilling was largely confined to the high grade southern end of the pipe, where 91 holes totalling 9 282 m were drilled on a 50 m square grid to provide information on grade at depth. The 200 mm-diameter core was divided into 20 m sample intervals of about 1.5 t each for crushing and processing through an HMS plant.

(4) *Shaft sinking:* Six shafts of 2.0 × 2.4 m dimensions were sunk to depths of 43 m to 64 m to check LDC grade results, to obtain metallurgical data, and to check for variations in diamond quality at depth.

By the end of 1982, 408 391 CM of diamond had been recovered from 62 842 t of pipe material during the evaluation work.

(5) *Ore-reserve estimation:* This was carried out by geostatistical methods, using a separate inverse distance calculation and the polygonal method as comparative checks. Estimated ore reserves are given in Table 6.

These reserves are estimated to RL200 m (100-200 m below ground surface). Additional resources are present below this level and in the north of the pipe for

TABLE 6. ARGYLE, AK1 PIPE, ORE RESERVES

Category	*Tonnage (Mt)*	*Grade (CM/t)*	*Diamond (000's CM)*
Proven	61	6.8	414.8
Probable	14	6.1	85.4

future evaluation. Mining of the Argyle pipe commenced in December 1985 (Fig. 7). A treatment rate of 3 Mt/a, producing some 25 $\times$ 10^6 CM annually, is envisaged. This represents an increase of about 50% on previous world production of natural diamonds. All mining of the Argyle deposits is conducted by *Argyle Diamond Mines Joint Venture,* a wholly owned subsidiary of the joint venture companies, registered on 1 November 1982. This company is charged with responsibility for the development, mining and management of the Joint Venturers' diamond interests in the Argyle and Ellendale Mining Lease areas.

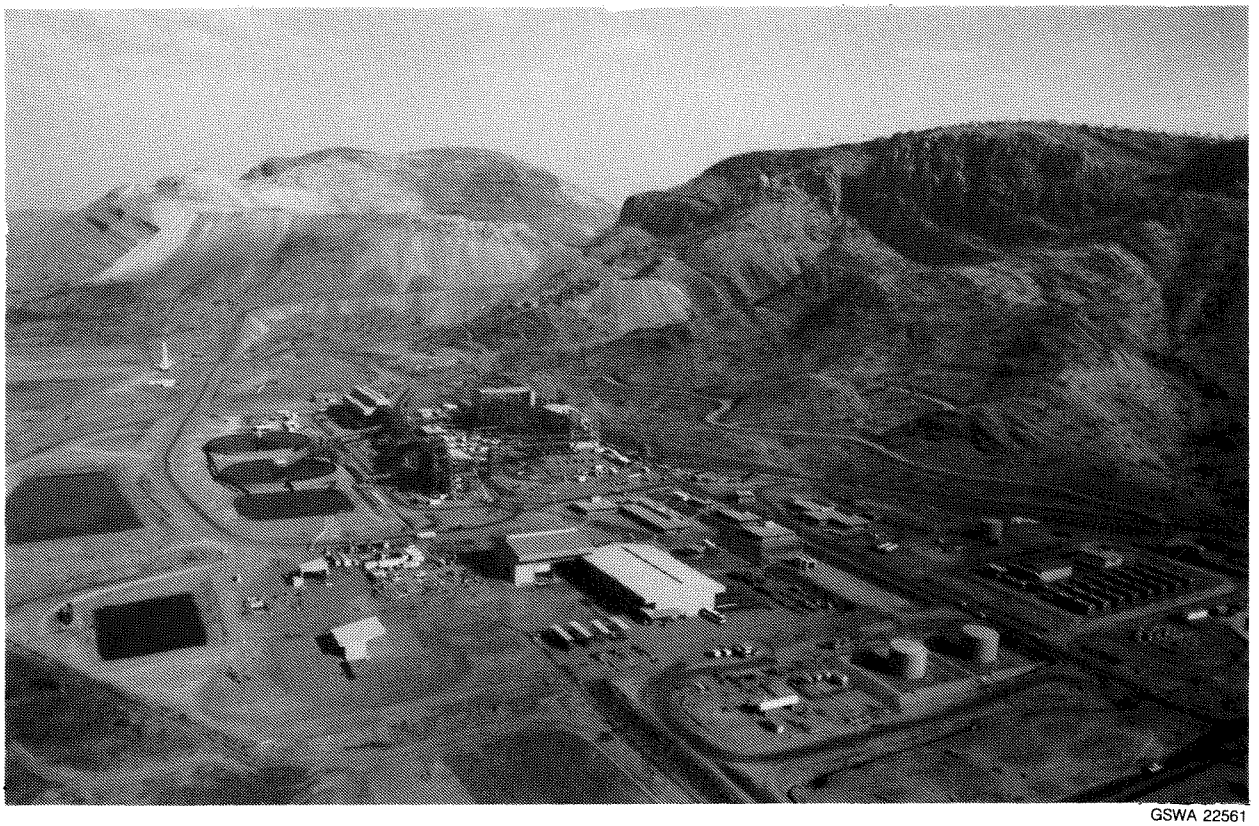
Post-Argyle exploration in the Kimberley area.

Many of the larger exploration programmes begun about the time of the Ellendale discovery, continued with renewed vigour, and expanded budgets after the announcement of the discovery of the Argyle deposits. In addition, as happened after the Ellendale annoucement, a "diamond rush" ensued in which all ground surrounding the AJV titles was pegged or taken under Temporary Reserve. Prominent among those holding ground around Argyle were Stockdale Prospecting, Monarch Petroleum, Samantha Exploration, Afro West, and Gem Exploration. Dredging claims were also taken out on the lower reaches of the Ord River by Gem Exploration and Carpentaria Exploration P/L.

The most successful of these companies has been Gem Exploration and Minerals Ltd, who tested alluvial gravels at several points along the Ord River below Lake Argyle and showed that diamonds were present. The diamonds recovered resemble Argyle stones in appearance and seem likely to have been transported by river from the Argyle pipe, a distance of about 150 km. The grade of the Ord River alluvials is too low tobe economic; details of the finds are given in Table 7.

Gem Exploration also obtained title to the lower reaches of Limestone Creek, above its confluence with the Ord River system (Lake Argyle) and about 20 km below the Argyle pipe. The area has been explored under a joint venture with Freeport of Australia Inc., as the Bow River Joint Venture. Initial exploration in 1983 outlined four gravel terraces, similar to those found by Meakins (1983) on the Lower Smoke Creek; grades and mean stone size decrease from the older and higher terraces to the modern river channel deposits (Table 8).

The largest stone recovered from this programme weighed 5 CM and was of industrial quality. More recently, the partners have reported a minimum resource of about 5 Mt of gravel yielding 0.67 CM/t associated with a larger volume of diamondiferous gravels of lower grade. Valuations from initial parcels of diamonds have given about US$19/CM and up to 30% gem quality. Whilst the grades are considerably lower than those of



GSWA 22561

Figure 7. Argyle Diamond Mines processing facility nearing completion, August 1985. The mine site is in the background. Compare the Razor Ridge and West Ridge with frontispiece. East Ridge is in the foreground (Photo: CRAE)

TABLE 7. DIAMONDS RECOVERED BY GEM EXPLORATION AND MINERALS LTD FROM THE ORD RIVER

Locality	*Distance by river from AK1 (km)*	*Material treated (t)*	*Diamonds recovered*	*Total weight (CM)*	*Mean stone size (CM)*	*Grade (CM/100t)*
Ord Dam Wall	80	1 000	16	1.556	0.097	0.155
Buttons Gap	150	150	25	0.802	0.032	0.534

the alluvials being worked by the Argyle Diamond Mines Joint Venture, the valuation of the stones is considerably higher. Evaluation of the deposit is continuing, with the operation of a 300 t/d pilot plant in 1985.

Despite intensive search following the discovery of Argyle, few other kimberlitic or lamproitic source rocks have been located in the east Kimberley. In 1980 after following up indicator minerals found in a stream sample, the AJV located the 25 km-long Bow lamprophyric dyke swarm. The most prominent indicator is andradite, but chromite, chrome pyrope, and chrome diopside, are also common (Atkinson and others, 1984a). The dykes are up to 7 m wide, and often give rise to a surface expression of lines of trees. Unfortunately, no diamonds were recovered from the dykes.

Later in 1980 the AJV located the Lissadell Road dyke, which is situated about 10 km southwest of the Argyle pipe. The dyke consists of discontinuous small dykes and stringers, it is diamondiferous, but too small to be of economic interest.

Exploration in the Kimberley area is still being actively pursued by a number of companies. Exploration licences have been taken up in the central Kimberley, and a major part of the endeavour is concentrated in the north Kimberley on a search for the primary source of alluvial diamonds in the King George River. The Pteropus Creek pipe has been reexamined by BHP and 40 t of material treated by jig plant to produce abundant chromite and zircon but no further diamonds. More successful has been a programme on Casuarina Creek, to the east of the King George River, where a bulk gravel sample of 10 t produced 50 small diamonds, a result repeated in a number of follow-up samples (M.J. Gunn, pers.comm.).

Exploration south of the Kimberley area

The success of the AJV led CRA Exploration to explore for diamonds in its own right. In 1978, a reconnaissance stream-sampling survey along the edge of the Carnarvon Basin, near the western margin of the Pilbara Block, recovered chrome pyrope, chrome diopside, and chromite on Wandagee and Middalya stations, 140 km northeast of Carnarvon. An airborne magnetic survey of the surrounding region delineated a number of discrete dipole anomalies, similar to those associated with the Ellendale lamproites. Drilling located 16 diatremes and sills with kimberlitic affinities. Stockdale Prospecting Ltd have since located five more bodies in this, the Wandagee Province. Twelve of the bodies are small tuff pipes, mostly <3 ha in size although geophysical evidence suggests the largest may be 14 ha. Four of the diatremes are concealed by up to 158 m of unconformable Cretaceous cover. The sills are a porphyritic peridotite with abundant groundmass diopside, and are petrographically and geochemically distinct from both kimberlites and lamproites. Prospecting operations have shown the pipes to be virtually barren of diamond (Atkinson and others, 1984a).

The exploration discoveries in the north of Western Australia have encouraged a number of mining companies to explore throughout the state in search of diamonds. Large regional exploration programmes have been executed. These programmes, however, have mostly been on "open ground" and for proprietary reasons the results remain confidential.

Large areas of the state have been covered by regional gravel and loam sampling, in particular the Pilbara Block, Gascoyne region and the northern Yilgarn Block. Parts of the eastern and southern Yilgarn Block have also been covered in some detail and in an effort to detect indicator minerals carried down by the major drainage from the Yilgarn parts of the southern Officer Basin have been prospected. Informally it is known that a small number of a variety of indicator minerals have been recovered from widely scattered localities. A few small diamonds have also been found but no source rock located.

In a reconnaissance loam-sampling programme on the southeastern margin of the Yilgarn Block Stockdale

TABLE 8. DIAMONDS RECOVERED BY BOW RIVER JOINT VENTURE FROM LIMESTONE CREEK

Gravel terrace	*No. of samples*	*Total material treated (t)*	*Diamonds recovered*	*Mean stone size (CM)*	*Grade (CM/100t)*
T1	4	350	684	0.280	56.02
T2	3	300	728	0.146	35.60
T3	5	500	212	0.138	5.86
T4	10	1 000	659	0.076	5.03
Undifferentiated	2	200	88	0.140	7.80

Prospecting Ltd found low-magnesium ilmenite near the Fraser Range (Joyce and Marx, 1981). Subsequent detailed prospecting located "parakimberlite" dykes in this area and southeast of Norseman (R V Danchin, pers.comm.; Danchin and others, 1985).

The result of exploration over the last twenty years has been the delineation of four provinces containing diamond bearing intrusion of lamproitic and kimberlitic affinities. These separate provinces and their structural setting will be described in detail in subsequent chapters.

NOMENCLATURE

In describing any group of rocks or rock bodies it is convenient to divide and sub-divide them in order to indicate similarities and differences. In this bulletin we have adopted both a geographic and petrographic scheme which requires some explanation.

Province: The concept of an "igneous province" to describe a group of intrusions of similar composition and associated in space and time, is well established.

Well known examples are the Roman Volcanic Province of Italy and the Tertiary Igneous Province of Scotland. In this bulletin, the geographic element is emphasized and the term "province" used to delimit various areas in which lamproites or kimberlites are intruded. In general, the intrusions in any given province will be of similar age and and form part of the same lineage; but, for example, in the East Kimberley Province, this may not be so.

Field: This term is used purely to define a geographical subset within a province. Thus, within the West Kimberley Province there are concentrations of lamproite intrusions in the Ellendale, Calwynyardah, and Noonkanbah areas; and each is designated a "field". Although each of these fields differs slightly in age and composition, this does not affect our use of the term. Isolated intrusions, away from any designated field, will be referred to the province.

Rock nomenclature: The large variations in texture and mineralogy which characterize kimberlitic and ultrapotassic rocks in general have lead to the formulation of numerous definitions, classification schemes, and rock names, many of which are specific to particular localities. In the case of kimberlites, many definitions have been proposed since the term was first introduced by Lewis (1887) and the nomenclature has been extensively reviewed (Dawson, 1967, 1971; Frantsesson, 1970; Clement and others, 1977; Skinner and Clement, 1979; Mitchell, 1979; Dawson, 1980; Clement, 1982; Clement and others, 1984; Smith, 1984b). As pointed out by Smith (1984b), the historical emphasis on diamond and the macrocryst assemblage has been replaced by greater emphasis on the nature of the groundmass. In this bulletin we have adopted the definition of Clement and others (1984) and followed the classification scheme of Skinner and Clement (1979). The full definition of Clement and others (1984) is:

> Kimberlite is a volatile-rich, potassic, ultrabasic, igneous rock which occurs as small volcanic pipes, dykes, and sills. It has a distinctively inequigranular texture resulting from the presence of macrocrysts set in a finer-grained matrix. This matrix contains, as prominent primary phenocrystal and/or groundmass constituents, olivine and several of the following minerals: phlogopite, carbonate (commonly calcite), serpentine, clinopyroxene (commonly diopside), monticellite, apatite, spinels, perovskite and ilmenite. The macrocrysts are anhedral, mantle-derived, ferromagnesian minerals which include olivine, phlogopite, picroilmenite, chromian spinel, magnesian garnet, clinopyroxene (commonly chromian diopside), and orthopyroxene (commonly enstatite). Olivine is extremely abundant relative to the other macrocrysts, all of which are not necessarily present. The macrocrysts and relatively early-formed matrix minerals are commonly altered by deuteric processes, mainly serpentinization and carbonatization. Kimberlite commonly contains inclusions of upper mantle-derived ultramafic rocks. Variable quantities of crustal xenoliths and xenocrysts may also be present. Kimberlite may contain diamond but only as a very rare constituent.

The classification scheme for kimberlites adopted by Skinner and Clement (1979) is based on the primary mineral constituents. Olivine is ubiquitous in kimberlities but its abundance in the rock is of limited value for classification as the proportion of olivine xenocrysts and olivine derived directly from the magma cannot be assessed with certainty. The mineralogical classification of kimberlites proposed by Skinner and Clement (1979) is therefore:

> ...in addition to olivine, any one of five other minerals may be present as a major primary constituent of kimberlite. These minerals are diopside, monticellite, phlogopite, calcite and serpentine. Accordingly we propose the recognition of five basic subdivisions of kimberlite depending upon (and named after) whichever one of these five minerals is volumetrically more abundant...
>
> Further subdivision can be made if one or more of these or any other mineral is present in sufficient abundance for it to qualify as a characterizing accessory or modifier. We have found it useful to accept, as characterizing accessories, those minerals which are present to the extent of, or exceed two-thirds of the volumetric abundance of the dominant mineral. ...in addition to the five minerals listed above, some other mineral may occur as a major constituent of kimberlite. In this event our primary subdivision could be extended.

Where material permits precise classification we have followed the scheme of Skinner and Clement (1979) but more often the West Australian kimberlite dykes are thoroughly altered and primary mineralogy has been destroyed. Identification is then based on the nature and chemical characteristics of the heavy-mineral suite and the material is best labelled *kimberlitic.*

Proliferation of local rock names is particularly evident amongst lamproites, lamprophyres, and other ultrapotassic rocks (Sahama, 1974; Gupta and Yagi, 1980). Prider, in his descriptions of the West Kimberley lamproites, adopted a locality based system of nomenclature based on the presence or absence of one or more of a suite of typical minerals (Wade and Prider, 1940; Prider 1960).

The names used were:

Fitzroyite:	phlogopite-leucite lamproite
Cedricite:	diopside-leucite lamproite
Wyomingite:	phlogopite-diopside-leucite lamproite
Mamilite:	magnophorite (potassic richterite)-leucite lamproite
Wolgidite:	phlogopite-diopside-magnophorite (potassic-richterite)-leucite lamproite.

It was noted also that each may carry olivine (commonly altered to nontronite) and that priderite is a constant accessory. This scheme, however, gives little consideration to the proportion of an individual mineral present; thus a few flakes of phlogopite would transform a cedricite into a wyomingite even though they were part of the same rock body. The result is that rocks of very similar chemistry might be given different names depending on their degree of crystallinity. An additional problem is that under Prider's classification olivine was essentially ignored although it might vary in abundance from 0-15% in rocks which were otherwise mineralogically similar. With the discovery of olivine-rich, leucite-poor (or absent) varieties in the Ellendale Field it was realized that olivine must be taken into account in defining and naming the rocks.

No satisfactory definition of lamproite existed prior to the discovery of the olivine lamproites at Ellendale. The name had been coined by Niggli and used by Troger (1935) to group potash and magnesia-rich lamprophyres from Spain, Wyoming and Antarctica. Prider (Wade and Prider, 1940) used the name to describe the leucite-rich rocks of the west Kimberley. Following the form of a definition of kimberlite by Clement and others (1977), this definition of lamproite was given by Jaques and others (1984a) and is used in this bulletin:

> Lamproite is defined as:
> * a potash and magnesia-rich lamprophyric rock of volcanic or hypabyssal origin belonging to the ultrapotassic rock series. Minerals commonly present as major primary constituents include one or more of the following: olivine, clinopyroxene (typically diopside), phlogopite (typically titaniferous), leucite, amphibole (typically potassic richterite), orthopyroxene, sanidine, and glass. Accessory phases may include priderite, apatite, nepheline, spinel, perovskite, wadeite, and ilmenite.
> * Xenoliths and xenocrysts (including olivine, pyroxene, garnet, and spinel) of upper mantle origin may be present, and diamond may be present as a rare accessory.
> * Lamproite may be of either basic or ultrabasic composition, and is characterised by high K_2O/Na_2O ratios (>3) and high abundances of Rb, Sr, Ba, Ti Zr, Nb, Pb, Th, U, and light-rare-earth-elements (LREE).

A similar definition was given by Scott-Smith and Skinner (1984a) who considered leucite, or glass with the potential to crystallize leucite, to be an essential mineral, although this condition was omitted in a later paper (Scott-Smith and Skinner, 1984c).

It will be noted that there are many mineralogical similarities to kimberlite as defined above, but the list of minerals potentially useful for classification is much wider and includes leucite, sanidine, nepheline, and amphibole, minerals not found as primary phases in kimberlite; the titania-rich compositions of minerals such as phlogopite and the presence of rare minerals such as wadeite and priderite is also distinctive.

When naming the rocks, we have followed the example of Clement and others (1984) in their classification of kimberlite quoted above and suggest that the lamproite suite be subdivided and named according to the primary minerals present (including olivine), the names of which should be added as a prefix in ascending order (Jaques and others, 1984a). Additional minerals used as modifiers to the dominant phase should be present to the extent of at least two thirds of the abundance of the major phase. Glass should not be used as a mineral qualifier; but where especially prominent the rock name may be given the general prefix "glassy" or "glass-rich". Where necessary to closely define a rock this system may produce cumbersome names, such as olivine-diopside-phlogopite-leucite lamproite but the name is informative; furthermore the presence of another phase in accessory amounts does not require changing a rock name.

Pyroclastic rocks: For pyroclastic rocks we have followed the nomenclature and classification recommended by the IUGS Subcommission on the Systematics of Pyroclastic Rocks (Schmid, 1981) which has been widely adopted. We have followed the terminology of Fisher and Schminke (1984) in the recognition of types of pyroclast (e.g. juvenile, cognate, and accidental), and for terminology of polymodal pyroclastic rocks. This scheme, essentially descriptive, is preferred to the genetic textural classification proposed for kimberlite by Clement and Skinner (1979), Clement and Skinner (1982), McCallum and others (1982), and Clement (1982); since, although the West Australian kimberlites and lamproites can be broadly assigned to the crater, diatreme, or hypabyssal facies (Atkinson and others, 1984a), many of the West Kimberley pipes rocks which on petrographic examination alone would be assigned to the hypabyssal facies (see also Dawson, 1980, p. 51) are juxtaposed and commonly overlie pyroclastics in the volcanic crater. Many of the West Australian rocks were erupted in the crater environment and these may be adequately described using standard pyroclastic terminology.

CHAPTER 2

THE STRUCTURAL SETTING OF WEST AUSTRALIAN KIMBERLITE AND LAMPROITE PROVINCES

The four major areas of kimberlite and lamproite intrusion outlined by recent diamond exploration in Western Australia occupy diverse structural settings (Fig. 8). The North Kimberley Province is located in the gently folded Proterozoic cover rocks of the Kimberley Block; the East Kimberley Province is associated with the Halls Creek Mobile Zone on the eastern margin of the craton; and the West Kimberley Province is associated with a shelf area and deep graben formed between the southwest margin of the Kimberley Block and the adjacent Canning Basin, although a few lamproites intrude the King Leopold Mobile Zone

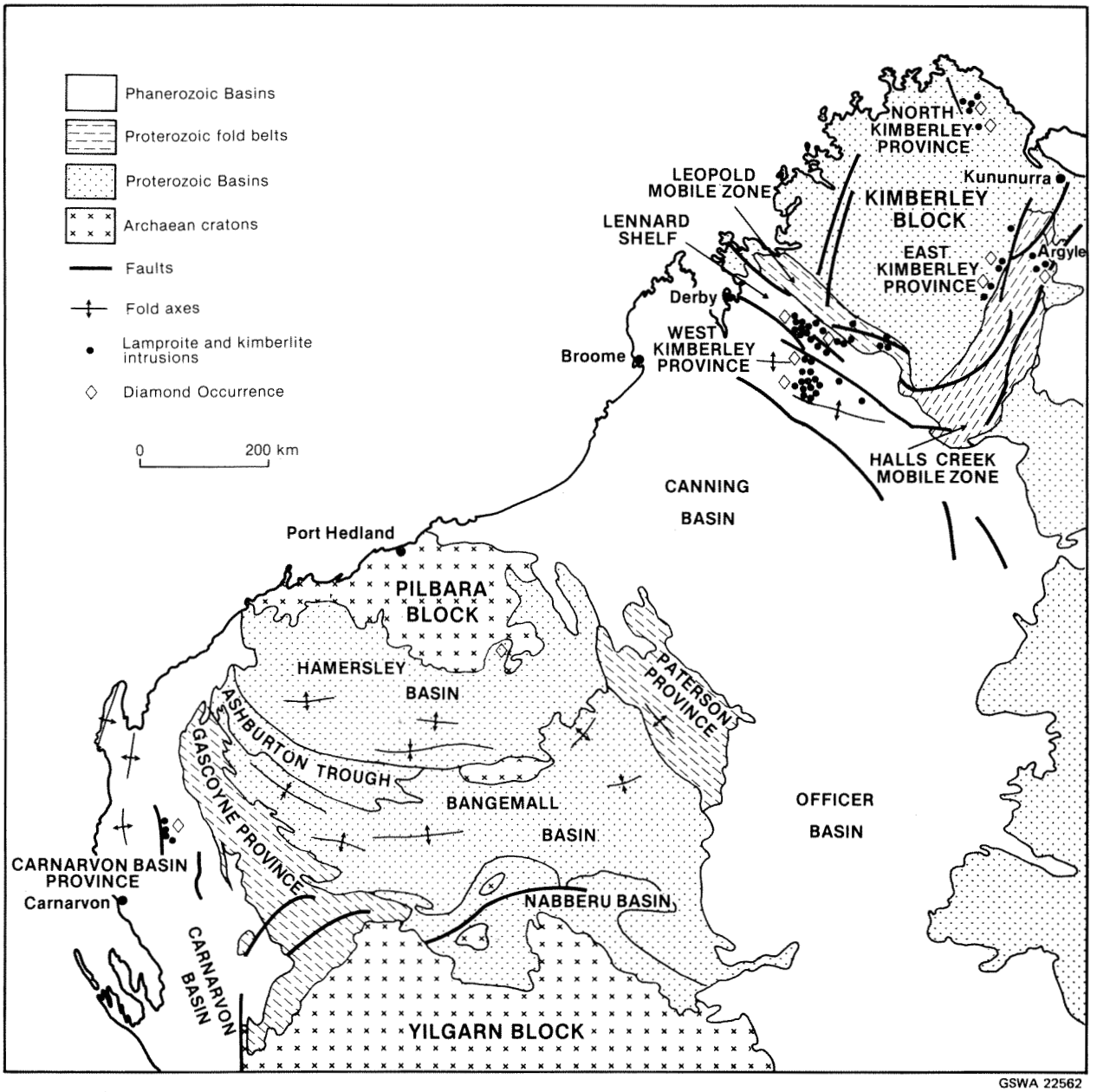


Figure 8. Tectonic units of Western Australia and the location of kimberlite and lamproite provinces.

marginal to the block. The alkali picrite pipes and sills of the Wandagee Province are associated with major rift faulting and a horst block within the Phanerozoic Carnarvon Basin. The age of the intrusions is equally diverse, ranging from ≈ 1 150 Ma for the Argyle Pipe in the East Kimberley to ≈ 20 Ma for the leucite lamproites of the West Kimberley Province. In the account which follows, this diversity of age and structural setting will be related to the structural evolution of Western Australia.

EVOLUTION OF THE STRUCTURAL FRAMEWORK OF WESTERN AUSTRALIA

The evolution of Western Australia is a history of progressive cratonization around the three ancient nucleii of the Yilgarn, Pilbara, and Kimberley Blocks. This took place during the Proterozoic and has been fully described by Plumb (1979) and Gee (1979). During the Phanerozoic, the Australian continent separated from India and sedimentary basins formed along the West Australian coast, a process documented by Veevers (1981).

THE ARCHAEAN NUCLEII

The Yilgarn Block occupies the southwestern quarter of Western Australia and is the largest of the three Archaean nucleii. Extensive north-trending greenstone belts in the Eastern Goldfields province of the block contain komatiite flows up to 3 290 Ma old (Claoué-Long and others, 1984) and felsic volcanics about 3 000 Ma old (Fletcher and others 1984). These were intruded by granites at about 2 750-2 650 Ma (de Laeter and others, 1981a). The western margin of the block is a more highly metamorphosed gneiss terrain about 3 000 Ma old (Fletcher and others, 1985), with isolated areas up to 3 350 Ma old (de Laeter and others, 1981b), and may represent the pre-greenstone basement (Gee, 1979). The youngest major event within the Yilgarn Block was the widespread emplacement, in the Eastern Goldfields, of small stocks of alkali granite at about 2 500 Ma (Libby and de Laeter, 1981), and an extensive basic dyke swarm at about 2 400 Ma (Turek, 1966), since which time the craton has remained stable.

The Pilbara Block is a smaller Archaean craton to the north of the Yilgarn Block (Fig. 8). It contains large granite batholiths, about 3 000 Ma old, that intrude greenstone belts only slightly older (de Laeter and others, 1981a), and post-tectonic "younger" granites 2 700-2 600 Ma old (de Laeter and Blockley, 1972). The southern half of the craton is covered by the gently folded volcanics, sediments and banded iron-formations of the Hamerlsey Basin, where a few inliers of granitic basement are exposed. These deposits were originally thought to be between 2 300 and 2 100 Ma old (de Laeter and others, 1974), but are now thought to be up to 2 700 Ma old (Hickman and de Laeter, 1977; Trendall, 1983, 1984).

The Kimberley Block is the most problematic of the three nucleii as the basement rocks are everywhere concealed beneath up to 5 km of very gently folded Proterozoic sediments and basalts of the Kimberley Basin succession (Plumb and Gemuts, 1976; Plumb and others, 1981). The extent of the block is not in doubt as the flat-lying basinal sediments contrast sharply with the granites and steeply dipping metasediments of the surrounding Proterozoic mobile zones; also the gravity field is easily distinguished from surrounding terrains (Wellman, 1976). An Archaean basement has been postulated by Gellatly (1971), while Plumb and Gemuts (1976) and Plumb and others (1981) prefer a continuation beneath the basin of the Lower Proterozoic Halls Creek Group exposed in the adjacent mobile zones. More recently, Hancock and Rutland (1984) suggested a thin Archaean crust which originally may have underlain the mobile zone and Sturt Block to the east, as well as the Kimberley Basin. Whatever its original nature, the block underlying the Kimberley Basin has remained stable since at least early Proterozoic times as the age of the Halls Creek Group is about 2 150 Ma (Page, 1976).

PROTEROZOIC MOBILE BELTS AND PROGRESSIVE CRATONIZATION

Structural development of Western Australia during Proterozoic times involved the development of mobile belts marginal to the Archaean nucleii, and the formation of two large cratons — the West Australian Shield (Gee, 1979) in the south, and the North Australian Craton (Plumb, 1979) across much of northern Australia.

The West Australian Shield was formed by the welding together of the Yilgarn and Pilbara blocks by the Capricorn Orogen, a major orogenic zone involving geosynclinal sedimation, metamorphism, basement reworking and granitoid emplacement (Gee, 1979). The basin was probably developed on a thin gneissic crust, a northward extension of the Western Gneiss Terrain of the Yilgarn Block. Tectonism brought remnants of this basement, intruded by younger granites, to the surface to form the Gascoyne Province, the oldest rocks of which are dated at 2 000-2 400 Ma and which were extensively intruded by granite at around 1 600 Ma (Fletcher and others, 1983b). Sedimentation and further deformation of the basement continued east of the Gascoyne Province throughout the deposition of the Lower Proterozoic Nabberu Basin (Bunting and others, 1976; Bunting, 1986) and the Upper Proterozoic Bangemall Basin (Muhling and Brakel, 1985). Sedimentation and folding in the basins reflect the continued tectonic activity of basement blocks, and final stability was not reached until about 1 000 Ma.

Concurrent with the development of the Capricorn Orogen the Albany-Fraser Province (Doepel, 1975) was forming on the southeast margin of the Yilgarn Block. This mobile belt is over 1 100 km long and up to 200 km wide, and contains strongly deformed ortho- and paragneisses of amphibolite to granulite facies, and includes the Fraser Complex, a large disrupted layered

gabbro (Myers, 1985), and a broad zone of post-tectonic granite intrusion. The margin between the Albany-Fraser Province and the Yilgarn Block is a zone of intense ductile deformation rather than faulting (Myers, 1985). The eastern margin of the mobile belt is a normal fault with a possible sinistral wrench component (Gee, 1979). Age determinations from the mobile belt range from 1 800-1 600 Ma for an early tectonic and metamorphic episode (Thom and others, 1981) to 1 300-1 200 Ma for the high-grade metamorphism, and 1 100 Ma for post-tectonic granite intrusion and low-grade metamorphism (Turek and Stephenson, 1966; Arriens and Lambert, 1969; Bunting and others, 1976). Recent Sm-Nd ages for the western end of the mobile belt give the age of the gneisses as 2 010-2 170 Ma and the granites as 1 810-2 020 Ma (Fletcher and others, 1983a).

In the west, the Yilgarn Block is terminated by the Darling Fault and the basement is concealed beneath the thick sedimentary pile of the Perth and Carnarvon Basins. A few relatively small Proterozoic inliers such as the Leeuwin and Northampton Blocks are exposed; but, otherwise, the basement has been intersected only by a small number of oil-exploration wells. Age determinations by Fletcher and others (1985) have produced Sm-Nd ages of 1 780-2 010 Ma for the Northampton Block, Mullingarra Inlier and the basement beneath the Perth Basin.

Little is known of the Paterson Province, a Proterozoic mobile zone which wraps around the eastern and northern margins of the Pilbara Block, beyond the broad geological outline provided by Chin and others (1980, 1982). Ortho- and paragneisses with a complex history, and several ages of granite intrusion probably continue the trend of the Musgrave Block of Central Australia (Plumb, 1979). No age determinations are available from the metamorphic complex, but an age of 614 Ma from the Mount Crofton Granite in the east and a similar age for a granite concealed beneath the marginal sediments of the Canning Basin (Trendall, 1974) attest that the mobile belt was active over a prolonged time span.

The North Australian Craton (Plumb, 1979) occupies a large area north of the Musgrave Block in central Australia and west of the Mount Isa Orogen in Queensland. In Western Australia, the craton includes the Kimberley Block and the adjacent Halls Creek and King Leopold mobile zones and, beneath a cover of younger rocks, the Sturt Block to the east, and the basement of part of the Canning Basin to the south.

The Halls Creek Mobile Zone is a narrow, fault-bounded belt of Early Proterozoic sediments, metamorphics, and granites, about 400 km long and 100 km wide, trending north-northeast along the margin of the Kimberley Basin. The earliest rocks exposed are the Halls Creek Group (Dow and Gemuts, 1969), a thick geosynclinal sequence about 2 150 Ma old (Page, 1976). Their metamorphosed equivalents, the Tickalara Metamorphics, together with intruded dolerite, gabbro, ultrabasics, and syntectonic granite, form the Early Lamboo Complex (Gemuts, 1971), about 1 920 Ma old (Bofinger, 1967, recalc.), with post-tectonic Whitewater Volcanics and the Bow Hill Granite forming the Late Lamboo Complex between 1 815 and 1 834 Ma (Bofinger, 1967, recalc.).

Hancock and Rutland (1984) propose an early extensional phase of tectonism during which the Halls Creek Group was deposited on a thinned Archaean crust. This was followed by phases of uplift and compression between 1 920 Ma and 1 830 Ma when the mobile belt finally cratonized and took on its present form. Compression was from a little west of north, resulting in sinistral strike-slip displacement on the boundary faults — the Halls Creek and Glenvale Faults — and the formation of northeast-trending *en echelon* faults within the belt. The compressional phase was also accompanied by limited subduction of the lithosphere beneath the margin of the Kimberley Block (Hancock and Rutland, 1984).

The pronounced linearity of the mobile zone is governed by the Halls Creek Fault, a major geosuture which was possibly present in the Archaean basement and controlled sedimentation in the early mobile zone (Hancock and Rutland, 1984). This fault, and internal faults parallel to it, remained active throughout the remainder of the Proterozoic. The Carr Boyd Group, for example, results from repeated cycles of marine transgression and regression produced by subsidence and uplift of a narrow strip between the Halls Creek and Dunham-Glenhill-Ivanhoe faults (Plumb and Gemuts, 1976). The age of these sediments ranges from about 1 158 Ma for the Golden Gate Siltstone to 891 Ma for the uppermost Pincombe Formation (Bofinger, 1967, recalc.). Activity continued on a number of the faults throughout the Paleozoic during the deposition over the northern part of the mobile zone of the Bonaparte Basin sediments.

The King Leopold Mobile Zone, on the southwestern margin of the Kimberley Block, is very similar to the Halls Creek Mobile Zone. The zone contains metamorphosed sediments equivalent of the Halls Creek Group which have been intruded by syntectonic gabbros and granites, and unconformably overlain by the Whitewater Volcanics. Post-tectonic granites, notably the Lennard Granite, intrude the older rocks. The age of this part of the Lamboo Complex is essentially the same as that found in the Halls Creek Mobile Zone. The two mobile zones meet in the Halls Creek area and a number of major faults in the Halls Creek Mobile Zone appear to swing round into the King Leopold Mobile Zone, notably the Greenvale Fault which, through the Little Gold Fault, appears to connect with the Sandy Creek Shear, the major fault of the western mobile belt. Much of the Halls Creek Mobile Zone, however, is not represented in the exposed part of the King Leopold Mobile Zone, although it probably exists, concealed beneath the sediments of the Fitzroy Trough and northern Canning Basin. This is shown by the major gravity high which coincides with the Bow Granite in the Halls Creek zone but swings round to follow the

Fitzroy Trough in the west. By contrast, the Lennard Granite is located over a gravity low. In general, the exposed portions of the King Leopold Mobile Zone are equivalent only to the westernmost zone of the Halls Creek Mobile Zone (Hancock and Rutland, 1984).

Because of the geometric and age relations of the two mobile zones, Hancock and Rutland (1984) propose that they were formed by the same extensional and compressional episodes, with pressure from the Kimberley Block directed from a little west of north. The admitted difficulty with this scheme is the lack of any evidence for major dextral faulting in the King Leopold Mobile Zone — the only major fault, the Sandy Creek Shear, shows a small sinistral displacement. However, much of the zone is covered by later sediments of the northern Canning Basin, and it is possible that the dextral wrench faulting on the Fitzroy Trough, in Late Triassic-Early Jurassic times (Forman and Wales, 1981), might be evidence for late reactivation of older dextral basement faults. Alternatively, Plumb and Gemuts (1976), noting the dominance of sinistral strike- slip faulting in the Halls Creek Mobile Zone with a total displacement of at least 110 km on the Halls Creek Fault, and the dominance of overfolding in the King Leopold Mobile Zone where a shortening of 80 km has been calculated (Sofoulis and others, 1971), propose that the Kimberley Block moved south-southwest, parallel to the Halls Creek Fault. However, they note that the age of the intense folding is about 600 Ma, and that there was a possible earlier metamorphic event at 1 550 Ma (Bennett and Gellatly, 1970), neither of which ages correlate with major displacements of the Halls Creek Fault.

The Kimberley Basin is approximately coincident with the area of the underlying Kimberley Block and contains a succession of fluviatile and marine sediments up to 5 km thick. The Carson Volcanics, a thick sequence of tholeiitic basalts, occurs in the middle of the succession, and sills of Hart Dolerite up to 1 800 m thick underlie the whole basin and intrude all sedimentary units (Plumb and Gemuts, 1976). The older age limit of the basin is fixed by the underlying post-tectonic granites of the Halls Creek Mobile Zone at about 1 830 Ma and the younger limit by the Hart Dolerite at 1 750 Ma (Bofinger, 1967, recalc.). The central part of the basin is only mildly deformed, but in a narrow zone adjacent to the mobile zones folding increases markedly.

PHANEROZOIC RIFTING OF THE WESTERN CONTINENTAL MARGIN

In a series of papers by Veevers and Cotterill (1976, 1978), Veevers and others (1975), and Veevers (1981), the western margin of the Australian continental shelf has been described as a fully developed, mature rift system analogous to the younger and less developed East African Rift.

Rifting on the northwest margin of the continent, adjacent to the Kimberley Block, may have begun in the Carboniferous as a precursor to continental breakup (Warris, 1973), although Veevers and others (1975) have argued that the region may have been open to the sea. Further south, off the present Pilbara coast, a rifted northeast-trending arch system developed, on which much of the offshore Carnarvon Basin was deposited. This system finally separated at about 160 Ma (Veevers and Cotterill, 1978). A southeasterly extension of the rift in Early Cretaceous times ($\approx$ 125 Ma) separated Greater India from Australia in the region of the Perth and southern Carnarvon Basins (Veevers and others, 1975; Veevers and Cotterill, 1978). The complete rift system has been likened by Veevers and Cotterill (1976) in its dimensions and the geometric relation of its parts to the East African Rift.

Within this scheme of events, the Fitzroy Trough is a failed rift trending east-southeast from a triple point on the northern arm of the main rift system. The trough, however, has a considerable pre-Triassic history, with the main period of subsidence along the marginal faults — the Fenton and Pinnacle Faults — taking place during Devonian times (Towner and Gibson, 1983; Forman and Wales, 1981). Sediments from Ordovician to Jurassic age were deposited in the trough, generally about 8 km, but up to 18 km thick in the southeast. The marginal faults were reactivated in the Late Triassic-Early Jurassic with a strong dextral strike-slip movement producing a set of east-west folds (Smith, 1968). The faults themselves are major structures with a throw on the Fenton Fault up to 4 km in places; they were active over a considerable time span with a variety of normal, reverse, and strike-slip displacements. It is probable that they are related to structures in the crystalline basement, which is possibly a wider extension of the King Leopold Mobile Zone.

From a triple point on the main rift at about Latitude 22° S another failed rift developed as the south-trending Merlinleigh Sub-basin of the main Carnarvon Basin. The sub-basin is bounded to the west by the Wandagee Fault and filled by a thick wedge of mostly Permian sediments. The fault is also the eastern margin of a narrow, concealed horst of basement rocks, the Wandagee-Yanrey Ridge, which together with the Ajana Ridge separates the marginal sub-basin from the major basin to the west.

KIMBERLITE AND LAMPROITE PROVINCES

NORTH KIMBERLEY PROVINCE

Little can be said about the structural setting of the North Kimberley kimberlite dykes and pipes, as they intrude flat-lying sediments and volcanics of the Lower Proterozoic Kimberley Group and any controlling structures are in the unexposed basement. Individually the dykes and pipes all trend northeast, parallel to the Halls Creek Mobile Zone, a prominent structural trend throughout the Kimberley area. The dykes as a group, however, form a northwest-trending group, parallel to the north coast of the Kimberley area.

The age of the dykes is about 800 Ma (Pidgeon and Smith, in prep.), a time of no presently known tectonic activity in the Kimberley Basin or the surrounding

mobile zones. The age of the enclosing sediments and volcanics is about 1 800 Ma and the youngest folding about 1 550 Ma (Plumb and Gemuts, 1976), although an intense deformation of the Elgee Siltstone and Carson Volcanics in the Yampi area, on the southwest margin of the Kimberley Block, has been dated at 630 Ma (Bennett and Gellatly, 1970). Possibly the pattern of kimberlite intrusion relates to the structures responsible for the development of the Bonaparte Basin; the intrusions are located at the margin of the Kimberley Block close to the northwest-trending downwarp separating the craton from the basin. Immediately offshore from the North Kimberley area is the Petrel Sub-basin, a northwest oriented graben or failed rift, similar to the Fitzroy Trough on the southwest margin of the Kimberley Block. Little is presently known of the offshore geology of the Bonaparte Basin, but onshore the basin developed only in the Silurian-Devonian period, thus any relationship between basin development and kimberlite intrusion must be through basement structures of long standing.

EAST KIMBERLEY PROVINCE

Kimberlite and lamproite intrusion in the East Kimberley Province is closely associated with major faults of the Halls Creek Mobile Zone — the Argyle pipe with the Glenhill and Halls Creek Faults, the Bow Hill Dykes with the Bow Hill Fault and the small kimberlite dykes of the Maude Creek and Devils Elbow area with the Greenvale Fault. However, it is only with the Argyle pipe that lamproite intrusion can be directly correlated with tectonic activity. The Argyle pipe intrudes the Carr Boyd Group, which was laid down in an area of subsidence between the Halls Creek and Glenhill faults. The pipe intrudes along a splay fault of the Glenhill Fault and is only a few kilometres from the Halls Creek Fault. The Golden Gate Siltstone, near the base of the Carr Boyd Group, has been dated at 1 158 ± 123 Ma (Bofinger, 1967, recalc.), a similar age to the lamproite, which was intruded between 1 045 Ma and 1 253 Ma (*see* Chapter 4, Table 20). Thus the tectonism which allowed the deposition of the Carr Boyd Group, occurred at the same time as the lamproite emplacement.

The Bow Hill Dykes form an *en echelon* swarm between the Bow Hill Fault and a smaller unamed fault trending north-northeast (Fig. 39). The age of the dykes is ≈ 800 Ma (Table 9) but the principal movement on the Bow Hill Fault would have been in the final phase of cratonization of the mobile zone, at about 1 800 Ma. However, the smaller northerly fault displaces the Cambrian Antrim Plateau Volcanics, which suggests that minor tectonism continued into the Palaeozoic.

The kimberlite dykes to the west have not been dated, but by analogy with the North Kimberley and nearby Bow Hill dykes are thought to be about 800 Ma old. The dykes are spatially associated with the marginal folds of the Kimberley Basin succession and with the Greenvale Fault, which is the western boundary fault of the Halls Creek Mobile Zone.

WEST KIMBERLEY PROVINCE

The lamproites of the West Kimberley Province are a uniform group of intrusions yet occur in widely differing structural settings, from the Proterozoic King Leopold Mobile Zone to the Paleozoic Fitzroy Trough. The age of the lamproites is early Miocene, 20-25 Ma, but the region had been essentially stable since the Jurassic. A few intrusions in the north of the area (Mount Rose, McKinrick Hill) appear to be spatially related to the Sandy Creek Shear, a major Early Proterozoic fault. Many of the lamproites intruding the Palaeozoic are associated with major faults parallel to the northern margin of the Fitzroy Trough. Ellendale 4 and 38, Camarotoechia Creek, Spielers Bore, and Oscar, are aligned with the Oscar Fault along the southwest face of the Oscar Range; Ellendale 17, 39 and 46 are probably associated with a concealed fault along the face of the Napier Range, a lineament which continues east to include the Big Spring pipes and possibly Hooper West. The main part of the Ellendale Field is located on a subsurface fault block which sits astride the northwesterly projection of the Oscar Fault. This fault does not extend into the area, but the form of the pre-Palaeozoic basement (Fig. 54) suggests that other major basement faults are present. The Calwyngardah Field clusters about the Pinnacle-Harvey Fault system, the northern margin of the Fitzroy Trough, but the Noonkanbah Field shows no obvious relationships to faults mapped at the surface.

Although the distribution of lamproites appears to be related to ancient faults within the basement, probably initiated during the Proterozic, the shape of many individual intrusions is elongated east-west, parallel to the axes of shallow folds in the Palaeozoic sediments. Smith (1968) has argued that those folds developed in response to dextral strike-slip movement on the boundary faults of the Fitzroy Trough during Late Triassic to Early Jurassic times the lamproites thus exploited east-west lines of weakness in the sedimentary cover during their emplacement (Atkinson and others, 1984a).

A feature of the West Kimberley Province is the concentration of most intrusions into relatively compact fields — the Ellendale, Calwynyardah and Noonkanbah fields — which occur on a north-south line. Further, it has been shown that the age of the bodies increases uniformly from south to north (Jaques and others, 1984c), leading to the suggestion that movement of the Australian continent northwards over a "hot spot" at about 3.7 cm/a can best explain the distribution (Smith, 1984a)

WANDAGEE PROVINCE

The association of the alkali picrite sills and diatremes of the Wandagee Province with the Wandagee Fault is obvious, as all are found within a few kilometres east of the fault. The fault was probably initiated in the late Carboniferous (≈ 300 Ma) and displacements continued until the Early Cretaceous (≈ 140 Ma) (Hocking and others, in press). The age of the picrites is 160 ± 10 Ma

(Atkinson and others, 1984a), concident with the age of breakup of the continental margin (Veevers, 1981) and the greatest movement on the fault. The picrites are therefore associated with a major fault which cuts the crystalline basement and is probably related to older structures within the basement.

DISCUSSION

Current theories of diamond genesis suggest that the mineral forms at depths of 100-150 km in a depleted mantle, *i.e.* a portion of the mantle low in oxygen fugacity from which basaltic and/or komatiitic magma has been extracted, leaving a refractory residuum (Boyd and Gurney, 1982). For these reasons, it is unlikely that an appropriate environment existed in early Archaean times while there was considerable volcanicity, mantle degassing, convective overturning in the mantle, and a presumed high heat flow. Neverthless, these processes led to the development of an appropriate lithosphere and refractory sub-cratonic mantle; and diamonds from South Africa have been found to have Sm-Nd ages of 3 200-3 300 Ma, although they were erupted with kimberlites only 90 Ma old (Richardson and others, 1984). Field evidence from southern Africa and the Soviet Union also supports this theory: diamondiferous kimberlites are apparently confined to old cratonic areas, stable for at least 1 500 Ma, while surrounding mobile zones contain intrusions of non-diamondiferous kimberlite, carbonatite and alkali volcanics (Clifford, 1966; Dawson, 1970, 1980).

In Western Australia, cratonization and development of the lithosphere in the Archaean nucleii of the Yilgarn and Pilbara Blocks should provide a suitable environment for diamond generation and kimberlite eruption. However, despite reported finds of a few small diamonds of unknown provenance no kimberlites are known from the Yilgarn Block. The only alkaline rocks are the late Archaean syenites of the Eastern Golfields (Libby and de Laeter, 1981), a carbonatite dated at 2 020 Ma (Collerson, 1982; Goode, 1981), and a few small dykes of alnöite or melilitite on the eastern margin, close to the Albany-Fraser Mobile Zone (Danchin and others, 1985). In the Pilbara Block, no alkaline intrusives are known, and the source of the diamonds at Nullagine remains to be discovered.

In the Kimberley region, the Archaean basement to the Kimberley Block is not exposed, but the voluminous outpouring of tholeiitic basalts to form the Carson Volcanics and the Hart Dolerite sills in the Early Proterozoic must have assisted in the production of the depleted mantle environment thought necessary for diamond formation. The presence of leucite lamproites in the surrounding mobile belts might be thought to be equivalent to the zone of non-diamondiferous kimberlites and alkaline intrusives surrounding the Transvaal Craton in South Africa, and provided the first incentive to explore the area (Chapter 1). A few small kimberlite dykes and pipes, and a number of diamonds, have been found in the North Kimberley, but the principal discoveries were made in the surrounding mobile zones at Argyle and Ellendale with the finding of the previously unknown diamondiferous olivine lamproites.

The Halls Creek and King Leopold Mobile Zones were active in the Early Proterozoic, between about 2 150 Ma and 1 800 Ma, but were then cratonized to form part of the North Australian Craton (Plumb, 1979). Some lithospheric development took place during cratonization, although Hancock and Rutland (1984) suggest that it was minor. Later underplating probably thickened the crust and further depleted the mantle. A study of mantle xenoliths from the Argyle pipe and Ellendale indicates the presence of a refractory harzburgitic and lherzolitic mantle, possibly with eclogite and granulite in parts (*see* Chapter 8). Subsequent to cratonization, the mobile zones have acted as rigid tectonic units subject only to brittle fracture and faulting. Minor folding and tilting have resulted from fault movements, particularly from strike-slip displacements on the major faults, but thermal metamorphic, and plastic deformation events have been absent since about 1 800 Ma. These faults continued to serve as locations for the dissipation of the major stresses which acted on North Western Australia through to the Jurassic. Not surprisingly these zones of weakness were exploited at the time of kimberlite and lamproite emplacement both in the East and West Kimberley Province.

The basement beneath the Perth and Carnarvon Basins is very poorly known, but was certainly cratonized in the Proterozoic. It has since remained a focus for structural activity extending into the Phanerozoic, eventually marking the site of rifting and the breakup of Gondwana. Once again, a major rift fault, possibly reflecting an ancient basement structure, acted as a focus for the emplacement of the alkali picrite diatremes at Wandagee.

The classical setting for kimberlites in southern Africa and the Soviet Union has commonly been thought of as the central portions of Archaean cratons. However, the relationship of kimberlite intrusion to the structures of the crystalline basement is generally obscure as in both areas the kimberlites mostly intrude sedimentary platform cover and only the larger basement structures, which reflect in the sediments, are known. Nevertheless, the general dependence of kimberlite emplacement on basement structures is widely recognized in some areas, *e.g.* Lesotho, where the alignment of pipes and dykes is striking. In Western Australia, these basement relationships are much more clearly visible as, except in the North Kimberley, much of the basement is exposed. The principal structural setting is around the margins of the Archaean nucleii, within Early Proterozoic mobile belts subsequently cratonized but still subjected to periodic brittle deformation, and related to major strike-slip faults which were active over a long period thus providing a conduit for deep seated kimberlite and lamproite magmatism.

CHAPTER 3

THE NORTH KIMBERLEY PROVINCE

Six small kimberlites, two pipes and four dykes, are known from the North Kimberley, in the area between the Berkeley and Drysdale rivers, adjacent to the Bonaparte Gulf (Fig.9). They were discovered between 1974 and 1976 by the Kalumburu Joint Venture and were the first rocks with strong kimberlitic affinities known in Western Australia. Extensive exploration of the area by a number of mining companies has recovered a considerable number of small diamonds and indicator minerals from gravels in the King George River and other rivers and creeks of the north Kimberley. No source for most of the diamonds is known although it is probable that other small dykes and pipes remain undiscovered. Of the six kimberlitic bodies which at present comprise the North Kimberley Province, only one pipe, and possibly one dyke, are known to contain occasional diamond.

This part of the north Kimberley area has an average annual rainfall of about 900 mm, and is tropical woodland savannah country supporting a bloodwood

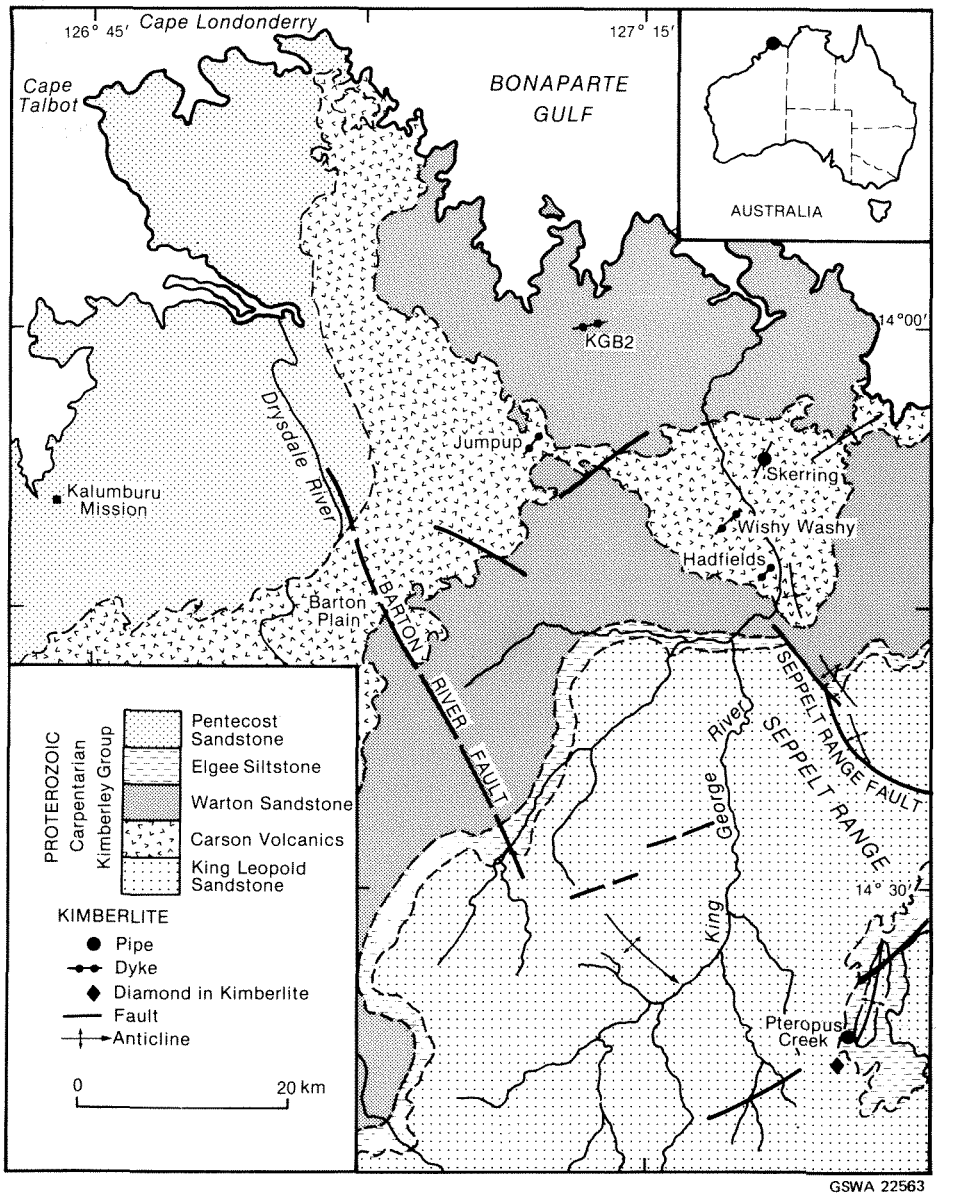


Figure 9. Location of kimberlites in the North Kimberley Province.

and stringybark vegetation belonging to the *Eucalyptus tetradonta — E. miniata* alliance of Beard (1979). The *E. tectifica — E. grandifolia* alliance occurs where the Carson Volcanics outcrop. Tall grass (*Sorghum* sp.) grows during the wet season as a dense understorey.

Access to the area is difficult. A moderately maintained graded road extends from Gibb River cattle station, 367 km east-northeast of Derby, a further 310 km to Kalumburu Mission at the mouth of the King Edward River (Fig. 9). The kimberlites can be approached from the Carson River crossing, about 18 km south of Kalumburu, via poorly maintained station tracks for a further 120 km to the King George River at Geebung airstrip. Access to the Forrest River Aboriginal Reserve on the east bank of the King George River is restricted. For some months during the summer wet season, all roads and tracks are impassable. Supplies of food and fuel must be obtained in Derby.

PHYSIOGRAPHY, REGIONAL GEOLOGY, AND STRUCTURE

Physiographically, the north Kimberley area is part of the broad, dissected Kimberley Plateau. It lies at elevations between 100 m and 200 m, and forms part of the Karunjie Plateau sub-province of Wright (1964). Erosion and weathering of siltstone and volcanics, interbedded with resistant sandstone, has produced a series of escarpments and isolated mesas.

The regional geology consists of a relatively flat-lying succession of sandstones, minor shales, and basaltic volcanics, belonging to the Kimberley Group. The oldest member of this group to occur in the region is the King Leopold Sandstone which outcrops near the mouth of the Drysdale River. A very gentle dip to the southeast, combined with increasing elevation, causes successively younger stratigraphic units to be exposed southeastwards as far as the Collison Range (Fig. 9). Minor domical structures expose inliers of Carson Volcanics in the lower King George River area, and of Warton Sandstone and Elgee Siltstone at Pteropus Creek.

Two prominent faults, the Barton River and Seppelt Range Faults, trend north-northwest parallel to the margin of the Bonaparte Basin. Throw on the Barton River Fault is small, but the Seppelt Range Fault has a throw of about 200 m (Gellatly and Sofoulis, 1969). The kimberlite dykes, and the Skerring pipe, are orientated northeast, sub-parallel to the Halls Creek Mobile Belt and the northwest Kimberley coastline. This same direction is followed by a number of long dolerite dykes of post-Pentecost Sandstone age. They are part of a swarm that seldom outcrops but has been detected and mapped on the basis of aeromagnetics for several hundred kilometres across the Kimberley Plateau.

AGE OF INTRUSION

The six kimberlites all cut rocks of the Kimberley Group for which a minimum age is given by the 1 760±25 Ma Hart Dolerite (Bofinger, 1967), which intrudes this succession, and a maximum age of 1 940±10 Ma from the Whitewater Volcanics at the base of the succession.

Surficial weathering, oxidation, silicification, and lateritization, have precluded use of near-surface samples from these kimberlites for dating purposes. However, zircon macrocrysts from the Skerring and Pteropus pipes have proved amenable to U-Pb and fission-track dating, the results of which are given in Table 9 (Pidgeon and Smith, in prep.).

TABLE 9. U-PB AND FISSION-TRACK ZIRCON AGES FROM THE NORTH KIMBERLEY

Kimberlite body	*U-Pb*	*Fission track*
Pteropus Creek	804±5 Ma	510±30 Ma
Skerring	800±7 Ma	No result

After Pidgeon and others, in prep.

Pidgeon and Smith interpret these results as implying an age of emplacement of 802±10 Ma for North Kimberley kimberlites and suggest the younger fission-track date is the result of later resetting, perhaps caused by a heating event such as may have accompanied the extrusion, during the Cambrian, of the Antrim Plateau lavas. Alternatively, the U-Pb date may represent the time of crystallization of the zircon; and the fission-track age, the date of emplacement of the kimberlite.

GEOLOGY OF THE KIMBERLITES

The five northern bodies, including the Skerring pipe, are of micaceous kimberlite and carry abundant kimberlite indicator minerals, particularly picroilmenite. The isolated southerly occurrence at Pteropus Creek is a silicified breccia pipe containing abundant blocks of sandstone and minor indicator minerals, chiefly chromite and zircon.

SKERRING PIPE

The Skerring Pipe, located at 127°22'E, 14°07'S (KING GEORGE, GR: 223393)*, lies about 3.5 km east of the King George River, within the Forrest River Aboriginal Reserve. It is 450 m long by a maximum of 75 m wide (1.75 ha) and is oriented north-northeast (Fig. 10). Ground magnetics and heavy-mineral loam-dispersion patterns indicate that the pipe is a localized expansion on an unexposed kimberlite dyke, that it extends 3.5 km southwest to near the King George River, and that it extends for an unknown distance to the northeast.

Silicified kimberlite float, and an abundance of megacrysts and xenoliths of both crystal and mantle types, strew the ground in the vicinity of the pipe. Pitting and trenching show the pipe to be composed of two varieties of kimberlite with sharp contacts between them (Muggeridge and others, 1978):

(1) A green, massive, and porphyritic variety containing abundant macrocrysts of garnet,

**Grid references:* Names of National Topographic Series 1:100 000 -scale sheets are given in full capitals. Eastings and northings are given as a six-digit number that refers to the Australian Map Grid.

picroilmenite, brown mica and chrome diopside, together with minor chromite, zircon, and large rutile. Xenoliths of shale, sandstone, and rare Carson Volcanics, mica schist, and foliated granite, are present. Silicified mantle xenoliths have also been recognized.

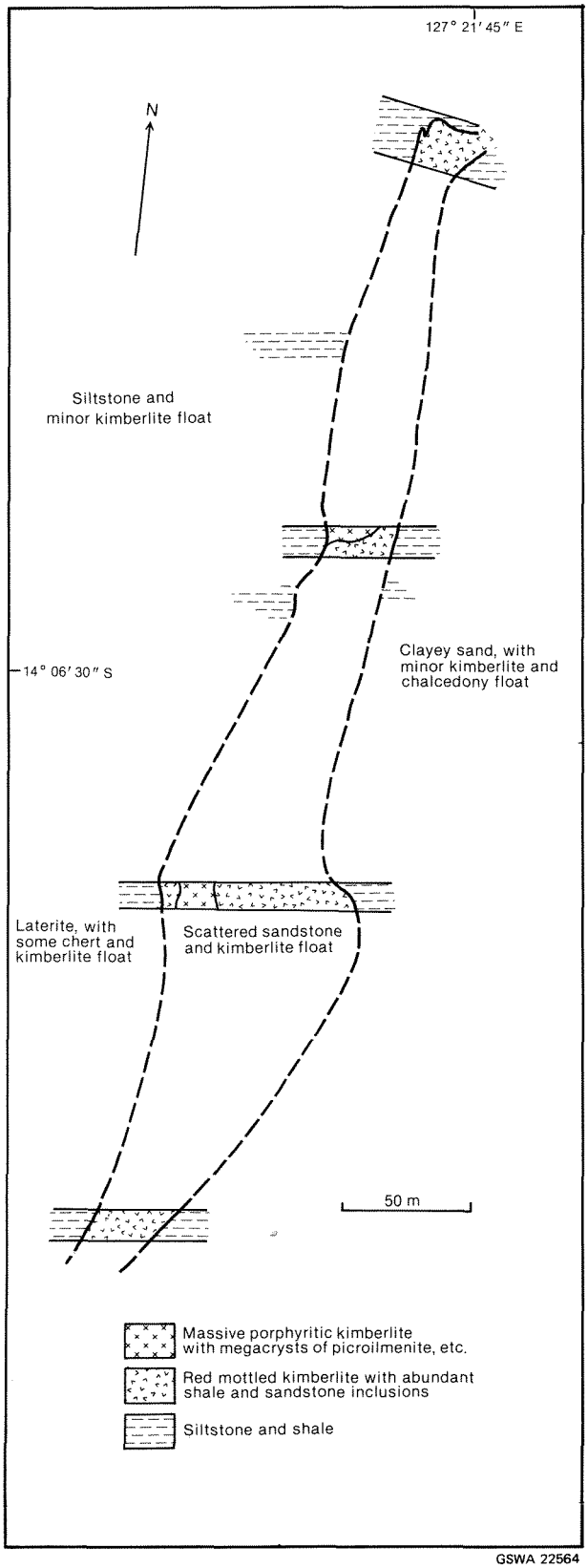


Figure 10. Sketch map of the Skerring Pipe and the geology of bulk-sample trenches (modified after Muggeridge and others, 1978).

(2) A red, mottled variety packed with xenoliths of red country-rock shale, rare rounded sandstone xenoliths, and abundant picroilmenite. The rock is often rubbly in appearance.

The relationship between the two varieties is unknown, although the more massive green variety probably intrudes the red, mottled kimberlite.

The country rock adjacent to the pipe is flat-lying grey shale forming the upper part of the Carson Volcanics. Contacts between country rock and kimberlite are sharp and near vertical; and, except for minor impregnation with carbonate, the shales are undisturbed.

Xenoliths in the kimberlite are dominated by crustal types: shales from the adjacent Carson Volcanics sequence (but no basalt fragments from higher in the sequence), subrounded Proterozoic quartzites, and rare schist and granite. Silicified mantle xenoliths found on the ground have been interpreted from textural evidence to range from dunite to garnet peridotite (Atkinson and others, 1984a) and are up to 28 cm across. Unaltered garnet occurs occasionally in the mantle xenoliths, but olivine and pyroxene are totally silicified and have been identified from relic fracture cracking and cleavage textures. Graphic-textured intergrowths between manganiferous picroilmenite and silica (Fig. 16) have also been found as xenoliths and it is presumed the silica replaces former pyroxene.

Petrographically, the massive green kimberlite from the pipe consists of abundant, large, rounded, talc pseudomorphs after olivine, set in a microporphyritic groundmass crowded with sub- to euhedral olivines, typically 0.2 mm diameter and pseudomorphed by talc, small phlogopite flakes, scaly talc, serpentine, chlorite, carbonate, Mn-ilmenite, rutile and minor spinel of < 10 μm diameter.

A chemical analysis of the Skerring kimberlite is given in Table 10. The material analyzed, although the freshest available, is from weathered material only 3 m below the surface. Silicification is apparent from the high SiO_2 value. The high MgO, Cr, Ni, Nb, Sr, and Zr

TABLE 10. ANALYSIS OF MASSIVE KIMBERLITE FROM SKERRING PIPE

Major components (%)		*Minor components (ppm)*	
SiO_2	54.3	Cr	1 600
TiO_2	2.9	Co	75
Al_2O_3	2.2	Ni	835
FeO(a)	9.53	Sr	260
MgO	19.3	Zr	340
CaO	1.8	Nb	120
K_2O	0.15	Ba	430
Na_2O	0.40		
P_2O_5	0.39		
Rest	0.49		
Total	**91.46**		

(a) Total iron reported as FeO.

Analysis by Analabs, Perth. XRF, except Co and Ni by atomic absorption.

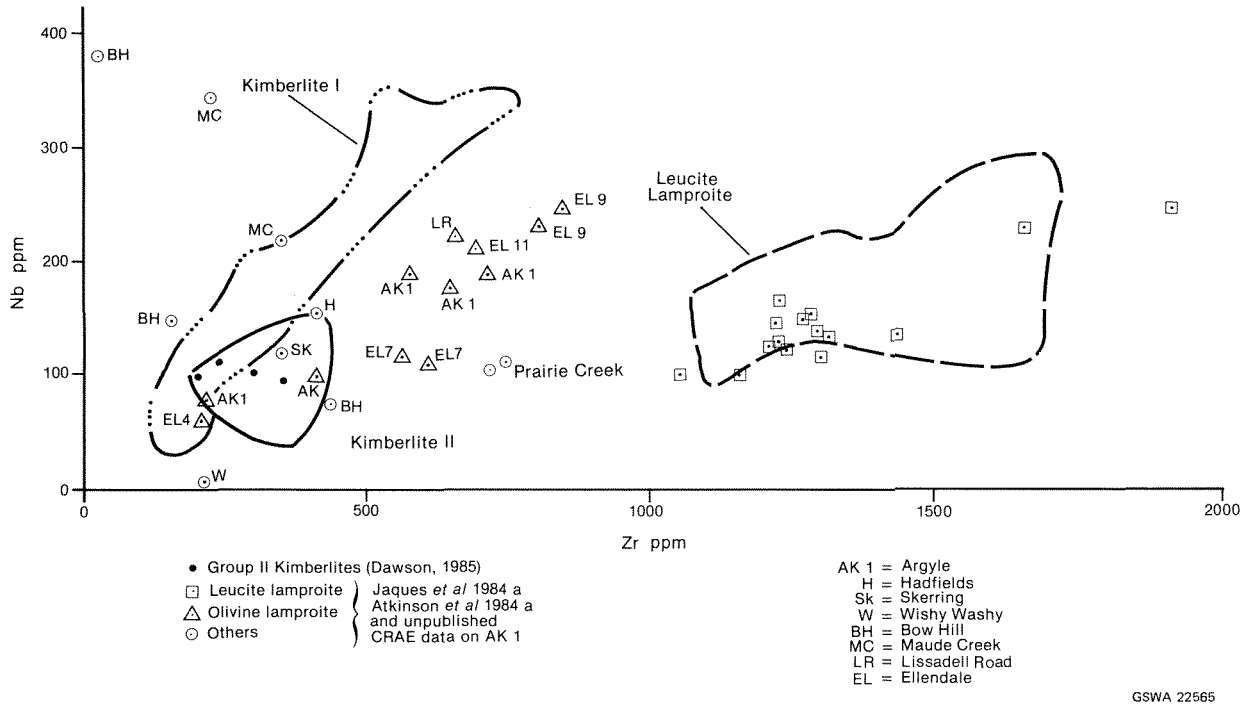


Figure 11. Nb *versus* Zr plot for some West Australian kimberlites and lamproites, together with compositional fields for kimberlites and lamproites, after Scott-Smith and Skinner (1984a), and Dawson (1985).

values, are in keeping with a kimberlitic origin, but the degree of alteration and leaching makes it difficult to use the analysis to distinguish it from lamproite.

Scott-Smith and Skinner (1984a) have used Nb and Zr, both relatively resistant to leaching, in a plot to distinguish kimberlite from lamproite. A plot of Nb *versus* Zr values for a number of Western Australian kimberlitic and lamproitic rocks, together with the fields for kimberlite type I, kimberlite type II and leucite lamproite (Scott-Smith and Skinner, 1984a; Dawson, 1985) is given in Fig. 11. On this plot, the Skerring analysis lies within the overlap between the fields of kimberlites of types I and II and the field covered by olivine lamproites.

WISHYWASHY DYKE

This dyke takes its name from the rather indeterminate, sporadic and swampy nature of the adjacent creek which yielded the indicator minerals that led to the dyke's discovery (KING GEORGE, GR: 195320). However, the dyke itself proved difficult to locate in trenches excavated across the trend of indicators found in surface loam samples. The indicator mineral abundances from the grid loam samples show the dyke to be traceable for some 2.5 km with a northeast strike. However, only in two closely spaced shallow tenches were heavily weathered and altered kimberlite dykes actually identified (Fig. 12; Paltridge and Smith, 1977). In these trenches the dyke has a maximum width of approximately 1 m, is vertical in attitude, and is largely altered to white, yellow and green clay with magnesite patches.

Country rock in the trenches was basalt, altered to brown clay; but, further southwest, the country rock was the shale that forms the upper part of the Carson Volcanics succession. The dyke could not be recognized

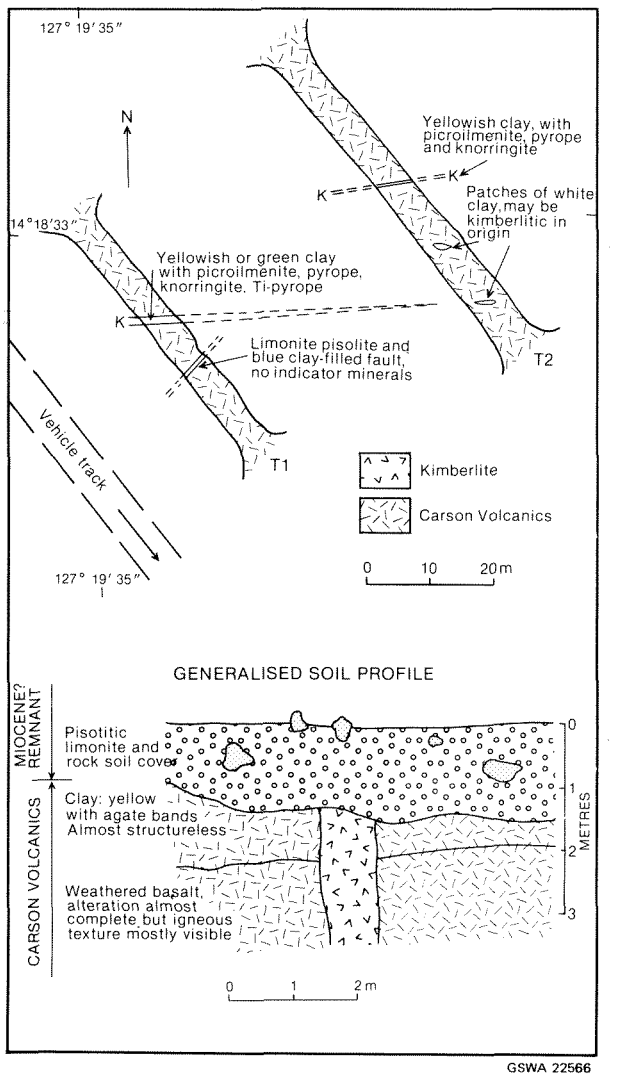


Figure 12. Geological sketch map of the Wishywashy Dyke (after Paltridge and Smith, 1977).

in other trenches along its presumed strike length, and it is thought to be represented elsewhere by hairline stringers similar to the Hadfields and KGB2 dykes described below. No bulk sampling of the dyke for diamonds was carried out because of its small size and consequent lack of economic potential.

Trace-element chemistry of this weathered dyke (Table 11) is not helpful in distinguishing its kimberlitic nature from the adjacent basalt country rock. The analysis is low in both Nb and Zr; and, on Fig. 11, the analysis plots outside the fields of kimberlite and olivine lamproite. However, picroilmenite and garnet were recovered from small samples of the altered dyke; and the presence of a diamond in a loam sample immediately above the trench site, and a number of stones in the adjacent Wishywashy Creek, would suggest the dyke is probably diamondiferous.

TABLE 11. TRACE-ELEMENT ANALYSES OF HADFIELDS AND WISHYWASHY DYKES

	Hadfields (ppm)	*Wishywashy (ppm)*
Cr	1 500	580
Co	75	35
Ni	515	140
Sr	250	150
Zr	400	200
Nb	160	9
Ba	2 800	340

Analysis by Analabs, Perth. XRF, except Co and Ni by atomic absorption.

HADFIELDS DYKE

This dyke (KING GEORGE, GR: 221279), marked at the surface by dispersion of kimberlite indicator minerals, chiefly picroilmenite, was exposed in two bulldozer cuts. The dyke occurs as a set of thin, pinching and swelling, lenticular stringers up to 14 cm wide but averaging only 2 or 3 cm (Paltridge and Smith, 1977). The stringers strike northeast and occur within a 1.5 m-wide zone in shales of the Carson Volcanics succession (Fig. 13).

Within the shallow bulldozer trenches, the kimberlite has been altered to soft chocolate-coloured clay, which contains visible indicator minerals, chiefly picroilmenite, and occasional lumps of hard, white silicified kimberlite. The very small size of the dyke precluded any bulk sampling operations, and it is not known if the kimberlite is diamondiferous.

The trace-element geochemistry of Hadfields Dyke (Table 11) shows the kimberlitic characteristics of high ultramafic-association elements (Ni, 515 ppm; Cr, 1 500 ppm) combined with high incompatible elements (Nb, 160 ppm; Zr, 400 ppm; Ba, 2 800 ppm). On the Nb *versus* Zr plot, Fig. 11, the dyke falls close to the area of overlap between kimberlite and olivine lamproite, near the similar plot for the Skerring kimberlite.

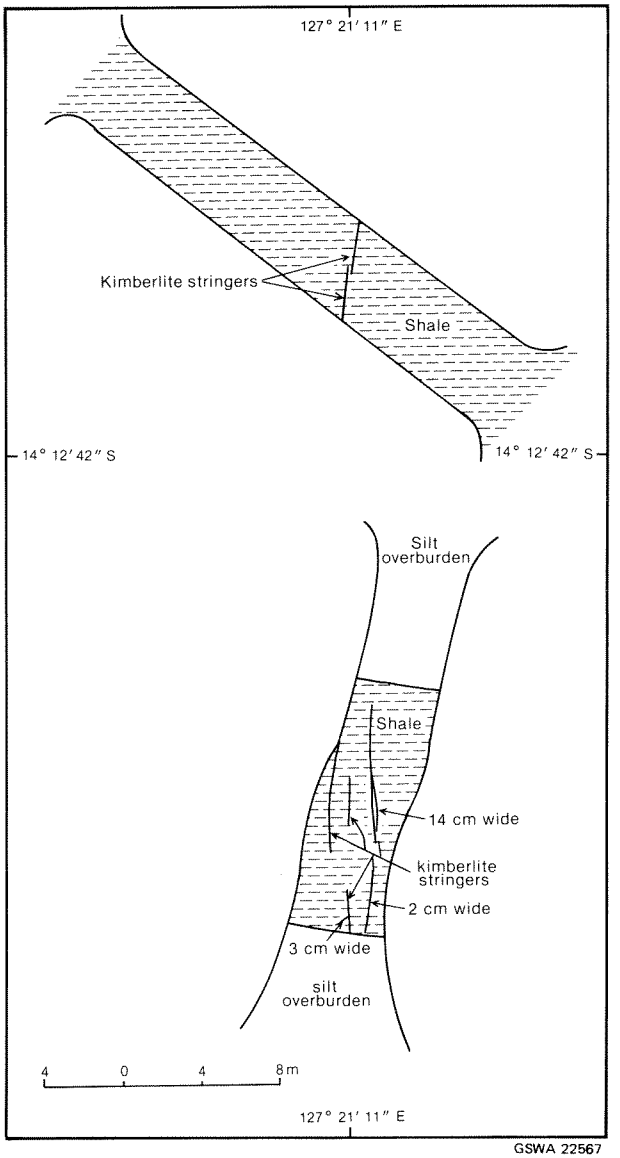


Figure 13. Geological sketch map of the Hadfields Dyke (after Paltridge and Smith, 1977).

Judging from the occurrence of abundant fresh kimberlite indicator minerals in loam samples taken at the sites of airphoto lineaments, other kimberlite dykes are believed to exist nearby. Examples of these are the Geebung Airport and Dearn's Gulley occurrences (Paltridge and Smith, 1977). Trenching at the airstrip failed to locate a dyke, and it is thought these occurrences may be represented by hairline kimberlite stringers similar to Hadfields Dyke, or even thinner.

KGB2 DYKE

A bulldozer cut, made into a lateritic surface over which picroilmenite and lateritized kimberlite float was spread, exposed a northeast-trending stringer of ferruginized micaceous kimberlite a few centimetres wide. It has not been traced beyond the area of discovery. Country rock consists of shales interbedded within the Warton Sandstone.

The dyke was also intersected by two 60° angle diamond drillholes and two percussion holes at depths of 26 m and 42 m. Most intersections were stringers a

few centimetres wide, but diamond drillhole DH2 showed a true width of 0.25 m of kimberlite and percussion hole PH2 recovered kimberlite chips mixed with sandstone chips over a true width of 2.5 m. Even at a depth of 43 m, the kimberlite was represented by heavily altered "yellow ground", and the core rapidly disintegrated to powder. The dyke was too thin to bulk sample and its diamond content is unknown.

A chemical analysis of drill core (Table 12) suggests that many of the more mobile elements (*e.g.* K,Ni,Co, Mg) have been strongly leached. In contrast, the dyke has seemingly been strongly enriched in the immobile elements — *e.g.* Ba, 1.8%; Sr, 1.3%; and Nb, 2 300 ppm. There are also high values for rare-earth elements — *e.g.* Ce, 1 850 ppm; Nd, 990 ppm.

TABLE 12. ANALYSIS OF KGB2 DYKE

Major components (%)		*Minor components* (ppm)		*Minor components cont'd* (ppm)	
SiO_2	42.3	Ni	30	La	1 500
TiO_2	12.0	Cr	2 500	Ce	1 850
Al_2O_3	19.5	Rb	15	Pr	264
Fe_2O_3	1.0	Sr	13 000	Nd	900
FeO	0.15	Y	170	Sm	104
MnO	0.01	Zr	1 050	Eu	23
MgO	0.03	Nb	2 300	Gd	60
CaO	1.1	Ba	18 000	Dy	27
K_2O	0.06	Ta	150	Ho	38
Na_2O	0.02	Th	450	Er	7
CO_2	0.55	U	20	Yb	7
P_2O_5	7.35	Sc	26		
SO_3	0.16				
LOI	8.90				
Rest	5.00				
Total	**98.13**				

Analysis by Analabs, Perth. XRF and chemical methods; Co and Ni by atomic absorption; REE by ICP.

JUMP UP DYKE

This dyke was named for its proximity to the escarpment or "jump up" of Warton Sandstone that the bush track from Drysdale River to the King George River has to ascend. The position of the dyke (KING GEORGE, GR: 988392) is known from concentrations of picroilmenite and pyrope in surface loams associated with a photo lineament (Smith, 1978a). The lineament is marked on the ground by a line of *Eucalyptus* trees. A shallow bulldozed costean across the lineament failed to expose recognizable kimberlite in the basaltic country rocks of the Carson Volcanics. It is likely that the dyke is formed by hairline stringers of kimberlite similar to Hadfields Dyke.

PTEROPUS BRECCIA PIPE

A small, low hill, about 100 m in diameter, covered with sandstone float and occasional blocks of brecciated rock, and located in a prominent bend in Pteropus Creek, marks the site of this pipe of approximately 2 ha (14°38'00"S, 127°27'45"E; COLLISON, GR: 307820) (Muggeridge and others, 1978). On the southwest side of the hill, there is a small lateritized and silicified outcrop of breccia, the only exposure of the pipe breccia. The outline of the pipe (Fig. 14) was determined by a gravity survey which showed a discrete low of 0.6 mgal over an oval area 190 m × 60 m, oriented east-west, and was confirmed by percussion drilling which outlined a pipe with essentially vertical margins, 190 m × 100 m (Shaw and others, 1985).

The pipe has been emplaced within Proterozoic Warton Sandstone at the southwest corner of, and close to the faulted axis of, a northeast-trending domical structure (Fig. 9).

The breccia that fills the pipe consists of abundant, cream- to fawn-coloured, angular blocks of siltstone and sandstone, and occasional well-rounded, smooth, egg-shaped boulders of sandstone; these are set in a quartz-rich tuffaceous matrix of detrital quartz grains and sparse macrocrystal zircon, chromite, garnet, and picroilmenite, and traces of mica and rutile. Grains of tourmaline found in heavy-mineral concentrates are probably derived from the wall rocks. Locally the breccia is full of voids and has a clinkery or scoriaceous appearance; one piece of float appeared to be bedded and tuffaceous.

Narrow zones — giving a strong magnetic response, both in the pipe and in the surrounding country — have been interpreted by Ryan (1982a) as possible concealed kimberlite dykes. Small patches of clay and chalcedony within the breccia may also represent weathered magmatic kimberlite.

Detailed gravel sampling in Pteropus Creek, close to the pipe, has recovered 16 small diamonds weighing 0.792 CM (Muggeride and others, 1978). None of the diamonds exceeds 3 mm and most are less than 1 mm in diameter. Only one irregular fragment of diamond, 0.16 mm in diameter, has been recovered from the crushed breccia (Fitton, 1980).

The distribution of indicator minerals in Pteropus Creek and its tributaries suggests that other kimberlites may occur in the general area, probably as narrow dykes.

The petrography of the breccia is obscured by thorough alteration and silicification. Fragments of sandstone, siltstone, and silicified shale — up to 8 mm across — can be identified in thin section, and there are often abundant rounded grains or angular fragments of quartz in the matrix. Rare examples of silicified olivine and pyroxene, identified by relic fracture and cleavage patterns, are also present. The sparse clay matrix in these "sandy" tuffs is often thoroughly ferruginized; but, where it forms larger masses, it consists of banded aggregates of submicroscopic kaolin filling voids within the rock. In one such specimen, the kaolin encloses large fragments of partly leucoxenized picroilmenite up to 1 mm across: a kimberlitic origin for the clay fraction is suggested. Clay veins within the breccia contain abundant large kaolin flakes up to 0.5 mm, possibly pseudomorphing an original micaceous mineral. Possible

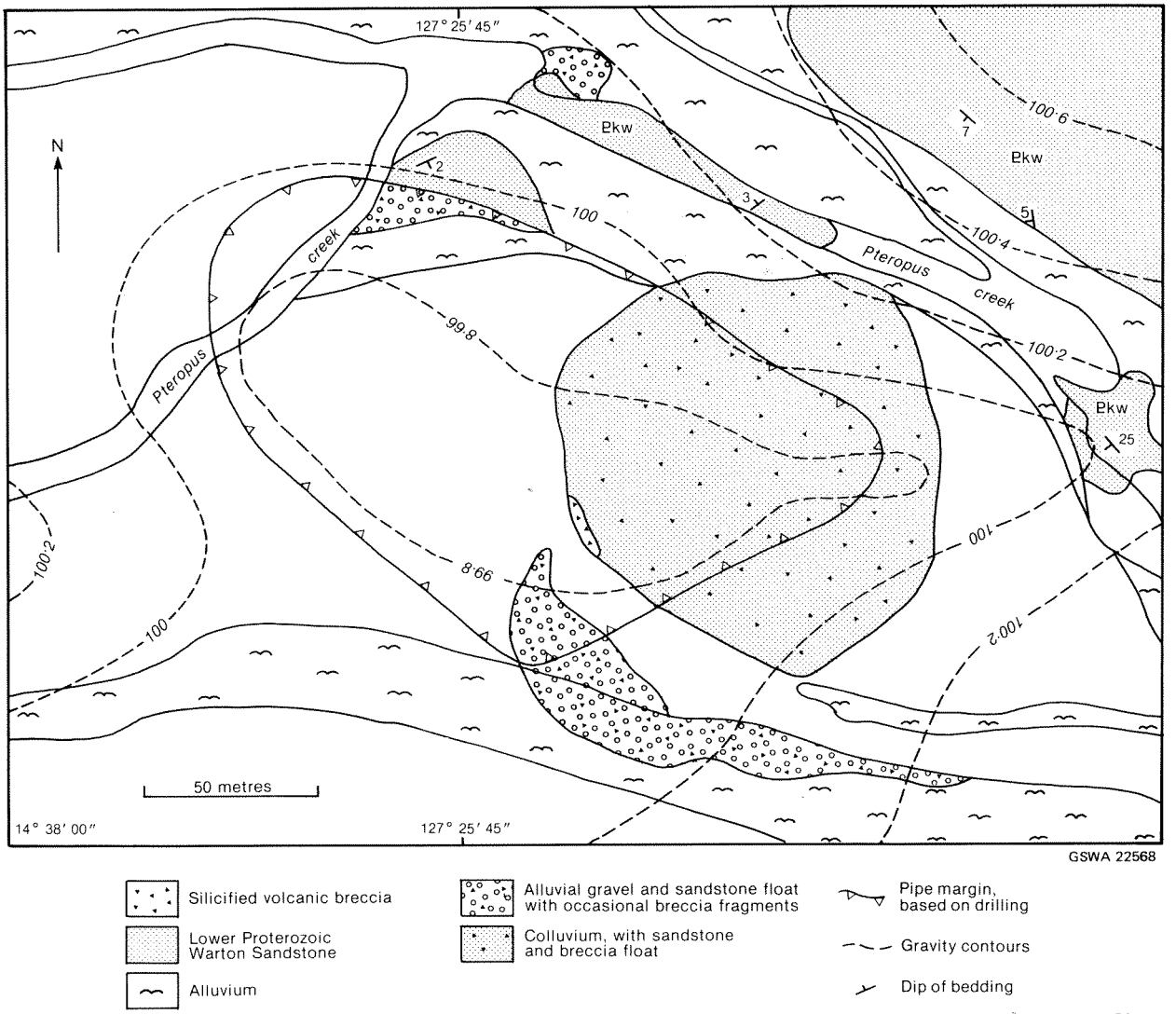


Figure 14. Surface geology and gravity contours of the Pteropus Breccia Pipe (after Muggeridge and others, 1978; Shaw and others, 1985).

bedding and small accretionary lapilli are present in some specimens; and the overall impression of the pipe rocks is of bedded tuffs and agglomerate, rich in accidental material. Kimberlitic material, including macrocrysts, tuff matrix, and small dykes and stringers, is probably more common than is evident in the silicified samples available but nevertheless forms only a minor proportion of the pipe deposits.

Drill cuttings from thirty percussion holes have been analyzed for eleven trace elements; a summary of the results, with selected analyses, is given in Table 13 (Shaw and others, 1985). The relatively low mean values, and the wide range of values for many elements in the breccia, are indicative of the high and variable dilution of kimberlitic material by wall-rock sandstone. The highest values for certain elements, such as Nb (600 ppm), La (620 ppm) and Ce (1 000 ppm), might suggest a lamproitic rather than kimberlitic magma, although these exceptional values are not from the same specimen. Specimens from the Warton Sandstone are chemically characterized by a narrower range of values and a significantly lower standard deviation for most element concentrations. Although there is a wide overlap between analyses of the breccia and the wall-rock, the concentrations of a number of elements, particularly Cr, Co, Ni, and Nb, are sufficiently elevated in the breccia that they serve to distinguish it from the sandstone. By contrast, and despite the presence of kimberlitic zircon in the breccia, Zr is higher in the wall rock (mean 353 ppm) than in the breccia (mean 246 ppm); apart from a few high values, Ba is about the same in both rocks.

MINERALOGY

Heavy-mineral concentrates were obtained from each known kimberlite dyke and pipe in the North Kimberley Province during diamond exploration. The composition of these concentrates is shown in Table 14.

Surficial weathering, silicification, and lateritization, have resulted in destruction of many of the heavy minerals; as a result, these may remain undetected, except where deep pitting or drilling has been carried out to expose relatively fresh rock. In the climate of the north Kimberley, the most resistant minerals appear to be spinel, rutile, and zircon, followed by ilmenite. Garnet is markedly less resistant to the processes of alteration, and pyroxenes are the most readily destroyed of all.

TABLE 13. TRACE-ELEMENT GEOCHEMISTRY OF THE PTEROPUS BRECCIA PIPE AND HOST-ROCK SANDSTONE.

	Pteropus Breccia (a)			*Warton Sandstone (b)*			*Pteropus Breccia*		*Warton Sandstone*	
	mean (ppm)	*range (ppm)*	*std. dev. (ppm)*	*mean (ppm)*	*range (ppm)*	*std. dev. (ppm)*	*(c) (ppm)*	*(d) (ppm)*	*(e) (ppm)*	*(f) (ppm)*
Cr	97	(210-25)	68	25	(60- 5)	19	275	75	40	10
Co	28	(75- 5)	18	6	(20- 5)	4	15	40	5	15
Ni	199	(620-10)	166	15	(70- 5)	14	85	335	15	70
Cu	21	(110- 5)	26	6	(45- 5)	2	30	5	5	5
Zn	52	(170-10)	39	14	(70- 5)	15	30	110	5	70
Zr	246	(440-50)	73	353	(930-140)	226	270	210	400	220
Nb	83	(600- 5)	99	22	(130- 3)	24	120	50	15	80
Ba	293	(1 100-95)	205	249	(690- 95)	170	570	180	200	690
La	88	(620-25)	100	36	(100- 20)	21	110	60	45	45
Ce	164	(1 000-60)	160	78	(220- 30)	44	200	120	80	75
Pb	19	(220- 5)	39	10	(95- 5)	18	30	5	5	5

(a) Sample contains 33 items. (b) Sample contains 24 items. (c) (d) Pteropus Breccia; PDH 5 (18-19m); PDH 26 (28-29m). (e) (f) Warton Sandstone; PDH 18 (4-4.6m); PDH 3 (13-14m). After Shaw and others, 1985.

TABLE 14. CONCENTRATE MINERALS AND THEIR ABUNDANCE IN KIMBERLITES FROM THE NORTH KIMBERLEY PROVINCE

Kimberlite	*Pyrope*	*Picroilmenite*	*Cpx*	*Opx*	*Spinel*	*Zircon*	*Rutile*	*Diamond*
Skerring	A	A	M	—	T	T	—	—
Wishywashy	M	A	—	—	M	—	—	(T)
Hadfields	A	A	—	—	T	T	—	—
KGB2	—	A	—	—	M	—	A	—
Jump-up	—	A	—	—	—	—	—	—
Pteropus	T	T	—	—	M	M	—	(T)

Cpx = clinopyroxene, Opx = orthopyroxene, A = abundant, M = minor, T = trace, (T) = one stone.

Extensive pitting and drilling has only been carried out to date at the Skerring and Pteropus pipes, which are, therefore, the best known of the North Kimberley Province kimberlites.

SKERRING PIPE

The heavy-mineral concentrates of the Skerring kimberlite are dominated by picroilmenite and garnet in almost equal proportions, and contain minor amounts of diopside, chromite, zircon, and rutile. Orthopyroxene is noticeably absent. No diamond was recovered during bulk-sampling operations in which 55 m^3 of kimberlite was excavated and processed through a heavy-media separation plant (Muggeridge and others, 1978).

Picroilmenite

Magnesium-rich ilmenite occurs as large, rounded macrocrysts up to 9 cm across, and as graphic intergrowths with silica (Atkinson and others, 1984a). When fractured, the internal texture of the macrocrysts varies from those showing smooth, glossy, conchoidal fractures to those having a granular mosaic internal texture. Representative analyses are given in Table 15: MgO values are typically 8-10%, and Fe_2O_3 is generally less than 10%. The edges are zoned towards a slight increase in FeO and MnO (which usually totals $<0.5\%$). Fig. 15 shows that, on an $MgTiO_3$-$FeTiO_3$-Fe_2O_3 plot, the ilmenite compositions fall within, or are marginal to, the kimberlite field of Mitchell (1977).

TABLE 15. REPRESENTATIVE ANALYSES OF ILMENITES FROM THE SKERRING PIPE

	Macrocrysts						*I-S nodule*	
	1	*2*	*3*	*4*	*5*	*6*	*7c*	*8r*
	(%)	*(%)*	*(%)*	*(%)*	*(%)*	*(%)*	*(%)*	*(%)*
SiO_2	nd	nd	nd	nd	nd	nd	0.25	0.35
TiO_2	52.97	51.22	51.55	50.26	49.26	47.18	53.59	50.99
Al_2O_3	0.70	0.64	0.64	0.70	nd	nd	0.83	0.62
V_2O_3	nd	0.35	0.30	nd	0.41	nd	nd	nd
Cr_2O_3	0.25	0.16	0.27	0.26	0.15	0.31	0.33	0.32
Fe_2O_3	6.89	9.45	7.96	9.91	11.90	16.54	5.23	2.51
FeO	28.40	28.07	30.15	30.22	30.55	31.12	28.49	39.60
MnO	nd	nd	nd	0.24	nd	nd	0.17	4.34
MgO	10.80	10.10	9.10	8.40	7.72	5.80	11.12	1.28
Total	**100.01**	**99.99**	**99.97**	**99.99**	**99.99**	**99.95**	**100.01**	**100.01**

Fe determined as FeO and calculated to Fe_2O_3 and FeO from stoichiometry. nd = not detected, detection limit = 0.1 - 0.2 wt%. I-S nodule = ilmenite-silica graphic intergrowths in nodules.

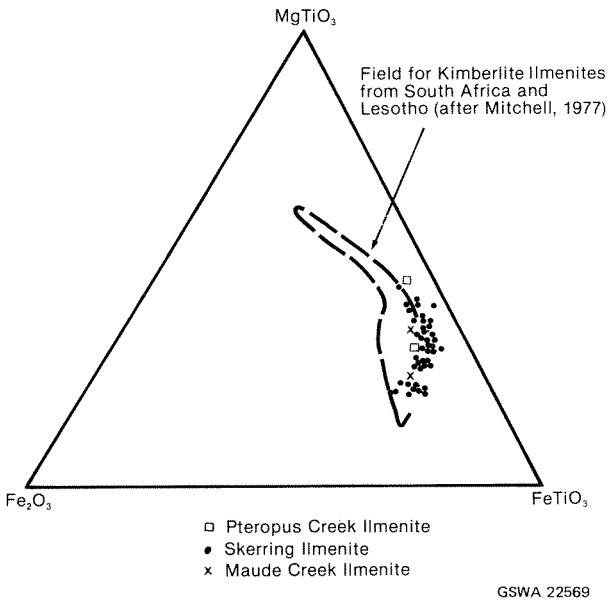


Figure 15. $MgTiO_3$-$FeTiO_3$-Fe_2O_3 plot for ilmenite macrocrysts from North and East Kimberley kimberlites.

Ilmenite from the graphic intergrowths with quartz shows higher contents of FeO and MnO; the latter ranges up to 4.34%. Representative analyses are given in Table 15. The appearance of these intergrowths (Fig. 16) is similar to ilmenite-silicate nodules described from South Africa and elsewhere (Boyd and Nixon, 1973; Gurney and others, 1973). The quartz presumably replaces clinopyroxene.

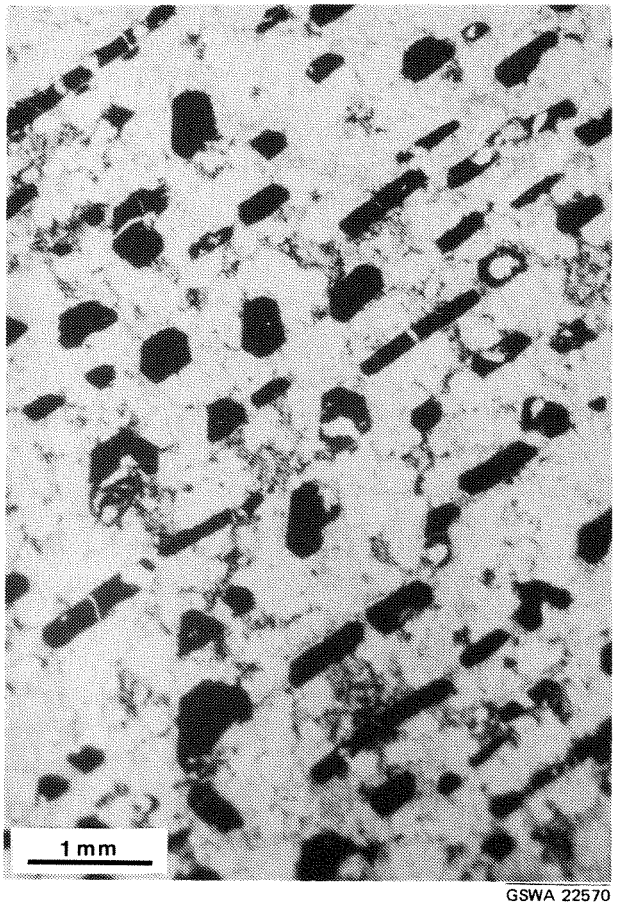


Figure 16. Ilmenite-silica graphic intergrowth, Skerring Pipe (Photo: CRAE).

Garnet

A variety of garnets occurs in the Skerring concentrates as illustrated in the MgO-FeO-CaO plot (Fig. 17), which also shows fields for the garnet cluster groups of Dawson and Stephens (1975). Garnets range up to 2 cm or more in size. Representative analyses are given in Table 16.

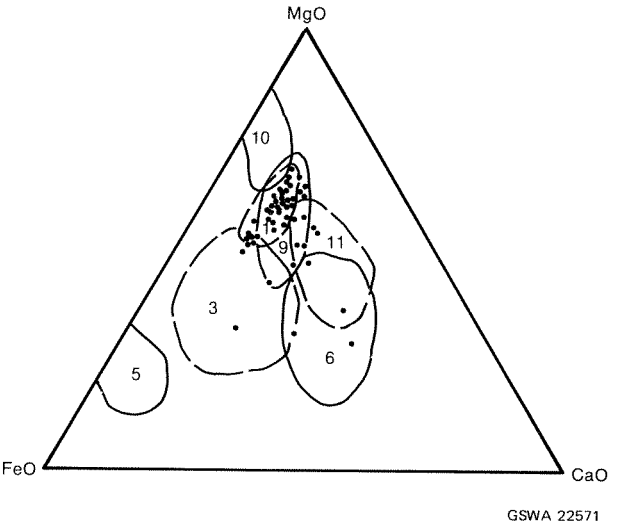


Figure 17. MgO-FeO-CaO plot of garnet macrocrysts from the Skerring Pipe, with fields for cluster groups after Dawson and Stephens (1975).

Almost one-half of the garnets are low-chrome pyrope (Dawson and Stephens, Group 9); about one-quarter are red or reddish-orange titanian pyrope (Group 1); and occasional Group 2, 3, 6 and 11 garnets also occur. Garnets of eclogitic nature and garnets of possible crustal origin are not common in the Skerring Pipe.

Low-calcium chrome pyropes belonging to the Dawson and Stephens Group 10 have not been found at Skerring. However, a CaO *versus* Cr_2O_3 plot (Fig. 18) of all the garnets analyzed from this pipe (n = 85) shows that five garnets fall within Gurney's (1984) high-chrome, low-calcium field for "G10" chrome pyropes from diamond inclusions and diamond-bearing kimberlites from southern Africa.

Gurney (1984) has shown that the distribution of "G10" garnets in southern Africa is confined to the long stabilized Kaap-Vaal and Rhodesian cratons. The Skerring "G10" garnets therefore suggest that the north Kimberley is underlain by old cratonic basement. The lack of diamonds in the Skerring Pipe, however, suggests that the view of Gurney, that the presence of "G10" garnets is an indicator of the presence of diamond, may not necessarily hold for all instances, particularly outside southern Africa.

Clinopyroxene

Bright-green to grey-green clinopyoxenes of predominantly blocky to elongate shape are the dominant pyroxene. Almost all are sub-calcic diopsides (cluster group 1 of Stephens and Dawson, 1977) and have Ca/(Ca + Mg) values of 0.31-0.35 (Fig. 19); 100 Mg/(Mg + Fe) values are typically 87-90; TiO_2 values average 0.32%, and the Cr_2O_3 content averages 0.59%. Representative analyses are given Table 17. This main

TABLE 16. REPRESENTATIVE ANALYSES OF GARNET MACROCRYSTS FROM SKERRING PIPE

	1	2	3	4	5	6	7	8	9	10	11	12
						Percent						
SiO_2	41.98	43.32	41.35	42.74	42.62	42.02	42.16	42.17	41.50	41.90	40.67	40.12
TiO_2	nd	0.88	0.41	0.93	0.13	nd	0.87	nd	0.17	0.45	0.62	0.22
Al_2O_3	14.84	21.92	13.25	22.13	22.10	18.81	20.33	22.86	23.35	22.60	22.35	22.96
Cr_2O_3	12.00	1.67	12.86	1.65	3.08	6.64	3.25	2.33	0.22	0.14	0.16	0.14
FeO	5.73	6.41	6.16	6.73	7.27	7.00	7.65	8.11	8.51	12.70	12.86	16.97
MnO	0.42	0.15	0.44	0.33	0.34	0.48	0.33	0.42	0.15	0.49	0.31	0.49
MgO	20.99	21.16	19.96	20.89	19.40	18.37	20.00	19.59	12.72	17.23	11.43	11.62
CaO	4.24	4.47	5.56	4.59	5.08	6.68	5.00	4.52	13.38	4.48	11.29	7.42
Total	**100.20**	**99.98**	**99.99**	**99.99**	**100.02**	**100.00**	**99.57**	**100.00**	**100.00**	**99.99**	**99.69**	**99.94**
Mg(a)	86.7	85.5	85.2	84.7	82.6	82.4	82.4	81.1	72.7	70.07	61.3	55.0
						Ratio						
Ca(b)	0.112	0.115	0.146	0.188	0.135	0.177	0.129	0.119	0.355	0.117	0.303	0.201
Mg(b)	0.770	0.757	0.728	0.747	0.715	0.678	0.717	0.715	0.469	0.625	0.427	0.439
Fe(b)	0.118	0.129	0.126	0.135	0.166	0.145	0.154	0.166	0.176	0.258	0.270	0.360
Group	**10?**	**1**	**11**	**2**	**9**	**9**	**1**	**9**	**6**	**3**	**4**	**3**

(a) Mg = 100 Mg/(Mg + Fe). (b) Ca = Ca/(Mg + Ca + Fe), Mg = Mg/(Mg + Ca + Fe), Fe = Fe/(Mg + Ca + Fe)

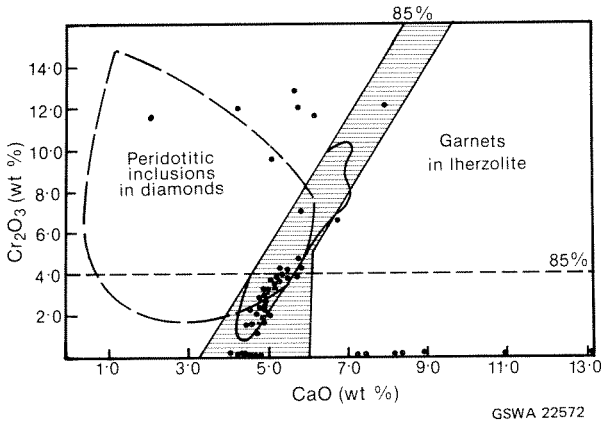


Figure 18. CaO *versus* Cr_2O_3 plot for macrocryst garnets from the Skerring Pipe. Field of lherzolitic garnets (Sobolev and others, 1973) shown as hatched area. Field enclosed by solid line refers to calcium saturated garnets from Finsch peridotites (Shee and others, 1982), and area labelled "peridotitic inclusions in diamond" is from Gurney (1984). The diagonal line designated 85% discriminates Ca-poor (G10) garnets from Ca-saturated (G9) garnets lying on the Ca-rich side of the line; 85% of garnet inclusions in diamonds plot above or to the left of the two lines marked 85% (Gurney, 1984).

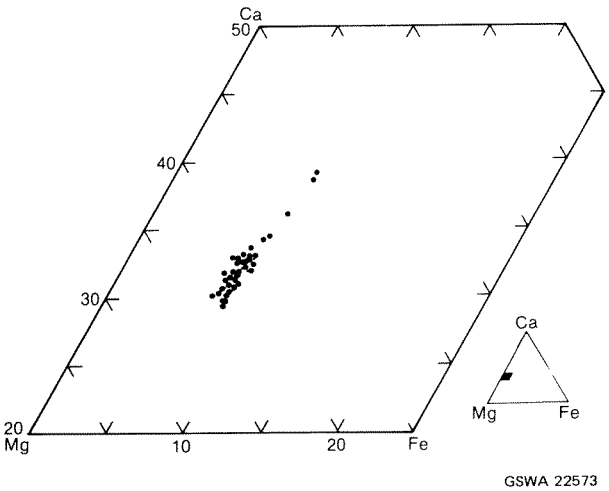


Figure 19. Ca-Mg-Fe plot for pyroxenes from Skerring Pipe.

TABLE 17. REPRESENTATIVE ANALYSES OF CLINOPYROXENES FROM THE SKERRING PIPE

	1	2	3	4	5
			Percent		
SiO_2	55.41	55.26	55.35	55.06	55.09
TiO_2	0.16	0.13	0.27	0.20	0.35
Al_2O_3	1.92	1.96	1.84	2.26	1.99
Cr_2O_3	0.87	0.76	0.44	0.47	0.40
FeO	4.83	4.90	5.11	5.16	5.50
MgO	21.10	20.54	19.92	19.68	18.89
CaO	14.33	15.55	16.06	15.99	16.80
Na_2O	1.00	0.91	0.91	1.07	0.97
Total	**99.62**	**100.01**	**99.90**	**98.89**	**99.99**
Mg(a)	88.6	88.2	87.4	87.2	86.0
			Ratio		
Ca(b)	0.302	0.324	0.336	0.337	0.355
Mg(b)	0.619	0.596	0.580	0.578	0.555
Fe(b)	0.079	0.080	0.084	0.085	0.091

(a) Mg = 100 Mg/(Mg + Fe). (b) Ca = Ca/(Mg + Ca + Fe), Mg = Mg/(Mg + Ca + Fe), Fe = Fe/(Mg + Ca + Fe).
All MnO below detection limit (<0.2 wt%).

group of subcalcic diopsides is similar in chemistry to the "sheared lherzolite" or "discrete nodule" pyroxenes from kimberlites in northern Lesotho (Nixon and Boyd, 1973).

Chromite

Small macrocrysts of spinel occur in the concentrates and vary from rounded anhedral forms to well-developed octahedral crystals. Representative analyses are given in Table 18 and spinel prism plots in Fig. 20. The spinels are magnesiochromites with variable Cr/(Cr + Al) ratios of 0.49-0.76, and more uniform 100 Mg/(Mg + Fe) ratios of 54-66. Titanium dioxide contents range from nil to 3% and Fe_2O_3 contents from 1-6%. Such chemistry is typical of kimberlitic macrocryst spinels.

Groundmass spinel from the massive green kimberlite ranges in composition from titaniferous chromite to chrome-bearing titaniferous magnetite (Table 19, and Figs. 20 and 21). This trend in spinel composition differs from that found by Mitchell (1985) to characterize

TABLE 18. REPRESENTATIVE ANALYSES OF MACROCRYST SPINELS FROM THE SKERRING PIPE

	1	*2*	*3c*	*4r*	*5*	*6*	*7*
				Percent			
SiO_2	0.61	0.62	0.60	0.17	0.32	0.42	0.26
TiO_2	0.21	0.20	0.21	3.23	nd	3.06	3.40
Al_2O_3	29.09	24.48	23.07	20.11	14.63	10.80	8.55
V_2O_3	nd	0.20	0.14	nd	0.16	0.30	nd
Cr_2O_3	34.30	39.21	40.89	38.74	53.05	51.91	55.71
Fe_2O_3	6.25	6.17	5.88	6.75	4.08	2.62	1.03
FeO	13.99	14.12	14.75	16.61	14.37	18.03	19.95
NiO	nd	0.24	nd	0.35	nd	0.32	nd
MnO	0.25	nd	0.34	nd	nd	0.34	nd
MgO	15.21	14.67	14.04	13.81	13.30	11.95	11.00
Total	**99.91**	**99.91**	**99.92**	**99.77**	**99.91**	**99.75**	**99.90**
				Ratio			
Mg(a)	0.660	0.649	0.629	0.597	0.623	0.541	0.496
Cr/R^{3+}(b)	0.411	0.481	0.505	0.515	0.674	0.736	0.802
Fe^{3+}/R^{3+}(b)	0.071	0.072	0.069	0.085	0.049	0.035	0.014

All Fe determined as FeO; and FeO and Fe_2O_3 calculated from stoichiometry. nd = not detected. Detection limits (EDS) are 0.1 - 0.2 wt%.
(a) Mg = $Mg/(Mg + Fe^{2+})$ (b) $R^{3+} = Cr + Al + Fe^{3+}$.

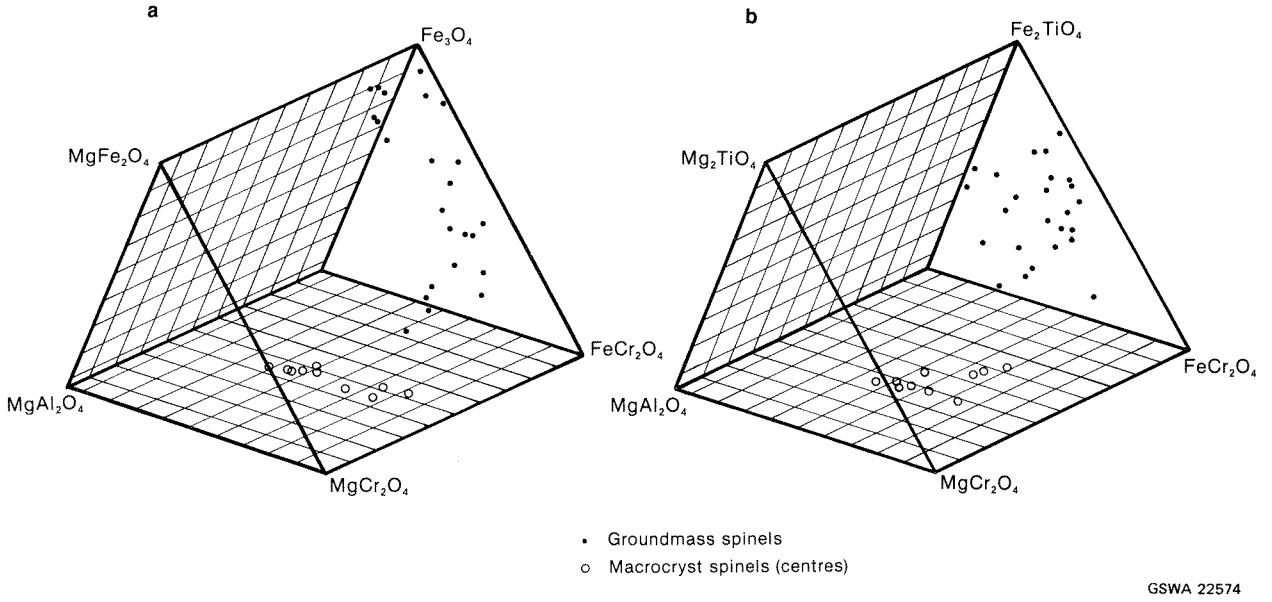


Figure 20. Spinel prism plots for spinels from Skerring Pipe.

kimberlite (Fig. 21) and suggests that the micaceous ultramafic rock of the Skerring Pipe might be classified as an ultrapotassic magnesian lamprophyre rather than a kimberlite under Mitchell's definition. It should be noted, however, that minerals characteristic of lamproite, such as leucite, potassic richterite, priderite, and wadeite, have not been found at the Skerring, or at any other kimberlitic intrusion of the North Kimberley Province.

Zircon

Occasional, pale, buff-coloured, rounded, and blocky zircon megacrysts have been recovered. The uranium content of the zircon has been determined as 5 ppm (Pidgeon and Smith, in prep.), which is amongst the lowest values recorded for kimberlitic zircon.

WISHYWASHY, HADFIELDS, AND JUMP UP DYKES

Concentrates from these bodies appear generally similar to the Skerring and are dominated by picro-ilmenite and to a lesser extent by chrome pyrope and titanian pyrope garnets, the composition of which is similar to those analyzed from the Skerring Pipe (*see* Table 16). The apparent lack of pyroxene is due to concentrates having been largely obtained from surface loams, and extremely weathered rock in shallow

TABLE 19. REPRESENTATIVE ANALYSES OF GROUNDMASS OXIDES IN THE SKERRING PIPE

	1	2	3	4	5	6	7	8
					Percent			
SiO_2	0.06	nd	nd	0.05	0.08	nd	nd	0.04
TiO_2	10.23	9.95	9.54	9.97	11.32	3.08	4.26	53.00
Al_2O_3	5.49	10.18	6.79	4.93	4.92	6.07	2.24	nd
V_2O_3	0.24	0.35	0.15	0.18	0.14	nd	0.33	nd
Cr_2O_3	38.55	33.69	31.72	32.73	29.64	5.34	2.15	0.08
FeO(a)	34.22	35.51	41.95	42.84	46.70	75.85	80.62	26.00
MnO	0.83	1.25	2.12	2.25	4.40	0.53	0.53	11.16
NiO	0.14	nd	nd	0.18	0.17	nd	nd	nd
MgO	9.92	8.15	6.23	5.67	0.75	2.92	3.40	0.05
CaO	0.03	nd	nd	0.03	0.02	nd	nd	0.04
ZnO	—	nd	nd	—	—	0.75	0.60	—
Total	**99.71**	**99.08**	**98.50**	**98.83**	**98.13**	**94.54**	**94.13**	**100.36**
Fe_2O_3(a)	9.02	7.52	13.60	13.64	10.80	51.88	57.29	
FeO(a)	26.10	28.75	29.72	30.57	36.98	29.17	29.07	
Total(a)	**100.61**	**99.84**	**99.87**	**100.20**	**99.20**	**99.74**	**99.87**	
					Ratio			
Mg(b)	0.404	0.336	0.272	0.248	0.035	0.151	0.173	
Cr/R^{3+}(c)	0.697	0.601	0.579	0.617	0.627	0.084	0.036	
Fe^{3+}/R^{3+}(c)	0.155	0.128	0.236	0.245	0.217	0.774	0.909	

(a) All Fe determined as FeO; Fe_2O_3 and FeO calculated from stoichiometry. (b) Mg = $Mg/(Mg + Fe^{2+})$. (c) R^{3+} = Cr + Al + Fe^{3+}
nd = not detected, detection limit = 0.1 - 0.2 wt%.
1,3,4,5 — Titaniferous chromite. 2 — Titaniferous aluminous chromite. 6, 7 — Titaniferous chrome-bearing magnetite.
8 — Manganiferous ilmenite.

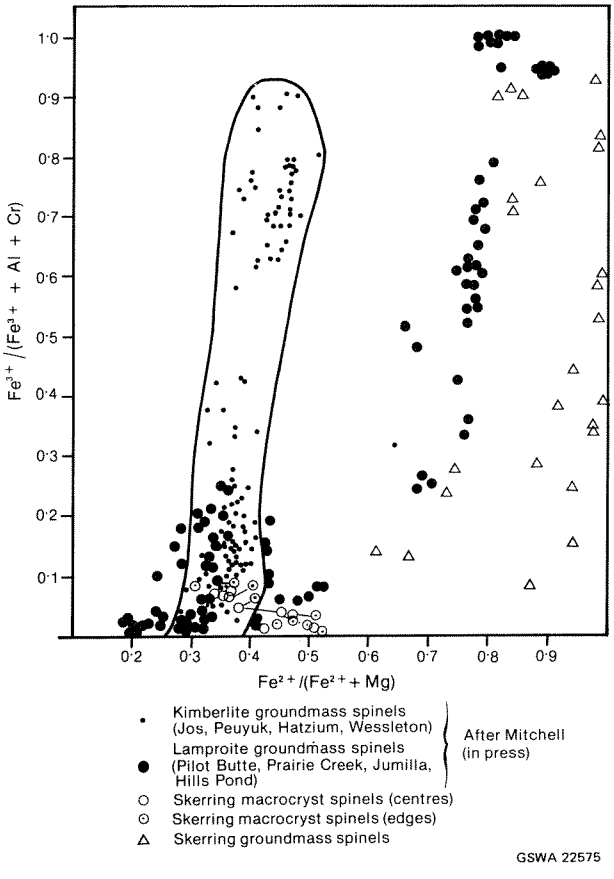


Figure 21. Plot of the Fe^{2+}/Mg face of the oxidized spinel prism for spinels from Skerring Pipe.

costeans. It is probable that pyroxene was present, but has been destroyed by weathering processes.

KGB2 DYKE

This dyke contains concentrates dominated by large blocky to rounded grains of rutile and ilmenite, together with minor amounts of spinel. Garnet appears to be absent. Ilmenite and chromite compositions are similar to those from the Skerring and Pteropus pipes. The rutile contains minor amounts of Nb and Cr.

PTEROPUS BRECCIA PIPE

Chromite is the most abundant mineral in Pteropus concentrates and spans a broad range in chemical compositions: the Cr/(Cr + Al) ratios are 0.37-0.97, and the 100 Mg/(Mg + Fe) ratios are 16-71. TiO_2 contents range from 1-5%, and Fe_2O_3 from 0.12%. The chromites are typical of kimberlitic macrocryst spinels.

Ilmenites are similar to those from Skerring in composition, but range up to slightly higher MgO contents (Fig. 15).

Garnets recorded from Pteropus are predominantly low- chrome pyropes, Group 9 of Dawson and Stephens (1975).

Zircon occurs as pale-coloured, buff and faintly pink blocky grains with a low uranium content; two analyzed grains have values of 9.5 and 16.1 ppm U. The ratio of zircon to chromite in drill core material is 1:5 (Shaw and others, 1985).

CHAPTER 4

THE EAST KIMBERLEY PROVINCE

Nine occurrences of kimberlite, lamproite, and related rocks, have been located in the East Kimberley area (Fig. 22). The largest body, the Argyle Pipe (AK 1) of 50 ha surface area, is richly diamondiferous and, together with associated alluvial deposits, is the site of the only operating diamond mine in Australia (Atkinson and others, 1984a,b,c).

The East Kimberley Province covers part of the Halls Creek Mobile Zone and the eastern edge of the Kimberley Plateau. The plateau occurrences are in the Durack Ranges, which form the folded and faulted margin to the Kimberley Basin immediately west of the Greenvale Fault System, which marks the western boundary of the Halls Creek Mobile Zone. The four occurrences in the Durack Ranges: Maude Creek, Duck Creek, Blackfellow Creek, and Devils Elbow, are kimberlite dykes. Argyle Pipe, Seagull's Dyke, and Lissadell Road Dyke, are lamproites intruded into the mobile zone close to its eastern margin, and the Bow Hill Dyke is a micaceous, andradite-bearing "lamprophyre" intruded towards the centre of the mobile zone. No true kimberlites are known within the mobile zone.

Six of the occurrences either outcrop or have been

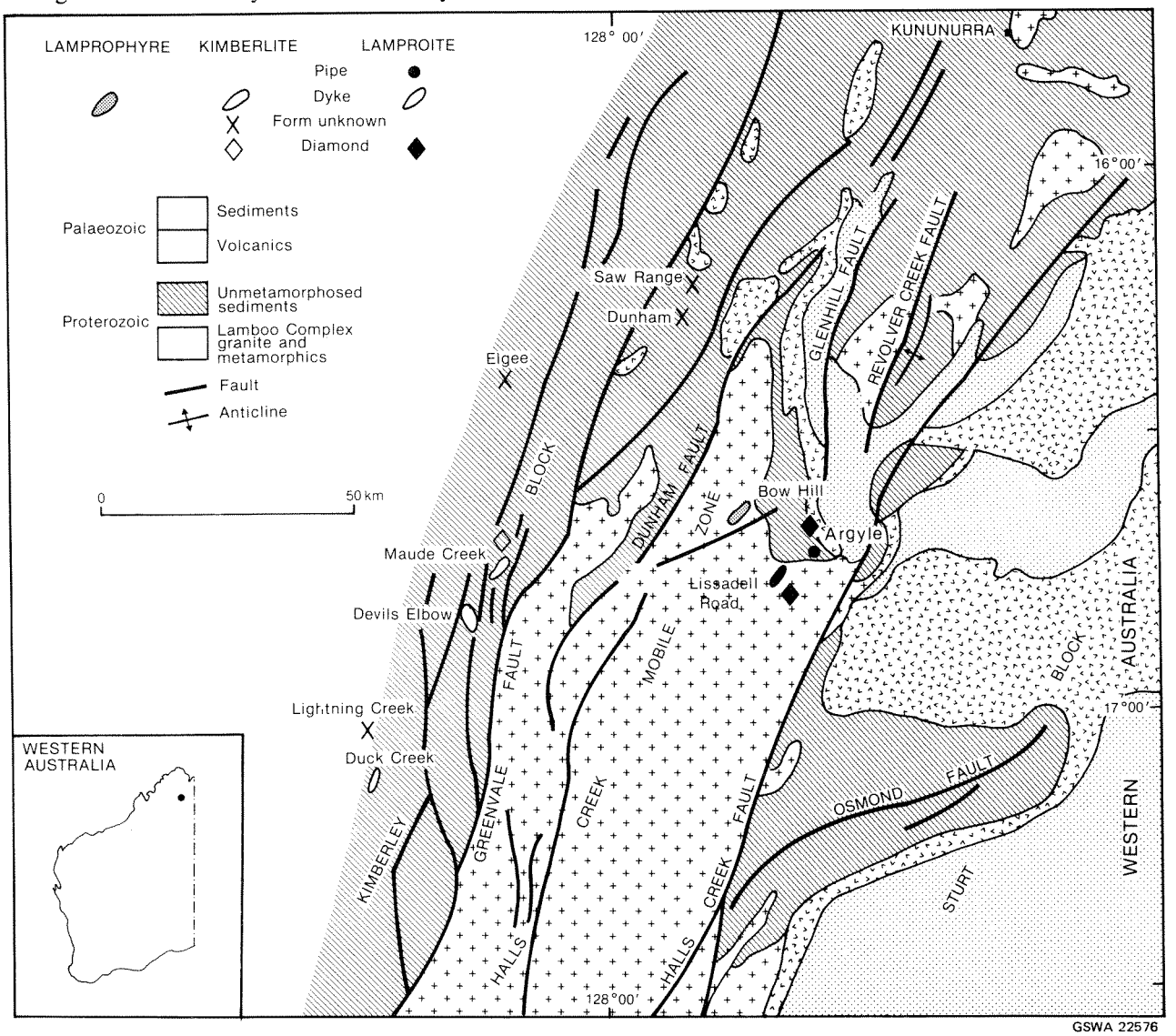


Figure 22. Location of kimberlites and lamproites in the East Kimberley Province.

exposed by pitting or drilling during diamond prospecting operations. The remaining three are dykes whose exact position has been established by detailed heavy-mineral loam sampling and geophysical techniques, but they have no outcrop and have not been exposed by pitting. Dispersion patterns of kimberlite indicator minerals in stream drainages show that many additional occurrences of kimberlite or related rocks are present in the Durack Ranges, although their precise location is still unknown.

Physiographically the area is very varied, and there is a strong relationship between topography and bedrock (Plumb, 1968). In the west, the Durack Ranges and the Kimberley foothills bordering the Kimberley Plateau form a rugged topography of north-northwest-trending hogbacks and cuestas of resistant sandstone that rise 200-300 m above narrow valleys eroded in less resistant sediments and dolerite sills. In the east, the sediments of the Carr Boyd and Ragged Ranges form similarly rugged topography with relief of up to 450 m, dissected by narrow valleys and gorges. In the central part of the mobile zone, the Bow River Hills are of relatively low relief and are developed on granitic rocks of the Lamboo Complex.

The region has a tropical savannah climate with an average annual rainfall between 500 mm and 750 mm. The rain is monsoonal and largely confined to a short summer wet season between December and March. Vegetation on the thin rocky soil of most of the region is spinifex grass and occasional stunted eucalypts. In thicker alluvial soils, other coarse perennial grasses are present together with isolated large specimens of the boab tree. Watercourses generally support denser stands of larger trees; and, in some gorges, pandanus and other palms are present.

Access to the region is from the Great Northern Highway, which traverses the area from north to south. Off the main road, station tracks of variable quality give reasonable access to most areas, but in the Durack Ranges long detours are often necessary to cross strike ridges, and large areas of the Kimberley Plateau and Carr Boyd Ranges are trackless. All tracks are impassable during the wet season and many washouts remain unrepaired. For ease of access, most exploration activity in the region is conducted with helicopter support. The Argyle Pipe is approached by an all-weather road from the Great Northern Highway but access to the mine site and the country around is restricted and must be negotiated before arrival.

REGIONAL GEOLOGY AND STRUCTURE

Kimberlite and lamproite volcanism in the East Kimberley Province is related to the Halls Creek Mobile Zone, a 400 km-long north-northeast-trending belt of deformed Precambrian metamorphic, igneous, and sedimentary rocks, overlain in part by a younger platform cover of Palaeozoic sediments and volcanics. The mobile zone separates the older cratons of the Sturt Block and the Kimberley Block and is about 60 km wide and bounded by two major faults, the Halls Creek Fault to the east and the Greenvale Fault to the west. The regional geology has been described in detail in a series of explanatory notes to 1:250 000 geological maps (Lissadell — Plumb, 1968; Dixon Range — Dow and Gemuts, 1967) and in memoirs by Dow and Gemuts (1969) and Gemuts (1971).

The oldest rocks in the mobile zone are the Halls Creek Group consisting of greywackes, slate, schist, and minor basalt flows of probable Lower Proterozoic age ($\approx$ 2 200 Ma, Page, 1976). These were metamorphosed at about 1 920 $\pm$ 30 Ma to form the Tickalara Metamorphics and intruded by pre- or syntectonic granites and gabbros. Following uplift and erosion, the Whitewater Volcanics were deposited and intruded by post-tectonic granites about 1 834 $\pm$ 32 Ma old, principally the Bow River Granite, a linear batholith 300 km long and up to 30 km wide which occupies much of the central area of the mobile zone. Further uplift and erosion was followed, at the end of the Early Proterozoic, by deposition of the Revolver Creek Formation in the mobile zone and its lateral equivalent over the Kimberley Block to the west (Dow and Gemuts, 1969). Minor tectonism and sedimentation continued into the Upper Proterozoic with the deposition and folding of the Carr Boyd Group, to be followed by the widespread deposition of Lower Cambrian to Devonian volcanics and sediments over much of the Sturt Block to the east and parts of the mobile zone.

In the area covered by the East Kimberley Province (Lissadell and parts of Dixon Range map sheets), the eastern third of the Halls Creek Mobile Zone consists of a belt 20 km wide containing Tickalara Metamorphics intruded by small pods of pre- and syntectonic Mabel Downs Granodiorite and MacIntosh Gabbro. The remainder of the mobile zone consists of Bow River Granite, containing large inclusions of MacIntosh Gabbro, and elongate, fault-bounded inliers of Whitewater Volcanics and Castlereagh Hill Porphyry. All the lower units are unconformably overlain in the northern part of the area by folded and faulted sediments of the Revolver Creek Formation and Carr Boyd Group.

West of the Greenvale Fault, the Kimberley Group sediments covering the Kimberley Block are flat-lying or only slightly deformed. The margin of the block, however, is dominated by splay faults of the Greenvale Fault which give rise to wedges of steeply dipping Speewah Group sediments and, in the area of the Speewah Valley, a large domical structure (Plumb, 1968).

The structure and evolution of the Halls Creek Mobile Zone has been explained by Hancock and Rutland (1984) in terms of successive extension and compression during Proterozoic times. They propose that the Halls Creek and Greenvale Faults are major geosutures, which, in the early Proterozoic, localized lithospheric stretching in the area of the present mobile zone. A basin resulted, and this was fed by sediments derived from a stable Kimberley island-continent block.

During subsequent convergence between the Kimberley and Sturt Blocks, the sediments were deformed and metamorphosed, and syn- and post-tectonic granites were emplaced. The main pressure during convergence was directed from a few degrees west of north with the result that the major boundary faults show extensive sinistral strike-slip movement; and, within the mobile zone, there are a number of northeast trending *en echelon* shears such as the Bow River Fault. Limited subduction of the thin lithospheric basement beneath the Kimberley Block (A-subduction) also took place.

The location of kimberlite and lamproite intrusions appears to be strongly controlled by the structure of the Halls Creek Mobile Zone, particularly the faulting. Kimberlitic dykes in the Durack Ranges, on the eastern margin of the Kimberley Block, are located in the zone of splay faults from the Greenvale Fault. As this fault dips beneath the Kimberley Block at depth (Hancock and Rutland 1984), the dykes are probably directly related to the major western boundary fault of the mobile zone. To the east, the Argyle Pipe is located about 6 km west of the Halls Creek Fault. Major sinistral displacement on the boundary fault has caused the southern end of the Matsu Range to be strongly folded and faulted in the area of the Argyle Pipe, which is also close to the extension, beneath a Palaeozoic cover, of the Glenhill Fault. The Bow Hill Dykes are intimately related to the Bow River Fault, a shear zone up to 100 m wide that trends east-northeast across the mobile zone. The dykes form a small swarm, which splays with increasing northerly trend from the Bow River Fault to almost join a north-northeast trending fault parallel to the trend of the mobile zone (Fig. 39).

AGE OF INTRUSION

No radiometric dating has been made on the kimberlitic dykes in the western part of the area because of the lack of availability of suitable material. Outcrop and near-surface samples are heavily weathered, and drill-core material is extensively altered. Six of the dykes are highly micaceous kimberlite dykes, resembling those of the North Kimberley Province, and similarly intrude Proterozoic rocks of the Kimberley Group. Accordingly, these dykes may be of a similar Late Proterozoic age, ≈ 800 Ma (*see* Chapter 3).

The Lissadell Road dykes are lamproitic, similar to the Argyle pipe, and likely to be of similar age. The Argyle pipe intrudes the Carr Boyd Group, of Upper Proterozoic age, including the Lissadell Formation for which an age of approximately 1 100 Ma is indicated by the dating of the overlying Glenhill Formation at $1\,057 \pm 80$ Ma and the underlying Golden Gate Siltstone at 1158 ± 23 Ma (Bofinger, 1967).

The Argyle pipe has been dated by the Rb-Sr whole-rock method, and model ages have been determined on micas by the Rb-Sr and K-Ar methods (Pidgeon and Smith, in prep.). The results are tabulated in Table 20 and range between 1 253 Ma and 1 048 Ma. The implication of these results is that the lamproite was emplaced close to the age of deposition of the Proterozoic country rock. This is in agreement with the geological evidence (Boxer and others, in prep.) that the Argyle pipe was intruded into unconsolidated sediments.

TABLE 20. Rb-Sr and K-Ar AGES OF THE ARGYLE PIPE

Method	*Material dated*	*Age*
Rb-Sr (whole rock)	Lamproite tuff with abundant country rock clasts.	$1\,100 \pm 300$ Ma
Rb-Sr (whole rock)	Magmatic lamproite	$1\,045 \pm 160$ Ma
Rb-Sr (model ages)	Mica	1 048 Ma, for $R_i = 0.710$ 1 231 Ma, for $R_i = 0.705$
K-Ar	Mica	$1\,253 \pm 26$ Ma

After Pidgeon and others, in prep.

The Bow Hill lamprophyre dykes cut the Bow River Granite, dated at $1\,834 \pm 32$ Ma (Bofinger, 1967). The dykes are micaceous and the micas have been dated by the Rb-Sr and K-Ar methods (Pidgeon and Smith, in prep.). The results given in Table 21 show a wide scatter, but an approximate age of 800 Ma seems the most likely from these results. Two observations are warranted; firstly, the East Kimberley Province contains at least two periods of intrusion, and in this respect differs from other provinces in Western Australia. Secondly, the age of the Bow Hill Dykes, at about 800 Ma, is probably similar to that of the North Kimberley kimberlites (Chapter 3).

TABLE 21. Rb-Sr AND K-Ar AGES OF THE BOW HILL DYKES. DYKES.

Method	*Age*
Rb-Sr (model ages)	568 Ma, for $R = 0.7166$ 752-819 Ma, for $R_i = 0.710$
K-Ar	804 ± 5 Ma to 826 ±4 Ma

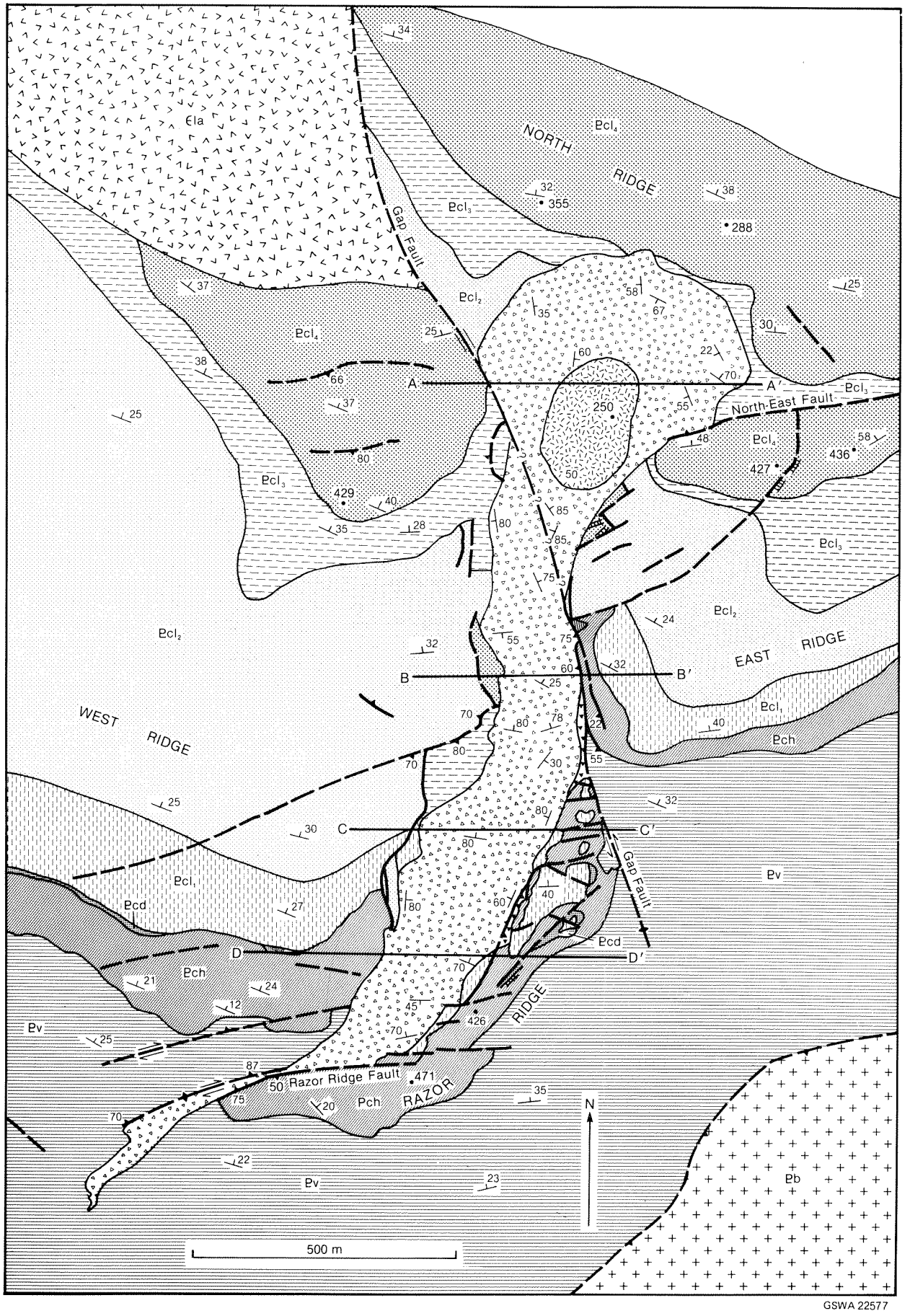
After Pidgeon and others, in prep.

THE ARGYLE PIPE (AK 1)

The Argyle diatreme is located in a small valley near the eastern end of the Matsu Range, in the headwaters of Smoke Creek (BOW, GR:347527). The pipe was discovered in October 1979 by tracing diamonds found in the alluvial gravels of Smoke Creek to their source (Atkinson and others, 1984b). Small exposures of bedded tuff were found at the northern end of the pipe, which was otherwise concealed beneath a thin cover of soil and scree from the surrounding hills that rise sharply up to 300 m above the valley floor. The pipe is named after the nearby Lake Argyle and was originally given the acronym AK 1, for Argyle Kimberlite No. 1. However, no other large kimberlitic bodies have been discovered in the area and the pipe is now recognized to be lamproitic rather than kimberlitic. The pipe is now known as the Argyle Pipe and the diamond mine established on it is the Argyle Mine.

LOCAL STRATIGRAPHY

The oldest rocks in the vicinity of the Argyle Pipe are the igneous and metamorphic rocks of the Lamboo Complex, which are poorly exposed about a kilometre


NORTH RIDGE
EAST RIDGE
WEST RIDGE
RAZOR RIDGE
Gap Fault
North-East Fault
Razor Ridge Fault
A
A′
B
B′
C
C′
D
D′
N
500 m
GSWA 22577

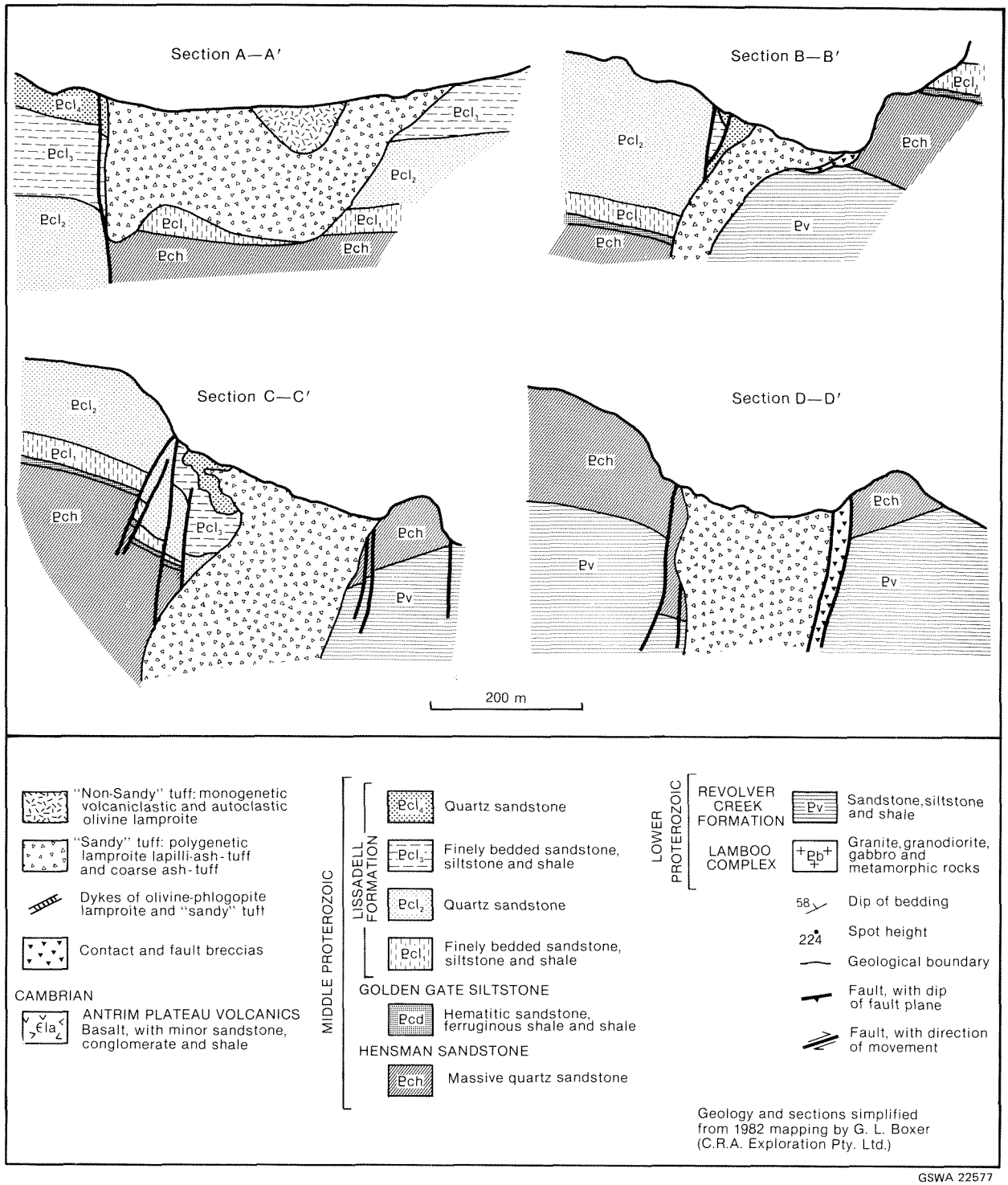


Figure 23. Geological map and cross sections of the Argyle Pipe.

south of the pipe. In this area, the Lamboo Complex is faulted against the Lower Proterozoic Revolver Creek Formation; but, to the east, the sediments unconformably overlie the crystalline rocks. The Revolver Creek Formation consists of a basal unit of amygdaloidal basalt overlain by an alternating sequence of sandstone, siltstone, and shale; it outcrops south and west of the Argyle Pipe and forms the base of the Matsu Range (Fig. 1). Unconformably overlying the Revolver Creek Formation, and forming the main ridge of the Matsu Range, is the Carr Boyd Group of Upper Proterozoic age. In the vicinity of the Argyle Pipe, the Carr Boyd Group comprises the Hensman Sandstone, the Golden Gate Siltstone, and the Lissadell Formation. The Hensman Sandstone is a massive silicified quartz sandstone which is overlain by shales and siltstone of the Golden Gate Siltstone, dated at 1 184 ± 123 Ma (Bofinger, 1967). To the west of Argyle, the Golden Gate Siltstone has a basal unit of sandy hematite (the Pompey's Pillar iron ore deposit) and ferruginous sandstone. There is an unconformity at the base of the Lissadell Formation, which consists of alternating shale and siltstone, and massive quartz sandstone units.

To the east of the Argyle Pipe, the Carr Boyd Group is unconformably overlain by the Lower Cambrian Antrim Plateau Volcanics and the Ragged Range

Conglomerate Member of the Upper Devonian Cockatoo Formation.

To the west of the Argyle Pipe, the sedimentary sequence dips to the north at about 30°; but, east of the pipe, the sediments have been deformed by sinistral movement on the Halls Creek Fault 5 km to the east. The drag produced by this movement has deformed the rocks at the eastern end of the Matsu Range, causing isoclinal folding in the Carr Boyd Group and overturning of the Revolver Creek Formation. This deformation was pre-Devonian, as the Ragged Range Conglomerate unconformably overlies all earlier formations.

The Argyle diatreme itself was elongated during this deformation by sinistral movement along the Gap and Razor Ridge Faults (Fig. 23). Along the southwestern margin of the diatreme, the country rocks have been down-folded and faulted along faults trending sub-parallel to the pipe margin. Movement along these faults has caused successively higher stratigraphic units to be successively juxtaposed against the pipe so that the stratigraphy youngs inwards towards the diatreme contact.

GEOLOGY OF THE ARGYLE PIPE

Shape of the pipe

The Argyle diatreme is an elongate body 2 km long, varying in width from 500 m to 150 m, with a surface area of 50 ha (Atkinson and others, 1984a,b,c). The shape has been modified by faulting and by a tilt of 30° to the north, thus presenting an oblique slice through the diatreme at the present level of erosion. At depth the diatreme is variable in shape (Fig. 23).

At its northern end, the pipe is bowl shaped, and roughly circular with a maximum diameter of about 500 m and a depth to country rock of up to 230 m below surface.

This part of the pipe probably represents a vent, open at depth; but extensive drilling has failed to locate the conduit. The remainder of the diatreme is narrow and dyke-like, and dips steeply to the west.

Immediately south of the northern bowl, the pipe narrows to about 150 m wide and trends south for 500 m before turning south-southwest and widening to about 200 m for a further 750 m length to the southern termination of the main body of the pipe. In the narrowest section the body dips at about 50° west; but, in the southern section, the area now being mined, the eastern contact dips consistently at 75° west while the western "hanging wall" varies in dip from 60° west in the north to near vertical at the southern end. South of the Razor Ridge (Fig. 23) is a small dyke-like "tail" about 400 m long and 30 m wide. This pod, almost separated from the diatreme, is known as the Southern Extension. Drilling in the central and southern parts of the pipe, and in the Southern Extension, to depths up to 300 m below surface indicates that the body is open at depth throughout its length.



GSWA 22578

Figure 24. Slickensides in the Hensman Sandstone, eastern wall of the Argyle Pipe. Gap Fault is a sinistral reverse fault which displaces the northern part of the pipe to the north. At this point the fault plane dips 60°W and the slickensides plunge 15°N. (Photo: CRAE).

The present shape of the pipe is governed by post-emplacement faulting along two major faults, the Gap Fault and the Razor Ridge Fault, which subtend an angle of about 80° (Fig. 23). Southeast compression of the West Ridge block has given rise to sinistral strike-slip movement on the Gap Fault and dextral movement on the Razor Ridge Fault. Most obvious is the 250 m dextral displacement on the Razor Ridge Fault, which has almost detached the Southern Extension from the main body of the pipe. Much of the northern margin of the extension is faulted; the fault plane dips nearly vertically to the north. The Gap Fault dips from vertical to 60° west and has produced spectacular horizontal slickensides in the Hensman Sandstone which forms the western end of the East Ridge (Fig. 24). The fault is easily traced north of the pipe, and appears to intersect the pipe between the northern bowl and the southern dyke-like section with a sinistral displacement of about 200 m. Prior to faulting, the Argyle Pipe was a more regular dyke-like body with a rapidly diminishing "tail" at its southern end, and a broad expansion at its northern end.

Contact relations of the Argyle Pipe

At the present erosional level, the Argyle Pipe is in contact with lithologies of the Revolver Creek Formation and the Carr Boyd Group. Xenoliths of granitic and gabbroic rocks within the diatreme indicate that the pipe intruded through rocks of the Lamboo Complex, but no clasts of the Antrim Plateau volcanics or the Ragged Range Conglomerate have been identified within the diatreme.

The contacts of the diatreme with the surrounding rocks consist largely of faulted remnants of an original marginal breccia. In the northern part of the diatreme, where faulting has been less intense, a distinct contact breccia can be identified at the outer margin of the diatreme. This breccia is often very complex and variable in detail but consists of a mixture of brecciated and/or deformed country rocks in a matrix of quartz-rich lapilli ash-tuff (Fig. 29). The nature of the country-rock fragments indicates conditions varying from brittle fracture through plastic deformation to rare instances of textures indicative of almost liquefaction of the country-rock sandstone. This wide variation in the nature of the contact breccia is probably a reflection of the variable nature of the volcanic processes at work in the diatreme, the depth of formation of the breccia, and the competence of the country rocks.

Tuffisite dykes: Narrow dykes, usually less than one metre wide, of ferruginous quartzose lapilli-ash tuff intrude the country rock around the margins of the diatreme. These tuffisite dykes appear similar in texture to the matrix of the contact breccia and are probably contemporaneous. The largest dyke, Seagulls Dyke, is located about 1 km west of the Argyle Pipe; the dyke trends north-northeast and is 370 m long and about 20 m wide.

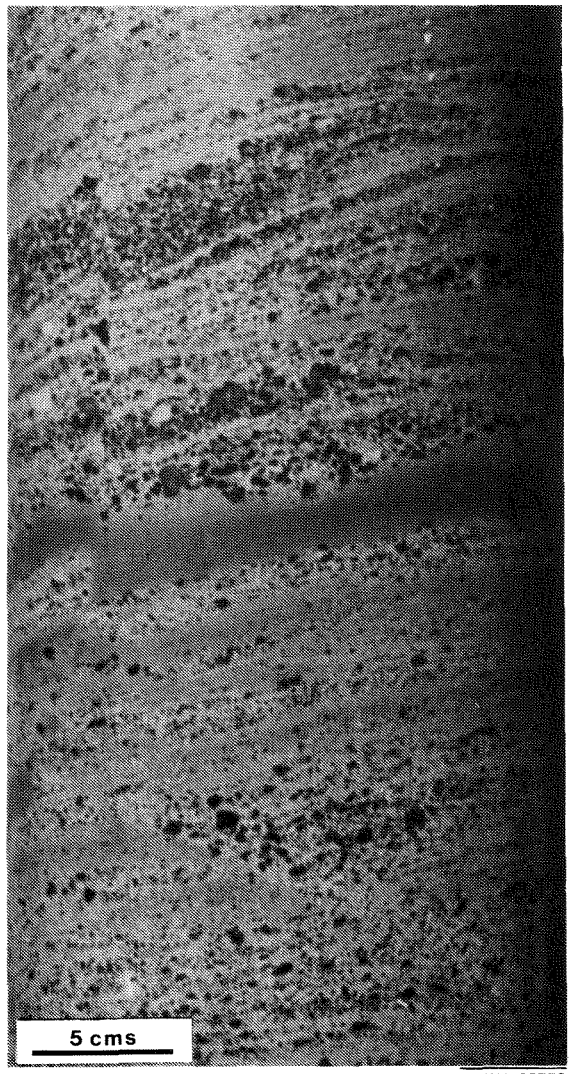
Diatreme lithologies

The Argyle diatreme comprises a faulted and disrupted sequence of varied pyroclastics and subordinate dykes of olivine lamproite (Atkinson and others, 1984a). The pyroclastics are divided into two major groups for which the mine terms "sandy" tuff (polygenetic, quartzose tuffs) and "non-sandy" tuff (monogenetic, non-quartzose) have been applied. The "sandy" tuffs predominate; the "non- sandy" tuffs are mainly confined to the northern and central areas of the diatreme (Atkinson and others, 1984b). The pyroclastic rocks are predominantly lapilli-ash-tuff and coarse ash-tuff, but there are lesser amounts of fine ash-tuff and rare pyroclastic breccia.

"Sandy" tuff: The "sandy" tuff is composed of juvenile lamproite and accidental clasts set in matrix of recrystallized lamproite ash and ash-sized quartz fragments derived from the country-rock sandstones (Atkinson and others, 1984a). The juvenile clasts range from light-coloured, irregularly shaped glassy types that are commonly vesicular, to dark coloured, blocky, dense, microcrystalline, porphyritic clasts. The matrix varies from dark to light grey: this reflects the proportion of lamproite ash to quartz in the matrix and the intensity of secondary alteration; the lightest colours indicate progressive alteration of finely disseminated anatase to leucoxene. Outcrop samples are typically reddish brown, and rich in hematite. The "sandy" tuffs are mostly massive or poorly bedded mass-flow deposits; this, combined with faulting and probable disruption in the diatreme during or immediately following eruption, makes it difficult to determine the internal stratigraphy.

Bed forms within the "sandy" tuff unit are massive to planar and broadly equivalent to the massive facies of Wohletz and Sheridan (1979). The thickness of the bedded units ranges up to 1 m. In planar bedded sections, individual beds are typically less than 10 cm and commonly only 1 cm thick (Figs 25, 28a). In places, as in the northern and central regions, plane-parallel bedded units grade into cross-bedded and, commonly, lenticular horizons. Beds are usually poorly sorted, but normal and reverse grading has been observed in some of the well-bedded units. The bedding and associated low-angle cross-bedding ($\pm 10°$) is similar to that described from base-surge deposits; and, in particular, those deposits forming the rim of maar volcanoes (Fisher and Schminke, 1984).

Slump and water-escape structures are also present in places and indicate the presence of water (Fig. 28a). Water- escape structures of Lowe's (1975) type 1 (soft-sediment mixing bodies) and type 2 (soft-sediment intrusion) are present in the tuffs. Lowe's type 4 (consolidation) structures are present in sandstone interbedded with tuffs in the northern part of the Argyle Pipe. Accretionary lapilli, some as large as 1 cm across, occur in particular horizons forming beds up to 20 cm thick. Most are avoid to spherical in shape, but some show evidence of compaction in the form of flattening, and some have carbonate deposited as crescent-shaped rims in pressure shadows associated with compaction



GSWA 22579

Figure 25. Bedded "sandy" tuff in drill-core. Note the rapid variation in thickness of lapilli-ash-tuff beds and the small fault displacing the beds. LDC 81, 92 m. (Photo: CRAE).

of formerly spheroidal accretionary lapilli (Figs. 28b, 29d).

In addition to the quartz clasts, accidental rock fragments form a widespread but minor constituent of the "sandy" tuffs. Clasts include Proterozoic sandstone, siltstone, shale, lesser amounts of mafic igneous and granitoid material derived from the Lamboo Complex, and, extremely rarely, serpentinized mantle peridotites.

Non-sandy" tuff: The "non-sandy" tuff is a massive to very poorly bedded unit of monogenetic volcaniclastic rocks ranging from hyalotuffs to hyaloclastite to autobrecciated lamproite flows. Both the hyalotuffs and hyaloclastites are massive volcaniclastic rocks, composed of lapilli-sized vitric clasts in a matrix of ash-sized lamproite fragments. But they differ in their degree of vesicularity; the hyalotuffs are the more vesicular. The hyaloclastite clasts are generally characterized by more planar boundaries (Honnorez and Kirst, 1975) than those in the hyalotuffs, but a continuum exists between the two types and no quantitative discrimination is possible. The hyaloclastites show little or no evidence of transport; and, in places, are underlain by autobrecciated and/or magmatic lamproite. The "non-sandy" tuffs vary from brown to dark greenish black: the colour depends largely on the extent of alteration. The range and size of juvenile clasts is similar to that of the "sandy" tuffs; but the proportion of clasts is greater, typically above 30%. The matrix of the "non-sandy" tuff is generally dark and turbid, but relic angular shards can be discerned in places. The "non-sandy" tuff appears to cross-cut "sandy" tuff sequences, and probably represents a later volcanic phase. Xenoliths of country rock are extremely rare in the "non-sandy" tuff, but peridotite nodules have been recorded (Atkinson and others, 1984a), some of which contain diamond (Hall and Smith, 1984).

Olivine(-phlogopite) lamproite dykes and olivine lamproite flows: Late-stage (phlogopite)-olivine lamproite dykes intrude the "sandy" tuff (Fig. 26) and locally may have breached the surface of the crater to form flows (see below). The dykes are typically less than 1 m wide, and are of limited extent; some appear to form *en-echelon* groups. The dykes are composed of olivine phenocrysts and macrocrysts (now replaced by talc) set in a micaceous (phlogopite) groundmass containing altered second-generation olivine, opaque oxides, and carbonate. The variety of contact features associated with the dykes indicates that intrusion took place over a long period of time and that dyke intrusion was both synchronous with, and post-dated deposition of, the



GSWA 22580

Figure 26. Dyke of phlogopite-olivine lamproite intruding "sandy" tuff close to the western wall of the pipe (*see also* Fig. 31).

"sandy" tuffs. Three types of dyke contact have been observed: dykes with chilled margins, which indicate a definite post-tuff age of intrusion; dykes that show no contact effects; and dykes that show autobrecciated contacts and represent intrusion into unconsolidated, and/or water saturated, tuff. The presence of lava flows is less certain, but features such as a chilled lower contact, combined with an autobrecciated upper contact, aligned amygdales of carbonate, and skeletal chromite, indicate that olivine lamproite flows are probably present in the sequence. However, identification of flows is difficult in outcrop because of weathering and oxidation; it is also difficult in drill core unless the above features are well developed.

Eruptive sequence

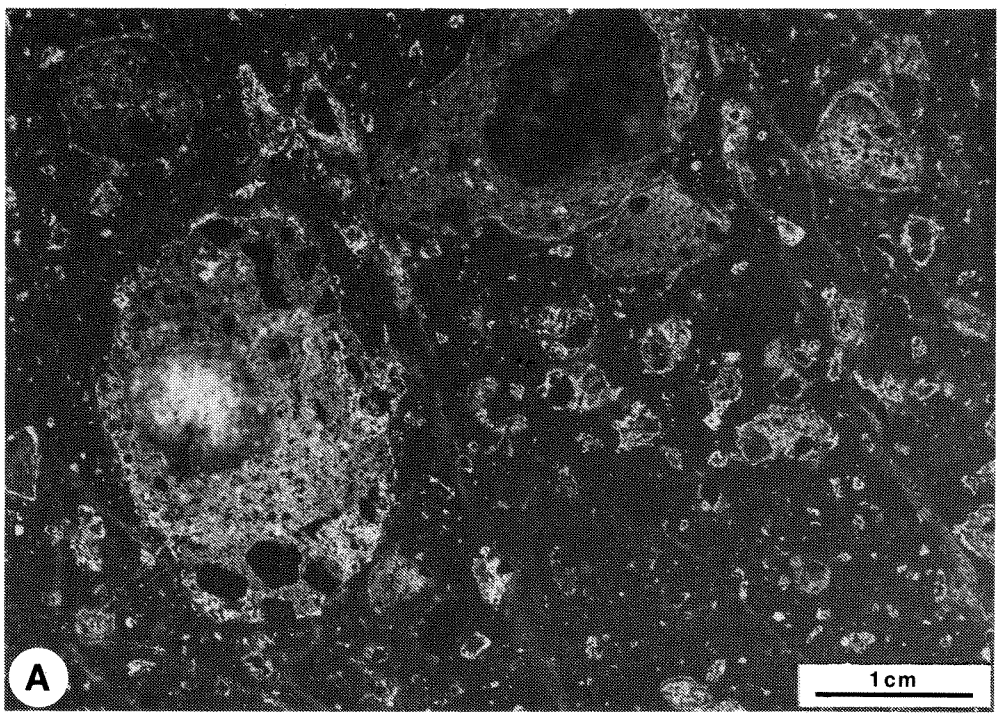
The study of the different pyroclastic types, and the relationships between them and the dykes present in the pipe, has led to the development of the following model for the sequence of eruption in the Argyle pipe. The model is similar to that proposed by Lorenz (1973, 1975, 1984) for the formation of maars by alkali basalt/kimberlite volcanism. A feature of the model is the recognition of the role of ground, or meteoric, water in the eruption, particularly the importance of the interaction of magma with groundwater in the crater environment. Many features commonly ascribed to, or taken as evidence strongly favouring, a hydrovolcanic or phreatomagmatic origin (Fisher and Schminke, 1984; Lorenz, 1979, 1984; Sheridan and Wohletz, 1983), are present in the Argyle pipe. These include the comparatively well-bedded nature of many of the "sandy" tuffs, the small size of the clasts, the low degree of sorting, the abundance of country rock fragments, the glassy (chilled) nature of the juvenile lapilli, the low degree of vesiculation of the pyroclasts overall, the angularity of the pyroclasts, together with the presence of water-escape features, impact sags, base-surge deposits, accretionary lapilli, inferred lahars, and the common inclusion of accidental fragments in juvenile clasts.

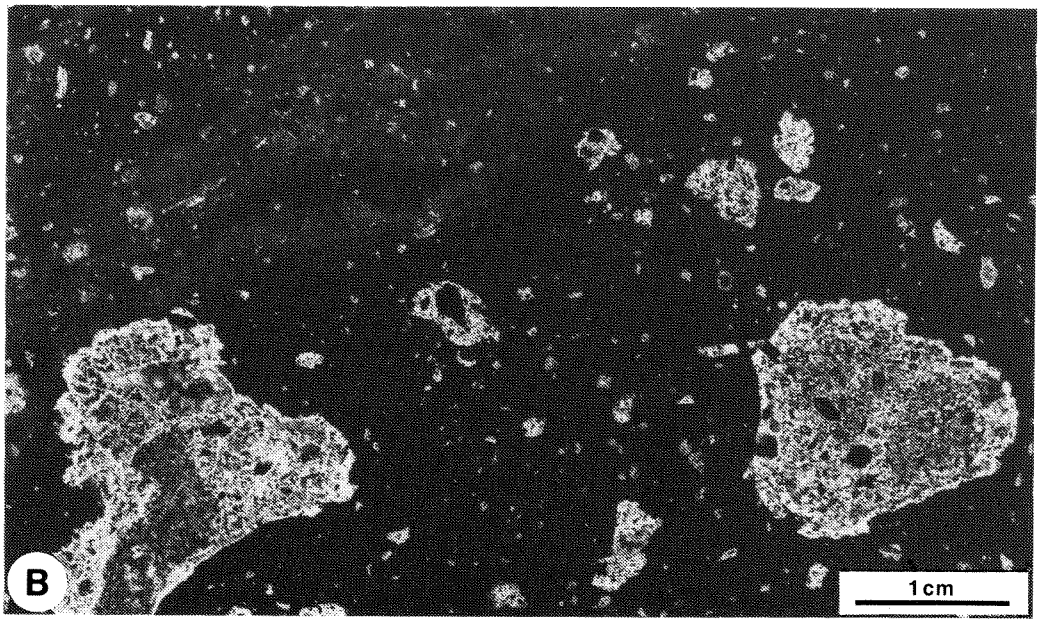
The model envisages a body of olivine lamproite magma rising towards the surface, where it began to vesiculate because decreasing confining pressure allowed exsolution of dissolved volatiles (CO_2, H_2O) under high magmatic volatile partial pressure. The magma continued to ascend into the crust through basement rocks of the Lamboo Complex, perhaps along a pre-existing fault or fault zone, to the unconformity separating the crystalline rocks from the less competent overlying sediments of the Revolver Creek Formation, where hydraulic fracturing of the sandstone units occurred. This fracturing may have been assisted by groundwater contained in the sandstone and/or water contained in the fault zones, which, on contact with the magma, flashed to steam initiating small vapour explosions enhancing disaggregation of the sandstone. The effect of combining magmatic and meteoric water increased water pressure and small vapour explosions which resulted in the shattering of the overlying country rock to the surface to form the basic tapered diatreme shape. During the pre-vent stage of eruption, tuffisite dykes were intruded into fractures and along planes of weakness in the country rock and through the fractured zone.

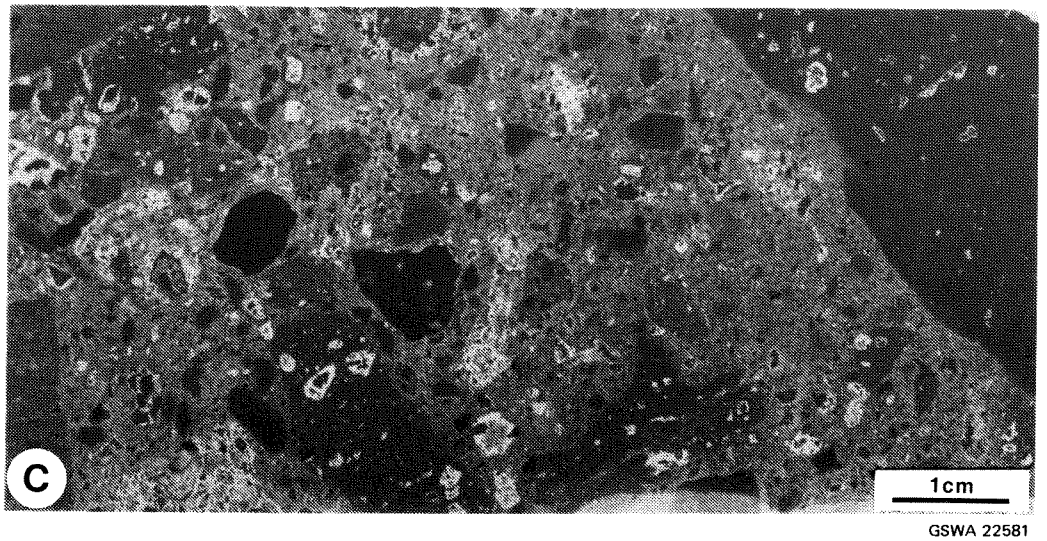
The pipe flared markedly when rocks of the Carr Boyd Group were encountered, which, being much younger than those of the Revolver Creek Formation, were less competent, had higher porosity, and may have constituted groundwater aquifers. Direct interaction of magma and water within the zone of fractured country-rock sandstones, penetrated by tuffisite dykes, resulted in fuel-coolant interaction (Lorenz, 1979; Sheridan and Wohletz, 1983; Wohletz and Sheridan, 1983; Fisher and Schminke, 1984) which generated explosive eruptions gradually enlarging the vent by destruction of the fractured zone. The conduit is envisaged as relatively confined, essentially to the centre of the zone of fracturing, and up to three conduits were possibly present throughout the length of the diatreme. Excavation of the vent increased the magma-water contact area and resulted in increased explosive activity and eruption of pyroclastics, predominantly as base-surge deposits.

Continued eruption resulted in a change in the relative proportions of accidental and juvenile clasts: the proportion of accidental fragments of quartz and quartzite from the fractured country rocks was progressively diluted by an increased proportion of juvenile pyroclastics. Variations in the morphology and vesicularity of the juvenile clasts are inferred to result from changes in the physical conditions of the magma, such as temperature, degree of crystallinity, viscosity, and, particularly, to changes in the mass ratio of coolant to fuel (*cf.* Wohletz and McQueen, 1984). The well-bedded units are inferred to have resulted from base-surge eruptions and to have formed a rim of bedded pyroclastics. Continued eruptions resulted in ejection of the fractured rocks and subsidence of the pyroclastic units, which left remnants of the fractured country rocks (now the contact breccia) at the margins of the diatreme. The presence of abundant water resulted in periodic eruptions, which assisted in homogenization of formerly bedded units by mixing of the pyroclastics in the vent. This is evidenced by the common occurrence of cognate pyroclastic fragments, mainly fine ash-tuff. Massive units are inferred to have been formed by mass movement, possibly lahars, down oversteepened slopes on the inner crater walls.

Late in the eruptive sequence, dykes of (phlogopite)-olivine lamproite were intruded intermittantly into the pyroclastic pile. Some penetrated high enough in the pile to encounter water-saturated pyroclastics, resulting in autobrecciation. Near the end of the volcanic sequence, magma extruded into the crater lake and fragmented, with limited vesiculation and venting, to form the "non-sandy" tuff and, where fragmentation was restricted, to form "rootless" lava flows. Erosion of the pyroclastics that formed the tuff-ring, deposited epiclastic sediments into the crater. Subsequent faulting, tilting, and erosion,







GSWA 22581

have resulted in the present shape and level of exposure of the diatreme.

PETROGRAPHY

"Sandy" tuff

Lapilli-ash-tuff and ash-lapilli-tuff: The lapilli-ash- tuffs and ash-lapilli-tuffs are polygenetic and polymodal volcaniclastics containing variable, but generally small, amounts (less than 35%) of lithic lapilli (> 2 mm across; Schmid, 1981) set in matrix of lamproite ash and fragmented quartz grains (Figs 27,28).

The lithic fragments are mostly juvenile lapilli and coarse ash of very fine-grained crystalline to cryptocrystalline, formerly glassy, olivine lamproite. The juvenile fragments include several textural types:

Dense vitric clasts: These clasts are blocky to equant with subangular to subrounded margins, and are either non-vesicular or contain only very sparse vesicles. They are composed of anhedal macrocrysts up to 5 mm and much smaller second-generation euhedral microphenocrysts of olivine (now talc ± carbonate) set in a formerly glassy groundmass with accessory euhedral chromite. In some clasts, the olivine grains are rimmed by feathery phlogopite or tetraferriphlogopite.

Dense porphyritic clasts: These clasts have a similar form to the vitric clasts, but the groundmass is more crystalline and contains small sub- to euhedral pseudomorphs after leucite (now K-feldspar) up to 40 μm diameter and, in many clasts, fine flakes of phlogopite or tetraferriphlogopite, together with accessory euhedral chromite granules and prisms of apatite.

Vesiculated vitric clasts: These pyroclasts are generally blocky to equant, have subangular to slightly scalloped margins, and contain a low to moderate amounts of spherical to subspherical vesicles, now infilled with calcite, or, less commonly, K-feldspar. The only crystalline primary phases are sparse anhedral macrocrysts and euhedral microphenocrysts of altered olivine, and granular to skeletal chromite grains.

Scoriaceous vitric clasts (pumice and fiamme): These clasts have a highly irregular, commonly strongly elongated shape and angular to scalloped margins. Vesicles are abundant, range from spherical to elongate, and are commonly flattened or deformed. The clasts are wholly vitric or contain only sparse anhedral macrocrysts and euhedral microphenocrysts of talcose olivine and accessory groundmass chromite, which is commonly skeletal, in a formerly glassy to cryptocrystalline groundmass. Eutaxitic textures are common.

Cored and composite lapilli: These are mostly vitric lapilli (chiefly dense rather than vesicular) with a core or nucleus of lapilli to coarse ash-sized fragments of quartz, or cognate or accidental lithic material (Fig. 27a). Less commonly, the lapilli are cored by a crystal fragment, usually macrocrystal talcose olivine. Some lapilli contain more than one lapillus-sized inclusion. In many cases the inclusions are of differing types (*e.g.* cognate and accidental); but some are of similar type. Composite lapilli composed of small juvenile lamproite lapilli enclosed in dense lamproite also occur. Similar lapilli elsewhere are inferred to have formed in the presence of water (Lorenz, 1975).

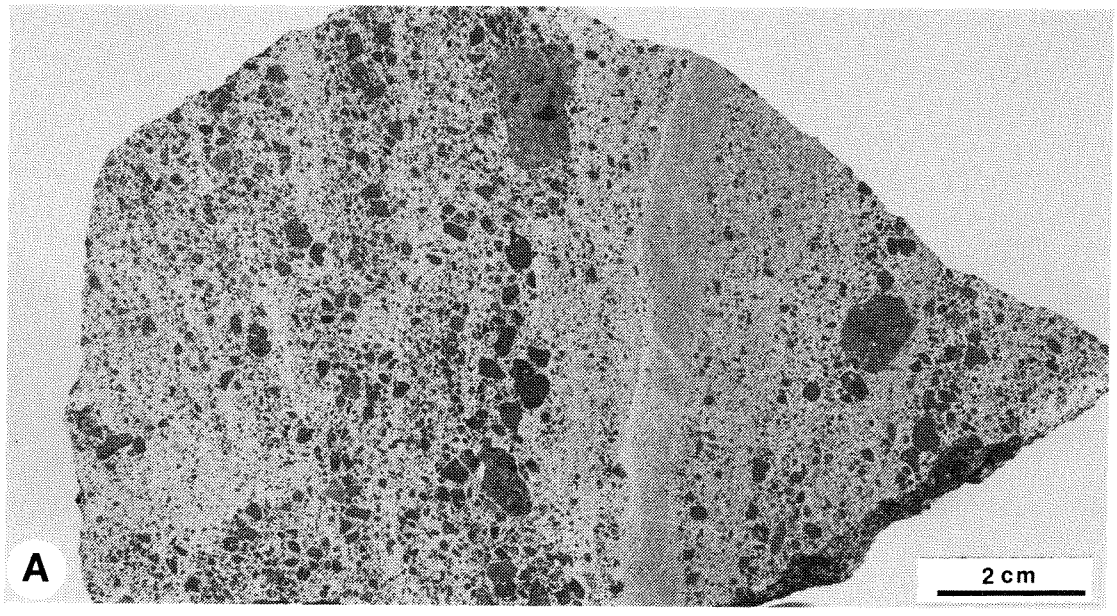
A proportion of the lapilli have dark oxidized skins; and, in many vesicular pyroclasts, the vesicles are typically surrounded by dark oxidized rims. According to Heiken (1974) oxidized skins are a characteristic feature of pyroclasts from magmatic eruptions. However, it is possible that the oxide-rich (mostly anatase) rims simply reflect, at least in part, the effect of relative differences in porosity of the clasts and matrix on fluids associated with the secondary alteration of the Argyle pipe.

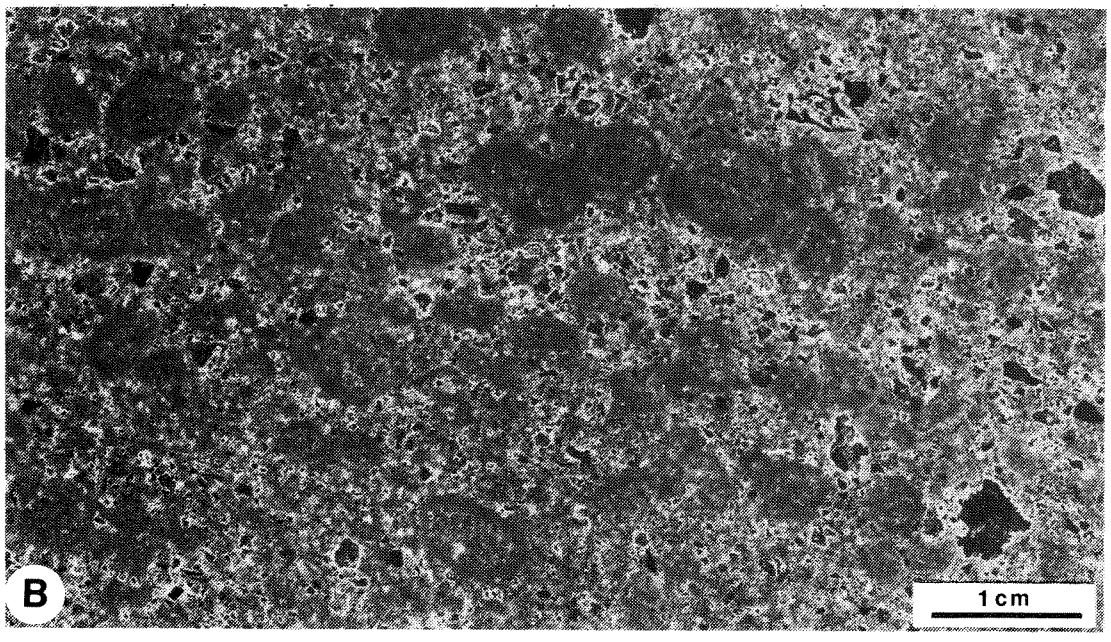
A feature of many of the juvenile fragments is the presence, as inclusions, of small fragmental quartz grains and lithic fragments. Unlike the cored lapilli, the included fragments, mostly quartz, are randomly distributed, and commonly show corroded margins. In some lapilli, the included quartz grains are concentrated at the rims, suggesting that accretion on, as well as inclusion within, the juvenile pyroclasts was an important process. Some of these resemble armoured lapilli.

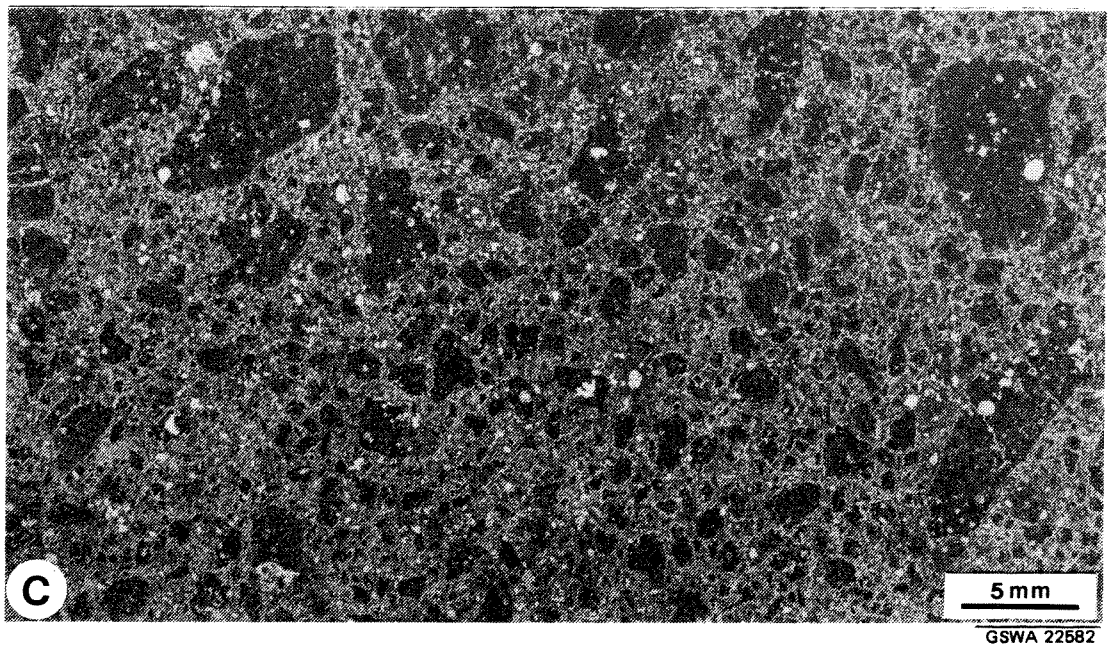
All the juvenile olivine lamproite fragments have been altered; both the olivine macrocrysts and microphenocrysts have been altered to talc ± carbonate ± sulphides, or serpentine. All leucite is altered, mainly to K-feldspar, and the glassy groundmass is now a turbid intergrowth of fine mica, serpentine and smectite. Other pervasive secondary phases include granular sphene and anatase, ragged irregular grains of Mn-ilmenite, small blebs of sulphide, talc, serpentine, smectite, and anhedral patches of carbonate, which typically infills vesicles or forms anhedral sparry patches in the groundmass.

In addition to the juvenile fragments, cognate lapilli of porphyritic, micaceous, olivine lamproite, and fine ash-tuff are present in many, if not most, of the lapilli ash-tuffs. The cognate magmatic lamproite fragments are slightly coarser grained than the juvenile clasts, and typically contain abundant groundmass phlogopite flakes and apatite prisms up to 200 μm, together with pseudomorphs after leucite; the coarsest grained types contain patches of K-feldspar in the groundmass. Many of the clasts are petrographically similar to the olivine-phlogopite lamproite dykes, and indicate incorporation of earlier formed subvolcanic rocks in later eruptive

Figure 27. Polished drill core of tuffs from the Argyle Pipe: A — Cored lapilli in massive lapilli-ash-tuff. Cores (nuclei) consist of recrystallized granitoid and talcose former olivine macrocrysts. Note angular blocky lamproite inclusions in the larger, and altered olivine phenocrysts in the smaller, lapilli; also bleached matrix and margins of lapilli due to formation of leucoxene; DDH 143, 75.5 m (BMR 83211039). B — Very weakly bedded to massive lapilli-ash tuff with sparse, partially leucoxenized matrix of quartz grains and lamproite ash. Note dark, altered macrocrystal olivines in the pyroclasts; DDH 113, 196.5 m (BMR 83211036). C — Coarse lapilli-ash tuff/agglomerate with both blocky clasts of country-rock and weakly vesiculated juvenile clasts in an ash matrix; DDH 17, 250.2 m (BMR 83211009).







GSWA 22582

phases. The lithic fragments of fine ash-tuff contain abundant ash-sized fragments of quartz, together with variable amounts of lamproite ash.

Accidental fragments occur in variable amounts in the tuff. Rock types present include tuffaceous sandstone and siltstone, quartz sandstone, orthoquartzite, variolitic-textured spilitic basalt, shale, quartz-biotite schist and gneiss, medium-grained granitoids ranging from hornblende-bearing tonalites to pink granite and adamellite, felsic gneiss, and altered dolerite and gabbro. The crystalline rocks are inferred to be derived from the Lamboo Complex and various granitoid intrusives whereas the sediments are probably derived from the local country rocks, both the Revolver Creek Formation and Carr Boyd Groups.

Crystal fragments, particularly talcose olivine macrocrysts up to 5 mm across, are common; but crystal fragments are subordinate to lithic fragments. Other conspicuous, but rare, crystal fragments include red-brown biotite (commonly deformed), zircon, and diamond.

The matrix consists of ash-sized particles of olivine lamproite and serpentinous or talcose olivine together with a large percentage, commonly 30 to 50%, of quartz grains. The larger quartz grains are rounded to well rounded; whereas the more comminuted grains are increasingly angular, and the fine ash-sized fragments are highly angular. Many of the quartz grains exhibit undulose extinction and have recrystallization textures and some are sagenitic; most appear to have a metamorphic provenance. The quartz grains have many similarities with quartz grains in the country-rock orthoquartzites of the Carr Boyd Group, but lack the authigenic overgrowths characteristic of many of the orthoquartzites from these formations. This implies emplacement of the Argyle pipe prior to lithification of the sediments. In addition to the quartz grains, the matrix also contains fine, ash-sized particles of altered lamproitic glass (some shard-like), talc, phlogopite, granular chromite, and apatite needles, together with secondary anatase, sphene, illite, montmorillonite, calcite, chlorite, dolomite, sulphides (including pyrite, pentlandite, chalcopyrite, sphalerite, galena), K-feldspar, and, rarely, zircon. The light colour of the matrix of some of the tuffs is inferred to result from alteration of finely disseminated anatase to leucoxene.

Coarse ash-tuff

Coarse ash-tuff is the most abundant lithology in the "sandy" tuff unit: it is a polygenetic volcaniclastic rock composed dominantly of lamproite ash and quartz fragments, and subordinate (typically 3 - 15%) lamproite lapilli. The same range of pyroclastic material is present in the coarse ash-tuffs as in the lapilli-tuffs; but, in general, the modal abundance of quartz clasts is greater. The coarse ash-tuffs are dominantly polymodal, but grade into moderately well-sorted types which are generally bedded.

Pumiceous pyroclastics appear to be poorly represented in such rocks; this suggests some reworking and sorting. The matrix in these tuffs consists of fine ash.

Fine ash-tuffs

The fine ash-tuffs represent fine-grained variants of the more common coarse ash-tuffs. In thin section they are composed of abundant small quartz fragments with angular to highly angular outlines, and fine lamproite ash, now largely altered to clay, talc, chlorite and/or serpentine. Within bedded units, a grading towards coarse ash-tuff and ash-lapilli-tuff horizons is apparent.

Accretionary lapilli tuff

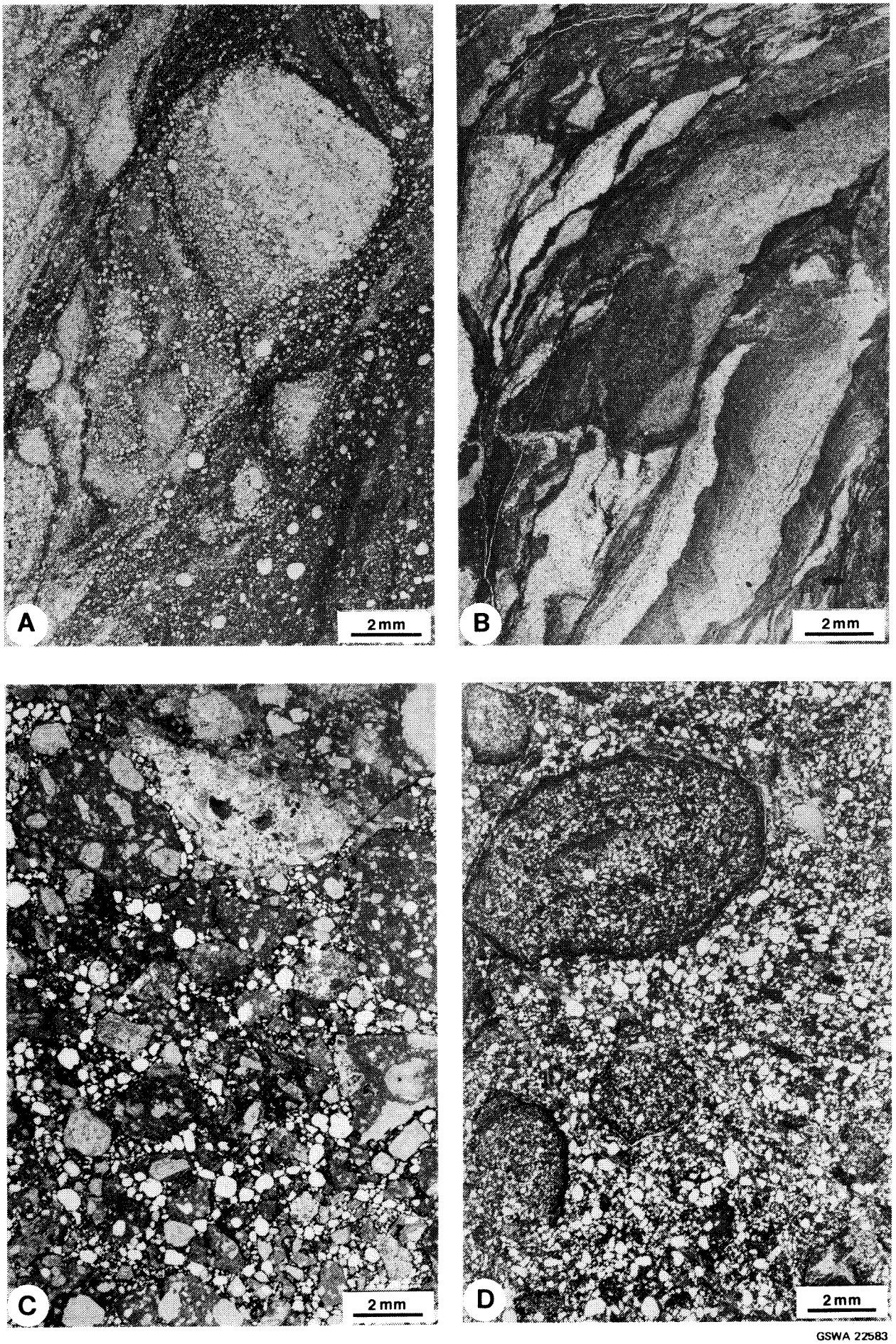
The accretionary lapilli-tuffs are composed of ash-tuff with abundant quartz fragments in a fine ash matrix. The lapilli, which are as large as 1 cm in diameter, are spherical to ovoid in shape and occur in thin beds (Fig.28b). The elongation (flattening) of some of the lapilli is parallel to the bedding and suggests compaction by the overlying pyroclastics. Individual lapilli have a core of coarser grained ash enclosed by a rim of very fine ash up to 1 mm wide which is clearly distinguishable on cut surfaces (Fig. 29d). Accretionary lapilli are commonly associated with Surtseyan or phreatomagmatic (hydroclastic) eruptions and rarely occur in magmatic eruptions (Walker and Croasdale, 1972; Fisher and Schminke, 1984).

Non-sandy" tuff

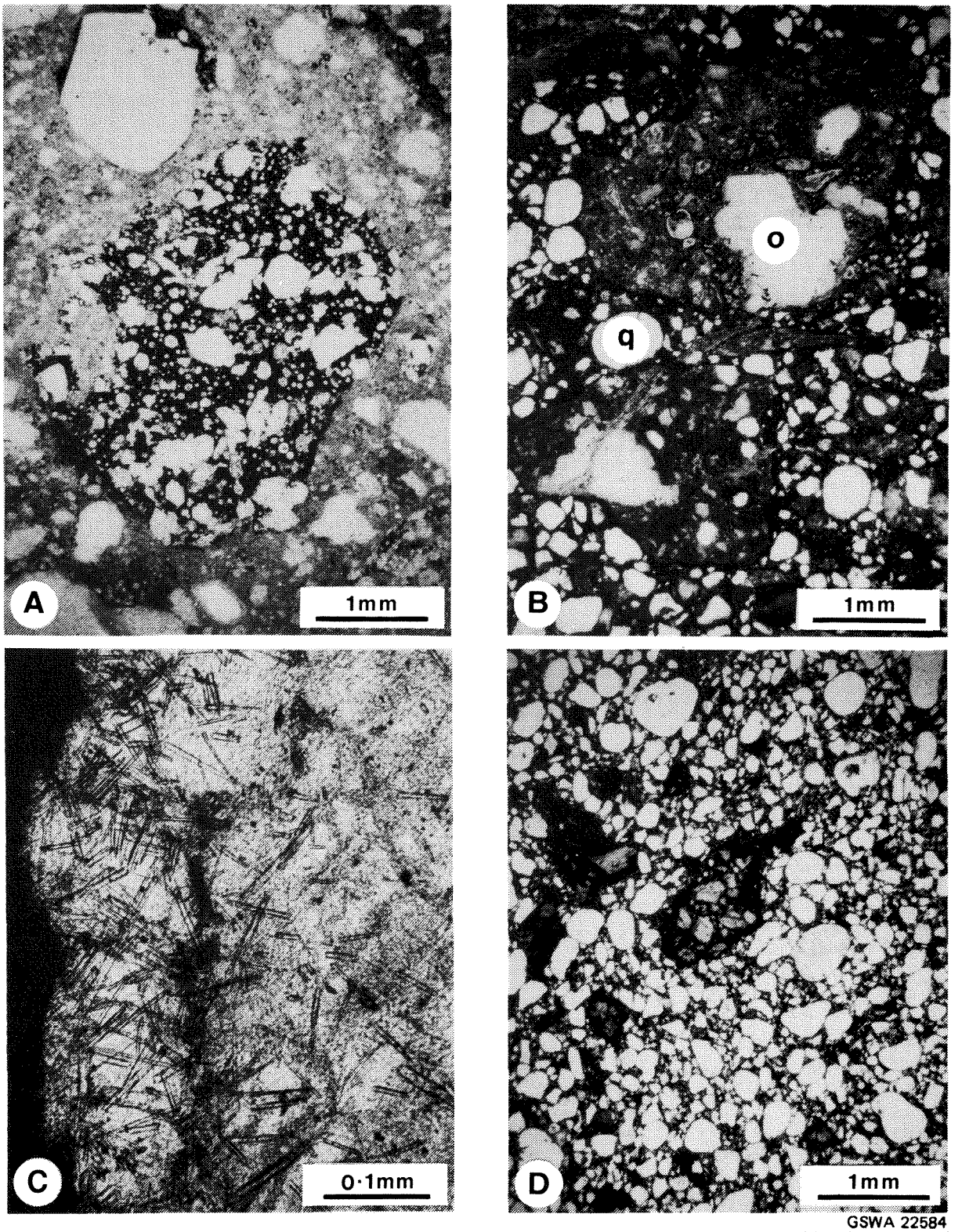
This unit consists of essentially monogenetic volcaniclastic and autoclastic rocks in contrast to the polygenetic "sandy" tuff. Additional features of this unit are the much higher proportion of lapilli-sized fragments than in the "sandy" tuffs, and the abundance of vitric clasts.

Vesiculated vitric lapilli tuff (hyalotuffs): These tuffs are polymodal, monogenetic lapilli-tuffs, consisting of some 30 to 45% of weakly vesiculated, angular to subangular lapilli, set in a matrix of lamproite ash (Fig.31a). Lithic clasts consist mostly of juvenile lapilli — typically 3 to 4 mm across, but up to 10 mm across — of glassy to very fine microcrystalline olivine lamproite that contains sparse spherical vesicles (now infilled by calcite, dolomite or K-feldpar). The olivine lamproite is composed of macrocrysts up to 3 mm, and smaller, euhedral, second-generation phenocrysts and microphenocrysts of altered olivine (now serpentine or talc); these are set in a turbid, brown, formerly glassy to cryptocrystalline, micaceous groundmass that contains accessory granular chromite, fine flakes of phlogopite, and, in more crystalline varieties, small pseudomorphs after leucite. Cognate lithic clasts are much subordinate, and consist mainly of dense glassy

Figure 28. Polished slab and drill core of tuffs from the Argyle Pipe: A — Bedded fine ash-tuff, coarse ash-tuff and lapilli-ash-tuff, with possible water-escape feature (light zone). Quarry BS 132 (BMR 83211005). B — Lapilli-ash-tuff showing accretionary lapilli composed of fine ash and ash-sized juvenile lamproite fragments; note weak bedding (BMR 83211072). C — Former palagonitic tuff with blocky to weakly vesicular vitric clasts (amygdales filled by calcite) in a brown, formerly palagonitic ash matrix; DDH 31, 140.3 m (BMR 83211016).



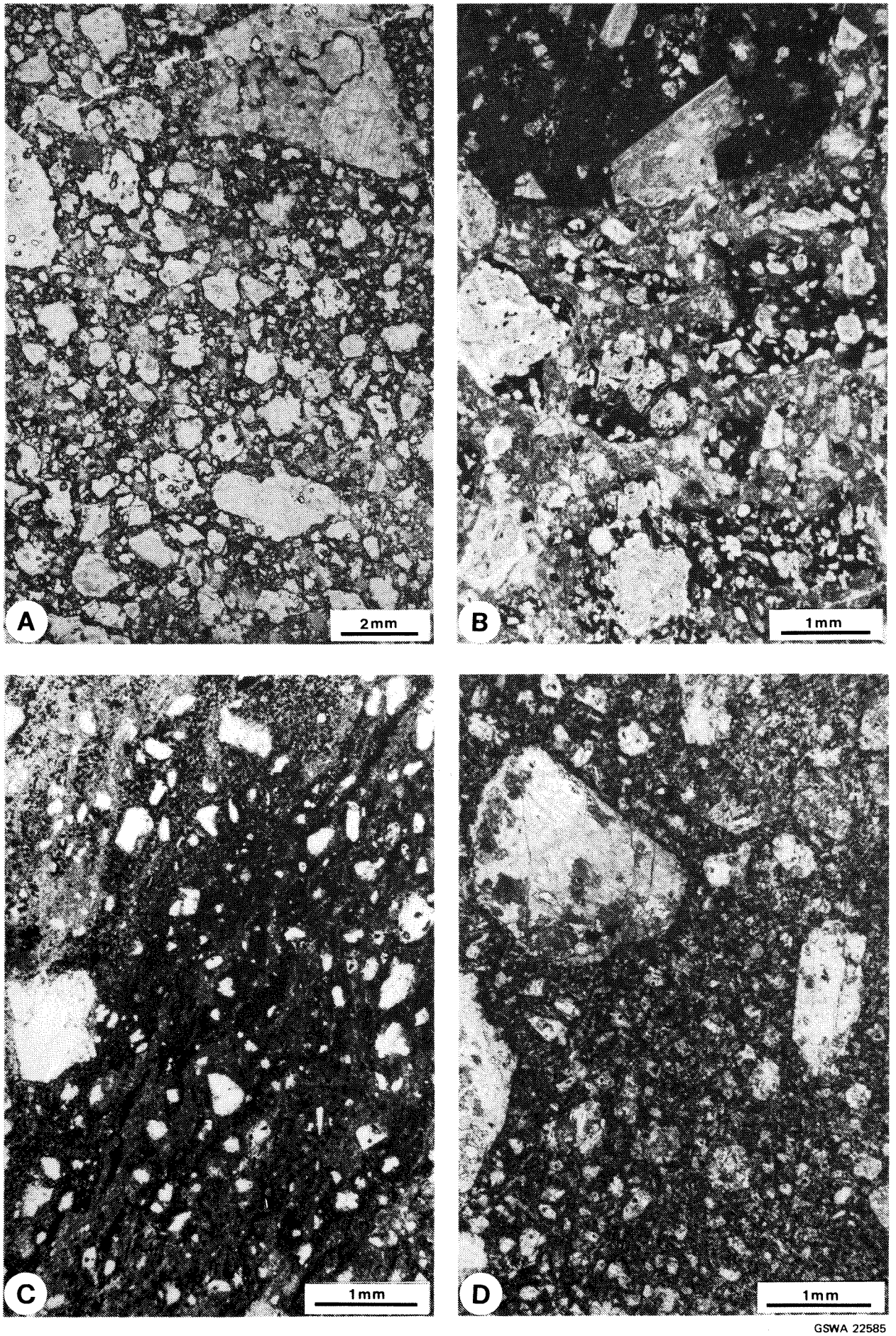
GSWA 22583



GSWA 22584

Figure 30. Photomicrographs of tuff from Argyle Pipe: A — Dark oxidized pumiceous lapilli of porphyritic olivine lamproite in coarse lapilli-tuff; DDH 59, 140.3 m (BMR 83211027). B — Juvenile porphyritic to weakly vesiculated lapilli with altered olivine macrocrysts (o) in a quartz-rich (q) matrix. Lapilli-ash-tuff; DDH 59, 126.5 m (BMR 83211026). C — Secondary arfvedsonitic amphibole needles in former olivine macrocryst (now talc), in weakly bedded lapilli-ash-tuff; DDH 59, 117.2 m (BMR 83211025). D — Dark, oxidized, vesiculated, vitric, juvenile clasts in (lapilli)-ash-tuff. Note altered former olivine crystals in lapilli; matrix mostly rounded to subrounded quartz grains; DDH 17, 246.5 m (BMR 83211008).

Figure 29. Photomicrographs of contact breccia and tuffs from Argyle Pipe: A — Contact breccia of disaggregated siltstone and rounded fragments of fine-grained sandstone with interstitial clay matrix; DDH 143, 204.8 m (GSWA 71704). B — Contorted and brecciated marginal shale and siltstone; DDH 141, 100.5 m (GSWA 71707). C — Lapilli-ash-tuff: lapilli of olivine lamproite with prominent altered olivine macrocrysts in a matrix of quartz grains and oxidized interstitial clay; DDH 106, 202.8 m (GSWA 71733B). D — Accretionary lapilli composed of small quartz fragments and clay (altered fine lamproite ash) in a "sandy" ash matrix. AC 6, 88.7 m (GSWA 71724).



GSWA 22585

olivine lamproite, but include crystalline porphyritic olivine-phlogopite lamproite, tuffaceous siltstone and fine ash-tuff. The porphyritic olivine-phlogopite lamproite is characterized by groundmass phlogopite-tetraferriphlogopite and apatite, as well as chromite. Accidental lithic clasts are rare, but include talcose quartz sandstone, tuffaceous siltstone, and fine ash-tuff, and, very rarely, serpentinized garnet (now spinel symplectite; *see* Fig. 32) lherzolite. The matrix consists of ash-sized fragments of glassy (now serpentinized) lamproite and talcose olivine, together with granular chromite, smectite, serpentine, carbonate, sphene, and, in some cases, fragmented quartz grains derived from the country rocks. A few samples contain very small amounts of zircon.

Hyaloclastite: The hyaloclastites are monogenetic, polymodal volcaniclastics, and are composed largely of vitric clasts. In a number of sections they are underlain by either autobrecciated or magmatic lamproite. They are composed of some 30 to 50% weakly vesiculated to dense, highly angular pyramidal to angular blocky, vitric juvenile clasts, set in a fine matrix of fragmented vitric clasts and serpentinized or talcose olivine fragments. The juvenile clasts consist of anhedral, commonly embayed, macrocrysts up to 3 mm across and small, euhedral, second-generation microphenocrysts of altered olivine (now mostly serpentine with thin talc rims) set in a brownish, commonly serpentinous, formerly glassy, groundmass with tiny (<20 μm) accessory chromite. Many of the second-generation olivines, and some of the chromite grains, exhibit skeletal textures formed by quenching on eruption. The matrix consists of highly angular, pyramidal fragments of serpentinous, formerly glassy, olivine lamproite, together with fragments of serpentinized olivine, chromite granules, and abundant secondary serpentine, smectite, calcite, dolomite, sphene, rutile, anatase, Mn-rich ilmenite, sulphide, and, in some cases, priderite.

Palagonitic hyaloclastites are characterized by brown, dense to sparsely vesicular, clasts set in a pale yellow-brown matrix with abundant serpentinous former palagonitic glass (Fig. 28c). The margins of the fragments and the rims of the sparse vesicles are characterized by dark, oxidized rims composed mainly of very fine granular sphene.

The low degree of vesicularity, coupled with the glassy nature, the pyramidal shape of the clasts, and the inferred presence of former palagonite, together with the close association with magmatic or autobrecciated lamproite, implies an origin essentially by fragmentation as a result of rapid chilling of lamproite magma, probably by water. Some hyaloclastites show minor vesiculation.

Autoclastic breccia: The autoclastic breccias are composed of up to 50% of angular blocky clasts of dense, magmatic, mostly glassy to microcrystalline porphyritic olivine lamproite, set in a magmatic matrix of similar material (Fig. 31b). Distinction between clasts and matrix is difficult, and only small differences in crystallinity exist among clasts and between the clasts and matrix. Clasts consist of olivine lamproite with embayed macrocrysts, up to 5 mm, and euhedral microphenocrysts of altered olivine in a groundmass which was formerly either glassy to cryptocrystalline or microcrystalline. The glassy to cryptocrystalline groundmass is commonly micaceous and contains accessory chromite, whereas the microcrystalline groundmass is composed of abundant small flakes of tetraferriphlogopite, prisms of apatite up to 60 μm, pseudomorphs after leucite, up to 80 μm, and accessory chromite, together with secondary anatase, sphene, Mn-ilmenite, rutile, priderite, serpentine, talc, smectite, and carbonate.

All the "non-sandy" tuffs have undergone low-temperature alteration. Olivine is entirely replaced by serpentine or talc $\pm$ carbonate, leucite is replaced by K-feldspar or very fine intergrowths of mica and K-feldspar; and the former glass is altered to smectite, serpentine, talc, and carbonate.

Olivine(-phlogopite) lamproite dykes

The olivine(-phlogopite) lamproite dykes are either massive or autobrecciated. They are composed of olivine macrocrysts — typically with textures indicating marginal resorption — and euhedral microphenocrysts of altered olivine in a groundmass rich in pleochroic (orange to red) tetraferriphlogopite with accessory apatite prisms and granular titaniferous magnesiochromite (Fig. 31d). In coarser grained types, K-feldspar forms a base interstitial to the mica flakes, which may be up to 0.2 mm across. Secondary phases consist of serpentine, talc, and carbonate, and a complex assemblage of Ti-bearing phases. Of these, sphene, anatese, rutile, and manganoan ilmenite are the most common, but other phases include priderite, a priderite-like mineral (Fe-bearing potassium titanate), and a complex Ti,Zr silicate. Traces of pentlandite, chalcopyrite and sphalerite are also present.

MINERALOGY

Silicate phases

Olivine: Despite the total alteration of all olivine in the Argyle lamproites, two generations of olivine are clearly distinguishable on the basis of the form of the pseudomorphs. Grains of the first generation, of macrocrystal olivines, range up to 5 mm across, but are

Figure 31. Photomicrographs of "non-sandy" tuff and olivine lamproite dykes from Argyle Pipe: A — Vesiculated vitric-lapilli-tuff (hyalotuff) composed of weakly vesiculated blocky lapilli of formerly glassy, olivine lamproite in an ash matrix of small shards of glassy lamproite. Many of the lapilli and vesicles are rimmed by dark leucoxene; DDH 31, 130.3 m (GSWA 71728A). B — Autoclastic breccia, dark, oxidized, amoeboid lapilli of formerly glassy olivine lamproite in a matrix of finely crystalline altered olivine lamproite; DDH 43, 117 m (GSWA 71715). C — Olivine lamproite dyke or pod from the Southern Extension of Argyle Pipe. Serpentinized olivine macrocysts and talcose microphenocrysts in a weakly flow-banded formerly glassy, groundmass (GSWA 71716B). D — Olivine-phlogopite lamproite dyke (Fig. 26) containing altered talcose olivine in a phlogopite-rich groundmass with minor calcite and secondary opaques (GSWA 71747).

typically 2 to 3 mm across. These grains are typically anhedral, and are characterized by resorbed and embayed margins, suggesting reaction with the host lamproite magma. Inclusions of chromite are typically absent. Second-generation olivines are less than 1 mm across, typically sub- to euhedral, and show little evidence of resorption, although skeletal forms, particularly hopper types, are common in the more glassy lamproites as a result of rapid quenching of the magma. Tiny inclusions of chrome spinel up to 20 μm, but typically less than 10 μm, are common.

The dominant alteration product of olivine in the Argyle pipe is talc: it occurs as very fine grained aggregates, commonly with carbonate. In many rocks, the olivine pseudomorphs, in addition to the fine-grained aggregates of white talc, contain greenish-yellow pleochroic flakes of chlorite. Olivine in a number of the hyaloclastites and hyalotuffs has been altered to pale yellowish-green serpentine, commonly intergrown with septechlorite.

Phlogopite: Phlogopite — typically with reverse pleochroism (X = orange red >Y = Z = pale orange/yellow) — is widespread in the olivine-phlogopite lamproite dykes, where it forms discrete flakes and poikilitic plates, which range up to 0.8 mm but average 0.5 mm or less across. Zoning is apparent in the coarsest types, from pale-orange cores to dark reddish-brown rims richer in Fe. Mica is poorly developed in the majority of juvenile clasts of the "sandy" tuff unit and also in the finer grained juvenile clasts of the "non-sandy" tuff, where it is restricted to microcrystalline flakes in the groundmass, commonly rimming macrocrystal and microphenocrystal olivine pseudomorphs. Many of these micas proved too small for microprobe analysis.

Microprobe analysis shows that the Argyle micas have the high Ti and low Al contents (2-9% TiO_2 and Al_2O_3) characteristic of lamproite micas. Most of the micas have low Cr content (< 0.2% Cr_2O_3) and are moderately enriched in Fe (9-14% FeO) with 100 Mg/(Mg+Fe) ratios of 80 or less (Table 22). They are thus more Fe-rich than the majority of the micas in the West Kimberley olivine lamproites (Jaques and others, 1984a). The Argyle micas have low Na and Ba contents and low to moderate F content (mostly <0.2% Na_2O, up to 0.6% BaO and 2% F), and resemble the more evolved of the West Kimberley micas. A number of the Argyle micas show a deficiency in cations in the X site. This presumably reflects degradation of the mica by late-stage alteration and/or weathering.

Leucite: Fine-grained (typically <0.01 mm) pseudomorphs after leucite are common in the groundmass of many of the dense microporphyritic clasts and in the groundmass of many of the juvenile lamproite clasts of the "sandy" tuff. Leucite pseudomorphs are less common in the glassy juvenile clasts of the "non-sandy" tuff and largely absent from the coarser grained olivine(-phlogopite) lamproite dykes, some of which contain potash feldspar in a crystalline groundmass. The absence of relic fresh leucite in the Argyle pipe is not surprising since leucite is readily altered and rarely preserved in rocks older than Tertiary. In the Argyle pipe, leucite is typically altered to very fine K-feldspar or intergrowths of K-feldspar and groundmass mica or secondary talc or smectite.

TABLE 22. REPRESENTATIVE ANALYSES OF MICA IN ARGYLE LAMPROITES

	1	*2*	*3*	*4*
		Percent		
SiO_2	39.61	39.76	39.78	37.25
TiO_2	6.32	6.25	6.34	5.38
Al_2O_3	5.93	5.28	5.68	5.05
Cr_2O_3	0.01	0.03	nd	0.05
FeO	10.01	10.24	9.56	14.14
MnO	0.08	0.07	0.02	0.12
NiO	0.07	0.07	0.07	0.09
MgO	21.43	21.13	21.38	19.80
CaO	0.03	0.04	0.04	0.05
BaO	0.46	0.33	0.44	0.30
Na_2O	0.03	0.03	0.03	0.11
K_2O	10.25	9.76	9.83	9.70
F	1.43	1.30	0.56	0.24
Cl	0.00	0.03	0.02	0.01
Total	**95.66**	**94.31**	**93.74**	**92.29**
$-0 \equiv F,Cl$	0.60	0.56	0.24	0.10
Total	**95.06**	**93.75**	**93.50**	**92.19**
Mg(a)	79.2	78.6	79.9	71.4

All Fe as FeO. nd = not detected (<0.02%).

(a) Mg = 100 Mg/(Mg+Fe)

1-2.—(1) Pale pleochroic core to microphenocryst. (2) Orange-red pleochroic groundmass mica. Sample 83211040, olivine-phlogopite lamproite dyke.

3-4—(3) Pale brown core. (4) Orange rim on core. Sample 83211033, olivine-phlogopite lamproite dyke.

Potash Feldspar: Potash feldspar (orthoclase) is present as a probable primary groundmass phase in the coarser grained olivine-phlogopite lamproite dykes, where it forms an interstitial base. Compositions are poor in Na and Ba, and contain little Fe.

Chrome spinel

Chrome spinel is present in the groundmass of all the Argyle lamproites examined, where it typically occurs as euhedral to subhedral granules up to 60 μm but averaging less than 20 μm across. In the more glassy lamproites, particularly the hyaloclastites, the spinels are skeletal as a result of quenching of the glass. In the coarser grained lamproites, the chrome spinels may be rimmed by sphene or Mn-ilmenite.

The Argyle spinels are mostly titaniferous magnesiochromites (TMC) containing some 3 to 4% TiO_2 and 50 to 60% Cr_2O_3 (Table 23). Most TMC grains have low Al (<10%, typically 3-7% Al_2O_3) and high Cr/(Cr+Al) ratios in the range 0.80 to 0.90. The TMCs contain a range of Fe and Mg contents (16-30% Fe as FeO, 5-15% MgO) and Mg/(Mg+Fe^{2+}) ratios range up to 0.70. Titaniferous aluminous magnesiochromite (TMAC) with up to 14% Al_2O_3 occurs as discrete groundmass grains and as inclusions in former olivines in some of the more mafic olivine lamproites present in the "non-sandy" tuffs. The TMAC grains are more Mg-rich and Fe-poor than the TMC grains (up to 16% MgO, FeO as low as 15%) and have Mg/(Mg+Fe^{2+}) ratios in the range 0.50 to 0.72. Ti content in the TMAC grains is generally slightly lower than in the TMC, and

TABLE 23. REPRESENTATIVE ANALYSES OF GROUNDMASS SPINEL, ARGYLE PIPE.

	1	2	3	4	5
			Percent		
SiO_2	0.12	0.15	0.05	nd	0.06
TiO_2	2.84	2.80	3.48	3.13	3.18
Al_2O_3	12.57	8.23	3.98	4.16	3.60
Cr_2O_3	52.93	57.23	55.73	60.49	57.51
V_2O_3	0.10	0.07	0.03	0.04	0.04
FeO(a)	15.26	16.64	27.81	21.12	27.95
MnO	0.20	0.22	1.26	0.36	0.72
NiO	0.13	0.10	0.13	0.10	0.05
MgO	15.86	14.73	6.17	11.14	6.98
CaO	0.03	0.03	0.12	0.04	0.02
Total	**100.04**	**100.20**	**98.76**	**100.58**	**100.11**
Fe_2O_3(a)	3.32	3.71	3.60	3.20	4.12
FeO(a)	12.28	13.30	24.57	18.24	24.25
Total	**100.37**	**100.57**	**99.12**	**100.90**	**100.53**
			Ratio		
Mg(b)	0.649	0.612	0.284	0.484	0.308
Mg(c)	0.699	0.666	0.312	0.523	0.342
Cr/R^{3+} (d)	0.708	0.784	0.857	0.868	0.862
Al/R^{3+} (d)	0.250	0.168	0.091	0.089	0.080
Fe^{3+}/R^{3+} (d)	0.042	0.048	0.052	0.043	0.058

nd = not detected, <0.02% (a) FeO = Fe determined as FeO and calculated to Fe_2O_3 and FeO based on stoichiometry.
(b) Mg = Mg/Mg + Fe as FeO. (c) Mg = $Mg/(Mg + Fe^{2+})$. (d) R^{3+} = Cr + Al + Fe^{3+}.

1-3-(1) Titaniferous magnesian aluminious chromite core; (2) Titaniferous magnesian chromite rim; (3) Titaniferous magnesian chromite groundmass discrete grain. Sample 83211017, 'Non-Sandy Tuff'.

4-5-(4) Titaniferous magnesian chromite, inclusion in former olivine phenocryst. (5) Titaniferous magnesian chromite, groundmass. Sample 83211033, olivine-phologopite lamproite dyke.

Si content, higher (0.1-0.2% SiO_2). The TMAC grains are commonly zoned to more Al-poor, Fe-rich TMC rims. Titaniferous chromite (TC) occurs as small groundmass subhedra and, in some rocks, as narrow rims on TMC grains. The TC grains are rich in Cr (> 50% Cr_2O_3) and very poor in Al and Mg (< 3% Al_2O_3, < 5% MgO), and have high Fe content (> 30% Fe as FeO). Most TC grains have Cr/(Cr + Al) ratios of 0.80 to 0.90 and $Mg/(Mg+Fe^{2+})$ typically less than 0.1. The TCs are also richer in Ti (up to 5% TiO_2) and Mn (up to 4% MnO) than either the TMAC or TMC grains. The evolutionary trend of the Argyle spinels is therefore one of decreasing Al and Mg and increasing Cr and Fe^{2+}, followed by increasing Fe^{2+}, Ti and Fe^{3+}. The trend toward titaniferous magnetite or chromian ulvöspinel is much less marked than that shown by the west Kimberley lamproites (*see* Chapter 5).

Accessory phases

Sphene: Sphene is widespread, occurring in the groundmass of most Argyle rocks as sub- to anhedral granular aggregates up to 100 μm, but individual grains are considerably smaller. Sphene is particularly common in the "non-sandy" tuffs. Compositions are typically low in Al, Fe, and Na, but contain variable amounts of Sr, REE and Nb. Sphene is rare in kimberlites and lamproites, which generally contain perovskite, although sphene has been reported from the Yakutia (USSR) kimberlites (Dawson, 1980). The irregular habit of the sphene in the Argyle pipe indicates a secondary origin as a result of alteration, possibly of perovskite.

Anatase and rutile: Anatase is also widespread in all phases within the pipe, and occurs as discrete granules up to 60 μm and larger granular aggregates, commonly in association with manganiferous ilmenite. Rutile is less common, but occurs in the cores of ragged intergrowths with Mn-ilmenite, priderite, and zircon. Compositions contain variable amounts of Nb (up to 2% Nb_2O_5) and subordinate Fe. Anatase has been reported in kimberlites as a result of alteration of ilmenite (Dawson, 1980); however, the occurrence of anatase in the Argyle lamproites is believed to be due to the alteration of Ti-rich groundmass, particularly glass. Alteration of anatase to leucoxene results in the bleached appearance of some of the Argyle tuffs.

Mn-ilmenite: Ilmenite containing up to 7% MnO forms ragged, irregular anhedra up to 200 μm across in many of the "non-sandy" tuffs and lamproite dykes, where it is commonly associated with carbonate and sphene. Microprobe analyses show the ilmenites to be poor in Mg (1% MgO or less) and to contain subordinate Nb (0.5% Nb_2O_5). Secondary Mn-rich ilmenite also occurs in some of the West Kimberley lamproites (*see* Chapter 5), in the Skerring pipe (Chapter 3), and has been reported in kimberlites both as secondary rims on ilmenite megacrysts and in the groundmass (Haggerty and others, 1979; Boctor and Meyer, 1979; Wyatt, 1979; Agee and others, 1982).

Priderite: Priderite and priderite-like minerals — CrFeBa- and NbFeK-titanates — occur as small prismatic rods and needles in the groundmass of some of the hyaloclastites and hyalotuffs where they form small (up to 150 μm, typically <60 μm) prismatic rods and needles. These phases are closely associated with rutile, anatase, sphene, Mn-ilmenite, and carbonate; and are also thought to be of secondary origin. In addition to these phases, very rare tiny grains of zircon and an undetermined Zr,Ti,Fe silicate (Atkinson and others, 1984a) have been found in the olivine(-phlogopite) lamproite dykes.

Sulphides: Disseminated sulphide grains are present in most of the Argyle lamproites. Ni,Cu,Fe sulphides, pentlandite and pyrrhotite, occur with talc in olivine pseudmorphs and, together with other sulphides including chalcopyrite, pyrite, sphalerite and galena (Atkinson and others, 1984a), in the groundmass.

Xenocryst suite

Xenocryst phases recovered from Argyle heavy-mineral concentrates include magnesiochromite, almandine, occasional chrome diopside and orthopyroxene, and very rare grains of pyrope garnet (Atkinson and other, 1984a). Diamond is present at grades which range from an average of 6.8 CM/t in the rich southern part to less than 1 CM/t in the northern part of the pipe (Atkinson and others, 1984b): Picroilmenite is absent.

Spinel: Chrome spinel is the most common xenocryst phase recovered from the Argyle pipe. The spinels range

in composition from magnesian aluminous chromite through to magnesiochromite. The xenocryst spinels are distinguished from the groundmass spinels by their larger size, irregular shape, and uniformly magnesian, Ti-poor (< 1% TiO_2) compositions (Table 4: Atkinson and others, 1984a). The Argyle xenocryst spinels are generally similar to the xenocryst spinels in the West Kimberley lamproites, but do not extend to the magnesian aluminous chromian pleonaste compositions recovered from nodules and from concentrates in some of the Ellendale pipes (*see* Chapter 5).

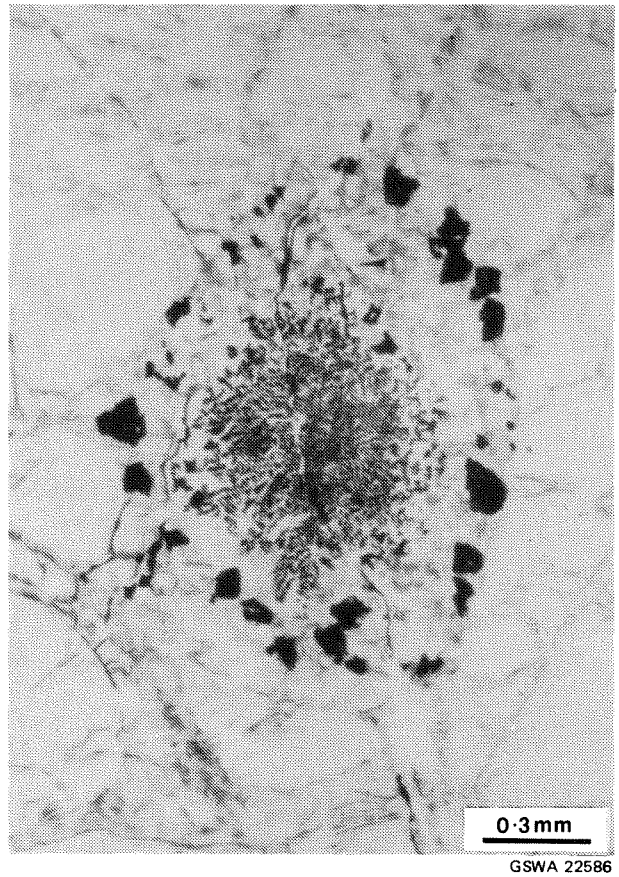
Garnets: The garnets are titanian and chrome pyropes belonging to groups 1 and 9 of the Dawson and Stephens (1975) classification. Representative analyses are given in Atkinson and others (1984a). The chrome pyropes are calcium-saturated, contain up to 6% Cr_2O_3 and CaO, and are similar to the chrome pyrope xenocrysts in the West Kimberley lamproites (Atkinson and others, 1984a; Jaques and others, 1984a; *see* Chapter 5). The titanian pyropes are moderately chrome-rich (up to 2% Cr_2O_3) and commonly poorer in Fe than Dawson and Stephens (1975) average group 1 garnets.

Pyroxenes: The chrome diopsides and enstatites are similar to groups 5 and 1 respectively of the Stephens and Dawson (1977) classification of pyroxenes. The chrome diopsides are rich in Mg, very poor in Al (commonly < 1% Al_2O_3) and Na (< 1% Na_2O), and have high Ca/(Ca + Mg) ratios. They are thus similar to the chrome diopside xenocrysts recovered from the West Kimberley lamproites, which are inferred to have been derived from relatively refractory peridotite at comparatively low temperatures within the garnet or garnet-spinel lherzolite field (Jaques and others, 1984a) (*see* Chapter 5). The enstatites are also very magnesian and have very low Al contents consistent with derivation from a depleted peridotite. The very low Al contents, if equilibrated with garnet, indicate an origin deep in the upper mantle, probably within the diamond stability field.

XENOLITHS

Rare, rounded to discoidal shaped peridotite xenoliths ranging up to 10 cm across, occur in the "non-sandy" tuff (Atkinson and others, 1984a). Most are extensively altered to talc and serpentine; but relics of the primary phases are commonly preserved, and primary textures can generally be discerned. The nodules are typically characterized by three marked concentric zones. A black, fine-grained outer zone, some 3 to 10 mm wide, is composed of lizardite and talc, and forms a shell around a yellowish-green zone, in which the original coarse textures are preserved but the primary mineralogy is replaced by lizardite, yellowish-green montmorillonite, and talc. This zone encloses a dark-coloured core with coarse texture and relic primary olivine, pyroxene, reddish-brown anhedral pseudomorphs after garnet and, in some cases, chrome spinel.

The peridotites are predominantly coarse-grained (terminology of Harte, 1977). Curvilinear grain boundaries are common; some grains, particularly the garnet pseudomorphs, have strongly lobate and embayed boundaries. The outlines of the garnet pseudomorphs in the Argyle nodules appear to be more irregular than the rounded forms commonly found in coarse-textured garnet peridotites described from elsewhere. This, coupled with the complete elimination of garnet, together with the radiating and quench-like form of the spinel and pyroxene, is interpreted to be the result of incongruent? melting of the garnet and subsequent quenching of the glass, Al-rich spinel, and pyroxenes (Fig. 32).



GSWA 22586

Figure 32. Spinel-pyroxene pseudomorph after garnet in a peridotite nodule from the "non-sandy" tuff, Argyle Pipe (Photo: CRAE).

The nodules are composed of olivine (typically 2 to 8 mm across), pyroxene (mainly enstatite, up to 6 mm across), and some smaller chrome diopside and garnet pseudomorphs, typically 1 to 4 mm across. Discrete anhedra of magnesiochromite, up to 0.5 mm (typically 0.1-0.3 mm) across, occur in some nodules. Although all of the nodules examined contain pseudomorphs and symplectic intergrowths after garnet, none now contains primary garnet; all garnet has undergone subsolidus reaction to Al-Cr spinel and Al-rich pyroxene. Modal analysis shows that the nodules were diopside-bearing (garnet) harzburgites, (garnet) harzburgites, and chromite-bearing (garnet) harzburgites.

All the nodules have undergone moderate solid-state deformation, probably at low to moderate temperatures; undulose extinction and kink-bands are common in both olivine and pyroxene. The peridotites appear to have undergone little recrystallization as there are few small,

strain-free polygonal neoblasts located along kink-bands and grain boundaries.

Two primary assemblages are recognized in the Argyle peridotites. The first, designated P1, consists of olivine, orthopyroxene, former garnet ± clinopyroxene ± chromian spinel, and corresponds to an equilibrium assemblage in the garnet lherzolite facies. The second, P2, is found in the garnet pseudomorphs and comprises the assemblage Al-orthopyroxene ± Al-clinopyroxene ± Cr-Al spinel; this is interpreted as having formed by breakdown of the garnet within the spinel lherzolite facies.

Superimposed on the two primary assemblages are several assemblages of secondary minerals which form either vein or pervasive alteration. The first of these secondary assemblages, designated S1, is associated with the alteration of the garnet pseudomorphs. Calcite, serpentine, phlogopite, and K-feldspar, have been determined optically; and illite, by x-ray diffraction. Also commonly associated with the garnet alteration are fine (mostly <50 μm) veinlets of red-brown, reversely pleochroic mica which cut the P1 pyroxenes where they are located in cleavage traces. A second assemblage, S2, consist of serpentine + magnetite + calcite + smectite. In the least altered peridotites, this assemblage is present as fine veinlets, mostly between 0.05 and 0.2 mm wide. Most of these veinlets are filled by serpentine that contains trains of fine granular or "dust" magnetite and rare Ni,Fe sulphides. A large number, however, contain blebs of calcite, commonly oriented transverse to the veinlet; serpentine (and magnetite) form a base or margin to the central calcite infilling; and yellowish-green, weakly pleochroic smectite partly replaces olivine. In extensively altered peridotites, the assemblage is present as a pervasive alteration of olivine and pyroxene to serpentine ± magnetite ± talc. A third, cross-cutting assemblage, S3, consists of veinlets, up to 2 mm but mostly less than 0.2 mm wide, of fine (<40 μm, mostly <20 μm), reversely pleochroic phlogopite, fine (mostly <30 μm) granular euhedra of reddish-brown chromite, and occasional Mn-rich ilmenite. This alteration is clearly associated with the entrainment of the nodule by the lamproite host magma: the micas, spinels and ilmenites, are of similar composition to those in the Argyle lamproites; and, in some nodules, mica-rich veinlets extend inwards from a rind of lamproite.

A number of the nodules contain diamonds at high grades — several carats per tonne (Hall and Smith, 1984). The mineral chemistry of the nodules and their conditions of equilibration are discussed elsewhere (O'Neill and others, in prep.).

GEOCHEMISTRY

Major elements

The geochemsitry of the Argyle pipe rocks is complicated by extensive pervasive alteration and the presence of accidental inclusions in the pyroclastic rocks, particularly the "sandy" tuffs. The effect of inclusion of accidental lithic fragments, particularly quartz fragments derived from the country rocks, is clearly apparent in Figure 32,where the variation in SiO_2 with MgO content is shown. The "sandy" tuffs are distinctly richer in SiO_2 and poorer in MgO as a consequence of mixing of fragments of country rock quartzites with lamproite. Inclusion of quartz fragments results in an increase in SiO_2 accompanied by a comensurate dilution of all other major elements, although element ratios are generally not affected. However, inclusion of country shale, such as the Revolver Creek formation, results in modification of some element ratios (*e.g.* K_2O/Al_2O_3). The effects of weathering and surface oxidation of samples from Argyle is severe as shown by the displacement of two samples towards Fe-rich compositions in the geochemical variation diagrams (Figs 33-35). These samples, which contain abundant hematite and secondary silica, are also strongly leached of Mg and the alkali and alkaline earth metals. Apart from the strongly oxidized samples, the 100 Mg/(Mg + total Fe as FeO) ratio does not appear to have been significantly modified by alteration, in contrast to ratios such as K_2O/Al_2O_3 which show the effects of severe leaching of K in all surface samples whether oxidized or not. The 100 Mg/(Mg + total Fe as FeO) ratios of all except the oxidized Argyle rocks are greater than 70 and typically in the range 75 to 85. These high ratios are consistent with the abundance of both macrocrystal and phenocrystal/microphenocrystal olivine and imply that the olivines were highly magnesian, probably Fo_{90} or more.

The ultrapotassic nature of the Argyle rocks is shown by the high K_2O/Na_2O ratios of the least altered rocks (Fig. 33), which are typically greater than 25. Surface samples, particularly where oxidized, have much lower values. The least-altered samples also have high K_2O/Al_2O_3 ratios, typically 0.75 to 1, and several samples are perpotassic (Fig. 33). Weathered and oxidized samples have both lower K_2O/Al_2O_3 and K_2O/Na_2O ratios, and the "sandy" tuffs show K_2O/Na_2O ratios ranging up to very high values.

Chemical variation within the suite is shown by the oxide versus 100Mg/(Mg + total Fe as FeO) diagrams (Fig. 34). Also shown are representative analyses of the country rocks in the immediate vicinity of the pipe, since much of the variation in the "sandy" tuffs results from simple mixing of lamproite and country-rock quartz and quartzite. This is demonstrated by the similarity in 100 Mg/(Mg + total Fe as FeO) ratio of the "sandy" tuffs, the "non-sandy" tuffs and the olivine-phlogopite lamproite dykes. Excluding the oxidized outcrop samples, silica contents in the "non-sandy" tuffs and olivine-phlogopite lamproite dykes lie in the range 35 to 55%; and 100 Mg/(Mg + total Fe as FeO) ratios typically lie in the range 76 to 86. The "non-sandy" tuff rocks are the most magnesian and show less variation in 100 Mg/(Mg + total Fe as FeO) than the other units. The "non-sandy" tuff and olivine-phlogopite lamproite dyke rocks have high TiO_2 contents, typically 3 to 4%, in common with lamproites elsewhere (Jaques and others, 1984a) (*see* Chapter 5). The oxidized surface samples have even higher TiO_2 contents, up to 6%. With

TABLE 24. REPRESENTATIVE ANALYSES OF ARGYLE (AK1) LAMPROITES AND ASSOCIATED COUNTRY ROCKS

	1	2	3	4	5	6	7	8	9	10	11	12	13
							Percent						
SiO_2	62.28	78.75	60.74	41.73	38.44	49.86	40.85	48.44	94.84	98.85	72.33	99.24	98.63
TiO_2	2.06	0.92	4.21	2.80	3.23	3.04	3.70	0.78	0.19	0.06	1.44	0.01	0.01
Al_2O_3	5.67	4.30	8.13	4.08	4.83	6.96	4.55	20.86	1.49	0.63	16.36	0.40	0.66
Fe_2O_3	1.65	0.80	9.72	2.85	2.50	1.77	2.29	12.67	2.01	<0.01	0.73	0.04	0.03
FeO	3.36	1.85	0.39	4.90	5.97	5.60	6.93	0.56	0.09	0.11	0.68	0.11	0.10
MnO	0.06	0.08	0.05	0.18	0.22	0.08	0.10	0.05	<0.01	<0.01	<0.01	<0.01	<0.01
MgO	11.57	3.94	5.23	21.75	20.51	15.39	18.98	2.43	0.06	0.02	0.36	0.01	0.03
CaO	3.40	2.61	1.96	5.22	7.37	3.99	7.54	0.20	<0.01	<0.01	<0.01	<0.01	<0.01
Na_2O	0.09	0.02	0.01	0.19	0.04	0.12	0.09	0.05	0.01	<0.01	0.05	<0.01	<0.01
K_2O	4.90	1.85	0.02	4.85	1.35	5.86	2.18	8.47	0.26	0.09	3.18	0.09	0.21
P_2O_5	0.69	0.27	1.56	0.94	0.99	1.02	1.20	0.12	0.02	0.02	0.05	0.01	<0.01
H_2O^+	2.47	1.71	4.93	3.59	4.35	4.85	4.78	3.97	0.27	0.23	2.91	0.16	0.43
H_2O^-	0.18	0.58	1.92	0.24	0.91	—	0.54	0.90	0.03	0.08	0.20	0.06	0.05
CO_2	1.39	2.45	0.08	5.23	7.81	—	4.76	0.25	0.47	0.12	1.29	0.08	0.01
Rest	0.74	0.31	0.87	1.05	1.15	1.04	1.19	0.34	0.03	0.02	0.25	0.02	0.01
Total	**100.51**	**100.44**	**99.82**	**99.60**	**99.67**	**99.58**	**99.68**	**100.09**	**99.77**	**100.23**	**99.83**	**100.23**	**100.17**
							Parts per million						
Ba	1654	402	75	1579	222	2368	1011	508	27	28	233	41	35
Li	54	17	79	68	116	52	69	6	5	1	22	2	2
Rb	130	39	2	288	137	208	230	290	10	4	140	3	6
Sr	533	143	464	1041	643	755	1220	38	8	24	66	4	4
Pb	18	16	19	19	405	27	233	26	6	5	9	3	4
Th	12	9	21	18	20	17	20	21	2	1	23	2	1
U	3	3	5.5	4	4	4	4.5	5	1.5	0.5	5.5	1	1
Zr	594	321	1215	590	695	888	762	149	62	43	433	26	28
Nb	135	56	301	194	234	217	273	15	3	<2	23	<2	<2
Y	20	14	30	20	24	23	22	22	8	5	49	2	2
La	70	43	118	123	127	104	150	78	47	43	60	12	8
Ce	164	89	277	249	270	239	305	161	107	103	135	20	9
Nd	55	30	91	82	80	83	89	52	24	23	47	8	4
Sc	10	7	19	12	15	13	15	21	3	<2	22	<2	<2
V	69	49	84	114	140	114	143	150	46	5	174	<2	2
Cr	695	252	838	1316	1833	1097	1682	156	14	9	102	7	7
Ni	560	154	994	969	1090	517	952	42	4	1	11	5	1
Cu	32	14	54	35	54	27	54		9	2	91		
Zn	42	32	179	40	110	199	115	66	2	1	25	2	1
Sn	2	4	6	2	5	3	2	3	<2	4	5	<2	3
Mo	<3	3	<3	3	3	<3	<3	5	<3	<3	<3	<3	<3
Ga	8	8	15	4	9	13	10	29	2	1	22	1	1
As	7.5	2	6.5	0.5	24	10	<0.5	3	1	0.5	5	<0.5	<0.5
F	2200	1600	3700	3200	5400	2900	4100	1800	<300	<300	500		

1 — "Sandy" tuff, lapilli ash tuff, DDH 108/154.4 m, BMR 83211032. 2 — "Sandy" tuff, lapilli ash tuff, DDH 17/135.15 m, BMR 8321106. 3 — "Non-sandy" tuff, highly oxidized olivine lamproite pyroclastic, outcrop, southern end of pipe, BMR 33211062. 4 — "Non-sandy" tuff, autobrecciated phlogopite-olivine lamproite, DDH 153/85.5 m, BMR 83211049. 5 — "Non-sandy" tuff, vitric lapilli tuff, DDH 17/300 m, BMR 83211010. 6 — Phlogopite-olivine lamproite dyke, DDH 31/188 m, BMR 83211018. 7 — Olivine-phlogopite lamproite dyke, DDH 106/160 m, BMR 83211037. 8 — Revolver Creek Formation, shale, contact zone, DDH 56/250.1 m, BMR 83211023. 9 — Revolver Creek Formation, quartzite, DDH 56/180.8 m, BMR 83211024. 10 — Lissadell Formation, orthoquartzite, DDH GT 2/92.5 m, BMR 83211056. 11 — Lissadell Formation, shale, DDH GT 2/137 m, BMR 83211057. 12 — Golden Gate Sandstone, orthoquartzite, DDH GT 2/157.2 m, BMR 33211058. 13 — Hensman Quartzite, orthoquartzite, DDH GT 2/180.7 m, BMR 83211059.

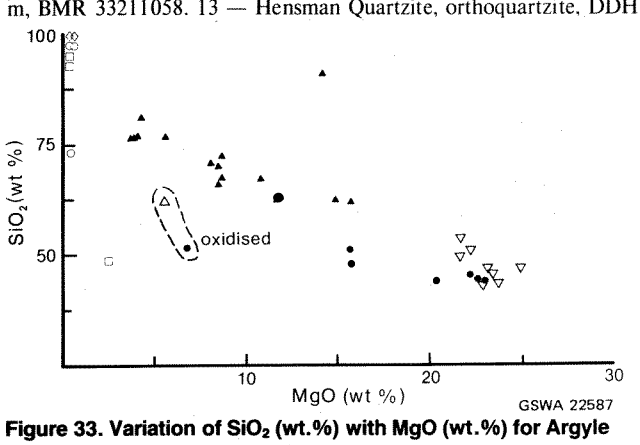


Figure 33. Variation of SiO_2 (wt.%) with MgO (wt.%) for Argyle lamproites and country rocks. Data plotted on H_2O^-- and CO_2-free basis. Symbols: filled triangles = "sandy" tuffs; inverted triangles = "non-sandy" tuffs; filled circles = olivine-phlogopite lamproite dykes; squares = Revolver Creek Formation; open circles = Lissadell Formation; diamonds = Golden Gate Siltstone and Hensman Sandstone. The trend of the "sandy" tuffs away from the magmatic compositions, represented by the dykes and monogenetic "non-sandy" tuffs, is consistent with mixing of quartz fragments derived from the country-rock quartzite units.

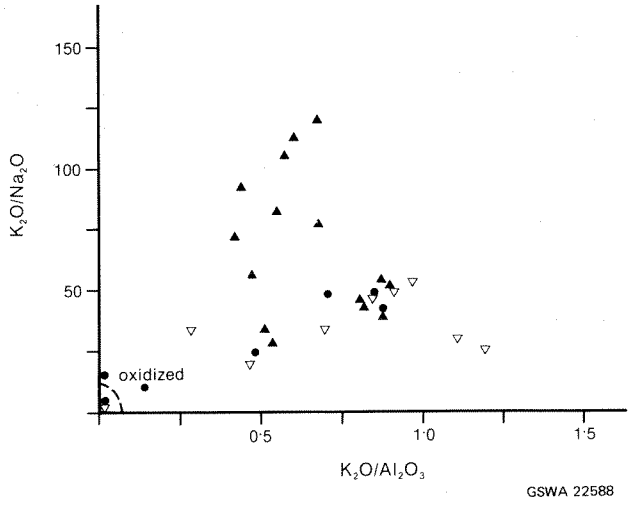


Figure 34. Variation in K_2O/Na_2O *versus* K_2O/Al_2O_3 of Argyle lamproites. Symbols as for Fig. 33. Note the range of values for the "sandy" tuffs and the very low ratios of oxidized and other leached surface samples.

the exception of the oxidized samples, Al_2O_3 contents are uniformly low (3.8 to 7%) in the "non-sandy" tuff and olivine-phlogopite lamproite dykes units, and up to 8% in the "sandy" tuff rocks. The higher Al_2O_3 contents in the "sandy" tuffs may result from incorporation of variable amounts of shale from the Revolver Creek and Lissadell Formations. Most of the Argyle rocks contain less than 10% Fe as FeO, and Fe contents in the "non-sandy" tuff and olivine-phlogopite lamproite dykes increase with decreasing 100 Mg/(Mg + total Fe as FeO) whereas the "sandy" tuffs are progressively depleted in Fe by dilution with SiO_2 (Fig. 34). The CaO contents in the Argyle rocks exhibit a wide range, consistent with the variable degrees of carbonate alteration observed in

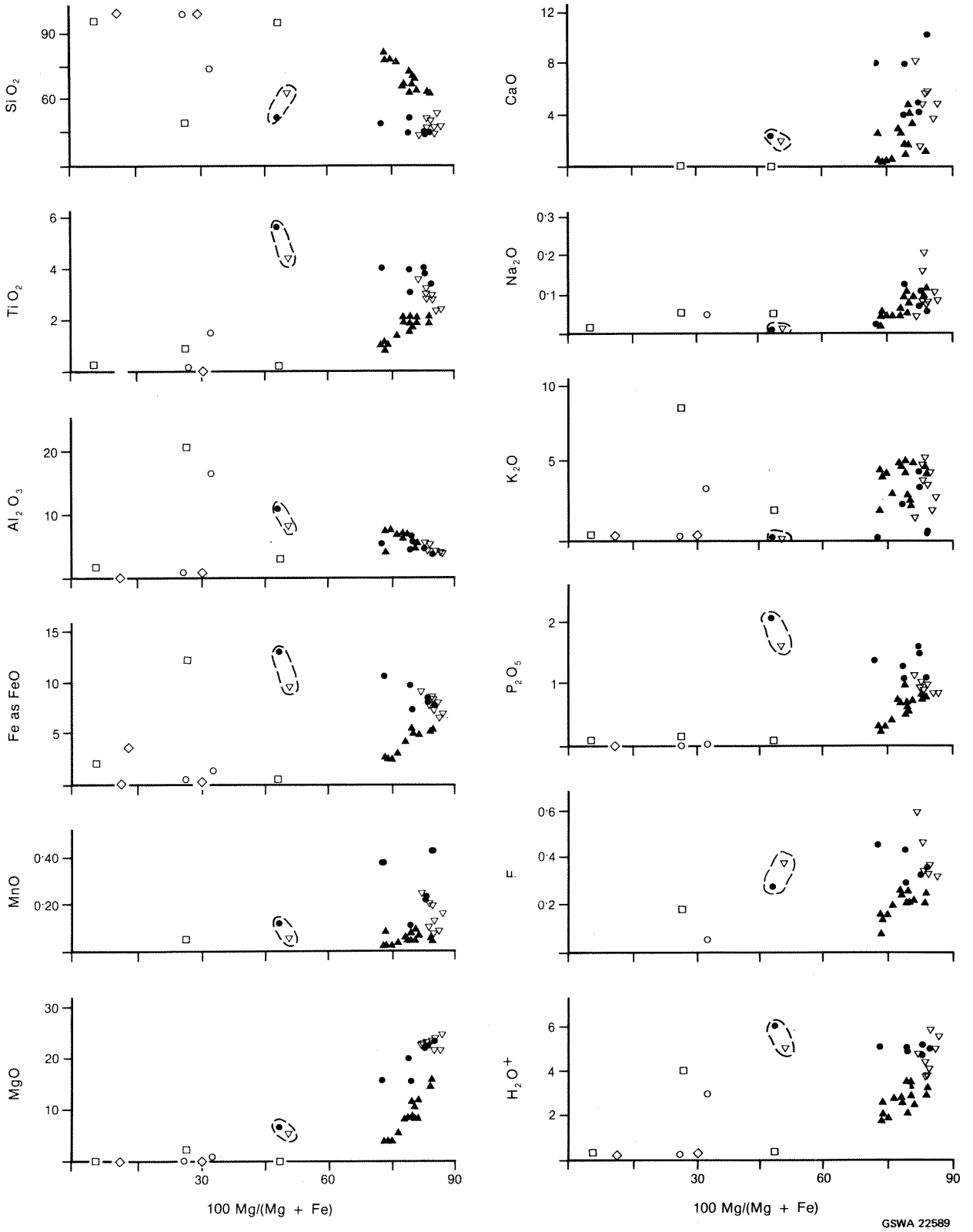


Figure 35. Variation in major elements with 100Mg/(Mg + tot Fe as FeO) for Argyle lamproites and country rocks. All data plotted on H_2O^-- and CO_2-free basis. Symbols as in Fig. 33.

the rocks. The least carbonated samples have low CaO contents (4%) similar to the olivine lamproites of the West Kimberley (Jaques and others, 1984a) (*see* Chapter 5). The Argyle rocks have exceptionally low Na_2O contents (0.2% or less), and this probably reflects both the Na-poor primary composition and the effects of leaching of alkalis during alteration. The oxidized samples are almost totally leached of Na. Potash contents range from exceptionally low values in the leached surface samples to high values (4-6%) characteristic of lamproites (Fig. 34). In contrast, the oxidized samples are enriched in P compared to the bulk of the "non-sandy" tuff and olivine-phlogopite lamproite dykes which have comparatively high P contents (1-1.5% P_2O_5). Both F and H_2O^+ contents are high, ranging up to 0.6% and 6% respectively.

Trace elements

Variation in trace elements within the Argyle pipe rocks is shown in the element *versus* 100 Mg/(Mg + total Fe as FeO) diagrams (Fig. 35). Ba contents range from very low values in the oxidized and leached surface samples to much higher values (up to 3 000 ppm) in some of the dykes (Fig. 36).

The Rb and Sr contents range from comparatively high values in the "non-sandy" tuff and olivine-phlogopite lamproite dykes (300-400 ppm Rb, 750-1 250 ppm Sr) to much lower values in the "sandy" tuffs and the leached and oxidized surface samples. The Rb/Sr ratios range from mean values of about 0.2 to 0.35 to higher values, particularly in the "sandy" tuffs, and lower values in the leached and oxidized surface samples. Although similar in terms of Rb and Sr contents and Rb/Sr ratio, the Argyle lamproites are much less enriched in Ba than the West Kimberley rocks (Jaques and others, 1984a) (*see* Chapter 5).

Lead contents are typically 20 to 30 ppm or less, but some very high Pb contents reflect the presence of galena and other sulphides. Thorium and uranium contents are typically lower than found in the West Kimberley lamproites (Jaques and others, 1984a) (*see* Chapter 5). Significantly, the U contents of the oxidized samples are higher than the remainder of the samples despite the fact that U in the oxidized (VI) valence state is very soluble under a wide range of pH and is readily leached.

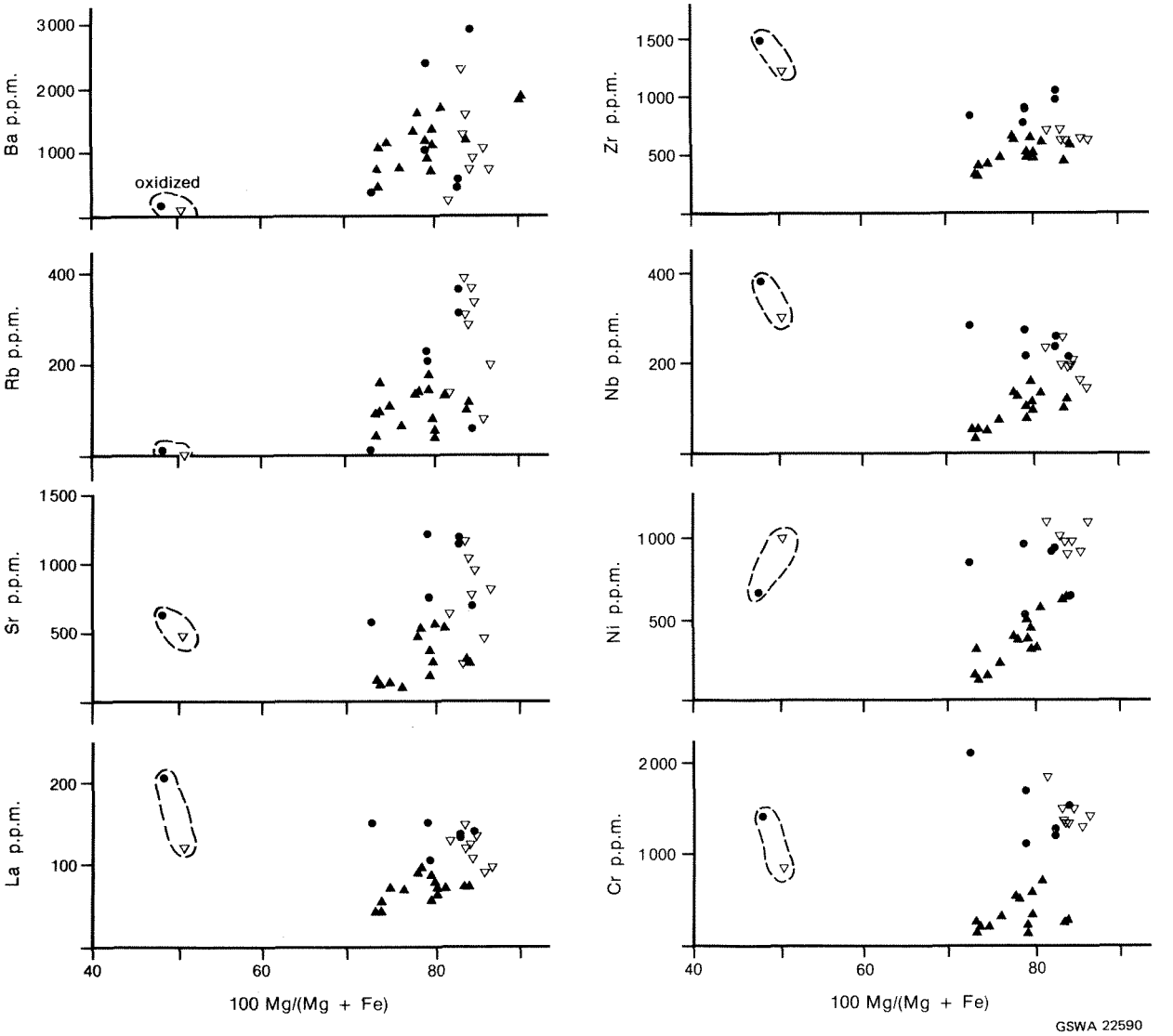


Figure 36. Variation in trace elements with 100Mg/(Mg + tot Fe as FeO) for Argyle lamproites and country rocks. Symbols as in Figure 33.

Zirconium and niobium contents are high, averaging 650 to 900 ppm Zr and 150 to 300 ppm Nb in the "non-sandy" tuff and olivine-phlogopite lamproite dykes. Zirconium and niobium contents in the oxidized samples are slightly higher than the remainder of the suite (Fig.36). The Zr/Nb ratios typically lie in the range 3 to 4 for "non- sandy" tuff and olivine-phlogopite lamproite dyke rocks, but range up to 9 in the "sandy" tuffs.

The Argyle rocks have high abundances of light rare earth elements (LREE) as shown by the high contents of La (90-150 ppm) and Ce (200-300 ppm) in the "non-sandy" tuff and olivine-phlogopite lamproite dyke samples. Yttrium contents are low (20-30 ppm), indicating that the Argyle lamproites are strongly enriched in LREE relative to heavy REE. The Argyle lamproites are much less enriched in LREE than the West Kimberley lamproites which contain LREE at 500 to 2000 times chondritic abundance (Jaques and others, 1984a).

The "non-sandy" tuff and olivine-phlogopite lamproite dyke rocks have similar high Ni and Cr contents (average 800-1100 ppm Ni, 1100-1800 ppm Cr) in accord with their high 100 Mg/(Mg + total iron as FeO) ratios. The "sandy" tuffs are progressively depleted in Ni and Cr (Fig.35). Vanadium contents lie in the range 50 to 150 ppm, whereas Sc contents range from 5 ppm in the "sandy" tuffs to 25 ppm in the oxidized samples.

The overall similarity of the least altered "non-sandy" tuff and olivine-phlogopite lamproite dykes is shown by their strongly overlapping fields on the variation diagrams examined. The similarity is further enhanced on "incompatible element" ratio plots such as Zr/Nb versus Ti/Zr (Fig. 37). On all the diagrams examined, the "sandy" tuffs form a field which overlaps all or part of the fields defined for the "non-sandy" tuff and olivine-phlogopite lamproite dyke fields. This strongly implies that the three units are in fact comagmatic and that the small geochemical differences betwen them reflect different degrees of crystallization and, possibly, the effects of alteration.

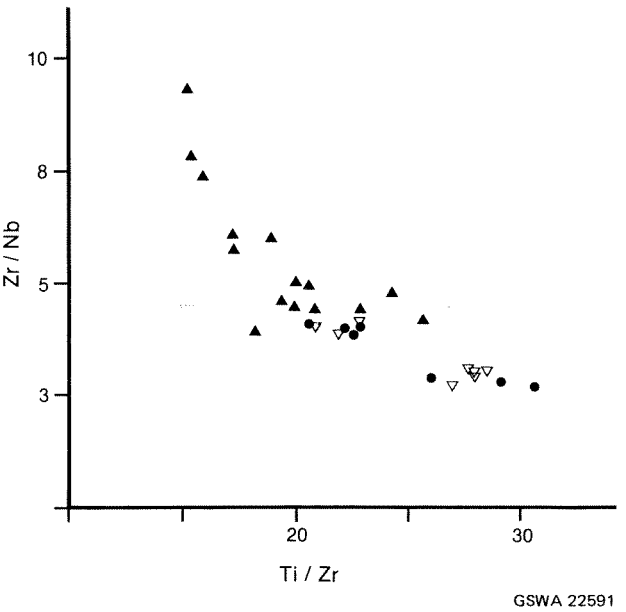


Figure 37. Zr/Nb *versus* Ti/Zr diagram for Argyle lamproites, showing the wide variation in "sandy" tuffs (filled triangles), and the overlap of "non-sandy" tuffs (inverted triangles) and olivine-phlogopite lamproite dykes (filled circles).

LAMPROITE AND LAMPROPHYRE DYKES

LISSADELL ROAD DYKES

The Lissadell Road Dykes (Fig. 38) form a discontinuous *en echelon* series of small stringers and dykes trending for 2.5 km northeastwards towards the Argyle Pipe and intruding the Bow River Granite of the Lamboo Complex. The individual dykes vary from a few millimetres to one metre in width, and exposures in prospecting trenches show typical dyke orientations to be 300°-320°, despite the east-northeast trend of the dykes overall. Each dykelet can rarely be traced more than 10 m before it pinches out; the structural implication is that the dyke has been emplaced in tension gashes resulting from shear movement along the Lissadell dyke trend.

Closely associated with the Lissadell Road Dykes are quartz veins, which preferentially intrude the dykes and follow the same orientation. Disseminated sulphides of copper, cobalt, nickel, iron, and lead, are prominent and testify to the use of this fracture zone as a channel for migrating ore fluids as well as magma. Surface outcrops of quartz, plus minor carbonate, occasionally mark the position of the dyke where the associated quartz veins are sufficiently wide and robust. Two boreholes, LRD-2 and LRD-5 were drilled to intersect the dykes at depth (Fig. 40). LRD-2 intersected a lamproite dyke 3 m wide at a depth of 46 to 50 m; LRD-5 encountered 0.75 m of lamproite at 31 m depth. Both holes encountered chloritic stringers cutting the granitic country rock close to the main lamproite contacts; these are probably very thin lamproite dykes.

Bulk-sampling operations yielded 6.41 CM of diamond from 42 m^3 of dyke and country rock material. Country-rock contamination could not be avoided as the bulldozed costeans were much wider than the dyke. The diamond grade is probably very high but insufficient material is available. The diamonds recovered strongly resemble those from the Argyle Pipe: they are predominantly brown, rounded dodecahedral stones with characteristic hexagonal surface depressions.

The mineralogy and texture of near-surface material from prospect trenches has been largely destroyed by silicification and carbonation. Some surface samples, however, preserve a relic texture of large macrocrysts of former olivine up to 6 mm across and smaller groundmass olivine up to 1 mm, now totally replaced by quartz, in a green chloritic groundmass with blebs of leucoxene (possibly replacing perovskite), minor sphene, secondary iron oxides, and accessory apatite. In less silicified samples, the olivine is replaced by talc; and the groundmass chlorite appears to have replaced original mica plates up to 1 mm long. Minor carbonate alteration is ubiqitous. Even at a depth of 50 m in borehole LRD-2, the rock is still altered to a quartz-

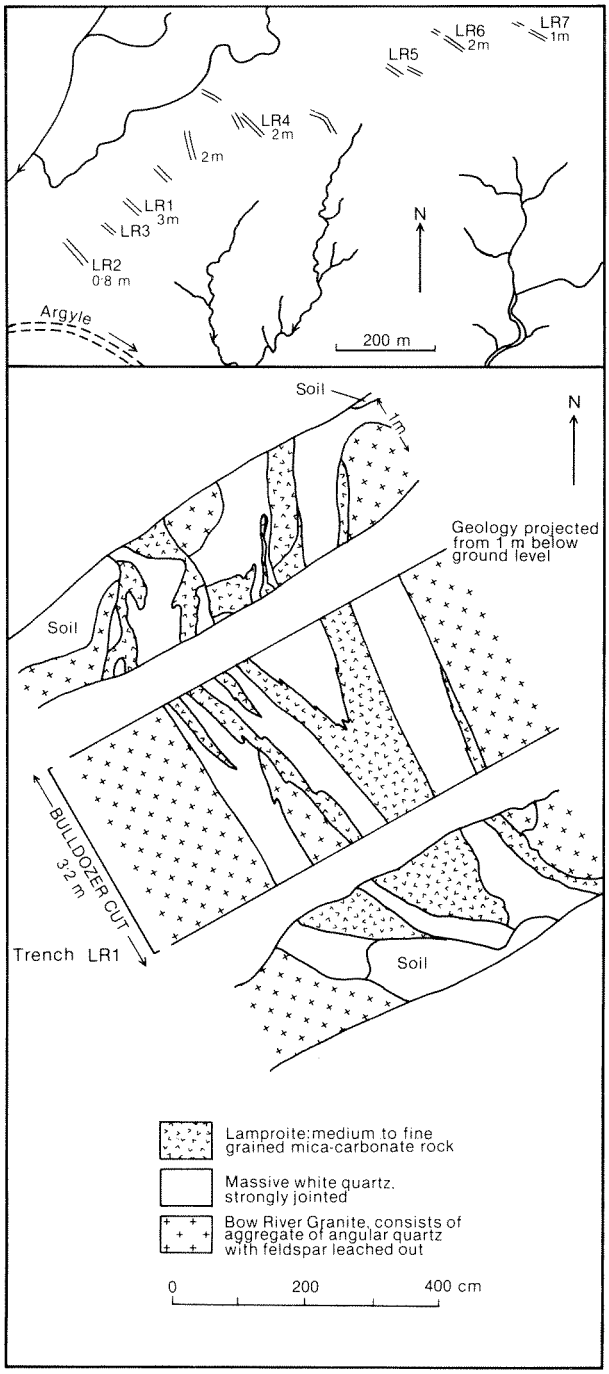


Figure 38. Geological sketch map and trench section of the Lissadell Road Dykes (after Ryan, 1982b).

chlorite-calcite assemblage. The quartz forms rounded to elongate patches, which preserve the general shape and, occasionally, fracture patterns suggestive of former olivine. The chlorite is a highly magnesian variety; it forms irregular patches interstitial to the quartz, and preserves shapes suggestive of mica plates up to 1 mm. Accessory minerals include squat, orange-yellow prisms of rutile, associated with leucoxene; traces of sphene, apatite, and chrome spinel; and disseminated fine grains of cobaltite, chalcopyrite, pyrite, and galena.

A chemical analysis of material from the drill core LRD-2 is given in Table 28. Many of the more mobile elements such as K_2O and Na_2O are strongly leached and reflect the high degree of alteration. Nevertheless, the high Cr, Ni, and Co, are in keeping with an ultramafic rock; and the kimberlitic affinity is indicated by the moderate to high values for Nb, Zr, Sr, and La.

The Lissadell Road Dykes are too altered to enable their true character to be determined. However, the chemistry indicates an alkaline ultramafic rock, and the Nb *versus* Zr plot (Fig. 11) falls within the field of olivine lamproite. The petrography suggests that the original mineralogy may have been predominantly mica plus olivine. The only kimberlite indicators recovered were chromite and diamond, an assemblage that is characteristic of olivine lamproites. The morphological resemblance of the diamonds to the Argyle stones, the geographic proximity to Argyle, and the trend of the dyke towards the pipe, suggest that this dyke is probably related to the Argyle lamproite.

BOW HILL DYKES

The Bow Hill dykes, a suite of micaceous ultrabasic-basic lamprophyres, occur at 128°13′E, 16°43′ S, some 120 km southwest of Kunnurra, and 22 km west of the Argyle pipe. They were discovered in 1980 after detrital andradite garnet and lamproitic chromite were detected by reconnaissance stream-sediment sampling conducted by CRA Exploration P/L as managers of the Ashton Joint Venture.

The Bow Hill Dykes intrude the Early Proterozoic Bow River Granite of the Lamboo Complex, which underlies much of the Halls Creek mobile Zone. Rb-Sr and K-Ar dating of phlogopite has established an emplacement age for the dykes of 815 Ma (Pidgeon and Smith, in prep.). Eight individual dykes, ranging in thickness from a few centimetres to 13 m, and up to 2 km long, are emplaced *en echelon* over a strike length of 19 km that extends from the O'Donnell Brook some 7 km southwest of Bow Hill (Fig. 39). The strike direction is approximately 030° and is sub-parallel to the major structures, such as the Dunham and Halls Creek Faults, that define the tectonic grain of the Halls Creek Mobile Zone. This close relationship with structure is apparent even on a hand-specimen scale where thin dykes (1-3 cm wide) fill tension fractures and joints, some with conjugate pattern. Exposures are mostly poor because of the deep weathering of both dykes and country rocks, and alluvial cover from the creeks.

The dykes are surrounded by a fenite zone, up to 1 m wide, containing pale-green chlorite (penninite) and pleochroic blue-green amphibole (magnesio-arfvedsonite), both in veinlets and as a pervasive alteration of the granite. In addition, the feldspar phenocrysts in the granite adjacent to the dykes, which in outcrop are salmon pink in colour, are seen in thin section to be altered to sericite.

Petrography

Three main rock types are present in the dykes: fine-grained ultramafic rocks composed largely of secondary minerals; ultramafic olivine-phlogopite lamprophyre; and garnet-phlogopite pegmatite.

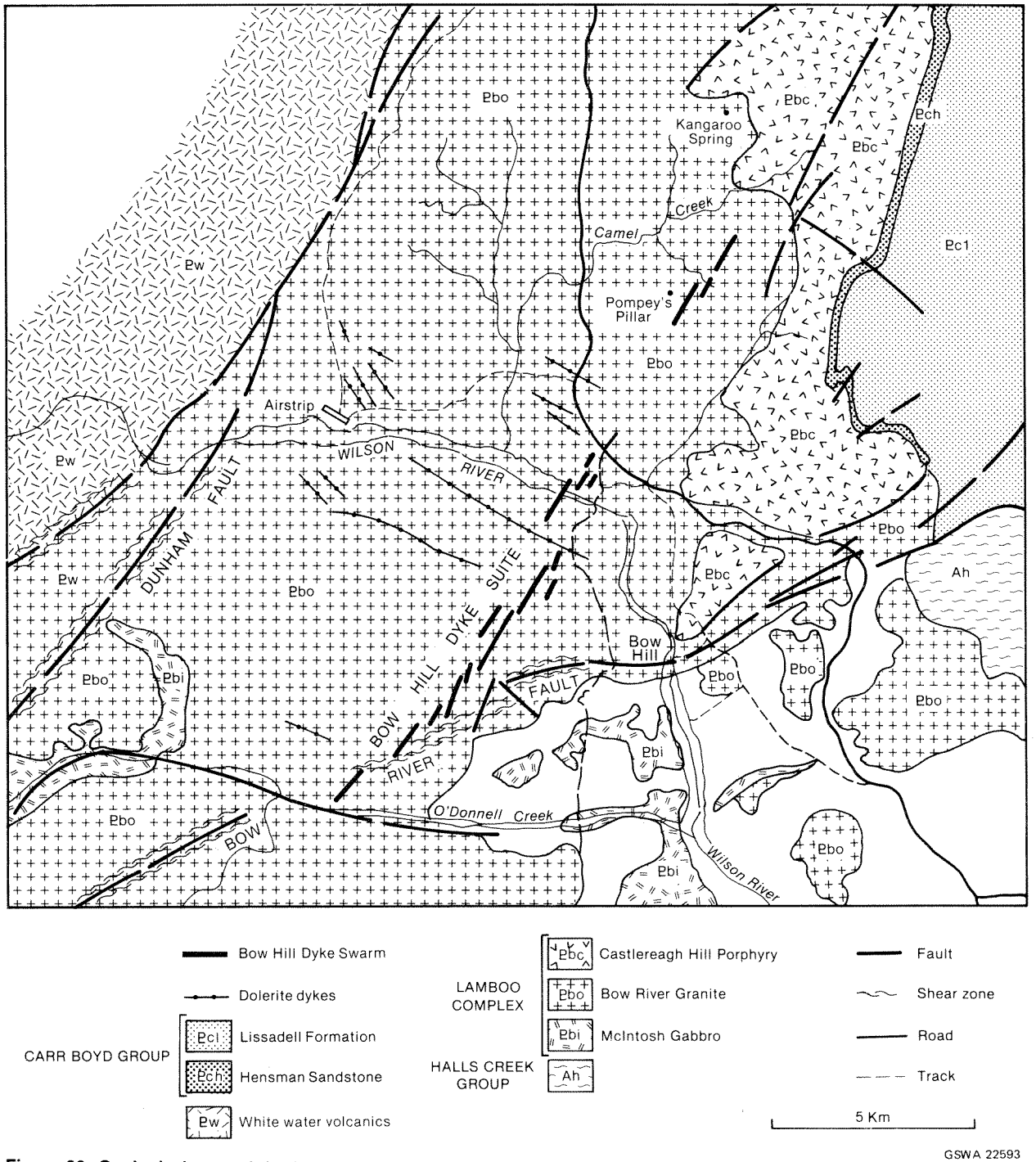


Figure 39. Geological map of the Bow Hill Dykes.

The fine-grained ultramafic rocks typically occur at the margins of the dykes, where they occur as green "chilled" selvedges, and in the smallest dykes, where the primary silicates are totally replaced by green chlorite (peninite) and blue-green alkali amphibole of richterite to magnesio-arfvedsonite composition. Relic chrome spinel is rimmed by magnetite and/or hematite.

The olivine-phlogopite lamprophyre (Fig. 41a) consists of abundant olivine (now altered to serpentine or talc + magnetite) up to 4 mm across and plates of weakly pleochroic mica (pale greenish-tan cores with some red-brown reversely pleochroic tetraferriphlogopite rims) up to 1.5 mm long, together with granular to prismatic clinopyroxene and lesser amounts of interstitial carbonate, apatite, dark red-brown perovskite, spinel, and richteritic amphibole, commonly replacing pyroxene. Interstitial melanite garnet, commonly rimmed by dark turbid granular epidote and sphene, is also present in some olivine-phlogopite lamprophyres. The lamprophyre grades into, and in places is cut by, segregation veinlets, both on a microscopic and on a macroscopic scale up to several millimeters across; these veinlets contain abundant sparry calcite, coarse prismatic diopside, with rims of green pleochroic aegirine-augite, up to 2 mm long, pale alkali amphibole, interstitial clinozoisite, and apatite.

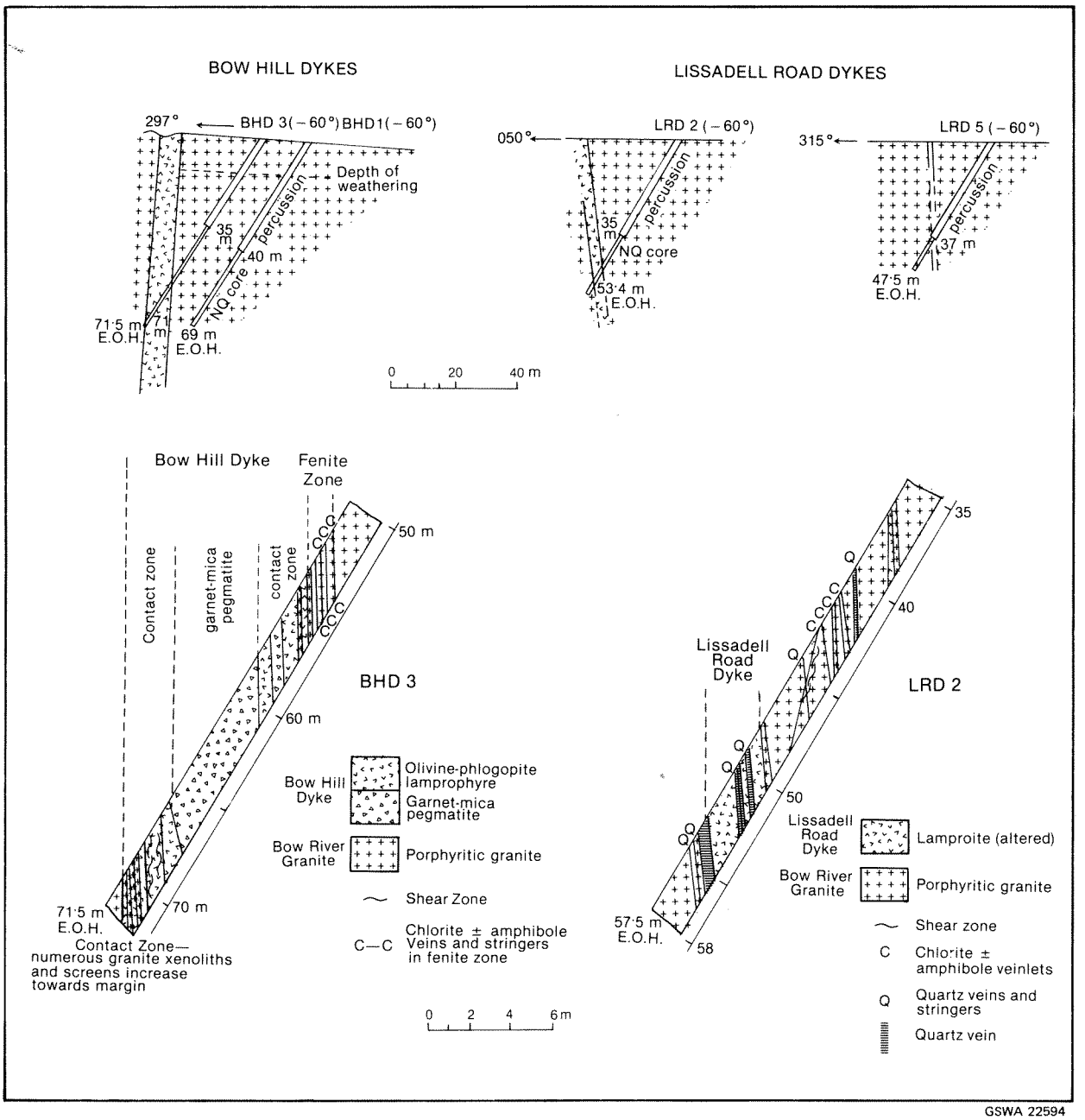


Figure 40. Detailed sections through Bow Hill and Lissadell Road dykes (after Fielding, 1983a).

The garnet-phlogopite pegmatites, which are in places banded, occur both near the margins and in the inner portions of the dykes. Drilling of one dyke showed that garnet-phlogopite pegmatite occupied the entire central portion and comprised nearly half of the dyke (Fig. 40). The garnet-phlogopite pegmatite is composed of abundant, coarse, individual phlogopite plates, up to 4 mm across, and mica aggregates up to 7.5 mm, together with large (up to 1 cm) anhedral to poikilitic garnets with irregular margins. The garnets, which commonly contain inclusions of mica and apatite, are spectacularly zoned in concentric fashion from dark red-brown melanite cores through pale tan to colourless andradite (Fig. 40b). These are set in crystalline groundmass, which contains diopsidic clinopyroxene and apatite prisms, some up to 1 mm, (enclosed by radial intergrowths of carbonate, clinozoisite, and sphene) with abundant richteritic amphibole arranged in sheaf-like form; K-feldspar is present in more altered samples.

Olivine is typically altered, but microprobe analyses of relics show them to be highly magnesian — $Mg_{92-92\cdot8}$ — and to have high Ni contents. The micas show a wide range of compositions (Table 25) from rare Ti-rich biotite cores (Mg_{62-66}, 6% TiO_2) to more typical Al-rich phlogopite (13-15% Al_2O_3, Mg_{89-76}) with variable TiO_2 contents (0.2-3.6%). Tetraferriphlogopite rims have low Ti and Al contents. The pyroxenes range from Na- and Al-poor diopside microphenocrysts to aegirine-augite with up to 6% Na_2O; all have very low Al and Cr contents (Table 26). The amphiboles are colourless richterites containing significant K_2O (up to 1.6%). The spinels (Table 27) range from titaniferous chromite with up to 55% Cr_2O_3 through to titaniferous magnetite with up to 10% TiO_2; all are Mg-poor, contain less than 9% MgO, and thus differ from groundmass spinels in typical kimberlite. The garnets show a wide

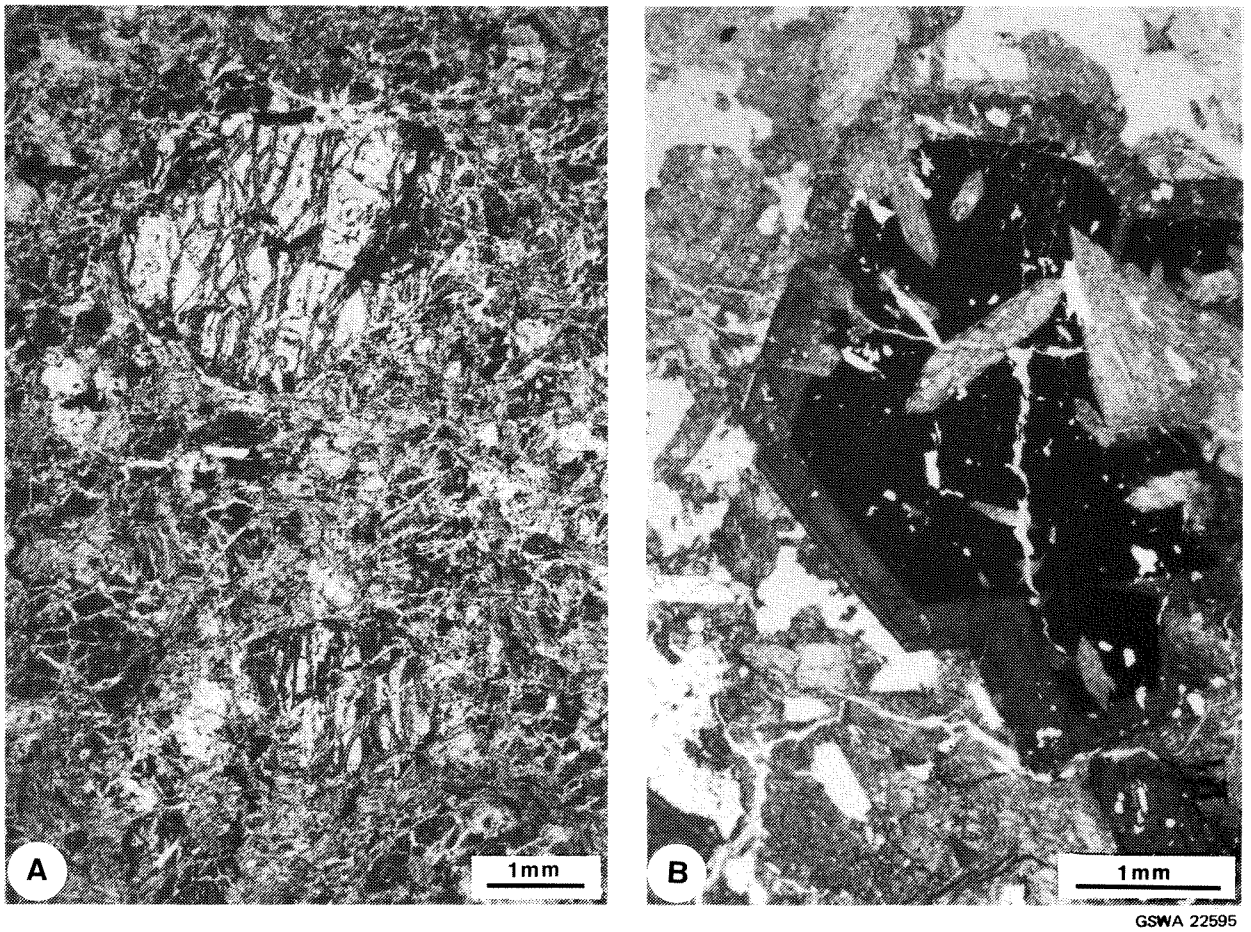


Figure 41. Photomicrographs of the Bow Hill Dykes: A — Altered olivine-phlogopite lamprophyre (GSWA 65999A). B — Garnet in a garnet-phlogopite-diopside pegmatite. The dark, red-brown core is schorlomite enclosing diopside and apatite; the outer pale-coloured zone is melanite/andradite (GSWA 71765).

range in composition, from dark-coloured melanite-schorlomite, with up to 14% TiO_2 and appreciable Zr and Nb, to colourless andradite with <1% TiO_2 (Table 26).

TABLE 25. REPRESENTATIVE ANALYSES OF MICA IN BOW HILL DYKES

	1	*2*	*3*	*4*	*5*	*6*
			Percent			
SiO_2	34.78	37.92	38.36	37.97	37.92	39.28
TiO_2	6.13	1.62	0.28	1.82	1.97	0.07
Al_2O_3	13.78	12.02	5.36	13.83	13.93	13.16
Cr_2O_3	0.33	0.04	nd	nd	nd	nd
FeO	14.97	7.20	11.23	9.06	8.37	9.54
MnO	0.14	0.07	0.12	0.12	0.07	0.12
NiO	nd	0.11	nd	nd	nd	nd
MgO	13.78	23.35	24.93	21.47	22.09	22.08
CaO	0.07	0.12	0.11	0.05	0.02	0.00
BaO	0.70	0.47	0.11	0.90	1.13	1.02
Na_2O	0.40	0.46	0.44	0.42	0.27	0.24
K_2O	9.70	9.70	9.14	9.36	9.74	9.66
F	0.50	1.29	1.02	1.14	0.79	1.06
Cl	0.05	0.03	0.02	0.00	0.00	0.00
Total	**95.32**	**94.39**	**91.12**	**96.16**	**96.29**	**96.23**
$-0\equiv F,Cl$	0.22	0.55	0.44	0.48	0.33	0.45
Total	**95.10**	**93.84**	**90.68**	**95.68**	**95.96**	**95.78**
Mg(a)	62.1	85.3	79.8	80.9	82.5	80.5

(a) Mg = 100 Mg/(Mg + Fe) nd = not detected, detection limit = 0.02% for CaO, 0.04% for NiO.

1-3 — (1) Biotite core; (2) Phlogopite phencryst core; (3) Phlogopite phenocryst rim, olivine-phlogopite lamprophyre, BMR 83211078.

4-6 — (4) Phlogopite inclusion in garnet; (5) Phlogopite core; (6) Green phlogopite rim, garnet-mica pegmatite, BMR 83211077.

Macrocryst minerals recovered from concentrates include chrome spinel (magnesian aluminous chromite), chrome pyrope, and chrome diopside. No diamond was recovered in the bulk-sampling programme.

The Bow Hill Dykes exhibit many petrographic and mineralogical differences from both kimberlite and lamproite. Melanite garnet, in particular, is found in a range of alkaline igneous rocks, but Zr-rich garnets appear to be restricted to a carbonatite paragenesis (Deer and others, 1982). In terms of the composition of the micas and spinels, and the presence of melanite and andradite garnet, sodic amphibole, and epidote; the Bow Hill dykes broadly resemble alnöites. Similar, although more undersaturated, melilite-bearing alnöites occur at Alnö, Sweden (Von Eckermann, 1967), Île Bizzard, Canada (Gold, 1972; Mitchell, 1979) and McKellar Harbour, Canada (Platt and Mitchell, 1982). The apparent absence of melilite and the presence of groundmass diopside in the Bow Hill dykes indicates that they are not as undersaturated as alnöites; however, the above features clearly indicate affinities with carbonatites.

Chemistry

Representative analyses of the Bow Hill dykes are given in Table 28. They indicate intrusions which are ultrabasic (37-44% SiO_2, 15-22% MgO), slightly nepheline normative and peralkaline in the olivine-

TABLE 26. REPRESENTATIVE ANALYSES OF PYROXENES (1-3), AMPHIBOLE (4), CLINOZOISITE (5), APATITE (6), PEROVSKITE (7) AND GARNET (8-10) FROM THE BOW HILL DYKES.

	1	2	3	4	5	6	7	8	9	10
						Percent				
SiO_2	53.06	53.36	51.88	56.69	38.62	0.99	nd	28.89	33.01	35.49
TiO_2	0.53	0.45	1.25	1.00	0.05	nd	49.81	13.82	5.11	0.64
Al_2O_3	0.68	0.47	0.77	0.20	28.60	nd	0.08	0.90	1.42	3.39
Cr_2O_3	0.40	nd	0.03	0.03	nd	nd	0.04	nd	nd	nd
Fe_2O_3	2.89	4.26	14.54	—	6.41	0.16	—	18.48	26.37	26.16
FeO(a)	2.86	3.73	2.79	2.48	—	—	2.23	2.66	—	—
MnO	0.13	0.22	0.36	0.05	nd	nd	nd	0.42	0.33	0.07
NiO	0.09	0.07	nd	nd	nd	nd	nd	nd	nd	nd
MgO	14.50	13.35	7.40	22.92	0.10	nd	nd	0.79	0.51	0.23
CaO	24.50	23.31	15.87	6.90	23.21	51.62	32.56	32.36	33.45	34.42
Na_2O	0.73	1.32	5.56	6.08	0.07	0.16	1.67	0.27	0.10	nd
K_2O	0.00	0.02	0.00	2.43	0.00	0.03	—	nd	nd	nd
P_2O_5	0.03	0.04	nd	nd	0.05	39.45	—	—	—	—
Nb_2O_5	—	—	—	—	—	—	4.11	1.00	0.28	nd
ZrO_2	—	—	—	—	—	—	nd	0.83	0.07	nd
Total	**100.40**	**100.56**	**100.45**	**98.78**	**97.11**	**92.41**	**90.58**	**100.42**	**100.65**	**100.40**
Mg(b)	82.6	75.9	45.4	94.3	—	—	—	6.81	9.59	1.71

(a) Fe determined as FeO; Fe_2O_3 and FeO calculated from stoichiometry. (b) Mg = 100 Mg/(Mg + Fe).

1-3 — (1) Granular diopside; (2) Elongate diopside; (3) green pleochroic aegirine augite rim; Olivine-phlogopite lamprophyre, BMR 83211078.

4 — Colourless richterite replacing pyroxene. (5) Granular clinozoisite. 6 — Apatite; olivine-phlogopite lamprophyre, BMR 83211078. 7 — Dark red brown perovskite; olivine-phlogopite lamprophyre, BMR 83211073. 8-10 — (8) Dark red-brown schorlomite core; (9) Pale tan melanite rim; (10) Colourless andradite outer rim; garnet-mica pegmatite, BMR 83211077.

TABLE 27. REPRESENTATIVE ANALYSES OF GROUNDMASS SPINELS FROM THE BOW HILL DYKES

	1	2	3	4
		Percent		
TiO_2	3.28	3.47	9.82	7.38
Al_2O_3	1.49	1.38	3.22	0.29
V_2O_3	0.13	nd	nd	0.15
Cr_2O_3	54.94	32.16	2.99	0.41
Fe_2O_3(a)	10.20	29.82	43.90	54.04
FeO	21.80	29.42	36.90	35.75
MnO	0.48	2.22	1.51	1.19
MgO	8.58	2.26	1.50	0.63
CaO	nd	0.13	nd	nd
Total	**100.90**	**100.85**	**99.84**	**99.85**
Mg (b)	0.412	0.120	0.068	0.030
Cr/R^{3+}(c)	0.821	0.514	0.060	0.008
Fe^{3+}/R^{3+}(c)	0.145	0.454	0.843	0.984

(a) Fe determined as FeO; FeO and Fe_2O_3 calculated from stoichiometry. (b) Mg = $(mg + Fe^{2+})$. (c) $R^{3+} = Cr + Al + Fe^{+3}$. nd — not detected, detection limit (EDS) = 0.06—0.10%.

1-2 — Titaniferous chromite. 3 — Titaniferous chromian magnetite. 4 — Titaniferous magnetite. Olivine-phlogopite lamprophyre, BMR 83211073.

phlogopite lamprophyes to Mg-poor, Ca-rich (<10% MgO, >20% CaO) compositions which are saturated to slightly oversaturated in silica in the garnet-mica pegmatites. All have high K_2O contents (1.5-6%) and high K_2O/Na_2O ratios (5-20). Calcium oxide increases from modest values (<10%) in the olivine-phlogopite lamprophyres to very high in the carbonate-rich, garnet-mica pegmatites (up to 32%); this is reflected in the presence of larnite in the CIPW norm. The olivine-phlogopite lamprophyres have moderatley high Ni and Cr contents (600-1300 ppm). The Bow Hill dykes show slight to moderate enrichment in incompatible elements such as Ba, Rb, Ti, Nb, and F (Table 28). The dykes show a decrease in Zr content from the olivine-phlogopite lamprophyres to the garnet-mica pegmatites as a consequence of crystallization of Zr-rich garnet.

TABLE 28. ANALYSES OF EAST KIMBERLEY LAMPROITIC AND KIMBERLITIC DYKES

	1	2	3	4	5
			Percent		
SiO_2	44.8	34.9	37.4	40.3	23.1
TiO_2	2.85	2.06	2.30	1.59	4.1
Al_2O_3	4.65	6.80	10.70	8.74	3.2
Fe_2O_3	0.34	—	—	—	—
FeO	4.45	(a)10.30	(a)10.84	(a)6.65	(a)9.7
MnO	0.45	0.38	0.31	0.18	—
MgO	7.6	9.49	15.8	19.4	9.0
CaO	16.3	24.5	13.4	9.79	23.4
BaO	—	0.22	0.60	0.49	0.04
K_2O	<0.01	2.81	4.89	6.24	0.15
Na_2O	0.02	0.29	0.39	0.95	—
P_2O_5	0.91	2.47	0.64	0.34	0.66
SO_3^+	0.16	—	—	—	—
H_2O^+	3.60	—	—	—	—
H_2O^-	0.15	—	—	—	—
CO_2	13.2	—	—	—	—
LOI	—	4.71	1.85	4.69	—
Rest	0.44	0.53	0.40	0.35	0.32
Total	**99.92**	**99.46**	**99.52**	**99.71**	**(73.67)**
			Parts per million		
Cr	1050	36	462	561	570
Co	105	53	74	66	75
Ni	850	68	179	668	460
Rb	—	—	—	—	5
Sr	210	905	309	410	780
Y	—	34	22	15	—
Zr	690	17	75	164	340
Nb	210	373	417	216	220
Ba	40	1980	5350	4400	350
La	120	1100	617	197	—
Ce	—	1300	715	277	—
Nd	—	458	245	113	—
Sm	—	57	41	17	—
Eu	—	10	6	2	—
Yb	—	<2	<2	<2	—
Sc	—	17	29	29	—

(a) Total Fe as FeO

1 — Lissadell Road Dyke, CRA958119. 2,3,4 — Bow Hill Dyke, CRA958106, 958107, 958108. 5 — Maude Creek Dyke, CRA MACK

Analyses by Analabs, Perth. Co, Ni, by atomic absorption; REE by ICP; Na_2O, SO_3, FeO, CO_2 by chemical methods; remainder by XRF.

The Bow Hill dykes are strongly enriched in LREE at 300-750 times chondrites, and have very low abundances of Sc and HREE. One sample of garnet-mica pegmatite contained extremely high LREE (La = 1100 ppm).

The Bow Hill lamprophyres have many of the chemical features of alnöites and kimberlites, but are not as undersaturated in silica. They are considered to be mica lamprophres of carbonatitic affinity. Their similarity in age (815 to 854 Ma; Pidgeon and Smith, in prep.) and in Nd and Sr isotopic compositions (Sun and others, 1986) suggests that the Bow Hill dykes may be related to the Cummins Range carbonatite, which lies some 350 km to the south, at the intersection of the King Leopold and Halls Creek Mobile Zones.

KIMBERLITIC DYKES

MAUDE CREEK DYKE

The Maude Creek Dyke (Smith, 1978b) is a 1.5 m-wide kimberlite dyke located at 127°46'E, 16°45' S (CHAMBERLAIN, GR:785478). The dyke occupies a slight, clay-filled depression between rocky outcrops of Proterozoic Hart Dolerite. The dolerite forms a sill, about 500 m thick, which was intruded into the Luman Siltstone of the Speewah Group close to its contacts with the overlying King Leopold Sandstone of the Kimberley Group. The kimberlite dyke trends north-northeast, and has been exposed in a bulldozer cut along a strike length of 22 m (Fig. 42). However, a photo lineament associated with the dyke extends for 2 km, and kimberlite indicator-mineral patterns from stream-drainage sampling suggest that the dyke is associated with this lineament over its full length.

In the bulldozed costean, the dyke has sharp contacts with the dolerite, and dips west at 70 to 90°. The kimberlite is weathered to a pale greenish yellow and is extensively carbonated. Xenoliths make up approximately 2% of the rock and are mainly angular dolerite blocks up to 30 cm across, although one rounded, decomposed, coarse-grained granitic xenolith was seen. The central zone of the dyke contains abundant, rounded, altered dunitic xenoliths from 0.5 to 2 cm diameter, and rare nodules of green, chloritized mica up to 1.5 cm have also been recorded.

Prospecting operations on the Maude Creek Dyke yielded one diamond weighing 0.05 CM from the treatment of +0.8 mm material from a bulk sample of 4.6 t. A further five microdiamonds were recovered from processing 80 kg of kimberlite down to 0.15 mm.

The distribution of kimberlite indicator minerals in stream gravels from the Maude Creek area suggests the presence of a further eight or more kimberlite dykes (Fielding, 1983a), none of which have been positively located.

Petrography

Kimberlite from the marginal zone is porphyritic with subhedral to rounded serpentinized olivines from 0.5 to 4 mm across. The olivine pseudomorphs are frequently

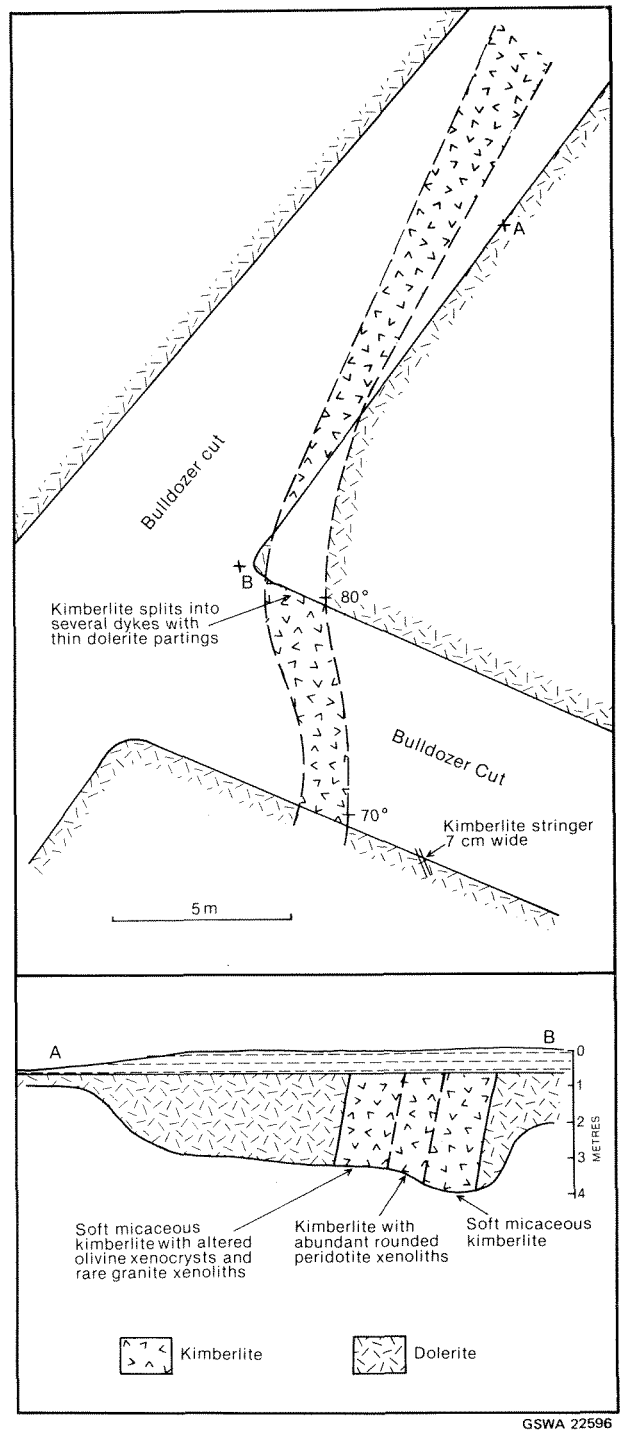


Figure 42. Geological sketch map of Maude Creek Dyke (after Smith, 1978).

bordered by titanomagnetite granules containing small amounts of chrome (Figs 44, 45). In some specimens, ragged plates of pale brown to colourless phlogopite up to 1.5 mm, partly altered to pale green chlorite are common. The mica encloses small spinels and turbid patches of leucoxene. The groundmass contains abundant secondary calcite and accessory apatite, sphene, perovskite, and xenotime.

Specimens from the central zone are strongly carbonated and consist of small, rounded, sepentinized ultramafic nodules, 0.5 to 2 cm diameter, and less common, rounded picroilmenites, up to 1 cm, in a groundmass of carbonate, chlorite, mica, granular



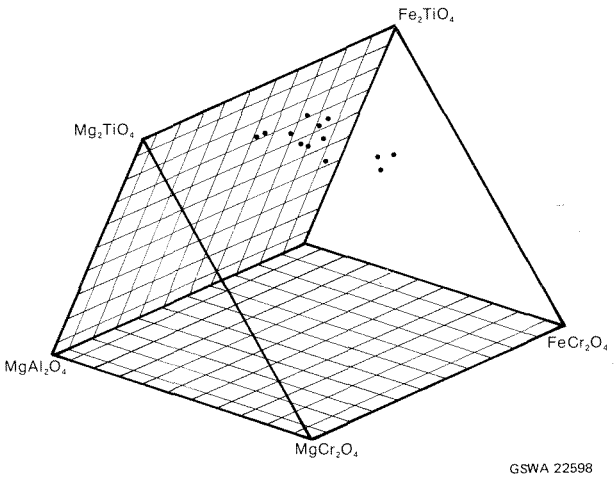
GSWA 22597

Figure 43. Photomicrograph of Maude Creek kimberlite, with rounded, serpentinized dunitic nodules in a groundmass of carbonate, serpentine, chlorite, and secondary spinels (GSWA 65992).

chromite, and secondary spinels (Fig. 43). Rare macrocrysts of pyrope and chrome diopside are also present. The nodules preserve no recognizable relic textures; and are commonly a mass of serpentine that has been veined by secondary magnetite. Many of the nodules are rimmed by chlorite and a narrow zone of fibrous calcite. Less altered portions of the groundmass preserve a texture similar to that of the marginal kimberlite. The rock is also traversed by late calcite veins about 0.2 mm wide.

Mineralogy and chemistry

No macrocrystal spinels have been recovered from Maude Creek Dyke. Analyses of groundmass spinels, which border the olivine pseudomorphs, are given in Table 29 and plotted in Figs 44 and 45. The plots show some scatter, but describe an overall trend from chromite towards titanomagnetite; however, there is an apparent compositional gap in the middle of the range. Figure 45 shows that the spinels fall outside the field for kimberlitic spinels as defined by Mitchell (1985) because of their high $Fe^{2+}/(Mg + Fe^{2+})$ ratios.



GSWA 22598

Figure 44. Spinel prism plot (using Ti, Al, Cr and Fe^{2+}) of groundmass spinels from Maude Creek dyke.

TABLE 29. REPRESENTATIVE ANALYSES OF ILMENITES AND SPINELS FROM MAUDE CREEK, DUCK CREEK, AND DEVILS ELBOW NO. 3 DYKES.

	Ilmenite							*Chromite*				*Spinel*			
	1	*2*	*3*	*4*	*5*	*6*	*7*	*8*	*9*	*10*	*11*	*12*	*13*	*14*	*15*
								Percent							
SiO_2	nd	nd	nd	nd	0.02	0.01	0.03	nd	0.03	0.04	0.10	nd	nd	nd	nd
TiO_2	49.88	49.06	53.00	51.22	50.46	44.77	44.77	0.01	1.28	1.61	1.91	13.44	12.40	18.18	10.27
Al_2O_3	0.34	0.67	0.72	nd	0.32	nd	nd	24.59	10.67	3.49	5.58	7.01	3.90	7.17	12.26
V_2O_3	nd	0.32	nd	0.43	—	—	—	—	—	—	—	nd	nd	0.27	nd
Cr_2O_3	0.31	0.61	0.48	0.42	0.99	3.20	0.71	45.66	49.95	61.59	55.91	nd	4.65	14.84	2.96
Fe_2O_3(a)	11.57	11.70	8.77	9.30	9.23	17.09	17.61	0.65	8.66	5.28	5.08	40.48	41.75	12.67	33.73
FeO(a)	29.22	29.45	23.60	29.11	30.14	29.16	30.51	13.94	17.60	15.05	20.19	27.45	26.32	40.31	35.97
MnO	0.16	0.19	nd	nd	0.26	0.23	0.24	0.52	0.59	0.69	0.65	1.07	1.34	2.21	0.93
MgO	8.68	8.12	13.43	9.51	8.37	6.19	5.37	13.90	10.73	11.89	8.71	10.55	8.66	4.21	3.59
CaO	nd	nd	0.09	nd	nd	nd	nd	nd	0.01	nd	nd	nd	0.30	nd	0.30
Total	**100.16**	**100.12**	**100.09**	**99.99**	**99.78**	**100.64**	**99.24**	**99.28**	**99.53**	**99.64**	**98.13**	**100.00**	**(b)100.00**	**100.00**	**100.00**
Mg(c)	34.6	32.9	50.3	36.8	33.1	27.5	23.9	64.1	52.8	58.5	43.9	40.7	37.0	15.7	15.1
								Ratio							
Cr/R^{3+}(d)								0.550	0.674	0.855	0.810	—	0.093	0.395	0.056
Fe^{3+}/R^{3+}(d)								0.008	0.111	0.070	0.070	0.787	0.792	0.321	0.602

nd = not detected. (a) Fe determined as FeO and calculated to Fe_2O_3 and FeO from stoichiometry. (b) Includes 0.66% ZnO. (c) Mg = 100Mg/(Mg+Fe). (d) $R^{3+} = Cr + Al + Fe^{3+}$.

1-2 — Macrocryst ilmenite, Maude Creek. 3-4 — Macrocryst ilmenite, Duck Creek. 5-6 — Macrocryst ilmenite, Devils Elbow No.3. 8-11 — Macrocryst chromite, Devils Elbow No.3. 12-15 — Groundmass spinel, Maude Creek.

Analyses 1-4, 12-15 by EDS (A. Benn, analyst, CRAE), analyses 12-15 normalized to 100%. Analyses 5-11 by WDS, data from Garlick (1982).

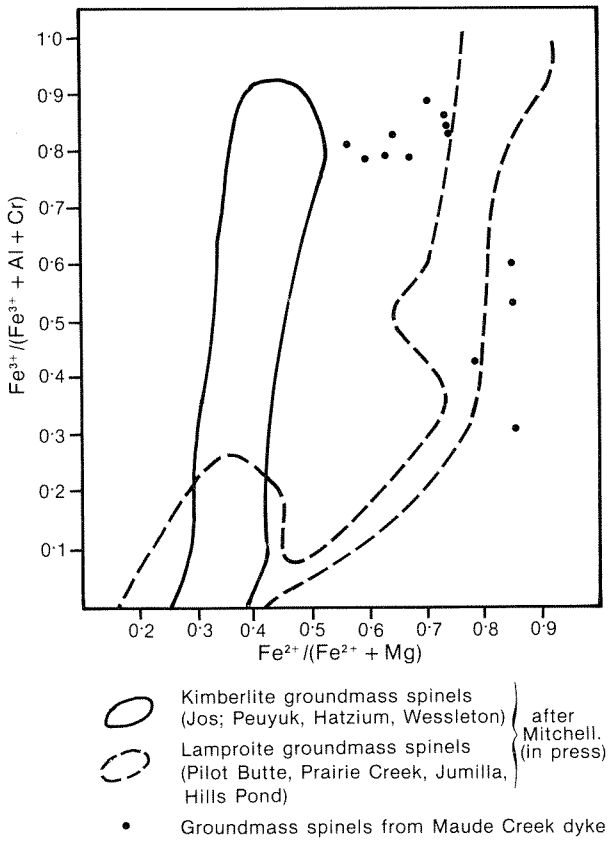


Figure 45. Plot of Fe^{2+}/Mg face of the oxidized spinel prism for groundmass spinels from Maude Creek dyke.

An $MgTiO_3$-$FeTiO_3$-Fe_2O_3 plot for the ilmenite macrocrysts (Fig. 46) shows that they fall within the kimberlitic field as defined by Mitchell (1977). Clinopyroxene compositions plotted on a Ca-Mg-Fe diagram (Fig. 47) show that some are subcalcic, as are to those of the Skerring kimberlite of the North Kimberley Province; and that they resemble pyroxenes from sheared lherzolite nodules from Lesotho

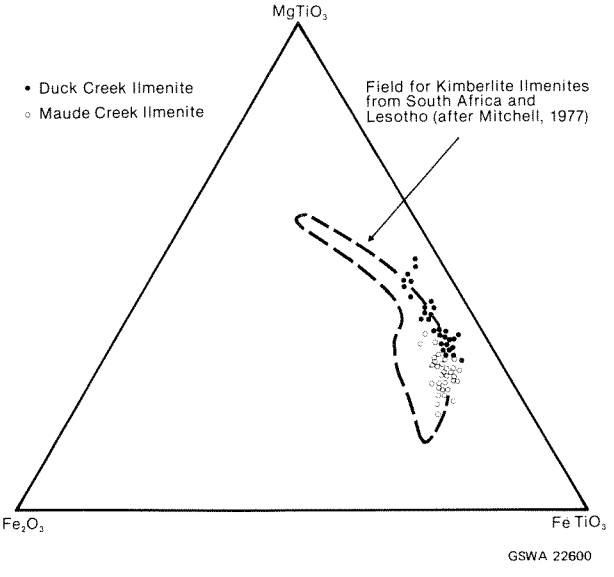


Figure 46. $MgTiO_3$-$FeTiO_3$-Fe_2O_3 plot for ilmenite macrocrysts from Maude Creek and Duck Creek kimberlite dykes.

kimberlites (Nixon and Boyd, 1973); whereas the remainder fall close to the field for Lesotho granular lherzolite clinopyroxenes.

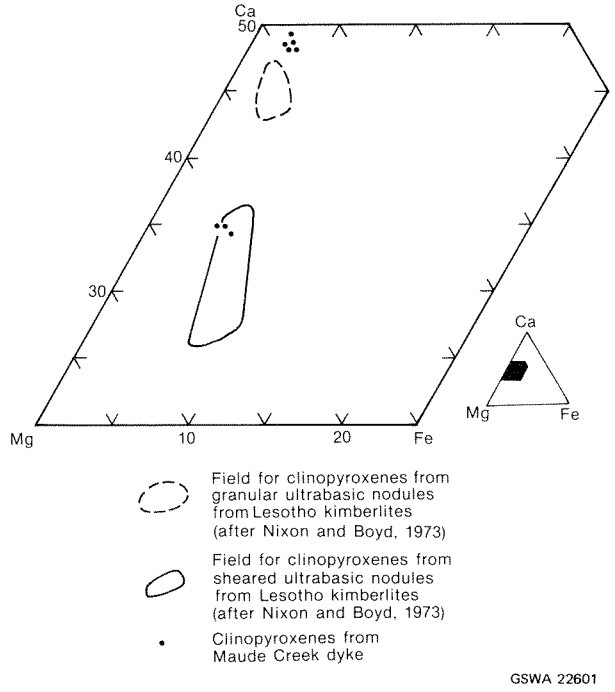


Figure 47. Ca-Mg-Fe plot for clinopyroxene macrocrysts from Maude Creek dyke.

Garnets (Table 30, Fig. 48) are pyropes with varying Ti and Cr contents. They range from groups 1 and 2 through to 9, 10 and 11 of Dawson and Stephens (1975). The CaO *versus* Cr_2O_3 plot (Fig. 49) shows that, while most of the garnets plot within the normal lherzolite field, a small proportion of low calcium, "G10" garnets (Gurney, 1984) also occur.

The extreme carbonation of the dyke is reflected in the analysis in Table 28. Calcium oxide at 23.4% is dominant, and SiO_2 at 23.1% and MgO at only 9.0% are low for a kimberlitic rock. Alkalis have been almost completely leached. The trace-element analysis shows the expected high Cr, Co and Ni values of a kimberlitic rock, associated with high Nb, Sr, Ba and Zr contents. On a Nb *versus* Zr plot (Fig. 11) the Maude Creek composition lies closer to the field for kimberlites than for lamproites.

The petrography shows that the Maude Creek Dyke is a mica peridotite containing abundant picroilmenite and pyrope macrocrysts, dunitic xenoliths, and traces of diamond. In this respect it resembles kimberlite, and no minerals characteristic of the lamproite association (*e.g.* leucite, potassic-richterite, priderite, etc.) have been seen. The Nb *versus* Zr plot (Fig. 11) is more suggestive of kimberlite than lamproite, however the groundmass spinel compositions (Figs 44, 45) are not typical of kimberlite as defined by Mitchell (1985).

DEVILS ELBOW DYKES.

The distribution of kimberlite indicator minerals in stream samples from the Devils Elbow area suggests the presence of five or more kimberlitic bodies (Fielding,

TABLE 30. REPRESENTATIVE ANALYSES OF DIOPSIDE AND GARNET FROM MAUDE CREEK AND DEVILS ELBOW NO. 3 DYKES.

	Diopside				*Garnet*							
	Maude Creek				*Maude Creek*					*Devil's Elbow No. 3*		
	1	*2*	*3*	*4*	*1*	*2*	*3*	*4*	*5*	*6*	*7*	*8*
					Percent							
SiO_2	54.23	53.81	56.11	55.91	41.93	42.25	41.06	41.94	41.07	41.89	42.25	43.43
TiO_2	nd	nd	nd	nd	nd	0.21	nd	0.74	0.95	0.11	0.01	0.03
Al_2O_3	3.60	2.79	1.21	1.42	17.49	20.88	17.51	21.67	21.30	17.63	16.96	21.82
Cr_2O_3	1.42	1.22	1.48	1.02	8.40	3.85	8.16	0.92	0.85	7.38	8.32	2.05
FeO(a)	1.40	1.60	2.88	3.58	5.78	6.12	7.13	10.05	11.52	6.97	7.08	7.75
MnO	nd	nd	nd	nd	0.32	0.26	0.16	0.32	0.34	0.47	0.48	0.35
MgO	15.74	16.93	20.53	20.65	22.27	21.69	19.45	20.19	19.48	19.62	18.73	20.34
CaO	22.27	23.13	16.49	16.39	3.80	4.73	6.52	4.17	4.48	6.87	7.26	5.38
Na_2O	1.22	0.52	1.07	1.05	nd	nd	nd	nd	nd	—	—	—
Total	**99.88**	**100.00**	**99.77**	**100.02**	**99.99**	**99.99**	**99.99**	**100.00**	**99.99**	**100.95**	**101.09**	**101.16**
Mg(b)	95.2	95.0	92.7	91.1	87.3	86.3	82.9	78.2	75.1	83.4	82.5	82.4
					Ratio							
Ca(c)	0.492	0.483	0.348	0.342	0.097	0.119	0.167	0.104	0.110	0.172	0.187	0.135
Mg(c)	0.484	0.491	0.604	0.600	0.788	0.760	0.691	0.700	0.668	0.684	0.671	0.712
Fe(c)	0.024	0.026	0.048	0.058	0.115	0.120	0.142	0.196	0.222	0.144	0.142	0.152
Cluster Group	—	—	—	—	10	9	9	1	2	9	9	9

nd = not detected. (a) All Fe as FeO. (b) Mg = 100Mg/(Mg+Fe). (c) Ca = Ca/(Ca+Mg+Fe), Mg = Mg/(Ca+Mg+Fe), Fe = Fe/(Ca+Mg+Fe).

Analyses from Maude Creek by EDS (A. Benn, analyst, CRAE). Devils Elbow No. 3 analyses by WDS data from Garlick (1982). Cluster Group from Dawson and Stephens (1975).

1983a). The locations of three of these are known, and all are dykes a metre or less in width. Two of the dykes cut sills of Hart Dolerite and the others are presumed to intrude sediments of the Proterozoic Speewah Group.

Devils Elbow No. 1: This dyke is located at 127° 43′ 27″E, 16° 50′ 55″S (Fig. 22), 3.3 km west of Devils Elbow and 2 km southwest of the fuselage of a crashed Sycamore helicopter, which forms a striking local landmark of shiny stainless steel. Picroilmenite indicator minerals in the soil clearly show the trend of a dyke striking 066° (Smith, 1978b), but a costean bulldozed across the anomaly revealed only weathered dolerite country rock. The dyke is presumed to be a thin stringer petrographically similar to the picroilmenite-rich dykes of Maude Creek and Devils Elbow No. 3 kimberlites.

Devils Elbow No. 2: This dyke is exposed in the bank of MacDonald Creek at 127° 45′ 32″E, 16° 49′ 60″S, 3.6 km north of Devils Elbow and 2.9 km east-northeast of the Sycamore helicopter (Fielding, 1983a). The dyke is 1 m wide and heavily weathered in outcrop. It lacks the abundant picroilmenite which characterizes other dykes in the Devils Elbow/Maude Creek area, but contains abundant, coarse andradite garnet similar to that found in the Bow Hill Dykes. The rock type is probably a micaceous peridotite with lamprophyric affinities. No diamonds were recovered from a bulk sample of 1.1 t processed through a heavy-media plant.

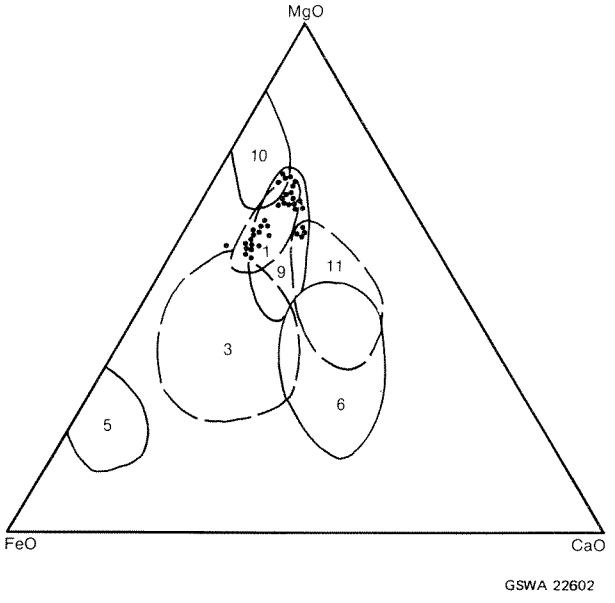


Figure 48. MgO-FeO-CaO plot of garnets from Maude Creek dyke, with fields for cluster groups of Dawson and Stephens (1975).

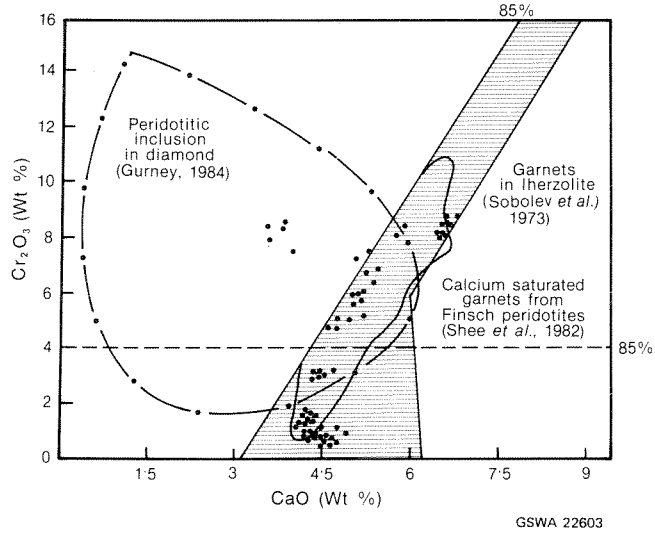


Figure 49. CaO *versus* Cr_2O_3 plot for garnets from Maude Creek dyke. For explanation of the fields see Fig. 18.

Devils Elbow No. 3: This small picroilmenite and pyrope-rich dyke is located on a tributary of Maude Creek (CHAMBERLAIN, GR: 691432). The dyke intrudes the Hart Dolerite and has been exposed by trenching over a distance of 120 m; it strikes about 210°, dips from near vertical to 75° northwest, and has an average width of about 1 m (Garlick, 1982). A 50 t sample of the dyke material was tested for diamond, but none was recovered.

Chromite, picroilmenite, pyrope, and occasional chrome diopside have been recovered from concentrates; representative analyses are given in Tables 29 and 30. The pyropes belong to Group 9 of the Dawson and Stephens (1975) classification and show a wide range in Cr_2O_3 content. Most have high CaO and fall, with rare exceptions (Fig. 50), on the Ca-saturated side of the 85% line separating Ca-poor and Ca-rich pyropes as defined by Gurney (1984). The picroilmenites range from 5.4 to 10.6% MgO and contain variable amounts of Cr (up to 3.2% Cr_2O_3). The chromites show a wide range in Cr_2O_3 content (41-62%) and include Ti-poor (< 1% TiO_2) and Ti-rich (up to 4.3% TiO_2) varieties, as shown in Fig. 51.

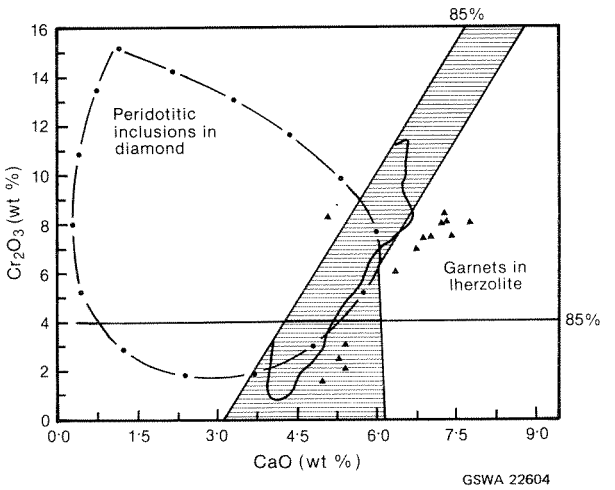


Figure 50. CaO *versus* Cr_2O_3 plot for garnets from Devils Elbow No. 3 dyke. For explanation of the fields see Fig. 18.

OTHER DYKE OCCURRENCES

The distribution patterns of picroilmenite and pyrope garnet in stream samples suggest the presence of kimberlitic bodies, probably dykes, in the Elgee, Dunham and Saw Ranges areas (Fielding, 1983b,c; Smith, 1978b), and in an area about 25 km northeast of Bedford Downs homestead (Gilfillan and Smith, 1977; Gilfillan, 1977) (Fig. 22). Only near Bedford Downs have any of these been located, and both are thought to be kimberlitic dykes petrographically similar to the Maude Creek Dyke although they do not outcrop and have not been exposed by trenching.

Duck Creek Dyke: From the distribution of kimberlite indicator minerals in loam samples, this dyke is traceable for about 1 km along a north-south strike. The dyke is located at 126°33'15"E, 17°7'8"S and intrudes Whitewater Volcanics. The kimberlite contains abundant picroilmenite, Ti-pyrope and Cr-pyrope. Analyses of picroilmenite macrocrysts are given in Table 29, and Fig. 46 shows that their chemistry is similar to picroilmenites from southern Africa.

Blackfellow Creek Dyke: This dyke is located at 127° 34' 58"E, 17°0'40"S, about 12 km north of Duck Creek and west of the Wilson River. The dyke was recognized from the distribution pattern of picroilmenite and garnet in loam samples and has a maximum length of 1 km with a north-south strike.

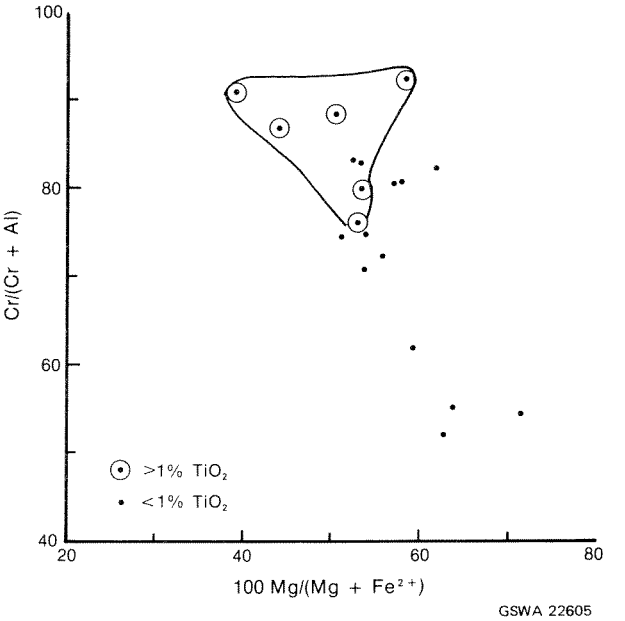


Figure 51. 100Mg/(Mg + Fe^{2+}) *versus* Cr/(Cr + Al) for chromite from Devils Elbow No. 3 dyke.

CHAPTER 5.

THE WEST KIMBERLEY PROVINCE

DISTRIBUTION OF PIPES AND MODE OF EMPLACEMENT

The West Kimberley Province includes all the lamproite bodies discovered in the early period of exploration in Western Australia; and, in addition, the first major diamond discovery at Ellendale. Over one hundred separate lamproite intrusions are known from an area approximately 150 km in diameter (Plate 1). The province occupies an area along the southwest margin of the Kimberley Block and includes parts of the King Leopold Mobile Zone, the Lennard Shelf, and a large part of the Fitzroy Trough. The intrusions are not evenly distributed, but occur as two major concentrations, the Ellendale and Noonkanbah Fields, and several smaller groups.

The largest concentration of lamproite intrusions within the West Kimberley Province is the Ellendale Field (Plate 2), where 48 bodies are known to intrude the Devonian and Permian sediments of the Lennard Shelf. All but three of the bodies are intruded along a subsurface extension of the northwest-trending ridge which forms the core of the Oscar Range; the remainder are found to the northeast, along the foot of the Napier Range. Most of the bodies are covered with several metres of windblown sand; they were discovered using geophysical methods (see Chapter 1) and have been drilled and trenched during exploration for diamonds. The Ellendale Field includes the well-known Mount North and 81 Mile Vent intrusions, but most noteworthy are a number of unexposed leucite-free and leucite-poor olivine lamproite bodies, particularly Ellendale No. 9 and Ellendale No. 4,* which contain significant concentrations of diamond. These were the first major discovery of the host rock of diamonds in Western Australia.

The Noonkanbah Field is located entirely within the Fitzroy Trough in the central and southern portions of the Quanbun Syncline. Of a total of 24 known intrusions, 16 are well exposed and include most of the classic locations of Wade and Prider (1939) and Prider (1960). Mount Abbott was early explored for diamond (Jeppe 1971) without success, although trace amounts have since been found in this and a number of other intrusions in the field (Boxer and Haebig, 1980a). Walgidee Hills, also within the Noonkanbah Field, is the largest lamproite body known in Western Australia: it has a diameter of 3 km, and contains a number of rare minerals such as wadeite, priderite, jeppeite and "noonkanbahite" (shcherbakovite).

A small concentration of lamproite intrusions is found near the northern margin on the Quanbun Syncline and is probably related to the Pinnacle Fault, a major fault system which forms the northern margin of the Fitzroy Trough. The Calwynyardah Field contains seven intrusions in the vicinity of Calwynyardah homestead (Plate 1) and up to five smaller intrusions closely associated with the fault system. Only one intrusion, Hanson's Bore, is partly exposed, but the field includes two of the largest bodies known, Calwynyardah (128 ha) and Layman's Bore East (103 ha).

Other groupings of lamproite bodies are found at Big Spring on the northern margin of the Lennard Shelf, and near Old Leopold homestead, where they intrude the granites of the Leopold Mobile Zone. At Big Spring, there is a closely spaced group of five lamproite bodies from which the first *in situ* diamonds in the West Kimberley Province were recovered. The eastern group is more widely spaced, but appears to straddle the boundary between the Lennard Shelf and the Leopold Mobile Zone. Four lamproites intruding the granites of the Lamboo Complex, including Old Leopold Hill and Prairie Hill East, are exposed; but the remaining four, which intrude Devonian sediments, are unexposed.

Throughout the province, there are a number of isolated lamproite intrusions. The most isolated, Bruten, in the south, and Mount Rose, in the north, bear no obvious relation to any previously mentioned grouping, but four widely spaced bodies from Camarotoechia Creek to Oscar form a line parallel to the Oscar Range and may be related to an unexposed fault. Similarly, Rice Hill is isolated from the nearby Calwynyardah and Noonkanbah fields whereas Kalyeeda and The Sisters may be outlying members of the Noonkanbah Field.

MODE OF EMPLACEMENT

A variety of volcanic forms — including dykes, sills, plugs, and diatremes — is evident among the lamproite bodies which constitute the West Kimberley Province. However, most intrusions are complex and show a

* The numbers referred to were given by CRA Exploration P/L to each body. The numbers initially referred to geophysical anomalies and run from 1 to 46. Not all anomalies, however, proved to be over lamproite bodies so the run of numbers is not complete, although a number of anomalies proved to be over two bodies which may then be numbered *e.g.* 21 and 21a. As most bodies are unexposed it is convenient to follow the CRAE system although well-exposed and easily accessible bodies have been separately named, *e.g.*, Ellendale 5 is 81 Mile Vent.

combination of at least two forms. Contrary to the description of Prider (1960), there is no evidence for the surface outflow of lavas, although magma probably filled the open vents of many of the diatremes as lava lakes or "blisters".

Small, late-stage dykes are found in a number of bodies — *e.g.* Machell's Pyramid — where a number of thin dykes, 1-3 m thick, radiate from the central plug. The only well-exposed bodies in which the dyke form predomintes are Oscar (Fig. 137) and Old Leopold Hill (Fig. 97); and, in both, the lamproite magma has filled what were probably tension fractures: there is no evidence of explosive activity.

Small sills are common in many diatremes, and form a major part of the central complex of 81 Mile Vent. Only three sills unrelated to explosive vents are known, however: at Rice Hill, Ellendale 2, and Nerrima. The well-exposed sill at Rice Hill is about 45 m thick and conformably intrudes gently dipping sandstone beds (Fig. 133).

The overwhelming majority of lamproite bodies in the West Kimberley Province are associated, to some degree, with explosive volcanic activity, which is now represented by a variety of tuffs and breccias. In some plugs, pyroclastic rocks may form only a minor feature: the body consists predominantly of a central core of hypabyssal lamproite. At the other extreme, there are diatremes in which hypabyssal rocks are rare or absent and the body consists almost entirely of tuffs and breccias. The commonest situation, throughout the province, is to find a combination of diatreme and hypabyssal rocks coexisting in the same body.

The best-exposed example of a volcanic plug is Brutens (Fig. 135), where a small lamproite stock 50 m in diameter is exposed for a height of about 10 m above a conical talus-covered pedestal of enclosing sediments. The cylindrical shape of the body is shown by radial and tangential joints on top of the exposure, and horizontal, columnar joints on the sides of the body. The stock occupies a "blow" at one end of a short, breccia-filled dyke; but, around the margin of the stock, there is only a narrow (< 1 m), discontinuous zone of breccia. By contrast, the much larger stock that forms Machell's Pyramid (Fig. 107) is surrounded by a tuff or breccia zone 30 m wide.

A number of the unexposed lamproite bodies, particularly in the Ellendale Field, are pyroclast-filled diatremes; their structures have been revealed by diamond drilling. The best exposed example, however, is White Rocks (Fig. 131), in the Noonkanbah Field, where late-stage hypabyssal intrusions occupy only a small part of the vent; this vent is filled mainly by lamproite lapilli-tuff which in parts is well bedded. Mount Abbott (Fig. 105) is a distinct type of diatreme, in which the principal rock type exposed is a very coarse boulder-breccia of country rock, veined and disrupted by "sandy" tuffs, lamproite tuffs, and lapilli-tuffs.

Most commonly, the lamproite intrusions of the West Kimberley Province show an early explosive phase that formed tuffs and breccias, followed by the quiet intrusion of a central hypabyssal stock or complex of sills and stocks. In most exposed bodies, the pyroclastic deposits show no obvious bedding and appear to be a chaotic in-filling of the vent. At Mount Cedric, Mount Ibis, and particularly at 81 Mile Vent, however, the pyroclastics are well bedded; drilling and trenching on a number of the Ellendale bodies suggests that bedded tuffs are the norm rather than the exception. The central hypabyssal core of the intrusion may be a simple stock, as at Noonkanbah Hill, or a complex of stocks, as at Mount Cedric; at 81 Mile Vent, an early sill complex that was intruded into bedded tuffs is, itself, intruded by a later central stock.

Little evidence is available for the overall subsurface shape of most lamproite bodies: some smaller plugs appear to be simple pipes with near-vertical contacts, but a number of larger bodies show indications of a rapid narrowing of the volcanic pipe with depth. Exploratory drilling of a number of the pipes at Ellendale and Calwynyardah has, however, shown a consistent pattern of vents which narrow rapidly with depth to a very small conduit at a few hundred metres depth (Atkinson and others, 1984a). The overall shape is, therefore, that of a champagne glass, where the stem represents the narrow conduit. The central magmatic core, where delineated by drilling, appears to be of similar shape; it rises from a narrow conduit and spreads out as the present-day land surface is approached. In a number of intrusions, it has been possible to drill through the magmatic rocks into underlying tuffs. Most bodies are relatively isolated from one another and appear to have arisen from some point source of weakness in the underlying basement; the alignment and close proximity of other vents suggest, however, a dyke-like source at no great depth.

It is probable that most of the larger lamproite bodies conform to this "champagne glass" shape. In this, they differ significantly from the "carrot" shape postulated by Hawthorne (1975) for kimberlite pipes in South Africa, where the margins of the pipe dip inwards at $80°$ or more and the diatreme extends to great depth. Further differences are observed in the proximity of diatreme and hypabyssal-facies rocks in the lamproite vents, and in the bedded nature of much of the lamproite pyroclastic deposits. In the kimberlite pipe model, the diatreme is filled with one or more columns of chaotic tuff and breccia, and the hypabyssal-facies feeder dykes and sills are only encountered at great depth, close to the point from which the pipe begins to flare. In the lamproite pipes, the common situation is that magmatic rocks have intruded through the pyroclastic pile to occupy a high level within the vent. Tuff within a kimberlite pipe is believed to be rarely bedded, except where it has been washed back into the pipe from an external tuff ring (*e.g.* Hawthorne, 1975; Dawson, 1980). In the lamproite pipes of the west Kimberley, however, well-developed bedding is a common feature and has been shown by drilling to continue throughout the pyroclastic pile. Some of the bedding may be the result of redeposition from water; but, for the most part, it

appears to be the result of volcanic processes similar to pyroclastic base-surge deposits. Such deposits, often finely laminated and showing small-scale dune and cross-bedded structures, have been shown to originate from maar type volcanic eruptions (Fisher and Waters, 1970; Fisher and Schminke, 1984).

Maar volcanism is characterized by phreatomagmatic explosive activity as a result of rising magma coming into contact with groundwater (Lorenz, 1973, 1975), and the products include air-fall and pyroclastic surge deposits composed of juvenile and wall-rock materials. As the vent enlarges, the inward slump of wall-rock material along ring faults results in the subsidence and preservation of bedded tuff deposits. The classic areas for such pyroclast-filled diatremes are the Eiffel district of Germany and the Massif Centrale of France (Lorenz, 1973), and the Fife coast of Scotland (Francis, 1970). In Scotland, it has been shown that subsidence of at least 500 m has taken place. The similarity of bedded tuffs in maars and in a number of the West Kimberley lamproites is obvious, but the latter are preserved within a "champagne glass" shaped vent with no evidence of substantial subsidence along ring-faults. A similar "champagne glass" shape is, however, postulated by Hearn (1968) for the upper parts of diatremes in Montana, where the shape was thought to have been produced by low-angle faults slumping blocks of country rock and early tuff into the vent. At depth, these faults become steep ring-faults, but it is possible that, in the West Kimberley, faulting never developed beyond the low-angle slumping stage.

The role of groundwater in the formation of the lamproite tuffs is uncertain. Unlike the European maars, which are generally located in valleys where copious ground and surface water is available (Lorenz 1973, 1984), the West Kimberley lamproite bodies are often located on topographic highs, which were probably similarly elevated during the early Tertiary. Nevertheless, it is probably noteworthy that the best examples of bedded tuff are from the Ellendale Field where the lamproites intrude groundwater aquifers, such as the sandstones of the Grant Group and limestones of the Napier Formation. In the Noonkanbah Field, the lamproites are intruded into finer grained compact sandstones, siltstones, and mudstones; and bedded tuffs are less-well developed. Exceptions are the lamproite body at Mount Abbott, which intrudes coarse sandstone, and those at Mount Ibis and "P" Hill, which lie close to the Fitzroy River.

A further similarity between maar volcanism and lamproite intrusion is the close association of pyroclastics with hypabyssal intrusions. If the supply of water to the erupting maar is exhausted, then phreatomagmatic eruptions cease; and magma may intrude the tuffs as plugs, dykes, or sills (Lorenz 1973). As described earlier, this is the common situation found in lamproite intrusions, which differ in this respect from the classical kimberlite pipes.

No kimberlite or lamproite volcano has been observed during eruption; but the Ukinrek maars of Alaska, which formed during April 1977 (Kienle and others, 1980), may provide a model for lamproite volcanism. Two small maars, about 170 m and 300 m in diameter, formed during ten days of phreatomagmatic activity. Steam and ash clouds reached a height of about 6 km and a rim deposit of tuff and ejecta up to 30 m thick was formed. The depth of the larger crater was about 70 m; and, after a few days of activity, a lava pool formed, cooling as a dome up to 40 m high. In the West Kimberley Province, lamproite volcanism appears to have begun with an explosive, possibly phreatomagmatic, phase. As the lamproite magma was probably more volatile-rich than the basaltic magma giving rise to most maars, the water to drive the explosive volcanism probably came from both juvenile magmatic and groundwater sources. As activity proceeded, the vent was enlarged, partly by exfoliation from the wall rock, but principally by the inward slump of large blocks of country rock along low-angled faults; these blocks of sandstone were disaggregated and incorporated into the tuff to give the quartz-rich tuffs and lapilli-tuffs common in the lower parts of the pyroclastic sequence in the lamproite pipes. The continued eruption of fragmental juvenile material produced the lamproite-rich lapilli-tuffs of the upper parts of the sequence. The cessation of a supply of groundwater — or more probably the isolation of the vent from groundwater by a thick sequence of tuffs — and the degassing of the magma column, led to the final stage of quiet intrusion of lamproite magma. In some pipes, sills and plugs of magmatic material intrude or displace the pyroclastics, but in a number of instances it seems likely that the magma reached the surface to form a lava lake within the volcanic crater. The time scale of this activity is difficult to assess; the small Ukinrek maars formed over a period of ten days, and it seems plausible that a number of the smaller lamproite bodies with very simple geology took no longer to emplace. Except in the rare instances where adjacent intrusions have coalesced, few of the larger lamproites have a complex geology which might suggest multiple phases of activity. Thus it appears likely that in individual bodies, volcanic activity lasted no more than a few weeks, or for large intrusions such as Mount Abbott or Walgidee Hills, a few months. Throughout each individual lamproite field, and throughout the West Kimberley Province as a whole, however, volcanic activity was spread over a considerable time span, which will be considered in the next section.

At the cessation of volcanic activity, a common feature of maar-type volcanism is the formation of a crater lake. In the West Kimberley, erosion has removed any former tuff ring or open crater that the lamproite volcano may have produced, and no crater lakes have been preserved. At Calwynyardah, however, a thick bed of reworked silty tuff with intercalated lignite beds overlies a considerable proportion of the pipe and probably represents sediments deposited in a former crater lake.

THE AGE OF INTRUSION

The West Kimberley lamproites are of early Miocene age. Recent K-Ar and Rb-Sr dating (Jaques and others, 1984b) has confirmed the early Miocene ages obtained by Wellman (1972). Wellman had previously disputed the Jurassic ages proposed on the basis of limited Rb-Sr dating by Prider (1960) and Kaplan and others (1967), and presented concordant K-Ar ages of 17 to 20 Ma on a variety of mineral separates. In a recent study, phlogopite and diopside separates from 13 leucite lamproite intrusions were dated by the K-Ar method; and Rb-Sr ages were obtained from phlogopite - whole-rock pairs for Mt Percy, 81 Mile Vent, Ellendale No. 9, and Walgidee Hills (Jaques and others, 1984b). With the exception of Walgidee Hills, the Rb-Sr and K-Ar dates are in reasonable agreement, and indicate that the K-Ar ages provide reliable estimates of the age of intrusion. Ages given by a poorly defined isochron obtained on mineral separates from several whole-rock samples and by phlogopite - whole-rock pairs for the Walgidee Hills intrusions are younger than those obtained by K-Ar. The Walgidee Hills Rb-Sr ages are considered unreliable in view of the variation in $^{87}Sr/^{86}Sr$ ratios within the intrusion and the widespread late-stage alteration in Walgidee Hills rocks.

The K-Ar ages of Wellman (1972) and Jaques and others (1984b) are in excellent agreement, and show a range from 20 to 22 Ma in the Ellendale Field to the north and 18 to 20 Ma in the Noonkanbah Field in the south (Fig. 51), suggesting a southward migration of volcanic activity with time. An exception to this is Walgidee Hills which gave a younger apparent age of 17.5 Ma (Jaques and others, 1984b). This apparently anomalous age could result from isotopic resetting owing to the slow cooling of the intrusion or late deuteric alteration.

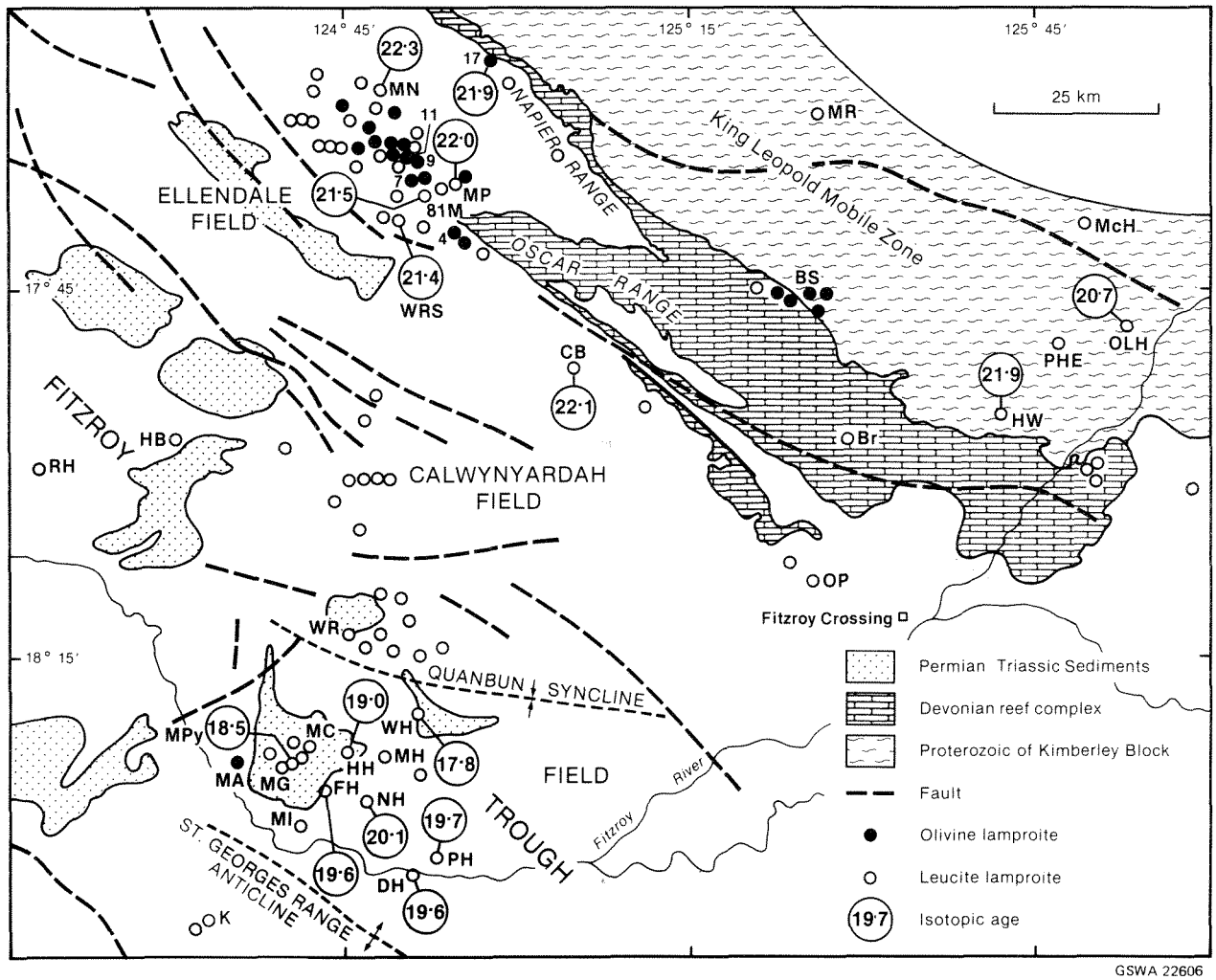


Figure 52. Distribution of lamproites in the West Kimberley Province, showing Ellendale, Calwynyardah and Noonkanbah fields, and a summary of K-Ar isotopic ages. Main lamproite bodies, from north to south, are: MN = Mount North, MR = Mount Rose, 4 = Ellendale 4, 7 = Ellendale 7, 9 = Ellendale 9, 11 = Ellendale 11, 17 = Ellendale 17, MP = Mount Percy, 81-M = 81 Mile Vent, WRS = Water Reserve Sill "A", CB = Camarotoechia Creek, McH = McKinrick Hill, BS = Big Spring, OLH = Old Leopold Hill, PHE = Prairie Hill East, HW = Hooper West, BR = Brooking Creek, RH = Rice Hill, HB = Hansons Bore, OP = Oscar, WR = White Rocks, WH = Walgidee Hills, MC = Mount Cedric, HH = Howes Hill, MH = Mamilu Hill, MA = Mount Abbott, MG = Mount Gytha, MPy = Machells Pyramid, FH = Fishery Hill, NH = Noonkanbah Hill, MI = Mount Ibis, PH = "P" Hill, DH = Djada Hill, K = The Sisters. Modified after Jaques and others (1984b).

The Miocene age of volcanism in the West Kimberley does not correspond with any known tectonic activity in the Kimberley region or Canning Basin, although Forman and Wales (1981) recorded some diastrophism, tilting, and faulting offshore in the region of the Rowley Shoals. Nor does it correspond with the major deformation and metamorphism in Timor associated with collison between the northward-moving Australian continent and the Inner Banda Arc which took place in the late Cainozoic — <15 Ma — (Berry and Grady, 1981).

The southward migration of volcanic activity with time is analogous to volcanism attributed to "hot-spots". The direction and apparent rate of movement of the Australian continent (Ellendale-Noonkanbah, 30 mm/a) is broadly comparable with that proposed for the Tertiary volcanism in eastern Australia by Wellman and McDougall (1974a,b) who suggested northwest movement of the Australian continent at approximately 66 ± 5 mm/a over a hotspot or hotspots. These rates compare favourably with spreading rates of 50 mm/a along the Antarctic Ridge in the Southern Ocean in the Miocene (Weissel and Hayes, 1971; Cande and Mutter, 1982). Sutherland (1983), on the other hand, ascribed the Cainozoic volcanism of eastern Australia to northward movement of Australia over former spreading sites in the Coral Sea.

An alternative approach is provided by paleomagnetism. Hurley (1985) sampled the lamproite core of Ellendale 38 and the metamorphased Devonian limestone within a few metres of the contact. Both sets of samples showed reversed polarity and a calculated paleolatitude of 37.3° S, compared with a present-day latitude of 18° S. The pole position falls close to the "best estimate for 25 Ma" pole of Embleton (1981), thus confirming the Tertiary age of the lamproite. The calculated rate of northward drift of the Australian continent — 20° of latitude in ≈ 22 Ma, or about 100 mm/a — is rather high, but of the same order as suggested by Wellman and McDougall (1974a,b).

At least locally, however, the major factor controlling the distribution of intrusions appears to have been structural: west-northwesterly trending faults at the margin of the Fitzroy Trough, northerly-trending fractures in the Kimberley Block, and east-west *en-echelon* faults and folds within the Fitzroy Trough.

THE ELLENDALE FIELD

The Ellendale Field (Plate 2) includes the greatest concentration of lamproite intrusions within the West Kimberley Province. A total of 45 bodies are enclosed within a northwest-trending area 40 km long by 15 km wide northwest of the Oscar Range. A further three intrusions are located 15 km to the northeast along the base of the Napier Range.

The lamproite intrusions are located approximately 150 km east of Derby, and access is via the Gibb River Road, which after 65 km of bitumen surface is a well formed "beef road" and tourist access to the interior of the Kimberley region. A public road along the Lennard River gives access to the unexposed lamproites at the base of the Napier Range, and four-wheel-drive station tracks lead from this road to the prominent exposures of Mount North and Mount Percy. Ellendale 38, in the southeast of the field, may be reached on station tracks, but access to the majority of the intrusions is along a well-formed private road built by C.R.A. Exploration Pty Ltd during diamond exploration of the area. The area is covered by two cattle stations, Fairfield and Kimberley Downs; and the occupants of Fairfield form the only permanent population of the area of Plate 2. During the winter tourist season (May to November), a ranger of the National Parks Service is stationed at Windjana Gorge. Supplies of fuel and food must be obtained from Derby, and, except in the immediate vicinity of the limestone areas, water is scarce.

The topography of the region is dominated by the limestone cliffs of the northwest trending Napier and Oscar Ranges. At several localities, *e.g.* Windjana Gorge (Fig. 55) and Tunnel Creek, rivers have cut spectacular gorges through the ranges, giving rise to scenically attractive areas frequented by tourists. In some caves and ravines there are numerous rock paintings, attesting to a considerable Aboriginal population in former times. Between the Napier and Oscar Ranges, there is the wide and flat Fairfield Valley drained by numerous small creeks that feed into the Lennard River. The valley is floored by black-soil plains, which are impassable during the wet season. Extending northwest from the Oscar Range is a low ridge of sandplain country on which are located most of the lamproite intrusions. Small mesas and low sandstone hills, rarely more than 30 m high, often mark the location of lamproite pipes; the Mount North lamproite, rising 90 m above the plain is a landmark visible from most quarters.

The limestone ridges are usually karstic and bare of vegetation except in gullies and gorges where a variety of shrubs and eucalypts are found. Soil-covered slopes within the limestone ranges generally support spinifex *(Triodia)* and other grasses with scattered trees — mainly various species of *Eucalyptus,* some wattles *(Acacia),* and boab trees *(Adamsonia).* The black-soil plain of the Fairfield Valley is covered with a variety of coarse grasses — principally spear grass — and scattered stands of eucalypts and occassional wattles. Patches of pindan scrub — dense wattle scrub with some eucalypts and an understorey of spear grass — are present on the sandy soils; but most of the area is open eucalypt woodland and dense spear grass. In drier areas of sandy soil, spinifex dominates.

GEOLOGY AND STRUCTURE OF THE FIELD

The Ellendale Field lies entirely within the Lennard Shelf, the northeast marginal unit of the Canning Basin. The shelf is a shallow-marine feature, about 500 km long and up to 60 km wide, overlain by up to 3 km of Ordovician, Devonian, and Permian sediments. To the southwest, the Lennard Shelf is bounded by the Pinnacle

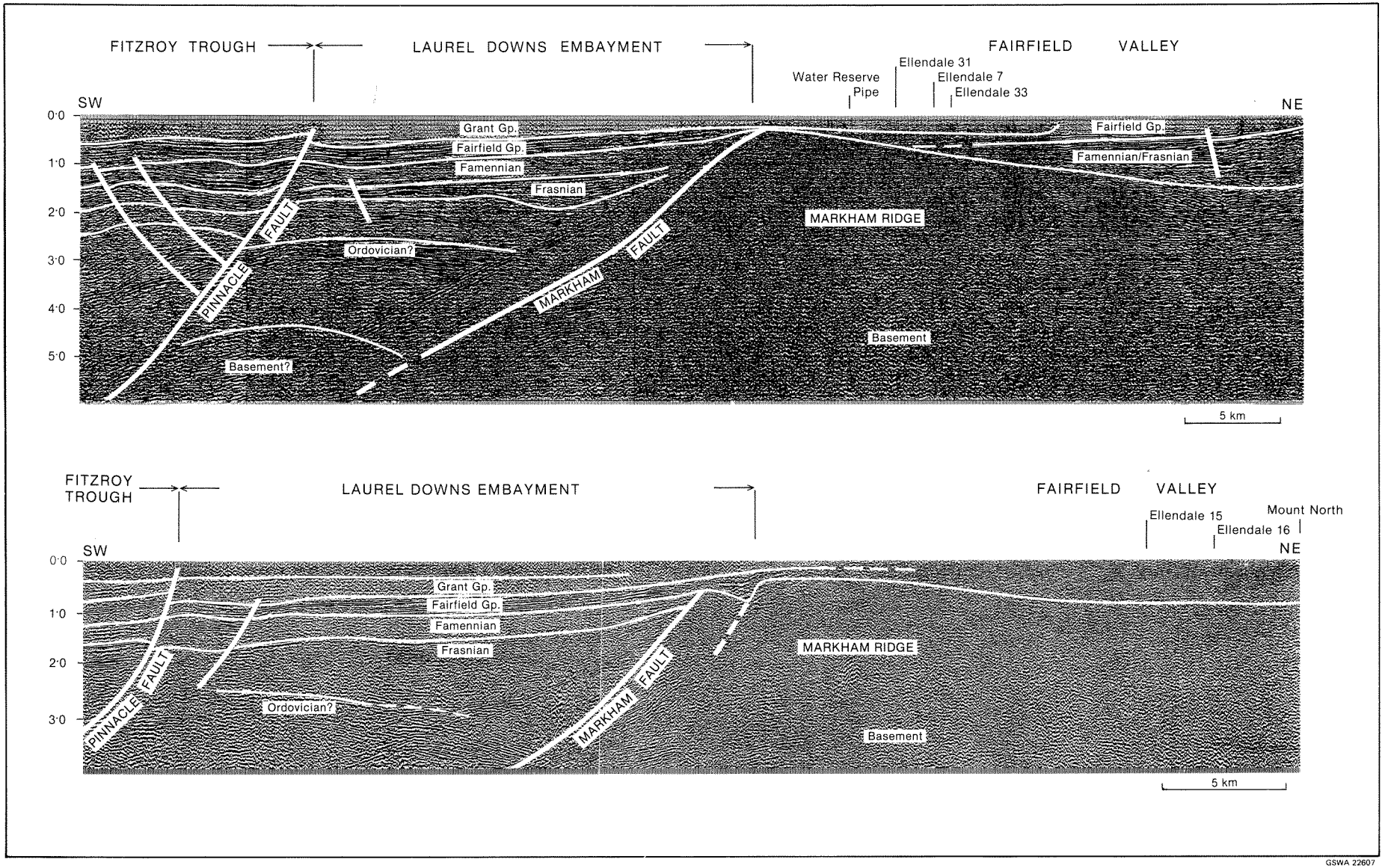


Figure 53. Seismic profiles across the Lennard Shelf. Upper line: ED 81-10 (1981), courtesy of IEDC; Lower line: C-3 (1970), courtesy of WAPET. (location of lines marked on Plate 2).

Fault and the Beagle Bay Fault systems, which separate it from the Fitzroy Trough.

Recent descriptions of the geology of the Canning Basin have been given by Towner and Gibson (1983) and Yeates and others (1984). The evolution of the Basin was described by Forman and Wales (1981), and the structure deduced from seismic work by Purcell and Poll (1984). The geology of the Lennard Shelf in the vicinity of the Ellendale Field, including adjacent areas of the Precambrian Leopold Mobile Zone, was described by Derrick and Playford (1973). The most significant geological features of the Ellendale Field area, apart from the lamproites themselves, are the reef complexes of the Napier and Oscar Ranges, which have been extensively studied by Playford and Lowry (1966) and Playford (1980,1984).

Structure

The Canning Basin was initiated during Early Ordovician times with a gentle downwarping of the eroded Precambrian basement and the widespread deposition of shallow-marine sediments. Major tectonism, including northwest faulting parallel to the basin margin took place in the Lennard Shelf area during the Middle Devonian. At this time, through the development of the Pinnacle and Fenton Faults (Yeates and others 1984), the Fitzroy Trough acquired its graben-like characteristics and the Lennard Shelf became a separate area of deposition. At the same time, the northeast margin of the Lennard Shelf was subjected to block faulting, giving rise to rugged topography with local relief of several hundred metres on which the late Devonion reef complexes of the Napier and Oscar Ranges were established (Playford 1980). Recognition of block faulting has been important for the interpretation of the Devonian reef complexes, as the Oscar Range appears as a fringing reef to an island of Precambrian schist (Playford and Lowry, 1966; Hurley, 1985), which was separate from the main part of the Leopold Mobile Zone, whereas the Emanuel Range reefs were established on a fault block of Ordovician dolomite (Playford 1980). Block faulting also appears to be important with respect to the emplacement of the Ellendale lamproites as the main part of the field intrudes an unexposed block of Precambrian basement.

Figure 53 presents two seismic lines which traverse the Lennard Shelf in the vicinity of Ellendale Field; the position of the lines are marked on Plate 2. Both lines show the Pinnacle Fault, which marks the southwest margin of the Lennard Shelf, and a basement ridge, the Markham Ridge, on which are located the Ellendale

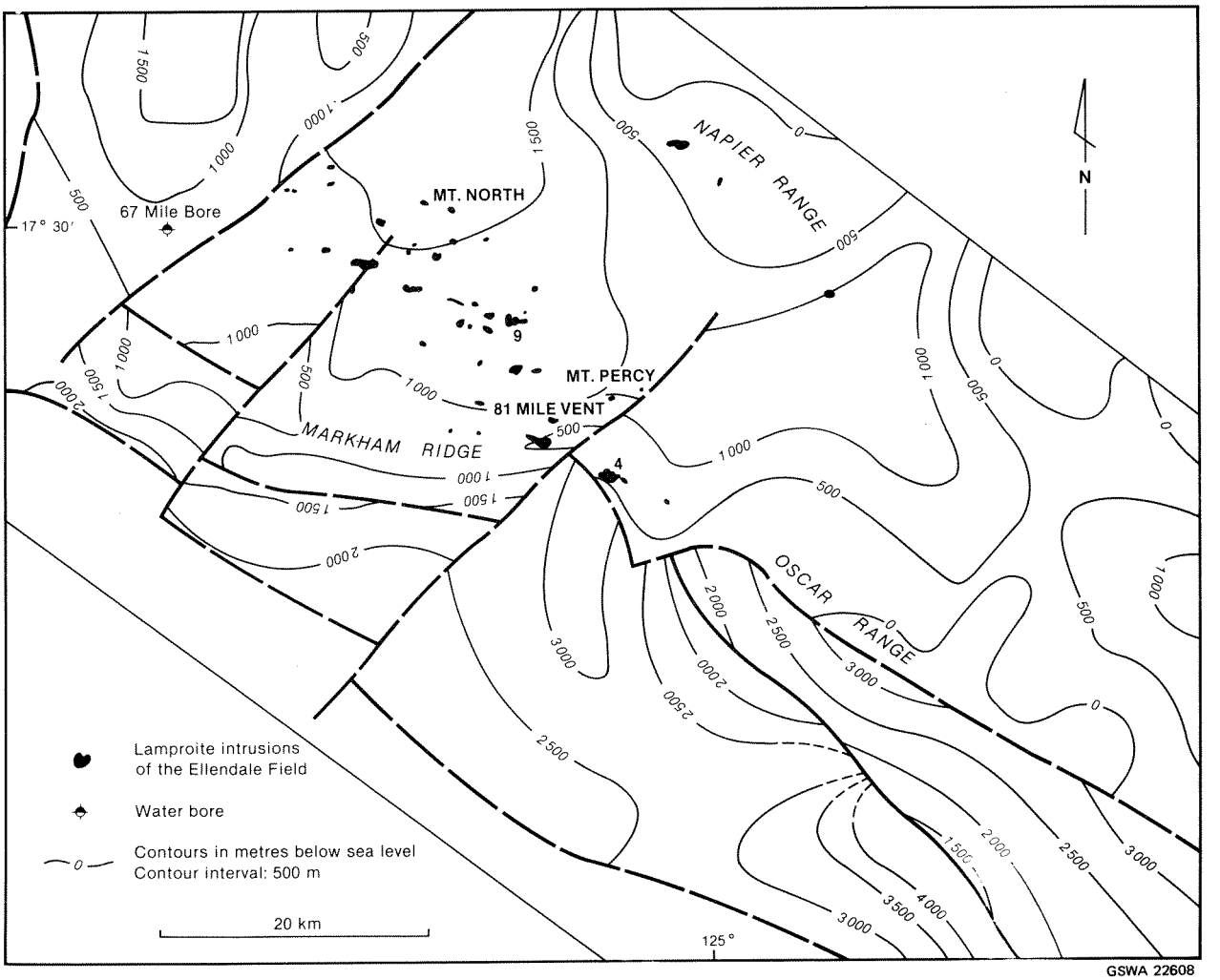


Figure 54. Depth to magnetic basement of part of the Lennard Shelf (modified, after MacLean, 1972).

lamproites. Another feature of the sections is the relatively thick sequence of Ordovician(?) to Permian sediments south of the ridge which contrasts with the thin sequence to the north. For the present purpose, however, the important feature is the Markham Ridge. In Fig. 53, the seismic profiles have been interpretated, with some changes of nomenclature, in the same manner as Purcell and Poll (1984). The southern face of the Markham Ridge thus appears as a fault — the Markham Fault — also noted in Forman and Wales (1981). In the uninterpreted profiles, however, there is little indication of the presence of a fault, and sedimentary reflectors appear either to pinch out as the ridge is approached, or thin as the beds cover the ridge. An alternative interpretation is that the contact is erosional and that the "Markham Fault", as marked, is the Upper Devonian land surface. The margin of the Canning Basin in this area is erosional (Towner and Gibson, 1983), and the Devonian reef structures of the Napier and Oscar Ranges grew on eroded surfaces of the Precambrian rocks (Hurley, 1984). Post Devonian tectonism was very limited in the Lennard Shelf area, particularly in this region (Playford and Lowry, 1966), which further suggests that the contact between the Markham Ridge and later sediments is depositional rather than faulted.

A study of the basement features of the Lennard Shelf, as deduced from aeromagnetic data, has been presented by MacLean (1972) and block faulting in the vicinity of the Oscar Range is well illustrated (Fig. 54). A major fault parallel to, and southwest of, the Oscar Range coincides, in part, with the Pinnacle Fault, while another major fault trends along the length of the range to give a basement depth of up to 3 000 m close to the Oscar Range, where Precambrian basement rocks are exposed. Surface faulting in the Fairfield Group, which was deposited along the front of the southeast part of the Oscar Range (Derrick and Playford 1973), may be a later reactivation of part of this fault. To the northwest of the Oscar Range, the basement is cut by three northeast-trending faults that divide the basement ridge into several blocks with steeply dipping faces to the southwest and shallow gradients to the northeast. It thus appears that the basement in the Ellendale area consists of a number of fault blocks, tilted towards the basin margin, and that the Precambrian core of the Oscar Range forms the exposed portion of one such block. The lamproite intrusions are located on the northern dip slope of one such block, and it appears that the depth to basement is between 1 000 m and 1 500 m, although the only reliable depth known is at 67 Mile Bore on an adjacent block, where Precambrian rocks were intercepted at 770 m below the present surface (Forman and Wales, 1981).

The block faulting of this part of the Lennard Shelf, and the straight line of Devonian reef outcrop along the margin of the King Leopold Mobile Zone suggests that a basement fault along the foot of the Napier Range should also be present. Such a fault was not detected by MacLean (1972) or any account given of this part of the basin margin. Possibly the margin is monoclinal, or consists of a number of parallel small faults; but, equally, the lack of a recognized fault may be an artefact of the data which were not collected far into the fold belt.

Geology

The geology of the exposed Precambrian basement in the vicinity of the Ellendale Field has been briefly described by Derrick and Playford (1973), and in more detail by Gellatly and others (1968). The Oscar Range succession has been described by Derrick and Gellatly (1971).

The main area of Precambrian rocks is found north and east of the Napier Range and forms part of the King Leopold Mobile Zone. The oldest rocks are the strongly folded phyllitic siltstones, sandstones, and greywackes, of the Halls Creek Group. These are generally metamorphased to greenschist or, in places, to almandine-amphibolite facies. The age of the metasediments may be Archaean (2 700 Ma: Bofinger, 1967), although metamorphic ages of 1 465-1 700 Ma, and the lack of a strong unconformity with the overlying Whitewater volcanics, may indicate a Lower Proterozoic age (Bennett and Gellatly, 1970). The Halls Creek Group is intruded by granites and dolerites of the Lamboo complex; but, in part, the junction between the sediments and the Lamboo rocks is a sinistral splay fault from the Sandy Creek Shear (Gellatly and others, 1968). The Lamboo Complex consists largely of elongated batholiths, and smaller stocks of a great variety of granites, granodiorites, and quartz gabbros, which make up the greater part of the King Leopold Mobile Zone. Within this sequence of intrusives is found the Whitewater volcanics, a series of rhyodacite and dacite tuffs, ash flow tuffs, tuffaceous siltstone, and minor sandy sediments. The total thickness of the volcanics may be as much as 12 km, but they now occur as steeply dipping sheets in narrow downwarped belts adjacent to granite plutons (Derrick and Playford, 1973). The age of the Whitewater Volcanics is given by Bennett and Gellatly (1970) as 1 940 ± 110 Ma, and of the granites that intrude the volcanics, 1 880 ± 160 Ma.

The exposed portion of the Oscar Range block consists of isoclinally folded and strongly faulted Precambrian metasediments. The dominant rock is quartzite, but there are some conglomerates and phyllites, and minor amounts of limestone and volcanics. The succession appears to dip and thicken towards the southwest, and its total thickness is about 11.5 km. The grade of metamorphism is lower greenschist facies (Derrick and Gellatly, 1971). The age of the sediments is probably Late Proterozoic, but the absence of granite clasts in the conglomerates suggests that the granitic basement to the northeast of the Oscar Range was not exposed. Probable glacial sediments correlate with similar rocks in the East Kimberley that have been dated by Bofinger (1967) at 740 ± 30 Ma and have a Cambrian metamorphic age of 580 Ma (Bennett & Gellatly 1970); but the Spielers Volcanics, the topmost

member of the succession, has an apparent metamorphic age of about 357 Ma.

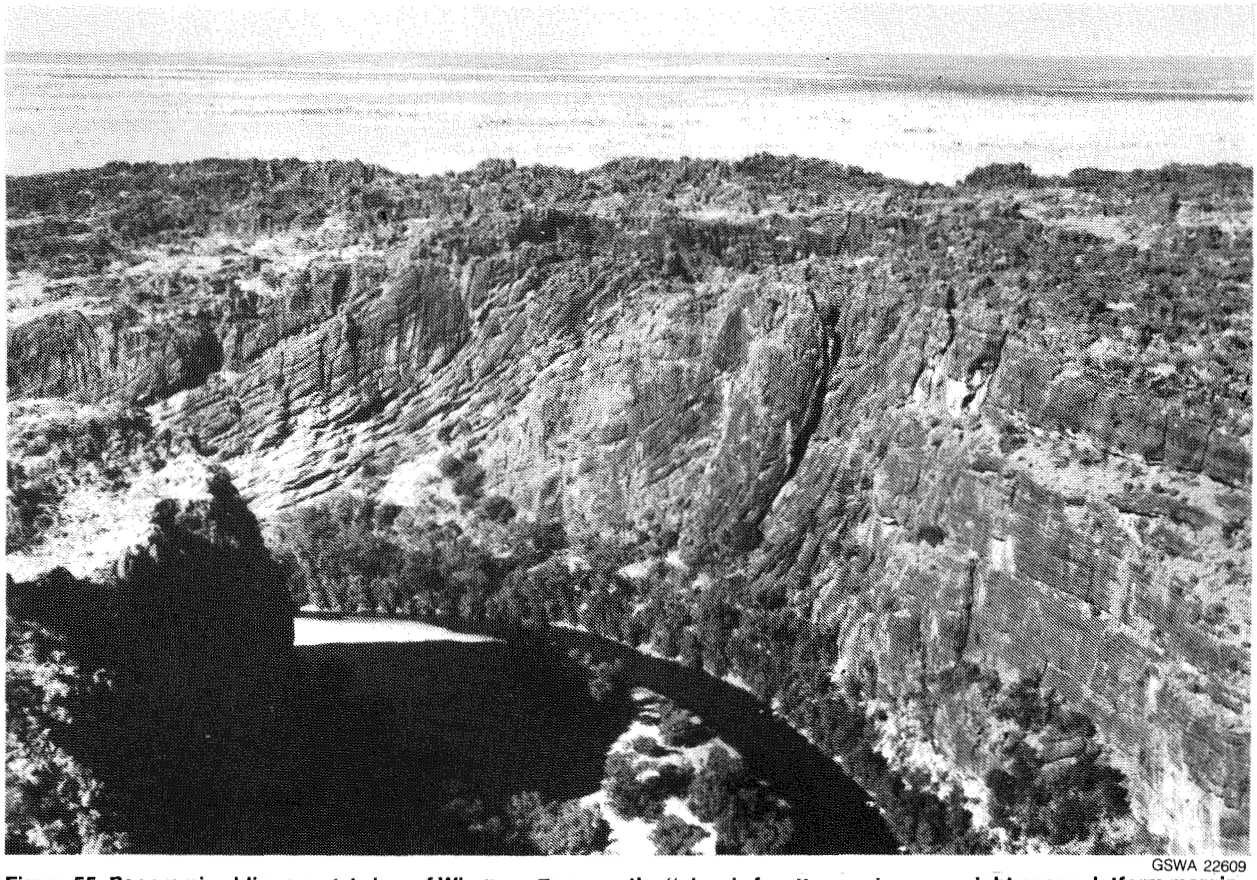
The remainder of the basement complex of the Lennard Shelf is nowhere exposed, but a number of bores have penetrated the sediments to intersect Precambrian quartzites and schists. The 67 Mile Bore (Plate 1), intersected Precambrian rocks at 770 m and continued for a further 148 m in quartzite and schist (Playford and Lowry, 1966). Similarly, Meda 1, Langoora 1, and Hawkstone Peak 1, all intersected Precambrian schist, probably similar to the Oscar Range succession. Napier 1, however, located about 10 km southwest of the Napier range, intersected banded granitic gneiss at 1 773 m (Newstead, 1969).

The Oscar Range succession, and the basement of the Lennard Shelf generally, is both younger than, and lithologically different from, the King Leopold Mobile Zone. It appears possible that the quartzites, schists, phyllites, and subordinate volcanics, represent deposition in a narrow basin in late Precambrian times of sediments which were later folded and faulted between the Kimberley Block and the crystalline basement of the present Canning Basin in the Early Paleozoic.

Overlying the basement rock, the oldest exposed Phanerozoic sediments in the Ellendale area are the Devonian reef complexes of the Napier and Oscar Ranges. To the southeast, at the foot of the Emanuel Range, Ordovician limestones, dolomites, shales, and sandstones, up to 1 km thick, are exposed (Playford and Lowry, 1966); and Purcell and Poll (1984) have interpreted seismic sections to show Ordovician sediments to the southwest of the Markham Ridge (Fig. 53), although they have not been intersected by drilling.

The oldest Devonian sediment is the Behn Conglomerate — of Givetian to Frasnian age and found in the Napier Range north of Fairfield Homestead. The conglomerate contains rounded boulders, cobbles, and pebbles, of Precambrian granite, quartzite, schist, and acid volcanic rocks, all in an arkosic matrix (Playford and Lowry, 1966). The clasts were derived locally from the Halls Creek Group and Lamboo Complex of the King Leopold Mobile Zone, and are overlain, with some interfingering at the contact, by the Famennian reef complex of the Napier Range. The contact between the Behn Conglomerate and the Halls Creek Group is probably faulted; and, if so, indicates a reactivation of faulting in Upper Devonian times.

Devonian reef complexes form a prominent topographic feature throughout the Ellendale area — rising, sometimes as a sheer limestone cliff, up to 90 m above the plain. The reefs grew — in Middle and Upper Devonian times — along the mainland shore of the King Leopold Mobile zone to form the Napier Range, and around an island of Precambrian rocks to form the Oscar Range. Overall, the reef complex is about 350 km long, up to 50 km wide, and forms a Palaeozoic analogue of the Great Barrier Reef (Playford, 1980). The typical reef complex consists of a platform facies, a marginal-slope facies grading into a basin facies, and along the margin of the platform a reef-margin subfacies — the



GSWA 22609

Figure 55. Panoramic oblique aerial view of Windjana Gorge — the "classic face"; exposing an upright-scarp platform margin. Dipping marginal-slope facies (Napier Formation) is on the left; flat-lying, reef-fringed platform facies (Pillara Limestone) is on the right (Photo: P.E.Playford).

original fringing reef (Playford and Cockbain 1976). In the Ellendale area these features are well shown in the classical Windjana Gorge section, where the Lennard River cuts through the Napier Range (Fig. 55 and Plate 2).

Two cycles of reef development are recognized, the Pillara Cycle of Givetian to Frasnian age, and the Nullara Cycle of Famennian age (Playford, 1984). The platform sediments of the Pillara Cycle consist of medium-bedded limestones, commonly near horizontal and rich in organic material — dominantly stromatoporoids and corals (Cockbain, 1984). The Frasnian platforms were essentially low-relief banks; and reef growth, built primarily by stromatoporoids and cyanobacteria, only became prominent in the Late Frasnian. The Pillara Cycle ended at the Frasnian-Famennian boundary with a brief regression and exposure of the platforms above sea level. Renewed subsidence initiated the Nullara Cycle: reef growth was vigorous and dominated by cyanobacteria and stromatolites, and the platform sequence is dominantly well-bedded cryptalgal calcarenite and oolite with some interbeds of sandstone and siltstone (Playford and Cockbain, 1976). The marginal-slope facies of both cycles is the Napier Formation; it consists of limestones with interbedded calcareous sandstone, conglomerate, and megabreccias, which are interpreted as talus derived from the growing reef. Dips of 35° are common adjacent to the reef, but flatten progressively down-slope towards the basin (Derrick and Playford, 1973).

In the Ellendale area (Plate 2), both cycles of reef formation are present in the Napier Range and Oscar Range areas. In the Napier Range, Windjana Gorge shows the type section of the Windjana Limestone (Fig. 55), the reef-margin sub-facies of the Nullara cycle; these overlie and interfinger with the Napier Formation and older Pillara Cycle reefs and platform sequence. In the Oscar Range area, recent mapping by Hurley (1985) shows that the central area of Frasnian platform facies, the Pillara Limestone, is surrounded by reefs of similar age, and succeeded by Famennian Windjana Limestone in the north, at Morown Cliffs, and on the southwest side of the range. The northwest extremity of the Oscar Range is made up of the type locality of the Nullara Limestone, the platform facies of the Famennian sequence. Outcrops of Napier Formation are found in both areas and underlie the whole of the Fairfield Valley.

Reef formation ceased towards the end of the Famennian, possibly as a result of shallowing of the depositional basin or an increased influx of terrigenous sediment (Playford and Lowry, 1966). The resulting sediments of the Fairfield Group (Druce and Radke, 1979) were laid down conformably on the sediments of the inter-reef basins and consist of thin-bedded limestones, shales, siltstones, and sandstones. The maximum thickness of the group is about 900 m in the southeastern part of the depositional area; but, in the Ellendale area, only the lowermost formation, the Gumhole Formation, remains, and it is probably less than 150 m thick (Druce and Radke, 1979). Thin-bedded limestones with minor shale horizons are exposed over a wide area north of Mount Percy and probably underlie much of the Fairfield Valley. In the Ellendale area, the age of the Fairfield Group rocks is uppermost Famennian; but, elsewhere, the group extends into the lower Carboniferous.

A major marine regression followed the deposition of the Fairfield Group, and was followed in turn, after a period of erosion during much of the Carboniferous, by deposition of the Grant Group of Late Carboniferous to Early Permian age. In the Ellendale area, only the uppermost part of the Grant Group, the Carolyn Formation, is present; it consists of fine to coarse feldspathic sandstones, often cross-bedded, and subordinate conglomerates. The sandstone is generally soft and friable, except where hardened by surface silicification, and it outcrops as small isolated mesas. In the Ellendale area, contact metamorphism by lamproite intrusions results in small rounded hills of baked quartzite surrounding a number of pipes, particularly Ellendale 4, 6, and 16. The unconformable nature of the Grant Group is shown by comparing outcrops at Mount Percy, where the sandstones directly overlie the limestones of the Fairfield Group, and in the nearby Oscar Range, where the Permian sandstones overlie the Pillara and Nullara Limestones. An excellent exposure of sandstone infilling a Devonian karst is found by the side of the road between 81 Mile Vent and Ellendale 4 (Fig 56). The outcrop of the Grant Group extends north to the Mount North Creek and Lennard River; and most lamproites in the Ellendale Field are emplaced in it. The maximum thickness of the Grant Group is in excess of 2 900 m in the central Canning Basin; but, in this part of the Lennard Shelf, only 305 m were intersected by the 67 Mile Bore.

Sedimentation continued throughout the Permian with the deposition of the sandstones, siltstones, shales, and subordinate limestones of the Noonkanbah and Liveringa Formations, which are exposed to the southwest of the Ellendale area. However, apart from the possibility of some Tertiary laterites, the youngest strata intruded by the lamproites are those of the Grant Group.

The lamproite intrusions

The distribution of lamproite intrusions within the Ellendale Field appears to be governed by a number of factors, all derived from the basement structure. The field can be divided into two parts, the major concentration of intrusions, which extends northwest from, and on-line with, the Oscar Range, and a group of three intrusions along the base of the Napier Range. There is no obvious reason for this distribution unless the major basement fault, which marks the southwest front of the Oscar Range, influenced tensional forces in the adjacent block that contains the Markham Ridge (Fig 54). The intrusions along the base of the Napier Range may be located along a fault that is marginal to the Lennard Shelf, although no such fault was located



GSWA 22610

Figure 56. Exhumed karst in the Devonian Nullara Formation, infilled by Permian Grant Group sandstone; remnants of sandstone fill the hollows between the limestone pinnacles, and flat-lying sandstone is just visible in the background.

during the aeromagnetic survey of MacLean (1972).

Most intrusions are located on two basement fault blocks, which were formed by northeast cross-faults perpendicular to the Oscar Range trend, principally on the Markham Ridge block. A number of lamproites lie on, or close to, these cross-faults; but, nevertheless, the intrusions in general do not appear to be directly related to known faulting.

Perhaps the most significant feature of the Ellendale lamproites is the dominant east-west elongation of the larger bodies and the similar alignment of groups of smaller intrusions. Ellendale 9 and 4 are composite bodies formed by the coalescing of two or more separate vents, but Ellendale 22 and 15 are complex elongate bodies probably from single vents. The most prominent alignment is between Ellendale 41,42,43 and 25 but a number of other east-west alignments is also evident. A subsidiary alignment trending 120° is shown by the elongation of Ellendale 6 and 13.

The east-west alignment is parallel to the dominant structural trend in the Phanerozoic rocks of the adjacent Fitzroy Trough. This alignment has been interpreted by Smith (1968) and Rixon (1978) to result from dextral wrench-fault movement in mid-Jurassic times. This direction is also parallel to the trend of the Markham Ridge in the Precambrian basement beneath the lamproites. Wrench faulting may have influenced basement fracturing, but it appears more likely that the east-west trend is an inherent feature of the basement into which the lamproites were intruded.

The size of the lamproites in the Ellendale Field range from a surface area of 106 ha for Ellendale 6, down to 0.4 ha for Ellendale 38. Within this range, the distribution appears to be logarithmic, with two thirds of the bodies less than 10 ha in area (Fig. 6). There is a slight concentration of intrusions in the central part of the field between Ellendale 9 and 22 but otherwise there is no pattern to the lamproite distribution either by size or location. The overwhelming majority of lamproites have no surface expression, except perhaps a rim of baked sandstone wall rock. A few, however, such as Mount North and 81 Mile Vent, are well exposed, although there are no obvious differences in rock type or form of the intrusion to explain the discrepancy.

As discussed earlier, the Ellendale lamproites are of early Miocene age (20-22 Ma); all except Ellendale 38 and the three intrusions along the foot of the Napier Range intrude Lower Permian Grant Group sandstones. No geomorphological studies of the West Kimberley have been published, it is therefore difficult to estimate the extent to which the lamproites have been reduced by erosion. The strongly flared, "champagne glass", shape of some vents, as shown by drilling, suggests that little erosion has occurred; on the other hand, the exposures of Mount North and Mount Percy indicate a minimum of 90 m of erosion in their vicinity. The

baked sandstone rim rocks of a number of pipes (*e.g.* Ellendale 6 and 7) also rise 20-30 m above the surrounding plain. The presence in the area of a few small flat-topped mesas possibly provides an indication of the original land surface. Mesas adjacent to Ellendale 31 and 19, for example, rise about 20-25 m above the plain, and their upper surface appears to be lateritized, although no laterite now remains. Laterite pebbles are found incorporated in the pyroclastic deposits of Ellendale 26, 81 Mile Vent, and, less commonly, in other pipes; they were presumably derived from laterites which once covered the surface represented by the tops of the mesas. No age is known for this surface, but in the Northern Territory Hays (1967) has suggested that the

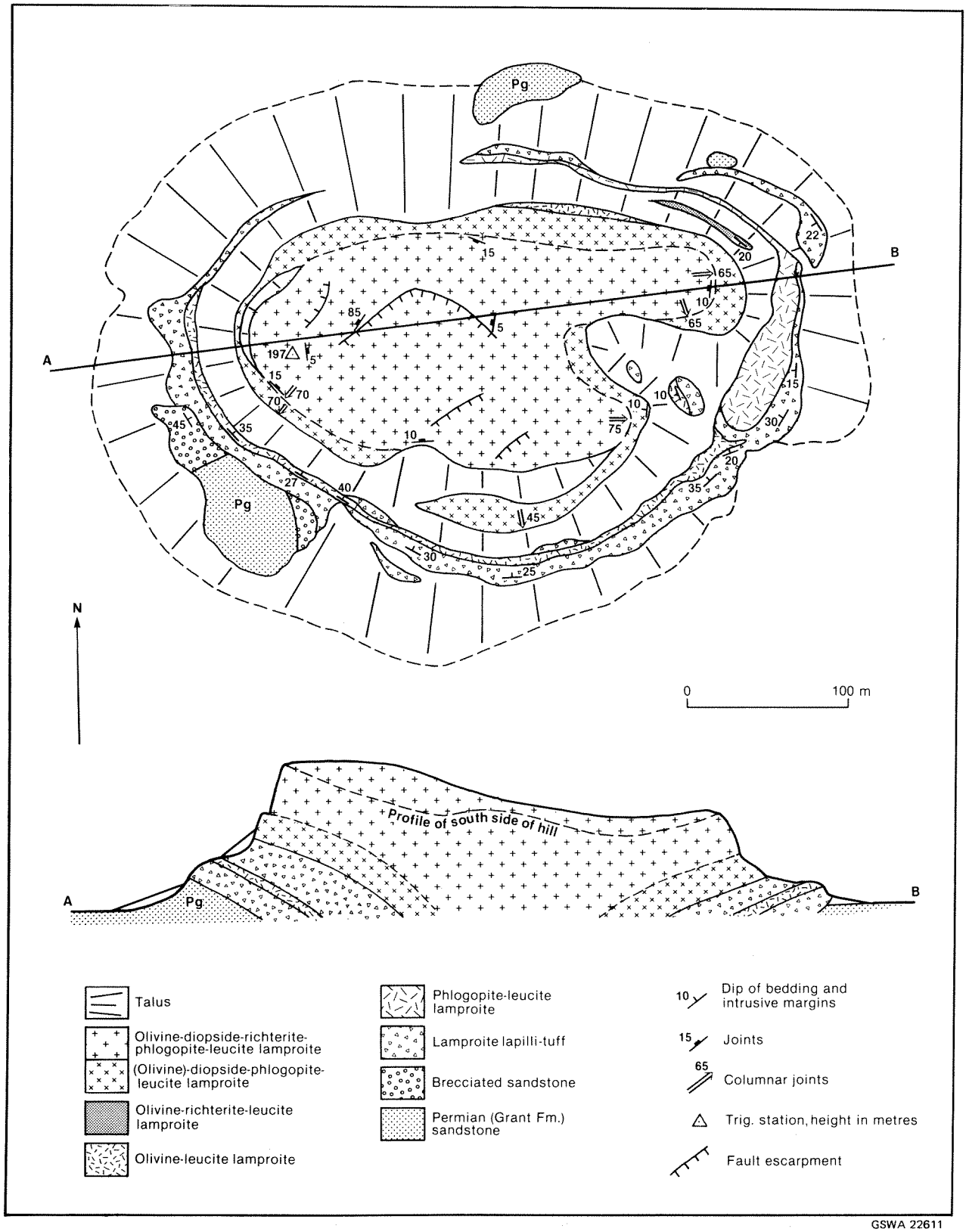


Figure 57. Geological map of Mount North.

lowest lateritized surface, the Wave Hill Surface, is of Miocene-Pliocene age and that it extends into the northern Kimberley area. If this surface can be correlated with that found in the Ellendale area of the west Kimberley, then it appears that the lamproites intruded a lateritized surface no more than 30 m or so above the present day land surface. All indications are that recent erosion in the Lennard River valley and Fairfield Valley areas has lowered the modern land surface somewhat more than on the ridge to the south, thus accounting for the greater erosion observed at Mount North and Mount Percy.

In the sections which follow, all exposed lamproites, as well as a number of the more important concealed bodies for which data is available from exploration activities, will be fully described. Brief notes and petrographic descriptions are given for the remaining bodies. The location of all intrusions is shown on Plate 2.

MOUNT NORTH

Mount North (Fig. 27) forms a prominent landmark throughout much of the Ellendale area, particularly when viewed from the north and west in the vicinity of the Napier Range. Steep cliffs of columnar-jointed lamproite rise above a talus slope to a height of about 90 m above the plain. The hill is distinctly layered: two tiers of columnar lamproite overlie lamproitic pyroclastics with thin interlayered lamproite sills. The Permian Grant Group sandstones, into which the lamproite is emplaced, are only exposed on the southwest side of the hill, near its base. Overall, the Mount North intrusion is oval shaped, approximately 500 × 300 m, and elongated east-west.

The wall rocks of Grant Group sandstone are well exposed only on the southwest margin of Mount North; it is a well-bedded, medium-grained sandstone containing cross-bedded units 30-40 cm thick. The bedding is near horizontal and does not appear to have been disturbed, despite its proximity to the vent. However, flanking this area of undisturbed sandstone, there are smaller outcrops of brecciated and recemented sandstone that contain angular fragments — generally 5-10 cm across, but up to 30 cm across — close packed in a sandstone matrix. These breccias contain no obvious lamproite fraction, and probably resulted from the initial explosive activity of the vent. A crude apparent bedding, at one point, suggests an inward dip of 45° for these breccias. Small outcrops of similar sandstone are found on the northern side of the hill, but consist only of isolated boulders.

The earliest lamproitic products of the Mount North vent were pyroclastics, the bulk of which are concealed beneath talus deposits of weathered lapilli-tuff and boulders from the columnar lamproites above. The best exposures of lapilli-tuff can be seen where they have been protected beneath sills of fine-grained lamproite, particularly around the southern and eastern parts of the vent. The pyroclastics are well bedded, and range from fine tuff through lapilli-tuff to coarse tuff-breccia that contains fragments of lamproite, sandstone, and, rarely, shale, in varying proportions. In the tuffs exposed at the eastern extremity of the hill (Fig. 58), there are excellent exposures of fine-grained laminated tuffs showing poorly developed cross-bedding. These are interbedded with lapilli-tuffs containing sandstone fragments up to 5 cm across; the whole assemblage dips 15° towards the centre of the vent. On the southeast side of the hill, well exposed over a distance of 30 m in a prominent gully, is a tuff-breccia layer, 1 m thick, that contains plentiful angular sandstone blocks up to 45 cm across. Most exposures, however, consist of lapilli-tuffs with fragments generally less than 1 cm diameter and rarely more than 5 cm diameter. Bedding is generally obscured by a thin scree of weathered-out fragments, but, where measurable, dips at about 30° towards the centre of the vent.

The pyroclastics outcrop beneath a series of thin sills, which form a prominent marker horizon around most of the hill. A few small outcrops of lapilli-tuff can be found above the sills, and it is presumed that pyroclastics underlie the deep talus that has formed below the upper, coarse lamproite layer. The total exposed thickness of the pyroclastics probably exceeds 50 m in places. The sills vary from 1-4 m thick and are possibly absent from the northwest sector of the hill; they occupy approximately the same stratigraphic position throughout; although, in the northeast sector, two thin lenticular sills are found higher in the tuff sequence. The rock is mostly a fine-grained, grey, olivine-leucite lamproite, but in parts it contains plentiful small phlogopite flakes.

These sills were originally described by Prider (1960) as flows interbedded with the tuff. However, the existence of flows is doubtful: at the eastern end of the hill, in a 10 m-high cliff section, thin veins of lamproite, 10-30 cm thick and similar to the overlying sill, can be seen to crosscut the bedding in the tuffs and, more rarely, other thin lamproite veins. At the western end of Mount North, the top of the sill is reasonably well exposed as a network of interconnecting veins, each up to 60 cm thick, enclosing lenticular patches of pyroclastics, including lapilli-tuff, and two large blocks of sandstone 40 cm across. At this point, the main part of the sill, 2 m thick, is patchily vesicular, and has a crude, 10-20 cm diameter, columnar jointing. There is a crude layering of vesicles, parallel to the dip of the sill and dipping at 35° towards the centre of the hill. Throughout its outcrop, the sill encloses xenoliths of sandstone and shale, sometimes amounting to 5% by volume. Although mapped as a single unit, there is sufficient variation to suggest that several intrusions are involved. The western and southern outcrop are grey, often scoriaceous, and columnar jointed: the eastern outcrops weather rusty brown, are compact, and not columnar. In a deep gully on the southeast side of the hill, the eastern part of the sill is seen to be about 2 m higher than the western sill; but there is no visible connection between the two.

The most impressive outcrops on Mount North are those that form the columnar-jointed cliffs of the upper

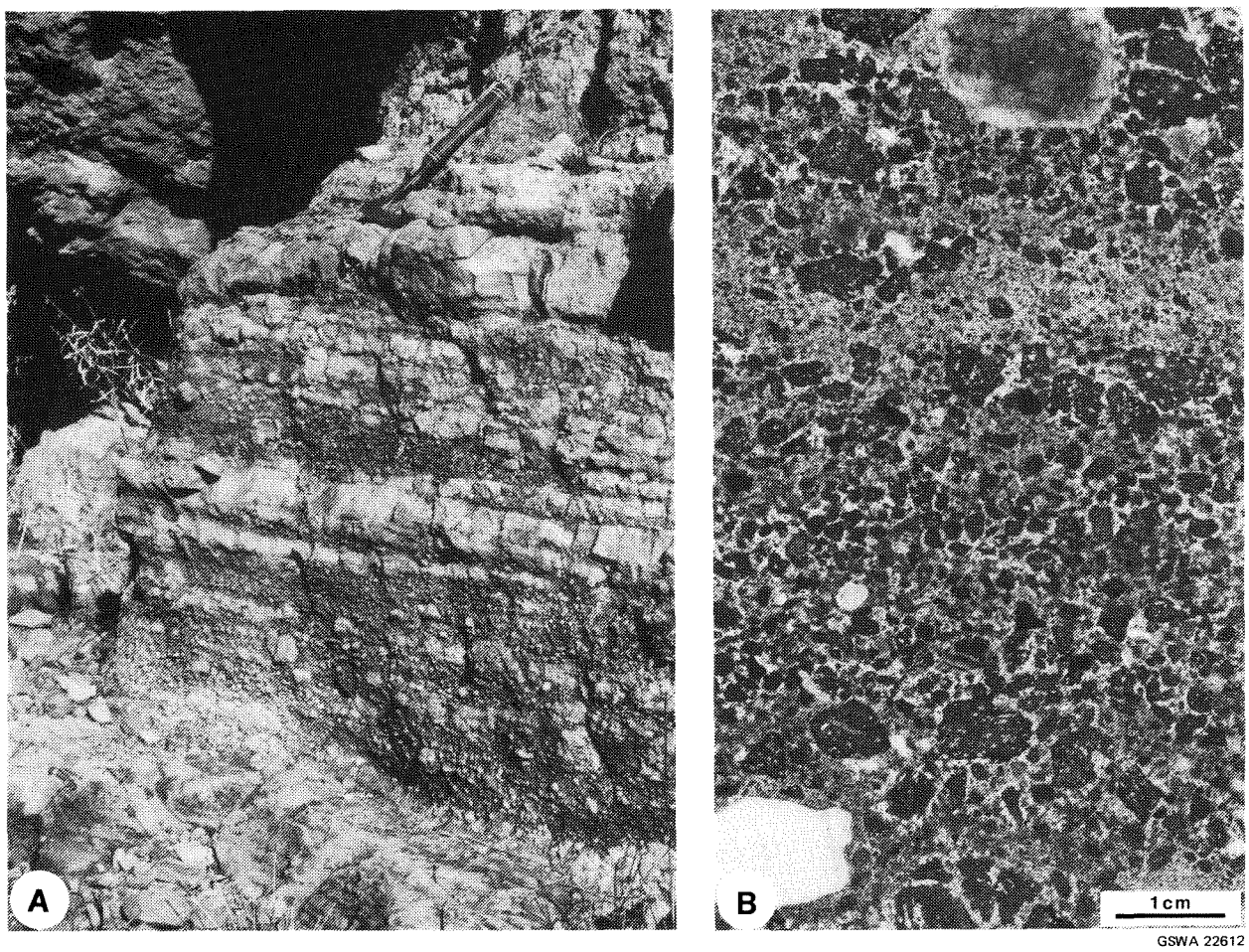
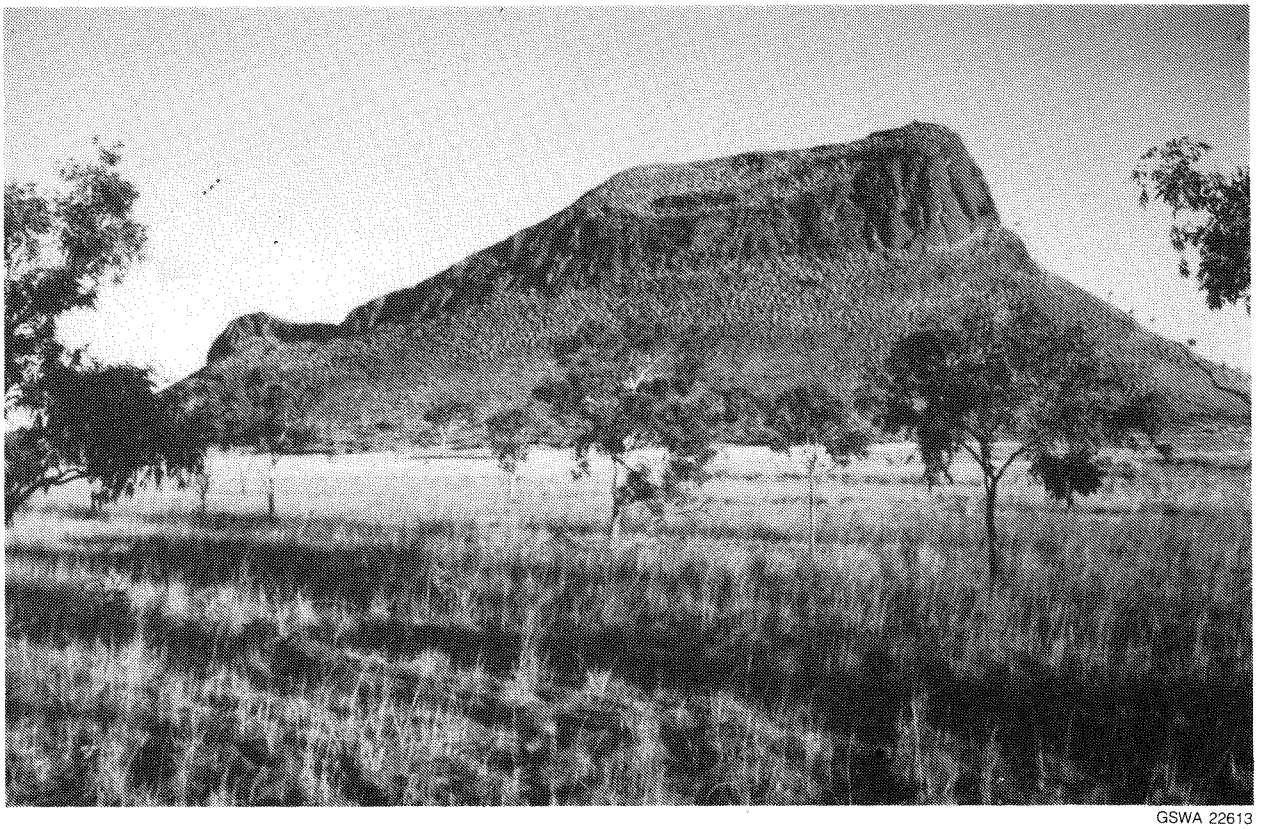


Figure 58. Bedded "sandy" lapilli-tuffs at the eastern end of Mount North. A — Alternating beds of light-coloured, quartz-rich, and dark, quartz-poor "sandy" lapilli tuff with country-rock fragments up to 10 cm across. Note the impersistence of some beds. B — Polished slab of the same tuff, showing bedding, vesiculated juvenile lapilli, quartzite fragment and interstitial quartz grains (BMR 83210319).

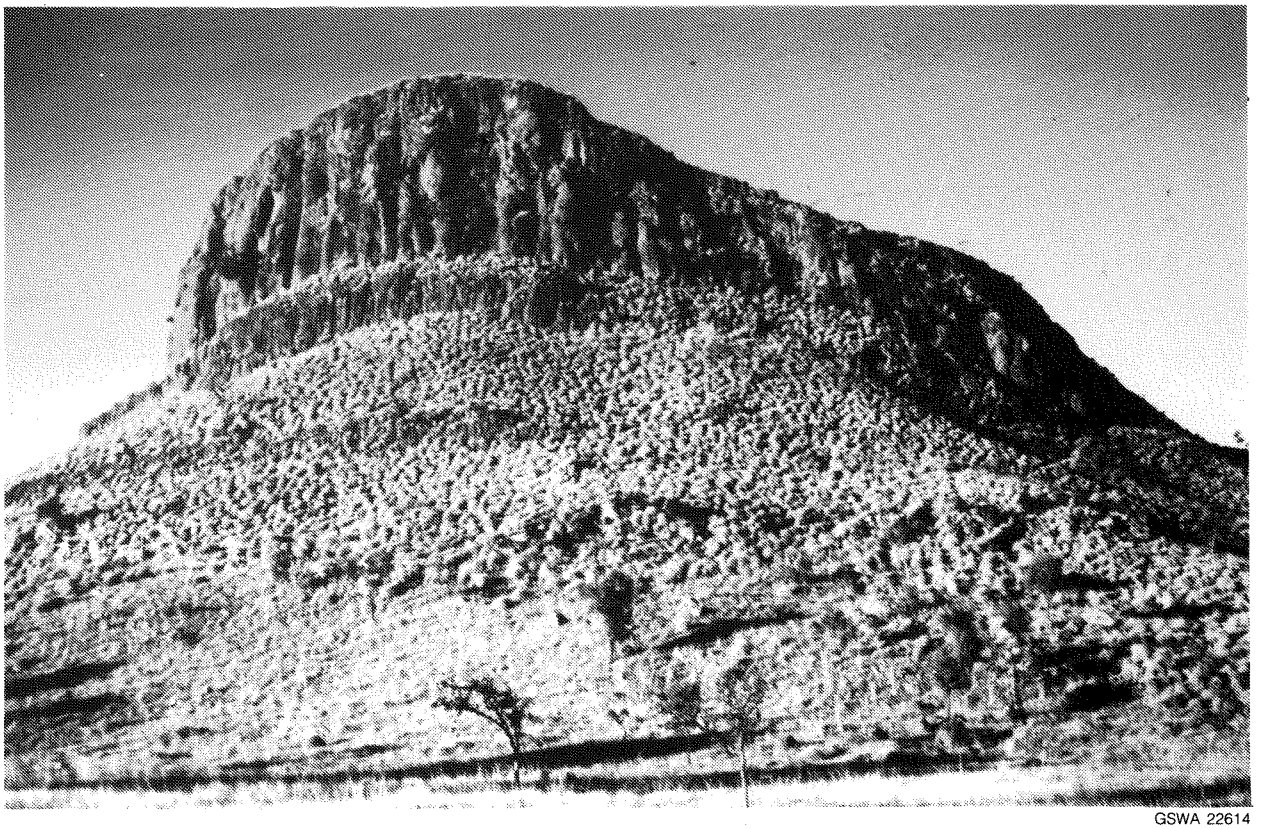
two "flows" of Prider (1960) (Figs 59 and 60). The upper tier, with columns 1-2 m in diameter, is about 30 m thick, whereas the lower tier, with columns 30-60 cm diameter, is about 18 m thick. A talus-covered ledge separates the outcrops of the two tiers of columns throughout most of the circumference of the hill; and, at the eastern end, where columnar jointing in the lower tier is poorly developed, the lower part of the outcrop is covered with boulder scree. Nevertheless, on the southwest side of the hill, the outcrop is continuous, and it can be seen that the two units form part of the same rock body. There is no scoriaceous material or intrusive margin between the two units to indicate successive flows or sills; instead, a number of small columns of the lower unit merge over a height of a metre or so to form the large columns of the upper unit. In the field, the rock type of each unit is indistinguishable, except that the upper unit is slightly coarser grained; both are coarse-grained green rocks with plentiful phlogopite. The two tiers of columnar jointing appear to be a cooling phenomenon: the smaller and lower columns represent relatively rapid cooling as the magma came into contact with cold, and possibly water-laden, tuffs, whereas the larger columns represent the slower cooling of the interior of the mass. The lower surface of the mass, in contact with the tuffs, is nowhere seen; and the upper surface has been eroded; but it appears that the upper lamproite unit of Mount North formed part of a large lava blister that filled the vent of the volcano. The columnar jointing, of both tiers, dips steeply outward from the hill, indicating an inward dip for the base of the mass of about 30°.

A further feature, particularly prominent in the upper parts of the mass, is a set of closely spaced, flat-lying joints or partings, coated with chalcedony and/or zeolite. The joints are usually 1-3 mm thick and spaced 1-5 cm apart; the bands are continuous over a distance of 30-40 cm and give a distinct layered appearance to fresh surfaces. However, the zeolite has not filled true joints as the rock shows no tendancy to fracture or weather along such surfaces. In places, flow-aligned phlogopite flakes are parallel to the zeolite veins; but, in general, the veins show no consistent relationship to other features. Commonly, the veins dip inward towards the centre of the vent, but usually at a lower angle than that indicated by columnar jointing. On top of the hill, the veins may dip steeply and radically change their orientation over a short distance. The origin of these veins is not known, but they are almost certainly not joints and are probably related to late cooling features of the mass.



GSWA 22613

Figure 59. Mount North, from the north, showing the columnar jointing of the central core. (Photo: G. Derrick, BMR).



GSWA 22614

Figure 60. Mount North, from the west. The upper and lower tiers of columnar jointing in the central core are prominent and the lower sill is visible on the spinifex covered lower slopes. (Photo: G. Derrick, BMR).

The volcanic sequence

Mount North is typical of a number of diatremes in the Ellendale Field which indicate an initial explosive phase of volcanism followed by the "quiet" emplacement of a magmatic core. Unlike other diatremes, however, that at Mount North has been eroded to remove much of the pyroclastic material and to leave the central core exposed.

Bedding in the lapilli-tuff indicates that the vent walls dip inward at about 30°, and suggests a rapid contraction to a relatively small conduit at no great depth. Although the tuffs which now occupy the vent contain a proportion of fragmented wall-rock, the initial explosive phase of volcanism fragmented and cleared a large volume of sedimentary rock from the vent. Unexposed basal pyroclastics probably contain a larger proportion of accidental material, but the only remnant of the initial activity now exposed is the sandstone breccia found on the southwest flank of the hill.

The pyroclastics now preserved were deposited entirely within the vent. The coarser and less well-bedded layers were probably plastered directly on the vent wall, but other beds were probably of air-fall origin. The well-bedded, laminated, and sometimes cross-bedded tuffs, however, are similar to base-surge deposits. The explosive phase of volcanism continued for a considerable but indeterminate length of time and consisted of numerous pulses of varying intensity, as indicated by the variety of pyroclastics present.

At the conclusion of the explosive phase, the volcano would have consisted of an extensive tuff-ring surrounding a deep crater partly filled by pyroclastics. No time sequence can be established for the intrusion of magmatic lamproite, but the thin sills intruding the tuff beds probably represent the earliest magmatic pulse. The final magmatic phase is represented by the coarse columnar lamproite, which would have filled the vent to form a lava lake or large volcanic blister. The development of columnar jointing suggests that the pyroclastics filling the vent were relatively cool when the lava lake formed, the larger upper columns indicating a slower cooling rate for the interior of the mass.

Erosion since the Miocene has removed all direct evidence of the final form of the Mount North volcano. The general land surface has been lowered by at least 90 m, destroying the original tuff ring and removing much of the pyroclastic material which filled a vent about three times the area of the present outcrop.

The present upper surface of Mount North appears to be related to the upper tier of large columns and shows a number of features related to post emplacement subsidence. Near the summit of the hill there are a number of small vertical scarps; in particular, an arcuate scarp about 100 m long has a vertical face of 2-3 m and is situated above a depression about 6 m deep and up to 80 m across. This depression was probably caused by the withdrawal of magma while the central portions of the mass were still liquid, and may have lead to a partial collapse of the overlying solidified rock. The scarp thus represents a small fault developed in the still-cooling mass and probably marks the location of the major conduit of the volcano.

The general slope of the top of Mount North is to the east at about 20°; but, at the eastern end, a smaller block appears to be tilted west at about 30°. At the low point, where the two slopes intersect, there is strong jointing, and a small stream flowing to the southeast has cut back a steep-walled gully. Prider (1960) suggested this location as a second centre of subsidence and the location of a second feeder for the lava lake. As in the earlier example, the features here are confined to the central coarse lamproite and are not reflected in the underlying pyroclastics. There is thus the possibility that Mount North consists of two vents which coalesced in their latest phase. However, considering the regular oval shape of the vent, it is more probable that the original vent was elongated, perhaps dyke-like, and later became enlarged at one or two points.

Petrography

Pyroclastics: Despite a few layers of very coarse material the dominant rock type is a fine-grained lapilli-ash tuff consisting mainly of disaggregated quartz grains, small juvenile lamproite lapilli, and minor accidental lithic fragments of wall rock, set in a sparse tuff matrix. A typical specimen of bedded pyroclastics from the southeast of the hill is crudely layered on a 2-5 cm scale: fine-grained quartz-rich tuff layers are interbedded with lapilli-tuff layers containing lamproite and wall-rock fragments from 1-2 cm across. Although, in some field exposures, sharp margins may be observed between the beds, in this specimen the margins are irregular and gradational.

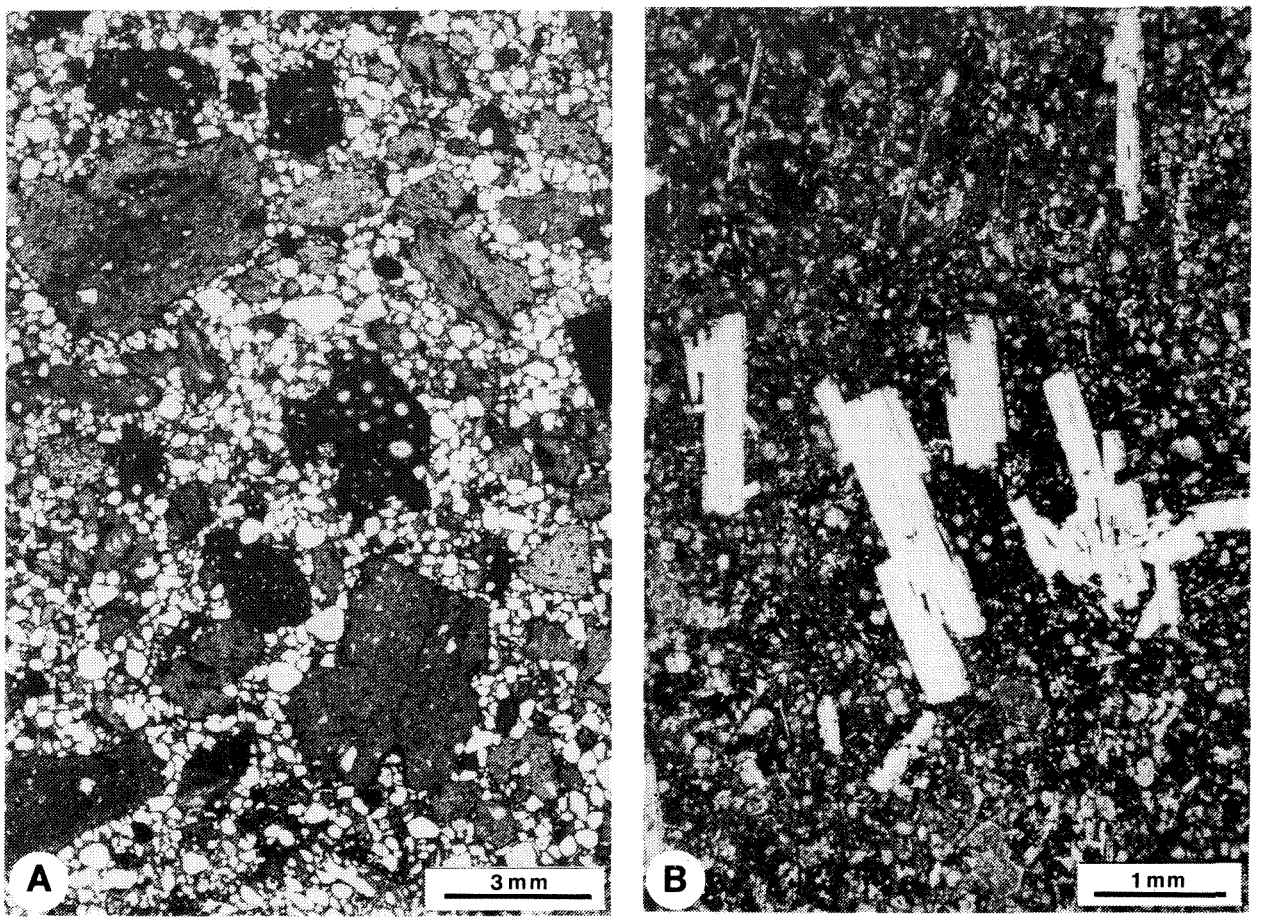
The quartz-rich tuff layers consist of about 70% of rounded to sub-angular quartz grains, about 0.2 mm across, and about 20% of slightly larger rounded juvenile lamproite fragments set in a sparse matrix of clay minerals derived from lamproite dust. The more abundant lapilli-tuff consists of 30-50% of poorly sorted, angular to rounded quartz grains, 40-60% of altered glassy and vesicular lamproite lapilli up to 10 mm across, and rare accidental lithic fragments of quartzite in an altered, clay-rich ash matrix. The glassy lamproite sometimes encloses a few quartz grains or fragments of crystalline lamproite that contain microphenocrysts of phlogopite, leucite, and olivine. Similar porphyritic, dense, lamproite also occurs as discrete cognate lapilli. A few examples are also found of spherical concretionary lapilli, from 1-6 mm across, consisting of quartz fragments cemented by clay minerals which may have originally been glassy lamproite ash. One such lapillus contains several grains of tourmaline and zircon. Rarely, the content of quartz grains is minimal and the rock becomes a lamproite lapilli-tuff. In the coarser lapilli-tuff layers, where lamproite fragments are often >10 mm across, the rock still contains up to 30% of rounded disaggregated quartz grains but, in addition, contains a significant proportion of wall-rock lapilli. Angular to sub-angular fragments of fine-grained

sandstone-siltstone predominate, but most prominent are a small number of ironstone nodules, up to 20 mm across, which were mostly probably derived from laterites which overlay the area of the vent. No limestone fragments from the underlying Devonian rocks have been observed, but a few fine-grained silica-rich fragments show textures suggestive of fossil shell fragments and may represent silicified limestone. One such pebble, 30 mm across, has the appearance of being a drop-stone within the finer grained tuffs.

Other pyroclastics observed at Mount North vary only slightly from those described above. A specimen from the northern side of Mount North carries no glassy juvenile lamproite fragments; but, in addition to quartz grains, has about 50% of fine-grained, cognate, olivine-leucite lamproite fragments. Another specimen, from the southern side of the hill, contains the only evidence of lamproite fragments ejected while still plastic. The lapilli-tuff consists of quartz grains and angular lapilli of juvenile lamproite glass up to 5 mm across and minor amounts of vesicular lamproite, olivine-leucite lamproite, accretionary lapilli, and country rock fragments. In addition, there are rare and striking lapilli of unusual type: one, an amoeboid mass of vesicular lamproite glass, the other a pumiceous mass of glass, which appears to have rolled, while still plastic, to enclose a mass of quartz-rich tuff, thus streaking out the vesicles in the glass.

The lower sill complex: These sills, each about 2-3 m thick, form an almost complete girdle around the lower flanks of Mount North (Fig. 60). At least three sills can be distinguished on the basis of petrography and by their relative stratigraphic position within the pyroclastic sequence.

The most extensive sill, and lowest stratigraphically, encircles the southern and western parts of the hill; it is very fine grained, grey to black, often vesicular, and, near the margins, pumiceous and brecciated. Small xenoliths of sandstone are occasionally seen, and two small xenoliths of plagioclase-bearing igneous rock, presumably from the basement complex, have been noted in thin-section. The rock is an olivine-leucite lamproite and commonly contains plentiful, small, subhedral microphenocrysts of olivine up to 1 mm across. Olivine is usually replaced by fibrous green aggregates of nontronite and other clay minerals, although one sample contains a few small fresh olivine crystals. The groundmass varies from fine-grained to microcrystalline, and consists largely of small, euhedral, former leucite crystals, and minute prisms of priderite, enclosed either in poikilitic prisms of colourless potassic richterite or turbid brown interstitial clay minerals. In



GSWA 22615

Figure 61. Photomicrographs of tuff and lamproite from Mount North: A — "Sandy" lapilli-tuff, southeast side of Mount North. Weakly vesicular, blocky lapilli of formerly glassy lamproite, rare lapilli of leucite lamproite, and accretionary lapilli, in a quartz-rich tuff matrix (GSWA 71807). B — Diopside-phlogopite-leucite lamproite, upper tier of the central core of Mount North. Note the alignment of phlogopite flakes and acicular diopside in a fine-grained matrix of altered leucite and interstitial potassic richterite (GSWA 71412).

some parts, the interstitial material includes small irregular flakes of phlogopite; and, in some specimens, there are microphenocrysts of phlogopite. The marginal facies of this sill is a dark, vesicular, autobrecciated, cryptocrystalline rock, in which minute leucite crystals are barely visible; and it consists of fragments and fiamme enclosed in a material of the same composition.

The eastern sill, of similar thickness, and encircling the northern and eastern parts of the hill, is emplaced about 3 m higher in the tuff sequence than the western sill. It is a pale-brown, fine-grained rock, which, in thin section, is seen to consist of small microphenocrysts of altered olivine, generally less than 0.5 mm across and set in a groundmass of minute altered leucite euhedra, small flakes of phlogopite, accessory priderite, and sparse, turbid matrix. The rock is distinguished from the western sill by the presence of phlogopite and the absence of potassic richterite. The thin veins of lamproite associated with this sill at the eastern end of the hill are of somewhat coarser grain size; the olivine phenocrysts are replaced by silica, and the phlogopite flakes up to 1 mm long. Subordinate apatite and a trace of diopside can also be distinguished in the groundmass. The margins of these veins against the tuff are contorted and indistinct, and suggest that the veins were intruded into unconsolidated tuff.

A thin sill on the northeast flank of the hill is coarser grained and contains many small, altered olivine phenocrysts in a groundmass of turbid leucite, poikilitic, strongly pleochroic, potassic richterite, and interstitial dark turbid material. A few small interstitial flakes of phlogopite are strongly coloured and zoned to dark red-brown titanium-rich margins.

The central core: Although there are small petrographic differences between the rocks forming the upper and lower tiers of columnar jointing within the central core of Mount North, little difference can be observed in hand specimens. Both are compact, medium-grained, pale-green rocks with prominent flow-aligned phenocrysts of phlogopite. On surfaces broken parallel to the alignment, the phlogopite forms rosettes up to 5 mm across. A few altered xenoliths of sedimentary rock and early-formed lamproite, up to 10 cm across, were noted, more commonly towards the base of the mass. Talus conceals the junction between the central core and the underlying tuff; but, at the base of the cliffs on the southwest side of the hill, there appears to be a chilled margin of darker fine-grained rock at least 1 m thick.

The chilled marginal zone is microscopically similar to the western sill which underlies it, and is a fine-grained olivine-leucite lamproite with small plates of poikilitic potassic richterite in the groundmass. In part, the rock is fragmental and consists of fiamme, droplets, and shards of similar material. Olivine has been altered to green nontronite.

The main mass of the lower tier is a medium-grained porphyritic rock with plentiful phenocrysts of phlogopite up to 2 mm long, and some small phenocrysts of olivine up to 1 mm across, which have been altered to pale-green nontronite. The groundmass consists of small euhedra of former leucite, usually turbid, small prismatic and acicular diopside crystals, small flakes of phlogopite, and much interstitial, turbid, green or brown, indeterminate clay minerals. Minor and accessory minerals include interstitial prisms of potassic richterite, acicular apatite, and many small prisms of priderite. In some specimens, a few minute prisms of wadeite were noted. The phlogopite phenocrysts typically have pale-coloured, twinned cores, which are strongly pleochroic from near colourless to pale red-brown, and are enclosed by narrow mantles of darker, more titanferous and less pleochroic mica. The mantles typically enclose many small priderite and some leucite crystals. Groundmass phlogopite is more uniformly dark red-brown in colour. Pseudomorphs after olivine microphenocrysts are common in some specimens, but mostly account for less than 5% of the rock; the original crystals were euhedral to subhedal and often occur as small aggregates.

The rocks of the upper tier of Mount North are essentially similar in mineralogy and texture to those of the lower tier. The only significant difference is the constant presence and relative abundance of interstitial potassic richterite, which commonly comprises 10-15% of the rock and forms large poikilitic plates enclosing priderite and leucite. Olivine, pseudomorphed by nontronite, while still a minor constituent, is more evenly distributed through the rock. Minute prisms of wadeite were found in all samples examined. The zeolite-filled partings, so prominent in hand specimen, are seen in thin section to be a series of sub-parallel anastomosing veinlets filled with colourless clear zeolite; similar material sometimes forms patches in the groundmass of the rock.

The petrography of the rocks of the central core of Mount North confirms the conclusion of the field survey that, despite initial impressions to the contrary, the rocks of the upper and lower tiers form a single mass. Slight differences that do occur can be explained by varying rates of cooling in different parts of the body.

Chemistry

The Mount North lamproites possess all the distinguishing chemical features of the West Kimberley lamproites, such as very high K_2O/Na_2O (typically >10), and molecular K_2O greater than Al_2O_3. However, compared to the suite as a whole, the compositional range of the Mount North rocks is limited, as shown in Table 31.

The central core rocks are of broadly uniform composition with comparatively low SiO_2 (typically 45-47% on an H_2O^--free basis), Al_2O_3 (5-7%), and K_2O (5-8%), and a moderate MgO content (10-12%). This composition is close to the mean of the West Kimberley lamproites. The upper tier exhibits little variation, apart from slightly lower MgO contents in the centre relative to the top and bottom of the unit. Greater variation is exhibited by the lower tier, which includes some MgO-poor types (8% MgO, 47-48% SiO_2). The central core rocks also show variation in the ratio 100 Mg/(Mg +

TABLE 31. REPRESENTATIVE ANALYSES OF MOUNT NORTH LAMPROITES

	1	2	3	4	5
			Percent		
SiO_2	48.17	42.84	44.59	44.68	49.00
TiO_2	6.42	7.53	8.13	6.84	5.85
Al_2O_3	8.22	5.45	6.17	5.78	6.20
Fe_2O_3	5.60	6.34	6.35	5.43	4.60
FeO	0.92	1.44	1.87	1.56	1.89
MnO	0.04	0.09	0.10	0.08	0.07
MgO	7.80	11.24	10.36	11.50	11.20
CaO	2.75	3.98	4.15	4.05	3.47
Na_2O	0.18	0.46	0.64	0.72	0.83
K_2O	11.23	7.37	8.91	6.53	7.73
P_2O_5	2.37	2.02	1.98	1.37	1.74
H_2O^+	2.33	3.80	2.46	4.01	1.97
H_2O^-	1.53	2.99	1.16	3.00	2.22
CO_2	0.24	0.43	0.28	0.41	0.14
Rest	1.86	3.24	2.77	3.68	2.02
total	**99.66**	**99.22**	**99.92**	**99.64**	**98.93**
			Parts per million		
Ba	4 124	17 084	11 273	22 076	7149
Li	9	9	11	9	11
Rb	711	653	694	666	342
Sr	1 999	1 996	1 722	1 897	1 640
Pb	95	93	101	77	48
Th	57	74	102	55	35
U	5.5	11	11	7	2
Zr	2 340	2 472	2 611	2 102	1 926
Nb	244	299	308	254	151
Y	37	38	38	33	15
La	489	486	716	336	385
Ce	967	1 045	1 734	719	718
Nd	326	471	695	377	—
Sc	15	16	18	12	21
V	158	225	242	178	162
Cr	630	546	665	521	406
Co	—	—	—	—	35
Ni	538	280	356	443	857
Cu	35	63	67	58	66
Zn	84	97	104	85	85
Sn	11	16	18	9	13
Ga	22	16	18	13	14
S	—	—	—	—	570
F	5 000	3 500	3 900	3 900	5 250
Cl	—	—	—	—	105

1 — Fine-grained olivine-phlogopite-leucite lamproite; lower sill, BMR 83210320. 2 — Olivine-phlogopite-leucite lamproite; tier 1, BMR 83210326. 3 — Olivine-bearing, diopside - potassic-richterite - phlogopite - leucite lamproite; base tier 2, BMR 83210323. 4 — Olivine-bearing phlogopite - potassic-richterite - leucite lamproite; top of tier 2, BMR 83210321. 5 — Phlogopite - olivine - potassic-richterite -leucite lamproite; sill northeast corner, offshoot from centre, GSWA 71803.

Fe), from ≈67 in the Mg-poor parts of the lower tier to ≈76 at the top of the upper tier. However, Mg/(Mg + Fe) ratios do not correlate strongly with other parameters of differentiation such as K_2O content and abundances of Ni, Cr, and Zr. A feature of the central core rocks is their high TiO_2 and Ba contents (6.4-7.8% TiO_2, 13 000-26 000 ppm Ba), which serve to distinguish the central core from the lower sill rocks.

Rocks from the lower sill complex, in contrast to the central core rocks, are characterized by more silica-rich and felsic compositions (49-55% SiO_2, 6-9% Al_2O_3, 8-11% K_2O). CIPW norms show greater normative orthoclase content and, commonly, normative quartz, in contrast to the central core lamproites. Apart from the olivine-rich sill in the northeast, which contains ≈11% MgO, the sills generally have lower MgO contents (6.5-8%) than the central core rocks. Nickel and chromium contents are very similar, however; but Ti and Ba contents are distinctly lower in the sill rocks than those of the central core (5-8% TiO_2 3600-5000 ppm Ba).

The Mount North lamproites, as a group, have high abundances of Sr, Pb, Zr, Y, Ti, Nb, and LREE, compared to the West Kimberley suite as a whole. The extremely fractionated nature of the Mount North rocks is shown by their extreme enrichment in LREE (1 500-2 400 times chondritic), and very high Rb/Sr ratio (0.2-0.4).

MOUNT PERCY

The lamproites of Mount Percy were known to Prider (1960): but, because of the apparent small size of the intrusion, they have not been previously studied in any detail. Mount Percy itself is composed of sandstones which rise as a conical hill about 60 m above the plain, forming a prominent landmark. The principal lamproite outcrops occupy a small area, about 100 × 150 m, at the foot of the hill on its northeast side. However, much of the vent is unexposed and the intrusion has affected much of the sandstone of Mount Percy which is intruded by dykes of lamproite, tuff, and breccia (Fig. 62).

Mount Percy forms part of an outlier of Grant Group sandstones, which, in the immediate vicinity, unconformably overlie the Gumhole Formation, the lowest unit of the Fairfield Group. Flaggy limestones of the Gumhole Formation outcrop to the north and east, within a few hundred metres of Mount Percy, and dip gently towards the hill. Although the Permian sandstones once covered the whole area, it appears they owe their present preservation, in part, to a depression in the limestone surface. The depression is possibly the result of adjacent strata sagging during the formation of the Mount Percy vent. Sedimentary structures in the sandstone have been largely destroyed by the effects of the lamproite intrusion; but, on the northern side of the hill, the sandstones are well-bedded mature sediments with sub-horizontal beds up to 1 m thick. Cross-bedding and rare pebble-sized conglomerate beds can also be found.

Volcanism began at Mount Percy with an explosive, gas-rich phase, which penetrated the sandstone to form a vent filled with sandstone breccia and arcuate dykes of similar composition. Most of this early vent is now obscured by eluvium and soil, but isolated outcrops can be found of a coarse sandstone breccia with fragments up to 10 cm across, close packed, and recemented by interstitial sand-size quartz grains. The margin of the vent is marked on the southeastern side by small rounded outcrops of baked sandstone and on the western side by the mass of Mount Percy. On the hill itself, the regular bedding of the Grant Group sandstone has been disrupted by the formation of narrow lenticular dyke-like masses of sandstone breccia. These dykes are particularly evident on the summit ridge where they are several metres wide and up to 80 m long. The breccia dykes are concentric with the main vent and appear to form a discontinuous set of cone-sheets, dipping towards the vent at about 80°. In addition to the breccia dykes,

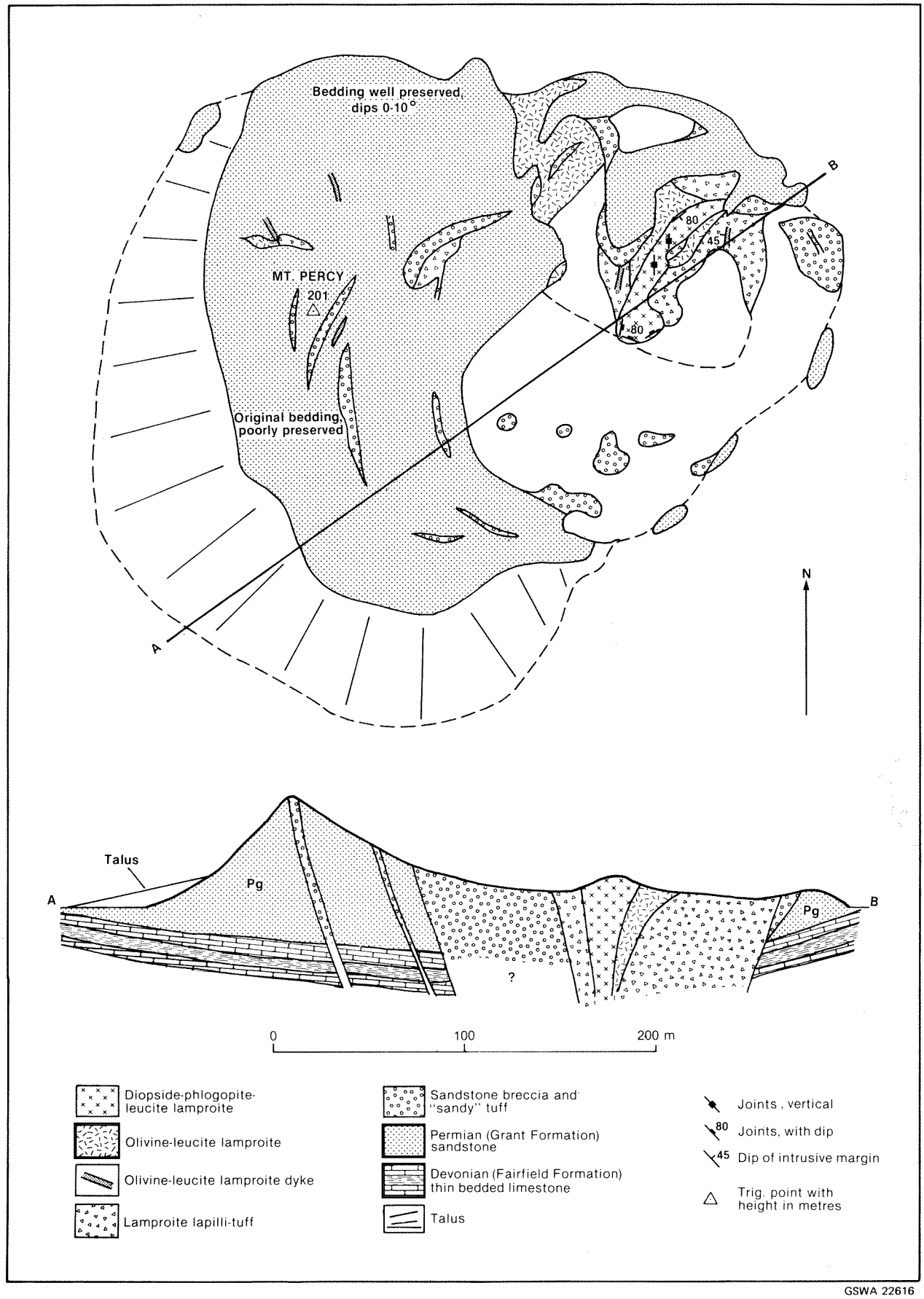


Figure 62. Geological map of Mount Percy.

but not marked on Fig. 62, Mount Percy contains a number of thin veins of fine-grained lamproite and lamproite tuff up to 50 cm wide; these probably relate to a later volcanic phase.

The lamproite phase of volcanism resulted in the emplacement of lamproite tuffs and lapilli-tuffs, fine-grained olivine-leucite lamproite, and a dyke-like central intrusion of phlogopite-leucite lamproite. The locus of this activity was displaced to the northern margin of the early vent. Much of the lapilli-tuff is soil covered; but, where exposed, it is fairly uniform, unbedded, and has a distinctive blue-green colour on fresh surfaces. Fine-grained olivine-leucite lamproite forms irregular masses, thin sills, and dykes, within the lapilli-tuff; and both have been cut by the central core of relatively coarse-grained, brown phlogopite-leucite lamproite. The central core is a dyke-like mass about 100 m long and 10 m wide; it trends northeast and has a bulbous expansion, about 20 m diameter, at the southwest end. Jointing, and exposures of the margin, indicate a body with margins dipping steeply inwards at 80°-90°.

Adjoining the main vent to the north is a complex area of sandstone breccia and intrusions of fine-grained olivine-leucite lamproite. A framework is provided by ribs of baked sandstone margined by a thin skin, up to a metre wide, of brecciated sandstone. Larger areas of sandstone breccia represent small vents, or enlarged breccia dykes similar to those on Mount Percy, and these have been intruded by fine-grained lamproite, leaving narrow screens of breccia between successive intrusions.

About 300 m northwest of Mount Percy is a low hill of Grant Group sandstone, about 20 m high, in the form of an oval amphitheatre 150 m across and open to the east. The formation suggests the possibility of a concealed lamproite vent occupying the central depression. However, there is no evidence of lamproite veining or contact metamorphism of the sandstones. The presence of numerous man-made flakes attest to the former use of this rock by aborigines for the manufacture of stone implements.

Volcanism

The general pattern of volcanism at Mount Percy is similar to that at Mount North: an initial phase of explosive volcanism was followed by successive intrusions of fine-grained magmatic lamproite and a central core of coarser grained lamproite. In detail, however, the pattern shows considerable variation from Mount North and many similar intrusions, in particular the shape of the vent and the eccentric nature of successive events.

The initial explosive phase led to the formation of the sandstone breccia and dykes of similar material in the surrounding country rocks. The force of the explosive activity, however, was not sufficient to clear the material from the vent; and, unlike Mount North where little such material remains, the Mount Percy vent is largely filled with brecciated sandstone. The breccia, and the lamproite pyroclastics of the succeeding volcanic phase, are unbedded chaotic vent infillings. The margins of the vent dip steeply inwards at about 80°; and, although Mount Percy is eroded to a somewhat lower level than Mount North, the lack of any evidence for a flaring of the vent cannot be because the vent has been eroded to the level of the "root zone": the difference in erosion level is only about 60 m or so. If the Mount Percy vent did continue to the surface as a steep-sided, carrot-shaped vent, similar to the model for kimberlite volcanism of Hawthorne (1975), then the "cone-sheet" form of the brecciated sandstone bodies possibly provides an insight into the formation of the flared vent more characteristic of lamproite volcanism. The sandstone breccia dykes represent zones of weakness concentric with the vent. During the active phase of volcanism, they would have been open to the passage of gas and allowed large blocks of country rock to subside into the vent. As no limestone or crystalline basement fragments are seen in the breccias, it can be assumed that there was little mass transport through the dykes, which must have been superficial features connecting with the main vent at no great depth. Had volcanic activity continued in a forceful way for any length of time, successive blocks would have spalled from the vent walls and would have been cleared from the vent by the force by the volcanic gases — thus giving rise to the typical flared "champagne glass" shaped vent. At Mount Percy, however, the process has been arrested at an intermediate stage, the sandstone breccia dykes being the equivalent of the ring-faults associated with maars, as noted by Lorenz (1973, 1975), and the faults in the upper parts of the Montana diatremes, as shown by Hearn (1968).

At the conclusion of this initial phase of activity at Mount Percy, it seems probable that there was a period of quiescence because the lamproite pyroclastics and intrusives occupy an area eccentric to the sandstone-breccia-filled vent. This secondary vent probably broke through fresh sandstone to form the northern complex, and invaded part of the original vent to emplace lamproite lapilli-tuffs and the central lamproite core. The narrow veins of lamproite in the country rock are probably related to this phase of activity as they are found predominantly in the northern half of the Mount Percy mass. The main tuff deposit is a medium-grained lamproite lapilli-tuff with only a minor wall-rock component; it is an unbedded, chaotic, vent filling. At the northern end of the central core, there is a small area of lapilli-tuff with a streaky appearance that is associated with fine- grained lamproite. The final phase of activity was the intrusion of the dyke-like central core, which possibly formed a small lava lake in the crater of the secondary vent.

Petrography

Pyroclastics: In thin section, the sandstone-rich breccias often appear to be normal mature sandstones; but, on weathered surfaces, their brecciated nature is apparent. The angular sandstone fragments, up to 10 cm across, are set in a sparse matrix of rounded quartz

grains, and the fragments can only be distinguished by the presence of quartz overgrowths that form the original cement of the sandstone. By attrition of the fragments and increase in the quartz-rich matrix, brecciated sandstone grades into tuff-breccia and tuff composed of accidental fragments and quartz grains with a small proportion of clay minerals and rare olivine pseudomorphs from the lamproite magma. In many of the finer grained tuffs, the quartz grains are fractured and shard-like; and, in some, there are accretionary lapilli up to 3 mm across of small quartz grains and clay minerals. Juvenile fragments of lamproite glass are common in some quartz-rich tuffs from the northern complex and in some small dykes which intrude Mount Percy; fiamme of fine-grained olivine-leucite lamproite often incorporate numerous quartz grains. The sandstone-rich breccias and tuffs commonly contain sedimentary grains of tourmaline; and some contain rare grains of zircon.

The lamproite lapilli-tuff varies from almost quartz-free, to material containing as much as 25% accidental quartz grains. The lamproitic material consists of angular, cognate and juvenile fragments, from 5-20 mm across, in a matrix that includes, besides quartz grains and rare quartzite and shale lapilli, many ash-sized lamproite fragments. The most common lamproite fragments are dense, fine-grained, porphyritic olivine-leucite lamproite that contain nontronite pseudomorphs after euhedral microphenocrysts of olivine in a matrix of small leucite euhedra and turbid, brown devitrified glass containing tiny prisms of priderite. Rare anhedral macrocrysts of altered olivine, up to 2 mm across, are also present. Other cognate lamproite types, present in some specimens, carry microphenocrysts of phlogopite or poikilitic groundmass potassic richterite. One specimen from the northern complex is richer in juvenile fragments; it consists of equal proportions of small fragments of a fine-grained welded tuff, and fragments and shards of a pumiceous lamproite glass.

In some pyroclastics there are, in addition to the angular fragments of crystalline lamproite, small lapilli and irregular blebs of lamproite which were evidently incorporated into the tuff while still plastic. More rarely, the proportion of such material rises to the extent that the lapilli-tuff consists of lamproite fragments in a matrix of similar magmatic lamproite. The rock resembles an autobreccia, but was probably formed by magma invading an earlier tuff. A final variety of tuff, which has a distinctive streaky appearance, occurs in a small area adjacent to the central core. In thin section, it is seen to consist of drawn out fiamme of fine-grained olivine-leucite lamproite, interlayered and mixed with quartz grains and fragments of grains from the brecciated wall rocks.

Intrusive lamproite: The fine-grained lamproite intrusive rocks are a uniform grey-green in hand-specimen, and contain euhedral microphenocrysts of former olivine in a matrix of minute euhedral and skeletal grains of altered leucite, set in brown turbid "clay minerals". The leucite grains, 10-20 μm diameter, are often cruciform or "snowflake" shaped: four or eight arms grow from a central nucleation point, but the typical leucite crystal form is not completely developed. Very small acicular prisms of priderite are present in most specimens with accessary apatite and prismatic diopside; one specimen contains indistinct poikilitic potassic richterite in the groundmass. The olivine is usually replaced by green nontronite, but in some specimens, by secondary silica. Marginal parts of the intrusions often incorporate small xenoliths of quartz-rich tuff, are vesicular, and have developed small flakes of phlogopite in the groundmass. The rock is in general similar to the rock fragments forming the lamproite tuffs.

The minor dyke rocks found intruding the lapilli-tuffs and the wall-rocks of Mount Percy are distinguished only by the presence of small flakes of phlogopite in the groundmass; one specimen contains a number of small euhedra of barite in the matrix.

The rocks of the central core are distinctive because of the numerous small phenocrysts of phlogopite; these are commonly about 1 mm long but may be up to 4 mm. The phenocrysts are strongly flow aligned, parallel to flow banding that is evident in the matrix. The phlogopite is strongly pleochroic and multiply twinned, but is distinctive in that it has developed no strongly coloured mantles or rims, and, apart from rare former olivine microphenocrysts, is free of inclusions. A few small altered olivine phenocrysts, up to 1 mm long, together with many small leucite crystals, up to 0.5 mm diameter, are set in a groundmass composed principally of brown turbid alteration products with small acicular crystals of diopside, small interstitial flakes of red-brown phlogopite, minor amounts of apatite, and accessory granules of priderite and perovskite.

Chemistry

The Mount Percy lamproites (Table 32) show a similar compositional range to that exhibited by the Mount North lamproites. Silica and MgO contents range from $\approx 46\%$ and $\approx 10\%$, respectively, in the phlogopite-leucite lamproites at the centre of the body to $\approx 60\%$ and $\leq 5\%$ in the olivine-leucite lamproites at the margins of the vent (analyses on H_2O^--free basis). However, some of the high SiO_2 and low MgO content of the olivine-bearing lamproites is attributed to leaching of Mg and silicification of altered olivine, because the MgO content of these rocks correlates poorly with observed modal percentages of olivine pseudomorphs and measured Ni contents, which range up to 700 ppm. Other major elements show less variation: TiO_2 contents lie in the range from 5 to 6.8%; K_2O contents, in the range from 8 to 10.8%; and Al_2O_3 contents, between 5.8 and 9.2%.

Large variations in alkalis and alkaline-earth metals occur within the suite, particularly Ba, Rb, and Sr. The highest Ba and Rb values (typically 10 000-20 000 ppm Ba, 500-600 ppm Rb) are associated with the phlogopite-rich lamproites of the central core, although a sample of an olivine-leucite lamproite near the summit of

TABLE 32. REPRESENTATIVE ANALYSES OF MOUNT PERCY LAMPROITES.

	1	2	3
	Percent		
SiO_2	45.60	51.20	52.40
TiO_2	6.65	5.31	5.54
Al_2O_3	6.60	8.20	8.50
Fe_2O_3	7.40	5.30	5.10
FeO	0.77	1.33	1.04
MnO	0.11	0.08	0.05
MgO	10.30	6.00	6.69
CaO	3.87	2.99	2.32
Na_2O	0.38	0.69	0.43
K_2O	9.83	9.95	10.80
P_2O_5	2.07	1.71	1.41
H_2O^+	2.58	2.12	2.20
H_2O^-	0.95	1.84	1.34
CO_2	0.08	0.27	0.05
Rest	3.60	2.59	1.63
Total	**100.79**	**99.58**	**99.50**
	Parts per million		
Ba	21 947	15 461	5 716
Li	10	11	8
Rb	649	259	318
Sr	1 875	996	1 254
Pb	80	58	75
Th	59	27	28
U	1	1	2
Zr	1 831	1 467	1 633
Nb	276	116	129
Y	29	19	18
La	520	386	435
Ce	610	570	749
Sc	23	18	17
V	124	178	278
Cr	419	320	283
Co	44	34	37
Ni	156	342	522
Cu	90	38	46
Zn	101	66	74
Sn	—	17	10
Ga	10	14	19
S	40	1 020	360
F	4 697	3 010	3 600
Cl	87	53	80

1 — Phlogopite-leucite lamproite; centre of vent, GSWA 71403. 2 — Olivine-leucite lamproite tuff; small pod to northwest of centre of vent, GSWA 71399. 3 — Olivine-leucite lamproite; dyke in tuff near centre of vent, GSWA 71838.

Mount Percy contained the extreme value of 2042 ppm Rb. In general, the phlogopite-rich lamproites are also enriched in many other "incompatible" elements over the phlogopite-poor olivine-leucite lamproites, despite the fact that the two groups are not greatly different in terms of Mg/(Mg + Fe) and Ni and Cr contents: the phlogopite-rich lamproites typically have slightly higher Mg/(Mg + Fe) ratios, but slightly lower Ni contents. All the Mount Percy rocks are strongly enriched in LREE (La = 860-1 600 times chondritic abundance) and have low abundances of HREE.

81 MILE VENT

The 81 Mile Vent was one of the first lamproite intrusions to be discovered after renewed interest in these rocks in the 1960's (Derrick & Gellatly, 1972). Although its outcrop is relatively insignificant compared with Mount North and many lamproites of the Noonkanbah Field, it is an ideal body in which to study lamproite volcanism. The body is named after the 81 mile post on the nearby telegraph-line track, but access has been improved as it lies beside the newly built haulage road to several of the diamond prospects of the Ellendale Field.

The main outcrop is a sill complex which forms a roughly circular ridge about 200 m in diameter and 15 m high, open to the southeast. The central depression is occupied by a core of phlogopite-rich lamproite (Figs. 63 and 64). Low outcrops of pyroclastics surround the central complex, but over half the surface area of the vent is covered by a thin layer of sand and soil up to 5 m thick. The overall outline of the pipe has been determined from shallow RAB drilling by CRA Exploration Pty Ltd; it occupies a roughly rectangular area 450 × 300 m, aligned northwest.

The wall rocks of the 81 Mile Vent are nowhere exposed, but drilling, and the presence of sandstone xenoliths in the pyroclastics, proves them to be Grant Group sandstones. Within the vent area, there is a thick sequence of tuffs and lamproitic lapilli-tuff, partly exposed beneath and between sills of fine-grained lamproite. In the western part of the vent, the pyroclastics are pale-coloured, thick-bedded (15-30 cm), and quartz-rich, lapilli-tuffs, but there is a small proportion of larger subrounded pebbles and blocks of sandstone up to 20 cm across. In the more easterly exposures, the pyroclastics are more thinly bedded and variable. They range from pale, fine-grained, laminated quartz tuff, with only a very minor lamproite component, to medium-grained lamproite-rich lapilli-tuff, bedded on a scale of 5-15 cm. A few larger cobbles of quartzite and, even more rarely, lamproite, are present, along with a variety of volcanic structures which will be considered later.

Towards the centre of the vent, the lapilli-tuffs are somewhat darker in colour, less quartz-rich, and appear more massive and tougher. They form a small ridge, 2-3 m high, across the outcrop of the eastern exposures. In part, this feature marks a real distinction in that the central lapilli-tuffs are comparatively lamproite-rich, but a close inspection reveals well-developed bedding indistinguishable from the lower tuffs. The principal cause of difference is that the central part of the tuff pile has been slightly metamorphosed by intrusive lamproite sills, now eroded, and numerous small veins and pods of similar lamproite.

On the northeast hill formed by the sill complex, thin slices of pyroclastic rock are found between the sills. Between the two lower sills there is about 1.5 m of bedded lapilli-tuff, similar to the main body of pyroclastics. It is a medium-grained lapilli-tuff containing small clasts of lamproite in a quartz-rich matrix; bedding is well developed on a 5 cm scale. A second screen of pyroclastic rock, between the upper two sills, is generally much thinner, but is very distinctive (Fig. 65). Throughout most of its length, the screen is only 30-50 cm thick, but it is crowded with angular fragments of sandstone and shale, 2-5 cm across, and a few larger fragments up to 20 cm across; the matrix consists of rounded quartz grains and phlogopite-bearing juvenile lamproite lapilli. At its northern end, where the overlying sill has been removed by erosion, this unit

presents itself as a small boulder field of large sandstone blocks. Both pyroclastic horizons are part of the main tuff-pile, although no rocks similar to the coarse breccia-lapilli-tuff are exposed elsewhere.

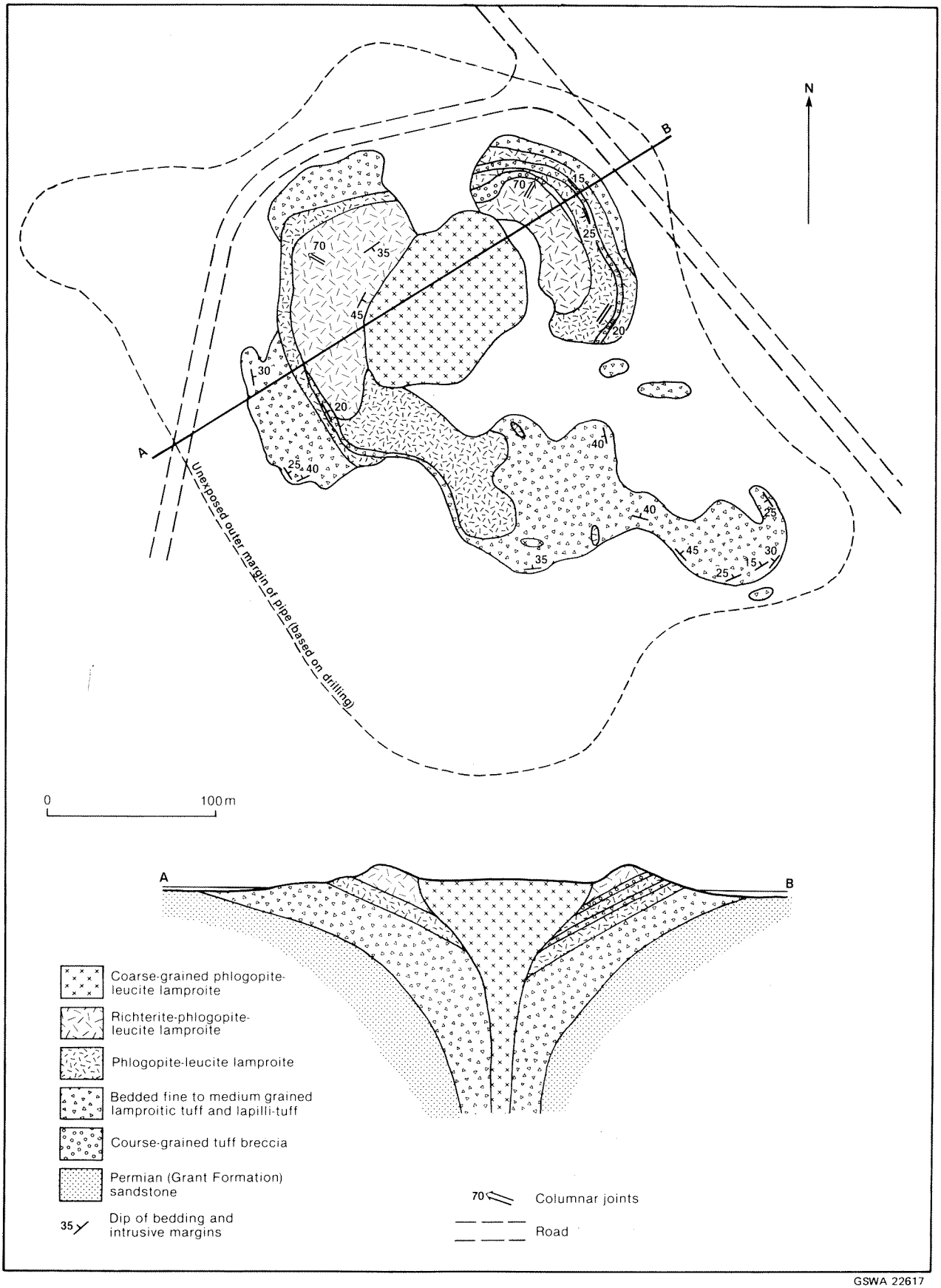


Figure 63. Geological map of 81 Mile Vent.



GSWA 22618

Figure 64. 81 Mile Vent: oblique view from the southwest. The upstanding rim is formed by lamproite sills and the central depression is occupied by the central core of phlogopite-leucite lamproite. (Photo: G. Derrick, BMR).



GSWA 22619

Figure 65. Thin screen of tuff-breccia between the upper and middle sills of the northern hill of 81 Mile Vent.

The main topographic expression of the 81 Mile Vent is formed by two small hills, each made up of a number of sills of fine-grained grey-brown lamproite. On the northeast hill, three sills can be distinguished, each separated by a thin screen of pyroclastic rock. On the western hill, the screens are less well developed; and, although three sills appear to be present, only the uppermost sill can be certainly correlated with the uppermost sill of the northeast hill. That the units are sills, rather than flows, as suggested by Derrick and Gellatly (1972), is shown by their sharp margin against the tuffs, and the inward dip of the bodies.

On the northeastern hill, the lowermost sill is about 2-3 m thick; formed by a very fine-grained, close-jointed, grey-weathering lamproite; and is partly obscured by soil cover and scree. The rock is distinctive in that, on fractured surfaces, the central portion is fresh and black, almost glassy, whereas the basal portions are pink-brown, autobrecciated, and intermixed with tuff. The lower slopes of the western hill are scree covered, and the sill is not traceable, with certainty, into this area. On the south side of this hill, there are small exposures of a thin sill, 1.5 m thick, which may be an extension of the lower sill.

The middle sill, exposed on the northeastern hill, is about 3 m thick, and similar in appearance to the lower sill. Where visible, the margins of the sill against screens of pyroclastics are sharp, and dip towards the centre of the vent at 15-25°. Immediately adjacent, on the western hill, this sill appears to be absent; but, to the southeast, separated from a lower sill by a thin tuff screen, there is a large area of poorly exposed lamproite of similar appearance which probably forms part of the middle sill.

The upper sill is distinctive and forms the capping of both the northeastern and western hills. It is formed by a fine-grained, grey-brown weathering lamproite, is up to 10 m thick on the western hill, and, in parts, is notable for columnar jointing. On the northeastern hill, the upper sill is separated by a screen of breccia-lapilli-tuff from the middle sill; but, on the western hill, it appears to directly overlie the middle sill. The columnar joints, about 20 cm diameter, dip outwards at 70°, and indicate an inward dip for the sill of about 20°. On the western hill, the ends of the columnar joints are exposed and indicate a progressively increasing dip for the upper surface of the sill of 35-45° towards the centre of the vent. On the northeastern hill, bulldozer scrapes — made during diamond exploration activities — show a similarly increasing dip of the sill towards the centre. At this point, there appears to be very little, if any, tuff separating the upper sill from the rocks of the central core.

Rock of a similar appearance to that forming the sill complex occurs as small pods, veins, and dykes, in the central parts of the pyroclastic outcrop and these are, no doubt, connected to the sills at depth.

The central core of the 81 Mile Vent is a medium-grained, brown rock containing prominent flow-aligned phenocrysts of phlogopite up to 5 mm across. The mass is roughly circular, about 120 m diameter, and ocupies a central depression that is partly encircled by the ridges of the sill complex. The natural exposure, partly obscured by soil cover, consists of boulders and scattered small exposures, but exploration activities have opened up some extensive exposures in pits.

Volcanism

The sequence of volcanic activity in the 81 Mile Vent is the same as that at Mount North. An initial explosive phase formed a pyroclast-filled vent; the pyroclastic rocks were then intruded by sills; and, finally, the vent was sealed by the emplacement of a central magmatic core. Although the central core appears as a lava lake in the cross section of Fig. 63, it is not known whether this was so in the original volcano. Compared with Mount North, however, the ratio of magmatic to pyroclastic deposits is much lower in the 81 Mile Vent, and late erosion has relatively reversed the topography: at Mount North the central core forms the bulk of the hill; at the 81 Mile Vent it occupies a topographic depression.

The initial explosive phase of volcanism excavated a large crater, which is now filled predominantly with well-bedded lapilli-tuffs. The low-angle dip of the bedding, commonly less than 30° in marginal areas, and the lack of any evidence of ring faulting, indicates a rapid constriction of the vent with depth to form a "champagne glass" shaped pipe. The irregular shape of the vent may have been caused by parallel elongated vents, but is probably the result of large joint-controlled blocks sliding into the vent, a similar mechanism to that proposed for Mount Percy. The straight southwest margin of the vent is an obvious candidate for joint control.

The pyroclastics are well exposed in certain areas and provide excellent examples of pseudo-sedimentary structures related to the style of volcanism. Fine-grained laminated quartz-rich tuff layers provide examples of low-angle cross-bedding that resulted from base-surge style deposition (Fig. 66c); and some of the larger rounded pebbles in the tuff, up to 20 cm across, are drop-stones which have disrupted the bedding of the tuff beneath them (Fig. 66a). Small-scale slump features, including zig-zag bedding, are common because of the steep depositional angles of the tuff, and later compaction (Fig. 66d). At one point, a trough, 1 m wide and 30 cm deep, has been cut into the fine-grained tuffs and is filled by coarser lapilli-tuff and overlain by more bedded tuff (Fig. 66b).

The best exposures of the pyroclastics outcrop parallel to the vent margin, and beds are only exposed for a few centimetres down dip. Nevertheless, it is evident from the regularity, lateral continuity, and dip of the bedding, that the internal structure of the tuff results from volcanic processes rather than from later reworking by water or wind. The various bedding structures represent air-fall deposits in the coarser layers, and drop-stones and base-surge deposits in the finer-grained layers. The structures are similar to those illustrated by Fisher and

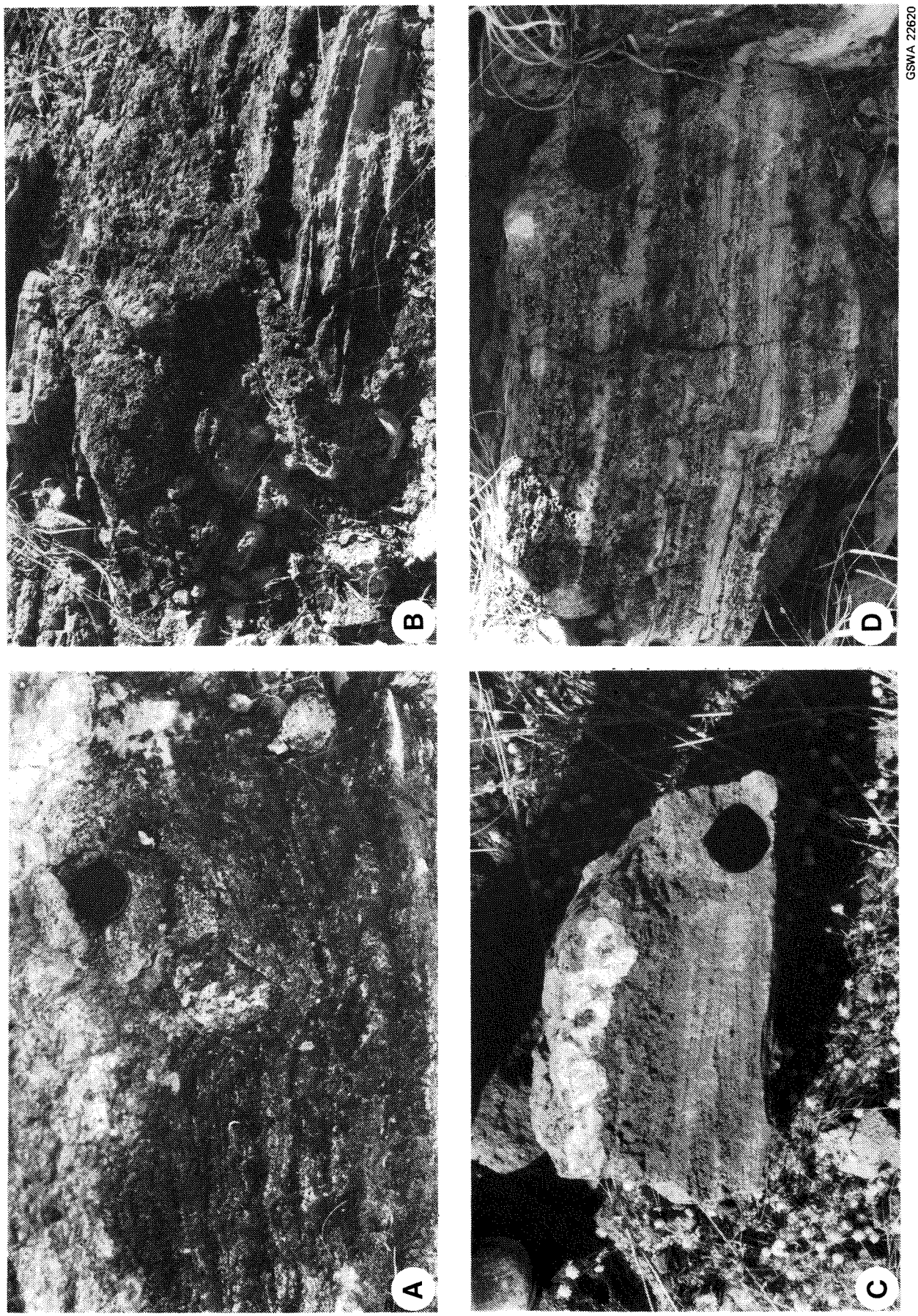
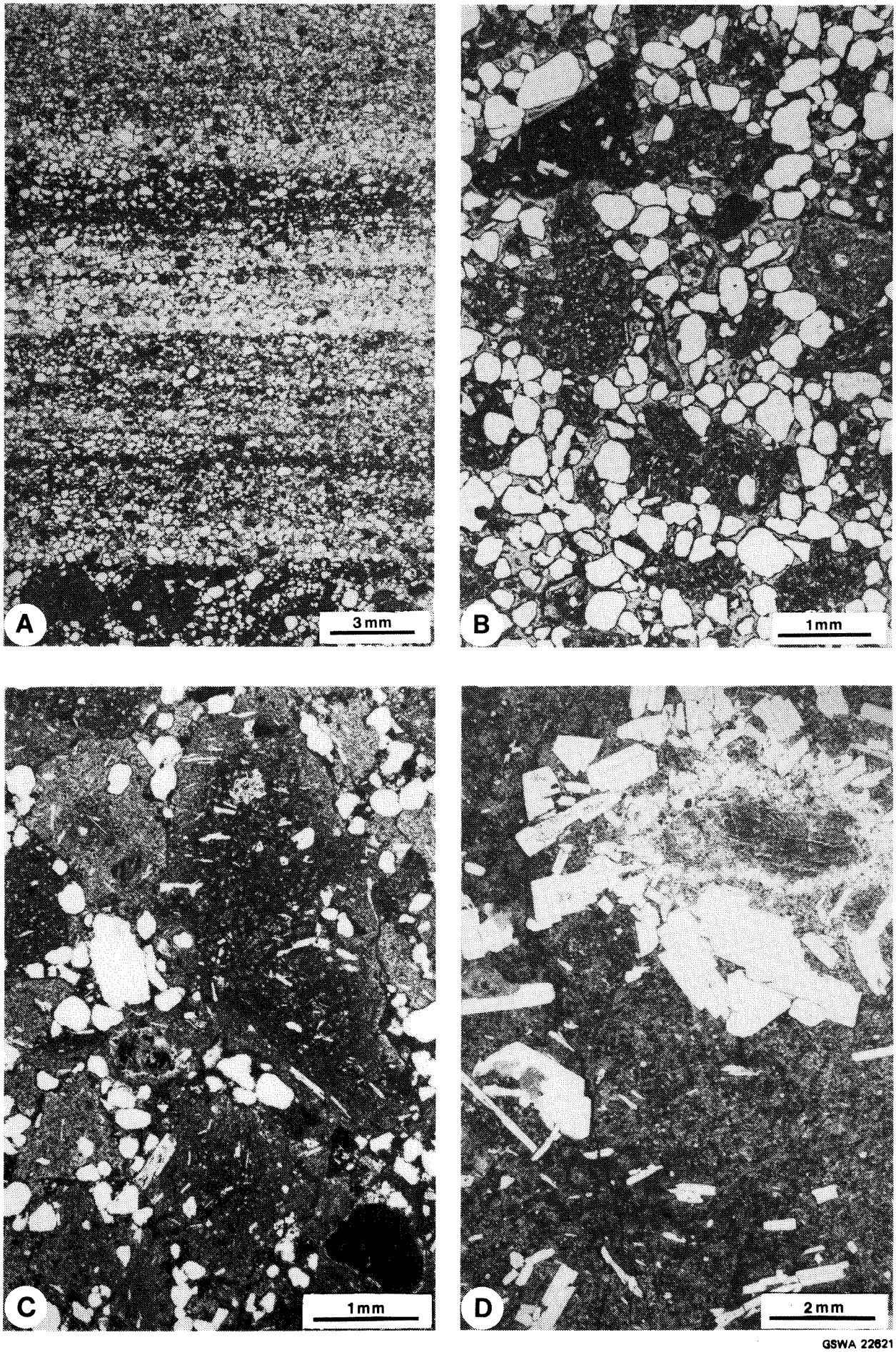


Figure 66. Structures in the pyroclastic deposits of 81 Mile Vent: A — Subrounded dropstone of lamproite: the lamellar bedding is disrupted around the stone. B — Radial channel about 1 m wide cut into thin-bedded "sandy" tuff, filled by coarse lapilli-tuff and overlain by more "sandy" tuff. Probably the result of slumping within the vent. C — Cross-bedding of fine-grained quartz-rich tuff. D — Minor slumping and disruption of well-bedded fine-grained tuffs.


A
3 mm
B
1 mm
C
1 mm
D
2 mm
GSWA 22621

Waters (1970) for a number of maar volcanoes and by Leys (1983) from Iceland.

The sill complex and central core are slightly displaced to the northeast from the geometric centre of the vent, but probably indicate the location of the original conduit. The sills, the earliest magmatic phase, were emplaced in a tuff pile that, although of unknown extent, was much larger than the present vent outline. By comparison with the baked sandstone rim rocks of nearby Ellendale 6, a minimum of 30 m of erosion is indicated, and the tuff-pile extended upwards to form a cone or tuff-ring. The two, lower, fine-grained sills were probably contemporaneous, and were possibly emplaced in a relatively cool tuff-pile. The upper sill, however, displays crude columnar jointing suggestive of a slower cooling rate. This may have been caused by the heating of the tuff-pile on the emplacement of the final magmatic phase, the central phlogopite rich core.

Petrography

Pyroclastics: The pyroclastics within the 81 Mile Vent vary from tuff to lapilli-tuff and consist essentially of mixtures, in variable proportions and grain size, of quartz grains and lamproite fragments. Although large blocks of sandstone are seen in outcrop, smaller xenoliths are very rare in thin sections; and the most prominent accidental lapilli are laterite pebbles.

The fine-grained laminated tuffs are particularly quartz-rich and contain overall about 70% rounded and fractured quartz grains up to 0.5 mm across; the remainder are small ash-sized lamproite fragments, phlogopite flakes, and interstitial, very finely comminuted lamproite dust (Fig. 67a). Individual laminae are from 0.5-2 mm thick, and are either quartz rich, with only rare lamproite ash and phlogopite flakes, or are composed predominantly of lamproitic debris. The margins between laminae vary from sharp to gradational, and there is a sharp margin against underlying coarser lapilli-tuff. Within some quartz-rich laminae, there is evidence of graded bedding; larger rounded grains are found at the base and smaller fractured grains at the top.

The most common pyroclastic is a lapilli-tuff, composed of about 30% of rounded quartz grains up to 1.5 mm across, rare rounded pyroclasts of shale and laterite, up to 5 mm, and the remainder, juvenile lamproite fragments 3-6 mm across (Fig. 67 b,c). The quartz grains are derived from disaggregated wall-rock sandstone, and the grains are less fractured than those of the laminated tuffs; rare grains of tourmaline and zircon are derived from the same source. The lamproite lapilli are of uniform composition and vary only in the degree of crystallinity. They are a fine-grained phlogopite-leucite lamproite with small flakes of phlogopite 0.1-0.5 mm long in a matrix crowded with minute euhedral and skeletal leucite crystals. The groundmass varies from glassy to cryptocrystalline, and is sometimes vesicular. A few of the lamproite fragments are angular or sub-rounded, but predominantly they are irregular, and appear to be small lapilli incorporated into the tuff while still plastic; some lapilli have incorporated quartz grains. The preservation of complex shapes is further evidence that the bedded tuffs are of air-fall or surge origin rather than reworked lacustrine deposits.

The sparse suite of accidental pyroclasts consists predominantly of small, rounded, laterite pebbles, fragments of siltstones, and a single example of a rounded fossiliferous limestone fragment, 20 mm long and cored by laths of barite. The shale and limestone xenoliths probably come from the underlying Fairfield Group, and the laterite pebbles from early Tertiary deposits overlying the Grant Group sandstones.

The coarse tuff-breccia forming a screen between the two upper sills of the northeastern hill is distinctive only for the presence of numerous accidental pyroclasts of quartzite and shale up to 5 cm across in addition to laterite pebbles, lamproite lapilli and rounded quartz grains.

Lapilli-tuffs collected close to the centre of the vent are quartz-poor and have a matrix rich in lamproite shards. In addition, the presence of a few large anhedral olivine crystals, up to 3 mm across and pseudomorphed by nontronite, suggests that later tuffs are more magnesian than the earlier products of the vent. Metamorphism of the tuffs by the sills and the central core has recrystallized the quartz grains to a fine- grained mosaic.

Sill complex: The two lowest sills are petrographically very similar, both are very fine grained phlogopite-leucite lamproites containing small flakes of phlogopite up to 0.5 mm long in a turbid matrix crowded with very small euhedral and skeletal crystals of altered leucite. The matrix also contains minute prisms of priderite and, in some specimens, is marked by incipient crystallization of phlogopite and potassic richterite. The phlogopite is crudely flow-aligned and the rock sometimes flow-banded. Most specimens contain a few rounded quartz grains derived from the tuff.

The basal 20-30 cm of the lowest sill commonly shows autobrecciation and a strong admixture with the underlying tuff; this results in textures with the appearance of a coarse lapilli-tuff. Quartz grains and laterite pebbles have been caught up in the advancing magma, which is further distinguished by the presence of small altered olivine euhedra, perhaps concentrated near the base by flow-differentiation.

The upper, columnar-jointed, sill is petrographically similar to the lower sills except for the prominent

Figure 67. Photomicrographs of tuffs and lamproite from 81 Mile Vent: A — Laminated, fine-grained, quartz-rich tuff overlying lapilli-tuff, from the bedded pyroclastics exposed on the southeast side of the vent (GSWA 76107B).B — "Sandy" lapilli-tuff; same location as A. (GSWA 71829). C — Lapilli-tuff with "sandy" matrix; note abundant microphenocrysts of phlogopite in the leucite-rich lamproite lapilli. Tuff screen between the two lower sills, north side of vent (GSWA 71815). D — Phlogopite-leucite lamproite, central core. Phenocrysts of phlogopite surround an altered "spongy" leucite with abundant pleonaste granules; the altered groundmass is leucite-rich (GSWA 71812).

development in the matrix of poikilitic potassic richterite prisms up to 1 mm long; in addition, a few small euhedral olivine pseudomorphs are generally present.

Central core: The most prominent feature of this intrusion in hand specimen is the abundance of large flow-aligned flakes of phlogopite, 2-3 mm long, often forming aggregates up to 8 mm across (Fig. 67d). The phlogopite is relatively pale-coloured, twinned, and shows only a very narrow dark-coloured titaniferous rim. A few altered phenocrysts of olivine up to 2 mm across are also present, and small laths of apatite are plentiful. The matrix is a fine-grained, altered, turbid mass of greenish clay minerals in which can be distinguished altered leucite, diffuse poikilitic potassic richterite, and small prisms of diopside and priderite. A small pod of similar material in the south of the vent differs only in having wide coloured margins to the phlogopite flakes that enclose small priderite prisms.

Chemistry

The 81 Mile Vent lamproites show a restricted range of compositions (47-54% SiO_2, 6.3-11% MgO, 6-11% K_2O). All are oversaturated in SiO_2, contain abundant normative orthoclase (>30%), and have high TiO_2 content (5.4-8.1%). Representative analyses are given in Table 33.

The most Mg-rich rocks of 81 Mile Vent are the medium-grained phlogopite-leucite lamproites at the centre of the vent. These contain 10 to 11% MgO, and have higher Mg/(Mg + Fe) ratios (≈0.75) and Ni and Cr contents than most of the other lamproites of 81 Mile Vent. The central lamproites also contain higher TiO_2, Zr, Nb, Pb, Sr, and La, than the other intrusive phases of the body indicating extreme enrichments in these incompatible elements.

The sills are of similar composition, but have lower MgO and higher SiO_2 and K_2O than the central lamproites (Table 33). The lower sill is notable for the extreme Rb abundances (8 600 and 7 500 ppm) found in two samples.

All the 81 Mile Vent lamproites contain consistently higher Sr, Pb, Th, U, Zr, Nb, and LREE, than most of the West Kimberley leucite lamproites. Abundances of F, Ta, and Hf, are also approximately 1.5 times those of the average West Kimberley leucite lamproite, and very similar to those of Mount Percy.

TABLE 33. REPRESENTATIVE ANALYSES OF 81-MILE VENT LAMPROITES

	1	*2*	*3*	*4*	*5*
			Percent		
SiO_2	53.20	49.62	53.50	52.40	49.50
TiO_2	5.87	5.86	5.72	5.65	7.36
Al_2O_3	7.10	6.83	7.00	6.50	5.70
Fe_2O_3	5.10	4.76	4.20	4.80	6.10
FeO	0.61	0.49	1.27	0.88	1.29
MnO	0.06	0.03	0.07	0.06	0.13
MgO	7.11	7.85	7.39	7.88	11.00
CaO	2.36	2.70	2.61	2.38	2.68
Na_2O	0.10	1.01	0.70	0.49	0.28
K_2O	9.74	6.03	10.00	10.40	8.48
P_2O_5	1.83	1.34	1.37	1.25	1.44
H_2O^+	2.43	4.96	1.56	1.87	2.69
H_2O^-	1.84	4.74	0.89	1.28	0.86
CO_2	0.06	0.42	0.08	0.05	0.11
Rest	2.04	3.04	2.51	2.79	2.16
Total	**99.45**	**99.68**	**98.87**	**98.68**	**99.68**
			Parts per million		
Ba	8 002	9 568	12 059	15 264	7 970
Li	6	6	8	5	7
Rb	404	7 470	315	341	550
Sr	1 625	2 560	1 930	1 861	1 600
Pb	85	101	68	78	100
Th	33	53	27	32	30
U	2	5.5	2	3	4
Zr	1 939	1 653	1 865	1 784	1 800
Nb	138	194	135	132	300
Y	34	—	19	19	40
La	488	419	441	473	600
Ce	767	851	789	769	950
Nd	—	332	—	—	—
Sc	18	11	17	15	25
V	236	205	160	153	520
Cr	199	357	234	201	300
Co	24	—	32	39	50
Ni	325	272	249	285	380
Cu	60	44	83	42	70
Zn	90	91	108	73	94
Sn	14	9	16	9	10
Ga	21	29	19	18	14
S	60	—	980	340	200
F	5 390	3 800	4 960	4 660	5 300
Cl	58	—	79	78	—

1 — Phlogopite-leucite lamproite; pod in tuff on east side of vent, GSWA 71828. 2 — Phlogopite-leucite lamproite; lower sill, BMR 83210305. 3 — Phlogopite-leucite lamproite; middle sill, GSWA 71818. 5 — Medium-grained phlogopite-leucite lamproite; central plug, GSWA 30493.

ELLENDALE 2

Ellendale 2 is a group of thin, unexposed sills that intrude the limestones and mudstones of the Fairfield Group, and are located about 3 km east-northeast of Mount Percy. The sills were discovered by an airborne magnetometer survey, followed by a ground proton magnetometer survey and air-core drilling (Hughes, 1978; Smith, 1979).

Outcrop in the area is poor. It consists of small areas of flat-lying, flaggy, fossiliferous limestone that protrude through a thin layer of black-soil or calcrete up to 3 m thick. From borehole data, the limestone is associated with green and grey calcareous mudstones with occasional fossiliferous horizons. (Fig. 68).

Contours of total magnetic intensity show two well-defined dipole patterns with maximum contrasts of 60 and 110 nT against a uniform background of 50 195 ± 5 nT. The dipoles are centred near the subcrop of two major sills: the smaller sills encountered in drilling had little discernible magnetic effect.

The two major sills of phlogopite-olivine lamproite are approximately 8 m and 5 m thick; the larger, eastern, sill strikes east-west and dips at 10° to the north whereas the western sill strikes east-northeast and dips northwards at about 15°. In the sections drawn on Fig. 68 the sills are shown as relatively uniform in thickness throughout; but, in a trench excavated in the sub-crop of the western sill, the body is seen to pinch and swell from a maximum of 5 m thick to about 20 cm as it intrudes and contorts the mudstones of the Fairfield Group. The sill also encloses thin septa of mudstone a few centimetres thick and several metres long. Drilling in the area between the two major sills revealed several thin sills of similar lamproite up to 2 m thick.

Petrographically, the rock type is phlogopite-olivine

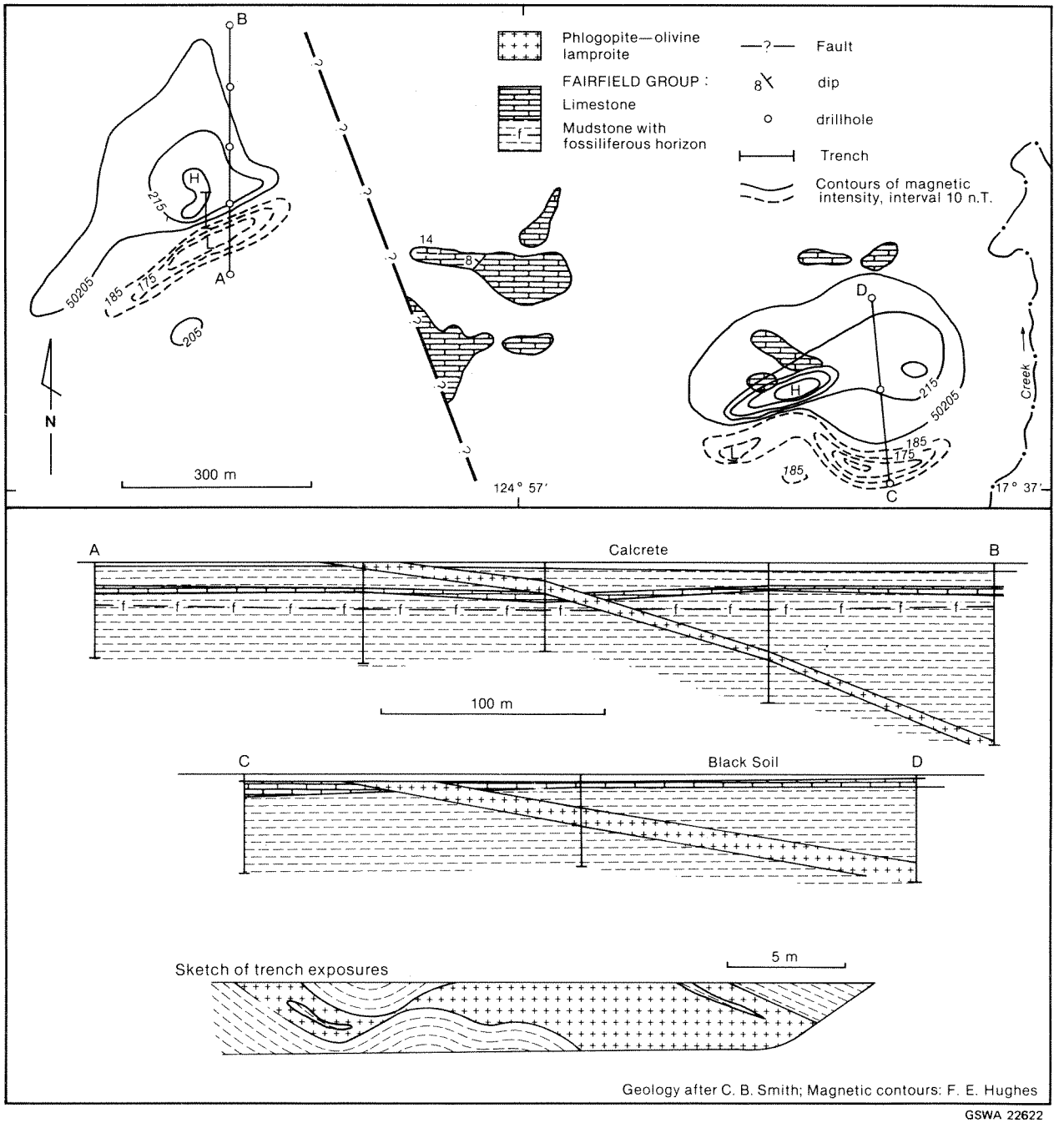


Figure 68. Geology and total magnetic intensity of Ellendale 2.

lamproite, distinguished from earlier descriptions by the complete lack of leucite. Olivine makes up about 20-30% of the rock and occurs in two generations: anhedral to subhedral macrocrysts 2-6 mm across; and small euhedral microphenocrysts < 1 mm long. The macrocrysts are commonly rounded or corroded to irregular shapes, and a single fresh example shows undulose extinction and polygonization. Apart from small relics, the olivine is pseudomorphed by talc, carbonate, or fine-grained clay minerals. Phlogopite forms small irregular, poikilitic flakes up to 1 mm across that enclose much groundmass material; it is generally a uniform orange-brown, but some examples show darker rims. The groundmass is thoroughly altered, and only accessory minerals can be clearly identified: many small grains of greenish perovskite, plentiful acicular apatite, and a little chromite and wadeite. The bulk of the groundmass is a brown turbid alteration product, but preserves a texture suggestive of many small diopside laths enclosed in glass. Most specimens contain irregular patches of carbonate and zeolitic material, and a few contain carbonate-filled vesicles and rare veins of carbonate. The source of the carbonate is almost certainly the enclosing limestones of the Fairfield Group and is not magmatic.

Chemically, the rocks are intermediate between the bulk of the leucite lamproites and the olivine lamproites of Ellendale 4 and 9. Table 34 gives the analyses of specimens from four thin sills and shows that for olivine lamproites MgO, at 17-18%, is low while CaO and K_2O are relatively high. The high CaO content is largely related to the degree of carbonation of the samples and

TABLE 34. REPRESENTATIVE ANALYSES OF ELLENDALE 2 LAMPROITES.

	1	2	3	4
		Percent		
SiO_2	42.50	37.10	37.40	39.60
TiO_2	4.63	4.60	4.79	4.59
Al_2O_3	4.30	4.40	4.70	4.20
Fe_2O_3	5.50	6.40	6.50	5.60
FeO	2.79	2.94	2.79	2.69
MnO	0.13	0.14	0.14	0.16
MgO	17.70	15.80	16.30	17.70
CaO	4.60	7.25	6.21	5.65
Na_2O	0.88	0.63	0.86	0.96
K_2O	4.34	3.35	3.47	4.11
P_2O_5	1.44	2.10	1.87	1.21
H_2O^+	5.65	4.89	5.16	5.71
H_2O^-	3.15	5.35	5.24	3.34
CO_2	0.28	2.56	1.68	1.41
Rest	1.82	1.88	1.99	2.11
Total	**99.71**	**99.29**	**99.10**	**99.04**
		Parts per million		
Ba	4 906	5 306	6 239	7 676
Li	60	41	55	61
Rb	538	362	358	471
Sr	1 613	1 975	1 874	1 659
Pb	80	75	77	80
Th	98	59	61	66
U	4	<1	1	2
Zr	1 371	1 648	1 618	1 550
Nb	259	207	211	229
Y	29	26	24	21
La	511	623	616	618
Ce	669	1 186	1 137	1 131
Sc	27	29	32	25
V	56	50	56	30
Cr	952	695	633	698
Co	58	51	51	61
Ni	600	627	632	706
Cu	56	53	60	53
Zn	96	81	75	80
Sn	—	15	13	5
Mo	3	<1	2	<1
Ga	4	6	6	7
S	300	260	160	490
F	6 072	4 900	5 500	4 660
Cl	60	86	80	60

1 — Olivine-phlogopite lamproite; core 2AC8 24m, GSWA 71440. 2 — Carbonated olivine-phlogopite lamproite; core 2AC3 22m, GSWA 71436. 3 — Olivine-phlogopite lamproite; core 2AC4 26m, GSWA 71437B. 4 — Leucite?-olivine-phlogopite lamproite; 2AC9 22-25m, GSWA 71442.

is reflected in the CO_2 analyses. Although up to 4.5% of K_2O is present, there is no evidence of leucite in the rocks.

ELLENDALE 4

Ellendale 4, at 76 ha, is one of the largest lamproite bodies in the Ellendale Field, and is perhaps the most complex structurally. It was discovered in November 1976 as a result of stream-gravel sampling, and was the first concealed pipe to be found in the area by the Ashton Joint Venture. Ellendale 4 is the richest diamond-bearing pipe in the Ellendale Field; and, as a result, has been subject to the most extensive drilling and sampling programme, although the grades recovered do not warrant mining under present conditions. The pipe is located at the northwest end of the Oscar Range, at the end of the haul road constructed by the AJV from the Gibb River Road.

At the present level of erosion, the pipe largely intrudes Permian sandstones of the Grant Group, while a small area in the northeast intrudes the Devonian Nullara Limestone, the platform facies of the Famennian reef cycle that forms much of the Oscar Range. Drilling has shown that the maximum thickness of Permian sediments overlying the limestone and calcareous mudstone formation is about 75 m around the southern margin of the pipe. In the vicinity of the pipe, the limestones are flat-lying and poorly exposed; but, around the southern margin of the pipe, the Permian sandstones are well exposed and form a low ridge up to 10 m high. Close to the pipe margin the sandstones have been baked and indurated; bedding structures have been disrupted and contorted and the rocks weather to rounded forms. Contact effects rarely extend beyond about 50 m from the pipe, and much of the sandstone outcrop is well bedded and flat-lying. Small, rounded exposures of indurated sandstone found around the northern margin of the pipe have, in parts, been brecciated and recemented.

The magmatic and pyroclastic rocks of Ellendale 4 are entirely concealed beneath a cover of sand and residual soil up to 5 m thick. Typically 1-2 m of red sand overlies a greenish residual clay of varying thickness derived from the underlying lamproite. In some sections, a thin calcrete horizon is present above the clay. The following account of the geology of the pipe is based largely on drilling records and core specimens, supplemented by surface pits excavated during exploration for diamonds (Onley and Smith, 1980; Smith, 1981)

In plan view, the pipe is a complex body in the shape of a figure of eight (Fig.69). The larger, eastern lobe is irregular in outline and approximately 850 m diameter, whereas the western lobe is 650 m × 400 m; the two are joined by a narrow neck about 150 m wide. The shape results from the coalescing of two major eruptive centres; but, as will be shown later, each lobe is itself a complex structure. Much of the surface area of the pipe is occupied by a central magmatic core of olivine lamproite, and pyroclastic rocks are confined to relatively small marginal zones. Drilling, however, has shown that in many areas, the magmatic material overlies lapilli-tuff at no great depth; and, overall, about 50% of the vent is filled by pyroclastics. The shape of the pipe will be considered in detail later; but, in general, it narrows rapidly to a number of narrow conduits at about 300 m depth (Atkinson and others, 1984a).

The pyroclastics are variable, both in grain-size and lamproite content, and range from quartz-rich tuff, a pale-green tuffaceous "sandstone" with little lamproite content, to dark-coloured lamproite lapilli-tuffs with little or no wall-rock component. Coarse layering in the tuffs can be reconstructed from drill logs, particularly near the margin of the pipe, and is illustrated in the cross sections of Fig. 69. An exploration pit excavated near the southern margin of the eastern lobe shows well bedded lapilli-tuff dipping at about 35° towards the centre of the vent (Fig. 70). Bedding is on a 10 cm scale; and, although there is minor faulting because of compaction, there is no evidence of major slumping. These pyroclastics are probably surge deposits and contain a few large dropstones of sandstone up to 10

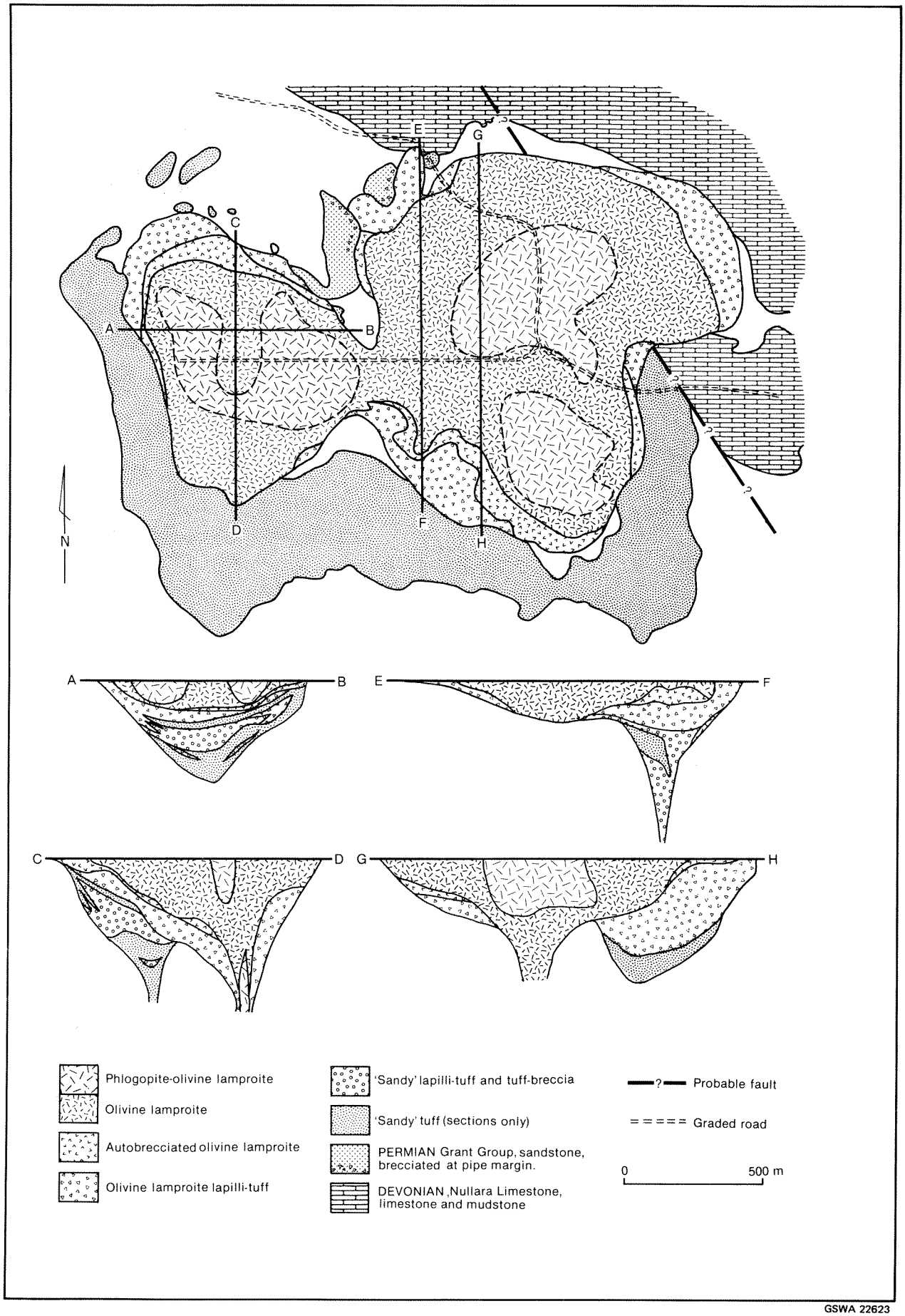


Figure 69. Geological map of Ellendale 4 (after Onley and Smith, 1980).



GSWA 22624

Figure 70. Bedded "sandy" lapilli-tuffs exposed in an exploration pit near the southern margin of Ellendale 4. The dip of the tuffs is depositional. (Photo: CRAE).

cm across. The pit also exposed a large mantle nodule, 30 cm diameter, weathered to a yellow clay.

In other pipes that have been drilled, and in exposed pyroclastics of the 81 Mile Vent and Mount North, lapilli-tuffs generally grade upwards from quartz tuffs and lapilli-tuffs with a significant accidental component at the base, to essentially monogenetic lamproite lapilli-tuffs without significant wall-rock content at the top of the pyroclastic pile. At Ellendale 4, the several varieties of pyroclastic rock are often interbedded, suggesting a more complex volcanic history than the gradual clearing from the conduit of wall-rock fragments. Quartz tuff, the initial product of the disaggregation of the wall-rocks, is usually the lowest deposit; but, as shown in section A-B of Fig. 69, beds of similar material may occur higher in the sequence, and lenses of more lamproite-rich tuff may be interbedded in the basal material. The interfingering of the several pyroclastic facies might result from the slumping of earlier deposits from the surrounding tuff-ring back into the vent, but the well-developed bedding suggests surge deposits from closely spaced vents erupting sequentially.

The central magmatic core of both eastern and western lobes is an olivine lamproite with prominent olivine macrocrysts up to 1 cm across. The magmatic material appears to have been erupted from at least two narrow conduits and probably formed a lava lake or magmatic blister in an open vent. From the cross sections of Fig. 69, it will be seen that the magma flowed out across the underlying pyroclastics and generally formed a relatively thin sheet. Two features of the magmatic core are noteworthy: firstly a basal layer, not always present, of autobrecciated olivine lamproite; and, secondly, large central areas of coarser grained lamproite with macroscopic phlogopite. The autobrecciated lamproite is the chilled marginal phase of the body, which was disrupted by the advance of the magma and the release of volatiles from the underlying pyroclastic deposits. The rock is usually glassy, rewelded, and has incorporated a few fragments from the tuff. Similar brecciated basal layers up to a metre thick are found in many lamproite intrusions but at Ellendale 4, autobrecciated zones up to 50 m thick have been recorded in some drill holes. The central zones of coarser phlogopite-olivine lamproite probably result from the slower cooling rate of the centre of the mass. The areas of phlogopite-rich lamproite are rootless zones extending to a depth of up to 130 m. Phlogopite is present throughout the olivine lamproite as small interstitial flakes, but only in the coarser variety is it visible in hand specimen.

Drill holes through the pyroclastic deposits have intersected a number of thin sheets of olivine lamproite. These are probably sills and intimately connected with the emplacement of the main lamproite core. Only one example of an intrusion later than the main core is known, from the neck of the conduit feeding the western lobe of the vent (section C-D, Fig. 69). A drill hole penetrated 318 m of magmatic lamproite, mostly a uniform olivine lamproite with groundmass phlogopite; the final 100 m, however, is quite different in character and contains large phlogopite flakes and a concentration

of olivine macrocrysts. This body represents a later pulse of magma cooled under a considerable cover of earlier lamproite.

Structure and volcanism

Drilling has been sufficiently extensive to allow the construction, with a reasonable degree of confidence, of contoured maps of the pipe wall and the base of the magmatic core (Onley and Smith, 1980) (Fig. 71). The maps reveal a complex system of small vents that coalesce to form the present pipe, and a lesser number of conduits feeding the magmatic core.

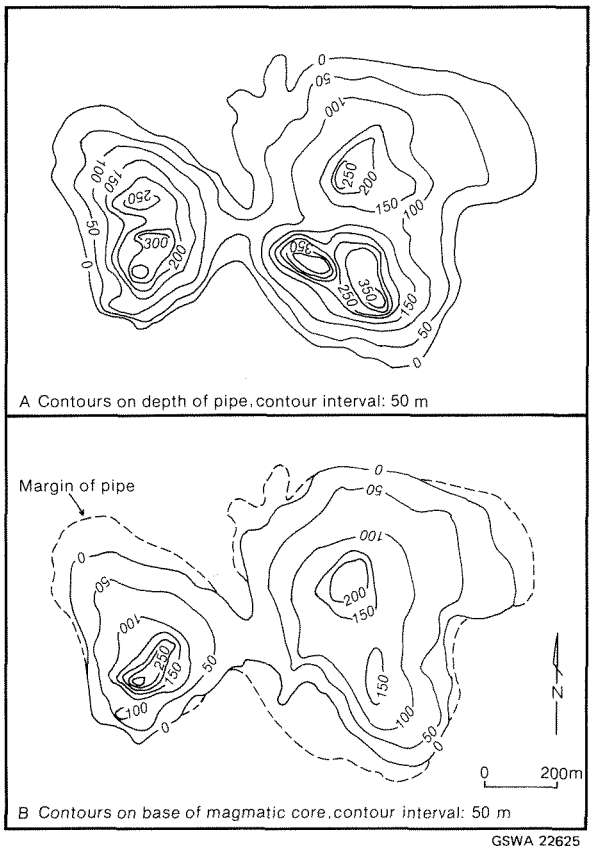


Figure 71. Structural contours of the Ellendale 4 pipe (after Onley and Smith, 1980).

The contours on the wall of the pipe show, firstly, that Ellendale 4 contains two major eruptive centres; both the western and eastern lobes are contoured to depths of 300-350 m, but the narrow neck joining them is no more than 60 m deep. The western lobe consists of three vents arranged north-south along the axis of the body, the two larger vents having been traced by drilling to 300 m and the smaller vent to 250 m. The overall shape of the complex, in which the contours merge at depths less than 150 m to form a single oval pattern, suggests that the vents were active simultaneously to form the final western vent.

The eastern lobe of Ellendale 4 also contains three vents, each of which can be contoured to a depth of 350 m. The two southern vents are very steep sided and coalesce above 250 m to form an elongate trough along the southern margin of the pipe. The larger northern vent is strongly flared and is responsible for the shape of the northern half of the lobe. Only at about 75 m depth do the three vents of the eastern lobe merge.

Contours on the base of the magmatic core outline a much simpler structure; only one conduit in each of the lobes produced magma. In the western lobe, only the southernmost vent was active in the final stage, and its products blanketed the two smaller vents. In the eastern lobe, the northern vent was the only major source of magma.

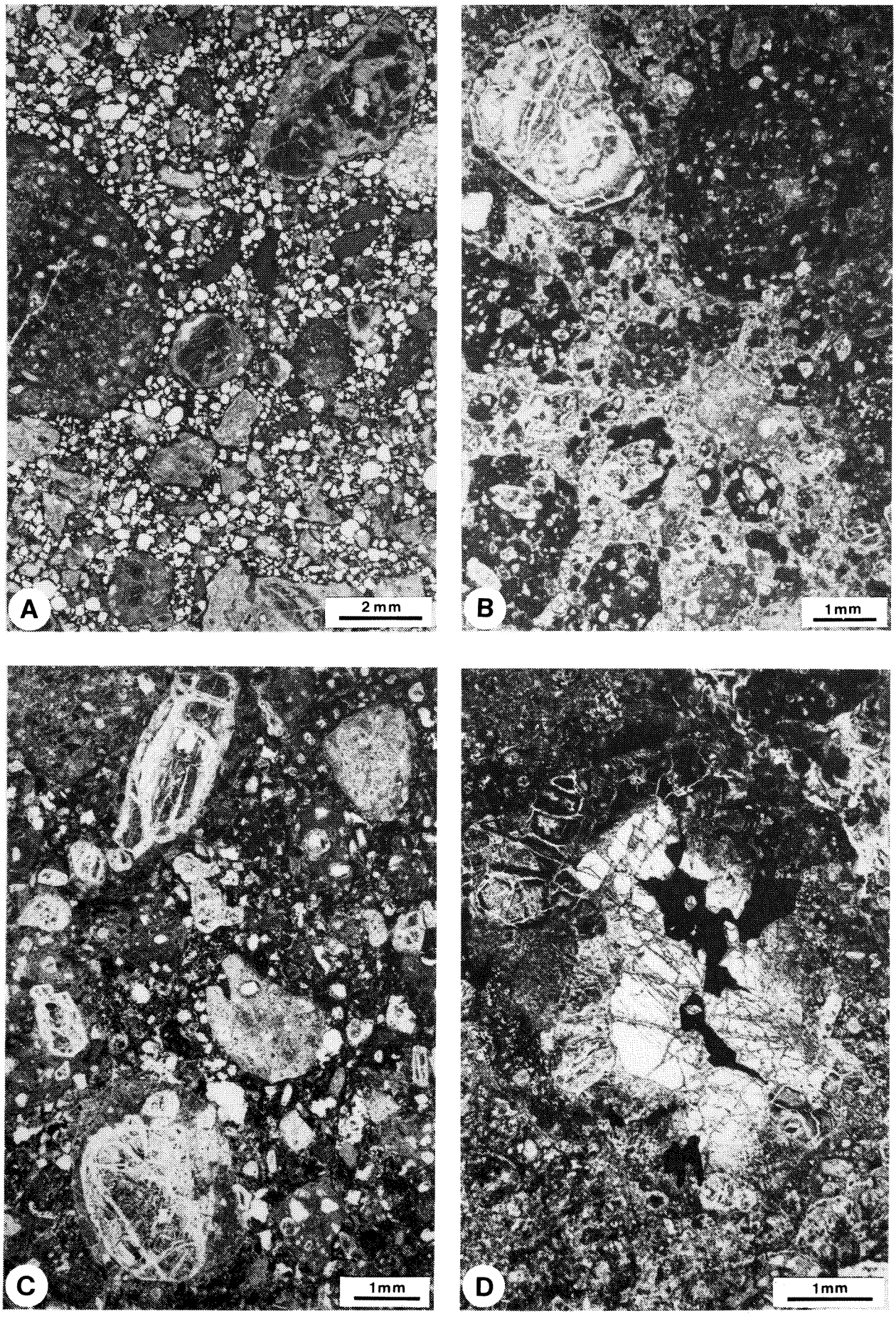
The eruptive sequence of these two grops of nested vents is difficult to determine; but, in the western lobe, activity probably moved from north to south. In the section C-D of Fig.69 the central vent is filled with quartz tuff overlain by "sandy" lapilli-tuff, probably the products of this vent. Overlying this sequence is more quartz tuff and lamproite lapilli-tuff, the product of the southern vent. In the final phase, magma welled up the southern vent blanketing the pyroclastics. Contours on the base of the magmatic material indicate that the northern vents had been obliterated as topographic features prior to the final eruption.

In the eastern lobe, the two southern vents are almost entirely pyroclast-filled, and contain a thick sequence of quartz tuff, "sandy" lapilli-tuff and lamproite lapilli-tuff. Section E-F of Fig.69 shows a thick lens of quartz tuff overlying "sandy" lapilli-tuff in the western vent. The tuff in this vent is in fact a distinctive tuff-breccia unit with plentiful large cobbles of sandstone up to 20 cm across; the lens of fine-grained quartz tuff is possibly the early product of a neighbouring vent slumped into the crater after the main eruption of the western vent. The overlying lamproite lapilli-tuffs are probably also the product of a neighbouring vent, blanketing the former crater. Magmatic activity at this vent was minor — a drill hole a little further east in the trough intersected several thin sills of olivine lamproite at levels not accessible to magma from the northern vent. The southwestern vent, not shown on cross sections, is similarly pyroclast-filled, but one drill hole into it did intersect an olivine lamproite plug in the vent, overlain directly by autobrecciated lamproite and olivine lamproite from the northern vent.

The main magmatic centre of the eastern lobe was the northern vent, the products from which spread out and blanketed the two earlier vents. Lamproite lapilli-tuffs from this vent probably filled much of the earlier, craters but the contours of Fig. 71b suggest that magma flowed out and filled the minor depressions that remained. No significant differences have been noted between the magmatic products of the two main vents, and no junction between the two lobes has been found in the vicinity of the neck joining the lobes. It is probable that the two vents were active simultaneously and that the magmas flowed together to form one large lava lake.

Diamonds

Exploration methods employed in assessing the diamond content of Ellendale 4 have been outlined in Chapter 1. The overall grade at surface of the most prospective area, above the trough on the southern



GSWA 22626

margin of the eastern lobe, is 14 CM/100 t (Table 3) but this includes local variations from 3.1 to 24.5 CM/100 t (Smith, 1981). The same variation is noted in samples from deep holes and is related broadly to the type of pyroclastic deposit sampled. Lamproite lapilli-tuffs, with little or no admixture of country rock material, range from 3-30 CM/100 t but "sandy" lapilli-tuff, because of dilution, rarely contains more than 4CM/100 t and quartz tuff rarely more than 1 CM/100 t. Pyroclastics of the western lobe show a similar range and variation, depending on the type of tuff sampled.

Magmatic material from the central core is very poor in diamonds. The grade recovered ranges from zero up to about 1.5 CM/100 t and averages about 0.5 CM/100 t. Of unknown significance, however, is the diamond content of the autobrecciated marginal lamproite. This is essentially the chilled marginal portion of the central magmatic core, and grades recovered have been as high as 21.8 CM/100 t (Smith, 1981). In general, the grades are intermediate between those of the lamproite lapilli-tuff and the magmatic core.

Petrography

Quartz tuff: The initial product of volcanism was a tuff consisting essentially of disaggregated wall rock, with only minor admixture of lamproitic material. Typically the tuff consists of rounded or fractured quartz grains from the Grant Group sandstones with a sparse matrix of clay minerals. In some specimens, small accretionary lapilli of angular quartz fragments and clay minerals (former volcanic ash) are present, and in others lapilli of olivine lamproite, siltstone, and altered olivine crystals. Where siltstone and mudstone has been incorporated into the tuff, the sediments have been metasomatized and plastically deformed to wisps of fine-grained chlorite-quartz rock. In one such specimen, small fragments of garnet, zircon, and rutile, are prominent accessories.

Tuffs intermediate between the quartz tuff and lapilli-tuff are rare, but there are examples in which quartz grains comprise less than 50% of the rock, the remainder being ash-sized particles of olivine lamproite or devitrified lamproite glass and interstitial lamproite dust. Other samples may contain 20-30% of small olivine lamproite lapilli 2-3 mm across, but contain quartz grains and lamproite ash as the dominant components (Fig. 72a). Tuffs composed entirely of ash-sized lamproite pyroclasts are very rare but may be found interbedded with coarser lapilli-tuff.

Lapilli-tuff: The dominant pyroclastic deposit within the vent is a lapilli-tuff consisting of lapilli of olivine lamproite up to 1 cm across, minor amounts of acidental lapilli of siltstone and shale, and a tuffaceous matrix of lamproite ash (Fig 72b). Some deposits, relatively early in the sequence, contain a proportion of quartz and microcline grains in the matrix and have been named "sandy" lapilli-tuffs; this provides a useful field distinction, as such tuffs can be recognized by the gritty surface of the drill-cores.

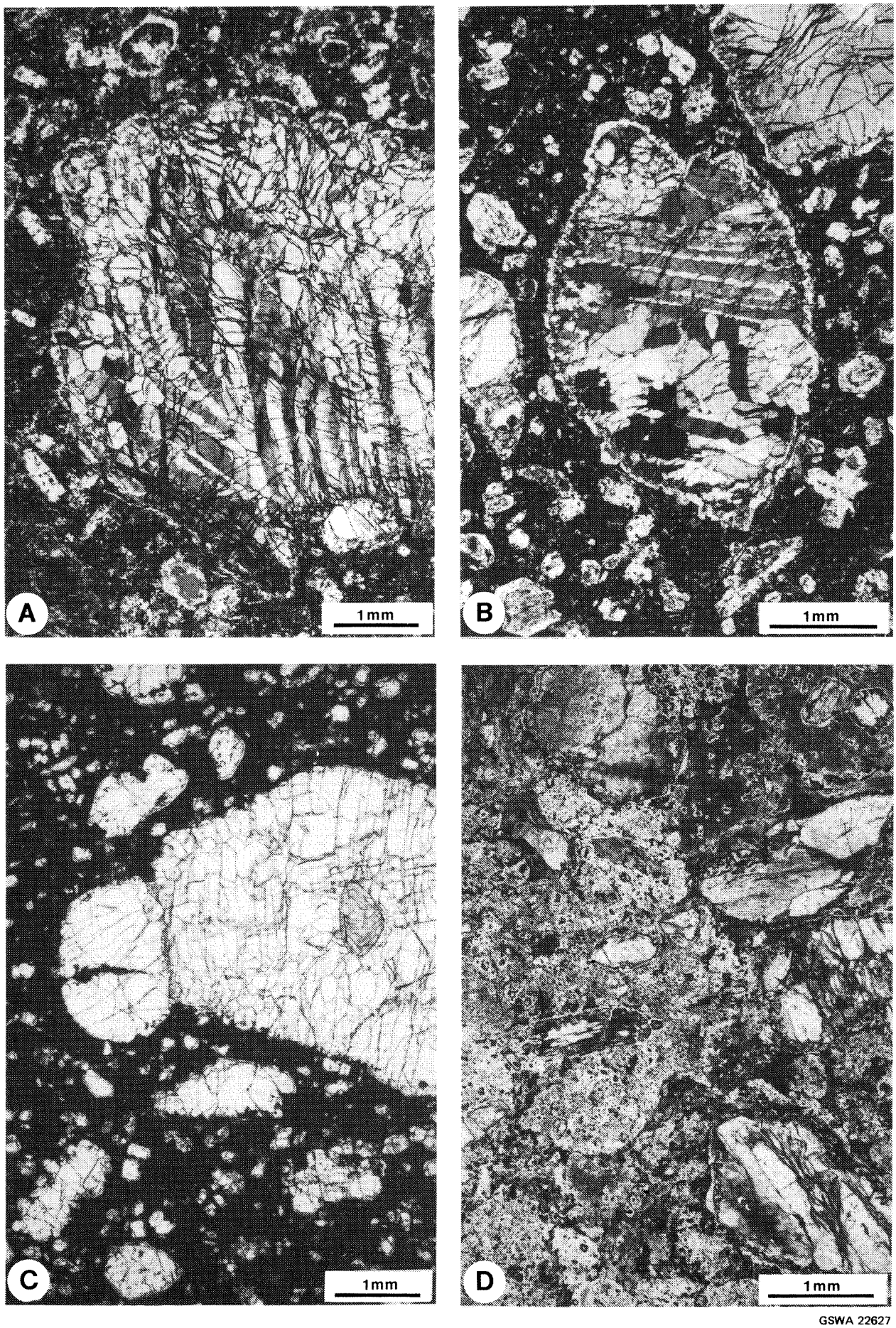
Apart from the presence of quartz grains and sparsely disseminated tourmaline in the tuffaceous matrix, the only difference between the "sandy" and "non-sandy" lapilli-tuff is a tendancy for the pyroclasts in the sandy variety to be glassy and for the olivine macrocrysts, typical of most of the lapilli-tuff, to be less common. The glassy lapilli often enclose a number of quartz grains. The proportion of quartz grains varies up to 20% of the rock, although most commonly only a few scattered grains are present. The source of these quartz grains is probably the wall-rock sandstones, but one specimen contains a few percent of microcline grains and these are possibly derived from the basement rocks.

The main body of lapilli-tuff is a lithic lapilli-tuff with pyroclasts of olivine lamproite from <1 mm to 1 cm across and isolated olivine macrocrysts up to 6 mm forming the bulk of the rock. Angular to rounded accidental pyroclasts of shale, up to 1 cm diameter, may be locally abundant but are generally rare or absent. The tuffaceous matrix of the rock consists of ash-sized lamproite fragments, crystals of altered olivine, and occasional phlogopite, in a structureless mass of clay minerals and other alteration products of lamproite dust. Most lapilli-tuffs are matrix-supported, and contain about 50% of lapilli >2 mm; but a few are clast-supported, and tuffaceous material occupies the interstices between lapilli.

Olivine lamproite pyroclasts are characterized by two generations of olivine: anhedral macrocrysts up to 6 mm across; and small euhedral groundmass phenocrysts <1 mm long. The matrix is a fine-grained clay-mineral aggregate containing minute grains of perovskite and accessory chromite. Some clasts are vesicular, and the groundmass is evidently an altered devitrified glass which lacks perovskite grains. The olivine is uniformly pseudomorphed by talc, and a little carbonate. Larger macrocrysts of olivine are often present as isolated crystals, often with a thin skin of glassy lamproite adhering. A few of the pyroclasts are angular, but most are rounded or have lobate margins and irregular shape and were plastic when ejected. In some examples, concentric structures are seen in the pyroclasts; these are probably the result of spinning while in flight.

A distinctive component of the lapilli-tuffs is a small number of phlogopite-bearing lapilli. Most commonly phlogopite occurs as isolated flakes, up to 1 mm long, with rounded resorbed margins, in olivine lamproite lapilli. A few lapilli, however, are crowded with small phlogopite phenocrysts in a fine-grained, brown, clay-

Figure 72: Photomicrographs of tuffs from Ellendale 4: A — "Sandy" lapilli-tuff; note the cored and accretionary lapilli, and altered olivine macrocrysts; 4 AC 147, 226 m (GSWA 76009E). B — Olivine lamproite lapilli-tuff; note the concentric structure of the large lapilli and the altered ash matrix; 4 AC 162, 165 m (GSWA 71468J). C — Olivine lamproite lapilli-tuff; the clear patches in the altered ash matrix contain secondary vesuvianite; 4 AC 185, 119 m, (GSWA 71482D). D — Small mantle xenolith in lamproite lapilli-tuff. The unaltered minerals are picrochromite (dark), and orthopyroxene, with minor chrome diopside; 4 AC 162, 137 m, (GSWA 71468H).



GSWA 22627

mineral matrix containing a few small olivine phenocrysts. No similar olivine-phlogopite lamproite is known from sills or larger bodies, and the poikilitic phlogopite of the central intrusive is a late-stage growth not a phenocryst phase. A few large phlogopite flakes with resorbed margins are also present in the tuffaceous matrix.

In twenty-five thin sections of lapilli-tuff, three contained small xenoliths of mantle origin, each enclosed in a lapillus of olivine lamproite. One nodule, 5 mm across, is completely altered to clay minerals except for vermicular red-brown picrochromite and can be recognized only by relic textures, while another fragment only 2 mm across preserves a crystal of orthopyroxene. The largest nodule, 6 mm diameter, has an altered and metasomatized marginal zone surrounding a core of orthopyroxene, vermicular chromite and diopside, and is enclosed by a thin "skin" of olivine lamproite (Fig. 72d). This nodule is similar to the fresh diopside-chromite-bearing harzburgite reported by Jaques and others (1984a). In the tuffaceous matrix, rare xenocrysts of red-brown chromite, often with an opaque, iron-rich alteration rim, orthopyroxene, and a single diopside grain have been noted. A few macrocrysts of olivine enclosing vermicular chromite are also present; the whole suite probably represents xenoliths of diopside-bearing harzburgite to lherzolite composition, similar to xenolith 80210127, which was recovered from the magmatic phase of Ellendale 7.

The tuffaceous matrix of the lapilli-tuffs consists of ash and dust-sized material similar to the lapilli. In most specimens, the fine ash fraction is completely altered to clay minerals, sometimes veined or partly replaced by carbonate. Some specimens also contain vesuvianite in the matrix or replacing individual tuff fragments (Fig. 72c). The mineral is colourless but has a variety of anomalous birefringent colours from khaki to red-brown to intense Berlin blue; it is also optically positive, which suggests a high (OH) content (Deer and others, 1962).

Central magmatic core: The magmatic rocks which occupy most of the surface area of Ellendale 4 are olivine lamproites (Fig 73c). Differing cooling histories have led to variations in grainsize, texture, and mineralogy, particularly with respect to the presence or absence of phlogopite and potassic richterite, but otherwise the rocks form a single petrographic unit. The lamproite is characterized by two generations of olivine crystals, macrocrysts and small groundmass phenocrysts, and by poikilitic groundmass phlogopite and a fine-grained matrix of clay minerals containing minute perovskite and chromite euhedra.

Olivine constitutes between 30% and 40% of the lamproite; macrocrysts and groundmass phenocrysts are in roughly equal amounts. The groundmass phenocrysts are small, up to about 0.5 mm long, commonly euhedral to subhedral, and extensively altered to talcose minerals. Macrocrysts range up to 1 cm diameter, are rounded to irregular in shape, and show undulose extinction, glide twinning, and kink bands (Fig.73a,b), indicative of progressive solid state deformation in the mantle source region. Undulose extinction is ubiquitous in unrecrystallized macrocrysts: with increased strain, kink bands and glide twins form, usually as a set of irregular lamellae and, rarely, as two intersecting sets (Fig.73a). Syntectonic recrystallization gives rise to small, strain-free neoblasts, 20-30 μm across, which form intergranular mosaics, often surrounding larger, strained porphyroclasts. This may also be the source of a number of small granular olivine aggregates 2-3 mm across. Primary static annealing (Mercier, 1979) has partially recrystallized many of the macrocrysts to polygonal strain-free neoblasts up to 300 μm across.

Most specimens of olivine lamproite contain small poikilitic phlogopite flakes in the groundmass. Slower cooling of central portions of the mass has generated larger poikilitic plates and aggregates of phlogopite up to 2 mm across; these enclose many groundmass grains of perovskite, diopside, and apatite. The smaller flakes are generally only weakly zoned and pale in colour, but the larger phlogopites are zoned to a dark red-brown titaniferous rim.

Potassic richterite, like coarse phlogopite, is found only in the coarser grained central parts of the mass, where it forms small interstitial grains or diffuse poikilitic patches up to 1 mm across and is usually associated with phlogopite.

The groundmass of the rock is made up largely of clay minerals that contain abundant minute grains of perovskite and less common chromite euhedra. Many specimens contain identifiable diopside, apatite, and wadeite. Perovskite grains are yellow-green in colour, euhedral, and range from 3 μm up to 100 μm diameter in the coarser central varieties. The larger grains are often anomalously birefringent. Minute laths of diopside, about 10 μm long, in the marginal parts of the mass grew to distinct prisms in the slower cooled central parts and, in rare instances, are up to 0.5 mm long. Occasional small prisms of apatite and wadeite are found in many samples, particularly the coarser potassic-richterite - phlogopite varieties. In addition to small euhedra of chromite up to 50 μm diameter, some of the more evolved rocks contain late-stage interstitial opaque grains which may be ilmenite; in a few specimens, rare prismatic grains of priderite, a mineral normally found

Figure 73. Photomicrographs of olivine lamproite from Ellendale 4: A — Kink-banding in an olivine macrocryst. Note two sets of kink-bands, (crossed polars); 4 AC 191, 244 m, (GSWA 71478J). B — Polygonization and glide-twinning in an olivine macrocryst: half the macrocryst has recrystallized to smaller neoblasts, and the remainder shows narrow, unstrained twin-bands in a crystal that retains undulose extinction, (crossed polars). 4 AC 191, 304 m, (GSWA 71478M). C — Olivine lamproite: olivine macrocrysts with resorbed margins, and olivine microphenocrysts, in a fine-grained, diopside and phlogopite-rich groundmass. The large macrocryst encloses a rounded grain of chrome diopside; 4 AC 112, 165 m, (GSWA 71469D). D — Autobrecciated marginal olivine lamproite: altered olivine macrocrysts in a brecciated, formerly glassy groundmass; 4 AC 228, 128 m, (GSWA 71486C).

only in leucite-bearing lamproites, are present. For almost all samples of olivine lamproite there is no evidence for the presence of leucite, either as phenocrysts or as groundmass crystallites. In most specimens, the clay minerals of the matrix form a fine-grained, brown, structureless mass, probably derived from a glassy or microcrystalline material close to phlogopite in composition. In the coarser matrix of the central parts of the body, the brown clay minerals pseudomorph small prismatic crystals of an unidentified mineral. This mineral is clearly not diopside or apatite, both of which occur as unaltered prisms within the matrix. In the interstitial areas between these pseudomorphs, there are patches of fine-grained colourless clay minerals which in a few specimens form distinct circular or octagonal "spots", from about 50-100 μm in diameter; these may be pseudomorphs after leucite. Such pseudomorphs are typically found only in the most evolved and coarse-grained portions of the olivine lamproite mass.

The autobrecciated basal parts of the olivine lamproite are distinctive both in drill-core and thin section, and often appear to be a coarse, rewelded lapilli-tuff with no interstitial tuffaceous material. However, the rock fragments are uniform in each sample; and, overall, the rock is an olivine lamproite with macrocrysts and groundmass phenocrysts of olivine in a devitrified, glassy, and sometimes vesicular, matrix. In most specimens, the totally rewelded nature of the rock, the contorted flow structures, and the complete absence of an interstital tuffaceous matrix, are sufficient to distinguish it from the lapilli-tuff (Fig. 73d).

Chemistry

The magmatic rocks of Ellendale No. 4 are olivine lamproites containing 22-28% MgO and 35-42% SiO_2. Representative analyses are given in Table 35. All have low contents of Al_2O_3 (1.8-4%) and CaO (2.5-6%), very low Na_2O (< 1%, typically $\leq$0.5%), and high TiO_2 and K_2O contents (2.2-4% TiO_2, 1.8-5% K_2O). Ni and Cr contents are high, typically 800 to 1 400 ppm. All except those samples with very high modal proportions of xenocrystal olivine are olivine and hypersthene normative. Apart from Ba, which shows a wide range

TABLE 35. REPRESENTATIVE ANALYSES OF ELLENDALE 4, AND ELLENDALE 4 SATELLITE LAMPROITES AND PYROCLASTICS

	1	*2*	*3*	*4*	*5*	*6*	*7*	*8*	*9*	*10*
					Percent					
SiO_2	39.10	45.00	38.80	37.70	42.20	38.60	38.00	38.70	35.20	37.40
TiO_2	2.31	3.20	2.22	3.81	3.41	2.25	3.54	3.89	2.49	3.72
Al_2O_3	2.30	4.00	2.00	3.20	3.60	2.20	2.90	3.70	2.00	3.40
Fe_2O_3	4.90	4.40	5.10	6.10	4.10	5.30	5.70	5.40	5.40	6.10
FeO	2.16	2.44	1.92	2.16	3.62	2.17	2.45	2.81	1.59	1.98
MnO	0.12	0.14	0.10	0.12	0.12	0.11	0.13	0.12	0.08	0.12
MgO	27.80	16.00	27.80	24.60	23.00	27.70	25.00	22.00	23.60	23.00
CaO	2.46	4.91	2.71	3.84	4.55	2.60	3.90	4.16	6.90	4.92
Na_2O	0.05	0.30	0.08	0.43	0.47	0.09	0.49	1.05	0.12	0.35
K_2O	2.10	6.56	2.17	5.69	4.89	3.20	5.26	3.63	1.37	2.41
P_2O	1.56	2.71	1.70	1.66	1.64	1.34	1.81	1.49	2.93	1.34
H_2O^+	10.00	4.34	8.94	6.61	3.18	8.57	6.21	5.13	7.25	7.57
H_2O^-	3.93	3.06	4.82	1.32	2.35	3.30	1.97	4.05	5.47	4.40
CO_2	0.30	0.63	0.22	0.27	0.46	0.46	0.23	0.39	3.20	0.40
Rest	1.48	3.04	1.63	2.26	2.59	1.60	2.11	2.89	1.76	1.91
Total	**100.57**	**100.73**	**100.21**	**99.77**	**100.18**	**99.49**	**99.70**	**99.41**	**99.36**	**99.02**
					Parts per million					
Ba	6 000	17 020	6 853	8 071	11 986	6 446	7 317	16 187	6 576	5 354
Li	4	9	7	9	11	7	10	8	8	9
Rb	300	400	291	554	383	333	607	392	187	378
Sr	850	1 700	987	1 491	1 455	1 093	1 430	1 271	1 083	1 530
Pb	40	80	35	58	53	44	59	42	56	58
Th	35	60	45	64	52	49	62	43	57	63
U	<2	10	2	1	1	3	2	4	6	1
Zr	800	1 200	926	1 470	1 244	845	1 378	1 163	1 269	1 430
Nb	150	150	110	181	166	104	175	159	137	189
Y	18	27	11	17	16	11	14	13	16	21
La	300	450	293	512	449	359	471	393	409	425
Ce	480	700	493	926	783	609	888	622	740	821
Sc	20	20	17	26	22	16	25	21	18	24
V	32	287	77	122	205	39	47	83	43	60
Cr	800	450	833	1 214	1 076	795	1 149	859	804	1 121
Co	85	60	70	75	73	83	74	71	65	68
Ni	1 500	640	1 257	1 068	967	1 396	1 117	931	925	954
Cu	40	45	40	52	65	40	48	50	35	59
Zn	68	72	61	75	74	66	71	66	50	66
Sn	4	4	20	9	11	5	12	5	8	17
Ga	2	2	3	4	4	2	5	3	2	5
S	200	400	230	80	150	60	140	380	1 000	1 110
F	1 617	5 453	2 170	5 720	5 530	2 100	5 180	4 300	3 550	5 450
Cl	—	—	122	142	105	125	113	256	127	117

1 — Olivine lamproite lapilli-tuff. 2 — Olivine lamproite lapilli-tuff, ('sandy tuff'). 3 — Glassy olivine lamproite; 4E, 4AC11 45m, GSWA 71498. 4 — Phlogopite-olivine lamproite; 4E, 4AC209 85m, GSWA 71467B. 5 — Olivine lamproite; 4E, 4AC162 145m, GSWA 71468I. 6 — Olivine lamproite; 4W, 4AC189 143m, GSWA 71479G. 7 — (Phlogopite)-olivine lamproite; 4W, 4AC137 57m, GSWA 71466B. 8 — (Diopside)-phlogopite-olivine lamproite; 4W, 4AC191 310m, GSWA 71478N. 9 — Olivine lamproite lapilli-tuff; 4 satellite, 4AC 212 117m, GSWA 71491F. 10 — Phlogopite-olivine lamproite; 4 satellite, 4AC206 34m, GSWA 71492A.

in concentration (4 000-13 000 ppm), abundances of trace elements lie within ranges of concentrations typical of the West Kimberley olivine lamproites, e.g. 900-1 600 ppm Zr, 100-210 ppm Nb, 360-590 ppm La.

The magmatic olivine lamproites from the satellite pipe are poorer in MgO, typically containing 20-25% MgO; they also have lower Ni contents (800-1000 ppm) than the olivine lamproites of the main pipe (Fig.74). Many have abundant secondary calcite, which is manifested in higher than averge CaO and CO_2 contents in the analysis.

The magmatic rocks of the western and eastern lobes of Ellendale 4 have similar chemistry as shown by the overlap in compositional fields (Fig 74, 75). The magmatic rocks of the satellite pipe overlap the Mg-poor compositions from the main pipe, both in terms of major- and trace-element abundances (Fig.74) and in terms of ratios of "incompatible" elements (Fig.75), suggesting that the two lobes and the satellite are comagmatic. However, the range in "incompatible" element ratios together with small differences in Sr and Nd isotopic compositions (McCulloch and others, 1983, WAK 20 and 21) implies that a suite of magmas with slightly differing trace elements and isotopic compositions is present.

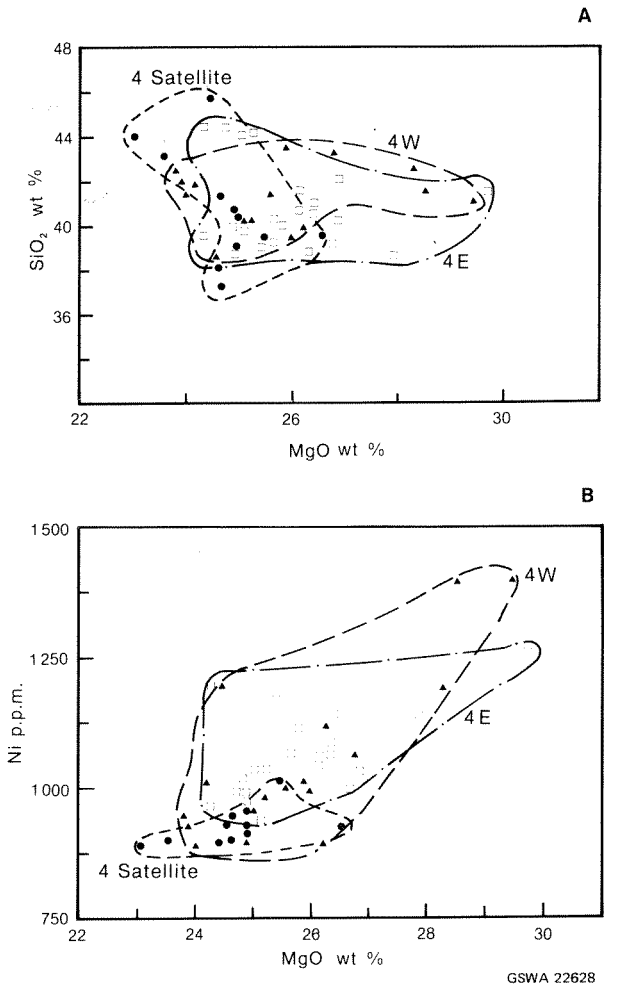


Figure 74. Variation of SiO_2 and Ni with MgO for olivine lamproites from Ellendale 4 and 4 Satellite. The fields 4W and 4E refer to the western and eastern lobes of the main body.

The magmatic rocks of Ellendale 4 are compositionally similar to other olivine lamproites from the Ellendale Field, but differ in terms of the greater proportion of high-MgO olivine lamproite containing abundant macrocrystal olivine. Similar high-MgO olivine lamproites are found only at Ellendale 9, 11, and 7, which are the only bodies carrying diamond at grades higher than 1 CM/100t. Although trace diamond occurs in many of the more evolved leucite lamproites of the Ellendale Field significant concentrations of diamond are restricted to pipes where magmatic rocks of ultramafic composition, resembling kimberlite, are present.

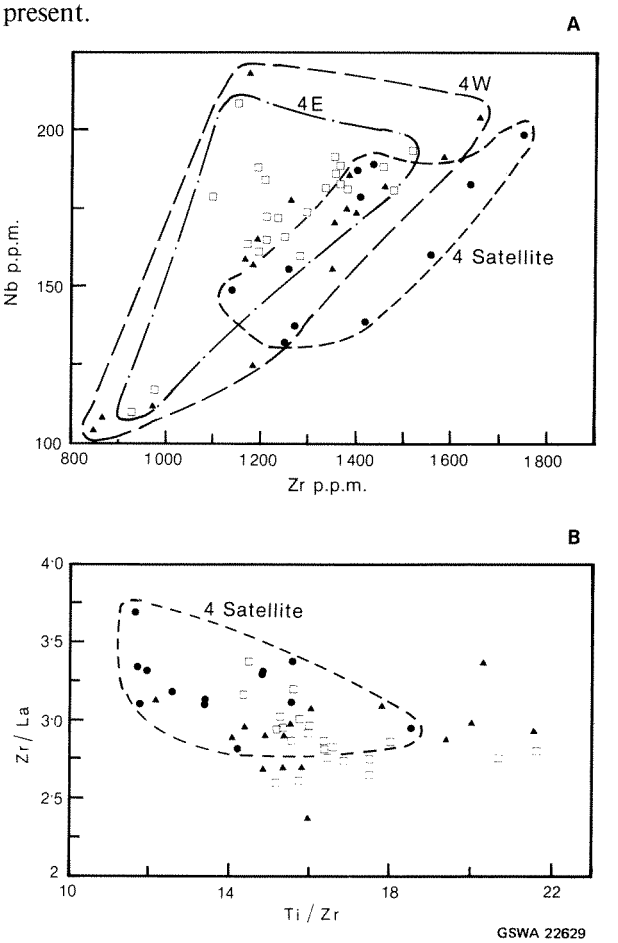


Figure 75. Nb *versus* Zr and Zr/La versus Ti/Zr variation diagrams for olivine lamproites from Ellendale 4 and 4 Satellite.

The olivine lamproite tuffs of Ellendale 4 range from Mg-rich compositions (25-28% MgO) in the more macrocrystal olivine-rich parts to Mg-poor compositions (typically 12-20% MgO) in the more crystal-poor tuffs. The "sandy" lapilli-tuffs range to very Mg-poor (< 10% Mg(O), silica-rich (75% SiO_2) compositions reflecting the modal proportions of disaggregated country rock quartz grains.

ELLENDALE 4, SATELLITE PIPE

The small satellite pipe of Ellendale 4 is located 100 m east of the main diatreme. It is an oval body — 500 × 250 m, or 8 ha in area — and lies concealed beneath 2-3 m of red sand and calcrete. The pipe intrudes poorly exposed, flat-lying Devonian limestones, which are

brecciated marginal to the lamproite. Small outcrops of the overlying Permian sandstone are found southwest of the pipe (Fig. 76).

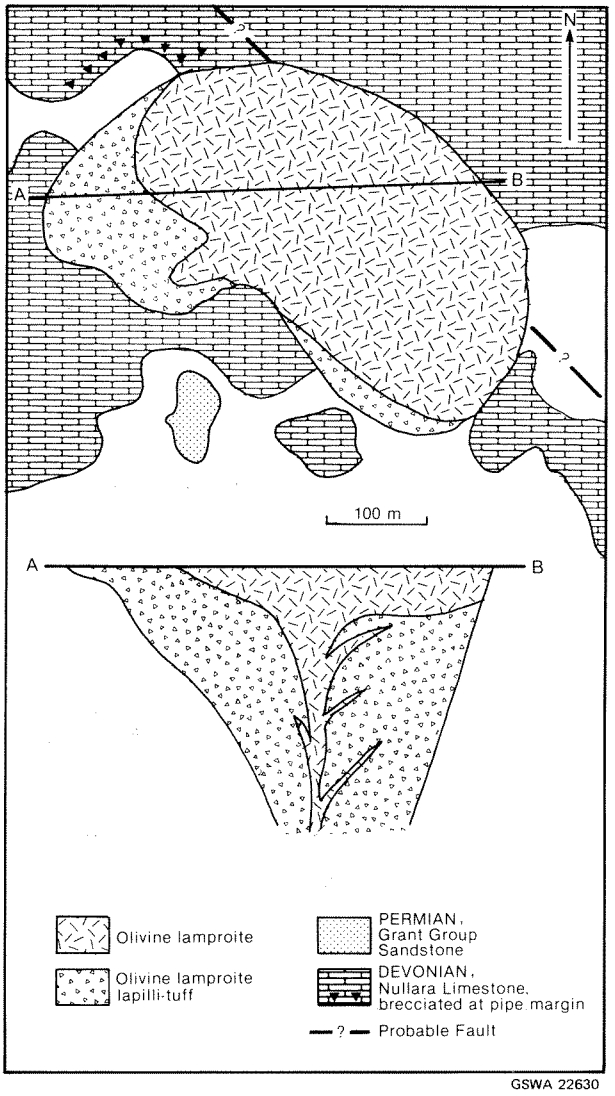


Figure 76. Geological map of Ellendale 4 Satellite pipe (after Onley and Smith, 1980).

The present area of the pipe is occupied mostly by a mass of olivine lamproite, but there are small areas of lamproite lapilli-tuff around the southern and western margins. Overall, the pipe is filled mostly with lapilli-tuff, and the olivine lamproite forms a thin capping over the pyroclastic deposits.

Extensive drilling has shown that the walls of the vent dip steeply at angles between 45° and 70° towards a presumed conduit that is eccentrically located close to the northeast side of the vent. The conduit drawn on the cross-section of Fig. 76 is schematic, as, apart from thin sills, olivine lamproite was not encountered at depths greater than 50 m. From drilling records, the olivine lamproite forms a sheet uniformly about 50 m thick except close to its margins. The sheet may originally have been a sill, unroofed by late erosion, but more probably formed as a lava lake in the open vent. In some drill sections, the basal lamproite is auto-brecciated.

The pyroclastic deposits are generally lamproite lapilli-tuffs with little or no wall-rock component, but, on more shallow dipping parts of the vent wall, there is often a lens of quartz tuff.

The Ellendale 4 Satellite pipe forms part of the same group of vents which make up the much larger Ellendale 4 and was probably active at about the same time. The volume of the satellite vent is equal to all but the largest of the Ellendale 4 vents. There is no obvious pattern to the group of vents as a whole, although the general east-west trend probably reflects a basement structure.

Exploration of the pipe for diamond has not been as extensive as at the nearby Ellendale 4, but 6 bulk samples of surface pyroclastics totalling 1 888 t yielded 126.3 CM of diamond, a grade of 6.69 CM/100 t. Individual samples ranged from 5.1 to 11.6 CM/100 t, while 7 smaller samples from a Wirth auger hole, drilled to a depth of 212 m, showed a similar variation, from 5.3 to 13.6 CM/100 t. Samples from the magmatic material produced few diamonds and the overall grade was 0.1 CM/100 t (Smith, 1981).

From the limited number of thin sections examined, the lapilli-tuffs of the Satellite pipe appear very similar to the lamproite lapilli-tuffs of Ellendale 4. The lapilli, up to 1 cm across, are of olivine lamproite, and the matrix is of ash- and dust-sized particles of the same material. Accidental material is very rare; only a few carbonate fragments were noted. No mantle xenoliths or minerals of mantle origin, other than the olivine macrocrysts, were noted. Most of the lapilli-tuffs have been thoroughly altered by the development of secondary barite and the replacement of the matrix by carbonate.

The olivine lamproite, which occupies much of the surface area of the pipe, is similar to much of the central core of Ellendale 4, although fresh olivine is rare. Macrocrysts and groundmass phenocrysts of olivine are set in a fine-grained matrix of clay minerals, which contains small poikilitic flakes of phlogopite, granular perovskite, and sparse chromite. Minute prisms of diopside are often present and in some specimens, the groundmass is strongly carbonated. A specimen from the central part of the mass shows a weak development of poikilitic potassic richterite.

The few relic olivine macrocrysts preserved show undulose extinction but no glide twinning or polygonization. A specimen from a sill within the tuff has many fresh macrocrysts, which show no undulose extinction or other features common to macrocrysts of Ellendale 4.

The chemistry of the magmatic rocks of the satellite pipe and their relation to similar rocks of the main body of Ellendale 4 has been described earlier.

ELLENDALE 6

This is the largest lamproite body (106 ha) in the Ellendale Field, and is located a little over 1 km south of 81 Mile Vent. The lamproite itself is concealed beneath an overburden of windblown sand up to 18 m thick, but Grant Group sandstones outcrop around the

margin of the vent to form a prominent ridge that rises to 40 m above the sandplain (Fig. 78). The sandstones are well bedded and flat lying; dips from 3-10° have been recorded. Induration and disruption of the sandstones caused by the emplacement of the vent do not extend beyond a few metres from the vent margin.

The main body of lamproite is a plug of phlogopite-olivine-leucite lamproite, approximately 850 m diameter, which occupies the eastern part of the vent (Fig. 77). Small areas of lapilli-tuff are present around the eastern margin of the plug, but the main area of pyroclastic rock extends as a broad tongue 1 100 m to the northwest. At the western extremity of this tongue, the tuffs form a relatively thin layer overlying the sandstone. The main vent is occupied by the lamproite plug, but there may be smaller vents, or a tuff-filled fissure, that give rise to the western tongue of tuffs.

Because of the thick cover of sand, diamond

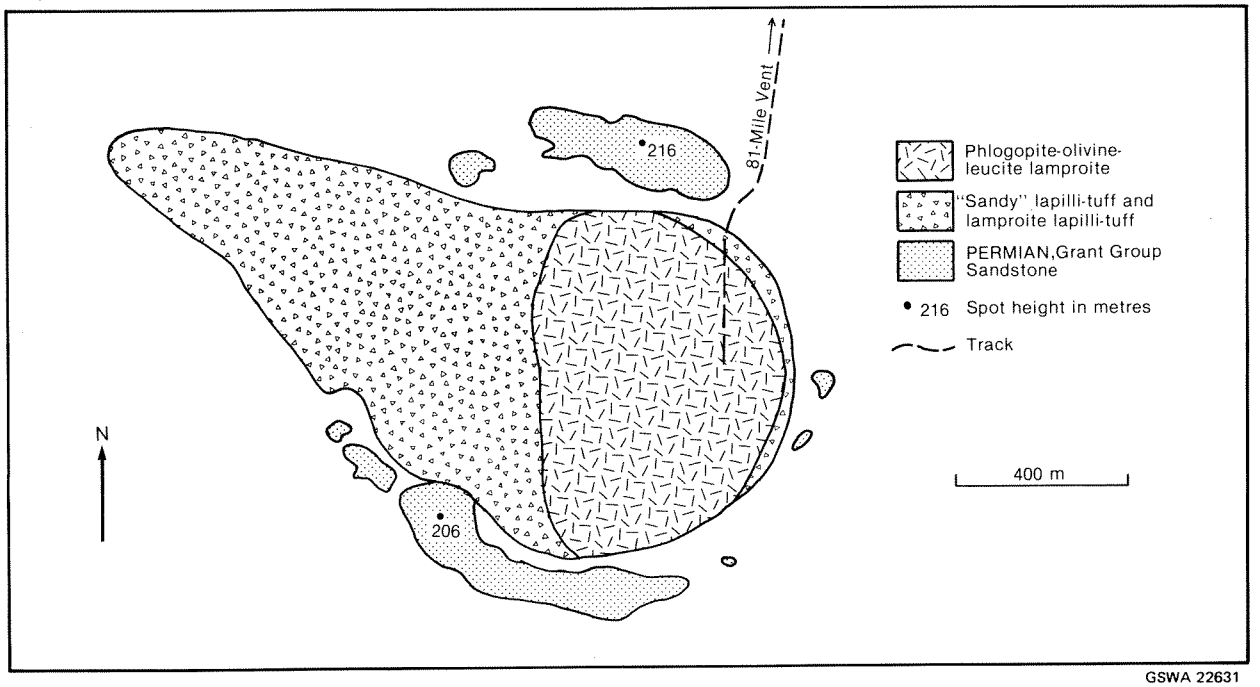


Figure 77. Geological map of Ellendale 6 (after Onley and Smith, 1980).

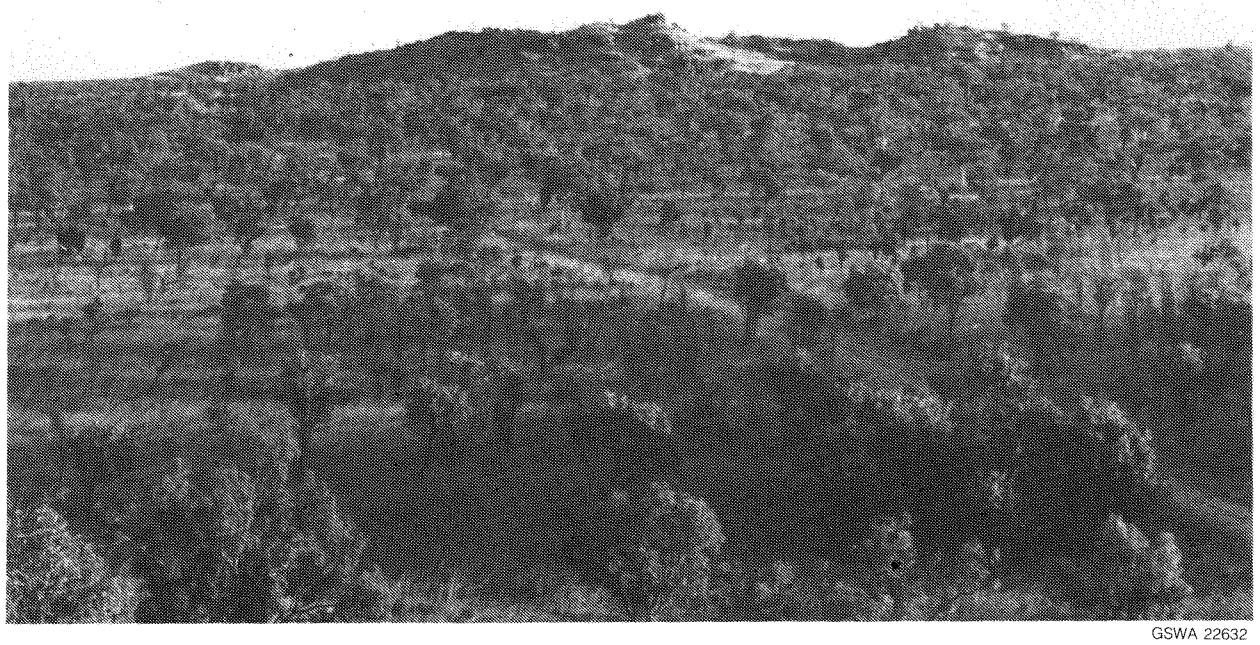

GSWA 22632

Figure 78. Sandstones of the Grant Group forming a ridge round the eastern end of Ellendale 6, viewed from 81 Mile Vent.

exploration was carried out with a Williams auger. A total of 1 063 t of material was processed from 21 samples; and 11 diamonds, weighing 0.61 CM, were recovered, of which the largest weighed 0.20 CM. Diamonds were recovered from both the pyroclastics and from weathered lamproite (Onley and Smith, 1980).

The pyroclastic rocks are vitric lapilli-tuffs: they contain angular fragments of glassy lamproite and country rock up to 1 cm across, a variable proportion of rounded quartz grains up to 0.5 mm diameter, and a sparse matrix of clay minerals and lamproite ash. The lamproite fragments are predominantly of altered, devitrified glass, flow-banded, sometimes vesicular and often enclosing quartz grains; microlites of leucite and small pseudomorphs after olivine can be identified. A few fragments of crystalline lamproite are present, commonly a very fine-grained phlogopite-leucite lamproite with accessory priderite needles. Accidental lapilli of wall rock make up a small proportion of the rock; shale and phyllite are the most common types, but siltstones and fine-grained sandstones are also present. The quartz grains are derived from the surrounding Grant Group rocks and may account for up to 30% of particular tuff specimens. The grains are either rounded, or angular and fractured, and often show the effects of partial resorption by the lamproite magma.

The central lamproite plug is a fine-grained, porphyritic phlogopite-olivine-leucite lamproite. Small phenocrysts of euhedral olivine, 0.2-0.5 mm long and altered to talc or nontronite, make up about 15% of the rock and are set in a groundmass of altered leucite, <0.1 mm diameter, diopside laths up to 1 mm, and abundant small flakes of phlogopite. Interstitial material is mainly dark-brown clay minerals, but includes abundant poikilitic potassic richterite, grains of priderite, and accessory apatite. The central parts of the mass are coarser grained; and olivine phenocrysts, up to 1.5 mm long, and dark-pink pleochroic potassic richterite are prominent in the groundmass. In addition to interstitial flakes of poikilitic phlogopite, all specimens contain a few large corroded phenocrysts up to 2 mm long, each surrounded by a zone containing abundant acicular priderite.

ELLENDALE 7

The large, unexposed lamproite vent of Ellendale 7 is located in the centre of the Ellendale Field, 3 km south of the CRA plant site, and is traversed by the main haul road to Ellendale 4. The vent is marked, around its southern and western margins, by ridges of baked sandstone rising 30 m above the sandplain. The sandstones are part of the Permian Grant Group, and, except close to the vent margin, are sub-horizontally disposed. Towards the base of the outcrop, the sandstone is cross-bedded but generally the rocks are massive, arkosic sandstones.

Ellendale 7 is an oval vent, approximately 900 × 600 m, or 34.7 ha in area, elongated east-west (Fig. 79). It is concealed by up to 10 m of loose, windblown, red sand, which overlies a thin laterite horizon. Scout drilling has outlined a large central core of olivine lamproite, emplaced in a thick pyroclastic sequence which fills most of the vent. A small area of olivine lamproite near the eastern end of the vent probably indicates a second smaller vent.

Two features of this pipe are distinctive: the presence of relatively abundant mantle nodules; and the close association of leucite-bearing lamproite with magnesia-rich olivine lamproite. The pyroclastic deposits, particularly in the western part of the vent, contain beds of coarse agglomerate with pyroclasts 25 cm or more in diameter. Trenching of these deposits at the surface recovered a number of well-rounded, altered mantle nodules from 10 cm diameter to ovoid masses 30 × 20 cm across. Unfortunately, the nodules are thoroughly altered to a mass of yellow clay minerals in which

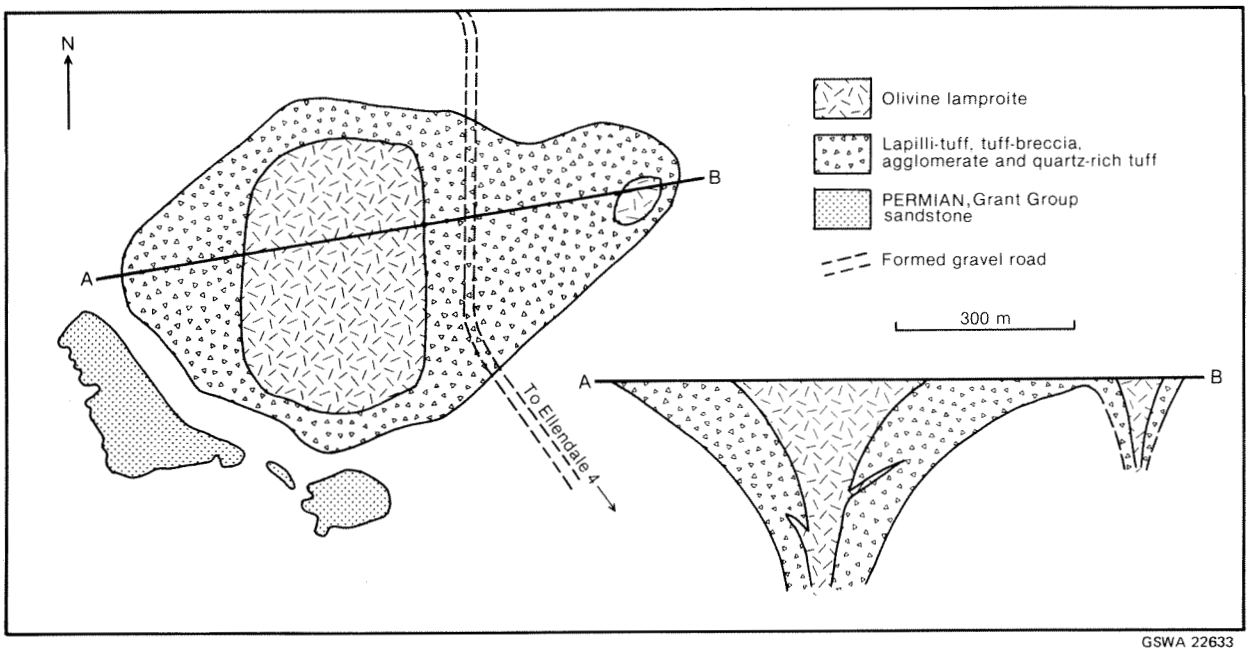


Figure 79. Geological Map of Ellendale 7 (modified, after Onley and Smith, 1980).

original textures are moderately preserved, together with minor relic chromite and chrome-diopside.

The pyroclastic deposits range from coarse block agglomerates to a variety of lapilli-tuffs and basal beds of quartz-rich tuff. In all but the quartz-rich tuff, fragments of leucite lamproite are found, mixed with the dominant olivine lamproite pyroclasts. In the block agglomerate, the blocks, up to 25 cm and more across, are of leucite lamproite, sandstone, and dolerite, with small lapilli of olivine lamproite and lamproite tuff forming the matrix. It is evident that the olivine lamproite magma invaded a prexisting mass of leucite lamproite but otherwise, the volcanic sequence and the relationship between the two magmas is not determinable. No intermediate rock types are present, and it may be fortuitous that the olivine lamproite utilized the same conduit as an earlier leucite lamproite diatreme.

From the few deep drill holes into the mass little information is available on the subsurface form of the central olivine lamproite core. From the available data it seems likely that it is similar to the olivine lamproite of Ellendale 4, a broad sheet-like body of magmatic lamproite overlying a pyroclastic sequence and fed from a narrow central conduit. A number of thin sills intruding the tuffs have been intersected by drilling.

Ellendale 7 was one of four pipes extensively sampled for diamonds by the Ashton Joint Venture (*see* Chapter 1). Initial scout sampling from small trenches showed grades of up to 4 CM/100 t, but subsequent bulk sampling and deep auger holes gave an average grade of a little over 1 CM/100 t. Twenty-three scout and auger samples totalling 1 957 t produced 198 diamonds weighing 19.76 CM, while four bulk samples totalling 2 573 t produced 172 stones weighing 28.09 CM. Three of the bulk samples of pyroclastic material averaged 1.25 CM/100 t, while a sample of weathered olivine lamproite produced only 0.48 CM/100 t.

Petrography

Pyroclastics: A range of petrographic types is evident among the quartz tuffs. Some are composed almost entirely of quartz grains and contain only small amounts of interstitial apple-green chloritic material and a few opaque grains. The quartz forms a fine-grained mosaic, but a relic texture shows rounded and angular grains about 0.2 mm diameter, each coated with a thin layer of chloritic material. Others contain only about 50% of accidental material, principally rounded quartz grains up to 0.5 mm, smaller angular grains, and accessory tourmaline. The matrix is very fine-grained kaolinitic clay with a poorly preserved fragmental texture. Both types represent the early products of volcanism — fine-grained tuffs composed primarily of disaggregated wall-rock sandstone.

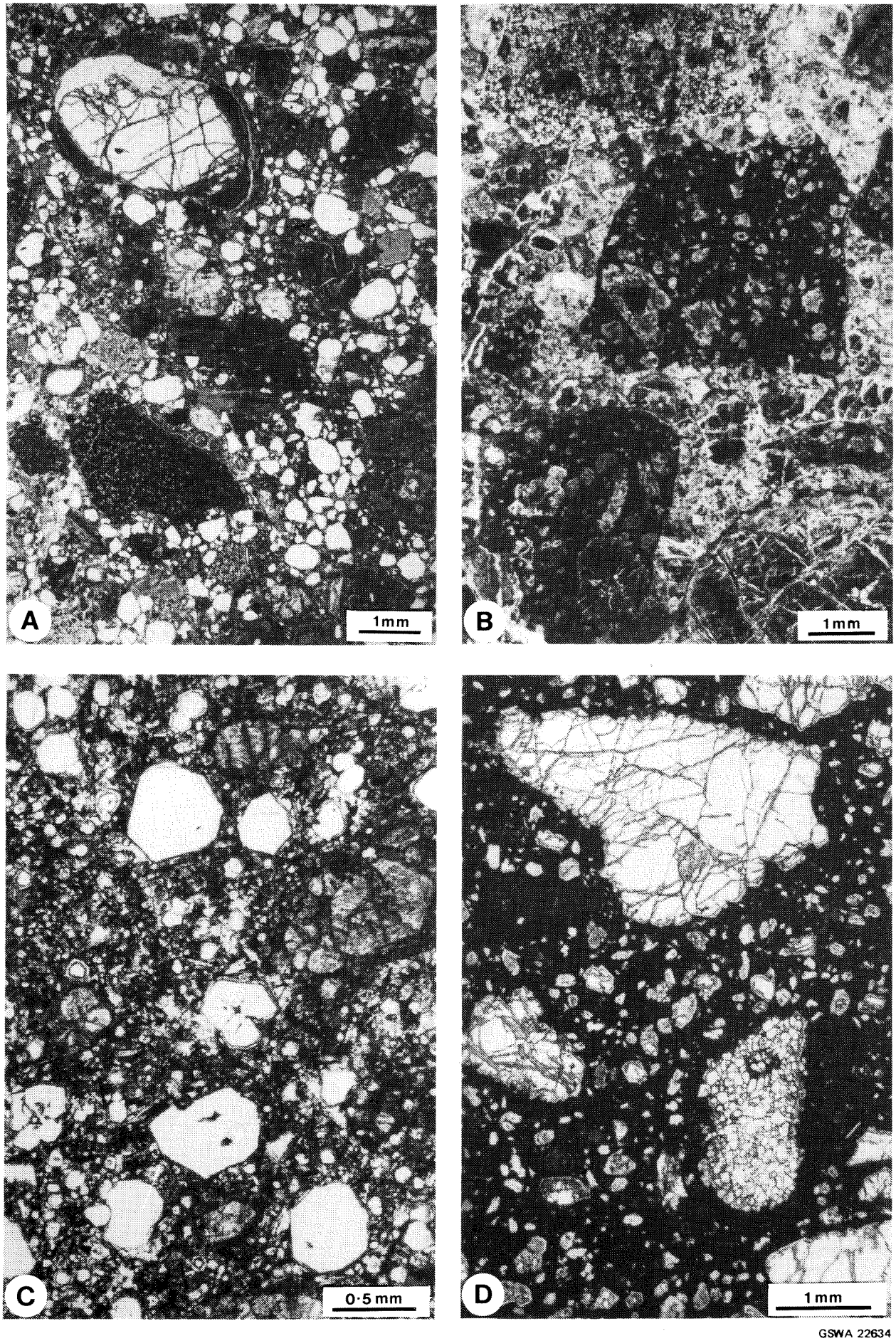
The dominant pyroclastic rock type is lapilli-tuff containing angular to rounded fragments up to 3 cm diameter of olivine lamproite, leucite lamproite, and, less commonly, metadolerite, schist, and limestone (Fig. 80a). The average clast size is about 5 mm, and the lapilli-tuff is matrix supported; the matrix is predominantly clay with lamproite ash, altered olivine crystals, and occasional garnet, orthopyroxene, clinopyroxene, and chromite, from cognate mantle xenoliths. Some specimens are of "sandy" lapilli-tuff containing up to 10% of accidental rounded quartz grains in the matrix (Fig. 80b). In these specimens, all from the western end of the vent, and early in the volcanic sequence, the proportion of leucite lamproite pyroclasts is high; and olivine lamproite is represented by ash-sized particles. The "sandy" lapilli-tuff also contains pyroclasts of fossiliferous limestone and the best examples of minerals from mantle nodules, including a large rounded garnet-phlogopite intergrowth, 3 mm across, that shows a well-developed kelyphitic rim (Fig. 80a).

Most commonly, the lapilli-tuff contains no accidental quartz; and leucite lamproite pyroclasts are subordinate to olivine lamproite. The olivine lamproite is similar to that of the central core: it contains large irregular to rounded macrocrysts of altered olivine up to 6 mm across and abundant small, euhedral olivines in a very fine-grained to glassy and vesicular groundmass. Minute chromite euhedra are present; as are, in some specimens, perovskite grains and small phlogopite flakes. The pyroclasts are generally angular, but some show evidence of plasticity on eruption. The matrix is commonly altered to clay minerals or, in some specimens, replaced by fine-grained carbonate; but there is often a poorly preserved texture of ash-sized particles.

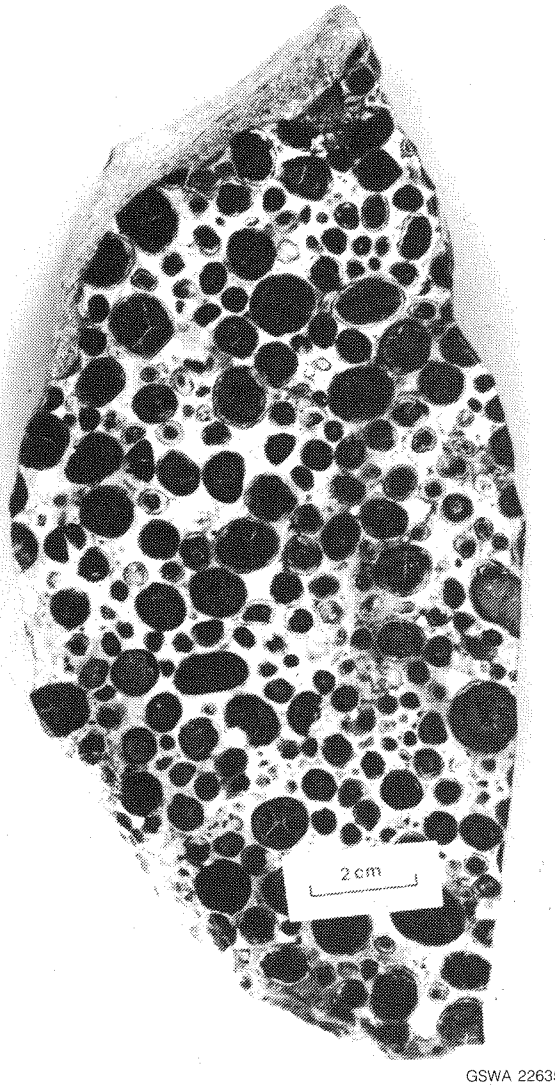
Small isolated accretionary lapilli can be found in some lapilli-tuffs, but in a near-surface trench sample the accretionary lapilli are well developed (Fig. 81). The large accretionary lapilli, or autoliths, are up to 8 mm diameter, spherical, and mostly replaced by iron oxides; some appear to have nucleated around rock fragments. The matrix is thoroughly silicified, but relic textures show that it was composed of minute spherical accretions, <0.1 mm diameter, and small lamproite pyroclasts.

The block agglomerate contains both cognate and accidental pyroclasts, although the group to which the leucite lamproites belong is not clear. Also present are mantle nodules, which are altered to a yellow-clay mineral, possibly hydrotalcite; and, although there is some silicification, textures of a coarse-grained mosaic, probably olivine, are moderately well preserved. The only relic minerals are a few grains of clinopyroxene and vermicular chromite. The chromite is generally dark-coloured picrochromite and occurs as distinct "finger prints", 2-3 mm across, intergrown with diopside. The original nodule was probably lherzolitic or diopside-chromite-bearing harzburgite, similar to that reported by Jaques and others (1984a).

Two distinct types of leucite lamproite pyroclasts are present: a fine-grained, porphyritic phlogopite-leucite lamproite; and a coarser grained, porphyritic olivine – potassic-richterite – leucite lamproite (Fig. 80c). The phlogopite-rich variety contains phenocrysts of phlogopite up to 3 mm long in a fine-grained, leucite-rich matrix with small amounts of potassic richterite,



GSWA 22634



GSWA 22635

Figure 81. Ferruginized and silicified lapilli-tuff, Ellendale 7.

pleochroic from pink to lemon yellow, priderite, and abundant small prisms of apatite. The coarser rock is characterized by abundant small phenocrysts of olivine and leucite 1 mm diameter in a groundmass of small leucite euhedra, poikilitic potassic richterite, a few diopside laths, and priderite, and sparse interstitial clay minerals. Individual specimens may be rich in diopside or potassic richterite and contain minor amounts of phlogopite. One specimen is particularly rich in small grains of wadeite, not seen in other examples. A further feature in some specimens is the presence of fresh leucite phenocrysts (analyses 2, 3; Table 60) and fresh interstitial glass.

Accidental pyroclasts incorporated into the agglomerate and lapilli-tuff are predominantly from the pre-Devonian basement rather than from the wall-rock of the vent. A few limestone fragments were noted in the lapilli-tuff, together with quartz grains derived from the Grant Group sandstones; but quartzite clasts in the agglomerate are of metasedimentary origin, and the quartz forms a flattened mosaic with oriented stringers of sericite and chlorite. Other metasediments noted include talc schist and quartz-chlorite schist. Most characteristic of the suite, however, are pyroclasts of metadolerite, metabasalt, metagabbro, and chlorite-amphibole-quartz rocks, possibly of meta-basic tuff origin. This suite is characteristic of Ellendale 7 and has not been found in other pipes.

Magmatic core: The central olivine lamproite is similar to that of Ellendale 4. Macrocrysts of olivine, commonly 2-3 mm but up to 8 mm across, are abundant, together with small euhedral groundmass phenocrysts up to 1 mm long. The macrocrysts typically show undulose extinction and incipient glide twinning; and many are partly polygonized and have crenulated resorbed margins (Fig. 80c). A number of specimens also contain fine-grained granular aggregates of olivine which appear to be small dunite xenoliths. The groundmass is of fine-grained clay minerals containing small poikilitic phlogopite flakes, abundant acicular diopside, granular perovskite, and accessory chromite euhedra.

Chemistry

The two lamproite types present in Ellendale 7 differ markedly in composition (Table 36). The olivine lamproites have high MgO (24-28%), and low TiO_2 (2.5-3%) and K_2O ($\approx$4%) compared to the leucite lamproites which have much lower MgO (10% or less) and higher TiO_2 (5-7%) and K_2O (5-8%). There are also marked differences in trace-element abundances: the olivine lamproites contain 1000 to 1500 ppm Ni and 500 to 600 ppm Zr, compared to values of 300 to 400 Ni, and 1 200-2 000 ppm Zr in the leucite lamproites. More importantly, however, are the differences in incompatible-element ratios and isotopic compositions: Zr/La ratios, for example, are less than 3 (2.6-3) in the olivine lamproite, and greater than 4 in the leucite lamproites. Zr/Hf ratios are similar in both rock types ($\approx$40), but La/Yb ratios are appreciably different, 160 in the olivine lamproites compared to 250 in the leucite lamproites. (Jaques and others, in prep.). There are also marked differences in Rb/Sr ratios (0.35 compared to 1.17) and initial $^{87}Sr/^{86}Sr$ (0.71037 compared to 0.71677), $^{143}Nd/^{144}Nd$ (0.51142 compared to 0.51103) and Pb isotopic compositions (McCulloch and others, 1983; Nelson and others, in press). These data appear to preclude a comagmatic relationship between the olivine lamproite and leucite lamproite in Ellendale 7.

ELLENDALE 9

Ellendale 9 is a large, complex, concealed body of olivine lamproite and pyroclastic rock in the centre of the Ellendale Field, a kilometre northeast of the CRA

Figure 80. Photomicrographs of tuffs and lamproite from Ellendale 7: A —"Sandy" lapilli-tuff: fragments of fine-grained leucite lamproite and amphibolite, and juvenile lapilli of olivine lamproite, in a matrix of quartz grains and lamproite ash. Note the garnet xenocryst with phlogopite and kelyphitic rim; 7 AC 18, 165 m, (GSWA 71449F). B — Lamproite lapilli-tuff, containing accidental fragments of leucite lamproite; 7 AC 11, 119 m, (GSWA 65828C). C — Olivine-diopside-leucite lamproite, with unaltered leucite microphenocrysts. Boulder in coarse breccia; 7AC 18, 147 m, (GSWA 71449C). D — Olivine lamproite, containing olivine macrocrysts and fine-grained, granular, dunitic aggregate; 7 AC 17, 80 m, (GSWA 71448C).

TABLE 36. REPRESENTATIVE ANALYSES OF ELLENDALE 7 LAMPROITES.

	1	2
	Percent	
SiO_2	41.52	49.26
TiO_2	2.68	5.41
Al_2O_3	3.54	7.27
Fe_2O_3	4.57	5.47
FeO	3.90	1.02
MnO	0.13	0.10
MgO	26.90	8.29
CaO	4.38	2.56
Na_2O	0.36	0.45
K_2O	4.10	7.74
P_2O_5	0.62	0.64
H_2O^+	4.13	5.29
H_2O^-	1.60	2.97
CO_2	0.19	0.30
Rest	1.97	4.47
Total	**100.59**	**101.24**
	Parts per million	
Ba	10 093	31 447
Li	6	6
Rb	386	1 459
Sr	959	1 075
Pb	20	50
Th	18	14
U	<1	1
Zr	564	1 238
Nb	118	123
Y	16	19
La	185	308
Ce	261	368
Sc	18	18
V	46	139
Cr	1 250	316
Co	81	42
Ni	1 500	390
Cu	55	145
Zn	90	88
Sn	6	12
Mo	1	3
Ga	5	18
S	120	800
F	1 950	3 200
Cl	50	70

1 — Olivine lamproite; core 7AC17, 128m, GSWA 71448F.
2 — Olivine - potassic-richterite - leucite lamproite; core 7AC18, 107m, GSWA 71449A.

plant site. The pipe, which has a surface area of 46.9 ha, consists of an irregular oval-shaped western lobe 700 × 350 m, elongated north-south, and a larger eastern lobe, 1000 × 400 m, elongated east-west (Fig. 82). The pyroclastics of the western lobe have proved to be the second richest source of diamonds among the Ellendale pipes, with the result that extensive drilling by the Ashton Joint Venture has allowed the subsurface form of the vent to be determined.

The vent is emplaced in Permian Grant Group sandstones, which are poorly exposed at a number of localities around the margin of the pipe, typically as low, rounded boulders of baked sandstone a few metres across. The only notable outcrop is on the northern side of the pipe, between the western and eastern lobes, where a narrow septum of baked sandstone extends into the vent, and shows that the two lobes formed as independent vents, which later coalesced to give the present outline.

The pyroclastics and olivine lamproite of the pipe are concealed beneath an overburden of sand, laterite, calcrete, and clay, from 1 to 6 m thick. The cover is thickest over pyroclastic rocks, where the calcrete and clay horizons, derived from weathered lapilli-tuffs, are well developed: over magmatic lamproite there is often only a metre or so of red wind-blown sand and sandy laterite.

The western lobe of the vent is underlain by a thick sequence of lapilli-tuffs and tuffs, with a central core of olivine lamproite and phlogopite-olivine lamproite. Where exposed in exploration trenches, the pale-green, weathered pyroclastics are well-bedded surge deposits that dip towards the centre of the vent. Lapilli-tuffs containing olivine lamproite lapilli, commonly about 1 cm across, but up to 5 cm across in coarser beds, occupy most of the vent. At the southern end of the vent, there are "sandy" lapilli-tuffs containing varying amounts of tuff-sized quartz grains in the matrix, and sparse sub-rounded to rounded pyroclasts of quartzite up to 10 cm across. Within the "sandy" lapilli-tuffs, there are beds of fine-grained, quartz-rich tuff, particularly close to the base of the pyroclastic sequence.

The olivine lamproite core of the western lobe is about 300 m diameter at the surface, and eccentrically located in the northern part of the vent. Drillhole data show that it narrows rapidly with depth to a conduit less than 50 m diameter (Onley and Smith, 1980). Most of the core is a fine-grained olivine lamproite with prominent olivine macrocrysts, but in the central part of the mass, where cooling was slower, there is an area of coarser grained phlogopite-olivine lamproite. The chilled marginal phase of the lamproite is glassy and often autobrecciated, and resembles the margins of the magmatic core of Ellendale 4.

The eastern lobe of Ellendale 9 is about 1 000 m long but very irregular in shape, ranging from a maximum of 500 m wide to a "neck" only 150 m across. The surface area of the lobe is occupied mainly by olivine lamproite, but contains a central zone of coarser phlogopite-olivine lamproite running the length of the vent. Pyroclastic rocks, similar to those of the western lobe, subcrop only in discontinuous narrow strips around the margin of the vent, although drilling has shown that the magmatic lamproite often forms only a thin cover over the pyroclastic deposits.

Structure and volcanism

Extensive deep drilling, particularly in the western lobe of the vent, has allowed the contouring of the vent walls and the base of the magmatic core to depths up to 200 m (Onley and Smith, 1980). The western lobe appears to be quite simple: a single major vent is present, located beneath the area of phlogopite-olivine lamproite in the central core, and this was the conduit for both pyroclastic and magmatic rocks in the vent (Fig. 82a, section A-B). In detail, the vent is a little more complex. The embayment on the western margin of the vent is formed by a large block of country rock which protrudes into the vent to form a subsurface vertical cliff 40 m high. If the mechanism for vent enlargement proposed earlier for Mount Percy is applicable, the embayment represents a block of country rock which failed to be

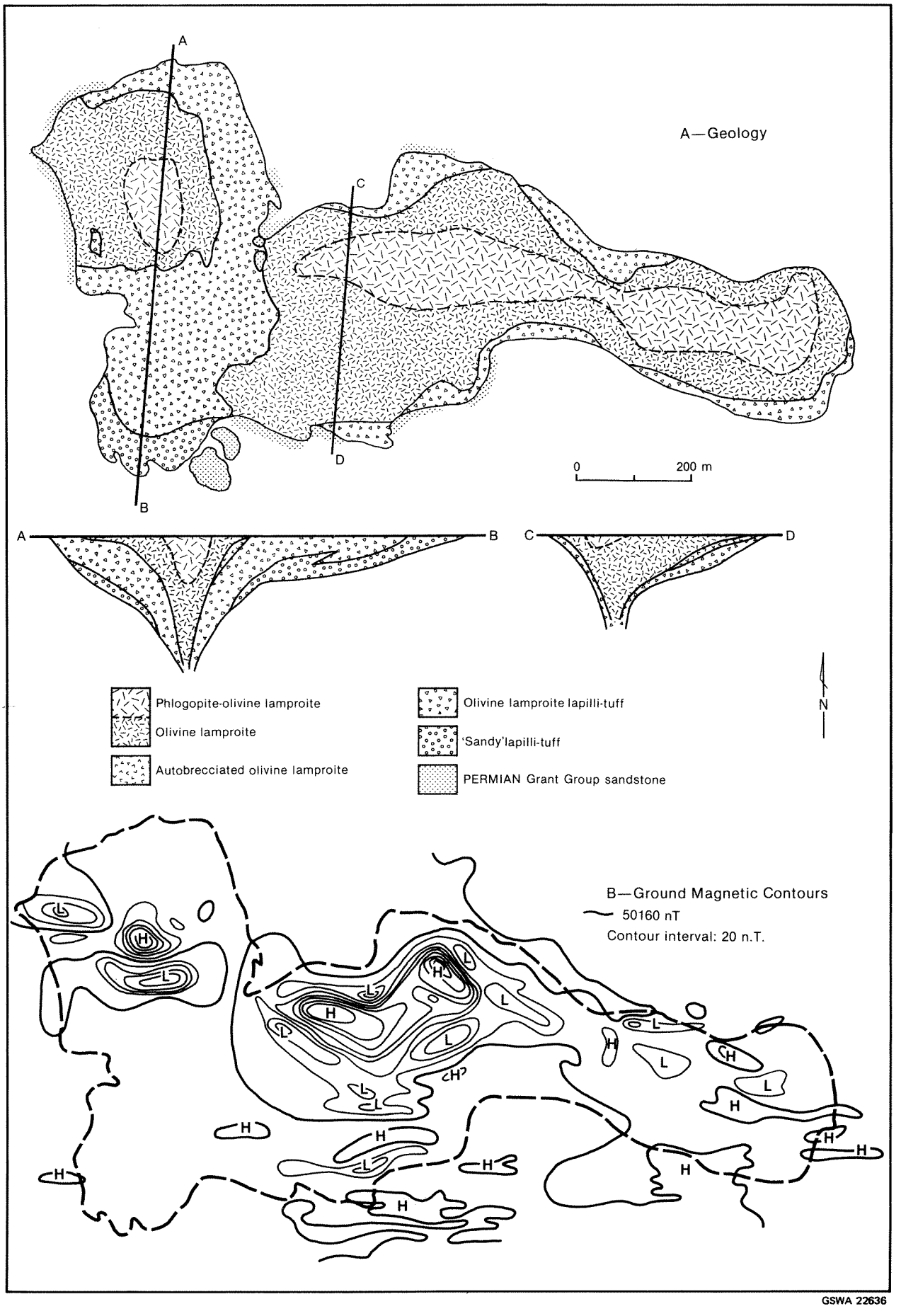
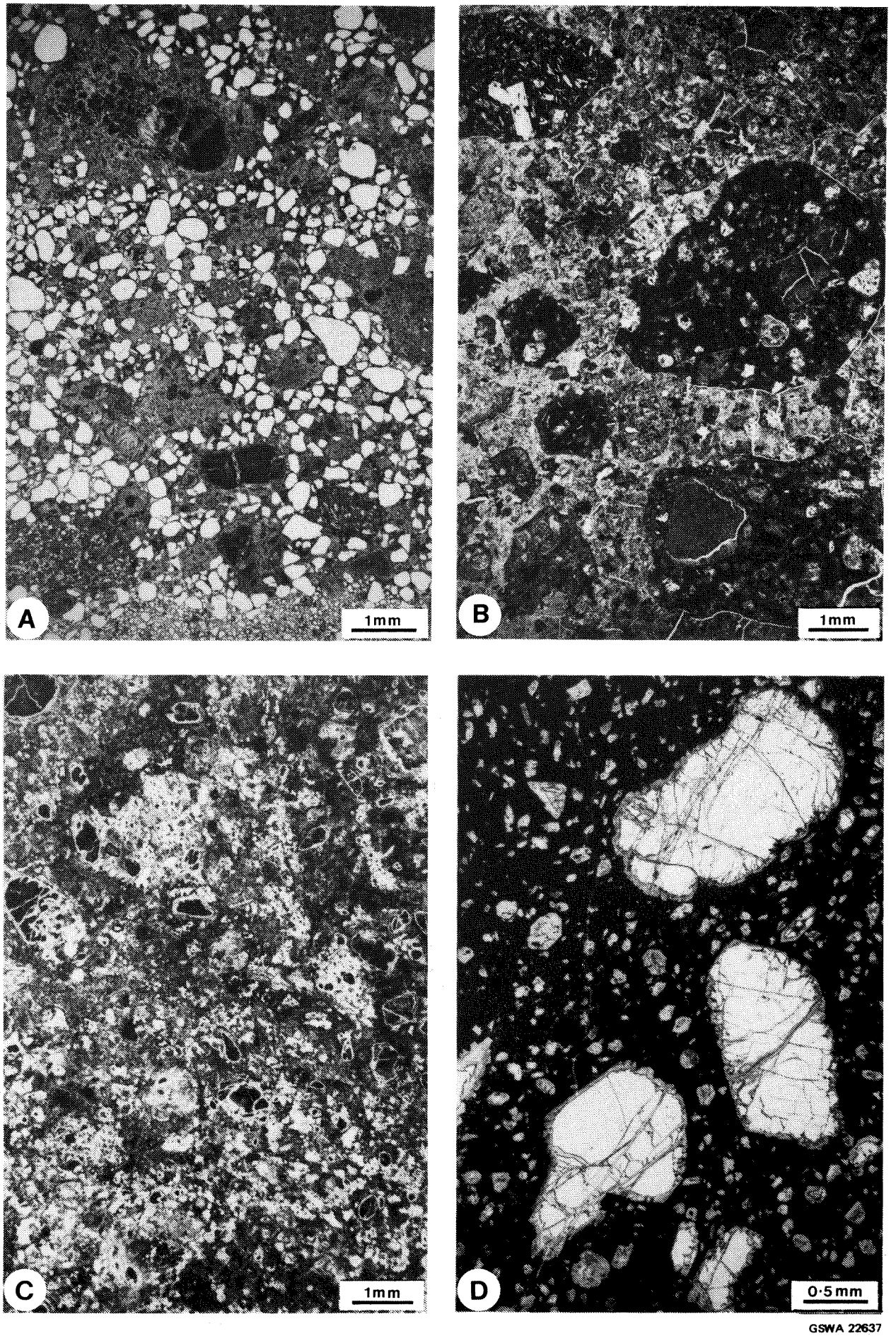


Figure 82. Geology and ground magnetic contours of Ellendale 9 (after Onley and Smith, 1980).



GSWA 22637

detached and slide into the vent. A few hundred metres north of the embayment, there is a small apophysis projecting westward from the vent. This may represent a small satellite vent, or a dyke-like sheet of lamproite extending from the main conduit. Drilling records suggest a satellite vent while ground magnetic contours (Fig. 82b) indicate an elongate body.

The eastern lobe has not been drilled as extensively as the western lobe and is therefore more difficult to interpret. In general the lobe is occupied by olivine lamproite, and pyroclastics form only a small proportion of the body (Fig. 82a, section C-D). To the east of the narrow neck, the lobe occupies a shallow trench about 50 m deep; whereas, in the western half of the lobe, drilling has outlined a broad area at least 120 m deep. It appears that the olivine lamproite magma erupted from a vent in the vicinity of section C-D of Fig. 82a and flowed out to fill the vent. However, a single vent is unlikely to have formed a body the shape of the eastern lobe. Initial pyroclastic volcanism most probably took place along a fissure, or set of fissures, and only the final magmatic phase seems to have been confined to a single vent. Ground magnetic contours (Fig. 82b) show several strong dipole anomalies in the western part of the lobe; and perhaps indicate a major fissure along the northern margin of the vent, and an *en echelon* fissure to the southwest, which would include the eruptive centre of the western lobe; both fissures trend about 300°. Alternatively, a single lineament might include both a fissure eruption in the east, with an expansion to form the final conduit of the eastern lobe, and the vent of the western lobe. Throughout most of their volcanic history, the two lobes formed separate vents; a north-south trending subsurface ridge separates the vents less than 40 m below the present surface.

The volcanic sequence is similar to, but less complex than, the events at Ellendale 4. Explosive volcanism from a central vent in the west and a fissure in the east excavated the vents and laid down thick deposits of pyroclastic rocks. The earliest deposits were quartz-rich tuffs, the product of disaggregation of the wall-rocks; these were followed by progressively more lamproite-rich "sandy" lapilli-tuff and lamproite lapilli-tuff. The pyroclastics are commonly well-bedded surge deposits, but unlike Ellendale 4, there is no interbedding of the various tuff types and no evidence that the vents erupted sequentially. Activity probably proceeded simultaneously in both lobes, although activity on the fissure was soon confined to a vent near its western end. The final volcanic event was the upwelling of olivine lamproite magma to form two separate lava lakes; the eastern vent also filled the former fissure vent.

Diamonds

Exploration and evaluation methods employed in assessing the diamond content of Ellendale 9 have been outlined in Chapter 1. Most effort was expended on the large area of pyroclastics of the western lobe, where an average grade of 5.3 CM/100 t was obtained (Table 3) from surface trenches and deep auger holes. Within the lobe, however, the grade varies from 3.03 CM/100 t to 8.04 CM/100 t. The lower grades relate, though not exclusively, to the "sandy" lapilli-tuffs (Onley and Smith, 1980).

Deep auger holes did not produce such consistent results as those for similar holes in Ellendale 4. Small sample size and a few large stones produced anomalously high grades in individual samples of quartz-rich tuff and magmatic lamproite.

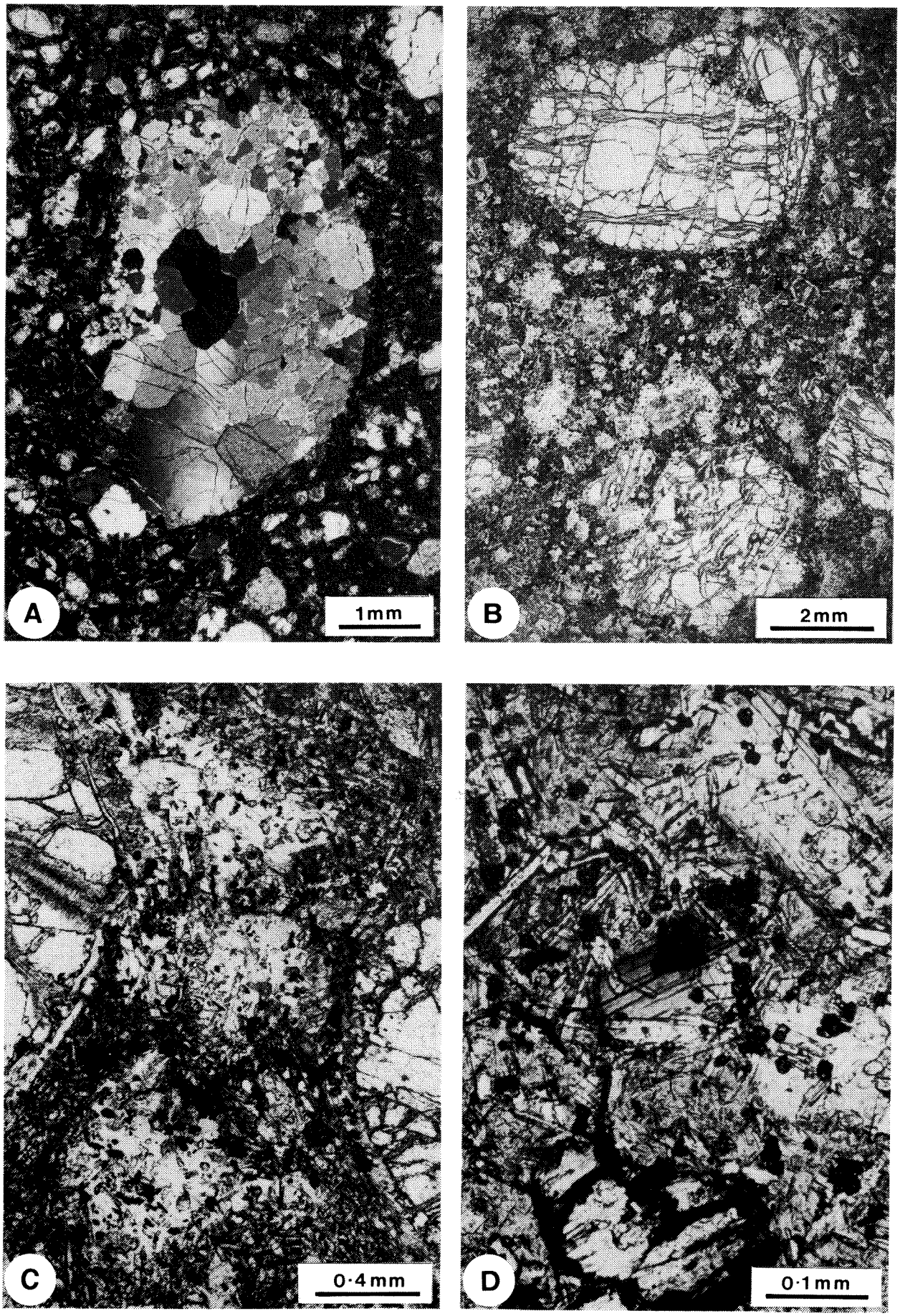
The magmatic lamproite of the western lobe is relatively diamond-rich, when compared with similar olivine lamproites of Ellendale 4. The overall grade is 2.1 CM/100 t, with 2.3 CM/100 t in the main body of lamproite and 1.0 CM/100 t in the central phlogopite-rich zone (Smith, 1981). Only one sample of marginal autobrecciated olivine lamproite was processed, it produced a grade similar to that of the main body of lamproite.

The eastern lobe of Ellendale 9 has not been tested as extensively as the western lobe, but the lapilli-tuffs produced grades of 3.0 to 8.1 CM/100 t, similar to those of the western lobe. The magmatic lamproite, with grades between 0.4 and 0.9 CM/100t (average, 0.6 CM/100 t) is significantly less diamondiferous than the lamproite of the western lobe. This may reflect a less diamond-rich magma or, more probably, greater resorption in a larger, slower cooling mass.

Petrography

Pyroclastics: The quartz-rich tuffs at the base of the pyroclastic succession range from almost pure "sandstone" to tuffs with only about 50% quartz grains of wall-rock origin. In one specimen, poorly sorted but well-rounded quartz grains up to 1.5 mm diameter are cemented by carbonate and secondary silica; occasional ash-sized grains of altered glassy olivine lamproite indicate its pyroclastic origin. The tuff is finely layered and includes thin beds of very fine-grained, fractured quartz grains. These quartz-rich tuffs grade upwards into mixed quartz-lamproite tuffs and finally to "sandy" lapilli- tuffs (Fig. 83a). The bulk of the pyroclastic deposit is fine-grained lapilli-tuff that contains juvenile olivine lamproite lapilli up to 6 mm across which form at least 50% of the rock; the remainder are cognate lamproite lapilli, accidental shale fragments, ash-sized lamproite

Figure 83. Photomicrographs of tuffs and lamproite from Ellendale 9: A — Quartz-rich lapilli-ash-tuff: lapilli of fine-grained olivine lamproite, containing altered olivine macrocrysts, in a matrix of quartz grains and lamproite ash; 9 AC 30, 120 m (GSWA 71465G). B — Lamproite lapilli-tuff: olivine lamproite lapilli in a matrix of altered lamproite ash. Note small phlogopite-bearing lapilli; 9 AC 60, 126 m(GSWA 76008E). C — Autobrecciated marginal olivine lamproite: altered olivine macrocrysts in a brecciated, formerly glassy groundmass; 9 AC 29, 127 m (GSWA 71464D). D — Olivine lamproite: olivine macrocrysts, veined and marginally altered to serpentine, and altered olivine microphenocrysts, in a fine-grained diopside-phlogopite groundmass; 9 AC 27, 67 m, (GSWA 71464C).



GSWA 22638

and quartz grains, and interstitial clay minerals (Fig. 83b). The proportion of quartz grains varies up to 30%; but, in the "sandy" lapilli-tuff, is commonly about 10%; the grains are angular to rounded and often show the effects of resorption by the lamproite magma. The juvenile lapilli are thoroughly altered, glassy, and often vesicular olivine lamproite, and have rounded to amoeboid shapes. Olivine macrocrysts up to 4 mm and microphenocrysts up to 0.2 mm, both replaced by talc, clay, or carbonate, are set in a brown or green devitrified vesicular glass. The vesicles are filled with carbonate or clay minerals and, in some lapilli, are flattened and streaked out to show flow structures. A few lapilli are formed by discrete olivine macrocrysts, some with a thin skin of adhering magma.

As with the lapilli-tuffs of Ellendale 4, there is the constant presence of a small proportion of cognate lapilli of olivine-phlogopite lamproite. These consist of altered euhedral olivines up to 0.4 mm, abundant small phlogopite crystals about 0.2 mm long, and a few phlogopite phenocrysts up to 1.5 mm long, in a dark, altered, devitrified glass. The phlogopite is pale coloured, and twinned; and the phenocrysts often have an almost colourless outer zone: they are unlike the poikilitic phlogopite found in the magmatic lamproite.

Apart from quartz grains there is little accidental material in the lapilli-tuffs. A few small shale fragments, probably from the underlying Fairfield Group, are present in most thin sections. Limestone, quartzite, and occasional granite and schist xenoliths, were recovered from trench samples, together with several pieces of fossilized wood.

The lapilli-tuffs are predominantly matrix-supported: the matrix consists of ash-sized lamproite fragments, interstitial clay, and in the "sandy" lapilli-tuffs, quartz grains.

Mantle-derived material is very rare, one small lherzolite nodule was intersected during drilling, and one altered fragment of a nodule with relic clinopyoxene was found in thin section. Heavy-mineral concentrates from diamond recovery produced chromite, kyanite, corundum, a little pyrope garnet, and, rarely, chrome-diopside (Onley and Smith, 1980).

Magmatic lamproite: The magmatic cores of Ellendale 9 are olivine lamproites, petrographically similar to those of Ellendale 4 and 7, but showing distinct differences in the development of phlogopite and in the olivine macrocrysts. Within Ellendale 9, there are also subtle differences probably related to cooling history, between the lamproites of the eastern and western lobes.

The olivine lamproite core of the western lobe is predominantly fine-grained and contains about 40% olivine as macrocrysts up to 6 mm across and euhedral microphenocrysts up to 0.4 mm. The groundmass is very fine grained and phlogopite-rich; it contains small prisms of diopside, and grains of perovskite and chromite. The olivine macrocrysts are commonly 2-3 mm diameter, subhedral to rounded, and marked by resorbed margins (Fig. 83d). Much of the olivine is pseudomorphed by serpentine, talc, or more rarely, carbonate; but where fresh, it shows undulose extinction and partial polygonization (Fig. 84a). Unlike the macrocrysts of Ellendale 4, there is only a poor development of kink bands, glide twinning, and granulation of the macrocrysts. Rare dunitic fragments, composed of a mosaic of strained olivine grains, are also present.

Groundmass olivine microphenocrysts are commonly pseudomorphed by talc or clay minerals but a few relics of fresh olivine remain. The groundmass itself is very fine-grained to glassy and phlogopite-rich, with abundant small flakes of red-brown phlogopite up to 30 μm across, small needles of diopside up to 30 μm long, and interstitial clay. Minute grains of perovskite, commonly <5 μm but up to 50 μm diameter, are abundant, with scattered euhedra of chromite, Very scarce wadeite, about 20 μm across, and tiny prisms of apatite are also present. Some specimens also contain a little groundmass potassic richterite, which is usually strongly coloured and often confined to small phlogopite-free areas of unknown origin. Such specimens also contain a little priderite in addition to perovskite.

In the central, more slowly cooled, parts of the mass, phlogopite becomes an essential mineral and forms large poikilitic plates up to 1.5 mm across (Fig. 84 b,c); these enclose numerous small prisms of diopside up to 100 μm and perovskite grains up to 50 μm. The phlogopite is strongly coloured and zoned to a red-brown titaniferous rim. Nearly colourless, weakly pleochroic potassic richterite is prominent in the more evolved varieties, and forms irregular poikilitic plates up to 1 mm across. Olivine macrocrysts and microphenocrysts, partly or completely pseudomorphed by serpentine or clay, are present in proportions similar to that in the common olivine lamproite. The matrix of the phlogopite-olivine lamproite contains abundant diopside and perovskite (set in a mass of brown clay minerals), chromite (commonly with titaniferous rims on magnesiochromite cores), secondary magnetite, hematite, and accessory wadeite and apatite. The clay minerals often pseudomorph an unidentified prismatic mineral, and a number of specimens contain circular to rounded spots of colourless clay mineral or zeolite (harmotome), up to 100 μm diameter, which probably represent former leucite (Fig. 84d). Ilmenite and sulphides are also present in some of the coarser grained rocks of the western lobe.

The autobrecciated marginal phase of the olivine lamproite is not so well developed as at Ellendale 4. Specimens available include a vesicular variety, in which

Figure 84. Photomicrographs of olivine lamproite from Ellendale 9: A — Partially recrystallized olivine macrocryst. Small, unstrained neoblasts, with a relic of the original strained macrocryst. Note the abundant acicular diopside in the groundmass; (crossed polars), 9 AC 110, 56 m (GSWA 71475B). B — Phlogopite-olivine lamproite containing olivine macrocrysts and abundant poikilitic phlogopite (GSWA 65885A). C — Detail of B, showing irregular poikilitic phlogopite, groundmass diopside prisms, and minor interstitial potassic richterite (small clear areas in groundmass) (GSWA 65885A). D — Former leucite (rounded), diopside prisms, and perovskite grains (dark), as inclusions in phlogopite. Phlogopite-olivine lamproite; 9 AC 110, 56 m (GSWA 71475B).

fragments of fine-grained olivine lamproite are set in a matrix of vesicular olivine lamproite, and others in which the lamproite fragments are thoroughly rewelded (Fig. 83d). A surface sample, in which altered olivine macrocrysts and microphenocrysts are set in a strongly vesicular microcrystalline groundmass, is from an unbrecciated marginal phase. Vesicles make up about 30% of the rock, are spherical to ovoid, from 0.1 mm to 3 mm diameter, and are filled with calcite, barite, clay minerals, and secondary silica.

The bulk of the olivine lamproite from the eastern lobe is distinctive only in the preservation of fresh microphenocrysts of olivine. Macrocrysts and microphenocrysts of olivine constitute about 40% of the rock and are similar to those described from the western lobe. The groundmass is very fine-grained, rich in minute phlogopite flakes and diopside prisms up to 20 μm, abundant perovskite <5 μm, accessory chromite, and interstitial clay minerals. No potassic richterite or priderite has been noted in these rocks.

The phlogopite-olivine lamproites of the eastern lobe are characterized by the poorer development of phlogopite and potassic richterite, and the stronger development of diopside and leucite, relative to similar rocks of the western lobe. Phlogopite forms irregular poikilitic flakes up to 1 mm across and has not developed the crystal outlines found in other bodies. It is relatively dark in colour and has a dark red-brown rim. Smaller phlogopite flakes sometimes fringe the olivine phenocrysts. Diopside laths, about 0.25 mm long and twinned, are abundant in the groundmass, and are sometimes replaced by colourless potassic richterite. Interstitial poikilitic plates of potassic richterite are not generally present. Olivine, perovskite and chromite are similar to those described from the main body of rock, and there is much interstitial brown clay in the matrix. As in other examples of slowly cooled olivine lamproite, there are small clear-to-turbid, rounded patches of harmotome, K-feldspar and/or clay minerals, up to 50 μm diameter, which are interpreted as former groundmass leucite. In one specimen, the clear patches are of entirely K-feldspar and provide the best evidence that leucite was formerly present in some olivine lamproites of Ellendale 9.

Chemistry

Analyses of magmatic olivine lamproite from Ellendale 9 show a range in composition from approximately 22 to 30% MgO, and 38 to 48% SiO_2 (Fig. 85; Table 37). All have high K_2O (3.5-5%) and TiO_2 (2.5-3.6%), and low Al_2O_3 (3-4.6%) and CaO (5-6%), and contain abundant Ni and Cr (700-1 200, and 750-1 750 ppm respectively) typical of the olivine lamproites of Ellendale (Jaques and others, 1984a). The most magnesian rocks are the olivine lamproites from the western robe, which contain more than 25% MgO. These rocks are strongly olivine-normative (>40%) reflecting their high content of macrocrystal olivine, and the associated pyroclastics contain the highest diamond grades in the pipe. The less MgO-rich olivine lamproites are olivine-hypersthene normative, as is more typical of the West Kimberley olivine lamproites, and contain a greater percentage of normative felsic minerals. Some of these contain leucite in the CIPW norm but modal (former) leucite is mostly restricted to the more Mg-poor olivine lamproites. Apart from lacking the high-MgO rocks, the olivine lamproites of the eastern lobe are similar in composition to those of the western lobe.

TABLE 37. REPRESENTATIVE ANALYSES OF ELLENDALE 9 LAMPROITES.

	1	*2*	*3*	*4*	*5*	*6*
			Percent			
SiO_2	36.81	40.43	40.60	40.00	44.10	39.90
TiO_2	3.33	3.31	3.06	3.19	3.20	3.48
Al_2O_3	4.01	4.48	4.50	4.20	3.50	3.90
Fe_2O_3	5.38	4.22	4.40	4.70	4.50	5.20
FeO	4.00	4.42	4.08	3.82	3.09	3.02
MnO	0.14	0.14	0.14	0.14	0.12	0.13
MgO	23.40	21.60	22.60	22.70	21.30	22.10
Cao	5.80	5.67	5.31	5.16	3.74	5.15
Na_2O	0.47	0.60	0.74	0.31	0.93	0.58
K_2O	4.74	4.95	3.70	3.16	6.51	4.12
P_2O_5	2.85	1.60	1.41	1.62	1.13	1.66
H_2O^+	6.00	3.98	4.09	5.79	3.09	4.97
H_2O^-	1.12	1.11	1.75	2.62	2.54	3.08
CO_2	0.15	0.27	0.16	0.14	0.28	0.69
Rest	2.76	4.19	3.77	2.54	2.12	2.54
Total	**100.96**	**100.97**	**100.31**	**100.09**	**100.15**	**100.52**
			Parts per million			
Ba	13 465	27 674	23 990	12 825	9 416	12 286
Li	8	8	10	14	9	10
Rb	751	500	500	447	494	526
Sr	1 341	1 284	1 075	1 124	943	1 359
Pb	20	50	42	48	51	50
Th	58	68	51	57	72	68
U	<1	4	1	3	2	3
Zr	723	807	777	843	902	958
Nb	224	232	197	199	169	188
Y	19	19	14	16	19	17
La	372	366	396	400	427	437
Ce	742	591	556	680	767	763
Sc	23	22	17	22	20	21
V	40	49	84	97	195	68
Cr	1 084	888	874	916	816	855
Co	83	77	66	66	64	64
Ni	1 200	930	899	909	888	881
Cu	65	70	60	57	50	52
Zn	84	92	71	72	66	72
Sn	—	8	24	11	14	3
Ga	7	5	2	5	6	4
S	100	80	80	320	70	120
F	6 450	5 400	5 990	5 480	5 130	5 930
Cl	110	110	131	163	97	99

1 — Potassic-richterite - phlogopite - olivine lamproite; 9AC86 39m, GSWA 71456A. 2 — Phlogopite-olivine lamproite, 9AC52 91m, GSWA 71474B. 3 — Diopside-phlogopite-olivine lamproite; 9E, 9AC78 37m, GSWA 71458. 4 — Olivine lamproite; 9E, 9AC113 42m, GSWA 71460. 5 — Olivine lamproite; 9W, 9AC29 67m, GSWA 71464C. 6 — Olivine lamproite; 9W, 9AC30 85m, GSWA 71465D.

Large variations in the abundances of Ba (6 000-30 000 ppm) and, to a lesser extent, Th (20-97) occur within the suite. Other elements show a much smaller range in abundances. For example, Rb, Zr, and La concentrations, lie in the ranges 460-740, 620-1 010 and 300-450 ppm respectively, and correlate inversely with MgO content. However, trace element ratios, such as Ti/Zr, Zr/Nb, La/Yb and Zr/Hf, are uniform regardless of MgO content (Fig. 85) or element concentration, implying that the eastern and western lobes are essentially comagmatic. Small differences exist, however, in terms of Rb/Sr and initial $^{87}Sr/^{86}Sr$ ratios (Jaques and others, 1984c).

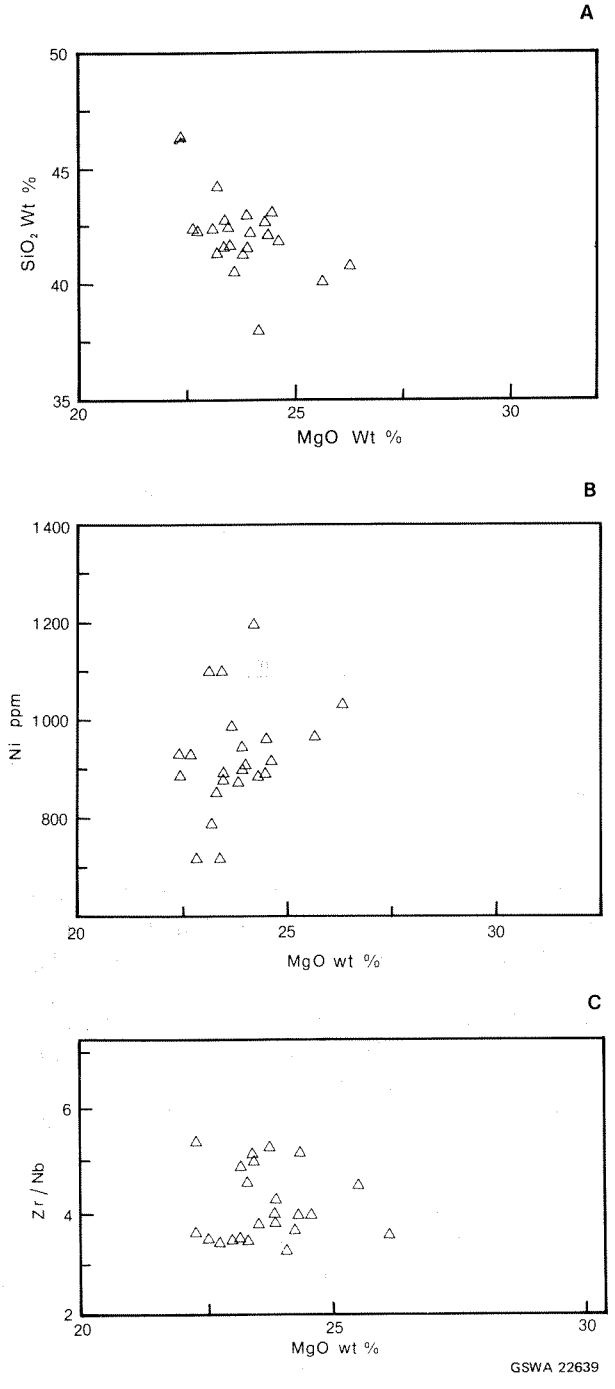


Figure 85. Variation of SiO_2, Ni, and Zr/Nb ratio with MgO for olivine lamproites of Ellendale 9.

ELLENDALE 11.

Ellendale 11 is a roughly circular pipe, 400 m diameter and 13.1 ha in area, and is located half a kilometre north of the CRA plant site and nearly one kilometre west of Ellendale 9. Significant diamond values were found in the marginal pyroclastics of the pipe with the result that the pipe has been extensively explored by aircore drilling and bulk sampling.

The pipe (Fig. 86) was emplaced in Permian sandstones of the Grant Group, which are poorly exposed at a few localities around the margin, usually as low, rounded boulders of baked sandstone. Drilling records show that the sandstone is rarely more than 50 m thick and around the eastern half of the pipe, no more than 20 m thick. Underlying the sandstones are mudstones and limestones of the Late Devonian Fairfield Group, xenoliths and boulders of which are incorporated in the pyroclastic deposits of the pipe.

Ellendale 11 is nowhere exposed; but, over the eastern half of the pipe, small cobbles and boulders of fresh olivine lamproite can be found in the thin soil horizon. Elswhere the overburden of red sand and clay is rarely more than 2 m thick.

The surface area of the pipe is mostly occupied by a large mass of olivine lamproite; pyroclastic rocks subcropping only in narrow marginal zones on the north and east and in a narrow pyroclast-filled tongue extending 200 m west from the pipe (Fig.86). However, drilling has shown that the olivine lamproite forms a cap, generally less than 50 m thick, over a pyroclast-filled vent. The pyroclastics are predominantly lamproite lapilli-tuffs, which contain olivine lamproite lapilli up to 1.5 cm across in a tuffaceous matrix, or "sandy" lapilli-tuffs with a high proportion of sand grains from disaggregated wall-rock in the matrix. Deep in the vent, the pyroclastics contain larger accidental pyroclasts of mudstone, limestone, and quartzite, and approach a tuff-breccia in composition. Breccias, composed of angular fragments of mudstone with little interstitial lamproitic material, are found close to the vent walls, together with fine-grained, quartz-rich tuff.

In general, the pyroclastics are moderately well-bedded surge deposits, and evolve upwards from "sandy" lapilli-tuff to lamproite lapilli-tuff. There is, however, some interbedding of these pyroclastics and lenses of "sandy" lapilli-tuff and quartz-rich tuff are found within the lamproite lapilli-tuffs.

The olivine lamproite of this vent has a form similar to that of the Ellendale 4 Satellite pipe — a thin sill-like sheet up to 50 m thick, fed from a narrow conduit. Several thin lamproite sheets intruding the pyroclastic rocks were intersected by drilling but the exact location of the conduit is unknown and the cross-section of Fig. 86 is diagrammatic only. There is no evidence of a central phlogopite-rich zone within the body.

The vent is very steep-sided, and "carrot shaped" below a depth of about 75 m, at which depth the vent is probably about 150 m in diameter. The pipe flares progressively above 75 m; and, in some marginal areas at the present surface level, the vent wall dips at shallow angles of 20° or less. The original vent was possibly a narrow fissure, which would explain the tongue of pyroclastic rocks extending westward from the main area of the vent. Such a fissure might be related to the subvolcanic system postulated to underly the Ellendale 9 pipe. Volcanic activity, however, was soon confined to the eastern end of the fissure; this gave the present form of the vent. Most activity was explosive and formed the thick pyroclastic deposits; but, in the final magmatic phase, olivine lamproite magma rose to form a shallow lava lake within the vent.

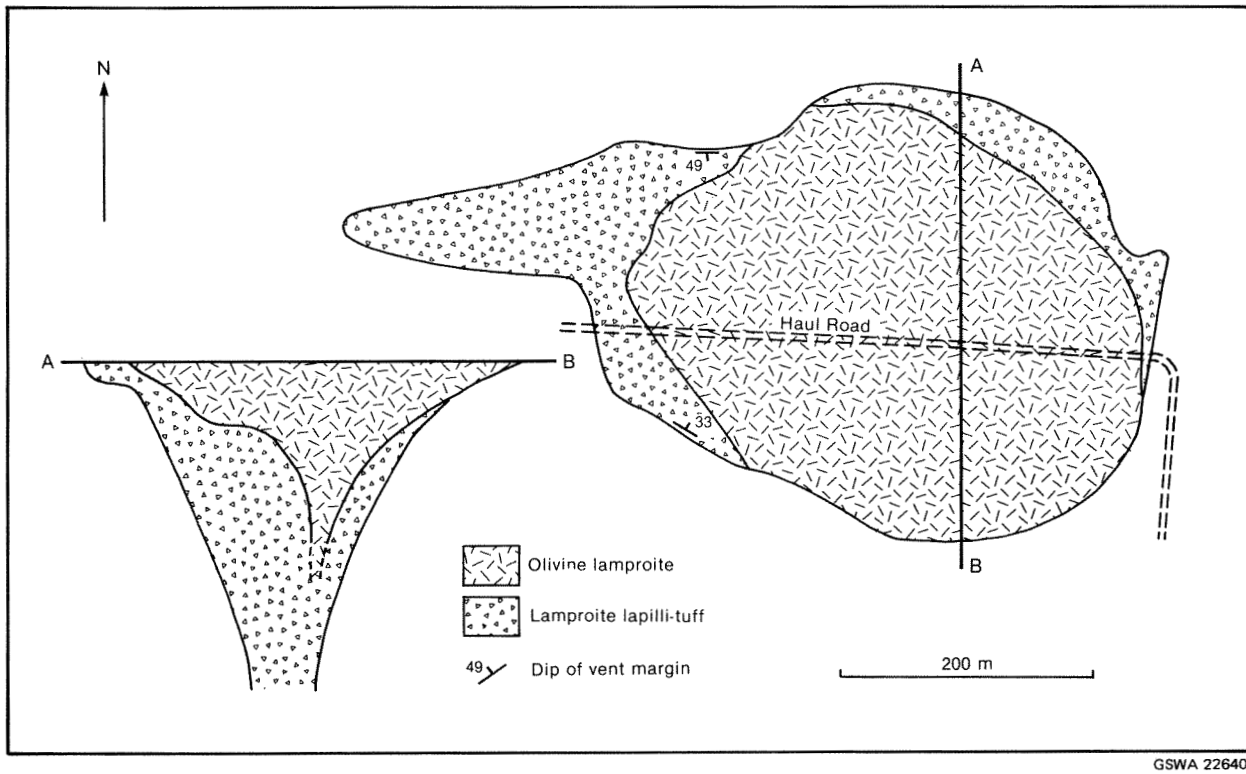


Figure 86. Geological map of Ellendale 11 (after Onley and Smith, 1980).

Diamonds

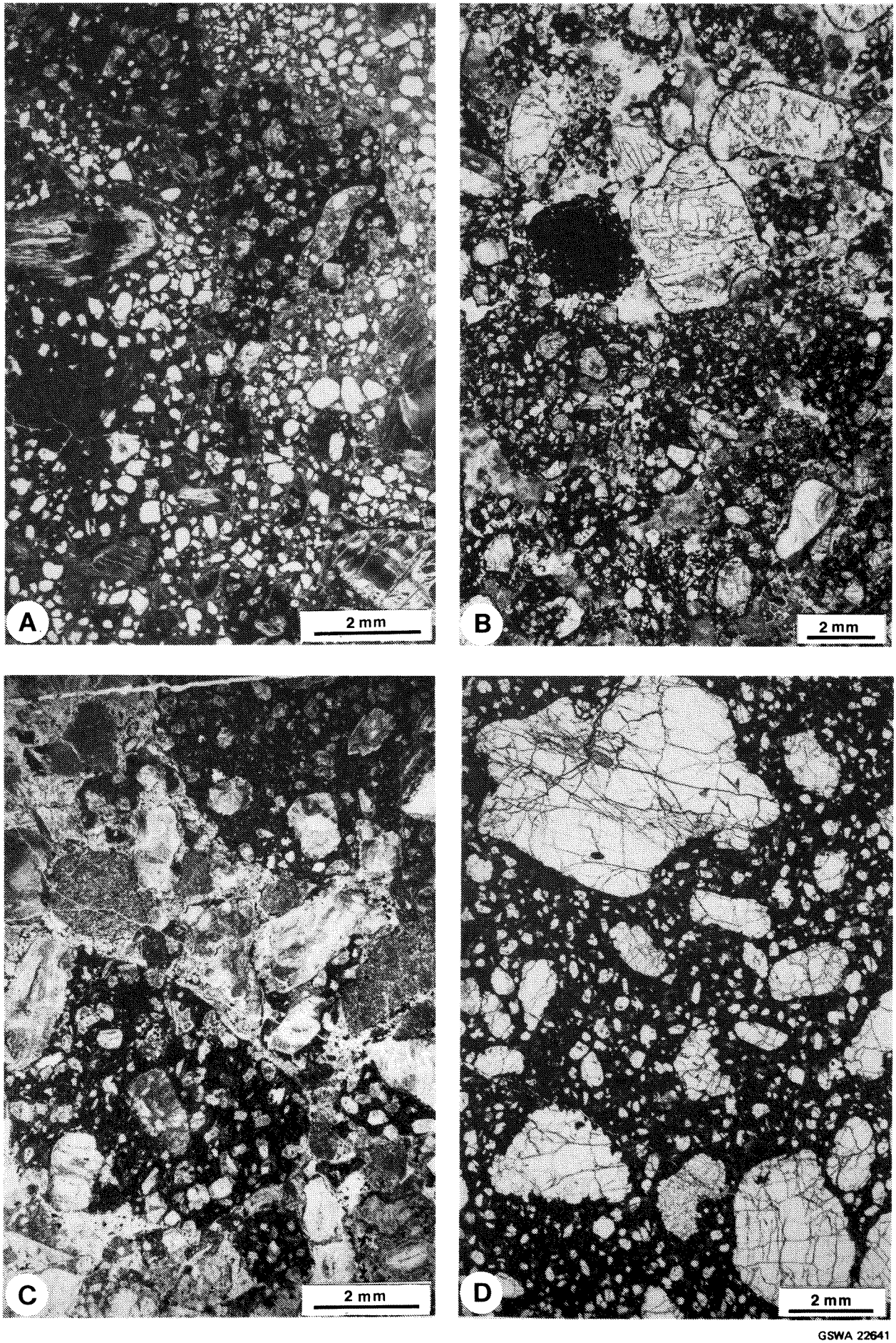
A total of over 4 600 t of material from surface trenches and deep auger holes was treated in the central plant for the recovery of 52.96 CM of diamond, an overall grade of 1.13 CM/100 t (Onley and Smith, 1980). Five initial scout samples of the pyroclastics, each of about 150 t, returned a grade of 1.99 CM/100 t, but four bulk samples totalling 3 108 t contained 1.03 CM/100 t. The difference between the grades is probably the result of the greater effect of surface concentration in the smaller samples. The deep auger samples proved that grades vary considerably but confirmed the lower results of the bulk sampling programme. Two scout samples of weathered olivine lamproite showed a grade of only 0.56 CM/100 t.

Petrography

Pyroclastics: Apart from the marginal breccias, no sample of which is available, the pyroclastics vary from quartz-rich tuffs, through "sandy" lapilli-tuffs to lamproite lapilli-tuffs with little or no accidental component. A specimen of quartz-rich tuff, interbedded with "sandy" lapilli-tuff, contains about 45% angular quartz and accessory tourmaline grains about 0.2 mm across, and 15% altered lamproite ash of similar size, in a clay matrix.

The lapilli-tuffs, both "sandy" and "non-sandy" varieties, contain lapilli of olivine lamproite, up to 15 mm across, in a tuffaceous matrix. The "sandy" lapilli-tuff contains up to 30% of rounded to angular quartz grains, together with ash-sized lamproite fragments and clay derived from fine lamproite ash. The proportion of juvenile pyroclasts varies between 30% and 50%, although in a few specimens, the pyroclasts are <2 mm across and the rock becomes a coarse tuff. In all specimens, the lamproite component of the matrix is thoroughly altered; secondary carbonate has developed in some, and vesuvianite in one specimen. The olivine lamproite lapilli are rounded to amoeboid in shape and usually vesicular (Fig. 87a). Rare, relatively fresh lapilli contain: altered olivine macrocrysts up to 4 mm; fresh groundmass olivine microphenocrysts up to 0.5 mm, in a vesicular, devitrified groundmass with abundant talc-filled vesicles 20-100 μm diameter; and perovskite and chromite grains up to 50 μm. A few larger vesicles, up to 1 mm diameter, are filled with talc and zeolite. More commonly the lapilli are thoroughly altered, and both olivine and groundmass are replaced by a mass of dark clay minerals. A few lapilli contain isolated small flakes of phlogopite. Accidental lapilli of shale, quartzite and quartz-mica schist are rare.

Figure 87. Photomicrographs of tuff and olivine lamproite from Ellendale 11: A — "Sandy" lapilli-tuff containing altered olivine macrocrysts, and dark, oxidized, amoeboid lapilli of formerly glassy olivine lamproite, in a matrix of quartz grains and lamproite ash; 11 AC 13, 90 m (GSWA 71451G). B — Lamproite lapilli-tuff with abundant altered olivine macrocrysts; 11 AC 15, 61 m (GSWA 71453E). C — Lamproite lapilli-tuff; 11 AC 16, 249 m (GSWA 71454I). D — Olivine lamproite: olivine macrocrysts and microphenocrysts in a fine-grained, diopside and phlogopite-rich groundmass. Note the small granular olivine aggregate, and the rounded crystal of chrome diopside enclosed in the large macrocryst; 11 AC 26, 24 m, (GSWA 71455A).



GSWA 22641

Lamproite lapilli-tuff consists almost entirely of olivine lamproite, either as lapilli up to 1.5 cm across or as ash-sized matrix fragments. The lapilli are similar to those in the "sandy" lapilli-tuff and thoroughly altered to talc and clay minerals (Fig. 87b,c). Most lapilli are of dense, crystalline lamproite; but there is a proportion of vesicular glassy lapilli, and some beds are made up entirely of lapilli and shards of pumiceous lamproite. Accidental pyroclasts are mostly small fragments of shale but a few examples of fossiliferous limestone are present. The tuffaceous matrix of lamproite ash is often thoroughly altered to clay, and all pyroclastic textures destroyed: secondary carbonate and barite are prominent in some specimens.

Phlogopite-olivine lamproite: Except in marginal areas, the magmatic core of Ellendale 11 is a uniform phlogopite-olivine lamproite containing abundant unaltered macrocrysts and microphenocrysts of olivine, and small poikilitic plates of phlogopite in a fine-grained, diopside-rich matrix. Perovskite and chromite grains, and accessory apatite, are abundant in the matrix.

Ellendale 11 is the most olivine-rich of the West Kimberley lamproites; about 45% of the rock consists of olivine macrocrysts up to 1 cm across and euhedral to subhedral microphenocrysts up to 0.4 mm. The macrocrysts are commonly 2-4 mm across, and rounded to subhedral, and have partially resorbed margins. They show undulose extinction, incipient glide twinning and granulation, and partial polygonization. A number of macrocrysts are actually micro-xenoliths of peridotite: they consist of several olivine crystals with interlobate margins, each showing undulose extinction; some enclose rounded crystals of clinopyroxene (Fig 87d).

The groundmass of the rock is predominatly a felted mass of small diopside prisms 50-100 μm long, but contains abundant small anhedral to subhedral flakes of poikilitic phlogopite up to 0.2 mm across. The phlogopite is red-brown in colour, but has a darker titaniferous rim, and encloses many small diopside and perovskite grains. Diopside prisms commonly show a poor alignment, probably the result of flow, and are set in a sparse interstitial matrix of clay minerals with abundant grains of perovskite 5-30 μm diameter and euhedra of chromite up to 50 μm across. In some evolved specimens, a little acicular priderite is present and the matrix may contain interstitial grains of colourless potassic richterite, and/or probable altered leucite, up to 30 μm across. In the more rapidly cooled parts of the body, both phlogopite and diopside are smaller and reduced in abundance; and, in marginal zones, the groundmass is a microcrystalline devitrified glass containing minute grains of perovskite and chromite, in parts vesicular.

Chemistry

Analyses of magmatic lamproite from Ellendale 11 (Table 38) are among the most MgO-rich olivine lamproites of the Ellendale Field: MgO is in the range 24.2-28.0%. All have high K_2O (2.0-4.0%) and TiO_2 (2.4-2.7%), and low Al_2O_3 (3.3-3.8%), CaO (4.5-5.6%), and SiO_2 (39.9-42.5%) contents and contain abundant Ni and Cr (960-1 157 ppm and 989-1 396 ppm respectively). The range of values for most elements is small: and the analyses are typical of the olivine lamproites of the Ellendale Field, and very similar to those from Ellendale 4 except for lower K_2O and higher SiO_2 contents.

TABLE 38. REPRESENTATIVE ANALYSES OF ELLENDALE 11 LAMPROITES.

	1	*2*
	Percent	
SiO_2	41.45	42.50
TiO_2	2.71	2.39
Al_2O_3	3.37	3.50
Fe_2O_3	4.27	4.70
FeO	4.32	3.54
MnO	0.13	0.12
MgO	28.00	25.70
CaO	4.79	4.77
Na_2O	0.34	0.53
K_2O	2.24	2.21
P_2O_5	1.33	1.35
H_2O^+	4.32	3.46
H_2O^-	1.05	2.09
CO_2	0.12	0.22
Rest	2.12	2.36
Total	**100.56**	**99.44**
	Parts per million	
Ba	9 080	12 200
Li	8	8
Rb	483	454
Sr	1 538	933
Pb	20	37
Th	61	46
U	8	2
Zr	700	645
Nb	206	173
Y	12	11
La	303	312
Ce	574	521
Nd	—	—
Sc	21	20
V	93	81
Cr	1 182	1 089
Co	89	85
Ni	1 200	1 110
Cu	70	51
Zn	68	63
Sn	2	5
Ga	4	3
S	150	120
F	4 200	4 540
Cl	40	76

1 — Phlogopite-olivine lamproite; Ellendale 11, core 11AC26, 24m, GSWA 714551. 2 — Olivine-lamproite; Ellendale 11, core 11AC12, 13m, GSWA 71450A.

ELLENDALE 16

Ellendale 16 is a roughly circular pipe, 450 m in diameter and 16.9 ha in area, located 3.5 km south-southwest of Mount North, and close to the main haul road that traverses the Ellendale Field (Fig. 88). The lamproite and minor pyroclastic rocks of the pipe are concealed beneath about 3.5 m of sandy overburden, which has a well-developed calcrete horizon over the central parts of the pipe.

The lamproite is emplaced in Permian sandstones of the Grant Group, which outcrop at a number of places around the margin of the pipe, particularly on the north side, where they form a prominent hill rising 30 m above

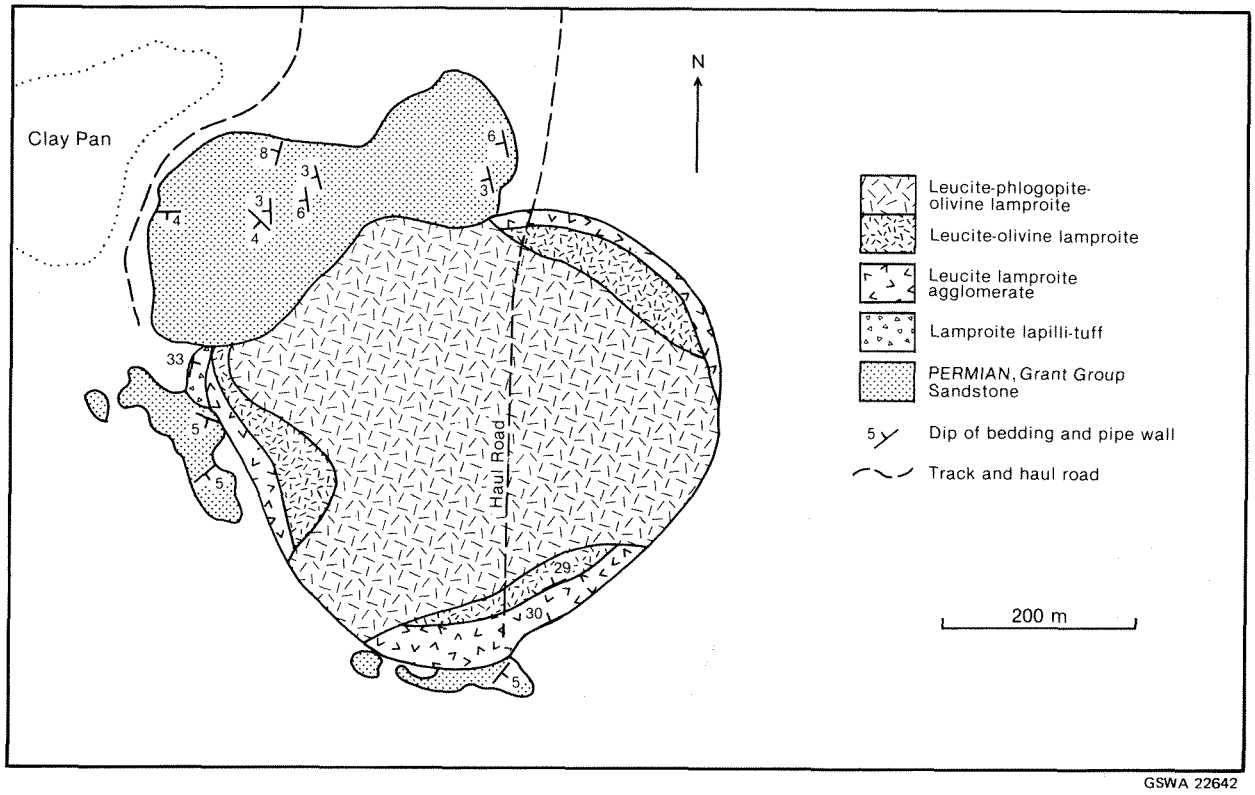


Figure 88. Geological map of Ellendale 16 (after Onley and Smith, 1980).

the plain. The sandstone is mostly fine-grained and well bedded, and away from the pipe margin is flat-lying and flaggy. Cross-bedding is evident in places and there are occasional coarse grit beds and pebble conglomerates. Close to the margin of the pipe, the sediments have been baked and indurated and the bedding disrupted. This is particularly evident to the north, where marginal effects can be found 50 m from the pipe.

Much of the area of the pipe is occupied by a coarse, thoroughly altered (leucite)-phlogopite-olivine lamproite. In surface trenches, the exposed rock has been largely replaced by carbonate in which clots of phlogopite 5 mm across are visible. Marginal to the main mass is a discontinuous zone of olive green, fine-grained olivine lamproite, which is probably a chilled facies of the central mass.

Pyroclastic rocks are poorly represented at the present level of erosion: there is only one small area of lapilli-tuff in the northwestern part of the pipe. There are, however, three marginal lenses of brecciated, vesicular, glassy lamproite agglomerate, pale grey to pale brown in colour, in which large rounded bombs of lamproite are welded together with a sparse matrix of lapilli and ash of similar material. The bombs range up to 50 cm across, and many show plastic deformation, lobate margins, and vesicles that show flow patterns parallel to the margins of the bombs. Angular blocks are also present, and there are large inter-block voids, often lined with secondary silica. The unit is a coarse bomb agglomerate that was erupted in the waning stages of the initial explosive volcanism.

Little drilling has been carried out on this pipe, but trenches close to the margin showed that the lamproite/sandstone contact dips 30-39° towards the centre. This suggests that the pipe narrows rapidly with depth to a small central conduit. A total of 717 t of surface material from five trenches was tested for diamond without result.

Petrography

The lapilli-tuffs and agglomerate are essentially grain-size variations of the same rock unit, both contain juvenile lapilli or bombs of the same, altered, fine-grained, vesicular leucite-olivine lamproite. In the lapilli-tuff, juvenile lamproite fragments are commonly from 4 mm to 5 cm across, rounded to amoeboid in shape, and set in a matrix of smaller lapilli and ash-sized lamproite shards. The lamproite contains occasional macrocrysts of olivine up to 4 mm across, and abundant euhedral microphenocrysts up to 0.3 mm; both are altered to talc and iron oxides or replaced by silica or barite, and set in a groundmass of clay minerals and abundant small altered leucite euhedra, minute flakes of phlogopite, and grains of perovskite (all <5 μm across) and small irregular shaped vesicles. Glassy lapilli are often strongly vesicular, and the vesicles are streaked out to show flow structures. Some glassy lapilli contain a little phlogopite. Accidental material in the lapilli-tuff includes a few small, rounded fragments of shale and siltstone up to 1 cm across.

The lamproite agglomerate is petrographically similar to the lapilli-tuff except for the proportion of vesicles. Most of the olivine lamproite bombs contain about 30% of spherical to ovoid vesicles up to 6 mm diameter; they are usually empty or lined by a thin coating of zeolite, but some are filled by barite. Interstitial areas in the agglomerate are filled by lapilli and lamproite ash.

The central magmatic core is a porphyritic (leucite)-

phlogopite-olivine lamproite containing abundant microphenocrysts of olivine, sparse olivine macrocrysts up to 3 mm — both pseudomorphed by talc — and poikilitic phlogopite flakes up to 0.7 mm across. Phlogopite forms subhedral to anhedral poikilitic plates enclosing diopside, perovskite, apatite, and former leucite grains. The mica is pale coloured and pleochroic from yellow to pink, and has a slightly darker marginal zone. The groundmass of the rock is predominantly a pale-brown chloritic material that pseudomorphs an unidentified prismatic mineral; but, in addition, there are abundant prisms of diopside, up to 100 μm long, interstitial pink potassic richterite, and euhedra of former leucite, perovskite, chromite, and accessory wadeite and apatite, each up to 30 μm across.

Carbonated specimens from the central part of the mass suggest a similar, but coarser grained, variety of the main phlogopite-olivine lamproite. Much of the texture and mineralogy has been replaced by carbonate and narrow veins of barite; but phlogopite flakes, up to 3 mm across, perovskite, potassic richterite, apatite, secondary magnetite, and rare wadeite are preserved. Some phlogopite encloses rare grains of former leucite. Olivine macrocrysts replaced by carbonate and serpentine (up to 4 mm across) are recognizable.

Specimens from the chilled marginal phase of olivine lamproite are petrographically similar to the main body except that phlogopite and diopside are less well developed. Phlogopite forms small groundmass flakes,or poikilitic plates up to 0.2 mm; and diopside prisms are usually < 50 μm long. Small altered leucites, < 30 μm across, are common in the groundmass and one specimen contains a diffuse mass of spongy altered leucite 3 mm across. In addition to perovskite, the marginal rocks also contain a little priderite.

Chemistry

Chemical analyses of bombs from the leucite-olivine lamproite agglomerate (Table 39) show the rocks to be low in MgO (6.3-9.7%) but high in K_2O (5.9-6.5%), TiO_2 (5.2-5.9%) and Al_2O_3 (6.5-7.2%). Trace-element contents are intermediate between the leucite lamproites and olivine lamproites, particularly Ni (≈ 550 ppm) and Cr (540 and 799 ppm), although V is very high (321 and 503 ppm).

The central (leucite)-phlogopite-olivine lamproite is, as expected from the petrography, more magnesian than the agglomerate. MgO at 15.6% is similar to that of the olivine lamproite of Ellendale 2, and K_2O at 2.6% is less than half that found in the associated agglomerate. TiO_2 and Al_2O_3 (4.4% and 4.8% respectively) are intermediate between leucite lamproite and olivine lamproite. Ni and Cr (737 ppm and 796 ppm) are only marginally higher than values for the agglomerate, but V at 87 ppm is much lower. Analyses 4 and 5 of Table 39 are from the centre of the mass; analysis 4 suggests a late-stage concentration of K_2O, but analysis 5 illustrates the effect of almost complete carbonation of the rock.

There is considerable variation between the composition of the early magma and the final magmatic intrusion — much greater than that found between the initial and final intrusions of Mount North, for example. Differentiation involving the settling of olivine macrocrysts would explain the MgO variation, but the trace elements present a confused picture: Ni and Cr indicate that the rocks may be co-magmatic, but V is strikingly different in the two rock types.

TABLE 39. REPRESENTATIVE ANALYSES OF ELLENDALE 16 LAMPROITES

	1	*2*	*3*	*4*	*5*
			Percent		
SiO_2	44.60	46.30	40.80	42.22	17.30
TiO_2	5.94	5.23	4.36	4.92	1.99
Al_2O_3	7.20	6.50	4.80	5.61	2.50
Fe_2O_3	10.60	7.80	7.80	7.61	4.80
FeO	0.77	0.27	1.00	1.35	0.22
MnO	0.09	0.07	0.09	0.10	0.20
MgO	6.28	9.69	15.60	13.49	19.00
CaO	3.41	4.25	4.94	5.54	17.30
Na_2O	0.21	0.29	0.40	0.62	0.21
K_2O	6.55	5.86	2.62	4.37	1.18
P_2O_5	2.47	1.57	1.45	1.67	0.63
H_2O^+	3.39	3.08	6.12	4.35	3.45
H_2O^-	4.42	5.09	8.11	3.76	3.59
CO_2	0.06	0.04	0.05	0.15	25.80
Rest	2.58	2.14	1.65	4.03	1.69
Total	**98.57**	**98.18**	**99.79**	**99.79**	**99.86**
			Parts per million		
Ba	9 954	9 048	3 551	24 572	8 688
Li	15	10	13	10	6
Rb	373	261	570	527	208
Sr	1 296	1 140	1 350	1 833	1 342
Pb	63	38	54	84	60
Th	72	53	57	83	32
U	2	2	1	10	<1
Zr	1 914	1 129	1 344	1 525	486
Nb	283	180	208	309	94
Y	29	17	15	37	12
La	648	335	470	419	266
Ce	1 173	600	830	760	379
Sc	45	25	26	17	12
V	321	503	87	158	33
Cr	799	540	796	830	277
Co	37	23	56		35
Ni	578	540	737	606	360
Cu	74	59	75	54	65
Zn	91	82	95	86	54
Sn	9	6	8	<2	
Ga	10	7	8	12	2
S	620	1 610	30		600
F	7 300	5 430	6 670	5 400	3 300
Cl	81	64	81		530

1,2 — Leucite-olivine lamproite; agglomerate bombs, NW margin of pipe, GSWA 71857B, 71859. 3 — Leucite-phlogopite-olivine lamproite; NW margin of central magmatic core, GSWA 76015A. 4 — Phlogopite-leucite-olivine lamproite; centre of pipe, BMR 83210316. 5 — Carbonated lamproite; centre of pipe, GSWA 71860C.

ELLENDALE 23

Ellendale 23 is one of only four new exposed lamproites discovered during exploration of the Ellendale Field: the others are Ellendale 31, 37, and 38. The outcrop, however, consists only of a small boulder-strewn rise, about 20 × 10 mm in an area and less than 1 m high. The exposed coarse-grained lamproite represents part of the 180 × 100 m core of a vent about 300 m in diameter that is concealed beneath 1-4 m of colluvial sand. A small outcrop of baked sandstone occurs close to the northeast margin of the plug, and there are scattered outcrops of ferruginized Grant Group sandstones in the surrounding area.

An exploration trench shows that the bulk of the vent is filled with a fine-grained tuffaceous lamproite containing veins and dykes of similar non-tuffaceous rock. The tuffaceous lamproite contains small, angular fragments of several lamproite types, and a small proportion of polygonized and recrystallized quartz grains; but the most prominent component is amoeboid lapilli of fine-grained phlogopite-leucite lamproite up to 2 cm across. The lapilli are commonly irregular in shape, and have a diffuse margin. The matrix appears to be a glassy variety of the same magma, but contains very small phlogopite flakes and skeletal leucite. Much of the groundmass is thoroughly altered, and consists of fine-grained, blue-green chloritic material. The fine-grained, lamproite veins contain many small flow-aligned phlogopite flakes, commonly <0.1 mm long, in a matrix of close-packed, minute euhedra of leucite and needles of priderite. A few small spherical vesicles up to 1 mm diameter are filled by secondary silica and rimmed by tangential flakes of phlogopite.

The central core is a plug of coarse-grained potassic-richterite — phlogopite — diopside — leucite lamproite and contains minor amounts of altered olivine and priderite, accessory jeppeite, apatite, and rare grains of wadeite. Diopside occurs in two generations, principally as euhedral prismatic phenocrysts up to 4 mm long, which are often twinned and marginally zoned, and as later acicular prisms up to 2 mm long. Phlogopite also occurs in two generations, as corroded phenocrysts up to 3 mm long, and as plentiful poikilitic groundmass plates and aggregates about 1 mm across. The phenocrystal phlogopite often shows a reaction rim containing small needles of priderite; it lacks the strongly coloured marginal zone of the groundmass phlogopite, and is pleochroic to colourless. Leucite is seriate, from large crystals, up to 2 mm across, to minute groundmass euhedra; it is completely altered to a mosaic of potash feldspar. Apart from a small proportion of dark-brown interstitial alteration products, there are large plates of poikilitic potassic richterite, strongly pleochroic from pale red to pale yellow-green, and marginally altered to a green amphibole. Of the minor minerals, olivine pseudomorphs are up to 2 mm across, and acicular priderite is commonly about 1 mm long. The matrix also contains numerous opaque needles and small prisms of probable jeppeite. An alaysis of the core rock is given in Table 40.

ELLENDALE 31

This lamproite body occupies a small pipe, about 200 m diameter, at the eastern end of a prominent flat-topped sandstone mesa that rises about 25 m above the surrounding plain. (Fig 89). The main pipe is poorly exposed, and its outline has been delineated by drilling. Outcrop consists of a few large boulders of lamproite, less than a metre high, and surrounding float. On the southern side of the sandstone mesa, however, there is a well-exposed, pod-like mass of mixed lamproite and tuff about 100 m long; and at the eastern end of the mesa two thin lamproite dykes.

The country rock is sandstone of the Grant Group, medium- to coarse-grained, sometimes cross-bedded, though the principal bedding planes are horizontal. Only in the immediate vicinity of the lamproite intrusions is the bedding disrupted; and the sandstone adjacent to the main pipe is baked for a distance of several metres.

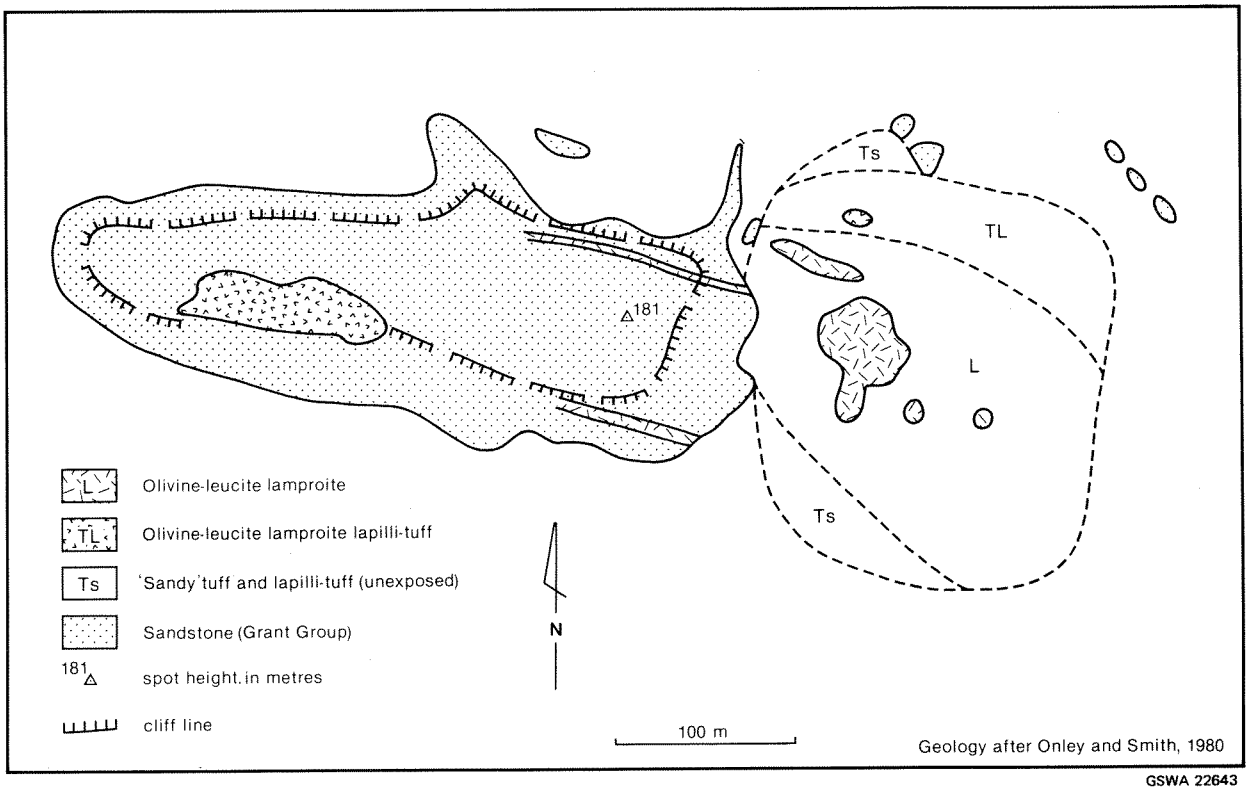


Figure 89. Geological map of Ellendale 31.

The pipe itself consists of a central core of medium-grained olivine-phlogopite-leucite lamproite with arcuate marginal zones of lamproite lapilli-tuff and quartz-rich tuff. The western pod and dykes are olivine-leucite lamproite, usually with some tuff content.

The form of the pipe at depth is not known, although the presence of quartz-rich tuffs suggests that the pipe is now seen at a relatively high level. The sandstone mesa indicates a minimum of 25 m of erosion, and the minimal baking of the enclosing sandstones suggests a pipe that narrows rapidly with depth and was little larger than the present area. The pod-like mass of tuff to the west has essentially vertical margins.

The quartz-rich tuff consists essentially of a disaggregated sandstone with rare lapilli of fine-grained lamproite and sandstone, and a sparse matrix of clay material of lamproite origin. About half the quartz grains are unfractured, rounded grains 0.5-1 mm across; the remainder are angular fragments <0.1 mm across. Some of the small fragments have aggregated with lamproitic material to form accretionary lapilli up to 10 mm across. This tuff unit is found only in lenses marginal to the vent; the source of 90% of its components is wall-rock sandstone.

The lamproite lapilli-tuff consists of lapilli of juvenile lamproite, up to 8 mm across, in a matrix of tuffaceous lamproite ash, quartz grains, and a few phlogopite flakes up to 3 mm long. The lamproite lapilli are predominantly olivine-diopside-phlogopite-leucite lamproite, similar to that in the central core of the vent but there are also cognate lapilli of olivine-leucite lamproite and some of earlier formed quartz-rich tuffs.

The pyroclastics are intruded by veins and small dykes of fine-grained potassic-richterite - olivine - leucite lamproite, the potassic richterite occurring as small prisms in the groundmass along with plentiful priderite. A coarser grained variety, with euhedral leucite pseudomorphs up to 0.5 mm diameter, contains about 20% olivine pseudomorphs and an opaque mineral, probably jeppeite, in the matrix.

The central core of this pipe is an olivine-phlogopite-leucite lamproite, in which small phenocrysts of altered olivine, phlogopite, altered leucite and very small prisms of diopside, are set in a dark-brown devitrified glass. Accessory amounts of yellow-green perovskite granules are also found in the groundmass. The olivine is pseudomorphed by green nontronite and a little barite; and leucite is altered to potash feldspar. A few small xenoliths of metasomatized shale are present along with irregular aggregates of diopside prisms up to 2 mm across. These aggregates may represent metasomatized limestone xenoliths.

The western pod consists of fine-grained phlogopite-leucite lamproite which has invaded a quartz-rich tuff. Quartz is present as rounded xenocrysts throughout the rock, and as blebs and stringers of tuff caught up in the advancing magma. The magmatic fraction consists of small microphenocrysts of corroded phlogopite, up to 0.5 mm long, rare pseudomorphs after olivine, and many small, altered, skeletal leucite grains in a dark devitrified glassy groundmass. Veins of fine-grained olivine-leucite lamproite are also present.

Analyses of the central olivine-phlogopite-leucite lamproite and an olivine-leucite lamproite vein from the western pod are given in Table 40.

TABLE 40. REPRESENTATIVE ANALYSES OF ELLENDALE 23, 31, AND 38 LAMPROITES.

	1	*2*	*3*	*4*
		Percent		
SiO_2	49.84	55.00	52.00	51.60
TiO_2	5.62	5.67	5.38	6.86
Al_2O_3	7.76	7.30	7.60	6.80
Fe_2O_3	5.55	4.80	5.00	5.60
FeO	2.36	0.70	1.26	1.40
MnO	0.08	0.03	0.05	0.07
MgO	7.84	6.04	7.89	9.37
CaO	4.74	2.51	2.52	2.93
Na_2O	0.79	0.35	0.58	0.35
K_2O	8.67	8.53	9.28	9.15
P_2O_5	0.89	1.24	1.02	0.70
H_2O^+	2.32	3.01	2.49	2.51
H_2O^-	0.87	2.22	2.05	1.06
CO_2	0.44	0.10	0.10	0.07
Rest	2.96	2.28	1.79	2.22
Total	**100.73**	**99.78**	**99.01**	**100.69**
		Parts per million		
Ba	18 069	11 485	8 325	11 968
Li	11	8	9	10
Rb	331	1 060	238	398
Sr	1 398	1 538	1 084	1 078
Pb	40	67	56	40
Th	31	24	17	26
U	2	2	1	1
Zr	1 287	1 371	1 280	1 491
Nb	154	94	93	136
Y	21	14	16	21
La	285	304	323	324
Ce	491	463	463	386
Sc	20	14	17	18
V	179	176	221	143
Cr	302	173	341	663
Co	45	35	46	40
Ni	240	258	609	228
Cu	120	84	89	86
Zn	104	84	96	78
Sn	13	10	14	—
Mo	2	9	<1	4
Ga	13	17	18	13
S	1 050	1 340	360	80
F	4 000	3 600	3 240	3 450
Cl	160	56	79	136

1 — Potassic-richterite - phologopite - diopside - leucite lamproite; magmatic core of Ellendale 23, GSWA 65912.
2 — (Phlogopite) - leucite lamproite; pod west of main vent, Ellendale 31, GSWA 71847. 3 — Olivine-leucite lamproite; central core, Ellendale 31, GSWA 71849. 4 — Diopside-phlogopite-leucite lamproite; magmatic core, Ellendale 38, GSWA 71417.

ELLENDALE 37

The small Ellendale 37 vent is located on the northwest margin of the Ellendale Field, about 5 km northwest of Ellendale 23. The outcrop consists of surface float and boulders of welded lapilli-tuff covering an area of about 50 m diameter. Much of the vent is concealed beneath about 2 m of sand and is oval in shape (200 × 125 m, 1.8 ha); it is filled with pyroclastics and a small lamproite plug.

Surface specimens of the tuff are thoroughly silicified and difficult to determine. One bedded specimen contains small rounded clasts of lamproite, up to 2 mm diameter, quartz grains, and interstitial silicified material. Phlogopite and rare grains of olivine and leucite can be recognized in some clasts that are now converted to

dark-green chloritic material. Another part of the same specimen consists largely of spherical accretionary lapilli up to 3 mm diameter; these contain quartz grains and fine lamproite dust. Interstitial areas are now thoroughly silicified.

The welded lapilli-tuff contains small glassy vesicular lamproite clasts, up to 3 mm, and a few shale clasts, as the matrix to large amoeboid lapilli of olivine-leucite lamproite. Small skeletal olivine phenocrysts, up to 0.3 mm across and replaced by orange and green chloritic material, are set in a groundmass of minute, altered leucites, clay, and priderite needles.

No diamonds were recovered from 89 t of weathered material processed through the central plant.

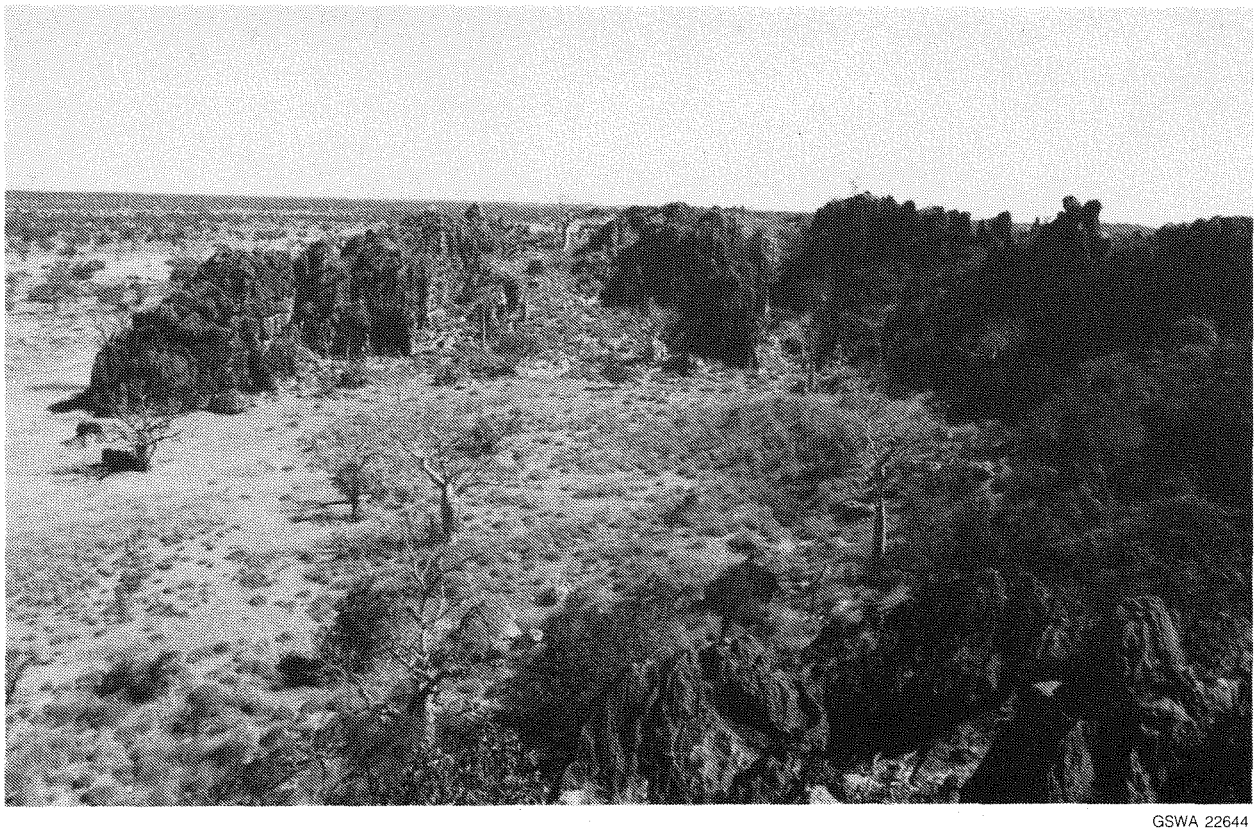
ELLENDALE 38

Ellendale 38 is a small intrusion, about 70 m diameter, and is located on the southwestern face of the Oscar Range about 5 km southeast of Ellendale 4. It is the only exposed lamproite in the Ellendale Field to intrude the Devonian reef complexes at the present level of erosion. The intrusion occupies a small embayment in the limestone cliffs which at this point are 20-25 m high (Fig. 90).

The floor of this natural amphitheatre consists of a melange of remobilized-limestone veins, stringers of lamproite, and blocks of limestone. An oval plug of coarse lamproite, 40 × 20 m, intrudes the northern margin of the vent, and forms a small spinifex-covered hill about 5 m high (Fig. 91).

The host rocks to Ellendale 38 are thick-bedded, grey calcarenites of the Napier Formation — the marginal slope deposits of the Famennian reef limestones. The beds dip at up to 35° to the southwest. Erosion along numerous joints has led to the formation of a karstic topography. The cliff line, which cuts the reef and marginal-slope facies of the Famennian reef complex — and to the southwest, the earlier Frasnian complex — probably represents the locus of the Oscar Fault: the lamproite probably intruded along this line of weakness.

The principal filling of the vent is a cream to pale-brown weathering carbonate, commonly with small, visible flakes of phlogopite. The rock does not appear to be fragmental; it contains many irregular veins of lamproitic material a few centimetres thick, and wider zones of mixed carbonate and lamproite. In thin section, the carbonate is a fine-grained mosaic of calcite, containing scattered small flakes of phlogopite and euhedral diopside; the rock also has veins of very fine-grained carbonate that contain abundant phlogopite, diopside and, commonly, numerous small fragments of priderite. The lamproite veins, which are strongly carbonated and show diffuse margins, are similar to the lamproite of the central plug but thoroughly altered. Phlogopite, diopside, and minor amounts of priderite and apatite remain fresh; pseudomorphs after olivine and leucite can also be found. Some phlogopite has been exfoliated by the emplacement of calcite along the basal cleavage, giving rise to small balls of calcite-phlogopite up to 6 mm across. The textures throughout the rock



GSWA 22644

Figure 90. Ellendale 38 from the east. The lamproite vent occupies most of the embayment in limestone cliffs of Devonian Napier Formation. The lamproite plug forms the small spinifex-covered hill to the right, at the foot of the cliffs.

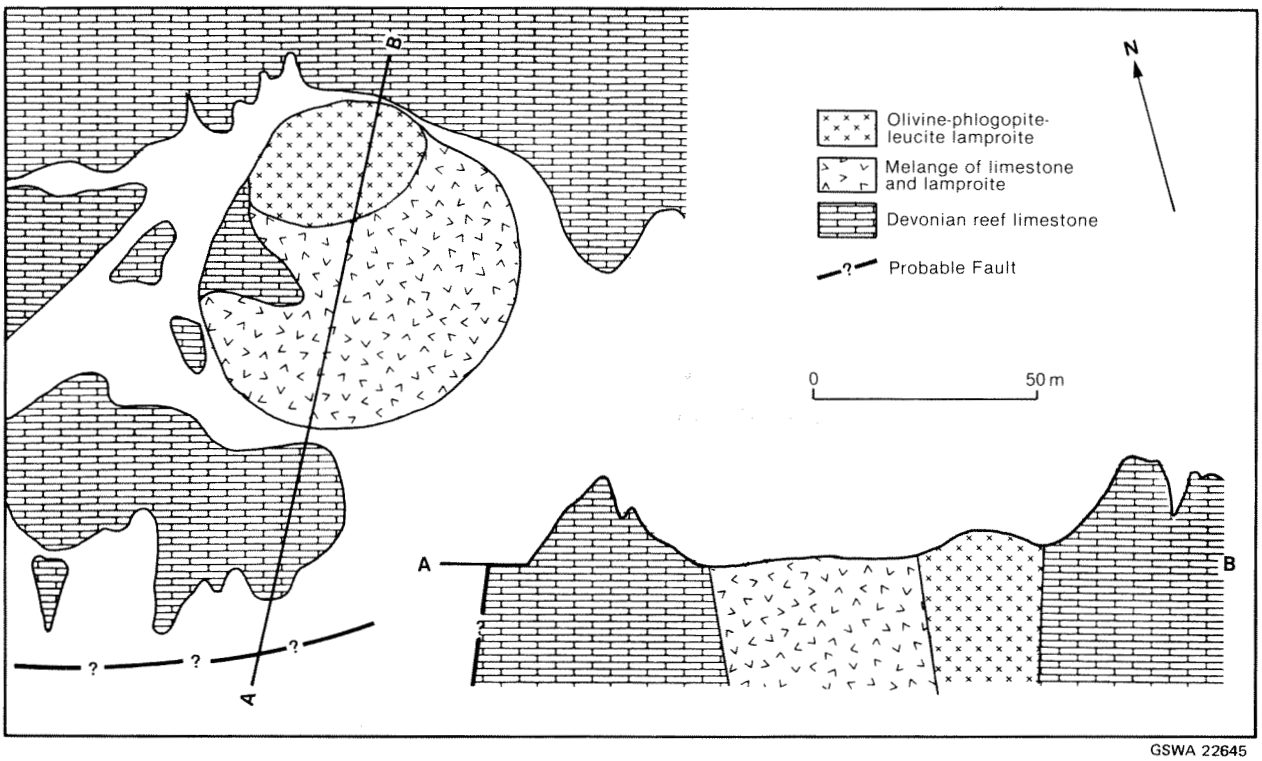


Figure 91. Geological map of Ellendale 38.

are generally of secondary origin. They result from recrystallization of carbonate and *in situ* carbonation of lamproite; a few patches remain, however, which indicate that the rock was originally fragmental. Some large blocks of relatively unaltered limestone remain; and, in the northwest of the vent, a large tongue of limestone protruding into the vent probably represents a large foundered block.

The small plug of coarse lamproite is in contact with the enclosing limestones along its northern margin, but the margin with the limestone melange is obscured by scree. The rock is a uniform coarse-grained olivine-phlogopite-leucite lamproite with a finer grained marginal zone containing potassic richterite but little phlogopite. Olivine occurs as euhedral pseudomorphs of green nontronite up to 2 mm across and commonly as aggregates of smaller crystals; fresh phlogopite, as twinned crystals up to 3 mm long, is the most prominent mineral. In the marginal zone, the few phlogopite crystals are often corroded, partially resorbed, and fringed with minute priderite needles. Leucite occurs in two generations: as prominent altered phenocrysts up to 2 mm across, and as small euhedra in the groundmass. Diopside, as small prisms and acicular crystals, is common in the groundmass, as are fine flakes of dark red-brown mica. Potassic richterite is present in accessory amounts throughout the body, but in the marginal zones is found as large poikilitic plates, up to 1 mm across, that enclose many small leucite pseudomorphs. About 30% of the rock consists of a groundmass of greenish clay minerals and minor amounts of priderite and accessory apatite. An analysis of the rock is given in Table 40.

Contact metamorphism of the limestone country rock is immediately visible in that, within a few metres of the lamproite, the limestones become granular and have a distinctive blue-grey rather than grey colour. From specimens collected on the northern margin of the vent, the recrystallization of the limestone to a coarse mosaic extends to about 4 m, at which point relic textures, including recognizable fossil fragments, become dominant. Small patches and rosettes of colourless chlorite in this specimen are probably of metamorphic origin. Within 2 m of the contact, small highly birefringent grains and prisms of spurrite ($2Ca_2(SiO_4).CaCO_3$) and probable polysynthetically twinned merwinite ($Ca_3Mg(Si_2O_8)$) have developed along calcite grain boundaries. The assemblage calcite-spurrite-merwinite indicates formation at high temperatures and very low pressure; the data of Walter (1965) suggest that the co-existence of merwinite and calcite indicates temperatures of 820 °C or more, and CO_2 pressure below 5 MPa. This estimate of wall-rock temperature on emplacement of the lamproite is even higher than the temperature deduced by Nicoll (1981) from the discoloration of conodonts in the wall rock of the Brooking Creek lamproite, and is consistent with a magma temperature of about 1 200 °C — close to the incongruent melting point of leucite.

OTHER LAMPROITE INTRUSIONS

In addition to the bodies so far described, there are a further 29 lamproites known in the Ellendale Field and located on Plate 2. All are concealed bodies, and most are small, although Ellendale 22 is the third largest lamproite in the field and has a surface area of 54.6 ha. The pipes were first located as aeromagnetic anomalies (Fig. 4), and the presence of lamproite proved by shallow rotary air-blast drilling. Most have been bulk sampled for diamonds and a few small stones recovered, but none

were sufficiently diamondiferous to warrant further exploration work by the Ashton Joint Venture, or by Seltrust Mining who discovered two of the lamproites. The result is that little is known about the bodies beyond the bare outline of the pipe and the petrography of weathered, near-surface specimens. Although exploration of the area has been thorough there are probably a few more small dykes and sills present, but no major pipe.

The following notes summarize present knowledge, and are drawn chiefly from the unpublished reports of diamond exploration by Onley and Smith (1980) and Smith (1981), supplemented by brief petrographic details where samples are available.

Ellendale 8

Two small bodies of 1.4 and 1.8 ha, about 100 m apart, were intersected by scout drilling beneath a sandy overburden up to 5 m thick. The larger body is a plug of phlogopite-olivine-leucite lamproite: the smaller body is a lamproite plug intruding "sandy" lapilli-tuff that contains altered glassy and phlogopite-rich lapilli with abundant quartz grains and a clay matrix. The lamproite is porphyritic: it contains small phenocrysts of olivine, partly fresh and up to 0.5 mm long, and rare altered macrocrysts up to 2 mm, together with ragged phenocrysts of dark red-brown phlogopite up to 1 mm long and fringed by priderite needles, all in a matrix of small diopside prisms, abundant altered leucite, groundmass phlogopite, and small priderite needles.

A bulk sample of 242 t of pyroclastics and weathered lamproite produced 0.83 CM of diamond.

Ellendale 10

Ellendale 10 is a roughly oval body, 330 × 290 m (8.3 ha), concealed beneath 6-10 m of windblown sand and sandy laterite. A central core of olivine-phlogopite-leucite lamproite is emplaced in lapilli-tuffs. Large marginal areas of the central core are vesicular, brecciated, and lack phlogopite.

During exploration, three trench samples, totalling 474 t, and five auger samples, totalling 187 t, were treated in the central processing plant for the recovery of 29 diamonds weighing 1.17 CM. A further 13 microdiamonds, none larger than 0.8 mm, were recovered after HF digestion of two samples of drill spoil from the pyroclastic and magmatic material.

The pyroclastics include quartz-rich tuffs, in which rounded quartz grains up to 1 mm diameter make up 30% of the rock; and a further 30% is composed of small fractured grains and flattened accretionary lapilli of quartz fragments, all in a clay matrix. The remainder of the rock consists of lamproite ash, occasional lamproite lapilli, and interstitial clay. The lamproite is a poorly preserved, olivine-rich glassy lamproite with small phlogopite phenocrysts.

The lapilli-tuffs contain abundant fragments of juvenile, olivine-rich lamproite up to 1 cm across in a matrix of lamproite ash. The rock is thoroughly altered to clay minerals, but olivine macrocrysts up to 8 mm and microphenocrysts up to 0.25 mm can be recognized in a vesicular groundmass that probably carried many small leucite crystals.

Magmatic rocks from the central core contain macrocrysts of olivine up to 3 mm, and microphenocrysts up to 0.5 mm, partly altered to talc and clay, and poikilitic phlogopite up to 0.7 mm in a groundmass of small diopside prisms, close-packed altered leucite ≈ 50 μm diameter and interstitial yellow clay mineral, possibly an altered glass. Minor groundmass minerals include perovskite, priderite, chromite, and potassic richterite. A finer grained marginal sample contains abundant unaltered olivine microphenocrysts, rare altered macrocrysts and small leucite euhedra, with phlogopite only as small groundmass flakes.

Ellendale 12

Ellendale 12 is an irregular shaped vent with maximum dimensions of 500 × 400 m (13.5 ha), concealed beneath 3-5 m of windblown sand. The vent is filled by a plug of medium-grained phlogopite – potassic-richterite – olivine – leucite lamproite with marginal zones of fine-grained vesicular and brecciated lamproite.

A total of 513 t of weathered lamproite was tested for diamond, and 16 stones weighing 0.66 CM were recovered.

The main plug is olivine-rich, and contains anhedral macrocrysts up to 4 mm and euhedral microphenocrysts 0.2-0.4 mm across. The macrocrysts are altered to serpentine with a marginal talc zone, and the smaller olivines are altered to talc. Poikilitic phlogopite, up to 1 mm, and ragged prisms of potassic richterite up to 1.5 mm, are abundant, both enclosing many altered leucite grains. The groundmass consists of altered leucite euhedra up to 100 μm, priderite, jeppeite; occasional diopside, perovskite, apatite, and accessory wadeite; and interstitial clay. The priderite forms prismatic crystals and irregular interstitial masses up to 0.2 mm, and some are mantled by opaque jeppeite. Wadeite is rare but forms large prismatic crystals 0.25 mm long.

The marginal facies is an altered, formerly glass-rich olivine(-leucite) lamproite. Small altered crystals of olivine (up to 0.2 mm) and rare altered macrocrysts are set in a clay groundmass that contains minute priderite needles. The groundmass is an altered glass and the high K_2O content (9.6%, *see* Appendix 2) indicates that the rock is potentially leucite-bearing. In some specimens, the groundmass contains abundant minute grains (< 5 μm) of altered leucite and small flakes of phlogopite. The rock is usually sparsely vesicular, carries rare xenoliths of shale and siltstone, and, in places, is brecciated and veined by barite.

Ellendale 13

Ellendale 13 is a large (21.4 ha), dyke-like body, 1 200 m long by a maximum of 250 m wide, elongated west-northwest, and concealed beneath 4-12 m of sandy

overburden. The vent is probably the result of a fissure eruption; and at the present level of erosion is filled by a central mass of phlogopite-olivine-leucite lamproite and, at each end of the vent, olivine-rich tuffs and lapilli-tuffs.

Diamond is present in Ellendale 13 at above average concentration for leucite-bearing rocks. Four trench samples and five smaller auger samples totalling 790 t produced 88 diamonds weighing 2.65 CM, while a 50 kg sample of drill spoil from the leucite lamproite produced a further 24 microdiamonds after HF digestion. Heavy-mineral concentrates from this pipe contained trace quantities of chromite, pyrope, chrome-diopside, corundum, and kyanite.

The pyroclastic deposits range from lamproite ash-tuff to lamproite lapilli-tuff depending on the proportion of lapilli present. The pyroclastics are monogenetic, and the bulk of the deposit consists of angular ash-sized fragments 0.2-0.5 mm diameter; these are altered to clay and set in a sparse interstitial clay matrix. Much of the ash-sized material appears to be altered fragments of olivine. Some lapilli consist of altered olivine macrocrysts up to 4 mm across, often with a thin skin of magmatic glass. Most lapilli are amoeboid in shape, up to 6 mm across, and composed of thoroughly altered, olivine-rich lamproite that contains both macrocrysts and abundant microphenocrysts in a formerly glassy, vesicular groundmass. A few small flakes of phlogopite and rare accidental grains of tourmaline are present in the matrix.

The central magmatic core is rich in olivine ($\approx 30\%$), which occurs as altered macrocrysts up to 3 mm and altered microphenocrysts up to 0.5 mm across. Poikilitic phlogopite up to 1 mm is abundant, and encloses perovskite and diopside grains. Diffuse patches of potassic richterite, up to 1.5 mm across, are equally abundant in the groundmass, which consists of yellow clay minerals pseudomorphing probable diopside, abundant small perovskite grains (< 30 μm), priderite (up to 100 μm), and rare chromite (< 50 μm).

The leucite-bearing lamproite contains altered olivine macrocrysts up to 3 mm, and abundant, partly altered groundmass olivine totalling about 20% of the rock. Small ragged flakes of poikilitic phlogopite enclosing diopside laths and a few leucite euhedra are common. The groundmass contains abundant altered leucite (30-50 μm), diopside laths (up to 150 μm), prismatic priderite, and minute interstitial needles of priderite. Some larger leucite crystals have unaltered cores; and a few small masses of altered spongy leucite contain abundant grey-green pleonaste granules.

The leucite-bearing lamproite is found as a broad band on the eastern margin of the central olivine lamproite, and as a small plug at the western end of the mass. No analyses are available of the two rock types; but petrographically, the leucite lamproite is not a chilled marginal facies of the central mass. The phlogopite-olivine lamproite is more olivine-rich than the leucite lamproite and the two may be related by settling of the macrocrysts; the leucite lamproite was the first pulse of magma, and was followed shortly afterwards by the olivine-rich magma.

Ellendale 14

Ellendale 14 is a small, oval body (400 × 250 m, 7.7 ha), elongated east-west, and concealed beneath 2-3 m of sand. A central core of diopside-olivine-leucite lamproite intrudes lapilli-tuffs and autobrecciated, fine-grained phlogopite-leucite lamproite. About 100 m west of the vent is a small satellite plug of diopside-olivine-leucite lamproite about 90 m diameter.

Two trench samples of weathered lamproite and pyroclastics, totalling 337 t, were processed for diamond. The heavy-mineral concentrate contained abundant chromite and one small diamond of 0.02 CM.

The lapilli-tuff is clast-supported and contains mostly angular lapilli of dense or sparsely vesicular phlogopite-leucite lamproite, and lesser amounts of glassy, amoeboid, and vesicular phlogopite-bearing lapilli, and small clasts of shale. The sparse tuff matrix is composed of lamproite ash and a few rounded quartz grains up to 0.3 mm. The lapilli are commonly up to 6 mm across and both dense and vesicular varieties are probably juvenile. The altered leucite in the dense lapilli are usually < 20 μm diameter, although skeletal crystals may be up to 50 μm. Rare cognate xenoliths of phlogopite-olivine-leucite lamproite are also present.

Fine-grained, vesicular phlogopite-leucite lamproite with scattered xenocrysts of quartz occurs as an autobrecciated unit; secondary silica fills voids and vesicles. Apart from the vesicles the lamproite is similar to the dense lapilli in the pyroclastic unit.

The central magmatic core is a porphyritic diopside-olivine-leucite lamproite. Small euhedral phenocrysts of olivine, 0.2-0.3 mm across, and pseudomorphed by talc, make up about 20% of the rock and are set in a groundmass of altered leucite (30-150 μm), abundant acicular diopside prisms (up to 0.4 mm), red-brown phlogopite (up to 150 μm), prismatic and interstitial priderite, a few grains of apatite, and abundant interstitial glass. The glass is usually devitrified and altered to a brown clay; but some specimens preserve altered dendritic crystallites, and one contains fresh glass.

Ellendale 15

Ellendale 15 is an east-west trending dyke-like body about 1 000 m long and 50-100 m wide (10.0 ha), with a central expansion up to 250 m wide. The lamproite is concealed beneath 4-7 m of sand. Pyroclastics are present at the eastern end of the vent and around the central swelling, but much of the vent is occupied by a dyke of phlogopite-olivine-leucite lamproite 800 m long and 50 m wide. A small pyroclast-filled vent, 1.5 ha in area, is located about 150 m from the western end of the main vent.

The treatment of four trench samples and two auger samples, totalling 683 t, recovered 21 diamonds weighing 0.33 CM, Heavy-mineral concentrates

contained chromite, pyrope, chrome diopside, and magnetite.

Like Ellendale 13, this lamproite originated as a fissure vent; and the magmatic lamproite was emplaced passively into an open, elongate vent.

The pyroclastic rocks are fine-grained lapilli-tuffs with clasts of altered, juvenile, glassy, vesicular, phlogopite-bearing olivine-lamproite, usually 2-3 mm across but up to 6 mm, and rounded clasts of shale and siltstone in a matrix of lamproite ash and interstitial clay. The lamproite carries altered macrocrysts of olivine (replaced by barite) up to 3 mm across, and abundant microphenocrysts.

The lamproite core is olivine-rich ($\approx 30\%$); it contains euhedral phenocrysts and anhedral macrocrysts, up to 3 mm across, and abundant microphenocrysts, up to 0.4 mm, both pseudomorphed by talc. One specimen contains small unaltered olivine crystals up to 0.2 mm. Phlogopite occurs as small groundmass flakes or as poikilitic plates up to 0.3 mm. The groundmass is composed of clay minerals in which abundant former leucite can be recognized, together with perovskite, apatite, and a little diopside. Marginal specimens are autobrecciated, and contain altered olivine in a very fine-grained clay matrix, which, in places is strongly vesicular.

Ellendale 17

Ellendale 17 is a large (41.8 ha) irregularly shaped vent located in the black-soil plain at the foot of the Napier Range. It is the largest of a group of three lamproites separated from the main area of the Ellendale Field. The lamproite intrudes mudstones and limestones of the Late Devonian to Early Carboniferous Fairfield Group and is concealed beneath 3 m of black soil, and 2-3 m of calcrete and thoroughly carbonated lamproite.

The main part of the vent is about 550 m diameter but a broad tongue of lamproite extends 600 m west from the northwest margin and a smaller tongue extends 250 m west from the southern margin of the vent. At the present level of erosion the vent is occupied by coarse-grained phlogopite-olivine lamproite with, in parts, a broad marginal zone of finer grained olivine lamproite. A large block of limestone, probably a slumped block ≈ 100 m diameter, is enclosed by the lamproite near the northern margin of the vent.

A total of 1 006 t of weathered lamproite from six samples was processed for diamond to recover six small stones weighing 0.91 CM; the heavy-mineral concentrate contained chromite and chrome-diopside. After HF digestion, three samples of drill spoil produced seven small diamonds, the largest 0.6 mm diameter. Two other samples were barren.

The typical lamproite specimen available from exploration trenches is thoroughly altered and veined by carbonate and a little barite. Calcrete has progressively replaced textures and minerals until only phlogopite, interleaved with carbonate, perovskite, and the outlines of former olivine macrocrysts remain. In better preserved samples, the lamproite is olivine-rich (20-25%) with rounded macrocrysts up to 6 mm across and altered euhedral microphenocrysts ≈ 0.5 mm across. The macrocrysts are usually replaced by carbonate or serpentine, but unaltered relics in some specimens show undulose extinction. Three poikilitic mineral phases are present: phlogopite, diopside, and potassic richterite. Phlogopite, in well formed plates up to 2 mm, is unzoned, twinned, pale coloured (pleochroic from pink-yellow), and encloses only perovskite and apatite grains. Diopside and potassic richterite form large, open poikilitic masses up to 4 mm across, which enclose up to 60% groundmass minerals. The diopside forms roughly prismatic crystal outlines, but poikilitic potassic richterite is anhedral and, in some specimens, is pervasive as small interstitial grains. The presence of poikilitic diopside distinguishes this lamproite from all others in the Ellendale Field. The groundmass consists of clay minerals, rarely chlorite or nontronite, and a felted mass of unidentified prismatic mineral with a hexagonal cross-section; this mineral is enclosed both by diopside and potassic richterite. Identifiable minerals in the groundmass include abundant perovskite (< 50 μm), chromite, apatite, wadeite, and rare grains of priderite. The wadeite occurs as equant prisms 0.25 mm long and as small poikilitic masses.

Petrographic variations include specimens in which one or both of diopside and potassic richterite are absent. The chilled marginal facies is an olivine lamproite and is similar to the main mass except that it contains only small phlogopite flakes in a fine-grained groundmass with abundant interstitial potassic richterite. Leucite has not been found in any of the samples examined.

Ellendale 18

Ellendale 18 is a near-circular pipe, 550 m diameter (25.7 ha), concealed beneath about 6 m of windblown sand. In the vicinity of the pipe, the Grant Group sandstone is thin; and calcareous mudstone of the Fairfield Group was encountered in a number of drill holes close to the vent, suggesting the possibility of local doming around the vent. At the present level of erosion, the pipe is filled largely by "sandy" lapilli-tuff which also contains a few large blocks of siltstone, sandstone, quartzite, limestone, and quartz-biotite schist, together with rare, small, altered peridotite nodules up to 3 cm across. In the central part of the vent is a small area of "non-sandy" lapilli-tuff intruded by olivine lamproite and marking the site of the final vent.

The diamond grade of the pyroclastics is variable; and, because a number of early samples returned grades of about 1 CM/100 t, the pipe was extensively sampled. As a result, 15 samples totalling 1 769 t were processed to recover 68 diamonds weighing 4.48 CM, an overall grade of only 0.25 CM/100 t. A further 11 microdiamonds were recoverd after HF digestion of 5 samples of drill spoil. The heavy-mineral concentrate from this pipe contained abundant pyrope, chromite, and occasional chrome-diopside; the pipe is richer in pyrope than any other Ellendale diatreme.

The "sandy" lapilli-tuff contains altered juvenile lapilli

of vesicular, glassy olivine lamproite up to 1 cm across in a tuff matrix of rounded quartz grains (10-30%), lamproite ash, and interstitial clay. The lapilli are olivine-rich: macrocrysts and microphenocrysts, replaced by talc and iron oxides, and a few small phlogopite flakes, are set in a vesicular, formerly glassy, groundmass of clay. One clast encloses a small, altered peridotite nodule 6 mm across.

The central olivine lamproite contains about 25% olivine, partly as altered macrocrysts (<2 mm) replaced by talc and clay, and partly as fresh microphenocrysts (<0.4 mm). Small poikilitic phlogopite flakes (<0.5 mm) are abundant and often mantle the olivine crystals. The groundmass is an indeterminate mass of fine-grained yellow-brown clay minerals that contains abundant granules of perovskite (<20 μm), small interstitial plates of potassic richterite and rare grains of chromite.

Ellendale 19

Ellendale 19 is a small, oval vent (425 × 350 m, 11.3 ha) concealed beneath 3-5 m of windblown sand and clay. The vent is emplaced in Grant Group sandstone, which outcrops in two small mesas to the southwest and northwest of the pipe. The vent is mostly filled by a variety of pyroclastic rocks, including quartz-rich tuffs and "sandy" lapilli-tuffs, veined by altered glassy lamproite. A small irregularly shaped central magmatic core is of leucite-poor olivine lamproite.

The diamond content of the pipe is low, four trench samples of total weight 518 t were processed to recover 0.12 CM of diamond and small amounts of chromite, kyanite and staurolite in the heavy-mineral concentrate. A further two microdiamonds were recovered after HF digestion of drill spoil.

The quartz-rich tuff contains about 60% of rounded to angular quartz grains and a few small fragments of shale in a matrix of altered lamproite ash, small phlogopite flakes, and interstitial clay. In the lapilli-tuff, juvenile, vesicular, glassy lapilli, up to 5 mm, predominate, and are composed of partly fresh, isotropic, colourless glass that is crowded with small vesicles from 5-150 μm diameter and often streaked out to show flow structures. The lapilli contain a little altered olivine, and some also contain phlogopite as microphenocrysts or as minute flakes <10 μm. The tuff matrix contains variable proportions of quartz grains, lamproite ash, and phlogopite flakes. In some specimens, accidental quartz is absent, and the tuff is clast supported.

A number of lamproite veins within the pyroclastic unit are composed of altered, devitrified, vesicular olivine lamproite that is similar to the juvenile material in the tuffs, but there are some veins in which numerous small leucite euhedra <5 μm across are present.

The magmatic core is moderately olivine-rich ($\approx$15%) and contains macrocrysts, up to 4 mm, and abundant microphenocrysts, pseudomorphed by talc. Small phenocrysts of phlogopite, up to 0.8 mm, are sparsely distributed, and many are marginally corroded and bent. The groundmass is mostly a brown clay mineral that pseudomorphs an unknown original prismatic mineral, and lesser altered leucite (<100 μm) and small interstitial flakes of phlogopite. Subordinate minerals include priderite, potassic richterite, apatite, and accessory diopside and wadeite.

Analyzed specimens from an olivine-leucite lamproite vein in the pyroclastics and a lamproite from the central magmatic core are chemically distinct: Magnesia is nearly doubled (from 8.9% to 16.9%), but K_2O is reduced to one third in the central core (from 8.5% to 3.4%). This is similar to differences noted earlier for the lamproites of Ellendale 16, and may be the result of the settling of olivine macrocrysts, which are present in the core rocks but not in the early pyroclastics.

Ellendale 21

Two vents comprise Ellendale 21, a larger body about 500 m diameter (19.3 ha) and a smaller vent 200 m northeast of the main body and 200 m in diameter (4.0 ha). Both vents are filled by pyroclastics, and contain a small central intrusion of olivine-rich lamproite.

Diamond exploration recovered two small stones weighing 0.2 CM from 920 t of pyroclastic and weathered magmatic rock. Chromite and chrome-diopside are present in the heavy-mineral concentrate.

The pyroclastics of the larger vent are well-bedded lapilli-tuffs and quartz-rich tuffs. Juvenile lamproite lapilli are angular to subrounded, up to 6 mm across, and composed of altered vesicular glass that contains small altered olivines. Cognate lapilli that contain small phenocrysts of phlogopite, small accretionary lapilli, and accidental clasts of shale and limestone, are sparsely distributed. The tuff matrix is composed of quartz grains and lamproite ash and varies from about 10% of the rock in clast-supported lapilli-tuffs, up to 50% in the more common "sandy" lapilli-tuff.

Veins within the pyroclastics are of fine-grained, porphyritic, phlogopite-leucite lamproite that contains pale, unzoned phenocrysts of phlogopite up to 1 mm in a groundmass crowded with altered leucite (<50 μm) and minute needles of priderite.

The central magmatic core is a phlogopite-olivine-leucite lamproite that contains abundant (15%) small altered olivine phenocrysts (<0.5 mm) and phlogopite up to 1.5 mm. The groundmass is composed of green clay minerals that contain abundant small, altered leucite euhedra, traces of priderite, diopside, and interstitial phlogopite.

Tuffs from the smaller body, Ellendale 21a, are poorly preserved lapilli-tuffs, in which altered olivine-rich lapilli up to 5 mm are set in a matrix of similar olivine-rich material that contains about 20% altered olivine macrocrysts and microphenocrysts. Phlogopite is present as small poikilitic plates or groundmass flakes. The groundmass contains abundant altered leucite; acicular diopside, perovskite, and priderite; and interstitial green clay.

Ellendale 22

Ellendale 22 is a large (54.6 ha), complex lamproite vent, 1 700 m long by up to 500 m wide, elongated east-west, and concealed beneath 2-3 m of red, windblown sand. The pipe intrudes Grant Group sandstone; but, around its margins, there are lenses of micaceous mudstone from the underlying Fairfield Group, mudstones in which the bedding is often contorted. These may indicte pre-eruption doming in the vicinity of the vent. Within the vent, there are several rafted blocks of mudstone and sandstone, up to 120 m across, which are brecciated and veined by carbonate.

Pyroclastic deposits occupy about 30% of the area of the vent, and consist of thick-bedded, quartz-rich tuffs and "sandy" lapilli-tuffs, in parts of which large rounded clasts of micaceous mudstone make up 10% of the deposit. Magmatic lamproite occupies the remainder of the vent, and is mostly a massive, micaceous, leucite-poor, olivine lamproite that contains prominent, altered olivine macrocrysts. A marginal, chilled facies is non-micaceous and, in parts, is vesicular and brecciated.

Seven bulk samples of weathered lamproite and pyroclastic rock, totalling 948 t, were processed to recover 6 diamonds weighing 0.23 CM.

Quartz-rich pyroclastics are found at each end of the vent. The quartz-rich tuff is composed of well-sorted angular fragments of quartz (60%), lamproite ash, small phlogopite flakes, and interstitial clay. Most of the pyroclastics are "sandy" lapilli-tuffs that contain about 30% juvenile, glassy, lamproite lapilli up to 6 mm across, and abundant accidental lapilli of shale and siltstone in a tuff matrix of lamproite ash, quartz grains, sparse microcline, and interstitial clay. The altered, glassy, lamproite lapilli contain abundant small olivines; and some lamproite clasts form the cores of accretionary lapilli that have a marginal zone of quartz fragments and former ash, now clay.

The magmatic lamproite is a fine-grained, porphyritic olivine(-phlogopite-leucite) lamproite. Olivine macrocrysts with strongly resorbed margins, and small euhedral microphenocrysts, together comprise about 20% of the rock and are mostly replaced by talc. The groundmass is a fine-grained aggregate of small phlogopite, leucite and diopside crystals; rare grains of perovskite; interstitial potassic richterite; and accessory chromite, priderite, and wadeite. In some specimens, the phlogopite is up to 0.2 mm across, but generally the grain-size is <30 μm; and the perovskite, <10 μm diameter. Samples from the margins of the mass are very fine-grained and consist of former olivine in a matrix of minute phlogopite flakes and clay minerals, and accessory chromite and priderite. Some marginal samples are autobrecciated, vesicular, and contain clasts of shale and lamproite from the pyroclastics.

Ellendale 24

Ellendale 24 is a concealed oval vent, 500 × 350 m (14.2ha), occupied mostly by a plug of massive, porphyritic phlogopite - olivine - leucite - potassic-richterite lamproite intruded into lapilli-tuff. The lamproite intrudes mudstones and siltstones of the Fairfield Group, which is overlain, in part, by a thin cover of Permian sandstone.

Four samples of weathered surface rock totalling 850 t were processed for diamond; 6 stones weighing 0.21 CM, with trace amounts of chromite in the heavy-mineral concentrate, were recovered.

The lapilli-tuff contains juvenile lapilli of altered vesicular, glassy lamproite, up to 3 mm across, and a few accidental lapilli of shale, siltstone, and laterite, in a lamproite ash matrix containing rare grains of phlogopite and microcline. The magmatic lamproite contains euhedral phenocrysts of olivine, commonly <1 mm long and replaced by talc and nontronite, minor plates of phlogopite enclosing a few leucite grains, and abundant large prismatic plates of poikilitic potassic richterite up to 3 mm across that enclose leucite, minor and accessory minerals, and rare grains of phlogopite. The groundmass is mostly dark-brown clay minerals with abundant small (<100 μm) leucites, altered to zeolite; small flakes of phlogopite; and prisms of diopside, priderite, and perovskite and apatite. The most striking feature of this lamproite is the strongly pleochroic (pink to yellow) plates of potassic richterite, which make up about 25% of the rock.

Ellendale 25

This small kidney-shaped vent (500 × 300 m, 11.2 ha) is concealed beneath 7 m of sand and clay. A marginal zone, mapped from drill chips as "grey micaceous mudstone", is probably a coarse breccia derived from the underlying Fairfield Group, and in places, overlies the Permian wall-rock sandstone. An irregular central area of tuff and lapilli-tuff contains altered juvenile glassy and vesicular lamproite lapilli up to 3 mm across, abundant ferruginous siltstone, and laterite clasts in a matrix of lamproite ash, quartz grains, phlogopite, and interstitial clay that contains irregular patches of secondary barite. One lamproite clast containing recognizable small altered leucites suggests that the magma was potash-rich.

The tuff is relatively rich in diamond: five small auger samples weighing 156 t produced 10 diamonds weighing 0.79 CM, and three samples of drill spoil produced 11 microdiamonds up to 0.5 mm across after digestion in HF.

Ellendale 26

Ellendale 26 is a very small oval vent (250 × 150 m, 2.9 ha) concealed beneath 4 m of red sand. The vent is filled by lapilli-tuff and a very small plug of olivine-leucite lamproite.

As a result of the toughness of the silica-cemented pyroclastics, this body has not been tested for diamond.

The marginal tuffs contain small juvenile lapilli of glassy lamproite and scattered siltstone clasts and quartz-rich accretionary lapilli, up to 3 mm across, in a sparse matrix of lamproite ash, rounded quartz grains, and small phlogopite flakes. The lamproite carries abundant

microphenocrysts of phlogopite and the central devitrified parts of some lapilli contain minute cruciform skeletal leucite crystals. The bulk of the lapilli-tuff is clast-supported and partly welded, but contains very little tuffaceous matrix. Lapilli are amoeboid, up to 10 mm across, vesicular, and carry minute euhedra of leucite and small phlogopite phenocrysts in a formerly glassy matrix. Accidental material includes siltstone and laterite clasts; and voids in the deposit are lined by secondary silica.

The lamproite plug is a glass-bearing olivine-leucite lamproite, petrographically similar to the Oscar Dyke from the Noonkanbah Field (*see* below). Euhedral olivine microphenocrysts, up to 0.8 mm and replaced by talc, are set in a groundmass of turbid leucite (up to 150 μm) and abundant pale-yellow interstitial glass. Acicular prisms of priderite up to 0.3 mm are abundant, and smaller phlogopite, diopside, and accessory apatite crystals are present.

Ellendale 27

Ellendale 27 is a roughly rectangular vent (350 × 225 m, 6.9 ha), covered by up to 8 m of clay and windblown sand. "Sandy" lapilli-tuff is intruded by sheets and veins of fine-grained olivine(-leucite) lamproite, but most of the vent is occupied by a plug of olivine-rich leucite lamproite.

Four samples of weathered lamproite and pyroclastics totalling 600 t were processed to recover 7 diamonds weighing 0.41 CM; occasional chromite and chrome diopside are also present in the heavy-mineral concentrate.

The tuff is composed of ash and lapilli-sized (0.5-3 mm) rounded fragments of altered lamproite glass that contain abundant flattened and streaked vesicles and a few small phlogopite flakes. Rounded quartz grains and rare laterite clasts make up the remainder of the rock. Some specimens are partly replaced by carbonate. Lamproite sills within the pyroclastics contain abundant small altered olivines about 0.2 mm across and a few small phlogopite phenocrysts in a very fine-grained groundmass of clay, phlogopite, and rare grains of priderite. The unaltered groundmass was probably leucite-rich.

The central plug of phlogopite-olivine-leucite lamproite contains about 25% of altered olivine as embayed macrocrysts up to 5mm and microphenocrysts up to 1mm across; these are set in a groundmass of altered leucite and small phlogopite flakes, scattered diopside and perovskite (<100 μm), accessory apatite and interstitial potassic richterite, and abundant dark-brown interstitial clay. Rare xenocrystal phlogopite forms corroded flakes up to 2 mm long in some specimens. Analyses of a lamproite vein from the pyroclastics, and a partly carbonated lamproite from the central plug (*see* Appendix 2), show that, as in Ellendale 16, there is strong chemical differentiation between the early and late magmas: MgO increases from 7.5 to 13.1%, and in K_2O deceases from 6.8 to 3.8%.

Ellendale 33

Ellendale 33 is a small, (6.8 ha) irregular-shaped vent filled mostly with quartz-rich lapilli-tuff. The pyroclastics are emplaced in Grant Group sandstone, and concealed beneath 10-20 m of sand and clay overburden.

Five samples of weathered material totalling 415 t yielded 13 small diamonds, weighing 0.93 CM, and abundant pyrope and chromite in the heavy-mineral concentrate.

The pyroclastics include bedded quartz-rich tuffs and lapilli-tuffs that contain juvenile glassy lamproite lapilli and cognate olivine-leucite lamproite clasts up to 6 mm across.

Accidental clasts include shale, siltstone, quartzite and abundant quartz-rich accretionary lapilli. The tuff matrix includes lamproite ash, rounded quartz grains, microcline, interstitial clay, and a single small garnet with a kelyphitic rim was noted. One drill hole intersected a mass of altered phlogopite-olivine-leucite lamproite containing abundant small olivines, groundmass phlogopite and leucite, accessory priderite, and much interstitial clay.

Ellendale 34

Ellendale 34 is a very small elongate vent (300 × 100 m, 2.6 ha), concealed beneath a metre or so of sandy soil. Several small, rounded outcrops of baked and brecciated Permian sandstone mark the outline of the vent on its northern side. The vent is filled by "sandy" lapilli-tuff and a small plug of very fine grained phlogopite-leucite lamproite.

A bulk sample of pyroclastic material weighing 160 t yielded 0.33 CM of diamond.

The pyroclastic rock contains about 50% of rounded lapilli up to 8 mm across in a matrix of rounded quartz grains and lamproite ash. Juvenile lapilli are of altered vesicular glassy lamproite that contain small phlogopite phenocrysts and minute groundmass leucite. Cognate lapilli are coarser grained, dense, phlogopite-olivine-leucite lamproite and contain poikilitic phlogopite and groundmass potassic richterite. Accidental lapilli include siltstone and limestone; there are also accretionary lapilli composed of small quartz fragments and clay minerals. The small lamproite plug encountered in drilling is a very fine grained assemblage of leucite, clay minerals, priderite, and microphenocrysts of phlogopite and, rarely, altered olivine. It appears to be a massive variety of the juvenile lamproite found in the pyroclastics, and carries a few quartz grains and xenoliths of coarser lamproite.

Ellendale 35.

This very small vent of only 1.5 ha is located 600 m east of Ellendale 12. Lamproitic pyroclastics were intersected beneath 6 m of sandy overburden by five drill holes. The body was considered too small to sample for diamonds, and no specimens are available.

Ellendale 36

Ellendale 36 gave a strong magnetic anomaly, but the lamproite was intersected by only one drill hole, beneath about 5 m of overburden. The body is probably a dyke of olivine-rich lamproite; but no samples are available, and it has not been sampled for diamond.

Ellendale 39

Ellendale 39 is located at the foot of Cycad Hill, a prominent conical limestone outcrop in the Napier Range. The lamproite vent is elongated east-west (440 × 100 m, 4.0 ha), and is intruded into flaggy limestones of the fore-reef Napier Formation. Only limited drilling was carried out to prove the presence of pyroclastics and leucite lamproite.

Three small bulk samples from Williams auger holes, totalling 192 t, were processed to recover 0.83 CM of diamond.

A specimen from the pyroclastics is a clast-supported lapilli-tuff composed of juvenile lamproite lapilli 2-8 mm across, small numbers of accidental lapilli of shale and laterite, and a sparse matrix of turbid clay containing a few quartz grains. The altered lamproite clasts are glassy, and vesicular; they contain some altered olivine and phlogopite microphenocrysts, and abundant small former leucites.

Several varieties of magmatic leucite lamproite are present in the vent; they probably form sheets within the pyroclastics. A fine-grained olivine-leucite lamproite contains small altered microphenocrysts of olivine, up to 1 mm, in a groundmass of altered leucite (< 50 μm), and sparse phlogopite, acicular priderite, and interstitial green chlorite. A coarser grained porphyritic variety contains altered olivine and leucite phenocrysts, up to 0.8 mm, in a groundmass of small leucite grains, phlogopite, priderite, and abundant interstitial clay. A few small masses of spongy leucite contain grains of pleonaste. The most magnesian lamproite present is a diopside-phlogopite-olivine-leucite lamproite that contains sparse euhedral olivine macrocrysts, up to 3 mm and altered to talc, and abundant microphenocrysts of unaltered olivine and phlogopite; all set in a groundmass of small altered leucites (< 50 μm), flow aligned acicular diopside (< 150 μm), scattered priderite and apatite, and interstitial clay.

Ellendale 40

Ellendale 40 is a small oval vent elongated east-west (340 × 130 m, 3.2 ha) and concealed beneath 3-5 m of sand and sandy clay material. The vent is filled by pyroclastics containing only small sheets and veins of olivine-leucite lamproite. The vent intrudes Grant Group sandstone, which outcrops at a number of places around the margins.

Two bulk samples, total weight 610 t, were processed for diamonds, but none were recovered; however, one small stone of 0.2 mm diameter was recovered from HF digestion of drill spoil.

The pyroclastic deposit is a uniform "sandy" lapilli-tuff dominated by welded lapilli of juvenile olivine lamproite, up to 10 mm across; sparse clasts of shale and siltstone, and quartz-rich accretionary lapilli, in a tuffaceous matrix with abundant rounded quartz grains. The lamproite is uniform in all specimens and contains abundant altered olivine microphenocrysts and a few small phlogopite flakes in a brown or green altered groundmass, which varies from vesicular and glassy to dense and cryptocrystalline and contains minute altered leucite and phlogopite. A vein of magmatic lamproite, intersected by drilling, is of similar material and contains abundant groundmass leucite and phlogopite, and accessory priderite.

Ellendale 41

Ellendale 42 is located at the northwest extremity of the Ellendale Field and is the largest of a group of three small pipes aligned east-west. The pipe is oval, about 400 × 300 m (9.3 ha), and is concealed beneath about 5 m of sand and clay overburden. The vent contains a small magmatic core of olivine-leucite lamproite intruding lapilli-tuffs.

Three trench samples of pyroclastics and weathered magmatic rock (total weight 440 t) were processed to recover 0.11 CM of diamond.

Two varieties of pyroclastics are present, an early "sandy" lapilli-tuff, and a later, welded lapilli-tuff. The early tuff contains altered glassy juvenile clasts up to 8 mm across, rounded to lobate, and containing sparse flakes of phlogopite and altered olivine. The matrix consists of rounded and corroded quartz grains and altered lamproite ash. Accidental lapilli of mudstone and laterite are also present. The welded lapilli-tuff, apart from a few small clasts of siltstone and laterite, consists of flattened lapilli and ash of an olivine-rich lamproite that contains former olivine macrocrysts and microphenocrysts in an altered glassy, or microcrystalline, leucite-rich groundmass. Rocks from the central core are also olivine rich, and contain macrocrysts (up to 6 mm) and euhedral microphenocrysts (up to 1 mm), uniformly altered to talc; and a few flakes of phlogopite up to 1 mm, in a microcrystalline groundmass of former leucite, prisms of potassic richterite, accessory priderite, and abundant interstitial clay.

Ellendale 42

Ellendale 42 is a small oval vent (500 × 250 m, 8.7 ha), located about 600 m east of Ellendale 41. The pipe is pyroclast-filled except for a small central magmatic core about 100 m diameter. Two trench samples of weathered tuff weighing 324 t were processed to recover 0.35 CM of diamond.

The pyroclastics are welded lapilli-tuffs containing lobate lapilli of altered, glassy, vesicular lamproite up to 3 cm across, sparse, accidental, rounded clasts of siltstone and shale, and a sparse tuff matrix. The lamproite contains phlogopite phenocrysts up to 1 mm long and a little altered olivine in a groundmass of brown clay derived from altered glass. Some cognate lapilli

contain abundant phlogopite. Most samples are veined by barite and secondary silica.

Magmatic rocks are of olivine-phlogopite-leucite lamproite, and contain abundant small olivines (<0.2 mm), altered to talc, in a groundmass of altered leucite, phlogopite, accessory priderite; and abundant interstitial clay.

Ellendale 43

This small (4.6 ha) pyroclast-filled vent is located about 200 m east of Ellendale 42. No specimens of the rock are available and no diamonds were recovered from a bulk sample of 212 t.

Ellendale 44

Ellendale 44 is a small, concealed body of less than 1 ha area, located in the northwest part of the Ellendale Field. The body gives a strong magnetic response but was intersected by only one drill hole. The rock has not been sampled for diamonds and no specimens are available.

Ellendale 45

This small body, about 2 km west of Ellendale 7, is less than 1 ha in area. It has been intersected by scout drilling but not sampled for diamonds. No specimens are available.

Ellendale 46

Ellendale 46 is located at the foot of the Napier Range, 4 km southeast of Ellendale 17. It is a dyke-like body of olivine-phlogopite-leucite lamproite (290 m long by about 50 m wide), aligned north-south and concealed beneath about 12 m of sand and black soil. The shallow water table in the area, at about 10 m depth, prevented the recovery by auger drilling of bulk samples for diamond testing.

The lamproite contains abundant phenocrysts of phlogopite and olivine up to 1 mm long, in a clay-rich groundmass with abundant, small, former leucite euhedra (<50 μm) and diopside prisms (<100 μm), groundmass phlogopite, and accessory apatite and priderite. The olivine is altered to talc, and the phlogopite phenocrysts and groundmass diopside show strong flow alignment.

Water Reserve Pipe

The Water Reserve was a small area excluded from the original Ellendale Temporary Reserves taken out by the Ashton Joint Venture to cover the magnetic anomalies discovered in the region between Mount North and Mount Percy. The reserve was claimed by Haoma Gold NL and Northwest Mining; and, under a joint venture, Seltrust Mining located two lamproite bodies, a pipe and a thin sill.

The Water Reserve Pipe (Plate 2) is on the southwestern edge of the Ellendale Field, 1.4 km north of the old telegraph-line track. It is a lozenge-shaped body (375 × 230 m) and about 3.2 ha in area, concealed beneath 3 m of windblown sand and detrital laterite. Most of the pipe is filled by a plug of fine-grained leucite lamproite, but there are marginal areas of lamproite lapilli-tuff. The pipe intrudes sandstones of the Permian Grant Group, and drilling records indicate that the pipe margin dips inwards at about 70°-80°.

A total of 229 m^3 of decomposed lamproite and lapilli-tuff from three trenches were treated for diamond but none were recovered (Gregory, 1980).

The pyroclastics are fine-grained lapilli-tuffs containing clasts of olivine-leucite lamproite, shale, and siltstone, up to 5 mm across, in a sparse matrix of ash-sized lamproite fragments and clay minerals. The lamproite is glassy, and contains microphenocrysts of altered olivine, skeletal former leucite, and minute needles of priderite; some fragments also contain phlogopite flakes up to 0.5 mm long. The lapilli-tuff appears to have been invaded by olivine lamproite magma which, in part, forms a matrix to the lapilli. This lamproite contains pseudomorphs after anhedral olivine macrocrysts (up to 3 mm across) and small olivine microphenocrysts in a phlogopite-rich groundmass containing chromite and leucoxenized perovskite.

The magmatic core of the pipe is a fine-grained olivine-leucite lamproite. Abundant small olivines, up to 0.5 mm and replaced by talc, are set in a leucite-rich groundmass containing minute laths of diopside, phlogopite, and less common potassic richterite, and abundant priderite.

Sill "A"

A thin sill of lamproite, a few metres thick underlies an area 375 m diameter located about 600 m east-southeast of the Water Reserve Pipe. The rock is an olivine-phlogopite lamproite containing macrocrysts of olivine up to 6 mm across that have been replaced by serpentine and secondary silica; abundant olivine microphenocrysts have been similarly altered; and phlogopite flakes up to 2 mm long are partly corroded. Apart from small interstitial phlogopite flakes, the groundmass is an indeterminate mass of dark, earthy, clay minerals and sparse accessory chromite, priderite, and perovskite. The rock is similar to some specimens of the Ellendale 2 sills, which also contain much phlogopite.

A small bulk sample of 5 m^3 was tested for diamonds but with negative results (Gregory, 1981a).

EASTERN LENNARD SHELF FIELD

The Ellendale Field is confined to a relatively small area in and around the Fairfield Valley; it is bounded to the northeast by the line of the Napier Range and to the southwest by the Markham Ridge, a subsurface extension of the Oscar Range. These southeast-trending structures continue parallel to the margin of the Kimberley Basin into a broad area north of the township of Fitzroy Crossing, in which there are fifteen widely scattered and generally small lamproite intrusions (Plate

1). These intrusions are here designated the Eastern Lennard Shelf Field.

From the Great Northern Highway, access to the area is entirely on unformed gravel roads and station tracks. Big Spring is close to the well-used tourist road which passes along the front of the Napier Range and across the southeast end of the Oscar Range to join the main highway west of Fitzroy Crossing. From the vicinity of Big Spring homestead, a good track leads eastward passing close to Prairie Hill East and Old Leopold. The small, unexposed lamproites south of the Fitzroy River in the vicinity of J.K. Yard may be reached by station tracks, but a number of intrusions, including Mount Rose and Brooking Creek, are relatively innaccessible. During the summer wet season, all tracks are impassable, and access to some areas depends on the maintenance of creek crossings by the local pastoralist. Supplies of food and fuel may be obtained at Fitzroy Crossing, and water is easily available from numerous bores. Apart from the small settlement of Fitzroy Crossing, the population of the area comprises the three pastoral homesteads of Fossil Downs, Brooking Spring and Leopold Downs (Big Spring).

The topography of the area varies greatly from the open flood plain of the Fitzroy River and its major tributaries, to the sharp strike ridges of the Hooper Hills and the Proterozoic core of the Oscar Range. The Devonian reef complexes present a cliff line up to 60 m high on the southeast margin of the area, and the Fitzroy River and Brooking Creek have cut deep, scenically attractive gorges through the limestone. The granite areas in places consist of tors, whalebacks, and low rounded hills of bare rock but generally present a subdued boulder-strewn topography. The local relief rarely exceeds 100 m.

The vegetation is predominatly open grassland with scattered eucalypts. Spear grass predominates on the black-soil plains of the Oscar Plateau; but elsewhere, spinifex and an assortment of perennial grasses. Stands of eucalyptus and wattles cover the metasediments of the Oscar Range and Hooper Hills; and, along watercourses, there is usually a dense stand of eucalypts, including large river gums (*E. papuana*), paperbark, and many smaller species.

GEOLOGY AND STRUCTURE

The regional geology of the Eastern Lennard Shelf Field is similar to that previously described for the Ellendale area and will not be detailed further. The principal references are: for the regional framework, Derrick and Playford (1973); for the Devonian reef complexes, Playford (1980, 1984); and for the Lamboo Complex, Gellatly and others (1968).

The Lennard Shelf, strictly speaking, comprises only the areas of Devonian reef complex. About half the lamproites intrude these limestones, but only near the northeast margin close to the outcrop of the underlying Lamboo Complex. The remainder of the lamproites are exposed within the granitic rocks of Proterozoic age. Nevertheless it is convenient to name this group the Eastern Lennard Shelf Field.

The location of many of the lamproites in this field appears to be structurally controlled. In the Ellendale Field, it was noted that apart from the main concentration of intrusions, there was an isolated group of three lamproites intruded along the foot of the Napier Range, possibly controlled by a concealed fault that marks the margin of the Leopold Mobile Zone. This lineament, if continued to the southeast, would include the intrusions of Big Spring, Big Spring West, Cajaput Creek, Hooper, and possibly, the J.K. Yard bodies. There is no direct evidence of a fault in the area, but the contrast between the granites of the Lamboo Complex and the probably younger metasediments of the Oscar Range indicates a profound and abrupt change in geology across this lineament.

A principal structural element of this part of the Leopold Mobile Zone is the Sandy Creek Shear, a sinistral transcurrent fault zone, largely obscured by Sandy Creek itself (Gellatly and others, 1968). The main shear in the vicinity of Sandy Creek has a sinistral displacement of up to 10 km; and, to the northwest and southeast of this portion, the fault zone branches and is accompanied by complimentary dextral faults. The Mount Rose lamproite is situated close to the shear zone where it bifurcates to the northwest; similarly McKinrick Hill lamproite is located at the intersection of a southeasterly branch of the shear zone and a north-trending complimentary fault. Old Leopold Hill is located close to a southerly branch of the shear zone, and Prairie Hill East is located on a fault which may be complimentary to the Sandy Creek Shear Zone. In these instances, it is clear that major basement faults have influenced the intrusion of lamproite magma. The same is probably true throughout the West Kimberley Province, where the basement is hidden beneath a thick cover of Phanerozoic sediments.

BIG SPRING

The Big Spring lamproite was first reported by Derrick and Gellatly (1972), who described the outcrop as "a low mound of loose bouldery breccia about 8 m by 5 m". Subsequent exploration and drilling has shown that there are five unexposed lamproite bodies present, four pipes ranging in surface area from 10.4 ha to 1.0 ha and a sill or dyke of at least 1.0 ha in extent (Fig. 92) (Haebig, 1983a). The Big Spring pipes have a certain historical importance in diamond exploration in Western Australia because, in 1976, they provided the first unequivocal source rock for diamonds in Western Australia, and the first specimens of olivine lamproite. Bulk testing of the pipes, however, showed grades of only 0.1 CM/100 t and the largest stone recovered was only 0.1105 CM (Haebig, 1983a).

The lamproite pipes are intruded at the edge of the present-day outcrop of the Devonian Pillara Limestone where it unconformably overlies McSherry's Granodiorite, part of the Proterozoic Lamboo Complex. The

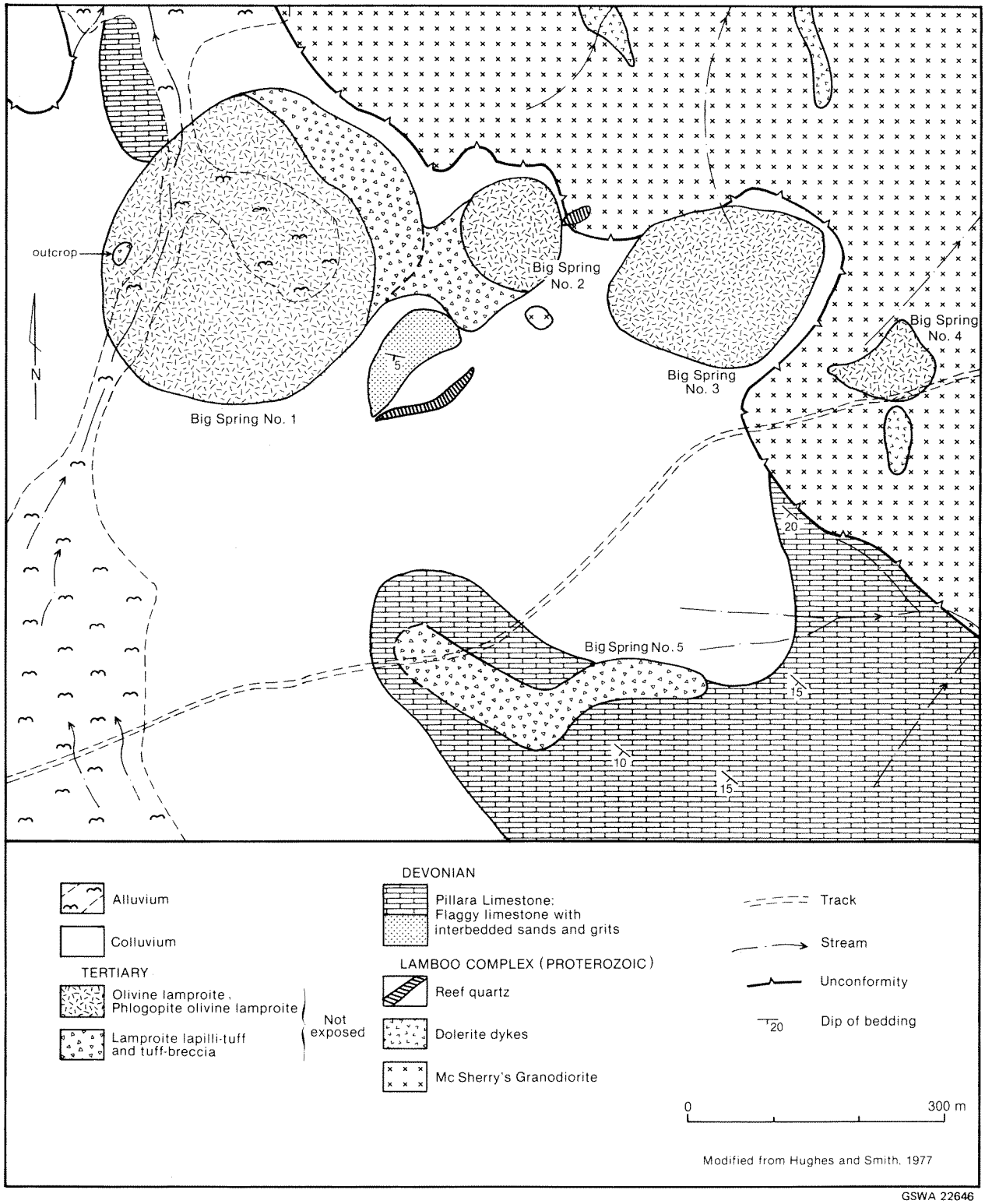


Figure 92. Geological map of the Big Spring lamproites.

granodiorite is a medium- to coarse-grained, moderately foliated, grey to pink rock, intruded by irregular dykes and pods of dolerite. This rock is the source of most of the country rock xenoliths in the lamproite pipes.

Unconformably overlying the granodiorite is the gently dipping Pillara Limestone of Frasnian age. The limestone is moderately well exposed on the low drainage divide southeast of the largest pipe, where it is a thin bedded, flaggy limestone, interbedded with some sandstone and grit beds and occasional pebble conglomerates. The basal sediments, visible near the unconformity, are grits with thin limestone partings. The Pillara Limestone is apparently undeformed, and dips regularly at 10-15° to the southwest.

Four lamproite pipes, ranging in diameter from 375 m to about 100 m, have been emplaced along a line that trends almost east-west; two of the pipes coalesce in outcrop, and the entire group occupies a distance of only about 1 000 m. It is apparent that the emplacement of the pipes was governed by a concealed, deep-seated,

linear feature, probably a fault. A fifth, irregularly shaped lamproite intrusion, 400 m to the south, is a dyke or sill-like body, probably related to the pipes. The following field description relies on the unpublished reports of Hughes and Smith (1977, 1978a) and Haebig (1979a, 1983a).

Two of the pipes, Big Spring 3 and 4, are occupied entirely by plugs of olivine lamproite concealed beneath a metre of so of sandy soil or calcrete. The rock exposed by trenching is, in each case, an olive-green, weathered lamproite containing large pseudomorphs after olivine, veins of carbonate and sparse xenoliths of granite and sandstone from the wall rocks.

The two pipes, Big Spring 1 and 2, each contain a small proportion of tuff in marginal zones, and central cores of olivine lamproite. In the smaller pipe, a tuff-breccia contains, in addition to phlogopite-olivine lamproite lapilli, about 25% country-rock pyroclasts up to 40 cm across; these are almost entirely of granite but some are sandstone, limestone or other lamproitic pyroclastics. In the larger pipe, Big Spring 1, a narrow zone of pyroclastics is present on the northeastern margin of the pipe. A coarse, lamproite lapilli-tuff, or tuff-breccia, is present; it contains autoliths up to 15 cm diameter, and granitic pyroclasts (< 5%) up to 20 cm, but commonly 2-4 cm, in diameter. Tuff-breccia, composed mainly of granite and metasedimentary fragments and only a minor lamproitic component, gives rise to two small outcrop areas, but its distribution is not known in sufficient detail to distinguish it on Fig 92. One of these outcrops, originally reported by Derrick and Gellatly (1972) is essentially a large xenolith in the magmatic core of the vent.

Little can be inferred about the subsurface shape of the Big Spring pipes, but three drill holes close to the northeast and southeast margin of Big Spring 1 intersected granitic wall-rock at shallow depth, indicating an inward dip of the vent wall of 51° to 62°. These dips suggest a flared vent similar to those of the Ellendale Field.

Big Spring 5 is an irregularly shaped, elongate body, probably formed by a "blow" on a dyke or steeply dipping sill complex. Both magmatic and pyroclastic phases are present, together with granite and/or arkose, which appears to form screens between different rock types. The body is emplaced in limestone, but the granite basement is only a few metres below the present surface. Drill logs (Fig. 93) from different parts of the body illustrate the complexity of Big Spring 5.

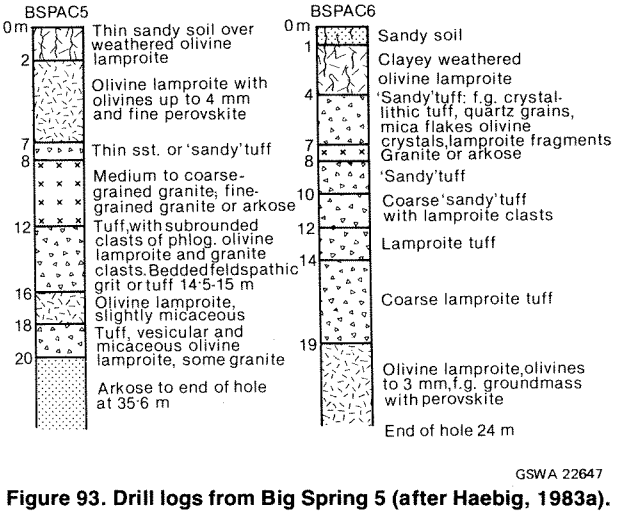


Figure 93. Drill logs from Big Spring 5 (after Haebig, 1983a).

Petrography

Pyroclastics: The two small outcrops of diverse types of tuffs and breccias are considerably altered by superficial silicification. Commonly the tuff comprises fragments of microcline, up to 2 mm across, and patches of chlorite after biotite, in a matrix of secondary silica and sparse carbonate. Textures indicate that some of the silica has pseudomorphed former plagioclase. This tuff represents a disaggregated granite with no obvious lamproite component. A very fine-grained variety, in which quartz and microcline fragments < 0.1 mm across are set in a chlorite- and silica-rich matrix, contains 14% K_2O, and is rich in Ba, F, and Rb: these elements may have been added from the lamproite gaseous phase (Table 41). Other varieties contain angular fragments of fine-grained shale in addition to granitic fragments; but only one specimen contains possible altered lamproite fragments.

Tuffs from Big Spring 5 contain both lamproitic and granitic material. The lamproite is a fine-grained olivine lamproite containing talcose pseudormorphs after olivine macrocrysts up to 4 mm across and microphenocrysts about 1 mm long. The granitic material consists of microcline, quartz, and altered plagioclase fragments and small granitic xenoliths. One large, rounded pyroclast, about 2 cm diameter, consists of microcline, biotite, and sericitized plagioclase; and is surrounded by a thin skin of olivine lamproite.

Lamproite lapilli-tuffs are widely distributed in the marginal zones of Big Spring 1 and 2, and consist, essentially, of close-packed fragments of olivine lamproite in a sparse lamproite ash matrix. Autoliths and rare accidental granitic pyroclasts were observed in exploration trenches, but none were present in the few thin sections available. The lapilli-tuff is thoroughly altered and often veined by carbonate and barite.

Central core lamproite: Only near-surface samples are available; the rock is thoroughly altered, and few original minerals are present. The rock is often extensively veined with carbonate and barite. Two rock types are present, an olivine lamproite with only sparse phlogopite, and an olivine-poor variety in which phlogopite is prominent. The common variety comprises two generations of olivine; both are pseudomorphed by talc, carbonate, chlorite or barite, and are contained in a fine-grained chloritic matrix in which the only original minerals remaining are scattered granular and euhedral yellow-green perovskite, and small interstitial flakes of phlogopite. In some specimens, small groundmass prisms of colourless potassic richterite are also present. Olivine accounts for about 30% of the rock; the euhedral phenocrysts range up to 1 mm, and the macrocrysts, up to 8 mm across. The macrocrysts are generally well

rounded; but some have "saw toothed" outlines, probably caused by overgrowth crystallization during the ascent of the magma. Some specimens are poor in olivine, particularly the macrocryst phase: the mineral makes up only 10-15% of the rock. This variety, however, contains abundant poikilitic groundmass flakes of phlogopite up to 1 mm across. The relationship between the two varieties is unknown.

Chemistry

Chemically, the Big Spring lamproites (Table 41) are intermediate between the leucite lamproites of the Eastern Lennard Shelf and the MgO-rich olivine lamproites of the Ellendale Field. The closest analogy is with the lamproites of Ellendale 2, although the Big Spring rocks are richer in Al_2O_3 (6.0%) and CaO (6.3%), and slightly poorer in TiO_2. Trace-element contents are similar except that Zr and LREE are somewhat lower in the Big Spring lamproites. The degree of alteration is indicated by the high Ba content (3.13% BaO).

BIG SPRING WEST

A small exposure of leucite lamproite occurs about 3 km west of the Big Spring pipes (LEOPOLD DOWNS, GR:512366). The body produces a strong magnetic anomaly (Hughes and Smith, 1978b), but the outcrop consists only of thin lamproite veins (up to 15 cm thick) intruding green-stained sandstone beds within the Pillara Limestone. The veins are found over a small area, about 30 m square, and the main body of lamproite might be concealed beneath colluvium, or perhaps never reached the surface.

The rock type is a xenocryst-bearing olivine-leucite lamproite. The angular xenocrysts, up to 3 mm across, are of microcline and quartz; they are presumably derived from the basement granite, and make up about 10% of the rock. A few, small xenoliths of granite and siltstone are also present. Small olivine euhedra, < 1 mm across and pseudomorphed by talc, make up about 15% of the rock; the remainder is a turbid, dark, devitrified glass, in which are embedded many small altered leucite euhedra, minute needles of priderite, and a few small flakes of phlogopite. Some veins are distinctly fragmental, and contain vesicular lamproite clasts and a matrix partly replaced by carbonate and a little barite. A chemical analysis of an olivine-leucite lamproite vein that is relatively free of xenocrystic material is given in Table 41. The rock is chemically similar to other leucite lamproites of the Eastern Lennard Shelf Field (Table 42).

TABLE 41. REPRESENTATIVE ANALYSES OF LAMPROITES FROM BIG SPRING

	1	*2*	*3*	*4*
		Percent		
SiO_2	40.40	30.20	60.50	49.00
TiO_2	4.12	3.79	0.62	3.79
Al_2O_3	6.00	4.10	15.10	7.40
Fe_2O_3	8.00	6.90	2.30	6.40
FeO	0.90	0.26	0.85	0.87
MnO	0.11	0.14	0.01	0.06
MgO	15.20	9.45	1.27	9.03
CaO	6.31	15.70	1.76	4.33
Na_2O	0.82	0.21	0.10	0.55
K_2O	3.99	2.68	14.05	6.60
P_2O_5	0.67	0.39	0.09	1.52
H_2O^+	5.63	5.12	1.10	5.07
H_2O^-	4.50	5.06	0.31	3.97
CO_2	0.38	10.60	0.43	0.08
Rest	4.14	5.28	0.98	2.54
Total	**101.17**	**99.88**	**99.47**	**101.21**
		Parts per million		
Ba	27 968	29 504	6 113	11 523
Li	8	7	4	13
Rb	507	409	424	192
Sr	1 334	967	82	1 601
Pb	40	40	40	90
Th	33	21	18	52
U	2	1	1	4
Zr	938	849	186	1 079
Nb	203	152	13	167
Y	20	26	16	28
La	392	356	165	552
Ce	417	340	115	783
Sc	23	18	15	21
V	59	40	97	170
Cr	622	389	79	523
Ni	540	410	26	500
Cu	85	65	30	80
Zn	74	70	68	73
Ga	6	4	13	13
S	100	4 600	140	1 000
F	5 260	3 300	1 086	3 540
Cl	120	110	149	440

1 — Potassic-richterite - olivine lamproite lapilli-tuff; Big Spring 3, GSWA 71388. 2 — Carbonated phlogopite-olivine lamproite; Big Spring 1, GSWA 71386. 3 — Fine-grained, quartz-rich tuff vein; Big Spring 1, GSWA 71385. 4 — Olivine-leucite lamproite; Big Spring West, GSWA 71382.

CAJAPUT CREEK

Three small plugs of leucite lamproite are reported to outcrop about 4 km east of the Big Spring pipes (LEOPOLD DOWNS, GR:590353). The lamproites intrude the McSherry's Granodiorite and give a strong magnetic response (Hughes and Smith, 1978b).

The intrusions have not been mapped, but the specimens available are diopside-phlogopite-olivine-leucite lamproites. One specimen contains about 15% of small olivine phenocrysts — pseudomorphed by talc and nontronite — and acicular, flow-aligned diopside up to 2mm long, in a matrix of small, altered leucite crystals and phlogopite flakes and an interstitial feathery mass of chloritic material. Large poikilitic plates of priderite and prisms of apatite are prominent accessory minerals. A second variety is less olivine-rich, but contains abundant aligned phlogopite flakes up to 2 mm long.

MOUNT ROSE

The Mount Rose plug is the most remote and difficult of access of the lamproites of the Eastern Lennard Shelf Field. It has been visited, very briefly, by only one of the authors (CBS); and the map (Fig. 94) and description are, with permission, taken largely from the account of Derrick and Gellatly (1972).

The Mount Rose lamproite intrudes the metasediments of the Halls Creek Group and is located about 3 km southeast of Mount Rose. It lies 1 km north of a large branch of the Sandy Creek Shear, a transcurrent fault that gives a sinistal displacement of 5 km to the Woodward Dolerite. The phyllites of the Halls Creek Group are moderately well exposed and dip between 40° and 70° to the south. The contact with the lamproite

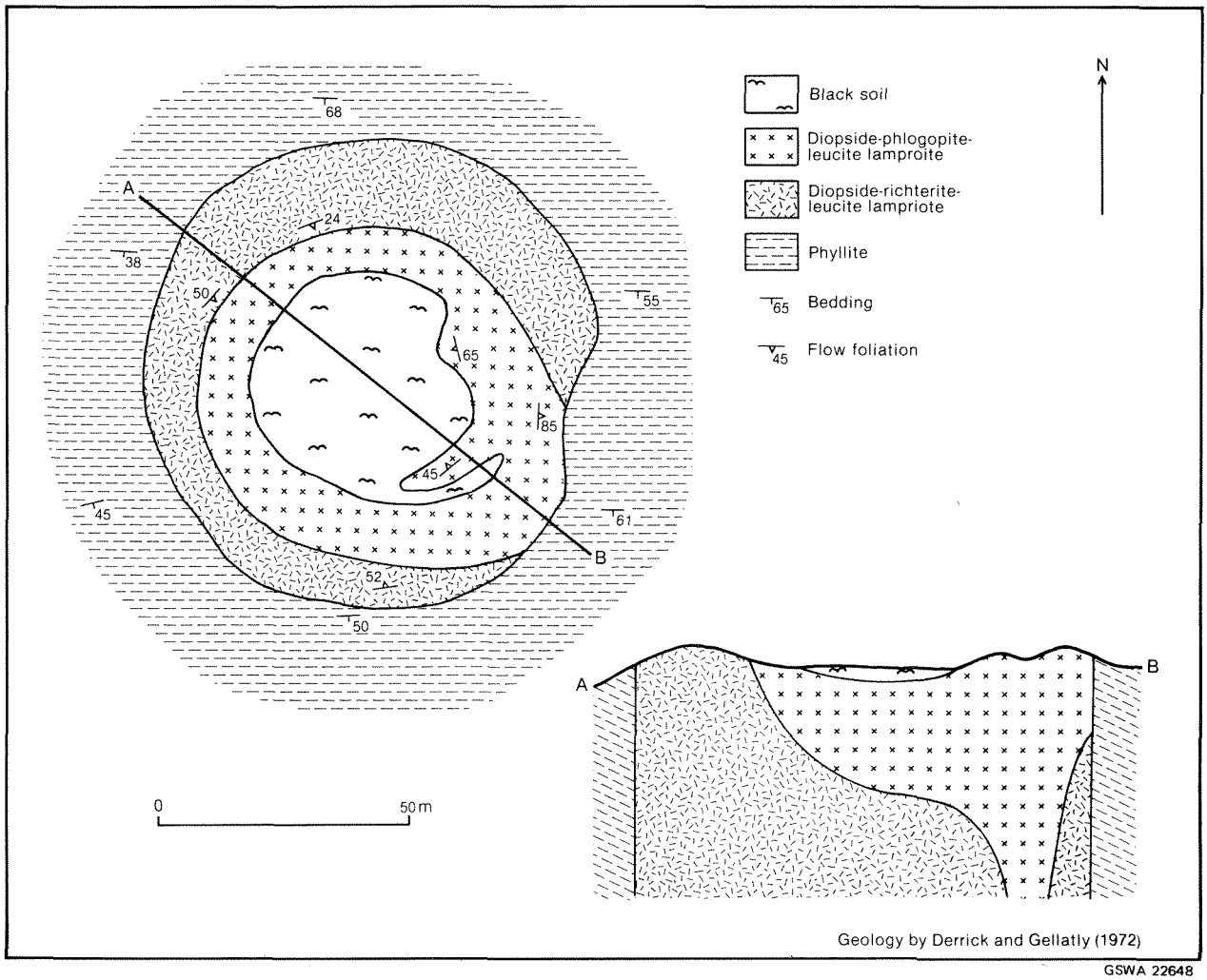


Figure 94. Geological map of Mount Rose.

shows only slight metamorphism and no deformation of the phyllites.

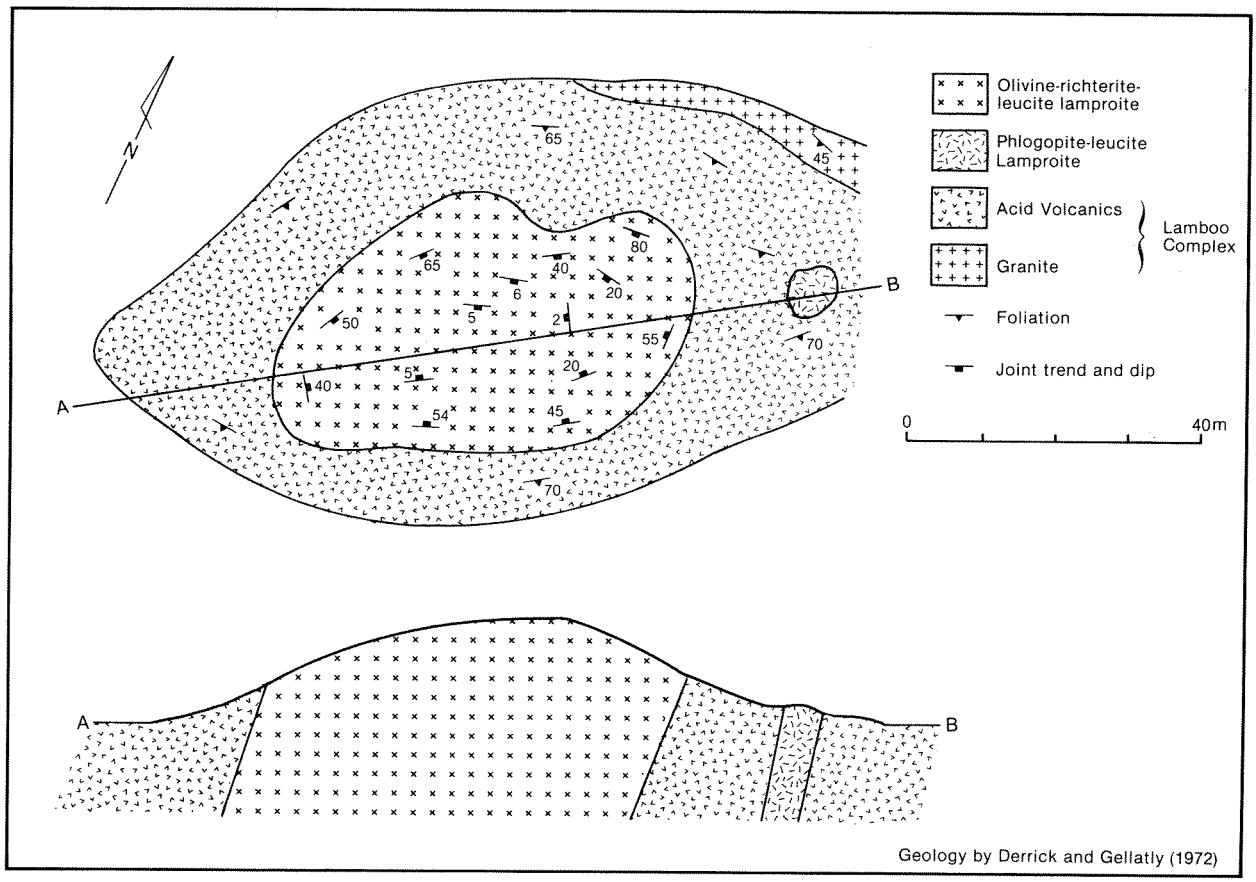
The lamproite plug is roughly circular in outcrop and about 80 m in diameter. It consists of an outer zone of friable, weathered, grey-green diopside - potassic-richterite - leucite lamproite and an eccentric inner zone of diopside-phlogopite-leucite lamproite with conspicuous phenocrysts of phlogopite and diopside up to 3 mm long. The central part of the plug is obscured by phlogopite-bearing black soil and lamproite debris.

Flow foliation within the plug commonly dips inward at 50°-65°; but, near the eastern margin, close to a vertical contact with the surrounding phyllites, it dips outward at 85°.

Petrographically the outer zone is a diopside - potassic-richterite - leucite lamproite containing small phenocrysts of altered leucite, occasional phlogopite, minor quantities of diopside and olivine pseudomorphs, all in a groundmass crowded with small leucite pseudomorphs (average diameter 50 μm) and abundant poikilitic potassic richterite crystals that are studded with small leucite inclusions. Small prismatic crystals of priderite and apatite are present in accessory amounts. Leucite is entirely altered to potash feldspar and clay. Some of the leucite crystals form irregular, amoeboid masses that contain tiny, green pleonaste grains (Jaques and Foley, 1985). Some of the hydrotalcite pseudomorphs after olivine contain minute (20 μm) granules of chrome spinel.

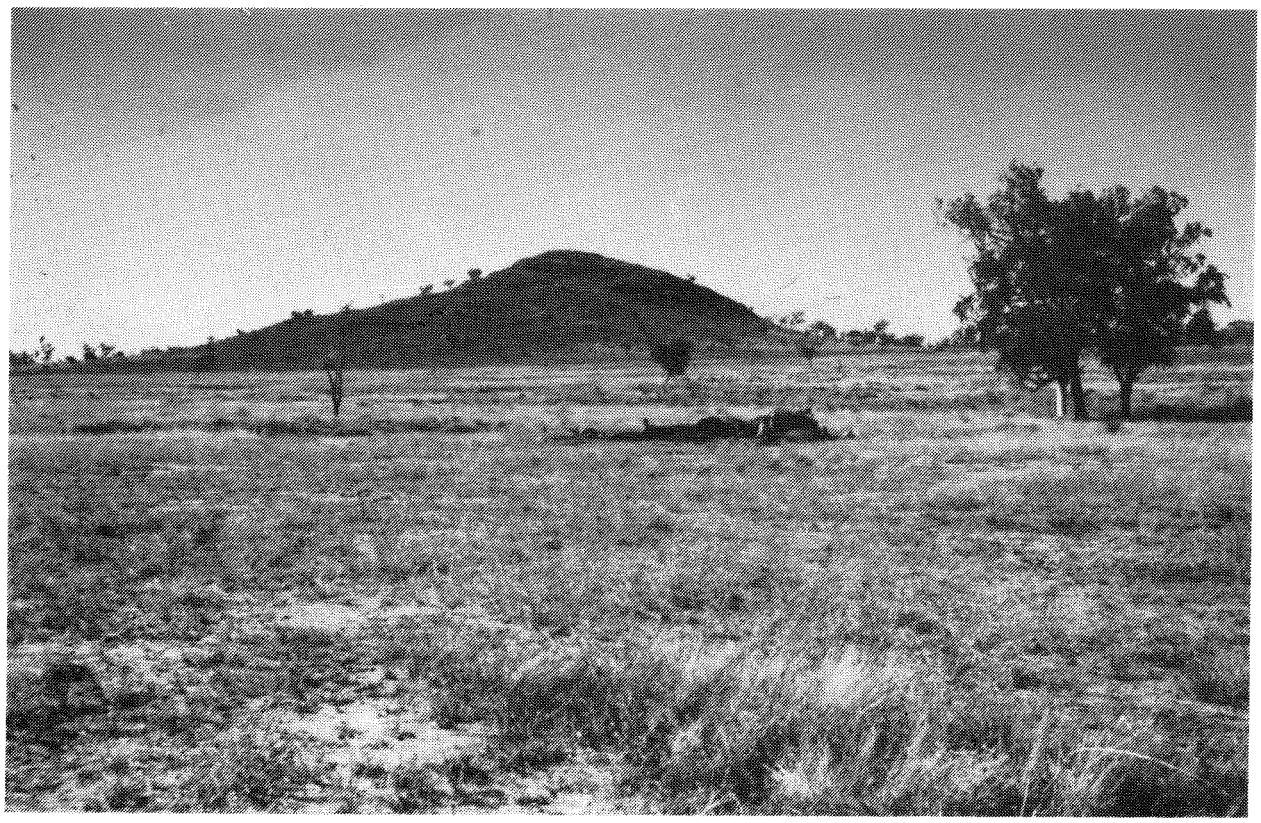
The inner zone is a diopside-phlogopite-leucite lamproite that contains abundant phenocrysts (up to 3 mm long) of phlogopite, and aggregates (up to 6 mm diameter) with diopside prisms. The phlogopite is zoned to a marginal red-brown colour and is often strongly corroded. In some specimens the phlogopite contains internal zones that are studded with minute crystals of leucite. Diopside phenocrysts are less numerous, and range from stout prisms, up to 2 mm long, to elongate prisms 4 mm long. Leucite, now completely altered to potash feldspar, and clay, is seriate, and ranges from prominent euhedra, 1.5 mm diameter, to small groundmass grains. The groundmass is a cryptocrystalline mass of greenish-yellow chlorite that contains small diopside crystals and phlogopite flakes, and large plates of poikilitic potassic richterite that enclose many small leucite crystals, together with prisms of priderite, apatite, and, more rarely, wadeite. The rim of some potassic richterite is zoned to greenish-brown alkali amphibole, and pleochroic green aegirine or aegirine-augite forms small, interstitial, feathery growths on diopside and amphibole.

Mount Rose lamproite is typical of most of the Eastern Lennard Shelf lamproites in being oversaturated



GSWA 22649

Figure 95. Geological map of McKinrick Hill.



GSWA 22650

Figure 96. McKinrick Hill from the south. (Photo: G. Derrick, BMR).

in silica, poor in MgO (<10%), and rich in K_2O and normative orthoclase (>40%). Representative analyses of two samples described by Derrick and Gellatly (1972) are given in Table 42.

McKINRICK HILL

McKinrick Hill has been visited only very briefly by the present authors; and, as with Mount Rose, the map (Fig. 95) and description is adopted largely from the original account by Derrick and Gellatly (1972).

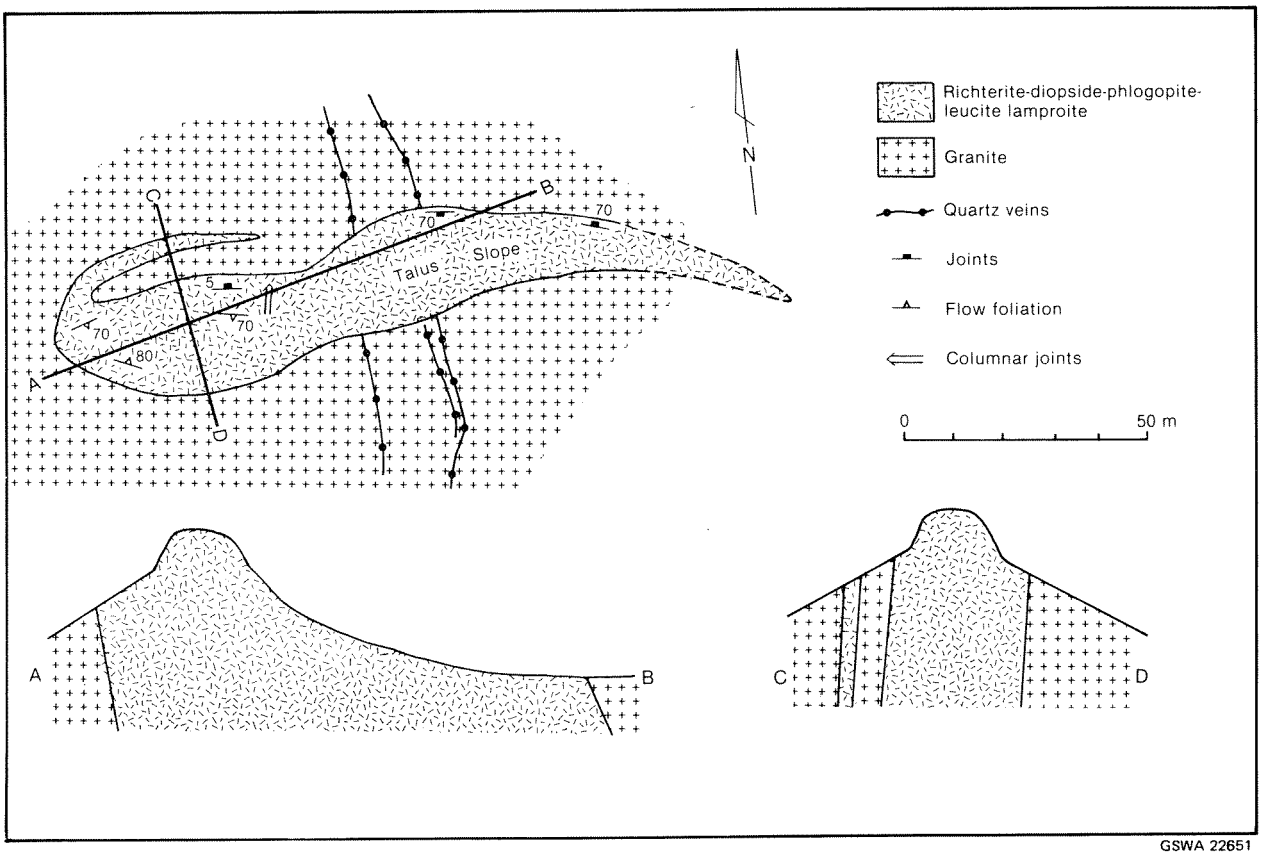
McKinrick Hill is located 45 km southeast of the Mount Rose lamproite and lies very close to an easterly branch of the Sandy Creek Shear. A north-trending fault, complimentary to the shear zone, probably assisted the location of the lamproite. The lamproite is intruded into rhyodacite flows and tuffs of the Proterozoic Whitewater Volcanics, a tongue of which separates two masses of the Lennard Granite, also of Proterozoic age. Foliation in the volcanic sequence dips steeply to the south.

The lamproite plug is roughly oval in shape, about 55 × 35 m and elongated northeast, and occupies most of a low spinifex covered hill about 20 m high (Fig. 96). A small pod of weathered lamproite, a few metres across, occurs about 15 m northeast of the main mass. The main lamproite is massive and fine-grained, and contains plentiful, small xenoliths of metamorphosed acid volcanics and granite and, rarely, xenoliths of red jasper. Joint planes from 10 cm to 1 m apart outline elongate, saucer-shaped structures with dips that range from 80° near the margin to near horizontal at the pipe centre; many of the joints are coated with zeolitic material. These features suggest that the lamproite pipe plunges steeply to the southwest.

Petrographically, the main mass is a uniform, very fine-grained olivine - potassic-richterite - leucite lamproite containing 10-20% xenoliths and xenocrysts derived from the country rock. Microphenocrysts of altered olivine are abundant (usually <0.2 mm,but up to 1 mm across) and entirely pseudomorphed by talc. A few small, corroded flakes of phlogopite, up to 0.5 mm long, are also present. The matrix is very fine grained, and consists of a mass of minute prisms of potassic richterite, and flakes of chlorite containing abundant small crystals of altered leucite and minute needles of priderite.

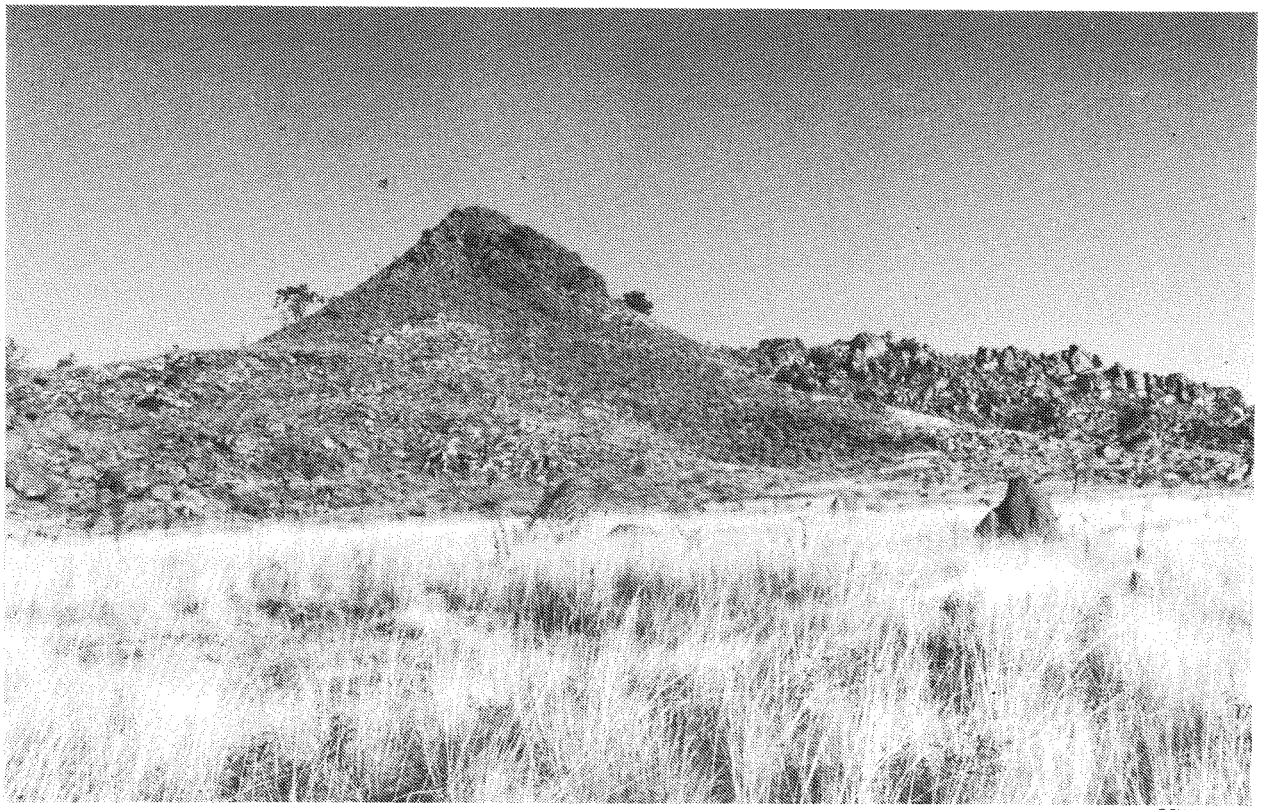
Xenocrysts are dominantly microcline, more rarely quartz; all show considerable corrosion, and are rimmed by chlorite. The xenoliths, usually less than 2 cm across, are of porphyritic rhyodacite, which contains phenocrysts of plagioclase, microcline, and few granitic xenoliths of similar size in a fine-grained matrix.

The McKinrick Hill lamproites range from compositions very similar to those of Mount Rose (in terms of SiO_2, MgO and K_2O) to more SiO_2- and K_2O-rich, and Mg-poor compositions (8.8 - 5.8% MgO, 8.0 - 11.7% K_2O). The two samples analyzed (Table 42) show marked differences in Sr (2 027 and 1 416 ppm) and Ba contents (1 600 and 8 000 ppm). Abundances



GSWA 22651

Figure 97. Geological map of Old Leopold Hill.



GSWA 22652

Figure 98. Old Leopold Hill from the east. The lamproite forms a small peak of dark rock surrounded by well- jointed, pink granite.

of trace elements are broadly similar to, or slightly higher than, those of Mount Rose.

OLD LEOPOLD HILL

This intrusion is located 15.7 km south-southeast of McKinrick Hill and 3 km north of the abandoned Old Leopold homestead, after which it is named. Access is from the main easterly track from Big Spring homestead.

The lamproite intrudes the Lennard Granite, a leucocratic, sparsely porphyritic, coarse-grained granite, veined by aplites and quartz. The granite forms low rounded hills, almost devoid of vegetation, with intervening grassy plains. Against the pink of the granite outcrops, Old Leopold Hill is conspicuous by its dark colour and conical form rising about 30 m above the granite outcrop. (Figs. 97 and 98).

Harms (1959) described Old Leopold Hill as a dyke of leucite lamproite, whereas Derrick and Gellatly (1972) described it as a plug. In plan, the intrusion is an irregular dyke-like body about 150 m long, up to 25 m wide, and elongated east-west. At its western end, a narrow apophysis, a few metres wide, runs parallel to the northern margin of the main mass. For much of its length, the margin of the intrusion is sharp and easily found; but, in the west, it is obscured by talus from the hill; and, in the east, the intrusion narrows and terminates beneath soil cover. The northern and southern margins are irregular and variable; they dip between 70° north and 70° south; and the lamproite is chilled to a finer grained variety. On the hill at the western end of the body, crude columnar jointing is subhorizontal, and flow foliation dips inwards at 70-80°. Together this evidence indicates that the lamproite is essentially a vertical dyke-like body.

Apart from the narrow, chilled margins, a few metres wide, the lamproite is essentially uniform; and prominent phlogopite, diopside, and leucite, are visible in hand specimen. Except in the marginal, chilled zones, no xenoliths were noted; but, on the northern and eastern slopes, the lamproite contains large masses of pale-green to cream opaline silica.

Petrographically the rock is a porphyritic potassic-richterite – diopside – phlogopite – leucite lamproite. The most prominent phenocrystal phase is leucite, which forms crystals up to 3 mm diameter; the larger crystals often show complex growth forms. Leucite is also prominent as small crystals in the groundmass where, like the phenocrysts, it is altered to potash feldspar. Phlogopite is moderately abundant, forming flakes up to 3 mm across, which are often overgrown on the leucite phenocrysts; it usually shows complex lamellar twinning, and commonly has a reaction rim containing priderite prisms. Diopside typically forms small euhedral twinned prisms about 1 mm long but which in some specimens is up to 3 mm long. The groundmass is a brown, turbid material, possibly former sanidine; small former leucite and diopside crystals, interstitial phlogopite, and abundant small priderite prisms are also present. Accessory apatite and occasional wadeite are also present. Most notable, however, is abundant poikilitic, strongly pleochroic potassic richterite, which occurs as prismatic masses up to 1 mm long. The potassic richterite is zoned to greenish-yellow rims of potassic magnesio-arfvedsonite. Pleochroic green

aegirine and aegirine-augite form feathery outgrowths and small stubby prisms on potassic richterite and diopside.

Samples from the chilled margin in the central part of the dyke are fine-grained phlogopite-olivine-leucite lamproite with xenocrysts of microcline and small xenoliths and xenocrysts, phlogopite has been of leucite and diopside found in the main mass; and the phlogopite phenocrysts are smaller more elongate and with less complex twinning. Olivine microphenocrysts, 0.3-1 mm long and altered to greenish talc, make up about 10% of the rock. The groundmass is a brown turbid mass containing many small altered leucite euhedra, interstitial phlogopite, and small prisms of potassic richterite. In reaction zones around some xenoliths, and xenocrysts, phlogopite has been suppressed, and prismatic potassic richterite is well developed, along with rare patches of poikilitic colourless richterite. A further feature of this rock is the presence of accessory grains of both perovskite and priderite; both are absent in the reaction zones around xenoliths.

The relationship between the two rock types is obscure. The fine-grained rock is not merely a chilled variety of the main mass yet no intrusive margin is visible. Possibly two pulses of magma were involved, an earlier olivine-bearing variety, and a later leucite-rich magma.

The Old Leopold Hill lamproite is of uniform composition — oversaturated in silica and poor in MgO-similar to the Mount Rose lamproite (Table 42). Analysis of the samples described by Derrick and Gellatly (1972) gave anomalously high (55-59%) SiO_2 as a consequence of the secondary quartz and chalcedony in these samples. Nickel and Cr contents in the Old Leopold Hill lamproite are very low compared to most of the other leucite lamproites (*i.e.* <100 ppm Ni, <300 ppm Cr).

OLD LEOPOLD WEST

This small exposed pipe, about 250 × 50 m across, is reported by Gellatly (1979) to occupy a gentle depression on top of a granite "whaleback" 800 m north-northwest of Old Leopold Hill (HOOPER, GR:053274). The rock is reported to be a leucite lamproite, but no further information is available.

PRAIRIE HILL EAST

Prairie Hill East lamproite plug was discovered in 1966 and first described by Derrick and Gellatly (1972), it is located 10.6 km west-southwest of Old Leopold Hill, and 1 km south of the main station track east from Big Spring.

Two small lamproite intrusions and one small outcrop of brecciated granite or arkose associated with volcanism lie on a low northeast-trending ridge (Fig. 99). The main lamproite plug occupies a depression in the centre of a small (15 m high) hill formed by granite and Devonian sandstones (Fig. 100). About 100 m to the northeast a second smaller lamproite, which is rimmed by baked sandstones, forms a small rise on the ridge (Fig. 101). Including the brecciated area, the lamproites extend over a distance of about 500 m. The lamproites occur in an open sand plain with extensive spinifex cover, and only in the vicinity of the intrusions is there any rock outcrop.

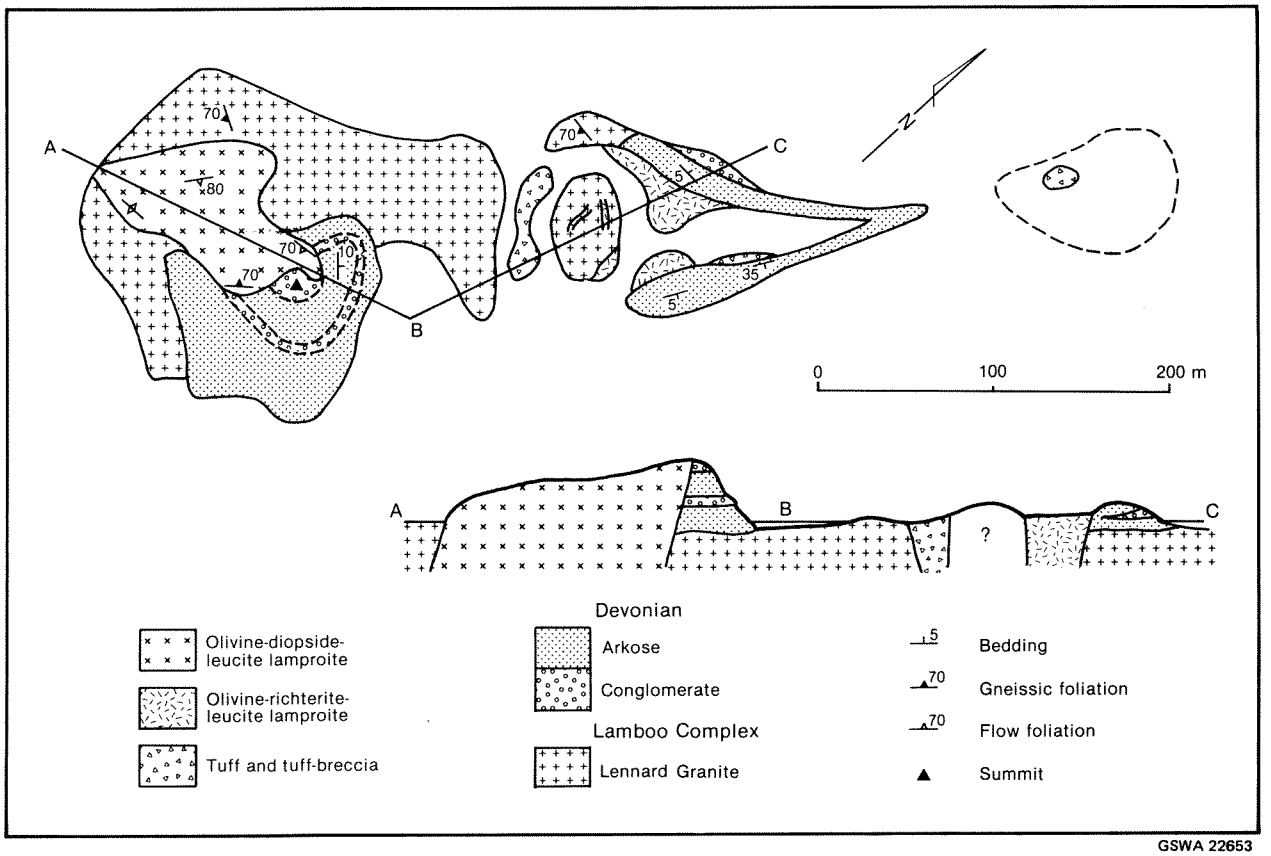
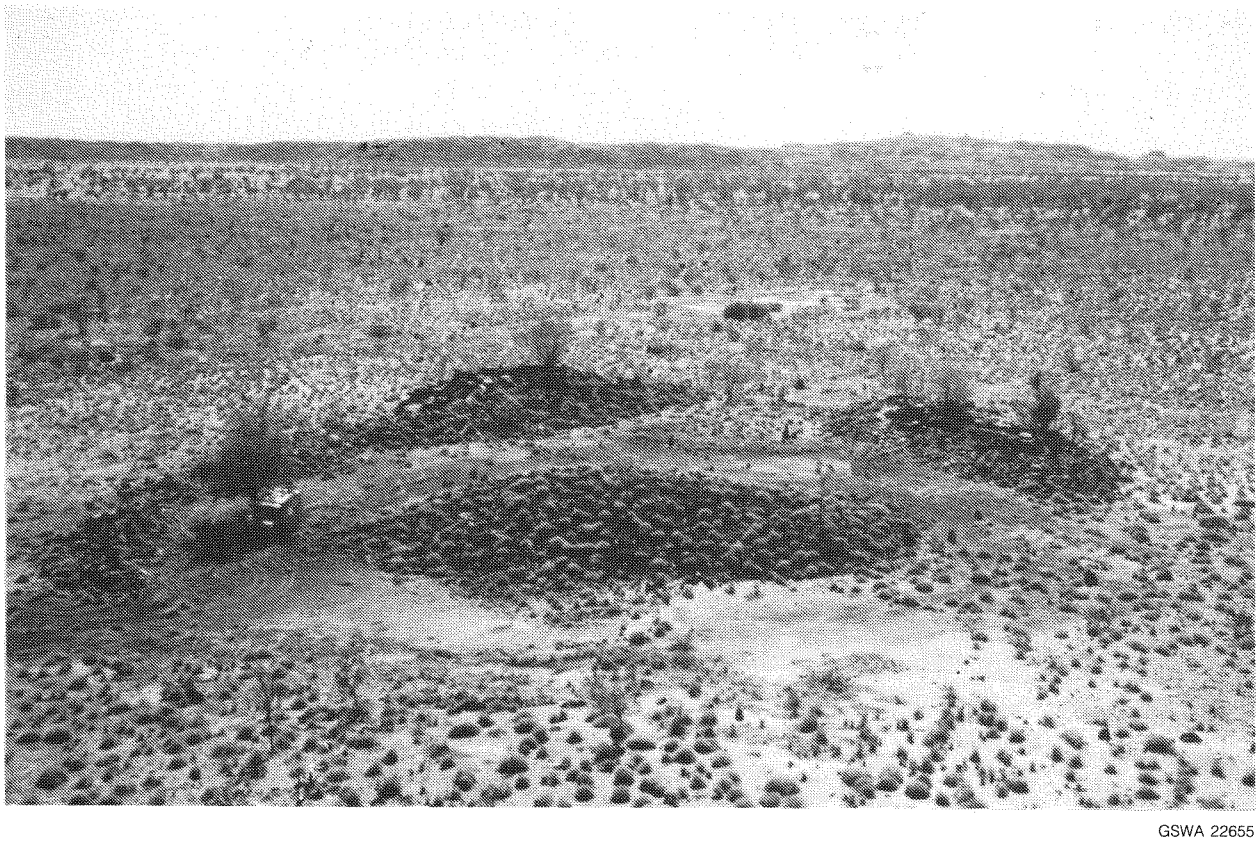


Figure 99. Geological map of Prairie Hill East.



GSWA 22654

Figure 100. Prairie Hill East from the northwest. The main lamproite plug is surrounded by flat-lying Devonian arkose and conglomerate on the east, and Proterozoic Lennard Granite to the west.



GSWA 22655

Figure 101. Satellite vent of Prairie Hill East, viewed from the main plug. The outer rim is composed of baked and brecciated sandstone and granite; the central hill is of boulders of brecciated granite veined by lamproite, with lamproite occupying the surrounding depression. (Photo: G. Derrick, BMR).

The basement rock is Lennard Granite, a coarse-grained pink granite, part of the Proterozoic Lamboo Complex. Uncomformably overlying the granite is a horizontally bedded sequence of arkose, grit, and pebble conglomerate, of Devonian age. It is evident, when the north and south sides of the main hill are compared, that the granite rises almost as high as the arkose. Just below the summit on the north side, a small exposure shows arkose overlapping the granite with the granite-sediment contact almost vertical. On the south side, the granite is at the level of the plain, and the face of the hill is composed entirely of an arkosic sandstone with two conglomerate horizons. The unconformity may be seen on the southwest of the hill, where fine-grained arkose forms the matrix between boulders of granite up to half a metre across. It appears that, in Devonian times, the unconformity in the area was marked by a small cliff, 10-15 m high, against which granite boulders were banked. The coincidence of this feature and the later intrusion of lamproites suggests the presence of a fault, a suggestion reinforced by the linear arrangement of the lamproite intrusions. Except locally, within a metre or so of the margin of the intrusion, the sandstones have not been disrupted by the emplacement of the lamproite.

The main lamproite plug is an irregularly shaped body, about 130 m long and a maximum of 75 m wide, and elongated east-west. The rock is coarse-grained, dark green-grey in colour, and shows prominent platy flow structures parallel to the margins of the body. The only metamorphic effects visible are a slight baking and toughening of the sediments, and a characteristic green staining close to the intrusion. Several small veins of lamproite and breccia penetrate the sediments.

The smaller lamproite intrusion is outlined by two low ridges of flat-lying arkose and basal conglomerate in the shape of a wishbone. To the northeast, where the ridges join, the outcrop is baked and silicified arkose. Between the arms of the wishbone is a low area containing a poor outcrop of a fine-grained, grey, olivine-leucite lamproite, a narrow marginal zone of brecciated granite, and a small central boulder covered hill about 3 m high. The boulders, rounded to sub-angular and about 30 cm across, are of granitic material, sometimes a medium-grained granite breccia. The central location of this "granite" hill led Derrick and Gellatly (1972) to describe the olivine-leucite lamproite as a ring-dyke: but between the boulders are many small veins of lamproite; and it is possible that the hill is the original coarse breccia infilling of the vent that was invaded by lamproite magma.

About 200 m northeast of the outcropping lamproite, there is a dark, oval photofeature about 100 m across. On the surface, this is marked by a slight vegetation change and a slightly darker soil, which is composed largely of disaggregated granite or arkose. To one side, however, are a few very small outcrops of dark brecciated rock with the green staining typical of lamproite metasomatism.

Petrography

Tuffs and breccias: The breccias found marginal to the northeast lamproite and in the blind pipe, appear to be entirely of granitic origin: there are no lamproite fragments and little lamproitic component. One variety consists of angular to sub-rounded microcline and quartz grains 1-2 mm across, a sparse sericitic matrix, and a little apple-green chloritic material typical of lamproite alteration. Another variety is banded: the banding is marked by fragments of a granitic gneiss (up to 8 mm across) in the coarser bands, and fine-grained bands of angular quartz grains (0.1 mm across) and oxidized biotite flakes. Much of the sparse matrix in this sample is stained green.

One sample is of a tuff partly assimilated by lamproite magma: it consists of about 50% corroded and embayed microcline and quartz grains; numerous irregular vughs (2-3 mm across) lined with opaline silica; and a matrix of devitrified glass containing numerous microlites of microcline, green chlorite, green amphibole, rutile, and patches dusted with opaque grains. The only evidence for a lamproite component is the prominence of rutile, presumably derived from the Ti component of the lamproite magma.

A granite sample collected from the central mound shows extensive remelting and possible brecciation; it consists of lobate, corroded microcline and patches of mosaic quartz, separated by melt channels. The melted material has crystallized as microlites and feathery masses of feldspar with minor green chloritic material and accessory amphibole microlites.

Breccia veinlets from the main hill are often bright-green in colour, but are similar to the finer grained tuffs described earlier. One sample contains a remarkable concentration of zircon in a narrow band.

A sample of the breccia over the blind pipe is similar to the coarser tuff-breccias described, except that it contains fresh biotite.

Lamproite: The main lamproite plug is a coarse-grained, porphyritic, olivine-diopside-leucite lamproite. Euhedral olivine phenocrysts, 1-2 m, long have been replaced by a pale-green talcose material, possibly hydrotalcite. Some contain tiny grains of chromite. Altered leucite euhedra, about 1 mm across, make up about 30% of the rock; and fresh prismatic or acicular diopside, up to 3 mm long, makes up the phenocryst suite. The groundmass of the rock is a dark brownish turbid mass of chloritic minerals containing identifiable small euhedra of altered leucite, flakes of phlogopite, and abundant small priderite and apatite crystals. Some specimens also contain isolated, corroded phlogopite grains, up to 2 mm across; these are usually surrounded by a reaction rim of leucite and priderite needles. Pleochroic, green, feathery prisms of aegirine form rims on groundmass diopside and potassic richterite in some samples.

Near the summit of the hill is a finer grained marginal phase of olivine-leucite lamproite, lacking diopside and phlogopite, but containing prominant acicular apatite and prismatic priderite. These rocks have been partly

silicified and contain secondary barite. A thin vein of lamproite in the arkose on the southeast side of the hill is a vesicular, olivine-leucite lamproite that contains leucite and small phlogopite flakes in the groundmass.

The lamproites of the northeasterly body are fine- to medium-grained potassic-richterite – olivine – leucite lamproites. Microphenocrysts of altered olivine are abundant, but much of the remainder of the rock is a seriate mass of altered leucite euhedra up to 0.5 mm across. The sparse matrix contains abundant interstitial and acicular potassic richterite, accessory apatite, and many opaque grains, some of which are dark-coloured priderite and others, possibly, jeppeite. Some specimens also contain a little acicular diopside.

A narrow lamproite vein from the granitic central mound of this body is a medium-grained olivine-diopside-leucite lamproite, very similar to the lamproite of the main plug except for the presence of abundant groundmass potassic richterite.

Chemistry

Prairie Hill lamproites range from Mg-poor (4-7% MgO), silica-rich compositions in the main plug, to more Mg-rich (8-12% MgO, 750 ppm Ni) compositions in the satellite or ring dyke (Table 42). The more Mg-rich, olivine-bearing lamproites have slightly lower SiO_2, K_2O, and TiO_2 contents, and a generally lower abundances of incompatible elements. Large variations occur in the abundances of Ba, Rb, Sr, and U; much of this variation probably reflects the greater mobility of these elements under the strong weathering experienced by Prairie Hill.

BROOKING CREEK

Dr P.E. Playford of the G.S.W.A. first noted the Brooking Creek lamproite in 1972, while studying the carbonate sediments of the area. It is located 4 km southeast of the Leopold Downs airstrip (LEOPOLD DOWNS, GR:617132). The only published report of the intrusion is by Nicoll (1981), who studied the alteration

TABLE 42. REPRESENTATIVE ANALYSES OF EASTERN LENNARD SHELF LAMPROITES.

	1	*2*	*3*	*4*	*5*	*6*	*7*	*8*
				Percent				
SiO_2	50.47	55.06	52.11	52.60	51.70	49.10	51.67	47.72
TiO_2	5.67	5.78	5.90	6.14	5.42	6.82	4.17	6.67
Al_2O_3	7.38	6.90	8.96	7.60	7.90	8.60	8.92	8.81
Fe_2O_3	5.72	6.12	5.11	5.70	4.70	6.90	2.88	8.25
FeO	1.62	1.32	1.17	1.47	2.37	1.23	3.19	0.32
MnO	0.09	0.08	0.05	0.09	0.08	0.10	0.08	0.06
MgO	9.12	6.85	5.78	6.95	8.82	5.90	9.09	5.53
CaO	4.15	3.33	1.98	3.88	3.30	3.13	3.73	2.00
Na_2O	0.44	0.47	0.08	1.00	0.88	0.19	0.27	0.06
K_2O	8.80	8.37	11.67	9.36	8.78	8.92	8.40	9.66
P_2O_5	0.75	0.96	1.51	0.91	0.69	1.38	0.93	1.49
H_2O^+	2.64	1.54	1.83	1.10	2.17	2.68	2.67	3.62
H_2O^-	0.41	0.59	0.91	0.44	1.65	1.53	1.98	2.95
CO_2	0.75	0.22	0.21	0.15	0.01	0.08	0.24	0.23
Rest	2.05	1.90	1.84	2.71	1.92	2.85	1.43	1.86
Total	**100.06**	**99.49**	**99.11**	**100.10**	**100.39**	**99.41**	**99.65**	**99.23**
				Parts per million				
Ba	11 253	9 660	8 565	16 710	10 089	16 411	7 158	7 222
Li	10	10	13	7	25	22	5	5
Rb	341	328	245	338	219	287	512	446
Sr	777	835	1 416	1 196	924	1 040	1 038	1 120
Pb	37	31	57	40	26	52	33	78
Th	27	27	23	16	18	27	17	64
U	3	4	1	<1	<1	1	1	5
Zr	1 225	1 233	1 147	1 250	989	1 192	927	1 618
Nb	166	181	117	122	108	150	81	227
Y	15	16	19	18	13	19	7	36
La	245	212	317	295	269	351	172	637
Ce	355	325	450	303	290	400	266	1 028
Nd	—	—	—	—	—	—	—	420
Sc	—	—	—	21	20	27	—	—
V	204	240	614	148	160	315	153	303
Cr	490	408	266	255	445	449	220	635
Co	33	32	—	30	38	47	—	—
Ni	235	181	241	143	749	318	337	475
Cu	70	70	36	88	98	94	38	56
Zn	78	76	87	89	70	94	61	87
Sn	6	7	7	—	8	13	9	16
Mo	—	—	4	3	1	<1	5	6
Ga	13	14	24	12	15	14	14	22
As	2	4	2	—	<1	1	1	2
S	—	—	—	780	930	2 960	—	-
F	3 900	4 600	3 700	4 036	2 920	3 920	1 900	2 200
Cl	—	—	—	227	<20	20	300	—

1 — Phlogopite-leucite lamproite; inner zone, Mount Rose, BMR 67160338 (Derrick and Gellatly, 1972). 2 — Diopside-phlogopite-leucite lamproite; Mount Rose, BMR 69161334. 3 — Vesicular phlogopite-leucite lamproite; McKinrick Hill, BMR 80210069. 4 — Phlogopite - potassic-richterite - diopside - leucite lamproite; main plug, Old Leopold Hill, GSWA 71371. 5 — Diopside-olivine-leucite lamproite; satellite or ring dyke, Prairie Hill East, GSWA 71887A. 6 — Diopside-olivine-leucite lamproite; main plug, Prairie Hill East, GSWA 71890A. 7 — Olivine-leucite lamproite; Brooking Creek, BMR 80210125. 8 — Olivine-phlogopite-leucite lamproite; Hooper West, BMR 80210083.

of conodont colour in the metamorphic aureole within the surrounding limestones, but not the lamproite itself.

The sketch map of Nicoll (1981) shows three small rounded pods of lamproite, the largest only 15 m diameter, intruding the gently dipping limestones of the Napier Formation. The outcrops consist of low mounds of lamproite rubble, and the limestone within 1 m of the contact is baked to dark grey or black. The lamproite is a porphyritic olivine-leucite lamproite, black on fresh fractured surfaces and remarkably fresh.

In thin section, the rock is seen to consist of microphenocrysts of fresh olivine and leucite (up to 1 mm across) in a cryptocrystalline matrix. The olivine crystals range from euhedral to subhedral prisms and include skeletal and hopper types; many have tiny inclusions of chromite. A few, large, irregular, xenocryst olivines, some 2 mm in diameter, show undulose extinction. The leucite phenocrysts exhibit polysynthetic twinning, and amoeboid aggregates of leucite often contain granules of green pleonaste (Jaques and Foley, 1985). The groundmass is unaltered and crowded with minute leucite euhedra, equally small prisms of diopside and priderite, rare ilmenite granules, sparse interstitial devitrified glass, and rare phlogopite grains. A few small spherical vesicles are filled with green chloritic material. An analysis of this rock is given in Table 42.

Limestones within 1 m of the margin of the lamproite have been metamorphosed. From an examination of the conodonts and their discoloration, Nicoll (1981) estimated that the limestone at the contact had reached temperatures in excess of 600 °C. The limestones at the contact contain spurrite, merwinite, Fe-periclase, perovskite, and gehlenite, as well as calcite. This assemblage indicates metamorphism under very low pressures and high temperatures, possibly as high as 820 °C, based on the coexistence of merwinite and calcite (Walter, 1965). This is similar to the temperatures estimated for the wall rock of Ellendale 38 and indicates a magmatic temperature of about 1 200 °C.

J J BORE

This lamproite pipe was discovered by Gellatly (1979) and is located in rough karst terrain of the Devonian Pillara Limestone, 2.5 km south-southeast of the Brooking Creek lamproite (LEOPOLD DOWNS, GR:622107). The body is about 350 m long by 100 m wide, and elongated north-northeast. The pipe has good outcrop and is filled with leucite lamproite tuff. Approximately 300 m east of the pipe is a 400 m-long leucite lamproite dyke that fills an east-southeast trending fracture (Gregory, 1981a). The area is extremely difficult of access and has not been visited by the authors; no further information or samples are available.

UNEXPOSED LAMPROITES

A number of unexposed lamproites have been located by mining companies during exploration for diamonds. All the bodies are small, and contain leucite lamproite tuffs and intrusive rocks, the least prospective rock type for diamond. It is probable that a number of other lamproites are present, as many aeromagnetic anomalies have not been followed up. The following is a list of the intrusions with details as known.

Hooper West

This small irregularly shaped diatreme was first reported by Gellatly (1980); it is located 14.5 km southwest of Prairie Hill East (HOOPER, GR:865138). Geologically it occupies a similar position to the Big Spring pipes and is located close to the unconformity between Devonian limestones and the Proterozoic Lennard Granite. Country-rock outcrop is poor, and the diatreme itself is concealed beneath several metres of soil.

The lamproite is about 2 ha in area, about 250 m long, and elongated east-west. The vent is filled by a tuff-breccia containing angular fragments of lamproite up to 5 cm across, and rounded granite xenoliths up to 10 cm across. The eastern end of the body widens to about 120 m and includes a small plug of olivine-phlogopite-leucite lamproite. Phlogopite phenocrysts up to 7 mm long have been separated from this rock and dated by Jaques and others (1984b) at 21.9Ma.

The tuff-breccia, apart from the altered granite xenoliths, contains a variety of lamproite inclusions and clasts of early formed, fine-grained tuff in a sparse matrix of lamproite ash and fragments of microcline and biotite. The whole is traversed by anastomosing veins of calcite. The clasts of tuff are angular and consist of small fragments of microcline, quartz, and biotite, in a clayey matrix altered from lamproite. The larger juvenile lamproite lapilli have lobate margins that indicate incorporation into the tuff while still plastic; they are of fine-grained olivine-diopside-leucite lamproite. In one example, the turbid matrix contains small flakes of phlogopite, prisms of priderite, and a few partly leucoxenized perovskite grains; in another vesicular example, the matrix is a devitrified glass with many small perovskite grains. The olivine in both examples is pseudomorphed by talc. Another, more altered, variety appears to have been olivine-rich, with little leucite, and large grains of perovskite.

The small plug at the eastern end of the pipe is of fine-grained olivine-phlogopite-leucite lamproite and contains sparse small xenoliths of altered fine-grained sediments and granitoids, together with cognate fragments of finer grained lamproite. Sparse, altered macrocrysts (up to 3 mm) and smaller (up to 1 mm) phenocrysts of olivine, now replaced by nontronite and/or hydrotalcite, together with euhedral to rounded and embayed macrocrystal phlogopite, are set in a turbid groundmass of abundant altered leucite euhedra, prisms of priderite, and interstitial green-brown clay. The phlogopite flakes are generally pale coloured, weakly pleochroic, and free of inclusions; some have kink-bands indicating solid-state deformation.

The Hooper West olivine-phlogopite-leucite lamproites are broadly similar to some of the Mg-poor, phlogopite-rich lamproites of the Ellendale Field, *e.g.*

Mount North, Mount Percy, and 81 Mile Vent, in terms of their comparatively low SiO_2, moderate to high K_2O, high TiO_2, and high Ni content (Table 42). The Hooper West lamproites share the extreme enrichment in incompatible elements Rb, Pb, Th, Zr, Nb, and LREE, which characterizes the phlogopite-rich lamproites of the Ellendale Field.

Brooking Gorge

A small lamproite body is located 17 km north of Fitzroy Crossing and 5 km east of the entrance to Brooking Gorge (FITZROY CROSSING, GR:744049) (Boxer, 1980a). The body is approximately 0.1 ha in area, 50 × 25m, and is concealed beneath 1.5-6 m of soil and calcrete. The lamproite intrudes the limestones of the Devonian Napier Formation.

J K Yard

Three small lamproites were located by ground magnetometer surveys in an area south of the Fitzroy River and about 15 km south of Old Leopold Hill. Exploration work on these concealed bodies has been reported by Boxer (1980b). The location and size of each body is as follows: J K Yard, 1.8 ha in area, located 2.5km southwest of J K Yard (HOOPER, GR: 983110); J K Yard East, 1.6 ha, 2.8 km southeast of Blue Bush Yard (HOOPER, GR:079131), and J K Yard Southeast, 0.3 ha, 5.6 km south-southeast of Blue Bush Yard (HOOPER, GR:067092). The intrusions are concealed beneath 3-6 m of sand and clay, part of the alluvial deposit of the Fitzroy River, and are located geologically near the trace of the unconformity between Devonian limestone and siltstones and the underlying granite and granite gneisses of the Lamboo Complex. These bodies therefore form part of the same group as the Big Spring and Hooper West lamproites.

J K Yard is emplaced in Devonian limestone and, from drill logs, contains both lamproitic tuffs and hypabyssal rocks. J K Yard East is similar, but emplaced in granite and granite gneiss. J K Yard Southeast appears to be a small lamproite plug emplaced in granite. No samples are available for examination, and Haebig (1983b) reports that no microdiamonds were found in drill-spoil digested in HF.

Stoney Creek

This small, partly exposed, lamproite is located at 125° 58'E, 17° 59'S (HOOPER, GR: 138078), about 30 km northeast of Geikie Gorge. The intrusion consists of a circular plug about 110 m diameter and a smaller satellite body immediately to the northwest. Lamproite from the main body is a fine-grained phlogopite-leucite lamproite, while the satellite plug is a coarser diopside-leucite lamproite.

The plug intrudes sandstones and conglomerates (Devonian or ?Permian), which outcrop along the western edge of the main body. Ground traversing showed a magnetic anomaly of 161 nt over the lamproite.

CALWYNYARDAH FIELD

Within a few kilometres of Calwynyardah homestead, there are two large and five small concealed lamproites. This small group of intrusions forms the core of the Calwynyardah Field and covers an area of less than 50 km^2 (Fig.102). A few outlying lamproites, including Hansons Bore in the west and Fishers Dam in the east, are considered to belong to the same field, which is distinct from the Ellendale Field to the north and the Noonkanbah Field to the south (Plate 1). The lamproites of the Calwynyardah Field lie along the northern margin of the Fitzroy Trough, a fault bounded graben and major structural feature of the northern Canning Basin; their location is probably controlled by major basement faulting.

All the lamproites of the Calwynyardah Field were discovered by the Ashton Joint Venture after groundmagnetic follow-up of aeromagnetic anomalies located during a regional survey that followed the discovery of the Ellendale Field.

Access to the area is good, as the Great Northern Highway traverses the area and there are many good station tracks. However, only one lamproite in the field is exposed, Hansons Bore, and then only an insignificant outcrop of weathered tuff and thin tuffisite veins.

The topography is very subdued: there are broad, open sandplains, low ridges, and some low sand dunes in the south of the area. The vegetation is either open grassland or dense pindan scrub: the latter comprises small eucalypts, acacia, and an understorey of tall grasses.

GEOLOGY AND STRUCTURE

The regional geology of the Calwynyardah area has been described by Derrick and Playford (1973) and Crowe and Towner (1981). The area is underlain by poorly outcropping rocks of the Permian Noonkanbah and Hardman Formations and the Triassic Blina Shale. The Noonkanbah Formation consists of grey micaceous mudstone and interbedded calcareous sandstone; it outcrops in The Sisters synclinal structure to the northwest of Calwynyardah homestead. The mudstones are overlain conformably by the fine to coarse, well-bedded sandstones of the Hardman Formation. This unit forms the principal outcrop of the Warrawadda and Mount Wynne anticlinal structures west of Calwynyardah and the low ridge on which the homestead stands. The mudstones of the Blina Shale unconformably overlie the Permian rocks, and small outcrops are found in the west of the area.

Structurally, the area lies along the northeast margin of the Fitzroy Trough, the most important structural feature of the northern Canning Basin. The margin of the trough is marked by a series of overlapping, southeast-trending normal faults, each stepping down to the southwest. The sedimentary sequence on the adjacent Lennard Shelf is up to 2 km thick; but, within the trough, at least 8 km of sediments, from Ordovician to Jurassic in age, overlie the crystalline Precambrian

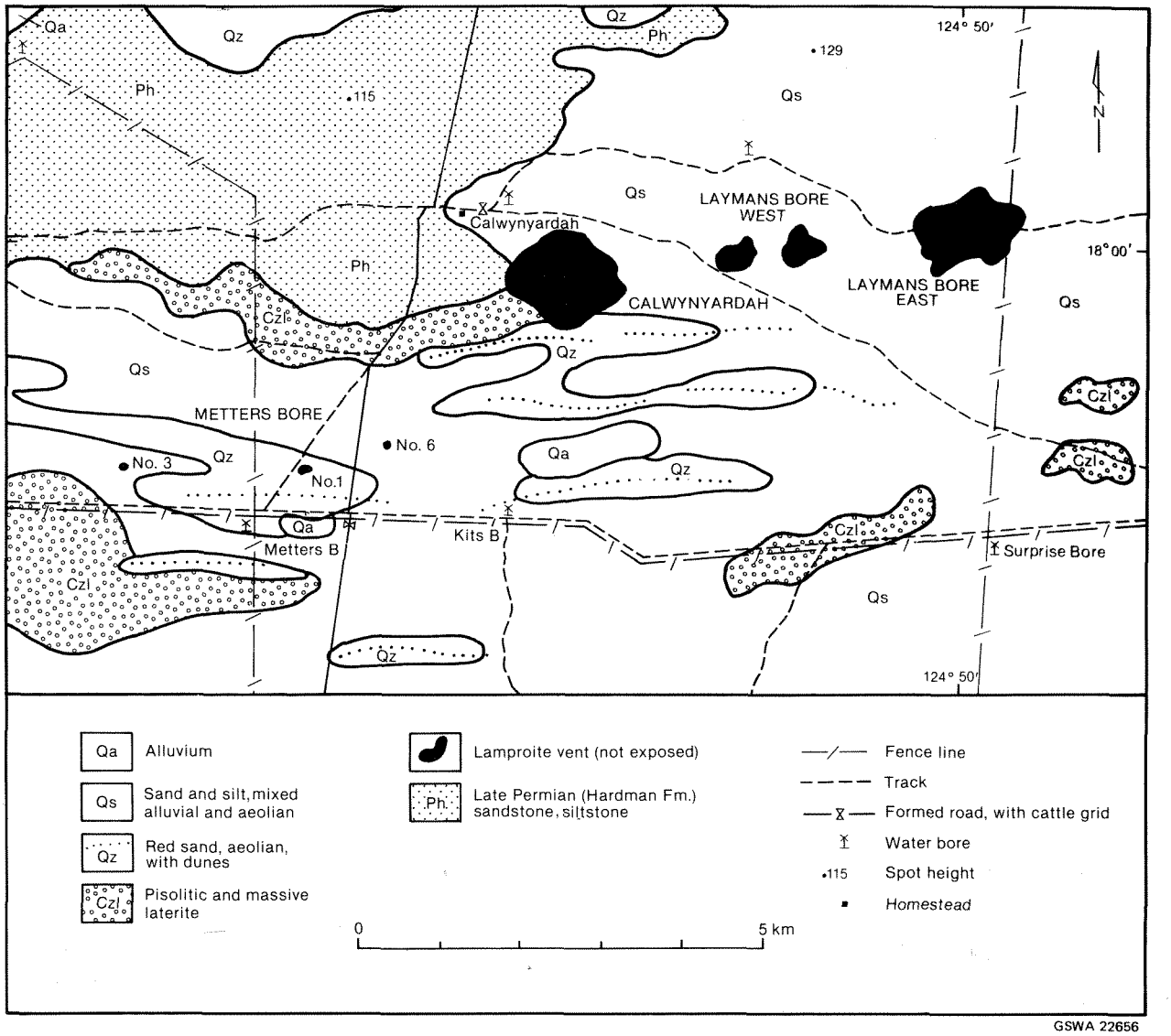


Figure 102. Geology of the Calwynyardah area.

basement. The trough was initiated in the Middle Devonian as a tensional structure; and the boundary faults continued to grow, as deposition proceeded, until Early Permian times. In Triassic or Early Jurassic times, tectonism was renewed, and the faults reactivated under a compressional, dextral-wrench stress field, probably arising from the breakup of Gondwana (Veevers and Cotterill, 1976). This last phase of faulting probably gave rise to most of the minor east-west folds and north-south faults found throughout the Fitzroy Trough (Smith, 1968).

In the Calwynyardah area, the principal boundary fault is the Harvey Fault, which forms part of the Pinnacle Fault System. It outcrops within the Sisters Structure and passes a few kilometres north of the main group of Calwynyardah lamproites. The folding associated with the Sisters Structure, and the nearby Warrawadda and Mount Wynne structures, may be reverse drag anticlines associated with the growth of the Harvey Fault (Forman and Wales, 1981) but Rixon (1978) has shown by clay modelling that similar small scale structures could be concentrated along the margin of the trough by wrench-faulting.

The Calwynyardah Field is located, therefore, in the vicinity of major faults that extend to the basement, faults which no doubt influenced the emplacement of the lamproites; but, with the possible exception of Hansons Bore, which intrudes the crest of the Warrawadda Structure, the lamproites are not related to the minor folding in the sediments.

CALWYNYARDAH

The Calwynyardah pipe is, after Walgidee Hills, the largest known pipe in the West Kimberley Province. It is slightly oval in shape, 124 ha in area, and has maximum dimensions of about 1.5 km east-west and 1.2 km north-south (Fig. 103). The pipe is located less than a kilometre southeast of Calwynyardah homestead and is concealed beneath 3-9 m of sand and laterite.

The geology of the Calwynyardah vent is known only from a small number of drill holes up to 292 m deep, scout drilling, and bulk sampling for diamonds (Haebig, 1979b, 1983c; Boxer and Haebig, 1980a,b). The pipe is distinctive in being almost entirely pyroclast-filled; only small intrusions of magmatic hypabyssal lamproite are known. The tuff sequence includes "sandy" tuff — tuffs

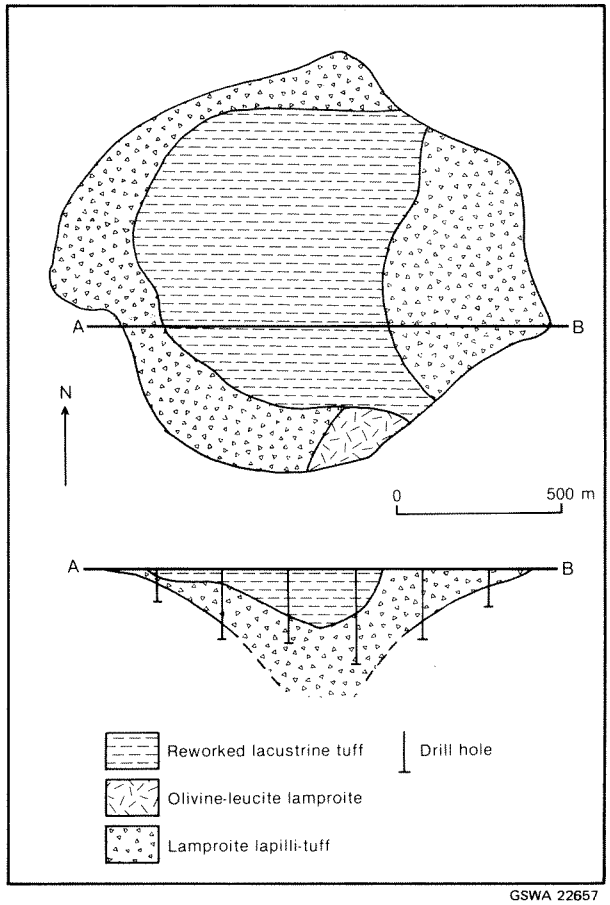


Figure 103. Geological map of Calwynyardah pipe. (after Boxer and Haebig, 1980a).

and lapilli-tuffs rich in accidental lithic fragments derived from disaggregated wall-rock — and olivine lamproite tuff, often autolithic. These are intruded by thin lamproite sheets and a small lamproite plug on the southeast margin of the pipe. The pyroclastics are overlain by a thick sequence of mudstone or reworked silty tuff which occupies much of the surface area of the vent. Thin lignite seams in the silty tuff have yielded palynomorphs of mid-Miocene to early Pliocene age (Atkinson and others, 1984a). The reworked tuffs and sediments are up to 150 m thick near the centre of the vent.

The geometry of the vent, as revealed by drilling, is similar to that found in many of the Ellendale pipes — the broad surface feature narrows rapidly with depth to a relatively small conduit, giving a "champagne glass" shape to the pipe overall. The drilling also showed that the fine-grained silty tuff or mudstone unit is rootless, and fills a depression in the main pyroclastic deposits. The sequence at Calwynyardah thus preserves a further stage not seen in other vents, namely sediments of a crater lake. Following the initial explosive pyroclast-forming phase and the quiet intrusion of magmatic lamproite (a minor feature of the Calwynyardah vent) there was a further phase in which decomposed tuff from the surrounding tuff ring was washed back into the vent to form reworked tuffaceous lake-bed deposits. The lignite horizons were formed by decomposing lake vegetation; the coarser lapilli-tuff intercalations may have resulted from renewed volcanic activity, but are more likely to represent less decomposed tuff slumped into the crater from the tuff ring; the tuff ring itself has been removed by later erosion. The crater lake formed in the vent shortly after cessation of volcanic activity, and the form of the lake bed would have been considerably modified by the compaction resulting from the deposition of reworked tuffs, but it appears likely that the small plug of lamproite on the southeast side of the vent originally formed a small lava blister within the vent.

Because of its size, the Calwynyardah pipe has been extensively prospected for diamonds. However, thirty bulk samples, totalling approximately 1 330 t, yielded only one diamond (0.015 CM) when processed through an HMS plant. The HF digestion of 21 samples from air-core drilling (each of about 25 kg) yielded a further 48 microdiamonds — only three samples were barren; a further four microdiamonds were obtained from air-blast drill chips (Haebig, 1983c). All the diamonds were obtained from the coarser tuff; the reworked tuffaceous lake deposits were not tested.

Petrography

A variety of tuffs are present in the Calwynyardah vent. They range from fine-grained tuffs, rich in accidental lithic material and resembling siltstone, to olivine-lamproite tuffs incorporating few accidental wall-rock clasts.

The finest grained tuffs are reconstituted wall rock and consist essentially of siltstone with no obvious juvenile component. The rock is usually bright-green in hand specimen, and shows obvious brecciation and disruption. In thin section, the rock contains abundant yellow-green chloritic material in addition to quartz and small muscovite flakes. Similar fine-grained tuffs, which, however, have a lamproite-derived clay matrix, are found interbedded with lamproite lapilli tuff throughout the vent.

The reworked lacustrine tuff which occupies the central area of the vent is a uniform cream-coloured rock that consists of a small proportion of quartz and microcline grains in a fine-grained matrix of chlorite, clay minerals, and carbonate. Only a few small flakes of phlogopite can be identified as of lamproitic origin. A poorly preserved relic fragmental texture allows the identification of a few lamproite fragments and pseudomorphs after olivine.

The dominant pyroclastic filling the vent is a carbonated phlogopite-olivine lamproite lapilli-tuff (Fig. 104) that consists of rounded juvenile and cognate lapilli of lamproite, a few rounded pyroclasts of shale up to 6 mm across, and flakes of phlogopite up to 3 mm long, in a matrix of comminuted ash-sized lamproite and secondary carbonate. Occasional xenocrysts of garnet and picrochromite have been observed in some thin sections. Many of the juvenile lapilli appear to have been magmatic droplets rather than fragments rounded by attrition. Some lapilli are cored with nuclei of altered olivine macrocrysts or shale fragments; but many olivine

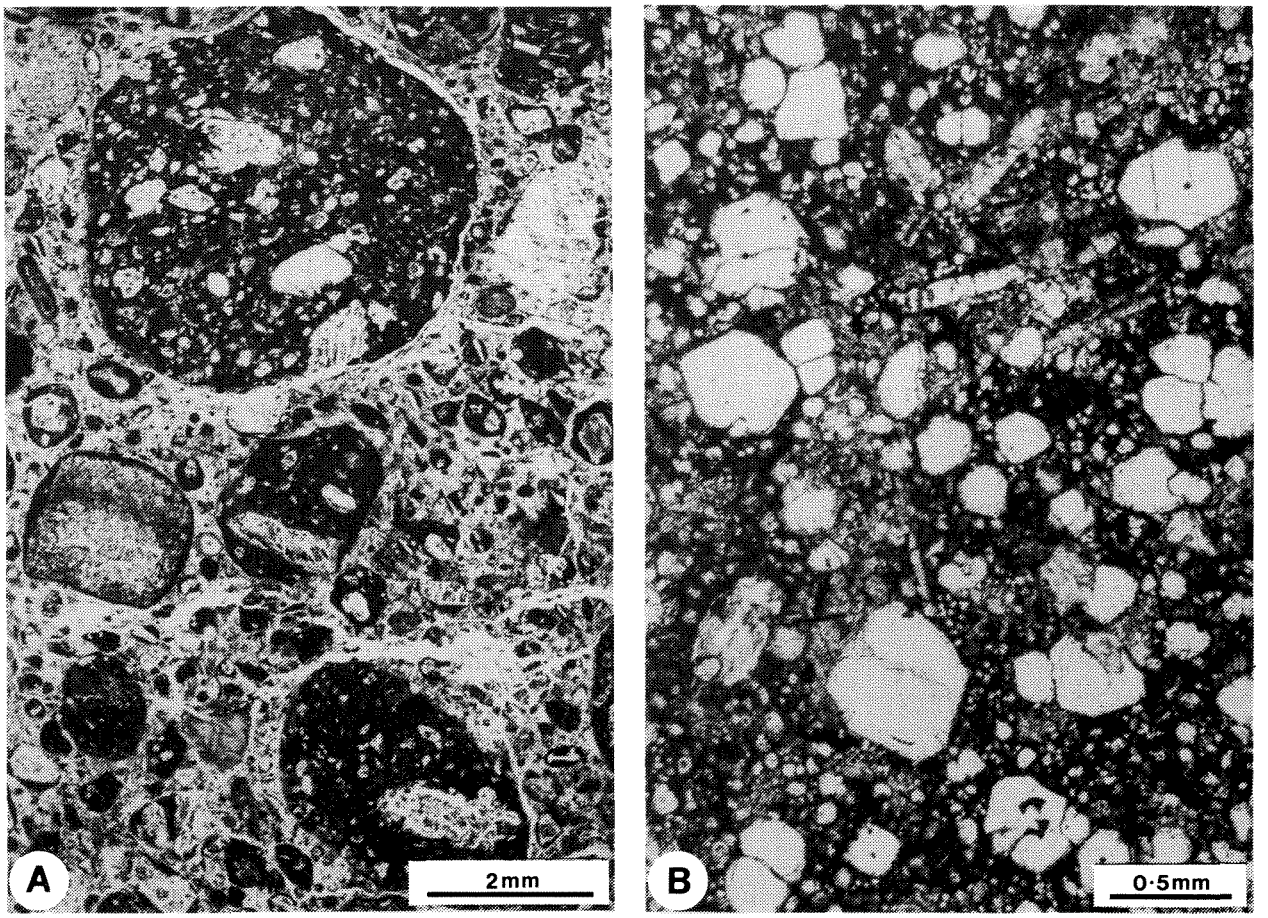


Figure 104. Photomicrographs of Calwynyardah lamproite: A — Lapilli-tuff with spheroidal lapilli of phlogopite-olivine lamproite in an altered ash matrix (GSWA 76075). B — Diopside-leucite lamproite with minor groundmass potassic richterite and small, dark prisms of priderite (GSWA 76076A).

macrocrysts and phlogopite flakes have only a thin magmatic skin adhering to them. The juvenile lapilli are of phlogopite-olivine lamproite containing former macrocrystal olivines up to 3 mm across, and microphenocrysts of olivine and phlogopite in a brown chloritic matrix. The rock has been extensively veined by carbonate, and the olivine replaced by carbonate or talc. Some tuffs also contain a small proportion of accidental lithic clasts predominantly derived from the wall rock.

No sample is available from the small lamproite stock, but drill holes and trenches intersected a number of veins and sheets of leucite lamproite intruding the tuff pile. These are probably of a similar rock type to the stock. Two varieties of lamproite are found, diopside - potassic-richterite - olivine - leucite lamproite and a fine-grained olivine-leucite lamproite (Fig. 104). Both varieties are rich in small euhedral olivine crystals, now pseudomorphed by talc. The coarser variety has leucite crystals up to 1.5 mm across — many with fresh cores, small prisms of diopside and poikilitic potassic richterite up to 1 mm across. The potassic richterite is very strongly pleochroic from orange to purplish-red. The matrix, which contains abundant priderite, is glassy; and, where fresh, the glass is pale apple-green in colour. The finer grained variety is crowded with small leucite euhedra in a matrix containing minute diopside prisms, abundant priderite, a little phlogopite, and green interstitial feathery chlorite after devitrified glass.

LAYMANS BORE EAST

The Laymans Bore East vent lies 6 km east of Calwynyardah homestead (Fig.102) and is an irregular shaped pipe 103 ha in area, approximately 1 300 × 1 000 m. The vent is concealed beneath sand, clay, and laterite deposits, up to 26 m thick. Laymans Bore East is very similar to Calwynyardah: it contains a thick sequence of olivine lamproite tuffs overlain by a silty tuff, up to 77 m thick, which is probably of lacustrine origin. There is, however, no evidence of a plug of magmatic lamproite: the vent is entirely filled by pyroclastics.

Drilling, to a maximum of 224 m, has established the geometry of the pipe, which is of "champagne glass" shape and similar to Calwynyardah.

The results of diamond exploration are given by Boxer and Haebig (1980c). Fifteen bulk samples, totalling 592 t, yielded 4 diamonds totalling 0.075 CM. The largest stone being 0.045 CM. HF digestion of drill samples recovered a further 79 microdiamonds. In this pipe, samples from the silty tuff crater-lake deposits were also examined, and the microdiamond count was not signifantly different from the main body of tuff.

Petrography

The tuff that fills most of the vent is a lapilli-ash tuff containing abundant, sub-rounded, altered fragments of olivine lamproite, and a few fragments of shale up to 5 mm across. The matrix is of comminuted lamproite ash, but contains a proportion of rounded quartz grains that were derived from the wall rock and a little secondary carbonate. The lamproite contains fine-grained microphenocrysts of olivine in an indeterminate groundmass. A few altered olivine macrocrysts, up to 3 mm across, are found as isolated crystals. One large composite lapillus, about 6 mm across, is an aggregate of smaller accretionary lapilli.

Interbedded with the lamproite lapilli-tuffs are finer grained tuffs with a high content of angular quartz grains; some have been coloured bright green by the development of nontronite.

The reworked silty tuff occupying the central part of the vent is very similar to that found in the Calwynyardah vent. Very small grains of quartz and microcline can be identified in a clay matrix which preserves a poor, relic, fragmental texture.

LAYMANS BORE WEST

These two smaller pyroclast filled vents of 12 ha and 16 ha area complete the east-west line of vents extending east from Calwynyardah homestead (Fig.102). The lamproitic tuffs are concealed beneath a sandy overburden 7-10 m deep. No samples of the tuff are available; but, as these two vents are closely allied to Calwynyardah and Laymans Bore East and appear to arise from the same east-west structure, it is reasonable to suspect that the tuffs are very similar petrographically.

The only specimens available from Laymans Bore West are a few drill chips of leucite lamproite. A fine-grained variety is olivine-leucite lamproite with abundant small altered olivines and leucite set in a sparse, dark-coloured matrix of devitrified glass and prisms of priderite. A coarser grained variety contains, in addition, small prisms of diopside, interstitial potassic richterite and infrequent interstitial phlogopite.

Sampling for diamonds by Hughes auger gave 13 samples, totalling 372 t, from which 5 small diamonds weighing 0.045 CM were recovered: the largest was 0.025 CM and came from the smaller western pipe. A further 12 microdiamonds were recovered from HF digestion of drill chips (Haebig, 1983c).

HANSONS BORE

The Hansons Bore lamproite is the only outcropping vent in the Calwynyardah Field. It is approximately 8.6 ha in area (400 × 325 m), but the outcrop consists only of a few scattered masses of lamproitic lapilli-tuff veined by fine-grained tuffisite over an area about 20 m square. The vent is located on the crest of a low ridge about 1 km south of the Great Northern Highway (ELLENDALE, GR:673252); this ridge also marks the crest of the Warrawadda anticlinal structure, although the relationship is probably accidental.

The lamproite intrudes fine-grained siltstone of the Hardman Formation, which has been stained apple green for some distance from the vent. Within the pipe, early formed lamproite lapilli-tuffs are intruded by a plug of olivine-rich leucite lamproite about 300 m in diameter. Unfortunately, no sample of the central plug is available; but the lapilli-tuffs were excavated during exploration activity, although no diamonds were recovered (Boxer and Haebig, 1980b).

Both in the limited outcrop and in trench samples, the tuff is a uniform fine- to medium-grained lapilli-tuff that contains a few small shale pyroclasts as well as grains of quartz and microcline from the wall rock. The matrix comprises small lamproite shards and blebs, and is partly carbonated. The lamproite lapilli range up to 10 mm across: a few cognate lapilli are of dense, fine-grained, porphyritic phlogopite-leucite lamproite; but most are of irregular to lobate shape, weakly vesicular, and contain phlogopite phenocrysts up to 2 mm long, and altered leucite microlites, in a glassy base.

The tuffisite veins observed in outcrop are fine-grained, and consist of a homogeneous mixture of small ash-sized lamproite fragments, quartz grains, and phlogopite, up to 0.5 mm across, and a few larger lapilli of lamproite and shale, and occasional olivine pseudomorphs up to 3 mm.

MINOR LAMPROITE INTRUSTIONS

In addition to the larger lamproite vents, a number of smaller bodies are known from the Calwynyardah Field; all are less than 2.5 ha in area and unexposed. All have been examined for microdiamonds and reported by Boxer and Haebig (1980a,b).

Metters Bore

Of six aeromagnetic anomalies in the Metters Bore area, ground magnetic traverses and scout drilling proved three to be small lamproite bodies. The lamproites are aligned roughly east-west, parallel to, but 3.5 km southwest of, the Calwynyardah alignment (Fig. 102). Brief details of the lamproites are as follows:

Metters Bore No. 1: 2.5 ha in area, located 1 km north-northwest of Metters Bore (HARDMAN, GR:860062), concealed beneath 2 m of sandy soil and 1.5 m of pisolitic laterite. Drilling and trenching have shown that both pyroclastic and intrusive varieties of leucite lamproite are present.

No specimen of the pyroclastics is available; the intrusive lamproite is a porphyritic olivine-diopside-leucite lamproite. Altered phenocrysts of leucite and olivine up to 2 mm across, and small prisms of fresh diopside, are contained in a matrix of minute leucite euhedra, interstitial devitrified glass, and acicular priderite. Minute octahedra of chromite are present, and a large spongy leucite mass contains grains of a grey-green spinel, probably pleonaste.

A total of about 500 t of material was processed through an HMS plant for diamonds without success,

i.e. without recovering diamonds of 0.8 mm diameter or more. However, HF digestion of two 25 kg samples of drill core proved the body to be rich in microdiamonds. A total of 37 microdiamonds were recovered, none larger than 0.2 mm diameter.

Metters Bore No.3: 2.5 ha in area, located 1.9 km east of Metters Bore (HARDMAN, GR:838062), concealed beneath 3 - 6 m of windblown sand, laterite, and clay. From drilling records, the vent contains leucite lamproite lapilli-tuff. Thirteen microdiamonds, all <0.2 mm diameter, were recovered from two samples.

Metters Bore No.6: 2.0 ha in area, located 1.3 km east-northeast of Metters Bore (HARDMAN, GR:871065), concealed beneath 2 m of laterite. This small plug of phlogopite-leucite lamproite produced 2 microdiamonds from 50 kg of sample after HF digestion.

Merrilees Bore

This small lamproite, 0.8 ha in area and concealed beneath 8-11 m of sand, is located 1 km southwest of Merrilees Bore (ELLENDALE, GR:769147). Two microdiamonds were recovered from drill chips (Haebig, 1982).

Billys Bore

Two small concealed lamproites are located close to a fault which forms part of the Pinnacle Fault System (Plate 1).

Billys Bore West: 1.6 ha in area, located 3 km north-northwest of Billys Bore (ELLENDALE, GR:920234). One 25 kg sample produced a single microdiamond of 0.10 mm diameter. Trenching to a depth of 5 m revealed a variety of lamproitic pyroclastics.

Near surface specimens of the pyroclastics are strongly silicified, losing all but a relic fragmental texture in thin section. Fresher samples show a lapilli-tuff with xenoliths of shale in a carbonated matrix of comminuted lamproite ash and a few quartz fragments. Some cognate lamproite lapilli, up to 8 mm across, are of a fine-grained porphyritic phlogopite-leucite lamproite that contains phlogopite flakes up to 3 mm in a dark matrix crowded with minute altered skeletal leucite. Most of the lamproite component, however, is juvenile, and consists of irregularly shaped lapilli of glassy material and similar phlogopite phenocrysts. The lapilli sometimes enclose fragments of earlier lamproite.

The core of the vent is of fine-grained phlogopite-leucite lamproite, and is similar to the fragments found in the lapilli-tuff except that the phlogopite phenocrysts are darker coloured. The rock contains a few xenocrysts of quartz and microcline, and small xenoliths of shale. Irregular chloritic patches suggest that the mass has been autobrecciated.

Billys Bore East: a single drill hole intersected leucite lamproite lapilli-tuffs in this small body of about 0.3 ha, located 4 km north of Billys Bore (ELLENDALE, GR:948241). No microdiamonds were recovered.

Fishers Dam

This small pyroclast-filled vent is 0.5 ha in area and located 7.2 km northeast of Fishers Dam (ELLENDALE, GR:066191). No microdiamonds were recovered.

THE NOONKANBAH FIELD

The Noonkanbah Field covers a large area in the central part of the Fitzroy Trough and is the "classic" locality for lamproite intrusions. Although not so numerous as the lamproites of the Ellendale Field, many more are exposed and available for study. Seventeen intrusions are exposed; and, except for one small dyke, all have previously been described by Wade and Prider (1940) or Prider (1960). Exploration activity in the 1970's has discovered a further twelve concealed pipes (Plate 3, Table 2). The Noonkanbah Field provides a variety of intrusions from the large breccia pipe of Mount Abbott and the "volcanic spine" of Machells Pyramid, to the isolated dyke of Mount Cedric North and the large pluton-like body of the Walgidee Hills. Mount Abbott provided the first known source rock for chrome pyrope in Western Australia (Jeppe, 1971), and a number of the pipes are known to carry diamond, although not in economic quantities.

The topography is generally very subdued except for the small peaks formed by the lamproite plugs and a few low mesas of Permian sandstone. A broad area in the south and east is occupied by the floodplain of the Fitzroy River at about 60 m above sea level. The central area is a broad ridge at 80-100 m, and the sandstone mesa of Mount Hardman rises to 132 m; and the northeast, rising gently to 140 m, is a dune-field with numerous east-west dunes averaging about 8 m high.

The vegetation over much of the area of interest is an open grassland of spinifex and a variety of coarse perennial grasses. In sand dune areas, spinifex is the principal cover, but isolated large eucalypts and boab trees occur. The grassland passes into areas of low scrub; and the river courses, particularly the Fitzroy River, support dense stands of eucalypts and paperbark. Access is generally good; moderately well formed and maintained gravel roads run south from the Great Northern Highway through Calwynyardah to Noonkanbah homestead and along the northern side of the Fitzroy River. Most of the lamproites can be reached by station tracks, or cross-country, in four-wheel-drive vehicles. A few intrusions in the floodplain of the Fitzroy River may only be reached on foot, if the relevant creek crossing has not been maintained. These notes apply only in the dry season, from May to October; during the summer wet season, many tracks are flooded and impassable, and river crossings washed out. Supplies of food and fuel must be obtained in Derby or Fitzroy Crossing; potable water is available from a number of widely scattered bores.

Much of the Noonkanbah Field is covered by the Noonkanbah pastoral lease, which is occupied by the Yungngora Aboriginal Community. A number of the

lamproite intrusions are sites sacred to the community, and it is therefore advised that visitors inform the community elders of their intentions on arrival. The community requests that no alcohol be brought onto the station.

GEOLOGY AND STRUCTURE

The Noonkanbah Field (Plate 3) is located in the central part of the Fitzroy Trough, about 30 km south of the Calwynyardah Field. The main area of lamproite intrusion is found in the Quanbun Syncline, which is underlain by Permian and Triassic rocks; but a few lamproites are found south of the Fitzroy River in Permian rocks of the Saint George Ranges Anticline. The regional geology has been decribed by Crowe and Towner (1981) and the structure of the trough by Smith (1968) and Forman and Wales (1981).

Bedrock is very poorly exposed throughout most of the area except in a few small mesas, such as Mount Hardman, or in the vicinity of the lamproite plugs, such as Mount Abbott or Fishery Hill. The usual outcrop pattern is loose rubble on a wind deflated surface; although, in many areas where soil cover is thin, the basic stratigraphy and structure is revealed on air photographs. The main area of lamproite intrusion is underlain by the Late Permian Liveringa Group, principally the three members of the Hardman Formation; these are regressive marine and lagoonal sediments: sandstone, siltstone, mudstone, and subordinate calcareous siltstone and limestone. Some sandstones are cross-bedded. Good exposures of the lowest part of the succession, the mudstone and fine sandstone of the Kirkby Range Member, may be found on the northern bank of the Fitzroy River, north of Mount Ibis. The overlying Hicks Range Sandstone is well exposed on Mount Noreen and particularly on Mount Abbott, where it has been extensively disrupted by the lamproite intrusion. Thin-bedded sandstones of the Cherrabun Member are well exposed on Mount Hardman, and north and east of Mount Cedric. Except where disrupted by the intrusion of lamproite, the bedding dips gently at 15° or less, north or east towards the axis of the Quanbun Syncline.

The central part of the syncline is underlain by Blina Shale of early Triassic age, which overlies, possibly with slight angular unconformity (Crowe and Towner, 1976), the Permian Hardman Formation. The rocks are thin-bedded mudstones, sandy mudstones, and subordinate sandstones; these are very poorly exposed and often lateritized. Small exposures of lateritized shale may be found in roadside gravel pits north of the Walgidee Hills lamproite, and of the sandstones, in the vicinity of White Rocks lamproite.

A few lamproites outcropping in the floodplain of the Fitzroy River, and south of the river, are associated with small outcrops of Early to Middle Permian mudstones, shales, siltstones, and sandstones; of the Lightjack and Noonkanbah Formations.

Structurally, the Noonkanbah Field is located in the central and southern part of the Fitzroy Trough, and the lamproites have penetrated through a sediment pile up to 8 km thick, ranging in age from Ordovician to Triassic. Unlike the Pinnacle Fault System forming the northeast margin of the trough, where a number of parallel faults step down successively into the trough, the Fenton Fault System on that part of the southwest margin adjacent to the Noonkanbah area is a single normal fault with a downthrow to the northeast of at least 4 km (Crowe and Towner, 1981). The fault has not influenced the emplacement of the lamproites directly, but Late Triassic to Early Jurassic dextral wrench movement has given rise to east-west and north-south structures (Smith, 1968), which may have controlled emplacement.

The main structures within this part of the Fitzroy Trough are the Saint George Ranges Anticline and the Quanbun Syncline; both trend east-southeast and were formed as a result of dextral wrench movement on the Fenton Fault System. A third-order structure is small-scale north-south faulting. These faults are particularly well represented in the Saint George Ranges, where normal faults up to 20 km long are spaced from 1-2 km apart but rarely have a throw exceeding 200 m. A similar series of faults is found on the southern limb of the Quanbun Syncline in the main area of lamproite volcanism. The smaller number of faults mapped in this area is probably the result of poor outcrop rather than lack of faulting.

The lamproite intrusions are concentrated on the southern flank of the Quanbun Syncline, but an equal number are found scattered throughout the area of the syncline. The largest body, Walgidee Hills, intrudes the axial zone of the syncline; but a number, including White Rocks, lie north of the axis. Similarly, a few lamproites have been intruded south of the Quanbun Syncline, and the Sisters intrusions probably lie on an extension of the Saint George Ranges Anticline. It does not appear, therefore, that lamproite intrusion is related to the major surface structures within the Fitzroy Trough. A few lamproites, Mount Ibis and Fishery Hill for example, lie on or close to north-south faults; but most of the faults mapped have no association with lamproites: and most lamproites are not located on known faults. At most, these faults had only a local influence on a few lamproites.

The lamproite volcanism of the Noonkanbah Field is more probably related to basement structures not seen at the surface. The present folding within the sedimentary pile is the result of minor tectonism and transcurrent movement on the boundary faults in Late Triassic to Early Jurassic times — the Fitzroy Movement of Forman and Wales (1981). Crowe and Towner (1976), however, suggest that the area of the Saint George Ranges Anticline was active before this time. For example, the early Permian Poole Sandstone is thicker in the axial region of the anticline than on the flanks to the north or south, while the underlying Wye Worry Member is thinnest in the axial region. This suggests that the basement to the Fitzroy Trough is not a simple block but is made up of a number of fault-

bounded blocks or slices which subsided independently of each other. The location of folding during the Fitzroy Movement may, therefore, have been governed by pre-existent structures in the basement and sedimentary pile. It appears equally probable that the location of lamproite intrusions was governed by the same basement faults and they are only fortuitously concentrated on the southern limb of the Quanbun Syncline.

MOUNT ABBOTT

Mount Abbott forms a low, rounded, scrub covered hill rising about 45 m above the plain. The hill is capped by well-bedded sandstone, and much of the area east of the summit has good exposures of boulder-sized sandstone breccia with blocks commonly 1 m or more across. It was these signs of disturbance, and the induration caused by the underlying lamproite, that Hardman (1884) first noticed, and which led Prider (1960) to describe Mount Abbott as a cryptovolcanic vent. Most of the hillside is covered by sand, soil, and small amounts of calcrete, and the only evidence of lamproite appears to be the characteristic green staining of some of the sandstone.

Wade (Wade and Prider, 1940) suspected the presence of igneous rocks in some of the narrow gullies between outcrops of sandstone breccia, but it was Jeppe (1971) who first discovered weathered lamproitic pyroclastics beneath the soil cover, and recovered chrome pyrope from the rock and surface gravels. Detailed mapping and drilling by CRA Exploration in 1978 outlined a roughly circular body about 1 200 m × 1 300 m, about 90 ha of which is underlain by tuff or sandstone breccia, (Fig. 105; Boxer and Haebig, 1980a).

The summit area of Mount Abbott is formed by a distinct cap of sandstone about 400 m across, and marked by a small scarp about 10 m high. The sandstones are well-bedded, slightly indurated, and weather to smooth rounded forms. In contrast, the poor exposures of the same Permian sandstones outside the pipe are flaggy and friable. Bedding within the sandstone cap generally dips at a low angle, but around the margins of the block it is disrupted and dips up to 60° are common. Brecciation of the cap rocks is not prominent, but a few thin veins of tuff have been noted.

Near the northern margin of the pipe, and particularly in the northeastern parts, there are large rounded outcrops of strongly indurated sandstone. The bedding in these areas has been extensively disrupted and the rock is, in part, brecciated; but, in general, the sandstones are similar to those of the summit area.

Large areas of Mount Abbott, particularly the ridge east of the summit, expose a very coarse breccia of sandstone, which is composed of large blocks of sandstone in a very sandy matrix. The angular blocks range up to a metre or more across, but the only evidence of lamproite activity is the common green coloration of the matrix. This "megabreccia" is the most easily observed volcanic feature of Mount Abbott.

The presence of lamproitic tuff was suspected by Wade, but not found by Prider (1960); although difficult to find, it is now known to underlie much of Mount Abbott. Both the northern and southern slopes of the hill are deeply gullied by small streams, and it is in these gullies and along the foot of the scarp on the northern side of the summit sandstones that the best exposures occur. In addition, close examination of the soils reveals a small amount of pyroclastic "float" on which much of the mapping in Fig. 105 is based. Two broad types of tuff are seen, a very quartz-rich "sandy" tuff, often pale and having the appearance of a sandstone; and a dark green lamproite-rich lapilli-tuff that has a distinct fragmental texture. The "sandy" tuffs can usually be recognized as a tuff by the presence of a few lamproite fragments.

The "sandy" tuff occupies a broad east-west zone through the central part of the diatreme. Exposures north and south of the summit sandstones show a crude layering which dips beneath the sandstones at about 15°, as if the sandstone is floating on a bed of "sandy" tuff. This zone also includes the most prominent outcrops of sandstone megabreccia, and smaller areas of lamproite tuff.

The northern and southern parts of the vent contain poorly outcropping lamproite lapilli-tuffs, fewer areas of sandstone megabreccia, and little "sandy" tuff.

No magmatic core is known at Mount Abbott, and a dyke-like mass of altered olivine lamproite near the southwest margin of the pipe is the only non-pyroclastic rock encountered: it does not outcrop and was found only in a number of drillholes. The pipe is essentially filled by pyroclastics: and this is indicated by the ground magnetic pattern over the body, which does not show the strong dipole expected over a magmatic core, but instead is a complex pattern of small east-west trending highs and lows (Boxer and Haebig, 1980a)

Mount Abbott has been intensely prospected for diamonds, beginning with Stellar Minerals in 1968-1971. From about 200 t of material, including surface gravels and tuffs excavated from trenches, the company recovered indicator minerals but no diamonds (Jeppe, 1971). Between 1978 and 1980, CRA Exploration treated nine bulk samples of lamproitic tuff and "sandy" tuff totalling 560 t and recovered three small diamonds weighing 0.04 CM. In addition, two diamonds totalling 0.015 CM were recovered from a gravel sample, and 19 microdiamonds from 8 samples digested in HF (Boxer and Haebig, 1980a).

Volcanism

The style of volcanism exhibited by Mount Abbott is significantly different from that of other intrusions in the West Kimberley Province. Elsewhere, an initial explosive phase shaped the vent, cleared it of most of its original contents, and filled the vent with lamproite-rich pyroclastics that contained greater or lesser amounts of remaining wall-rock fragments. This explosive phase was generally followed by the quiet upwelling of magma to form sills within the tuff pile, or a lava lake within the vent. The result is a concentric arrangement of an

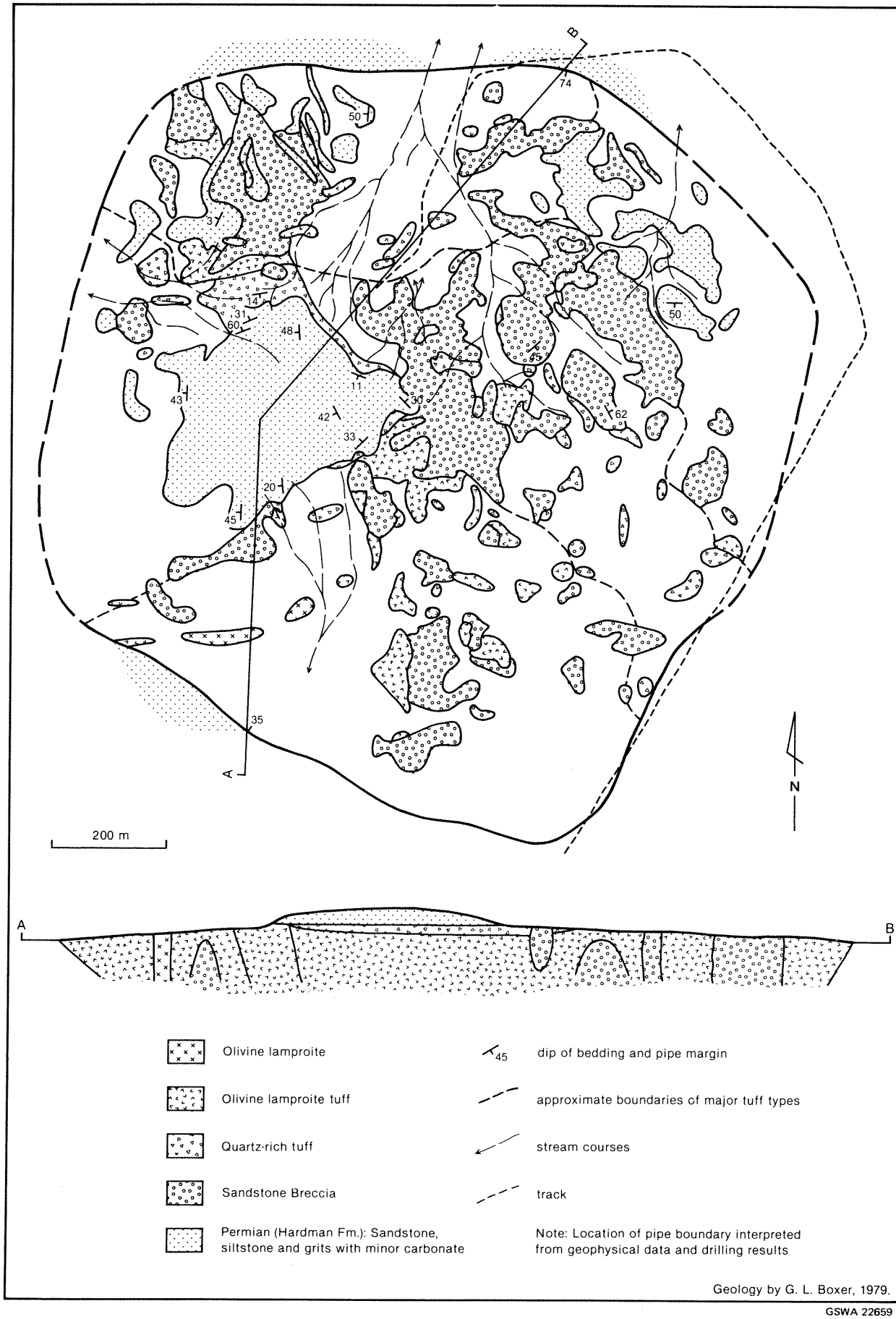


Figure 105. Geological map of Mount Abbott.

outer pyroclastic zone and a central magmatic core; this arrangement is preserved even where two vents coalesce.

At Mount Abbott, large volumes of country rock remain within the vent, and much of the tuff consists of disaggregated sandstone. The summit area may represent a large block that slumped into the vent after the initial explosive phase, but it is stratigraphically equivalent to the wall-rocks and cannot have slumped any great depth. Similarly, the presence of large areas of sandstone megabreccia indicates that the vent was not cleared in the initial phase. The distribution of lamproite tuff in areas on the north and south sides of the vent might suggest that two nearby vents coalesced, leaving the summit sandstones as a partial septum, but the overall shape of the vent is circular and the sandstone megabreccia is distributed throughout all areas.

In contrast to other lamproite vents in the West Kimberley, volcanic activity at Mount Abbott appears to have been relatively less violent but was probably of longer duration. The initial, most violent, phase was sufficient only to fracture the rocks over the area of the vent to form the sandstone megabreccia. It left the present summit area as a relatively undisturbed block, but was not sufficiently intense to remove the fractured rock from the vent. At this stage, little magma was involved, only volcanic gases, which were channeled through the megabreccia and which, by attrition of the sandstone, produced the quartz-rich tuffs. These now occupy a marginal position around the summit rocks and the numerous small vents within the sandstone megabreccia. Had activity proceeded no further, Prider's (1960) description of Mount Abbott as a cryptovolcanic vent would have been accurate. However, continued gaseous activity, and the ingress of lamproitic magma, led to the formation of small vents of lamproite tuff, and to the concentration of activity into certain areas in the north and south of the vent. Whether the several tuff zones were active simultaneously or successively is not determinable; but, if "sandy" tuff vents had formed in the northern and southern parts of the vents, they were either destroyed by later activity, or transformed by the addition of lamproite pyroclastics.

Apart from the sandstone megabreccia, the pyroclastics of Mount Abbott are uniformly fine-grained. The overall picture presented is one where volcanic activity, largely gaseous and involving magma only in the later stages, took place over a long period at a number of small vents. This activity was not explosive, as in other vents; and there is no evidence of vent-wide, bedded, base-surge deposits, although the presence of accretionary lapilli in many tuffs indicates subaerial activity. Except by attrition, the force of the volcanic activity was insufficient to remove the brecciated country rock from the vent.

Petrography

The quartz-rich "sandy" tuff is variable, but generally fine-grained, and contains at least 50%, and up to 80%, of small, angular grains of quartz and microcline, about 0.1 mm across, and a little accessory tourmaline, in a yellowish clay-rich matrix. A pyroclastic appearance is given to the rock by a few small fragments of glassy lamproite and larger iron-stained quartz aggregates which possibly represent an earlier tuff. In some sections, flakes of muscovite and small lapilli of metasomatized shale are present, and a very fine-grained specimen contains numerous spherical accretionary lapilli up to 6 mm across.

Some varieties of "sandy" tuff are slightly coarser grained, contain a higher proportion of lamproitic material, and are often dark-green in colour. One such tuff, in addition to quartz and microcline, contains many dark-green chloritic grains and partly altered brown biotite flakes. Accessory minerals include, in addition to minor tourmaline and rare rutile grains, flakes of phlogopite and numerous small grains of garnet and zircon. Some zircons are well rounded and zoned, whereas others are unzoned and euhedral. Large rounded rutile and widely scattered picrochromite grains are found in similar rock types. A study of the heavy minerals obtained from 100 kg of drill spoil showed, in addition to the minerals listed, barite, arfvedsonite, 5 grains of chrome diopside, and about 13 000 chromite grains, all in the +0.4 mm fraction (Hughes and Smith, 1978c). Of about 650 garnets found, 150 were of orange or violet pyrope, some were ellipsoidal and with surface pitting similar to that found on kimberlitic garnets. Microprobe analysis confirmed that these were low-chrome and high-chrome pyropes, typical of the megacryst and mantle-nodule suite found with kimberlites. Priderite, potassic richterite, and other minerals typical of the leucite lamproites, were not found in the heavy-mineral suite and have not been seen in thin section.

The "yellow ground" of Jeppe (1971) is a buff-coloured clayey mass, preserving a distinct fine-grained fragmental texture. In thin section, relic textures of fine-grained olivine lamproite lapilli are preserved with rare small pyroclasts of schist. A few small octahedra of picrochromite were obtained from the sample. Other samples of lamproite lapilli-tuff are thoroughly carbonated but preserve a texture similar to that of the tuffs from Calwynyardah. The tuff contains small, spherical, juvenile lapilli, up to 4 mm across, and a few xenoliths of shale in a tuffaceous matrix containing accidental quartz and microcline grains.

MOUNT NOREEN

Mount Noreen is a small spinifex-covered sandstone mesa about 15 m high, formed of well-bedded sandstones of the Hicks Range Sandstone, similar to those in the vicinity of Mount Abbott. The sandstones dip gently at 5° or less to the northeast. At the foot of a small scarp which forms the southern end of the mesa, there is a prominent circular photofeature caused by a shallow claypan, about 350 m diameter, that overlies a lamproite pipe. The pipe was first detected as an aeromagnetic anomaly by CRA Exploration who outlined an oval

body (350 × 275 m, 6.3 ha) by drilling and trenching (Boxer and Haebig, 1980a).

The pipe is predominantly filled by pyroclastics, which are cut by veins and dykes of leucite lamproite. The only exposures are of a coarse sandstone breccia that contains blocks up to 30 cm across and forms the pipe margin at the foot of the sandstone mesa. Narrow, brecciated zones, typically stained green, are also found a few metres from the margin. The dip of the pipe margin exposed in trench sections is 75-87°, indicating a "carrot shaped" pipe.

Near surface samples of the pyroclastics from exploration trenches are extensively carbonated, but sufficient textures and mineralogy are preserved to outline their main characteristics. Most are lapilli-tuff; they typically contain lamproite pyroclasts, up to 10 mm across, rare rounded xenoliths of shale, siltstone, and schist, and abundant quartz grains in a secondary carbonate matrix. The lamproite fragments are of potassic-richterite – diopside – leucite lamproite with accessory priderite and, sometimes, a glassy matrix. Some specimens of tuff preserve a relic texture of spherical droplets of lamproite, possibly an olivine-leucite lamproite. The heavy-mineral suite from the lapilli-tuffs, present as matrix grains, includes abundant barite, phlogopite, diopside, fibrous pyroxene, potassic-richterite, priderite, perovskite, and chromite.

The lamproite veins within the tuff are of olivine-leucite lamproite and phlogopite-leucite lamproite. The olivine-rich variety contains sparsely disseminated, altered olivine macrocrysts, up to 3 mm across, and abundant microphenocrysts, up to 0.5 mm; both have been replaced by talc and barite. The groundmass is glassy and, in addition to altered leucite, contains a little priderite, diopside, and interstitial phlogopite. The second variety contains sparse, corroded phlogopite flakes, up to 2 mm, which are set in a fine-grained mass of altered leucite, and interstitial potassic richterite and priderite.

Eight bulk samples of tuffaceous material, totalling about 450 t, were processed to recover one diamond of 0.24 CM. In addition, 34 small diamonds, the largest 0.35 mm diameter, were recovered from 3 loam samples; and 2 more from 25 kg of drill chips (Boxer and Haebig, 1980a). These grades, while of no economic interest, clearly show that Mount Noreen, a leucite-rich lamproite, is diamond bearing.

MOUNT GYTHA

Mount Gytha is a spinifex covered hill about 30 m high and located 500 m west of Machells Pyramid and 1.7 km southeast of Mount Noreen. It comprises a small, oval vent, about 75 × 100 m across, which is truncated at its southern end by faulting (Fig. 106).

The vent cuts through sandstones of the Hardman Formation, which are moderately well-exposed on the southern and western margins of the body. The sandstones are well-bedded and only moderately indurated. Along the southern margin of the vent, the sandstones appear to be faulted against the tuffs and breccias of the vent.

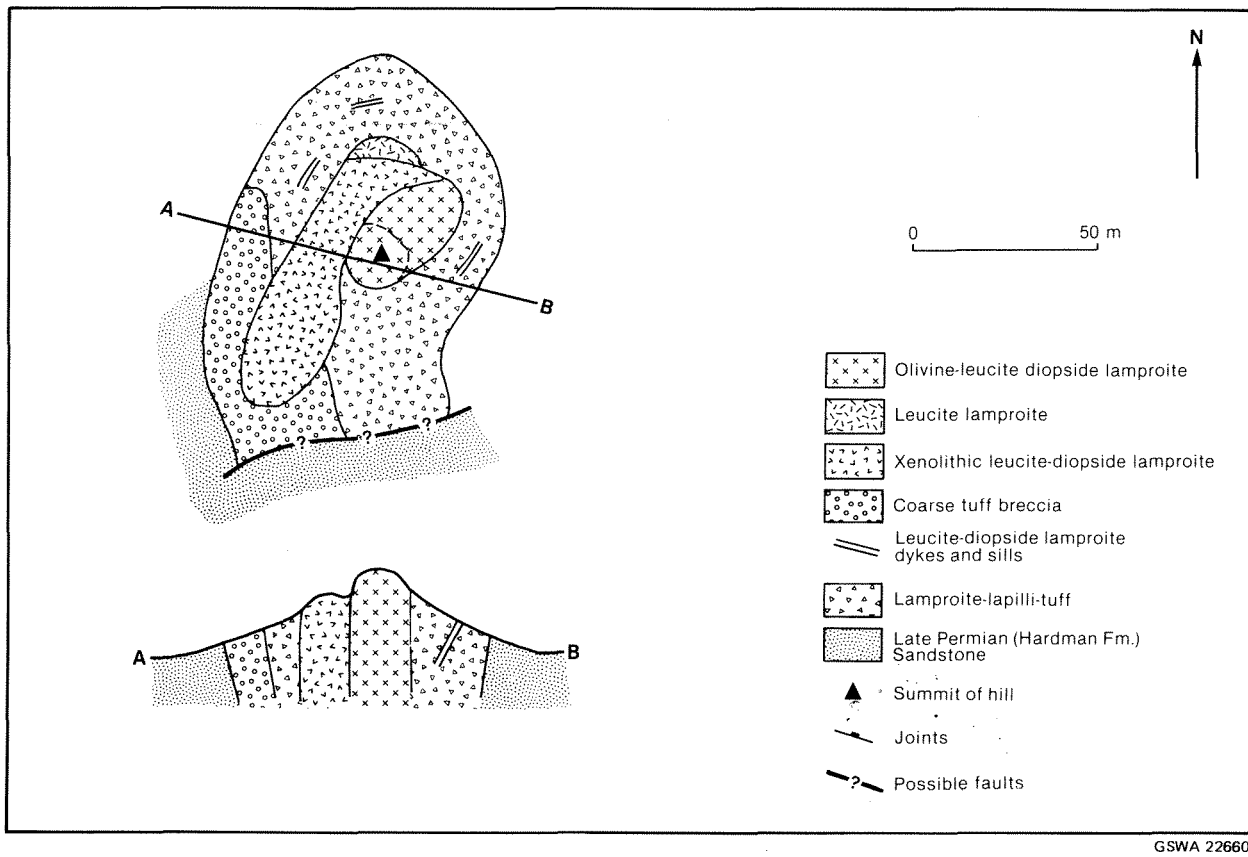


Figure 106. Geological map of Mount Gytha.

The vent is largely filled by tuffs and breccias, principally a lamproite lapilli-tuff, but in the south and west by a very coarse breccia of country-rock sandstone with very little interstitial lamproitic material. The lamproite lapilli-tuffs are scree covered, but appear to be bedded, and dip towards the centre of the vent. Thin sills of leucite lamproite up to 1 m thick intrude the tuff pile.

The central ridge of Mount Gytha is a coarse breccia that has been cemented by lamproite. At the southern end, the ridge consists of a chaotic pile of sandstone blocks, up to 3 m square and 0.5 m thick; the intervening spaces are filled with a fine-grained lamproite. Northwards, the blocks decrease in size, and the unit becomes a lamproite, crowded with sedimentary xenoliths up to 50 cm across, and many smaller cognate lamproite xenoliths. It is probable that lamproite magma invaded the tuff pile without displacing the larger blocks of sandstone: the large blocks at the southern end of the ridge differ little from the surrounding breccia except for the presence of a lamproite cement. Prider (1960) reported fossiliferous limestone blocks, now altered to collophane, within this breccia.

The summit of the hill is formed by a small circular plug, about 15 m diameter, of fine-grained olivine-leucite-diopside lamproite that contains numerous xenoliths of sediments and lamproite, up to 10 cm across. To the north of the plug, and a few metres below the summit, is a platform of fine-grained, blue-grey lamproite which is petrographically similar to the central plug but carries few xenoliths. Closely spaced, flat shear or joint planes dip at about 20° towards the centre of the vent, and crude columnar jointing dips at 70°, suggesting that this unit is a sill derived from the central lamproite.

Petrographically, the lapilli-tuff consists of small juvenile lapilli of glassy olivine-leucite lamproite, up to 1 cm across, and rare shale xenoliths in a matrix of comminuted lamproite ash and a few angular quartz and microcline grains. The lamproite is commonly vesicular and carries sparse phlogopite and altered leucite phenocrysts. Olivine, now replaced by a pale-green chloritic material, forms euhedral crystals, <0.5 mm across, and rare anhedral macrocrysts, up to 4 mm across.

Sills that intrude the tuff-pile are generally similar to the central plug, a diopside-leucite lamproite; but one larger sill-like body is a fine-grained leucite lamproite that carries occasional microphenocrysts of olivine and diopside, and numerous priderite and diopside laths, all in a fine-grained leucite-rich matrix.

The central plug, and a number of the sills, are of a distinctive fine-grained diopside-leucite lamproite, in which small, stumpy prisms of groundmass diopside, generally about 0.1 mm long, are prominent. Small phenocrysts of altered olivine, fresh leucite showing complex twinning, and prisms of diopside (up to 1.5 mm), with rare phlogopite flakes (up to 1 mm), are abundant. In addition to diopside, the groundmass contains altered leucite, abundant small phlogopite flakes, grains of priderite, and a yellow interstitial devitrified glass. In one specimen, small leucites, with sparse interstitial diopside and phlogopite, are found in glomeroporphyritic masses up to 3 mm across. Small xenoliths of sandstone, shale, and lamproite tuff are found in most specimens.

Chemical analysis of a diopside-leucite lamproite from Mount Gytha (Table 43) shows it to be similar to the analysis presented by Wade and Prider (1940). Apart from having higher contents of CaO and CO_2 because of the presence of secondary calcite, the Mount Gytha lamproite is very similar to the average West Kimberley leucite lamproite composition. The Mount Gytha lamproite is very similar to the Machells Pyramid lamproites in terms of major- and trace-element abundances, but there are small differences in trace-element abundance ratios.

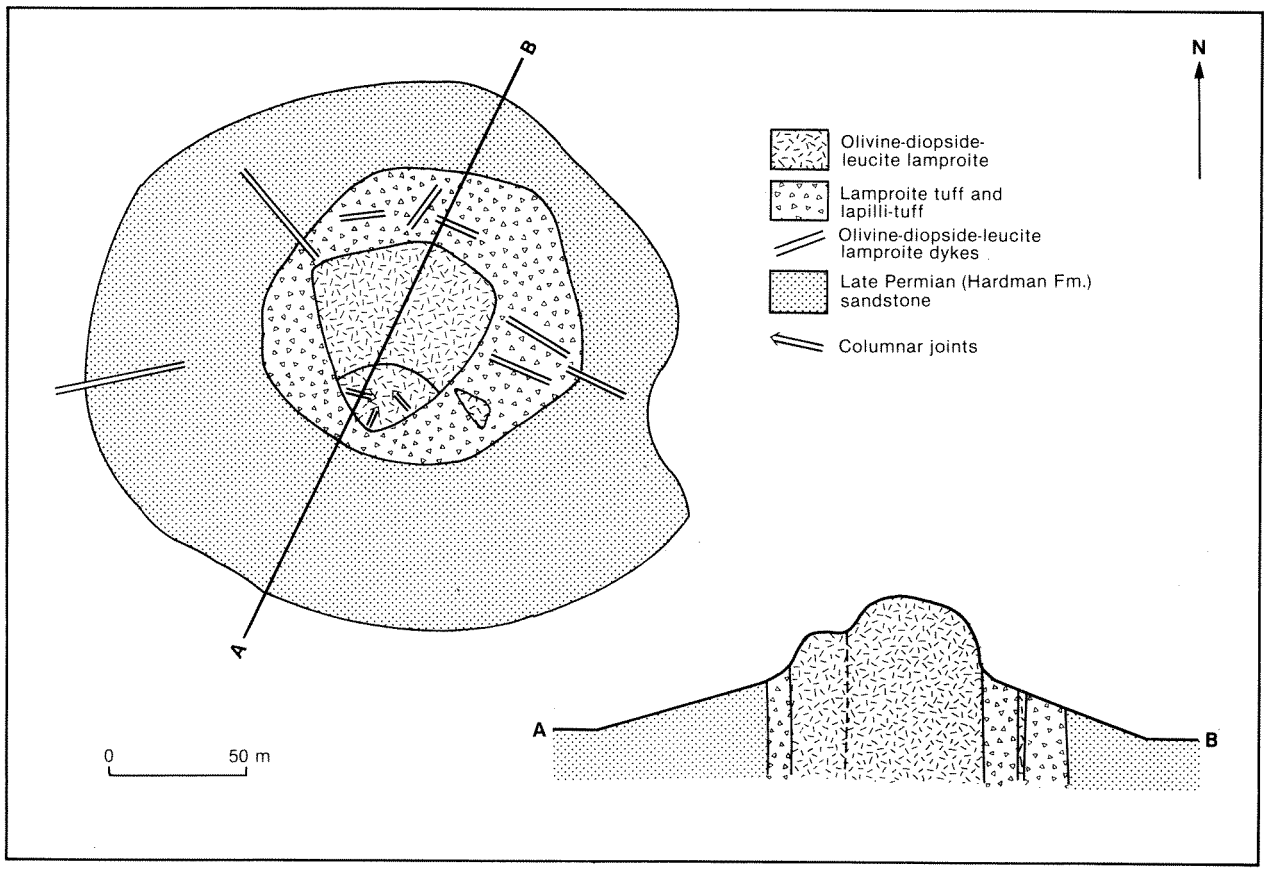
MACHELLS PYRAMID

Machells Pyramid, although not the largest, is perhaps the most striking of all the lamproite intrusions in the Noonkanbah Field; it forms a landmark that is visible over a wide area. The peak is formed by a vertical-sided pillar of lamproite, about 60 m diameter, which rises 30 m above a conical plinth of sediments and tuffs to a total height of about 50 m above the plain (Figs 107, 108).

The lamproite intrudes flat-lying, thin-bedded sandstones of the Hardman Formation, which are poorly exposed on the spinifex covered conical base of the hill. The lamproite itself consists of a roughly triangular plug of olivine-diopside-leucite lamproite, about 60 m across, and was intruded into unbedded pyroclastics which fill a nearly circular vent about 120 m diameter. A number of lamproite dykes intrude the pyroclastics and the surrounding sediments, but no sills are present. It is probable that, unlike the nearby Mount Gytha, the lamproite occupies a near vertical-sided pipe.

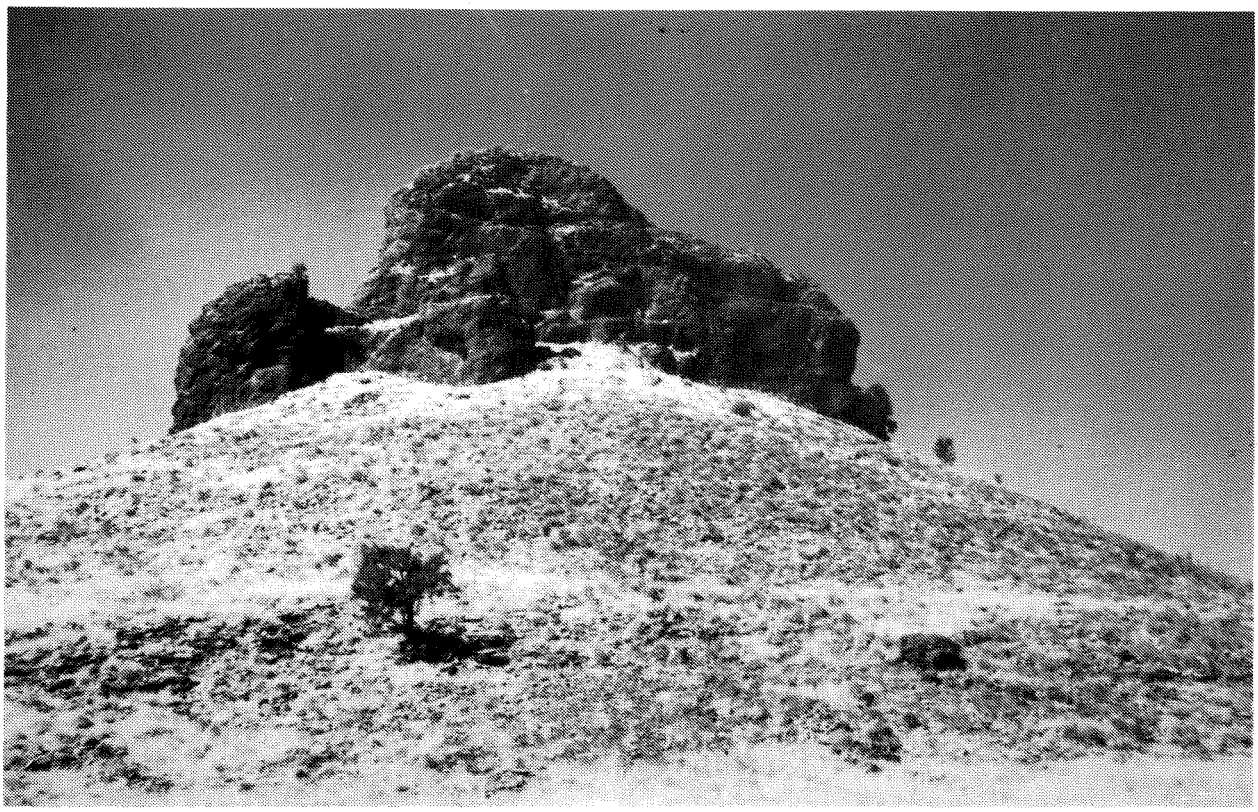
The margins of the lamproite plug are crowded with sedimentary xenoliths and fragments of early formed lamproite. Parts of the mass are also vesicular, and the vesicles sometimes contain barite. The xenoliths are mostly only a few centimetres across, but range up to half a metre. It is also noticeable that the proportion of xenoliths decreases towards the centre of the mass; this suggests that they were derived from the surrounding pyroclastic rocks, although at the present level of erosion these contain little sedimentary material.

On the southern corner of the plug, there is well-developed columnar jointing, the columns plunging at less than 5° towards the centre of the mass. The columns are radially disposed around what is possibly a separate, smaller intrusion of the same magma. This secondary plug forms a distinct notch on the cross section of the hill (Fig. 108) and carries fewer xenoliths. Columnar jointing is absent or very poorly developed elsewhere. Another, separate, small plug of similar material, only a few metres across intrudes the tuffs to the southeast of the main plug.



GSWA 22661

Figure 107. Geological map of Machells Pyramid.



GSWA 22662

Figure 108. Machells Pyramid from the southeast. (Photo: G. Derrick, BMR).

A number of small dykes of olivine-diopside-leucite lamproite intrude the tuffs and surrounding sediments. The dykes are near vertical and vary in width from 0.5 m to 3 m. The most prominent strike direction is about 280°, but there are other dykes which suggest a radial pattern and, on the northern side of the plug, two possibly tangential dykes. The largest dyke, on the eastern side of the mass, is vesicular in parts; the vesicles are elongated and plunge at about 70° towards the central plug. The magma filling the dyke fissure apparently moved upwards and outwards from the plug, either before or during the emplacement of the plug. There is no evidence that the dykes cut the central plug, although it is cut by prominent joints parallel to the dykes.

The pyroclastic rocks are medium-grained lamproite lapilli-tuffs that contain a small proportion of shale pyroclasts. The juvenile lamproite lapilli are of fine-grained olivine-leucite-diopside lamproite, and are similar to the rock of the central core; but a coarser grained variety with close-packed leucite euhedra and small phenocrysts of diopside is also present, as are a few fragments with porphyritic phlogopite. The lapilli and xenoliths range up to 1 cm across and are close-packed in a sparse matrix of lamproite ash. Small pods and dyke-like masses of fine-grained, quartz-rich tuff are composed of accidental quartz and feldspar grains; there is only a small lamproite component.

The dyke rocks are generally a fine-grained olivine-diopside-leucite lamproite that contain altered phenocrysts of olivine, up to 2 mm, and acicular diopside, up to 1 mm long; some of the olivine carries small chromite euhedra. The groundmass is glassy, but contains small altered leucites, phlogopite flakes, and accessory priderite. One dyke on the southeast side lacks phlogopite, and the diopside is overgrown by zoned, pleochroic, potassic richterite. A number of these dykes contain secondary barite, and many are vesicular.

The rocks of the central core are variable in gross texture and xenolith content. In the marginal zone of the plug, the lamproite is commonly vesicular and, in places, autobrecciated. Most xenoliths are highly metasomatized shale fragments. The lamproite is a uniform, fine-grained, porphyritic, olivine-diopside-leucite lamproite that carries altered olivine phenocrysts up to 3 mm. Diopside varies from minute prisms up to phenocrysts 2 mm long, and altered leucite, from minute crystalites up to euhedra 1 mm across. The matrix is a dark devitrified glass that contains small phlogopite and priderite grains. In one specimen the groundmass contains minute perovskite grains and small prisms of a highly birefingent mineral — pleochroic from colourless to yellow — possibly shcherbakovite.

The Machells Pyramid lamproites show a small to moderate range in composition (Table 43); MgO contents are in the range 4.9 to 10%. The widest range in compositions is shown by the dykes; the most magnesian rock is a vesicular olivine-diopside-leucite lamproite on the northern side of the body. The most evolved rocks are from a diopside-leucite lamproite dyke on the western side of Machells Pyramid; these have the lowest MgO and Ni contents and the highest contents of TiO_2, K_2O, Zr, Y, and LREE.

TABLE 43. REPRESENTATIVE ANALYSES OF MACHELLS PYRAMID (1-5) AND MOUNT GYTHA (6) LAMPROITES.

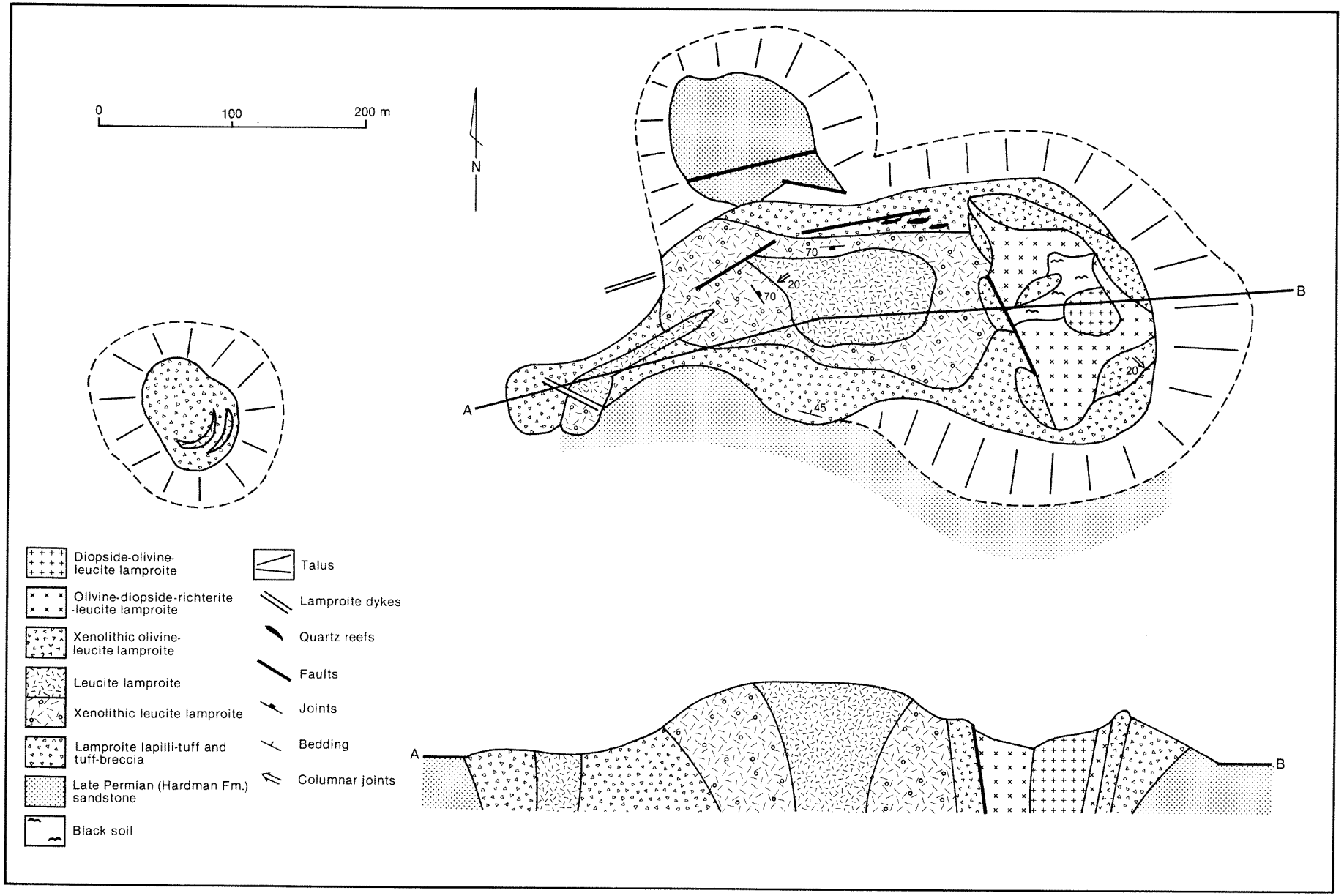
	1	*2*	*3*	*4*	*5*	*6*
			Percent			
SiO_2	48.40	52.91	46.85	51.45	49.00	49.14
TiO_2	5.14	4.94	6.81	5.43	5.25	5.35
Al_2O_3	8.03	7.66	9.30	6.98	6.76	7.51
Fe_2O_3	6.37	5.70	8.42	5.17	5.24	6.40
FeO	0.85	1.17	1.25	1.56	1.20	1.02
MnO	0.07	0.10	0.10	0.10	0.06	0.10
MgO	8.65	7.14	4.80	9.19	10.07	7.78
Cao	6.99	6.37	2.60	4.38	4.00	6.26
Na_2O	0.36	0.61	0.25	0.47	0.27	0.50
K_2O	7.78	8.21	10.58	9.36	7.33	8.51
P_2O_5	1.15	1.20	1.60	0.61	1.01	1.17
H_2O^+	2.58	1.98	2.49	1.80	3.28	2.26
H_2O^-	1.34	0.48	1.05	0.95	3.77	1.10
CO_2	0.20	1.15	0.71	1.00	0.55	0.92
Rest	1.96	1.24	2.44	1.39	1.63	1.84
Total	**99.87**	**100.86**	**99.25**	**99.84**	**99.42**	**99.86**
			Parts per million			
Ba	11 516	5 245	14 445	6 084	7 542	9 401
Li	10	8	10	7	11	8
Rb	316	293	271	182	135	525
Sr	1 139	1 130	914	1 104	1 084	1 192
Pb	40	35	45	34	44	35
Th	31	26	35	23	21	28
U	3	1	4	<1	3.5	1
Zr	1 167	1 026	1 301	1 102	1 240	1 066
Nb	148	130	167	102	134	134
Y	20	19	30	18	21	17
La	201	174	311	229	218	214
Ce	261	225	410	461	390	291
Nd	—	107	223	141	159	157
Sc	—	12	18	10	11	11
V	109	125	255	198	163	214
Cr	291	258	375	440	436	280
Ni	158	160	121	512	496	246
Cu	58	46	38	44	50	58
Zn	80	67	69	73	79	77
Sn	4	12	14	17	19	12
Ga	14	12	16	14	21	15
As	2	1	6	2	4.5	2
F	2 700	2 800	3 900	1 800	3 100	3 500

1 — Diopside-leucite lamproite; centre of Machells Pyramid, BMR 67165018. 2 — Diopside-phlogopite-leucite lamproite; eastern margin of Machells Pyramid, BMR 81210157. 3 — Olivine-bearing leucite-lamproite dyke; western margin of Machells Pyramid, BMR 81210155. 4 — Diopside-leucite lamproite; dyke on eastern margin of Machells Pyramid, BMR 81210156. 5 — Vesicular olivine-diopside-leucite lamproite; dyke on northern margin of Machells Pyramid, BMR 83210270. 6 — Diopside-leucite lamproite with cognate xenoliths of diopside and leucite; eastern flank of Mount Gytha, BMR 81210154.

MOUNT CEDRIC

Mount Cedric, located on the crest of a low ridge of poorly outcropping Permian sandstone 3.5 km northeast of Machells Pyramid, is one of the larger and more complex lamproite intrusions of the Noonkanbah Field. The main body of lamproite forms a low rounded hill, 400 × 200 m and about 40 m high. To the west, a small satellite vent of 75 m diameter forms a conical hill about 25 m high.

The lamproite intrudes thin-bedded sandstones of the Cherrabun Member, the youngest rocks of the Late Permian Hardman Formation. Poor outcrops of flaggy sandstone are found along the southern margin of the



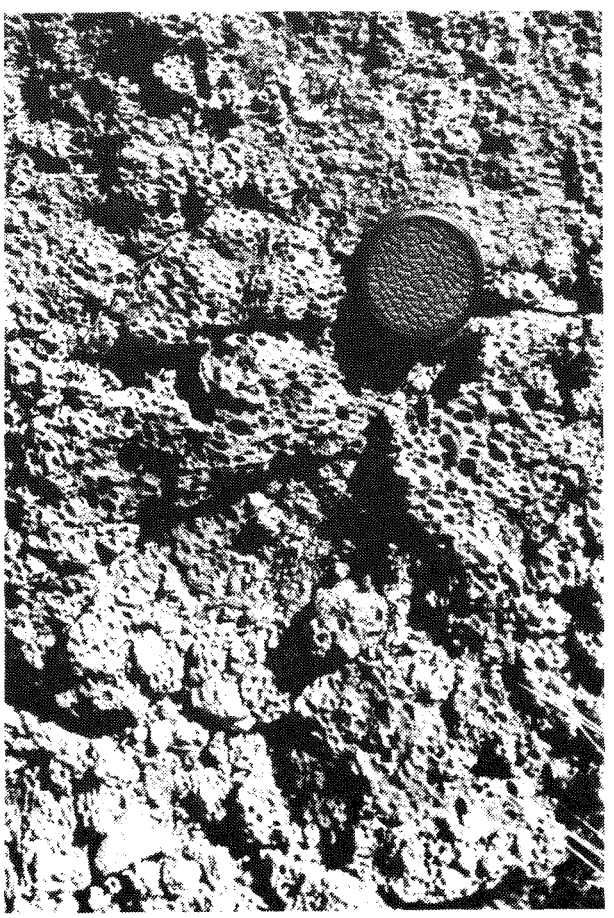
GSWA 22663

Figure 109. Geological map of Mount Cedric.

lamproite; but, on the northwestern flank of the hill, there is a small flat-topped mesa of more massive, horizontally bedded sandstone. A narrow gully between sandstone and lamproite suggests a faulted junction at this point (Fig. 109).

Two centres of intrusion are present on Mount Cedric: the earlier western centre that includes the summit of the hill and occupies about 60% of the area; and the later eastern centre that has given rise to a crater-like erosional depression about 100 m diameter and 25 m deep (Fig. 111). In addition, a narrow tongue of tuff and lamproite extends southwest for about 150 m from the western end of the mass to a small satellite vent, and 200 m further west is the larger satellite vent.

The earliest volcanic activity produced pyroclastics, well-exposed on the northern and southern flanks of the hill, but obscured by spinifex and talus around the eastern end of the vent. The pyroclastics are mostly lapilli-tuffs, well bedded and dipping towards the centre of the vent at about 45°. The basal unit on the northern flank, below the small sandstone mesa, is a bedded, coarse, tuff-breccia of siltstone and shale fragments up to 20 cm across; above the small fault marked in this area the pyroclastics grade into lapilli-tuff. Associated with this fault are several elongate quartz reefs with a distinctive spherulitic texture. Similar coarse tuff-breccia that contains large siltstone xenoliths, but is unbedded, occupies the small satellite vent on the southwest of Mount Cedric. On the southern flank the basal unit is a coarse pyroclastic breccia that contains pumiceous blocks of lamproite up to half a metre across (Fig. 110).



GSWA 22664

Figure 110. Breccia of vesicular lamproite at the base of the pyroclastic succession, Mount Cedric.

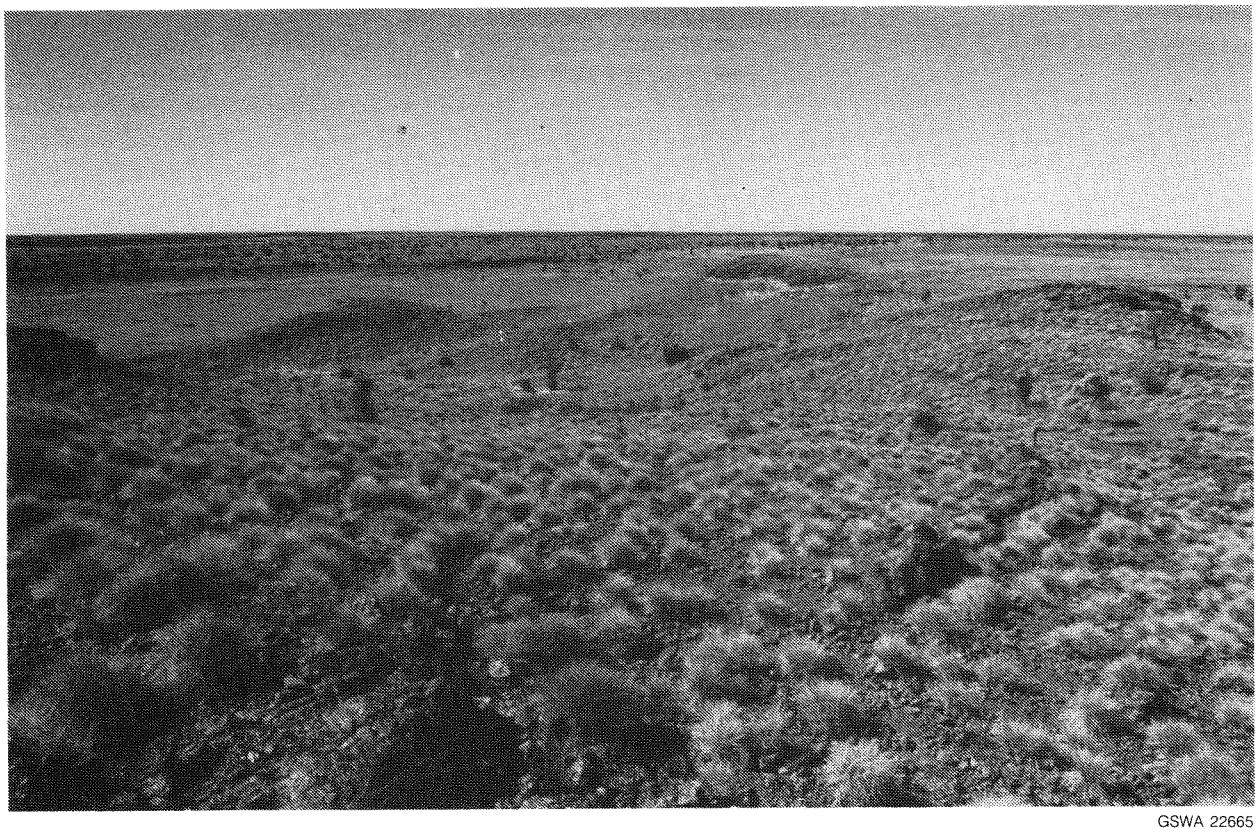
The pyroclastics were intruded by massive fine-grained leucite lamproite which also forms the magmatic core to Centre I. The lower part of the intrusion contains numerous small xenoliths, but these become rare or absent towards the summit of the hill. In places, the change from xenolithic to homogeneous lamproite is abrupt, and marked by a small step in the topography. West of the summit, small, columnar joints mark the boundary, dipping outwards at 20°. Joints in the underlying xenolithic lamproite dip inwards, consistent with an igneous contact dipping at 70°. To the east, however, the contact is possibly gradational. The rocks do not differ greatly, except in xenolith content, and it is possible that two pulses of the same magma were involved, the early pulse entraining xenoliths from the wall rocks.

Centre II, at the eastern end of the hill, did not involve renewed pyroclastic eruption. The earliest intrusion was of xenolithic olivine-leucite lamproite, which forms a number of small hills surrounding the crater-like depression (Fig. 111). Columnar jointing is well developed on one body, and indicates an inward dip of 70°. The western side of Centre II is faulted; this fault dips towards the centre at about 70°. The xenolithic lamproite intrusions thus form an irregular and incomplete cone sheet.

Most of the central depression of Centre II is occupied by a fine-grained olivine – diopside – potassic-richterite – leucite lamproite. The shape of this body is irregular, and probably governed by the surrounding xenolithic lamproite intrusions. Marginally, the lamproite is in places strongly vesicular. The vesicles are flattened and elongated in the direction of flow, and some are filled with barite or zeolites. A small pod of tuff is enclosed by the lamproite, and probably represents a large foundered block rather than a late vent. Close to the eastern side of the depression is a small, rubble-covered dome about 40 m diameter and a few metres high; it is distinctive because of the presence of nodules and incrustations of secondary magnesite. Beneath the rubble is a medium-grained, black, diopside-olivine-leucite lamproite that has weathering pits, up to 5 mm across, after olivine. This body was the final intrusion of Centre II.

The relative age of the small satellite vent on the southwest flank of the hill is not known: but a dyke of vesicular phlogopite-leucite lamproite, 10 m wide, which extends from a small plug of similar composition, is known to cut the core of Centre I. In addition to the dyke, this vent also includes tuff-breccia, lapilli-tuff, and a small plug of xenolithic leucite lamproite. A number of small phlogopite-leucite dykes, not marked on Fig. 109, cut the pyroclastics and most units of Centre I; but are not found in Centre II.

The small vent 500 m west-southwest of Mount Cedric is about 75 m diameter and composed largely of lamproite lapilli-tuff that contains a few thin sills of phlogopite-leucite lamproite. The conical hill is



GSWA 22665

Figure 111. Centre II of Mount Cedric, from the summit. The small hills are intrusions of xenolith-bearing olivine-leucite lamproite and form a partial cone-sheet. The light-coloured patches within the central depression are formed by magnesite from weathered olivine-rich leucite lamproite.

surrounded by a talus slope; and, although there are no exposures between it and the southwestern extremity of Mount Cedric, there is little doubt that this is a separate small vent.

Volcanism

The generallized eruptive sequence at Mount Cedric is simlar to that at other vents — an initial explosive pyroclastic phase followed by the intrusion of magmatic rocks. Dips in the bedding of the lower pyroclastics indicate that the explosive phase opened a vent which narrows rapidly with depth; and the well-developed bedding, itself, suggests deposition by pyroclastic surge. The magmatic phase at Mount Cedric, however, is more complex in that four eruptive centres are involved, and the two major centres appear to form part of a single vent.

The vents are probably located along a complex fracture system. The two major vents, Centres I and II, lie east-west; and Centre I is elongated in the same direction: these vents almost certainly lie on a single fissure. The small satellite vent on the southwest flank of the hill, and the broad dyke which passes from it towards Centre I, indicate a fracture that trends 240°. The larger satellite vent lies due west; and again suggests that two parallel east-west fractures and a cross fracture are involved. These fractures exist in the Mesozoic rocks, but may be related to similarly oriented basement fractures.

Centres I and II do not represent two adjacent vents that have coalesced, or successive vents along the same fracture. Unlike Ellendale 9 and Big Spring 1 and 2, where vents have coalesced and separate pyroclastic deposits may be ascribed to each vent, there is no tuff unit at Mount Cedric that is specifically associated with Centre II. The original vent was elongated, probably developing from a dyke at no great depth, and the lamproites of Centre I are the completion of the first phase of activity. Some time later, intrusive activity was renewed at the eastern end of the original vent, and the lamproites of Centre II were emplaced. The magmatic core of Centre I possibly formed a lava lake or blister in an open vent, but this is unlikely for the lamproites of Centre II. The xenolithic lamproite "cone-sheet" was intruded into the core rocks of Centre I as well as the earlier pyroclastics, and these rocks probably remained as a cap to the later intrusions. The minor faulting in the rocks of Centre I is probably related to the emplacement of the later centre, and indicates that it had cooled sufficiently to undergo brittle fracture.

Petrography

Pyroclastics: The bulk of the pyroclastic rocks are lapilli-tuffs: the lamproite lapilli range up to 1 cm as do about 10% of similar-sized xenoliths of shale and siltstone. The tuffs are clast-supported, and contain only a sparse matrix of lamproite ash, clay minerals, and rare grains of quartz. The juvenile lamproite lapilli are generally fine-grained olivine-leucite lamproite, sometimes vesicular, that contain rare olivine macrocrysts up to 2 mm. Cognate lapilli include coarse varieties of olivine-leucite lamproite and a few clasts of phlogopite-

leucite lamproite that contain phenocrysts of phlogopite up to 1.5 mm. Pumiceous lamproite from the basal breccia on the south side of the hill consists of close-packed, small leucite euhedra, small altered olivines, and accessory priderite, in a devitrified glass; the vesicles in this rock are unfilled.

The small vent to the west is filled by lamproite lapilli tuffs that contain rare shale xenoliths, and a sparse matrix of secondary silica and barite. The lamproite lapilli are of phlogopite-leucite lamproite that contain abundant phlogopite up to 2 mm and a devitrified, glassy groundmass studded with small leucites. The thin sills intruded into the mass are of a similar rock type, and vesicles are sometimes filled with quartz or barite.

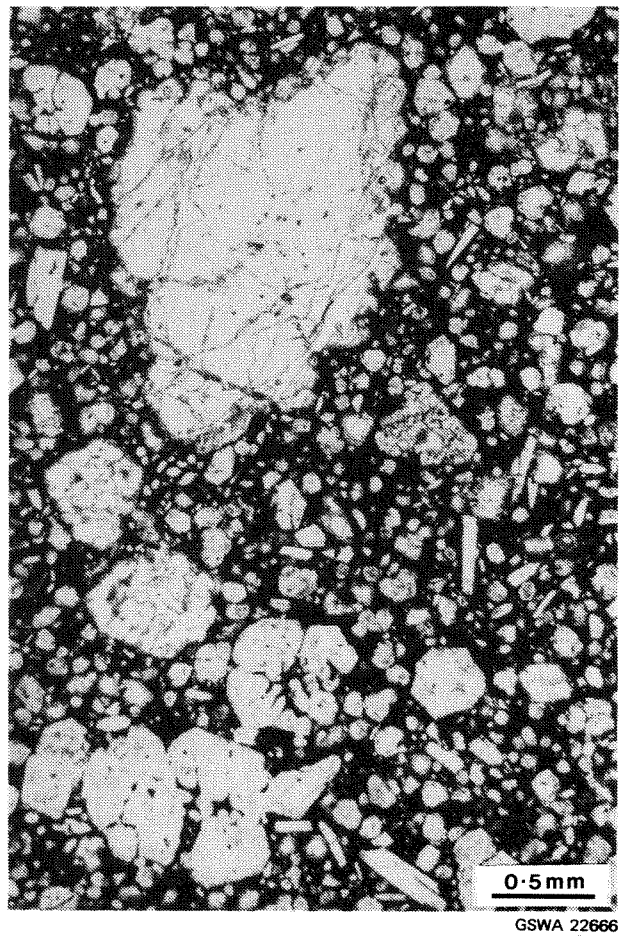
Centre I: The outer zone of the magmatic core of Centre I is a very fine-grained leucite lamproite that contains a few large anhedral olivines up to 2 mm, and abundant groundmass olivines less than 0.1 mm across; the olivine is pseudomorphed by green nontronite or colourless clay minerals. The groundmass is a devitrified glass with minute needles of priderite and abundant altered leucites up to 0.1 mm. Xenoliths of metasomatized shale, up to 6 mm across, are abundant and, with rare xenoliths of siltstone, make up about 10% of the rock. The central, xenolith-free zone of Centre I, is a similar leucite lamproite; but, towards the centre of the mass, it is slightly coarser grained and contains small prisms of diopside and a little interstitial potassic richterite.

The quartz reefs on the north side of Centre I have a distinctive appearance on weathered surfaces caused by many small spherical pits up to 5 mm across. In thin section, the whole rock is seen to consist of interlocking spherulites of quartz and spherulites of calcite. The pits result from the weathering of the carbonate.

Dykes cutting the major units of Centre I are of fine-grained phlogopite-leucite lamproite; vesicular examples often show vertical flow alignment of vesicles and phlogopite.

Centre II: The xenolithic olivine-leucite lamproite of Centre II is generally similar to the xenolith-bearing rocks of Centre I — a fine-grained leucite lamproite that contains two generations of olivine and a devitrified glassy groundmass rich in leucite and priderite. Olivine, however, is more prominent, and there are rare phenocrysts of phlogopite up to 2 mm. Xenoliths of metasomatized shale are present; but small fiamme of lamproitic glass, and cognate xenoliths of phlogopite-leucite lamproite, are more common; grains of quartz and microcline, and xenoliths of granite, are rare.

Inside the ring of xenolithic lamproite is a large mass of fine-grained olivine - diopside - potassic-richterite - leucite lamproite. Small altered leucite grains, up to 0.5 mm, together with small (< 1 mm) euhedral and sparse anhedral macrocrystal olivine (up to 4 mm), abundant diopside laths up to 1 mm, and interstitial potassic richterite, make up the bulk of the rock. A sparse matrix is altered to clay minerals and contains accessory priderite and rare grains of phlogopite. The diopside laths show a strong flow alignment not seen in hand specimen.



GSWA 22666

Figure 112. Photomicrograph of diopside-olivine-leucite lamproite, Centre II, Mount Cedric. Note the macrocrysts of olivine, microphenocrysts of altered leucite, and prismatic diopside. (GSWA 71312).

The small central core of Centre II is a distinctive olivine-rich rock that contains abundant anhedral to embayed olivine macrocrysts (up to 4 mm across) which show undulose extinction (Fig. 112). These macrocrysts are often partly recrystallized to an olivine mosaic, and many show a narrow overgrowth-zone, marked by small inclusions. Phenocrysts of euhedral olivine range up to 2 mm, but are mostly less than 0.5 mm, slightly corroded, and rimmed by phlogopite. Altered leucite ranges up to 2 mm across, and diopside forms abundant small prisms and acicular crystals up to 1 mm. The groundmass is commonly a very fine-grained mass of dark clay minerals, probably a devitrified glass, that contains minute granules of perovskite. Where the groundmass was originally more crystalline, small prisms of priderite replace perovskite. Small euhedra of chromite commonly occur as inclusions in olivine. A narrow dyke of this rock in the surrounding lamproite shows flow alignment of olivine and diopside, and contains large masses of spongy leucite up to 6 mm across, set in a crystalline groundmass of abundant priderite and interstitial potassic richterite. In weathered specimens of this rock, the olivine is replaced by a pale-green, micaceous mineral, identified by Prider and Cole (1942) as hydrotalcite.

Chemistry

The Mount Cedric lamproites range from the comparatively MgO-rich (up to 16% MgO, <50% SiO_2), in the olivine-rich leucite lamproites of the central core of Centre II, to unusual MgO-poor, SiO_2-rich (<10%, typically 6-8% MgO, >50% SiO_2) lamproites that are comparable with the cedricite analyses of Wade and Prider (1940) and Prider (1960). Representative analyses are given in Table 44. All are saturated to oversaturated in silica; the most MgO-rich lamproites contain appreciable (>10%) normative olivine; but the unusual MgO-poor types contain normative quartz, abundant normative orthoclase (>40%), and abundant modal leucite. The most Mg-poor rocks are the phlogopite-leucite lamproite sills and dykes, which contain as little as 5% MgO; TiO_2 and K_2O contents show a comparably wide range (4 - 7.2% TiO_2, 6.3 - 11.6% K_2O). Nickel and Cr contents are low in the Mg-poor lamproites (< 500 ppm), as is typical of the leucite lamproites of the Noonkanbah Field, but range up to moderate levels in the most olivine-rich rocks (600 ppm Ni, 750 ppm Cr). A feature of all except the phlogopite-bearing samples is the comparatively low Rb contents and Rb/Sr ratios of the Mount Cedric rocks (typically 150-260 ppm Rb, ≈0.2 Rb/Sr); the phlogopite-bearing lamproites have Rb contents and Rb/Sr ratios more typical of the West Kimberley suite as a whole. Other trace-element abundances fall either within the range established for the leucite lamproites; or, in the case of the more MgO-rich compositions, extend toward the compositions of olivine lamproites. The more MgO-rich Mount Cedric lamproites are similar to the olivine-phyric, diopside-olivine-leucite lamproites at Mount Ibis and The Sisters Southwest, whereas the leucite-rich lamproites are typical of the Noonkanbah Field leucite lamproites.

TABLE 44. REPRESENTATIVE ANALYSES OF MOUNT CEDRIC LAMPROITES.

	1	*2*	*3*	*4*	*5*	*6*
			Percent			
SiO_2	50.30	48.68	49.44	50.20	50.30	50.00
TiO_2	6.63	4.64	5.73	6.86	6.71	7.16
Al_2O_3	8.00	6.44	7.05	8.10	8.90	9.50
Fe_2O_3	5.70	3.85	5.02	6.10	7.10	6.80
FeO	1.58	2.02	1.26	0.86	0.76	0.75
MnO	0.12	0.10	0.07	0.05	0.08	0.05
MgO	7.74	16.19	9.97	7.29	6.18	5.24
Cao	2.88	3.28	3.40	2.32	1.83	2.51
Na_2O	0.52	0.74	0.71	0.13	0.12	0.06
K_2O	10.25	7.26	8.66	10.68	11.61	10.82
P_2O_5	1.01	0.48	0.56	1.19	1.49	1.93
H_2O^+	2.54	3.57	2.90	3.09	2.51	2.64
H_2O^-	1.29	1.00	1.94	2.03	1.20	1.20
CO_2	0.22	0.23	0.26	0.10	0.09	0.15
Rest	1.30	1.37	2.34	1.44	1.45	1.69
Total	**100.08**	**99.85**	**99.31**	**100.44**	**100.33**	**100.50**
			Parts per million			
Ba	4 461	6 148	14 094	5 534	5 871	7 699
Li	6	10	10	7	14	12
Rb	228	143	177	267	262	273
Sr	1 111	954	1 174	1 285	1 099	731
Pb	60	39	51	58	73	83
Th	16	18	23	24	23	21
U	1	3	3	1	1	2
Zr	1 270	1 042	1 263	1 199	1 167	1 206
Nb	131	107	141	119	124	136
Y	23	17	19	15	22	34
La	371	197	246	331	348	434
Ce	469	357	449	430	507	528
Nd	—	137	221	—	—	—
Sc	20	10	11	23	23	22
V	186	143	171	231	375	282
Cr	366	677	468	360	224	276
Co	36	—	—	38	33	23
Ni	381	528	417	628	277	190
Cu	92	52	66	104	76	71
Zn	82	62	67	77	86	85
Sn	16	13	18	17	8	85
Mo	<1	3	3	<1	<1	<1
Ga	18	20	18	18	24	25
As	<1	2	3	<1	3	7
S	380	—	—	100	470	820
F	2 620	1 700	2 100	2 550	2 620	3 700
Cl	40	—	—	20	20	40

1 — (Diopside) - potassic-richterite - leucite lamproite; central plug, centre I, GSWA 71868A. 2 — Diopside-olivine-leucite lamproite; central zone, centre II, BMR 83210275. 3 — Diopside-olivine-leucite lamproite; inner zone, centre II, northern side, BMR 83210277. 4 — (Diopside)-olivine-leucite lamproite; inner zone, centre II, southern side, GSWA 71870D. 5 — Vesicular phlogopite-leucite lamproite; dyke at western end of hill, GSWA 71874B. 6 — Phlogopite-leucite lamproite; Mount Cedric satellite plug, sill in tuff, GSWA 71875C.

MOUNT CEDRIC NORTH

This lamproite, located about 2 km west of Mount Cedric, is a dyke-like body. The largest exposure is about 150 m long and 25 m wide and trends at 060°; a small exposure of the same dyke is found 300 m to the west-southwest. The dyke probably occupies parts of a fracture at least 450 m long. The main mass is a medium-grained olivine-leucite lamproite that contains a small amount of diopside, potassic richterite, and priderite. Occasional macrocrysts of altered olivine are also present (Boxer and Haebig, 1980a). The smaller mass was described by Mitchell (1981) as a phlogopite-leucite lamproite.

MOUNT IBIS

Mount Ibis is located in the floodplain of the Fitzroy River, at the eastern end of a low outcrop of thin-bedded sandstones of the Lightjack Formation, the oldest member of the Late Permian Liveringa Group. Mount Ibis itself is a prominent, steep-sided mass of lamproite tuff-breccia, which rises from a conical talus slope to a height of about 30 m above the surrounding alluvial and black-soil plains. Further tuffs and lamproites are exposed as a series of small hills up to 15 m high to the north and west. The tuffs intrude flat-lying sandstones which are baked and disrupted only within a few metres of the vent.

The Mount Ibis vent is roughly circular in outline, 375 × 330 m, but most of the lamproite is hidden beneath black soil. A slight rise marks the vent margin in the southeast, and scout drilling has proved the margin in the south, beneath a metre or so of black soil (Gregory, 1980). On the northern and western sides, the vent-wall appears to dip inwards at about 70°.

The earliest unit exposed is the lapilli-tuff which forms the small hills west of the central pillar. The tuffs are fine-grained, but contain scattered xenoliths of country rock up to 10 cm across. Outcrop is generally covered by scree, but poorly preserved bedding dips 30° towards the centre of the vent. Drilling has shown that the tuffs

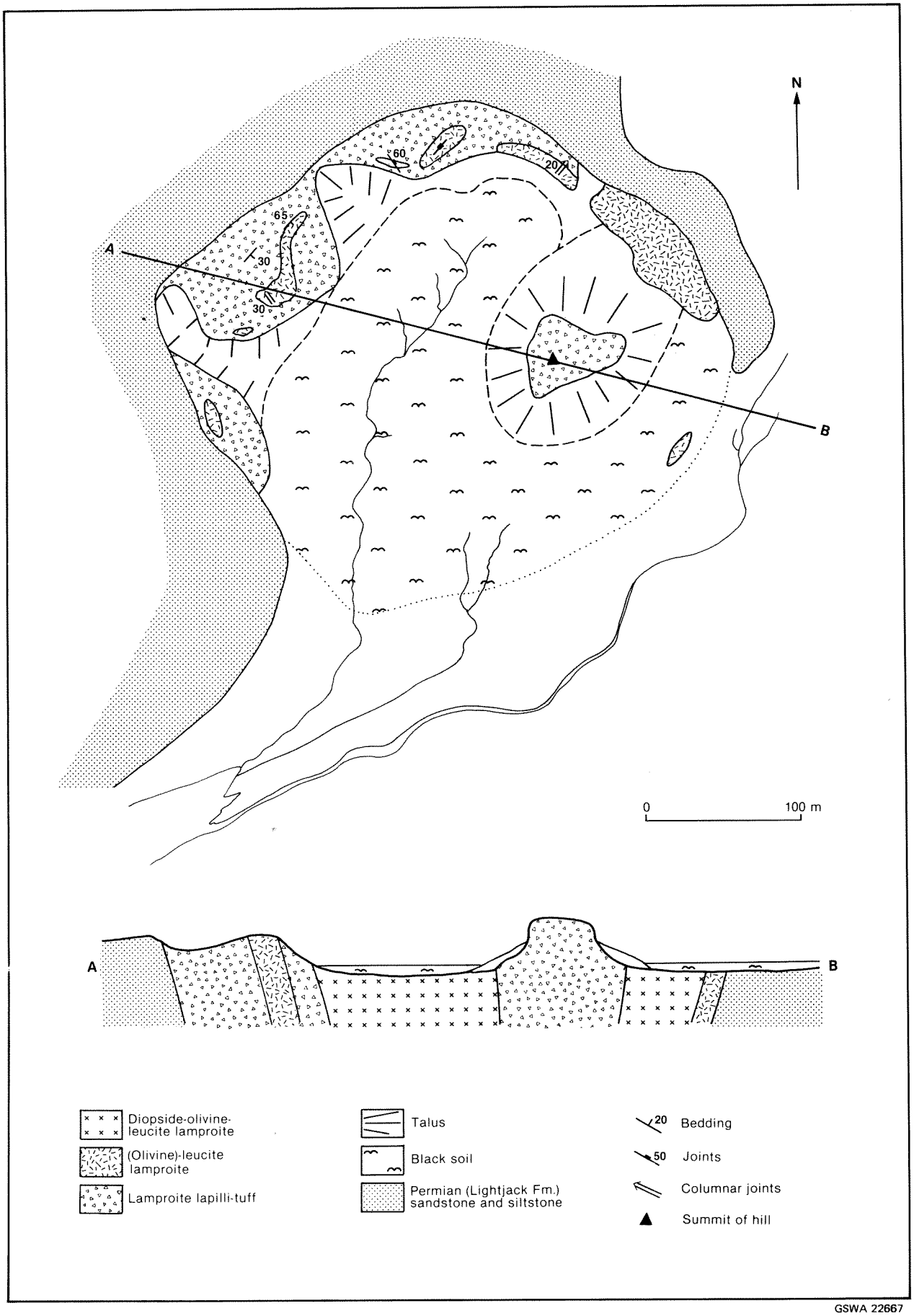


Figure 113. Geological map of Mount Ibis.

are confined to the crescentic area of the present outcrop. The lapilli-tuffs and tuff-breccias of the central pillar of Mount Ibis are not obviously bedded, but otherwise appear similar to the marginal tuffs, except that sedimentary xenoliths are larger, up to 15 cm, and more numerous. The tuff-breccias do not contain fragments of the olivine-leucite lamproite intrusive core, as would be expected if they were the result of a late resurgence of explosive activity. It seems probable that they represent a remnant of the original vent filling.

The marginal pyroclastics are intruded by small irregular sheets of very fine-grained, dark, leucite lamproite. Crude columnar jointing is developed at a number of locations; the small columns, 15 cm diameter, indicate a dip of 60-70° towards the centre of the vent.

Drilling has shown that the black-soil area is underlain by an olivine-rich leucite lamproite similar to the final intrusion of Centre II of Mount Cedric. The diopside-olivine-leucite lamproite forms a roughly circular mass about 250 m diameter and almost surrounds the central mass of pyroclastics. Exploration trenches have shown that there is a narrow zone of lapilli-tuff, similar to the exposed tuffs, around the southern margin of the mass, and a wider zone of fine-grained lamproite. This is a chilled marginal phase of the main mass, distinct from the small exposed lamproite sheets.

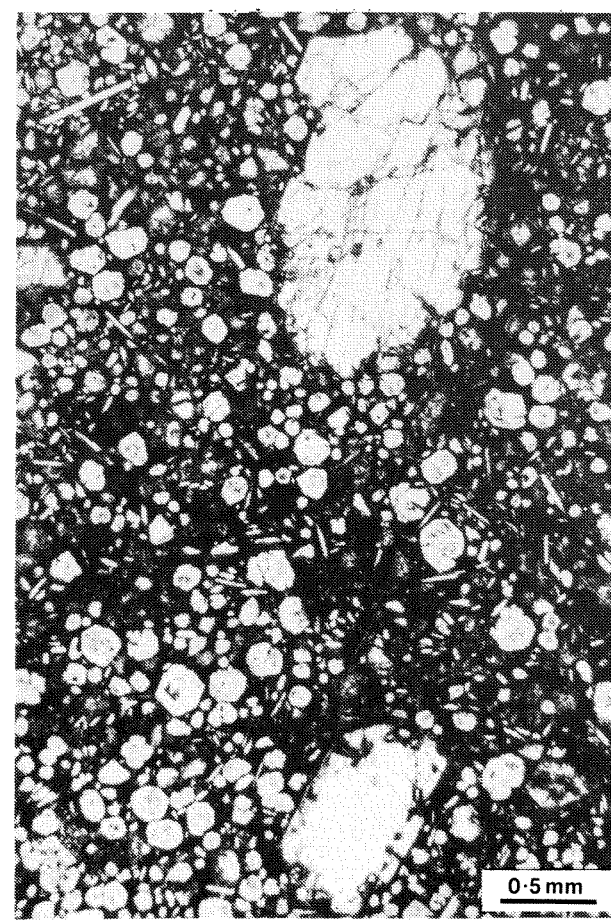
The Mount Ibis vent has been prospected for diamonds; approximately 200 t of weathered rock from six trenches in the central magmatic core were treated in a trommel-jig plant. Pyrope and picrochromite were recovered, but no diamonds. HF digestion of drill chips recovered one small diamond (Gregory, 1980, 1981).

Petrography

Pyroclastics from the western margin of the vent are fine-grained lapilli-tuffs containing angular to sub-rounded lapilli of glassy, juvenile lamproite, shale and metasomatized siltstone, up to 1 cm across, in a tuffaceous matrix of comminuted lamproite ash, and rare accidental grains of quartz, microcline, and plagioclase. The juvenile pyroclasts are of olivine-leucite lamproite, which is typically vesicular and glassy and in which only small altered olivines, less than 0.2 mm across, are visible. More crystalline varieties in which minute altered leucites are abundant may be cognate. Small amounts of phlogopite are present in both lapilli and matrix. Pyroclastics from the central area of Mount Ibis are mostly lapilli-tuffs of very similar composition to the western tuffs. The lapilli are close-packed and partly welded; and there is only a sparse tuffaceous matrix, which includes fragments of quartz, microcline, and plagioclase. Xenolithic fragments of shale, siltstone, and, rarely, granite, are common, and, in the tuff-breccias, range up to 15 cm across.

The lamproite sheets that were intruded into the lapilli-tuff are of similar composition to the lamproite fragments of the tuff — olivine-leucite lamproite, and altered olivines, up to 0.2 mm, in a very fine-grained matrix carry abundant, minute former leucites and accessory priderite. The groundmass also carries a little interstitial phlogopite, and, in some specimens, potassic richterite. Small xenoliths of shale are common; and xenocrysts of quartz, microcline, and plagioclase, are present. The rock shows varying degrees of autobrecciation.

The concealed central intrusion is of fine-grained, pseudo-porphyritic, diopside-olivine-leucite lamproite; and relatively fresh specimens are available from exploration trenches (Fig. 114). Anhedral to rounded macrocrystal olivine, up to 4 mm across, is common, and small euhedral olivines up to 0.3 mm are abundant in the groundmass. Apart from iron-stained margins and cleavages, many of the larger olivines are unaltered and commonly show undulose extinction and polygonization. Groundmass olivine is usually strongly iron-stained. Euhedral leucite, seriate from minute grains up to 0.3 mm, and altered to a turbid zeolitic material, is the most abundant mineral. Diopside is also abundant, and forms minute groundmass prisms and larger acicular crystals up to 0.5 mm long. The interstitial material is a brown mass of submicroscopic clay minerals, probably a devitrified glass, and makes up about 15% of the rock; it contains accessory euhedral perovskite and chromite. The perovskite is greenish yellow, up to 0.1 mm across, and anomalously birefringent. Priderite is present only as rare, minute grains, often fringing perovskite.



GSWA 22668

Figure 114. Photomicrograph of diopside-olivine-leucite lamproite, Mount Ibis. Note the macrocrysts of olivine and abundant diopside and leucite in the groundmass. Compare with Fig. 112. (GSWA 76043A).

Other specimens from the central intrusive contain olivine that has been replaced by talc, and may contain priderite rather than perovskite. Some specimens show flow-alignment of the diopside and sparse phlogopite in the groundmass. The chilled marginal phase shows the development of potassic richterite and relatively abundant groundmass phlogopite.

Chemistry

Chemical analyses (Table 45) of the tuffs and breccias that form Mount Ibis show them to be composed of leucite lamproite typical of most of the Noonkanbah Field lamproite: it contains 6 to 8% MgO, 50 to 53% SiO_2, and 9 to 11% K_2O. The olivine-diopside-leucite lamproites are much richer in MgO (up to 19%), and poorer in SiO_2 (<45%) and K_2O (5-10%), and closely resemble the olivine-rich lamproites of Centre II of Mount Cedric. These rocks are transitional to the more Mg-poor olivine lamproites of the Ellendale Field. In terms of trace-element abundances and abundance ratios, however, they are closer to leucite lamproites; for example, Ni and Cr contents are less than 750 ppm and Zr/Nb ratios are approximately 10 and thus closer to leuctie lamproites than to olivine lamproites which have Zr/Nb ratios near 4.

TABLE 45. REPRESENTATIVE ANALYSES OF MOUNT IBIS LAMPROITES

	1	*2*	*3*
	Percent		
SiO_2	51.69	42.43	50.47
TiO_2	4.27	5.77	4.85
Al_2O_3	8.31	4.44	7.11
Fe_2O_3	5.09	4.94	4.18
FeO	2.03	2.37	2.45
MnO	0.08	0.11	0.09
MgO	6.04	19.04	10.47
CaO	3.77	4.06	2.43
Na_2O	0.70	0.63	0.68
K_2O	10.79	5.11	8.98
P_2O_5	2.20	0.80	0.84
H_2O^+	1.70	4.93	2.54
H_2O^-	0.75	2.32	1.88
CO_2	0.40	0.70	0.38
Rest	2.04	1.25	1.14
Total	**99.86**	**98.90**	**98.49**
	Parts per million		
Ba	12 147	4 009	4 020
Li	12	5	24
Rb	286	300	236
Sr	2 692	1 150	1 374
Pb	53	22	50
Th	29	22	28
U	3	2	2
Zr	885	1 215	1 092
Nb	92	130	114
Y	26	12	25
La	256	161	279
Ce	372	293	422
Nd	—	97	172
Sc	—	9	11
V	248	140	186
Cr	194	1 033	275
Ni	223	673	265
Cu	23	54	43
Zn	54	61	91
Sn	7	19	9
Mo	4	—	—
Ga	12	7	17
As	3	2	2
F	—	1 700	1 600

1 — Diopside-leucite lamproite tuff-breccia; central pillar, BMR 80210093. 2 — Diopside-olivine-leucite lamproite; 60m depth, hole MI 100 south, BMR 81210169. 3 — Olivine-diopside-leucite lamproite; 38-44m depth, hole MI 101 south, BMR 81210170C.

FISHERY HILL

Fishery Hill is located 7.6 km south-southeast of Mount Cedric and is formed by an arcuate ridge of brecciated and tuffaceous lamproite that rises 30 m above the plain (Fig. 116). The lamproite vent intrudes flat-lying sandstone of the Hicks Range Member of the Hardman Formation, which is well exposed on the western and southern faces of the hill, and is undistrubed to within a few metres of the vent. On the northern side of the intrusion, thin-bedded, flaggy siltstones and shales, which dip at 10° to the north, are fractured and disrupted over a 20 m-wide zone.

The vent is about 150 m diameter and consists of an outer, incomplete ring of pyroclastic rock with positive relief that surrounds a poorly exposed central magmatic stock (Fig. 115). The southern part of the tuffaceous phlogopite-leucite lamproite, including the highest part of the ridge, varies from tuff and lapilli-tuff to autobrecciated lamproite. The pyroclastics contain many small sedimentary xenoliths and, particularly in the less tuffaceous parts, are veined by small dykes and sheets of lamproite, which are often vesicular.

On the northern side of the central intrusion is a large area of lamproite lapilli-tuff, typically massive but with a distinct radial joint pattern around its southern margin. The contact of this unit with the central magmatic core is marked by a small vertical cliff about 3 m high in which crude, vertical columnar jointing has developed. The core rocks appear to dip under the tuff at a low angle.

Most of the central magmatic core is concealed beneath black soil that contains abundant nodules of secondary magnesite up to 10 cm across. The core occupies a depression around the margins, of which there are small outcrops of a fine-grained olivine-diopside-leucite lamproite; these margins probably represent the chilled marginal facies of the main mass. Elsewhere, magnesite nodules are associated with the weathering of olivine-rich lamproites — as at Mount Cedric and Mount Abbott — and have been reported from the soil above concealed olivine-rich bodies. It seems likely that the core of Fishery Hill is also of olivine-rich lamproite.

In most areas, there is no evidence that the contact between magmatic core and pyroclastics does not dip steeply; but, on its northern margin the tuff forms a partial roof to the body, and the lamproite dips under it at a shallow angle. The radial jointing and crude columnar jointing in the pyroclastics are probably related to the emplacement of the core, which rose only to its present level and probably did not reach the open vent.

The pyroclastics are cut by a number of small dykes and sills. A 3 m-wide dyke in the southwest and a smaller dyke in the north of the vent, are of phlogopite-leucite lamproite, and similar to that which forms lapilli in the

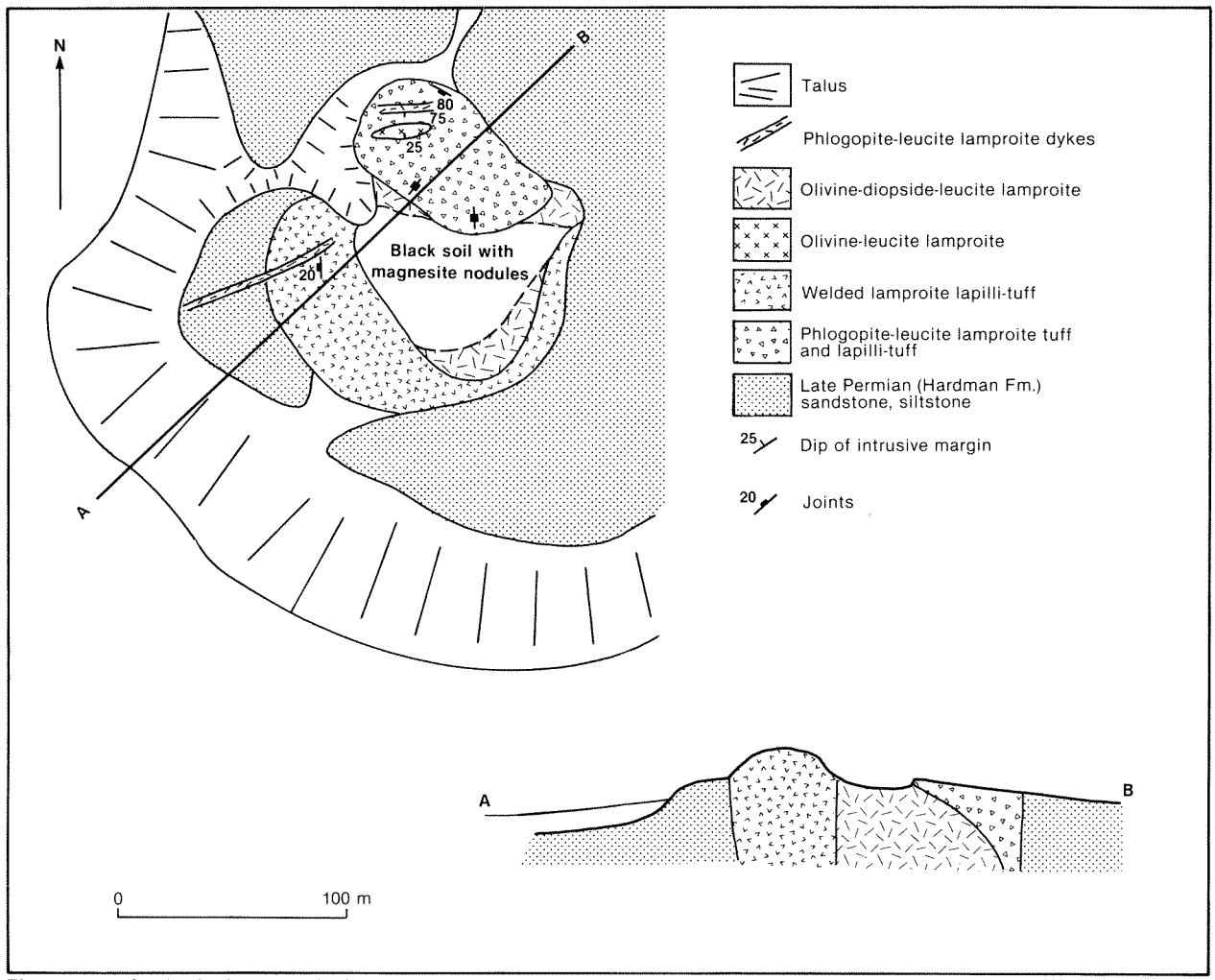


Figure 115. Geological map of Fishery Hill.

GSWA 22669



GSWA 22670

Figure 116. Fishery Hill from the south. Flat-lying sandstone outcrops around the base of the hill, with welded lapilli-tuff forming the summit ridge.

tuff. These dykes were probably intruded shortly after the emplacement of the tuff. A small sill of olivine-leucite lamproite, which intrudes the northern tuff, dips 25° north, and is probably related to the magmatic core rocks.

Petrographically the northern tuff is a fine-grained lamproite lapilli-tuff that contains only very little accidental lithic material, mostly shale fragments, and grains of quartz and microcline. Angular juvenile lapilli of phlogopite-leucite lamproite, up to 5 mm across, are supported by a matrix of abundant smaller lamproite fragments, lesser phlogopite flakes, quartz and microcline grains, and a few olivine pseudomorphs up to 3 mm across. Some larger, more rounded, lamproite lapilli have a narrow, chilled margin; some are vesicular and pumiceous. The main ridge of tuffaceous lamproite on the southern margin of the vent is a lapilli-tuff of similar composition. The lapilli are close-packed, commonly welded, and give the impression of an autobrecciated, xenolith-bearing, phlogopite-leucite lamproite.

Phlogopite-bearing lamproite dykes are uniformly fine-grained and composed of scattered microphenocrysts of phlogopite (strongly embayed and corroded), and altered olivine and leucite, set in a very fine-grained groundmass of small former leucite euhedra, phlogopite, interstitial clay minerals, and accessory priderite.

Specimens available from marginal areas of the central core are fine-grained olivine-diopside-leucite lamproites. Abundant microphenocrysts of altered olivine and acicular diopside are set in a matrix of small former leucite euhedra, potassic richterite, clay minerals, and accessory priderite. Rare, corroded microphenocrysts of phlogopite are present.

The small sill in the northern tuff, and several small, impersistent dykes in the southern tuff, are petrographically similar to the central core. In the dykes, the diopside laths show a strong flow alignment. These small intrusions are probably offshoots from the the main mass.

The Fishery Hill lamproites show little variation in composition: 5.5-9.3% MgO, 50-54% SiO_2 (Table 46) and lie close to the average West Kimberley leucite lamproite. Like other Noonkanbah Field lamproites, all are saturated to oversaturated in silica. The most MgO-poor (5.5% MgO) are the phlogopite-leucite lamproite dykes. The Fishery Hill lamproites, however, appear to be distinguished by their very high initial $^{87}Sr/^{86}Sr$ ratio, 0.71865 (McCulloch and others, 1983), and low $^{208}Pb/^{204}Pb$ and $^{206}Pb/^{204}Pb$ ratios (Nelson and others, 1986) compared to the other West Kimberley lamproites analyzed to date.

TABLE 46. REPRESENTATIVE ANALYSES OF FISHERY HILL LAMPROITES

	1	2	3	4	5
			Percent		
SiO_2	49.95	50.80	51.10	53.90	50.10
TiO_2	6.45	6.65	5.89	6.23	7.02
Al_2O_3	7.12	7.40	8.60	7.90	8.90
Fe_2O_3	4.66	4.83	4.80	5.90	6.60
FeO	1.54	1.43	1.71	0.71	0.71
MnO	0.09	0.08	0.08	0.07	0.06
MgO	9.27	8.48	7.77	5.54	6.62
CaO	3.24	3.35	2.56	1.81	1.88
Na_2O	0.68	0.88	0.64	0.38	0.22
K_2O	9.00	9.26	10.70	10.47	11.45
P_2O_5	0.72	0.62	0.62	1.41	1.45
H_2O^+	4.16	1.97	1.98	1.90	2.33
H_2O^-	0.79	1.76	0.53	0.91	1.10
CO_2	0.23	0.24	0.53	0.47	0.09
Rest	2.36	2.31	2.11	1.95	1.59
Total	**100.26**	**100.06**	**99.62**	**99.55**	**100.12**
			Parts per million		
Ba	14 027	12 763	11 723	8 530	6 351
Li	12	17	8	8	10
Rb	268	275	284	380	381
Sr	1 420	1 420	1 393	1 530	1 337
Pb	43	55	71	90	73
Th	20	23	21	28	22
U	1	3	1	3.5	2
Zr	1 214	1 399	1030	1 493	1 217
Nb	110	147	114	177	139
Y	15	21	18	27	27
La	286	296	351	411	419
Ce	560	539	459	778	585
Nd	175	258	—	284	—
Sc	8	12	17	15	23
V	245	232	159	234	180
Cr	400	433	231	347	220
Co	—	—	31	—	29
Ni	349	453	318	275	300
Cu	64	78	94	54	72
Zn	68	77	101	85	86
Sn	16	24	17	16	13
Mo	—	3	<1	<3	<1
Ga	13	18	19	34	24
As	2	3	1	3.5	<1
S	—	—	540	—	190
F	2 100	2 500	3 020	3 500	3 680
Cl	—	—	70	—	20

1 — Diopside-leucite lamproite; western side of vent, BMR 81210152. 2 — Olivine-diopside-leucite lamproite; western side of vent, BMR 83210280. 3 — Phlogopite-leucite lamproite; dyke in centre of vent, GSWA 71877. 4 — Phlogopite-leucite lamproite dyke; western margin of vent, BMR 83210284. 5 — (Phlogopite)-olivine-leucite lamproite; dyke on northern side, GSWA 71880.

NOONKANBAH HILL

Noonkanbah Hill is a small conical hill, about 30 m high, that rises sharply from the flat alluvial plains of the Fitzroy River. It is located 6 km east-southeast of Fishery Hill, and intrudes flat-lying, thin-bedded sandstones of the Kirkby Range Member of the Hardman Formation. To the west of the vent, the sandstones are poorly exposed; but, on the eastern flank, the sediments form the base of the hill, and are well exposed over a height of about 15 m. Except for patchy green staining, the sediments are not disrupted beyond a few metres from the vent margin, although the margin on the eastern flanks is in places difficult to determine.

The main vent is roughly oval in shape, about 150 × 100 m. It is a crescentic mass of pyroclastics that forms the hill itself, and that has been intruded by a nearly circular magmatic plug which occupies a depression to the west of the summit (Fig. 117). The pyroclastics are quite variable and massive; normally they are fine-grained lapilli-tuffs, with rare fragments up to 10 cm, and few obvious sedimentary pyroclasts. From the summit ridge eastwards, however, the proportion and size of the sedimentary xenoliths increases until the marginal zone is a chaotic megabreccia of locally derived sandstone blocks up to 2.5 m across and sparse lamproite tuff cement (Fig. 119).

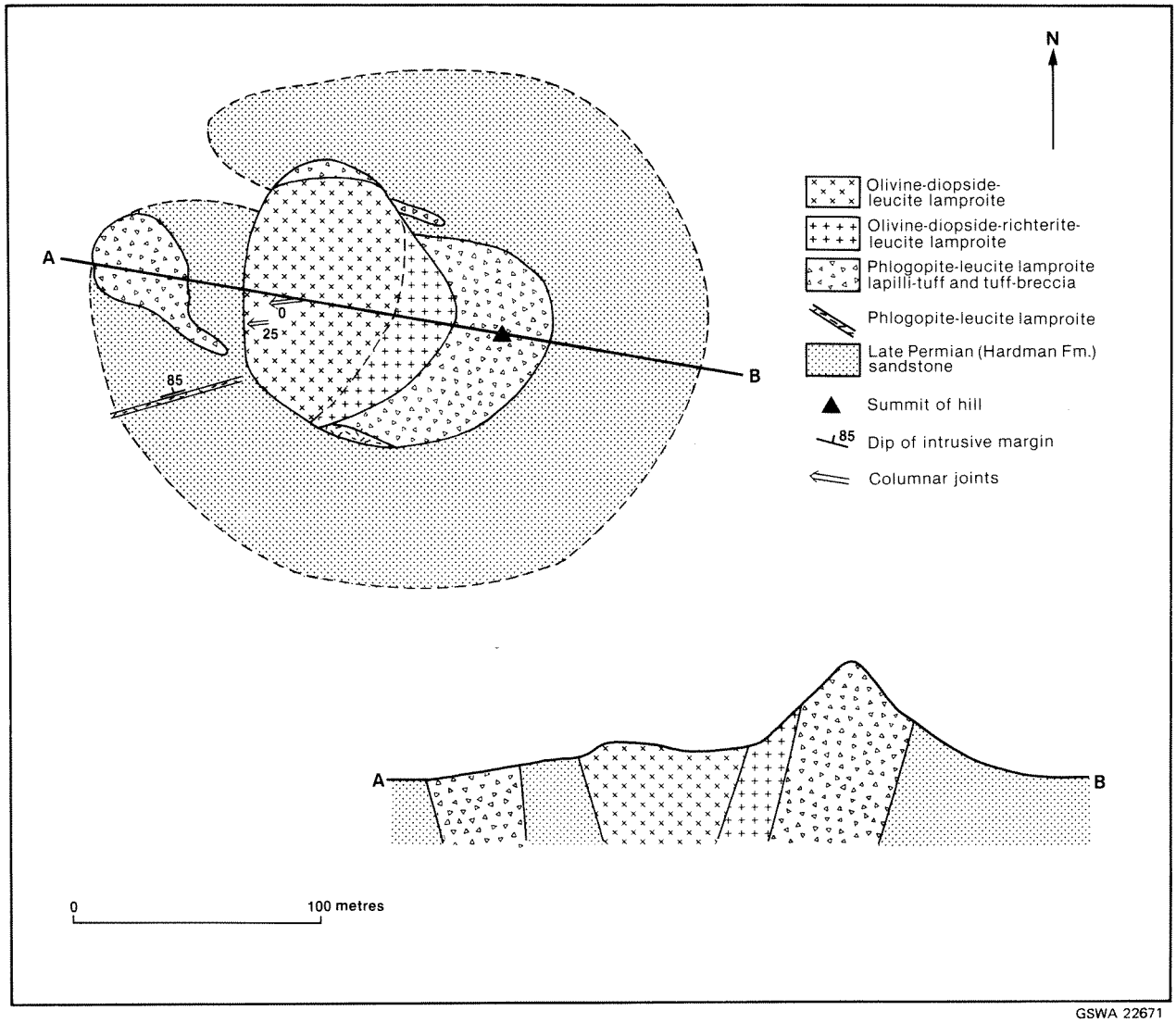


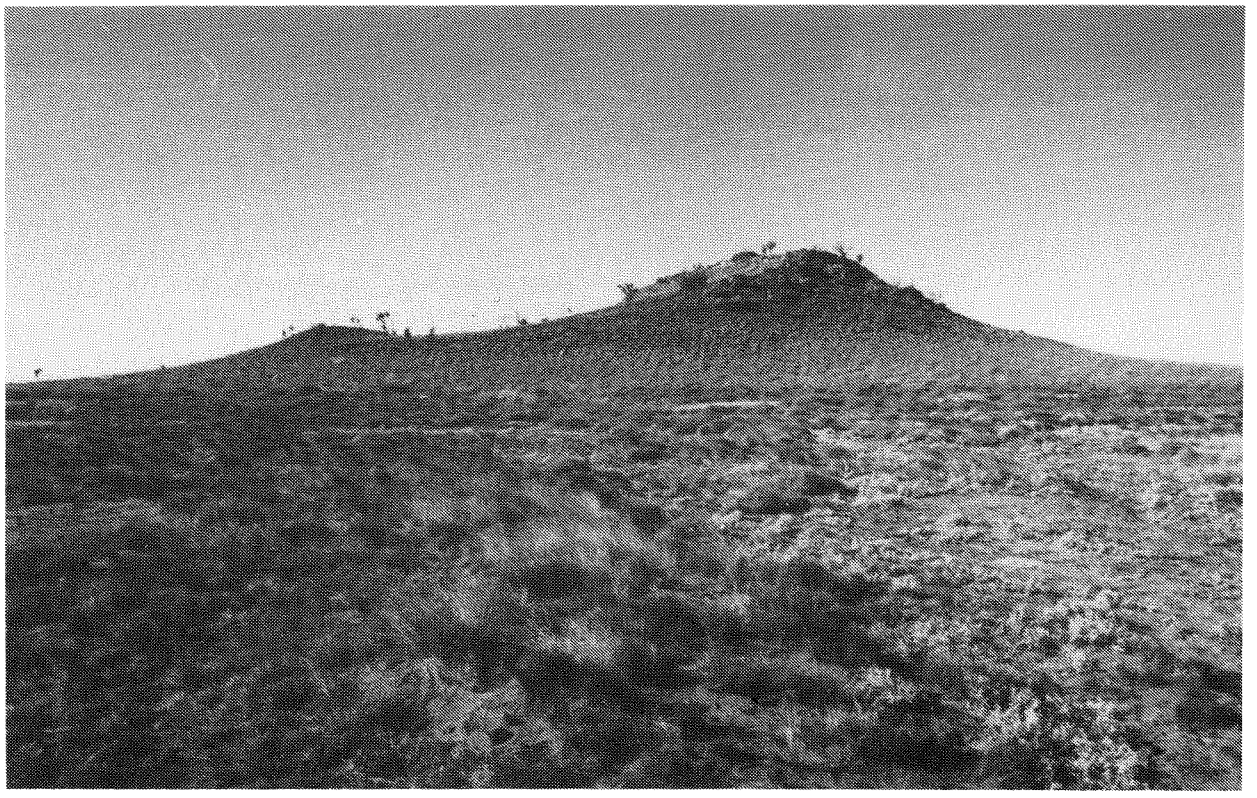
Figure 117. Geological map of Noonkanbah Hill.

This megabreccia, which is similar to that found on Mount Abbott and Mount Gytha, is probably the remains of the initial explosive activity; the intensity of the volcanism was insufficient to remove the blocks from the steep-sided vent. Continued activity brought more lamproitic material into the vent, and probably removed the sedimentary blocks by attrition. The centre of activity appears to have moved slightly westward, towards the position of the central plug; and, on the northern side of the vent, two lenses of lapilli-tuff are seen to be cut by the plug. On the south side of the vent is a small lens of phlogopite-leucite lamproite which is similar to the lamproite lapilli in the tuff, and a narrow dyke which may also be part of the initial phase of activity. The dyke is 60 cm wide, near vertical, and contains prominent flow-aligned phlogopite and flattened vesicles. The dyke neither joins nor cuts the central core of the vent.

A few metres to the west of the main vent is a poorly exposed satellite vent of lamproite lapilli-tuff. The tuff is largely hidden beneath thin soil and sandstone scree; its relationship to the main vent is not obvious.

The central magmatic plug intrudes the pyroclastics on its eastern and northern margins and is in direct contact with sediments elsewhere. The contact is nowhere directly seen; but flow alignment of small diopside laths on the eastern side is nearly vertical, whereas columnar jointing on the western margin indicates an inward dip of between 65 ° and vertical. The main mass of the core is a compact, dark-coloured, olivine-diopside-leucite lamproite; but, on the eastern margin, there is a wide lens of slightly coarser grained, lighter coloured, and strongly jointed rock which also contains potassic richterite. The two rock types form part of the same body, and the margin between them is transitional.

Pyroclastics forming the summit ridge are fine-to medium-grained lapilli-tuffs that contain angular fragments of lamproite, shale, and siltstone, up to 1.5 cm across. The juvenile clasts are of vesiculated, fine-grained, phlogopite-leucite lamproite that contains embayed phenocrysts of phlogopite, up to 1 mm, set in a matrix of turbid clay minerals studded with small former leucite euhedra. Lamproite ash of less than 1 mm



GSWA 22672

Figure 118. Noonkanbah Hill from the south. The hill is composed of chaotic, unbedded lapilli-tuff and coarse breccia; flat-lying Permian sandstone outcrops on the lower slopes.



GSWA 22673

Figure 119. Breccia of sandstone blocks up to 2.5 m across with minor interstitial lamproite tuff, on the eastern flank of Noonkanbah Hill.

diameter is present, but relatively uncommon, and there is no other matrix. The deposit was unconsolidated, and the fragments are now cemented by secondary silica.

The main mass of the central plug is an olivine-diopside-leucite lamproite that contains abundant microphenocrysts of olivine, pseudomorphed by nontronite and up to 1 mm across, and altered leucite, seriate from 1 mm to 0.1 mm diameter. Abundant small prisms of diopside and accessory priderite are enclosed in a dark, turbid, altered matrix. The marginal zone on the eastern side of the plug is similar to the main mass except that poikilitic potassic richterite is very well developed in the matrix. The diopside prisms, which are a little larger and more abundant than in the main mass, show strong flow-alignment; and a little phlogopite is present in the groundmass.

The phlogopite-leucite lamproite dyke is petrographically similar to the fragments in the tuff — flow-aligned phlogopite, up to 1.5 mm long and set in an altered leucite-rich groundmass that contains minute flakes of phlogopite and acicular priderite. The vesicles are lined by secondary zeolites and clay minerals. In the small lens on the southern margin of the vent, phlogopite phenocrysts have developed a dark-coloured rim; phlogopite and poikilitic potassic richterite are prominent in the matrix.

The Noonkanbah Hill lamproites, like those of Fishery Hill, show only small compositional variation between petrographic types. Compositions are typical of the leucite lamproites of the Noonkanbah Field (Table 47).

HOWES HILL

Howes Hill forms a small, rounded, spinifex-covered hill about 150 m diameter and 10 m high; it is located 7 km east of Mount Cedric and on the northern slope of a low ridge of Cherrabun Member siltstones and sandstones.

The lamproite vent is semicircular in outline, and the northern margin is faulted. Lamproite, pyroclastics, and a central plug of phlogopite-diopside-leucite lamproite, abut against disrupted, baked, flaggy siltstones and sandstones that dip at about 80° to the south. Poor outcrops of similar flaggy siltstones to the south and east of the lamproite appear to be flat lying.

The lamproite tuffs, which are mostly fine-grained and massive, occupy a crescentic area around a central magmatic plug. Thin sheets of diopside-leucite lamproite, a metre or so thick, have been intruded parallel to the margin of the plug and appear to dip steeply towards it. The tuffs also enclose, east of the plug, a thick vertical slice of brecciated siltstone that is up to 5 m wide and about 40 m long. This slice is a screen of brecciated wallrock preserved within the vent.

The lamproite plug is about 75 m diameter and is located eccentrically within the vent. It is composed of medium-grained, dark-coloured, phlogopite-diopside-leucite lamproite. The northen margin of the plug is truncated against a fault, but the southern margin is sparsely vesicular, and flow foliation indicates an inward dip of 70° to 80° for the contact with the tuffs.

A few hundred metres to the southwest, Jeppe (1971) reports a small lamproite, Howes Hill West, which

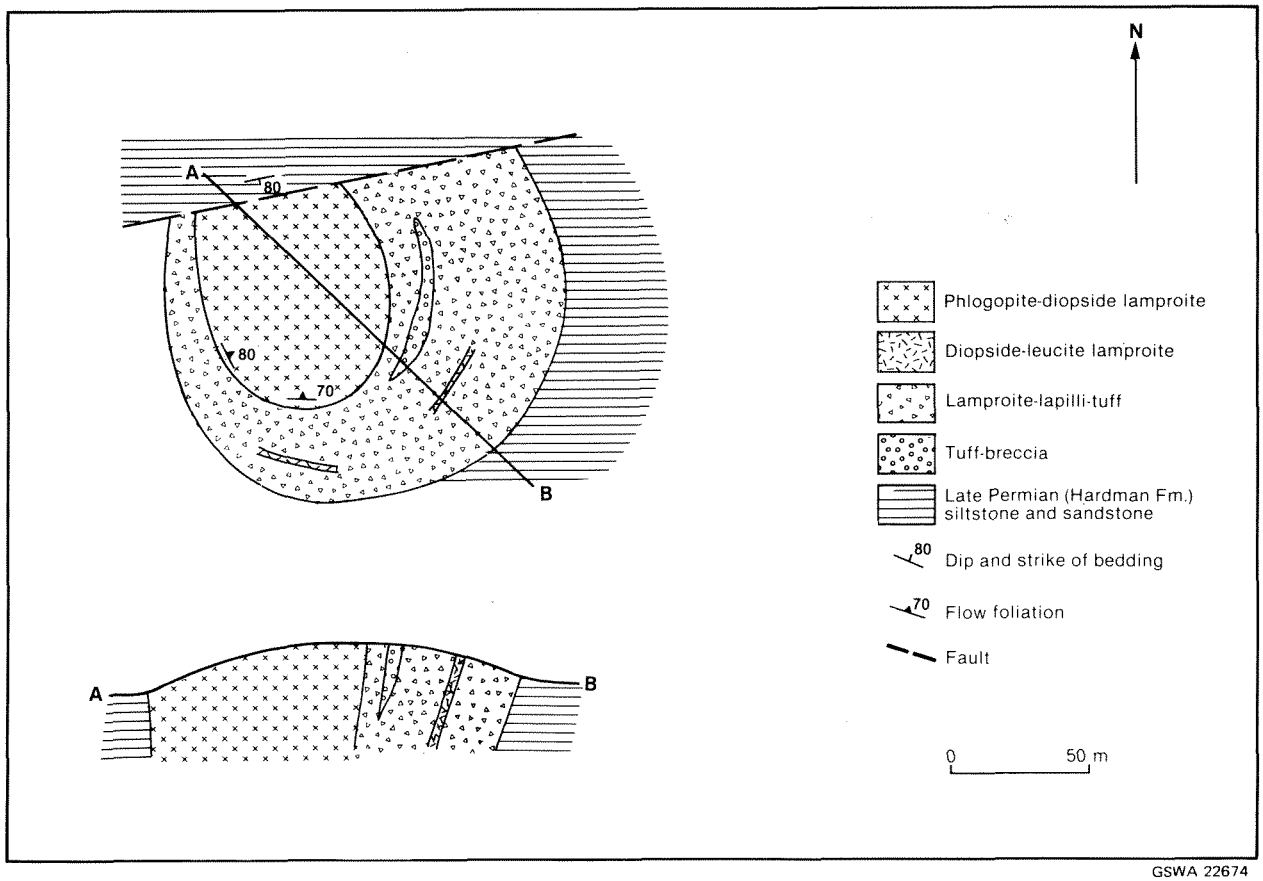


Figure 120. Geological sketch map of Howes Hill.

TABLE 47. REPRESENTATIVE ANALYSES OF NOONKANBAH HILL LAMPROITES.

	1	2
	Percent	
SiO_2	50.75	50.60
TiO_2	5.68	6.18
Al_2O_3	7.59	7.95
Fe_2O_3	4.82	5.73
FeO	1.34	1.23
MnO	0.07	0.07
MgO	9.18	7.09
CaO	3.70	4.00
Na_2O	0.92	0.61
K_2O	8.69	9.67
P_2O_5	0.53	0.65
H_2O^+	2.44	1.89
H_2O^-	1.70	1.38
CO_2	0.22	0.13
Rest	1.66	2.05
Total	**99.29**	**99.23**
	Parts per million	
Ba	8 167	11 190
Li	11	10
Rb	243	203
Sr	1 254	1 190
Pb	39	44
Th	22	23
U	2	2
Zr	1 235	1 311
Nb	118	134
Y	19	21
La	228	242
Ce	419	437
Nd	182	218
Sc	12	14
V	178	188
Cr	461	506
Ni	354	443
Cu	70	75
Zn	64	63
Sn	20	24
Mo	<3	3
Ga	16	21
As	2.5	2.5
F	1 900	2 300

1 — Amygdaloidal diopside-leucite lamproite; southwest margin, BMR 83210265. 2 — Olivine-diopside-leucite lamproite; northeast of central mass, BMR 83210266.

TABLE 48. REPRESENTATIVE ANALYSES OF HOWES HILL LAMPROITES.

	1	2
	Percent	
SiO_2	52.30	51.50
TiO_2	5.14	6.53
Al_2O_3	8.90	7.90
Fe_2O_3	4.90	5.20
FeO	2.00	1.63
MnO	0.05	0.08
MgO	7.21	7.28
CaO	1.88	3.57
Na_2O	0.22	0.65
K_2O	8.87	9.42
P_2O_5	1.07	0.85
H_2O^+	3.07	1.87
H_2O^-	2.53	1.03
CO_2	0.12	0.04
Rest	2.04	1.94
Total	**100.30**	**99.49**
	Parts per million	
Ba	10 193	9 832
Li	29	11
Rb	224	237
Sr	1 269	1 190
Pb	70	42
Th	18	19
U	<1	1
Zr	1 030	1 029
Nb	103	91
Y	19	16
La	381	298
Ce	420	308
Sc	19	16
V	191	164
Cr	292	255
Co	20	32
Ni	700	280
Cu	100	95
Zn	85	80
Sn	—	15
Ga	19	16
As	2	<1
S	300	930
F	3 000	3 160
Cl	310	<20

1 — Potassic-richterite - leucite lamproite; sill in tuff, GSWA 71885. 2 — Diopside - potassic-richterite - olivine - phlogopite - leucite lamproite; centre of plug, GSWA 71882A.

probably intrudes along the same fault that forms the northern margin of the main body.

The lapilli-tuff contains a variety of cognate and juvenile lamproite fragments, up to 2 cm across, together with a few small xenoliths of metasomatized siltstone and shale; they are contained in a matrix of lamproite ash, clay minerals, quartz, and phlogopite. The juvenile lapilli are of fine-grained, olivine-leucite lamproite; but coarser, probably cognate, clasts also contain altered leucite phenocrysts, and there are abundant cognate clasts of phlogopite-leucite lamproite. The screen of coarse, sediment-rich breccia consists of plastic, metasomatized fragments of siltstone in a very fine-grained, silica-rich matrix. The presence of a lamproite component is shown by nontronite pseudomorphs of small olivines in the matrix.

The lapilli-tuff has been intruded by sheets of medium-grained, diopside-leucite lamproite that contains altered leucite, up to 0.5 mm, and flow aligned acicular diopside 1 mm long. The diopside is partly altered to colourless, weakly pleochroic potassic richerite and the green chloritic matrix contains some pink potassic richterite in addition to priderite and phlogopite.

The main mass of the magmatic core is a medium-grained olivine-diopside-leucite lamproite; the named minerals occur as phenocrysts, up to 1 mm across, in a groundmass of dark clay, small, altered leucite crystals, priderite and scattered, large, poikilitic plates of potassic richterite. The rock also contains large altered masses of spongy leucite, up to 5 mm across, and quartz-filled vesicles up to 1 mm diameter. A specimen from the northern margin of the plug is similar, but has less phlogopite and more abundant poikilitic potassic richterite.

Howes Hill lamproites exhibit little compositional variation and, apart from slightly lower CaO and lower Rb and Rb/Sr ratio, lie close to the average West Kimberley leucite lamproite in composition. Representative analyses are given in Table 48.

MAMILU HILL

The topographic feature known as Mamilu Hill is a low, rounded hill of thin-bedded sandstones of the Cherrabun Member of the Hardman Formation, 8 km southwest of Walgidee Hills. The Mamilu Hill lamproite

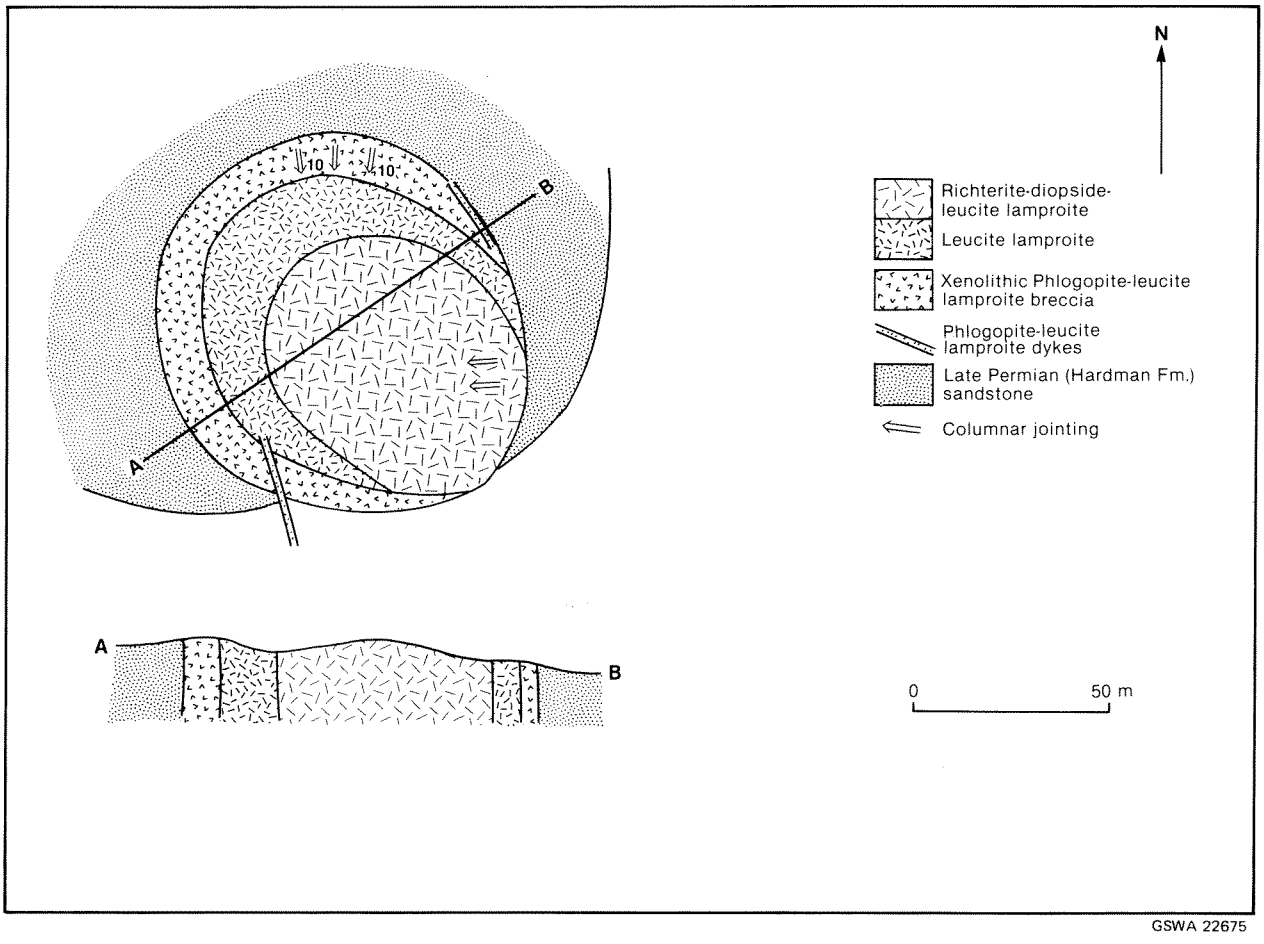


Figure 121. Geological map of Mamilu Hill

does not form a marked topographic feature, but occurs as a low rise on the southern flank of the hill; it is a small body, about 90 m diameter, and consists of concentric, crescentic zones of lamproite breccia and magmatic lamproite. The intrusion of the lamproite has had little effect on the surrounding sandstones, which remain flat lying and undisturbed to within a few metres of the intrusion.

The outer zone of the pipe is a phlogopite-leucite lamproite that contains numerous small sedimentary xenoliths. In places the rock is brecciated and fragmental, and sometimes vesicular. Around the northern margin, small columnar joints dip 10° towards the centre; elsewhere, close-spaced radial joints are common. The available evidence indicates that Mamilu Hill lamproite is a plug which occupies a nearly vertical cylindrical pipe, as suggested by Prider (1960).

The central magmatic plug consists of a marginal zone of poorly exposed, grey, fine-grained leucite lamproite, up to 12 m wide and partly enclosing a nearly circular central zone 60 m in diameter, which forms a small central rise. This central plug of potassic-richterite – diopside – leucite lamproite abuts directly against the enclosing sediments on the southeast margin; crude, flat-lying columnar jointing is present. Prider (1960) noted that the two zones of the central plug are chemically similar and that the outer zone was probably the chilled margin of the inner zone. The disposition of units in Fig. 121 suggests that the central zone was probably a second pulse of magma after the first had partly crystallized.

Two small dykes are marked on Fig.121; both are of fine-grained, earthy, brown, phlogopite-leucite lamproite; and the phlogopite is strongly aligned by vertical platy flow.

A small vent of lamproite tuff, a few metres across, was noted by Jeppe (1971) on the adjacent hill to the southwest.

The outer pyroclastic zone is a xenolith-rich lapilli-tuff. The xenoliths, up to 1 cm across, are of siltstone, shale, laterite pebbles, and rare grains of quartz and microcline. The juvenile lapilli are of phlogopite-leucite lamproite that contains corroded phlogopite, up to 1.5 mm, and a brown, devitrified, glassy groundmass, studded with small altered leucites.

The outer zone of the central magmatic plug is a fine-grained olivine-leucite lamproite. Small altered olivine crystals, about 0.3 mm across, and rare corroded phlogopite flakes, are set in a mass of small euhedra of altered leucite, interstitial clay minerals, and priderite. The core of the plug is a similar, fine-grained, leucite-rich lamproite that contains a few small olivines which have been replaced by green nontronite. The rock lacks phlogopite, but there is abundant interstitial potassic richterite and much small prismatic diopside.

Mamilu Hill is characterized by extremely leucite-rich compositions: 50 to 55% SiO_2; and 9 to 12% Al_2O_3 and K_2O. The new analyses (Table 49) are very similar to

those presented by Wade and Prider (1939) and Prider (1960), and support Prider's contention that the mineralogical and petrographic variation within the body is attributable to different rates of cooling from magma of uniform composition.

TABLE 49. REPRESENTATIVE ANALYSES OF MAMILU HILL LAMPROITES.

	1	*2*
	Percent	
SiO_2	53.61	53.90
TiO_2	5.66	5.26
Al_2O_3	9.85	9.60
Fe_2O_3	5.66	5.90
FeO	1.22	1.48
MnO	0.11	0.08
MgO	4.99	4.79
CaO	2.13	2.34
Na_2O	0.67	0.61
K_2O	11.22	10.30
P_2O_5	0.72	0.81
H_2O^+	1.53	2.00
H_2O^-	0.48	1.12
CO_2	0.30	0.09
Rest	1.93	1.64
Total	**100.08**	**99.92**
	Parts per million	
Ba	10 105	6 652
Li	6	10
Rb	322	252
Sr	1 033	1 085
Pb	71	80
Th	25	17
U	3	<1
Zr	1 215	1 014
Nb	129	106
Y	18	17
La	409	342
Ce	552	479
Sc	—	17
V	282	185
Cr	296	267
Co	30	35
Ni	263	450
Cu	51	85
Zn	77	93
Sn	4	—
Ga	23	23
As	1	1
S	—	100
F	3 200	3 430
Cl	—	160

1 — Diopside-leucite lamproite; centre of plug, BMR 79211048.
2 — Potassic-richterite - leucite lamproite; inner core of plug, GSWA 71310.

HILLS CONE

Hills Cone is located 1 km east of Mayborough Bore on the main road north of Noonkanbah Homestead. Two small conical hills, about 10 m high and 100 m apart, each have a central depression that gives the appearance of a small volcanic crater. The "craters", however, are erosional features in the central intrusions of two small vents. Overall, Hills Cone is an irregularly shaped pipe, about 225 × 130 m, which has a dyke-like apophysis extending northwards, and which is filled, mainly, with a variety of tuffs (Fig. 122).

The pipe intrudes flat-lying, flaggy sandstones of the Hardman Formation, which are poorly exposed around the western margin of the vent. The sandstones are not disturbed except within a few metres of the vent margin.

The vent, which is filled mainly with lamproite lapilli-tuff, is moderately well exposed in the vicinity of the two small hills; but, elsewhere, it is marked by a weathered, rubbly outcrop. On the southern flank of the western hill there is a suggestion of bedding that dips inwards; but, otherwise, the pyroclastics appear to be a chaotic infilling of a steep-sided vent. Variations in the tuff include, on the eastern hill, a welded lapilli-tuff that lacks the dark lateritic material of the main tuff. This unit probably represents a final phase of intrusive tuff; the body shows distinct columnar jointing, the columns dipping outwards at 20°. Elsewhere the lapilli-tuff grades into a tuff-breccia containing angular blocks of country rock.

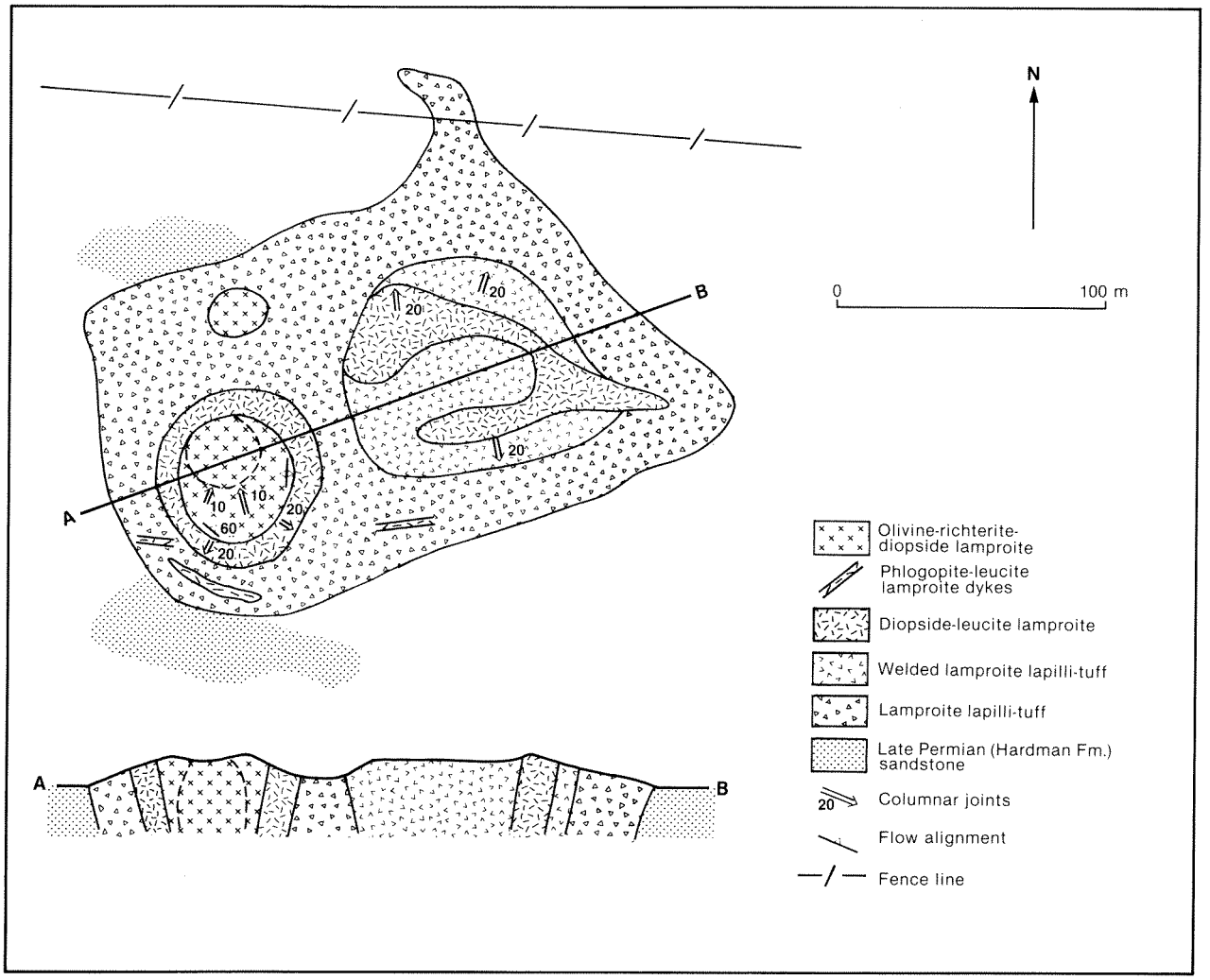
A number of small dykes and sills of phlogopite-leucite lamproite intrude the pyroclastic pile, but these are probably late-stage intrusions. The main magmatic intrusion of the eastern vent is a complex body of fine-grained lamproite that forms a partial ring-dyke and extends eastwards as a dyke-like body. Columnar jointing indicates an inward dip of 70° for the margins of the body, the outcrop of which forms the rim of the "crater" on the eastern vent.

The western vent is filled by a zoned plug of lamproite about 50 m diameter. An outer, relatively fine-grained zone, about 10 m wide, forms a low rim surrounding a central depression that formed over coarser grained, more easily weathered lamproite. There is no obvious intrusive contact between the two units, and the rim rocks are probably the chilled marginal facies of the plug. Columnar and radial jointing are prominent, except in a small area on the north side of the plug. The columns in the marginal rocks indicate an inward dip of 70° for the margin of the plug, whereas columns in the central area indicate an outward dip of 80°. Flow alignment of vesicles in parts of the body shows a dip between vertical and 60° inwards.

North of the western plug is a small, poorly outcropping area of coarse-grained diopside-leucite lamproite, probably a small plug about 20 m diameter.

Hills Cone appears to be essentially a single pyroclast-filled vent with two major centres of magmatic intrusion. The main pyroclastic deposit is uniform throughout the vent, but a later phase, as well as an irregular body of lamproite, is associated with the eastern vent. The western, and possibly younger, vent is occupied by a lamproite plug. The arrangement of the two vents probably reflects a source zone elongated northeast.

Petrographically, the main pyroclastic unit is a medium-grained, clast-supported, lapilli-tuff that contains angular fragments of lamproite, and accidental clasts of laterite, siltstone, and shale, up to 15 mm across. The juvenile lamproite lapilli are strongly vesicular and contain sparse phenocrysts of olivine and phlogopite in a devitrified glassy groundmass containing abundant small altered leucites. The matrix is of lamproite ash that has been altered to clay minerals and much secondary silica, and a few quartz grains. The central tuff of the eastern vent is a fine-grained lapilli tuff, containing clasts



GSWA 22676

Figure 122. Geological map of Hills Cone.

up to 4 mm, and is matrix-supported. The lamproite fragments are a glassy leucite lamproite similar to those of the main tuff unit; but both olivine and phlogopite are less prominent. Accidental material includes shale fragments and grains of quartz and microcline in the matrix. The matrix is predominantly altered to clay minerals, pale green or pale brown in colour, but includes many small, altered, leucite euhedra, some with a skin of lamproite glass, and much secondary silica. A welded lapilli-tuff from the base of the western hill is similar but contains streaked out lapilli up to 4 cm long.

The magmatic intrusion of the eastern vent is a fine-grained diopside-olivine-leucite lamproite containing abundant microphenocrysts of altered olivine up to 1 mm and former leucite up to 0.7 mm, in a groundmass of small altered leucites, acicular diopside, and accessory priderite with interstitial clay minerals and small flakes of phlogopite. In the dyke-like extension of this body, olivine and diopside are less common and there is a little poikilitic potassic richterite that forms prismatic grains up to 1 mm long. Large spongy masses of altered leucite, up to 3 mm across and enclosing tiny grey-green grains of pleonaste, are also found in this rock.

The most significant difference between the centre and the margin of the plug in the western vent is grain size, particularly with respect to diopside and potassic richterite. The central mass is an olivine - diopside - potassic-richterite - leucite lamproite: olivine phenocrysts range up to 1 mm, often in glomeroporphyritic aggregates, and often replaced by nontronite and quartz. Diopside forms abundant prismatic crystals up to 3 mm long, together with small, acicular, groundmass crystals. The bulk of the rock is composed of altered leucite, which occurs as small crystals 0.2-0.4 mm across, or as spongy masses up to 3 mm; and the interstitial material is dark clay minerals, abundant masses of pink potassic richterite, and accessory priderite. In the marginal zone, the diopside is reduced to small acicular prisms; and the potassic richterite is colourless, and often forms as overgrowths on the diopside. A further distinction is that the groundmass contains small phlogopite flakes.

Although it lacks potassic richterite, the small plug to the north of the western vent is similar in appearance to the central part of the main plug, particularly in regard to the glomeroporphyritic olivine and prismatic diopside. The groundmass of the rock, however, is a brown, turbid devitrified glass with many small priderite prisms and phlogopite flakes.

Hills Cone lamproites are highly uniform in

composition, as are the other Noonkanbah Field leucite lamproites. Representative analyses (Table 50) show only small differences in composition between the western and eastern vents.

TABLE 50. REPRESENTATIVE ANALYSES OF HILLS CONE LAMPROITES

	1	*2*	*3*
	Percent		
SiO_2	51.90	52.20	51.70
TiO_2	5.16	5.92	6.11
Al_2O_3	9.40	8.40	8.80
Fe_2O_3	5.70	5.90	5.80
FeO	1.23	1.26	1.84
MnO	0.07	0.07	0.09
MgO	5.86	6.63	5.92
CaO	2.96	2.67	3.32
Na_2O	0.20	0.36	0.74
K_2O	10.50	9.70	9.27
P_2O_5	1.99	0.97	0.79
H_2O^+	2.50	2.21	1.87
H_2O^-	0.94	1.63	1.11
CO_2	0.21	0.18	0.06
Rest	1.65	2.12	2.16
Total	**100.27**	**100.22**	**99.49**
	Parts per million		
Ba	7 265	11 666	12 363
Li	8	11	7
Rb	277	305	313
Sr	1 229	1 086	1 057
Pb	90	60	60
Th	23	17	16
U	2	<1	<1
Zr	1 108	1 103	1 129
Nb	112	98	94
Y	23	16	20
La	418	337	317
Ce	548	403	394
Sc	16	17	19
V	203	186	169
Cr	267	246	226
Co	35	30	35
Ni	320	540	370
Cu	85	110	120
Zn	79	84	79
Mo	<1	1	1
Ga	23	18	15
As	<1	2	<1
S	300	500	400
F	3 360	3 200	3 160
Cl	140	160	140

1 — Leucite lamproite dyke; eastern vent, GSWA 71325. 2 — Olivine-diopside-leucite lamproite, centre of eastern vent, GSWA 71326. 3 — Potassic-richterite - olivine - diopside - leucite lamproite; centre of western vent, GSWA 71327.

"P" HILL

"P" Hill is the most accessible of the lamproites of the Noonkanbah Field; it is situated by the side of the Fitzroy River Road, 9 km east of Noonkanbah Homestead, in the alluvial plain of the Fitzroy River. It forms a distinct, double peak: a small knob of lamproite breccia rises abruptly from a broad conical hill to a height of about 35 m; and a lower rounded hill of dark lamproite rises a few metres to the southwest (Fig. 124). The lamproite intrudes Early Permian sediments of the Noonkanbah Formation, which are exposed at several localities around the base of the hill. The sediments are flat-lying, thin-bedded sandstones and siltstones, often iron-stained and ferruginized.

The vent is oval, about 125 × 75 m, elongated east-northeast, and is filled mostly with fine-grained lamproite lapilli-tuff. Exposure of the tuff is poor, but it is probably an unbedded, chaotic vent-filling deposit. A small dyke of tuff, 3 m wide, can be traced for 50 m east southeast from the main body of tuff, where it disappears beneath alluvium.

The summit of the hill is formed by a mass of lamproite agglomerate intrusive into the lapilli-tuffs. The lamproite component of the mass is pale green with wisps of pale-brown material; it has the appearance of a welded lapilli tuff, or autobrecciated lamproite; but, in parts, is more recognizably pyroclastic, and has inclusions of vesicular lamproite. More important, however, is the accidental component of the rock. Xenoliths of green-stained siltstone are plentiful in the upper parts of the body and on the northeast face, and large blocks, 1-2 m across, are common. This body appears have formed in the waning phase of pyroclastic activity, or as a short-lived renewal of activity before the intrusion of the lamproite plug; it probably occupies the neck of the original volcano. The body displays large columnar joints which dip at less than 10° to the northeast. A number of thin, impersistent veins of tuffisite, up to 15 cm across, cut the body, particularly near the summit, and probably represent the final degassing of the magma.

The main lamproite intrusion is a zoned plug about 50 m diameter. The western half of the plug is coarse-grained and rich in potassic richterite, whereas the eastern half is strongly porphyritic, has a fine-grained groundmass, and lacks potassic richterite. Petrographic differences, and the presence of crude columnar jointing that dips 20° southwest, suggest an internal contact, although none was found, and the two rocks appear to grade into each other. The plug was probably deflected from the original vent by the earlier emplacement of the spine of lamproite agglomerate, and probably cooled slowly beneath a cover of tuff.

Petrographically, the main pyroclastic deposit is a fine-grained, matrix-supported lapilli-tuff. The lapilli, usually 2-5 mm but up to 2 cm across, are of leucite lamproite that contains sporadic phlogopite and abundant small altered leucites in a devitrified glassy matrix. Accidental material includes a few, small, shale fragments and grains of quartz and microcline. The matrix makes up about 50% of the rock, and is thoroughly altered to clay minerals, although small shards and fragments of lamproite ash can be identified, together with abundant isolated leucite crystals, and a few phlogopite flakes.

The intrusive lamproite agglomerate "spine" appears at first sight to be a sparsely phlogopite-bearing leucite lamproite that encloses large xenoliths of shale, sandstone, siltstone, and laterite, and xenocrysts of quartz and microcline. Closer examination reveals a distinct pyroclastic texture of lamproite lapilli in a matrix of comminuted lamproite. Post-emplacement welding of both lapilli and matrix has given a uniform appearance to the rock; the original lapilli are distinguished from the greenish matrix only by their pale-brown colour. Apart from the degree of welding and the size of the xenoliths, the "spine" is very similar to the surrounding lapilli-tuffs.

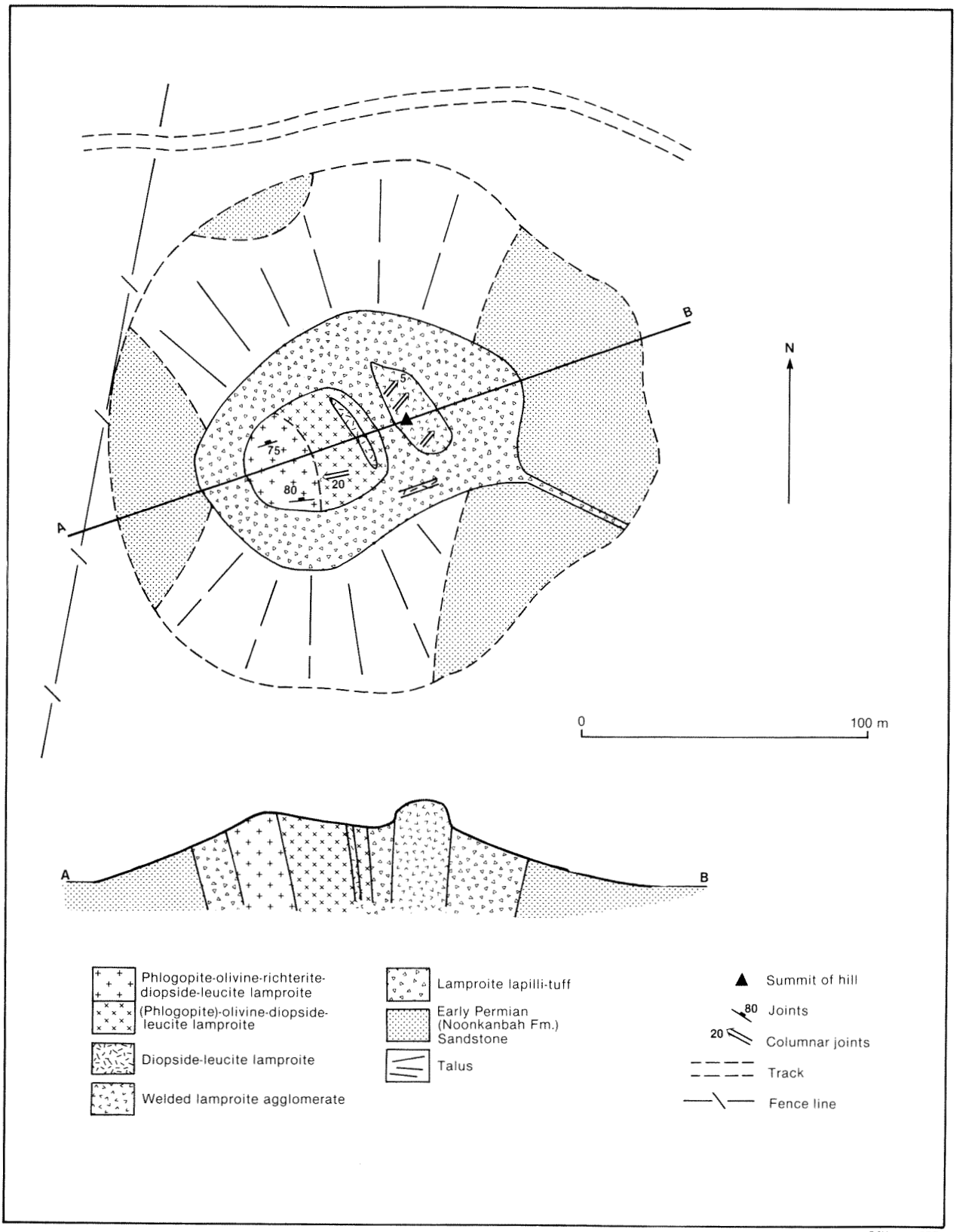
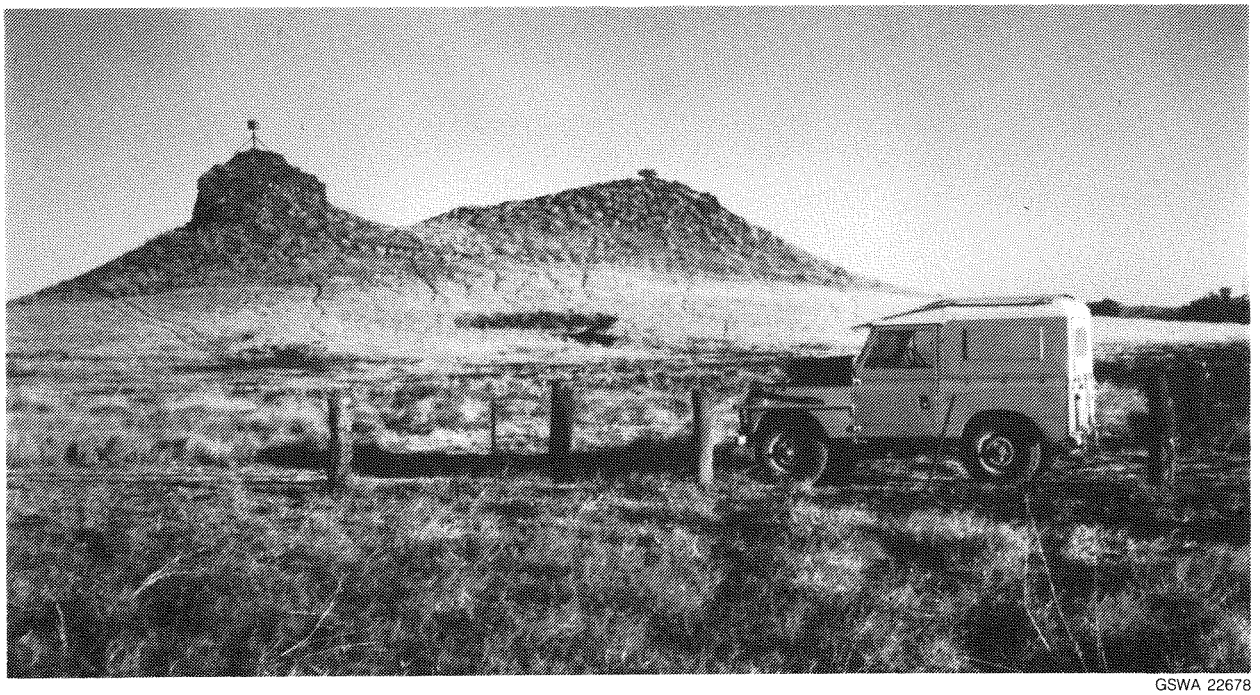


Figure 123. Geological map of "P" Hill.

The central lamproite of "P" Hill is one of the coarser grained lamproites of the West Kimberley. Leucite occurs as altered phenocrysts up to 3 mm diameter, but is usually about 1 mm across. Diopside is found as prisms up to 4 mm long; and abundant nontronite pseudomorphs after olivine are 1 mm long and often form glomeroporphyritic aggregates. A few corroded flakes of phlogopite are present. The groundmass, apart from numerous small leucite and diopside crystals, consists of large poikilitic masses of potassic richterite, up to 3 mm across, and patches of dark clay minerals with small interstitial flakes of phlogopite. Accessory minerals include priderite, apatite, and wadeite. The finer grained portion of the plug is distinctly porphyritic;



GSWA 22678

Figure 124. "P" Hill from the north: the steep sided knob on the left is a spine of intrusive lamproite agglomerate. (Photo: G. Derrick, BMR).

leucite, up to 1.5 mm, and smaller olivine pseudomorphs make up about 30% of the rock. The groundmass contains abundant small diopside laths and a few phlogopite flakes up to 1 mm long but, otherwise, consists of clay minerals enclosing minute leucite and priderite grains. The leucite and olivine phenocrysts suggest a relationship with the coarse-grained part of the plug; but, otherwise, the two rocks are very different.

Little variation in composition is evident between the different rock types of "P" Hill. All, like most other Noonkanbah Field lamproites, have high SiO_2 (50-55%) and K_2O (9-11%), and low MgO (5-8%). There are small differences apparent between the coarser grained potassic richterite-bearing lamproites of the western half, such as lower MgO, Ni, and Cr, and slightly higher SiO_2 and Al_2O (Table 51), but overall petrographic differences appear to result from different rates of cooling rather than differences in rock chemistry.

TABLE 51. REPRESENTATIVE ANALYSES OF 'P' HILL LAMPROITES

	1	*2*	*3*
	Percent		
SiO_2	53.47	52.13	52.42
TiO_2	6.43	5.60	6.36
Al_2O_3	8.27	8.13	8.04
Fe_2O_3	5.52	5.11	5.43
FeO	1.56	1.66	1.46
MnO	0.09	0.10	0.09
MgO	5.38	7.00	6.63
CaO	2.95	3.50	3.48
Na_2O	0.68	1.07	0.73
K_2O	10.36	9.79	10.29
P_2O_5	0.66	0.39	0.55
H_2O^+	1.09	1.56	1.98
H_2O^-	0.62	0.82	0.79
CO_2	0.16	0.81	0.28
Rest	1.81	1.62	1.87
Total	**99.05**	**99.29**	**100.40**
	Parts per million		
Ba	9 509	8 758	9 622
Li	7	8	10
Rb	236	192	248
Sr	1 166	1 119	1 191
Pb	38	32	44
Th	23	20	23
U	2	2	3
Zr	1 107	1 007	1 300
Nb	100	95	132
Y	17	16	22
La	235	197	241
Ce	332	291	446
Nd	174	146	210
Sc	11	12	15
V	165	154	213
Cr	317	265	396
Ni	179	380	342
Cu	69	69	86
Zn	100	69	85
Sn	25	12	21
Ga	14	12	21
As	2	2	2.5
F	3 000	2 000	2 600

1 — Phlogopite - diopside - potassic-richterite - leucite lamproite, southerwestern end of western plug, BMR 81210145. 2 — Olivine-diopside-leucite lamproite; eastern margin of western plug, BMR 81210147. 3 — Diopside - potassic-richterite - leucite lamproite; summit of western plug, BMR 83210259.

DJADA HILL

This small lamproite body is located in the floodplain south of the Fitzroy River, 7 km southwest of Noonkanbah Homestead and close to the track which leads south towards the Saint George Ranges. The hill is now known as Djada Hill but previous spellings have been Dadja Hill (Wade and Prider, 1940; Prider, 1960) and Barjar Hill (Simpson, 1925).

The lamproite forms a small circular hill, 100 m diameter and 15 m high, on the bank of a large billabong. (Figs. 125, 126). The centre of the hill has been eroded and a large depression, open to the south, is floored by black soil. A small stream to the east and north almost makes an island of the intrusion, thus obscuring its relationships with the sediments of the Noonkanbah Formation which it intrudes.

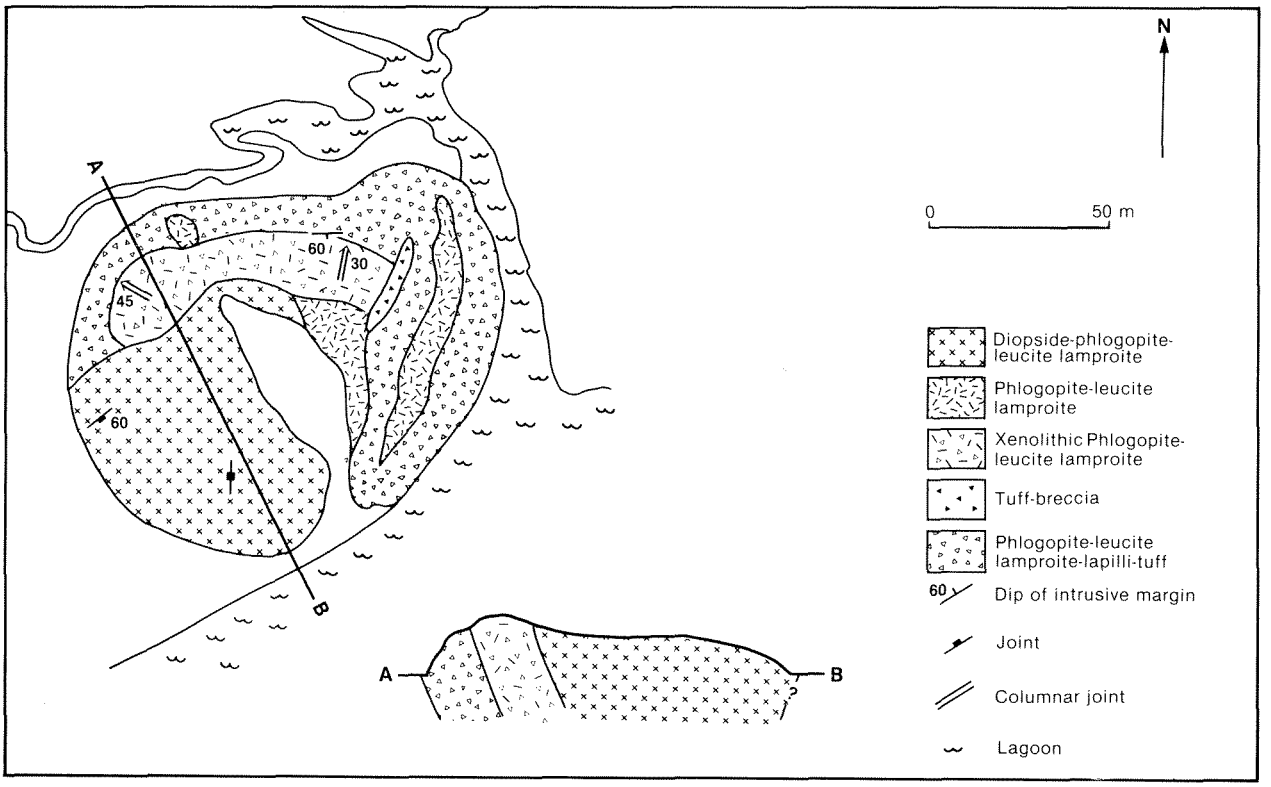


Figure 125. Geological map of Djada Hill.

Djada Hill lamproite is a complex body; it consists of lamproite lapilli-tuff intruded by a variety of crescentic lamproite sheets and an eccentric plug of coarse lamproite. Pyroclastics occupy the northern and eastern sectors of the hill, and are uniform, medium- to fine-grained, very poorly bedded lapilli-tuffs. Intruding the tuff on the northern side of the vent is a thick sheet of xenolith-bearing phlogopite-leucite lamproite, which forms the summit ridge of the hill. This rock is similar to xenolith-bearing intrusions at other locations, notably "P" Hill, and contains numerous small sedimentary xenoliths up to 3 cm across. At the eastern end of the ridge xenoliths are larger and more numerous; occasionally blocks range up to 1 m across. The sheet dips at between 45° and 60° to the south, as is shown by well-developed columnar joints (Fig. 127) and exposed intrusive margins on the northern side. The eastern end of this body is truncated by a small, vertical, intrusive lens of coarse tuff-breccia, which contains sandstone and shale blocks up to 1 m across in a sparse lamproitic matrix.

Intruding the lapilli-tuff of the eastern sector are two steeply dipping sheets of phlogopite-leucite lamproite that have prominent flow-aligned phlogopite. A small pod of similar material is found near the northwest margin of the vent.

The lamproite plug is a nearly circular body, about 60 m diameter, but its eastern part is hidden beneath the soil filling the central depression of Djada Hill. The plug is of diopside-phlogopite-leucite lamproite, and little variation can be seen in the field except that it is slightly coarser grained in the central parts. Throughout the length of the western margin of the plug, which forms a small cliff a few metres high, there is a prominent jointing that dips 60° southeast. The jointing is parallel to the dip of the xenolithic lamproite sheet, but its significance is not clear. On the ridge there is also close-spaced vertical jointing trending north-south.

The pyroclastics are welded lapilli-tuffs of phlogopite-leucite lamproite that contain abundant small pyroclasts of shale and siltstone. The sparse matrix of lamproite ash carries a few xenocrysts of quartz and microcline, but has been welded to such a degree that the rock has lost much of its tuffaceous texture. The lapilli are up to 10 mm across and contain microphenocrysts of phlogopite to 1 mm, and smaller altered microphenocrysts of leucite and olivine, all in a groundmass of devitrified glass that contains abundant small altered leucites. Olivine has been replaced by nontronite and quartz. The intrusive sheet of xenolithic lamproite is petrographically very similar to the lapilli-tuffs, except that wall-rock xenoliths are more abundant and include sandstone in addition to shale and siltstone. The rock may be a thoroughly welded lapilli tuff, the final phase of tuff formation that is similar to the summit rocks of "P" Hill.

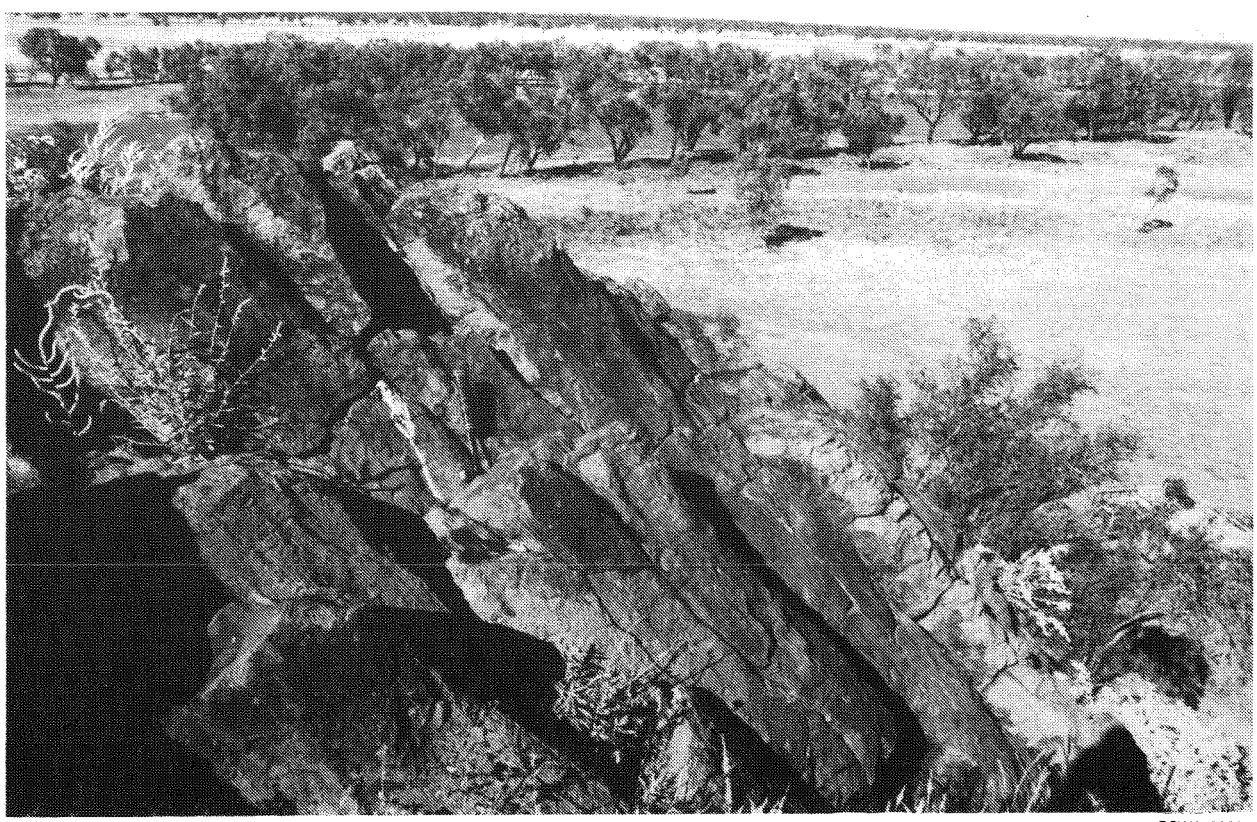
The sheets of phlogopite-leucite lamproite that have intruded the tuffs contain very little olivine; but consist of phlogopite up to 2 mm long, in a matrix of altered leucite and interstitial clay minerals, phlogopite, and priderite needles. The body on the eastern side of the central depression also contains sparse interstitial potassic richterite and a little diopside; it may be a chilled marginal phase of the main plug.

The lamproite plug is a fairly uniform, porphyritic diopside-phlogopite-leucite lamproite that contains



GSWA 22680

Figure 126. Djada Hill from the west.



GSWA 22681

Figure 127. Columnar jointing in a sheet of xenolith-bearing phlogopite-leucite lamproite, summit of Djada Hill.

variable amounts of interstitial potassic richterite. Small phenocrysts of phlogopite, prismatic diopside, and olivine, each up to 2 mm across, are moderately abundant in a leucite-rich groundmass. A few altered leucite crystals reach 2 mm but are usually less than 1 mm. Olivine is replaced by nontronite and quartz, and occurs in glomeroporphritic aggregates with diopside. Pale-coloured phlogopite phenocrysts are corroded and fringed by priderite needles; small interstitial phlogopite flakes are more strongly coloured. Interstitial materials are mostly brown clay minerals, phlogopite, abundant acicular diopside, and accessory priderite. Interstitial potassic richterite is present in all samples; but only near the northern margin does it form large poikilitic masses and become an essential mineral. Elsewhere, it forms small interstitial prisms or overgrowths on diopside needles.

The Djada Hill lamproites have uniform composition in terms of MgO (5.8-7.4%), SiO_2 (51-55%), and K_2O (10-11.4%). The phlogopite-leucite lamproite sheets on the eastern side of the intrusion have distinctly lower TiO_2, but higher Sr contents (1 700-1 850 ppm) and are exceptionally enriched in LREE — La is 1 600 times chondritic abundance. These values contrast with the values of 6.5 to 7% TiO_2, 1 000-1 450 ppm Sr and LREE abundances of 1 000 times chondrites or less in the main plug. However, TiO_2 and Zr contents and Zr/La ratios are much higher in the plug than in the dykes and sheets (Table 52).

TABLE 52. REPRESENTATIVE ANALYSES OF DJADA HILL LAMPROITES

	1	*2*	*3*
	Percent		
SiO_2	51.47	51.01	53.96
TiO_2	7.73	7.71	5.67
Al_2O_3	7.92	8.11	8.30
Fe_2O_3	5.70	5.55	5.42
FeO	0.81	0.90	1.06
MnO	0.06	0.06	0.06
MgO	6.07	5.81	6.24
CaO	3.06	2.95	1.94
Na_2O	0.29	0.25	0.43
K_2O	10.41	10.85	11.42
P_2O_5	0.58	0.57	1.18
H_2O^+	2.07	2.33	1.85
H_2O^-	1.39	1.46	0.86
CO_2	0.68	0.21	0.20
Rest	2.13	2.48	1.97
Total	**100.37**	**100.25**	**100.56**
	Parts per million		
Ba	11 233	14 678	8 678
Li	15	15	14
Rb	374	351	308
Sr	1 369	1 238	1 712
Pb	51	49	95
Th	21	21	27
U	3	2.5	4
Zr	1 591	1 595	1 354
Nb	148	146	177
Y	21	20	31
La	250	266	436
Ce	459	489	764
Nd	239	283	268
Sc	14	13	13
V	162	163	296
Cr	367	366	475
Ni	304	316	339
Cu	78	75	62
Zn	70	66	87
Sn	25	23	10
Mo	3	3	<3
Ga	17	24	28
As	2.5	3.5	1.5
F	2 800	2 400	3 000

1 — Phlogopite-diopside-leucite lamproite; southwest margin, BMR 83210340. 2 — Phlogopite-diopside-leucite lamproite; central plug, BMR 83210341. 3 — Phlogopite-leucite lamproite; eastern margin (dyke), BMR 83210342.

THE SISTERS

These two small lamproites are located south of the Fitzroy River, close to the main all-weather track south-east from Nerrima Homestead, and 17 km west-southwest of the abandoned Kalyeeda Homestead. In earlier publications, the bodies have been referred to as the Kalyeeda Hills (Wade and Prider, 1940; Prider, 1960), but this name properly belongs to a group of low sandstone hills 20 km east.

The lamproites form two small hills rising 10-15 m from the flat alluvial and sand plains of the Fitzroy River. Despite their small size they are, in open country, good landmarks. The two vents are 1.6 km apart and are intruded along a fault trending east-northeast; the larger northeastern vent is itself elongated in this direction. Prospecting by Stellar Minerals found several small patches of lamproite tuff and breccia along the line of the fault between the two vents (Jeppe, 1971). Bedrock exposures throughout the sandplain are very poor; but, along the northern side of the northeast vent there are exposures of coarse grits and thin-bedded, flaggy sandstones and shales, possibly of the Noonkanbah Formation, that show little disruption even close to the vent margin.

Sisters Southwest

The vent forms a small circular hill about 10 m high and 110 m diameter (Fig. 128). Only the central core of welded lapilli-tuff is naturally well exposed, but numerous bulldozer scrapes, the result of diamond exploration activities, have cleared scree and exposed the marginal rocks.

On the south side of the vent, bedded fine- to medium-grained lamproite tuffs and lapilli-tuffs are exposed; but, on the northeast margin there is a zone of pyroclastic breccia that contains boulders of green-stained sandstone, up to 3m across, shale blocks, up to 0.5 m, and a sparse lamproitic matrix. The northwest margin of the vent is occupied by lenticular intrusions of fine-grained, grey leucite lamproite and a lens of dark-green to grey, olivine-leucite lamproite. This latter rock type shows two distinct generations of olivine on weathered surfaces; there are altered macrocrysts up to 5 mm across and smaller euhedral olivines.

The tuffs, breccias, and magmatic intrusions, are disposed as lenticular bodies surrounding a central core of pale-grey, welded lapilli-tuff. The mass shows a strong, streaky flow texture that dips vertically, or steeply inwards, parallel to the margins of the cylindrical mass. It seems probable that the core is the result of the final phase of explosive activity, when gas generation had waned considerably. The lenticular masses of lamproite post-date the central core and were emplaced in the tuffs surrounding it. The alternative interpretation, that the

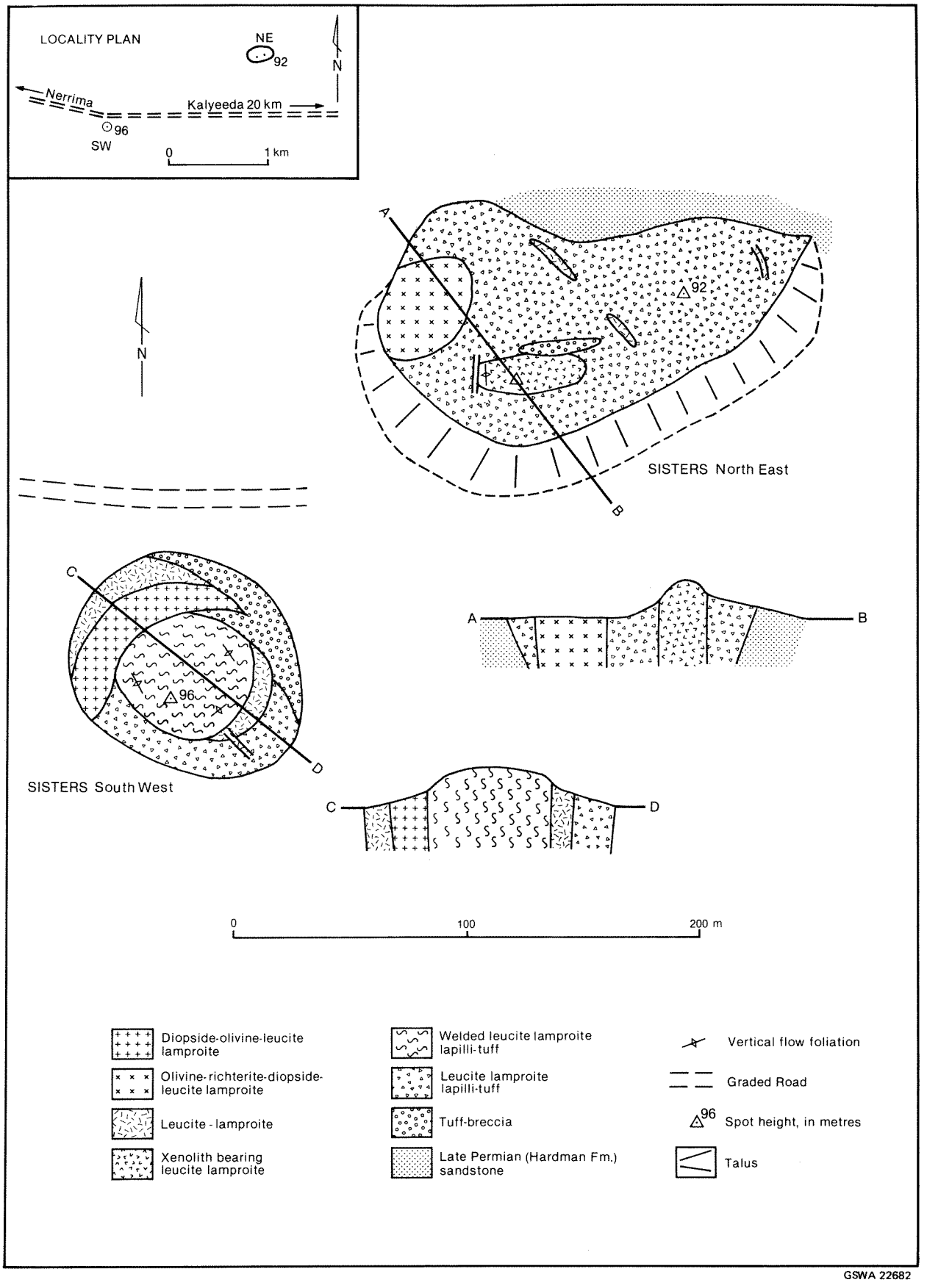


Figure 128. Geological map of The Sisters.

core indicates a resurgence of explosive activity is less probable, as the central core carries no xenoliths of magmatic rock, and the intrusions show no evidence of brecciation.

The lamproite lapilli-tuff is fine-grained; it contains amoeboid and angular lapilli of altered, glassy, leucite lamproite, up to 5 mm, and a few small xenoliths of shale and sandstone, in a matrix of lamproite shards and ash, and abundant, angular quartz and microcline grains of wall-rock origin. Very fine-grained tuff beds consist entirely of lamproite ash and sedimentary detritus, thoroughly welded to give a homogeneous rock.

The matrix of the very coarse volcanic breccia on the northern side of the vent is a strongly ferruginized "sandy" tuff, which contains spherical, accretionary lapilli of quartz grains and lamproitic material, up to 2 cm across, in a matrix of lamproitic ash. Alteration has destroyed the original mineralogy, and there is abundant secondary barite; but textures are well preserved.

The central core is a welded lapilli-tuff of leucite lamproite, similar in composition to the bedded lapilli-tuffs. The rock has a streaky appearance, and has incorporated small fragments of quartz and microcline, and occasional xenoliths of shale and siltstone. Only rarely is the original pyroclastic texture preserved; lapilli range up to 3 cm and many smaller ash-sized fragments are present.

The leucite lamproite intrusions are very fine-grained, flow-banded, and consist of minute, altered leucites in a clay-rich groundmass derived from devitrified glass. One specimen contains a little groundmass potassic richterite, and all specimens contain a few fragments of quartz and microcline, and small sedimentary xenoliths.

The intrusive sheet of diopside-olivine-leucite lamproite contains about 20% olivine, pseudomorphed by talc. Small, euhedral crystals, 0.5mm long, are most common; but larger euhedral and skeletal phenocrysts, up to 2 mm, and anhedral to rounded macrocrysts, up to 5 mm, are abundant. Small crystals of altered leucite, from 0.3 mm to minute interstitial grains, form the bulk of the rock; but there are abundant, small, acicular prisms of diopside, less than 1 mm long and flow-aligned, in a matrix of clay minerals. Also present is a little interstitial phlogopite, accessory priderite, and rare perovskite. This rock is very similar to the MgO-rich intrusives of Mount Cedric and Mount Ibis.

Sisters Northeast

This is the larger of the two vents; it is 200 m long by a maximum of about 110 m wide. It forms two small hills that rise about 15 m above the sandplain, but a large area of the vent on the northern side forms no positive feature, and is poorly exposed (Fig. 128). The vent is filled mainly with a variety of pyroclastics, including lapilli-tuffs and coarse tuff-breccias that contain shale and sandstone pyroclasts up to 15 cm across. On the northern side of the western hill, there is a vertical lens of particularly coarse volcanic breccia that contains blocks of sediment from 5 cm up to 1 m across in a sparse lamproite matrix. The eastern hill is entirely of lamproite lapilli-tuff, and is traversed by a number of thin, impersistent, lamproite veins. The tuffs do not appear to be bedded, except around the northern margin of the vent where there is some evidence of low-angle inward dips.

Small intrusions of fine-grained leucite lamproite form dykes and sills within the pyroclastic deposit. A larger mass of similar magma, but containing a small proportion of xenoliths, has intruded to form the summit ridge of the western hill. At the western end of this mass, strong, vertical, platy flow-banding has developed.

At the western end of the vent, a plug of coarse-grained olivine – potassic-richterite – diopside – leucite lamproite has been intruded. The plug is poorly exposed and formed during the final phase of magmatic activity in the vent.

The lapilli-tuffs show varying degrees of welding and silicification. Accidental xenoliths of shale and siltstone are rare, but most specimens include many small fragments of quartz and microcline from the wall-rock. The lamproite is a leucite lamproite with a few small flakes of phlogopite and abundant small altered leucites in a groundmass of clay minerals and interstitial phlogopite. The matrix to the lapilli is generally sparse and has been replaced by secondary silica.

The lamproite sheets intruding the tuff, and the xenolithic lamproite mass of the western hill, are very similar to the lamproite of the lapilli-tuffs, but richer in small phlogopite flakes, which are often zoned to a dark-coloured rim. The xenoliths are predominantly small siltstone clasts, up to 1 cm across, and make up about 5% of the rock.

The plug of lamproite is coarse-grained; it contains altered olivine and leucite, up to 2 mm across, and acicular and prismatic diopside, up to 3 mm long. The goundmass contains many smaller leucite and diopside crystals, and abundant acicular potassic richterite, accessory phlogopite and priderite, and interstitial clay minerals. Olivine is not so plentiful as in the olivine-leucite lamproite in the nearby Sisters Southwest, and there are no olivine macrocrysts.

The rocks of the two vents differ considerably in composition (Table 53). The Sisters Northeast is dominated by MgO-poor (<8%), SiO_2-rich (>50%), leucite-rich, lamproite with 10% or more K_2O. These rocks are very similar to the other leucite lamproites of the Noonkanbah Field. The Sisters Southwest contains MgO-rich, SiO_2-poor, lamproites (up to 13% MgO, 45-50% SiO_2) that are similar to the strongly olivine-phyric lamproites of Centre II at Mount Cedric and Mount Ibis (Tables 44 and 45). Similar abundance ratios of trace elements *e.g.* Rb/Sr, Sr/La, Zr/Nb, etc., suggest that the two centres may be essentially comagmatic and related by differentiation.

WALGIDEE HILLS

The Walgidee (formerly Wolgidee) Hills intrusion is the largest of the West Kimberley lamproites; it forms a roughly circular to heart-shaped body some 3 km in

TABLE 53. REPRESENTATIVE ANALYSES OF THE SISTERS LAMPROITES.

	1	2
	Percent	
SiO_2	48.18	50.24
TiO_2	5.27	6.13
Al_2O_3	6.65	8.36
Fe_2O_3	6.11	5.17
FeO	0.86	1.04
MnO	0.07	0.07
MgO	11.65	7.47
CaO	3.12	3.67
Na_2O	0.43	0.80
K_2O	7.45	9.96
P_2O_5	1.04	0.96
H_2O^+	3.58	2.05
H_2O^-	3.60	1.23
CO_2	0.27	0.30
Rest	1.86	2.63
Total	**100.14**	**100.08**
	Parts per million	
Ba	9 001	15 896
Li	21	12
Rb	252	296
Sr	1 398	1 466
Pb	56	50
Th	25	27
U	3	4
Zr	1 234	1 346
Nb	164	168
Y	25	21
La	233	259
Ce	365	479
Nd	176	267
Sc	11	14
V	167	229
Cr	772	308
Ni	519	267
Cu	49	74
Zn	78	69
Sn	15	16
Mo	<3	3
Ga	15	17
As	2.5	1.5

1 — Diopside-olivine-leucite lamproite; southern side of The Sisters Southwest, BMR 83210336. 2 — Potassic-richterite - diopside - leucite lamproite; southwest end of The Sisters Northeast, BMR 83210345.

diameter (Fig. 129), composed mainly of medium-grained, green, magmatic lamproite. The intrusion is poorly exposed; the most prominent topographic features are at the northern and northwestern margin of the intrusion where upstanding brecciated and silicified country rocks at the rim form low hills (Walgidee Hills) that rise some 20 m above the surrounding plain. At the centre of the intrusion, adjacent to the road from Noonkanbah station, which transects the intrusion, medium- to coarse-grained massive, strongly jointed, green lamproite, commonly veined by carbonate, forms a small hill of very low relief. Another low hill, composed of grey to brown amphibole-rich lamproite, lies immediately to the east of the central hill. Apart from the low hills at the centre of the intrusion, isolated discontinuous outcrops of fine-grained, olivine-phyric lamproite, and brecciated lamproite, occur at the margin of the intrusion. Elsewhere, exposure is limited to isolated subcrop, and most of the intrusion is covered by a thin veneer of eluvium that contains abundant, detrital minerals derived from the underlying lamproite.

The western half, particularly the southwestern third, of the intrusion is strewn by an angular rubble, up to 25 cm across, of fine-grained dense, magnesite. The surfaces of the magnesite concretions are highly irregular, and many have "cauliflower" or "breadcrust" textures. At the southern rim of the intrusion, immediately east of the road, brecciated lamproite and country-rock sandstone is covered by a thin layer of calcrete. Both the magnesite and the calcrete were clearly derived by weathering of the lamproite (Prider, 1960). Drilling has shown that the zone of weathering over the intrusion commonly extends to 40 m.

The Walgidee Hills intrusion intrudes both the flat-lying, dark-grey to brown mudstones and shales and the paler coloured sandstones and siltstones of the Triassic Blina Shale. Much of the rim of the intrusion is marked by a discontinuous breccia zone — typically some 10 to 30 m, but in the west, up to 125 m wide — in which country-rock shales, mudstones, and sandstones, are upturned and silicified. Rock fragments within this breccia zone range up to several metres across in places. The brecciated country rocks have been intruded in places by a pale-coloured, grey-brown breccia of fine-grained olivine-phyric lamproite. Bedding and cleavage in the sediments at the rim of the intrusion dip either towards or away from the intrusion at high angles, and the steeply dipping beds form a distinct rim at the northern and northwestern margin of the intrusion (Fig. 129). The outer zone — of dominantly brecciated country rock and sporadic intrusions of brecciated magmatic lamproite — passes inwards, into a finer grained, pale-grey to buff-brown tuff-breccia that is composed dominantly of angular fragments of country-rock sediments, set in a matrix of brecciated olivine-phyric lamproite. These pass inwards into fine-grained olivine-phyric lamproite, which may be brecciated or contain occasional angular inclusions of country rock. In places, the magmatic lamproite underlies, or possibly intrudes the tuff-breccia. Fine-grained, porphyritic olivine lamproite is found only at the margins of the intrusion, and contains conspicuous altered olivine phenocrysts and macrocrysts in a fine- to very fine-grained groundmass. This passes inwards into medium-grained, green, magmatic lamproite that contains conspicuous flakes of phlogopite, typically 2 to 3 mm across, together with altered olivine, diopside, potassic richterite, and priderite prisms; this forms the bulk of the body. The lamproite forming the core of the intrusion is medium- to coarse-grained and is cut by numerous veinlets of calcite that impart a mesh-like appearance. Coarse phases of the lamproite grade into, or are cut by, pegmatoid veins up to 1 m across that contain coarse-grained (up to several centimetres long) diopside, phlogopite, apatite, potassic richterite, altered sanidine, priderite, wadeite, jeppeite, and shcherbakovite.

The shape of the Walgidee Hills intrusion is uncertain. Prider (1960) suggested, on the basis of the columnar jointing at the centre of the intrusion, that the intrusion might be a flat-lying sheet (*i.e.* a laccolith) rather than

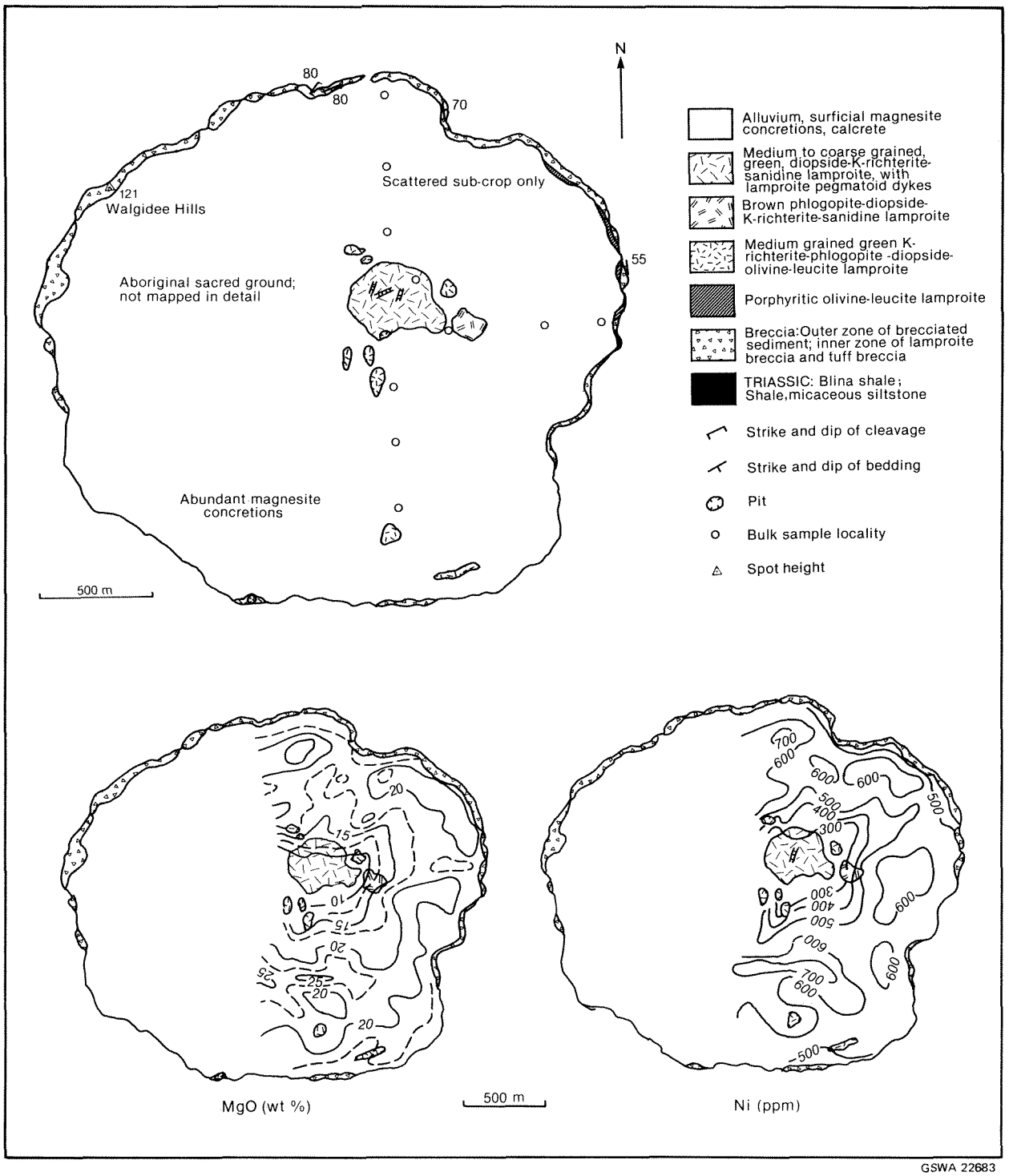


Figure 129. Geological map of the Walgidee Hills and contours of MgO and Ni content.

a steep-sided vertical body. Contacts between the country rock and the intrusion are mostly steep sided, however; and a programme of shallow (rotary) drilling of the eastern half of the intrusion showed that, in at least two localities, a thin horizon of fine-grained magmatic olivine lamproite laps over, or tongues into, flat-lying siltstone and shale. Elsewhere, the holes bottomed in lamproite, and were of insufficient depth (60 m maximum) to evaluate the shape of the body. The variation in rock types within the intrusion is gradational: the coarsest and most differentiated rock types are in the centre of the body. This, coupled with the geochemical zoning (*see* below), demonstrates that the Walgidee Hills intrusion is a zoned intrusion of magmatic lamproite which crystallized largely inwards from the margins.

Contact effects of the Walgidee Hills intrusion on the country-rock sediments appear slight, and limited to baking of the shales and siltstones; subordinate chlorite is developed in places. In addition, some biotite-rich sediments show evidence of incipient growth of biotite and possible growth of K-feldspar immediately adjacent to the intrusion.

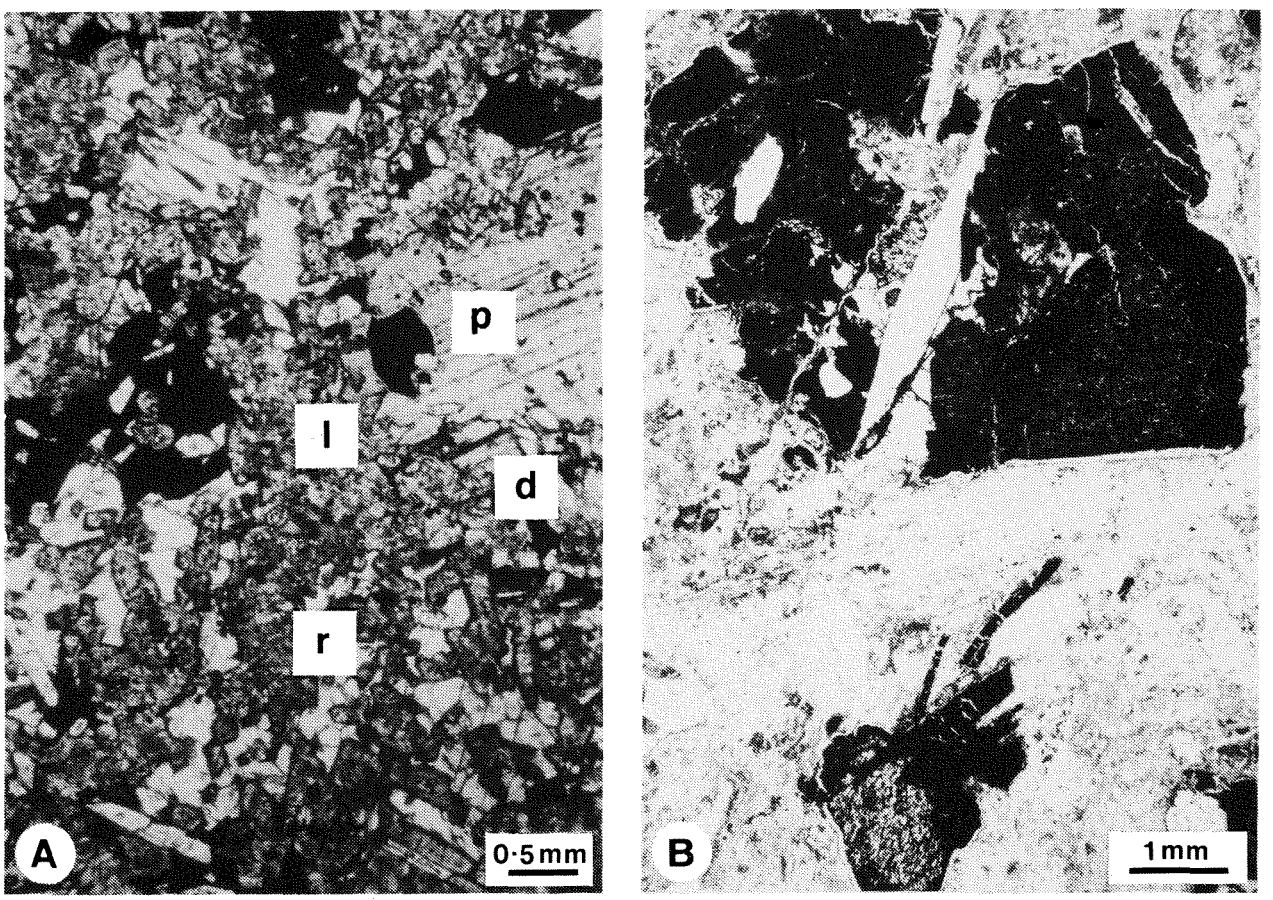
Petrography

Fine-grained, porphyritic olivine-leucite lamproite: The fine-grained porphyritic olivine lamproite found at the margin of the intrusion consists of sparse (2-5%) former olivine macrocrysts (many of which are probably xenocrysts judging by the degree of resorption) up to 3 mm across. They are accompanied by more abundant, euhedral, second generation, olivine phenocrysts and microphenocrysts (now serpentine and/or talc), some 100 to 600 μm across, together with prisms of diopside. All are set in an altered, very fine-grained groundmass that contains granular perovskite and chromite, flakes of pleochroic phlogopite (yellow to pale orange cores and dark orange to red rims, some with reverse pleochroism), prisms of apatite and wadeite, sparse pleochroic potassic richterite, and altered leucite, now a yellowish green celadonite.

Medium-grained, green, potassic-richterite — phlogopite — diopside — olivine — leucite lamproite: This lamproite (Fig.130) forms the bulk of the intrusion. It consists of sparse olivine macrocrysts (now talc or serpentine), up to 3 mm, together with euhedral, smaller, second-generation olivines (also altered: some to celadonite, and some to green nontronite), diopside prisms, granules of perovskite and chromite, prisms of apatite, wadeite, and priderite, and altered former leucite euhedra (now K-feldspar or yellow-green celadonite). These are partly enclosed by poikilitic plates of phlogopite (yellow to orange) that commonly show resorbed margins, and pleochroic (lemon yellow to pink) potassic richterite. This lamproite grades into more- and less-magnesian types by increase and decrease respectively in modal olivine, particularly macrocrystal olivine.

Grey-brown phlogopite — diopside — potassic-richterite sanidine lamproite: This lamproite is more fractionated than the more typical medium-grained green lamproite, and consists of euhedral diopside prisms, granular coarse perovskite, coarse prismatic wadeite and apatite with poikilitic plates of phlogopite, sanidine, and, particularly, poikilitic potassic richterite, and interstitial shcherbakovite. Secondary alteration products, including red-brown Fe oxides and turbid brown "clay" after feldspar are common.

Green diopside - potassic-richterite - sanidine lamproite: The green carbonated lamproite forming the central core of the intrusion contains coarse prisms of diopside, apatite, and wadeite; granular perovskite with polysynthetic twinning; priderite; jeppeite; and altered leucite. These are enclosed or partially enclosed by poikilitic potassic richterite, altered sanidine, or, less commonly, phlogopite. The matrix consists of greenish smectite/celadonite, together with secondary carbonate and K-feldspar.



GSWA 22684

Figure 130. Photomicrographs of Walgidee Hills lamproite: A — Medium-grained potassic richterite(r), diopside(d), phlogopite(p), altered leucite(l) lamproite with abundant priderite (dark) (BMR 81210184). B — Jeppeite (opaque) replacing priderite (dark) in pegmatoid lamproite; the colourless prismatic mineral is apatite (GSWA 71310).

Lamproite pegmatoid: The veins and small dykes of lamproite pegmatoid that intrude the core of the intrusion are typically altered and, in outcrop samples, strongly weathered and silicified. The most striking of these comprise coarse interlocking prisms of jeppeite, relic shcherbakovite, and potassic richterite. Additional primary phases, now replaced by clay, silica, K-feldspar and Fe oxides (goethite), include probable former wadeite, apatite, priderite, and sanidine.

Chemistry

Geochemical sampling of chips obtained from a 100 m grid-drilling programme over the eastern half of the Walgidee Hills intrusion reveals a systematic zoning of major- and trace-elements which coincides with the petrographic variation. The zoning is well displayed by the variation in MgO and Ni contents over the eastern part of the intrusion (Fig. 129). These show a concentric pattern: the more MgO- and Ni-poor rocks are located in the centre of the intrusion. The MgO and Ni contour diagrams show an outer ring of moderate to high MgO and Ni contents (16-18% MgO, 500-600 ppm Ni). It corresponds to the fine-grained, olivine-phyric lamproite, which passes inwards into a more Mg- and Ni-rich lamproite (18-22% MgO, 600-700 ppm Ni) that in turn, corresponds to the medium-grained potassic-richterite - phlogopite - diopside - olivine - leucite lamproite. These grade inwards into the coarse-grained amphibole-sanidine-rich lamproite at the centre of the intrusion, which contains less than 10% MgO and 300 ppm Ni. The most fractionated rocks are the pegmatoids; they contain 5% or less of MgO and less than 100 ppm Ni and Cr. The most Mg- and Ni-rich rocks occur in discontinuous zones in the south-central and southwestern parts of the intrusion, where the rocks contain up to 27% MgO and more than 700 ppm Ni (Fig. 129). The variation in Mg and Ni correlates directly with the modal proportion of olivine — particularly macrocrystal olivine — in the rock. Abundance of Cr shows a similar zonation to that of Ni, whereas incompatible major- and trace-elements show the reverse pattern: TiO_2, K_2O, Zr, LREE, and Ba for example, are highest in the core of the intrusion. The lamproite pegmatoids are exceptionally enriched in Ti, Zr, and Nb

TABLE 54. REPRESENTATIVE ANALYSES OF WALGIDEE HILL LAMPROITES

	1	*2*	*3*	*4*	*5*	*6*	*7*	*8*
				Percent				
SiO_2	44.89	44.31	40.23	33.40	48.50	36.11	59.55	47.32
TiO_2	4.00	4.36	4.15	9.14	5.24	5.27	11.97	5.49
Al_2O_3	6.13	5.13	5.74	3.80	6.10	4.72	0.41	5.54
Fe_2O_3	6.17	5.26	6.63	7.10	7.30	5.94	9.41	6.98
FeO	0.57	1.81	1.10	0.68	1.76	0.51	1.51	1.52
MnO	0.10	0.10	0.11	0.06	0.11	0.08	0.14	0.13
MgO	13.88	19.90	17.29	6.98	9.77	7.64	4.45	11.08
CaO	3.64	2.23	3.89	13.30	5.52	15.73	2.45	5.78
Na_2O	0.44	0.36	0.38	0.37	0.98	0.32	0.42	0.73
K_2O	5.79	3.72	7.78	6.44	8.28	7.40	4.28	8.73
P_2O_5	0.27	0.11	2.44	1.79	1.03	1.18	0.53	1.25
H_2O^+	5.12	6.74	1.42	2.89	1.73	1.91	1.00	1.80
H_2O^-	2.36	4.02	0.58	1.33	0.57	0.33	0.34	0.29
CO_2	1.03	—	5.74	10.00	0.15	10.41	1.51	0.48
Rest	4.42	1.35	2.50	2.70	3.28	2.22	2.17	3.26
Total	**99.35**	**99.40**	**99.98**	**99.98**	**100.32**	**99.77**	**100.14**	**100.38**
				Parts per million				
Ba	32 132	5 390	15 312	18 176	19 754	12 767	7 304	19 640
Li	5	7	5	8	6	3	13	6
Rb	543	417	582	324	395	447	470	452
Sr	812	867	1 223	1 743	1 600	1 839	1 080	1 614
Pb	9	28	25	30	50	10	110	39
Th	37	28	23	<5	21	14	14	25
U	2	4	2	<1	<1	2	6	3
Zr	1 057	1 167	1 598	676	1 928	2 462	6 011	2 320
Nb	105	153	107	87	135	96	294	143
Y	7	20	9	8	19	10	31	18
La	441	138	148	79	283	79	120	154
Ce	649	250	177	—	277	123	194	259
Nd	231	116	123	—	—	36	68	82
Sc	8	10	14	21	24	17	43	15
V	116	96	103	65	50	39	262	124
Cr	836	851	—	7	213	34	67	413
Ni	439	819	518	100	290	66	50	281
Cu	34	43	48	160	130	85	213	86
Zn	65	66	77	62	100	61	75	89
Sn	<2	12	10	—	—	20	60	20
Ga	11	10	11	8	12	12	<2	9
S	—	—	—	600	400	—	—	—
F	2 400	1 500	3 200	3 500	5 660	1 800	2 400	4 600
Cl	—	—		270	260	—	—	170

1 — Porphyritic diopside-phlogopite-olivine-leucite lamproite; eastern margin. BMR 81210201. 2 — Phlogopite-leucite-olivine lamproite; S3 BO, northern interior of pluton, BMR 84210349. 3 — Phlogopite-olivine-leucite lamproite; S11-E4, eastern interior of pluton, BMR 81210203. 4 — Carbonate - priderite - jeppeite - shcherbakovite - wadeite - potassic-richterite lamproite, central core, GSWA 71301. 5 — Potassic-richterite - diopside - leucite lamproite; central core, GSWA 71302. 6 — Carbonate - perovskite - wadeite - priderite - jeppeite - potassic-richterite lamproite; central core, BMR 81210195. 7 — Altered shcherbakovite-wadeite-priderite-jeppeite pegmatoidal lamproite; vein central core, BMR 81210196. 8 — Brown phlogopite - diopside - potassic-richterite - leucite lamproite; outcrop eastern hill at centre, BMR 81210197A.

(up to 12% TiO_2, 6 000 ppm Zr, and 300 ppm Nb). The pegmatoids also have higher abundances of V and Y, but similar or lower abundances of LREE than the other Walgidee Hills lamproites which suggests that LREE have been removed from residual liquids by crystallization of a LREE-enriched phases, probably perovskite and/or apatite. A detailed study of the petrology and geochemistry of the Walgidee Hills intrusion is in progress (Jaques and others, in prep). Representative analyses of Walgidee Hills lamproites are given in Table 54.

White Rocks

White Rocks is the most northerly exposed lamproite of the Noonkanbah Field; it is located 16 km northwest of Walgidee Hills and 2.5 km west of the main road to Noonkanbah Homestead. The vent is a few kilometres north of the axis of the Quanbun Syncline and is emplaced in Blina Shale, of Triassic age. The vent takes its name from a narrow ridge of bleached and disrupted sandstone, a few metres high, which is a landmark, and which forms the eastern margin of the body.

In general, the Blina Shale consists of thin-bedded fossiliferous mudstone and sandy mudstone with only minor sandstones. Exposures at White Rocks are of fine-grained, shallow-water sandstone, ripple marked and cross-bedded in places, and interbedded with coarser sandstones. Along the eastern margin of the vent, the sandstone beds dip from vertical to 60° inwards; and along the northern margin, from 25-60° towards the centre of the vent (Fig.131). In both areas, the outcrop is only a narrow zone of baked sandstone up to 15 m wide. On the northern margin the sediments are traversed by bands of brecciated sandstone up to metre wide, and parallel to the vent margin. The sediments dip steeply towards the centre of the vent, but there is no evidence that they are overturned. Possibly the sediments have slumped into the vent, either during eruption or during post-eruptive compaction of the pyroclastic deposits.

The vent is pear shaped, about 300 m long by a maximum of 230 m wide, and is filled largely with lamproite lapilli-tuffs. In areas with no wall-rock outcrop, the margin of the vent can be traced easily by changes in soil colour and the presence of sandstone float. At the southern end of the vent, the pyroclastics form a small hill; but, over much of the northern part, they are obscured beneath a thin sandy soil. Bedding in the lapilli-tuff is often obscured by scree, but a number of small outcrops near the northern and western margins show good bedding that dips 45-60° towards the centre. These tuffs are often noticeably "sandy", with quartz grains derived from the wall-rock, whereas tuffs from the hill at the southern end lack both bedding and a significant wall-rock component and probably mark the site of the final volcanic conduit.

The tuffs are intruded by a number of thin dykes and sills of phlogopite-leucite lamproite, often vesicular and rarely more than a metre thick. Along the northern margin of the vent there are lenses of similar rock several metres thick.

The intrusive magmatic phase is poorly developed at White Rocks. There is no central plug; but, in the narrow southern part of the vent, there is what may be described as a "cactolith" (Bates and Jackson,1980) of fine-grained leucite lamproite. A number of sills, radial dykes, and irregular veins, intrude the tuff over an area about 100 m diameter. The outcrop pattern of Fig. 131 is somewhat diagramatic, but the sills and dykes appear to be part of one body which presumably has a single pipe-like conduit. It is the permeation of the tuff by the magma that has given rise to the small hill at the southern end of the vent. The relationship of the body to the original volcanic vent is unknown, but its curious shape probably results from intrusion into unconsolidated pyroclastics.

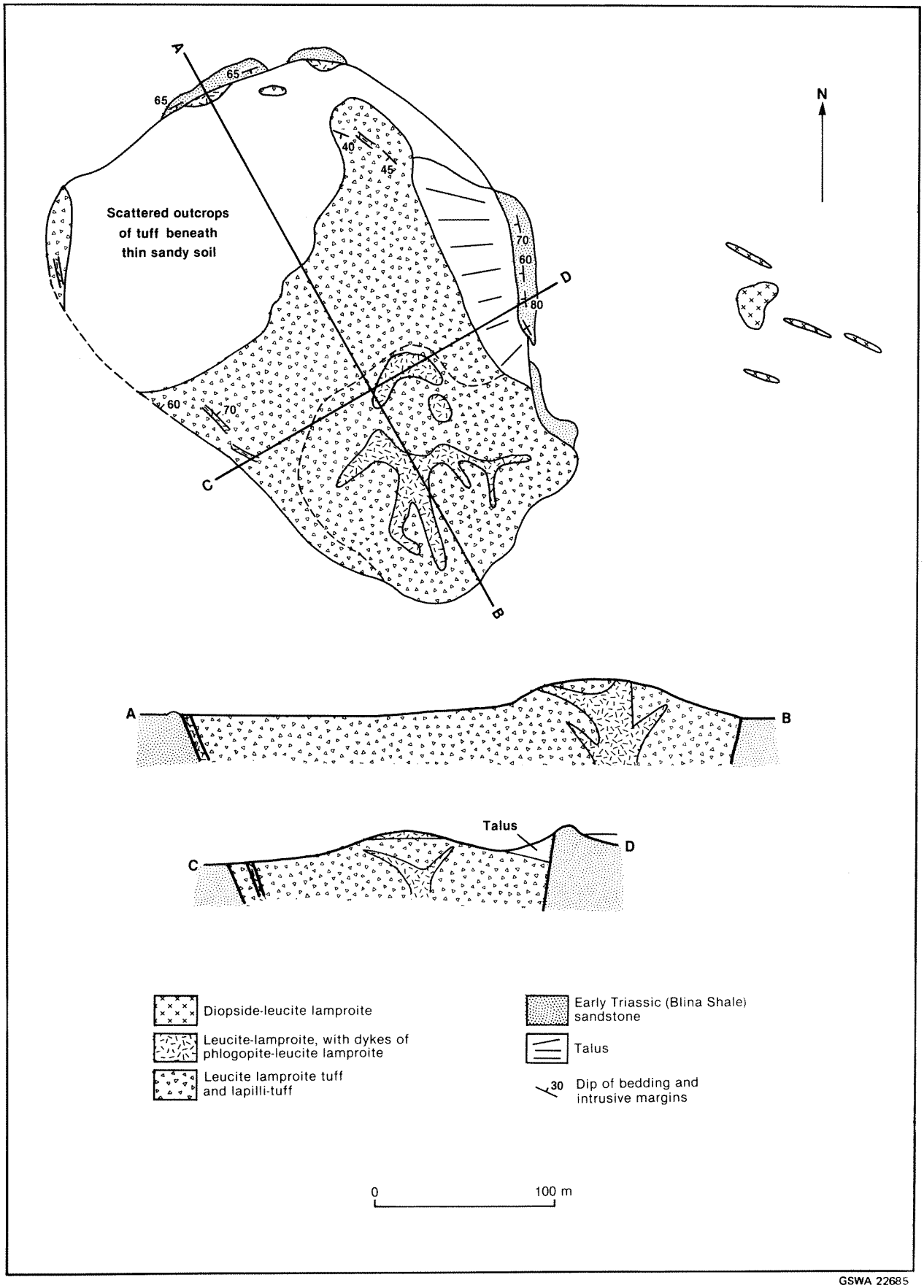
A hundred metres east of the main vent is a small hillock, 30 m across and 2 m high, composed of coarse-grained diopside-leucite lamproite. Associated with this small plug are a number of dykes of similar material up to 2 m wide and 40 m long, and trending west-northwest.

The stratigraphically lower pyroclastics, poorly exposed in the northern part of the vent, are fine-grained, matrix-supported "sandy" lapilli-tuffs that contain fragments of juvenile lamproite, up to 1 cm, and smaller shale clasts in a matrix of lamproite shards and ash that contains abundant rounded quartz grains of wall-rock origin. The lamproite pyroclasts are of devitrified glassy leucite lamproite, although a few fragments carry phlogopite or small olivines in addition. In the southern part of the vent, the lapilli-tuffs are clast supported, but have a sparse matrix of lamproite ash, clay minerals, and rare grains of quartz. The lamproite is a leucite lamproite, glassy and vesicular, and contains occasional phlogopite.

The thin dykes and sheets intruded into the pyroclastics are a uniform, fine-grained, altered phlogopite-leucite lamproite. Phlogopite, up to 2 mm, and a few small olivines, are set in a groundmass of small leucites, interstitial clay minerals, sparse potassic richterite, and needles of priderite. Vesicular specimens show strong flow-alignment of phlogopite.

The "cactolith" at the southern end of the vent is a fine-grained olivine-leucite lamproite that carries small, metasomatized xenoliths of shale and siltstone up to 15 mm across. Abundant, small, altered olivines and leucites, about 0.3 mm across,are set in a groundmass of clay minerals and minute former leucite grains. Towards the centre of the complex, the groundmass develops small laths of diopside, potassic richterite, and accessory priderite. Olivine is variably replaced by nontronite or talc, and sometimes by barite. The small intrusion to the east of the main vent is a slightly coarser variety of the "cactolithic" intrusion; it contains many small prisms of diopside and interstitial, pink, potassic richterite in the groundmass.

The White Rocks lamproites are characterized by low MgO (<8%), and high SiO_2 (>50%) and K_2O (8.7-12%). Compositions are all oversaturated with silica and have high normative orthoclase content (40-50%).



GSWA 22685

Figure 131. Geological map of White Rocks.

Representative analyses (Table 55) show that the pyroclastics are of similar composition to the magmatic phases, and that there is only a small range in compositions between phases. Apart from the highly leucitic compositions, which are amongst the most potassic of the West Kimberley lamproites, other features of the White Rocks lamproites are their high Sr and LREE contents which range up to 1 700 ppm and 1 600 times chondritic abundances respectively. Other features which strongly suggest that the extremely felsic (leucitic) compositions are the result mainly of fractional crystallization from more mafic parents are the low Mg/(Mg+Fe) ratios, the low Ni and Cr contents, and the relatively high abundance of elements such as Zr, Pb, Y, and V (Table 55, analyses 3 and 4).

TABLE 55. REPRESENTATIVE ANALYSES OF WHITE ROCKS LAMPROITES

	1	*2*	*3*	*4*
		Percent		
SiO_2	52.17	51.30	51.00	50.53
TiO_2	4.75	5.05	6.09	6.35
Al_2O_3	8.64	8.00	8.54	8.91
Fe_2O_3	3.84	5.90	5.60	6.52
FeO	1.90	0.66	1.05	0.64
MnO	0.09	0.07	0.08	0.09
MgO	7.73	6.65	5.74	5.14
CaO	2.92	2.97	2.24	1.62
Na_2O	0.52	0.60	0.50	0.32
K_2O	10.73	8.73	11.76	12.05
P_2O_5	1.31	0.65	1.27	1.03
H_2O^+	2.10	3.45	1.62	2.20
H_2O^-	0.53	1.90	0.79	0.68
CO_2	0.81	0.11	0.20	0.42
Rest	1.81	3.86	2.83	2.96
Total	**99.85**	**99.90**	**99.31**	**99.46**
		Parts per million		
Ba	11 419	22 102	16 244	18 290
Li	10	12	8	6
Rb	272	168	293	278
Sr	1 501	1 417	1 734	811
Pb	52	60	94	101
Th	14	18	29	30
U	2	<1	3	3
Zr	932	969	1 446	1 427
Nb	99	104	181	194
Y	18	18	31	32
La	219	421	450	496
Ce	298	417	801	856
Nd	—	—	344	363
Sc	—	17	14	15
V	164	188	288	271
Cr	198	253	345	340
Co	—	30	—	—
Ni	289	490	116	233
Cu	42	100	67	62
Zn	64	81	108	94
Sn	11	—	6	8
Mo	3	<1	4	4
Ga	13	16	34	35
As	2	1	4	4
S	—	2 600	—	—
F	—	2 940	3 600	3 400
Cl	—	290	—	—

1 — Leucite lamproite lapilli tuff; southwest margin, BMR 80210097.
2 — Olivine-leucite lamproite; southern centre of body, GSWA 71361.
3 — Phlogopite-leucite lamproite; northern margin, BMR 83210246.
4 — Phlogopite-leucite lamproite; western margin, MBR 83210249.

MINOR LAMPROITE INTRUSIONS

A further ten lamproite bodies have been located by mining companies during exploration activity. Most are unexposed, and all, except 33 Bore, are small. Little is known of these bodies except the brief reports from the mining companies, particularly Boxer and Haebig (1980a), Haebig (1983c) and for the Kalyeeda pipe Gregory (1980). Six of the bodies are located in the northeastern part of the Noonkanbah Field in dune covered areas; three occur within the main group of lamproites that intrude the rocks of the Liveringa Group on the southern limb of the Quanbun Syncline; and one lies concealed beneath alluvium on the south bank of the Fitzroy River.

19 Bore No. 1

Two small lamproite pipes totalling 3.7 ha in area are located approximately 7 km north-northwest of Number 19 Bore (HARDMAN GR:942924 and 940924). The larger body is about 200 × 50 m and elongated west-northwest; and the smaller body is about 70 m diameter and 200 m from the larger vent. Scout drilling showed the presence of both pyroclastics and a leucite lamproite core. No diamonds were recovered from a 13.5 m^3 bulk sample.

19 Bore No. 2

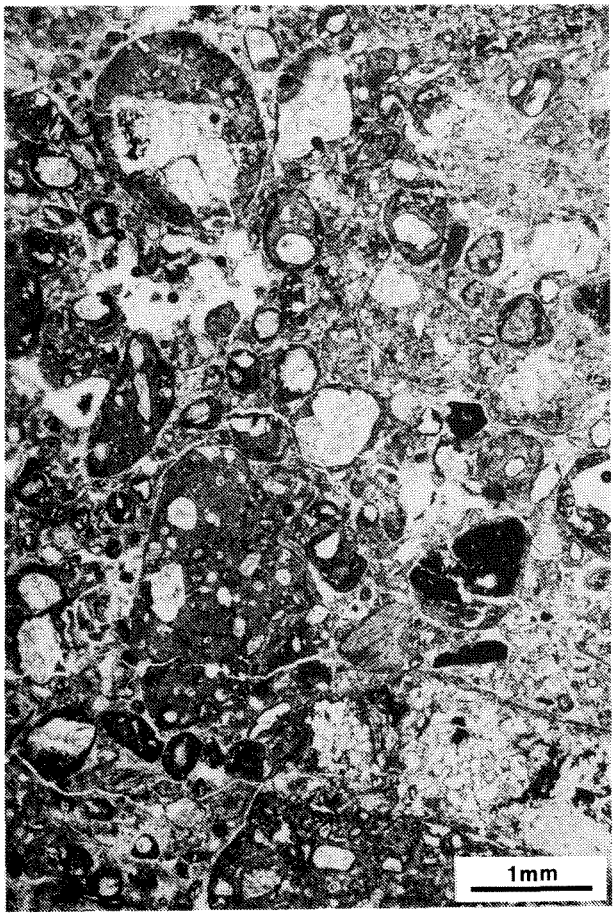
A small oval lamproite vent, 100 × 70m, or 0.8 ha, is located 3.5 km southeast of Number 19 Bore (HARDMAN GR:003845). The vent is filled by a distinctive autolithic lapilli-tuff that consists of subspherical autoliths of olivine lamproite and phlogopite-olivine lamproite, 1-10 mm diameter, and rounded fragments of shale and siltstone, in a fine-grained clay matrix that is extensively veined by secondary carbonate (Fig. 132). The autoliths contain anhedral to subrounded macrocrysts of altered olivine, 1-4 mm across, and microphenocrysts of euhedral olivine, up to 0.5 mm, in a fine-grained pale-brown, clay-rich matrix. Some autoliths also contain phenocrysts of phlogopite up to 2 mm long. Olivine and phlogopite also occur commonly as cores in nucleated autoliths that are surrounded by a thin skin of magma. Another feature of some autoliths is a marginal zone in which small phlogopite flakes are arranged tangentially; in some cases, this forms an outer skin to an autolith that is otherwise lacking phlogopite. The tuff contains a number of rounded, opaque grains, probably chromite, up to 1mm diameter, and one example of a clear, brown grain of picrochromite which is mantled by opaque, secondary, iron-bearing chromite.

A bulk sample of 15 m^3 and two HF digestions of drill chips failed to recover any diamonds.

20 Bore

This lamproite body is located 2 km north-northwest of Number 19 Bore (HARDMAN, GR:963879) and forms a circular vent 200 m diameter; there is a dyke-like extension westwards for a further 200 m. It is concealed beneath 8-10 m of wind-blown sand. From drilling records, both lapilli-tuff and a leucite lamproite core are present, but no samples are available.

No diamonds were recovered from a bulk sample of 15 m^3, but one microdiamond, 0.15 mm across, was recovered from HF digestion of drill chips.



GSWA 22686

Figure 132. Photomicrograph of lapilli-tuff from 19 Bore No. 2, containing spheroidal lapilli of phlogopite-olivine lamproite and rounded grains of chromite (GSWA 65937B).

33 Bore

Two large lamproite vents of 28 ha and 8 ha, aligned east-west, are located about 1 km southwest of Number 33 Bore (HARDMAN GR:056846 and 046845). The larger body is oval in shape, about 800 × 550 m; the smaller body, 500 m to the west, is about 350 m diameter. From drilling records, the vents are filled with pyroclastics, and only minor lamproite veins and sheets. A few drill chips are available of a fine-grained, quartz-rich tuff, and a fine-grained lamproite lapilli-tuff that contains devitrified glassy, phlogopite-rich, lamproite fragments.

Ten bulk samples weighing 235 t in total, were treated but no diamonds recovered. Three small diamonds, the largest 1.2 mm diameter, were recovered after HF digestion of three samples of drill chips.

Mamilu West

Haebig (1983c) refers to a small lamproite pipe, less than 1 ha in area, discovered in 1982 after following up an aeromagnetic anomaly. The location is 1 km south-southwest of Howes Hill (HARDMAN, GR:876685). Another very small lamproite in the same general area is Howes Hill West first noted by Jeppe (1971) and located 400m southwest of Howes Hill. Neither of these exposure has been visited by the authors.

Mount Cedric South

This small pipe is located midway between Mount Cedric and Machells Pyramid. The vent is roughly circular, 150 m in diameter and 1.8 ha in area, and filled with pyroclastics and a small, partly exposed, central lamproite core. The pyroclastic rock is a medium-grained tuff-breccia that contains about 30% of phlogopite-leucite lamproite clasts greater than 10 cm across, and clasts of dark-green shale in a fine-grained tuffaceous matrix. The magmatic core is a relatively coarse diopside – potassic-richterite – olivine – leucite lamproite with scattered macrocrysts of olivine, up to 3 mm across, altered to talc and iron oxides. The bulk of the rock consists of former leucite and phenocrystal olivine grains, each about 0.25 mm across, prismatic and acicular diopside, abundant poikilitic potassic richterite, and small prisms of priderite in a greenish, interstitial, chloritic groundmass. The pipe was bulk-sampled for diamonds but none was recovered.

A small, concealed, lamproite plug, 0.3 ha in area, is located about 150 m northwest of the main vent (Moore, 1986).

BHPM-2

This small pyroclast-filled vent was discovered in 1985 and is not marked on Plate 3; it is an oval body about 300 × 150 m and 3.3 ha in area, oriented east-west and, located 1 km south of Mount Cedric (HARDMAN, GR: 811688) (Moore, 1986).

Two small outcrops of pyroclastic rock are of lamproite lapilli-tuff; they contain close-packed spherical lapilli of juvenile phlogopite lamproite, 0.5-4 mm diameter, a few angular lapilli of leucite lamproite, and rounded fragments of shale and siltstone in a sparse altered matrix of secondary silica, zeolite, or carbonate. The juvenile lapilli are composed of phenocrysts of phlogopite in a brown clay matrix in which former leucite is often visible. Many of the larger lapilli are concentrically zoned and the phogopite aligned tangentially; this suggests that magma was liquid when erupted. Larger phlogopites, up to 1 mm, and in one specimen, occasional diopside prisms, form cores to some lapilli.

Kalyeeda

The Kalyeeda lamproite pipe, about 2 ha in area, is concealed beneath a seasonal swamp in the floodplain of the Fitzroy River, 2.5 km south of Quonga Waterhole (HARDMAN, GR:603556). Drilling revealed a small plug of fine-grained leucite lamproite that carries a few shale xenoliths. The plug forms a topgraphic high in the bedrock, rising to within 1-2 m of the surface. Sixty tonnes of material were treated in a jig plant,but no diamonds or indicator minerals were recovered (Gregory, 1980).

It should be noted that this intrusion is not the Kalyeeda Hills referred to by Wade and Prider (1940) and Prider (1960), which are now known as The Sisters. The name is for the Kalyeeda pastoral lease on which the intrusion occurs.

ISOLATED INTRUSIONS IN THE FITZROY VALLEY

In addition to those lamproites forming distinct clusters or fields, there is a small number of intrusions scattered throughout the Fitzroy valley. Bruten, for example, although petrographically similar to the lamproites of the Noonkanbah Field is 65 km distant from the nearest lamproite. Three intrusions are found in the Fitzroy Trough — Rice Hill, Nerrima, and Bruten; and four lamproites intrude the Laurel Downs Embayment, a narrow strip between the Lennard Shelf and the Fitzroy Trough. These four, including the well-exposed Oscar dyke, lie on a 50 km line, parallel to the fault-bounded Oscar Range. It is possible that they relate to a single basement fault or fault system.

RICE HILL

Rice Hill is located 14 km east-northeast of Camballin (WILLUMBAH, GR:394140) and is about 29 km west-southwest of Hansons Bore, the nearest lamproite in the Calwynyardah Field. The hill, which is formed almost entirely by a lamproite sill, rises about 45 m above its surroundings and is a prominent landmark. The lamproite is effectively an island: to the north of Rice Hill lies the Erskine Swamp, and to the south the former rice paddies of the Camballin irrigation scheme; access is along a levee bank from Willumbah Outstation, 5 km to the west.

Rice Hill is the name given on the 1:100 000-scale map, WILLUMBAH, which was produced by the Australian Survey Corps, and is the offical name. Earlier writers referred to it as Moulamen Hill, or because there is another "Moulamen Hill" some distance to the south, as Moulamen Hill North, and the local population refer to it as Moulamen Hill.

Rice Hill lamproite is a well-exposed mass, about 700 m across, with a narrow ridge extending about 800 m northwest (Fig. 133). The main mass is composed of medium-grained, green lamproite that contains abundant phlogopite, and forms a sill, about 45 m thick, that dips at about 10-14° northeast, as measured on prominent jointing in the rock. A number of small scarps within the mass are caused by erosion along these flat-lying joints, which are sometimes coated with carbonate.

The sill intrudes sandstones of the Permian Liveringa Group, which are moderately well exposed on the south and west, where they conformably underlie the sill. At the base of the sill, adjacent to the track, there are small outcrops of a fine-grained, grey lamproite and bands of tuffaceous material a few metres thick. This may be a chilled phase of the sill, but it is not seen elsewhere; and, a little further south, the base of the sill is marked by the more typical green lamproite, which, however, contains numerous boulder-sized xenoliths of sandstone up to a metre across.

There are no exposures of the upper margin of the sill, although the presence of sandstone float north of

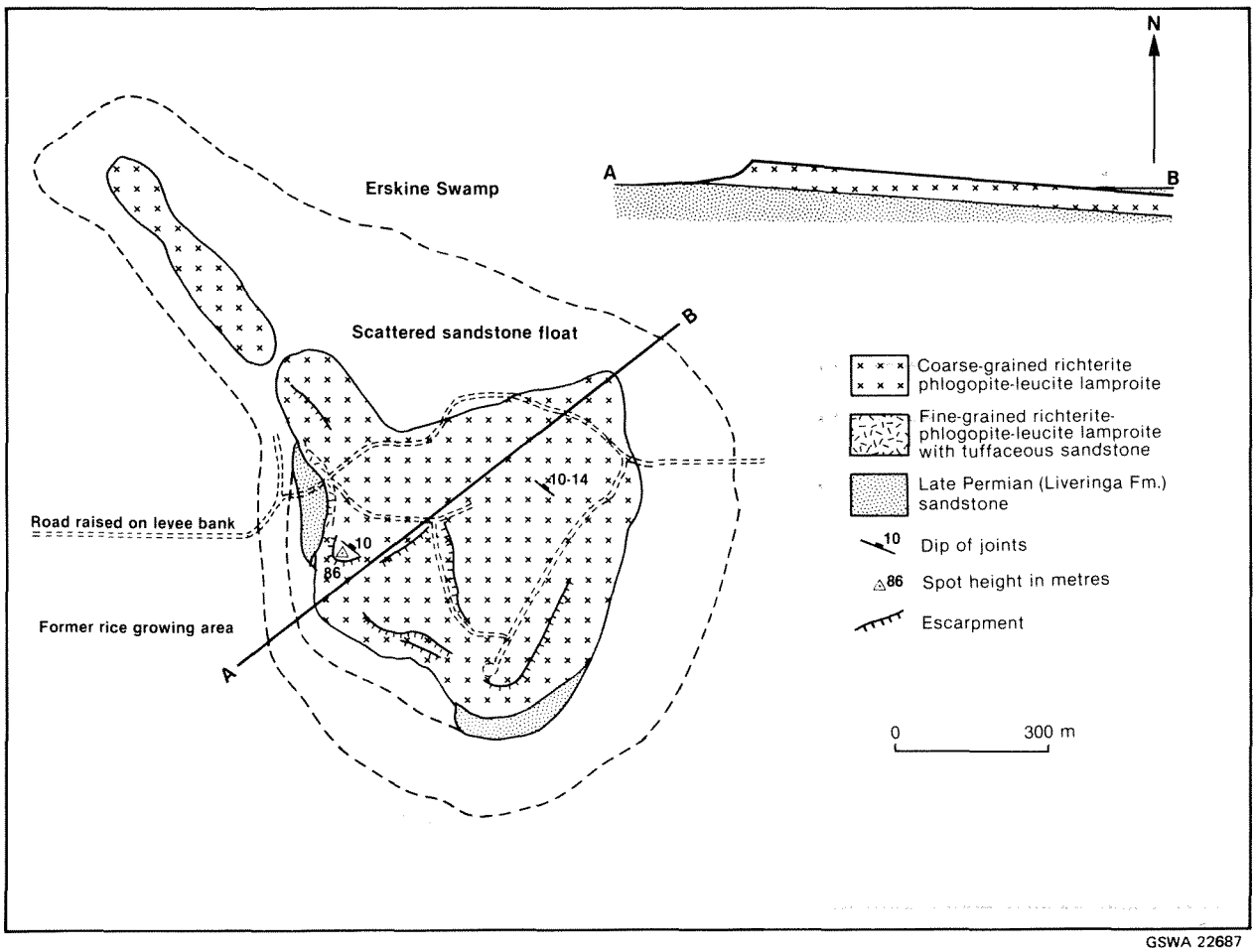


Figure 133. Geological map of Rice Hill.

the hill indicates that the roof is nearby. Drilling confirms this and shows that the northwest ridge is a dyke-like body of similar rock type to the main mass (Gregory, 1981).

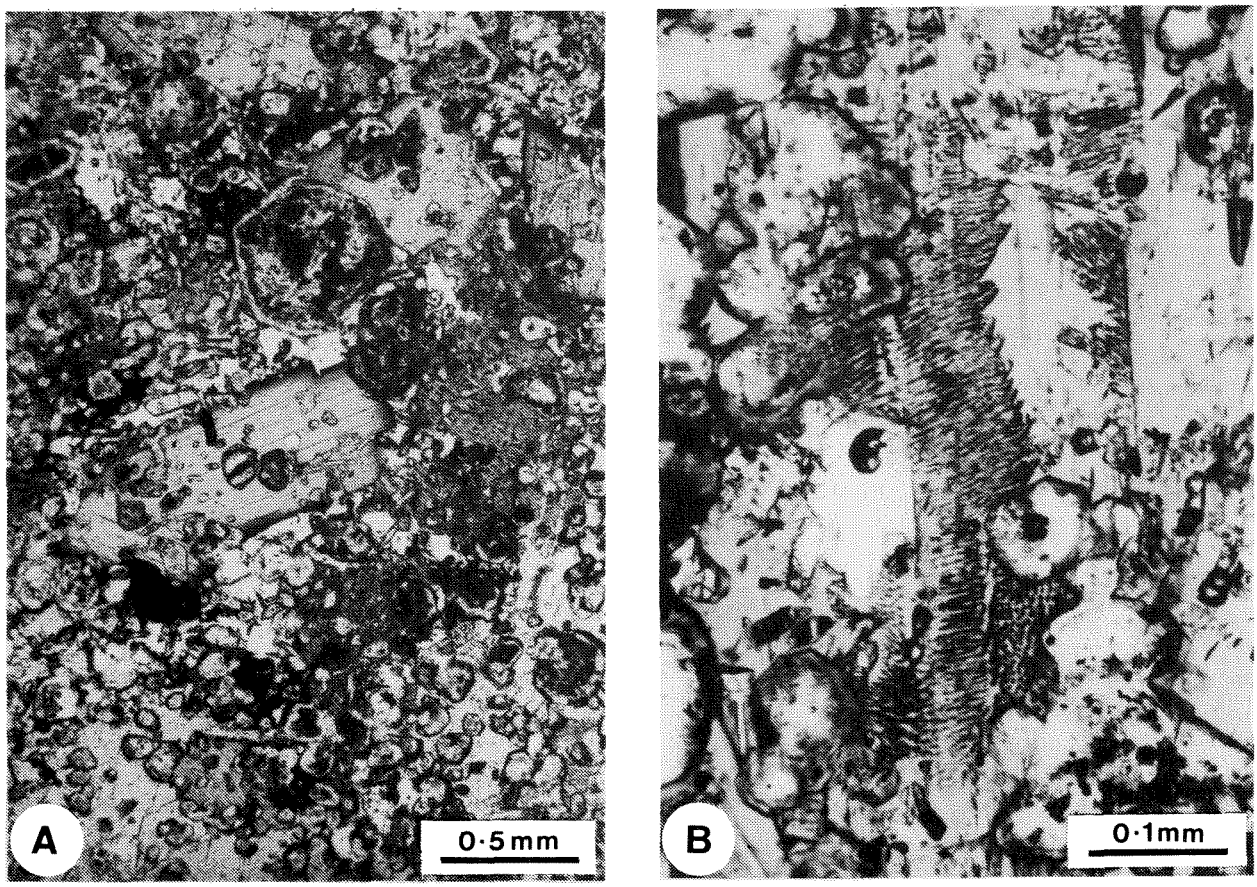
The tuffaceous material at the base of the sill is a fine-grained tuff containing angular fragments of quartz and microcline, flakes of muscovite, brown biotite, and abundant, green, chloritic material. The fine-grained lamproite associated with the tuff is thoroughly altered, and contains small phenocrysts of former olivine and abundant flakes of phlogopite in a groundmass of small former leucite crystals, acicular diopside, priderite, accessory apatite, and abundant interstitial clay minerals.

The principal rock is a medium- to coarse-grained potassic-richterite – phlogopite – leucite lamproite that contains abundant poikilitic phenocrysts of phlogopite, 2 mm across, which enclose numerous small altered leucites and small prisms of diopside. The phlogopite is strongly pheochroic with orange-yellow cores and dark red-brown rims. Olivine phenocrysts, 1-2 mm long and replaced by talc, are present in a number of samples. The bulk of the rock consists of altered leucite, small diopside prisms, and priderite up to 1 mm long; all are in a matrix of green nontronite, or enclosed in large irregular poikilitic, strongly pleochroic (pink-yellow green) plates of potassic richterite up to 3 mm across. The nontronitic groundmasss is possibly a devitrified glass. Accessory minerals include small prisms of green aegirine or aegirine-augite; some of these partly replace diopside, apatite, and sporadic grains of wadeite. A fine-grained sample from near the roof of the sill is an olivine – potassic-richterite – leucite lamproite, with a yellow-green matrix of devitrified glass. The northerly dyke is similar to the main mass, but contains proportionately more potassic richterite and less phlogopite.

The Rice Hill lamproites are chemically similar and characterized by high SiO_2 (48-53%), TiO_2 (5.8-7.1%) and K_2O (8.4-10.8%), and low MgO (4.8-9.2%). Representative analyses are given in Table 56. The most MgO-poor rocks are fine-grained phlogopite-leucite lamproites at the southern margin of Rice Hill; these also have the highest TiO_2, Zr, Nb, Sr, and LREE content. The available data suggest small compositional variations with stratigraphic height: the upper part of the sill is less Mg-rich.

BRUTEN

Bruten is the most isolated lamproite of the West Kimberley Province; it is located on the north bank of Christmas Creek (BRUTEN, GR:772303), approximately 65 km southeast of the Oscar dyke. Access to within a few kilometres of the intrusion is good, *via* the main gravel track to Cherrabun



GSWA 22688

Figure 134. Photomicrographs of lamproite from Rice Hill: A – Phlogopite – potassic-richterite – leucite lamproite. Note dark, titaniferous rims of phlogopite, and altered leucite phenocryst (GSWA 76050). B — "Herringbone" exsolution texture in potassic richterite. Potassic-richterite – diopside – phlogopite – leucite lamproite; the leucite is altered to K-feldspar (BMR 83210290).

TABLE 56. REPRESENTATIVE ANALYSES OF ISOLATED LAMPROITES IN THE FITZROY VALLEY.

	1	2	3	4	5	6
			Percent			
SiO_2	50.56	53.06	48.17	52.23	56.30	51.60
TiO_2	6.44	6.28	6.04	5.76	6.89	4.90
Al_2O_3	7.89	8.41	7.83	8.64	8.70	8.10
Fe_2O_3	5.22	4.89	5.88	5.17	5.40	5.10
FeO	1.80	1.38	1.34	0.98	0.97	1.51
MnO	0.08	0.08	0.11	0.08	0.04	0.07
MgO	8.42	6.44	8.53	6.28	4.96	7.07
Cao	3.83	3.38	3.79	3.55	0.91	3.09
Na_2O	0.95	0.80	0.49	0.61	0.16	0.32
K_2O	10.08	9.86	8.38	10.72	10.00	7.80
P_2O_5	0.37	0.53	0.37	1.00	0.89	1.13
H_2O^+	1.43	1.72	4.46	1.81	1.85	4.80
H_2O^-	0.43	1.38	1.66	0.83	1.42	2.80
CO_2	0.14	0.16	0.97	0.16	0.05	0.10
Rest	2.31	1.99	2.20	1.93	2.02	2.19
Total	**99.95**	**100.36**	**100.22**	**99.75**	**100.52**	**100.58**
			Parts per million			
Ba	13 245	10 271	12 179	10 346	8 777	12 933
Li	12	9	7	8	10	8
Rb	330	318	393	372	297	1 123
Sr	1 382	1 379	2 111	1 235	702	960
Pb	55	57	49	50	49	48
Th	25	24	25	20	16	<5
U	3	3	1	3	<1	<1
Zr	1 264	1 268	1 218	1 297	1 123	946
Nb	140	127	107	118	91	90
Y	24	28	20	20	20	<5
La	277	290	301	241	265	258
Ce	501	525	566	445	348	274
Nd	245	241	186	210	—	—
Sc	14	12	10	13	22	19
V	200	182	206	161	201	170
Cr	422	389	385	392	266	365
Ni	372	348	359	340	240	304
Cu	70	100	69	74	104	92
Zn	76	116	76	81	87	78
Sn	20	22	19	20	11	11
Ga	18	25	12	24	18	16
S	—	—	—	—	1 320	320
F	2 300	2 500	1 200	2 200	2 820	2 160

1 — Diopside - potassic-richterite - phlogopite - leucite lamproite; Rice Hill, northeast margin, BMR 83210290. 2 — Diopside - phlogopite - potassic-richterite - leucite lamproite; Rice Hill, western end, BMR 83210291. 3 — Phlogopite - potassic-richterite - leucite lamproite; Rice Hill, central ridge, BMR 81210230A. 4 — Phlogopite - potassic-richterite - leucite lamproite; Rice Hill, central ridge, BMR 83210288. 5 — Diopside - phlogopite - leucite lamproite; Brutens, main plug, GSWA 71894. 6 — Glassy olivine-leucite lamproite; Oscar, central dyke, GSWA 71893B.

homestead; but the lamproite is hidden in a dense stand of eucalyptus and paperbark which grows on the flood plain of the creek and the final kilometre is difficult to navigate.

The main intrusion of Bruten is a small, slightly oval plug, about 30 m diameter, it has a vertical exposure of about 10 m above a conical plinth of slightly baked shale and siltstones of the Permian Noonkanbah Formation. On the eastern side of the hill, a dyke of lamproite lapilli-tuff 5 m wide extends about 40 m, to end in a small swelling (Fig. 135).

The country-rock shales and siltstones are thinly bedded, flaggy and near horizontal. The contact between sediments and lamproite is usually obscured by scree; but, on the northeast side of the plug, the sediments are undisturbed to within a few centimetres of the intrusion. On the northwest and southern margins of the plug, a narrow zone of coarse tuff-breccia or brecciated siltstone, up to 1 m wide, and containing fragments up to 30 cm across, can be seen. In contact with the breccia is a zone, 2-3 m wide, of fine-grained grey lamproite that contains few xenoliths and forms a chilled margin to the main plug. This zone can be traced round the main plug, and extends into the easterly tuffaceous dyke. The central plug is a medium- to coarse-grained, greenish-black leucite lamproite that contains prominent phlogopite phenocrysts.

The tuffaceous dyke is variable but much of it is a coarse, lamproite lapilli-tuff that contains fragments 1-3 cm across. Close to the plug, fine-grained leucite lamproite intrudes a lapilli-tuff that contains many sedimentary fragments; but, in other parts of the dyke, fine-grained lamproite replaces the matrix of the lamproite lapilli-tuff.

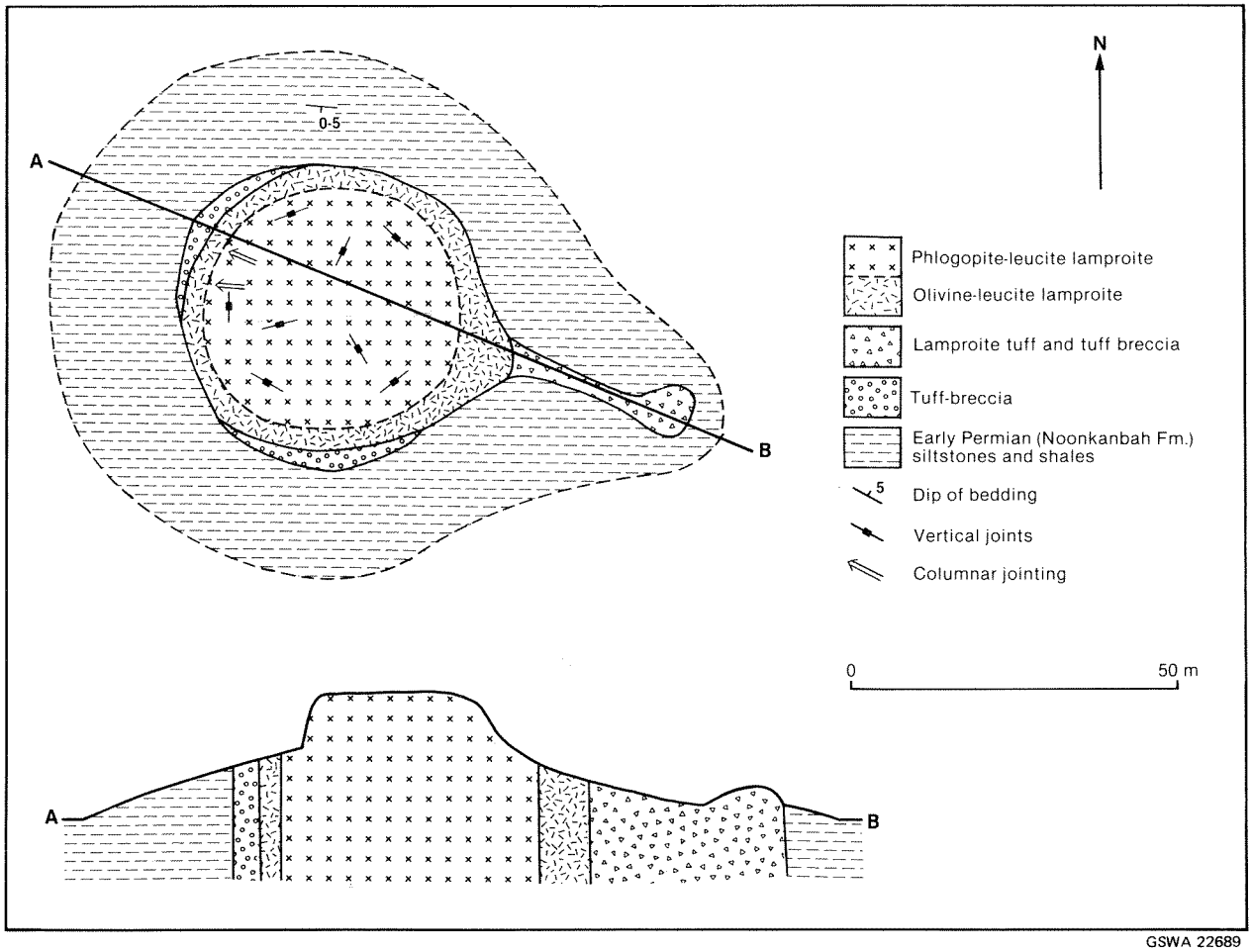
On the basis of horizontal planar structures in the main mass, Prider (1960) described Bruten as the remnant of a flow. These features are combined, however, with prominent radial and tangential jointing which is exposed on the flat top of the outcrop, and with polygonal jointing and horizontal columnar joints, which are well exposed on the western face of the body, to suggest that Bruten is, in fact, a small plug, probably an expansion on a small dyke. The earliest activity emplaced the tuffaceous dyke; but later activity expanded the western end, to allow the emplacement of the plug.

The tuffaceous dyke consists largely of unsupported lapilli of glassy leucite lamproite up to 2 cm across. Small, altered, leucite euhedra and sparse phlogopite are contained in a brown, streaky, and devitrified glass. The lapilli are close packed; and a few grains of quartz and xenoliths of shale are found interstitially and enclosed in lamproite lapilli. The rock is cemented by secondary silica. Some lapilli-tuffs within the dyke contain abundant xenoliths of shale and siltstone. The coarse breccia of the pipe margin contains more and larger sedimentary xenoliths, together with abundant lapilli of the same glassy leucite lamproite.

The chilled marginal zone of the lamproite plug is similar to the lamproite of the lapilli, but contains a few small, altered olivine phenocrysts, occasional corroded phlogopite and a sparse iron-stained clay matrix. The central portion of the plug is similar, but contains abundant phlogopite phenocrysts, up to 3 mm, and some prismatic diopside phenocrysts. Accessory priderite and secondary barite are also present.

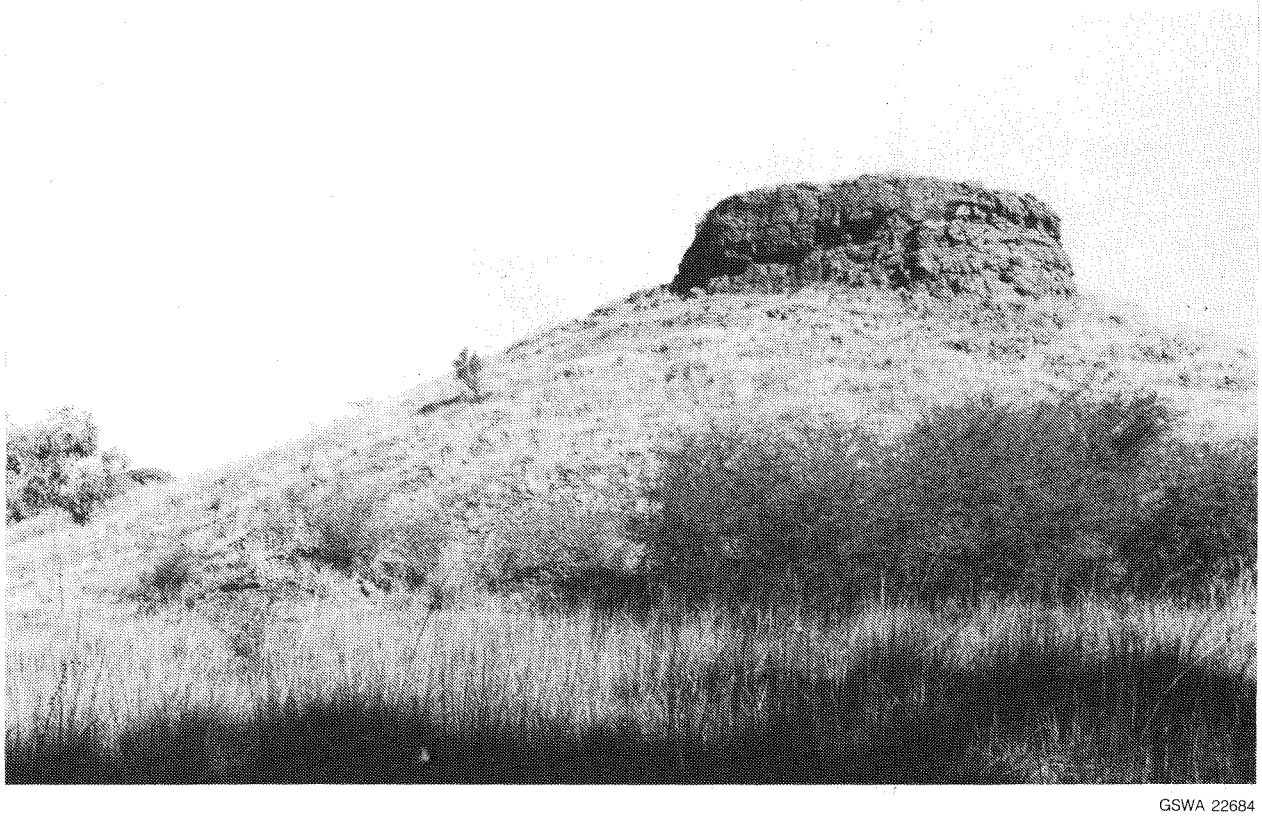
A few hundred metres southwest of the lamproite is Brutens Hill, a group of low hills, about 20 m high, that surround a circular depression about 500 m across. The flaggy siltstones forming the hills dip radially outward at about 5°, and the floor of the depression is covered with alluvium from Christmas Creek, which is diverted around the hills. Wade suggested that this formation might be an old volcanic crater (Wade and Prider, 1940). The structure is certainly suggestive of doming above a concealed lamproite, but a number of mining companies have investigated it and drilled the floor of the depression without encountering evidence of lamproite.

Chemical analyses of lamproites from Bruten show



GSWA 22689

Figure 135. Geological map of Bruten.



GSWA 22684

Figure 136. Bruten from the northwest. The ends of crude horizontal columnar joints can be seen on the western face.

high silica, but low MgO and Ni relative to the other Noonkanbah Field lamproites (Table 56). Although highly differentiated in terms of MgO, Ni, and 100 Mg/(Mg+Fe) (45-60), abundances of "incompatible" trace elements are lower than typically found in the Noonkanbah Field lamproites. For example, Sr contents are low (<800 ppm) and Rb/Sr ratios correspondingly high (0.34-0.42). Zirconium, Nb, Y, and LREE abundances are much lower than Noonkanbah Field lamproites of comparable TiO_2 and MgO content. The abundances of LREE, at 750 to 850 times chondrites, are also low by comparison.

OSCAR

Oscar Plug is the name that was given to a small plug of lamproite a few metres in diameter that Wade (Wade and Prider, 1940) discovered intruding a sandstone close to the Great Northern Highway 10 km west of Fitzroy Crossing (CUNNINGHAM, GR:563928). The small conical sandstone hill, about 20 m high, is visible from the highway and a good access track passes close to the outcrop.

Later investigation (Prider, 1982) has shown that the most important feature of this lamproite is a poorly outcropping dyke about 15 m wide by 200 m long and trending 060°, that intrudes the southern side of the hill (Fig. 137).

The sandstone, part of the Early Permian Carolyn Formation, is massive, well bedded, and sub-horizontal. Dips are less than 10°, and it forms a roughly triangular mass, apparently fault bounded to the south and west. On the southern side, close to the dyke, the sandstone is baked and indurated; and, on the southern margin of the dyke, there is a narrow outcrop of similar rock a few metres wide. The dyke, which dips about 70° northwards, probably occupies a fault. On the western side of the hill, there is a similar style of outcrop: a narrow linear gully about 10 m wide separates a small sandstone outcrop from the main mass. This probably marks a fault that trends 330°, but drilling has failed to reveal any lamproite dyke. At the intersection of these two faults lies the small lamproite mass noted by Wade. This body lies adjacent to a surface depression about 100 m in diameter, and a much larger photofeature that might conceal a large lamproite body; but again, drilling has failed to locate lamproite much beyond the present outcrop.

The main lamproite dyke is unexposed at its western end; but, in the central and eastern parts, there are small exposures of a fine-grained, close-jointed rock. On fractured surfaces, the rock shows a distinctive black and glassy core that is surrounded by a yellow-brown, earthy, weathered rind. At its eastern end, the dyke pinches and swells, and encloses septa of baked sandstone. A small dyke of green-stained, brecciated sandstone, about 30 cm wide, and parallel to the main dyke, marks the line of a small fault within the sandstone.

The lamproite pod at the western end of the dyke is complex. The pod, which is of fine-grained olivine-leucite lamproite, and about 10 m across, has a core, about 5 m acorss, of tuff-breccia containing sandstone

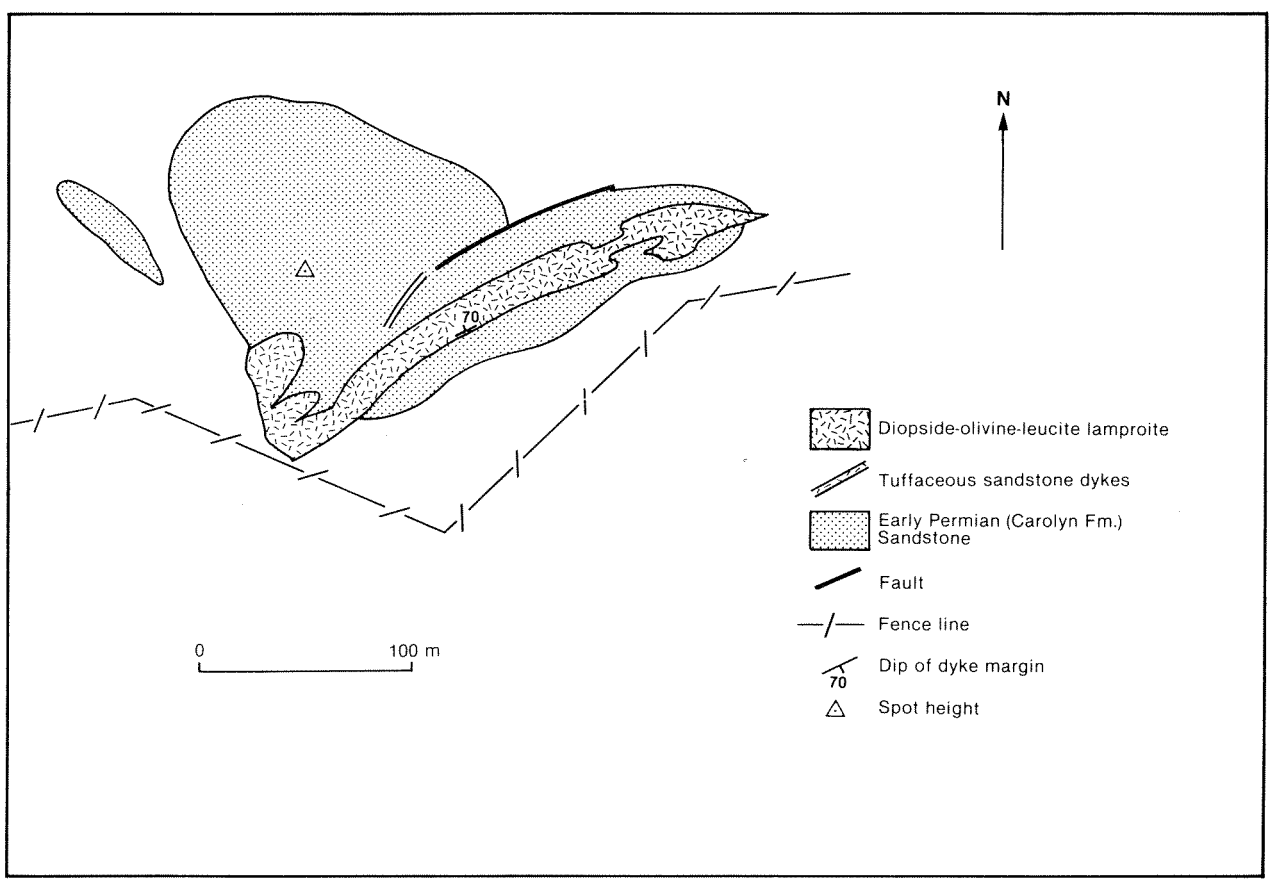


Figure 137. Geological map of Oscar.

cobbles up to 15 cm in diameter. In addition, there is a variety of tuffs, and a pod of fine-grained lamproite with a distinctive streaky appearance. The relationship of these rocks to the dyke is obscured beneath soil cover.

The main part of the dyke is occupied by a remarkably fresh, vitrophyric, olivine-leucite lamproite (Fig. 138). Small phenocrysts of prismatic olivine, up to 1 mm across, acicular skeletal olivine, up to 3 mm long, fresh leucite phenocrysts, up to 0.7 mm, and abundant minute groundmass leucites, are set in a pale-brown, fresh, volcanic glass. The glass also encloses abundant small flakes of phlogopite, and acicular prisms of priderite and diopside. The eastern portion of the dyke, beyond the constriction caused by the sandstone septa, is probably a different, and earlier, intrusion. The rock is an altered olivine-leucite lamproite that contains less olivine, closer packed leucite, and small groundmass laths of potassic richterite. Former glassy interstitial material is now altered to chlorite.



GSWA 22692

Figure 138. Photomicrograph of vitrophyric olivine-leucite lamproite from Oscar dyke; priderite forms small dark prisms, and the groundmass is unaltered glass (GSWA 71347).

The small plug at the western end of the dyke is similar to the eastern end of the dyke, an altered olivine-leucite lamproite that contains variable amounts of groundmass phlogopite and acicular diopside.

The streaky lamproite occupying a small pod adjacent to the western end of the dyke is a flow-banded olivine – potassic-richterite – leucite lamproite. The bands are alternately rich in groundmass phlogopite or green chloritic material; both contain abundant small prisms of potassic richterite. The rock is vesicular and includes a variable proportion of xenolithic quartz and microcline grains.

The Oscar lamproites exhibit a limited range of compositions (5-7.4% MgO, 4.9-6.3% TiO_2). All contain abundant orthoclase (45-50%) and some quartz in the CIPW norm. Prider (1982) drew attention to the fresh glass in the Oscar lamproite and presented microprobe analyses that showed excessively high SiO_2 and TiO_2, coupled with very low K_2O. Analysis of an identical sample by us has confirmed the very high TiO_2 ($\approx$ 10%), but found much lower SiO_2 ($\approx$ 55%), and much higher K_2O (10-13%) than that given by Prider (1982). The most likely reason for the discrepancy is volatilization of K_2O under the microprobe beam in Prider's analyses.

A feature of the Oscar lamproites is the extreme Rb content of some samples. McCulloch and others (1983) reported 3 400 ppm Rb in a glassy leucite lamproite, and values of around 2 000 ppm have been found in further samples.

CONCEALED LAMPROITE INTRUSIONS

Nerrima

Prider (1960) reports that the Nerrima 1 well, drilled by Associated Freney Oil Field N/L about 10 km north of Nerrima homestead (NERRIMA, GR:433642), intersected four sills of lamproite; the largest was 18 m thick and 68 m below the surface. The rock is described as a medium-grained wolgidite, *i.e.* a phlogopite – diopside – potassic-richterite – leucite lamproite.

No other lamproite intrusions are known in the area despite the intensive search in recent years. It must be presumed that these sills, which intrude the Noonkanbah Formation, did not reach the surface. Lamproite sills were intersected by an oil well drilled close to "P" Hill, but these were obviously related to the "P" Hill vent.

Gumhole

A small body of lamproite pyroclastics (less than 1ha) was intersected by two drill holes at a location 3.5 km northwest of the Oscar lamproite dyke (CUNNINGHAM, GR:534949). Drill spoil was checked for diamonds with negative results (Boxer and Haebig, 1980c).

Spielers Bore

A small concealed plug of diopside-olivine-leucite lamproite, overlain by 4-5 m of aeolian sand, is located 4.3 km east-southeast of Spielers Bore (LEOPOLD DOWNS, GR:346162). Drilling outlined an oval body, approximately 225 × 125 m, or about 2.5 ha, that consists entirely of intrusive lamproite, and contains no pyroclastic material; it intrudes Permian siltstones. The rock is fine-grained, and contains former olivine microphenocrysts, up to 0.6 mm; these have been pseudomorphed by talc and are in a groundmass of altered leucite, small diopside prisms, sparse phlogopite and acicular priderite and apatite; the interstitial material

is a dark clay mineral. Sporadic chromite grains are also present.

Five auger holes were drilled to obtain a 50 t bulk sample of weathered lamproite. This was treated in a jig plant, but no diamonds were recovered (Gregory, 1981).

Camarotoechia Creek

Camarotoechia Creek is a small leucite lamproite vent of about 3.5 ha, and is located 17 km northwest of Spielers Bore lamproite (LEOPOLD DOWNS, GR:202252). The vent intrudes Permian quartzite and calcareous sandstone, both of which are exposed in small, low outcrops on the southern margin of the vent. The lamproite is overlain by 2-3 m of aeolian sand and 1-2 m of detrital pisolitic laterite (Gregory, 1980).

The vent is irregular in shape; its maximum dimensions are 325 × 200 m. The southern two-thirds of the vent is occupied by a plug of porphyritic phlogopite-leucite lamproite, whereas the remainder is filled by bedded lapilli-tuffs. Where exposed by trenching the tuff dips 24° towards the centre of the vent; and it appears that the pipe narrows rapidly with depth.

The tuff is a uniform, fine-grained "sandy" lapilli-tuff, that contains glassy lamproite lapilli, up to 1 cm across, and rare pumiceous blocks and sedimentary xenoliths, up to 10 cm. The proportion of lapilli is variable but commonly about 50%: the remainder consists of a few small shale xenoliths, sporadic pisoliths and pisolitic aggregates, abundant rounded quartz grains, lamproite ash and sparse interstitial clay. The lapilli are of devitrified vesicular glass, and contain minute crystalites of altered leucite, microphenocrysts of altered olivine, and flakes of phlogopite up to 2 mm.

Two varieties of lamproite are present in the magmatic core, and may represent two phases of intrusion. The first is an olivine-phlogopite-leucite lamproite that contains altered olivine, up to 1 mm, and phlogopite, up to 3 mm long, in a fine-grained groundmass that is studded with small, altered leucite euhedra, groundmass phlogopite, and grains of priderite. A fragmental specimen composed entirely of vesicular clasts of a similar rock type may be a marginal autobrecciated phase of the same intrusion. The second lamproite type is a fine-grained olivine - diopside - potassic-richterite - leucite lamproite. Phenocrysts of partly unaltered olivine, up to 2 mm long, are set in a groundmass of close-packed leucite and interstitial prisms of diopside, poikilitic potassic richterite, acicular priderite, subordinate phlogopite, and devitrified glass. This rock is variable to olivine-leucite and olivine - potassic-richterite - leucite lamproite.

Three trenches were excavated, and a bulk sample of 279 m^3 of lamproite and pyroclastics treated by jig plant. No diamonds were recovered: but the heavy-mineral suite included barite, chromite, diopside, perovskite, and priderite, from the lamproite; and andalusite, corundum and almandine from (presumed) basement xenoliths. A 17 kg sample of the phlogopite-leucite lamproite yielded 6 microdiamonds after digestion in HF; the largest being 0.015 CM (Gregory, 1981).

MINERAL CHEMISTRY

OLIVINE

In many of the West Kimberley lamproites, olivine (or in altered or weathered rocks, pseudomorphs after olivine) is present as xenocrysts, early formed phenocrysts and microphenocrysts. Fresh olivine is found in outcrop samples of lamproite from Ellendale 11, Mount Cedric, Oscar Plug, The Sisters Southwest, and Brooking Creek lamproites; and in drill-core samples from a number of the Ellendale olivine lamproite pipes. In many intrusions, olivine is totally altered, commonly to serpentine or talc, as in many of the olivine lamproites of the Ellendale field, or to bright green nontronite as in many of the leucite lamproites (Prider and Cole, 1943). Olivine in the Walgidee Hills intrusion is totally altered to pale-green celadonite.

Two generations of olivine are present in the olivine lamproites of the Ellendale Field and in some of the olivine-bearing leucite lamproites. The coarser generation occurs as anhedral to slightly rounded grains up to 4 mm across, which typically exhibit undulose extinction and/or kink banding. These also commonly have embayed and partly resorbed grain boundaries. Resorption features are particularly pronounced in the, more evolved, olivine-bearing leucite lamproites, where the resorbed magnesian olivine grains are clearly xenocrystal. Many of the coarser olivines are clearly derived from disaggregated olivine-rich peridotites; fragments of dunite and, more rarely, harzburgite, up to 10 cm across and composed largely of aggregates of recrystallized olivines, typically mosaic textured and up to 10 mm across, are common in many of the Ellendale pipes.

The second-generation olivines are smaller (< 1 mm, commonly < 0.4 mm), and typically euhedral; glassy rocks commonly contain skeletal or "hopper" olivines with abundant melt inclusions. The second-generation olivines, which occur as phenocrysts and microphenocrysts or groundmass grains, are free of solid-state deformation and, unlike the xenocrystal olivines, commonly contain tiny (< 20 μm) inclusions of chromite.

The xenocrystal olivine ranges in composition from Mg_{88} to Mg_{93}, but histograms show that most lie in the range $Mg_{90\text{-}92.5}$ and that there is a population maximum at $Mg_{91\text{-}91.5}$ (Fig. 139). Second-generation olivines show a wider compositional range — $Mg_{82\text{-}93.5}$; but most are of similar composition or slightly more Mg-rich than the xenocrysts, and the bulk of the population lies in the range $Mg_{90.5\text{-}92.5}$ (Fig.139). This compositional range is similar to that found in other lamproites (*e.g.* Carmichael, 1967; Sheraton and Cundari, 1980; Kuehner and others, 1981; Venturelli and others, 1984; Scott-Smith and Skinner, 1984a, b), and in kimberlites (Dawson, 1980).

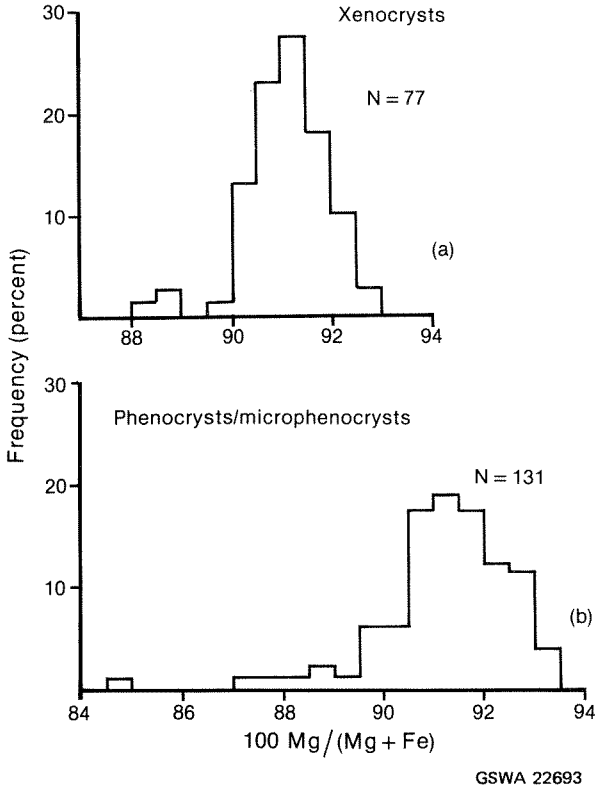


Figure 139. Frequency diagram of compositions of xenocrystal and phenocrystal/microphenocrystal olivines in West Kimberley lamproites.

The xenocrystal olivines are characterized by uniformly high Ni (0.3-0.5% NiO) and very low Ti, Al, and Ca (<0.05%), typical of mantle olivines (Table 57). The second-generation olivines typically have higher Ca (up to 0.5% CaO); and, in some cases, higher Ni contents, which range up to 0.6% NiO (Fig. 14). Similar high Ni values in olivines were reported from the Gaussberg leucitites by Sheraton and Cundari (1980), and the Spanish lamproites by Venturelli and others (1984). Both olivine generations show low Cr (<0.1%, typically 0.02-0.07% Cr_2O_3), and Cr contents appear to correlate with Mg/(Mg+Fe). Most of the olivines exhibit, only minor zoning; reverse and normal zoning of a few atom percent is widespread. Many of the xenocrystal olivines show reverse zoning, from cores of uniform composition to a narrow (< 100 μm, commonly < 50 μm) zone with higher Mg and Ca, and less abundant Ni (Fig. 140). This zone is enclosed by a normally zoned, thin, outer rim that contains higher Ca and Mn and lower Ni. Similar reverse zoning, on uniform phenocryst cores enclosed in an outer rim of normal zoning, is apparent on some of the phenocrysts (Fig. 140). The Ni zonation trend in the phenocrysts/microphenocrysts is of decreasing Ni and lower Mg/(Mg+Fe), and is similar to that observed in the outer part of the xenocrystic olivine rims (Fig. 141). The zoning in lamproitic olivines, therefore, differs from the complex zoning often described from kimberlitic olivines (*e.g.* Boyd and Clement, 1977). The reverse zoning in the West Kimberley lamproites is interpreted to indicate growth on mantle olivine and early formed phenocryst cores from the host lamproite melt at low temperature and, possibly, under more oxidizing conditions.

PHLOGOPITE

Phlogopite is present in the majority of the West Kimberley rocks, either as phenocrysts or in the groundmass. All except the most glassy olivine lamproites contain phlogopite in the groundmass, and some contain microphenocrysts up to 2 mm long, seriate to groundmass mica. In a few cases, the phlogopite microphenocrysts are bent and exhibit undulose extinction indicative of solid-state deformation. The microphenocrysts typically have pale, weakly pleochroic (pink to yellow) cores that are relatively free of inclusions, enclosed by more strongly pleochroic rims, and crowded with inclusions of diopside, chromite, perovskite, and apatite and/or leucite. The groundmass micas in the olivine lamproites are of two petrographic types: coarser (up to 1 mm), pale, pink-yellow, poikilitic plates, and smaller (< 100 μm), more strongly pleochroic (orange to red-brown) flakes, commonly with reverse pleochroism.

TABLE 57. REPRESENTATIVE ANALYSES OF OLIVINE.

	1	*2*	*3*	*4*	*5*	*6*	*7*	*8*
				Percent				
SiO_2	40.74	40.61	40.82	41.01	40.86	41.12	40.80	40.09
TiO_2	0.04	0.06	0.02	0.02	0.04	0.02	—	—
Al_2O_3	<0.02	<0.02	<0.03	<0.02	<0.02	<0.02	—	—
Cr_2O_3	0.05	0.02	0.07	0.05	0.10	0.08	0.07	0.04
FeO	9.02	8.30	6.95	7.26	7.69	7.75	7.14	11.17
NiO	0.41	0.22	0.40	0.32	0.34	0.51	0.64	0.29
MnO	0.05	0.16	0.08	0.10	0.17	0.11	0.09	0.17
MgO	49.71	50.34	51.36	50.76	49.93	50.34	51.02	47.51
CaO	0.03	0.27	0.10	0.00	0.24	0.10	0.12	0.23
Total	**100.04**	**99.98**	**99.81**	**99.52**	**99.39**	**100.06**	**99.86**	**99.48**
Mg(a)	90.8	91.5	92.9	92.6	92.0	92.0	92.7	88.4

(a) Mg = 100 Mg/(Mg + Fe).

1,2 — Xenocryst core (1) and rim (2), phlogopite-olivine lamproite; GSWA 71475B, Ellendale No 9 (E). 3 — Microphenocryst, phlogopite-olivine lamproite; GSWA 71475B, Ellendale No. 9(E). 4 — Xenocryst core, olivine-diopside-leucite lamproite; BMR 83210276, Mt Cedric. 5 — Microphenocryst, olivine-diopside-leucite lamproite; BMR 83210276, Mt Cedric. 6 — Microphenocryst, glassy olivine-bearing leucite lamproite; BMR 80210125, Brooking Cree. 7,8 — Microphenocryst core (7) and rim (8), glassy olivine-bearing leucite lamproite; BMR 71160408, Oscar Plug.

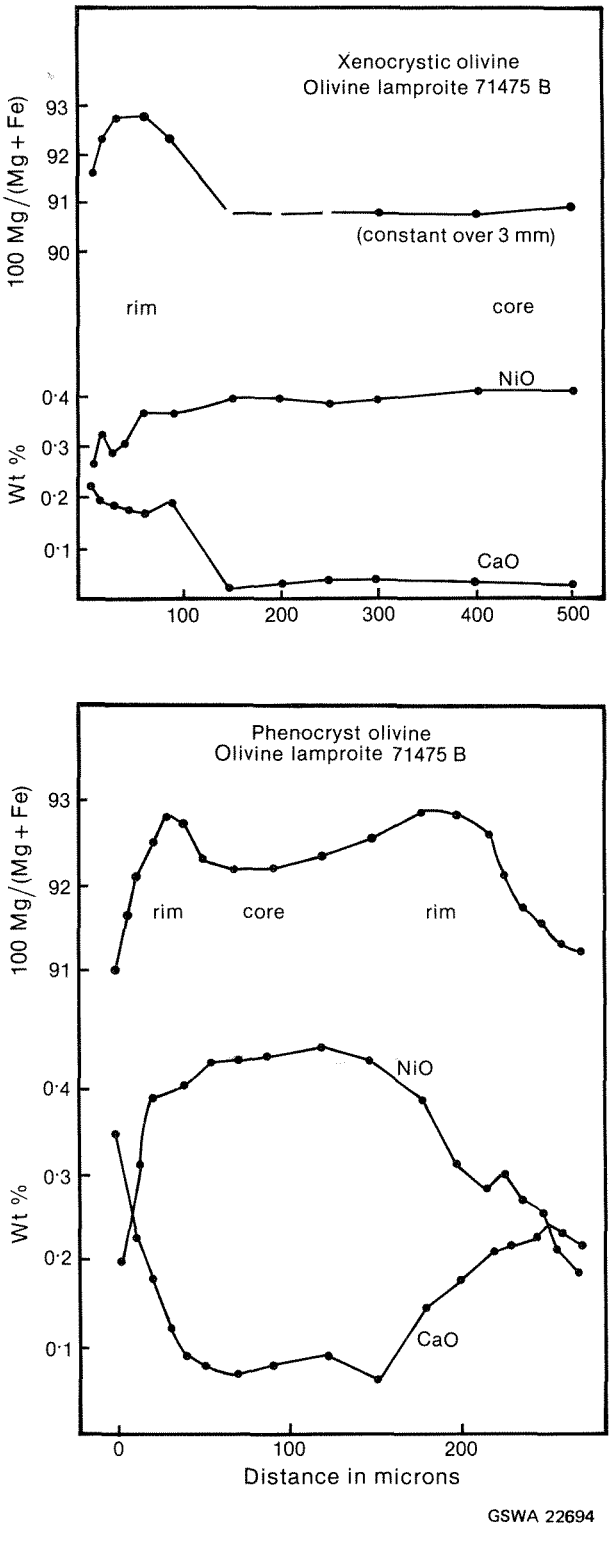


Figure 140. Profiles across xenocryst and phenocryst olivines from olivine lamproite GSWA 71475B, showing outer rim of reverse zoning with a normally zoned rim.

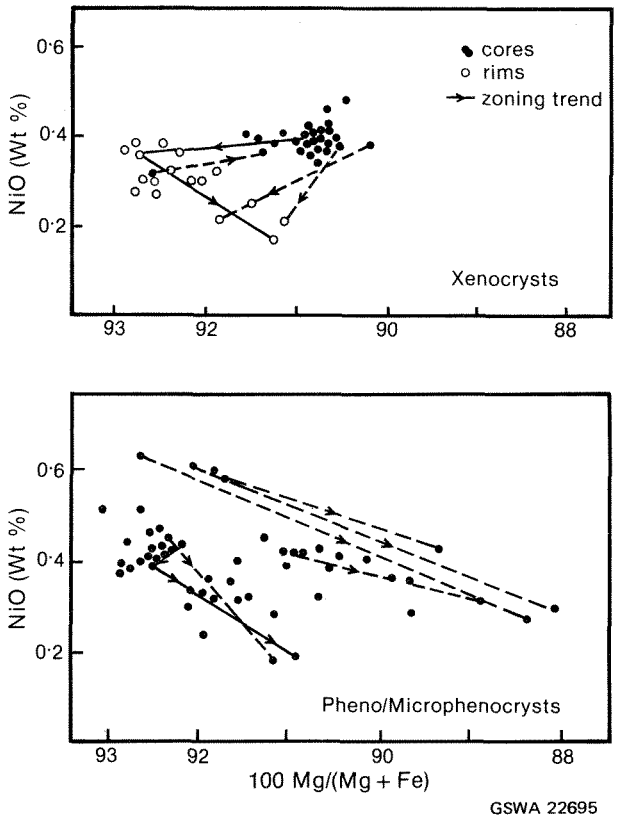


Figure 141. Variation of NiO content (wt.%) with 100Mg/(Mg + Fe) ratio in xenocryst and phenocryst/microphenocryst olivine from West Kimberley lamproites. Dashed lines and arrows indicate direction of zoning. Note trend in xenocryst olivines of initial increase in 100Mg/(Mg + Fe) followed by a decrease in both NiO and Mg in the outer zone.

The cores of the microphenocrysts are compositionally distinct from most groundmass micas: they are richer in Mg, Al, and Cr (Mg_{88-92}, 9-13% Al_2O_3, up to 1.3% Cr_2O_3) and poor in Na (<0.5%). BaO contents range up to 2% (Table 58). Many, however, are zoned to more Fe-rich, Al-poor rims with low Cr contents which overlap the groundmass mica compositions (Fig. 142). The poikilitic phlogopites, typically twinned and free of deformation, are zoned from pale-coloured cores of uniform composition (5-10% Al_2O_3, 4-8% TiO_2, <0.2% Cr_2O_3) to strongly coloured rims, richer in Ti, Fe, and Na, and poorer in Mg and Al (Fig. 142). The smaller groundmass micas exhibit a wide range in Al, Ti, and Fe, from moderately Al-rich types (up to 9% Al_2O_3, Mg_{88-80}) to small reversely pleochroic grains of tetraferriphlogopite (Mg_{84-74}, <4% Al_2O_3); all have low Cr and relatively high Na contents (<0.1% Cr_2O_3, up to 0.9% Na_2O; Table 58).

Phlogopite is a major, if not the dominant, ferromagnesian phase in the leucite lamproites; it occcurs both as a phenocryst and a groundmass phase. Phenocryst phlogopite in the strongly porphyritic, commonly glomeroporphyritic or flow-aligned, phlogopite-leucite lamproites and olivine-leucite-phlogopite lamproites of the Ellendale Field (*e.g.* Mount Percy, 81-Mile Vent, Camarotoechia Creek) are typically sub- to euhedral, pale straw-yellow, show little or no optical zoning in the cores, are twinned, and are free of inclusions. Some (*e.g.* Camarotoechia Creek) show extensive resorption and/or kink banding. These micas are characterized by high Mg, Al, and Cr (Mg_{88-92}, 10-12% Al_2O_3, up to 1.5% Cr_2O_3) as are the microphenocrysts in the olivine lamproites (Fig. 142), and are thought to have crystallized under higher pressure than the groundmass phlogopites. Mica in the coarser grained leucite lamproites from the Lennard Shelf (*e.g.* Mount North, Mount Rose) typically has

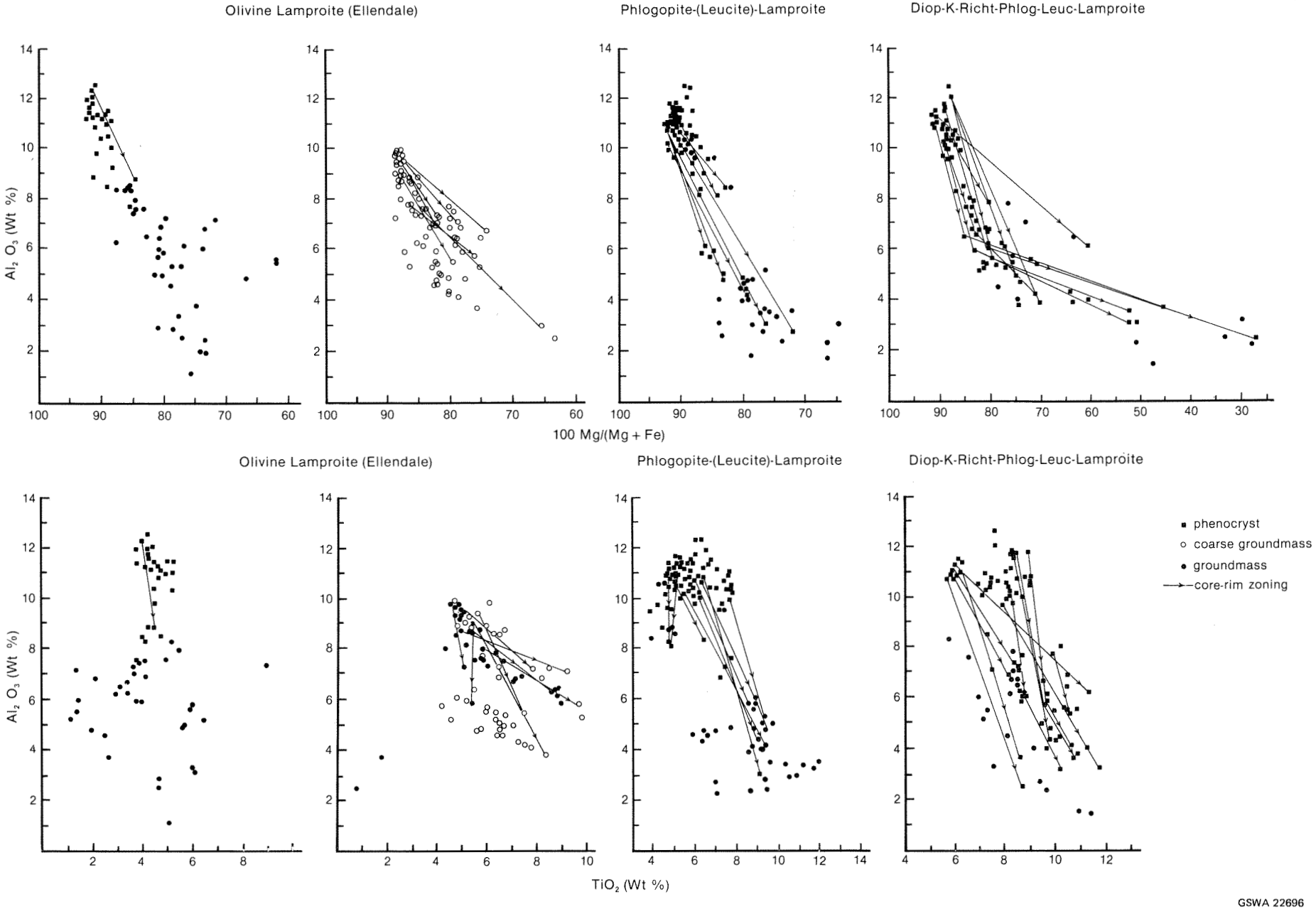


Figure 142. Variation in composition of West Kimberley micas in terms of Al_2O_3 (wt.%), 100Mg/(Mg + Fe) ratio, and TiO_2 (wt.%).

TABLE 58. REPRESENTATIVE ANALYSES OF PHLOGOPITE

	1	2	3	4	5	6	7	8	9	10	11	12	13	14	15	16
									Percent							
SiO_2	38.65	40.31	38.88	39.98	39.94	40.54	42.56	40.94	42.48	38.79	40.25	40.55	42.05	40.23	40.54	38.91
TiO_2	4.11	3.70	4.53	5.45	8.31	5.95	8.50	6.26	9.04	8.19	8.70	9.51	11.87	9.87	10.58	9.38
Al_2O_3	11.95	7.20	11.18	9.04	6.87	11.02	5.83	11.27	3.07	11.69	5.97	4.97	3.58	7.68	5.30	1.99
Cr_2O_3	1.25	0.01	0.78	0.05	0.01	0.94	0.01	1.31	0.01	1.65	0.01	0.00	0.00	0.01	0.00	0.00
FeO	3.67	8.71	4.16	5.43	9.25	3.42	5.80	3.56	10.74	4.37	7.41	10.88	11.11	7.21	10.15	23.03
MnO	0.03	0.06	0.08	0.04	0.03	0.03	0.03	0.02	0.05	0.04	0.03	0.05	0.05	0.04	0.05	0.21
NiO	0.05	<0.04	<0.04	0.07	<0.04	0.13	<0.04	0.16	0.07	0.09	0.08	0.06	<0.04	0.07	0.13	0.07
MgO	23.23	22.92	23.80	22.46	18.75	23.34	21.51	22.99	19.48	20.68	20.49	18.33	16.30	20.69	19.10	11.95
CaO	0.03	0.00	0.00	0.05	0.06	0.00	0.00	0.00	0.00	0.03	0.72	0.09	0.08	0.00	0.01	0.00
BaO	0.90	1.55	0.88	1.62	1.97	0.38	0.68	0.31	0.95	0.58	0.79	0.70	1.07	0.69	0.66	0.36
Na_2O	0.05	0.23	0.11	0.48	0.65	0.04	0.25	0.04	0.58	0.15	0.51	0.57	0.30	0.20	0.38	0.88
K_2O	10.49	10.05	10.80	9.45	9.20	10.72	10.68	10.55	9.61	10.39	9.55	9.59	10.04	10.22	9.89	9.59
F	1.71	4.83	3.21	5.63	2.13	1.63	2.65	1.60	2.70	1.34	2.75	1.81	3.42	2.12	1.06	0.48
Cl	0.00	0.00	0.02	0.03	0.01	0.01	0.00	0.01	0.01	0.02	0.02	0.03	0.02	0.02	0.00	0.01
Total	**96.22**	**99.57**	**98.43**	**99.78**	**97.18**	**98.14**	**98.49**	**98.71**	**98.78**	**98.01**	**97.28**	**97.14**	**99.89**	**99.05**	**97.85**	**96.86**
$^1O \equiv F,Cl$	0.72	2.03	1.35	2.38	0.90	0.69	1.12	0.67	1.14	0.57	1.17	0.77	1.44	0.90	0.45	0.20
Total	**95.50**	**97.54**	**97.07**	**97.40**	**96.28**	**97.45**	**97.37**	**98.04**	**97.64**	**97.44**	**96.11**	**96.37**	**98.45**	**98.15**	**97.40**	**96.66**
Mg(a)	91.9	82.4	91.1	88.1	78.3	92.4	86.9	92.0	76.4	89.4	83.1	75.0	72.3	82.8	77.0	48.1

(a) Mg = 100 Mg/(Mg + Fe) atomic.

1,2 — Microphenocryst (1) and groundmass (2), phlogopite-olivine lamproite; GSWA 71453M, Ellendale No. 11. 3 — Poikilitic plate, core, phlogopite-olivine lamproite; GSWA 71476D, Ellendale No. 4 (E). 4,5 — Poikilitic plate, core (4) and rim (5), Potassic-richterite - phlogopite - olivine lamproite; BMR 7911086, Ellendale No. 9. 6,7 — Phenocryst core (6) and rim (7), phlogopite-leucite lamproite; BMR 83210302, 81<Mile Vent. 8,9 — Phenocryst core (8) and rim (9), diopside - potassic-richterite - phlogopite - leucite lamproite; BMR 83210323, Mt North. 10,11,12 — Phenocryst core (10), mantle (11) and rim (12), diopside - potassic-richterite - phlogopite - leucite lamproite; BMR 67160336, Mt Rose. 13 — Groundmass, olivine-leucite lamproite, BMR 71160408, Oscar Plug. 14,15,16 — Poikilitic plate, core (14), rim (15) and groundmass (16), diopside - potassic-richterite - phlogopite - leucite lamproite; BMR 83210290, Rice Hill.

pale-yellow, weakly pleochroic, ovoid to anhedral cores that are free of inclusions and surrounded by mantles of more strongly pleochroic (yellow-orange) mica that contains abundant inclusions of priderite, diopside, apatite, barite, wadeite, and leucite. These micas are rimmed by strongly pleochroic, red-brown tetraferriphlogopite resembling that in the groundmass. The compositional trends in these rocks are characterized by strong depletion in Al, and increasing Ti, and a decreasing Mg/(Mg+Fe) ratio (Fig. 142). Rims in these micas are invariably Ti-rich (up to 10% TiO_2), poor in Cr, and low in Al (<5% Al_2O_3).

Phlogopite in the coarser grained lamproites of Walgidee Hills, Rice Hill, and Mount North, typically occurs as coarse, poikilitic, subhedral plates that show moderate pleochroism (orange-yellow) and are crowded with inclusions of diopside, leucite, priderite, wadeite and apatite. They have narrow rims of deep red-brown tetraferriphlogopite, show reverse pleochroism, and have high Fe and low Al contents. In contrast to the marked aluminium depletion shown by the phlogopites in the finer grained rocks, these micas are characterized by strong enrichment in Fe, moderate depletion in Mg and Al, and slight enrichment in tetrahedral ferric iron (Mitchell, 1981; Jaques and others, 1984a). TiO_2 is extremely high (6-11%).

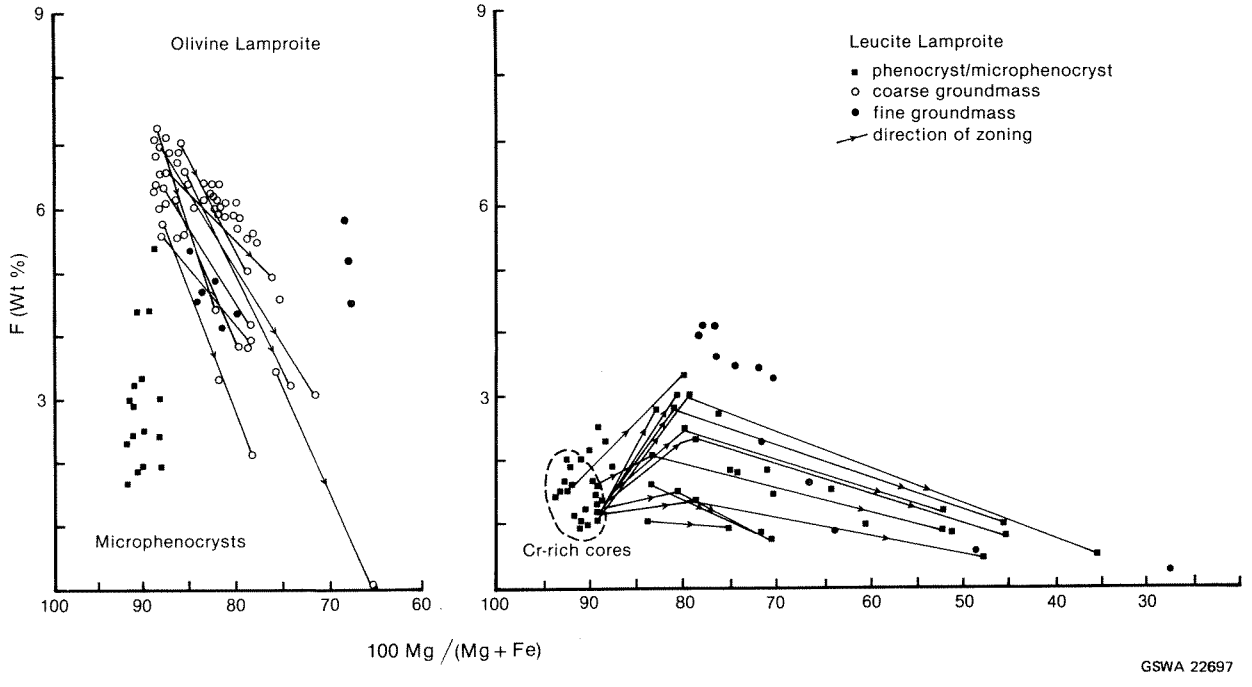


Figure 143. Variation of F content with 100Mg/(Mg + Fe) ratio of West Kimberley micas.

A feature of the West Kimberley micas is their very high Ti and F contents; TiO_2 ranges from 1 to 12%, and F ranges up to 7%. High Ti is typical of micas from ultrapotassic (lamproitic) rocks elsewhere, including Leucite Hills (Carmichael, 1967; Kuehner and others, 1981), Gaussberg (Sheraton and Cundari, 1980), and Spain (Venturelli and others, 1984). The high Ti contents, together with differences in Al, Fe, and Na, and the different zonation trends of the West Kimberley phlogopites, and phlogopites from other lamproites, distinguish them from the groundmass micas in kimberlites (Mitchell, 1981; Jaques and others, 1984a). High Ti in micas is favoured by low pressure, high temperature, and high oxygen fugacity (Robert, 1976; Arima and Edgar, 1981). High F contents also appear to be a feature of lamproite micas (Jaques, in prep.); and the West Kimberley micas are amongst the most F-rich to be found in ultrapotassic rocks.

The F contents of the West Kimberley phlogopites, and those of other lamproite suites, are an order of magnitude higher than typically found in phlogopite from kimberlite, where most micaceous kimberlites contain less than 1% F (Jaques, in prep.). In the West Kimberley lamproites, F contents in phlogopites exhibit complex relationships with other parameters. Microphenocrysts of mica in the olivine lamproites show an increase in F from $\approx 1.6\%$ in the most Mg and Cr-rich to $\approx 5\%$ in the more Mg-poor examples. In terms of Mg/(Mg + Fe), Ti and F contents they overlap the more Mg-rich groundmass micas. The groundmass micas in the olivine lamproites exhibit a strong negative correlation with Mg/(Mg + Fe). This implies that F is increasingly partitioned into the melt as Mg/(Mg + Fe) in phlogopite decreases (Fig. 143).

Micas in the leucite lamproites show similar relationships (Fig. 143): phenocryst cores show an initial increase in F with increasing Ti and decreasing Mg/(Mg + Fe); whereas the mantles on the phenocryst core show the expected decrease in F with increase in Ti and decreasing Mg/(Mg + Fe). This further supports the contention that some of the Mg,Cr,Al-rich cores to the phenocrysts in the lamproites may be xenocrystal, or, at least, have crystallized at higher pressure (Jaques and others, 1984a).

DIOPSIDE

Diopside is present in the groundmass of all except the most glassy West Kimberley lamproites and is present as a phenocryst phase in many of the leucite lamproites. In olivine lamproites, diopside is restricted to the groundmass, where it occurs as small ($< 100\ \mu m$), randomly oriented prisms or, in glassy rocks, as acicular quench crystals. The diopsides are of uniform composition: they lie close to the diopside-hedenbergite join, and exhibit little solid solution towards enstatite (Fig. 144). The diopsides are rich in Ti (1-3%, average 1.5% TiO_2), very low in Al ($< 0.9\%$, typically $< 0.3\%$ Al_2O_3), and contain minor Cr and Na (Table 59). Structural formulae typically show atomic proportions of Si + Al < 2, and commonly Na $>$ Al + Cr. They

TABLE 59. REPRESENTATIVE OF ANALYSES OF DIOPSIDE.

	1	2	3	4	5	6	7
				Percent			
P_2O_5	0.04	—	—	0.04	0.05	0.05	0.05
SiO_2	53.74	51.68	53.44	52.91	53.51	54.15	53.26
TiO_2	1.04	2.76	1.31	1.43	1.45	0.86	1.16
Al_2O_3	0.06	0.15	0.10	0.16	0.08	0.05	0.03
Cr_2O_3	0.31	0.22	0.84	0.74	0.39	0.08	0.25
FeO	2.68	2.86	2.35	2.10	2.17	2.51	2.59
MnO	0.10	0.08	0.10	0.06	0.06	nd	0.03
MgO	16.63	16.42	17.31	17.10	17.61	17.45	16.79
CaO	24.93	25.28	24.00	24.59	24.49	24.90	24.69
Na_2O	0.38	0.27	0.22	0.36	0.22	0.18	0.35
K_2O	0.02	0.06	0.12	0.02	0.01	0.02	0.05
Total	**99.94**	**99.78**	**99.70**	**99.52**	**100.04**	**100.25**	**99.25**
Mg(a)	91.7	91.1	92.9	93.5	93.6	92.6	92.1
				Ratio			
Ca(b)	0.497	0.502	0.481	0.492	0.483	0.487	0.493
Mg(b)	0.461	0.454	0.482	0.476	0.483	0.475	0.466
Fe(b)	0.042	0.044	0.037	0.033	0.033	0.038	0.040

(a) Mg = 100 Mg/(Mg + Fe). (b) Ca = Ca/(Ca + Mg + Fe); Mg = Mg/(Ca + Mg + Fe); Fe = Fe/(Ca + Mg + Fe).
nd = not detected, < 0.03 wt %. All contain < 0.05 wt % NiO, < 350 ppm Zr & Nb.

1 — Groundmass, phlogopite-leucite-olivine lamproite; BMR 83210316, Ellendale No. 16. 2 — Groundmass, (potassic-richterite - phlogopite) - olivine lamproite; GSWA 71456D, Ellendale No. 9. 3 — Microphenocryst, olivine-diopside-leucite-lamproite; GSWA 71449A, Ellendale No. 7. 4 — Phenocryst, diopside - potassic-richterite - phlogopite - leucite lamproite; BMR 83210290, Rice Hill. 5 — Phenocryst, phlogopite - potassic-richterite - diopside - leucite lamproite; BMR 80210079, Old Leopold Hill. 6,7 — Phenocryst, core (6) and rim (7), diopside - potassic-richterite - phlogopite - leucite lamproite; BMR 67160336 Mount Rose.

contain subordinate amounts of Cr (up to 0.6% Cr_2O_3) and Na (up to 0.5% Na_2O), and traces of P and K.

Pale-green (in handspecimen) to colourless (in thin section) diopside occurs as a phenocryst, or in glassy rocks, as a microphenocryst phase in many of the leucite lamproites. Diopside phenocrysts are conspicuous in the diopside-leucite lamproites (cedricites of Wade and Prider, 1940; Prider, 1960) of Mount Cedric, Mount Gytha, Machells Pyramid, Noonkanbah Hill, and Fishery Hill, and in the phlogopite-diopside-leucite lamproite of Old Leopold Hill, where they form elongate, flow-aligned phenocrysts up to 5 mm long. The phenocryst diopsides in the leucite lamproites are of similar composition to the groundmass diopsides in the olivine lamproites, but show less variation in Mg-Fe with greater solid-solution towards enstatite (Fig. 144). This implies higher crystallization temperatures. Both phenocryst and groundmass diopsides in the leucite lamproites have high Ti (0.7-2.3%, average 1.1% TiO_2) and very low Al contents (typically $< 0.5\%$ Al_2O_3, commonly $< 0.2\%$) and Si + Al < 2. Chromium in the diopside phenocrysts ranges up to high values ($\approx 1\%$, average 0.35% Cr_2O_3). The Fe^{3+} contents are calculated on the basis of stoichiometry and show a wide range ($Fe^{3+}/(Fe^{3+} + Fe^{2+})$ = 0.2-0.6); but they are generally comparatively low.

Groundmass and microphenocryst diopsides in the leucite lamproites overlap the compositions of the diopside phenocrysts and extend to more Fe-rich (salitic) compositions. Most are rich in Ca and plot near the diopside-hedenbergite join, although microphenocrysts

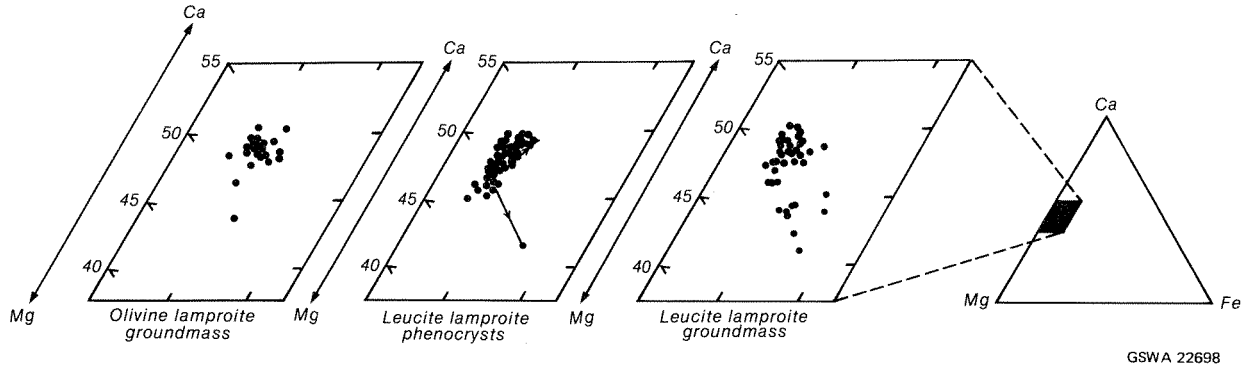


Figure 144. Compositional variation in Ca-Mg-Fe of West Kimberley phenocryst and groundmass pyroxenes. Arrow indicates direction of zoning from core to rim (after Jaques and others, 1984a).

from the glassy, leucite lamproites of Brooking Creek and Oscar Plug show a wider range in Ca contents. In general, the groundmass diopsides are poorer in Al and Cr, and richer in Ti, than the phenocrysts. This is consistent with crystallization from more evolved magmas at lower temperatures. Contents of Zr and Nb in both phenocrysts and groundmass grains are low (<350 and 200 ppm respectively). Most diopside grains exhibit only minor zoning (Table 59; Fig. 144): rims are slightly richer in Ca, Mg, and Ti, than cores; and a few grains have higher Fe contents at the rim. Some grains, however, show strong zoning in Ti and Ca-Mg-Fe, and the rims are distinctly poorer in Ca and richer in Ti and Fe.

The West Kimberley diopsides closely resemble the Ti-rich, Al-deficient diopsides found in other ultrapotassic suites, *e.g.* Spain (Venturelli and others, 1984), Leucite Hills (Carmichael, 1967; Kuehner and others, 1981), New South Wales (Cundari, 1973), and Gaussberg volcano (Sheraton and Cundari, 1980). Lamproitic diopsides, although similar in terms of Mg, Ca, Fe, Na, and Al, are much more Ti-rich than late-stage groundmass diopside found in kimberlites (Dawson and others, 1977).

LEUCITE

Leucite is present as a phenocryst or groundmass phase in all except the most olivine-rich and glassy lamproites of the West Kimberley. However, it is poorly preserved and typically pseudomorphed by K-feldspar (orthoclase), clay, chalcedony, or zeolite, commonly harmotome (Prider and Cole, 1942; Jaques and others, 1984a). In a number of samples, groundmass leucite and much of the groundmass (itself leucite-rich), is altered to K-feldspar, harmotome, and clay (Prider, 1960). Fresh leucite is preserved in the glassy lamproites of Oscar Plug (Prider, 1982), Mount Gytha (Prider, 1960), Brooking Creek, and Ellendale No. 7. In these rocks, the leucite is euhedral, weakly anisotropic and commonly twinned; this indicates a slow rate of cooling through the leucite inversion interval (≈600°C: Faust, 1963). The West Kimberley leucites are close to the ideal stoichiometry (Fig. 145) or show a slight excess of silica; they are unlike those of Leucite Hills (Carmichael, 1967; Kuehner and others, 1981), which show a significant molecular excess of alkalies and Si over Al and Fe^{3+}. Representative analyses of West Kimberley leucites are given by Carmichael (1967), Jaques and others (1984a), Jaques and Foley (1985), and in Table 60.

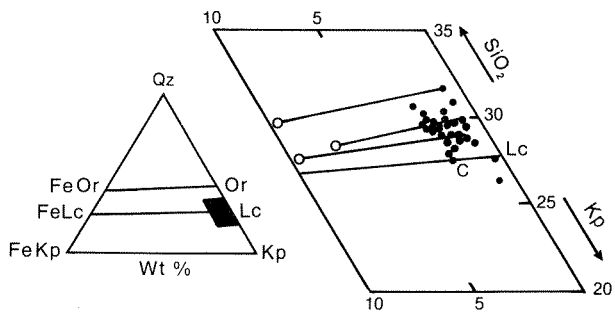


Figure 145. Composition of leucite in West Kimberley lamproites plotted in the system SiO_2 — $KFe^{3+}SiO_4$ — $KAlSiO_4$ (Carmichael, 1967). Open circles and tie-lines join analyses of leucite and Al-spinel inclusions with leucite host compositions. The letter C refers to leucite analysis by Carmichael (1967). Modified after Jaques and Foley (1985).

TABLE 60. REPRESENTATIVE ANALYSES OF LEUCITE

	1	*2*	*3*	*4*	*5*
			Percent		
SiO_2	55.90	55.35	56.06	56.12	55.33
TiO_2	0.11	0.10	0.16	0.17	0.27
Al_2O_3	22.01	21.21	21.17	21.85	21.03
Fe_2O_3	0.55	0.88	1.19	0.62	1.08
MnO	nd	nd	0.03	nd	nd
MgO	0.26	0.69	0.19	0.38	0.46
CaO	nd	nd	nd	nd	nd
Na_2O	0.10	0.02	0.14	0.08	0.09
K_2O	21.36	21.38	21.10	21.40	21.25
TOTAL	**100.29**	**99.53**	**100.04**	**100.62**	**99.42**

Fe determined as FeO and recalculated to Fe_2O_3. nd = not detected; detection limit = 0.02 wt %.

1 — Leucite phenocryst, glassy olivine-bearing leucite lamproite; BMR 80210125, Brooking Creek. 2,3 — Leucite phenocryst core (2), and rim (3), olivine-diopside-leucite lamproite; GSWA 71449A, Ellendale No. 7. 4,5 — Leucite phenocryst core (4), and rim (5), glassy olivine-bearing leucite lamproite; BMR 71160408, Oscar Plug.

Jaques and Foley (1985) described the occurrence of aluminous spinel (pleonaste-hercynite) inclusions in leucite phenocrysts in many of the West Kimberley leucite lamproites. The spinel inclusions, mostly <20 μm in size, occur mainly in aggregated, poorly crystallized leucites, and are compositionally distinct from the groundmass chrome spinels. Jaques and Foley

(1985) suggested that these aluminous, Cr-free spinels formed by exsolution under conditions of supersaturation from non-stoichiometric leucites that originally incorporated Mg, Al and Fe^{2+} in solid solution.

AMPHIBOLE

Pleochroic amphibole — potassic richterite (magnophorite of Prider, 1939) — is present in the groundmass of some of the coarser grained olivine lamproites and in many of the more evolved, coarsely crystalline leucite lamproites (wolgidites and mamilites of Wade and Prider, 1940; Prider, 1960). It typically occurs as coarse poikilitic plates up to several millimetres across and encloses diopside, leucite, chrome spinel, priderite, apatite, and/or wadeite. The plates are commonly zoned from pale, weakly pleochroic cores (X = pale yellow to colourless, Y = salmon pink, Z = lemon yellow) to strongly pleochroic rims (X = lemon yellow, Y = pinkish brown, Z = greenish yellow; Y>Z>X). Coarse poikilitic amphibole is particularly conspicuous at Rice Hill and in the central portion of the Walgidee Hills intrusion where it may comprise up to 50% of the mode. Extreme zoning to dark green-brown arfvedsonitic rims is present in a number of coarse-grained lamproites from Rice Hill and Mount North. Amphibole formed late in the crystallization sequence and typically encloses all other phases apart from the groundmass (and aegirine), as noted by Wade and Prider (1940).

Most of the amphiboles are of similar composition — titanian potassic richterite by Leake's (1978) classification — and characterized by high Mg/(Mg+Fe), high TiO_2 (2-7%, typically 4-6%) and alkali contents (Na_2O+K_2O >8%), and very low Al contents (<1%, commonly <0.5% Al_2O_3). The K_2O content is characteristically ≈5%, and K may exceed Na. There is insufficient Al to fill the tetrahedral site; this indicates that significant Fe^{3+}, and possibly Ti, are in fourfold coordination. The Ba is typically low (<0.1% BaO), probably as a consequence of the earlier ubiquitous crystallization of priderite. Fluorine contents are moderate to high (up to 4%, commonly 1-2%), whereas Cl contents are very low. Both the TiO_2 and Na/(Na+K) ratios correlate weakly with decreasing Mg/(Mg+Fe); and, in general, the Ti contents of the amphiboles in the olivine lamproites are lower than those in the the more felsic leucite lamproites (Fig. 146). The dark amphiboles rimming the potassic richterite are distinctly more sodic and more Fe-rich: they are potassic magnesio-arfvedsonites, which contain up to 7% Na_2O and have variable TiO_2 contents.

The West Kimberley potassic richterites are compositionally similar (Table 61) to amphiboles found in ultrapotassic volcanic rocks elsewhere, such as the Leucite Hills (Carmichael, 1967; Kuehner and others, 1981), and Prairie Creek (Scott-Smith and Skinner, 1984a). Amphiboles found in the Spanish (Venturelli and others, 1984) and New South Wales (Cundari, 1973) lamproites are richer in Al and have higher Na/(Na+K) ratios. The West Kimberley amphiboles differ from the potassic richterites found in the MARID suite (Dawson and Smith, 1977) and those in some veins in mantle harzburgites and lherzolites (Dawson and Smith, 1982) by virtue of their notably higher Ti.

CHROME SPINEL

Chrome-rich spinel is present as a primary groundmass phase in the Ellendale olivine lamproites and in many of the olivine-bearing leucite lamproites. Chrome spinel is generally not present in rocks

TABLE 61. REPRESENTATIVE ANALYSES OF TITANIAN POTASSIC RICHTERITE (1-7) AND POTASSIC MAGNESIO-ARFVEDSONITE (8).

	1	*2*	*3*	*4*	*5*	*6*	*7*	*8*
					Percent			
SiO_2	52.95	52.44	52.40	53.28	52.89	52.85	50.87	55.68
TiO_2	2.08	3.45	6.26	5.79	6.77	5.87	7.45	1.32
Al_2O_3	0.42	0.55	0.31	0.28	0.22	0.26	0.31	0.14
Cr_2O_3	0.01	0.00	0.01	0.04	0.10	0.01	0.00	0.00
FeO	3.28	3.70	3.50	3.23	5.84	3.81	6.75	10.99
MnO	0.10	0.14	0.13	0.06	0.12	0.07	0.10	0.12
NiO	0.05	0.03	0.03	0.06	0.03	0.03	0.09	nd
MgO	22.07	21.37	20.21	19.98	18.35	19.78	17.07	16.73
CaO	7.09	6.56	6.34	6.37	5.80	6.09	6.25	0.89
BaO	0.07	0.26	0.13	0.06	0.05	0.05	0.07	nd
Na_2O	3.86	3.65	3.66	3.74	3.99	3.81	3.95	6.88
K_2O	5.33	5.29	5.32	5.53	5.46	5.63	5.23	5.37
Cl	0.00	0.00	0.02	0.00	0.00	0.02	0.01	0.01
F	2.69	3.91	2.19	1.33	0.82	1.94	1.22	0.32
Total	**99.96**	**101.35**	**100.44**	**99.74**	**100.45**	**100.18**	**99.36**	**97.95**
$-O\equiv Cl,F$	1.13	1.65	0.92	0.56	0.35	0.83	0.51	0.14
Total	**98.83**	**99.70**	**99.52**	**99.18**	**100.10**	**99.35**	**98.85**	**97.81**
Mg(a)	92.3	91.2	91.1	91.7	84.8	90.3	81.9	83.1

(a) Mg = 100 Mg/(Mg + Fe). nd = not detected (<0.03%).

1,2 — Poikilitic plate, core (1) and rim (2) (potassic-richterite - phlogopite) - olivine lamproite; GSWA 71456D, Ellendale No. 9. 3 — Interstitial grain, diopside - potassic-richterite - phlogopite - leucite lamproite; BMR 83210323, Mount North. 4,5 — Poikititic plate, core (4) and rim (5), diopside - potassic-richterite - phlogopite - leucite lamproite; BMR 83210290, Rice Hill. 6,7 — Interstitial amphibole, core (6) and rim (7), diopside - potassic-richterite - phlogopite - leucite lamproite; BMR 67160336, Mount Rose. 8 — Potassic magnesio-arfvedsonite rim on potassic-richterite; BMR 83210290, Rice Hill.

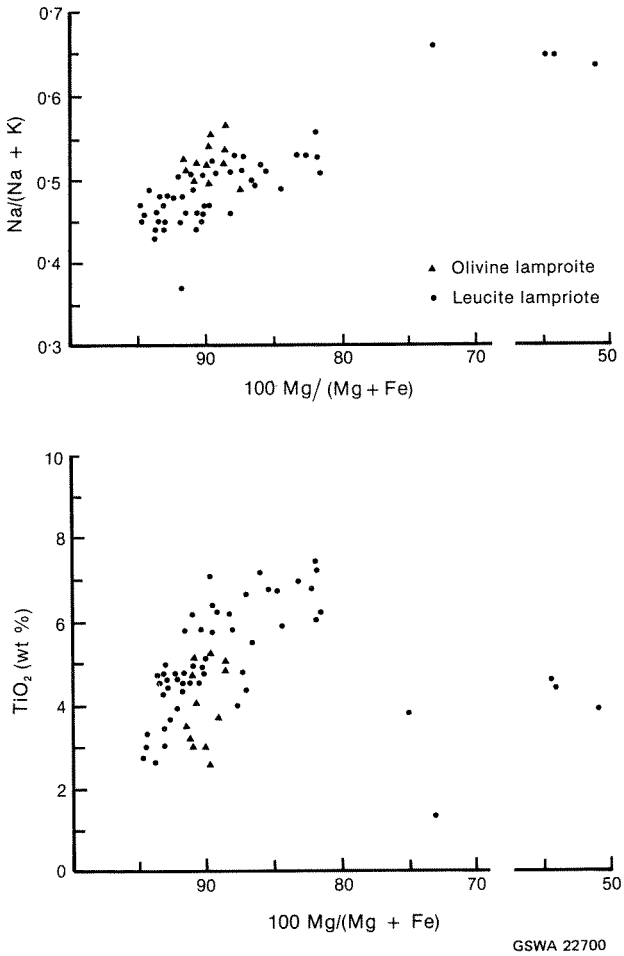


Figure 146. Compositional variation of amphiboles in West Kimberley lamproites in terms of 100Mg/(Mg + Fe) *versus* TiO_2, and Na/(Na + K). Modified after Jaques and others (1984a).

containing less than 8-10% modal olivine (corresponding to 7-8% MgO). The spinel typically occurs as small (< 100 μm, mostly < 40 μm) red-brown euhedra in the groundmass, or as smaller (typically < 20 μm) inclusions in olivine, phlogopite or other later crystallizing phases. Larger (up to 250 μm) rounded spinels are occasionally found in some of the olivine lamproites; these spinels, with cores of titaniferous magnesian aluminous chromite composition may be of xenocrystal origin, or have crystallized at higher pressure. In the more olivine-rich lamproites, the spinel is euhedral and of titaniferous magnesian aluminous chromite to titanian, magnesian chromite composition whereas in coarser grained and less Mg-rich lamproites the titaniferous magnesian chromite cores are rimmed by titaniferous chromian magnetite with ragged outlines.

The bulk of the spinels in the West Kimberley rocks are of titaniferous magnesian chromite to titaniferous chromite composition and are characterized by moderate Ti (3-6% TiO_2), low Al (< 10% Al_2O_3), and very high Cr (Cr/(Cr + Al) > 0.9, > 50% Cr_2O_3). The more magnesian of these contain up to 15% MgO and significant Ni (up to 0.2% NiO) and overlap the occasional titaniferous magnesian aluminous chromites (1-4% TiO_2, 10-13% Al_2O_3, Cr/(Cr + Al) = 0.75-0.9, 10-15% MgO). In the more coarsely grained lamproites, the cores of titaniferous magnesian chromite to titaniferous chromite are rimmed by titaniferous chromian magnetite (10-15% TiO_2, up to 25% Cr_2O_3, < 5% MgO) that contains significantly higher V (0.2-0.3% V_2O_3) and Mn (up to 1.3% MnO). Rare tiny grains of titaniferous magnetite (ulvöspinel-magnetite) are present in the groundmass of some of the coarser grained olivine lamproites (Table 62).

TABLE 62. REPRESENTATIVE ANALYSES OF SPINELS (1-10) AND ILMENITES (10-13).

	1	*2*	*3*	*4*	*5*	*6*	*7*	*8*	*9*	*10*	*11*	*12*	*13*
							Percent						
Nb_2O_5										nd		0.37	0.15
SiO_2	0.20	0.19	0.05	nd	0.21	0.09	0.05	0.04	0.09	0.09	0.10	0.10	0.10
TiO_2	2.06	2.15	3.07	3.91	2.94	3.88	4.35	3.52	12.89	15.75	55.03	53.39	54.30
Al_2O_3	12.31	11.37	4.38	2.78	7.72	2.24	1.5i	0.90	nd	nd	nd	nd	nd
Cr_2O_3	52.64	53.36	59.96	57.83	52.96	57.65	57.15	52.13	21.91	0.45	nd	0.03	0.16
V_2O_3	0.07	0.06	0.05	0.15	0.25	nd	0.05	0.03	0.30	0.14	0.61	0.28	nd
FeO(a)	16.71	17.88	18.57	22.59	24.18	28.68	27.25	37.76	67.58	74.57	35.77	37.63	40.41
MnO	0.19	0.27	0.29	0.27	0.28	0.66	0.31	0.97	1.05	1.23	0.56	1.33	1.55
NiO	0.13	0.15	0.14	0.23	0.13	0.11	0.16	0.12	0.34	0.11	0.11	0.06	0.05
MgO	15.00	14.08	12.80	11.86	11.68	7.19	8.95	3.61	3.58	2.81	7.40	6.98	3.35
CaO	0.06	0.05	0.02	nd	0.02	0.07	0.03	0.03	0.05	0.08	0.20	0.09	0.13
Total	**99.37**	**99.56**	**99.35**	**99.62**	**100.38**	**100.56**	**99.80**	**99.11**	**97.79**	**95.23**	**99.78**	**100.26**	**100.20**
Fe_2O_3(a)	4.49	4.33	3.52	5.82	6.72	4.50	5.65	10.07	23.36	38.68	0.31	7.03	1.51
FeO (a)	12.67	13.98	15.40	17.35	18.14	24.63	22.17	28.69	36.56	39.77	35.50	31.03	39.06
Total (a)	**99.82**	**99.99**	**99.70**	**100.20**	**101.06**	**101.01**	**100.37**	**100.11**	**100.13**	**99.11**	**99.81**	**100.96**	**100.36**
							Ratio						
Mg (b)	0.678	0.642	0.597	0.549	0.534	0.342	0.418	0.184	0.149	0.112	0.271	0.284	0.133
$Cr/(R^{3+})$(c)	0.699	0.717	0.859	0.857	0.747	0.883	0.882	0.826	0.496	0.004	—	—	—
$Fe^{3+}/(R^{3+})$(c)	0.057	0.055	0.048	0.082	0.090	0.066	0.083	0.152	0.504	0.996	—	—	—

nd = not detected. < 0.02wt%. (a) FeO and Fe_2O_3 calculated from stoichiometry. (b) Mg = Mg/(Mg + Fe^{2+}) (c) R^{3+} = (Cr + Al + Fe^{3+}).

1-3 — Groundmass titaniferous magnesium aluminous chromite (1); titaniferous magnesium aluminous chromite, inclusion in olivine $Mg_{91.6}$ (2); groundmass titaniferous magnesium chromite (3); phlogopite-olivine lamproite; Ellendale No. 11, GSWA 71453M. 4 — Titaniferous magnesium chromite inclusion in olivine $Mg_{89.9}$; glassy olivine-bearing leucite lamproite; Brooking Creek, BMR 80210125. 5,6 — Coarse titaniferous magnesium chromite, microphenocryst (5); groundmass titaniferous magnesium chromite (6); phlogopite-olivine lamproite; Ellendale No. 4 (W), GSWA 71480C. 7, — Groundmass titaniferous magnesium chromite; glassy olivine-bearing leucite lamproite; Oscar Plug, BMR 71160408. 8,10 — Groundmass, titaniferous chromite (8); titaniferous chromian magnetite (9); and titaniferous magnetite (10); Potassic-richterite - phlogopite - olivine lamproite; Ellendale, No. 9, BMR 79211086. 11 — Groundmass ilmenite, glassy olivine-bearing leucite lamproite; Brooking Creek, BMR 80210125. 12, — Groundmass ilmenite; potassic-richterite - phlogopite - olivine lamproite; Ellendale No. 9, BMR 79211086. 13 — Groundmass ilmenite; phlogopite-olivine lamproite; Ellendale No. 9 (E), GSWA 71475B.

The evolutionary trend of the West Kimberley spinels is initially one of decreasing Al and Mg and near-constant to slightly increasing Ti, and increasing Cr and Fe (*i.e.* titaniferous magnesian aluminous chromite to titaniferous magnesian chromite); followed by decreasing Mg and increasing Fe^{2+} and near constant Cr and Ti (titaniferous magnesian chromite to titaniferous chromite); followed by increasing Ti and Fe^{2+} and Fe^{3+}, and decreasing Cr and Mg (titaniferous chromite — titaniferous chromian magnetite). The evolutionary trend of the West Kimberley spinels differs from that of kimberlites: lamproite spinels show only limited solid solution towards $MgAl_2O_4$; and there is no late stage Mg-Al trend comparable with that observed in some kimberlites (Haggerty, 1975, 1976; Pasteris, 1983). In addition, lamproite chromites are generally more titaniferous than kimberlitic chromites; and, although exhibiting a late stage increase in Ti and Fe^{3+}, this trend is toward ulvöspinel-magnetite rather than magnesian ulvöspinel - ulvöspinel magnetite.

APATITE

Apatite is present as small (typically $< 100\ \mu m$) stubby prisms in the groundmass of all except the glassy lamproites. In the coarser grained lamproites forming the core of the Walgidee Hills intrusion, apatite forms prisms up to 2 mm long. The modal abundance of apatite increases from trace amounts in olivine lamproite to several percent in the more fractionated, coarse-grained leucite lamproites. Microprobe analyses show the West Kimberley apatites to be fluor-apatites that contain up to 4% F and are rich in Sr (up to 3.5% SrO in some samples from Walgidee Hills) and LREE, notably Ce (Mason, 1977; Jaques and others, 1984b).

PRIDERITE AND OTHER TITANATES AND TI-ZR SILICATES

Priderite: $(K,Ba)_{1\cdot33}(Ti,Fe^{3+})_8O_{16}$ (Norrish, 1951) — is present as small rods and prisms, typically 0.2-0.5 mm long, in the groundmass of all except the most olivine-, rich and glassy lamproites. The modal abundance of priderite increases from sparse tiny prisms in olivine lamproite to more than 10% by volume in some of the coarser grained leucite lamproites (Wade and Prider, 1940; Derrick and Gellatly, 1972). Priderite is particularly conspicuous in the coarser grained central part of the Walgidee Hills intrusion, where it is present as prisms up to 2 mm long. Microprobe analyses show little variation regardless of bulk-rock composition, apart from small intergrain and within-grain variation in Ba and K (Table 63). All contain only minor Cr, Nb, Na, and Ca; Si and Al contents are typically below 100 ppm. The priderite analyses given here are similar to those reported by Carmichael (1967) and Mitchell and Lewis (1983) for the West Kimberley lamproites, and differ from the original analysis of Norrish (1951) in having much lower Al and Na. A typical composition is $(K_{1\cdot1}Na_{0\cdot02}Ba_{0\cdot30})_{1\cdot42}(Mg_{0\cdot22}Fe_{0\cdot9}Ti_{6\cdot95}Cr_{0\cdot01})_{8\cdot07}O_{16}$.

Jeppeite: $(K,Ba)_2(Ti,Fe^{3+})_6O_{13}$ (Pryce and others, 1984). Jeppeite is found commonly only in the coarse-grained central core of the Walgidee Hills intrusion, where it forms isolated black-blue (in hand specimen) acicular to prismatic crystals, up to 1 mm long, commonly closely associated with priderite. Jeppeite is distinguished from priderite, on which it commonly forms overgrowths (Fig. 130), by its characteristic colour and pleochroism (X = slate grey, Y = dark green-brown, Z = olive buff; Y > Z > X). Microprobe analyses show minor zoning within grains and some intergrain differences in K, Ba, and Ti. The average composition is close to the ideal structure and composition reported by Pryce and others (1984) — apart from Zr which was typically at or below the limit of detection (< 170 ppm Zr). The analyses (Table 63) contain significant Mg, Na, Sr, and Nb, as shown by a typical structural formula:

$$(Na_{0\cdot09}K_{1\cdot18}Ba_{0\cdot67}Sr_{0\cdot02})_{1\cdot96}$$
$$(Mg_{0\cdot05}Fe_{0\cdot40}Ti_{5\cdot60}Nb_{0\cdot01})_{6\cdot06}O_{13}.$$

TABLE 63. REPRESENTATIVE ANALYSES OF TITANATES AND TI AND ZR SILICATES

	1	*2*	*3*	*4*	*5*	*6*	*7*	*8*	*9*
					Percent				
P_2O_5	0.00	—	—	—	—	—	0.00	0.02	—
Nb_2O_5	0.04	0.06	0.04	0.06	0.08	0.15	0.30	0.35	nd
ZrO_2	0.04	0.04	0.03	0.04	nd	nd	0.03	0.06	31.27
SiO_2	0.03	0.00	0.00	0.06	0.02	0.03	40.72	40.98	46.08
TiO_2	75.54	76.79	75.58	76.22	69.79	69.30	24.36	24.51	1.60
Al_2O_3	0.00	0.00	0.00	0.00	0.00	0.00	0.00	0.00	0.00
Cr_2O_3	0.04	0.16	0.03	0.04	nd	0.02	nd	nd	nd
FeO	9.82	8.70	10.52	9.09	4.43	4.54	1.79	2.22	nd
MnO	nd	nd	nd	nd	nd	nd	nd	nd	nd
MgO	1.22	1.35	1.10	1.29	0.32	0.33	0.56	0.45	0.01
CaO	0.02	0.00	0.02	0.17	0.04	0.02	3.01	2.63	0.00
SrO	nd	nd	nd	nd	0.26	0.26	0.02	nd	nd
BaO	6.30	5.71	6.25	5.36	15.98	16.76	14.14	13.98	0.08
Na_2O	0.07	0.09	0.08	0.08	0.43	0.41	3.77	4.04	0.00
K_2O	6.89	7.00	6.29	7.05	8.86	8.60	11.19	11.18	21.46
Total	**99.99**	**99.92**	**99.94**	**99.47**	**100.21**	**100.41**	**99.87**	**100.42**	**100.53**

Fe as FeO; nd = not detected, < 0.02 wt %.

1-4 — priderite; 5-6 — jeppeite; 7-8 — shcherbakovite; 9 — wadeite.

1 — Pegmatoidal, shcherbakovite - potassic-richterite lamproite; central Walgidee Hills, BMR 81210197B. 2 — Diopside - potassic-richterite - phlogopite - leucite lamproite; Rice Hill, BMR 8210290. 3 — Priderite rimmed by jeppeite; coarse, altered, titania-rich diopside - potassic-richterite lamproite; central Walgidee Hills, BMR 81210195. 4 — Olivine-diopside-leucite lamproite; Mount Ibis, BMR 81210169. 5,6 — Jeppeite rimming priderite, (6); jeppeite rim; Walgidee Hills, BMR 81210195. 7,8 — Shcherbakovite core (7); and rim (8); Walgidee Hills, BMR 8120197B. 9, — Wadeite; Walgidee Hills, BMR 81210197B.

Shcherbakovite: (Noonkanbahite of Prider, 1965) — a batisite of general formula $NaKBaTi_2Si_4O_{14}$. Scherbakovite is found in the coarse-grained central part of the Walgidee Hills intrusion, where it occurs as millimetre-length prismatic grains that show marked pleochroism (X = Y = colourless to straw yellow, Z = golden yellow). Microprobe analyses (Table 63) show compositions close to that given by Prider (1965) apart from lower Si and higher Ti. The average structural formula is:

$$(Na_{0.75}K_{1.42}Ba_{0.54}Ca_{0.29})_{3.00}$$
$$(Nb_{0.01}Fe_{0.16}Ti_{1.84})_{2.01}Si_{4.05}O_{14}$$

Small intergrain differences are found in Fe, Mg, Ca, Na, and K.

Perovskite: This mineral is present as tiny euhedral granules in the groundmass of all except the most glassy olivine lamproites of the Ellendale area and in some of the more olivine-rich lamproites of the Noonkanbah field such as Mount Ibis. Perovskite is ubiquitous in the olivine lamproites of the Walgidee Hills intrusion, where it increases in size and abundance from small granules in the fine-grained rocks of the rim to the coarse-grained, fractionated lamproites forming the core, where it may be as large as 1 mm across. Many of the Walgidee Hills perovskites are characterized by anomalous birefringence, colour zoning (from yellow cores to colourless rims), and striking, complex, polysynthetic twinning as observed by Wade and Prider (1940). Microprobe analyses show them to be rich in Nb (up to 1% Nb_2O_5), Sr (up to 3% SrO), and light rare-earth elements ($\approx$2% REE, predominantly Ce). REE patterns are extremely fractionated: LREE abundances are up to 10 000 times chondritic abundances: and HREE abundances only 6 times chondritic *i.e.* La/Yb $\approx$730 (Mason, 1977). Other elements present include Na (up to 1% Na_2O), Fe, Ba, Th, and U.

Wadeite: $Zr_2K_4Si_6O_{18}$ — originally described by Prider (1939) and later determined by Henshaw (1955) — occurs as colourless prisms in the groundmass of many of the West Kimberley lamproites including most of the olivine lamproites of the Ellendale area. It is readily distinguished, even in fine-grained rocks, by its strong fluorescence under the electron beam. Wadeite is conspicuous in the coarse-grained lamproites of the central core of the Walgidee Hills intrusion, where it forms strongly birefringent, tabular grains and prisms up to 1.5 mm long. As noted by Prider (1939) many of these are partly replaced by calcite. Microprobe analyses (Table 63) show compositions similar to that reported previously from the West Kimberley by Carmichael (1967), who showed that natural wadeites have deficiencies in the K site. Apart from TiO_2 which is present at 1-2%, and traces of Ba, Mg, and Sr, most other elements were not detected by microprobe (Table 63; *see* Mason, 1977). An average composition is therefore $(Zr_{1.98}Ti_{0.16})_{2.14}K_{3.56}Si_{5.98}O_{18}$.

Ilmenite: Small groundmass granules of ilmenite (<20 μm) occur in some of the West Kimberley lamproites, but are comparatively rare (Jaques and others, 1984a). The most Mg-rich contain up to 7.5% MgO, and are poor in Cr and Mn (Table 62). Many of the ilmenite grains in the coarser lamproites (such as BMR 79211086 from Ellendale 9) have ragged outlines and are rich in Mn (up to several percent; Table 62) and poor in Mg. These grains formed late in the crystallization sequence and appear to have been modified by, or even crystallized as the result of, late-stage deuteric or secondary processes. These grains are generally not as Mn-rich as the secondary groundmass ilmenites found in the Argyle lamproites (*see* Chapter 4), the Skerring Pipe (Chapter 3), and reported from several kimberlites elsewhere (*e.g.* Boctor and Boyd, 1979; Agee and others, 1982).

OTHER PHASES

Alkali pyroxene: Aegirine and aegirine augite are present in the groundmass of some of the coarser grained evolved leucite lamproites. Aegirine is conspicuous in the diopside - phlogopite - potassic-richterite - leucite lamproites of Rice Hill and Old Leopold Hill (Derrick and Gellatly, 1972), where it occurs as interstitial subhedra that rim earlier crystallized diopside, leucite, or potassic richterite. Both the aegirine and aegirine augite are strongly pleochroic (X = emerald green, Y = green, Z = yellow green) and clearly distinguishable from diopside when forming rims and extensions along common crystallographic axes.

Microprobe analyses (Table 64) show a compositional range from aegirine augite (Na/(Na + Ca + K) $\approx$ 0.5) to aegirine (Na/(Na + Ca + K) $\approx$ 0.9). Aluminium is low (<0.9%, typically <0.5% Al_2O_3), whereas Ti ranges from high values in aegirine augite and Ca-bearing

TABLE 64. REPRESENTATIVE ANALYSES OF AEGIRINE-AUGITE AND AEGIRINE.

	1	*2*	*3*
	Percent		
P_2O_5	0.02	0.02	0.02
SiO_2	52.14	52.30	51.12
TiO_2	2.18	3.8	5.11
Al_2O_3	0.06	0.23	nd
V_2O_3	—	1.05	—
Cr_2O_3	0.88	nd	0.05
Fe_2O_3(a)	16.27	22.33	24.45
FeO(a)	1.60	3.75	2.36
MnO	0.11	0.08	0.08
MgO	6.93	1.94	1.43
CaO	11.43	2.60	1.80
Na_2O	7.61	11.81	12.65
K_2O	0.07	0.16	0.40
Total	**99.30**	**100.09**	**99.47**
Mg(b)	88.5	48.0	51.9
	Ratio		
Ca(c)	0.339	0.109	0.079
Mg(c)	0.286	0.113	0.087
Fe(c)	0.375	0.778	0.834

(a) Fe_2O_3 and FeO calculated from stoichiometry.
(b) Mg = 100Mg/(Mg + Fe^{+2}).
(c) Ca = Ca/(Ca + Mg + Fe); Mg = Mg/(Ca + Mg + Fe); Fe = Fe/(Ca + Mg + Fe).
nd = not detected, <0.02 wt%.

Diopside - potassic-richterite - phlogopite - leucite lamproite; BMR 83210290, Rice Hill.

aegirine (up to 6% TiO_2) to low values (< 1% TiO_2) in Ca-poor aegirine. Many of the aegirines also have very high V contents (up to 1% V_2O_3); Manganese is very low. The Fe^{3+} contents, estimated from stoichiometry, exhibit considerable variation. Variation in pyroxene composition in terms of Na-Mg-(Fe^{2+} + Mn), and amphibole composition in terms of Na-Mg-Ca is shown in Fig. 147 for a phlogopite — diopside — potassic-richterite-leucite lamproite from Rice Hill. The compositional fields of early formed diopside and late- stage aegirine are separated by the crystallization fields, firstly, of potassic richterite and then of magnesio-arfvedsonite. This is consistent with the existence of a "miscibility gap" between Ca-rich and Na-rich pyroxene during which alkali amphibole crystallized (Ferguson, 1978).

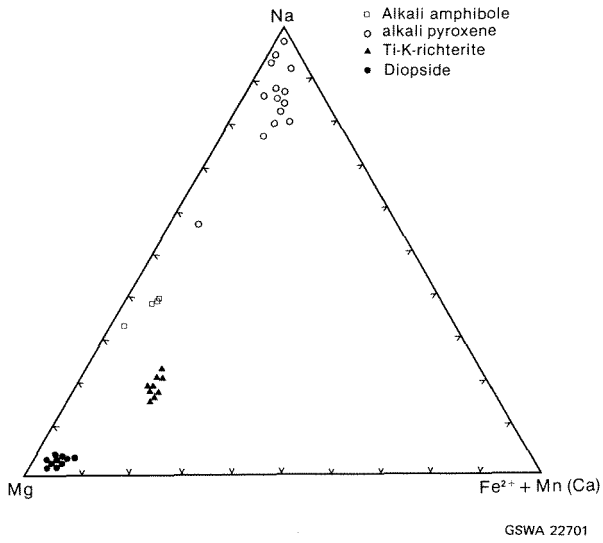


Figure 147. Compositional variation of pyroxenes in terms of Mg — Ca — Na, and amphibole in terms of Mg — (Fe^{2+} + Mn) — Na in sample BMR 83210290 from Rice Hill (after Ferguson, 1978).

The crystallization of alkali pyroxene in the the West Kimberley lamproites indicates that the residual liquids were distinctly peralkaline (*e.g.* Bailey, 1969). The crystallization of late Na-pyroxene after alkali amphibole is not uncommon in alkaline suites (Ferguson, 1978), and has been attributed to increasing Na and oxygen fugacity in the magma (Nicholl and Carmichael, 1969), and/or crystallization of the amphibole in the presence of significant volatiles, followed by a decrease in volatile pressure (*e.g.* Ferguson, 1978).

Potash Feldspar: Sanidine is present as a primary phase in the groundmass of some of the coarser grained diopside - phlogopite - potassic-richterite - (leucite) lamproites from Mount North, Walgidee Hills, and, possibly, Djada Hill, Old Leopold Hill, Rice Hill, and "P" Hill. It is both difficult to recognize, because of extensive alteration to turbid brown "clay" or amorphous material, and difficult to distinguish, in many cases, from the widespread secondary K-feldspar. The modal abundance ranges from trace to 40% in the coarse pegmatitic lamproites at the centre of Walgidee Hills, where it forms altered plates poikilitically enclosing earlier crystallised phases. Compositions are very rich in K, and poor in Ca and Na (Table 65). Iron is low, in contrast to the Fe-rich sanidines found in the Leucite Hills lamproites (Carmichael, 1967).

TABLE 65. REPRESENTATIVE ANALYSES OF SANIDINE.

	1	*2*
	Percent	
SiO_2	64.91	64.30
Al_2O_3	18.11	16.98
Fe_2O_3	0.32	0.83
CaO	0.03	0.13
Na_2O	0.06	0.15
K_2O	17.03	16.74
Total	**100.46**	**99.13**

1 — Poikilitic feldspar; priderite - jeppeite - diopside - potassic-richterite lamproite, central Walgidee Hills, BMR 81210195. 2 — Interstitial feldspar; diopside - potassic richterite - phlogopite - leucite lamproite, Mount North, BMR 83210323.

Secondary phases: The West Kimberley lamproites contain a variety of secondary minerals; these include serpentine, talc, nontronite, celadonite, orthoclase, chalcedony, harmotome, hematite, montmorillonite, illite, and devitrified glass.

XENOCRYST PHASES

Heavy-mineral concentrates of the West Kimberley lamproites contain abundant barite, olivine, chrome-rich spinel, and smaller amounts of garnet, chrome diopside, enstatite, diamond, moissanite, ilmenite (Mg-poor), corundum, kyanite, andalusite, staurolite, zircon, and tourmaline — the last six minerals presumably derived from Proterozoic basement rocks. Olivine, garnet, chrome diopside, enstatite, and diamond, are more abundant in olivine lamproite than leucite lamproite. Representative microprobe analyses of xenocryst phases are given in Table 66, and by Atkinson and others (1984a) and Jaques and others (1984a).

Olivine: By far the most abundant xenocryst phase in the West Kimberley lamproites is olivine; it occurs both as discrete anhedra and in dunite fragments. Compositions range from Mg_{88-93}; and the olivines have high Ni contents, but very low Al, Ca, and Mn, typical of mantle peridotite (Table 66).

Chromian spinel: Red-brown, subhedral to anhedral grains of chromian spinel up to 1 mm diameter occur in heavy-mineral concentrates. These spinels, which range in composition from magnesian chromian pleonaste through magnesian aluminous chromite to magnesiochromite, are distinguished from the smaller groundmass spinels by their size, and by their low Ti (typically 1% TiO_2 or less) and high Al (Table 66). The xenocryst spinels are uniformly magnesian — Mg/(Mg + Fe^{2+}) ratios in the range 0.45-0.75 — and exhibit a wide range of Cr contents and Cr/(Cr + Al) ratios (Fig. 148). There is also a marked negative correlation of Mg/(Mg + Fe) and Cr/(Cr + Al). The West Kimberley xenocryst spinel compositions are similar to those of spinels found in the spinel-diopside-bearing harzburgite from the Ellendale area and in peridotite

TABLE 66. REPRESENTATIVE ANALYSES OF XENOCRYSTS

	Olivine	*Opx*	*Cpx*	*Ga*	*Spinel*				
	1	*2*	*3*	*4*	*5*	*6*	*7*	*8*	*9*
				Percent					
SiO_2	40.84	57.42	54.99	41.26	—	—	—	—	—
TiO_2	0.03	nd	nd	0.17	0.13	0.20	0.17	0.13	1.50
Al_2O_3	nd	1.58	0.21	19.32	7.92	10.63	23.71	37.24	13.83
V_2O_3	—	—	nd	—	0.36	0.28	0.28	nd	0.16
Cr_2O_3	0.04	0.38	1.85	5.97	63.53	62.21	46.41	32.29	51.00
FeO(a)	8.92	4.55	2.10	8.27	13.42	13.12	14.71	13.72	18.71
MnO	0.07	0.13	nd	0.67	0.52	0.44	0.83	0.71	0.63
NiO	0.42	—	—	—	—	—	—	—	—
MgO	49.79	35.08	17.82	18.99	13.92	13.61	14.35	16.08	13.94
CaO	0.04	0.59	22.52	5.96	nd	nd	nd	nd	nd
Na_2O	—	—	0.55	nd	—	—	—	—	—
Total	**100.15**	**99.74**	**100.06**	**100.61**	**99.81**	**100.49**	**100.47**	**100.17**	**99.77**
Fe_2O_3(a)					2.01	0.30	1.48	0.99	5.59
FeO (a)					11.61	12.85	13.38	12.83	13.68
Total (a)					**100.01**	**100.52**	**100.61**	**100.27**	**100.33**
Mg (b)	90.9	93.2	93.8	80.4	68.1	65.4	65.6	69.1	64.5

(a) Fe_2O_3 and FeO calculated from stoichiometry; nd = not detected (analyses by EDS except for 1). (b) Mg = 100 Mg/(Mg + Fe^{2+}).

1 — Olivine; Ellendale No. 9. 2 — Orthopyroxene (enstatite); Ellendale No. 9. 3 — Clinopyroxene (chrome diopside); Water Reserve Pipe. 4 — Garnet (chrome pyrope); Walgidee Hills. 5-9 — Cr-Al spinels; Water Reserve Pipe.

nodules elsewhere (*e.g.* Smith and Dawson, 1975). As noted by Jaques and others (1984a) they closely resemble those occurring in the garnet and chromite-lherzolites and harzburgites from Pipe 200, northern Lesotho (Carswell and others, 1979).

The most Al-rich xenocryst spinels overlap the magnesian chromian pleonaste grains found in peridotite nodule 958164 from Ellendale 7 (Fig. 148). These spinels are very similar to those described from peridotites that are believed to have equilibrated near the spinel-garnet lherzolite boundary (*e.g.* Ferguson and others, 1977).

Spinels in nodule 958164 show similar trends to the xenocryst spinels (*e.g.* variation in Mg/(Mg + Fe^{2+}) with Cr/(Cr + Al), as a consequence of subsolidus equilibration under slightly different P and T conditions. The negative correlation between Mg/(Mg + Fe^{2+}) and Cr/(Cr + Al) is broadly consistent with equilibration with Mg-rich olivine of near constant composition at near constant temperature (Irvine, 1965). Such a wide range in Cr/(Cr + Al) ratios of the spinels suggests derivation from a range of peridotite types with differing bulk-rock Al_2O_3 and Cr_2O_3 contents which have been equilibrated over a wide range of pressures and a smaller range of temperature. The variation in Al and Cr contents of the peridotites is inferred to reflect (at least in part) differing degrees of depletion in the mantle caused by differing degrees of partial melting, and equilibration of pyroxene and in some cases garnet, over a range of pressures. Some of the most Cr-rich spinels approach (but do not overlap) the extremely refractory magnesiochromites found in the peridotitic suite of diamond inclusions (Jaques and others, 1984a); however, the magnesiochromites from the West Kimberley lamproites are not as magnesian as the inclusions in diamonds (Fig. 148), or from kimberlites elsewhere.

Chrome diopside: Xenocrysts of chrome diopside are very rare and are clearly distinguished from Cr-rich diopside phenocrysts in the lamproites by their marked difference in Ti content. The xenocryst diopsides have

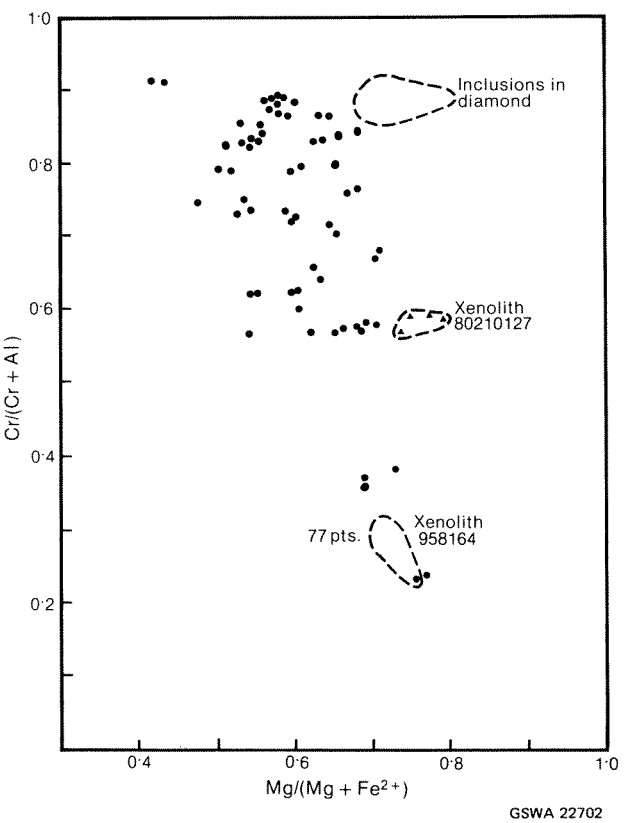


Figure 148. Mg/(Mg + Fe^{2+}) versus Cr/(Cr + Al) variation of West Kimberley xenocryst spinels, and spinels from West Kimberley peridotite nodules 958164 and BMR 80210127.

very low Ti (<0.1% TiO_2), Al (0.2-1.5% Al_2O_3), and Na (<1% Na_2O), and high Cr (up to 1.8% Cr_2O_3) contents (Table 66). They have high Mg/(Mg + Fe) and Ca/(Ca + Mg) ratios, and correspond to Group 5 diopsides of the Stephens and Dawson (1977) classification (Atkinson and others, 1984a; Jaques and others, 1984a). The xenocryst diopsides closely resemble diopside in the diopside-bearing harzburgite xenolith from Ellendale in terms of their very low Al and Na contents and high Mg/(Mg + Fe) ratios (*see* below).

Apart from having lower Al and Na contents the West Kimberley chrome diopsides are similar to diopside in granular lherzolites (*e.g.* Nixon and Boyd, 1973). The compositions suggest equilibration of depleted peridotite at comparatively low temperatures within the garnet or garnet-spinel lherzolite facies (Fig. 149).

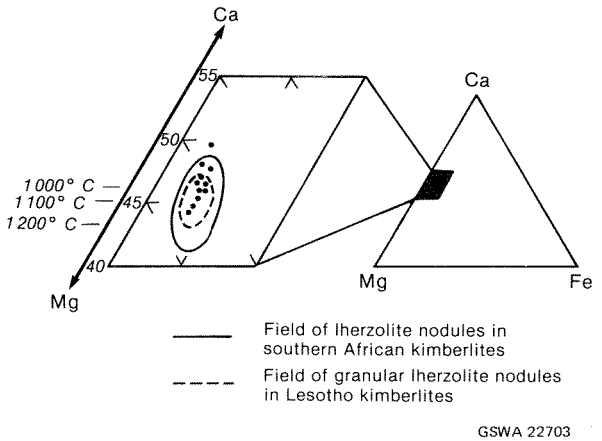


Figure 149. Composition of chrome diopside xenocrysts in West Kimberley lamproites (after Jaques and others, 1984a). Fields of clinopyroxenes from granular lherzolite nodules from Lesotho (Nixon and Boyd, 1973), and lherzolite nodules from southern Africa (McGregor, 1975), are shown by dashed and solid lines. Positions of the enstatite-diopside solvus temperatures taken from the 30 kb data of Mori and Green (1975).

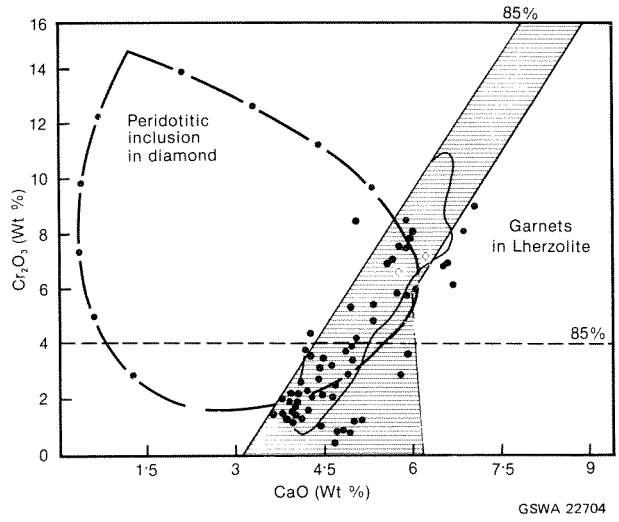


Figure 150. CaO *versus* Cr_2O_3 in Cr-bearing West Kimberley garnets (dots) compared with the field of lherzolitic garnets (Sobolev and others, 1973) shown as hatched area. Field labelled "garnets in lherzolite" refers to calcium-saturated garnets from Finsch peridotites (Shee and others, 1982), and area labelled "peridotitic inclusions in diamond" is from Gurney (1984). The diagonal line designated 85% discriminates Ca-poor (G10) garnets from the Ca-saturated (G9) garnets lying on the Ca-rich side of the line; 85% of garnet inclusions in diamonds are above or to the left of of the two lines marked 85% (Gurney, 1984). Diamond symbols indicate garnets from diamond-bearing peridotites from Finsch (Shee and others, 1982)

Garnet: Xenocrysts of garnet have been recovered from some of the West Kimberley intrusions; but, except in the case of certain of the olivine lamproites, are rare. The garnets range from pyrope to almandine-pyrope composition, corresponding to groups 1, 3, 5 and 9 of the Dawson and Stephens (1975) classification (Atkinson and others, 1984a). The chrome pyropes are poor in Ti, and have moderate to high Ca and Cr contents (Table 66). The West Kimberley Cr-pyropes have Ca and Cr contents which fall, with very few exceptions, within the the range of Ca- saturated pyropes belonging to the lherzolite facies (Fig. 150). As such, they are more Ca-rich than the low-Ca (G10) chrome pyropes typically found in diamonds and in diamond-bearing kimberlites from southern Africa (Boyd and Gurney, 1982; Gurney, 1984). The more Cr-rich of the West Kimberley garnets resemble the Ca- and Cr-rich pyropes found in the more depleted garnet and garnet-chromite lherzolite nodules from Pipe 200, Thaba Putsoa, and Mothae, northern Lesotho, described by Nixon and Boyd (1973b) and Carswell and others (1979). These are also similar to the pyropes reported in concentrates from the Finsch pipe (Gurney and others, 1979) and from two diamond-bearing peridotite xenoliths from the Finsch pipe (Shee and others, 1982).

Enstatite: Enstatite belonging to Group 1 of the Stephens and Dawson (1977) classification occurs rarely in concentrates although it is often more common than chrome diopside xenocrysts, and is also found infrequently in thin sections of olivine lamproite (Atkinson and others, 1984a; Jaques and others, 1984a). These compositions typically have low to moderate Al contents and are very similar to that of the enstatite in the diopside-bearing harzburgite nodule (Table 66).

Rutile: occurs rarely in concentrates as dark-brown to black rounded grains and occasional prisms. The rutiles typically contain $\approx 0.2\%$ Cr_2O_3 and 0.25 to 0.5% Nb_2O_5.

Moissanite: Broken blue grains of moissanite have been found in concentrates from leucite lamproite but are exceptionally rare, as they are in kimberlite (*e.g.* Dawson, 1980).

MANTLE XENOLITHS

Apart from dunite fragments, mantle xenoliths are rare and commonly highly altered. The dunite xenoliths, typically 0.5-2.5 cms across, are common in both magmatic and tuffaceous olivine lamproite. The dunites are typically composed of large (up to 8 mm), strained olivine porphyroclasts together with smaller (30-300 μm) strain-free, polygonal neoblasts of similar composition. Many of the larger, discrete, anhedral, deformed (kink-banded) olivine grains are clearly derived from disaggregated dunite xenoliths.

In addition to the dunite fragments, rare xenoliths, up to 50 cm diameter, of coarse-textured harzburgite that contains little enstatite and chrome-rich spinel, and ocasional chrome diopside and garnet, have been recorded (Atkinson and others, 1984a). These are most abundant in Ellendale 7, where a number of small xenoliths were encountered in drill core. Jaques and others (1984a) reported a diopside-chromite-bearing harzburgite xenolith, approximately 3 cm across, with a coarse texture (average grainsize 3-5 mm) comprising

76% olivine, 20% enstatite, 4% chrome diopside, and a little chromite. Average mineral compositions are given in Table 67. All phases are uniformly magnesian, and have very low Ti contents. The pyroxenes are low in Al and Na, and rich in Cr, as is the magnesiochromite. The pyroxenes resemble the Al-poor, Cr-rich pyroxenes in the granular, garnet-poor peridotites described from Pipe 200, Kao, and Thaba Putsoa (Nixon and Boyd, 1973b; Carswell and others, 1979; MacGregor, 1979). Assuming equilibrium between all phases, nominal equilibration temperatures of ≈880 °C were obtained for coexisting pyroxenes by the Wells (1977) calibration, ≈1 100 °C for coexisting olivine-spinel (Fabries, 1979), and ≈930 °C for orthopyroxene-spinel following Sachtleben and Seck (1981). Equilibration pressures are not known. Equilibration at low temperature is consistent with the coarse (granular) texture (*i.e.* <1 100 °C according to Boyd and Nixon, 1978). The symplectic intergrowth of spinel and chrome diopside is inferred to result from re-equilibration of garnet (and olivine) at lower pressure.

TABLE 67. AVERAGE MINERAL COMPOSITIONS IN HARZBURGITE XENOLITH BMR 80210127, (1-4) AND SPINEL (5) FROM XENOLITH 958164, ELLENDALE 7

	1 *Ol* *[9]*	*2* *Opx* *[7]*	*3* *Cpx* *[4]*	*4* *Sp* *[4]*	*5* *Sp* *[1]*
			Percent		
SiO_2	41.20	57.68	54.69	0.14	nd
TiO_2	—	nd	nd	0.09	nd
Al_2O_3	—	1.41	1.33	22.2	46.08
Cr_2O_3	nd	0.29	0.91	46.52	23.07
Fe_2O_3(a)	—	—	—	4.29	0.70
FeO(a)	7.50	4.71	1.33	9.03	11.07
NiO	0.22	—	—	—	nd
MnO	0.08	0.09	nd	0.82	0.28
MgO	50.90	35.41	17.75	16.70	18.14
CaO	nd	0.41	23.60	0.22	nd
Na_2O	—	—	0.44	—	—
Total	**99.90**	**100.00**	**100.05**	**100.01**	**99.44**
Mg (b)	92.4	93.1	96.0	76.7	74.5

(a) Fe determined as FeO; FeO and Fe_2O_3 calculated from stoichiometry. (b) Mg = 100Mg/(Mg + Fe^{2+}). nd = not detected, <0.05 wt %. (EDS analyses).

Values in parentheses indicate number of grains averaged. 01 = olivine, Opx = orthopyroxene, Cpx = clinopyroxene, Sp = spinel.

CHEMISTRY

Approximately 470 rock samples obtained from outcrop, diamond-drill core and drill cuttings have been analyzed for major and trace elements. Samples included in the database for geochemical comparison are of magmatic material which, from thin section examination, contains little or no accidental country-rock fragments. The majority of the samples exhibit some degree of alteration such as serpentinization of olivine and replacement of leucite, but samples showing secondary silicification, or containing secondary hematite or abundant secondary carbonate or barite, have been excluded from the data base. Comparison of samples, altered as described above, with equivalent unaltered samples that contain primary phases shows that the effects of such alteration are mostly limited to addition of H_2O and, in some cases, CO_2, increase in Fe_2O_3/FeO ratio, small decreases in MgO contents, and (mostly) small variations in abundances of the alkali and alkaline earth metals (particularly Ba and Cs). These differences lead to a greater scatter when the data are plotted on variation diagrams than would be obtained for the unaltered material, but do not obscure the igneous trends and correlations (Jaques and others, 1984a). Statistics (*e.g.* mean compositions) based on the entire database have only slightly higher standard deviations than do those obtained using selected unaltered material, where available.

Analytical methods are described in Appendix 1 and the individual analyses are listed in Appendix 2 (microfiche, in pocket).

MAJOR ELEMENTS

The early analyses of Wade and Prider (1940) and Prider (1960) showed that the leucite lamproites were characterized by extremely high contents of K_2O, TiO_2, ZrO_2, BaO, and F, and very low levels of Na_2O; and it was pointed out that K_2O commonly exceeded Al_2O_3. Jaques and others (1984a) and Atkinson and others (1984a) showed that these chemical features, which are now recognized as charactistic of ultrapotassic rocks in general and the lamproite association in particular, also apply to the newly discovered olivine lamproites, and that the West Kimberley lamproite suite forms a chemical continuum from ultrabasic, peridotitic compositions represented by the olivine lamproites, to the more basic compositions represented by the leucite lamproites.

The West Kimberley lamproites are all characterized by high K_2O contents (2-12%), very low Na_2O contents (typically <0.5%), and very high to extreme K_2O/Na_2O ratios (>10, averaging 30). Contents of K_2O typically exceed Al_2O_3 with the average K_2O/Al_2O_3 ratio for the suite being 1.2±0.15. The perpotassic (mol. K_2O > mol. Al_2O_3) nature of the suite and the presence of potassium metasilicate (ks) in the CIPW norm indicate that the West Kimberley lamproites are extreme members of the ultrapotassic rock series.

Chemical variation within the suite is shown in the weight percent of major-element oxides *versus* weight percent MgO diagrams, because the greatest variation within the suite is in MgO content (Jaques and others, 1984a; Fig. 151). The total range of MgO is from 29% in the most mafic olivine lamproites from the Ellendale pipes (*e.g.* Ellendale No. 9, 11, 4) to less than 5% in the more leucite-rich lamproites, such as found at Prairie Hill East, The Sisters, Noonkanbah Hill, and Mamilu Hill. Compositions range from ultrabasic (38-45% SiO_2) in the olivine lamproites to basic (>50%, up to 60% SiO_2) in the leucite lamproites. The suite as a whole is saturated to oversaturated in silica, ranging from olivine-hypersthene normative compositions in the olivine lamproites to quartz normative in the more felsic of the leucite lamproites. The West Kimberley rocks follow an orenditic differentiation trend of increasing SiO_2 with decreasing MgO content and Mg/(Mg+Fe) ratio (Fig.

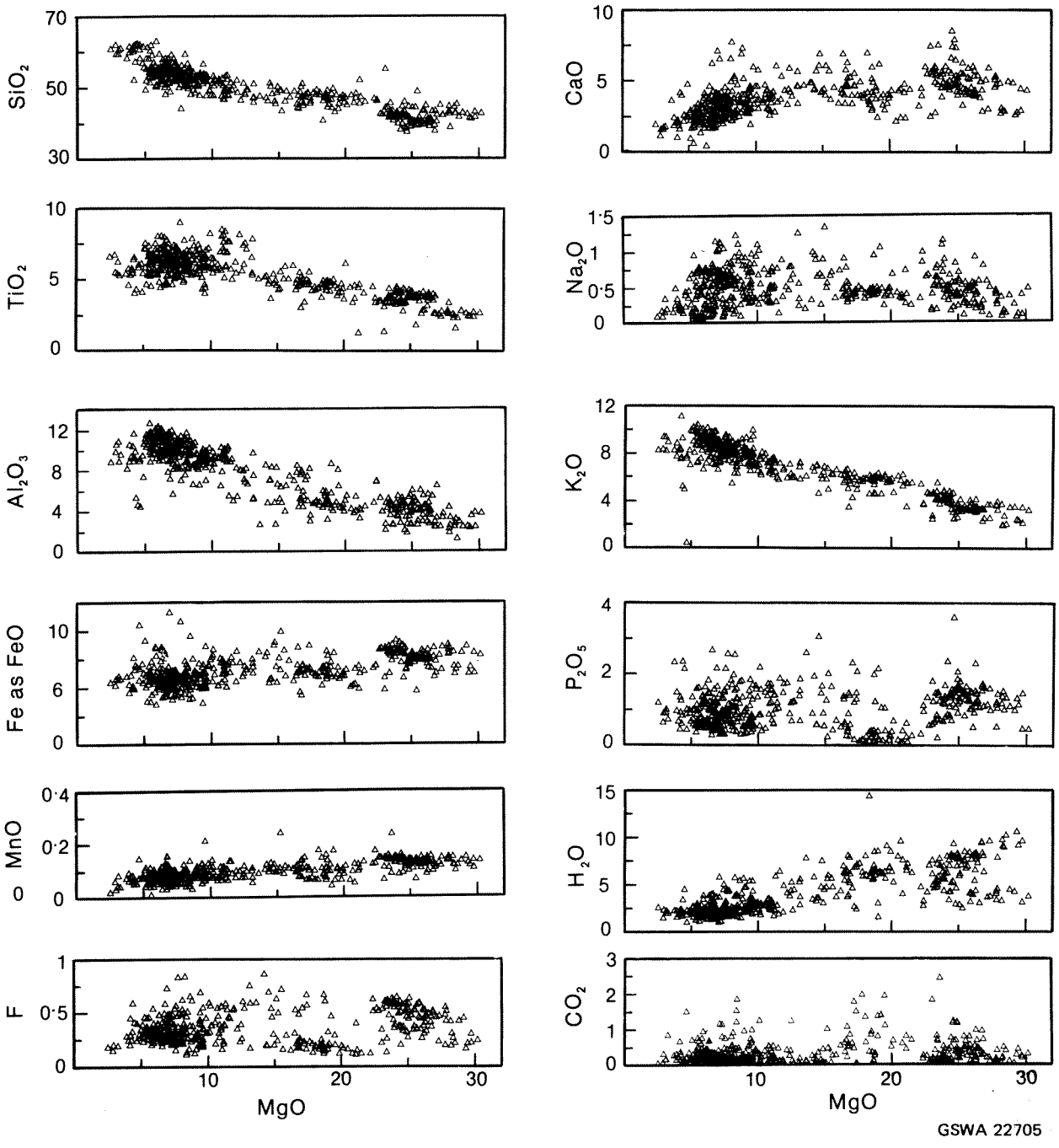


Figure 151. Major element *versus* MgO variation in West Kimberley lamproites. All data except CO_2 and F plotted in weight % on a CO_2- and H_2O^-- free basis.

151). The majority of the West Kimberley rocks have 10% or more of MgO and less than 50% of SiO_2; the mean of 470 samples is 13.9±7.9% MgO and 49.3±5.8% SiO_2. Most of the West Kimberley lamproites have Mg/(Mg+Fe as FeO) ratios greater than 0.65 within a total range of 0.43 to 0.87. These high Mg/(Mg+Fe) values are consistent with either derivation from the mantle, or derivation from the mantle followed by limited crystal fractionation.

The West Kimberley lamproites are characterized by very high contents of TiO_2, K_2O,and P_2O_5, which increase as MgO decreases, except for the most MgO-poor lamproites where TiO_2 decreases. The TiO_2 content ranges from 2.5%, in the most MgO-rich olivine lamproites, to extreme values (up to 12%) in the lamproite pegmatoid dykes and veins in the Walgidee Hills intrusion; most contain between 3 and 7% TiO_2. The K_2O content shows a similar range, from 3% in the most MgO-rich lamproites to 12% in the leucite-rich lamproites of White Rocks, Mamilu Hill, Djada Hill, Oscar Plug, Noonkanbah Hill and Mount Cedric. The P_2O_5 content commonly reaches 2% in the leucite lamproites and locally ranges up to 3% in apatite-rich samples.

Other features of the West Kimberley rocks are their low Al_2O_3 and CaO, and extremely low Na_2O contents (Jaques and others, 1984a; Fig. 151). The range in Al_2O_3 content is from very low values (<4%) in the olivine

lamproites, similar to those found in kimberlites, to ≈10% in the most leucite-rich lamproites: values higher than these result from contamination by country-rock shales. Primary CaO contents in the suite are low compared to kimberlites and other basic to ultrabasic rocks, and show a decrease from low values in the olivine lamproites (4-6%) to very low values (≈2%) in the more fractionated leucite-rich lamproites (Fig. 151). Higher values are found in samples containing secondary carbonate. For example, lamproites at the centre of the Walgidee Hills intrusion, with abundant vein and pervasive carbonate, contain up to 20% CaO and CO_2. Similarly, all or parts of lamproites which intrude the Devonian limestones are also strongly carbonated. For example, some samples from Ellendale 17 are totally carbonated and contain up to 40% CaO. All the West Kimberley lamproites have very low Na_2O contents, less than 1% and, commonly, less than 0.75%. In general, Na_2O contents increase with decreasing MgO (Fig.151); but primary trends are partially obscured by leaching of Na in some surface samples.

Total Fe content in the West Kimberley lamproites is low (typically <8% Fe as FeO) and, like MnO content, decreases with MgO (Fig. 151). Jaques and others (1984a) suggested that this decrease resulted from crystallization and removal of priderite. The ratio of Fe_2O_3/FeO in the West Kimberley rocks is high (0.4-1) and increases with decreasing MgO. This trend may partly reflect greater surficial oxidation because of weathering of the exposed leucite lamproites relative to the oxidation of the unexposed olivine lamproites for which the analyzed samples were taken from drill core. It is, nevertheless, believed to be a primary trend because the chrome spinels (where present) in the leucite lamproites are also more oxidized than those in the olivine lamproites. Volatile contents, mainly H_2O^+, in the lamproites are high and also exhibit a decrease with MgO content (Fig.151). Jaques and others (1984a) pointed out that a feature of the West kimberley rocks was their high F contents (commonly 0.2-0.6%, up to 0.8%) and low CO_2 contents (usually <0.5%, commonly <0.25%).

TRACE ELEMENTS

Jaques and others (1984a) showed that the West kimberley lamproites are characterized by very high to extreme levels of "incompatible" elements, the abundances of which either exceed, or fall at the high end of the range established for kimberlites. Strictly speaking the term "trace element" is often misleading when applied to the West Kimberley lamproites, because elements, such as Ba, which are present in common igneous rocks at trace levels, are present at the weight-percent level. Nevertheless, for convenience, these elements are included with the trace elements in this discussion. The range and variation in trace element abundances in the West Kimberley rocks are summarised on the element (ppm) *versus* MgO (wt.%) variation diagram (Fig. 152).

Barium contents are high to extreme, typically greater than 5 000 ppm, and commonly up to 20 000 ppm with a mean of 10 800 ppm. Large variations are found within individual intrusions and no systematic variation is apparent within the suite. The highest Ba content, 86 260 ppm (9.63% BaO), was found in a sample from Walgidee Hills. Part of the variation could be the result of leaching in weathered surface samples, as both Ba and Sr appear to be depleted in the more weathered samples when these are compared to less weathered equivalents. Barite of probable secondary origin is present in many of the samples with anomalously high Ba.

Rubidium and strontium contents are high and correlate weakly with MgO content (Fig. 152): the average is 500 ppm Rb and 1 300 ppm Sr in the olivine lamproites, and slightly less in the leucite lamproites. The mean values for the suite are 460 ppm Rb and 1 290 ppm Sr. Extreme concentrations of Rb (>1 000 ppm) and Sr (>2 000 ppm) occur in certain samples from 81 Mile Vent, Oscar, Mount Percy, and Mount North. Two separate samples from 81 Mile Vent contain 8 626 and 7 470 ppm Rb respectively. Carbonated samples can contain in excess of 2 000 ppm Sr. The K/Rb ratios are low, but increase from about 70 in the olivine lamproites to about 250 in the leucite lamproites; the values are similar to those reported for kimberlites and other ultrapotassic rocks (Kay and Gast, 1973; Fesq and others, 1975; Wedepohl and Muramatsu, 1979). The Rb/Sr ratios are high, higher than typically found in kimberlites and other alkaline ultrabasic magmas: they average 0.3 to 0.4.

Lithium content is typically less than 20 ppm (mean, 10 ppm), but ranges up to higher values in samples contaminated by country-rock and xenoliths, and in some altered lamproites (*e.g.* Ellendale 2). The West Kimberley rocks also have high abundances of Pb, Th, and U: they typically contain 40 to 60 (mean = 53) ppm Pb, 30 to 60 (mean = 40) ppm Th, and 2 to 8 (mean = 3) ppm U. The highest Pb, Th, and U, values (up to 120 ppm Pb, 100 ppm Th and 12 ppm U) occur in certain samples from Mount North, 81 Mile Vent, Mount Percy, and Ellendale 27 and 12. Extreme Pb (up to 300 ppm) and Th (up to 100 ppm) also occur locally in carbonated samples from Walgidee Hills, and in samples contaminated by country rock inclusions.

Zirconium and niobium contents of the West Kimberley lamproites are also high: Zr ranges from about 600 to 700 ppm in the more mafic olivine lamproites to approximately 1 500 ppm in the Mg-poor, leucite-rich lamproites (Fig. 152) and averages 1 313 ppm for the suite. Higher values (2 000 — 2 500 ppm) occur in some samples from 81 Mile Vent, Mount North, Mount Percy, and in central core of Walgidee Hills, and extreme values (>3 000 ppm) are found in Ti-rich samples from Ellendale 12, 21, and 27, and in the lamproite pegmatoid dykes and veins in the Walgidee Hills intrusion, where an exceptionally Ti-rich sample (12% TiO_2) was found to contain 6 000 ppm Zr.

Unlike Zr,which exhibits a negative correlation with MgO content, Nb shows a weak positive correlation with MgO content (Fig. 152). In general, Nb content

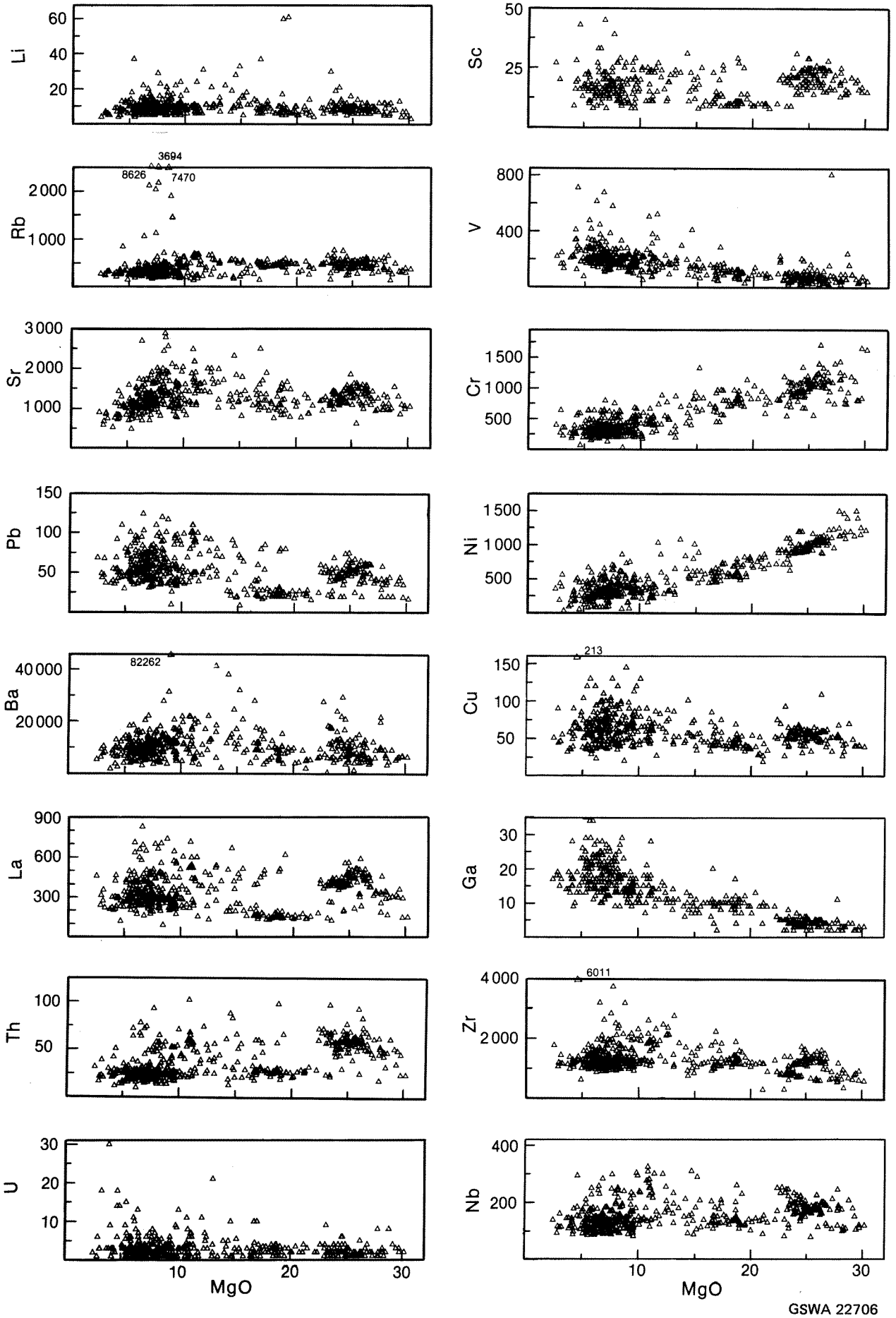


Figure 152. Trace element (ppm) *versus* MgO (wt.%) variation in West Kimberley lamproites.

decreases from around 200 ppm (175-200) in the olivine lamproites to values in the range 100 to 150 ppm in the leucite lamproites: the mean for the suite is 158 ppm. However, many leucite lamproites have Nb contents higher than these, particularly the Zr-rich rocks from Mount North, Mount Percy, 81 Mile Vent, Walgidee Hills and Ellendale 12, 16, 21, and 27: the highest Nb contents (>300 ppm) occur in rocks from 81 Mile Vent. The Zr/Nb ratio increases from about 3 to 4 in the most mafic olivine lamproites to about 10 in the leucite lamproites as a consequence of the decrease in Nb with MgO content which Jaques and others (1984a) attributed to early separation of Nb-rich perovskite.

The West Kimberley lamproites exhibit a wide range in Ni and Cr contents which correlate with MgO content (Fig. 152) and Mg/(Mg+Fe) ratio. The olivine lamproites are characterized by very high Ni and Cr (>1 000 ppm, up to 1 300 ppm Ni and 1 600 ppm Cr) contents, whereas the most Mg-poor leucite lamproites are strongly depleted in Ni (<100 ppm) and to a lesser extent Cr (<200 ppm). Most of the West Kimberley lamproites, however, contain more than 300 ppm and have a mean of 566 ppm Ni and 600 ppm Cr, which is consistent with their high Mg/(Mg+Fe) ratios.

An additional feature of the West Kimberley lamproites is their low Sc and V contents (Jaques and others, 1984a); Sc contents average 18 ppm (range 10-30 ppm), whereas V contents increase from very low values in the olivine lamproites (40-80 ppm) to much higher values (100-300 ppm) in the more Mg-poor leucite lamproites (Fig. 152).

Copper and zinc concentrations are typically low (mostly <100 ppm), and Cu exhibits a negative correlation with MgO. Tin concentrations are also low, mostly less than 20 ppm, typically 5 to 15 ppm. Gallium concentrations are similar or slightly higher than Sn: they range up to 30 ppm in certain leucite lamproites and, like Al, are negatively correlated with MgO (Fig 152).

The West Kimberley lamproites are exceptionally enriched in LREE (500 to 2 000 times chondritic abundances) and have extremely fractionated REE patterns. Abundances of HREE and Y are very low: HREE contents are typically 3 to 6 times chondrites, and Y contents typically lie in the range 10 to 25 ppm, but range up to higher values in strongly fractionated lamproites and samples contaminated by country rocks. The REE patterns in the olivine lamproites and leucite lamproites are similar, differing only in the relative abundance of REE. Typically the leucite-rich lamproites contain greater abundances of REE, although there is considerable overlap (Fig. 153). Such strongly fractionated REE patterns are characteristic of kimberlites (Fesq and others, 1975; Mitchell and Brunfelt, 1975; Frey and others, 1977; Nixon others, 1977; Nixon and others, 1981). Minettes, and other alkaline basic and ultrabasic rocks, also have strongly fractionated REE patterns, but are not enriched in LREE to the same extent as the West Kimberley lamproites; nor do they have much higher abundances of HREE (Kay and Gast, 1973; Bachinski and Scott, 1979; Roden, 1981; Rogers and others, 1982). The West Kimberley lamproites share the low abundances of HREE characteristic of kimberlites, but are even more enriched in LREE (Jaques and others, 1984a).

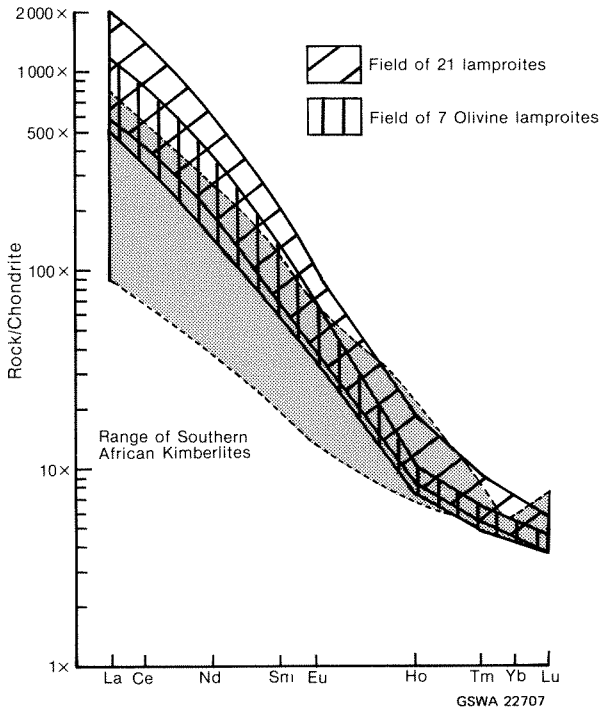


Figure 153. Chondrite-normalized REE diagram, showing REE abundances in West Kimberley lamproites compared to southern African kimberlites (after Jaques and others, 1984a).

ISOTOPIC COMPOSITIONS

Recent studies by McCulloch and others (1983) and Jaques and others (1984b) have confirmed the high initial $^{87}Sr/^{86}Sr$ ratios originally reported for the Fitzroy Lamproites by Powell and Bell (1970), and have demonstrated that the initial $^{87}Sr/^{86}Sr$ ratios of the West Kimberley lamproites range from 0.711 to 0.720. The Rb/Sr ratios and initial $^{87}Sr/^{86}Sr$ ratios of the West Kimberley rocks are amongst the highest reported for mantle-derived ultrabasic and basic rocks. In general, the leucite lamproites are more radiogenic and exhibit a wider range of initial $^{87}Sr/^{86}Sr$ ratios than the olivine lamproites. The broad correlation of Sr isotopic composition and MgO content also extends to diamond content; the pipes with the highest diamond contents have the lowest initial ratios. Jaques and others (1984b) pointed out that only the lamproites from Walgidee Hills overlapped the initial $^{87}Sr/^{86}Sr$ ratios of the olivine lamproites from the Ellendale Field. In addition to the variation in initial $^{87}Sr/^{86}Sr$ observed between adjacent intrusions, there is also variation in Sr isotopic composition within single intrusions. This variation ranges from small differences, as observed in olivine lamproites from Ellendale 4 and 9, to larger differences between similar lamproites types in the Walgidee Hills intrusion (0.71160 and 0.71252), to large differences between olivine lamproite (0.710370) and leucite lamproite (0.71677) observed in Ellendale 7 (McCulloch and others, 1983; Jaques and others, 1984b). The West

Kimberley lamproites have more radiogenic Sr than kimberlites, particularly non-micaceous (Group I) kimberlites (Berg and Allsopp, 1972; Barrett and Berg, 1975; Smith, 1983). Micaceous (Group II) kimberlites are more radiogenic than Group I and have isotopic compositions which range up to (but do not overlap) the least radiogenic of the West Kimberley lamproites.

The West Kimberley lamproites have low $^{143}Nd/^{144}Nd$ ratios (0.5110-0.5112); with ϵ_{Nd} values are in the range -7.4 to -15.4 (McCulloch and others, 1983; Nixon and others, 1984). As with Sr there is a broad correlation between Nd isotopic composition and rock type composition, and diamond content; the leucite lamproites (Mg-poor) have distinctly more negative ϵ_{Nd} values than the diamond-bearing olivine lamproites of Ellendale Field (McCulloch and others, 1983). Differences in Nd isotopic composition are evident within individual pipes of similar rock type, and larger variations are evident in pipes containing both olivine-rich and leucite-rich lamproite (McCulloch and others, 1983). The West Kimberley lamproites have much higher ϵ_{Nd} values than kimberlites: Group 1 kimberlites typically have ϵ_{Nd} values close to 0 ($\epsilon_{Nd} = -1$ to $+4$) whereas ϵ_{Nd} values in Group II kimberlites range up to values which overlap the end of the range of ϵ_{Nd} values exhibited by the Ellendale olivine lamproites, *i.e.* -10 (Basu and Tatsumoto, 1980; Smith, 1983; Basu and others, 1984).

Lead isotopic data on the West Kimberley lamproites has been presented by Nelson and others (1986) who show that the West Kimberley lamproites have low $^{206}Pb/^{204}Pb$ (17.23-17.86) and high $^{207}Pb/^{204}Pb$ (15.69-15.8) ratios. These values differ considerably from values reported for kimberlites (Smith, 1983) and most other basic and ultrabasic rocks: they fall to the left of the "geochron" on a $^{207}Pb/^{204}Pb$ versus $^{206}Pb/^{204}Pb$ diagram.

McCulloch and others (1983) and Jaques and others (1984a) interpreted the Sr and Nd systematics of the West Kimberley lamproites in terms of mixing of depleted and enriched mantle components, and proposed that ancient enrichment events (>1 000 Ma) were required to explain the observed Sr and Nd isotopic compositions. The Pb-Pb isotope correlations displayed by the West Kimberley lamproites are consistent with the mixing of a high $^{207}Pb/^{204}Pb$, low $^{206}Pb/^{204}Pb$ component with more typical mantle Pb, and the modelling of the Pb and Nd isotopic compositions indicates that the sources of the unusual high $^{207}Pb/^{204}Pb$ component cannot have differentiated from the mantle less than about 2.1 Ma ago (Nelson and others, 1986).

CHAPTER 6

THE WANDAGEE PROVINCE (CARNARVON BASIN)

Following reconnaissance stream-sediment sampling and aeromagnetic surveys, sixteen small kimberlite-like diatremes and associated picritic sills and dykes were discovered in 1978 by CRA Exploration P/L in the vicinity of Wandagee Hill, 125 km northeast of the town of Carnarvon, on the Winning Pool and Kennedy Range 1:250 000 map areas (Atkinson and others,1984a; *see* Plate 4). Subsequent exploration by Stockdale Prospecting Ltd has located an additional diatreme and a number of sills and dykes in the same area (Marx, 1984a,b). A total of 22 bodies, 14 diatremes and 8 sills and dykes, are now known from the Wandagee Province.

Physiographically the area is one of very subdued relief; it occupies the floodplain of the Minilya River and its tributaries. Wandagee Hill, about 100 m high and the only major eminence in the area, is formed by a resistant outlier of Permian Kennedy Group sandstones. Much of the region is a well-developed etch plain which has been developed on the fine-grained sediments of the Byro Group by the downcutting and lateral shifting of river courses during Pliocene and Pleistocene times (Hocking and others, in press). Extensive alluvial fans and dunes have developed, primarily in the Late Pleistocene.

The area, with an annual rainfall of about 200 mm, is arid to semi-arid. The vegetation is mostly open hummocky grass and spinifex-covered plains; but there are areas of open acacia scrub and stands of river gums along the main watercourses. Access is good: there is a well-formed gravel road from the North West Coastal Highway to Wandagee pastoral station, and an abundance of station tracks throughout the area. However, only sill M88 and nearby dyke PK4 (Table 68), are exposed in the banks of the Minila River.

REGIONAL GEOLOGY AND STRUCTURAL SETTING

The Carnarvon Basin is a Phanerozoic trough which developed along the margin of the continent to the west of the Proterozoic Gascoyne Province and the Archaean Yilgarn Block. It is infilled with terrestrial and marine clastic sediments. The trough was initiated in the Silurian, during a period of rifting and instability that preceded the separation of the western margin of Australia from the Indian Plate during the Cretaceous (Veevers, 1981).

The basin is divided by the north-trending Wandagee-Yanrey Ridge, a basement horst block which separates the Merlinleigh Sub-basin to the east from the onlapping Gascoyne Sub-basin to the west (Figs. 154,155). The ridge is bounded to the east by the Wandagee Fault System, a series of normal faults with a maximum downthrow to the east of about 4 km in the vicinity of Wandagee Hill (Hocking and others, in press). The western margin of the horst is the Marilla Fault, a smaller, west-block-down normal fault, 15 km west of the Wandagee Fault.

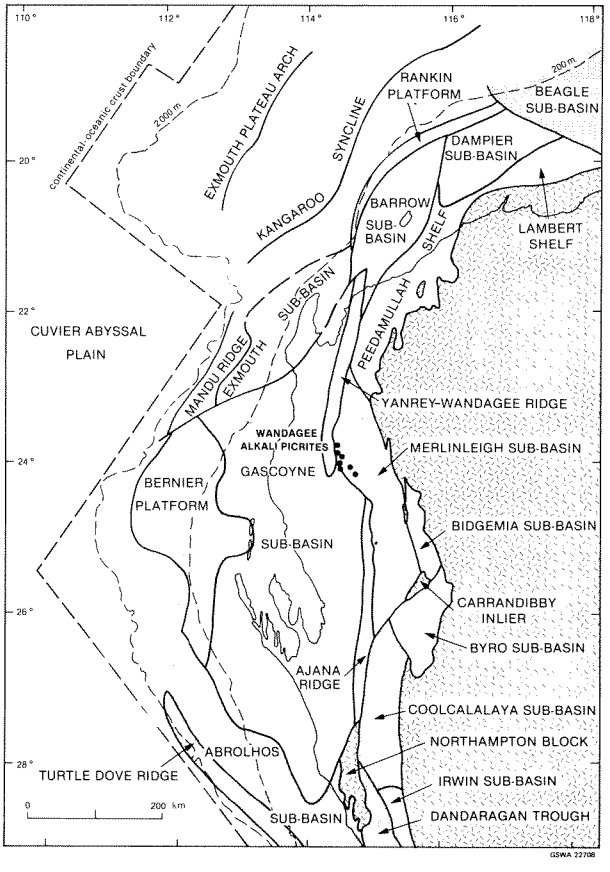


Figure 154. Structural divisions of the Carnarvon Basin (after Hocking and others, in press).

The crystalline basement of the Wandagee Ridge, which cannot be traced south of Hutton Creek (see Plate 4), is covered by 1-2 km of Silurian and Devonian sediments, which are overlain by Late Cretaceous rocks, although at Mia Mia, north of Wandagee, granitic basement was encountered at 153 m in a drill hole (C.J. Gregory, 1982). The Merlinleigh Sub-basin, to the east of the ridge, is a half-graben filled with up to 6 km of

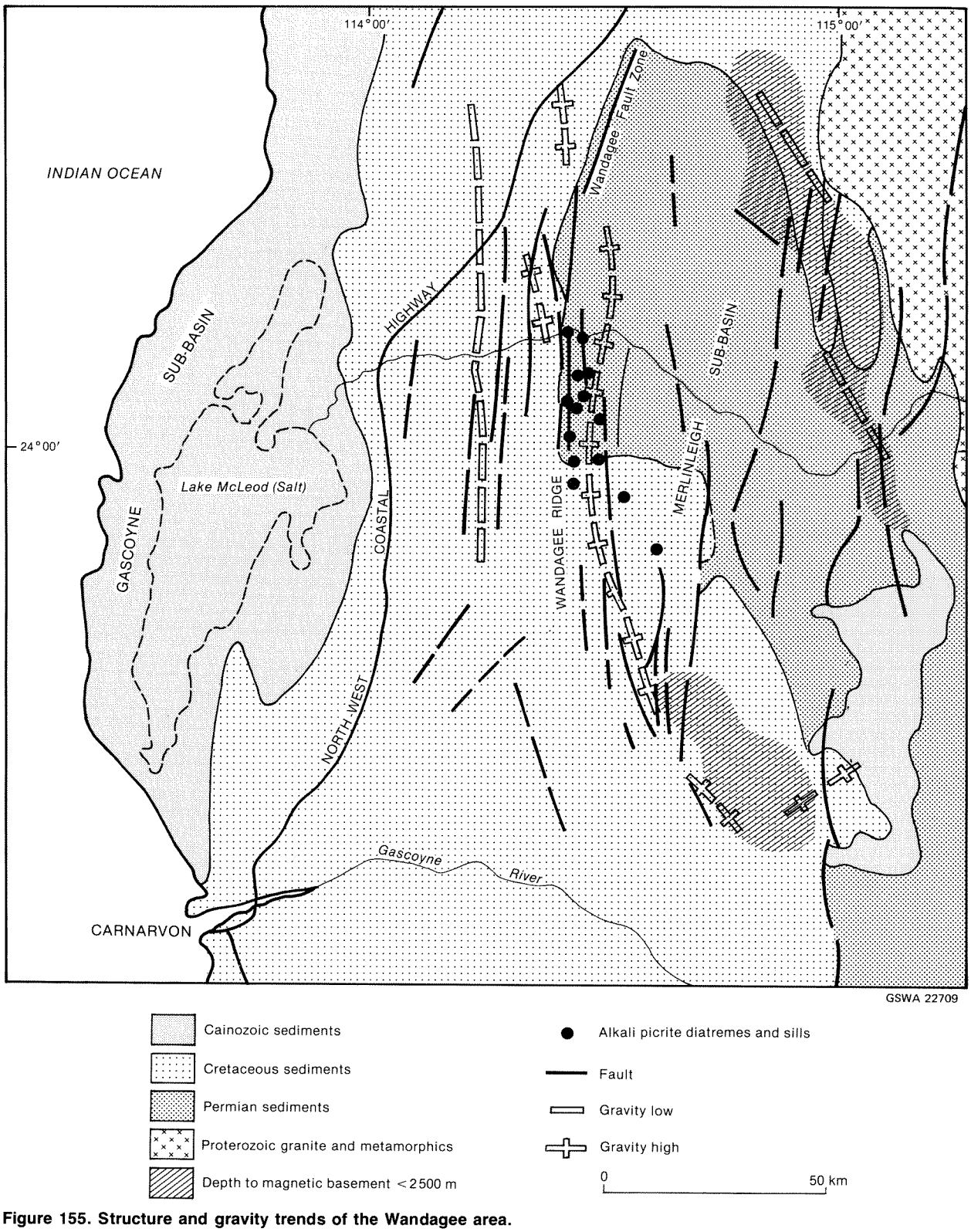


Figure 155. Structure and gravity trends of the Wandagee area.

mainly Permian sediments (Thomas and Smith, 1976; Hocking and others, in press).

Basement to the Carnarvon Basin is not exposed in the Wandagee area, but granulites of 1 054 ± 50 Ma are known in the Northampton Block 500 km south (Compston and Arriens, 1968). This inlier is the southerly extension of the Ajana Ridge, which is similar to the Wandagee-Yanrey Ridge (Fig. 154). To the east of the Carnarvon Basin, the age of formation of the Gascoyne Province is between 2.0 and 2.4 Ga (Fletcher and others, 1983), but there were further igneous events around 1.6 Ga and uplift at about 750-800 Ma (Williams and others, 1978).

The Wandagee diatremes and hypabyssal intrusions are emplaced along the eastern margin of the Wandagee-Yanrey Ridge in a cluster that is elongated north-south, parallel to the trend of the Wandagee Fault System. The main phase of movement on the faults is post-Triassic and pre-Middle Cretaceous, close to the age of emplacement of the diatremes, but there was also some

reverse movement in the Late Tertiary.

Apart from the Wandagee diatremes, igneous activity in the Carnarvon Basin has been minor. Alkaline hypabyssal intrusions were intersected between depths of 354 m and 2 749 m in the Edel 1 offshore petroleum-exploration well. These sills have been described by Le Maitre (1975) as trachytes, nosean phonolites, and "lamprophyres"; and are quite unlike any other alkaline rock in Western Australia. Potassium-argon ages of micas from these rocks range from 241 ± 7 Ma to 261 ± 5 Ma (mid-Triassic to Early Permian); and there is a general increase in age with depth (Ocean Ventures, 1972), indicating that the rocks are considerably older than the Wandagee diatremes. In the offshore Dampier Sub-basin, the Enderby 1 well intersected possible rhyolitic flows interbedded with minor amounts of sandstone between 2 081 m and 2 149 m depth. Palynology indicates a Late Permian-Early Triassic age (Hocking and others, in press).

GEOLOGY OF THE DIATREMES AND INTRUSIVES

The 22 intrusions of the Wandagee Province lie within a belt 50 km long by about 15 km wide. Most of the bodies have been plotted on Plate 4, but information on some was obtained after the map had been compiled. The size and type of each body is given in Table 68: the thirteen diatremes range from less than 1 ha to approximately 14 ha, and the sills and dykes range from 1-15 m thick.

TABLE 68. DETAILS OF WANDAGEE DIATREMES, DYKES, AND SILLS.

Name	*Description of body*	*Size*
M88	Sill	2-4 m thick
M89	Diatreme	3.75 ha
M92B	Diatreme	3.0 ha
M94A	Diatreme	2.4 ha
M94B	Diatreme, 78.5 m Cret. cover	1.0(?) ha
M97	Diatreme	3.0 ha
M98	Diatreme, 89 m Cret. cover	3.0(?) ha
M100B	Sill	15 m thick
M103	Sill, partly exposed	
M104	Sill	3.5 m thick
M105	Sills	1 and 3 m thick
M113A	Diatreme	0.5 ha
M113B WEST	Diatreme	1.5 ha
M113B EAST	Diatreme	3.0 ha
M129	Diatreme, 71 m Cret. cover	2.25(?) ha
M142	Diatreme	0.5 ha
M154	Diatreme, 154 m Cret. cover	14(?) ha
PK1	Diatreme, 1.5 km north of M89	1 ha
PK2	Dyke, 1 km west of M100B	
PK3	Sill	3 m thick
PK4	Dyke, exposed in bank of Minilya River, 500m northwest of M88	1-2m thick
PK5	Small diatreme? associated with PK4	

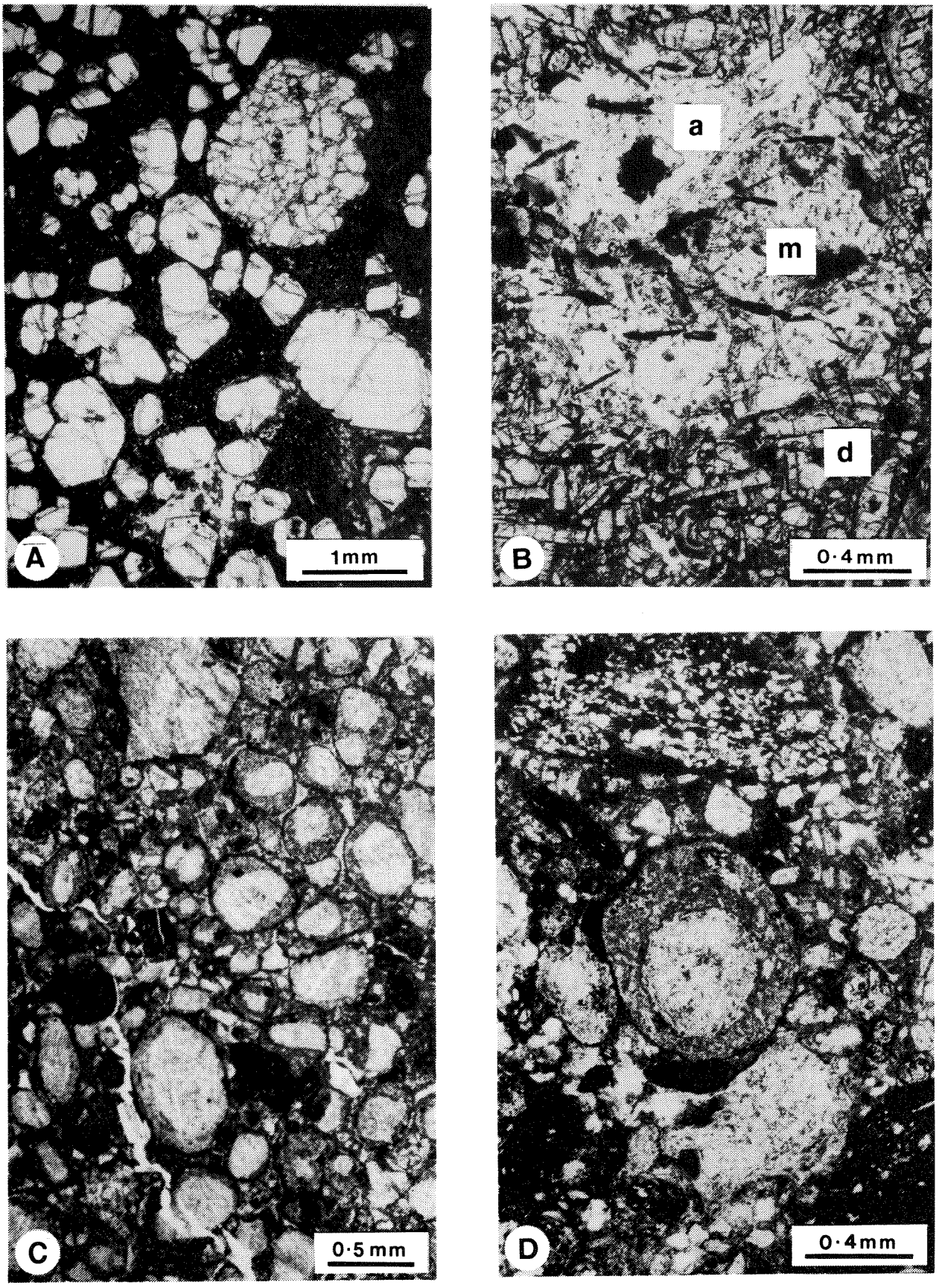
All the Wandagee bodies intrude black shales and siltstones of the Permian (Artinskian) Byro Group. However, four of the diatremes were located by drilling aeromagnetic anomalies and are concealed beneath up to 158 m of Cretaceous (Albian/Aptian) cover of Windalia Radiolarite and grey shale. The remaining bodies are covered at surface by no more that 1-3 m of Recent colluvial silty sheetwash and eluvial soil; one sill, M88, and the dyke PK4, outcrop close to the Minilya River.

The lower Cretaceous age of the overlying rocks was confirmed by palynology (C.J.Gregory, 1981); and a 50 m^3 bulk sample of the Windalia Radiolarite from a quarry near Wandagee Hill produced numerous kimberlitic garnets, ilmenite, and chrome diopside (Joyce and Marx, 1981b), presumably incorporated from the eroded diatremes. Uranium-lead dating of zircon megacrysts from diatreme M142 gave a Jurassic age of 160 ± 10 Ma (Atkinson and others, 1984a; Pidgeon and Smith, in prep.), which is in agreement with the geological evidence for the age of the intrusions.

The sills and dykes are concentrated towards the northern end of the Wandagee cluster and are of uniform, fresh, dense, dark, and porphyritic ultramafic appearance, and contain sparse macrocrysts of olivine up to 1 cm across. Specimens from outcrops of M88, close to the Minilya River, are weathered and extensively veined by carbonate. Drilling at M105 showed that two sills, 1 m and 3 m thick, are present; M104, 500 m to the east-northeast, probably represents the same sill complex. The magnetic anomalies which led to the original discoveries may simply represent places where the undulating sill is nearer the surface, or where the rock is more strongly magnetic. These minor magmatic intrusives are not usually associated directly with diatremes; but ground magnetics over PK4 have been interpreted as showing a northwest-trending dyke, about 700 m long, associated with a small diatreme, PK5, neither of which has been sampled (Marx, 1984b).

The diatremes are steep-sided, pipe-shaped bodies filled with pyroclastic deposits. Where the margins of the diatremes were exposed by trenching, they were sub-vertical, and contact effects were minimal. In contrast to the lamproite pipes of the Kimberley area, the Wandagee diatremes are thought to have been eroded to the pipe zone; no crater facies is present, and bedding in the pyroclastics is very poorly developed or absent (Atkinson and others, 1984a). No magmatic phases have been recognized within the diatremes, except as juvenile clasts in the pyroclastics; and, in contrast to the sills and dykes, the pyroclastics are thoroughly decomposed and friable. The pyroclastics range from lapilli-tuffs to coarse tuff-breccias. In shallow costeans, abundant angular to rounded cobbles of Permian shale and siltstone were readily identified; but it was difficult to determine the nature of the tuffaceous matrix or any juvenile clasts. Veins of gypsum, which are extremely abundant in the shale country rock, also cross-cut the pyroclastics. In drill core, sub-horizontal bedding and imbrication of clasts can occasionally be observed within the tuffs; but the general massive appearance would suggests that some form of mass-flow process has operated during emplacement.

Most of the diatremes have been tested for diamond by costeaning and processing a bulk sample through a



GSWA 22710

Figure 156. Photomicrographs of Wandagee alkali picrites and tuffs: A — Alkali picrite with phenocrysts of olivine and microxenolith of granular-textured dunite (BMR 8321008). B — Segregation vesicle of analcime(a) and mica(m) enclosed by groundmass, with abundant stubby prisms of diopside(d) (BMR 83212012). C — Lapilli-tuff with many small lapilli cored by altered olivine; M94B, ACH 10, 92 m, (GSWA 37921). D — Cored spheroidal lapilli in Wandagee tuff (BMR 83212037).

rotary diamond pan. Large bulk samples of gravel have also been processed from the Minilya River and Barabiddy Creek, which drain the area. However, only three very small diamonds were recovered from this programme — from pipes M92b and M154, and from a loam sample over M142 (Kerr, 1983; Atkinson and others, 1984a). Heavy minerals recovered from this programme are listed in Table 71.

PETROGRAPHY

SILLS AND DYKES

The sills and dykes are petrographically similar; all are dark, porphyritic, magmatic rocks with abundant (typically 30-60%) phenocrysts and microphenocrysts of sub- to euhedral olivine — 0.5 to 1.5 mm, but up to 3 mm across — and rare macrocrysts up to 8 mm. In most samples the olivine has undergone marginal or partial alteration to serpentine; in some sills, *e.g.* M100b, olivine is only preserved in the marginal zones; and, elsewhere, is totally altered to serpentine and calcite. Sparse fragments of country-rock sandstone, siltstone, and shale, and mantle peridotite (dunite), up to 1 cm across, occur in some of the dykes (Fig. 156a). The groundmass contains abundant pale-green diopside microphenocrysts up to 0.5 mm, and seriate to fine lath-like prisms (100 μm or less), which form a felted mass together with abundant subhedral opaques up to 60 μm across and rarely up to 200 μm in coarser grained sills. In sill M88, two generations of diopside are present, small groundmass prisms and microphenocrysts up to 1 mm long. The opaques consist of sub- to euhedral or, in some cases, partly rounded cores of Ti- and Al-rich chromian spinel rimmed by titaniferous magnetite. The interstitial base is mostly cryptocrystalline (formerly glassy) and composed largely of Al-rich serpentine; but, in places, alkali feldspar and/or analcime is discernable. Also present are small needles and prisms of kaersutite, flakes of biotite, skeletal Ti-magnetite and, in coarser grained rocks, needles of apatite.

A feature of the dykes and sills is the variation in groundmass crystallinity and the presence of patches and veinlets, up to 4 mm across, which are largely infilled by calcite, alkali feldspar, analcime, and/or serpentine. The more rounded and regular-shaped of these might represent former vesicles (Atkinson and others, 1984a); but many have irregular shapes and microlitic textures with dendrites of clinopyroxene (including pale mauve-brown titanian salite), kaersutite, mica, and alkali feldspar projecting into them (Fig. 156b). In sill M88, such patches are particularly prominent, and titanian salite and kaersutite form prisms up to 0.5 mm long. Some patches are filled by near-isotropic analcime, probably replacing former glass.

The inclusions typically show extensive alteration, chiefly by serpentine and carbonate. The dunite fragments and olivine macrocrysts show solid-state deformation, *e.g.* kink bands and undulose extinction, and range from coarse-textured types, grain size 3 to 4 mm, to granular types with polygonal, strain-free subgrains approximately 0.03 mm across.

The magmatic dykes and sills at Wandagee exhibit petrographic and mineralogical differences from kimberlite *s.s.* as defined by Clement and others (1984). In particular, the presence of feldspar, analcime, and hornbelende, with the compositional trend of the pyroxenes (to Ti-Al-rich salite) and spinels (to Mg-poor titanomagnetite) distinguish the Wandagee rocks from kimberlite. In terms of their abundance of olivine, and Ti-Al-rich clinopyroxene, they resemble the meimechites and picritic porphyrites of Yakutia; but they differ fom meimechite in terms of the lesser abundance of olivine, and from both meimechite and picritic porphyry in the presence of analcime and feldspar (Frantsesson, 1970; Egorov, 1970). Since the most distinctive feature of these rocks is their picritic nature, the name alkali (analcime) picrite is the most appropriate.

PYROCLASTICS

Pyroclastics from Wandagee diatremes are extensively altered, clast-supported tuffs and lapilli-tuffs that contain clasts, typically 0.5 to 5 mm across, and occasionally larger fragments of country rock up to 5 cm across (Fig. 156c). Juvenile clasts of coarse ash to fine lapilli size predominate; but accidental lithic fragments, typically of pyritic shale, siltstone, and quartz-rich and quartz-poor sandstone, occur in all samples examined and may be locally abundant. Other accidental clasts include limestone, quartzite (metamorphic), and occasional rare altered granitoid (tonalite).

Many of the juvenile fragments are nucleated (Fig. 156d), typically with cores of sub- to euhedral olivine — now altered to serpentine $\pm$ carbonate — surrounded by a thin selvage of very fine grained crystalline to formerly glassy(?) magmatic material that is composed mainly of serpentine and carbonate with sub- to euhedral Ti-rich, Al-Cr spinels up to 100μ, but mostly 20-50 μm across. Many juvenile clasts contain pale phlogopite, typically as groundmass flakes up to 200 μm; but, in a large proportion of clasts the phlogopite occurs as microphenocrysts up to 0.5 mm long, and seriate to the groundmass flakes. Other, less common, juvenile clasts contain abundant former pyroxene prisms up to 250 μm long (in some cases in weakly fluidal texture), now replaced by amphibole. These clasts more closely resemble the magmatic dykes and sills.

In addition to the lithic fragments, most of the tuffs contain a high proportion of crystal fragments, typically serpentinized olivine but also including macrocrystal phlogopite up to 6 mm long. The phlogopite is commonly altered, in part, to green chlorite $\pm$ pyrite, and is weakly pleochroic (X = neutral, Y = Z = pale tan) and similar in colour to the groundmass mica. Many of the large phlogopite grains are deformed and show undulose extinction and kink-bands. Macrocrystal phlogopite forms cores to some of the nucleated lapilli. Also common in some tuffs are quartz grains up to 2 mm across. Many of these have embayed margins, show undulose extinction, and are probably of metamorphic provenance; but some have authigenic overgrowths and

are likely to have been derived from wall-rock sandstones. Many of the tuffs contain a significant proportion of small, angular quartz fragments, <100 μm across, which were probably derived from the siltstone wall rocks; and there are rare examples of spherical, quartz-rich accretionary lapilli up to 3 mm diameter. Smaller grains of feldspar (mostly microcline), rare grains of tourmaline, and even fewer grains of zircon also, occur in the tuffs.

The tuffs are cut by veins of calcite and serpentine up to 0.5 mm wide; and some juvenile clasts have been almost totally replaced by very fine-grained, granular, sparry calcite. In one sample, the sparse interstitial matrix has been largely replaced by calcite.

Although strongly altered, the tuffs display petrographic differences from the magmatic rocks — particularly in the presence of phenocrystal, macrocrystal, and groundmass phlogopite, and in the rarity of groundmass pyroxene. Petrographically the tuffs resemble micaceous kimberlite, but the apparent absence of perovskite suggests that they may not be as silica undersaturated as kimberlite.

MINERALOGY

OLIVINE

Phenocrystal olivines in the magmatic dykes and sills have uniformly magnesian cores, $Mg_{90.2-91.1}$, with high Ni (0.36 - 0.45% NiO) and low Ca ($\leq 0.1\%$ CaO); they show only slight zoning, typically to more Fe-rich (as low as $Mg_{86.8}$) and Ca-rich (up to 0.32% CaO) and Ni-poor (to 0.16% NiO) rims. Some samples, however, show reverse zoning and the more Mg-rich rims are similar to the microphenocryst olivines in the rock. The most Mg-rich of these, $Mg_{91.9}$, is also the most Ni-rich (0.47% NiO) and, like the other rim and groundmass olivines, has a high CaO content (0.17%). Representative analyses are given in Table 69.

CLINOPYROXENE

Groundmass clinopyroxenes in the alkali picrites show a wide range of compositions from diopside cores with low Ti (0.4-0.7% TiO_2), Al (1-2% Al_2O_3), and Na (0.2-0.3% Na_2O), and moderate Cr (up to 1% Cr_2O_3) contents, to rims of Ti- and Al-rich salite (up to 3% TiO_2, 8% Al_2O_3), with higher Na (up to 0.7% Na_2O) and negligible Cr (Table 69). The mauve-brown variolitic pyroxenes in the segregation patches extend to more Ti- and Al-rich salite with up to 5% TiO_2 and 11% Al_2O_3. These pyroxene compositions are distinctly unlike groundmass pyroxenes found in kimberlite (Dawson and others, 1977) which have very low Al, moderately low Ti and Na, and show little variation of Mg and Fe.

SPINELS

Spinels in the picrite dykes and sills show considerble variation in composition; there is extensive Mg-Fe and Cr-Al-Ti-Fe^{3+} substitution (Table 70). The earliest formed spinels, which occur as sub- to euhedral inclusions in olivine (typically 15-40 μm across) and as cores in larger (up to 250 μm) grains in the groundmass, are of titaniferous magnesian chromite (TMC) to titaniferous magnesian aluminous chromite (TMAC) composition. They contain 50% or more Cr_2O_3 (up to 60%), up to 10% Al_2O_3, and about 1% TiO_2, ($Cr/(Cr+Al) \geq 0.75$; $Mg/(Mg+Fe) = 0.45$-0.56). The TMAC and TMC cores are commonly zoned to, and in some cases rimmed by, more Fe- rich chrome spinel — titaniferous chromite (TC) and rare titaniferous aluminous chromite (TAC) — with similar Al and Cr contents to the TMAC and TMC grains but much lower contents of Mg ($<10\%$ MgO) and much higher Fe content ($Mg/(Mg+Fe) < 0.40$). Spinels of TC and rare TAC are common as 5 to 30 μm diameter sub- to euhedral grains in the groundmass where they, like many of the TMC and TMAC grains, are rimmed by titaniferous chromian magnetite (TCM, $<20\%$ Cr_2O_3)

TABLE 69. REPRESENTATIVE ANALYSES OF SILICATE PHASES IN THE WANDAGEE PICRITES

	1	*2*	*3*	*4*	*5*	*6*	*7*	*8*	*9*	*10*
					Percent					
SiO_2	40.87	40.98	40.04	51.27	44.23	44.02	38.77	32.94	51.68	63.48
TiO_2	—	—	—	0.83	3.28	3.61	5.25	5.45	nd	nd
Al_2O_3	—	—	—	2.03	8.37	8.23	14.15	15.74	25.60	20.24
Cr_2O_3	0.08	0.04	0.03	0.60	nd	nd	nd	nd	nd	nd
FeO(a)	8.89	9.58	11.71	4.56	8.22	8.47	11.53	13.53	0.07	0.87
NiO	0.37	0.38	0.15	0.08	nd	nd	nd	nd	nd	nd
MnO	0.15	0.10	0.20	0.11	0.18	0.28	0.15	0.24	nd	nd
MgO	50.10	49.71	47.50	16.28	11.75	11.37	12.29	15.14	nd	nd
CaO	0.09	0.08	0.28	23.85	23.35	23.39	11.86	nd	0.18	0.84
Na_2O	—	—	—	0.25	0.57	0.59	2.15	0.55	12.76	5.14
K_2O	—	—	—	0.00	0.00	0.00	1.18	8.30	0.04	8.87
Total	**100.53**	**100.87**	**99.91**	**99.86**	**99.96**	**99.95**	**97.32**	**91.88**	**90.33**	**99.44**
Mg(b)	90.9	90.2	87.9	86.4	71.8	70.5	65.5	66.6	—	—
					Ratio					
			Ca(c)	0.477	0.506	0.510			Ca(d)	0.041
			Mg(c)	0.452	0.354	0.345			Na(d)	0.449
			Fe(c)	0.071	0.139	0.144			K(d)	0.510

(a) All Fe as FeO. nd = not detected: detection limit = 0.02 wt % except for Ni and Mn (0.04%) (b) Mg = 100 Mg/(Mg + Fe). (c) Ca = Ca/(Ca + Mg + Fe); Fe = Fe/(Ca + Mg + Fe). (d) Ca = Ca/(Ca + Na + K); Na = Na/(Ca + Na + K); K = K/(Ca + Na + K).

1-3 — Olivine, (1) Macrocryst; (2) Phenocryst core; (3) Phenocryst rim; BMR 8321200B. 4-6 — Clinopyroxene; (4) Diopside microphenocryst core; (5) Ti-Al salite rim on microphenocryst; (6) Ti-Al salite microlite in groundmass; BMR 83212002B. 7 — Kaersutite, groundmass; BMR 832121002B. 9 — Analcime, segregation vesicle; BMR 83212001A. 10 — Sanidine, groundmass; BMR 83212001A.

and titaniferous magmatite (TM, <5% Cr_2O_3) containing up to 19% TiO_2.

Spinels in the tuff show a wide range of compositions (Table 70). TMAC with up to 50% Cr_2O_3 and 16% Al_2O_3, (1-3% TiO_2, 10-15% MgO, Mg/(Mg+Fe) = 0.45-0.55, Cr/(Cr+Al) = 60-76), occurs as discrete inclusions in olivine, as cores in larger (up to 80 μm) euhedra in the groundmass, and as rarer sub- to anhedral, fractured macrocrysts (>100 μm). The TMAC cores are typically zoned towards, and rimmed by spinel which contains less Cr and Mg and more Fe and Fe^{3+}, *i.e.* titaniferous aluminous chromite to titaniferous (aluminous) chromian magnetite composition. The TCM rims and smaller groundmass grains contain up to 30% Cr_2O_3 and higher Ti contents (>5% TiO_2, Mg/(Mg+Fe) >0.2) and moderate to high Al (5-8% Al_2O_3). The TCM grains are commonly rimmed by titaniferous magnetite that contains up to 15% TiO_2 and, commonly, appreciable Al, (Mg/(Mg+Fe) <0.2, 4-5% Al_2O_3, <1% Cr_2O_3).

Compared to the magmatic picrites, groundmass spinels in the tuff are more magnesian and aluminous, and do not show the pronounced enrichment in Fe/Mg (*i.e.* very high Fe/(Fe+Mg) ratios) exhibited by the spinels in the picrites. The groundmass spinels in the Wandagee pipes are similar to those in kimberlite, but show a larger range in Fe/(Fe+Mg) compared with kimberlite, where late-crystallizing spinels show extensive solid solution towards magnesian ulvöspinel-magnetite (Haggerty, 1976; Mitchell, 1979).

MICA

Mica is restricted to the groundmass in the picrites where it typically occurs as small flakes of dark brown, strongly pleochroic biotite in or near segregation patches. Compositions (Table 69) are rich in Ti (4-7% TiO_2) and Al, (13-16% Al_2O_3) and have Mg/(Mg+Fe) ratios in the range 0.58-0.68. All have very low Cr but contain significant Na, (0.4-0.6% Na_2O).

Phlogopite occurring as macrocrysts, phenocrysts or microphenocrysts, and in the groundmass of clasts in the tuffs, is of similar composition and distinct from the groundmass mica in the picrites. All have high Al (13-16% Al_2O_3) and moderate Ti contents (1-3% TiO_2) and typically have high Mg/(Mg+Fe) ratios (0.84-0.87). The macrocrysts, which are slightly zoned from more Mg-rich cores to more Fe-rich rims (≈1 mol percent variation), are more Mg-rich and have higher Cr and, typically, lower Na contents (≤0.2% Cr_2O_3, <0.3% Na_2O) than the groundmass and microphenocryst mica, which has very low Cr but higher Na contents. Micas of this composition are typical of kimberlite (*e.g.* Smith and others, 1978; Mitchell, 1979).

OTHER PHASES

Other phases present in the groundmass of the magmatic rock include brown pleochroic kaersutite (Mg/(Mg+Fe^{2+}) ≈65, 5% TiO_2, 12-14% Al_2O_3), apatite (Cl-poor), alkali feldspar (Ab_{40-50} Or_{60-50}), and analcime (Table 69).

XENOCRYST SUITE

The following macrocryst phases have been recovered from heavy-mineral concentrates from the Wandagee intrusions: chromite, diopside, garnet, ilmenite, olivine, mica, rutile, zircon, magnetite, pyrite, apatite, barite, tourmaline, staurolite, andalusitie, monazite, and

TABLE 70. REPRESENTATIVE ANALYSES OF GROUNDMASS SPINELS FROM WANDAGEE PICRITES AND TUFFS

	Picrites			*Tuffs*		
	1	*2*	*3*	*4*	*5*	*6*
			Percent			
SiO_2	0.12	0.31	0.12	0.07	0.06	0.03
TiO_2	1.08	17.73	17.38	3.10	13.63	10.43
Al_2O_3	6.66	3.93	5.37	13.53	6.62	5.34
V_2O_3	0.11	0.39	0.40	0.20	0.20	0.14
Cr_2O_3	58.83	6.75	0.12	44.37	1.65	0.06
FeO(a)	21.33	65.38	70.15	25.33	63.85	68.26
NiO	0.14	0.06	0.04	0.19	0.13	0.04
MnO	0.27	0.83	0.94	0.13	0.45	0.59
MgO	11.13	1.68	1.63	12.78	9.71	9.91
CaO	0.08	0.27	0.23	nd	0.44	0.16
Total	**99.73**	**97.32**	**96.36**	**99.71**	**96.74**	**94.96**
Fe_2O_3(a)	5.15	22.86	28.72	8.93	38.58	47.47
FeO(a)	16.70	44.81	44.31	17.30	29.14	25.55
Total (a)	**100.25**	**99.61**	**99.24**	**100.61**	**100.60**	**99.72**
			Ratio			
Mg (b)	0.543	0.063	0.061	0.568	0.373	0.409
Cr (c)	0.799	0.196	0.003	0.607	0.034	0.001
Al (c)	0.135	0.170	0.226	0.276	0.205	0.150
Fe^{3+} (c)	0.067	0.633	0.771	0.116	0.761	0.849

(a) Fe determined as FeO and Fe_2O_3 calculated from stoichimetry. nd = not detected (<0.02%). (b) Mg = Mg/(Mg + Fe^{2+}). (c) Cr = Cr/(Cr + Al + Fe^{3+}); Al = Al/(Cr + Al + Fe^{3+}); Fe^{3+} = Fe^{3+}/(Cr + Al + Fe^{3+})

Picrites 1 — Titaniferous magnesian aluminous chromite; core. 2 — Titaniferous chromian magnetite; rim. 3 — Groundmass aluminous magnetite. Tuffs 4 — Titaniferous magnesian aluminous chromite; core. 5 — Titaniferous magnesian-magentite; rim. 6 — Titaniferous magnesian megnetite.
(Analyses 1-3: Picrite, BMR 83212002B; 4-6: "Kimberlitic" tuff, Pipe M97, BMR 8421028).

amphibole. Many of these, including some of the zircon grains, are derived from the metamorphic basement, but a number of the zircons have uranium contents typical of kimberlite (Atkinson and others, 1984a). Table 71 summarizes the macrocryst assemblage recovered from individual intrusions and Table 72 gives representative analyses of the phases.

Garnet is predominantly of peridotitic origin, and falls within cluster group 1, 9, or 11, of the garnet classification scheme of Dawson and Stephens (1975). Occasional garnets can be assigned to group 3, the eclogitic suite. With rare exceptions, the Wandagee garnets plot well into the CaO-rich side of Gurney's (1984) 85% line separating the fields of garnets from diamond inclusions and garnets from lherzolite. Representative analyses are given in Table 72.

Chromites were recovered in concentrates from all bodies tested. They contain low to moderate Al (10-13% Al_2O_3) and high Cr (Cr/(Cr+Al) = 0.70-0.77) and comparatively high Mg/(Mg+Fe^{2+}) ratios, typically in the range 0.53 to 0.60. Titanium is comparatively high (1.8-5. 1% TiO_2). Rims are commonly depleted in Cr_2O_3, Al_2O_3, and MgO, and markedly enriched in TiO_2 and Fe_2O_3. The cores of the macrocrysts approach, and in part overlap, the composition of the coarser spinels found in the groundmass of the Wandagee intrusions. The magnetite-rich rims on the macrocrysts are very similar to the titaniferous chromian magnetite rims on groundmass chromites. Spinels of these high Ti contents are atypical of spinel derived from disaggregated mantle peridotite, but are similar to groundmass spinel in kimberlite (Haggerty, 1975).

Olivine macrocrysts are rare in the concentrates. Those found were uniformly magnesian (Mg_{90-92}) and similar to the xenocrystic olivines found in magmatic dykes and sills. These are characterized by low Cr and

TABLE 71. SUMMARY OF MACROCRYST MINERALS RECOVERED IN CONCENTRATES FROM THE WANDAGEE INTRUSIONS.

	Chromite	Diopside	Garnet	Ilmenite	Olivine	Mica	Rutile	Zircon	Magnetite	Barite	Tourmaline	Staurolite	Andalusite	Apatite	Monazite	Sulphide	Amphibole
Sills:																	
M88	*	—	—	—	—	—	—	—	—	—	—	—	—	—	—	—	—
M100B	*	*	*	—	*	—	—	*	—	*	—	*	—	—	—	*	*
M103	*	*	*	—	—	—	—	—	—	—	—	—	—	—	—	—	—
M104/105	No sample available																
Pipes:																	
M89	*	*	*	*	*	*	—	—	*	*	*	*	*	*	—	*	*
M92B	No sample available																
M94A	*	*	*	—	*	—	*	—	*	*	*	*	*	—	—	*	—
M94B	*	*	*	—	—	—	—	—	—	—	—	—	—	—	—	—	—
M97	*	*	*	*	—	*	—	—	—	*	*	*	*	—	—	*	*
M98	*	*	*	—	—	—	—	—	—	—	—	—	—	—	—	—	—
M113A	*	*	*	?	—	—	—	—	—	—	—	—	—	—	—	—	—
M113B east	*	*	*	—	—	—	—	—	—	—	—	—	—	—	—	—	—
M113B west	No sample available																
M129	*	—	*	—	—	—	—	—	—	—	—	—	—	—	—	—	—
M142	*	*	*	—	—	—	—	*	*	—	—	—	—	—	—	—	—
M265	*	*	*	—	—	—	—	—	—	—	—	—	—	—	—	—	—

TABLE 72. REPRESENTATIVE ANALYSES OF XENOCRYST PHASES FROM THE WANDAGEE DIATREMES BY MINERAL, AND INTRUSION NUMBER

	Garnet		*Opx*	*Clinopyroxene*				*Opx*	*Ilmenite*		*Magnetite*		*Spinel*			
	M97	*M97*	*M97*	*M89*	*M89*	*M142*	*M97*	*M97*	*M142*	*M142*	*M97*	*M97*	*M97 Centre*	*M97 Edge*	*M97 Centre*	*M97 Edge*
								Percent								
SiO_2	42.56	42.42	38.30	56.37	55.92	55.32	55.89	58.57	—	0.20	—	—	—	—	—	—
TiO_2	—	0.31	—	—	—	—	—	—	46.50	49.24	4.68	5.74	3.16	3.20	3.29	3.12
Al_2O_3	20.14	19.48	21.86	0.69	0.41	—	—	—	—	—	0.19	0.31	12.49	12.71	12.75	12.57
V_2O_3	—	—	—	—	—	0.33	—	—	—	—	0.59	0.70	0.24	—	0.28	—
Cr_2O_3	3.85	4.76	—	1.35	1.57	1.65	1.08	—	0.23	0.79	—	—	45.89	45.44	45.72	46.21
Fe_2O_3(b)	—	—	—	—	—	—	—	—	15.38	10.93	—	—	12.31	12.61	12.01	11.50
FeO(b)	6.72	6.82	34.07	3.15	3.02	1.82	2.76	4.86	32.46	30.91	92.63	91.15	13.29	12.98	13.22	14.53
NiO	—	—	—	—	—	—	—	—	—	0.27	—	—	—	0.38	—	—
MnO	—	—	0.21	—	—	—	—	—	0.44	0.37	0.19	0.29	—	—	—	—
MgO	21.30	20.75	4.60	19.04	19.07	17.22	18.95	35.68	5.00	7.28	1.75	1.75	13.84	13.95	13.94	13.16
CaO	5.43	5.47	0.94	19.39	19.56	23.65	21.31	0.89	—	—	—	—	—	—	—	—
Na_2O	—	—	—	—	0.47	—	—	—	—	—	—	—	—	—	—	—
Total	**100.00**	**100.01**	**99.98**	**99.99**	**100.02**	**99.99**	**99.99**	**100.01**	**100.00**	**99.99**	**100.03**	**99.94**	**101.02**	**101.27**	**101.21**	**101.09**
Cluster Gp	9	9	—	2	5	2 or 5	2 or 5	1	—	—	—	—	—	—	—	—

(a) Fe_2O_3 calculated from stoichiometry. After Atkinson and others, 1984a. Analyst: A. Benn, CRAE.

Ca (<0.05% CaO) and moderate to high Ni (>0.37% NiO). Olivine also occurs as inclusions within chromites; these range to more Fe-rich compositions (Mg_{86-90}) and contain significant Cr.

Chrome diopside was recovered in concentrates from most of the intrusions examined. Compositions are Al- and Na-poor (<2.5% Al_2O_3, <1% Na_2O) with low Ti (<0.7%, typically <0.5% TiO_2) and variable Cr (up to 2% Cr_2O_3). Calcium oxide contents are high and the clinopyroxenes belong to cluster groups 2 (diopside) and 5 (chrome diopside) of the Stephens and Dawson (1977) classification.

Ilmenite is rare in the concentrates (Table 72). Those recovered have moderate to high MgO contents (7.9-20.3 wt%) and contain significant Cr (up to 1.25% Cr_2O_3).

CHEMISTRY

The alkali picrites of the Wandagee dykes and sills are uniformly magnesian (Table 73), contain 21 to 28% MgO, and are very rich in normative olivine (40-50%). They range from slightly undersaturated (<5% Ne) to barely saturated, and have appreciable normative diopside (up to 20%) and similar normative feldspar contents. Alkali contents are low ($Na_2O + K_2O$ <2.5%) and Na_2O/K_2O ratios show a wide range from less than unity to near 5. Most contain appreciable CO_2, reflecting the abundance of calcite in the rock. All the picrites contain abundant Ni (850-1 200 ppm) and Cr (1 500-2 200 ppm) but have low levels of "incompatible" elements. For example, Ba contents are typically around 600 ppm; Rb contents are mostly less than 40 ppm and Sr contents less than 600 ppm. Zirconium and niobium contents are low (70-110 ppm, and 30-45 ppm respectively) and Zr/Nb ratios very low. The Wandagee alkali picrites have low abundances of REE, and have fractionated patterns with La/Yb ratios of near 40, LREE abundances of approximately 100 to 120 times chondritic abundances, and HREE approximately 3 to 4 times. These abundances and the degree of fractionation are similar to those from kimberlite and similar highly undersaturated rocks (Fesq and others, 1975; Frey and others, 1979).

Chemical characterization of the tuffs is hindered by their fragmental nature and degree of alteration. Analyses of the groundmass in the juvenile clasts by microprobe (using a defocussed beam or raster) gave compositions similar to, although less MgO-rich than, the picrites (*see also* Atkinson and others, 1984a). This suggests that the Wandagee tuffs and the picrites may be closer in terms of their bulk compositions than is suggested by the differences in mineralogy and mineral chemistry.

TABLE 73. REPRESENTATIVE ANALYSES OF WANDAGEE INTRUSIONS

	1	*2*	*3*
	Percent		
SiO_2	39.30	39.83	49.30
TiO_2	1.36	0.96	0.87
Al_2O_3	5.44	6.12	8.70
Fe_2O_3	4.97	5.34	4.15
FeO	5.36	4.67	3.89
MnO	0.19	0.15	0.07
MgO	23.22	27.51	16.10
CaO	10.33	2.13	1.30
Na_2O	0.87	0.71	1.43
K_2O	0.63	0.12	2.70
P_2O_5	0.27	0.25	0.23
H_2O^+	3.77	8.35	(6.30)
H_2O^-	0.93	2.16	4.05
CO_2	2.62	1.19	0.55
Rest	0.77	0.59	0.35
Total	**100.03**	**100.08**	**100.34**
	Parts per million		
Ba	566	323	680
Li	40	64	—
Rb	25	7	120
Sr	618	99	180
Pb	5	5	—
Th	5	5	—
U	1	1	—
Zr	101	84	200
Nb	44	34	55
Y	10	10	15
La	41	35	80
Ce	77	68	110
Nd	25	22	—
Sc	19	17	—
V	253	221	180
Cr	1 918	1 566	670
Ni	917	866	425
Cu	74	62	—
Zn	70	70	—
Ga	10	10	—
As	2	1.5	—
F	2 100	1 700	—

1 — Picrite, dyke, BMR 83212002B. 2 — Picrite, sill M100B, BMR 83212015. 3 — "Kimberlitic" tuff (Atkinson and others, 1984a).

CHAPTER 7

DIAMONDS

The impetus for the growing interest in, and recent research on, lamproites has been the discovery of diamonds associated with these rocks, and the search for economic deposits of this valuable commodity. The presence of diamonds in rocks so radically different from the "classical" kimberlites of southern Africa and elsewhere presents many problems for the genesis of diamond and the characterization of stones from various sources. However, research on the diamonds recovered from the Argyle mine and the Ellendale pipes is at an early stage, and this chapter presents only a preliminary appraisal of the morphology, colour, and mineral inclusions of West Australian diamonds.

ARGYLE DIAMONDS

LAMPROITE DIAMONDS

Diamonds have been won, both from the Argyle lamproite, and from the nearby Lissadell Road dykes. The diamonds from these two sources strongly resemble each other.

The Lissadell Road dykes carry diamond in high grade, probably comparable to the Argyle pipe. The dykes form small stringers and lenses of little strike length and width; they are usually traceable only for a few metres and, hence, are of no commercial interest as there is insufficient lamproite volume available for any kind of mining operation.

The 50 ha Argyle Pipe has an overall surface diamond grade of about 5 CM/t, with a diamond value of US$6.50/CM. The low value is the result of a high content of industrial stones (Table 74). The surface grade varies according to the pipe geology: the "non-sandy" tuff at the northern end of the pipe has a grade of less than 1 CM/t (Atkinson, and others, 1984b). The commercial mining operation is being developed at the rich southern end of the pipe where grades of 6.8 CM/t have been estimated (*see also* Chapter 1).

Hall and Smith (1984) described the morphology of Argyle stones and noted that irregular shapes are dominant, but that lesser amounts of macles and crystal aggregates occur (Fig. 157). Most stones are strongly resorbed dodecahedra or octahedra-dodecahedra combination forms. Cubes have not been seen. The dominant colour of the stones is brown: less than 20% are yellow and colourless (Fig. 158). Green and pink stones occur very rarely, but pink fancies may become a special trading feature of the Argyle production. Most

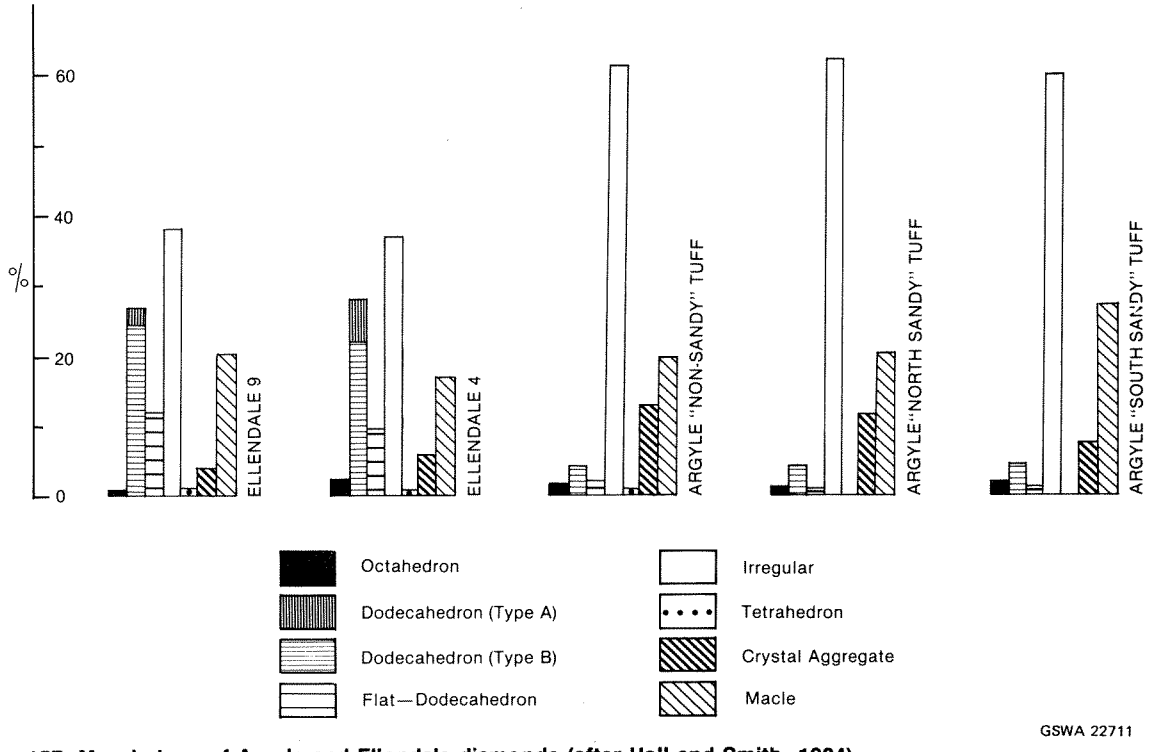


Figure 157. Morphology of Argyle and Ellendale diamonds (after Hall and Smith, 1984).

Argyle stones are heavily frosted and cut by etch channels. Flat-bottomed hexagonal surface depressions are common.

TABLE 74. QUALITY OF ARGYLE DIAMONDS

	Alluvial	*Argyle pipe*
Gem (wt.%)	10	5
Cheap gem (wt.%)	35	40
Industrial (wt.%)	55	55
Total	**100**	**100**
Average value 1982 (US$/CM)	11.00	6.50

Diamonds have been recovered from peridotite xenoliths in the "non-sandy" tuff; they are small, less than 0.4 mm, but occur in grades equivalent to several carats per tonne. These stones are brown, irregularly shaped, unresorbed, octahedral forms, aggregates, and macles. All are strongly frosted and show hexagonal pits. Occasional, similar, strongly frosted planar octahedra have been recorded in the smaller size ranges in concentrates from the Argyle lamproite, particularly from the "non-sandy" tuff.

TABLE 76. REPRESENTATIVE ANALYSES OF OLIVINE INCLUSIONS IN DIAMONDS FROM WESTERN AUSTRALIAN LAMPROITES.

	Ellendale 4		*Ellendale 9*	*Argyle (AK1)*	
	E1214	*E1413*	*E9111*	*A1211*	*A15*
			Percent		
SiO_2	40.06	40.19	40.47	40.38	40.63
FeO	9.02	7.47	7.22	9.08	6.98
MgO	50.92	52.34	52.31	50.54	52.39
Total	**100.00**	**100.00**	**100.00**	**100.00**	**100.00**

After Hall and Smith, 1984.
EDS analyses by SEM (Analyst A. Benn).

TABLE 75. SYNGENETIC MINERAL INCLUSIONS FROM ARGYLE (AK1) LAMPROITE DIAMONDS.

Geological subdivision within pipe	*Diamond reference number*	*Ultramafic suite olivine (no.)*	*Eclogetic suite*		
			Cpx (no.)	*Gar (no.)*	*Ky (no.)*
"Non-sandy" tuff	A1	—	—	1	—
Alluvials	A2	—	—	2	—
Alluvials	A3	—	1	1	—
Alluvials	A4	—	—	1	P
Alluvials	A5	—	—	1	—
Alluvials	A6	—	—	4	—
Alluvials	A7	—	—	1	—
Alluvials	A8	—	—	1	—
"Non-sandy" tuff	A9	—	—	4	—
"South sandy" tuff	A10	—	—	11	—
"South sandy" tuff	A12	1	1	2	—
"Non-sandy" tuff	A13	—	—	4	—
"Non-sandy" tuff	A14	—	—	2	2
"Non sandy" tuff	A15	—	—	—	—

Cpx = clinopyroxene. Gar = garnet. Ky = kyanite. After Hall and Smith, 1984.

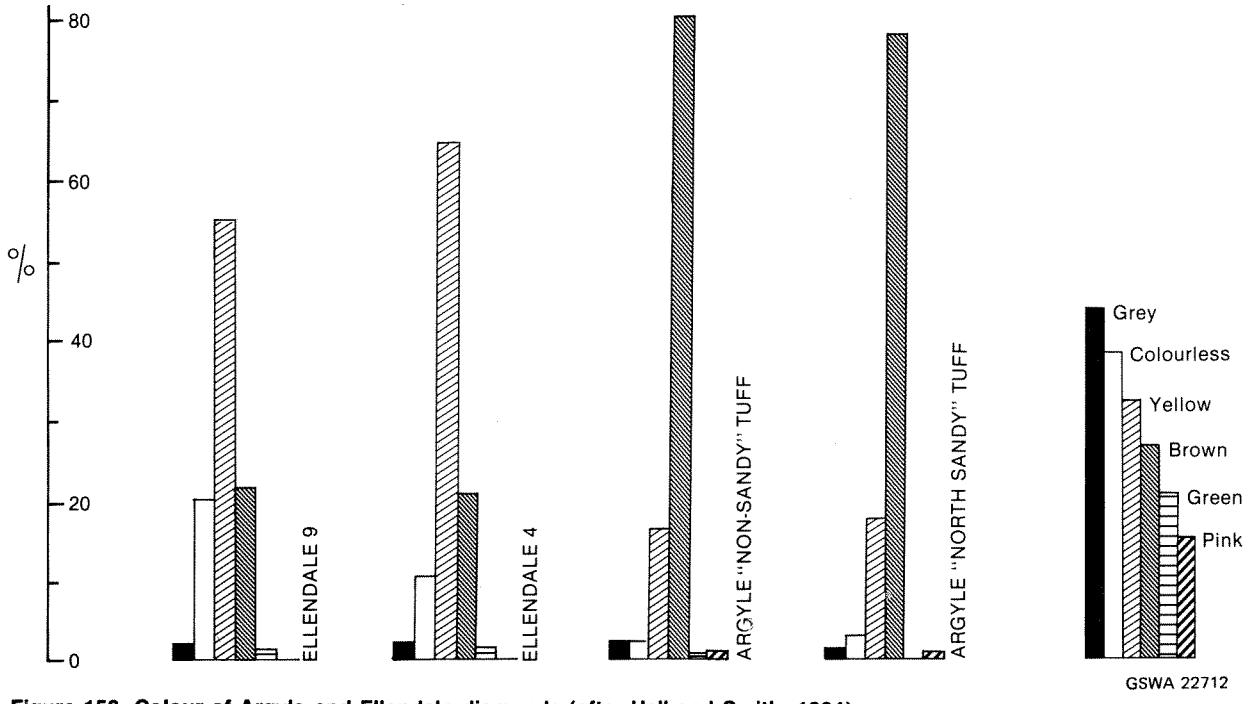
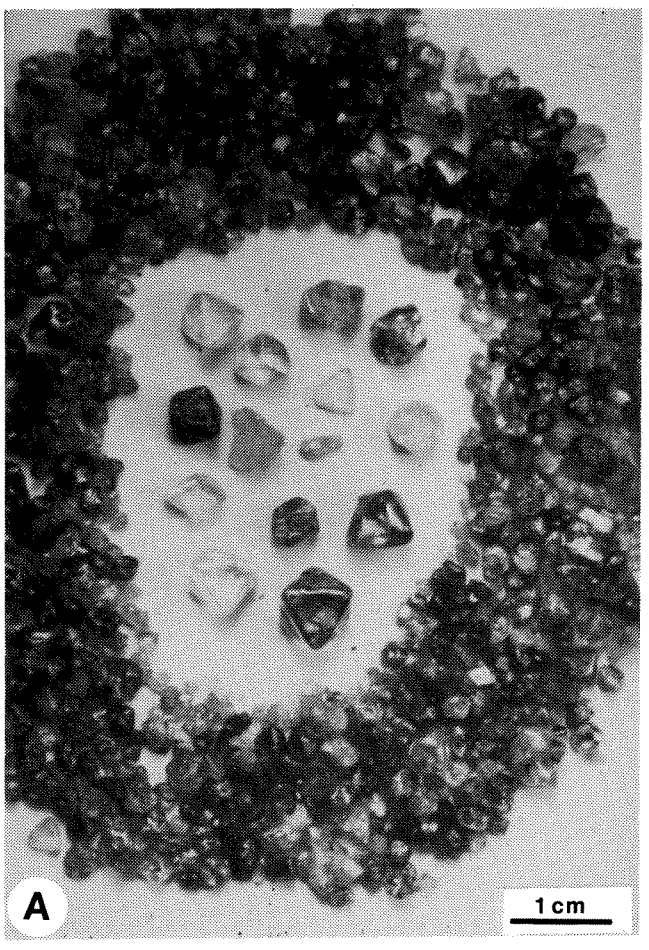
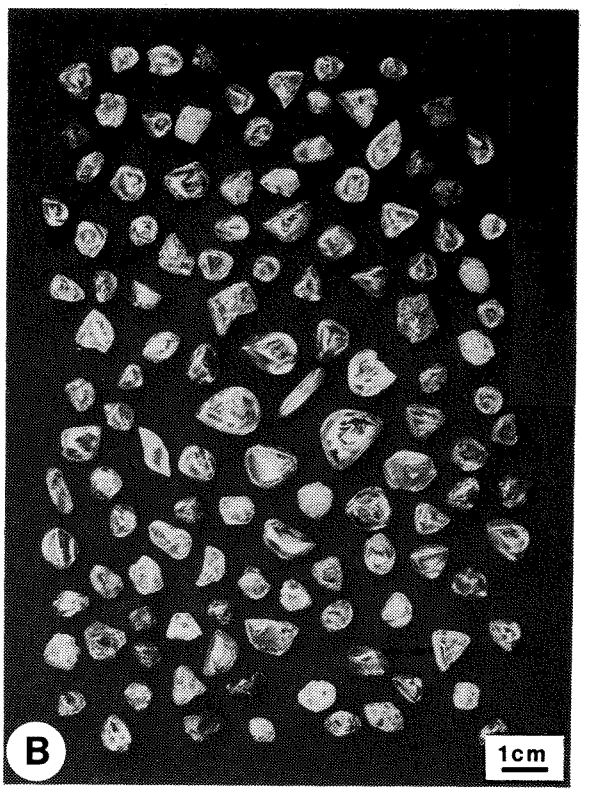
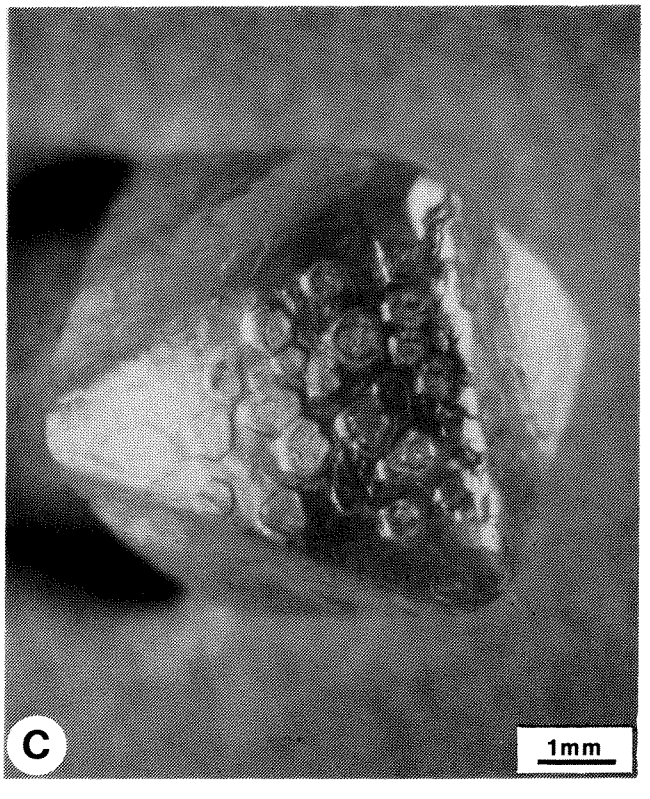
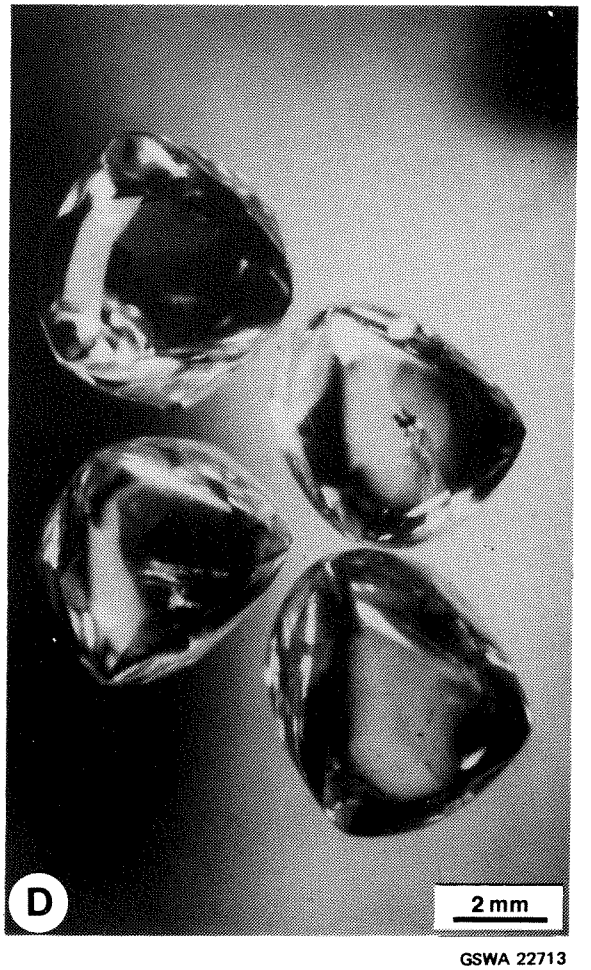


Figure 158. Colour of Argyle and Ellendale diamonds (after Hall and Smith, 1984).









GSWA 22713

Figure 159. Photographs of Argyle and Ellendale diamonds: A — General assortment of Argyle stones, with selected larger stones. B — Selection of typical + 1 CM stones from Ellendale 9. C — 1.5 CM octahedron, with characteristic hexagonal surface pits; Argyle. D — Typical shiny-surfaced dodecahedra from Ellendale (Photos: CRAE).

Graphite spots form the most common mineral inclusion in Argyle diamonds. Syngenetic mineral inclusions reported by Hall and Smith (1984) are given in Table 75, and representative analyses in Tables 76-79. The eclogitic suite of minerals is overwhelmingly dominant, and almandine-pyrope garnets with high Na_2O contents (up to 0.52%) predominate. The associated omphacitic diopsides contain up to 1.07% K_2O. Kyanite has also been reported, and more recently rutile and coesite have been identified. Potash feldspar inclusions have also been found, but it is uncertain whether they are of syngenetic or, more likely, of epigenetic paragenesis.

TABLE 77. REPRESENTATIVE ANALYSES OF PYROXENE INCLUSIONS IN DIAMONDS FROM WESTERN AUSTRALIAN LAMPROITES.

	Ellendale 4			*Ellendale 9*	*Argyle (AK1)*	
	Cpx	*Cpx*	*Opx*	*Cpx*	*Cpx*	*Cpx*
	E1111	*E1414*	*E1418*	*E9111*	*A1214*	*A1316*
	Percent					
SiO_2	55.48	55.72	57.85	54.35	55.86	55.91
TiO_2	0.34	0.15	nd	0.55	0.55	0.47
Al_2O_3	3.86	0.44	0.39	13.52	12.86	12.64
Cr_2O_3	nd	1.05	nd	0.08	nd	nd
FeO	6.27	2.15	4.37	1.82	4.54	2.45
NiO	nd	nd	nd	0.04	nd	nd
MnO	nd	nd	nd	0.03	nd	nd
MgO	15.17	18.97	36.96	8.77	6.90	8.56
CaO	16.67	20.26	0.35	13.50	10.63	12.29
K_2O	0.14	nd	nd	0.77	0.88	1.07
Na_2O	2.07	1.26	0.08	4.92	7.78	6.60
Total	**100.00**	**100.00**	**100.00**	**98.35**	**100.00**	**100.00**

nd = below limit of detection. A1214: EDS analysis by SEM (Analyst A. Benn). E1111, E1414, E1418: EDS analyses by SEM except for Na_2O and Al_2O_3 determined by WDS analysis by electron microprobe (Analyst A. Benn). E9111: WDS analysis by electron microprobe (Analyst A.L. Jaques). After Hall and Smith, 1984.

ALLUVIAL DIAMONDS

Erosion of diamonds from the Argyle Pipe has given rise to the adjacent alluvial diamond deposits of Smoke and Limestone Creeks. At Smoke Creek, the diamonds are found in gravels, both within the modern drainage channel and associated flood plain, and within nearby higher level gravel terraces. At Limestone Creek, the deposits again consist of gravels within the modern drainage channel plus an older duricrusted alluvial fan (Meakins, 1983; Atkinson and others, 1984b).

The alluvial deposits at both creeks have been rapidly deposited during flash-flood conditions and have not been upgraded by the reworking and chemical weathering that characterizes many tropical alluvial diamond deposits, such as the Birim Placer in Ghana (Hall and others, 1985) and those in Sierra Leone (Thomas and others, 1985). As a result, the grades of the deposits in proximity to the pipe (*see also* Chapter 1, Table 4, for grades) are similar to that of the Argyle Pipe, *i.e.* reserve figures range from 3.0 to 4.6 CM/t compared to the approximate overall grade of 5 CM/t for the Argyle lamproite. The quality of diamonds in the alluvials is somewhat higher than that of the pipe diamonds through elimination of some of the more cracked, etched, and friable stones, by wear and tear during transportation. The average value of alluvial stones was estimated in 1980 as US$11.00 compared to US$6.50 for the pipe stones (Table 74).

TABLE 79. REPRESENTATIVE ANALYSES OF CHROMITE, KYANITE AND RUTILE INCLUSIONS IN DIAMONDS FROM WESTERN AUSTRALIAN LAMPROITES.

	Ellendale 4	*Argyle (AK1)*	*Ellendale 9*
	Chromite	*Kyanite*	*Rutile*
	E15	*A1318*	*E919*
	Percent		
SiO_2	nd	36.84	nd
TiO_2	0.31	nd	99.00
Al_2O_3	8.13	63.16	nd
Cr_2O_3	61.01	nd	0.65
Fe_2O_3	4.98	—	—
FeO	10.43	nd	0.35
MnO	nd	nd	nd
MgO	15.13	nd	nd
Total	**100.00**	**100.00**	**100.00**

nd = below limit of detection. EDS analyses by SEM, Fe_2O_3 content in chromite estimated from stoichiometry (Analyst A. Benn). After Hall and Smith, 1984.

TABLE 78. REPRESENTATIVE ANALYSES OF GARNET INCLUSIONS IN DIAMONDS FROM WESTERN AUSTRALIAN LAMPROITES BY LAMPROITE.

	Ellendale 4			*Ellendale 9*		*Argyle (AK1)*					
	E2I1	*E3I1*	*E13I2*	*E9I18*	*E10I1*	*A6I1*	*A8I1*	*A9*	*A12I6*	*A13I4*	*A14I1*
	Percent										
P_2O_5	0.01	0.04	0.02	0.12	0.02	0.13	0.20	0.08	0.32	0.07	0.24
SiO_2	40.50	40.80	42.18	40.90	39.63	40.04	40.76	41.10	39.51	40.43	40.64
TiO_2	0.24	0.29	0.04	0.54	0.47	0.89	0.43	0.11	0.94	0.79	0.78
Al_2O_3	23.50	23.71	18.42	23.35	22.86	22.24	22.88	23.50	21.77	22.66	21.63
V_2O_3	nd	nd	nd	nd	nd	nd	nd	nd	nd	nd	nd
Cr_2O_3	nd	nd	6.84	0.09	nd	nd	0.06	nd	nd	nd	nd
FeO	14.22	11.86	5.36	9.05	15.71	16.67	9.60	9.12	17.61	12.10	14.25
MnO	nd	nd	nd	0.18	nd	nd	0.19	nd	nd	nd	nd
MgO	15.25	15.03	24.32	12.89	8.76	13.32	12.10	11.98	7.63	11.88	13.56
CaO	6.19	8.12	2.76	13.09	12.40	6.49	13.20	13.87	11.82	11.60	8.38
Na_2O	0.08	0.14	0.06	0.18	0.14	0.23	0.30	0.23	0.25	0.48	0.52
Total	**100.00**	**100.00**	**100.00**	**100.38**	**100.00**	**100.00**	**99.74**	**100.00**	**100.00**	**100.00**	**100.00**

nd = below limit of detection. All analyses except E9I18 and A8I1: EDS analyses by SEM, except for P_2O_5, TiO_2 and Na_2O determined by WDS analyses by electron microprobe (Analyst A. Benn). Analyses E9I18 and A8I1: WDS analyses by electron microprobe (Analyst A.L. Jaques). After Hall and Smith, 1984.

Further downstream from Argyle, the grades of alluvials steadily fall away because of dilution from non-diamond-bearing tributary streams. Grades of less than 1 CM/t are the norm at the lower end of Smoke and Limestone Creeks (*see* Chapter 1, Table 8).

Below the confluences of Smoke Creek and Limestone Creek with Lake Argyle, occasional diamonds have been recorded from Ord River gravels as far downstream as the Argyle Dam and Buttons Gap at 80 km and 150 km downstream from the Argyle pipe respectively (Table 7). These stones have the distinctive morphological appearance of Argyle diamonds, and their original source seems likely to be the Argyle Pipe — with, perhaps, a small contribution from the Lissadell Road dykes, drainage from which also runs into the Ord River system.

WEST KIMBERLEY DIAMONDS

Diamonds are widely distributed throughout the West Kimberley lamproite province. They have been recorded from 30 lamproites in the Ellendale Field (Fig. 6) and a further 15 bodies throughout the province (Table 2). Occasional stones occur in the adjacent river systems. All these stones have similar characteristics — with the exception of those reported by Transoil/Exoil from the Lennard River, and described below.

LAMPROITE DIAMONDS

Lamproites from which diamond has been recovered are listed in Fig. 6 and Table 2. In almost every case, only the occasional stone has been recovered from treatment of very large tonnages of lamproite during exploration work; or microdiamonds, usually less than 1 mm across, have been recovered from HF digestion of drill spoil. Only at Ellendale (Atkinson, and others, 1984a; Hall and Smith, 1984) have diamond grades approaching economic levels been reported. Ellendale pipes 4, 7, 9 and 11, all contain a variety of tuffs and lapilli-tuffs with grades of 1 CM/100 t or better, and the higher grade tuffs of pipes 4 and 9 average 14 CM/100 t and 5 CM/100 t respectively. However, even with a value of US$100/CM, the Ellendale deposits are not currently considered economically viable. The most diamondiferous lamproites are rich in olivine and poor in leucite (Fig. 2); they also tend to be large, rather than small, pipes. At any given pipe, the early pyroclastic phase is more diamondiferous than the later magmatic phase.

The West Kimberley lamproite diamonds have a distinctive morphological appearance (Hall and Smith, 1984). In the commercial size range, the stones are typically resorbed, rounded, dodecahedral, yellow, very shiny, smooth-surfaced forms (Fig. 159). With steady increase in size the dodecahedra become increasingly more strongly curved about the long axis of the dodecahedron until the form starts to take on the shape of an octahedron, even though it has no octahedral faces. Below 1 mm size, the dominant crystal form is a planar, step-layered, frosted, unresorbed octahedron, usually colourless or pale brown.

Of some 100 000 diamonds recovered at Ellendale during prospecting operations, only 3 stones exceeded 6 CM in weight: the largest was 6.47 CM from pipe Ellendale 9.

Hall and Smith (1984) report on the extraction of syngenetic mineral inclusions from diamonds from pipes Ellendale 4 and 9 (Table 80). The table divides the mineral inclusion species present into ultramafic and eclogitic suites as defined by Meyer and Boyd (1968, 1972). From this initial work, the two suites appear to be present in roughly equal proportions in these two pipes. Analyses of the mineral inclusions are given in Tables 76-79. The ultramafic suite inclusions are dominated by olivine (Fo_{91-93}), but diopside, enstatite and high-chrome, low-calcium garnet (Group 10 garnets under the classification of Dawson and Stephens, 1975) also occur. Almandine-pyrope garnets are common in

TABLE 80. SYNGENETIC MINERAL INCLUSIONS FROM ELLENDALE OLIVINE-LAMPROITE DIAMONDS.

Diamond	*Ultramafic suite*					*Eclogitic suite*			
Ref. No.	*Ol*	*Cpx*	*Opx*	*Gar*	*Chr*	*Cpx*	*Gar*	*Rut*	*Coes*
Pipe 4:									
E1	—	—	—	—	—	—	2	—	—
E2	—	—	—	—	—	—	1	—	—
E3	—	—	—	—	—	—	5	—	—
E7	2	—	—	—	—	—	—	—	—
E11	—	—	—	—	—	4	—	—	—
E12	4	—	—	—	—	—	—	—	—
E13	—	—	—	2	—	—	—	—	—
E14	7	3	1	—	—	—	—	—	—
Pipe 9:									
E4	4	—	—	—	—	—	—	—	—
E5	1	—	—	—	—	—	—	—	—
E6	1	—	—	—	—	—	—	—	—
E9	—	—	—	—	—	3	31	4	3
E10	—	—	—	—	—	—	1	—	—
E15	—	—	—	—	1	—	—	—	—

Ol = olivine. Cpx = clinopyroxene. Opx = orthopyroxene. Gar = garnet. Chr = chromite. Rut = rutile. Coes = coesite. After Hall & Smith, 1984.

the eclogitic suite and are associated with clinopyroxene, rutile and coesite.

ALLUVIAL DIAMONDS

Drainages leading away from the known diamondiferous lamproite pipes carry only occasional diamonds. These stones are a rarity, except in the immediate vicinity of the pipes. Such stones have been recorded in Pidgeon Creek, downstream from the Big Spring Pipes, and in the small creek which drains Ellendale 4 and flows north past Mount Percy. All these alluvial stones (with the exception of the Lennard River occurrence described below) show the characteristics of the West Kimberley lamproite diamonds. Stones of this kind have not been recorded from the Lennard River; no diamonds have been reported from the Fitzroy River. The lack of development of alluvial diamond deposits is no doubt a response to the preservation of the crater-facies of the West Kimberley lamproites. The lamproites have been emplaced within a syneclisal or basinal areas subjected to minimal erosion.

As suggested by Gold (1984), it is unlikely that many alluvial diamonds in syneclisal areas would be eroded from subjacent pipes; and, if diamonds are found in such areas, their provenance may be from distant, more heavily eroded anticlisal regions. The occurrence of diamonds reported by Transoil/Exoil from the Lennard River may be of this ilk. Nine stones totalling 1.65 CM were recovered from about 1 t of alluvial gravel. Haynes (1971) describes two of these stones as cube-octahedra combination forms, and another two are described as octahedra. AMDEL (1970) describe the usual form as striated octahedra, and state that, with one exception, a smokey-coloured stone, they are colourless to white. No cubes or cube-combination forms have been recorded from the Ellendale lamproite diamonds. In the size range of the Transoil/Exoil stones (mean size 0.18 CM), less than 1% of Ellendale stones would be octahedral. Of the Ellendale stones 50-70% are yellow and only 10-16% are colourless (white). Not one of the nine Transoil/Exoil stones is described as yellow. This evidence supports the conclusion of Haynes (1971) that the stones from the Lennard River occurrence are not representative of the surrounding area.

KIMBERLEY PLATEAU DIAMONDS

The archives of the Benedictine Mission at Kalumburu (near the North Kimberley coast) record the claim of a prospector to have discovered diamonds nearby in the Prince Frederick Ranges (and also near Mount Hann in the West Kimberley). Recent exploration by the Ashton Exploration Joint Venture and others has failed to detect the presence of diamonds in the Prince Frederick Ranges. However, diamonds in the North Kimberley were found at Pteropus Creek by the Kalumburu Joint Venture in 1973 and subsequently in the King George River.

In 1976 the Ashton Joint Venture processed 22 m^3 of alluvial gravels from the Morelli's Fox site on the King George River and recovered 242 stones totalling 11.08 CM. The site was named after Dr Bruno Morelli, a director of Sibeka, whose encouragement of the Joint Venture never to lose sight of the diamonds it had found was made memorable by his use of the well known French proverb, *"quand vous avez le renard par le queue, ne le lachez pas!"* (when you have the fox by the tail, never let him go!). However, the fox's lair still remains to be found: exploration by many companies during the late seventies and 1980's has shown that occasional similar diamonds are spread widely across the northeast and central parts of the Kimberley Plateau; and the Fox site appears to be just a good trap for alluvial concentration of the stones. The location of their primary kimberlitic source is still to be discovered.

Diamonds from the Kimberley Plateau show a family resemblance. They are generally small, less than 1 CM. The mean stone size at Morelli's Fox site was 0.05 CM. They are predominantly colourless to pale brown, often with green or brown surface spots, have fewer inclusions, and are generally of a better quality than Argyle stones. Irregular shapes predominate, but good crystal forms are common. Octahedra, dodecahedra, and macles, occur in about equal proportions. The planar octahedra show pronounced step layering and light to no frosting; the dodecahedra often have characteristic, coarse, roll-like relief. There is a minor content of "Argyle-type" stones — rounded, brown, frosted dodecahedra with hexagonal surface depressions. There are occurrences of cubes, a form which has not been recorded from the West Kimberley (except for the Transoil/Exoil find in the Lennard River) nor at Argyle.

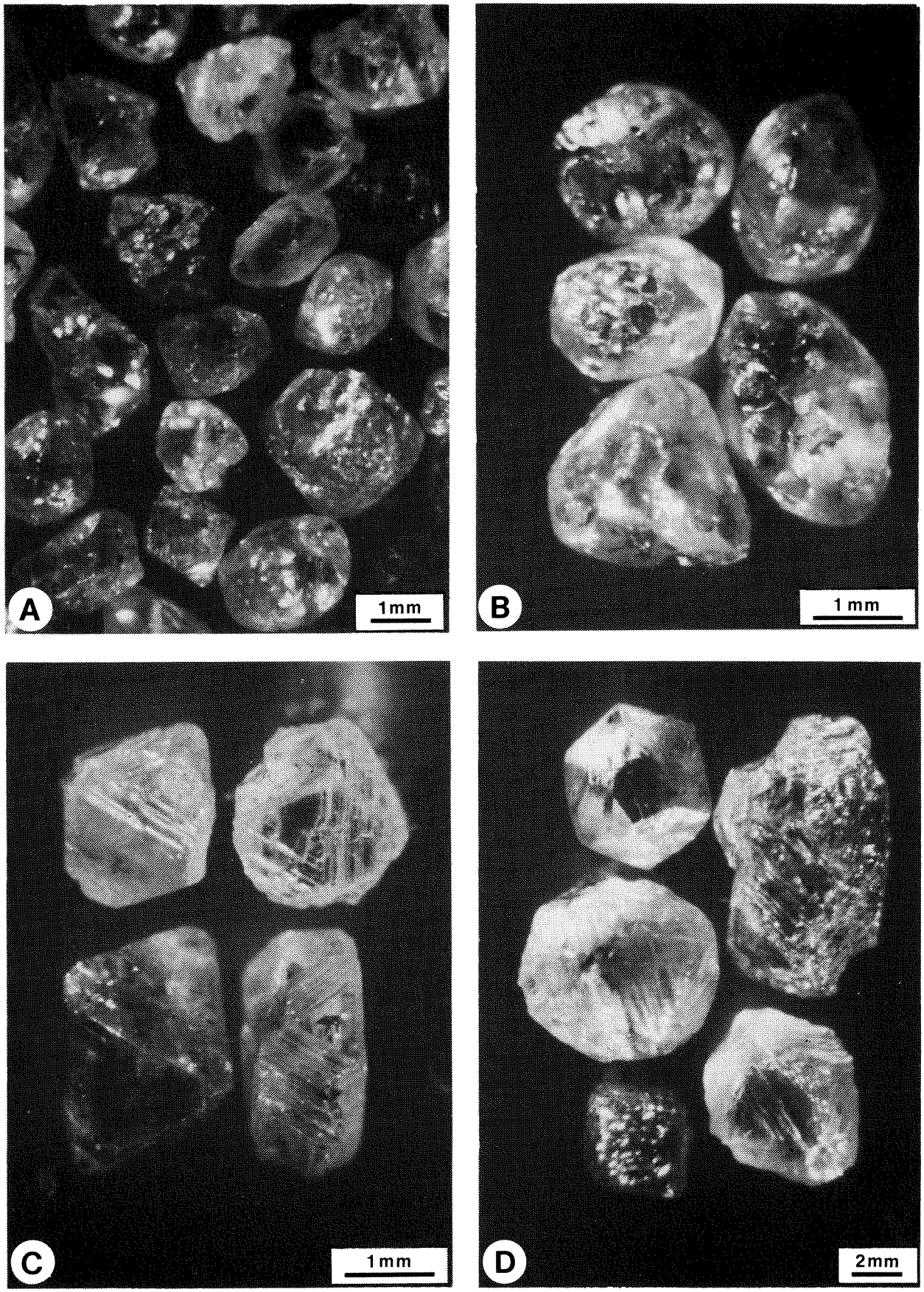
The varied characters of the stones present on the Kimberley Plateau is suggestive of a mixed population originating from several distinct sources. Pteropus Creek stones are thought to originate in the Pteropus Breccia pipe (1 stone has been found in the breccia itself), but some of the plateau stones, such as those similar to Argyle stones, may be far travelled.

NULLAGINE DIAMONDS

Diamonds have occasionally been won at Nullagine as a by-product of alluvial gold mining and prospecting since just before the turn of the century (Groom, 1896; Simpson, 1951). Renewed prospecting during the last 20 years, principally by Dr J Jeppe, but also by CRA Exploration and Mining Advisers, has shown that Tertiary fluviatile conglomerates are the source of many of the stones (Carter, 1974), but others have been obtained from nearby younger alluvials. No primary kimberlite or lamproite source for these stones is known.

Although no reliable estimate can be made of numbers of diamonds found at Nullagine, the total seems unlikely to exceed more than a few hundred. The largest recorded is 3.5 CM but the average stone recovered would probably weigh 0.2 CM or less.

Morphological examination of a small number of stones won by Dr J.Jeppe from the Nullagine alluvials showed them to be mostly of good crystal shape, and



GSWA 22714

Figure 160. Photographs of diamonds from Morelli's Fox site, King George River: A — Assortment of typical stones from the King George River. B — Rounded, resorbed forms with hexagonal surface pits; similar to Argyle stones. C — Step-layered planar octahedra. D — Four dodecahedral forms showing roll-type relief, and one cube form. (Photos: CRAE).

roughly equally divided in numbers between octahedra, dodecahedra, aggregates and macled forms. The stones are pale brown or green. Green and brown surface spots are common. Green spots are thought to be produced by alpha particle radiation damage in an alluvial or weathered kimberlite environment, and brown spots have been produced experimentally from green ones when diamond is heated to 500°C (Vance and others, 1973). Hence, the Nullagine diamonds may have been subjected to a post-kimberlite heating event, such as burial within a sedimentary sequence subjected to low-grade metamorphism. Such an argument implies the kimberlitic primary source for these diamonds may well date back to the Proterozoic or earlier, as metamorphic rocks of Palaezoic or younger age are unknown from the Pilbara and adjoining regions.

WANDAGEE DIAMONDS

Early exploration sampling in the vicinity of the Wandagee pipes (Atkinson and others, 1984a) yielded 3 microscopic diamonds, one from drill core of pipe M154, one from a loam sample over pipe M142, and one from a trench sample from pipe M92b. Subsequent evaluation bulk sampling of the Wandagee pipes did not produce any commercial-sized diamonds.

COMPARISON OF LAMPROITE AND KIMBERLITE DIAMONDS

Hall and Smith (1984) compared the properties of diamonds from Western Australian lamproites with those from kimberlite diamonds from other parts of the world. None of the morphological types of diamond seen is unique to lamproite. Likewise, the surface markings of lamproite diamonds are all found on kimberlite diamonds. The mineral inclusion species found within the lamproite diamonds fall within the same two associations, the ultramafic and eclogitic suites of Meyer and Boyd (1968, 1972) that characterize minerals included within kimberlite diamonds. No mineral inclusion unique to lamproite diamonds has yet been found.

Carbon isotope measurements made by J.W.Smith on West Australian lamproite diamonds so far show similar small negative $\delta^{13}C$ values such as characterize kimberlite diamonds (Table 81).

TABLE 81. CARBON ISOTOPE MEASUREMENTS ON WEST AUSTRALIAN LAMPROITE DIAMONDS.

Source	$\delta^{13}C$ PDB ‰
Argyle (AK1)	−11.1
	−7.8
	−7.5
Ellendale Pipe 9	−2.8
	−5.7
	−3.5

After Hall and Smith, 1984.

Modern beliefs are that diamond is a xenocryst in kimberlite (Gurney and Harris, 1982; Meyer, 1979), and Hall and Smith (1984) conclude that the Western Australian lamproites were, similarly, solely the transporting medium for diamond crystals formed within the mantle.

CHAPTER 8

PETROGENESIS

The kimberlitic and lamproitic rocks described in this bulletin — although similar in that all can be loosely termed alkaline ultrabasic or broadly "kimberlitic" in character, and in that many might be considered as part of a kimberlite clan (Dawson, 1985) — have a number of significant and, in some cases, distinctive differences from "classical" kimberlites. The age, structural setting, and petrologic type of the various intrusives in the four provinces differ considerably (Chapter 2). The late Proterozoic (800 Ma) North Kimberley intrusions resemble classical kimberlites in most respects, and lie near the margin of the Kimberley Block. The East Kimberley Province comprises kimberlite and lamprophyre dykes both of late Proterozoic age (800 Ma), in the west and central parts of the Halls Creek Mobile Zone, and the older, mid Proterozoic (1 150 Ma) lamproites of Argyle pipe and Lissadell Road dykes in the eastern part of the mobile zone. The leucite- and olivine-rich lamproites of the West Kimberley are Miocene in age (20 Ma) and straddle the Proterozoic King Leopold Mobile Zone and the Phanerozoic Fitzroy Trough. The Wandagee alkali picrites and associated "kimberlitic" pipes are mid-Jurassic in age (160 Ma) and intrude Phanerozoic sediments of the Carnavon Basin. Within each of these provinces the location of the individual intrusions is strongly influenced by structure (Atkinson and others, 1984a; *see also* Chapter 2), particularly by reactivated ancient major faults.

At least four major periods of alkaline ultramafic magmatism are indicated: mid Proterozoic (lamproite), late Proterozoic (kimberlite, lamprophyre), Jurassic (alkali picrite and "kimberlite"), and Miocene (lamproite). The repetition of lamproite magmatism within the Kimberley region, separated by approximately 1 100 Ma, is particularly striking.

On the basis of their early studies, Atkinson and others (1984a) and Jaques and others (1982, 1984a) showed that the lamproite magmatism of the Kimberley region of Western Australia exhibited a number of mineralogical, petrological, and geochemical differences to the classical kimberlites of southern Africa. Atkinson and others (1984a) also pointed out that the kimberlitic rocks of Wandagee differed from both North and East Kimberley kimberlites and the West Kimberley and Argyle lamproites. The differences between all the kimberlitic and lamproitic rocks of Western Australia are now re-examined in the light of the new data with a view to assisting in the determination of their petrogeneses.

RELATIONSHIPS BETWEEN THE KIMBERLITIC AND LAMPROITIC ROCKS OF WESTERN AUSTRALIA

PETROLOGICAL AND MINERALOGICAL DIFFERENCES

Detailed drilling and mapping has shown that West Kimberley lamproite pipes have a different geometry to the kimberlite pipe model proposed by Hawthorne (1975) based on the southern African pipes (Atkinson and others, 1984a; *see also* Chapter 5). The West Kimberley lamproite pipes in particular, are characterized by a relatively large diameter of the crater zone compared to that of the feeder pipe and by the presence of magmatic rocks within the crater zone where they are commonly juxtaposed and, in some pipes, intercalated with, pyroclastic rocks. In both the West Kimberley and Argyle pipes, the pyroclastic and magmatic rocks are commonly glassy and have been quenched on eruption. An additional feature is the highly vesicular nature of many of the pyroclastics. In many of the pipes, the magmatic rocks probably crystallized from a lava lake within the open vent. Glassy pyroclastics and magmatic rocks have not been reported from the upper parts of kimberlite pipes (Hawthorne, 1975; Dawson, 1980, 1984a; Clement, 1982); magmatic phases are typically crystalline and confined to dykes and sills, or occur deep in the pipe beneath tuffs and breccias of the diatreme facies, where they comprise the hypabyssal facies or root zone (Dawson, 1984a). The kimberlites of the North and East Kimberley Provinces appear to conform more closely to this model inasmuch as the magmatic rocks are confined to dykes and deeply eroded pipes. Similarly, in the Wandagee intrusions, the magmatic alkali picrites are confined to dykes and sills, whereas the pipes are filled with tuffs and tuff-breccias. The juvenile lapilli in the Wandagee pipes, although strongly altered, differ from those of the West Kimberley in being largely crystalline and very poorly vesiculated.

The volcanological differences are also reflected in the mineralogy of the different suites. Both the West Kimberley and Argyle lamproite suites reflect their low-pressure equilibration and are characterized by low-pressure, high-temperature mineral assemblages, in particular, the assemblage leucite + olivine. The stability field of leucite + olivine is apparently restricted to <500 MPa in water-undersaturated lamproitic compositions (Barton and Hamilton, 1979, 1982) and

to 120 MPa under water-saturated conditions in the system $KAlSiO_4$-Mg_2SiO_4-SiO_2-H_2O (Luth, 1967), although it is stable to much higher pressures in the vapour-absent system (Wendlandt and Eggler, 1980a).

Much of the crystallization in the lamproite suites occurred as a consequence of quenching immediately prior to, or on, eruption, which was accompanied by strong vesiculation and volatile exsolution. The experimental data of Barton and Hamilton (1979), Arima and Edgar (1983), and Foley (1986), suggest eruption temperatures for the lamproites in the region of 1 200°C — higher than generally supposed for kimberlites.

In addition to leucite, the West Kimberley lamproites contain a number of other phases atypical of kimberlite (*sensu stricto*) notably potassic richterite, priderite, and wadeite. Primary calcite, serpentine, and monticellite, which are common groundmass phases in kimberlite (*e.g.* Clement and others, 1984), are not present in the lamproites. In addition the compositions and evolutionary trends of the micas and spinels in lamproites differ from those of kimberlite (*see* Chapter 5)

The alkali picrites of Wandagee differ in their groundmass mineralogy from both kimberlite and lamproite: they contain feldspar, analcime, and amphibole (kaersutite). The compositions of the groundmass spinels also differ from those in kimberlite (*see* Chapter 6). In these respects, the alkali picrites resemble the more undersaturated basaltic suites, *e.g.* olivine analcimites.

The Bow Hill dyke suite resembles kimberlite more than lamproite, but differs in its groundmass mineralogy from kimberlite (*s.s.*) as it contains richteritic amphibole. The dykes also have segregation veinlets of, and grade into, pegmatites containing alkali amphibole, melanitic and andraditic garnet, and clinozoisite, all of which rarely occur in kimberlite (Dawson, 1980).

LOW-PRESSURE FRACTIONATION

The low equilibration pressures of the West Kimberley lamproites have resulted in extensive modification of magma compositions by crystal fractionation. This is shown by the wide range of compositions (*see* Chapter 5); much of this range is explicable in terms of accumulation of variable amounts of xenocrystal olivine derived from mantle peridotite, and of high-level separation of olivine, chrome spinel, diopside, phlogopite, perovskite and priderite (Jaques and others, 1984a). Petrographic evidence for high-level crystal fractionation of the West Kimberley lamproites, particularly the leucite lamproites, is provided by the common occurrence of phenocrystal aggregates and cognate xenoliths of diopside, and phlogopite ± olivine ± chrome spinel. The dominant effect of the low-pressure crystal fractionation is the formation of more silica-rich derivative liquids, *i.e.* an orenditic differentiation trend. Coupled with the increase in SiO_2 and the decrease in MgO content and Mg/(Mg + Fe) ratio is an increase in Al_2O_3, K_2O, and (initially) TiO_2 content, and the abundance of Pb, La, V, Cu, Ga, and Zr. Decreases in Ni and Cr are attributable to olivine and chrome spinel crystallization respectively, and the decrease in CaO reflects the crystallization of diopside. The small decrease in FeO, MnO, and ultimately TiO_2, is thought to be the result of chrome spinel, priderite, and, to a lesser extent, perovskite crystallization. The effects of perovskite fractionation are well displayed in the Walgidee Hills intrusion, where the abundances of normally incompatible elements which substitute into perovskite (Nb, Th, Ta, Sr, and La) are largely buffered by significant perovskite crystallization. This leads to changes in certain incompatible-element ratios such as Zr/Nb, Nb/Ta, La/Nb, and Zr/Hf (Jaques and others, 1986).

Although crystal fractionation has played a role in the evolution of the West Kimberley lamproites, the range of incompatible-element ratios and abundances, together with the isotopic data, indicate the existence of more than one parent magma and a number of lines of liquid descent. Jaques and others (1984a) proposed the existence of a spectrum of related magmas of variable MgO and SiO_2 content.

The effects of low-pressure crystal fractionation are not as marked in the Argyle lamproites as the West Kimberley lamproites even though they have also equilibrated largely at low pressure. Entrainment and accumulation of variable amounts of xenocrystic olivine is an additional important control on both the West Kimberley and Argyle lamproites.

In contrast to the lamproites, the kimberlites and other rocks show only limited crystal fractionation. Some of the Wandagee sills show minor compositional variation as a result of separation and accumulation of xenocrystal and phenocrystal olivine. The compositional variation between the olivine-phlogopite lamprophyres and the garnet-phlogopite pegmatites of the Bow Hill dykes is attributed to fractional crystallization: crystal separation was probably relatively unimportant.

HIGH-PRESSURE CRYSTALLIZATION

Evidence of multiphase high-pressure (deep-level) crystallization is displayed by a number of the West Australian kimberlites. These high pressure phases, described as discrete nodules by Nixon and Boyd (1973) and megacrysts by other workers, *e.g.* Binns and others (1970) and Dawson (1980), are believed to be high-pressure cognate phenocrysts in kimberlite or, possibly, the magmatic precursors to kimberlite (Nixon and others, 1981). Megacryst species recognized to date in the West Australian kimberlitic rocks include picroilmenite, red-brown titaniferous pyrope, chrome diopside, zircon and, possibly, chromite.

Ilmenite megacrysts are common in the Skerring pipe, where large (up to 9 cm) rounded picroilmenites and ilmenite-silicate nodules occur together. By analogy with the experimental studies of Green and Sobolev (1975), Wyatt (1977, 1978), and Rawlinson and Dawson (1979) these are inferred to be high-pressure cognate phenocrysts of the kimberlite host magma. The picroilmenite macrocrysts found in the other North

Kimberley kimberlites, the East Kimberley kimberlite dykes of Maude Creek, Duck Creek, and Devils Elbow, and in the Wandagee pipes, probably also represent high pressure cognate phenocrysts. All have appreciable Cr_2O_3 and MgO contents (up to 3.2% Cr_2O_3 and 12% MgO respectively) and are thus similar to megacryst ilmenite found elsewhere in kimberlite. The Cr contents of the Wandagee ilmenites are higher than the low values (<0.5% Cr_2O_3) commonly reported from ilmenites in alkali basalts (Jones, 1984).

Megacrysts of rounded, red-brown, titanian pyrope (Groups 1 and 2 of Dawson and Stephens, 1975), up to several centimetres across, have been recovered from the Skerring, Wishywashy, and Hadfields kimberlites in the North Kimberley, and the Maude Creek, Duck Creek, and Blackfellow Creek kimberlites in the East Kimberley. These garnets have high but variable TiO_2 contents (up to 1% TiO_2) and, in the case of the Skerring pipe, contain appreciable Cr (up to 3.6% Cr_2O_3). Similarly, some of the Ti-pyropes from the Wandagee intrusions may be cognate megacrysts since, as with the ilmenites, the Wandagee garnets are richer in Cr than commonly found in alkali basalts. Very rarely, macrocrystal Ti-pyropes (Group 1) recovered in concentrate from the Argyle and West Kimberley lamproite suites are of much smaller grain size, and are inferred to have been derived from disaggregated peridotite (*see below*) rather than crystallized under high pressures from the lamproite host.

Distinction of pyroxene and spinel megacrysts of cognate origin from xenocrysts derived from disaggregated mantle peridotite is less certain. Some of the large sub-calcic diopsides (group 1 of Stephens and Dawson, 1977) from the Skerring pipe are likely to be cognate in view of their size; but, in terms of their compositions, in particular their Ca/(Ca + Mg) ratios, they are comparable to diopside from high-temperature (sheared) peridotites (*e.g.* Nixon and Boyd, 1973). The pyroxenes recovered from the lamproite suites are all of a size and composition compatible with a mantle xenolith origin.

Some of the macrocrystal titaniferous magnesian

TABLE 82. COMPARISON OF THE CHEMICAL COMPOSITIONS OF WEST AUSTRALIAN KIMBERLITES AND LAMPROITES.

	1	*2*		*3*		*4*	*5*	
	range	*mean*	*std. dev.*	*mean*	*std. dev.*	*mean*	*mean*	*std. dev.*
				Percent				
SiO_2	—	45.7	4.28	41.5	2.15	53.2	42.3	2.31
TiO_2	—	2.83	0.34	3.62	0.44	5.84	1.08	0.16
Al_2O_3	—	4.33	0.33	3.64	0.72	8.34	6.05	0.88
FeO	—	7.46	0.66	8.10	0.62	6.60	9.85	0.63
MnO	—	0.14	0.05	0.13	0.02	0.08	0.17	0.03
MgO	—	22.02	1.06	25.00	1.40	7.80	25.01	3.33
CaO	—	4.85	1.70	4.99	1.03	3.22	6.37	3.31
Na_2O	—	0.11	0.05	0.46	0.22	0.57	1.01	0.32
K_2O	—	3.43	1.26	4.12	1.11	9.89	0.74	0.70
P_2O_5	—	0.91	0.06	1.68	0.50	0.98	0.27	0.83
H_2O	—	4.58	0.80	6.36	1.76	2.98	4.96	2.24
CO_2	—	3.43	2.38	0.45	0.36	0.50	2.07	1.37
				Ratio				
K_2O/Na_2O		31		9		17	0.73	
				Parts per million				
Ba	340-18 000	1 075	622	10 334	5 500	9 871	570	250
Li	—	91	57	9	3	10	56	17
Rb	5-16	264	112	479	112	275	29	35
Sr	150-13 000	767	300	1 312	173	1 184	330	198
Pb	—	68	138	50	13	52	7	3
Th	(450)	17	6	60	11	23	7	3
U	(20)	3	1	2	2	3	2	1
Zr	200-1 050	626	47	1 133	268	1 144	107	37
Nb	9-2 300	199	36	184	35	123	40	7
Y	—	20	4	16	4	20	12	4
La	—	117	19	421	61	292	42	8
Ce	—	240	40	734	135	435	77	16
Sc	(26)	12	2	21	4	14	15	3
V	—	110	22	85	88	210	219	24
Cr	370-2 500	1 428	181	1 006	146	348	1 812	361
Ni	140-835	986	74	1 004	138	346	958	162
Co	35-75	—	—	70	8	33	—	—
Cu	—	39	18	56	12	66	64	10
Zn	—	54	25	71	9	77	73	6
Sn	—	3	3	9	5	13	4	6
Mo	—	3	15	3	10	4	5	5
Ga	—	7	2	4	1	17	10	2
S	—	—	—	425	530	514	—	—
F	—	3 638	890	4 756	1 186	2 655	1 746	290
Cl	—	—	—	116	40	154	—	—

All analyses recalculated H_2O-free with all Fe as FeO.

1 — Range of compositions for Skerring, Hadfields, Wishywashy, KGB2 and Maude Creek Kimberlites. 2 — Mean and standard deviation of 8 'non-sandy' tuffs from Argyle pipe. 3 — Mean and standard deviation of 89 olivine lamproites from Ellendale 4 and 9. 4 — Mean of 100 leucite lamproites from the Noonkanbah Field. 5 — Mean and standard deviation of 13 alkali picrites from Wandagee.

aluminous chromites found in both the kimberlite and lamproite suites might represent moderate to high-pressure cognate phenocrysts. Megacryst and phenocryst spinels are difficult to distinguish from spinels derived from mantle xenoliths, although the spinels with very low Ti contents are inferred to have been derived from disaggregated mantle peridotite.

A number of the coarser, embayed and resorbed, Cr-rich mica phenocrysts in the West Kimberley lamproites appear to have crystallized at higher pressure than the groundmass micas (Jaques and others, 1984a; Chapter 5). These differ in composition from megacryst micas in kimberlite in terms of their much higher Ti contents, which may reflect, at least in part, higher crystallization temperatures.

Rounded, blocky, pale-buff zircon megacrysts occur in the Skerring and Pteropus Creek pipes, and in the Wandagee intrusions. Uranium ranges from very low values (5 ppm) in the Skerring, to values more typical of kimberlitic zircons (30-50 ppm) in the Wandagee intrusions (Atkinson and others, 1984a).

From this comparison, it is clear that, although there is evidence for accumulation and (probably) high level crystallization of olivine and chrome spinel, minerals characteristic of the kimberlite megacryst suite are lacking in the West Australian lamproite suites. This contrasts with the kimberlites of the North and East Kimberley Provinces, in which megacryst minerals are well represented. Jaques and others (1984a), in noting the lack of megacrysts and high temperature xenoliths, suggested that the lamproites may have originated at shallower levels and/or contained a lower proportion of "proto-kimberlite" magma.

CONTRASTING MAGMA TYPES

Previous geochemical comparisons have shown that significant compositional differences exist between the various kimberlitic and lamproitic suites of Western Australia, and between the West Australian rocks and kimberlites elsewhere (Atkinson and others, 1984a, Jaques and others, 1984b). Mean compositions for the various West Australian suites are given in Table 82.

The mean compositions of 89 olivine lamproites from Ellendale 4 and 9 is similar to the average of 21 olivine lamproites published by Jaques and others (1984a) apart from having slightly higher volatile, TiO_2, and P_2O_5 contents, and slightly lower Al_2O_3 and K_2O contents. The comparative uniformity of the olivine lamproite in the two diamondiferous pipes is noteworthy, and contrasts with the wide compositional range exhibited by the West Kimberley suite as a whole and by certain individual intrusions such as Walgidee Hills. The wide compositional range of the West Kimberley rocks means that little significance can be attached to average values; however, the mean of 100 Noonkanbah Field leucite lamproites is included for comparison and contrast with the olivine lamproites and with the other suites. The leucite lamproites are distinctly more siliceous and potassic and much less magnesian than the olivine lamproites; and abundances of incompatible elements are generally higher than those in more olivine-rich lamproites from the same field. Much of the variation in leucite lamproites is attributed to shallow-level crystal fractionation; but it is also clear from the abundances and abundance ratios of incompatible elements, and from isotopic compositions, that lamproites of equivalent Mg/(Mg + Fe) ratio from different fields and, in some cases, from different intrusions within the same field have different levels of enrichment in incompatible elements (Jaques and others, 1986).

The olivine lamproites of the Argyle pipe clearly have chemical as well as mineralogical affinities with the West Kimberley lamproites as previously pointed out by Atkinson and others (1984a); key features are the very high K_2O/Na_2O ratios and the high TiO_2 and K_2O contents. Compared to the olivine lamproites of the West Kimberley, however, the Argyle lamproites are slightly richer in SiO_2, poorer in MgO, and distinctly poorer in TiO_2, K_2O, and other incompatible elements. The level at which the incompatible elements in the West Kimberley lamproites are enriched relative to the Argyle lamproites is not uniform for all elements; for example, TiO_2 and K_2O contents in the mean Argyle "non-sandy" tuff are approximately 0.8 of those in the mean Ellendale 4 and 9 olivine lamproite, whereas Rb and Zr abundances are about 0.55, and La and Th abundances approximately 0.3 of those in the Ellendale 4 and 9 lamproites.

Geochemical data on unaltered material is not available for either the North or East Kimberley kimberlites. The few data that are available suggest that these rocks resemble kimberlite rather than lamproite (Atkinson and others, 1984a).

The mineralogical differences of the Wandagee intrusions from the lamproite and kimberlite suites are reflected in their chemistry. Key features of the Wandagee alkali picrites are their higher abundances of Al_2O_3, CaO, and Na_2O and, particularly, the much lower K_2O and TiO_2 contents (Table 82). The high Na_2O contents and very low K_2O/Na_2O ratio of the Wandagee rocks are distinctly unlike either kimberlite or lamproite. The Wandagee alkali picrites have very low abundances of incompatible trace elements — only about 10% of those in the strongly enriched West Kimberley lamproites.

The data show, as previously pointed out (Atkinson and others, 1984a; Jaques and others, 1984c), that the West Australian kimberlitic rocks comprise at least three chemical suites — kimberlite, lamproite, and alkali picrite. It has also been previously shown (Jaques and others, 1984a; Atkinson and others, 1984a) that, compared to published average compositions of micaceous and non-micaceous kimberlites, the lamproite suite, especially the West Kimberley lamproites, is characterized by higher SiO_2, TiO_2, K_2O, and P_2O_5 contents, and lower Al_2O_3 and FeO and particularly CaO and CO_2 contents, and much higher abundances of all the incompatible trace elements. The enrichment in incompatible elements over abundances in kimberlites is particularly evident in Ba, Rb, Th, LREE, Zr and

TiO_2. The lamproites are closer in composition to the micaceous kimberlites, as shown by the recent data of Dawson (1985), and also in terms of isotopic compositions (McCulloch and others, 1983; Smith, 1983), but differ appreciably from the non-micaceous kimberlites. Both lamproite and micaceous kimberlite appear to have been derived from mantle sources which have undergone long-term enrichment in Rb relative to Sr and Nd relative Sm, but the lamproite sources appear to have undergone a greater degree of enrichment. Dawson (1985) has highlighted the fact that the micaceous (Group II) kimberlites of southern Africa have greater chemical affinities with the olivine lamproites than with the non-micaceous (Group I) kimberlites.

XENOLITHS AND THE NATURE OF THE UPPER MANTLE BENEATH THE KIMBERLEY AND CARNARVON BASIN REGIONS

With the exception of the small number of serpentinized, spinel (formerly garnet)-bearing peridotite nodules recovered from the Skerring and Argyle pipes, and olivine-rich (dunitic) microxenoliths found, commonly in thin section, in a number of the intrusions from all provinces, mantle xenoliths are rare. Although incomplete, an estimate of the nature of the mantle underlying the various provinces can be obtained from the available xenoliths and from the nature of the minerals recovered from heavy-mineral concentrates.

Mantle xenoliths from the North Kimberley region, although altered (Chapter 3), have been interpreted as former dunite and garnet peridotite (Atkinson and others, 1984a). Fresh garnet is preserved in some of the peridotite xenoliths from Skerring; and the presence of chrome pyropes belonging to Dawson and Stephens (1975) Group 9 at the other localities suggests that the garnet lherzolite is widespread. The subcalcic nature of the chrome diopsides recovered, and the presence of uvarovite-pyrope garnets suggests that many of the lherzolites are likely to be of high-temperature origin and resemble deformed (sheared) nodules described from elsewhere (Nixon and Boyd, 1973). The presence of the high-Cr, low-Ca garnets in the concentrates may indicate, by analogy with southern Africa (Boyd and Gurney, 1982; Gurney, 1984), the existence of old cratonic basement beneath at least part of the North Kimberley region. The presence of occasional calcic pyrope-almandines suggests the existence of small amounts of eclogite and granulite beneath the region. In the absence of orthopyroxene, no P-T estimates for the xenoliths or minerals are possible, although the low Ca/(Ca + Mg) ratios of the diopsides suggest equilibration temperatures of 1 400 °C, or higher, depending on pressure.

The spinel (formerly garnet) lherzolite xenoliths recovered from the Argyle pipe are characterized by Al-poor orthopyroxene and calcic-diopside, indicating equilibration at high pressure (> 5 GPa) and low temperature, 1 100-1 200 °C (Hall and Smith, 1984; O'Neill and others, in prep.). Similar temperatures have been obtained for mineral inclusions in diamonds from Argyle (Hall and Smith, 1984). The compositions of the mineral phases and the bulk chemistry of the nodules are refractory, and indicate the existence of depleted mantle at depth beneath the region. The common occurrence of microxenoliths of dunite in the Argyle pipe and weathered dunite at some of the other intrusions (*e.g.* Maude Creek) also supports the presence of a refractory (olivine-rich) peridotite mantle. Occasional pyrope garnets recovered from the Argyle concentrate are not sub-calcic; but low-calcium, high-chrome, Group 10 garnets have been recovered from the Maude Creek dyke, confirming the existence of refractory mantle beneath the East Kimberley. The presence of occasional titanian pyrope and subcalcic diopside in the Argyle concentrate, and their more common occurrence in the kimberlites at the western margin of the Halls Creek Mobile Zone and the Kimberley Block, implies that lherzolite, deformed (sheared) at high temperature, is also present at depth beneath the region. Although no eclogite xenoliths have been recovered, the diamond inclusion suite at Argyle is dominantly eclogitic (Hall and Smith, 1984); and the very rare presence of calcic pyrope-almandine in the concentrate suggests that eclogite may be present in the mantle beneath the East Kimberley.

The very few mantle xenoliths recovered from either outcrop or drill core, and the microxenoliths observed in thin section from the West Kimberley lamproites, are either dunite, harzburgite, or spinel- and clinopyroxene-poor lherzolite (Atkinson and others, 1984a; Jaques and others, 1984a; *see* Chapter 5). All have coarse or granular texture, refractory, highly magnesian mineral compositions, and appear to have equilibrated at low temperature. Garnet and pyroxene compositions from concentrate are mostly Ti-poor and Ca- and Cr-rich and are inferred to have been derived from garnet- and diopside-poor lherzolite that equilibrated at low temperature. However, the rare presence of Ti-pyrope (as at Mount Abbot) suggests that the lamproites have also sampled some deformed, high-temperature mantle peridotites. As with the Argyle Pipe, no eclogite nodules have been found, but minerals of eclogitic paragenesis occur as inclusions in diamonds from Ellendale although they do not occur in the same relative proportions as in Argyle diamonds (Hall and Smith, 1984; Tables 75, 80). In addition, eclogitic garnets (dominantly calcic pyrope-almandine, but including some magnesian almandine) have been recovered from concentrate; this suggests the existence of eclogite and granulite beneath the region.

The nature of the mantle beneath the Wandagee region is even less well constrained as no mantle xenoliths have been found to date — apart from the coarse- to granular-textured dunitic microxenoliths. Garnets and pyroxenes in the mineral concentrates have compositions consistent with derivation, mostly, from depleted garnet lherzolite that equilibrated at low temperature and, in rare cases, eclogite.

ORIGIN OF THE MAGMA

MANTLE SOURCES

Kimberlite and kimberlite-like magmas are often considered to be small volume partial melts of carbonated phlogopite peridotite formed deep in the mantle (*e.g.* Dawson, 1980; Wyllie, 1980). The high abundances of K and other incompatible elements in kimberlite require that the degree of partial melting is small. However, since four-phase garnet lherzolite is not an adequate source, it is widely believed that either phases capable of hosting such elements, or perhaps an incompatible-element-rich melt or fluid, are also present in the source regions of kimberlites (Bailey, 1984; Dawson, 1984a). Mantle sources of lamproites are inferred to be at least as (if not even more than) enriched in incompatible elements as those of the kimberlites. In contrast to these conclusions, Kramers and others (1981) have argued, on the basis of apparently low values of clinopyroxene-kimberlite liquid REE partition coefficients, that kimberlites could be generated by melting of "ordinary" (*i.e.* oceanic island type) mantle. There is now a large volume of trace-element and isotopic evidence, both from xenoliths entrained in kimberlite (Boettcher and O'Neill, 1980; Menzies and Murthy, 1980; Gurney and Harte, 1980; Erlank and others, 1982; Jones and others, 1982: Harte, 1983; Kramers and others, 1983) and from the kimberlite host rocks themselves (Smith, 1983, Bailey, 1984; *but see* Basu and Tatsumoto, 1980; Basu and others, 1984), to indicate that the mantle in the region of many kimberlitic intrusions has been modified (enriched) by the introduction of incompatible elements in melts or fluids commonly characterized by high Rb/Sr and low Sm/Nd. Enrichment in incompatible elements by metasomatic-type processes is now recognized as a common feature in many, if not most, areas of alkaline magmatism, resulting in heterogeneous mantle compositions (Bailey, 1980, 1982; Boettcher and O'Neill, 1980, Menzies and Murthy, 1980; Hawkesworth and others, 1984). Metasomatism characterized by the development of replacement textures and/or hydrous phases has been termed patent (Dawson, 1984b) or modal (Harte, 1983) metasomatism, whereas elemental enrichment without petrographic modification of the host has been termed cryptic metasomatism (Dawson, 1984b).

Strontium, neodymium, and lead isotopic data from both kimberlites and lamproites indicate the existence of mantle sources differing widely in isotopic character (Kramers, 1977; Basu and Tatsumoto, 1980; McCulloch and others, 1983; Smith, 1983; Basu and others, 1984; Vollmer and others, 1984). Some, such as the non-micaceous kimberlites of southern Africa, are derived from undifferentiated to slightly depleted sources relative to bulk Earth, whereas others, in particular the lamproites of the West Kimberley and the micaceous kimberlites (Group II) of southern Africa, are derived from mantle sources which have undergone long-term enrichment in Rb/Sr and Nd/Sm. The Pb isotope data of Nelson and others (1986) suggest that the enriched component (low Sm/Nd, high Rb/Sr, variable U/Pb) may be 2 Ga or older. It is widely believed that the most likely storage reservoir for such components is the subcontinental lithosphere (Brooks and others, 1976; Jordan, 1978, 1981), although the origin and nature of the enrichment remains controversial. Recycling of oceanic lithosphere (including oceanic sediments) subducted deep into the lower mantle *via* diapiric rise from a "megalith" layer has been suggested as one possible mechanism (Hoffman and White, 1982; Ringwood, 1982, 1985, Thompson and others, 1984).

Metasomatism of mantle sources may also be directly linked with diamond formation because sub-calcic garnet inclusions in diamond from South African kimberlites give old model Sm-Nd and Rb-Sr ages (3.2-3.3 Ga) and apparently formed following enrichment of residual subcratonic mantle (Richardson and others, 1984). Detailed isotopic and trace-element studies of metasomatized mantle xenoliths in both kimberlite and alkali basalt show that metasomatic enrichment, commonly of formerly refractory mantle peridotite, may occur without mineralogical change, and that cryptic metasomatism, or enrichment events with no obvious mineralogical modification, may be much older than patent or modal metasomatism (Erlank and others, 1982; Kramers and others, 1983; Menzies and others, 1985). In a number of cases, modal metasomatism has been found to be of similar age to the host kimberlite (or alkali volcanics) and the metasomatic component to be of similar composition to the host (Kramers and others, 1983; Menzies and others, 1985). Modal metasomatism has, therefore, been inferred to have taken place in contact metamorphic aureoles surrounding magma conduits, while enrichment fronts occur further from the conduit and are a result of volatile gradients (Menzies and others, 1985). This model bears some similarities with that proposed by Wyllie (1980), who suggested that metasomatism was a consequence rather than a precursory cause of kimberlite magmatism and resulted from crystallization in the lower lithosphere, as a consequence of a thermal barrier on the solidus, of partially melted diapirs derived from deep in the asthenosphere.

CONDITIONS OF FORMATION

Kimberlite and kimberlite-like magmas are believed to form by partial melting of carbonated phlogopite peridotite in the presence of H_2O and/or CO_2; and experiments carried out in the system, peridotite-C-O-H, are relevant to their petrogenesis (Eggler, 1978; Wyllie, 1980). Despite the fact that this system has been studied intensively over the past decade (Eggler, 1978; Eggler and Wendlandt, 1979; Eggler and Baker, 1982; Wyllie, 1978, 1979, 1980; Wyllie and Huang, 1976; Ellis and Wyllie, 1980; Wendlandt and Eggler, 1980a,b; Brey and others 1983; Wendlandt, 1984) no consensus has emerged as to a detailed petrogensesis of kimberlite. Of particular importance are such variables as the oxidation state of the mantle, and the relative roles of gaseous CO_2, CH_4, and H_2, and of carbonate phases such as dolomite

and magnesite. However, there appears to be a consensus that oxygen fugacities in the mantle sources at depths appropriate for the genesis of diamond-bearing kimberlites must at least be as reduced as that constrained by carbonate-graphite-silicate buffers to allow formation of graphite and diamond. Under such conditions, kimberlitic melts may be produced by near solidus melting of carbonated (magnesite) peridotite at depths greater than about 150 km under a range of CO_2/H_2O conditions, where the solidus is essentially fluid-buffered. The experimentally determined solidus of kimberlite, as determined by Eggler and Wendlandt (1979), is consistent with derivation of kimberlite from phlogopite-carbonate peridotite at 150-180 km depth. Under more reducing conditions carbonate is not stable and fluids consist of CH_4, H_2 and H_2O rather than CO_2 and H_2O (Ryabchikov and others, 1981; Eggler and Baker, 1982; Green, 1985). The nature of near-solidus melts of peridotite under such reduced conditions is very poorly known; but melts are likely to be more silica-rich than equivalent melts under more oxidized conditons because CH_4 has a depolymerizing effect on silicate melts (Eggler and and Baker, 1982).

Lamproites and similar ultrapotassic lamprophyres are also inferred to be derived by small degrees of melting of phlogopite peridotite; and experimental studies of melting relations in simple systems (Modreski and Boettcher, 1973; Boettcher and others, 1975; Wendlandt and Eggler, 1980 a,b; Wendlandt, 1984) have shown that melting is governed by the decrease in the hypersolidus stability of phlogopite with increasing pressure, and that melts derived by breakdown of mica become increasingly silicic and potassic with pressure. Experimental studies on natural rock compositions, ranging from biotite mafurite to leucite lamproite (Edgar and others, 1976, 1980; Barton and Hamilton, 1979, 1982; Arima and Edgar, 1983), have shown that, while some compositions (*e.g.* biotite mafurite, madupite) are unlikely to have been derived from lherzolitic mantle under hydrous or anhydrous conditions, some might have formed from peridotite containing both H_2O and CO_2 or, alternatively, from modified mantle. In particular, Arima and Edgar (1983) suggested from their study of a potassic-richterite - diopside - phlogopite - leucite lamproite from Mount North that, if mantle-derived, it was most likely to have been derived from a phlogopite-rutile harzburgite. Jaques and others (1984a) proposed that the West Kimberley lamproites were derived by small degrees of partial melting under H_2O-and HF-rich and CO_2-poor conditions of a phlogopite-rich, metasomatized, formerly depleted, harzburgite or garnet-diopside-poor lherzolite, which had undergone long-term enrichment in incompatible elements. They suggested that high F contents enhanced the stability field of phlogopite and that partial melting under these conditions resulted in silica-saturated olivine lamproite melts rather than the undersaturated (larnite normative) melts formed under high pCO_2. These conclusions concerning the importance of H_2O- and HF-rich mixtures in the genesis of ultrapotasic rocks and the effect of F on mica stability are supported by a recent experimental study of the system $KAlSiO_4$-Mg_2SiO_4-SiO_2 by Foley and others (1986). As with kimberlites, a key variable in the petrogenesis of lamproites is oxygen fugacity because this will determine the role, if any, of carbonates. Evidence from spinel compositions (Foley, 1986; *see* also Chapter 5) suggests that the West Kimberley lamproites were derived under reducing conditions.

Estimates of oxygen fugacity in the mantle, based on studies of xenoliths and xenocrysts, indicate both reduced (near the iron-wustite buffer) and oxidized (near the quartz-fayalite-magnetite buffer) conditions exist (Arculus and Delano, 1981; Haggerty and Tomkins, 1983; Arculus and others, 1984). Highly reduced conditions seem appropriate for diamond formation in the mantle (Eggler and Baker, 1982; Taylor, 1985), but such conditions are not necessarily applicable to the genesis of kimberlite, particularly since recent dating of diamond inclusions (Kramers, 1979; Richardson and others, 1984) makes it likely that diamond is a xenocryst rather than a phenocryst in kimberlite; more oxidizing conditions might prevail during kimberlite formation. It is also possible that the mantle is layered with respect to both chemistry and oxygen fugacity (Nixon and others, 1981; Haggerty and Tomkins, 1983) and that a spectrum of oxygen fugacity conditions prevail in the mantle.

Nixon and others (1981) consider that kimberlite is a hybrid melt and propose a two-stage model for the genesis of kimberlite that involves interaction of the base of the lithosphere, which had formerly been depleted in lithophile elements by basaltic volcanism and gradually enriched in incompatible elements, with a "proto-kimberlite" magma formed by deep-seated diapiric upwelling and melting of relatively hot, fertile asthenosphere. This general model can directly, or in modified form, account for many of the features of kimberlite and kimberlitic rocks although many details remain to be resolved.

CONCLUSIONS

Although the details of the petrogenesis of kimberlites and lamproites remain areas of contention and active research, it is clear that both rock suites are low-volume melts derived from deep in the mantle, within the diamond stability field. The many broad similarities between kimberlite and lamproite and, in particular, between micaceous kimberlite and lamproite, mean that there must be many common links in their petrogeneses. Both sample sub-continental mantle of broadly similar character and the diamond-inclusion suites in kimberlite and lamproite diamonds are the same (Hall and Smith, 1984), implying that the mantle sources for both are essentially similar. Both kimberlite and lamproite appear to have been derived by partial melting of micaceous peridotite in the presence of H_2O, CO_2 and, in the case of the lamproites, probably HF. The peridotite sources of lamproites and micaceous kimberlites have undergone

long-term enrichment in Rb/Sr and Nd/Sm and, by association, other incompatible elements; and apparently differ from non-micaceous sources. The strong similarities between olivine lamproite and micaceous kimberlite have already prompted closer inspection of the petrographically and mineralogically diverse group of rocks termed "kimberlite"; and Dawson (1985) has proposed that — in view of this petrological diversity and the isotopic variation now known to exist amongst kimberlites — kimberlite be regarded as a group or clan rather than a single narrowly defined rock type. From a practical and economic point of view, a key factor to be considered is that early recognition that the differences in petrography, mineralogy, and geochemistry, between olivine lamproite and micaceous kimberlite were subordinate to the gross similarities facilitated successful exploration and discovery of the West Australian diamond deposits (Atkinson and others, 1984a,c). The fact that lamproite is now recognized, because of the newly discovered West Australian diamond deposits, to constitute an additional, new, primary terrestrial source of diamond will ensure that this rock type, formerly considered petrologically interesting but otherwise insignificant, remains a topic of active research by both industry and academic institutions in the foreseeable future.

APPENDIX 1

MINERAL ANALYSES

Mineral analyses presented in this bulletin were obtained on three different instruments by both energy-dispersive spectrometry (EDS) and wavelength-dispersive spectrometry (WDS) Almost all the mineral data presented in Chapter 3, and much of the xenocryst mineral data in Chapters 4, 5 and 6, were obtained by EDS following the method of Ware (1981) using an ISI scanning electron microscope equipped with a PGT energy dispersive analytical system operating at 15 kV and 5nA in the CRA Exploration Pty Ltd Belmont (Perth) laboratory, (A. Benn, analyst). The majority of the analyses of groundmass phases in Chapters 4, 5 and 6 were obtained by WDS by a fully automated Camebax (Cameca) microbeam in the joint Australian National University/Bureau of Mineral Resources (ANU/BMR) microprobe facility. Operating conditions employed an accerating voltage of 15 kV and a beam current of 30 to 40 nA. Analyses were made using pulse-height analysis with a variety of synthetic and natural standards and full ZAF corrections were applied using a computer program developed by N.G. Ware, (A.L. Jaques, analyst). Additional data were obtained by EDS on the TPD microprobe at ANU following the method of Reed and Ware (1975) and Ware (1981), (A.L. Jaques, analyst). Data from the three instruments are in reasonable agreement for major elements; but, as expected, discrepancies are evident in minor-element concentrations (< 1%) because of the much higher limits of detection of the EDS analyses (0.2% for Na, Ni, and Zn, 0.15% for Mn, 0.07-0.15% for Mg-Fe).

CHEMICAL ANALYSES

Chemical analyses were carried at the BMR (BMR samples) and West Australian Government Chemical Laboratories (GSWA samples) by a combination of x-ray fluorescence spectrometry (XRF), wet chemical methods, and atomic absorption spectroscopy (AAS). Additional analyses of trace elements and rare-earth elements (REE) were performed by instrumental neutron activation analysis at the Department of Geology, Australian National University by Dr B.W. Chappell. These will be presented elsewhere. A few of the analyses presented in Chapter 3 were carried out by Analabs (Perth) by a combination of XRF, wet-chemical analysis, and inductively-coupled plasma spectrophotometry (ICP).

The BMR samples were crushed in tungsten carbide mills except for the material used for Co determination where chrome-steel mills were used. Major elements were determined by XRF following the method of Norrish and Hutton (1969), and H_2O, CO_2, and FeO, by conventional methods. Trace elements were determined by XRF on pressed-powder pellets (Norrish and Chappell, 1979) except for Li, Cr, Ni, Cu, and Zn, which were determined by AAS. All high Cr values (>400 ppm) were repeated by XRF in order to avoid possible incomplete dissolution of chromite.

The GSWA samples were crushed in a tungsten carbide mill, and most major and trace elements were determined by XRF following the methods of Norrish and Hutton (1969) and Norrish and Chappell (1979). The MgO, Na_2O, Li, Ni, Co, Cu, Zn, and Pb values were determined by AAS, U by paper chromatography, F by selective ion electrode, and FeO, S, CO_2, and H_2O, by standard chemical methods.

NOTE: A complete listing of the analyses is given in Appendix 2, in the microfiche enclosed on the back cover of this bulletin.

REFERENCES

Note: Most unpublished company reports referenced are available on microfilm from the Geological Survey of Western Australia.

AGEE, J.J., GARRISON, J.R., and TAYLOR, L.A., 1982, Petrogenesis of oxide minerals in kimberlite, Elliot County, Kentucky: American Min., v. 67, p. 28-42.

AMDEL, 1970, Open file report No. MP1789-70: Australian Min. Dev. Labs. (unpublished).

ARCULUS, R.J. and DELANO, J.W., 1981, Intrinsic oxygen fugacity measurements: techniques and results for spinels from upper mantle peridotite and megacryst assemblages: Geochim. Cosmochim. Acta, v. 45, p. 899-913.

ARCULUS, R.J., DAWSON, J.B., MITCHELL, J.B., GUST, D.A., and HOLMES, R.D., 1984, Oxidation states of the upper mantle recorded by megacryst ilmenite in kimberlite and type A and type B spinel lherzolites: Contrib. Min. Pet., v. 85, p. 85-94.

ARIMA, M. and EDGAR, A.D., 1983, A high pressure experimental study on a magnesia-rich leucite lamproite from the west Kimberley area, Australia: Contrib. Min. Pet., v. 84, p. 228-234.

ARRIENS, P.A. and LAMBERT, I.B., 1969, On the age and strontium isotope geochemistry of granulite facies rocks from the Fraser Range, Western Australia, and the Musgrave Ranges, Central Australia: Geol. Soc., Australia, Spec. Publ. 2, p. 377-388.

ATKINSON, W.J., HUGHES, F.E., and SMITH, C.B., 1982, A review of the kimberlitic rocks of Western Australia, (abstract): Terra Cognita, v. 2, p. 204.

ATKINSON, W.J., HUGHES, F.E., and SMITH, C.B., 1984a, A review of the kimberlitic rocks of Western Australia, *in* Kimberlites I: Kimberlites and related rocks, *edited by* J. Kornprobst: Amsterdam, Elsevier, p. 195-224.

ATKINSON, W.J., SMITH, C.B., and BOXER, G.L., 1984b, The discovery and geology of the Argyle diamond deposits, Kimberley, Western Australia: Australasian Inst. Min. Met., Ann. Conf., Darwin, August 1984, p. 141-149.

ATKINSON, W.J., SMITH, C.B., and BOXER, G.L., 1984c, The discovery and evaluation of the Ellendale and Argyle lamproite diamond deposits, Kimberley Region, Western Australia: Denver, U.S.A, SME Conference, 1984.

BACHINSKI, W.S. and SCOTT, R.B., 1979, Rare earth and other trace element contents of minettes (mica lamprophyres): Geochim. Cosmochim. Acta, v. 43, p. 93-100.

BAILEY, D.K., 1969, The stability of acmite in the presence of H_2O: American Jour. Sci., v. 267-A (Schairer Vol.), p. 242-248.

BAILEY, D.K., 1980: Volatile flux, geotherms and the generation of the kimberlite-carbonatite-alkaline magma spectrum: Min. Mag., v. 43, p. 695-699.

BAILEY, D.K., 1982, Mantle metasomatism — continuing chemical change within the Earth: Nature, v. 296, p. 525-530.

BAILEY, D.K. 1984: Kimberlite, "The mantle sample" formed by ultrametamorphism, *in* Kimberlites I: Kimberlites and related rocks, *edited by* J. Kornprobst: Amsterdam, Elsevier, p. 323-333.

BARRETT, D.R. and BERG, G.W., 1975, Complementary petrographic and isotope ratio studies of South African kimberlites: Phys. Chem. Earth, v. 9, p. 619-675.

BARTON, M. and HAMILTON, D.L., 1979, The melting relationships of a madupite from the Leucite Hills, Wyoming, to 30 kb: Contrib. Min. Pet., v. 69, p. 133-142.

BARTON, M. and HAMILTON, D.L., 1982, Water-undersaturated melting experiments bearing upon the origin of potassium-rich magmas: Min. Mag., v. 45, p. 267-278.

BASU, A.R., RUBURY, E., MEHNERT, H., and TATSUMOTO, M., 1984, Sm-Nd, K-Ar and petrologic study of some kimberlites from eastern United States and their implication for mantle evolution: Contrib. Min. Pet., v. 86, p. 35-44.

BASU, A.R. and TATSUMOTO, M., 1980, Nd isotopes in selected mantle-derived rocks and minerals and their implications for mantle evolution: Contrib. Min. Pet., v. 75, p. 43-54.

BATES, R.L., and JACKSON, J.A., 1980, Glossary of geology (2nd. ed): Falls Church, Va., American Geol. Inst., 749 p.

BEARD, J.S, 1979, Vegetation survey of Western Australia, Kimberley 1:1 000 000 Vegetation Series, explanatory notes to sheet 1. The vegetation of the Kimberley area: University of Western Australia Press, 118 p.

BENNETT, R. and GELLATLY, D.C., 1970, Rb-Sr age determinations of some rocks from the west Kimberley region, Western Australia: Australia BMR, Rec. 1970/20 (unpublished).

BERG, G.W. and ALLSOPP, H.L., 1972, Low $^{87}Sr/^{86}Sr$ ratios in fresh South African kimberlites: Earth Plan. Sci. Letts., v. 16, p. 27-30.

BERRY, R.F. and GRADY A.E., 1981, Deformation and metamorphism of the Aileu Formation, north coast, East Timor, and its tectonic significance: Jour. Structural Geol., v. 3, p. 143-167.

BINNS, R.A., DUGGAN, M.B., and WILKINSON, J.F.G., 1970, High pressure megacrysts in alkaline lavas from northeastern New South Wales: American Jour. Sci., v. 269, p. 132-168.

BLATCHFORD, T., 1927, The geology of portions of the Kimberley Division, with special reference to the Fitzroy Basin and the possibilities of the occurrence of mineral oil: West Australia Geol. Survey, Bull. 93.

BOCTOR, N.Z. and MEYER, H.O.A., 1979, Oxide and sulfide minerals in kimberlite from Green Mountain, Colorado, *in* Kimberlites, diatremes and diamonds: Their geology, petrology and geochemistry, *edited by* F.R. Boyd and H.O.A. Meyer: Washington, American Geophys. Union, p. 217-228.

BOETTCHER, A.L., MYSEN, B.O., and MODRESKI, P.J., 1975, Melting in the mantle: phase relationships in natural and synthetic periodotite-H_2O and peridotite-H_2O-CO_2 systems at high pressures: Phys. Chem. Earth, v. 9, p. 855-867.

BOETTCHER, A.L. and O'NEILL, J.R., 1980, Stable isotope, chemical and petrographic studies of high pressure amphiboles and micas: evidence for metasomatism in the mantle source regions of alkali basalts and kimberlites: American Jour. Sci., v. 280A, p. 594-621.

BOFINGER, V.M., 1967, Geochronology of the east Kimberley area of Western Australia: Australian National University, Ph.D Thesis (unpublished).

BOXER, G.L., 1980a, Annual report on exploration completed within mineral claims 04/4055-4058, Brooking Gorge, Noonkanbah, Western Australia: CRA Exploration P/L, Report 130195 (unpublished).

BOXER, G.L., 1980b, Annual report on exploration completed within mineral claims 04/3611-16, 04/3680-83, 04/3676-79, J.K. Yard, Lennard River, Western Australia: CRA Exploration P/L, Report 130196 (unpublished).

BOXER, G.L., and HAEBIG, E.A., 1980a, Annual report for 1979 on exploration completed within mineral claims on the Hardman 1:100 000 map sheet 3861, West Kimberley Goldfield, W.A.: CRA Exploration P/L, Report 130191 (unpublished).

BOXER, G.L. and HAEBIG, E.A., 1980b, Annual report for 1979 on exploration completed within mineral claims in the Calwynyardah area, Ellendale 1:100 000 sheet, Western Australia: CRA Exploration P/L, Report 130192, (unpublished).

BOXER, G.L., and HAEBIG, E.A., 1980c, Annual report for 1979 on mineral claims 04/2777 and 04/2844-59, Gumhole, Noonkanbah, Western Australia: CRA Exploration P/L, Report 130197 (unpublished).

BOXER, G.L., SMITH, C.B., and LORENZ, V., 1986, Geology and volcanology of Argyle AK1 lamproite diatreme: Int. Kimberlite Conf., 4th, Perth, 1986, Extended Abstracts.

BOYD, F.R. and CLEMENT, C.R., 1977, Compositional zoning of olivines in kimberlite from the De Beers Mine, Kimberley, South Africa: Carnegie Inst., Washington, Yearbook for 1976, p. 485-487.

BOYD, F.R. and GURNEY, J.J., 1982, Low-calcium garnets: keys to craton structure and diamond crystallization: Washington, Carnegie Inst., Yearbook 1981, p. 261-267.

BOYD, F.R. and NIXON, P.H., 1973, Origin of the ilmenite-silicate nodules in kimberlites from Lesotho and South Africa, *in* Lesotho kimberlites, *edited by* P.H. Nixon: Lesotho Nat. Dev. Corp., Maseru, p. 254-268.

BOYD, F.R. and NIXON, P.H., 1978, Ultramafic nodules from the Kimberley pipes, South Africa: Geochim. Cosmochim. Acta, v. 42, p. 1367-1382.

BREY, G., BRICE, W.R., ELLIS, D.J., GREEN, D.J., HARRIS, K.L., and RYABCHIKOV, I.D., 1983, Pyroxene-carbonate reactions in the upper mantle: Earth Plan. Sci. Letts., v. 62, p. 63-74.

BROOKS, C., JAMES, D.E., and HARTE, S.R., 1976, Ancient lithosphere: Its role in young continental volcanism: Nature, v. 193, p. 1086-1094.

BUNTING, J.A., 1986, Geology of the eastern part of the Nabberu Basin: West. Australia Geol. Survey, Bull. 131.

BUNTING, J.A., de LAETER, J.R., and LIBBY, W.G., 1976, Tectonic subdivisions and geochronology of the northeastern part of the Albany-Fraser Province, Western Australia: West. Australia Geol. Survey Ann. Rept. 1975, p. 117-126.

CANDE, S.C. and MUTTER, J.C., 1982, A revised identification of the oldest sea-floor spreading anomalies between Australia and Antarctica: Earth Plan. Sci. Letts., v. 58, p. 151-160.

CARMICHAEL, I.S.E., 1967, The mineralogy and petrology of the volcanic rocks from the Leucite Hills, Wyoming: Contrib. Min. Pet., v. 15, p. 24-66.

CARSWELL, D.A., CLARKE, D.B., and MITCHELL, R.H., 1979, The petrology and geochemistry of ultramafic nodules from pipe 200, northern Lesotho, *in* The mantle sample: Inclusions in kimberlites and other volcanics, *edited by* F.R. Boyd and H.O.A. Meyer: Washington, American Geophys. Union, p. 127-144.

CARTER, J.D., 1974, Diamond exploration in Western Australia: West. Australia Geol. Survey, Ann. Rept. 1973, p. 73-79.

CHIN, R.J., HICKMAN, A.H., and TOWNER, R.R., 1982, Paterson Range, Western Australia (2nd ed.): West. Australia Geol. Survey, 1:250 000 Geological Series — Explanatory Notes.

CHIN, R.J., WILLIAMS, I.R., WILLIAMS, S.J., and CROWE, R.W.A., 1980, Rudall, Western Australia: West Australia Geol. Survey, 1:250 000 Geological Series — Explanatory Notes.

CLAOUÉ-LONG, J.C., THIRLWALL, M.F., and NESBITT, R.W. 1984, Revised Sm-Nd systematics of Kambalda greenstones, Western Australia: Nature, v. 307, p. 697-701.

CLEMENT, C.R., 1982, A comparative geological study of some major kimberlite pipes in the northern Cape and Orange Free State: Ph.D Thesis, University of Capetown, (unpublished).

CLEMENT, C.R. and SKINNER, E.M.W., 1979, A textural classification of kimberlitic rocks: Cambridge Kimberlite Symposium, 2nd, Abstracts (unpublished).

CLEMENT, C.R. and SKINNER, E.M.W., 1982, Kimberlite textures I: Terra Cognita, v. 2, p. 209.

CLEMENT, C.R. SKINNER, E.M.W., and SCOTT-SMITH, B.H., 1977, Kimberlite redefined: International Kimberlite Conf., 2nd, Santa Fe, Abstracts (unpublished).

CLEMENT, C.R., SKINNER, E.M.W., and SCOTT-SMITH, B.H., 1984, Kimberlite redefined: Jour. Geol., v. 92, p. 223-228.

CLIFFORD, T.N., 1966, Tectono-metallogenic units and metallogenic provinces of Africa: Earth Plan. Sci. Letts., v. 1, p. 421-434.

COCKBAIN, A.E., 1984, Stromatoporoids from the Devonian Reef Complexes, Canning Basin, Western Australia: West. Australia Geol. Survey, Bull. 129, 108 p.

COLLERSON, K.D., 1982, Age and strontium isotope systematics of the Mt Weld carbonatite, Western Australia: Report to Union Oil (unpublished).

COMPSTON, W. and ARRIENS, P.A., 1968, The Precambrian geochronology of Australia: Canadian Jour. Earth Sci., v. 5, p. 561-583.

COOPER, I.S., 1982, Fitzroy Joint Venture, annual report for 1981: Seltrust Mining Corporation (unpublished).

CROWE, R.W.A. and TOWNER, R.R., 1976, Permian depositional history of the Noonkanbah 1:250,000 sheet area, W.A: Australia BMR Rec. 1976/24 (unpublished).

CROWE, R.W.A. and TOWNER, R.R., 1981, Noonkanbah, Western Australia: West. Australia Geol. Survey, 1:250 000 Geol. Series — Explanatory Notes.

CUNDARI, A., 1973, Petrology of the leucite-bearing lavas in New South Wales: Geol. Soc. Australia Jour. v. 20, p. 465-492.

DANCHIN, R.V., BRISTOW, J.W., ROBEY, J.V.A., and SCOTT-SMITH, B.H., 1985, The petrolology of three suites of Australian kimberlitic intrusions: Int. Kimberlite Symposium, Yakutsk, U.S.S.R. (Abstract).

DAWSON, J.B., 1967, A review of the geology of kimberlite, *in* Ultramafic and related rocks, *edited by* P.J. Wyllie: New York, Wiley, p. 241-251.

DAWSON, J.B., 1970, The structural setting of African kimberlite magmatism, *in* African magmatism and tectonics, *edited by* T.N. Clifford and I.G. Gass: Edinburgh, Oliver & Boyd, p. 321-335.

DAWSON, J.B., 1971, Advances in kimberlite geology: Earth Sci. Rev., v. 7, p. 187-214.

DAWSON, J.B., 1980, Kimberlites and their xenoliths: Berlin, Springer Verlag, 250p.

DAWSON, J.B. 1984a, Petrogenesis of kimberlite, *in* Kimberlite occurrence and origin, *edited by* J.E. Glover and P.G. Harris: Univ. West. Australia, Geol. Dept. Publ. No. 8, p. 103-111.

DAWSON, J.B., 1984b, Contrasting types of upper mantle metasomatism? *in* Kimberlites II: The mantle and crust-mantle relationships, *edited by* J Kornprobst: Amsterdam, Elsevier, p. 289-294.

DAWSON, J.B., in press, The kimberlite clan: relationship to olivine and leucite-lamproites, and inferences for upper mantle metasomatism , *in* Alkaline rocks, *edited by* J.G. Fitton and B.G.J. Upton: London, Geol. Soc. Spec. Publ.

DAWSON, J.B. and SMITH, J.V., 1977, The MARID (mica-amphibole-rutile-ilmenite-diopside) suite of xenoliths in kimberlite: Geochim. Cosmochim. Acta, v. 41, p. 309-323.

DAWSON, J.B. and SMITH, J.V., 1982, Upper mantle amphiboles: A review: Min. Mag., v. 45, p. 35-46.

DAWSON, J.B., SMITH, J.V., and HERVIG, R.L., 1977, Late-stage diopside in kimberlite groundmass: N. Jb. Mineral., v. 2, p. 529-547.

DAWSON, J.B., and STEPHENS, W.E., 1975, Statistical analysis of garnets from kimberlites and associated xenoliths: Jour. Geol., v. 83, p. 589-607.

DEER, W.A., HOWIE, R.A., and ZUSSMAN, J., 1962, Rock-forming minerals, v. 1 (1st ed.): London, Longmans, 379 p.

DEER, W.A., HOWIE, R.A., and ZUSSMAN, J., 1982, Rock-forming minerals, v. 1A, Orthosilicates. (2nd ed.): London, Longmans, 919 p.

de LAETER, J.R. and BLOCKLEY, J.G., 1972, Granite ages within the Archaean Pilbara Block, Western Australia: Geol. Soc. Australia, Jour. v. 19, p. 363-370.

de LAETER, J.R., LIBBY, W.G., and TRENDALL, A.F., 1981a, The older Precambrian geochronology of Western Australia: Geol. Soc. Australia, Spec. Publ. No. 7, p. 145-147.

de LAETER, J.R., PEERS, R., and TRENDALL, A.F., 1974, Petrography, chemical composition and geochronology of two dolerite sills from the Precambrian Weeli Wolli Formation, Hamersley Group: West. Australia Geol. Survey, Ann. Rept 1973, p. 82-91.

de LAETER, J.R., WILLIAMS, I.R., ROSMAN, K.J.R., and LIBBY, W.G., 1981b, A definitive 3 350 m.y. age from banded gneiss, Mount Narryer area, Western Gneiss Terrain: West. Australia Geol. Survey, Ann. Rept 1980, p. 94-98.

DERRICK, G.M., and GELLATLY, D.C., 1971, The Precambrian geology of the Oscar Range Inlier, Lennard River 1:250 000 sheet area, SE51-8, Western Australia: Australia BMR, Rec. 1971/61 (unpublished).

DERRICK, G.M., and GELLATLY, D.C., 1972, New leucite lamproites from the West Kimberley: Australia BMR, Bull. 125, p. 103-120.

DERRICK, G.M., and PLAYFORD, P.E., 1973, Lennard River, Western Australia: Australia BMR, 1:250 000 Geological Series — Explanatory Notes.

DOEPEL, J.J.G., 1975, Albany-Fraser Province, *in* Geology of Western Australia: West. Australia Geol. Survey, Mem. 2, p. 94-102.

DOW, D.B. and GEMUTS, I., 1967, Dixon Range, Western Australia: Australia BMR, 1:250 000 Geological series — Explanatory notes.

DOW, D.B. and GEMUTS, I., 1969, Geology of the Kimberley region, Western Australia: The East Kimberley: Australia BMR, Bull. 106.

DRUCE, E.C., and RADKE, B.M., 1979, The geology of the Fairfield Group, Canning Basin, Western Australia: Australia BMR, Bull. 200.

EDGAR, A.D., CONDLIFFE, E., BARNET, R.L., and SHIRRAN, R.J., 1980, An experimental study of an olivine ugandite magma and mechanisms for the formation of its K-enriched derivatives: Jour. Petrol., v. 21, p. 475-497.

EDGAR, A.D., GREEN, D.H., and HIBBERSON, W.D., 1976, Experimental petrology of a highly potassic magma: Jour. Petrol., v. 17, p. 339-356.

EGGLER, D.H., 1978, The effect of CO_2 upon partial melting of peridotite in the system Na_2O-CaO-MgO-SiO_2-CO_2 to 35 kb, with an analysis of melting in a peridotite H_2O-CO_2 system: American Jour. Sci., v. 278, p. 305-343.

EGGLER, D.H. and BAKER, D.R., 1982, Reduced volatiles in the system C-O-H: Implications to mantle melting, fluid formation, and diamond genesis, *in* High pressure research in geophysics, *edited by* S.A. Kimoto and M.H. Manghnani: Tokyo, p. 237-250.

EGGLER, D.H. and WENDLANDT, R.F., 1979, Experimental studies on the relationship between kimberlite magmas and partial melting of peridotite, *in* Kimberlites, diatremes and diamonds: Their geology, petrology and geochemistry, *edited by* F.R. Boyd and H.O.A. Meyer: Washington, American Geophys. Union, p. 330-343.

ELLIS, D.E. and WYLLIE, P.J., 1980, Phase relations and their petrological implications in the system MgO-SiO_2-H_2O-CO_2 at pressures up to 100 kb: American Min., v. 65, p. 540-556.

EMBLETON, B.J.J., 1981, A review of the palaeomagnetism of Australia and Antarctica, *in* Paleoreconstruction of the Continents, *edited by* M.W. McElhinny and D.A. Valencio: American Geophys. Union, Geodynamics Ser. 2, p. 77-92.

ERLANK, A., ALLSOPP, H.L., HAWKESWORTH, C.J. and MENZIES, M.A., 1982, Chemical and isotopic characteristics of upper mantle metasomatism in peridotite nodules from the Bultfontein kimberlite: Terra Cognita, v. 2, p. 261-263.

FABRIES, J., 1979, Spinel-olivine geothermometry in peridotite from ultramafic complexes: Contrib. Min. Pet., v. 69, p. 329-336.

FARQUHARSON, R.A., 1920, Petrological work: West. Australia Geol. Survey, Ann. Rept 1919, p. 41-45.

FARQUARSON, R.A., 1922, Petrological work: West. Australia Geol. Survey, Ann. Rept 1921, p. 53-58.

FAUST, G.T., 1963, Phase transition in synthetic and natural leucite: Schweiz. Min. Petr. Mitt., v. 43, p. 165-195.

FERGUSON, A.K., 1978, The crystallization of pyroxenes and amphiboles in some alkaline rocks and the presence of a pyroxene compositional gap: Contrib. Min. Pet., v. 67, p. 11-15.

FERGUSON, J., ELLIS, D.E., and ENGLAND, R.N., 1977, A unique spinel-garnet lherzolite inclusion in kimberlite from Australia: Geology, v. 5, p. 278-280.

FERGUSON, J. and SHERATON, J.W., 1979, Petrogenesis of kimberlitic rocks and associated xenoliths of southeastern Australia, *in* Kimberlites, diatremes and diamonds: Their geology, petrology, and Geochemistry, *edited by* F.R. Boyd and H.O.A. Meyer: Washington, American Geophys. Union, p. 140-160.

FESQ, H.W., KABLE, E.J.D., and GURNEY, J.J., 1975, Aspects of the geochemistry of kimberlites from the Premier mine and other selected South African occurrences with particular reference to the rare earth elements: Phys. Chem. Earth, v. 9, p. 687-709.

FIELDING, D.C., 1983a, Final report on mineral claims 80/5359-5388, Maude Creek, and 80/5333-5358, Devils Elbow, Lissadell, Western Australia: CRA Exploration P/L, Report 130107 (unpublished).

FIELDING, D.C., 1983b, Final report on exploration completed on mineral claims 80/5671-5677, Elgee, Lissadell, Western Australia: CRA Exploration P/L, Report 13105 (unpublished).

FIELDING, D.C., 1983c, Final report on mineral claims 80/5464, 5647, Dunham, and 80/5662-5666, Saw Ranges, Lissadell, Western Australia: CRA Exploration P/L, Report 130106 (unpublished).

FISHER, R.V. and SCHMINCKE, H.-U., 1984, Pyroclastic Rocks: Berlin, Springer Verlag, 472 p.

FISHER, R.V., and WATERS, A.C., 1970, Base surge bed forms in maar volcanoes: American Jour. Sci., v. 286, p. 157-180.

FITTON, A., 1980, Annual report on exploration completed within Temporary Reserve 6576H and 6577H Forrest River, Drysdale, Western Australia: CRA Exploration P/L, Report 130260 (unpublished).

FITZGERALD, W.V., 1907, Reports on portions of the Kimberleys (1905-6): West. Australia, Parlt. Papers No. 19 of 1907.

FLETCHER, J.R., ROSMAN, K.J.R., WILLIAMS, I.R., HICKMAN, A.H., and BAXTER, J.L., 1984, Sm-Nd geochronology of greenstone belts in the Yilgarn Block, Western Australia: Precamb. Res., v. 26, p. 333-361.

FLETCHER, I.R., WILDE, S.A., LIBBY, W.G., and ROSMAN, K.J.R., 1983a, Sm-Nd model ages across the margins of the Archaean Yilgarn Block — II. Southwest transect into the Proterozoic Albany-Fraser Province: Geol. Soc. Australia, Jour., v. 30, p. 333-340.

FLETCHER, I.R., WILDE, S.A., and ROSMAN, K.J.R., 1985, Sm-Nd model ages across the margins of the Archaean Yilgarn Block, Western Australia — III. The western margin: Australian Jour. Earth Sci., v. 32, p. 73-82.

FLETCHER, I.R., WILLIAMS, S.J., GEE, R.D., and ROSMAN, K.J.R., 1983b, Sm-Nd model ages across the margins of the Archaean Yilgarn Block, Western Australia; northwest transect into the Proterozoic Gascoyne Province: Geol. Soc. Australia, Jour., v. 30, p. 167-174.

FOLEY, S.F., 1986, The oxidation state of lamproite magmas. Tsch. Min. Pet. Mitt., v. 34, p. 217-238.

FOLEY, S.F., TAYLOR, W.R., and GREEN, D.H., 1986, The effect of fluorine on phase relationships in the system KAlSiO-Mg_2SiO_4-SiO_2 and the solution mechanism of fluorine in silicate melts: Contrib Min. Pet.

FORMAN, D.J., and WALES, D.W., 1981, Geological evolution of the Canning Basin, Western Australia: Australia BMR, Bulletin 210.

FRANCIS, E.H., 1970, Bedding in Scottish (Fifeshire) tuff-pipes and its relevance to maars and calderas: Bull. Volc., v. 34, p. 697-712

FRANTSESSON, E.V., 1970, The petrology of kimberlite: Canberra, Australian National University Press.

FREY, F.A., FERGUSON, J., and CHAPPELL, B.W., 1977, Petrogenesis of South African and Australian kimberlitic suites: International Kimberlite Conf., 2nd, Santa Fe., Abstracts Volume, (unpaged).

GARLICK, H.J., 1982, Maude Creek kimberlite occurrence, Kimberley Goldfield, Western Australia: Gem Exploration P/L, (unpublished).

GEE, R.D., 1979, Structure and tectonic style of the Western Australian shield: Tectonophysics, v. 58, p. 327-369.

GELLATLY, D.C., 1971, Possible Archaean rocks of the Kimberley region, Western Australia: Geol. Soc. Australia, Spec. Publ. No. 3, p. 93-101.

GELLATLY, D.C., 1979, W.A. Diamonds Project (908): Amax Iron Ore Corporation (unpublished).

GELLATLY, D.C., 1980, Annual Report, Hooper Hills Bore area Kimberlite prospects: Amax Iron Ore Corporation (unpublished).

GELLATLY, D.C. and SOFOULIS, J., 1969, Drysdale and Londonderry, W.A: West. Australia Geol. Survey, 1:250 000 Geol. Series — Explan. Notes.

GELLATLY, D.C., SOFOULIS, J., DERRICK, G.M., and MORGAN, C.M., 1968, The older Precambrian geology of the Lennard River 1:250 000 sheet area, SE51-8, Western Australia: Australia BMR, Rec. 1968/126 (unpublished).

GEMUTS, I., 1971, Metamorphic and igneous rocks of the Lamboo Complex, East Kimberley Region, Western Australia: Australia BMR, Bull. 107.

GILFILLAN, M.A., 1977, Wilson River area, Kimberleys, W.A., final report on Temporary Reserves 6319H, 6323H and 6324H: CRA Exploration P/L, Report 130018 (unpublished).

GILFILLAN, M.A. and SMITH, C.B., 1977, Wilson River area, Kimberleys, Western Australia, Temporary Reserves 6319H, 6323H and 6324H — Annual Report for 1977: CRA Exploration P/L, Report 130018 (unpublished).

GOLD, D.P., 1972, Monteregian Hills: Diatremes, kimberlites, lamprophyres and intrusive breccias west of Montreal: Int. Geol. Congress, 24th, Montreal, Excursion Handbook B-10, 32 p.

GOLD, D.P., 1984, A diamond exploration philosophy for the 1980's: Penn. State Univ., Earth and Min. Sci. v. 53, No. 4, p. 37-42.

GOODE, A.D.T., 1981, Proterozoic geology of Western Australia, *in* Precambrian geology of the southern hemisphere, *edited by* D.R. Hunter: Amsterdam, Elsevier, p. 105-203.

GREEN, D.H., 1985, The upper mantle as the source for magmatic fluids, *in* Conference on stable isotopes and fluid processes in mineralization — 5, *edited by* H.K. Herbert: Univ. Queensland, Dept. Geol. Min., Abstract.

GREEN, D.H. and SOBOLEV, N.V., 1975, Coexisting garnets and ilmenites synthesized at high pressures from pyrolite and olivine basanite and their significance for kimberlite assemblages: Contrib. Min. Pet., v. 50, p. 217-229.

GREGORY, C.J., 1981, Annual report on exploration completed within mineral claims 09/2199-2216 and 09/3082-3106, Winning Pool and Kennedy Range, Western Australia: CRA Exploration P/L, Report 130301 (unpublished).

GREGORY, C.J., 1982, Final report on exploration completed within mineral claims 08/2873-2876 and 3171-3182, Mia Mia, Winning Pool, Western Australia: CRA Exploration P/L, Report 130341 (unpublished).

GREGORY, G.P., 1980, Mount Wynne Joint Venture, annual report for 1979: BP Minerals, (unpublished).

GREGORY, G.P., 1981a, Mount Wynne Joint Venture, annual report for 1980: BP Minerals, (unpublished).

GREGORY, G.P., 1981b, Fitzroy Joint Venture, annual report for 1980: BP Minerals, (unpublished).

GREGORY, G.P., 1984, Exploration for primary diamond deposits with special emphasis on the Lennard Shelf W.A., *in* The Canning Basin, W.A., *edited by* P.G. Purcell: Geol. Soc. Aust./ Pet. Expl. Soc. Aust., Symposium, Perth, 1984, Proceedings, p. 475-484.

GROOM, F.F., 1896, Report of a visit to Nullagine, Pilbara district, to examine the country reported to be diamond yielding. West. Australia Dept. Mines, Ann. Rept 1895, p. 27.

GUPTA, A.K. and YAGI, K., 1980, Petrology and genesis of leucite-bearing rocks. Berlin, Springer-Verlag.

GURNEY, J.J., 1984, A correlation between garnets and diamonds in kimberlites, *in* Kimberlite occurrence and origin, *edited by* J.E. Glover and P.G. Harris: University of Western Australia, Geol. Dept., Publ. No. 8, p. 143-166.

GURNEY, J.J., FESQ, H.W., and KABLE, E.J.D., 1973, Clinopyroxene-ilmenite intergrowths from Lesotho kimberlites: A reappraisal, *in* Lesotho Kimberlites, *edited by* P.H. Nixon: Maseru, Lesotho Nat. Dev. Corp., p. 238-253.

GURNEY, J.J. and HARRIS, J.W., 1982, Some observations relevant to the formation of natural diamonds: Terra Cognita, v. 2, p. 199.

GURNEY, J.J., HARRIS, J.W., and RICKARD, R.S., 1979, Silicate and oxide inclusions in diamond from the Finsch kimberlite pipe, *in* Kimberlites, diatremes, and diamonds: Their geology, petrology and geochemistry *edited by* F.R. Boyd and H.O.A. Meyer: Washington, American Geophys. Union, p. 1-15.

GURNEY, J.J. and HARTE, B., 1980, Chemical variations in upper mantle nodules from southern African kimberlites: Royal. Soc. (London) Phil. Trans., v. A297, p. 273-293.

GURNEY, J.J. and SWITZER, G.S., 1973, The discovery of garnets closely related to diamonds in the Finsch pipe, South Africa: Contrib. Min. Pet., v. 39, p. 103-116.

HAEBIG, E.A., 1979a, Annual Report for 1978 on mineral claims 04/1848-1851, 04/2149-2150 and 04/2282, West Kimberley Goldfield, W.A: CRA Exploration P/L, (unpublished).

HAEBIG, E.A., 1979b, Annual report for 1978, mineral claims on the Hardman 1:100,000 map sheet 3861, West Kimberley Goldfield, W.A: CRA Exploration P/L, Report 130041 (unpublished).

HAEBIG, E.A., 1982, Final report on mineral claim 04/2560, Merrilees Bore, Lennard River, Western Australia: CRA Exploration P/L, Report 130089 (unpublished).

HAEBIG, E.A., 1983a, Final Report on Exploration completed at Big Spring, Leopold Downs 1:100,000 map sheet 3962, Western Australia: CRA Exploration P/L, Report 130086 (unpublished).

HAEBIG, E.A., 1983b, Final Report on mineral claims 04/3611-16, 04/3680-83, 04/3676-79, J K Yard, Lennard River, Western Australia: CRA Exploration P/L, Report 130096 (unpublished).

HAEBIG, E.A., 1983c, Final report on exploration completed within mineral claims on the Hardman 1:100,000 map sheet, Noonkanbah, Western Australia: CRA Exploration P/L, Report 130093 (unpublished).

HAGGERTY, S.E., 1975, The chemistry and genesis of opaque minerals in kimberlites: Phys. Chem. Earth, v. 9, p. 295-307.

HAGGERTY, S.E., 1976, Opaque mineral oxides in terrestrial igneous rocks, *in* Reviews in mineralogy — v. 3, Oxide minerals, *edited by* D. Rumble: Min. Soc. America, p. 101-300.

HAGGERTY, S.E., HARDIE, R.B., and McMAHON, B.M., 1979, The mineral chemistry of ilmenite nodule associations from the Monastery diatreme, *in* The mantle sample: Inclusions in kimberlite and other volcanics, *edited by* F.R. Boyd and H.O.A. Meyer: Washington, American Geophys. Union, p. 249-256.

HAGGERTY, S.E. and TOMKINS, L.A., 1983, Redox state of Earth's upper mantle from kimberlitic ilmenites: Nature, v. 303, p. 295-300.

HALL, A.E. and SMITH, C.B., 1984, Lamproite diamonds — are they different? *in* Kimberlite occurrence and origin, *edited by* J.E. Glover and P.G. Harris: University of Western Australia, Geology Dept., Publ. 8, p. 167-212.

HALL, A.M., THOMAS, M.F., and THORP, M.B., 1985, Late Quaternary alluvial placer development in the humid tropics: The case of the Birim Diamond Placer, Ghana: Geol. Soc. (London) Jour. v. 142, p. 777-787.

HANCOCK, S.L. and RUTLAND, R.W.R., 1984, Tectonics of an early Proterozoic geosuture: The Halls Creek orogenic sub-province, northern Australia: Jour. Geodynamics, v. 1, p. 387-432.

HARDMAN, E.T., 1884, Report of the geology of the Kimberley district, Western Australia: West Australia, Parlt. Papers No.31 of 1884.

HARMS, J.E., 1959, The geology of the Kimberley Division, Western Australia and of an adjacent area of the Northern Territory: Adelaide Univ., M.Sc Thesis, (unpublished).

HARTE, B., 1977, Rock nomenclature with particular relation to deformation and recrystallization textures in olivine-bearing xenoliths: Jour. Geol., v. 85, p. 279-288.

HARTE, B., 1983, Mantle peridotites and processes — The kimberlite sample, *in* Continental basalts and mantle xenoliths, *edited by* C.J. Hawkesworth and M.J. Norry: U.K., Shiva, p. 45-91.

HAWKESWORTH, C.J., ROGER, N.W., van CALSTEREN, P.W.C., and MENZIES, M.A., 1984, Mantle enrichment processes: Nature, v. 311, p. 331-335.

HAWTHORNE, J.B., 1975, Model of a kimberlite pipe: Phys. Chem. Earth, v. 9, p. 1-15

HAYNES, R.W., 1971, Completion Report on Temporary Reserves Nos: 4665H, 5184H, and 5423H, Lennard River area, Western Australia: Exoil N.L., Transoil N.L., and Petromin N.L. (unpublished).

HAYS, J., 1967, Land surfaces and laterites in the north of the Northern Territory, *in* Landform studies from Australia and New Guinea, *edited by* J.N. Jennings and J.A. Mabbut: Canberra, Australian National University, 1967, p. 182-210.

HEARN, B.C., 1968, Diatremes with kimberlite affinitites in north-central Montana: Science, v. 159, p. 662-625.

HEIKEN, G., 1974, An atlas of volcanic ash: Smithsonian Contrib. Earth Sci., v. 12, 101 p.

HENSHAW, D.E., 1955, The structure of wadeite: Min. Mag., v. 30, p. 585-595.

HICKMAN, A.H. and de LAETER, J.R., 1977, The depositional environment and age of a shale within the Hardey Sandstone of the Fortescue Group: West. Australia Geol. Survey, Ann. Rept. 1976, p. 62-68.

HOCKING, R.M., MOORS, H.T. and van de GRAAFF, W.J.E., in press: The Geology of the Carnarvon Basin, W.A. West. Australia Geol. Survey, Bull. 133.

HOFFMAN, A.W. and WHITE, W.M., 1982, Mantle plumes from subducted oceanic crust: Earth Plan. Sci. Letts., v. 57, p. 421-436.

HONNOREZ, J. and KIRST, P., 1975, Submarine basaltic volcanism: Morphometric parameters for discriminating hyaloclastites from hyalotuffs: Bull. Volc., v. 39, p. 1-25.

HUGHES, F.E., 1978, Annual report for 1977, West Kimberley Goldfield, W.A: CRA Eploration P/L, (unpublished).

HUGHES, F.E., and SMITH, C.B., 1977, Annual report for 1976 on Big Spring mineral claims: CRA Exploration P/L, (unpublished).

HUGHES, F.E., and SMITH, C.B., 1978a, Annual report for 1977 on Big Spring mineral claims, West Kimberley Goldfield: CRA Exploration. P/L, (unpublished).

HUGHES F.E. and SMITH, C.B., 1978b, Annual report for 1977, mineral claim 04/2282, Big Spring West, West Kimberley Goldfield: CRA Exploration P/L, (unpublished).

HUGHES, F.E. and SMITH, C.B., 1978c, Annual report for 1977, Mineral Claim 04/2288, Mount Abbott, West Kimberley Goldfield: CRA Exploration P/L, (unpublished).

HURLEY, N.F., 1984, Geology of the Oscar Range (Devonian) reef complex, Canning Basin, Western Australia: A.A.P.G., Ann. Convention, May 1984 (Abstract).

HURLEY, N.F., 1985, Geology of the Oscar Range Devonian reef complex, Canning Basin, Western Australia: Univ. Michigan, Ph.D. Thesis, (unpublished).

HUTTON, G.J., 1985, Annual report on the Nullagine alluvial gold mine, Pilbara Mineral Field, Western Australia: Metana Minerals, (unpublished).

IRVINE, T.N., 1965, Chromian spinel as a petrogenetic indicator; Part 1, Theory: Canadian Jour. Earth Sci., v. 2, p. 648-671.

JAQUES, A.L., in prep., F-rich micas in the West Kimberley lamproites: Contrasts with kimberlites and other micaceous alkaline ultramafic intrusions:

JAQUES, A.L., CHAPPELL, B.W., SUN, S-S., LEWIS, J.D., and SMITH, C.B., 1986, The West Kimberley lamproites: Intraplate volcanism of extreme character: Int. Volcanol. Congress, New Zealand, (Abstract).

JAQUES, A.L., CREASER, R.A., FERGUSON, J., and SMITH, C.B., 1986, A review of the alkaline rocks of Australia: Geol. Soc. South Africa, Trans., v. 88.

JAQUES, A.L., FERGUSON, J., and SMITH, C.B., 1984c, Kimberlites in Australia, *in* Kimberlite occurrence and origin, *edited by* J.E. Glover and P.G. Harris: Univ. Western Australia, Geol. Dept., Publ. 8, p. 227-274.

JAQUES, A.L. and FOLEY, S.F., 1985, The origin of Al-rich spinel inclusions in leucite from the leucite lamproites of Western Australia: American Min., v. 70, p. 1143-1150.

JAQUES, A.L., GREGORY, G.P., LEWIS, J.D., and FERGUSON, J. 1982, The ultrapotassic rocks of the West Kimberley region, Western Australia and a new class of diamondiferous kimberlites: Terra Cognita, v. 2, p. 251-252.

JAQUES, A.L., LEWIS, J.D., SMITH, C.B., GREGORY, G.P., FERGUSON, J., CHAPPELL, B.W., and McCULLOCH, M.T., 1984a, The diamond-bearing ultrapotassic (lamproitic) rocks of the west Kimberley region, Western Australia, *in* Kimberlites I: Kimberlites and related rocks, *edited by* J. Kornprobst: Amsterdam, Elsevier, p. 225-254.

JAQUES, A.L., WEBB, A.W., FANNING, C.M., BLACK, L.P., PIDGEON, R.T., FERGUSON, J., SMITH, C.B., and GREGORY, G.P., 1984b, The age of the diamond bearing pipes and associated leucite lamproites of the West Kimberley region, Western Australia: BMR Jour. of Australian Geol. and Geophys., v. 9, p. 1-7.

JENKE, G., 1983, The role of geophysics in the discovery of the Ellendale and Fitzroy kimberlites: Australian Soc. Expl. Geophys., Conference Abstracts, Brisbane, p. 66-72.

JEPPE, J., 1971, Reports on Temporary Reserves Nos: 4630H-4637H, 4644H and 4659H: Stellar Minerals N.L. (unpublished).

JONES, A.P., SMITH, J.V., and DAWSON, J.B., 1982, Mantle metasomatism in 14 veined peridotites from Bultfontein Mine, South Africa: Jour. Geol., v. 90, p. 435-453.

JONES, D.J., 1984, Difficulties associated with using indicator minerals for diamond exploration in north Queensland: Australasian Inst. Min. Metall., Ann Conf, Darwin, 1984, p. 127-139.

JORDAN, T.H., 1978, Composition and development of the continental tectosphere: Nature, v. 274, p. 544-548.

JORDAN, T.H., 1981, Continents as a chemical boundary layer: Royal Soc. (London), Phil. Trans., v. A301, p. 359-373.

JOYCE, J. and MARX, M.R., 1981a, Final Report on Temporary Reserves 7724H to 7726H, 7728H to 7738H: Stockdale Prospecting Ltd (unpublished).

JOYCE, J. and MARX, M.R., 1981b, Final report on Temporary Reserves 7352H-7354H, Winning Pool, Western Australia: Stockdale Prospecting Ltd. (unpublished).

KAPLAN, G., FAURE, D., ELLOY, R., and HEILAMMER, R., 1967, Contribution à l'étude de l'orgines des lamproites: Centre Rech. PAU-SNPA, Bull. v. 1, p. 153-159.

KAY, R.W., and GAST, P.W., 1973, The rare earth content and origin of alkali-rich basalts: Jour. Geol., v. 81, p. 653-682.

KERR, I.D., 1983, Final report on exploration completed within mineral claims 09/2199-2216, 09/3082-3106, Wandagee, Winning Pool and Kennedy Range, Western Australia: CRA Exploration P/L, Report 13101 (unpublished).

KIENLE, J., KYLE, P.R., SELF,S., MOTYKA, R.J., and LORENZ, V., 1980, Ukinrek Maars, Alaska, 1 April 1977; eruption sequence, petrology and tectonic setting: Jour. Volcanol. Geotherm. Res., v. 7, p. 11-37.

KNOPF, D., 1970, Les kimberlites et les roches aparantées de Côte d'Ivoire: Direction des Mines et Géologie de Côte d'Ivoire, Bull Nr. 3.

KRAMERS, J.D., 1977, Lead and strontium isotopes in inclusions in diamonds and in mantle-derived xenoliths from southern Africa: Int. Kimberlite Conf., 2nd., Santa Fe, Abstract (unpaged).

KRAMERS, J.D., 1979, Lead, uranium, strontium, potassium and rubidium in inclusion-bearing diamonds and mantle-derived xenoliths from southern Africa: Earth Plan. Sci. Letts., v. 42, p. 58-70.

KRAMERS, J.D., RODDICK, J.C.M., and DAWSON, J.B., 1983, Trace element and isotope studies on veined metasomatic and "MARID" xenoliths from Bultfontein, South Africa: Earth Plan. Sci. Letts., v. 65, p. 90-106.

KUEHNER, S.M., EDGAR, A.D., and ARIMA, M., 1981, Petrogenesis of the ultrapotassic rocks from the Leucite Hills, Wyoming: American Min., v. 66, p. 663- 677.

LAWRENCE, M.J., 1971, The diamond search in Australia: Applications of a mobile prospecting unit and the concept of mineral-geochemistry: Australasian Inst. Min. Met., Ann. Conf., New Zealand (abstract).

LEAKE, B.E., 1978, Nomenclature of amphiboles: Canadian Mineralogist, v. 16, p. 501-520.

Le MAITRE, R.W., 1975, Volcanic rocks from Edel No. 1 petroleum exploration well, offshore Carnarvon Basin, Western Australia: Geol. Soc. Australia, Jour., v. 22, p. 167-174.

LEWIS, H.C., 1887, On a diamantiferous peridotite and the genesis of diamond: Geol. Mag. N.S., v. 5, p. 22-24.

LEYS, C.A., 1983, Volcanic sedimentary processes during formation of the Sæfell tuff-ring, Iceland: Royal Soc. Edinburgh, Trans. Earth Sci., v. 74, p. 15-22.

LIBBY, W.G. and de LAETER, J.R., 1981, Rb-Sr geochronology of alkaline granitic rocks in the Eastern Goldfields Province: West. Australia Geol. Survey, Ann. Rept 1980, p. 98-103.

LONGMAN, M.J., 1980, Location of kimberlite intrusives using landsat digital data, *in* Kimberlites and diamonds, *edited by* J.E. Glover and D.I. Groves: Univ. West. Australia, Geology Dept., Publ. 5, p. 89-95.

LORENZ, V., 1973, On the formation of maars: Bull. Volc., v. 37, p. 183-204.

LORENZ, V., 1975, Formation of phreatomagmatic maar-diatreme volcanoes and its relevance to kimberlite diatremes: Phys. Chem. Earth, v. 9, p. 17-27

LORENZ, V., 1979, Phreatomagmatic origin of the olivine melilitite diatremes of the Swabian Alb, Germany, *in* Kimberlites, diatremes and diamonds: Their geology, petrology, and geochemistry, *edited by* F.R. Boyd and H.O.A. Meyer: Washington, American Geophys. Union p. 354-363.

LORENZ, V., 1984, Explosive volcanism of the West Eifel Volcanic Field, Germany, *in* Kimberlites I: Kimberlites and related rocks, *edited by* J. Kornprobst: Amsterdam, Elsevier, p. 299-307.

LOWE, D.R., 1975, Water escape structures in coarse-grained sediments: Sedimentology, v. 22, p. 157-204.

LUTH, W.C., 1967, Studies in the system $KAlSiO_4$-SiO_2: I. Inferred phase relations and applications: Jour. Pet., v. 8, p. 372-416.

McCALLUM, M.E., COOPERSMITH, H.G., and HODGE, C.W., 1982, Mineralogical and textural-genetic classification of kimberlites in northern Colorado and southern Wyoming, U.S.A: Terra Cognita, v. 2, p. 209.

McCULLOCH, M.T., JAQUES, A.L., NELSON, D.R., and LEWIS, J.D., 1983, Nd and Sr isotopes from kimberlites and lamproites from Western Australia: An enriched mantle origin: Nature, v. 32, p. 400-403.

MacGREGOR, I.D., 1975, Petrologic and thermal structure of the upper mantle beneath South Africa in the Cretaceous: Phys. Chem. Earth, v. 9, p. 455-466.

MacGREGOR, I.D., 1979, Mafic and ultramafic xenoliths from the Kao kimberlite pipe, *in* The mantle sample: Inclusions in kimberlites and other volcanics, *edited by* F.R. Boyd and H.O.A. Meyer: Washington, American Geophys. Union, p. 156-172.

MacLEAN, H.D., 1972, Final Report, Lennard Shelf aeromagnetic survey, Canning district of northwest Australia: West Australian Petroleum Pty Ltd (unpublished).

McNEVIN, A.A., 1977, Diamonds in New South Wales: New South Wales Geol. Survey, Min. Res. Bull. 42.

MARX, M.R., 1982, Final Report, Temporary Reserves 7398H and 8033H, St George's Range, Western Australia: Stockdale Prospecting Ltd (unpublished).

MARX, M.R., 1984a, Winning Pool, mineral claim 09/3112, final report: Stockdale Prospecting Ltd. (unpublished).

MARX, M.R., 1984b, Winning Pool, mineral claims 09/3207 and 09/3208, final report: Stockdale Prospecting Ltd. (unpublished).

MASON, B., 1977, Elemental distribution in minerals from the Wolgidee Hills intrusion, Western Australia: New Zealand DSIR, Bull., v. 128, p. 114-120.

MEAKINS, A., 1983, Geology and genesis of the Argyle alluvial diamond deposits, Kimberley region, Western Australia, *in* Geochemical exploration in arid and deeply weathered environments. Geochemistry and genesis of ore deposits associated with weathering, *edited by* R. Davy, C.R.M. Butt, and T.A. Ballinger: Assoc. Expl. Geochemists, Regional Meeting, Perth 1983, Abstracts, p. 54-56.

MENZIES, M.A., KEMPTON, P., and DUNGAN, M., 1985, Interaction of continental lithosphere and asthenospheric melts below the Geronimo Volcanic Field, Arizona, U.S.A: Jour. Pet., v. 26, p. 663-693.

MENZIES, M.A. and MURTHY, V.R., 1980, Mantle metasomatism as a precursor to the genesis of alkaline magmas — Isotopic evidence: American Jour. Sci., v. 280A, p. 622-638.

MERCIER, J-C.C., 1979, Peridotite xenoliths and the dynamics of kimberlite intrusion, *in* The mantle sample: Inclusions in kimberlites and other volcanics, *edited by* F.R. Boyd and H.O.A. Meyer: Washington, American Geophys. Union, p. 197-212.

MEYER, H.O.A., 1979, Kimberlites and the mantle: Rev Geophys. Space Phys., v. 17, p. 776-789.

MEYER, H.O.A. and BOYD, F.R., 1968, Mineral inclusions in diamonds: Washington, Carnegie Inst., Yearbook 1967, p. 130-135.

MEYER, H.O.A. and BOYD, F.R., 1972, Composition and origin of crystalline inclusions in natural diamonds: Geochim. Cosmoschim. Acta, v. 36, p. 1255-1273.

MITCHELL, R.H., 1970, Kimberlite and related rocks - A critical reappraisal: Jour. Geol., v. 78, p. 686-704.

MITCHELL, R.H., 1977, Geochemistry of magnesian ilmenites from kimberlites in South Africa and Lesotho: Lithos, v. 10, p. 29-37.

MITCHELL, R.H., 1979, The alleged kimberlite-carbonatite relationship: Additional contrary mineralogical evidence: American Jour. Sci., v. 279, p. 570-589.

MITCHELL, R.H., 1981, Titaniferous phlogopites from the leucite lamproites of the West Kimberley area, Western Australia: Contrib. Min. Pet., v. 76, p. 243-251.

MITCHELL, R.H., 1985, A review of the mineralogy of lamproites: Geol. Soc. South Africa, Trans., v. 88.

MITCHELL, R.H. and BRUNFELT, A.O., 1975, Rare earth element geochemistry of kimberlite: Phys. Chem. Earth, v. 9, p. 671-686.

MITCHELL, R.H. and LEWIS, R.D., 1983, Priderite-bearing xenoliths from the Prairie Creek mica peridotite, Arkansas: Canadian Min., v. 21, p. 59-64.

MODRESKI, P.J. and BOETTCHER, A.L., 1973, Phase relationships of phlogopite in the system K_2O-MgO-CaO-Al_2O_3-SiO_2-H_2O to 35 kilobars: A better model for micas in the interior of the Earth: American Jour. Sci., v. 273, p. 385-414.

MOORE, A.C., 1986: Machells Pyramid area, Kimberley region, W.A., annual report for the period 30.4.85-29.4.86, Exploration License 04/183: BHP Minerals (unpublished).

MORI, T. and GREEN, D.H., 1976, Subsolidus equilibria between pyroxenes in the CaO-MgO-SiO_2 system at high pressures and temperatures: American Min., v. 61, p. 616-625.

MOSIG, R.W., 1980, Morphology of indicator minerals as a guide to proximity of source, *in* Kimberlites and diamonds, *edited by* J.E. Glover and D.I. Groves: Univ. West. Australia, Geol. Dept., Publ. 5, p. 81-88.

MUGGERIDGE, M.T., SMITH, C.B., and JENKE, J.P., 1978, Report for the year ending 30 June 1978. Temporary Reserves 6573H-6577H, Kimberley Goldfield, Western Australia: CRA Exploration P/L, Report 130030, (unpublished).

MUHLING, P.C. and BRAKEL, A.T., 1985, Geology of the Bangemall Group: The evolution of an intracratonic Proterozoic basin: West.Australia Geol. Survey, Bull. 128, 266 p.

MYERS, J.S., 1985, The Fraser Complex — A major layered intrusion in Western Australia: West Australia Geol. Survey, Rept 14, p. 57-66.

NELSON, D.R., McCULLOCH, M.T., and SUN, S-S, 1986, The origins of ultrapotassic rocks as inferred from Sr, Nd and Pb isotopes: Geochim. Cosmochim. Acta, v. 50, p. 231-246.

NEWSTEAD, P.G., 1969, Napier No. 1 well completion report: Lennard Oil N.L. (unpublished).

NICHOLL, J. and CARMICHAEL, I.S.E., 1969, Peralkaline acid liquids: A petrological study: Contrib. Min. Pet., v. 20, p. 268-294.

NICOLL, R.S., 1981, Conodont colour alteration adjacent to a volcanic plug, Canning Basin, Western Australia: BMR Journal of Australian Geology and Geophysics, v. 6, p. 265-267.

NIXON, P.H. and BOYD, F.R., 1973a, Petrogenesis of the granular and sheared ultrabasic nodule suite in kimberlite, *in* Lesotho kimberlites, *edited by* P.H. Nixon: Maseru, Lesotho Nat. Dev. Corp., p. 48-56.

NIXON, P.H. and BOYD, F.R., 1973b, The discrete nodule association in kimberlites from northern Lesotho, *in* Lesotho kimberlites, *edited by* P.H. Nixon: Maseru, Lesotho Nat. Dev. Corp., p. 67-75.

NIXON, P.H., ROGERS, N.W., GIBSON, I.L., and GREY, A., 1981, Depleted and fertile mantle xenoliths from southern African kimberlites: Ann. Rev. Earth Plan. Sci., v. 9, p. 285-309.

NIXON, P.H., THIRLWALL, M.F., BUCKLEY, F., and DAVIES, C.J., 1984, Spanish and West Australian lamproites: Aspects of whole rock geochemistry, *in* Kimberlites I: Kimberlites and related rocks, *edited by* J. Kornprobst: Amsterdam, Elsvier, p. 285-296.

NORRISH, K., 1951, Priderite, a new mineral from Western Australia: Min. Mag. v. 29, p. 496-501.

NORRISH, K., and CHAPPELL, B.W., 1977, X-ray fluorescence spectrometry, *in* Physical methods of determinative mineralogy, *edited by* J. Zussman, 2nd. ed: London, Academic Press p. 201-272.

NORRISH, K. and HUTTON, J.T., 1969, An accurate X-ray spectrographic method for the analysis of a wide range of geological samples: Geochim. Cosmochim. Acta, v. 33, p. 431-453.

OCEAN VENTURES PTY. LTD., 1972, Edel No. 1, well completion report: (unpublished).

O'NEILL, H.St.C., JAQUES, A.L., SMITH, C.B., and MOON, J., in prep., Diamond-bearing peridotite xenoliths from the Argyle (AK1) pipe: Int. Kimberlite Conf., 4th, Perth, Abstract Volume.

ONLEY, P.G. and SMITH, C.B. 1980, Annual report for 1979 on exploration completed within temporary reserves and mineral claims at Ellendale, Lennard River, W.A: CRA Exploration P/L, Report 130209 (unpublished).

PAGE, R.W., 1976, Reinterpretation of isotopic ages from the Halls Creek Mobile Zone, northwestern Australia: BMR Jour. Australian Geol. Geophys., v. 1, p. 79-81.

PALTRIDGE, I.M. and SMITH, C.B., 1977, Final report on King George Temporary Reserves, TR 6311H, 6312H, 6315H and 6317H: CRA Exploration P/L, Report 130020, (unpublished).

PASTERIS, J.D., 1983, Spinel zonation in the De Beers kimberlite, South Africa: Possible role of phlogopite: Canadian Min., v. 21, p. 41-58.

PIDGEON, R.T. and SMITH, C.B., in prep., The ages of kimberlite and lamproite emplacement in Western Australia: Int. Kimberlite Conf., 4th, Perth, Abstracts Volume.

PLATT, R.G. and MITCHELL, R.H., 1982, The Marathon Dikes, ultrabasic lamprophyres from the vicinity of McKellar Harbour, N.W. Ontario: American Min., v. 67, p. 907-916.

PLAYFORD, P.E., 1980, Devonian "Great Barrier Reef" of Canning Basin, Western Australia: A.A.P.G. Bull., v. 64, p. 814-840.

PLAYFORD, P.E., 1984, Platform-margin and marginal-slope relationships in Devonian reef complexes of the Canning Basin, *in* The Canning Basin, W.A., *edited by* P.G. Purcell: Geol. Soc. Aust/Pet. Expl. Soc. Aust. Symposium, Perth, 1984, Proceedings, p. 189-214.

PLAYFORD, P.E., and COCKBAIN,A.E., 1976, Revised stratigraphic and facies nomenclature in Devonian reef complexes of the Canning Basin: West. Australia Geol. Survey, Ann. Rept. 1975, p. 52-56.

PLAYFORD, P.E., and LOWRY, D.C., 1966, Devonian reef complexes of the Canning Basin, Western Australia: West. Australia Geol. Survey, Bull. 118.

PLUMB, K.A., 1968, Lissadell, Western Australia: Australia BMR, 1:250 000 Geological Series — Explanatory Notes.

PLUMB, K.A., 1979, The tectonic evolution of Australia: Earth Sci. Rev., v. 19, p. 205-249.

PLUMB, K.A., DERRICK, G.M., NEEDHAM, R.S., and SHAW, R.D., 1981, The Proterozoic of Northern Australia, *in* Precambrian geology of the southern hemisphere, *edited by* D.R. Hunter: Amsterdam, Elsevier, p. 205-307.

PLUMB, K.A. and GEMUTS, I., 1976, Precambrian geology of the Kimberley region, Western Australia: Int. Geol. Congress, 25th, Sydney, Excursion guide 44C, 69pp.

POWELL, J.L., and BELL, K., 1970, Strontium isotopic studies of alkalic rocks: Localities from Australia, Spain and Western United States: Contrib. Min. Pet., v. 17, p. 1-10.

PRIDER, R.T., 1939, Some minerals from the leucite-rich rocks of the West Kimberley area, Western Australia: Min. Mag., v. 25, p. 373-387.

PRIDER, R.T., 1960, The leucite lamproites of the Fitzroy Basin, Western Australia: Geol. Soc. Australia, Jour., v. 6 p. 71-118.

PRIDER, R.T., 1965, Noonkanbahite, a potassic batisite from the lamproites of Western Australia: Min. Mag., v. 34, p. 403-405.

PRIDER, R.T., 1982, A glassy lamproite from the west Kimberley area, Western Australia: Min. Mag., v. 45, p. 279-282.

PRIDER, R.T., and COLE, W.F., 1942, Some minerals from the leucite-rich rocks of the west Kimberley area, Western Australia: American Min., v. 27, p. 373-384.

PRYCE, W.M., HODGE, L.C., and CRIDDLE, A.J., 1984: Jeppeite, a new K-Ba-Fe titanate from Walgidee Hills, Western Australia: Min. Mag., v. 48, p. 263-266.

PURCELL, P.G. and POLL, J., 1984, The seismic definition of the main structural elements of the Canning Basin, *in* The Canning Basin, W.A., *edited by* P.G. Purcell: Geol. Soc. Aust./Pet. Expl. Soc. Aust. Symposium, Perth, 1984, Proceedings, p. 73-84.

RAWLINSON, P.J. and DAWSON, J.B., 1979, A quench pyroxene-ilmenite xenolith from kimberlite: Implications for pyroxene-ilmenite intergrowths, *in* The mantle sample: Inclusions in kimberlites and other volcanics, *edited by* F.R. Boyd and H.O.A. Meyer: Washington, American Geophys. Union, p. 292-299.

REED, S.J.B., and WARE, N.G., 1975, Quantitative electron microprobe analysis of silicates using energy-dispersive x-ray spectrometry: Jour. Petrol., v. 16, p. 499-519.

RICHARDSON, S.H., GURNEY, J.J., ERLANK, A.J., and HARRIS, J.W., 1984, Origin of diamonds in old enriched mantle: Nature, v. 310, p. 198-202.

RINGWOOD, A.E., 1982, Phase transformations and differentiation in subducted lithosphere: Implications for mantle dynamics, basalt petrogenesis and crustal evolution: Jour. Geol., v. 90, p. 611-643.

RINGWOOD, A.E., 1985, Mantle dynamics and basalt petrogenesis: Tectonophysics, v. 112, p. 17-34.

RIXON, L.K., 1978, Clay Modelling of the Fitzroy graben. Australian: BMR Jour. Australian Geol. Geophys., v. 3, p. 71-76.

ROBERT, J.L., 1976, Titanium solubility in synthetic phlogopite solid solutions: Chem. Geol., v. 17, p. 213-227.

RODEN, M.F., 1981, Origin of coexisting minette and ultramafic breccia, Navajo volcanic field: Contrib. Min. Pet., v. 77, p. 195-206.

ROGERS, N.W., BACHINISKI, S.W., HENDERSON, P., and PARRY, S.J., 1982, Origin of potash-rich basic lamprophyres: Trace element data from Arizona minettes: Earth Plan. Sci. Letts., v. 57, p. 305-312.

RYABCHIKOV, I.D., GREEN, D.H., WALL, V.J., and BREY, G., 1981, The oxidation state of carbon in the environment of the low velocity zone: Geokhimiya, v. 2, p. 221-232.

RYAN, D.M., 1982a, Final report on exploration completed within Temporary Reserves 6576H and 6577H Forrest River, Drysdale, Western Australia: CRA Exploration P/L, Report 130345 (unpublished).

RYAN, D.M., 1982b, Annual report on exploration within Temporary reserves 7216H-7217H, 7304H-7317H, 7321H-7323H, 7327H-7336H and 7386H-7390H Argyle, and the associated dredging and mineral claims, Lissadell, Western Australia: CRA Exploration P/L, Report 130353 (unpublished).

SACHTLEBEN, Th. and SECK, H.A., 1981, Chemical control of Al solubility in orthopyroxene and its implications on pyroxene gethermometry: Contrib. Min. Pet., v. 78, p. 157-165.

SAHAMA, Th., 1974, Potassim-rich alkaline rocks, *in* The alkaline rocks, *edited by* H. Sorensen: London, Wiley, p. 96-109.

SCHMID, R., 1981, Descriptive nomenclature and classification of pyroclastic deposits and fragments: Recommendations of the IUGS Subcommission on the Systematics of Igneous Rocks: Geology, v. 9, p. 41-43.

SCOTT-SMITH, H.H., and SKINNER, E.M.W., 1984a, A new look at Prairie Creek, Arkansas, *in* Kimberlites I: Kimberlites and related rocks, *edited by* J. Kornprobst: Amsterdam, Elsevier, p. 255-284.

SCOTT-SMITH, B.H., and SKINNER, E.M.W., 1984b, Kimberlite and American mines, near Prairie Creek, Arkansas, *in* Kimberlites III: Documents, *edited by* J. Kornprobst: Univ. Clermont-Ferrand, Ann. Sci., v. 74, p. 27-36.

SCOTT-SMITH, B.H., and SKINNER, E.M.W., 1984c, Diamondiferous lamproites: Jour. Geol., v. 92, p. 433-488.

SHAW, W.J., KELLY, M., MOORE, A.C., and CHAPMAN, S., 1985, Pteropus Creek area, east Kimberley Region, W.A., annual report to 25 Jan 1985, exploration licences E80/102 and E80/103: BHP Minerals Division (unpublished).

SHEE, S.R, GURNEY, J.J. and ROBINSON, D.N., 1982, Two diamond-bearing peridotite xenoliths from the Finsch kimberlite, South Africa: Contrib. Min. Pet., v. 81, p. 79-87.

SHERATON, J.W. and CUNDARI, A., 1980, Leucitites from Gaussberg, Antarctica: Contrib. Min. Pet., v. 71, p. 417-427.

SHERIDAN, M.F., 1979, Emplacement of pyroclastic flows: a review: Geol. Soc. America, Spec. Paper 180, p. 125-136.

SHERIDAN, M.F. and WOHLETZ, K.H., 1983, Hydrovolcanism: Basic considerations and review: Jour. Volc. Geotherm. Res., v. 17, p. 1-29.

SIMPSON, E.S., 1925, Contributions to the mineralogy of Western Australia, Series I: Royal Soc. West Australia, Jour., v. 12, p. 57-66.

SIMPSON, E.S., 1948, 1951, 1952, Minerals of Western Australia, 3 vols.: Perth, Government Printer.

SKINNER, E.M.W. and CLEMENT, C.R., 1979, Mineralogical classification of southern African kimberlites, *in* Kimberlites, diatremes and diamonds: Their geology, petrology and geochemistry, *edited by* F.R. Boyd and H.O.A. Meyer: Washington, American Geophys. Union, p. 129-139.

SMITH, C.B., 1978a, Final report on mineral claims MC 80/5923-5937, Kimberley Goldfield, Western Australia: CRA Exploration P/L, Report 130027 (unpublished).

SMITH, C.B., 1978b, Annual report on mineral claims 80/5333-5388, 80/5646-5647, 80/5662-5666 and 80/5671-5677, and annual and final report on mineral claims 80/5667-5670, Kimberley Goldfield, Western Australia: CRA Exploration P/L, Report 130029 (unpublished).

SMITH, C.B., 1979, Annual report for 1978, West Kimberley Goldfield, W.A.: CRA Exploration P/L (unpublished).

SMITH, C.B., 1984a, The genesis of the diamond deposits of the West Kimberley, W.A., *in* The Canning Basin, W.A., *edited by* P.G. Purcell: Geol. Soc. Aust./Pet. Expl. Soc. Aust. Symposium, Perth, 1984, Proceedings, p. 463-473.

SMITH, C.B., 1984b, What is a kimberlite? *in* Kimberlite occurrence and origin, *edited by* J.E. Glover and P.G. Harris: University of West Australia, Geol. Dept., Publ. No. 8, p. 1-18.

SMITH, Craig .B., 1983, Pb, Sr and Nd Isotope evidence for sources of southern African Cretaceous kimberlite: Nature, v. 304, p. 51-54.

SMITH, J.G., 1968, Tectonics of the Fitzroy wrench trough, Western Australia: American Jour. Sci., v. 266, p. 766 776.

SMITH, J.V. and DAWSON, J.B., 1975, Chemistry of Ti-poor spinels, ilmenites and rutiles from peridotite and eclogite xenoliths: Phys. Chem. Earth, v. 9, p. 309-322.

SOBOLEV, N.V., LAURENT'EV, Yu.G., POKHILENKO, N.P. and USOVA, L.V., 1973, Chrome-rich garnets from the kimberlites of Yakutia and their parageneses: Contrib. Min. Pet., v. 40, p. 39-52.

SOFOULIS, J., GELLATLY, D.C., DERRICK, G.M., FARBRIDGE, R.A., and MORGAN, C.M., 1971, The geology of the Yampi 1:250 000 sheet area, SE/51-3, Western Australia: Australia BMR, Rec. 1971/1 (unpublished).

STEPHENS, W.E. and DAWSON, J.B., 1977, Statistical comparisons between pyroxenes from kimberlites and their associated xenoliths: Jour. Geol., v. 85, p. 433-449.

STRACKE, K.J., FERGUSON, J., and BLACK, L.P., 1979, Structural setting of kimberlites in south-eastern Australia, *in* Kimberlites, diatremes and diamonds: Their geology, petrology and geochemistry, *edited by* F.R. Boyd and H.O.A. Meyer: Washington, American Geophys. Union, p. 71-91.

SUN, S-S., McCULLOCH, M.T., and JAQUES, A.L., 1986, Isotopic evolution of the Kimberley Block, Western Australia: Int. Kimb. Conf., 4th Perth, Abstracts Volume.

SUTHERLAND, F.L., 1983, Timing, trace and origin of basaltic migration in eastern Australia: Nature, v. 305, p. 123-126.

TAYLOR, W.R., 1985, A reappraisal of the nature of fluids included by diamond: A window to deep-seated mantle fluids and redox conditions, *in* Conference on stable isotopes and fluid processes in mineralization, *edited by* H.K. Herbert: Univ. Queensland, Dept. Geol. Min., Abstracts Volume, p. 72-73.

THOM, R., de LAETER, J.R., and LIBBY, W.G., 1981, Rb-Sr dating of tectonic events in the Proterozoic Mount Barren Group near Hopetoun: West. Australia Geol. Survey, Ann. Rept 1980, p. 109-112.

THOMAS, B.M. and SMITH, D.N., 1976, Carnarvon Basin, *in* Economic Geology of Australia and Papua New Guinea, *edited by* C.L. Knight: Australasian Inst. Min. Met., Monograph 7, p. 126-154.

THOMAS, M.F., THORP, M.B., and TEEUW, R.M., 1985, Palaeogeomorphology and the occurrence of diamondiferous placer deposits in Koidu, Sierra Leone: Geol. Soc. (London), Jour., v. 142, p. 789-802.

THOMPSON, R.N., MORRISON, M.A., HENDRY, G.L., and PARRY, S.J., 1984, An assessment of the relative roles of crust and mantle in magma petrogenesis: An elemental approach: Royal Soc. (London), Phil. Trans., v. A310, p. 549-590.

TOWNER,R.R., and GIBSON, D.L., 1983, Geology of the onshore Canning Basin, Western Australia: Australia BMR, Bull. 215.

TRENDALL, A.F., 1974, The age of a granite near Mount Crofton, Paterson Range sheet: West. Australia, Geol. Survey, Ann. Rept 1973, p. 92-96.

TRENDALL, A.F., 1983, The Hammersley Basin, *in* Iron-formations facts and problems, *edited by* A.F. Trendall and R.C. Morris: Amsterdam, Elsevier, p. 69-129.

TRENDALL, A.F., 1984, The Archaean/Proterozoic transition as a geological event — A view from Australian evidence, *in* Patterns of change in earth evolution, *edited by* H.D. Holland and A.F. Trendall: Berlin, Springer-Verlag, p. 243-259.

TRÖGER, W.E., 1935, Spezielle Petrographie der Eruptiv-gesteine, Ein Nomenklatur-Kompendium: Berlin, Deutsche Miner. Ges.

TUREK, A., 1966, Rubidium-strontium isotopic studies in the Kalgoorlie-Norseman area, Western Australia: Australian National University, Ph.D. Thesis (unpublished).

TUREK, A. and STPEHENSON, N.C.N., 1966, The radiometric age of the Albany Granite and the Stirling Range Beds, south-west Australia: Geol. Soc. Australia, Jour., v. 13, p. 449-456.

VANCE, E.R., HARRIS, J.W., and MILLEDGE, H.J., 1973, Possible origins of α-damage in diamonds from kimberlite and alluvial sources: Min. Mag., v. 39, p. 349-360.

VEEVERS, J.J., 1981, Morphotectonics of rifted continental margins in embryo (East Africa), youth (Africa-Arabia) and maturity (Australia): Jour. Geol., v. 89, p. 57-82.

VEEVERS, J.J. and COTTERILL, D., 1976, Western margin of Australia: A Mesozoic analog of the East African rift system: Geology, v. 4, p. 713-717.

VEEVERS, J.J. and COTTERILL, D., 1978, Western margin of Australia: Evolution of a rifted arch system: Geol. Soc. America, Bull. v. 89, p. 337-355.

VEEVERS, J.J., POWELL, C. McA., and JOHNSON, B.D., 1975, Greater India's place in Gondwanaland and in Asia: Earth Plan. Sci. Letts., v. 27, p. 383-387.

VENTURELLI, G., CAPEDRI, S., Di BATTISTINI, G., CRAWFORD, A., KOGARKO, L.N., and CELESTINI, S., 1984, The ultrapotassic rocks from southeastern Spain: Lithos, v. 17, p. 37-54.

VOLLMER, R., OGDEN, P., SCHILLING, J-G., KINGSLEY, R.H., and WAGGONER, D.G., 1984, Nd and Sr isotopes in ultrapotassic volcanic rocks from the Leucite Hills, Wyoming: Contrib. Min. Pet., v. 87., p. 359-368.

VON ECKERMAN, H., 1967, Progress of research on the Alnö carbonatite, *in* Carbonatites, *edited by* O.F. Tuttle and J. Gitting: New York, Wiley, p. 3-31.

WADE, A., 1924, Petroleum Prospects: Kimberley District of Western Australia and Northern Territory: Australia, Commonwealth Parlt. Paper No. 142.

WADE, A. and PRIDER, R.T., 1940, The Leucite-bearing rocks of the West Kimberley area, Western Australia: Quart. J. Geol. Soc., (London), v. 96, p. 39-98.

WALKER, G.P.L. and CROASDALE, R., 1972, Characteristics of some basaltic pyroclastics: Bull. Volc., v. 35, p. 303-317.

WALTER, L.S., 1956, Experimental studies on Bowen's decarbonation series, III: P-T univariant equilibrium of the reaction: spurrite + monticellite = merwinite + calcite and analysis of assemblages found at Crestmore, California: American Jour. Sci., v. 263, p. 64-77.

WARE, N.G., 1981, Computer programs and calibration with the PIBS technique for quantitative electron probe analysis using a lithium-drifted silicon detector: Computers Geosci. v. 7, p. 167-184.

WARRIS, B.J., 1973, Plate tectonics and the evolution of the Timor Sea, Northwest Australia: A.P.E.A. Jour., v. 13, p. 13-18.

WEDEPOHL, K.H. and MURAMATSU, Y., 1979, The chemical composition of kimberlites compared with the average composition of three basaltic magma types, *in* Kimberlites, diatremes and diamonds: Their geology, petrology and geochemistry, *edited by* F.R. Boyd and H.O.A. Meyer: Washington, American Geophys. Union, p. 300-312.

WEISSEL, J.K. and HAYES, D.E., 1971, Asymmetric seafloor spreading south of Australia: Nature, v. 231, p. 519-522.

WELLMAN, P., 1972, Early Miocene potassium-argon age for the Fitzroy lamproites of Western Australia: Geol. Soc. Australia, Jour., v. 19, p. 471-474.

WELLMAN, P., 1976, Gravity trends and the growth of Australia: A tentative correlation: Geol. Soc. Australia, Jour., v. 23, p. 11-14.

WELLMAN, P. and McDOUGALL, I., 1974a, Potassium-argon ages on the Cainozoic volcanic rocks of New South Wales: Geol. Soc. Australia, Jour., v. 21, p. 247-272.

WELLMAN, P. and McDOUGALL, I., 1974b, Cainozoic igneous activity in eastern Australia: Tectonophysics, v. 23, p. 49-65.

WELLS, P.R.A., 1977, Pyroxene thermometry in simple and complex systems: Contrib. Min. Pet., v. 62, p. 129-139.

WENDLANDT, R.F., 1984, An experimental and theoretical analysis of partial melting in the system $KAlSiO_4$-CaO-MgO-SiO_2-CO_2 and applications to the genesis of potassic magmas, carbonatites and kimberlites *in* Kimberlites I: Kimberlites and related rocks, *edited by* J. Kornprobst: Amsterdam, Elsevier, p. 359-369.

WENDLANDT, R.F. and EGGLER, D.H., 1980a, The origins of potassic magmas — 1. Melting relations in the system $KAlSiO_2$-Mg_2SiO_4-SiO_2 and $KAlSiO_4$-MgO-SiO_2-CO_2 to 30 kilobars: American Jour. Sci., v. 280, p. 385-420.

WENDLANDT, R.F. and EGGLER, D.H., 1980b, The origins of potassic magmas — 2. Stability of phlogopite in natural spinel lherzolite and in the system $KAlSiO_4$-MgO-SiO_2-H_2O-CO_2 at high pressures and high temperatures: American Jour. Sci., v. 280, p. 421-458.

WILLIAMS, S.J., ELIAS, M., and de LAETER, J.R., 1978, Geochronology and evolution of the eastern Gascoyne Province and the adjacent Yilgarn Block: West Australia, Geol. Survey, Ann. Rept. 1977, p. 50-56.

WOHLETZ, K.H. and McQUEEN, R.G., 1984, Experimental studies in hydromagmatic volcanism, *in* Studies in geophysics: explosive volcanism, inception, evolution and hazards, *edited by* F.R. Boyd: Washington, National Academy Press, p. 158-169.

WOHLETZ, K.H. and SHERIDAN, M.F., 1983, Hydrovolcanic explosions II: Evolution of basaltic tuff rings and tuffcones: American Jour. Sci., v. 283, p. 385-413.

WRIGHT, R.L., 1964, Geomorphology of the west Kimberley area: Australia CSIRO, Land Res. Series 9, p. 103-118.

WYATT, B.A., 1977, The melting and crystallization behaviour of a natural clinopyroxene-ilmenite intergrowth: Contrib. Min. Pet., v. 61, p. 1-9.

WYATT, B.A., 1978, Phase relationships in the system picroilmenite-clinopyroxene-Cr_2O_3: A preliminary assessment: Proc. Exper. Petrol., p. 181-185.

WYATT, B.A., 1979, Manganoan ilmenites from the Premier pipe: Kimberlite Symposium II, Cambridge 1979, Abstracts Volume (unpublished).

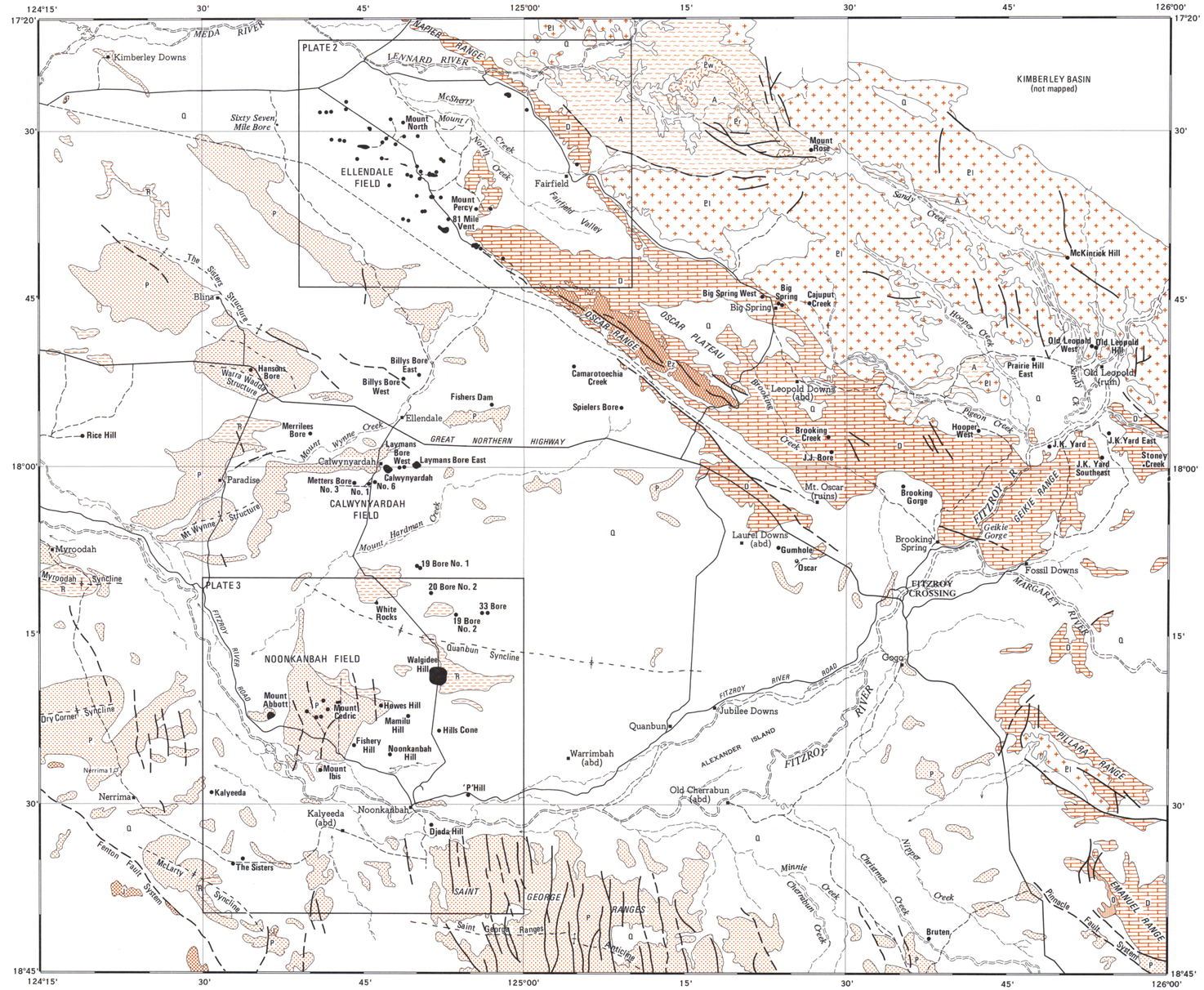
WYLLIE, P.J., 1978, Mantle fluid compositions buffered in peridotite-CO_2-H_2O by carbonates, amphibole and phlogopite: Jour. Geol., v. 86, p. 687-713.

WYLLIE, P.J., 1979, Magmas and volatile components: American Min., v. 64, p. 469-500.

WYLLIE, P.J., 1980, The origin of kimberlite: Jour. Geophys. Res., v. 85, p. 6902-6910.

WYLLIE, P.J. and HUANG, W.L., 1976, Carbonation and melting relations in the system $CaO-MgO-SiO_2-CO_2$ at mantle pressures, with geophysical and petrological applications: Contrib. Min. Pet., v. 54, p. 79-107.

YEATES, A.N., GIBSON, D.L., TOWNER, R.R., and CROWE, R.W.A., 1984, Regional Geology of the onshore Canning Basin, W.A., *in* The Canning Basin, W.A., *edited by* P.G. Purcell: Geol. Soc. Aust/Pet. Expl. Soc Aust. Symposium, Perth 1984, Proceedings p. 23-56.



REFERENCE

CAINOZOIC		Q	Alluvium and eolian sands and silt with minor conglomerate, calcrete and laterite
	MIOCENE		Lamproite plugs, diatremes and sills; small intrusions represented by a dot
MESOZOIC	JURASSIC	J	Sandstone, fine to coarse; mudstone, minor conglomerate; cross-bedded, rippled; marine to deltaic
	TRIASSIC	R	Mudstone, sandy mudstone, rippled, laminated to thin bedded; shallow marine. Sandstone, cross-bedded; continental
PALAEOZOIC	PERMIAN	P	Sandstone, mudstone, minor limestone; lagoonal to marine. Very minor glacial deposits
	DEVONIAN (WITH LOWER CARBONIFEROUS)	D	Limestone : reef, fore-reef and back-reef facies with minor conglomerates and sandstone. Calcarenite, calcirudite, shale, siltstone and minor sandstone : basin and marginal slope facies
	ORDOVICIAN	O	Dolomite, limestone, shale, sandstone; marine
PROTEROZOIC	OSCAR RANGE SUCCESSION	Er	Quartzite, conglomerate, feldspathic sandstone, siltstone, shale; phyllite and phyllitic sandstone; minor chlorite schist, epidotized basalt, tuff, rhyolite
	LAMBOO COMPLEX	Pi	Granite : leucocratic to mesocratic, biotite granite; granodiorite, minor tonalite; porphyritic micro-granite. Rhyodacite tuff; conglomerate, arkose; (Whitewater Volcanics)
		Ew	WOODWARD DOLERITE : uralitized porphyritic dolerite with minor ultramafic patches
		Pr	RICHENDA MICROGRANODIORITE : even-grained microgranodiorite, minor hornblende microgranodiorite and microtonalite. Rhyolite cone sheets
ARCHAEAN	HALLS CREEK GROUP	A	Grey phyllitic siltstone and greywacke; chloritoid, andalusite, staurolite, kyanite and garnet-mica schist

SYMBOLS

Geological boundary

Fault
- Accurate
- Approximate

Fold
- Anticline concealed
- Syncline concealed

Highway

Road

Track

Town

Homestead

Abandoned

River

Creek

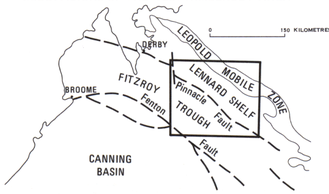
Petroleum exploration well

FITZROY CROSSING
■ Quanbun
(abd)

LOCATION DIAGRAM



LOCATION DIAGRAM AND MAJOR STRUCTURAL SUBDIVISIONS OF THE WEST KIMBERLEY AREA



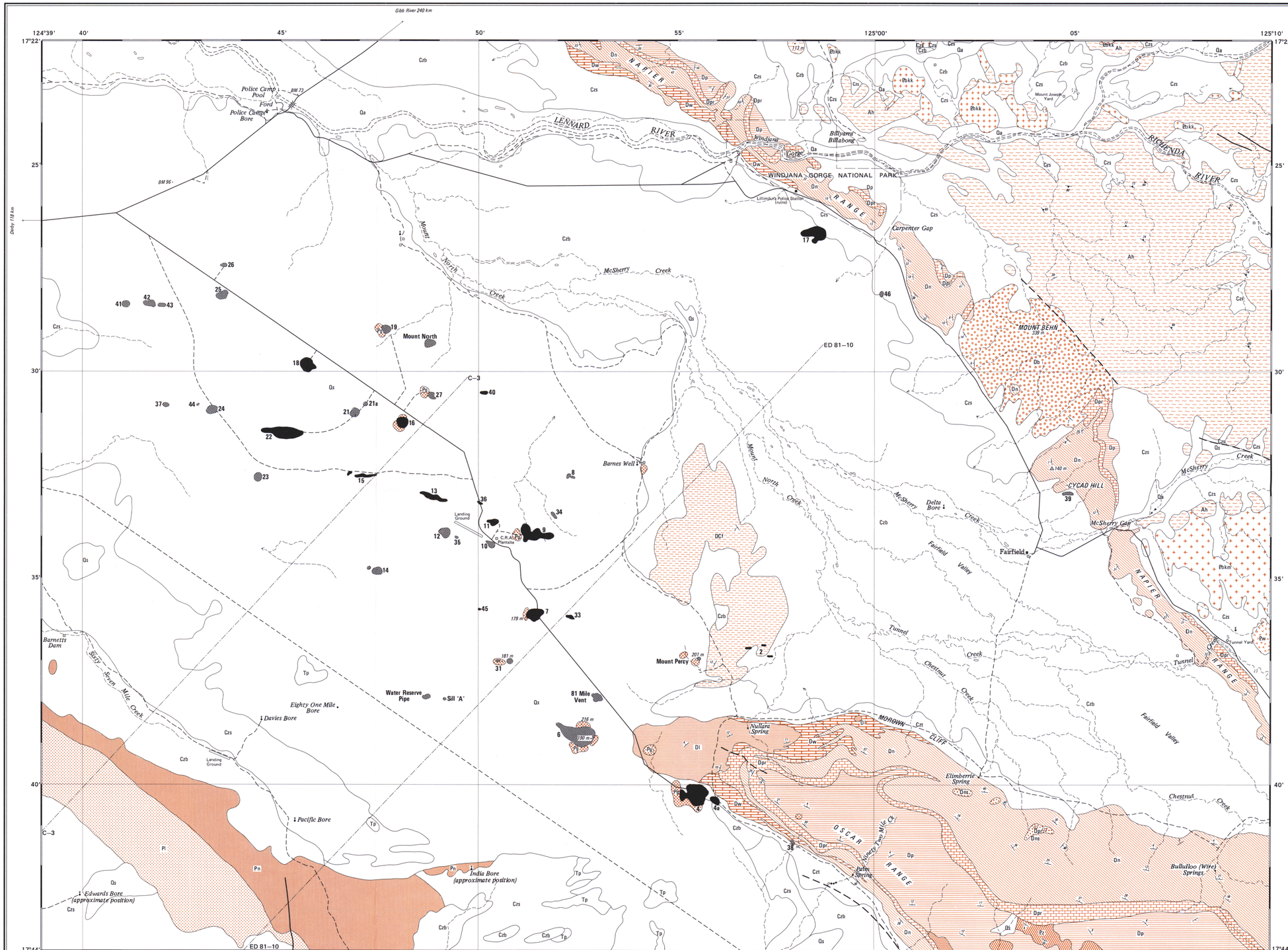
INDEX TO 1 : 250 000 SHEETS

DERBY SE 51-7	LENNARD RIVER SE 51-8	LANSDOWNE SE 52-5
MT ANDERSON SE 51-11	NOONKANBAH SE 51-12	MT RAMSAY SE 52-9
MCLARTY HILLS SE 51-15	CROSSLAND SE 51-16	MT BANNERMAN SE 52-13

HON. DAVID PARKER, M.L.A.
MINISTER FOR MINERALS AND ENERGY
A. F. TRENDALL, DIRECTOR, GEOLOGICAL SURVEY DIVISION
SCALE 1 : 500 000
10 0 10 20 30 40
KILOMETRES
Compiled by J.D. Lewis (G.S.W.A.)

LAMPROITE INTRUSIONS OF THE WEST KIMBERLEY AREA, W.A.

© Western Australia 1985



REFERENCE

QUATERNARY

- Qa — Alluvium
- Qs — Windblown sand, residual sand

TERTIARY

- Czt — Travertine, tufa (caliche)
- Czb — Residual black soil
- Czs — Sand and sandy soil
- Olivine lamproite diatreme
- Leucite lamproite diatreme
- Tp — Laterite, pisolitic ironstone, ferruginous sandstone

U.DEVONIAN TO L.CARBONIFEROUS

- Pl — LIVERINGA FORMATION : ferruginous, micaceous, silty sandstone and conglomeratic sandstone
- Pn — NOONKANBAH FORMATION : shale, siltstone, limestone, intraformational conglomerate
- Pg — GRANT GROUP : massive aqueoglacial unsorted silty sandstone, conglomeratic sandstone, tillite, siltstone, shale

DEVONIAN — FAMENNIAN

- DCl — FAIRFIELD GROUP : grey to yellow-brown coquinoid limestone, calcarenite, calcareous sandstone, siltstone and shale
- Dw — WINDJANA LIMESTONE : reef subfacies : yellow to white, massive, algal and stromatoporoid limestone, dolomitized in part
- Dl — NULLARA LIMESTONE : platform facies : well bedded cyanobacterial calcarenite and oolite with subordinate sandstone and siltstone
- Dn — NAPIER FORMATION : marginal-slope and basin facies : grey to red calcarenite, calcirudite and megabreccia; in part sandy and silty
- Dnv — ELIMBERRIE BIOHERMS : sponge-stromatolite bioherms

DEVONIAN — FRASNIAN

- Dpr — PILLARA LIMESTONE : reef subfacies : massive to bedded, stromatoporoid and cyanobacterial limestone, dolomitized in part
- Dp — PILLARA LIMESTONE : back-reef subfacies : yellow to light grey bedded stromatoporoid limestone : calcarenite, calcilutite; minor conglomerate and arkose
- Dc — BEHN CONGLOMERATE : boulder, cobble and pebble conglomerate with arkose matrix

PROTEROZOIC

- Pz — OSCAR RANGE SUCCESSION : quartzite, feldspathic sandstone, siltstone, shale, phyllite; minor conglomerate and basalt
- Pbkm — McSHERRYS GRANODIORITE : coarse-grained, porphyritic hornblende granodiorite and tonalite; minor adamellite and quartz gabbro
- Pw — WHITEWATER VOLCANICS : rhyodacite ashflow tuff, conglomerate, arkose; minor rhyodacite flows
- Pbkk — KONGDROW GRANITE : coarse-grained porphyritic biotite granite; remnant gneissic bands some granodiorite

ARCHAEAN

- Ah — HALLS CREEK GROUP : grey phyllitic siltstone and greywacke; chloritoid, andalusite, staurolite, kyanite and garnet-mica schist

SYMBOLS

- Geological boundary
- Fault
  - Accurate
  - Approximate
- Bedding
  - Inclined
- Seismic line
- Formed road
- Track
- Horizontal control, major — △ 140 m
- Homestead — ■ Fairfield
- Watercourse, intermittent
- Well, bore, spring
- Windmill
- Dam, tank, yard

LOCATION DIAGRAM



INDEX TO 1:100 000 SHEETS

MEDA 3763	LENNARD 3863	RICHENDA 3963
WILLUMBAH 3762	ELLENDALE 3862	LEOPOLD DOWNS 3962
NERRIMA 3761	HARDMAN 3861	CUNNINGHAM 3961

HON. DAVID PARKER, M.L.A.
MINISTER FOR MINERALS AND ENERGY
A. F. TRENDALL, DIRECTOR, GEOLOGICAL SURVEY DIVISION

SCALE 1 : 100 000

2 0 2 4 6 8
KILOMETRES

Geology by G.M. Derrick and P.E. Playford (1973), P.E. Playford (1981), N.F. Harley (1983-4), location of lamproite intrusions by C.B. Smith (C.R.A.E.), compiled by J.D. Lewis (G.S.W.A.)

LAMPROITE INTRUSIONS OF THE ELLENDALE FIELD, WEST KIMBERLEY, W.A.

© Western Australia 1985

124°30' 40' 50' 125°00'
18°10' 20' 30' 18°40'

Troy Lagoon
Mount Hardman Dam
Mount Hardman Creek
Darling Bore
Stocktrack Bore
Deadhorse Swamp Bore
Sears Bore
Mount Abbott Bore
Outcamp Bore
Centenary Bore
FITZROY RIVER
MOUNT HARDMAN 132 m
Boundary Bore
Rocky Yard
Mount Abbott 172 m
Mount Cedric North
Mount Cedric
Mount Cedric South
Howes Hill
Mount Noreen 108 m
Machells Pyramid 129 m
Mount Gytha
FITZROY RIVER ROAD
Shedforth Bore
Broken Wagon Pool
Fishery Hill 108 m
Mount Ibis
Noonkanbah Hill 92 m
Quonga Waterhole
Kalyeeda
Slaughter Hole
Backhouse Waterhole
Goosehole Billabong
Kalyeeda (abd)
Kalyeeda Creek
Baldocks Dam
The Sisters 92 m 96 m
Landing Ground
Duck Hole Billabong
Rock Hole Pool
Sandy Billabong
Noonkanbah Airfield
Noonkanbah
FITZROY RIVER
'P' Hill 98 m
FITZROY RIVER ROAD
Djada Hill
Balwynah Pool
One Tree Hole
KALYEEDA HILLS
Popes Bore
SAINT GEORGE RANGES
White Rocks 107 m
No. 20 Bore
20 Bore No. 2
No. 19 Bore
19 Bore No. 2
No. 33 Bore
33 Bore
No. 17 Bore
No. 18 Bore
No. 7 Bore
No. 8 Bore
Walgidee Hills 121 m
No. 6 Bore
No. 12 Bore
No. 13 Bore
Mamilu Hill 91 m
Mayborough Bore
Hills Cone
Lubys Tank
Mallallah Bore
Lubys Bore
Mickeys Bore
No. 5 Bore
No. 1 Bore
Paddys Bore

REFERENCE

QUATERNARY

- Qa — Alluvium
- Qs — Sand, silt, minor gravel : mixed alluvium and eolian
- Qz — Red sand, minor silt; sand dunes : eolian
- Qb — Black soil

TERTIARY

- Czl — Pisolitic and massive laterite
- Czh — WARRIMBAH CONGLOMERATE : conglomerate, cobble and pebble, unconsolidated : fluvial
- Lamproite diatremes and plugs

EARLY TRIASSIC

- Rb — BLINA SHALE : mudstone, sandy mudstone; minor sandstone; thin bedded, fossiliferous : brackish water
- Rm — MILLYIT SANDSTONE : sandstone; minor siltstone; thin bedded, ripple marks : continental

LATE PERMIAN

- Ph — HARDMAN FORMATION : sandstone, siltstone; thin bedded; ferruginized
- Pl — LIGHTJACK FORMATION : shale, siltstone, fine sandstone; fossiliferous : regressive marine
- Pn — NOONKANBAH FORMATION : mudstone, shale, fine sandstone, calcareous; minor limestone; fossiliferous marine

EARLY PERMIAN

- Pp — POOLE SANDSTONE : sandstone, mudstone : fluvial to marine
- Pc — CAROLYN FORMATION : sandstone, siltstone, claystone; minor poorly bedded glacial deposits

SYMBOLS

- Geological boundary
- Fault
  - Accurate
  - Approximate
- Formed road
- Track
- Horizontal control, major
- Spot height, height in metres — 121 m
- Homestead — Noonkanbah
- Watercourse, intermittent; pool — P
- Water tank
- Bore and windmill
- Dam
- Dam and windmill

LOCATION DIAGRAM



INDEX TO 1 : 100 000 SHEETS

WILLUMBAH 3762	ELLENDALE 3862	LEOPOLD DOWNS 3962
NERRIMA 3761	HARDMAN 3861	CUNNINGHAM 3961
CRAVEN ORD 3760	KALYEEDA 3860	DUKES DOME 3960

HON. DAVID PARKER, M.L.A.
MINISTER FOR MINERALS AND ENERGY
A. F. TRENDALL, DIRECTOR, GEOLOGICAL SURVEY DIVISION

SCALE 1 : 100 000

2 0 2 4 6 8
KILOMETRES

Geology by R.W.A. Crowe and R.R. Turner (1981), additional lamproite locations by G.L. Boxer and E.A. Haebig (1980), compiled by J.D. Lewis (G.S.W.A.)

LAMPROITE INTRUSIONS OF THE NOONKANBAH FIELD WEST KIMBERLEY, W.A.

© Western Australia 1985

114°22' 25' 30' 35' 114°40'
23°43' 45' 50' 55' 24°00' 05' 10' 24°12'

Colvin Well
Boorilya Well
Cundlego Well
MINILYA RIVER
Wandagee
Landing Ground
Nalbia Dam
WANDAGEE HILL 164 m
Mungadan Dam
Wandagee 1
Wandagee 2
Joolajugga Dam
Wyalong Tank
Billamberry Dam
Nerrie Dam
West Dam
Barrabiddy Creek
Wapet Bore
Quail T
Barrabiddy Outcamp
Barrabiddy Dam
Mulbia Dam
Yearlit Dam
Ulupnia Well
Hutton Creek
Whitby Dam
O'Briens Dam
Phillips Tank
2nd Parry Tank

M 88 Sill ~2.4 m
M 100 B Sill ~15 m
PK 3 Sill ~ 3 m
M 97 ~3 ha
M 103 Sill
M 104/105 Sills ~ 3 m
M 89 ~3.75 ha
M 94 A ~ 2.4 ha
M 113 A ~ 0.5 ha
M 92 B ~ 3 ha
M 142 ~ 0.5 ha
M 113 B East ~3 ha
M 113 B West ~1.5 ha
M 98 ~3 ha 89 m
M 94 B ~ 1 ha 78.5 m
M 129 ~2.5 ha 71 m
M 154 ~14 ha 158 m

REFERENCE

QUATERNARY
- PLEISTOCENE TO HOLOCENE — Qa — Alluvium, clay, silt, sand and gravel, locally calcreted
- PLEISTOCENE — Q — Eolian sands, calcarenite and dune deposits

TERTIARY
- PLIOCENE TO PLEISTOCENE — Czc — Older alluvium, consolidated clay, silt, sand and gravel

CRETACEOUS — K — Low energy marine shelf deposits, siltstone, radiolarite shale and calcilutite

JURASSIC
- M 89 ~3.75 ha — Kimberlitic tuff diatreme, with approximate surface area
- M 98 ~3 ha 89 m — Kimberlitic tuff diatreme, with approximate surface area and depth of Cretaceous cover
- M 100 B Sill ~15 m — Kimberlitic sill or dyke, with approximate thickness

PERMIAN
- Kennedy Group — PK — Quartz arenite, quartz wacke and siltstone, locally calcareous and ferruginized; shallow marine shelf
- Byro Group — PB — Quartz wacke, siltstone and shale, locally carbonaceous and calcareous; offshore and shallow marine

SYMBOLS

- Geological boundary
- Fault
  - Accurate
  - Approximate
- Bedding
  - Inclined
- Formed road
- Track
- Homestead — ■ Wandagee
- Horizontal control, major
- Watercourse, intermittent
- Well, bore
- Windmill
- Dam, tank
- Dam and windmill
- Petroleum exploration well, abandoned

LOCATION DIAGRAM



INDEX TO 1 : 100 000 SHEETS

MAUDS LANDING 1651	MIA MIA 1751	WINNING 1851
MINILYA 1650	BARRA-BIDDY 1750	GOOCH RANGE 1850
MACLEOD 1649	BOOLO-GOORO 1749	MARDA-THUNA 1849

HON. DAVID PARKER, M.L.A.
MINISTER FOR MINERALS AND ENERGY
A. F. TRENDALL, DIRECTOR, GEOLOGICAL SURVEY DIVISION

SCALE 1 : 100 000
2 0 2 4 6 8
KILOMETRES

Geology by R.M. Hocking (G.S.W.A.), location of diatremes and sills by I.D. Kerr (C.R.A.E.)

KIMBERLITIC INTRUSIONS OF THE CARNARVON BASIN, W.A.

© Western Australia 1985

Geological Survey of Western Australia

Bulletin No. 132

THE KIMBERLITES AND LAMPROITES OF WESTERN AUSTRALIA

by

A.L. Jaques, J.D. Lewis and C.B. Smith

1986

APPENDIX 2

CHEMICAL ANALYSES

The following chemical analyses were carried out in the analytical laboratories of the Division of Petroleum and Geochemistry, Bureau of Mineral Resources, and the West Australian Government Chemical Laboratories. Details of analytical techniques are given in Appendix 1. All data are stored on disk in a Hewlett-Packard 9825 desktop calculator at BMR, using storage, retrieval, and plotting programmes written by Dr M. Owen (BMR)

Analyses are stored under different categories by use of upper and lower case first letters in their 'Formation' and 'Locality' names. Analyses considered to have been chemically altered, or to contain crustal inclusions which could not be excluded during sample preparation, have been excluded from the geochemical data base used in this Bulletin, and are assigned lower case Formation names (e.g. fitzroy lamproites). Analyses used in the data base have upper case first letters in their 'Formation' and 'Locality' names.

The following abbreviations are used for the mineral qualifiers to lamproite (Lamp, L) in the 'Rock Name' (see Chapter 1 for nomenclature): A(p) - Apatite; Carb - Carbonated; D(i) - Diopside; J(p) - Jeppeite; Lc (Leuc) - Leucite; Ol - Olivine; KR (i) - Potassic Richterite; Ph(l) - Phlogopite; P(r) - Priderite; P(v) - Perovskite; Sh(ch) - Shcherbakovite; W(a) - Wadeite. Additional abbreviations used in rock descriptions are CG - Coarse grained; Cog Xen - Cognate Xenolith; FG - Fine grained; Gl(assy) - Glassy; Lam(p) - Lamproite; Por(ph) - Porphyritic; Ves - Vesicular; Xen - Xenolithic; ss - sandstone.

Argyle samples are described in terms of their rock units, as well as petrographic name. ST - 'Sandy' Tuff, NsT - 'Non-sandy' Tuff, OLD - Olivine (-Phlogopite) Lamproite Dyke.

Information regarding the exact location is given, as far as possible, in terms of 'Grid Reference' and relevant 1:100 000 map sheet, under 'Additional Information'. In the case of drill core samples, where known, the hole number and meterage are also given, e.g. 2AC 9/100m. Drill core locality information for Argyle Pipe samples is given under 'Locality'. The heading 'Bibliography' indicates the collector of the sample, and the analytical laboratory - (BMR or West Australian Government Chemical Laboratories - GSWA). Specimens were collected mainly by J.D. Lewis (JDL), and A.L. Jaques (ALJ), with additional samples kindly provided as follows: Donated, origin uncertain (Don, Donat); G.M. Derrick, formerly of BMR (GMD); John Ferguson, formerly of BMR (JF); G.P. Gregory of BP Minerals (GPG); and G. Halford of Dept of Geology ANU (GH).

ARGYLE LAMPROITES

Sample number	83211001B	83211001C	83211002	83211006	83211009A	83211009C	83211010	83211013	83211014	83211016
Formation	Argyle Lamproite	Argyle Lamproite	Argyle Lamproite	Argyle Lamproite	Argyle Lamproite	Argyle Lamproite	Argyle Lamproite	Argyle Lamproite	Argyle Lamproite	Argyle Lamproite
Rock type	OLD.Phl-Ol Lamproite	ST. Tuff Sandstone	OLD. Ol-Phl Lamp.	ST.Lapilli Ash Tuff	ST.Lapilli Ash Tuff	Tuff clast Ol-Lamp.	NsT. Lapilli Tuff	ST.Lapilli Ash Tuff	ST.Lapilli Ash Tuff	NsT. Lapilli Tuff
Locality	AK1.Quarry BS 131	AK1.Quarry BS 131	AK1.Quarry BS 131	AK1. DDH 17/135.15m	AK1. DDH 17/250.20m		AK1. DDH 17/300.00m	AK1. DDH 22/75.20m	AK1. DDH 22/96.00m	AK1. DDH 31/140.3m
Grid reference										
Map sheet	Bow	Bow	Bow	Bow	Bow	Bow	Bow	Bow	Bow	Bow
Additional data	carbonated		oxidized					Leucoxene		Hyaloclast
Biblio. ref.	ALJ-BMR	ALJ-BMR	ALJ-BMR	ALJ-BMR	ALJ-BMR	ALJ-BMR	ALJ-BMR	ALJ-BMR	ALJ-BMR	ALJ-BMR
SiO_2	37.72	76.68	42.83	28.75	77.15	51.32	38.44	64.27	64.87	41.42
TiO_2	2.92	1.04	3.56	0.92	0.80	1.52	3.23	2.03	1.91	2.79
Al_2O_3	3.49	7.49	4.90	4.30	7.62	12.53	4.83	7.24	6.91	4.43
Fe_2O_3	3.62	1.86	8.93	0.80	2.72	1.29	2.50	1.49	1.40	3.45
FeO	3.30	0.74	1.39	1.85		4.55	5.97	2.82	2.87	4.27
MnO	0.37	0.02	0.34	0.08	0.02	0.07	0.22	0.05	0.04	0.12
MgO	19.78	4.00	14.04	3.94	3.80	13.04	20.51	8.20	8.33	22.65
CaO	8.94	0.37	7.23	2.61	0.46	1.97	7.37	2.90	2.72	5.56
Na_2O	0.05	0.04	0.02	0.02	0.04	0.11	0.04	0.04	0.06	0.08
K_2O	0.48	4.22	0.08	1.85	4.52	7.35	1.35	4.81	4.64	4.26
P_2O_5	0.93	0.25	1.23	0.27	0.19	0.61	0.99	0.69	0.63	0.90
H_2O+	4.40	1.87	4.58	1.71	2.61	5.47	4.35	2.72	2.53	5.69
H_2O-	0.92	0.53	1.55	0.58		0.09	0.91	0.60	0.55	0.86
CO_2	11.61	0.12	8.40	2.45			7.81	1.96	1.98	2.40
Rest	1.17	0.42	1.01	0.31	0.31	0.65	1.15	0.68	0.70	1.02
Total	99.70	99.65	100.09	100.44	100.24	100.57	99.67	100.50	100.14	99.90
Ba	2885	1108		402	683	[illegible]	222	1291	1575	876
Li	87	28	98	17	17	72	[illegible]	32	36	32
Rb	60	104	6	39	92	177	137	133	138	337
Sr	699	131	569	143	107	284	643	463	526	957
Pb	61	17	20	16	10	23	405	23	20	63
Th	18	14	20	9	14	3	20	15	14	17
U	3	3	4	3	3.5	2	4	3.5	4	3
Zr	573	407	821	321	317	383	695	612	593	599
Nb	213	52	284	56	34	91	234	137	129	206
Y	16	20	23	14	18	9	24	27	24	19
La	139	69	150	43	41	55	127	88	95	132
Ce	249	126	289	89	88	118	270	177	191	265
Nd	136	41	83	30	28	36	80	61	64	79
Sc	13	8	18	7	5	3	15	14	12	14
V	136	81	138	49	62	66	140	87	85	139
Cr	1501	191	2096	252	129	839	1833	527	508	1475
Co										
Ni	635	150	840	154	307	551	1090	386	369	963
Cu	363	19	21	14	18	7	54	24	26	50
Zn	56	19	151	32	33	83	110	65	43	71
Sn	3	7	6	4	2	<2	5	2	7	2
Mo	<3	<3	<3	3	<3	<3	3	<3	<3	<3
Ga	6	10	8	8	10	13	9	11	11	8
As	1.5	1.5	21	2	57	0.5	24	4.5	3.5	4
S										
F	3100	1600	4100	1600	800	2600	5400	2600	2400	3500
Cl										

ARGYLE LAMPROITES

Sample number	83211017	83211018	83211030	83211032	83211033	83211034	83211035	83211037	83211048	83211049
Formation	Argyle Lamproite	Argyle Lamproite	Argyle Lamproite	Argyle Lamproite	Argyle Lamproite	Argyle Lamproite	Argyle Lamproite	Argyle Lamproite	Argyle Lamproite	Argyle Lamproite
Rock type	NsT. Lapilli Tuff	OLD. Phl-Ol Lamp.	NsT. Lapilli Tuff	ST.Lapilli Ash Tuff	OLD. Ol-Phl Lamp.	OLD. Ol. Phl. Lamp.	ST.Lapilli Ash Tuff	OLD. Ol-Phl. Lamp.	ST. Coarse Ash Tuff	NsT. Ol-Phl Lamp.
Locality	AK1. DDH 31/170.5m	AK1. DDH 31/188m	AK1. DDH 59/240.3m	AK1. DDH 108/154.4m	AK1. DDH 108/171.0m	AK1. DDH 82/159.80m	AK1. DDH 113/174.4m	AK1. DDH 106/160.8m	AK1. DDH 123/127.0m	AK1. DDH 153/85.50m
Grid reference										
Map sheet	Bow	Bow	Bow	Bow	Bow	Bow	Bow	Bow	Bow	Bow
Additional data	Autobrccia	contact								
Biblio. ref.	ALJ-BMR	ALJ-BMR	ALJ-BMR	ALJ-BMR	ALJ-BMR	ALJ-BMR	ALJ-BMR	ALJ-BMR	ALJ-BMR	ALJ-BMR
SiO_2	44.47	49.86	51.05	62.28	43.17	42.13	65.77	40.85	75.00	41.73
TiO_2	2.30	3.04	2.28	2.06	3.80	3.62	1.90	3.70	1.32	2.80
Al_2O_3	3.92	6.96	4.19	5.67	4.89	4.80	6.06	4.55	7.03	4.08
Fe_2O_3	2.45	1.77	1.99	1.65	3.30	3.34	1.30	2.29	0.94	2.85
FeO	4.38	5.60	4.45	3.36	5.06	5.02	3.66	6.93	2.17	4.90
MnO	0.15	0.08	0.08	0.06	0.21	0.22	0.04	0.10	0.03	0.18
MgO	23.69	15.39	20.95	11.57	21.55	21.52	10.68	18.98	5.41	21.75
CaO	4.60	3.99	3.71	3.40	4.21	4.77	1.78	7.54	0.49	5.22
Na_2O	0.08	0.12	0.10	0.09	0.10	0.07	0.05	0.09	0.04	0.19
K_2O	2.71	5.86	1.93	4.90	4.27	3.37	2.80	2.18	2.90	4.85
P_2O_5	0.80	1.02	0.81	0.69	1.53	1.43	0.58	1.20	0.36	0.94
H_2O+	5.37	4.85	4.92	2.47	4.60	4.99	3.51	4.78	2.72	3.59
H_2O-	0.90		0.62	0.18	0.87	1.32	0.43	0.54	0.58	0.24
CO_2	2.71		1.28	1.39	1.17	2.13	1.22	4.76	0.56	5.23
Rest	0.91	1.04	0.83	0.74	1.00	0.97	0.60	1.19	0.43	1.05
Total	99.44	99.58	99.19	100.51	99.73	99.70	100.38	99.68	99.98	99.60
Ba	704	2368	1028	1654	426	552	674	1011	718	1579
Li	70	52	55	54	46	52	81	69	34	68
Rb	200	208	80	130	365	312	79	230	63	288
Sr	817	755	461	533	1197	1141	279	1220	94	1041
Pb	9	27	22	18	3	4	9	233	10	19
Th	12	17	10	12	16	15	13	20	14	18
U	2	4	3	3	3	3	3.5	4.5	4.5	4
Zr	607	888	627	594	1030	952	629	762	462	590
Nb	146	217	162	135	259	237	161	273	76	194
Y	16	23	15	20	26	25	19	22	22	20
La	95	104	89	70	131	129	76	150	68	123
Ce	199	239	181	164	283	265	162	305	127	248
Nd	68	83	58	55	90	88	58	89	46	82
Sc	9	13	9	10	14	14	12	15	11	12
V	86	114	79	69	104	50	94	143	82	114
Cr	1393	1097	1275	695	1261	1180	560	1682	307	1316
Co										
Ni	1087	517	903	560	926	929	443	952	227	969
Cu	24	27	31	32	38	31	19	54	31	35
Zn	44	199	41	42	47	52	55	115	36	40
Sn	2	3	2	2	3	3	2	2	3	2
Mo	<3	<3	<3	<3	<3	<3	<3	<3	<3	3
Ga	8	13	6	8	10	8	10	10	10	4
As	1	10	3	7.5	2	2	1	<0.5	5.5	0.5
S										
F	3100	2900	2800	2200	3200	3200	2600	4100	2000	3200
Cl										

ARGYLE LAMPROITES

Sample number	83211050	83211054	83211055	83211060	83211062	83211063
Formation	Argyle Lamproite	Argyle Lamproite	Argyle Lamproite	Argyle Lamproite	Argyle Lamproite	Argyle Lamproit
Rock type	NsT. Ol-Lamproite	ST.Lapilli Ash Tuff	NsT. Ol-Lamproite	NsT. Ol-Lamproite	NsT. Ol. Lamproite	OLD. Ol. Lamproite
Locality	AK1. DDH 153/82m	AK1. DDH 110/57.8m	AK1. DDH 160/80m	AK1. DDH 130/74.2m	AK1. 600S 152. O/C	AK1. south end, O/C
Grid reference						
Map sheet	Bow	Bow	Bow	Bow	Bow	Bow
Additional data	Autobrccia				oxidized	oxidized
Biblio. ref.	ALJ-BMR	ALJ-BMR	ALJ-BMR	ALJ-BMR	ALJ-BMR	ALJ-BMR
SiO_2	43.39	77.22	49.29	47.23	60.74	50.07
TiO_2	2.79	1.05	3.16	2.71	4.21	5.53
Al_2O_3	4.12	7.65	4.44	3.79	8.13	10.84
Fe_2O_3	2.75	0.87	4.31	2.68	9.72	13.58
FeO	5.23	1.72	3.90	4.51	0.39	0.46
MnO	0.19	0.02	0.10	0.07	0.05	0.11
MgO	21.69	3.93	21.71	20.72	5.23	6.59
CaO	4.53	0.33	1.46	5.48	1.96	2.33
Na_2O	0.15	0.05	0.08	0.07	0.01	0.01
K_2O	4.54	4.14	3.72	3.42	0.02	0.15
P_2O_5	0.92	0.26	0.88	0.86	1.56	2.04
H_2O+	3.54	2.06	4.34	3.96	4.93	5.95
H_2O-	0.21	0.30	0.64	0.73	1.92	1.35
CO_2	4.38	0.62	0.35	2.67	0.08	0.11
Rest	1.04	0.39	1.23	0.90	0.87	0.96
Total	99.47	100.61	99.61	99.80	99.82	100.08
Ba	1238	1019	2251	703	75	156
Li	71	33	217	98	79	62
Rb	309	94	390	367	2	6
Sr	1167	126	269	778	464	619
Pb	13	13	5	4	19	9
Th	17	13	29	15	21	17
U	4	4	4	2.5	5.5	6
Zr	606	398	704	581	1215	1475
Nb	195	54	258	193	301	382
Y	18	23	25	19	30	52
La	118	53	145	106	118	204
Ce	235	104	302	216	277	440
Nd	74	36	113	68	91	153
Sc	12	10	13	11	19	25
V	114	78	107	104	84	133
Cr	1351	200	1483	1300	838	1408
Co						
Ni	991	124	1000	888	994	650
Cu	38	15	67	10	54	3
Zn	39	33	50	40	179	170
Sn	<2	2	<2	2	6	5
Mo	<3	<3	<3	<3	<3	<3
Ga	6	12	8	8	15	13
As	1	2.5	1.5	1	6.5	2
S						
F	3300	1400	4600	3200	3700	2700
Cl						

ARGYLE PIPE COUNTRY ROCKS

Sample number	83211023	83211024	83211052	83211056	83211057	83211058	83211059
Formation	Revolver Creek Fm.	Revolver Creek Fm.	Revolver Creek Fm.	Lissadell Fm.	Lissadell Fm.	Golden Gte Sandstone	Hensman Quartzite
Rock type	Shale at contact	Quartzite	Ortho-quartzite	Ortho-quartzite	Shale	Ortho-quartzite	Ortho-quartzite
Locality	AK1. DDH 56/250.1m	AK1. DDH 56/180.8m	AK1. DDH 87/164.0m	AK1. DDH GT 2/92.5m	AK1. DDH GT 2/137m	AK1. DDH GT2/157.2m	AK1. DDH GT2/180.7m
Grid reference							
Map sheet	Bow	Bow	Bow	Bow	Bow	Bow	Bow
Additional data	ferrug.		Country Rk	Country Rk	Country Rk		
Biblio. ref.	ALJ-BMR	ALJ-BMR	ALJ-BMR	ALJ-BMR	ALJ-BMR	ALJ-BMR	ALJ-BMR
SiO_2	48.44	94.84	93.81	98.85	72.33	99.24	98.63
TiO_2	0.78	0.19	0.07	0.06	1.44	0.01	0.01
Al_2O_3	20.86	1.49	2.97	0.63	16.36	0.40	0.66
Fe_2O_3	12.67	2.01	0.28	<0.01	0.73	0.04	0.03
FeO	0.56	0.09	0.11	0.11	0.68	0.11	0.10
MnO	0.05	<0.01	<0.01	<0.01	<0.01	<0.01	<0.01
MgO	2.43	0.06	0.19	0.02	0.36	0.01	0.03
CaO	0.20	<0.01	0.02	<0.01	<0.01	<0.01	<0.01
Na_2O	0.05	0.01	0.05	<0.01	0.05	<0.01	<0.01
K_2O	8.47	0.26	1.83	0.09	3.18	0.09	0.21
P_2O_5	0.12	0.02	0.02	0.02	0.05	0.01	<0.01
H_2O+	3.97	0.27	0.34	0.23	2.91	0.16	0.43
H_2O-	0.90	0.03	0.10	0.08	0.20	0.06	0.05
CO_2	0.25	0.47	0.15	0.12	1.29	0.08	0.01
Rest	0.34	0.05	0.08	0.04	0.25	0.02	0.01
Total	100.09	99.79	100.02	100.25	99.83	100.23	100.17
Ba	508	27	388	28	233	41	35
Li	6	5	2	1	22	2	2
Rb	290	10	52	4	140	3	6
Sr	38	8	45	24	66	4	4
Pb	26	6	9	5	9	3	4
Th	21	2	3	1	23	2	1
U	5	1.5	1	0.5	5.5	1	1
Zr	149	62	91	43	433	26	28
Nb	15	3	<2	<2	23	<2	<2
Y	22	8	7	5	49	2	2
La	78	47	11	43	60	12	8
Ce	161	107	21	103	135	20	9
Nd	52	24	7	23	47	8	4
Sc	21	3	<2	<2	22	<2	<2
V	150	46	6	5	174	<2	2
Cr	156	14	12	9	102	7	7
Co							
Ni	42	4	2	1	11	5	1
Cu		9	1	2	91		
Zn	66	2	5	1	25	2	1
Sn	3	<2	3	4	5	<2	3
Mo	5	<3	<3	<3	<3	<3	<3
Ga	29	2	2	1	22	1	1
As	3	1	<0.5	0.5	5	<0.5	<0.5
S							
F	1800	<300	<300	<300	500		
Cl							

MOUNT NORTH

Sample number	66160326	71407	71802	71803	71804	71806	71809	71810B	71812	71813
Formation	Fitzroy Lamproites	Fitzroy Lamproites	Fitzroy Lamproites	Fitzroy Lamproites	Fitzroy Lamproites	Fitzroy Lamproites	Fitzroy Lamproites	Fitzroy Lamproites	Fitzroy Lamproites	Fitzroy Lamproites
Rock type	Ol-Phl-Lc Lamproite	Phl-Lc Lamproite	Ol-Phl-Lc Lamproite	Phl-Ol-KRi -Lc Lamp.	Ol-Phl-Lc Lamproite	Ol-Di-KRi-Ph-Lc Lamp	Ol-KRi-Lc Lamproite	Vesic Ol-Lc Lamp.	Ol-Di-Phl-Lc Lamp.	Ol-Di-KRi-Ph-Lc Lamp
Locality	Mount North	Mount North	Mount North	Mount North	Mount North	Mount North	Mount North	Mount North	Mount North	Mount North
Grid reference	924655	924655	927656	927656	926656	925654	925653	924653	924653	925655
Map sheet	Lennard	Lennard	Lennard	Lennard	Lennard	Lennard	Lennard	Lennard	Lennard	Lennard
Additional data		dyke, Eend	sill 1 NE	sill NE	tier 1, NE	summit	sill 1, S	sill 1, SW	tier 2, SW	tier 2, N
Biblio. ref.	GMD-BMR	Lewis-GSWA	Lewis-GSWA	Lewis-GSWA	Lewis-GSWA	Lewis-GSWA	Lewis-GSWA	Lewis-GSWA	Lewis-GSWA	Lewis-GSWA
SiO_2	57.47	47.80	47.70	49.00	46.50	45.40	50.10	53.50	43.10	45.80
TiO_2	5.97	7.37	6.76	5.85	7.43	6.57	6.38	4.86	7.16	7.02
Al_2O_3	5.27	6.80	9.10	6.20	6.70	5.50	8.60	6.50	5.30	5.50
Fe_2O_3	5.08	6.50	6.20	4.60	6.40	6.00	5.20	3.70	6.30	5.60
FeO	1.55	1.32	0.72	1.89	1.80	1.26	1.01	1.30	1.11	1.68
MnO	0.05	0.09	0.05	0.07	0.08	0.09	0.04	0.05	0.05	0.07
MgO	7.77	7.63	7.20	11.20	8.13	11.70	6.56	8.86	12.00	11.70
CaO	2.66	3.46	2.90	3.47	4.44	3.59	2.89	2.65	4.18	3.90
Na_2O	0.35	0.80	0.14	0.83	0.82	0.62	0.41	0.67	0.30	0.73
K_2O	7.32	9.03	9.99	7.73	8.03	6.11	9.48	8.89	4.76	7.58
P_2O_5	1.46	2.01	2.57	1.74	2.10	1.41	1.95	1.31	2.12	1.41
H_2O+	2.12	2.08	2.31	1.97	2.12	4.09	2.26	2.57	5.08	2.14
H_2O-	0.34	0.99	1.82	2.22	1.31	4.22	2.29	1.84	4.59	3.27
CO_2	0.54	0.04	0.05	0.14	0.19	0.07	0.11	0.11	0.02	0.14
Rest	1.67	2.01	1.80	2.02	3.00	2.68	1.96	1.99	3.44	2.76
Total	99.62	98.29	99.31	98.93	99.05	99.31	99.24	98.80	99.51	99.30
Ba	5597	7192	3607	7149	15112	13149	6100	8112	18527	12970
Li	7	8	12	11	11	10	8	11	11	11
Rb	379	354	628	342	447	553	370	293	524	379
Sr	1490	1677	1702	1640	1895	1607	1703	1559	1982	1727
Pb	61	55	76	48	68	58	55	68	80	92
Th	54	48	49	35	39	39	45	35	56	49
U	7	2	3	2	2	3	2	2	4	6
Zr	1595	2121	2844	1926	2156	2128	2629	1942	2763	2372
Nb	193	199	168	151	186	172	160	120	195	181
Y	17	22	21	15	18	17	91	15	15	19
La	311	478	508	385	465	382	504	370	539	467
Ce	525	887	953	718	768	650	913	698	867	747
Sc		27	25	21	25	22	20	14	24	19
V	197	135	231	162	138	168	208	163	168	158
Cr	408	387	466	406	368	265	410	314	286	485
Mn		720	364	562	632	693	298	377	351	575
Co	29	34	30	35	40	41	34	31	38	45
Ni	331	449	436	857	396	329	421	439	269	320
Cu	56	44	50	66	80	76	62	66	86	88
Zn	76	77	76	85	84	86	80	79	94	85
Sn	7	15	13	13	13	18	7	2	14	22
Mo		<1	<1	<1	<1	<1	<1	<1	<1	<1
Ga	9	13	25	14	13	11	24	19	11	10
As	2									
S		210	50	570	340	80	100	580	40	370
F	5300	6200	5670	5250	6530	5430	4810	4300	5900	6050
Cl		90	83	105	74	601		99	100	114

MOUNT NORTH

Sample number	71814	83210320	83210321	83210322	83210323	83210324	83210326
Formation	Fitzroy Lamproites	Fitzroy Lamproites	Fitzroy Lamproites	Fitzroy Lamproites	Fitzroy Lamproites	Fitzroy Lamproites	Fitzroy Lamproites
Rock type	Phl-Ol-Lc Lamproite	Ol-Phl-Lc Lamproite	Di-Phl-KRi -Lc Lamp.	Di-Phl-KRi -Lc Lamp.	Di-KRi-Lc Lamproite	Ol-Lc Lamproite	Ol-Phl-Lc Lamproite
Locality	Mount North	Mount North	Mount North	Mount North	Mount North	Mount North	Mount North
Grid reference	926654	924655	924655	924655	924655	924655	924655
Map sheet	Lennard	Lennard	Lennard	Lennard	Lennard	Lennard	Lennard
Additional data	sill 1, SE	lower sill	summit	top tier	base tier2	lower sill	tier 1
Biblio. ref.	Lewis-GSWA	ALJ-BMR	ALJ-BMR	ALJ-BMR	ALJ-BMR	ALJ-BMR	ALJ-BMR
SiO_2	48.80	48.17	44.68	45.13	44.59	48.80	42.84
TiO_2	5.26	6.42	6.84	7.77	8.13	6.41	7.53
Al_2O_3	7.90	8.22	5.78	6.14	6.17	7.46	5.45
Fe_2O_3	5.80	5.60	5.43	6.07	6.35	5.85	6.34
FeO	1.28	0.92	1.56	2.05	1.87	1.24	1.44
MnO	0.08	0.04	0.08	0.11	0.10	0.07	0.09
MgO	7.46	7.80	11.50	9.39	10.36	7.35	11.24
CaO	3.59	2.75	4.05	4.33	4.15	3.64	3.98
Na_2O	0.64	0.18	0.72	0.88	0.64	0.59	0.46
K_2O	8.93	11.23	6.53	8.20	8.91	10.39	7.37
P_2O_5	2.14	2.37	1.37	1.60	1.98	1.95	2.02
H_2O+	2.10	2.33	4.01	2.94	2.46	2.43	3.80
H_2O-	2.76	1.53	3.00	1.75	1.16	1.51	2.99
CO_2	0.11	0.24	0.41	0.32	0.28	0.45	0.43
Rest	1.87	1.86	3.68	3.10	2.78	2.53	3.24
Total	98.72	99.66	99.64	99.78	99.93	100.67	99.22
Ba	5006	4124	22076	16234	11273	10961	17084
Li	6	9	9	10	11	8	9
Rb	314	711	666	628	694	509	653
Sr	1893	1999	1897	2035	1722	2010	1996
Pb	100	95	77	85	101	77	93
Th	58	57	55	71	102	52	74
U	4	5.5	7	8.5	11	5	11
Zr	2513	2340	2102	2316	2611	1974	2472
Nb	230	244	254	294	308	247	299
Y	25	37	33	38	38	32	38
La	665	489	336	510	716	466	486
Ce	1171	967	719	1083	1734	935	1045
Nd		326	377	457	695	374	471
Sc	27	15	12	16	18	16	16
V	170	158	178	184	242	157	225
Cr	197	630	521	536	665	600	546
Co	28						
Ni	423	538	443	345	356	530	280
Cu	82	35	58	59	67	46	63
Zn	76	84	85	73	104	91	97
Sn	8	11	9	14	18	9	16
Mo	<1	<3	<3	<3	<3	<3	<3
Ga	23	22	13	15	18	22	16
As		2.5	2.5	3	2.5	2.5	3.5
S	150						
F	4830	5000	3900	3100	3900	4700	3500
Cl	94						

MOUNT PERCY

Sample number	66160329	66160330	67160334	79211053	80210046	80210047	80210048	80210049	80210090	71403
Formation	Fitzroy	Fitzroy	Fitzroy	[illegible]roy	fitzroy	Fitzroy	Fitzroy	Fitzroy	Fitzroy	Fitzroy
Rock type	Lamproites Phl-Lc	Lamproites Ol-Di-Lc	Lamproites Phlog-L[illegible]	[illegible]tes [illegible]	lamproites Xeno-tuff	Lamproites Phl-Lc	Lamproites Ol-Lc	Lamproites Ol-Phl-Lc	Lamproites Phl - Lc	Lamproites Phl-Lc
Locality	Lamproite Mount Percy	Lamproite Mount Percy	Lamproite Mount Percy	[illegible]e [illegible]	breccia Mount Percy	Lamproite Mount Percy	Lamproite Mount Percy	Lamproite Mount Percy	Lamproite Mount Percy	Lamproite Mount Percy
Grid reference	043512	043512	043512	[illegible]2	043512	043512	043512	043512	043512	043513
Map sheet	Ellendale	Ellendale	Ellendale	Ellendale	Ellendale	Ellendale	Ellendale	Ellendale	Ellendale	Ellendale
Additional data					margin		fg margin	centre		centre
Biblio. ref.	GMD-BMR	GMD-BMR	GMD-BMR	GMD-BMR	JF.ALJ-BMR	JF.ALJ-BMR	JF.ALJ-BMR	JF.ALJ-BMR	GPG-BMR	Lewis-GSWA
SiO_2	51.43	60.56	46.04	45.50	58.67	44.10	58.29	48.51	45.65	45.60
TiO_2	6.02	5.12	6.59	6.59	4.15	6.79	5.99	6.56	6.64	6.65
Al_2O_3	8.34	7.12	6.85	7.00	7.66	6.87	7.86	6.89	7.11	6.60
Fe_2O_3	6.00	4.56	7.12	7.04	4.22	7.63	6.69	7.05	7.21	7.40
FeO	1.27	0.77	0.88	0.88	0.97	0.51	0.51	0.71	0.86	0.77
MnO	0.06	0.04	0.10	0.10	0.04	0.09	0.08	0.12	0.11	0.11
MgO	7.22	5.36	10.74	10.73	5.95	10.35	2.98	8.86	10.50	10.30
CaO	2.07	2.12	3.89	3.71	2.35	3.78	1.65	2.78	3.57	3.87
Na_2O	0.48	0.37	0.45	0.46	0.32	0.29	0.33	0.33	0.49	0.38
K_2O	10.02	9.37	9.67	9.81	8.41	9.35	8.55	9.28	9.64	9.83
P_2O_5	1.05	1.18	1.68	1.68	1.32	2.03	1.21	1.81	1.84	2.07
H_2O+	2.86	1.48	2.20	2.13	2.12	2.99	2.16	2.35	2.20	2.58
H_2O-	1.21	0.26	0.11	0.23	0.97	2.31	1.99	1.52	0.60	0.95
CO_2	0.48	0.35	0.23	0.24	<0.10	0.20	0.17	0.19	0.25	0.08
Rest	1.56	1.23	3.15	3.32	1.66	2.54	1.78	2.96	2.74	3.60
Total	100.07	99.89	99.70	99.42	98.81	99.83	100.24	99.92	99.41	100.79
Ba	6910	3943	18993	20776	9855	12415	10389	17214	17627	21947
Li	12	4	6	6	6	6	5	6	6	10
Rb	248	351	656	680	663	668	323	575	598	649
Sr	1092	1059	1620	1504	1026	1651	891	1665	1567	1875
Pb	69	67	92	88	54	102	68	85	84	80
Th	27	33	55	57	29	68	39	53	55	59
U	4	7	7	7	3	8	3	5	3	1
Zr	1281	1419	1651	1654	1061	1889	1451	1613	1586	1831
Nb	133	156	231	233	113	268	160	213	223	276
Y	24	14	13	8	11	21	19	14	15	29
La	335	327	436	441	278	599	355	449	440	520
[illegible]	502	518	619	633	411	1047	517	591	640	610
Nd						331				
Sc										23
V	270	190	109	117	168	72	134	96	77	124
Cr	275	216	440	394	195	430	221	385	427	419
Co	26	28	37	34						44
Ni	225	193	235	217	347	221	559	308	238	156
Cu	62	41	69	62	35	76	46	70	56	90
Zn	96	75	76	74	59	81	66	76	79	101
Sn	2	5	8	5	8	23	13	19	15	
Mo					<3	3	5	4	7	3
Ga	23	18	12	13	12	12	15	12	12	10
As	2	1	1	2	2	2	2	2	2	
S										40
F	3200	3200	3900	3800		3400		4300		4697
Cl			35			140				87

MOUNT PERCY

Sample number	71392	71399	71406	71830	71832	71834	71838	71841	71842	83210328
Formation	Fitzroy Lamproites	Fitzroy Lamproites	fitzroy lamproites	Fitzroy Lamproites	Fitzroy Lamproites	Fitzroy Lamproites	Fitzroy Lamproites	Fitzroy Lamproites	Fitzroy Lamproites	Fitzroy Lamproites
Rock type	Ol-Phl-Lc Lamproite	Ol-Lc Lamp Tuff	Xen Ol-Lc Lamp Tuff	(Ol)-Lc Lamproite	Phl-Lc Lamproite	Ol-Lc Lamproite	Ol-Lc Lamproite	Di-Ol-Lc Lamproite	Phl-Lc Lamproite	Phl-Lc Lamproite
Locality	Mount Percy	Mount Percy	Mount Percy	Mount Percy	Mount Percy	Mount Percy	Mount Percy	Mount Percy	Mount Percy	Mount Percy
Grid reference	043513	043513	043512	043512	043512	043512	043512	043512	043512	043512
Map sheet	Ellendale	Ellendale	Ellendale	Ellendale	Ellendale	Ellendale	Ellendale	Ellendale	Ellendale	Ellendale
Additional data	dyke in ss	o/c in NW	centre	N side	vesic71830	dyke in ss	dyke,centr	centre N	centre o/c	N side
Biblio. ref.	Lewis-GSWA	Lewis-GSWA	Lewis-GSWA	Lewis-GSWA	Lewis-GSWA	Lewis-GSWA	Lewis-GSWA	Lewis-GSWA	Lewis-GSWA	ALJ-BMR
SiO_2	50.00	51.20	54.20	58.30	48.50	50.20	52.40	48.50	49.40	46.36
TiO_2	6.09	5.31	5.05	6.32	6.76	5.21	5.54	5.78	6.09	6.80
Al_2O_3	8.50	8.20	7.40	7.90	9.20	7.50	8.50	7.10	5.80	6.66
Fe_2O_3	7.50	5.30	4.80	6.40	8.30	4.30	5.10	6.80	7.10	7.02
FeO	0.67	1.33	1.49	0.33	0.64	1.58	1.04	0.43	0.53	0.75
MnO	0.01	0.08	0.07	0.02	0.05	0.04	0.05	0.08	0.09	0.08
MgO	5.25	6.00	6.98	2.39	5.92	6.87	6.69	8.25	9.62	9.31
CaO	2.55	2.99	2.92	1.84	0.38	3.04	2.32	3.41	2.86	3.16
Na_2O	0.08	0.69	0.62	0.09	0.17	0.64	0.43	0.55	0.32	0.32
K_2O	9.89	9.95	8.96	8.49	9.27	8.14	10.80	8.02	8.11	9.63
P_2O_5	1.91	1.71	1.57	1.43	1.16	1.53	1.41	1.57	1.84	1.86
H_2O+	2.60	2.12	2.36	2.49	3.61	4.14	2.20	3.25	2.81	2.83
H_2O-	2.80	1.84	1.71	2.16	2.88	3.33	1.34	2.71	1.77	1.41
CO_2	0.01	0.27	0.09	0.05	0.04	0.10	0.05	0.04	0.11	0.39
Rest	1.56	2.59	1.70	1.45	2.32	1.93	1.63	2.50	2.35	3.11
Total	99.42	99.58	99.92	99.66	99.20	98.55	99.50	98.99	98.80	99.69
Ba	4439	15461	7684	5320	10820	7292	5716	13351	11140	17451
Li	11	11	13	4	8	9	8	8	8	6
Rb	306	259	523	275	264	2042	318	292	504	614
Sr	1170	996	1103	903	698	1343	1254	1321	1435	1917
Pb	60	58	70	69	65	74	75	63	99	90
Th	26	27	25	32	37	36	28	25	45	54
U	2	1	<1	2	8	2	2	1	2	9
Zr	1791	1467	1432	1777	1960	1462	1633	1655	2093	1969
Nb	141	116	110	139	150	116	129	130	234	303
Y	9	19	15	24	19	25	18	16	18	32
La	464	386	394	460	660	397	435	419	604	448
Ce	780	570	587	756	949	667	749	606	996	822
Nd										374
Sc	21	18	17	27	25	17	17	20	25	15
V	416	178	129	221	445	170	278	108	106	84
Cr	351	320	338	398	342	242	283	323	172	556
Co	27	34	34	44	49	38	37	51	45	
Ni	357	342	300	353	430	364	522	727	209	348
Cu	40	38	36	51	47	53	46	62	79	79
Zn	78	66	65	70	130	78	74	74	77	90
Sn	13	17	11	15	16	8	10	18	15	15
Mo	<1	1	<1	<1	<1	3	2	<1	<1	<3
Ga	22	14	15	17	21	19	19	13	10	17
As										3
S	50	1020	190	340	110	70	360	700	520	
F	4580	3010	2880	1800	4790	3910	3600	3750	3800	3100
Cl	58	53	93	63	96	73	80	87	77	

81 MILE VENT

Sample number	66160332	66160333	67160392	79211054	79211056	71426	30493	71427	71428A	71429
Formation	Fitzroy Lamproites	Fitzroy Lamproites	Fitzroy Lamproites	Fitzroy Lamproites	Fitzroy Lamproites	Fitzroy Lamproites	Fitzroy Lamproites	Fitzroy Lamproites	Fitzroy Lamproites	Fitzroy Lamproites
Rock type	Phlog-Leuc Lamproite	Di-Phl-Lc Lamproite	Phlog-Leuc Lamproite	Phl-Lc Lamproite	Phl-Lc Lamproite	Phl-Lc Lamproite	Phl-Lc Lamproite	KRi-Phl-Lc Lamproite	KRi-Phl-Lc Lamproite	KRi-Phl-Lc Lamproite
Locality	81-Mile Vent	81-Mile Vent	81-Mile Vent	81-Mile Vent	81-Mile Vent	81-Mile Vent	81-Mile Vent	81-Mile Vent	81-Mile Vent	81-Mile Vent
Grid reference	997497	997497	997497	997497	997497	997497	997497	997497	997497	997497
Map sheet	Ellendale	Ellendale	Ellendale	Ellendale	Ellendale	Ellendale	Ellendale	Ellendale	Ellendale	Ellendale
Additional data						centre cre	centre	top sill,N	top sill,S	mid sill,N
Biblio. ref.	GMD-BMR	GMD-BMR	GMD-BMR	GMD-BMR	GMD-BMR	Lewis-GSWA	Lewis-GSWA	Lewis-GSWA	Lewis-GSWA	Lewis-GSWA
SiO_2	52.62	47.60	61.15	48.12	51.75	46.80	49.40	52.40	55.20	54.30
TiO_2	5.49	7.83	5.28	8.12	6.08	7.30	7.36	5.65	5.65	5.85
Al_2O_3	6.88	6.29	6.43	5.97	7.47	6.40	5.70	6.50	6.90	7.30
Fe_2O_3	4.17	6.36	4.11	5.99	5.11	5.80	6.10	4.80	4.50	4.30
FeO	1.16	1.45	0.96	1.50	0.84	1.68	1.29	0.88	1.04	1.35
MnO	0.07	0.11	0.06	0.09	0.07	0.10	0.13	0.06	0.06	0.06
MgO	7.97	10.55	5.71	10.74	7.39	10.50	11.00	7.88	6.80	6.94
CaO	3.27	2.87	1.30	2.80	2.39	3.53	2.68	2.38	2.16	2.13
Na_2O	0.51	0.47	0.39	0.49	0.52	0.26	0.28	0.49	0.55	0.67
K_2O	10.00	9.21	8.94	9.56	10.92	8.62	8.48	10.40	9.80	9.88
P_2O_5	1.58	1.44	0.87	1.05	1.18	1.88	1.44	1.25	0.97	1.07
H_2O+	1.59	2.29	2.08	2.65	2.25	3.15	2.69	1.87	1.51	1.65
H_2O-	0.47	0.25	0.57	0.42	0.66	0.70	0.86	1.28	0.66	0.96
CO_2	1.22	0.47	0.31	0.25	0.32	0.09	0.11	0.05	0.05	0.07
Rest	2.48	2.69	1.74	2.08	2.47	3.22	2.16	2.79	2.39	2.32
Total	99.48	99.88	99.90	99.83	99.42	100.03	99.68	98.68	98.24	98.85
Ba	14611	14009	8105	10337	12960	16834	7970	15264	11575	10705
Li	6	7	6	7	6	10	7	5	6	6
Rb	385	669	331	667	442	664	550	341	420	353
Sr	2781	1770	757	1900	1799	2175	1600	1861	1907	1665
Pb	73	95	61	90	81	110	100	78	75	80
Th	43	60	39	59	47	68	30	32	29	33
U	5	4	6	6	6	1	4	3	1	3
Zr	1485	1855	1435	1914	1659	1950	1800	1784	1808	1971
Nb	151	250	155	250	172	281	300	132	135	141
Y	17	17	18	15	20	29	40	19	16	22
La	360	542	408	519	438	531	600	473	463	471
Ce	594	855	640	788	695	646	950	769	799	825
Nd										
Sc						23	25	15	17	13
V	220	198	187	215	268	312	520	153	120	180
Cr	286	421	264	389	329	503	300	201	202	225
Co	22	36	28	31	24	41	50	39	26	34
Ni	240	355	207	312	265	250	380	285	274	300
Cu	39	45	33	47	43	60	70	42	37	46
Zn	73	83	78	86	84	99	94	73	84	91
Sn	<2	9	2	9	<2		10	9	15	11
Mo						10	<1	<1	<1	2
Ga	16	12	18	13	22	15	14	18	20	20
As	2	1	1	<1	1		<10			
S						340	200	340	180	270
F		3600	4000		3700	5589	5300	4660	4630	4840
Cl		20				130		78	81	70

81 MILE VENT

Sample number	71818	71819	71823	71825	71828	83210302	83210304	83210305
Formation	Fitzroy Lamproites	Fitzroy Lamproites	Fitzroy Lamproites	Fitzroy Lamproites	Fitzroy Lamproites	Fitzroy Lamproites	Fitzroy Lamproites	Fitzroy Lamproites
Rock type	Phl-Lc Lamproite	Phl - Lc - Lamproite	Phl-Lc Lamproite	Ol-Phl-Lc Lamproite	Phl - Lc Lamproite	Ol-Phl-Lc Lamproite	Phl - Lc Lamproite	Phl - Lc - Lamproite
Locality	81-Mile Vent	81-Mile Vent	81-Mile Vent	81-Mile Vent	81-Mile Vent	81-Mile Vent	81-Mile Vent	81-Mile Vent
Grid reference	997497	997497	997497	997498	997498	997497	997497	997497
Map sheet	Ellendale	Ellendale	Ellendale	Ellendale	Ellendale	Ellendale	Ellendale	Ellendale
Additional data	mid sill,N	low sill,N	mid sill,S	centre, E	pod,E side	E flank	centre	lower sill
Biblio. ref.	Lewis-GSWA	Lewis-GSWA	Lewis-GSWA	Lewis-GSWA	Lewis-GSWA	ALJ-BMR	ALJ-BMR	ALJ-BMR
SiO_2	53.50	52.10	52.40	49.50	53.20	53.94	47.43	49.62
TiO_2	5.72	5.44	5.73	6.15	5.87	5.80	7.56	5.86
Al_2O_3	7.00	6.70	7.10	6.70	7.10	5.99	5.93	6.83
Fe_2O_3	4.20	4.30	5.10	6.40	5.10	5.41	5.78	4.76
FeO	1.27	0.84	0.46	0.86	0.61	1.12	1.32	0.49
MnO	0.07	0.04	0.03	0.12	0.06	0.09	0.08	0.03
MgO	7.39	6.48	6.26	8.85	7.11	7.81	10.19	7.85
CaO	2.61	2.78	2.32	2.55	2.36	2.07	2.85	2.70
Na_2O	0.70	0.92	0.12	0.32	0.10	0.33	0.39	1.01
K_2O	10.00	5.20	9.56	9.52	9.74	9.27	9.05	6.03
P_2O_5	1.37	1.63	1.84	1.63	1.83	1.28	1.37	1.34
H_2O+	1.56	5.32	3.02	2.18	2.43	2.26	2.22	4.96
H_2O-	0.89	3.77	3.00	1.84	1.84	1.56	2.11	4.74
CO_2	0.08	0.09	0.05	0.05	0.06	<0.01	0.11	0.42
Rest	2.51	3.20	1.92	2.50	2.04	2.39	3.73	3.01
Total	98.87	98.81	98.91	99.17	99.45	99.32	100.12	99.65
Ba	12059	11312	6432	11436	8002	11070	21754	9568
Li	8	6	8	6	6	5	7	6
Rb	315	8626	450	469	404	495	609	7470
Sr	1930	1827	1728	1534	1625	1608	2484	2560
Pb	68	74	60	93	85	89	100	101
Th	27	74	32	41	33	58	60	53
U	2	2	2	2	2	5.5	4.5	5.5
Zr	1865	1564	1967	2169	1939	1827	2168	1653
Nb	135	117	140	191	138	251	324	194
Y	19		19	23	34	32	36	
La	441	391	430	572	488	485	531	419
Ce	789	622	760	925	767	919	1060	851
Nd						365	496	332
Sc	17	15	16	27	18	13	15	11
V	160	151	678	214	236	199	232	205
Cr	234	125	233	308	199	526	48	357
Co	32	30	25	35	24			
Ni	249	277	252	486	325	427	353	272
Cu	83	87	58	68	60	40	52	44
Zn	108	79	75	85	90	78	84	91
Sn	16	8	11	17	14	9	13	9
Mo	<1	2	<1	<1	<1	<3	<3	<3
Ga	19	20	20	17	21	20	17	29
As						2.5	3	3
S	980	250	140	40	60			
F	4960	4650	4940	5020	5390	3600	2700	3800
Cl	79	62	80	68	58			

ELLENDALE 2

Sample number	71440	71436	71437B	71442
Formation	Fitzroy Lamproites	Fitzroy lamproites	Fitzroy lamproites	Fitzroy Lamproites
Rock type	Phl-Ol Lamproite	Carb. Phl-Ol Lamp	Phl-Ol-Lamproite	Phl-Ol-Lamproite
Locality	Ellendale No. 2	Ellendale No. 2	Ellendale No. 2	Ellendale No. 2
Grid reference	062519	063518	063518	063518
Map sheet	Ellendale	Ellendale	Ellendale	Ellendale
Additional data	2AC 8/24m	2AC 3/ 22m	2AC4/26m	2AC9/22-25
Biblio. ref.	Lewis-GSWA	Lewis-GSWA	Lewis-GSWA	Lewis-GSWA
SiO_2	42.50	37.10	37.40	39.60
TiO_2	4.63	4.60	4.79	4.59
Al_2O_3	4.30	4.40	4.70	4.20
Fe_2O_3	5.50	6.40	6.50	5.60
FeO	2.79	2.94	2.79	2.69
MnO	0.13	0.14	0.14	0.16
MgO	17.70	15.80	16.30	17.70
CaO	4.60	7.25	6.21	5.65
Na_2O	0.88	0.63	0.86	0.96
K_2O	4.34	3.35	3.47	4.11
P_2O_5	1.44	2.10	1.87	1.21
H_2O+	5.65	4.89	5.16	5.71
H_2O-	3.15	5.35	5.24	3.34
CO_2	0.28	2.46	1.68	1.41
Rest	1.82	1.88	1.99	2.11
Total	99.71	99.29	99.10	99.04
Ba	4906	5306	6239	7676
Li	60	41	55	61
Rb	538	362	358	471
Sr	1613	1975	1874	1659
Pb	80	75	77	80
Th	98	59	61	66
U	4	<1	1	2
Zr	1371	1648	1618	1550
Nb	259	207	211	229
Y	29	26	24	21
La	511	623	616	618
Ce	669	1186	1137	1131
Nd				
Sc	27	29	32	25
V	56	50	56	30
Cr	952	695	633	698
Co	58	51	51	61
Ni	600	627	632	706
Cu	56	53	60	53
Zn	96	81	75	80
Sn		15	13	5
Mo	3	<1	2	<1
Ga	4	6	6	7
As				
S	300	260	160	490
F	6072	4900	5500	4660
Cl	60	86	80	60

Sample number	71476F	30495A	30495E	30495G	30495H	71476D	71480C	71477B	71477E	71477H
Formation	Fitzroy Lamproites	Fitzroy Lamproites	Fitzroy Lamproites	Fitzroy Lamproites	Fitzroy Lamproites	Fitzroy Lamproites	Fitzroy Lamproites	Fitzroy Lamproites	Fitzroy Lamproites	Fitzroy Lamproites
Rock type	Ol. Lamp. (altered)	(Phl)-Ol-Lamproite	Ol - Lamp Tuff	Ol - Lamp Tuff	Ol - Lamp Tuff	Phl-Ol Lamproite	Phl-Ol Lamproite	Phl-Ol Lamproite	Phl-Ol Lamproite	(Phl)-Ol Lamproite
Locality	Ellendale No.4	Ellendale No.4	Ellendale No. 4	Ellendale No. 4	Ellendale No. 4	Ellendale No.4E	Ellendale No.4W	Ellendale No.4E	Ellendale No.4E	Ellendale No.4E
Grid reference	040453	040453	040453	040453	040453	040453	040453			
Map sheet	Ellendale	Ellendale	Ellendale	Ellendale	Ellendale	Ellendale	Ellendale	Ellendale	Ellendale	Ellendale
Additional data	4AC123/123	core,unkwn	core,unkwn	core,unkwn	core,unkwn	4AC123/96m	4AC203/50m	4AC188/41m	4AC188/90m	4AC188/137
Biblio. ref.	Lewis-GSWA	Lewis-GSWA	Lewis-GSWA	Lewis-GSWA	Lewis-GSWA	Lewis-GSWA	Lewis-GSWA	Lewis-GSWA	Lewis-GSWA	Lewis-GSWA
SiO_2	37.70	42.40	39.10	45.00	48.60	37.85	37.40	34.80	36.70	37.30
TiO_2	3.53	3.62	2.31	3.20	2.88	3.97	4.22	3.26	3.68	3.48
Al_2O_3	2.90	3.20	2.30	4.00	3.30	3.91	3.56	3.10	3.10	3.00
Fe_2O_3	5.60	4.10	4.90	4.40	3.60	5.77	5.96	6.80	6.30	5.40
FeO	2.54	3.48	2.15	2.44	1.94	2.84	3.01	1.96	1.89	2.38
MnO	0.12	0.15	0.12	0.14	0.13	0.13	0.13	0.12	0.12	0.13
MgO	24.70	26.10	27.80	16.00	16.00	23.20	23.70	24.70	23.20	23.40
CaO	3.67	5.24	2.46	4.91	4.56	4.51	4.43	4.55	4.39	4.08
Na_2O	0.34	0.55	0.05	0.30	0.30	0.28	0.36	0.17	0.32	0.26
K_2O	3.90	5.25	2.10	6.56	7.34	4.23	4.46	2.61	4.27	4.22
P_2O_5	1.71	1.30	1.56	2.71	1.74	1.68	1.89	1.77	1.53	1.48
H_2O+	7.20	2.99	10.00	4.34	5.12	7.20	7.73	8.65	7.30	6.82
H_2O-	3.40	1.19	3.93	3.06	2.62	2.02	1.52	4.00	4.05	3.57
CO_2	0.14	0.46	0.30	0.63	0.61	0.15	0.18	0.29	0.33	0.44
Rest	2.55	2.22	1.48	3.05	2.34	2.62	2.27	1.88	2.09	2.34
Total	100.00	102.25	100.57	100.74	101.08	100.36	100.82	98.66	99.27	98.30
Ba	12009	10030	6000	17020	12000	12760	9724	6111	7208	10464
Li	8	6	4	9	7	8	7	7	6	6
Rb	481	380	300	400	460	492	625	428	524	473
Sr	1576	1300	850	1700	1600	1433	1518	1247	1490	1560
Pb	60	60	40	80	60	50	40	49	56	53
Th	83	50	35	60	60	60	63	56	56	56
U	1	<2	<2	10	10	4	2	1	<1	<1
Zr	1269	1000	800	1200	1000	1149	1173	1245	1334	1329
Nb	196	200	150	150	150	210	222	190	168	161
Y	23	24	18	27	24	20	21	11	10	13
La	425	400	300	450	400	419	202	466	468	493
Ce	545	650	480	700	600	812	460	842	832	781
Nd										
Sc	22	15	20	20	15	22	24	24	19	21
V	54	32	32	287	76	23	59	20	65	67
Cr	1326	1000	800	450	450	982	972	1124	1014	1050
Co	70	80	85	60	45	73	75	75	68	69
Ni	880	1050	1500	640	660	1200	1200	1121	990	1038
Cu	109	60	40	45	45	68	63	48	48	58
Zn	68	78	68	72	65	88	76	66	65	66
Sn		6	4	4	4	7	9	10	10	5
Mo	10	<1	<1	<1	<1	2	1	<1	<1	<1
Ga	4	4	2	2	4	4	6	4	5	2
As		<10	<10	<10	<10	<1	<1			
S	40	100	200	400		130	440	420	1050	320
F	4703	4887	1617	5453	4848	4900	5050	4660	5250	3720
Cl	72					20	20	136	168	106

Sample number	71468D	71468G	71468I	71468M	71469D	71469H	71470A	71470F	71471B	71472B
Formation	Fitzroy Lamproites	Fitzroy Lamproites	Fitzroy Lamproites	Fitzroy Lamproites	Fitzroy Lamproites	Fitzroy Lamproites	Fitzroy Lamproites	Fitzroy Lamproites	Fitzroy Lamproites	Fitzroy Lamproites
Rock type	Olivine Lamproite	Olivine Lamproite	Olivine Lamproite	Olivine Lamproite	Olivine Lamproite	Olivine Lamproites	Phl-Ol Lamproite	Glassy Ol-Lamproite	Phl-Ol Lamproite	Phl-Ol Lamproite
Locality	Ellendale No.4E	Ellendale No.4E	Ellendale No.4E	Ellendale No.4E	Ellendale No.4E	Ellendale No.4E	Ellendale No.4E	Ellendale No.4E	Ellendale No.4E	Ellendale No.4E
Grid reference										
Map sheet	Ellendale	Ellendale	Ellendale	Ellendale	Ellendale	Ellendale	Ellendale	Ellendale	Ellendale	Ellendale
Additional data	4AC162/104	4AC162/134	4AC162/145	4AC162/223	4AC112/165	4AC112/254	4AC224/47m	4AC224/125	4AC218/45m	4AC192/105
Biblio. ref.	Lewis-GSWA	Lewis-GSWA	Lewis-GSWA	Lewis-GSWA	Lewis-GSWA	Lewis-GSWA	Lewis-GSWA	Lewis-GSWA	Lewis-GSWA	Lewis-GSWA
SiO_2	38.60	42.40	42.20	41.80	42.00	38.50	37.80	40.00	37.90	35.90
TiO_2	3.60	3.61	3.41	3.52	3.51	3.52	3.28	2.46	3.51	3.12
Al_2O_3	3.30	3.30	3.60	3.30	3.20	3.20	3.10	2.40	3.10	3.00
Fe_2O_3	5.20	4.40	4.10	4.70	4.40	4.60	5.80	4.50	5.90	6.30
FeO	2.76	3.48	3.62	3.29	3.36	3.03	1.64	2.56	1.84	2.10
MnO	0.12	0.12	0.12	0.12	0.12	0.12	0.09	0.11	0.11	0.13
MgO	24.80	23.60	23.00	23.70	24.00	23.10	24.50	25.50	23.80	25.90
CaO	5.65	4.86	4.55	4.94	5.22	7.31	5.28	2.70	3.72	4.37
Na_2O	0.41	0.51	0.47	0.65	0.48	0.76	0.16	0.74	0.27	0.21
K_2O	3.83	5.00	4.89	4.48	4.63	3.12	2.45	6.05	2.55	2.99
P_2O_5	1.39	1.27	1.64	1.45	1.70	1.60	1.40	1.91	1.04	1.67
H_2O+	5.10	2.78	3.18	2.69	2.37	4.29	7.72	5.99	7.38	7.27
H_2O-	2.52	2.08	2.35	1.91	1.48	2.40	3.70	1.75	5.09	3.44
CO_2	0.34	0.39	0.46	0.41	0.31	0.71	1.00	0.32	0.35	0.43
Rest	2.12	2.03	2.59	2.20	2.52	2.55	1.75	1.74	1.80	2.28
Total	99.74	99.83	100.18	99.16	99.30	98.81	99.67	98.73	98.36	99.11
Ba	9049	6645	11986	8318	12201	12146	5476	4275	4520	9109
Li	9	10	11	11	10	16	9	10	9	9
Rb	389	416	383	386	401	421	565	568	559	522
Sr	1356	1451	1455	1406	1349	1371	1298	1183	1381	1329
Pb	45	52	53	63	53	51	38	43	47	58
Th	53	58	52	59	55	54	59	51	64	53
U	1	<1	1	1	<1	2	2	4	1	1
Zr	1231	1333	1244	1296	1200	1171	1194	974	1378	1190
Nb	172	182	166	174	165	164	162	117	182	188
Y	15	16	16	13	13	14	12	11	15	13
La	451	473	449	455	456	414	425	375	470	457
Ce	776	876	783	862	755	766	794	651	875	789
Nd										
Sc	18	20	22	22	19	16	15	17	25	25
V	28	122	205	53	28	35	58	805	73	47
Cr	1014	1114	1076	1128	1024	1106	1048	940	1098	1141
Co	74	76	73	81	83	75	77	78	83	75
Ni	1076	994	967	1034	1034	1019	1066	1225	1043	1138
Cu	49	62	65	62	60	55	48	43	58	68
Zn	69	74	74	80	69	72	63	61	71	71
Sn	12	6	11	7	9	5	11	6	6	10
Mo	<1	<1	<1	<1	9	<1	<1	7	1	<1
Ga	3	4	4	6	5	3	4	2	5	4
As										
S	240	160	150	130	130	170	190	220	550	680
F	3770	5790	5530	5840	4720	5150	4090	4990	5290	5130
Cl	154	107	105	100	125	152	75	158	122	139

Sample number	71478B	71478D	71478F	71478J	71478L	71478N	71499B	71500B	71466B	71467B
Formation	Fitzroy	Fitzroy	Fitzroy	Fitzroy	Fitzroy	Fitzroy	Fitzroy	Fitzroy	Fitzroy	Fitzroy
Rock type	Lamproites (KRi)-Phl-Ol Lamp	Lamproites Phl-Ol Lamproite	Lamproites (KRi-Di)-Phl-Ol Lam	Lamproites (KRi-Di)-Ph-Ol-Lamp	Lamproites (KRi)-Phl-Ol - Lamp	Lamproites (Di)-Phl-Ol - Lamp	Lamproites Ol - Lamp Tuff	Lamproites Ol - Lamp Tuff	Lamproites (Phl) - Ol Lamproite	Lamproites Phl - Ol - Lamproite
Locality	Ellendale No.4W	Ellendale No.4W	Ellendale No.4W	Ellendale No.4W	Ellendale No.4W	Ellendale No.4W	Ellendale No.4	Ellendale No. 4	Ellendale No.4W	Ellendale No.4E
Grid reference	036452	036452								
Map sheet	Ellendale	Ellendale	Ellendale	Ellendale	Ellendale	Ellendale	Ellendale	Ellendale	Ellendale	Ellendale
Additional data	4AC191/58m	4AC191/126	4AC191/161	4AC191/244	4AC191/276	4AC191/310	4AC105/58m	4AC105/71m	4AC137/57m	4AC209/85m
Biblio. ref.	Lewis-GSWA	Lewis-GSWA	Lewis-GSWA	Lewis-GSWA	Lewis-GSWA	Lewis-GSWA	Lewis-GSWA	Lewis-GSWA	Lewis-GSWA	Lewis-GSWA
SiO_2	38.40	37.30	37.80	38.60	39.60	38.70	38.90	39.60	38.00	37.70
TiO_2	3.77	4.20	3.62	4.04	3.81	3.89	2.09	2.25	3.54	3.81
Al_2O_3	3.60	4.00	3.10	3.80	3.80	3.70	1.80	2.40	2.90	3.20
Fe_2O_3	5.70	5.30	5.40	5.50	5.00	5.40	5.80	5.40	5.70	6.10
FeO	2.68	3.34	2.85	2.79	3.03	2.81	1.58	1.93	2.45	2.16
MnO	0.13	0.13	0.13	0.13	0.12	0.12	0.11	0.11	0.13	0.12
MgO	22.60	22.50	23.40	22.30	22.20	22.00	25.80	25.70	25.00	24.60
CaO	4.18	4.54	3.72	4.53	4.17	4.16	2.47	2.83	3.90	3.84
Na_2O	0.40	0.41	0.55	0.81	1.00	1.05	0.06	0.07	0.49	0.43
K_2O	4.09	5.04	5.53	3.82	4.38	3.63	2.42	3.05	5.26	5.69
P_2O_5	0.97	1.97	1.87	0.92	0.78	1.49	1.56	1.87	1.81	1.66
H_2O+	6.47	5.19	5.50	5.72	5.32	5.13	8.85	9.00	6.21	6.61
H_2O-	3.95	2.60	2.36	3.50	2.70	4.05	5.11	3.64	1.97	1.32
CO_2	0.29	0.25	0.22	0.47	0.30	0.39	0.19	0.22	0.23	0.27
Rest	1.80	2.27	2.59	2.22	2.59	2.89	1.63	1.53	2.11	2.26
Total	99.03	99.04	98.64	99.15	98.80	99.41	98.37	99.60	99.70	99.77
Ba	6529	10839	13011	10520	12867	16187	7004	6066	7317	8071
Li	7	8	8	8	8	8	5	7	10	9
Rb	535	423	529	367	507	392	301	308	607	554
Sr	1238	1331	1085	1284	1108	1271	978	971	1430	1491
Pb	44	44	53	44	42	42	41	42	59	58
Th	44	51	52	47	47	43	43	42	62	64
U	1	3	3	2	1	4	3	2	2	1
Zr	1147	1137	1229	1192	1179	1163	857	906	1378	1470
Nb	162	174	165	165	157	159	99	107	175	181
Y	11	13	13	14	13	13	11	12	14	17
La	385	400	444	356	413	393	288	329	471	512
Ce	715	751	766	658	686	622	540	571	888	926
Nd										
Sc	14	21	25	15	14	21	14	16	25	26
V	97	53	91	69	97	83	59	68	47	122
Cr	930	946	1062	783	924	859	746	742	1149	1214
Co	65	87	73	68	70	71	79	74	74	75
Ni	998	910	1020	889	943	931	1464	1233	1117	1068
Cu	51	50	47	54	49	50	27	33	48	52
Zn	65	63	60	70	67	66	56	55	71	75
Sn	7	6	9	9	7	5	7	9	12	9
Mo	<1	<1	<1	<1	1	2	<1	<1	<1	<1
Ga	3	4	2	3	5	3	2	2	5	4
As										
S	280	190	230	760	210	380	230	110	140	80
F	3730	3560	4420	3850	5750	4300	1890	2290	5180	5720
Cl	116	192	159	131	<50	256	96	119	113	142

Sample number	71476B	71479B	71479D	71479G	71480F	71480I	71481A	71481C	71482A	71483B
Formation	Fitzroy	Fitzroy	Fitzroy	Fitzroy	Fitzroy	Fitzroy	Fitzroy	Fitzroy	Fitzroy	Fitzroy
Rock type	Lamproites Phl-Ol Lamproite	Lamproites Olivine Lamproite	Lamproites Phl-Ol Lamproite	Lamproites Olivine Lamproite	Lamproites Phl-Ol Lamproite	Lamproites Phl-Ol Lamproite	Lamproites (Glassy) Ol Lamp.	Lamproites (Glassy) Ol Lamp.	Lamproites Ol - Lamp Tuff	Lamproites Olivine Lamproite
Locality	Ellendale No.4E	Ellendale No.4W	Ellendale No.4W	Ellendale No.4W	Ellendale No.4W	Ellendale No.4W	Ellendale No.4W	Ellendale No.4W	Ellendale No.4W	Ellendale No.4W
Grid reference										
Map sheet	Ellendale	Ellendale	Ellendale	Ellendale	Ellendale	Ellendale	Ellendale	Ellendale	Ellendale	Ellendale
Additional data	4AC123/55m	4AC189/52m	4AC189/92m	4AC189/143	4AC203/153	4AC203/206	4AC187/65m	4AC187/92m	4AC185/60m	4AC108/68m
Biblio. ref.	Lewis-GSWA	Lewis-GSWA	Lewis-GSWA	Lewis-GSWA	Lewis-GSWA	Lewis-GSWA	Lewis-GSWA	Lewis-GSWA	Lewis-GSWA	Lewis-GSWA
SiO_2	37.60	37.20	37.20	38.60	41.10	38.30	36.70	39.60	39.60	37.30
TiO_2	3.94	3.72	3.90	2.25	3.56	3.56	3.49	2.28	2.39	3.98
Al_2O_3	3.90	3.00	3.10	2.20	3.00	3.00	2.90	1.80	2.10	2.90
Fe_2O_3	5.40	6.30	6.20	5.30	4.70	5.10	6.30	5.40	4.70	6.40
FeO	3.08	1.75	1.97	2.17	3.26	2.68	1.36	1.56	1.92	1.58
MnO	0.13	0.12	0.13	0.11	0.12	0.12	0.08	0.11	0.11	0.13
MgO	23.70	24.30	24.50	27.70	24.40	23.60	24.20	26.30	24.50	23.20
CaO	4.59	3.63	3.86	2.60	3.97	3.86	3.66	2.86	4.50	4.44
Na_2O	0.53	0.20	0.46	0.09	0.39	0.50	0.22	0.10	0.11	0.32
K_2O	3.71	3.20	4.20	3.20	5.11	3.61	3.21	2.85	2.11	3.57
P_2O_5	2.11	1.47	1.74	1.34	1.78	1.90	2.65	1.76	1.97	1.83
H_2O+	5.78	7.28	7.19	8.57	2.98	6.20	7.57	8.40	7.59	7.58
H_2O-	2.53	5.58	2.62	3.30	1.92	3.08	4.73	3.96	5.04	3.54
CO_2	0.20	0.71	0.35	0.46	0.58	0.69	0.54	0.23	0.98	0.23
Rest	2.32	1.91	2.51	1.60	2.99	2.98	1.91	1.62	1.47	2.19
Total	99.52	100.37	99.93	99.49	99.86	99.18	99.52	98.83	99.09	99.19
Ba	9882	5825	11052	6446	15048	13705	7280	6155	3686	7601
Li	10	8	8	7	8	8	8	6	7	9
Rb	463	568	496	333	420	498	550	349	273	528
Sr	1253	1539	1590	1093	1518	1498	1476	1120	1239	1852
Pb	46	49	65	44	55	56	51	38	49	75
Th	47	73	93	49	57	63	62	47	49	77
U	1	2	1	3	1	1	5	2	<1	2
Zr	1093	1622	1574	845	1352	1393	1346	969	1179	1654
Nb	179	200	191	104	171	174	156	112	125	205
Y	13	15	20	11	15	16	14	12	13	16
La	393	509	589	359	507	517	455	336	377	561
Ce	715	978	1056	609	806	901	817	566	692	1046
Nd										
Sc	23	25	25	16	24	24	25	16	16	29
V	163	54	61	39	23	44	68	58	156	75
Cr	988	1098	1098	795	1245	1182	1020	812	792	1061
Co	65	67	68	83	81	59	50	63	62	65
Ni	940	1046	998	1396	1011	1003	893	1191	1064	903
Cu	59	59	62	40	55	53	48	41	39	56
Zn	71	66	74	66	77	69	59	58	58	70
Sn	6	10	11	5	7	7	12	6	8	14
Mo	<1	<1	<1	<1	<1	<1	<1	<1	<1	<1
Ga	5	5	4	2	5	4	5	2	4	5
As										
S	50	980	790	60	130	3510	60	160	870	310
F	6370	3260	3430	2100	5900	5180	3030	3050	3670	4610
Cl	136	122	137	125	96	97	113	81	105	123

Sample number	71484	71485	71486A	71486C	71487A	71488	71489B	71489E	71496B	71497A
Formation	Fitzroy Lamproites	Fitzroy Lamproites	Fitzroy Lamproites	Fitzroy Lamproites	Fitzroy Lamproites	Fitzroy Lamproites	Fitzroy Lamproites	Fitzroy Lamproites	Fitzroy Lamproites	Fitzroy Lamproites
Rock type	Phl-Ol Lamproite	KRi-Phl-Ol Lamproite	Olivine Lamproite	Glassy Ol-Lamproite	Phl - Ol-Lamproite	Phl-Ol Lamproite	Phl-Ol Lamproite	Phl-Ol Lamproite	Phl - Ol - Lamproite	Phl-Ol Lamproite
Locality	Ellendale No.4W	Ellendale No.4W	Ellendale No.4W	Ellendale No.4W	Ellendale No.4E	Ellendale No.4E	Ellendale No.4E	Ellendale No.4E	Ellendale No.4E	Ellendale No.4E
Grid reference										
Map sheet	Ellendale	Ellendale	Ellendale	Ellendale	Ellendale	Ellendale	Ellendale	Ellendale	Ellendale	Ellendale
Additional data	4AC140/73m	4AC263/27m	4AC228/72m	4AC228/128	4AC129/38m	4AC263/27m	4AC190/41m	4AC190/109	4AC204/71m	4AC104/20m
Biblio. ref.	Lewis-GSWA	Lewis-GSWA	Lewis-GSWA	Lewis-GSWA	Lewis-GSWA	Lewis-GSWA	Lewis-GSWA	Lewis-GSWA	Lewis-GSWA	Lewis-GSWA
SiO_2	37.40	39.10	37.60	38.70	36.20	37.10	36.90	36.50	36.50	36.60
TiO_2	3.70	3.73	3.74	2.14	3.66	3.21	3.52	3.69	3.68	3.64
Al_2O_3	3.20	3.60	2.90	1.90	3.00	3.00	3.00	3.30	3.50	2.90
Fe_2O_3	6.10	7.70	6.90	5.00	6.50	6.40	6.10	6.20	5.80	5.20
FeO	2.09	0.98	1.12	2.44	1.63	1.85	1.66	2.12	2.40	2.26
MnO	0.13	0.08	0.10	0.11	0.09	0.11	0.10	0.13	0.13	0.09
MgO	23.20	22.50	23.50	26.60	24.60	23.60	24.60	24.70	23.40	22.70
CaO	3.93	4.20	3.92	2.65	3.50	4.02	3.97	4.03	4.51	5.86
Na_2O	0.20	0.40	0.36	0.10	0.20	0.22	0.26	0.37	0.32	0.31
K_2O	3.61	2.54	4.79	2.63	2.15	3.66	2.94	3.61	5.13	2.31
P_2O_5	1.93	1.00	1.80	1.55	1.91	1.44	1.26	1.69	2.18	1.89
H_2O+	7.38	7.41	6.57	9.46	8.73	7.39	7.35	7.51	6.50	7.46
H_2O-	3.57	4.65	3.14	3.43	4.71	4.39	5.04	2.54	2.01	4.87
CO_2	0.36	0.16	0.39	0.42	0.39	0.54	0.74	0.20	0.49	1.19
Rest	2.21	1.86	2.12	1.44	1.73	1.75	1.90	2.06	2.13	1.73
Total	99.01	99.91	98.95	98.57	99.00	98.68	99.34	98.65	98.68	99.01
Ba	9978	5820	7540	4594	4779	5853	5579	7438	8807	4423
Li	9	10	10	8	10	10	9	11	10	7
Rb	481	455	548	260	377	552	494	460	497	369
Sr	1434	1230	1626	1001	1086	1181	1424	1298	1380	1461
Pb	56	43	63	44	61	51	60	62	49	52
Th	58	51	69	47	68	54	64	68	64	63
U	2	<1	3	2	3	2	2	1	2	2
Zr	1380	1259	1458	861	1515	1204	1353	1450	1354	1365
Nb	186	178	182	108	194	184	187	189	191	184
Y	16	12	18	12	18	14	13	15	16	14
La	452	409	503	297	449	413	424	480	482	462
Ce	810	687	893	486	802	715	797	888	828	790
Nd										
Sc	29	18	25	15	28	22	24	24	25	23
V	88	79	122	159	51	68	86	33	88	43
Cr	1080	947	1038	924	1255	1072	1109	1211	1196	1122
Co	61	69	68	74	65	66	68	71	63	71
Ni	955	1012	982	1395	1001	1159	1035	1087	974	987
Cu	56	57	55	43	59	65	62	60	52	55
Zn	68	69	68	58	72	65	61	76	69	67
Sn	6	9	27	8	11	21	15	8	17	27
Mo	<1	<1	<1	<1	<1	<1	1	<1	<1	<1
Ga	4	5	5	3	4	4	4	5	6	4
As										
S	220	390	40	720	630	260	680	590	150	840
F	2680	5740	4760	2140	4120	3490	5170	4050	3150	4620
Cl	134	122	104	162	122	117	101	89	133	110

ELLENDALE 4

Sample number	71497C	71498	76009A	76009B	76009C	76009D	76009E
Formation	Fitzroy Lamproites	Fitzroy Lamproites	Fitzroy Lamproites	Fitzroy Lamproites	Fitzroy Lamproites	Fitzroy Lamproites	fitzroy lamproites
Rock type	Ol - Lamp Tuff	(Glassy) Ol Lamp.	Phl - Ol - Lamproite	Phl-Ol Lamproite	(Phl)-Ol- Lamproite	(Phl)-Ol- Lamp. Tuff	'Sandy' Tuff
Locality	Ellendale No. 4E	Ellendale No.4E	Ellendale No.4E	Ellendale No.4E	Ellendale No.4E	Ellendale No. 4E	Ellendale No. 4E
Grid reference							
Map sheet	Ellendale	Ellendale	Ellendale	Ellendale	Ellendale	Ellendale	Ellendale
Additional data	4AC104/52m	4AC11/45m	4AC147/33m	4AC147/102	4AC147/152	4AC147/161	4AC147/226
Biblio. ref.	Lewis-GSWA	Lewis-GSWA	Lewis-GSWA	Lewis-GSWA	Lewis-GSWA	Lewis-GSWA	Lewis-GSWA
SiO_2	43.70	38.80	37.10	36.30	37.80	44.80	53.90
TiO_2	1.60	2.22	3.49	3.40	3.37	3.41	2.15
Al_2O_3	3.20	2.00	3.30	3.00	3.00	4.30	3.90
Fe_2O_3	3.70	5.10	6.40	5.90	5.20	4.80	3.00
FeO	1.79	1.92	1.58	2.04	2.60	1.82	1.31
MnO	0.06	0.10	0.10	0.13		0.12	0.12
MgO	22.80	27.80	23.90	23.60	24.30	13.50	7.28
CaO	2.93	2.71	4.80	5.77	3.72	5.28	9.45
Na_2O	0.08	0.08	0.19	0.23	0.36	0.60	0.30
K_2O	2.28	2.17	2.65	3.77	3.62	7.70	4.15
P_2O_5	0.93	1.70	1.43	1.75	1.42	3.55	1.95
H_2O+	6.67	8.94	7.73	7.01	6.67	3.32	2.67
H_2O-	7.42	4.82	4.44	3.46	3.82	1.70	1.99
CO_2	0.82	0.22	0.81	0.51	0.50	0.36	5.56
Rest	0.93	1.63	2.00	1.99	2.65	3.10	1.37
Total	98.91	100.21	99.92	98.86	99.03	98.36	99.10
Ba	1313	6853	5955	7507	12901	15152	4397
Li	14	7	6	6	7	28	60
Rb	272	291	530	522	441	565	238
Sr	618	987	1348	1300	1444	2319	1256
Pb	25	35	60	67	58	91	48
Th	39	45	61	58	54	88	59
U	2	2	1	2	1	5	2
Zr	686	926	1359	1209	1280	1286	682
Nb	78	110	189	172	160	152	99
Y	14	11	14	14	10	26	18
La	215	293	466	441	429	669	379
Ce	398	493	797	761	718	1139	693
Nd							
Sc	14	17	20	17	23	23	13
V	77	77	86	68	67	410	73
Cr	554	833	1229	1117	1114	399	218
Co	52	70	71	69	73	41	44
Ni	925	1257	1117	1170	1141	502	309
Cu	33	40	56	56	60	57	41
Zn	51	61	81	82	80	90	71
Sn	11	20	8	4	7	6	8
Mo	<1	<1	<1	<1	<1	<1	<1
Ga	3	3	5	4	3	8	6
As							
S	1140	230	590	600	360	60	2030
F	3380	2170	5850	3380	4610	6930	3980
Cl	102	122	101	135	158	62	92

Sample number	71490C	71490E	71491B	71491C	71491F	71491L	71492A	71493B	71494A	71495B
Formation	Fitzroy Lamproites	Fitzroy Lamproites	Fitzroy Lamproites	Fitzroy Lamproites	fitzroy lamproites	Fitzroy Lamproites	Fitzroy Lamproites	Fitzroy Lamproites	Fitzroy Lamproites	fitzroy lamproites
Rock type	Phl - Ol-Lamproite	Ol - Lamp Tuff	Phl - Ol - Lamproite	Olivine Lamproite	Ol - Lamp Tuff	Ol - Lamp Tuff	Phl-Ol Lamproite	Ol - Lamp Tuff	Olivine Lamproite	Ol - Lamp Tuff
Locality	Ellendale No.4Sat	Ellendale No.4Sat	Ellendale No.4Sat	Ellendale No.4Sat	Ellendale No.4Sat	Fllendale No.4Sat	Ellendale No.4Sat	Ellendale No.4Sat	Ellendale No.4Sat	Ellendale No.4Sat
Grid reference	051449	051449		051449	051449					
Map sheet	Ellendale	Ellendale	Ellendale	Ellendale	Ellendale	Ellendale	Ellendale	Ellendale	Ellendale	Ellendale
Additional data	4AC214/31m	4AC214/68m	4AC212/36m	4AC212/73m	4AC212/117	4AC212/197	4AC206/34m	4AC210/39m	4AC202/38m	4AC236/34m
Biblio. ref.	Lewis-GSWA	Lewis-GSWA	Lewis-GSWA	Lewis-GSWA	Lewis-GSWA	Lewis-GSWA	Lewis-GSWA	Lewis-GSWA	Lewis-GSWA	Lewis-GSWA
SiO_2	36.70	38.00	37.80	35.20	35.20	36.00	37.40	40.50	39.30	33.10
TiO_2	3.62	3.07	3.50	3.90	2.49	3.42	3.72	2.45	3.48	2.98
Al_2O_3	3.00	2.30	3.40	2.80	2.00	2.40	3.40	2.90	3.40	2.20
Fe_2O_3	6.20	5.90	5.70	6.30	5.40	5.60	6.10	4.80	5.70	6.10
FeO	1.96	1.38	2.33	1.92	1.59	1.94	1.98	1.55	2.00	0.89
MnO	0.12	0.11	0.12	0.13	0.08	0.11	0.12	0.08	0.08	0.10
MgO	23.60	22.60	23.10	22.60	23.60	23.00	23.00	21.60	21.40	21.80
CaO	5.05	6.76	4.31	6.05	6.90	6.74	4.92	3.84	4.29	7.50
Na_2O	0.34	0.18	0.38	0.31	0.12	0.34	0.35	0.13	0.44	0.17
K_2O	2.69	2.41	3.96	3.88	1.37	3.40	2.41	1.76	2.35	1.56
P_2O_5	1.67	1.77	1.05	1.71	2.93	2.38	1.34	1.59	1.41	3.97
H_2O+	7.82	7.23	7.13	7.21	7.25	7.06	7.57	7.19	7.00	8.20
H_2O-	3.77	5.28	2.96	2.71	5.47	3.27	4.40	8.06	5.87	4.67
CO_2	0.45	0.70	0.40	1.20	3.20	1.22	0.40	0.78	0.30	1.25
Rest	1.79	1.51	2.16	2.43	1.76	2.08	1.91	1.86	1.91	3.46
Total	98.78	99.20	98.30	98.35	99.36	98.96	99.02	99.09	98.93	97.95
Ba	4100	3649	10117	10034	6576	6831	5354	7577	6397	20949
Li	6	8	6	8	8	8	9	12	10	7
Rb	410	303	493	558	187	430	378	237	335	241
Sr	1627	1471	1275	1578	1083	1496	1530	1162	1401	1117
Pb	49	54	<10	74	56	67	58	46	69	60
Th	62	66	47	70	57	67	63	58	60	60
U	1	6	1	6	6	4	1	3	2	4
Zr	1395	1551	1133	1743	1269	1633	1430	1249	1406	1255
Nb	187	161	149	200	137	183	189	133	179	156
Y	16	18	11	17	16	18	21	19	15	18
La	450	466	386	557	409	513	425	375	426	448
Ce	890	920	698	995	740	960	821	658	767	651
Nd										
Sc	22	18	17	25	18	19	24	19	25	20
V	93	52	73	35	43	29	60	190	113	32
Cr	1135	672	984	1136	804	943	1121	677	1083	880
Co	67	61	51	72	65	76	68	57	61	53
Ni	1010	939	912	931	925	920	954	893	900	901
Cu	50	40	40	56	35	49	59	41	58	31
Zn	62	58	59	70	50	57	66	58	65	58
Sn	11	10	4	14	8	8	17	5	5	6
Mo	<1	<1	<1	<1	<1	1	<1	<1	<1	<1
Ga	4	3	4	4	2	3	5	3	4	<2
As										
S	1170	150	390	1140	1000	370	1110	660	230	3040
F	5260	3650	3200	3520	3550	5740	5450	3690	4750	3280
Cl	111	116	154	167	127	147	117	105	116	124

ELLENDALE 4, SATELLITE PIPE

Sample number	71495F
Formation	Fitzroy Lamproites
Rock type	Ol - lamp Tuff
Locality	Ellendale No.4Sat
Grid reference	
Map sheet	Ellendale
Additional data	4AC236/100
Biblio. ref.	Lewis-GSWA
SiO_2	39.50
TiO_2	2.75
Al_2O_3	2.20
Fe_2O_3	4.90
FeO	1.55
MnO	0.10
MgO	20.60
CaO	6.62
Na_2O	0.16
K_2O	2.35
P_2O_5	2.01
H_2O+	6.74
H_2O-	5.68
CO_2	1.85
Rest	1.71
Total	98.72
Ba	6134
Li	13
Rb	284
Sr	1123
Pb	52
Th	57
U	3
Zr	1415
Nb	139
Y	15
La	383
Ce	690
Nd	
Sc	20
V	100
Cr	714
Co	57
Ni	891
Cu	44
Zn	60
Sn	4
Mo	<1
Ga	2
As	
S	840
F	3420
Cl	113

Sample number	80210126	80210127	80210128	71448G	71448F	71449A	71449D	71448C
Formation	Fitzroy Lamproites		Fitzroy Lamproites	Fitzroy Lamproites	Fitzroy Lamproites	Fitzroy Lamproites	Fitzroy Lamproites	Fitzroy Lamproites
Rock type	Olivine Lamproite	Spinel Lherzolite	Olivine Lamproite	Phl-Ol Lamproite	Olivine lamproite	Ol-KRi-Lc Lamproite	(KRi)-Phl-Lc Lamp	Olivine Lamproite
Locality	Ellendale No.7	Ellendale No.7	Ellendale No.7 (?)	Ellendale No.7	Ellendale No.7	Ellendale No.7	Ellendale No.7	Ellendale No.7
Grid reference				970535	970535	970535	970535	973533
Map sheet	Ellendale		Ellendale	Ellendale	Ellendale	Ellendale	Ellendale	Ellendale
Additional data	core	Nodule	core	7AC17/130m	7AC17,128m	7AC19/107m	7AC18,155m	7AC17/ 80m
Biblio. ref.	Donat-BMR	Donat-BMR	Donat-BMR	Lewis-GSWA	Lewis-GSWA	Lewis-GSWA	Lewis-GSWA	Lewis-GSWA
SiO_2	40.83	41.40	40.94	42.80	41.52	49.26	45.58	40.40
TiO_2	2.56	0.04	2.53	2.71	2.68	5.41	7.13	3.13
Al_2O_3	3.28	0.37	3.10	3.30	3.54	7.27	5.95	3.80
Fe_2O_3	4.55	1.95	4.38	4.90	4.57	5.47	6.69	5.10
FeO	3.88	5.16	3.98	3.52	3.90	1.02	1.18	3.41
MnO	0.13	0.12	0.13	0.12	0.13	0.10	0.06	0.13
MgO	28.24	45.51	29.09	24.90	26.90	8.29	10.50	21.90
CaO	4.21	0.27	4.17	4.30	4.38	2.56	3.90	5.49
Na_2O	0.35	0.05	0.44	0.51	0.36	0.45	0.48	0.52
K_2O	3.53	0.22	3.49	4.23	4.10	7.74	5.07	4.25
P_2O_5	0.55	0.01	0.55	0.60	0.62	0.64	1.17	0.83
H_2O+	2.97	3.46	3.61	3.74	4.13	5.29	5.45	4.59
H_2O-	1.91	0.20	0.86	1.74	1.60	2.97	5.82	2.10
CO_2	0.27	0.11	0.33	0.10	0.19	0.30	0.12	0.73
Rest	1.65	0.82	1.60	1.70	1.97	4.47	1.90	2.87
Total	98.91	99.69	99.20	99.17	100.59	101.24	101.00	99.25
Ba	6531	93	6414	6976	10093	31447	6043	17578
Li	4	<1	3	6	6	6	9	6
Rb	388	16	363	376	386	1459	457	426
Sr	1057	23	1044	986	959	1075	1440	1231
Pb	19	<2	17	20	20	50	50	27
Th	24	<2	24	25	18	14	49	22
U	3	<1	2	<1	<1	1	6	<1
Zr	620	14	592	603	564	1238	1995	634
Nb	120	3	118	113	118	123	215	108
Y	8	<2	11	17	16	19	31	9
La	146	4	149	232	185	308	419	260
Ce	260	6	279	270	261	368	1031	337
Nd	85	3	85					
Sc	15	3	15	17	18	18	23	18
V	49	39	43	80	46	139	149	48
Cr	1651	2801	1622	1703	1250	316	397	1047
Co				70	81	42	42	78
Ni	1157	2316	1217	1120	1500	390	410	1031
Cu	41	6	39	46	55	145	60	41
Zn	59	33	59	70	90	88	90	68
Sn	5	<2	4		6	12	14	12
Mo				4	1	3	1	<1
Ga	2	<2	3	3	5	18	14	4
As	2	<2	<1		<1	<1	<1	
S				100	120	800	130	1100
F	3000	1500	2400	2610	1950	3200	5850	2570
Cl				70	50	70	80	99

Sample number	79211086	80210129	71456B	71456G	30494A	71456A	71456D	71474B	71475B	71462B
Formation	Fitzroy Lamproites	Fitzroy Lamproites	Fitzroy Lamproites	Fitzroy Lamproites	Fitzroy Lamproites	Fitzroy Lamproites	Fitzroy Lamproites	Fitzroy Lamproites	Fitzroy Lamproites	Fitzroy Lamproites
Rock type	KRi-Phl-Ol Lamproite	Olivine Lamproite	Di-KRi-Phl -Ol Lamp	Phl-Ol Lamproite	Olivine Lamproite	KRi-Phl-Ol Lamp	(KRi)-Phl-Ol Lamp	Phl-Ol Lamproite	(Phl)-Ol Lamproite	Olivine Lamproite
Locality	Ellendale No.9	Ellendale No.9(?)	Ellendale No.9	Ellendale No.9	Ellendale No.9	Ellendale No.9	Ellendale No.9	Ellendale No.9	Ellendale No.9	Ellendale No.9
Grid reference			970970	970970	970570	970970	970970	970970	970970	972569
Map sheet	Ellendale	Ellendale	Ellendale	Ellendale	Ellendale	Ellendale	Ellendale	Ellendale	Ellendale	Ellendale
Additional data	drill core	core	9AC 86/52m	9AC86/127m	core,unkwn	9AC86/ 70m	9AC86, 70m	9AC52, 91m	9AC110/56m	9AC108/45m
Biblio. ref.	Don-BMR	Donat-BMR	Lewis-GSWA	Lewis-GSWA	Lewis-GSWA	Lewis-GSWA	Lewis-GSWA	Lewis-GSWA	Lewis-GSWA	Lewis-GSWA
SiO_2	42.61	41.31	40.60	40.40	45.30	36.81	40.09	40.43	40.71	38.90
TiO_2	3.19	3.15	3.34	3.64	3.61	3.33	3.54	3.31	3.31	3.18
Al_2O_3	4.40	3.89	4.40	4.00	3.70	4.01	4.62	4.48	4.51	4.20
Fe_2O_3	4.52	5.58	4.10	5.40	3.80	5.38	4.61	4.22	4.58	4.60
FeO	4.26	2.99	4.68	3.00	3.95	4.00	4.38	4.42	4.28	4.09
MnO	0.14	0.13	0.14	0.13	0.17	0.14	0.15	0.14	0.14	0.14
MgO	22.33	23.45	21.90	22.10	22.00	23.40	22.50	21.60	22.20	22.50
CaO	5.21	4.78	5.25	4.61	4.36	5.80	5.75	5.67	5.37	5.23
Na_2O	0.47	0.43	0.63	0.70	0.82	0.47	0.60	0.60	0.37	0.60
K_2O	4.03	4.44	3.69	4.58	6.65	4.74	4.58	4.95	4.51	3.43
P_2O_5	0.78	0.83	0.67	0.87	1.37	2.85	1.02	1.60	1.48	1.54
H_2O+	4.45	4.94	6.73	5.17	2.70	6.00	4.52	3.98	4.74	3.90
H_2O-	1.71	1.04	2.35	2.91	1.14	1.12	1.17	1.11	0.95	1.95
CO_2	0.17	0.52	0.08	0.13	0.19	0.15	0.15	0.27	0.21	0.12
Rest	2.05	1.97	1.96	2.45	1.90	2.76	3.18	4.19	3.16	4.38
Total	100.32	99.45	100.52	100.09	101.66	100.96	100.86	100.97	100.52	98.76
Ba	11393	9893	7423	11254	6450	13465	17435	27674	18281	29486
Li	7	5	10	10	6	8	7	8	7	9
Rb	611	428	648	646	460	751	764	500	486	473
Sr	1098	1263	1202	1438	1200	1341	1344	1284	1172	1145
Pb	39	20	58	55	60	20	20	50	50	35
Th	68	30	72	97	60	58	64	68	66	51
U	9	3	<1	1	<2	<1	2	4	4	2
Zr	841	729	845	991	900	723	832	807	796	752
Nb	244	143	252	221	250	224	245	232	233	190
Y	10	13	24	25	27	19	25	19	20	12
La	265	194	384	403	400	372	419	366	412	393
Ce	504	362	503	557	700	742	771	591	673	544
Nd	161	111								
Sc		17	19	22	20	23	22	22	21	24
V	107	87	80	79	221	40	52	49	32	55
Cr	1098	1341	1183	1088	800	1084	944	888	947	860
Co	57		58	64	70	83	74	77	73	84
Ni	792	963	720	720	930	1200	1100	930	1100	892
Cu	49	46	54	50	75	65	65	70	93	55
Zn	73	67	78	76	82	84	92	92	84	69
Sn	<2	3			4		1	8	5	3
Mo			<1	2	<1	1	7	2	1	<1
Ga	5	4	5	5	6	7	5	5	5	3
As	1	1			<10	<1	<1	<1	<1	
S			700	680	200	100	300	80	100	150
F		2000	5166	5539	6244	6450	6000	5400	5350	6050
Cl			69	44		110	70	110	140	120

ELLENDALE 9

Sample number	76008B	76008D	76008F	71457A	71457D	71458	71459B	71460	71461	71463
Formation	Fitzroy Lamproites	Fitzroy Lamproites	Fitzroy Lamproites	Fitzroy Lamproites	Fitzroy Lamproites	Fitzroy Lamproites	fitzroy lamproites	Fitzroy Lamproites	Fitzroy Lamproites	Fitzroy Lamproites
Rock type	Olivine Lamproite	Olivine Lamproite	Phl-Ol Lamproite	Phl-Ol Lamproite	Phl-Ol Lamproite	Di-Phl-Ol Lamproite	Carb. Ol Lamp. Tuff	Olivine Lamproite	Olivine Lamproite	Olivine Lamproites
Locality	Ellendale No.9	Ellendale No.9	Ellendale No.9	Ellendale No.9E	Ellendale No.9E	Ellendale No.9E	Ellendale No.9E	Ellendale No.9E	Ellendale No.9E	Ellendale No.9W
Grid reference										
Map sheet	Ellendale	Ellendale	Ellendale	Ellendale	Ellendale	Ellendale	Ellendale	Ellendale	Ellendale	Ellendale
Additional data	9AC60/80m	9AC60/117m	9AC60/193m	9AC49/ 32m	9AC49/ 36m	9AC78/ 37m	9AC22/ 51m	9AC113/42m	9AC48/ 40m	9AC63/111m
Biblio. ref.	Lewis-GSWA	Lewis-GSWA	Lewis-GSWA	Lewis-GSWA	Lewis-GSWA	Lewis-GSWA	Lewis-GSWA	Lewis-GSWA	Lewis-GSWA	Lewis-GSWA
SiO_2	38.20	39.00	38.50	38.60	40.00	40.60	35.60	40.00	39.50	39.60
TiO_2	3.38	3.67	2.97	3.21	3.27	3.06	2.29	3.19	3.16	3.53
Al_2O_3	3.80	3.90	3.90	4.50	4.50	4.50	3.50	4.20	4.40	4.10
Fe_2O_3	5.50	5.40	3.60	5.40	4.50	4.40	5.00	4.70	6.30	5.60
FeO	2.85	3.29	4.89	3.76	4.31	4.08	2.06	3.82	2.58	2.97
MnO	0.13	0.14	0.14	0.14	0.15	0.14	0.13	0.14	0.13	0.14
MgO	21.50	22.50	24.80	22.20	22.80	22.60	22.70	22.70	23.20	22.30
CaO	5.35	4.98	5.00	3.57	4.28	5.31	6.88	5.16	5.19	5.09
Na_2O	0.47	0.52	0.85	0.64	0.38	0.74	0.11	0.31	0.51	0.74
K_2O	4.72	3.82	4.45	3.21	4.49	3.70	1.31	3.16	3.11	3.77
P_2O_5	1.69	1.41	1.28	1.34	1.27	1.41	1.15	1.62	1.37	1.77
H_2O+	4.88	5.96	4.09	6.41	3.91	4.09	8.04	5.79	5.00	5.51
H_2O-	2.93	2.85	1.40	2.92	1.91	1.75	5.12	2.62	2.11	2.60
CO_2	0.43	0.21	0.24	0.54	0.15	0.16	4.07	0.14	0.07	0.18
Rest	3.14	1.79	2.37	2.16	3.57	3.77	1.53	2.54	2.97	2.27
Total	98.97	99.44	98.48	98.60	99.49	100.31	99.49	100.09	99.60	100.17
Ba	17992	5380	11416	8665	21973	23990	6229	12825	16864	9620
Li	12	21	12	13	10	10	11	14	10	19
Rb	519	459	482	572	557	500	208	447	479	465
Sr	1408	1231	1134	1179	1142	1075	725	1124	1126	1424
Pb	45	56	38	47	44	42	39	48	47	50
Th	58	69	57	58	58	51	47	57	58	66
U	2	2	1	4	2	1	3	3	2	3
Zr	841	1013	608	866	759	777	625	843	763	955
Nb	173	195	172	232	208	197	140	199	196	192
Y	13	18	12	16	14	14	14	16	16	17
La	396	443	435	384	405	396	302	400	403	442
Ce	651	816	736	640	601	556	533	680	636	743
Nd										
Sc	19	21	19	31	24	17	19	22	23	21
V	51	83	115	52	53	84	65	97	75	70
Cr	788	872	1062	1049	974	874	733	916	851	888
Co	59	64	77	73	77	66	60	66	69	68
Ni	855	878	1034	946	888	899	969	909	918	896
Cu	50	53	45	64	60	60	41	57	57	58
Zn	64	76	70	78	88	71	64	72	71	73
Sn	8	10	8	5	4	24	12	11	8	16
Mo	<1	<1	<1	<1	<1	<1	<1	<1	<1	<1
Ga	2	5	4	4	3	2	3	5	5	6
As										
S	140	80	120	390	370	80	870	320	130	120
F	6070	6320	5210	6170	5720	5990	3260	5480	5760	6160
Cl	109	92	65	163	106	131	126	163	124	143

ELLENDALE 9

Sample number	71464C	71465A	71465D
Formation	Fitzroy Lamproites	Fitzroy Lamproites	Fitzroy Lamproites
Rock type	Olivine Lamproite	KRi-Phl-Ol Lamproite	Olivine Lamproite
Locality	Ellendale No.9W	Ellendale No.9W	Ellendale No.9W
Grid reference			
Map sheet	Ellendale	Ellendale	Ellendale
Additional data	9AC29/ 67m	9AC30/ 32m	9AC30/ 85m
Biblio. ref.	Lewis-GSWA	Lewis-GSWA	Lewis-GSWA
SiO_2	44.10	37.60	39.90
TiO_2	3.20	3.08	3.48
Al_2O_3	3.50	4.10	3.90
Fe_2O_3	4.50	5.60	5.20
FeO	3.09	3.27	3.02
MnO	0.12	0.22	0.13
MgO	21.30	21.90	22.10
CaO	3.74	6.94	5.15
Na_2O	0.93	0.47	0.58
K_2O	6.51	2.33	4.12
P_2O_5	1.13	0.82	1.66
H_2O+	3.09	6.47	4.97
H_2O-	2.54	3.57	3.08
CO_2	0.28	2.46	0.69
Rest	2.12	1.64	2.54
Total	100.15	100.47	100.52
Ba	9416	4353	12286
Li	9	10	10
Rb	494	493	526
Sr	943	1117	1359
Pb	51	40	50
Th	72	55	68
U	2	1	3
Zr	902	781	958
Nb	169	207	188
Y	19	13	17
La	427	385	437
Ce	767	702	763
Nd			
Sc	20	21	21
V	195	89	68
Cr	816	977	855
Co	64	70	64
Ni	888	990	881
Cu	50	60	52
Zn	66	73	72
Sn	14	2	3
Mo	<1	<1	<1
Ga	6	4	4
As			
S	70	660	120
F	5130	5870	5930
Cl	97	65	99

Sample number	71453M	71455A	71453D	71453M	71450A	71451B	71451E	71453E	71453F	71453K
Formation	Fitzroy Lamproites	Fitzroy Lamproites	Fitzroy Lamproites	Fitzroy Lamproites	Fitzroy Lamproites	Fitzroy Lamproites	fitzroy lamproites	lamproites	Fitzroy Lamproites	Fitzroy Lamproites
Rock type	Olivine Lamproite	Phl-Ol Lamproite	Olivine Lamproite	Phl - Ol Lamproite	Phl-Ol- Lamproite	Olivine Lamproite	Ol-Lamp Tuff	Carb. Ol-Lamp. Tuff	Olivine Lamproite	Ol. Lamp. Tuff
Locality	Ellendale No.11	Ellendale No.11	Ellendale No.11	Ellendale No.11	Ellendale No.11	Ellendale No.11	Ellendale No. 11	Ellendale No.11	Ellendale No.11	Ellendale No.11
Grid reference	953 575	953 575	954574	954574	954574	954574	954574	954574	954574	954574
Map sheet	Ellendale	Ellendale	Ellendale	Ellendale	Ellendale	Ellendale	Ellendale	Ellendale	Ellendale	Ellendale
Additional data	core15/249	11AC26/24m	11AC15/56m	11AC15/249	11AC12/13m	11AC13/33m	11AC13/60m	11AC15/61m	11AC15/93m	11AC15/216
Biblio. ref.	Lewis-GSWA	Lewis-GSWA	Lewis-GSWA	Lewis-GSWA	Lewis-GSWA	Lewis-GSWA	Lewis-GSWA	Lewis-GSWA	Lewis-GSWA	Lewis-GSWA
SiO_2	41.30	41.45	40.10	41.90	42.50	39.90	50.20	37.70	40.50	47.50
TiO_2	2.72	2.71	2.64	2.72	2.39	2.43	1.21	1.75	2.44	1.13
Al_2O_3	3.70	3.37	3.50	3.70	3.50	3.70	2.50	2.90	3.80	3.20
Fe_2O_3	3.70	4.27	3.80	3.70	4.70	4.50	4.60	5.80	4.50	4.10
FeO	4.82	4.32	4.98	4.82	3.54	4.19	1.16	1.06	3.98	1.68
MnO	0.13	0.13	0.14	0.13	0.12	0.14	0.06	0.11	0.14	0.09
MgO	25.00	28.00	26.10	25.00	25.70	26.20	21.00	22.50	24.20	19.30
CaO	4.91	4.79	5.61	4.91	4.77	4.98	2.26	8.25	5.49	4.34
Na_2O	0.45	0.34	0.45	0.45	0.53	0.25	0.14	0.96	0.44	0.66
K_2O	4.02	2.24	3.46	4.02	2.21	2.32	1.86	1.89	3.28	2.92
P_2O_5	1.22	1.33	1.17	1.22	1.35	1.23	0.68	1.11	1.19	0.71
H_2O+	3.95	4.32	3.55	3.95	3.46	4.27	5.57	6.21	3.80	5.90
H_2O-	1.16	1.05	1.93	1.16	2.09	2.37	7.97	3.37	2.45	6.28
CO_2	0.14	0.12	0.12	0.14	0.22	0.13	0.15	3.63	0.38	0.83
Rest	1.54	2.12	2.11	1.54	2.36	2.07	0.68	1.60	1.83	0.98
Total	99.36	100.56	99.66	99.36	99.44	98.68	100.04	98.84	98.42	99.62
Ba	4192	9080	8966	4209	12200	9451	492	6782	7057	2027
Li	8	8	12	8	8	12	30	15	12	14
Rb	569	483	556	572	454	350	152	127	408	254
Sr	1078	1538	1245	1079	933	1024	1063	918	1124	866
Pb	40	20	40	40	37	36	22	14	36	24
Th	59	61	61	58	46	51	24	32	49	26
U	<1	8	1	<1	2	2	1	2	2	2
Zr	667	700	683	668	645	586	314	441	614	305
Nb	225	206	211	224	173	178	81	118	176	89
Y	18	12	19	17	11	10	5	8	12	7
La	302	303	344	324	312	321	141	243	323	137
Ce	435	574	415	441	521	554	242	378	554	262
Nd										
Sc	18	21	22	18	20	23	9	9	19	10
V	79	93	38	66	81	42	60	80	73	67
Cr	1398	1182	1396	1391	1089	989	546	726	1020	585
Co	80	89	82	80	85	91	55	62	80	58
Ni	1040	1200	960	1040	1110	1136	923	930	1076	863
Cu	48	70	52	48	51	54	27	33	51	27
Zn	106	68	72	106	63	65	42	60	67	49
Sn		2			5	3	1	2	6	
Mo	3		6	3	<1	<1	<1	<1	<1	<1
Ga	5	4	4	4	3	2	2	2	4	4
As		<1								
S	240	150	680	240	120	1110	200	1440	740	1030
F	4434	4200	4657	4434	4540	4220	2190	3740	4600	4010
Cl	85	40	59	85	76	129	69	119	118	77

Sample number	71454A	71454B	71454D	7'454F	76007A	83210296
Formation	Fitzroy Lamproites	Fitzroy Lamproites	Fitzroy Lamproites	fitzroy lamproites	Fitzroy Lamproites	Fitzroy Lamproites
Rock type	Phl-Ol-Lamproite	Phl-Ol-Lamproite	Ol. Lamp. Tuff	Carb. Ol-Lamp. Tuff	Olivine lamproite	Olivine Lamproite
Locality	Ellendale No.11	Ellendale No.11	Ellendale No.11	Ellendale No.11	Ellendale No.11	Ellendale No.11
Grid reference	954574	954574	954574	954574	954574	954574
Map sheet	Ellendale	Ellendale	Ellendale	Ellendale	Ellendale	Ellendale
Additional data	11AC16/15m	11AC16/26m	11AC16/57m	11AC16/186	o/c E side	E side
Biblio. ref.	Lewis-GSWA	Lewis-GSWA	Lewis-GSWA	Lewis-GSWA	Lewis-GSWA	ALJ-BMR
SiO_2	41.70	39.90	41.20	40.20	40.80	41.42
TiO_2	2.40	2.48	1.44	1.15	2.54	2.62
Al_2O_3	3.50	3.30	2.50	2.50	3.40	3.37
Fe_2O_3	4.20	5.70	5.20	4.10	5.50	4.79
FeO	4.15	3.22	1.92	2.26	3.52	3.68
MnO	0.14	0.14	0.09	0.09	0.13	0.13
MgO	26.50	27.50	25.90	21.80	26.30	25.87
CaO	4.51	4.56	2.64	7.00	4.95	4.71
Na_2O	0.31	0.22	0.13	0.35	0.40	0.37
K_2O	2.21	2.22	1.05	2.02	2.01	1.62
P_2O_5	1.38	1.16	1.14	0.74	1.35	1.40
H_2O+	3.07	3.98	8.12	6.52	3.80	3.13
H_2O-	1.90	2.60	6.22	4.82	2.06	2.27
CO_2	0.06	0.06	0.52	3.99	0.12	0.17
Rest	2.11	1.64	1.14	1.68	3.27	3.59
Total	98.14	98.68	99.21	99.22	100.15	99.14
Ba	9134	5249	3383	7555	19833	21726
Li	11	13	12	106	12	5
Rb	645	315	132	210	405	603
Sr	1276	1297	956	763	968	1102
Pb	35	36	20	18	29	42
Th	48	51	32	32	45	62
U	2	4	1	2	1	8
Zr	654	646	365	313	649	780
Nb	174	178	102	81	170	244
Y	6	10	6	7	10	23
La	344	316	166	167	335	256
Ce	553	587	328	272	503	441
Nd						202
Sc	20	19	14	9	19	13
V	94	59	241	160	93	59
Cr	1209	1109	739	682	1134	1432
Co	85	85	70	62	92	
Ni	1157	1135	1097	1013	1251	1134
Cu	47	49	33	28	51	52
Zn	64	65	49	42	64	66
Sn	3	4	1	3	6	<2
Mo	<1	<1	2	<1	<1	3
Ga	3	4	3	2	<2	11
As						2.5
S	460	350	760	1880	320	
F	4170	4480	2610	3600	4780	5500
Cl	70	76	86	109	78	

ELLENDALE 16

Sample number	71860C	71857B	71858A	71859	76015A	832103
Formation	fitzroy lamproites	Fitzroy Lamproites	Fitzroy Lamproites	Fitzroy Lamproites	Fitzroy Lamproites	Fitzroy Lamproites
Rock type	Carb Phl-KRi-Ol Lam	Ves Gls Ol Lamproite	Ves Gl Ol Lamp Brecc	Ves Gls Ol Lamp.	Di-Phl-Ol-Lc Lamp.	Phl-Lc-Ol Lamproite
Locality	Ellendale No.16	Ellendale No.16	Ellendale No.16	Ellendale No.16	Ellendale No.16	Ellendale No.16
Grid reference	912620	913619	913619	913619	913619	913619
Map sheet	Ellendale	Ellendale	Ellendale	Ellendale	Ellendale	Ellendale
Additional data	centtrench	centre NW	centre NW	centre NW	NW margin	centre pit
Biblio. ref.	Lewis-GSWA	Lewis-GSWA	Lewis-GSWA	Lewis-GSWA	Lewis-GSWA	ALJ-BMR
SiO_2	17.30	44.60	58.60	46.30	40.80	42.22
TiO_2	1.99	5.94	3.80	5.23	4.36	4.92
Al_2O_3	2.50	7.20	4.90	6.50	4.80	5.61
Fe_2O_3	4.80	10.60	7.60	7.80	7.80	7.61
FeO	0.22	0.77	0.28	0.27	1.00	1.35
MnO	0.20	0.09	0.06	0.07	0.09	0.10
MgO	19.00	6.28	4.08	9.69	15.60	13.49
CaO	17.30	3.41	3.91	4.25	4.94	5.54
Na_2O	0.21	0.21	0.16	0.29	0.40	0.62
K_2O	1.18	6.55	5.03	5.86	2.62	4.37
P_2O_5	0.63	2.47	2.77	1.57	1.45	1.67
H_2O+	3.45	3.39	3.23	3.08	6.12	4.35
H_2O-	3.59	4.42	4.00	5.09	8.11	3.76
CO_2	25.80	0.06	0.10	0.04	0.05	0.15
Rest	1.69	2.58	1.39	2.14	1.65	4.03
Total	99.86	98.57	99.91	98.18	99.79	99.79
Ba	8688	9954	2507	9048	3551	24572
Li	6	15	8	10	13	10
Rb	208	373	292	261	570	527
Sr	1342	1296	1049	1140	1357	1833
Pb	60	63	43	38	54	84
Th	32	72	51	53	57	83
U	<1	2	3	2	1	10
Zr	486	1914	1213	1129	1344	1525
Nb	94	283	178	180	208	309
Y	12	29	23	17	15	37
La	266	648	290	335	470	419
Ce	379	1173	592	600	830	760
Nd						333
Sc	12	45	28	25	26	17
V	33	321	712	503	87	158
Cr	277	799	556	540	796	830
Co	35	37	27	23	56	
Ni	360	578	476	540	737	606
Cu	65	74	53	59	75	54
Zn	54	91	79	82	95	86
Sn		9	6	6	8	<2
Mo	<1	<1	<1	2	2	3
Ga	2	10	9	7	8	12
As	<1					2
S	600	620	140	1610	30	
F	3300	7300	5900	5430	6670	5400
Cl	530	81	58	64	81	

Sample number	65912	76016B	71847	71848	71849	71850	71856A	76016A	76016D
Formation	Fitzroy	fitzroy	Fitzroy	Fitzroy	Fitzroy	Fitzroy	Fitzroy	Fitzroy	Fitzroy
Rock type	Lamproites KRi-Phl-Di -Lc Lamp.	lamproites Phl-Lc Lamp Tuff	Lamproites Phl - Lc Lamproite	Lamproites Gl-Di-Ol- Lc-Ph Lamp	Lamproites Fg Ol - Lc Lamproite	Lamproites Cg Ol-Lc Lamproite	Lamproites Di-KRi-Ol- Ph-Lc Lamp	Lamproites Phl - Lc Lamproite	Lamproites Phl - Lc Lamproite
Locality	Ellendale No.23	Ellendale No.23	Ellendale No.31	Ellendale No.31	Ellendale No.31	Ellendale No.31	Ellendale No.6	Ellendale No.23	Ellendale No.23
Grid reference	847597	847596	954513	954513	954513	954513	990479	847596	913619
Map sheet	Ellendale	Ellendale	Ellendale	Ellendale	Ellendale	Ellendale	Ellendale	Ellendale	Ellendale
Additional data	centre o/c	outer tuff	p 1,W vent	centre o/c	centre o/c	vein in tf	centre	dyke in tf	centre o/c
Biblio. ref.	Lewis-GSWA	Lewis-GSWA	Lewis-GSWA	Lewis-GSWA	Lewis-GSWA	Lewis-GSWA	Lewis-GSWA	Lewis-GSWA	Lewis-GSWA
SiO_2	49.84	59.60	55.00	46.60	52.00	56.40	48.40	53.80	48.40
TiO_2	5.62	4.51	5.67	5.52	5.38	5.42	6.15	6.10	6.45
Al_2O_3	7.76	7.80	7.30	6.50	7.60	6.30	6.60	7.90	8.70
Fe_2O_3	5.55	4.00	4.80	6.80	5.00	5.20	6.80	5.60	7.70
FeO	2.36	1.27	0.70	1.05	1.26	2.08	1.55	0.45	1.47
MnO	0.08	0.05	0.03	0.12	0.05	0.09	0.10	0.05	0.11
MgO	7.84	5.06	6.04	9.28	7.89	6.65	9.50	6.40	5.97
CaO	4.74	1.60	2.51	5.62	2.52	1.63	3.77	1.56	2.67
Na_2O	0.79	0.11	0.35	0.78	0.58	0.33	1.04	0.15	0.36
K_2O	8.67	10.23	8.53	8.61	9.28	8.60	7.59	9.46	9.94
P_2O_5	0.89	1.20	1.24	1.97	1.02	0.89	1.00	1.33	1.18
H_2O+	2.32	1.96	3.01	1.94	2.49	1.90	2.27	2.36	2.11
H_2O-	0.87	1.44	2.22	1.01	2.05	1.41	2.00	2.15	2.34
CO_2	0.44	0.08	0.10	0.44	0.10	0.18	0.05	0.03	0.04
Rest	2.96	1.48	2.28	2.76	1.79	1.77	2.60	1.70	1.98
Total	100.73	100.39	99.78	99.00	99.01	98.85	99.42	99.04	99.42
Ba	18069	5599	11485	15852	8325	8281	14576	5052	9002
Li	11	18	8	10	9	8	10	10	11
Rb	331	313	1060	421	238	291	412	353	318
Sr	1398	1241	1538	1328	1084	699	935	1306	842
Pb	40	76	67	52	56	57	45	60	47
Th	31	31	24	26	17	23	27	31	27
U	2	<1	2	1	1	1	1	2	2
Zr	1287	1131	1371	1348	1280	1308	1154	2108	1600
Nb	154	116	94	179	93	120	149	132	145
Y	21	20	14	13	16	16	12	27	36
La	285	285	304	356	323	297	293	414	600
Ce	491	425	463	488	463	491	399	670	647
Nd									
Sc	20	16	14	19	17	23	20	20	33
V	179	211	176	239	221	245	121	261	220
Cr	302	214	173	295	341	412	424	228	349
Co	45	24	35	46	46	49	51	25	47
Ni	240	193	258	290	609	509	481	295	284
Cu	120	50	84	120	89	86	90	51	94
Zn	104	77	84	78	96	97	105	100	80
Sn	13	7	10	19	14	14	16	12	13
Mo	2	<1	9	<1	<1	<1	3	1	1
Ga	13	17	17	10	18	13	11	25	16
As	<1	2							
S	1050	300	1340	760	360	470	230	50	40
F	4000	4600	3600	4510	3240	3300	5930	5840	4810
Cl	160	<20	56	93	79	83	59	53	<50

ELLENDALE 38 (PALM SPRINGS)

Sample number	71417	30496	83210308
Formation	Fitzroy Lamproites	Fitzroy Lamproites	Fitzroy Lamproites
Rock type	(ol)-Di-Ph -Lc Lamp	(Di)-Phl- Lc Lamp	Ol-Phl-Lc Lamproite
Locality	Palm Spring	EL38 Palm Springs	EL 38 Palm Spring
Grid reference	085432	085432	085432
Map sheet	Ellendale	Ellendale	Ellendale
Additional data	centre o/c	centre	centre
Biblio. ref.	Lewis-GSWA	Lewis-GSWA	ALJ-BMR
SiO_2	51.60	51.10	50.04
TiO_2	6.86	6.90	7.15
Al_2O_3	6.80	6.80	8.05
Fe_2O_3	5.60	5.50	6.01
FeO	1.40	1.44	1.21
MnO	0.07	0.11	0.06
MgO	9.37	8.86	6.99
CaO	2.93	3.04	2.39
Na_2O	0.35	0.32	0.50
K_2O	9.15	9.10	11.02
P_2O_5	0.70	1.02	1.04
H_2O+	2.51	2.59	2.30
H_2O-	1.06	0.87	0.73
CO_2	0.07	0.13	0.21
Rest	2.22	1.96	1.96
Total	100.69	99.74	99.66
Ba	11968	10030	9291
Li	10	7	5
Rb	398	320	361
Sr	1078	1000	1193
Pb	40	60	63
Th	26	25	28
U	1	4	3.5
Zr	1491	1400	1776
Nb	136	150	182
Y	21	18	22
La	324	350	326
Ce	386	460	615
Nd			252
Sc	18	20	16
V	143	178	222
Cr	663	500	622
Co	40	40	
Ni	228	300	285
Cu	86	90	78
Zn	78	84	81
Sn		10	19
Mo	4	<1	<3
Ga	13	14	27
As		<10	2.5
S	80	300	
F	3450	3119	2100
Cl	136		

Sample number	76012A	71862B	71862C	76003D	71861B	76013A	76014A
Formation	fitzroy lamproites	fitzroy lamproites	fitzroy lamproites	Fitzroy Lamproites	Fitzroy Lamproites	Fitzroy Lamproites	Fitzroy Lamproites
Rock type	Weathd Ol-Phl Lamp	Carb. Phl-Ol-Lamp	Carb. KRi-Di-Ph-Ol L	Glassy Ol-Lc ? Lamp	Di-Phl-Ol-Lc Lamp.	Ph-Di-Ol-Lc Lamp.	Phl-Ol-Lc? Lamproite
Locality	Ellendale No.18	Ellendale No.17	Ellendale No.17	Ellendale No.12	Ellendale No.8	Ellendale No.14	Ellendale No.15
Grid reference	871645	096703	096703	932570	987595	903554	894596
Map sheet	Lennard	Lennard	lennard	Ellendale	Ellendale	Ellendale	Ellendale
Additional data	silicified	trench	trench	trench	trench	trench	trench
Biblio. ref.	Lewis-GSWA	Lewis-GSWA	Lewis-GSWA	Lewis-GSWA	Lewis-GSWA	Lewis-GSWA	Lewis-GSWA
SiO_2	71.10	27.30	34.10	45.40	57.80	44.00	39.20
TiO_2	1.64	3.87	3.80	7.53	3.98	4.94	4.26
Al_2O_3	1.40	4.30	4.40	6.70	4.60	6.10	4.10
Fe_2O_3	5.30	7.20	6.90	8.20	6.30	7.20	7.70
FeO	0.05	0.81	1.18	0.50	1.23	1.26	0.60
MnO	0.15	0.10	0.14	0.06	0.05	0.09	0.14
MgO	6.20	12.00	13.20	6.17	4.13	10.80	16.50
CaO	1.54	17.80	14.00	4.34	3.69	4.81	4.51
Na_2O	0.12	0.25	0.52	0.19	0.13	0.33	0.39
K_2O	2.39	4.36	3.73	9.40	4.29	4.90	2.71
P_2O_5	0.98	1.34	1.39	3.15	2.49	1.96	2.19
H_2O+	2.81	3.79	4.03	2.99	4.19	4.44	6.18
H_2O-	4.94	3.73	4.32	2.42	4.60	6.09	8.51
CO_2	0.12	11.50	6.73	0.22	0.08	0.09	0.12
Rest	1.14	1.74	2.19	1.82	2.17	2.39	2.25
Total	99.88	100.09	100.63	99.09	99.73	99.40	99.36
Ba	3926	5845	10014	3007	10005	11051	7887
Li	12	15	18	13	8	11	17
Rb	279	431	383	428	844	399	437
Sr	312	1209	1208	1591	1294	1438	1532
Pb	46	53	53	124	50	51	77
Th	78	38	39	78	28	39	57
U	1	<1	<1	3	2	1	2
Zr	457	1160	1123	3200	1229	1415	1900
Nb	136	158	153	257	111	123	200
Y	29	14	14	38	13	23	21
La	574	406	448	830	298	383	492
Ce	840	749	760	1629	466	662	847
Nd							
Sc	18	17	11	33	20	24	29
V	93	67	53	203	277	140	66
Cr	285	733	697	507	587	885	836
Co	37	61	75	44	49	49	61
Ni	273	698	785	514	504	593	742
Cu	33	51	50	42	71	83	69
Zn	50	73	70	81	93	107	93
Sn	3	7	9	15	11	9	11
Mo	2	<1	1	<1	2	<1	<1
Ga	2	5	5	16	10	11	7
As	2						
S	820	550	960	100	1050	40	330
F	3680	5070	4530	4160	4100	5420	6670
Cl	<20	125	93	99	52	136	82

Sample number	76005A	76005D	76005E	76017	76018	71854	71855B	71864A	76019
Formation	Fitzroy Lamproites	fitzroy lamproites	Fitzroy Lamproites	Fitzroy Lamproites	Fitzroy Lamproites	Fitzroy Lamproites	Fitzroy Lamproites	fitzroy lamproites	fitzroy lamproites
Rock type	Di-Phl-Ol-(Lc?) Lamp	Ol-Lc? Lamp. Tuff	Ol-Lc? Lamproite	Phl-Lc Lamproite	KRi-Phl-Ol-Lc Lamp.	(Glassy) Ol-Lc Lamp	Phl - Ol Lamproite	Ol-Phl-Lc Lamproite	Phl - Lc Lamp. tuff
Locality	Ellendale No.22	Ellendale No.22	Ellendale No.22	Ellendale No.21	Ellendale No.24	Ellendale No.19	Ellendale No.19	Ellendale No.21a	Ellendale No.26
Grid reference	862616	862616	862616	893625	828627	905662	905662	898628	834692
Map sheet	Ellendale	Ellendale	Ellendale	Ellendale	Ellendale	Lennard	Lennard	Ellendale	Lennard
Additional data	trench	trench	trench	trench	trench	trench	trench	trench/alt	trench/alt
Biblio. ref.	Lewis-GSWA	Lewis-GSWA	Lewis-GSWA	Lewis-GSWA	Lewis-GSWA	Lewis-GSWA	Lewis-GSWA	Lewis-GSWA	Lewis-GSWA
SiO_2	41.90	44.80	41.30	46.00	42.70	47.50	41.00	40.50	61.70
TiO_2	4.58	3.91	4.69	6.99	5.94	5.95	4.92	4.24	3.64
Al_2O_3	5.70	5.30	5.80	8.70	6.20	6.00	4.40	5.20	6.00
Fe_2O_3	7.10	6.20	7.40	6.60	6.40	6.60	6.60	8.40	4.10
FeO	1.43	1.78	0.88	0.84	1.49	1.05	0.61	0.62	0.40
MnO	0.08	0.09	0.11	0.07	0.09	0.10	0.06	0.11	0.03
MgO	14.10	13.80	12.70	8.30	11.90	8.65	15.50	13.20	4.77
CaO	5.15	4.02	4.33	2.35	4.20	2.78	4.10	6.14	2.65
Na_2O	0.59	1.22	0.88	0.09	1.14	0.25	0.31	0.22	0.08
K_2O	3.56	4.71	4.26	10.20	4.66	8.26	3.11	2.35	6.45
P_2O_5	1.87	1.44	2.17	2.15	1.57	2.12	2.30	1.85	1.96
H_2O+	5.14	4.29	5.18	2.69	4.78	3.08	6.32	6.69	2.48
H_2O-	5.48	5.01	4.48	2.10	3.00	2.65	7.15	8.47	2.57
CO_2	0.08	0.06	0.19	0.02	0.08	0.11	0.04	0.06	0.11
Rest	3.65	2.46	5.62	1.94	5.85	3.65	3.12	2.37	1.65
Total	100.41	99.09	99.99	99.04	100.00	98.75	99.54	100.42	98.59
Ba	20833	11218	38114	3683	41378	20667	16345	11616	6427
Li	18	16	19	14	15	10	10	13	13
Rb	373	269	575	406	483	333	433	486	253
Sr	1432	1330	1344	1680	1645	1627	1889	1387	1179
Pb	64	72	41	117	71	96	85	50	48
Th	56	66	61	58	37	52	47	31	25
U	3	3	2	2	1	1	2	1	3
Zr	1751	1434	1710	3193	1462	1680	1839	1025	1225
Nb	206	181	211	239	160	234	196	158	97
Y	22	24	20	18	17	31	18	19	18
La	513	475	506	739	522	644	500	361	285
Ce	822	835	702	1393	708	1118	830	589	501
Nd									
Sc	25	21	31	27	22	24	24	20	12
V	151	201	88	279	137	194	142	77	214
Cr	642	618	595	268	379	448	558	818	166
Co	62	44	31	31	40	40	48	61	18
Ni	608	612	648	510	401	293	712	795	205
Cu	57	40	47	20	45	40	58	71	46
Zn	76	77	62	72	83	96	89	103	76
Sn	8	7	6	15	10	16	14	10	10
Mo	<1	<1	<1	<1	<1	2	2	<1	2
Ga	7	7	6	23	8	12	8	7	16
As									
S	370	540	40	50	50	1000	70	470	1370
F	7180	6290	8610	6140	7520	6910	5690	4600	5140
Cl	71	84	87	123	88	132	113	98	<50

Sample number	80210054	80210055	76011A	76001	76002A	76010	76004A	76004C	76006B	83210298
Formation	fitzroy lamproites	fitzroy lamproites	Fitzroy Lamproites	fitzroy lamproites	Fitzroy Lamproites	Fitzroy Lamproites	Fitzroy Lamproites	fitzroy lamproites	Fitzroy Lamproites	Fitzroy Lamproites
Rock type	Phl-Lc-Ol Lamproite	Phl-Ol Lamproite	Ol-Lc Lamproite	carb. Phl-Ol Lamp	Glassy Ol-Lc lamp.	Ol-Phl-Lc Lamproite	Ves Gl Ph-Ol-Lc Lamp	Phl-Ol-Lamp. tuff	Ol-Phl-Lc Lamproite	ol-Phl-Lc Lamproite
Locality	Water Reserve Sill	Water Reserve Sill	Ellendale No.39	Ellendale No.27	Ellendale No.27	Ellendale No. 46	Ellendale No. 41	Ellendale No. 41	Ellendale No. 42	Ellendale No.27
Grid reference	930496	930496	210585	926632	926632	127676	788673	788673	801673	926632
Map sheet	Ellendale	Ellendale	Lpld Downs	Ellendale	Ellendale	Richenda	Lennard	Lennard	Lennard	Ellendale
Additional data	LDH5-chips	costean	pit spoil	trench	trench	surface	trench	trench	trench	N pit
Biblio. ref.	JF.ALJ-BMR	JF.ALJ-BMR	Lewis-GSWA	Lewis-GSWA	Lewis-GSWA	Lewis-GSWA	Lewis-GSWA	Lewis-GSWA	Lewis-GSWA	ALJ-BMR
SiO_2	63.92	54.97	47.10	30.70	40.80	44.90	42.30	45.20	46.20	39.46
TiO_2	4.89	6.37	5.59	3.77	8.34	6.14	4.49	4.48	6.55	5.05
Al_2O_3	4.66	6.12	6.30	3.50	7.70	7.00	5.40	6.40	6.90	4.52
Fe_2O_3	5.52	12.63	5.20	6.20	10.00	8.20	8.00	7.40	6.90	9.13
FeO	0.25		1.41	1.72	0.86	1.00	0.36	0.26	0.64	0.81
MnO	0.06	0.26	0.04	0.10	0.08	0.20	0.08	0.08	0.05	0.22
MgO	3.91	4.77	7.76	12.60	7.13	9.02	12.10	10.40	7.65	13.86
CaO	2.18	0.16	4.89	16.00	4.18	4.14	4.16	3.13	3.96	5.50
Na_2O	0.17	0.13	0.15	0.44	0.25	0.29	0.17	0.12	0.22	0.50
K_2O	5.29	6.51	8.87	3.27	6.49	8.31	2.33	4.46	7.60	4.35
P_2O_5	1.44	0.39	1.84	1.82	2.97	2.00	2.89	2.10	2.96	2.29
H_2O+	2.59	3.41	3.66	4.45	3.96	3.18	6.93	5.73	3.52	5.43
H_2O-	2.31	1.73	3.84	4.30	5.05	2.92	10.00	8.37	4.19	5.31
CO_2	0.23	0.19	1.54	9.69	0.05	0.16	0.13	0.13	0.06	0.48
Rest	1.94	1.31	1.93	2.41	2.71	1.83	1.60	1.58	2.32	2.83
Total	99.36	98.95	100.12	100.97	100.57	99.29	100.94	99.84	99.72	99.74
Ba	10389	2757	9083	12125	7755	4806	2209	3454	5919	13845
Li	5	3	16	12	16	24	22	31	11	15
Rb	303	365	214	338	389	448	241	223	372	509
Sr	759	83	1435	1270	1659	1592	1709	1420	2441	1788
Pb	50	70	90	53	110	98	70	73	120	69
Th	43	58	36	25	93	52	44	47	65	51
U	3	6	2	2	2	1	1	1	2	5.5
Zr	1286	1677	1232	1159	3740	2005	1855	1783	2433	1670
Nb	182	239	158	136	298	225	179	167	241	289
Y	21	82	22	13	30	25	18	21	24	32
La	272	665	453	377	700	564	420	386	705	249
Ce	352	875	616	624	1194	1186	788	778	1175	422
Nd										190
Sc			17	15	39	29	23	27	29	18
V	141	212	189	87	267	203	298	176	193	66
Cr	561	1134	301	686	754	494	697	737	447	1330
Co			42	63	52	50	56	46	45	
Ni	543	884	385	752	687	402	1079	1031	612	889
Cu	38	76	70	48	48	39	52	27	57	56
Zn	121	95	97	68	91	65	96	107	121	90
Sn	20	29	10	9	15	13	7	8	14	4
Mo	3	7	2	<1	<1	<1	<1	<1	<1	<3
Ga	6	12	18	4	15	15	11	11	20	8
As	4	16	2							3
S			750	220	610	110	160	230	270	
F	3000	2400	3140	5190	8320	5490	5950	4480	8380	5000
Cl			60	117	126	97	81	75	84	

Sample number	69160398	69160399	69160400	71385	71382	71386	71388
Formation	fitzroy lamproites	fitzroy lamproites	fitzroy lamproites	fitzroy lamproites	Fitzroy Lamproites	fitzroy lamproites	fitzroy lamproites
Rock type	Xeno-tuff-breccia	Xeno-tuff-breccia	Xeno-tuff-breccia	fg xeno-tuff brecc	Ol-Lc Lamproite	Carb Phl-Ol Lamp	KRi-Ol-Lamp Tuff
Locality	Big Spring	Big Spring	Big Spring	Big Spring	Big Spring West	Big Spring 1	Big Spring 3
Grid reference	537354	536354	536353	537354	512366	543352	543352
Map sheet	Leopld Dwn	Leopld Dwn	Leopld Dwn	Lpld Downs o/c	Lpld Downs o/c	Lpld Downs loc unknow	Lpld Downs W trench
Additional data							
Biblio. ref.	GMD-BMR	GMD-BMR	GMD-BMR	Lewis-GSWA	Lewis-GSWA	Lewis-GSWA	Lewis-GSWA
SiO_2	60.99	61.58	61.21	60.50	49.00	30.20	40.40
TiO_2	0.74	0.58	0.66	0.62	3.79	3.79	4.12
Al_2O_3	14.01	14.84	15.45	15.10	7.40	4.10	6.00
Fe_2O_3	5.74	3.37	3.34	2.30	6.40	6.90	8.00
FeO	0.83	1.00	1.16	0.85	0.87	0.26	0.90
MnO		0.02		0.01	0.06	0.25	0.11
MgO	0.97	1.45	0.97	1.27	9.03	9.45	15.20
CaO	0.12	0.13	0.10	1.76	4.33	15.70	6.31
Na_2O	0.14	0.12	0.12	0.10	0.55	0.21	0.82
K_2O	14.39	14.78	15.02	14.05	6.60	2.68	3.99
P_2O_5	0.13	0.07	0.07	0.09	1.52	0.39	0.67
H_2O+	1.15	1.24	0.58	1.10	5.07	5.12	5.63
H_2O-	0.04	0.06		0.31	3.97	5.06	4.50
CO_2	0.27	0.47	0.28	0.43	0.08	10.60	0.38
Rest	0.70	0.63	1.05	0.94	2.33	4.25	4.12
Total	100.22	100.34	100.01	99.43	101.00	98.96	101.15
Ba	5026	4297	7928	6113	11523	29504	27968
Li	8	7	5	4	13	7	8
Rb	395	462	453	424	192	409	507
Sr	56	44	52	82	1601	967	1334
Pb	30	13	28	40	90	40	40
Th	26	21	25	18	52	21	33
U	3	6	6	1	4	1	2
Zr	206	219	285	186	1079	849	938
Nb	12	11	11	13	167	152	203
Y	9	2	8	16	28	26	20
La	25	20	25	165	552	356	392
Ce	40	32	34	115	783	340	417
Nd							
Sc				15	21	18	23
V	107	123	177	97	170	40	59
Cr	81	95	70	79	523	389	622
Co	6	10	6	10	35	45	40
Ni	16	80	13	26	500	410	540
Cu	6	11	7	30	80	65	85
Zn	13	32	14	68	73	70	74
Sn	<2	<2	<2				
Mo				1	<1	<1	<1
Ga	17	19	19	13	13	4	6
As	1	<1	1		<1	<1	<1
S				140	1000	4600	100
F				1086	3540	3300	5260
Cl				149	440	110	120

MOUNT ROSE, BROOKING CREEK

Sample number	67160336	67160338	69160333	69160334	78210847	80210125	30426B
Formation	Fitzroy Lamproites	Fitzroy Lamproites	Fitzroy Lamproites	Fitzroy Lamproites	Fitzroy Lamproites	Fitzroy Lamproites	Fitzroy Lamproites
Rock type	Phl-KRi-Lc Lamproite	Di-Phl-Lc Lamproite	Di-KRi-Phl -Lc Lamp	lamproite	Glassy Ol-Lc Lamp.	Glassy Ol-Lc Lamp.	Ol-Lc Lamproite
Locality	Mount Rose	Mount Rose	Mount Rose	Mount Rose	Brooking Creek	Brooking Creek	Brooking Creek
Grid reference	594603	594603	594603	594603	617132	617132	304368
Map sheet	Leopld Dmn	Leopld Dwn	Leopld Dwn	Leopld Dwn	Leopld Dwn	Leopld Dwn	Lpld Downs
Additional data			Cognte xen		Glassy	Glass	
Biblio. ref.	GMD-BMR	GMD-BMR	GMD-BMR	GMD-BMR	RSN-BMR	RSN-BMR	Lewis-GSWA
SiO_2	50.95	50.47	49.85	55.06	49.34	51.67	52.00
TiO_2	5.62	5.67	5.59	5.78	4.42	4.17	4.17
Al_2O_3	7.64	7.38	7.75	6.90	9.49	8.92	8.80
Fe_2O_3	5.56	5.72	5.33	6.12	3.73	2.88	3.20
FeO	1.68	1.62	1.83	1.32	2.80	3.19	2.96
MnO	0.07	0.09	0.07	0.08	0.08	0.08	0.08
MgO	8.91	9.12	9.86	6.85	9.14	9.09	9.07
CaO	3.45	4.15	3.49	3.33	4.31	3.73	3.63
Na_2O	0.48	0.44	0.52	0.47	0.28	0.27	0.35
K_2O	8.58	8.80	8.89	8.37	7.90	8.40	8.24
P_2O_5	0.65	0.75	0.48	0.96	0.95	0.93	0.91
H_2O+	2.28	2.64	2.66	1.54	3.36	2.67	3.48
H_2O-	0.64	0.41	0.88	0.59	2.44	1.98	1.35
CO_2	0.27	0.75	0.23	0.22	0.35	0.24	0.06
Rest	2.25	2.05	2.10	1.90	1.40	1.43	1.28
Total	99.03	100.06	99.53	99.49	99.99	99.65	99.58
Ba	12938	11253	11490	9660	7117	7158	8715
Li	10	10	10	10	6	5	8
Rb	309	341	290	328	567	512	
Sr	808	777	826	835	989	1038	
Pb	38	37	36	31	36	33	40
Th	26	27	24	27	18	17	
U	4	3	3	4	3	1	<1
Zr	1268	1225	1260	1233	1054	927	
Nb	157	166	138	181	93	81	
Y	14	15	13	16	4	7	
La	220	245	218	212	211	172	209
Ce	326	355	321	325	438	266	250
Nd					145		
Sc							
V	209	204	216	240	154	153	156
Cr	536	490	597	408	560	220	
Co	36	33	36	32	37		46
Ni	291	235	366	181	331	337	480
Cu	69	70	65	70	45	38	72
Zn	75	78	71	76	69	61	84
Sn	6	6	5	7	4	9	
Mo						5	
Ga	13	13	13	14	15	14	
As	2	2	2	4	2	1	
S							180
F	4000	3900	3800	4600		1900	1950
Cl			70			300	111

MCKINRICK HILL, HOOPER WEST

Sample number	66160016	80210069	80210083	80210084	80210085	80210086
Formation	Fitzroy Lamproites	Fitzroy Lamproites	Fitzroy Lamproites	Fitzroy Lamproites	Fitzroy Lamproites	Fitzroy Lamproites
Rock type	Ol-Lc Lamproite	Phl-Lc Lamproite	Ol-Phl-Lc Lamproite	Ol-Phl-Lc Lamproite	Ol-Phl-Lc Lamproite	Ol-Phl-Lc Lamproite
Locality	McKinrick Hill	McKinrick Hill	Hooper West	Hooper West	Hooper West	Hooper West
Grid reference	013422	013422	865138	865138	865138	865138
Map sheet	Hooper	Hooper	Hooper	Hooper	Hooper	Hooper
Additional data	xenoliths			Xenoliths	Xenoliths	
Biblio. ref.	GMD-BMR	GPG-BMR	GPG-BMR	GPG-BMR	GPG-BMR	GPG-BMR
SiO_2	49.57	52.11	47.72	47.57	47.27	46.73
TiO_2	4.81	5.90	6.67	6.13	6.45	6.87
Al_2O_3	7.37	8.96	8.81	8.19	8.97	9.11
Fe_2O_3	4.90	5.11	8.25	7.18	8.01	8.49
FeO	1.13	1.17	0.32	0.62	0.29	0.35
MnO	0.05	0.05	0.06	0.08	0.12	0.09
MgO	8.77	5.78	5.53	7.80	6.14	6.05
CaO	3.08	1.98	2.00	2.09	1.73	1.55
Na_2O	0.61	0.08	0.06	0.12	0.10	0.08
K_2O	8.03	11.67	9.66	7.87	9.10	9.29
P_2O_5	0.78	1.51	1.49	1.82	1.37	1.20
H_2O+	5.03	1.83	3.62	5.43	3.73	3.71
H_2O-	1.67	0.91	2.95	3.06	3.24	3.32
CO_2	0.57	0.21	0.23	0.31	0.26	0.31
Rest	2.03	1.84	1.86	2.36	1.96	1.80
Total	98.40	99.11	99.23	100.63	98.74	98.95
Ba	11753	8565	7222	10983	7858	6480
Li	9	13	5	7	6	6
Rb	499	245	446	357	461	487
Sr	2027	1416	1120	1516	1095	1010
Pb	58	57	78	80	103	84
Th	43	23	64	51	64	67
U	6	1	5	1	5	4
Zr	1328	1147	1618	1538	1659	1706
Nb	169	117	227	216	229	242
Y	18	19	36	54	59	51
La	280	317	637	557	692	579
Ce	456	450	1028	968	1177	963
Nd			420	363	427	388
Sc						
V	161	614	303	331	243	266
Cr	225	266	635	608	597	628
Co	28					
Ni	303	241	475	405	491	556
Cu	51	36	56	48	57	60
Zn	75	87	87	81	98	98
Sn	<2	7	16	16	17	19
Mo		4	6	5	6	5
Ga	10	24	22	17	21	23
As	1	2	2	2	2	2
S						
F		3700	2200	370[illegible]	2300	2700
Cl						

OLD LEOPOLD HILL

Sample number	66160001	66160002	66160003	66160004	71160401	79211007	80210079	80210080	71371
Formation	Fitzroy Lamproites	Fitzroy Lamproites	Fitzroy Lamproites	Fitzroy Lamproites	Fitzroy Lamproites	Fitzroy Lamproites	Fitzroy Lamproites	Fitzroy Lamproites	Fitzroy Lamproites
Rock type	Phl-Di-KRi -Lc Lamp	Phl-Di-KRi -Lc Lamp	Phl-Di-KRi -Lc Lamp	Phl-Di-KRi -Lc Lamp	Phl-KRi-Di -Lc Lamp	Di-Phl-KRi -Lc Lamp.	Phl-Di-KRi -Lc Lamp.	Phl-KRi-Di -Lc Lamp.	Phl-KRi-Di -Lc Lamp
Locality	Old Leop-old Hill	Old Leop-old Hill	Old Leop-old Hill	Old Leop-old Hill	Old Leop-old Hill	Old Leop-old Hill	Old Leop-old Hill	Old Leop-old Hill	Old Leop-old Hill
Grid reference	061272	061272	061272	061272	061272	061272	061272	061272	061272
Map sheet	Hooper	Hooper	Hooper	Hooper	Hooper	Hooper	Hooper	Hooper	Hooper
Additional data	cntr plug		E.ctr.plug						Main Plug
Biblio. ref.	GMD-BMR	GMD-BMR	GMD-BMR	GMD-BMR	GMD-BMR	GMD-BMR	GPG-BMR	GPG-BMR	Lewis-GSWA
SiO_2	59.01	55.06	57.55	54.26	53.65	52.50	50.59	51.14	52.60
TiO_2	5.68	5.98	5.43	6.18	6.06	6.22	6.44	6.53	6.14
Al_2O_3	7.02	7.44	6.91	7.82	7.29	7.47	7.98	8.08	7.60
Fe_2O_3	6.02	5.86	5.21	6.66	5.88	5.86	5.94	6.20	5.70
FeO	1.02	1.06	1.00	0.56	1.33	1.45	1.40	1.38	1.47
MnO	0.08	0.09	0.08	0.09	0.10	0.09	0.09	0.10	0.09
MgO	5.31	6.29	5.91	6.02	6.50	6.84	6.75	7.05	6.95
CaO	2.51	3.67	3.64	3.27	3.79	3.97	3.95	3.91	3.88
Na_2O	0.69	0.67	0.58	0.72	0.77	0.72	0.61	0.71	1.00
K_2O	8.67	9.20	8.67	9.59	9.33	9.44	9.74	9.48	9.36
P_2O_5	0.65	0.83	0.78	0.79	0.82	0.97	0.99	0.98	0.91
H_2O+	1.42	1.26	1.29	1.37	1.38	1.46	1.70	1.69	1.10
H_2O-	0.62	0.59	0.54	0.71	0.15	0.35	0.48	0.68	0.44
CO_2	0.18	0.35	0.45	0.45	0.24	0.15	0.30	0.21	0.15
Rest	1.33	1.59	1.72	1.77	1.74	1.96	2.31	2.07	2.71
Total	100.21	99.94	99.76	100.26	99.03	99.45	99.27	100.21	100.10
Ba	5734	7569	9268	8903	10608	12463	13713	11673	16710
Li	5	6	6	5	5	5	5	5	7
Rb	260	284	255	299	308	319	331	319	338
Sr	805	1057	1022	1041	1108	1288	1215	1079	1196
Pb	42	38	36	40	42	41	41	43	40
Th	25	23	19	24	26	25	26	27	16
U	15	13	11	10	4	4	3	2	<1
Zr	1220	1318	1233	1323	1279	1296	1229	1261	1250
Nb	145	136	110	139	142	140	134	141	122
Y	14	15	12	13	13	11	14	14	18
La	227	235	171	236	242	242	241	245	295
Ce	347	340	274	349	382	377	372	372	303
Nd									
Sc									21
V	216	231	224	200	239	228	200	203	148
Cr	201	224	221	242	228	209	234	295	255
Co	31	31	27	30	28				30
Ni	77	81	82	83	83	83	97	94	143
Cu	62	66	66	60	71	69	76	79	88
Zn	76	72	72	75	71	71	77	76	89
Sn	7	8	7	6	8	6	13	16	
Mo							5	5	3
Ga	13	13	11	15	13	11	13	14	12
As	1	1	2	1	1	2	2	2	
S									780
F	3500	3600	3100	4000			3900	3700	4036
Cl			15						227

Sample number	66160011	66160012	66160013	66160327	66160328	69160395	69160396	69160397	79211049	80210070
Formation	Fitzroy Lamproites	Fitzroy Lamproites	Fitzroy Lamproites	Fitzroy Lamproites	Fitzroy Lamproites	Fitzroy Lamproites	Fitzroy Lamproites	Fitzroy Lamproites	Fitzroy Lamproites	Fitzroy Lamproites
Rock type	Ol-Phl-Di-Lc Lamp	Ol-Di-Lc Lamproite	Ol-Di-Lc Lamproite	Ol-Di-Lc Lamproite	Ol-Di-KRi-Lc Lamp	Ol-Phl-Di-Lc Lamp	Ol-Di-Lc Lamproite	Di-Lc Lamproite	Ol-Lc Lamproite	Ol - Lc Lamproite
Locality	Prairie Hill East	Prairie Hill East	Prairie Hill East	Prairie Hill East	Prairie Hill East	Prairie Hill East	Prairie Hill East	Prairie Hill East	Prairie Hill East	Prairie Hill East
Grid reference	956252	956252	956252	956252	956252	956252	956252	956252	956252	956252
Map sheet	Hooper	Hooper	Hooper	Hooper	Hooper	Hooper	Hooper	Hooper	Hooper	Hooper
Additional data	NE side	S side	E side							
Biblio. ref.	GMD-BMR	GMD-BMR	GMD-BMR	GMD-BMR	GMD-BMR	GMD-BMR	GMD-BMR	GMD-BMR	GMD-BMR	GPG-BMR
SiO_2	59.54	54.67	58.72	58.75	59.66	58.75	41.90	49.30	44.37	51.98
TiO_2	5.45	5.86	5.06	5.13	5.56	5.64	4.99	5.10	5.33	5.12
Al_2O_3	7.23	7.90	8.58	7.96	7.47	7.29	6.61	8.34	6.95	9.35
Fe_2O_3	5.83	7.39	6.00	6.33	6.03	6.02	5.58	5.81	6.52	4.81
FeO	0.62	0.72	0.95	0.95	0.59	0.87	2.01	1.37	1.83	2.01
MnO	0.08	0.07	0.04	0.08	0.09	0.07	0.10	0.08	0.13	0.10
MgO	4.03	4.66	3.11	3.89	3.76	4.47	12.02	8.26	9.41	5.44
CaO	1.97	2.38	1.69	1.96	1.78	2.07	5.15	3.25	4.26	2.75
Na_2O	0.25	0.34	0.19	0.33	0.24	0.38	0.21	0.24	0.24	0.46
K_2O	8.61	9.10	9.21	9.10	8.62	8.64	8.84	8.07	9.13	10.18
P_2O_5	1.11	1.18	0.87	0.81	1.17	1.06	1.75	0.89	2.54	0.92
H_2O+	2.03	2.12	1.92	1.78	2.18	1.75	2.60	3.83	2.53	1.80
H_2O-	0.75	1.07	0.68	0.70	1.15	0.97	0.82	2.23	0.98	0.77
CO_2	0.37	0.35	0.85	0.22	0.15	0.22	4.52	0.24	1.26	0.61
Rest	1.77	2.26	1.47	1.39	1.52	1.62	2.38	2.05	3.09	2.73
Total	99.64	100.07	99.34	99.38	99.97	99.82	99.48	99.06	98.57	99.03
Ba	9699	13293	8198	6705	7453	9338	15929	11572	21883	18473
Li	9	6	5	4	7	7	12	15	19	10
Rb	269	356	328	276	298	333	494	1902	462	335
Sr	835	1005	747	838	767	1042	1018	1027	1212	921
Pb	39	45	37	36	40	44	52	36	57	35
Th	23	27	21	21	26	27	41	17	43	19
U	32	14	18	9	30	14	21	2	13	2
Zr	1225	1267	1157	1129	1384	1278	1063	1153	1173	1054
Nb	136	150	114	120	145	153	232	109	238	93
Y	12	15	22	10	10	12	21	3	23	23
La	211	263	220	203	221	230	357	257	381	291
Ce	325	387	332	323	347	358	530	333	557	313
Nd										
Sc										
V	251	208		214	221	183	187	229	222	224
Cr	261	356	351	294	180	345	193	292	201	323
Co	33	52		36	33	28	27	34	25	
Ni	167	342	30	258	185	248	307	544	320	436
Cu	56	62	55	35	58	63	42	60	41	61
Zn	71	75	79	64	69	78	96	73	103	75
Sn	5	5	4	5	5	6	<2	3	<2	6
Mo										4
Ga	15	15	17	13	14	13	14	14	12	16
As	3	4	3	2	3	3	7	6	7	3
S										
F	2900	3000	1900	2400	2800					2000
Cl										

PRAIRIE HILL EAST

Sample number	80210071	71374	71887A	71890A	83210240	83210241
Formation	fitzroy lamproites	Fitzroy Lamproites	Fitzroy Lamproites	Fitzroy Lamproites	Fitzroy Lamproites	Fitzroy Lamproites
Rock type	Xeno-tuff-breccia	(Ol)-Di-Lc Lamproite	Di-Ol-Lc Lamproite	Di-Ol-Lc lamproite	Ol-Di-Lc Lamproite	Ol-Di-Lc Lamproite
Locality	Prairie Hill East	Prairie Hill East	Prairie Hill	Prairie Hill	Prairie Hill East	Prairie Hill East
Grid reference	956252	955252	956423	956252	956252	956252
Map sheet	Hooper	Hooper	Hooper	Hooper	Hooper	Hooper
Additional data		main plugW	satel plug	main plug		NE margin
Biblio. ref.	GPG-BMR	Lewis-GSWA	Lewis-GSWA	Lewis-GSWA	ALJ-BMR	ALJ-BMR
SiO_2	61.54	49.00	51.70	49.10	52.36	55.82
TiO_2	2.02	6.54	5.42	6.82	6.60	5.77
Al_2O_3	9.60	8.60	7.90	8.60	8.28	7.40
Fe_2O_3	3.05	6.20	4.70	6.90	6.23	6.88
FeO	0.96	1.56	2.37	1.23	1.27	0.82
MnO	0.04	0.11	0.08	0.10	0.08	0.07
MgO	6.17	6.50	8.82	5.90	5.18	4.45
CaO	1.79	4.06	3.30	3.13	2.95	2.48
Na_2O	0.67	0.29	0.88	0.19	0.19	0.22
K_2O	8.89	9.51	8.78	8.92	9.45	8.75
P_2O_5	0.62	1.48	0.69	1.38	1.37	1.21
H_2O+	1.84	2.05	2.17	2.68	2.24	2.19
H_2O-	0.84	1.12	1.65	1.53	1.44	1.81
CO_2	<0.10	0.11	0.01	0.08	0.22	0.21
Rest	0.90	3.36	1.92	2.85	2.56	2.30
Total	98.93	100.49	100.39	99.41	100.42	100.38
Ba	5183	20458	10089	16411	13308	12175
Li	21	11	22	22	37	12
Rb	527	435	219	287	344	334
Sr	516	1372	924	1040	1159	1091
Pb	39	60	26	52	55	50
Th	20	27	18	27	30	25
U	4	2	<1	1	5.5	18
Zr	464	1446	989	1192	1577	1392
Nb	64	158	108	150	210	184
Y	19	24	13	19	32	22
La	117	362	269	351	362	274
Ce	186	422	290	400	550	472
Nd					285	222
Sc		23	20	27	19	16
V	92	117	160	315	477	181
Cr	135	645	445	449	644	588
Co		44	38	47		
Ni	247	284	749	318	221	444
Cu	26	86	98	94	70	65
Zn	43	88	70	94	76	74
Sn	7		8	13	12	12
Mo	<3	2	1	<1	<3	<3
Ga	12	16	15	14	29	19
As	2		<1	1	3.5	4.5
S		1820	930	2960		
F		4348	2920	3920	4500	4000
Cl		135	<20	20		

MOUNT GYTHA

Sample number	80210091	81210154	71353	71355
Formation	Fitzroy Lamproites	Fitzroy Lamproites	Fitzroy Lamproites	fitzroy lamproites
Rock type	Ol - Lc Lamproite	Ol-Di-Lc Lamproite	Ol-Lc-Di- Lamproite	Xen Ol-Di-Lc Lamp
Locality	Mount Gytha	Mount Gytha	Mount Gytha	Mount Gytha
Grid reference	773677	773677	773677	773677
Map sheet	Hardman	Hardman	Hardman	Hardman
Additional data	Xenoliths	E. flank	centr plug	sill, E
Biblio. ref.	GPG-BMR	ALJ-BMR	Lewis-GSWA	Lewis-GSWA
SiO_2	56.05	49.14	52.90	48.10
TiO_2	5.19	5.35	4.54	6.01
Al_2O_3	7.92	7.51	7.60	9.10
Fe_2O_3	6.21	6.40	6.20	7.10
FeO	0.93	1.02	1.47	1.76
MnO	0.07	0.10	0.10	0.10
MgO	3.56	7.78	7.00	6.75
CaO	3.47	6.26	6.93	4.06
Na_2O	0.15	0.50	0.58	0.24
K_2O	7.88	8.51	7.96	7.83
P_2O_5	2.81	1.17	1.03	0.71
H_2O+	2.18	2.26	2.02	3.15
H_2O-	1.70	1.10	0.94	2.90
CO_2	0.28	0.92	0.10	0.12
Rest	0.64	1.84	1.61	2.28
Total	99.04	99.86	100.98	100.21
Ba	1702	9401	7900	13537
Li	9	8	14	12
Rb	267	525	315	233
Sr	529	1192	973	1089
Pb	37	35	60	50
Th	30	28	22	25
U	3	1	<1	<1
Zr	1146	1066	915	1143
Nb	144	134	115	118
Y	26	17	29	22
La	209	214	305	350
Ce	322	291	373	408
Nd		157		
Sc		11	15	22
V	209	214	140	169
Cr	263	280	198	330
Co			35	45
Ni	91	246	240	440
Cu	32	58	100	70
Zn	47	77	97	78
Sn	17	12		
Mo	5		<1	1
Ga	14	15	14	17
As	7	2	1	1
S			200	100
F		3500	3200	2700
Cl			380	200

Sample number	67165018	80210116	80210118	81210155	81210156	81210157	81210158	71349	83210268	83210269
Formation	Fitzroy Lamproites	Fitzroy Lamproites	Fitzroy Lamproites	Fitzroy Lamproites	Fitzroy Lamproites	Fitzroy Lamproites	Fitzroy Lamproites	Fitzroy Lamproites	Fitzroy Lamproites	Fitzroy Lamproites
Rock type	Phl-Di-Lc Lamproite	Phl-Di-Lc Lamproite	Ol-Di-Lc Lamproite	(Ol)-Lc Lamproite	KRi-Di-Lc Lamproite	Phl-Di-Lc Lamproite	Di-Lc Lamproite	Ol-Di-Lc Lamproite	Di-Phl-Lc Lamproite	Ves Ol-Di-Lc Lamp.
Locality	Machells Pyramid	Machells Pyramid	Machells Pyramid	Machells Pyramid	Machells Pyramid	Machells Pyramid	Machells Pyramid	Machells Pyramid	Machells Pyramid	Machells Pyramid
Grid reference	789678	789678	789678	789678	789678	789678	789678	789670	789678	789678
Map sheet	Hardman	Hardman	Hardman	Hardman	Hardman	Hardman	Hardman	Hardman	Hardman	Hardman
Additional data		cogn xen		dyke,wflnk	dyke,Eside	cog. xen.	Cog. Xen.	centr plug	dyke SE	dyke N
Biblio. ref.	GMD-BMR	GPG-BMR	GPG-BMR	ALJ-BMR	ALJ-BMR	ALJ-BMR	ALJ-BMR	Lewis-GSWA	ALJ-BMR	ALJ-BMR
SiO_2	48.40	48.40	52.34	46.85	51.45	52.91	48.32	59.80	56.21	51.25
TiO_2	5.14	5.13	5.55	6.81	5.43	4.94	5.08	3.99	4.55	5.95
Al_2O_3	8.03	8.01	7.56	9.30	6.98	7.66	7.43	6.80	6.77	7.71
Fe_2O_3	6.37	5.95	4.63	8.42	5.17	5.70	6.10	5.60	5.30	5.84
FeO	0.85	1.16	2.12	1.25	1.56	1.17	1.03	1.11	0.95	1.58
MnO	0.07	0.08	0.08	0.10	0.10	0.10	0.10	0.08	0.15	0.10
MgO	8.65	8.47	7.11	4.80	9.19	7.14	7.78	4.76	6.51	7.76
CaO	6.99	6.51	2.90	2.60	4.38	6.37	7.31	4.61	6.00	4.13
Na_2O	0.36	0.40	0.08	0.25	0.47	0.61	0.55	0.44	0.52	0.31
K_2O	7.78	7.87	9.45	10.58	9.36	8.21	8.36	7.16	7.60	10.79
P_2O_5	1.15	1.10	1.78	1.60	0.61	1.20	1.29	1.09	1.10	0.74
H_2O+	2.58	2.02	2.09	2.49	1.80	1.98	1.77	2.01	1.29	1.70
H_2O-	1.34	1.51	1.50	1.05	0.95	0.48	0.88	1.56	0.82	0.80
CO_2	0.20	<0.10	0.26	0.71	1.00	1.15	0.13	0.16	0.17	0.18
Rest	1.96	1.97	1.59	2.44	1.39	1.24	1.96	1.00	1.55	1.38
Total	99.87	98.58	99.04	99.25	99.84	100.86	98.09	100.17	99.49	100.22
Ba	11516	13252	8452	14445	6084	5245	11089	3941	7394	4888
Li	10	10	6	10	7	8	8	13	11	9
Rb	316	313	247	271	182	293	472	150	253	278
Sr	1139	1056	1224	914	1104	1130	1179	838	1119	813
Pb	40	37	33	45	34	35	37	30	40	41
Th	31	31	23	35	23	26	27	14	26	21
U	3	2	4	4	<1	1	<1	<1	3.5	1.5
Zr	1167	1069	1069	1301	1102	1026	1049	627	1107	1357
Nb	148	136	109	167	102	130	130	107	155	143
Y	20	20	16	30	18	19	18	18	23	25
La	201	219	225	311	229	174	196	225	161	294
Ce	261	296	330	410	461	225	255	311	258	464
Nd				223	141	107	148		119	178
Sc				18	10	12	12	13	13	14
V	109	107	578	255	198	125	275	76	129	185
Cr	291	260	375	375	440	258	277	192	265	524
Co	28							40		
Ni	158	149	452	121	512	160	234	170	271	413
Cu	58	48	38	38	44	46	59	80	52	50
Zn	80	69	58	69	73	67	74	64	72	88
Sn	4	11	13	14	17	12	8		13	27
Mo		4						<1	3	<3
Ga	14	14	12	16	14	12	13	13	10	22
As	2	2	1	6	2	1	2	<1	3	3
S								100		
F	2700			3900	1800	2800	2600	2660	3400	3400
Cl								320		

MACHELLS PYRAMID

Sample number	83210270	83210271
Formation	Fitzroy Lamproites	Fitzroy Lamproites
Rock type	Ves Ol-Di-Lc Lamp.	Ves Ol-Di-Lc Lamp.
Locality	Machells Pyramid	Machells Pyramid
Grid reference	789678	789678
Map sheet	Hardman	Hardman
Additional data	dyke N	dyke N
Biblio. ref.	ALJ-BMR	ALJ-BMR
SiO_2	49.00	50.46
TiO_2	5.25	6.29
Al_2O_3	6.76	7.40
Fe_2O_3	5.24	5.56
FeO	1.20	1.55
MnO	0.06	0.07
MgO	10.07	7.61
CaO	4.00	3.17
Na_2O	0.27	0.61
K_2O	7.33	9.40
P_2O_5	1.01	0.71
H_2O+	3.28	2.20
H_2O-	3.77	1.37
CO_2	0.55	0.57
Rest	1.63	2.24
Total	99.42	99.21
Ba	7542	12444
Li	11	9
Rb	135	266
Sr	1084	1302
Pb	44	51
Th	21	26
U	3.5	2
Zr	1240	1412
Nb	134	128
Y	21	24
La	218	253
Ce	390	459
Nd	159	228
Sc	11	13
V	163	174
Cr	436	516
Co		
Ni	496	512
Cu	50	62
Zn	79	65
Sn	19	25
Mo	<3	3
Ga	21	24
As	4.5	5
S		
F	3100	2400
Cl		

Sample number	67165016	68165025	68165026	68165027	79211058	80210099	80210100	71312	71867A	71868A
Formation	Fitzroy Lamproites	Fitzroy Lamproites	Fitzroy Lamproites	Fitzroy Lamproites	Fitzroy Lamproites	Fitzroy Lamproites	fitzroy lamproites	Fitzroy Lamproites	Fitzroy Lamproites	Fitzroy Lamproites
Rock type	Ol-KRi-Di-Lc Lamp	Phl - Lc Lamproite	Ol-leucite Lamproite	(Ol)-Lc Lamproite	Ol-Di-Lc Lamproite	Ol - Lc Lamproite	Ol-Di-Lc Lamp. Tuff	Ol-Di-Lc Lamproite	Ol-Lc lamp (cogn xen)	Di-KRi-Lc Lamp
Locality	Mount Cedric	Mount Cedric	Mount Cedric	Mount Cedric	Mount Cedric	Mount Cedric	Mount Cedric	Mount Cedric	Mount Cedric	Mount Cedric
Grid reference	807703	807703	807703	807703	807703	807703	807703	812702	807703	807703
Map sheet	Hardman	Hardman	Hardman	Hardman	Hardman	Hardman	Hardman	Hardman	Hardman	Hardman
Additional data			Xenoliths	Cognte xen			xenoliths	centr creE	centre 1 W	centre 1
Biblio. ref.	GMD-BMR	GMD-BMR	GMD-BMR	GMD-BMR	GMD-BMR	GPG-BMR	GPG-BMR	Lewis-GSWA	Lewis-GSWA	Lewis-GSWA
SiO_2	50.11	49.69	50.23	52.12	50.87	51.38	48.59	48.30	50.40	50.30
TiO_2	6.17	6.92	5.48	5.14	5.85	6.27	5.79	4.41	5.59	6.63
Al_2O_3	7.54	8.62	7.73	8.17	7.34	8.76	9.38	6.60	8.00	8.00
Fe_2O_3	5.95	6.75	4.64	4.84	5.27	6.43	6.40	4.40	4.90	5.70
FeO	1.15	0.88	1.80	1.92	1.39	0.77	0.96	2.14	1.67	1.58
MnO	0.06	0.09	0.09	0.07	0.07	0.07	0.08	0.09	0.06	0.12
MgO	9.21	7.03	9.01	8.31	9.67	6.12	6.22	14.40	9.17	7.74
CaO	2.85	2.64	2.54	2.67	3.46	2.30	2.54	4.09	1.84	2.88
Na_2O	0.52	0.44	0.71	0.62	0.64	0.23	0.13	0.85	0.69	0.52
K_2O	9.53	10.15	8.80	10.21	8.74	11.88	10.96	6.34	9.45	10.25
P_2O_5	0.78	1.07	1.00	0.92	0.64	1.81	1.90	0.65	0.92	1.01
H_2O+	2.90	2.06	3.00	2.45	1.93	2.01	2.27	4.30	3.08	2.54
H_2O-	1.17	0.81	1.66	0.83	2.01	0.55	0.90	1.54	2.78	1.29
CO_2	0.69	0.23	0.63	0.49	0.32	0.29	0.26	0.07	0.13	0.22
Rest	2.05	2.18	2.65	1.31	1.26	1.15	2.67	2.61	1.36	1.30
Total	100.68	99.56	99.97	100.07	99.46	100.02	99.05	100.79	100.04	100.08
Ba	11485	12209	16734	5461	4705	4426	18897	17108	5451	4461
Li	9	7	9	10	9	6	7	10	16	6
Rb	234	429	276	226	202	353	275	216	220	228
Sr	1262	1070	1551	1362	1098	1537	1212	1178	1256	1111
Pb	56	59	60	48	38	70	57	20	54	60
Th	28	29	24	24	21	26	31	21	25	16
U	3	3	3	4	3	3	3	<1	1	1
Zr	1265	1428	1212	1171	1242	1311	1104	855	1066	1270
Nb	130	138	122	119	121	129	113	87	114	131
Y	20	23	17	22	12	14	22	17	21	23
La	254	317	307	275	234	338	309	251	317	371
Ce	392	459	451	412	355	501	443	242	429	469
Nd										
Sc								16	20	20
V	254	169	214	217	211	242	213	122	190	186
Cr	254	278	198	200	245	245	199	680	331	366
Co	29	36	29	31	30			44	33	36
Ni	558	407	471	452	308	254	234	550	314	381
Cu	63	58	56	49	46	36	30	74	113	92
Zn	74	74	78	78	67	70	71	74	76	82
Sn	10	12	2	6	12	10	10		16	16
Mo						4	6	9	<1	<1
Ga	16	17	15	17	10	23	17	9	17	18
As	2	3	3	1	2	2	3		<1	<1
S								120	220	380
F	2300	3000	2400	1600	3200			1980	2500	2620
Cl					10			70	60	40

Sample number	71869	71870B	71870D	71871	71874B	71875C	83210274A	83210274B	83210275	83210276
Formation	Fitzroy Lamproites	Fitzroy Lamproites	Fitzroy Lamproites	Fitzroy Lamproites	Fitzroy Lamproites	Fitzroy Lamproites	Fitzroy Lamproites	Fitzroy Lamproites	Fitzroy Lamproites	Fitzroy Lamproites
Rock type	Ol-Lc Lamp (cogn xen)	Di-KRi-Lc Lamproite	(Di)-Ol-Lc Lamproite	Ol-Di-Lc Lamproite	Phl-Lc Lamp	Phl-Lc Lamproite	Ol-Di-Lc Lamproite	Ol-Di-Lc Lamproite	Di-Ol-Lc Lamproite	Di-Ol-Lc lamproite
Locality	Mount Cedric	Mount Cedric	Mount Cedric	Mount Cedric	Mount Cedric	Mount Cedric sat	Mount Cedric	Mount Cedric	Mount Cedric	Mount Cedric
Grid reference	807703	807703	807703	807703	807703	803699	807703	807703	807703	807703
Map sheet	Hardman centre E	Hardman centre 2 E	Hardman centre 2 S	Hardman centre 2	Hardman dyke W	Hardman sill in tf	Hardman centre	Hardman centre	Hardman centre W	Hardman centre E
Additional data										
Biblio. ref.	Lewis-GSWA	Lewis-GSWA	Lewis-GSWA	Lewis-GSWA	Lewis-GSWA	Lewis-GSWA	ALJ-BMR	ALJ-BMR	ALJ-BMR	ALJ-BMR
SiO_2	51.20	51.10	50.20	48.10	50.30	50.00	50.15	50.89	48.68	48.74
TiO_2	5.35	6.73	6.86	4.69	6.71	7.16	5.73	5.61	4.64	4.46
Al_2O_3	8.60	8.00	8.10	6.70	8.90	9.50	7.28	7.16	6.44	6.59
Fe_2O_3	5.40	5.90	6.10	4.40	7.10	6.80	4.86	4.41	3.85	4.24
FeO	1.26	1.26	0.86	2.31	0.76	0.75	1.39	1.78	2.02	2.18
MnO	0.06	0.08	0.05	0.10	0.08	0.05	0.07	0.07	0.10	0.09
MgO	8.19	7.44	7.29	13.80	6.18	5.24	10.70	10.64	16.19	13.67
CaO	2.32	2.96	2.32	4.25	1.83	2.51	3.30	3.58	3.28	4.14
Na_2O	0.46	0.50	0.13	0.84	0.12	0.06	0.68	0.74	0.74	0.90
K_2O	10.59	10.23	10.68	6.72	11.61	10.82	8.66	8.40	7.26	6.65
P_2O_5	1.12	0.81	1.19	0.69	1.49	1.93	0.74	0.71	0.48	0.69
H_2O+	2.72	2.15	3.09	3.41	2.51	2.64	2.63	1.60	3.57	3.11
H_2O-	1.60	1.23	2.03	1.45	1.20	1.20	1.49	2.07	1.00	1.21
CO_2	0.12	0.17	0.10	0.14	0.09	0.15	0.54	0.25	0.23	0.17
Rest	1.70	1.64	1.44	2.18	1.45	1.69	1.41	1.43	1.37	2.28
Total	100.69	100.20	100.44	99.78	100.33	100.50	99.63	99.34	99.85	99.12
Ba	8120	7354	5534	13853	5871	7699	5553	6068	6148	13769
Li	12	9	7	9	14	12	10	10	10	10
Rb	275	242	267	171	262	273	246	175	143	204
Sr	1315	1133	1285	1030	1099	731	1079	1136	954	1213
Pb	57	66	58	21	73	83	47	50	39	26
Th	24	20	24	13	23	21	23	22	18	19
U	1	<1	1	1	1	2	4	1.5	3	3.5
Zr	986	1161	1199	764	1167	1206	1255	1221	1042	938
Nb	107	119	119	91	124	136	140	137	107	124
Y	18	17	15	15	22	34	21	19	17	20
La	286	312	331	222	348	434	259	236	197	193
Ce	393	419	430	241	507	528	455	432	357	354
Nd							164	168	137	164
Sc	19	17	23	15	23	22	13	11	10	11
V	166	180	231	134	375	282	199	207	143	148
Cr	288	355	360	514	224	276	546	519	677	718
Co	36	33	38	45	33	23				
Ni	596	627	628	510	277	190	413	360	528	538
Cu	99	130	104	101	76	71	65	66	52	57
Zn	86	86	77	64	86	85	70	65	62	67
Sn	14	19	17	12	8	10	18	21	13	8
Mo	<1	<1	<1	<1	<1	<1	<3	<3	3	3
Ga	18	18	18	10	24	25	28	18	20	13
As	2	1	<1	1	3	7	2.5	2.5	2	2.5
S	510	410	100	200	470	820				
F	2640	2780	2550	1920	2620	3700	2300	2100	1700	2000
Cl	60	40	20	<20	20	40				

MOUNT CEDRIC

Sample number	83210277
Formation	Fitzroy Lamproites
Rock type	Di-Ol-Lc Lamproite
Locality	Mount Cedric
Grid reference	807704
Map sheet	Hardman
Additional data	NW side
Biblio. ref.	ALJ-BMR
SiO_2	49.44
TiO_2	5.73
Al_2O_3	7.05
Fe_2O_3	5.02
FeO	1.26
MnO	0.07
MgO	9.97
CaO	3.40
Na_2O	0.71
K_2O	8.66
P_2O_5	0.56
H_2O+	2.90
H_2O-	1.94
CO_2	0.26
Rest	2.34
Total	99.31
Ba	14094
Li	10
Rb	177
Sr	1174
Pb	51
Th	23
U	3
Zr	1263
Nb	141
Y	19
La	246
Ce	449
Nd	221
Sc	11
V	171
Cr	468
Co	
Ni	417
Cu	66
Zn	67
Sn	18
Mo	3
Ga	18
As	3
S	
F	2100
Cl	

MOUNT IBIS

Sample number	80210093	81210159	81210169	81210170A	81210170B	81210170C
Formation	fitzroy lamproites	Fitzroy Lamproites	Fitzroy Lamproites	Fitzroy Lamproites	Fitzroy Lamproites	Fitzroy Lamproites
Rock type	Ol-Lc Lamp tuff-brecc	Phl-Lc Lamp Brecc	Di-Ol-Lc Lamproite	Ol-Di-Lc Lamproite	Di-Ol-Lc Lamproite	Di-Lc Lamproite
Locality	Mount Ibis	Mount Ibis	Mount Ibis	Mount Ibis	Mount Ibis	Mount Ibis
Grid reference	777592	776592	776592	776592	776592	776592
Map sheet	Hardman	Hardman	Hardman	Hardman	Hardman	Hardman
Additional data		margin	100 60-66m	MI 101 14m	101 26-36m	101 38-44m
Biblio. ref.	GPG-BMR	ALJ-BMR	ALJ-BMR	ALJ-BMR	ALJ-BMR	ALJ-BMR
SiO_2	51.69	52.83	42.43	45.96	45.77	50.47
TiO_2	4.27	4.57	5.77	5.57	5.60	4.85
Al_2O_3	8.31	7.92	4.44	5.82	5.79	7.11
Fe_2O_3	5.09	5.35	4.94	5.44	4.52	4.18
FeO	2.03	1.52	2.37	1.49	1.96	2.45
MnO	0.08	0.08	0.11	0.11	0.10	0.09
MgO	6.04	7.59	19.04	14.65	15.17	10.47
CaO	3.77	2.23	4.06	3.46	3.20	2.43
Na_2O	0.70	0.67	0.63	0.66	0.68	0.68
K_2O	10.79	9.96	5.11	6.06	6.48	8.98
P_2O_5	2.20	0.73	0.80	0.50	0.60	0.84
H_2O+	1.70	2.07	4.93	4.44	4.03	2.54
H_2O-	0.75	0.99	2.32	2.03	2.64	1.88
CO_2	0.40	0.16	0.70	0.28	0.56	0.38
Rest	2.04	1.97	1.25	1.66	1.19	1.14
Total	99.86	98.64	98.90	98.13	98.29	98.49
Ba	12147	11198	4009	8042	4086	4020
Li	12	14	5	11	14	24
Rb	286	321	300	284	266	236
Sr	2692	1414	1150	1219	1075	1374
Pb	53	51	22	29	33	50
Th	29	28	22	21	23	28
U	3	2	2	2	3	2
Zr	885	975	1215	1148	1218	1092
Nb	92	100	130	112	116	114
Y	26	25	12	14	15	25
La	256	279	161	198	211	279
Ce	372	408	293	383	406	422
Nd		203	97	121	130	172
Sc		11	9	9	9	11
V	248	183	140	136	159	186
Cr	194	221	1033	837	737	275
Co						
Ni	223	269	673	495	443	265
Cu	23	41	54	48	45	43
Zn	54	82	61	65	64	91
Sn	7	8	19	15	17	9
Mo	4					
Ga	12	16	7	9	10	17
As	3	2	2	2	1	2
S						
F		2200	1700	1600	1500	1600
Cl						

FISHERY HILL

Sample number	67165014	80210095	81210149	81210150	81210152	71876	71877	71878A	71880	71881
Formation	Fitzroy Lamproites	fitzroy lamproites	Fitzroy Lamproites	Fitzroy Lamproites	Fitzroy Lamproites	Fitzroy Lamproites	Fitzroy Lamproites	Fitzroy Lamproites	Fitzroy Lamproites	fitzroy lamproites
Rock type	Ol-Diop-Lc Lamproite	Ph-Lc Lamp Tuff	KRi-Di-Lc Lamproite	Phl-Lc Lamp Brecc	Ol-Di-Lc Lamproite	Di-Ol-Lc Lamproite	Phl-Lc Lamproite	Di-Ol-Lc Lamp dyke	Phl-Ol-Lc Lamproite	Xenolithic tuff
Locality	Fishery Hill	Fishery Hill	Fishery Hill	Fishery Hill	Fishery Hill	Fishery Hill	Fishery Hill	Fishery Hill	Fishery Hill	Fishery Hill
Grid reference	833633	833633	833633	833633	833633	833633	833633	832632	834634	835633
Map sheet	Hardman	Hardman	Hardman	Hardman	Hardman	Hardman	Hardman	Hardman	Hardman	Hardman
Additional data				Brecc.zone		sill	centre o/c	dyke. S	dyke, N	NE side
Biblio. ref.	GMD-BMR	GPG-BMR	GH-BMR	GH-BMR	GH-BMR	Lewis-GSWA	Lewis-GSWA	Lewis-GSWA	Lewis-GSWA	Lewis-GSWA
SiO_2	51.27	58.69	50.55	52.59	49.95	51.10	51.10	50.50	50.10	57.40
TiO_2	6.52	3.70	6.38	5.81	6.45	7.62	5.89	7.10	7.02	0.67
Al_2O_3	7.46	8.07	7.28	8.77	7.12	8.50	8.60	8.00	8.90	13.20
Fe_2O_3	4.91	6.27	4.50	4.43	4.66	6.20	4.80	6.20	6.60	8.10
FeO	1.62	1.07	1.63	2.16	1.54	1.40	1.71	0.92	0.71	1.14
MnO	0.09	0.09	0.09	0.09	0.09	0.09	0.08	0.05	0.06	0.14
MgO	8.60	4.42	8.76	6.77	9.27	6.60	7.77	7.21	6.62	1.78
CaO	3.30	1.63	3.15	1.81	3.24	2.85	2.56	2.68	1.88	0.78
Na_2O	0.77	0.12	0.71	0.98	0.68	0.72	0.64	0.26	0.22	0.09
K_2O	9.18	10.74	9.05	11.50	9.00	10.40	10.70	10.60	11.45	12.90
P_2O_5	0.61	1.34	0.65	0.63	0.72	0.82	0.62	1.15	1.45	0.61
H_2O+	2.08	1.47	2.21	0.99	4.16	1.94	1.98	2.74	2.33	1.56
H_2O-	0.58	0.48	1.39	0.36	0.79	1.11	0.53	1.52	1.10	0.42
CO_2	0.23	0.11	0.53	0.42	0.23	0.12	0.53	0.07	0.09	0.03
Rest	1.92	0.95	2.09	2.39	2.36	1.66	2.12	1.64	1.59	0.34
Total	99.14	99.15	98.97	99.70	100.26	101.13	99.63	100.64	100.12	99.16
Ba	10165	4334	11978	14471	14027	7944	11723	7402	6351	715
Li	9	7	11	6	12	10	8	11	10	14
Rb	295	306	258	318	268	277	284	275	381	350
Sr	1223	1040	1467	1333	1420	1034	1393	1357	1337	90
Pb	54	49	43	68	43	69	71	54	73	17
Th	25	21	21	32	20	17	21	19	22	7
U	4	3	1	2	1	1	1	2	2	1
Zr	1325	816	1182	1109	1214	1254	1030	1195	1217	180
Nb	124	80	107	116	110	126	114	120	139	14
Y	17	19	16	23	15	19	18	17	27	26
La	311	226	259	372	286	329	351	337	419	78
Ce	441	345	370	519	560	434	459	442	585	141
Nd			199	262	175					
Sc			8	8	8	22	17	20	23	14
V	236	224	191	226	245	182	159	162	180	121
Cr	310	220	266	240	400	319	231	252	220	68
Co	32					33	31	28	29	20
Ni	381	146	367	218	349	292	318	442	300	55
Cu	65	43	63	56	64	98	94	84	72	48
Zn	75	57	70	87	68	84	101	71	86	75
Sn	15	9	17	6	16	23	17	20	13	5
Mo		4				<1	<1	<1	<1	<1
Ga	13	16	14	22	13	18	19	19	24	15
As	1	3	2	2	2	<1	1	<1	<1	4
S						160	540	320	190	80
F	2600		2000	2400	2100	2860	3020	2980	3680	1380
Cl			130			40	70	<20	20	40

FISHERY HILL

Sample number	83210280	83210281	83210282	83210284
Formation	Fitzroy Lamproites	Fitzroy Lamproites	Fitzroy Lamproites	Fitzroy Lamproites
Rock type	Ol-Di-Lc Lamproite	Di-Lc Lamproite	Ol-Di-Lc Lamproite	Phl-Lc Lamproite
Locality	Fishery Hill	Fishery Hill	Fishery Hill	Fishery Hill
Grid reference	833633	833633	833633	832634
Map sheet	Hardman	Hardman	Hardman	Hardman
Additional data	margin W	N side	N side	dyke, N
Biblio. ref.	ALJ-BMR	ALJ-BMR	ALJ-BMR	ALJ-BMR
SiO_2	50.80	51.45	51.60	53.90
TiO_2	6.65	7.19	6.47	6.23
Al_2O_3	7.40	8.34	7.63	7.90
Fe_2O_3	4.83	5.87	5.07	5.90
FeO	1.43	0.80	1.13	0.71
MnO	0.08	0.04	0.06	0.07
MgO	8.48	6.56	8.19	5.54
CaO	3.35	1.62	2.75	1.81
Na_2O	0.88	0.24	0.57	0.38
K_2O	9.26	10.31	9.54	10.47
P_2O_5	0.62	1.10	0.79	1.41
H_2O+	1.97	2.35	3.65	1.90
H_2O-	1.76	1.94	0.11	0.91
CO_2	0.24	0.12	0.15	0.47
Rest	2.31	1.69	2.53	1.95
Total	100.06	99.62	100.24	99.55
Ba	12763	5568	13888	8530
Li	17	17	18	8
Rb	275	342	268	380
Sr	1420	1297	1760	1530
Pb	55	67	67	90
Th	23	24	24	28
U	3	3	2.5	3.5
Zr	1399	1542	1416	1493
Nb	147	163	156	177
Y	21	21	24	27
La	296	339	312	411
Ce	539	612	548	778
Nd	258	223	274	284
Sc	12	15	10	15
V	232	214	215	234
Cr	433	515	354	347
Co				
Ni	453	652	858	275
Cu	78	91	70	54
Zn	77	120	96	85
Sn	24	27	17	16
Mo	3	<3	<3	<3
Ga	18	28	27	34
As	3	2.5	3	3.5
S				
F	2500	4500	2600	3500
Cl				

Sample number	80210119	80210120	83210263	83210266
Formation	Fitzroy Lamproites	Fitzroy Lamproites	Fitzroy Lamproites	Fitzroy Lamproites
Rock type	Phl - Lc Lamproite	Ol-Di-Lc Lamproites	Ol-Di-Lc Lamproite	Ol-Di-Lc Lamproite
Locality	Noonkanbah Hill	Noonkanbah Hill	Noonkanbah Hill	Noonkanbah Hill
Grid reference	894614	894614	894614	894614
Map sheet	Hardman	Hardman	Hardman	Hardman
Additional data		Cogn Xen	S margin	Ne margin
Biblio. ref.	GPG-BMR	GPG-BMR	ALJ-BMR	ALJ-BMR
SiO_2	54.01	51.40	50.75	50.60
TiO_2	5.45	5.51	5.68	6.18
Al_2O_3	8.41	7.90	7.59	7.95
Fe_2O_3	5.14	4.96	4.82	5.73
FeO	0.83	1.24	1.34	1.23
MnO	0.09	0.08	0.07	0.07
MgO	5.57	8.69	9.18	7.09
CaO	2.17	3.81	3.70	4.00
Na_2O	0.08	0.76	0.92	0.61
K_2O	10.76	8.50	8.69	9.67
P_2O_5	1.63	0.40	0.53	0.65
H_2O+	2.15	2.16	2.44	1.89
H_2O-	1.06	2.10	1.70	1.38
CO_2	0.76	0.18	0.22	0.13
Rest	1.94	2.08	1.66	2.05
Total	100.05	99.77	99.29	99.23
Ba	12137	12314	8167	11190
Li	11	6	11	10
Rb	238	200	243	203
Sr	1496	1299	1254	1190
Pb	58	34	39	44
Th	22	23	22	23
U	1	3	2	2
Zr	1022	1056	1235	1311
Nb	101	88	118	134
Y	16	16	19	21
La	284	225	228	242
Ce	414	326	419	437
Nd			182	218
Sc			12	14
V	279	150	178	188
Cr	226	302	461	506
Co				
Ni	238	370	354	443
Cu	34	50	70	75
Zn	74	58	64	63
Sn	5	20	20	24
Mo	4	3	<3	3
Ga	21	11	16	21
As	2	2	2.5	2.5
S				
F		2800	1900	2300
Cl		45		

Sample number	71882B	71885	71882A
Formation	Fitzroy Lamproites	Fitzroy Lamproites	Fitzroy Lamproites
Rock type	Di-Ol-Phl-Lc Lamp	KRi-Lc Lamproite	Di-KRi-Ol-Ph-Lc Lamp
Locality	Howes' Hill	Howes' Hill	Howes' Hill
Grid reference	879696	879696	878697
Map sheet	Hardman	Hardman	Hardman
Additional data	centr plug	sill in tf	centr plug
Biblio. ref.	Lewis-GSWA	Lewis-GSWA	Lewis-GSWA
SiO_2	55.60	52.30	51.50
TiO_2	6.36	5.14	6.53
Al_2O_3	9.00	8.90	7.90
Fe_2O_3	6.50	4.90	5.20
FeO	1.20	2.00	1.63
MnO	0.06	0.05	0.08
MgO	4.18	7.21	7.28
CaO	1.56	1.88	3.57
Na_2O	0.19	0.22	0.65
K_2O	9.60	8.87	9.42
P_2O_5	1.02	1.07	0.85
H_2O+	2.10	3.07	1.87
H_2O-	1.00	2.53	1.03
CO_2	0.03	0.12	0.04
Rest	1.48	1.99	1.86
Total	99.88	100.25	99.41
Ba	6637	10193	9832
Li	13	29	11
Rb	266	224	237
Sr	820	1269	1190
Pb	50	70	42
Th	24	18	19
U	<1	<1	1
Zr	1193	1030	1029
Nb	98	103	91
Y	17	19	16
La	298	381	298
Ce	355	420	308
Nd			
Sc	19	19	16
V	294	191	164
Cr	251	292	255
Co	35	20	32
Ni	180	700	280
Cu	70	100	95
Zn	78	85	80
Sn			15
Mo	<1	<1	<1
Ga	17	19	16
As	1	2	<1
S	200	300	930
F	3240	3000	3160
Cl	160	310	<20

Sample number	79211048	80210110	80210111	81210218	81210219	81210220	81210221	71309	71310
Formation	Fitzroy Lamproites	Fitzroy Lamproites	Fitzroy Lamproites	Fitzroy Lamproites	Fitzroy Lamproites	Fitzroy Lamproites	Fitzroy Lamproites	fitzroy lamproites	Fitzroy Lamproites
Rock type	Diop-Leuc Lamproite	KRi-Di-Lc Lamproite	Ol - Lc Lamproite	Phl-Lc Lamp Brecc	Phl-Lc Lamproite	Di-KRi-Lc Lamproite	Di-KRi-Lc Lamproite	Di-Lc lamproite	Phl-KRi-Lc Lamproite
Locality	Mamilu Hill	Mamilu Hill	Mamilu Hill	Mamilu Hill	Mamilu Hill	Mamilu Hill	Mamilu Hill	Mamilu Hill	Mamilu Hill
Grid reference	923678	923678	923678	923678	923678	923678	923678	923677	923677
Map sheet	Hardman	Hardman	Hardman	Hardman	Hardman	Hardman	Hardman	Hardman	Hardman
Additional data				xenoliths				Xenoliths	inner cent
Biblio. ref.	GMD-BMR	GPG-BMR	GPG-BMR	ALJ-BMR	ALJ-BMR	ALJ-BMR	ALJ-BMR	Lewis-GSWA	Lewis-GSWA
SiO_2	53.61	51.48	49.96	53.17	49.20	53.12	52.19	52.70	53.90
TiO_2	5.66	6.09	5.21	4.66	5.54	5.89	6.01	5.45	5.26
Al_2O_3	9.85	9.10	10.63	9.80	9.77	9.38	9.25	11.00	9.60
Fe_2O_3	5.66	5.97	8.47	5.84	9.05	5.44	5.58	6.00	5.90
FeO	1.22	1.24	0.15	1.37	0.49	1.38	1.28	0.53	1.48
MnO	0.11	0.07	0.40	0.08	0.07	0.11	0.08	0.04	0.08
MgO	4.99	5.69	4.03	5.98	5.68	5.33	5.31	3.92	4.79
CaO	2.13	3.17	2.01	1.60	1.96	2.34	2.37	2.43	2.34
Na_2O	0.67	0.64	0.18	0.64	0.13	0.68	0.49	0.14	0.61
K_2O	11.22	10.84	11.16	11.46	11.82	11.52	11.23	10.90	10.30
P_2O_5	0.72	0.83	1.51	0.89	1.70	0.71	0.67	1.79	0.81
H_2O+	1.53	1.83	2.29	1.58	2.16	1.79	2.39	2.25	2.00
H_2O-	0.48	0.75	0.97	0.44	0.29	0.53	0.86	1.45	1.12
CO_2	0.30	0.95	0.30	0.39	0.36	0.50	0.77	0.12	0.09
Rest	1.93	1.65	2.11	1.94	1.93	1.76	2.22	2.05	1.54
Total	100.08	100.30	99.38	99.84	100.15	100.48	100.70	100.77	99.82
Ba	10105	9369	12894	9613	7889	8177	12591	9522	6652
Li	6	6	5	9	7	6	7	8	10
Rb	322	262	365	267	370	295	246	296	252
Sr	1033	1379	1428	1240	1071	1094	1053	1851	1085
Pb	71	50	92	76	87	63	53	110	80
Th	25	25	29	27	23	23	23	24	17
U	3	2	3	2	2	1	1	1	<1
Zr	1215	1302	1132	1049	1214	1167	1164	1078	1014
Nb	129	125	130	118	141	119	112	139	106
Y	18	21	21	22	24	20	17	20	17
La	409	329	464	414	490	390	335	602	342
Ce	552	493	611	721	920	691	644	733	479
Nd				222	295	216	202		
Sc				9	8	11	10	14	17
V	282	201	342	307	330	288	271	261	185
Cr	296	233	262	424	475	479	493	256	267
Co	30							25	35
Ni	263	166	246	255	158	421	325	180	450
Cu	51	42	39	46	29	56	57	60	85
Zn	77	52	68	81	92	80	71	93	93
Sn	4	17	5	3	5	19	11		
Mo		<3	4					<1	1
Ga	23	16	28	27	29	23	20	31	23
As	1	1	4	<1	16	2	2	1	1
S								200	100
F	3200			3300	5400	2500	2600	4060	3430
Cl								160	160

Sample number	68165029	79211046	79211050	81210223	81210224	71325	71326	71327	71331	71334
Formation	Fitzroy	Fitzroy	Fitzroy	Fitzroy	Fitzroy	Fitzroy	Fitzroy	Fitzroy	Fitzroy	fitzroy
Rock type	Lamproites Ol-Di-KRi-Lc Lamp	Lamproites Ol-Di-Lc Lamproite	Lamproites Ol-Di-KRi-Lc Lamp	Lamproites KRi-Di-Lc Lamproite	Lamproites KRi-Di-Lc Lamproite	Lamproites (Ol-KRi)-Lc Lamp	Lamproites Ol-Di-Lc Lamproite	Lamproites KRi-Ol-Di-Lc Lamp	Lamproites Di-KRi-Ol-Lc Lamp	lamproites Lc Lamp Tuff
Locality	Hills Cone	Hills Cone	Hills Cone	Hills Cone	Hills Cone	Hills Cone	Hills Cone	Hills Cone	Hills Cone	Hills Cone
Grid reference	974654	974654	974654	974654	974654	975653	975653	975653	975653	975653
Map sheet	Hardman	Hardman	Hardman	Hardman	Hardman	Hardman	Hardman	Hardman	Hardman	Hardman
Additional data						dyke, East	centre, E	Centre, W	centre, W	Xenoliths
Biblio. ref.	GMD-BMR	GMD-BMR	GMD-BMR	ALJ-BMR	ALJ-BMR	Lewis-GSWA	Lewis-GSWA	Lewis-GSWA	Lewis-GSWA	Lewis-GSWA
SiO_2	52.36	53.00	53.34	59.16	52.22	51.90	52.20	51.70	53.50	53.20
TiO_2	7.01	6.53	6.54	5.60	6.47	5.16	5.92	6.11	5.96	3.57
Al_2O_3	8.55	9.05	8.99	8.02	8.33	9.40	8.40	8.80	8.60	11.40
Fe_2O_3	5.79	5.39	5.49	5.58	5.24	5.70	5.90	5.80	5.90	5.80
FeO	1.58	1.54	1.46	0.78	1.63	1.23	1.26	1.84	1.24	1.77
MnO	0.08	0.08	0.07	0.06	0.09	0.07	0.07	0.09	0.09	0.05
MgO	6.36	5.61	5.44	4.01	6.33	5.86	6.63	5.92	5.23	4.40
CaO	2.23	2.64	2.18	0.98	2.83	2.96	2.67	3.23	2.18	1.61
Na_2O	0.50	0.73	0.73	0.25	0.70	0.20	0.36	0.74	0.50	0.12
K_2O	10.47	10.84	10.79	10.10	10.69	10.50	9.70	9.27	9.84	10.80
P_2O_5	0.48	0.59	0.59	0.54	0.50	1.99	0.97	0.79	0.75	1.29
H_2O+	2.03	1.47	1.51	2.27	1.46	2.50	2.21	1.87	2.59	2.17
H_2O-	0.54	0.71	0.84	0.62	0.44	0.94	1.63	1.11	1.22	1.01
CO_2	0.36	0.17	0.25	0.67	0.20	0.21	0.18	0.06	0.08	0.11
Rest	1.73	1.88	2.02	1.13	2.54	1.65	2.12	2.16	2.18	2.39
Total	100.07	100.23	100.24	99.77	99.67	100.27	100.22	99.49	99.86	99.69
Ba	9322	10648	11350	3648	15803	7265	11666	12363	11865	14982
Li	7	7	7	5	6	8	11	7	10	18
Rb	353	301	290	286	305	277	305	313	238	175
Sr	887	1065	1074	725	1108	1229	1086	1057	1086	1365
Pb	51	46	49	54	44	90	60	60	50	90
Th	20	24	23	22	21	23	17	16	18	21
U	6	6	2	1	2	2	<1	<1	<1	2
Zr	1302	1245	1302	1165	1122	1108	1103	1129	1037	831
Nb	120	107	110	116	98	112	98	94	95	92
Y	14	16	16	16	18	23	16	20	13	21
La	269	255	290	302	275	418	337	317	319	397
Ce	387	366	413	591	535	548	403	394	364	442
Nd				189	170					
Sc				9	10	16	17	19	16	16
V	216	267	335	338	345	203	186	169	198	248
Cr	204	172	146	388	377	267	246	226	192	200
Co	37	27	26			35	30	35	40	25
Ni	259	236	241	300	276	320	540	370	440	220
Cu	65	69	59	63	72	85	110	120	120	65
Zn	78	63	65	72	73	79	84	79	80	78
Sn	13	11	12	14	16					
Mo						<1	1	1	1	<1
Ga	16	14	16	18	16	23	18	17	17	23
As	2	2	2	1	2	<1	2	<1		2
S						300	500	400	1300	100
F	2400	2400	3000	2000	2400	3360	3200	3160	3550	2410
Cl						140	160	140	340	250

Sample number	67165015	81210145	81210146	81210147	71335	71338	71339	83210258	83210259	83210260
Formation	Fitzroy Lamproites	Fitzroy Lamproites	Fitzroy Lamproites	Fitzroy Lamproites	fitzroy lamproites	Fitzroy Lamproites	Fitzroy Lamproites	Fitzroy Lamproites	Fitzroy Lamproites	Fitzroy Lamproites
Rock type	Ol-Diop-Lc Lamproite	Ol-Phl-Di-KR-Lc Lamp	Di-KRi-Lc Lamproite	Ol-Di-Lc Lamproite	Xeno-tuff breccia	Phl-Ol-KRi Di-Lc Lamp	Phl-Ol-Di-Lc Lamp	Di - Lc Lamproite	Ol-Di-Phl-KR-Lc Lamp	Phl-Di-Lc Lamproite
Locality	"P" Hill	"P" Hill	"P" Hill	"P" Hill	"P" Hill	"P" Hill	"P" Hill	"P" Hill	"P" Hill	"P" Hill
Grid reference	022548	022548	022548	022548	022547	022547	022547	022548	022548	022548
Map sheet	Hardman	Hardman	Hardman	Hardman	Hardman	Hardman	Hardman	Hardman	Hardman	Hardman
Additional data		Wolg. zone				main plug	main plug	SE margin	top W hill	saddle o/c
Biblio. ref.	GMD-BMR	GH-BMR	GH-BMR	GH-BMR	Lewis-GSWA	Lewis-GSWA	Lewis-GSWA	ALJ-BMR	ALJ-BMR	ALJ-BMR
SiO_2	52.59	53.47	51.47	52.13	56.00	52.80	52.00	52.58	52.42	52.24
TiO_2	5.37	6.43	6.11	5.60	3.69	5.50	5.42	6.10	6.36	5.93
Al_2O_3	8.28	8.27	7.89	8.13	10.30	8.40	8.50	8.23	8.04	8.08
Fe_2O_3	5.05	5.52	4.99	5.11	5.60	5.60	5.90	4.67	5.43	5.06
FeO	1.69	1.56	1.59	1.66	1.95	1.55	1.52	1.58	1.46	1.71
MnO	0.08	0.09	0.08	0.10	0.06	0.09	0.09	0.09	0.09	0.08
MgO	7.28	5.38	7.81	7.00	3.74	5.97	6.63	6.84	6.63	6.98
CaO	3.53	2.95	3.39	3.50	1.66	3.96	3.64	3.46	3.48	3.43
Na_2O	1.01	0.68	0.71	1.07	0.12	0.70	1.10	0.68	0.73	1.09
K_2O	9.72	10.36	9.69	9.79	10.80	9.11	8.72	10.45	10.29	10.06
P_2O_5	0.50	0.66	0.48	0.39	1.36	0.60	0.69	0.49	0.55	0.47
H_2O+	1.79	1.09	2.40	1.56	2.26	2.66	1.94	1.70	1.98	1.47
H_2O-	0.56	0.62	1.18	0.82	0.79	1.31	1.63	1.03	0.79	0.73
CO_2	0.76	0.16	0.25	0.81	0.06	0.05	0.13	0.21	0.28	0.17
Rest	1.70	1.81	1.89	1.62	1.52	1.83	1.96	1.86	1.87	1.90
Total	99.91	99.05	99.93	99.29	99.91	100.13	99.87	99.97	100.40	99.40
Ba	9810	9509	10711	8758	7377	8986	10914	9814	9622	10318
Li	8	7	9	8	27	10	14	11	10	12
Rb	199	236	200	192	227	222	213	262	248	235
Sr	1176	1166	1321	1119	1291	1073	999	1231	1191	1119
Pb	35	38	36	32	80	50	50	41	44	44
Th	21	23	21	20	21	10	15	22	23	22
U	7	2	2	2	<1	<1	<1	3	3	3
Zr	1057	1107	1107	1007	784	975	975	1244	1300	1258
Nb	101	100	98	95	86	86	89	123	132	133
Y	17	17	15	16	21	20	18	20	22	20
La	189	235	236	197	291	264	282	228	241	228
Ce	286	332	335	291	429	340	331	418	446	419
Nd		174	181	146				196	210	202
Sc		11	11	12	16	16	17	14	15	13
V	162	165	194	154	236	140	184	177	213	224
Cr	267	317	257	265	151	243	327	389	396	455
Co	35				30	50	35			
Ni	363	179	258	380	140	260	330	354	342	352
Cu	66	69	68	69	130	120	110	80	86	75
Zn	71	100	70	69	90	98	74	99	85	76
Sn	2	25	15	12				21	21	18
Mo					<1	<1	<1	3	3	<3
Ga	12	14	14	12	23	14	14	25	21	21
As	1	2	2	2	1	<1	<1	2.5	2.5	3
S					700	2100	200			
F	1500	3000	2100	2000	1840	3200	3230	2300	2600	2000
Cl		300			410	400	260			

Sample number	68165021	79211051	79211052	79211055	79211057	83210339	83210340	83210341	83210342
Formation	fitzroy lamproites	Fitzroy Lamproites	Fitzroy Lamproites	Fitzroy Lamproites	Fitzroy Lamproites	Fitzroy Lamproites	Fitzroy Lamproites	Fitzroy Lamproites	Fitzroy Lamproites
Rock type	Ph-Lc Lamp breccia	Phl-Lc Lamproite	Ol-Di-Lc Lamproite	Phl-Lc Lamproite	Phl-Di-KRi -Lc Lamp	Phl-Di-KRi -Lc lamp.	Phl-Di-Lc Lamproite	Phl-Di-Lc Lamproite	Phl-Lc Lamproite
Locality	Djada Hill	Djada Hill	Dadja Hill	Djada Hill	Djada Hill	Djada Hill	Djada Hill	Djada Hill	Djada Hill
Grid reference	961499	961499	961499	961499	961499	961499	960498	960498	962498
Map sheet	Kalyeeda	Kalyeeda	Kalyeeda	Kalyeeda	Kalyeeda	Kalyeeda	Kalyeeda	Kalyeeda	Kalyeeda
Additional data	Xenoliths					W side	SW side	Sw end	Se [illegible]
Biblio. ref.	GMD-BMR	GMD-BMR	GMD-BMR	GMD-BMR	GMD-BMR	ALJ-BMR	ALJ-BMR	ALJ-BMR	ALJ BMR
SiO_2	56.36	55.42	51.84	51.64	52.19	52.31	51.47	51.01	53.96
TiO_2	4.43	4.62	6.03	5.39	6.72	7.23	7.73	7.71	5.67
Al_2O_3	8.86	9.02	8.33	8.47	7.90	8.06	7.92	8.11	8.30
Fe_2O_3	3.59	3.94	5.20	5.15	5.23	5.20	5.70	5.55	5.42
FeO	1.96	1.95	1.60	1.03	1.16	1.29	0.81	0.90	1.06
MnO	0.05	0.06	0.07	0.05	0.07	0.08	0.06	0.06	0.06
MgO	6.34	6.45	6.86	7.36	6.84	6.30	6.07	5.81	6.24
CaO	1.63	1.93	3.10	2.16	3.20	2.81	3.06	2.95	1.94
Na_2O	0.60	0.68	0.65	0.53	0.58	0.69	0.29	0.25	0.43
K_2O	11.03	11.15	10.06	9.96	9.98	10.70	10.41	10.85	11.42
P_2O_5	0.64	0.71	0.69	1.17	0.36	0.34	0.58	0.57	1.18
H_2O+	1.55	1.41	1.73	2.12	1.98	1.89	2.07	2.33	1.85
H_2O-	0.28	0.24	0.86	1.96	0.90	1.15	1.39	1.46	0.86
CO_2	0.17	0.28	0.21	0.17	1.17	0.19	0.68	0.21	0.20
Rest	1.71	1.94	2.28	2.07	2.22	2.17	2.13	2.48	1.97
Total	99.20	99.80	99.51	99.23	100.50	100.41	100.37	100.25	100.56
Ba	10023	10481	13939	10742	13149	12150	11233	14678	8678
Li	13	11	12	23	9	12	15	15	14
Rb	346	297	292	260	283	301	374	351	308
Sr	1230	1331	985	1842	1351	1467	1369	1238	1712
Pb	72	73	44	96	47	53	51	49	95
Th	23	23	21	28	20	22	21	21	27
U	7	2	3	4	4	2.5	3	2.5	4
Zr	1005	1075	1164	1241	1293	1483	1591	1595	1354
Nb	119	126	104	146	116	147	148	146	177
Y	19	18	15	24	13	21	21	20	31
La	298	332	259	447	281	277	250	266	436
Ce	443	490	361	647	398	497	459	489	764
Nd						244	239	283	268
Sc						13	14	13	13
V	232	263	215	271	206	183	162	163	296
Cr	337	326	205	370	329	368	367	366	475
Co	25	19	26	19	27				
Ni	281	231	383	321	188	287	304	316	339
Cu	47	38	61	48	63	64	78	75	62
Zn	85	81	70	82	62	66	70	66	87
Sn	<2	<2	7	<2	10	21	25	23	10
Mo						<3	3	3	<3
Ga	24	22	14	21	11	23	17	24	28
As	1	1	2	<1	2	3	2.5	3.5	1.5
S									
F		2800	2800	2100	2500	1900	2800	2400	3000
Cl			230						

THE SISTERS

Sample number	80210076	80210077	80210078	80210082	83210336	83210345
Formation	Fitzroy Lamproites	Fitzroy Lamproites	fitzroyite lamproites	Fitzroy Lamproites	Fitzroy Lamproites	Fitzroy Lamproites
Rock type	Ol-Lc Lamp breccia	Phl - Lc Lamproite	Lapilli-ash tuff	Di-Ol-Lc Lamproite	Di-Ol-lc Lamproite	KRi-Di-Lc Lamproite
Locality	TheSisters East Hill	TheSisters East Hill	TheSisters East Hill	TheSisters West Hill	The Sisters W	The Sisters E
Grid reference	650446	650446	650446	634441	634441	650446
Map sheet	Kalyeeda	Kalyeeda	Kalyeeda	Kalyeeda	Kalyeeda	Kalyeeda
Additional data			carbonated		trench W	SW end
Biblio. ref.	GPG-BMR	GPG-BMR	GPG-BMR	GPG-BMR	ALJ-BMR	ALJ-BMR
SiO_2	57.62	56.12	43.24	47.91	48.18	50.24
TiO_2	4.41	5.12	3.34	4.99	5.27	6.13
Al_2O_3	8.47	8.38	6.53	6.71	6.65	8.36
Fe_2O_3	4.42	4.73	3.98	6.23	6.11	5.17
FeO	1.44	1.74	0.61	0.98	0.86	1.04
MnO	0.06	0.07	0.03	0.07	0.07	0.07
MgO	3.74	5.12	4.99	12.36	11.65	7.47
CaO	2.30	1.76	12.73	3.19	3.12	3.67
Na_2O	0.47	0.92	0.09	0.51	0.43	0.80
K_2O	10.15	11.01	8.00	7.01	7.45	9.96
P_2O_5	1.79	0.64	1.12	0.80	1.04	0.96
H_2O+	1.52	1.21	1.68	3.46	3.58	2.05
H_2O-	0.68	0.28	0.39	2.87	3.60	1.23
CO_2	0.31	0.16	10.31	0.20	0.27	0.30
Rest	1.47	2.01	1.04	1.49	1.86	2.63
Total	98.85	99.27	98.08	98.78	100.14	100.08
Ba	8640	13010	5244	6012	9001	15896
Ii	9	8	11	7	21	12
Rb	216	255	211	207	252	296
Sr	1137	1179	1369	1215	1398	1466
Pb	55	51	38	45	56	50
Th	25	25	20	25	25	27
U	3	3	2	2	3	4
Zr	992	1038	767	1123	1234	1346
Nb	109	120	85	127	164	168
Y	24	21	16	20	25	21
La	300	271	183	273	233	259
Ce	432	387	283	454	365	479
Nd				150	176	267
Sc					11	14
V	221	346	265	208	167	229
Cr	209	256	123	867	772	308
Co						
Ni	113	162	112	651	519	267
Cu	36	36	26	52	49	74
Zn	75	88	55	68	78	69
Sn	5	5	3	17	15	16
Mo	3	4	4	4	<3	3
Ga	19	20	16	10	15	17
As	2	2	3	1	2.5	1.5
S						
F				1700	2300	2800
Cl						

Sample number	67165019	71160402	71160403	71160404	71160407	79211060	80210087	81210167B	81210167C	81210172
Formation	fitzroy lamproites	Fitzroy Lamproites	fitzroy lamproite	fitzroy lamproites	fitzroy lamproites	fitzroy lamproites	fitzroy lamproites	fitzroy lamproites	fitzroy lamproites	Fitzroy Lamproites
Rock type	Phl-Di-KRi -San? Lamp	Ol-Di-Lc Lamproite	Shch-KRi-San? Lamp	Ph-Lc Lamp tuff-brecc	Phl-Di-KRi -Lc? Lamp	P/J-Sh-Di-KR-Sa? Lp	P-Di-Ph-Ol -KR-S Lamp	Carb P-J-Sh-Ap-KR Lp	Carb P-J-Ph-Ol-KR Lp	Phl-Di-Ol-Lc Lamp.
Locality	Walgidee Hills	Walgidee Hills	Walgidee Hills	Walgidee Hills	Walgidee Hills	Walgidee Hills	Walgidee Hills	Walgidee Hills	Walgidee Hills	Walgidee Hills
Grid reference	974746		974746	unknown		974746	974746	974746	974746	W2-S2
Map sheet	Hardman	Hardman	Hardman	Hardman	Hardman	Hardman	Hardman	Hardman	Hardman	Hardman
Additional data	carbonated		carbonated	Xenoliths	altered			centre	centre	cuttings
Biblio. ref.	GMD-BMR	GMD-BMR	GMD-BMR	GMD-BMR	GMD-BMR	GMD-BMR	GPG-BMR	ALJ-BMR	ALJ-BMR	ALJ-BMR
SiO_2	35.86	45.28	31.06	59.65	23.23	40.58	35.87	30.40	34.86	43.35
TiO_2	5.32	4.96	4.21	2.59	4.73	3.66	4.65	12.55	5.30	4.19
Al_2O_3	5.29	6.53	4.23	7.43	0.99	6.82	4.24	3.40	4.55	5.69
Fe_2O_3	7.30	6.98	5.46	4.74	13.22	5.78	6.21	7.57	6.18	6.21
FeO	0.76	1.55	0.40	0.87	1.56	0.41	0.72	0.54	0.63	0.86
MnO	0.11	0.10	0.07	0.08	0.32	0.05	0.09	0.12	0.09	0.10
MgO	7.35	13.54	9.18	6.62	11.84	6.07	8.44	6.56	8.44	15.46
CaO	13.52	4.66	18.16	2.56	15.98	12.26	15.30	13.54	14.32	3.56
Na_2O	0.39	0.30	0.24	0.82	0.23	0.22	0.22	0.16	0.24	0.34
K_2O	7.59	8.13	6.07	9.06	3.08	8.89	6.12	6.46	6.11	6.60
P_2O_5	2.49	1.07	2.23	1.62	0.98	5.13	0.56	2.44	0.87	1.35
H_2O+	2.01	3.30	1.93	1.98	2.94	2.14	2.50	1.84	2.17	2.37
H_2O-	0.23	0.45	0.19	0.59	0.67	1.86	0.69	0.66	0.91	3.09
CO_2	5.04	0.28	14.37	0.35	17.85	4.04	10.32	10.17	9.90	1.79
Rest	2.99	1.98	1.48	0.89	1.82	1.37	2.33	2.83	2.17	2.45
Total	96.25	99.11	99.28	99.85	99.44	99.28	98.26	99.24	96.74	97.41
Ba	19984	11617	8803	5211	12092	6253	15709	21116	15106	14404
Li	7	7	3	18	18	4	5	5	5	11
Rb	536	540	416	363	762	538	482	428	402	479
Sr	2456	1173	1664	389	1404	3507	1407	2128	1911	1192
Pb	60	27	19	24	283	10	23	30	26	17
Th	28	32	4	19	8	8	21		16	30
U	9	5	5	12	13	4	4		3	2
Zr	2045	1291	1287	685	67	958	1653			1090
Nb	175	149	119	77	230	63	127		128	125
Y	22	9	8	18	63	10	10	13	13	13
La	113	190	40	40	108	76	75			179
Ce	123	241	44	85	105	89	85			302
Nd										93
Sc								14	17	14
V	121	196	59	160	260	42	65	155	100	100
Cr	100	424	78	117	164	32	254	21	200	967
Co	22	50	18	24	38	16				
Ni	66	838	48	276	70	34	189	81	132	536
Cu	72	44	65	22	20	47	63	118	75	41
Zn	66	80	54	42	191	51	67	57	64	70
Sn	17	6	10	5	<2	11	15	5	15	5
Mo							8			
Ga	8	9	7	10	6	5	6	8	8	9
As	4	2	2	<1	1	1	3	2	3	2
S										
F								1700	1700	2300
Cl										300

Sample number	81210168	81210173A	81210173B	81210175	81210176	81210177B	81210182	81210183	81210184	81210185
Formation	fitzroy lamproites	Fitzroy Lamproites	Fitzroy Lamproites	Fitzroy Lamproites	Fitzroy Lamproites	Fitzroy Lamproites	Fitzroy Lamproites	Fitzroy Lamproites	Fitzroy Lamproites	Fitzroy Lamproites
Rock type	Carb Ol-Di-KR-Lc-Lp	Di-KRi-Ol-Ph-Lc Lamp	Ph-Di-KRi-Ol-Lc Lamp	Di-KRi-Ph-Ol-Lc Lamp	Di-Ph-KRi-Ol-Lc Lamp	Ph-Di-KRi-Ol-Lc Lamp	Porph Di-Ol-Lc Lamp	Di-Phl-KRi Lc-Ol Lamp	Ph-Di-Ol-KRi-Lc Lam	Ph-Di-Ol-KR-Lc Lamp
Locality	Walgidee Hills	Walgidee Hills	Walgidee Hills	Walgidee Hills	Walgidee Hills	Walgidee Hills	Walgidee Hills	Walgidee Hills	Walgidee Hills	Walgidee Hills
Grid reference	977747									
Map sheet	Hardman	Hardman	Hardman	Hardman	Hardman	Hardman	Hardman	Hardman	Hardman	Hardman
Additional data	E centre	B0-S2	B0-S2 18m	E1-S2 16m	E1-S3 38m	W2-S3 50m	E5-S4 20m	E4-S5 42m	E1-S5 17m	B0-S5 15m
Biblio. ref.	ALJ-BMR	ALJ-BMR	ALJ-BMR	ALJ-BMR	ALJ-BMR	ALJ-BMR	ALJ-BMR	ALJ-BMR	ALJ-BMR	ALJ-BMR
SiO_2	32.23	46.09	43.41	43.24	41.79	41.76	44.77	41.33	43.48	44.57
TiO_2	4.68	4.69	4.36	4.25	4.01	4.07	4.34	3.95	4.05	4.59
Al_2O_3	4.46	6.08	5.30	5.49	4.83	4.66	5.62	5.02	5.09	5.30
Fe_2O_3	5.60	6.49	6.29	4.93	4.67	4.51	5.42	4.78	6.08	6.55
FeO	0.44	1.24	1.02	2.16	2.35	2.41	1.85	2.02	0.81	0.83
MnO	0.17	0.09	0.11	0.10	0.11	0.11	0.10	0.10	0.09	0.06
MgO	7.37	14.13	17.13	15.96	19.86	18.52	15.84	21.28	16.16	15.83
CaO	19.12	3.96	4.06	4.29	2.87	3.93	4.33	2.49	4.46	3.11
Na_2O	0.41	0.61	0.43	0.37	0.29	0.33	0.26	0.15	0.41	0.37
K_2O	6.09	7.83	5.12	7.44	4.22	4.74	7.47	3.16	4.36	4.55
P_2O_5	0.99	1.07	0.44	1.69	0.35	0.45	1.05	0.23	0.18	0.18
H_2O+	1.60	2.89	2.71	2.19	4.23	3.56	3.67	6.48	5.72	6.24
H_2O-	0.35	1.51	3.50	2.05	5.20	5.11	2.20	5.83	4.26	5.04
CO_2	12.57	0.46	0.82	1.52		0.62	0.52	0.84	1.99	0.48
Rest	3.23	1.94	1.94	2.27	1.45	1.80	1.78	1.32	1.90	1.80
Total	99.31	99.08	96.64	97.95	96.23	96.58	99.22	98.98	99.04	99.50
Ba	24914	9402	10262	13279	5970	8897	8998	5910	10071	8883
Li	3	33	8	11	9	8	37	8	7	7
Rb	413		413	420	462	526	444	388	425	457
Sr	1465	1151	1485	1193	1182	1338	1096	975	1158	1014
Pb	15	19	21	19	25	23	21	20	22	28
Th		29	30	28	29	29	28	24	26	32
U		1	1	3	2	2	2	2	2	4
Zr		1204	1152	1087	1286	1204	1110	1093	1285	1601
Nb		135	131	127	138	134	127	121	127	176
Y	14	16	16	12	12	11	13	11	8	11
La		194	191	163	179	174	167	124	153	179
Ce		341	344	325	326	326	313	231	277	316
Nd		106	113	106	91	100	106	77	86	100
Sc	17	12	10	13	10	10	13	9	9	9
V	135	148	110	170	97	95	159	53	121	125
Cr	149	926	825	963	809	946	920	692	704	568
Co										
Ni	95	1011	487	602	724	685	492	630	531	472
Cu	71	52	44	49	52	52	40	39	40	42
Zn	53	75	71	71	68	63	67	63	62	68
Sn	3	14	9	6	14	11	9	13	10	13
Mo										
Ga	9	10	9	10	9	9	9	8	10	10
As	2	1	1	2	1	2	1	1	1	2
S										
F	2600	3000	1600	1600	1200	1200	1800	1300	2100	2100
Cl										100

Sample number	81210186	81210187	81210188	81210190B	81210191	81210192	81210193	81210195	81210196	81210197A
Formation	Fitzroy	Fitzroy	Fitzroy	Fitzroy	Fitzroy	Fitzroy	Fitzroy	fitzroy	Fitzroy	Fitzroy
Rock type	Lamproites Di-Phl-Ol-KR-Lc Lamp	Lamproites Ph-Ol-Di-KR-Lc Lamp	Lamproites Ph-Di-Ol-KR-Lc Lamp	Lamproites P-J-Ph-Di-KR-Sa Lamp	Lamproites Porph Phl-Ol-Lc lamp	Lamproites Ph-Di-Ol-KR-Lc Lamp	Lamproites KRi-Di-Ol-Ph-Lc Lamp	lamproites Carb PJ-Ap-W-KR-Sa L	Lamproites Alt PJ-Ap-Sh-Sa Lamp	Lamproites W-Ph-Ol-Di-KR-Lc lam
Locality	Walgidee Hills	Walgidee Hills	Walgidee Hills	Walgidee Hills	Walgidee Hills	Walgidee Hills	Walgidee Hills	Walgidee Hills	Walgidee Hills	Walgidee Hills
Grid reference										
Map sheet	Hardman	Hardman	Hardman	Hardman	Hardman	Hardman	Hardman	Hardman	Hardman	Hardman
Additional data	W2-S5 15m	E2-S6 5-7m	E3-S6 20m	O/C centre	E2-S7 18m	E4-S7 18m	E6-S7 20m	pegmatoid	pegmatoid	E centre
Biblio. ref.	ALJ-BMR	ALJ-BMR	ALJ-BMR	ALJ-BMR	ALJ-BMR	ALJ-BMR	ALJ-BMR	ALJ-BMR	ALJ-BMR	ALJ-BMR
SiO_2	44.08	44.90	42.01	40.55	41.26	43.08	43.29	36.11	59.55	47.32
TiO_2	4.02	4.26	3.69	6.32	3.98	5.02	3.88	5.27	11.97	5.49
Al_2O_3	5.42	5.50	5.90	7.89	5.48	5.47	5.49	4.72	0.41	5.54
Fe_2O_3	6.11	6.63	6.15	6.55	6.30	6.46	6.37	5.94	9.41	6.98
FeO	0.69	0.70	1.06	0.63	1.05	0.71	0.69	0.51	1.51	1.52
MnO	0.06	0.07	0.10	0.07	0.10	0.07	0.09	0.08	0.14	0.13
MgO	16.66	15.35	18.66	7.70	17.82	15.25	17.68	7.64	4.45	11.08
CaO	3.47	3.69	3.14	4.36	3.64	4.24	3.45	15.73	2.45	5.78
Na_2O	0.30	0.36	0.22	0.28	0.32	0.34	0.36	0.32	0.42	0.73
K_2O	4.13	4.75	7.62	5.58	5.80	4.72	3.90	7.40	4.28	8.73
P_2O_5	0.10	0.31	1.25	1.09	0.46	0.45	0.18	1.18	0.53	1.25
H_2O+	7.38	6.01	6.05	4.02	5.13	5.78	7.91	1.91	1.00	1.80
H_2O-	5.62	4.94	1.52	4.28	5.79	3.81	4.76	0.33	0.34	0.29
CO_2	1.37	0.71	1.96	0.37	1.13	1.09	[illegible]	10.41	1.51	0.48
Rest	1.41	1.78	1.75	9.95	1.95	2.77		2.22	2.17	3.26
Total	100.82	99.96	101.08	99.64	100.21	99.26	[illegible]	99.7[illegible]	100.14	100.38
Ba	6181	9018	8215	82262	9819	17692		12767	7304	19640
Li	6	8	6	5	6	6		3	13	6
Rb	437	468	518	683	483	507	[illegible]0	447	470	452
Sr	755	1095	790	1183	1478	1217	843	1839	1080	1614
Pb	20	22	20	10	23	22	20	10	110	39
Th	25	27	27	37	26	42	19	14	14	25
U	2	1	1	4	3	3	2	2	6	3
Zr	1287	1338	1138	2045	1375	1107	1324	2462	6011	2320
Nb	133	134	118	135	123	153	120	96	294	143
Y	9	13	8	12	12	12	8	10	31	18
La	141	161	163	211	162	236	140	79	120	154
Ce	265	282	296	279	317	381	257	123	194	259
Nd	82	82	95	135	96	130	79	36	68	82
Sc	10	10	12	10	14	12	11	17	43	15
V	108	107	67	106	59	89	98	39	262	124
Cr	706	696	1135	212	911	697	722	34	67	413
Co										
Ni	567	504	576	64	533	449	535	66	50	281
Cu	40	42	33	67	41	41	48	85	213	86
Zn	65	68	65	74	66	66	62	61	75	89
Sn	10	7	7	5	9	6	11	20	60	20
Mo										
Ga	10	11	10	10	12	10	10	12	<2	9
As	2	2	2	5	2	2	2	3	7	3
S										
F	1900	2100	2900	1600	2000	2300	1900	1800	2400	4600
Cl				45						170

Sample number	81210197B	81210200	81210201	81210202	81210203	81210204	81210206	81210207	81210208	81210213
Formation	Fitzroy	Fitzroy	Fitzroy	Fitzroy	Fitzroy	Fitzroy	Fitzroy	Fitzroy	Fitzroy	Fitzroy
Rock type	Lamproites Alt PJ-KR-Sh-Sa Lamp	Lamproites Di-Ph-Ol-KR-Lc Lamp	Lamproites Ph-Ol-Di-KR-Lc lamp	Lamproites Ph-Di-Ol-KR-Lc lamp	Lamproites Porph Phl-Ol-Lc Lamp	Lamproites Ph-KRi-Di-Ol-Lc Lamp	Lamproites Por Ph-Di-Ol-Lc Lamp	Lamproites Ph-Di-KRi-Ol-Lc Lamp	Lamproites Phl-Di-Ol-KR-Lc Lamp	Lamproites Ph-Di-Ol-Kr-Lc Lamp
Locality	Walgidee Hills	Walgidee Hills	Walgidee Hills	Walgidee Hills	Walgidee Hills	Walgidee Hills	Walgidee Hills	Walgidee Hills	Walgidee Hills	Walgidee Hills
Grid reference										
Map sheet	Hardman	Hardman	Hardman	Hardman	Hardman	Hardman	Hardman	Hardman	Hardman	Hardman
Additional data	E centre	E[-S10 20m	E7-S10 20m		E4-S11 20m	E8-S11 20m	E9-S11 8m	E5-S12 20m	E4-S12 12m	E3-S13 16m
Biblio. ref.	ALJ-BMR	ALJ-BMR	ALJ-BMR	ALJ-BMR	ALJ-BMR	ALJ-BMR	ALJ-BMR	ALJ-BMR	ALJ-BMR	ALJ-BMR
SiO_2	45.35	44.22	44.89	44.13	40.23	42.70	43.36	43.56	43.68	42.98
TiO_2	6.59	4.31	4.00	4.00	4.15	4.37	4.63	3.34	4.54	4.60
Al_2O_3	5.92	5.49	6.13	5.28	5.74	5.58	6.06	5.41	5.21	4.93
Fe_2O_3	8.31	6.28	6.71	6.57	6.63	6.17	6.58	6.05	6.49	6.74
FeO	1.60	0.87	0.57	0.48	1.10	1.16	1.31	0.82	1.09	0.84
MnO	0.13	0.08	0.10	0.16	0.11	0.09	0.10	0.08	0.09	0.10
MgO	7.95	17.24	13.88	16.48	17.29	17.31	14.55	18.52	15.09	15.39
CaO	4.85	3.08	3.64	3.67	3.89	3.68	4.15	3.65	3.78	4.18
Na_2O	1.16	0.41	0.44	0.36	0.38	0.34	0.31	0.33	0.43	0.41
K_2O	9.66	5.02	5.79	4.34	7.78	4.43	6.78	4.56	5.66	4.90
P_2O_5	1.53	0.26	0.27	0.27	2.44	0.40	0.80	0.44	0.73	0.66
H_2O+	1.51	6.00	5.12	5.45	1.42	6.03	3.38	5.86	4.97	5.56
H_2O-	0.22	3.26	2.36	5.67	0.58	4.70	2.65	3.92	3.95	4.43
CO_2	1.86	0.95	1.03	0.65	5.74	0.34	0.29	0.53	0.64	0.87
Rest	4.07	1.82	4.42	2.16	2.50	1.64	1.73	1.72	2.15	2.20
Total	100.71	99.29	99.35	99.67	99.98	98.94	96.68	98.79	98.50	98.79
Ba	27866	9415	32132	12613	15312	8860	9094	9775	11700	12172
Li	9	6	5	6	5	11	11	5	6	6
Rb	436	458	543	473	582	400	430	471	531	510
Sr	1933	1094	812	1002	1223	1205	1248	1044	1457	1357
Pb	63	20	9	23	25	20	22	18	29	28
Th	14	28	37	22	23	27	29	21	21	26
U	3	3	2	2	2	1	1	2	1	2
Zr	1748	1212	1057	1334	1598	1290	1190	1071	1774	2240
Nb	182	136	105	121	107	139	138	101	128	119
Y	20	9	7	8	9	11	13	9	10	10
La	90	169	441	144	148	161	159	136	160	152
Ce	160	308	649	260	177	210	202	170	199	180
Nd	63	100	231	76	123	117	113	101	126	126
Sc	16	9	8	9	14	11	11	9	11	13
V	204	107	116	125	103	107	87	112	140	121
Cr	27	812	836	720						
Co										
Ni	57	533	439	538	518	586	571	699	459	450
Cu	96	44	34	48	48	50	45	36	72	60
Zn	96	67	65	63	77	73	73	64	73	75
Sn	25	9	<2	9	10	9	9	7	14	12
Mo										
Ga	9	10	11	10	11	10	10	9	10	10
As	3	2	3	2	3	2	2	1	2	3
S										
F	5100	1900	2400	1800	3200	1500	2900	1900	3100	2400
Cl										

Sample number	81210215A	81210215B	81210216	81210226	81210227	81210228	81210229A	81210229B	81210229C	71301
Formation	Fitzroy Lamproites	Fitzroy Lamproites	Fitzroy Lamproites	Fitzroy Lamproites	Fitzroy Lamproites	Fitzroy Lamproites	fitzroy lamproites	Fitzroy Lamproites	Fitzroy Lamproites	fitzroy lamproites
Rock type	Ph-Di-KRi-Ol-Lc lamp	Ph-Di-KRi-Ol-Lc Lamp	Porph Ol-Di-Lc lamp	Ph-Di-KRi-Ol-Lc lamp	Phl-Di-Ol-Lc Lamp	KR-Di-Phl-Ol-Lc Lamp	Carb Ph-Di KR-Ol-Lc L	Ph-Di-KRi-Ol-Lc Lamp	Ph-Di-KRi-Ol-Lc Lamp	Pri-Jp-Sh-Wd-Carb L
Locality	Walgidee Hills	Walgidee Hills	Walgidee Hills	Walgidee Hills	Walgidee Hills	Walgidee Hills	Walgidee Hills	Walgidee Hills	Walgidee Hills	Walgidee Hills
Grid reference										975747
Map sheet	Hardman	Hardman	Hardman	Hardman	Hardman	Hardman	Hardman	Hardman	Hardman	Hardman
Additional data	W1-S14 18m	W1-S14 2m	E6-S15	B0-S18	E3-S19 35m	E4-S19 20m	B0-S15A 14	B0-S15A 30	B0-S15A 60	central oc
Biblio. ref.	ALJ-BMR	ALJ-BMR	ALJ-BMR	ALJ-BMR	ALJ-BMR	ALJ-BMR	ALJ-BMR	ALJ-BMR	ALJ-BMR	Lewis-GSWA
SiO_2	44.20	44.21	42.07	41.09	42.58	42.57	39.89	41.97	41.66	33.40
TiO_2	4.24	4.35	4.44	4.00	4.18	4.32	3.07	3.45	3.67	9.14
Al_2O_3	5.23	5.42	5.78	5.00	5.33	5.66	4.98	5.36	5.02	3.80
Fe_2O_3	6.34	6.60	6.77	4.88	4.73	5.53	5.77	4.18	4.48	7.10
FeO	0.84	0.91	0.90	2.38	2.56	1.84	0.43	2.39	2.44	0.68
MnO	0.07	0.08	0.13	0.11	0.10	0.10	0.12	0.10	0.12	0.06
MgO	17.11	17.41	15.60	19.13	16.92	16.94	17.43	19.32	19.57	6.98
CaO	3.04	3.29	4.78	3.76	3.77	3.85	5.01	2.07	3.97	13.30
Na_2O	0.39	0.41	0.39	0.23	0.34	0.39	0.21	0.22	0.21	0.37
K_2O	5.37	5.32	5.45	3.75	4.73	5.44	3.53	3.96	3.96	6.44
P_2O_5	0.35	0.47	1.62	0.26	0.47	0.44	0.10	0.13	0.30	1.79
H_2O+	5.06	5.83	4.77	6.15	5.11	5.36	5.07	5.94	5.65	2.89
H_2O-	3.60	3.22	3.45	5.00	4.28	3.82	4.43	5.08	3.65	1.33
CO_2	0.37	0.87	0.55	0.46	0.14	0.39	2.78	0.18	0.72	10.00
Rest	1.91	1.77	2.10	1.26	1.61	1.93	1.09	1.15	1.27	2.70
Total	98.12	100.16	98.80	97.46	96.85	98.58	93.91	95.50	96.69	99.98
Ba	9362	7974	11447	4911	7688	10025	3929	4374	5233	18176
Li	6	6	10	5	5	6	7	5	4	8
Rb	509	474	403	408	434	502	374	392	377	324
Sr	1463	1441	1040	1248	1088	1294	787	820	1067	1743
Pb	25	27	20	21	22	21	19	19	16	30
Th	29	26	29	27	27	28	27	27	32	<5
U	2	1	1	2	2	3	2	2	3	<1
Zr	1437	1439	1239	1170	1198	1147	1146	1222	906	676
Nb	140	139	135	139	135	134	112	120	129	87
Y	12	12	13	12	12	12	10	10	11	8
La	193	147	172	137	148	180	140	141	153	79
Ce	349	275	323	229	274	321	266	270	266	<27
Nd	110	84	103	78	91	104	79	89	91	
Sc	11	11	13	9	9	10	9	9	8	21
V	126	123	46	82	99	63	75	83	72	65
Cr	746	799	967	734	800	907	687	648	769	7
Co										30
Ni	536	561	577	653	588	538	713	636	713	100
Cu	41	47	45	19	44	40	35	32	34	160
Zn	67	70	73	67	69	70	61	63	63	62
Sn	13	12	8	15	9	12	6	8	7	
Mo										<1
Ga	9	9	9	9	8	11	9	10	9	8
As	2	1	2	1	1	1	1	1	1	<1
S										600
F	2100	2500	2600	1100	1700	1900	1100	1100	1200	3500
Cl									170	270

Sample number	71302	84210349	84210350	84210354	84210360	84210361	84210366	84210367	84210368	84210369
Formation	Fitzroy Lamproites	Fitzroy Lamproites	Fitzroy Lamproites	Fitzroy Lamproites	Fitzroy Lamproites	Fitzroy Lamproites	Fitzroy Lamproites	Fitzroy Lamproites	Fitzroy Lamproites	Fitzroy Lamproites
Rock type	KRi-Di-Lc Lamproite	Di-Ph-KRi-Ol-Lc Lamp	Ph-Di-KRi-Ol-Lc Lamp	Ph-Di-KRi-Ol-Lc Lamp	Ph-Di-KRi-Ol-Lc Lamp	Di-Ph-KRi-Ol-Lc Lamp	Di-Ph-KRi-Ol-Lc lamp	PJ Ph-Di-Ol-KR-Lc L	Di-KRi-Ph-Ol-Lc Lamp	Di-Ph-KRi-Ol-Lc Lamp
Locality	Walgidee Hills	Walgidee Hills	Walgidee Hills	Walgidee Hills	Walgidee Hills	Walgidee Hills	Walgidee Hills	Walgidee Hills	Walgidee Hills	Walgidee Hills
Grid reference	975747									
Map sheet	Hardman	Hardman	Hardman	Hardman	Hardman	Hardman	Hardman	Hardman	Hardman	Hardman
Additional data	centre	B0-S3	B0-S4	B0-S14	E4-S16	E3-S15	E1-S13	E5-S10	W3-S14	W2-S15
Biblio. ref.	Lewis-GSWA	ALJ-BMR	ALJ-BMR	ALJ-BMR	ALJ-BMR	ALJ-BMR	ALJ-BMR	ALJ-BMR	ALJ-BMR	ALJ-BMR
SiO_2	48.50	44.31	43.49	45.48	45.70	46.10	45.63	41.71	44.87	43.49
TiO_2	5.24	4.36	4.13	4.37	3.94	4.00	3.96	4.87	4.18	3.83
Al_2O_3	6.10	5.13	4.97	5.45	5.45	5.45	5.59	5.26	5.72	5.35
Fe_2O_3	7.30	5.26	6.78	6.83	6.99	6.64	6.97	6.60	5.41	6.99
FeO	1.76	1.81				0.69		1.03	0.78	
MnO	0.11	0.10	0.10	0.04	0.06	0.07	0.06	0.07	0.06	0.09
MgO	9.77	19.90	17.37	17.51	16.57	16.77	17.38	15.66	19.26	18.49
CaO	5.52	2.23	5.52	2.21	3.65	3.78	2.71	5.82	2.01	3.72
Na_2O	0.98	0.36	0.36	0.40	0.42	0.47	0.44	0.50	0.38	0.39
K_2O	8.28	3.72	4.20	3.62	4.59	4.42	4.49	4.06	3.86	4.23
P_2O_5	1.03	0.11	0.15	0.17	0.15	0.14	0.09	0.29	0.17	0.34
H_2O+	1.73	6.74	6.05	5.78	5.44	6.88	5.92	7.31	7.47	6.35
H_2O-	0.57	4.02	4.86	6.45	4.98	3.27	4.84	4.10	3.90	4.04
CO_2	0.15									
Rest	3.28	1.35	1.39	1.18	1.34	1.31	1.42	2.05	1.20	1.77
Total	100.32	99.40	99.37	99.49	99.28	99.99	99.50	99.33	99.27	99.08
Ba	19754	5390	5293	3856	5463	4662	5948	9400	4340	8971
Li	6	7	9	9		9		9	7	7
Rb	395	417	425	294	451	441	456	473	331	477
Sr	1600	867	1075	946	1111	943	916	2496	772	1188
Pb	50	28	32	25	27	30	28	42	27	27
Th	21	28	31	24	30	28	26	24	27	26
U	<1	4	4	3.5	3.5	3.5	3	4.5	3.5	3
Zr	1928	1167	1438	1192	1198	1179	1286	1890	1155	1213
Nb	135	153	172	127	148	155	145	182	143	139
Y	19	20	18	15	19	19	19	24	18	23
La	283	138	159	144	132	133	146	137	147	146
Ce	277	250	260	269	224	230	257	242	262	232
Nd		116	110	118	98	97	105	136	112	111
Sc	24	10	11	10	10	9	9	13	10	10
V	50	96	81	104	108	112	126	120	92	85
Cr	213	851	886	756	795	795	852	605	829	825
Co	45									
Ni	290	819	793	680	581	725	617	541	755	799
Cu	130	43	43	40	36	40	49	66	39	38
Zn	100	66	65	64	62	67	64	78	76	66
Sn		12	17	8	9	10	12	19	8	11
Mo	<3	<3	<3	<3	<3	<3	<3	<3	<3	<3
Ga	12	10	9	11	12	10	17	9	13	9
As	<1	1.5	2	1.5	1.5	1.5	1.5	3	1.5	1.5
S	400									
F	5660	1500	1200	2100	1300	2300	1500	1700	1600	1200
Cl	260									

Sample number	80210097	80210098	71359	71361	71362	83210246	83210249	83210251
Formation	Fitzroy Lamproites	Fitzroy Lamproites	Fitzroy Lamproites	Fitzroy Lamproites	Fitzroy Lamproites	Fitzroy Lamproites	Fitzroy Lamproites	Fitzroy Lamproites
Rock type	Ol-Lc Lamp tuff-brecc	Ol-Lc Lamp Tuff	Ol-Lc Lamproite	Ol-Lc Lamproite	KRi-Ol-Lc Lamproite	Vesic Phl-Lc Lamp.	Phl - Lc Lamproite	Ol-Di-Lc Lamproite
Locality	White Rocks	White Rocks	White Rocks	White Rocks	White Rocks	White Rocks	White Rocks	White Rocks
Grid reference	873867	873867	872866	872866	872865	873867	871866	874865
Map sheet	Hardman	Hardman	Hardman	Hardman	Hardman	Hardman	Hardman	Hardman
Additional data			centre	centre o/c	centre o/c	N margin	W margin	dyke in tf
Biblio. ref.	GPG-BMR	GPG-BMR	Lewis-GSWA	Lewis-GSWA	Lewis-GSWA	ALJ-BMR	ALJ-BMR	ALJ-BMR
SiO_2	52.17	52.70	54.40	51.30	52.30	51.00	50.53	51.59
TiO_2	4.75	5.00	4.48	5.05	6.10	6.09	6.35	6.67
Al_2O_3	8.64	8.68	8.70	8.00	9.00	8.54	8.91	8.44
Fe_2O_3	3.84	4.29	4.30	5.90	7.10	5.60	6.52	5.93
FeO	1.90	1.85	2.00	0.66	0.75	1.05	0.64	0.98
MnO	0.09	0.09	0.12	0.07	0.04	0.08	0.09	0.06
MgO	7.73	6.45	6.57	6.65	5.50	5.74	5.14	5.74
CaO	2.92	2.73	2.43	2.97	2.08	2.24	1.62	2.49
Na_2O	0.52	0.53	0.70	0.60	0.38	0.50	0.32	0.49
K_2O	10.73	10.96	9.92	8.73	9.62	11.76	12.05	11.39
P_2O_5	1.31	1.16	0.72	0.65	0.70	1.27	1.03	0.70
H_2O+	2.10	1.65	2.60	3.45	2.75	1.62	2.20	2.32
H_2O-	0.53	0.57	1.26	1.90	2.04	0.79	0.68	1.16
CO_2	0.81	0.36	0.05	0.11	0.08	0.20	0.42	0.28
Rest	1.81	1.64	1.33	3.40	1.35	2.83	2.96	2.13
Total	99.85	98.66	99.58	99.44	99.79	99.31	99.46	100.37
Ba	11419	9918	4908	22102	4915	16244	18290	10925
Li	10	9	17	12	10	8	6	8
Rb	272	285	201	168	265	293	278	332
Sr	1501	1284	1177	1417	1117	1734	811	1348
Pb	52	53	60	60	70	94	101	70
Th	14	17	21	18	21	29	30	26
U	2	2	1	<1	<1	3	3	3.5
Zr	932	989	915	969	1156	1446	1427	1481
Nb	99	105	94	104	115	181	194	173
Y	18	20	25	18	23	31	32	29
La	219	292	314	421	381	450	496	358
Ce	298	363	452	417	447	801	956	597
Nd						344	363	267
Sc			15	17	18	14	15	12
V	164	167	167	188	149	288	271	206
Cr	198	225	230	253	254	345	340	440
Co			30	30	35			
Ni	289	250	470	490	590	116	233	406
Cu	42	40	100	100	130	67	62	71
Zn	64	57	83	81	80	108	94	79
Sn	11	12				6	8	19
Mo	3	4	<1	<1	<1	4	4	<3
Ga	13	14	17	16	19	34	35	20
As	2	2	1	1	<1	4	4	3
S			800	2600	200			
F			2500	2940	2780	3600	3400	2600
Cl			450	290	170			

Sample number	81210230A	81210230B	71366	83210287	83210288	83210289	83210290	83210291	83210292
Formation	Fitzroy	Fitzroy	Fitzroy	Fitzroy	Fitzroy	Fitzroy	Fitzroy	Fitzroy	Fitzroy
Rock type	Lamproites Di-Phl-KRi -Lc Lamp.	Lamproites Phl-Di-KRi -Lc Lamp.	Lamproites KRi-Phl-Lc Lamproite	Lamproites Phl-KRi-Lc Lamproite	Lamproites Phl-KRi-Lc Lamproite	Lamproites Di-Phl-KRi -Lc Lamp.	Lamproites Di-KRi-Phl -Lc lamp.	Lamproites Di-Phl-KRi -Lc lamp.	Lamproites Phl-Di-Lc Lamproite
Locality	Rice Hill	Rice Hill	Rice Hill	Rice Hill	Rice Hill	R ce Hill	Rice Hill	Rice Hill	Rice Hill
Grid reference	394141	394141	395138	395138	395139	395140	396141	393140	395138
Map sheet	Willumbah	Willumbah	Willumbah	Willumbah	Willumbah	Willumbah	Willumbah	Willumbah	Willumbah
Additional data				S side	uppr ridge	NE side	NE side	W side	S side
Biblio. ref.	ALJ-BMR	ALJ-BMR	Lewis-GSWA	ALJ-BMR	ALJ-BMR	ALJ-BMR	ALJ-BMR	ALJ-BMR	ALJ-BMR
SiO_2	48.17	50.89	51.00	48.06	52.23	51.87	50.56	53.06	48.86
TiO_2	6.04	5.96	6.04	5.95	5.76	6.35	6.44	6.28	7.10
Al_2O_3	7.83	8.28	7.70	8.23	8.64	8.65	7.89	8.41	9.59
Fe_2O_3	5.88	5.08	4.70	5.29	5.17	4.97	5.22	4.89	6.36
FeO	1.34	1.15	1.84	1.60	0.98	1.40	1.80	1.38	0.75
MnO	0.11	0.06	0.07	0.05	0.08	0.05	0.08	0.08	0.04
MgO	8.53	7.96	9.18	7.85	6.28	7.27	8.42	6.44	4.82
CaO	3.79	3.52	4.02	3.54	3.55	3.08	3.83	3.38	2.74
Na_2O	0.49	0.56	0.81	0.87	0.61	0.73	0.95	0.80	0.13
K_2O	8.38	9.44	9.24	8.90	10.72	10.79	10.08	9.86	10.25
P_2O_5	0.37	0.44	0.45	0.45	1.00	0.37	0.37	0.53	1.18
H_2O+	4.46	1.87	2.01	3.56	1.81	2.00	1.43	1.72	2.55
H_2O-	1.66	1.22	1.09	2.52	0.83	0.87	0.43	1.38	3.18
CO_2	0.97	0.14	0.06	0.47	0.16	0.18	0.14	0.16	0.15
Rest	2.20	2.14	2.05	2.54	1.94	2.11	2.31	1.99	2.01
Total	100.22	98.71	100.26	99.88	99.76	100.69	99.95	100.36	99.71
Ba	12179	12713	11673	14172	10346	11723	13245	10271	9553
Li	7	13	11	21	8	12	12	9	14
Rb	393	288	294	502	372	288	330	318	323
Sr	2111	1465	1197	2881	1235	1336	1382	1379	1586
Pb	49	45	60	61	50	58	55	57	75
Th	25	20	21	26	20	23	25	24	28
U	1	2	1	3.5	3	3	3	3	3.5
Zr	1218	1026	1113	1347	1297	1268	1264	1268	1584
Nb	107	92	94	146	118	128	140	127	175
Y	20	17	21	29	20	26	24	28	27
La	301	282	301	254	241	338	277	290	427
Ce	566	537	338	485	445	506	501	525	625
Nd	186	173		239	210	252	245	241	279
Sc	10	9	16	10	13	14	14	12	17
V	206	220	138	219	161	192	200	182	171
Cr	385	374	382	372	392	371	422	389	466
Co			30						
Ni	359	383	224	354	340	343	372	348	370
Cu	69	58	82	72	74	75	70	100	74
Zn	76	65	86	81	91	73	76	116	65
Sn	19	15		17	20	22	20	22	19
Mo			3	<3	<3	<3	3	3	3
Ga	12	17	14	25	24	26	18	25	26
As	1	1		3.5	2.5	2	2.5	2.5	2.5
S			180						
F	1200	1300	2745	1100	2200	2000	2300	2500	2300
Cl			202						

Sample number	71894	71895B	71897
Formation	Fitzroy Lamproites	Fitzroy Lamproites	Fitzroy Lamproites
Rock type	Di-Phl-Lc Lamproite	Phl-Ol-Lc Lamproite	Di-Phl-Lc Lamproite
Locality	Bruten Hill	Bruten Hill	Bruten Hill
Grid reference	775305	775305	775305
Map sheet	Bruten	Bruten	Bruten
Additional data	main plug	NW side	SE side
Biblio. ref.	Lewis-GSWA	Lewis-GSWA	Lewis-GSWA
SiO_2	56.30	60.40	60.10
TiO_2	6.89	6.54	6.23
Al_2O_3	8.70	8.10	7.40
Fe_2O_3	5.40	5.80	5.60
FeO	0.97	0.77	0.70
MnO	0.04	0.06	0.05
MgO	4.96	2.78	4.14
CaO	0.91	1.10	1.77
Na_2O	0.16	0.17	0.20
K_2O	10.00	9.59	9.04
P_2O_5	0.89	0.78	0.74
H_2O+	1.85	1.46	1.64
H_2O-	1.42	1.34	1.18
CO_2	0.05	0.07	0.02
Rest	1.71	1.27	1.36
Total	100.25	100.23	100.17
Ba	8777	6205	6307
Li	10	7	8
Rb	297	269	261
Sr	702	585	760
Pb	49	49	55
Th	16	17	12
U	<1	1	2
Zr	1123	1069	1050
Nb	91	93	88
Y	20	13	11
La	265	240	230
Ce	348	294	305
Nd			
Sc	22	20	16
V	201	165	126
Cr	266	270	267
Co	28	29	29
Ni	240	186	189
Cu	104	90	90
Zn	87	77	81
Sn	11	12	13
Mo	<1	1	<1
Ga	18	18	15
As	3	2	3
S	1320	720	920
F	2820	1480	2450
Cl	<20	<20	50

Sample number	71160408	71160409	71160410	71160411	71160412	80210072	80210073	71347	71891	71893B
Formation	Fitzroy Lamproites	Fitzroy Lamproites	Fitzroy Lamproites	Fitzroy Lamproites	Fitzroy Lamproites	Fitzroy Lamproites	Fitzroy Lamproites	Fitzroy Lamproites	fitzroy lamproites	Fitzroy Lamproites
Rock type	Ol-Di-Lc Lamproite	Ol-Di-Lc Lamproite	Ol-Leuc Lamproite	Ol-Phl-Lc Lamproite	Ol-Phl-Lc Lamproite	Ol-Phl-Lc Lamproite	Ol - Lc Lamproite	Glass Ol-Lc Lamp	Alt Ol-Lc Lamproite	Ol-Lc Lamproite
Locality	Oscar Plug	Oscar Plug	Oscar Plug	Oscar Plug	Oscar Plug	Oscar Plug	Oscar Plug	Oscar Plug	Oscar Plug	Oscar Plug
Grid reference	564926	564926	564926	564926	564926	564926	564926	563927	564926	565926
Map sheet	Cunningham	Cunningham	Cunningham	Cunningham	Cunningham	Cunningham	Cunningham	Cunningham	Cunningham	Cunningham
Additional data	glassy	glass				Xenoliths		dyke	W end plug	centr dyke
Biblio. ref.	GMD-BMR	GMD-BMR	GMD-BMR	GMD-BMR	GMD-BMR	GPG-BMR	GPG-BMR	Lewis-GSWA	Lewis-GSWA	Lewis-GSWA
SiO_2	50.37	50.36	56.87	50.31	51.81	50.79	57.15	51.20	58.80	51.60
TiO_2	4.95	4.97	5.25	5.77	6.29	6.25	5.19	4.86	5.33	4.90
Al_2O_3	8.84	9.17	8.95	9.12	9.72	9.29	8.97	8.20	8.30	8.10
Fe_2O_3	5.29	5.41	6.47	6.16	6.96	5.92	6.40	4.80	5.90	5.10
FeO	1.54	1.32	0.50	1.33	0.88	1.45	0.54	1.76	1.31	1.51
MnO	0.07	0.06	0.03	0.05	0.06	0.05	0.04	0.07	0.05	0.07
MgO	7.38	6.34	2.78	6.35	5.11	5.68	2.95	7.18	2.24	7.07
CaO	3.01	2.93	1.50	2.06	0.56	1.92	1.53	2.99	1.65	3.09
Na_2O	0.18	0.15	0.09	0.17	0.09	0.10	0.15	0.18	0.33	0.32
K_2O	7.90	8.29	10.13	10.56	11.15	11.05	10.46	7.67	9.26	7.80
P_2O_5	1.11	1.05	1.08	1.33	0.43	1.36	1.11	1.12	0.96	1.13
H_2O+	4.11	3.42	2.23	2.84	2.52	2.02	1.90	4.20	2.20	4.80
H_2O-	2.55	3.81	1.70	1.65	1.70	1.16	1.83	3.29	2.15	2.80
CO_2	0.21	0.22	0.32	0.15	0.28	0.35	0.16	0.08	0.01	0.10
Rest	2.95	2.21	1.78	1.89	2.49	1.42	1.40	2.63	1.75	2.19
Total	100.46	99.71	99.68	99.74	100.05	98.81	99.78	100.23	100.24	100.58
Ba	16409	10739	9251	9258	14446	7378	7626	15278	9905	12933
Li	6	9	6	8	9	8	6	9	8	8
Rb	3694	2124	242	302	331	377	316	2183	223	1123
Sr	902	918	677	1097	484	1006	857	1053	706	960
Pb	46	48	44	53	44	53	47	42	43	48
Th	21	21	22	24	28	26	23	<5	25	<5
U	8	3	6	5	9	2	3	<1	1	<1
Zr	1115	1214	1194	1321	1394	1364	1160	1092	1033	946
Nb	104	111	116	130	139	134	112	88	116	90
Y	2	2	10	11	17	25	17	47	16	<5
La	289	291	315	303	292	349	272	281	279	258
Ce	554	581	549	616	597	464	375	294	330	274
Nd	184	190	208	196	196					
Sc								19	24	19
V	213	225	246	253	289	192	167	159	157	170
Cr	552	623	640	611	631	261	354	503	461	365
Co	40	36	22	30	37			36	21	36
Ni	336	351	434	297	462	239	384	250	431	304
Cu	48	45	44	53	55	52	46	78	53	92
Zn	70	70	82	71	126	82	71	82	75	78
Sn	8	3	4	4	3	14	9		7	11
Mo						4	3	3	1	2
Ga	20	20	19	21	25	21	18	18	17	16
As	3	2	<1	2	2	1	1		1	4
S								140	540	320
F	2200	2700	2000	2700	3400			2348	1560	2160
Cl					10			139	<20	30

Sample number	71893C
Formation	Fitzroy Lamproites
Rock type	Ol-Lc Lamproite
Locality	Oscar Plug
Grid reference	565926
Map sheet	Cunningham
Additional data	dyke E end
Biblio. ref.	Lewis-GSWA
SiO_2	51.90
TiO_2	5.54
Al_2O_3	9.40
Fe_2O_3	6.60
FeO	0.69
MnO	0.07
MgO	5.22
CaO	2.15
Na_2O	0.15
K_2O	10.97
P_2O_5	1.17
H_2O+	2.88
H_2O-	2.66
CO_2	0.04
Rest	1.35
Total	100.79
Ba	5450
Li	8
Rb	280
Sr	942
Pb	47
Th	19
U	1
Zr	1084
Nb	106
Y	15
La	287
Ce	383
Nd	
Sc	23
V	183
Cr	414
Co	26
Ni	371
Cu	65
Zn	72
Sn	9
Mo	2
Ga	21
As	1
S	50
F	3000
Cl	<20